J. Indian Chem. Soc., Vol. LXIII, No. 1, Pp. 1-186

January 1986 JULY

CODEN: JICSAH LXIII, (1) (1986), 1-186

ISSN 0019-4522

JOURNAL OF THE INDIAN CHEMICAL SOCIETY

PROFESSOR SADHAN BASU 65TH BIRTHDAY COMMEMORATION ISSUE

Published by The Indian Chemical Society
92 Acharya Prafulla Chandra Road
Calcutta-700 009

INDIAN CHEMICAL SOCIETY

92 ACHARYA PRAFULLA CHANDRA ROAD

CALCUTTA-700 009

Price of Publications :

1. Catalogue of Physico-Chemical Standard Substances
   Reprinted from *Pure Appl. Chem.*, 1972, 29, 601-16
   (With the kind permission of the International Union of Pure and Applied Chemistry) :
   Price : Rs. 4.00 (Inland, inclusive of postage)
   Rs. 8.00 (Foreign, inclusive of postage by Surface Mail).

2. Acharya Prafulla Chandra Ray : Life and Achievements
   by Prof. N. R. Dhar :
   Price : Rs. 5.00 (Inland, inclusive of postage)
   Rs. 10.00 (Foreign, inclusive of postage by Surface Mail).

3. Reflections on Chemical Education
   by Prof. N. R. Dhar :
   Price : Rs. 12.50 (Inland, inclusive of postage)
   Rs. 25.00 (Foreign, inclusive of postage by Surface Mail).

4. History of Chemistry in Ancient and Medieval India
   Edited by Prof. P. Ray :
   Price : Rs. 30.00 (Inland, inclusive of postage)
   Rs. 75.00 (Foreign, inclusive of postage by Surface Mail).

5. Abstracts of XX-ICCC (held at Calcutta in December, 1979) :
   Price : Inland : Rs. 325.00 (Inclusive of postage by Regd. Surface Mail)
   Foreign : Rs. 425.00 or U. S. $ 50.00 (Inclusive of postage by Regd. Air Mail)

6. Calcutta (A Tourist Guide Book) :
   Price : Inland : Rs. 15.00 (Inclusive of postage)
   Foreign : Rs. 25.00 (Inclusive of postage by Surface Mail).

Annual Subscription (inclusive of postage) for the Journal of the Indian Chemical Society (for Non-Fellows) for 1986 :

Rs. 400.00 (Inland) ; U. S. $ 125.00 (Foreign), Air Postage Extra (May be paid in equivalent Indian Rupee).

Back issues of the Journal of the Indian Chemical Society and the Indian Journal of Applied Chemistry (upto 1972 ; discontinued from January, 1973) may be available, for which separate enquiries are to be made for the availability and rates.

I. Kar

Executive Secretary

J. Indian Chem. Soc., Vol. LXIII, No. I, Pp. 1-186 ISSN 0019-4522

January 1986

CODEN : JICSAH LXIII, (1) (1986), 1-186

JOURNAL OF THE INDIAN CHEMICAL SOCIETY

PROFESSOR SADHAN BASU 65TH BIRTHDAY COMMEMORATION ISSUE

Published by The Indian Chemical Society
92 Acharya Prafulla Chandra Road
Calcutta-700 009



Professor Sadhan Basu
D.Sc., F.N.A., F.R.S.C., F.A.Sc.

(*Born* : January 2, 1921)

FOREWORD

This issue of the *Journal of the Indian Chemical Society* containing invited articles from a number of distinguished scientists is dedicated to Professor Sadhan Basu, an eminent Physical Chemist and an outstanding teacher of the country, to commemorate his 65th Birthday. This is a fitting tribute to his pioneering contributions in the fields of quantum chemistry, molecular spectroscopy and polymer chemistry and to his long and dedicated service to the cause of chemical education. Professor Basu adorned the Chair of Sir Taraknath Palit Professor of Chemistry of the University of Calcutta from 1965 till his retirement on 31st January, 1986. He was the Director of the Indian Association for the Cultivation of Science, Calcutta during 1980-82. During his long research and teaching career in the University of Calcutta he introduced new dimensions in research and teaching of various branches of Quantum Chemistry and Molecular Spectroscopy and founded a well reputed school in these fields.

On the occasion of the 65th Birthday of Professor Basu a *National Conference on Spectroscopy and Theoretical Chemistry* was organised in the auditorium of the Saha Institute of Nuclear Physics, Calcutta on 5th and 7th December, 1986 and at the Indian Association for the Cultivation of Science, Calcutta on 6th December, 1986. Some of the articles contributed in this issue were also presented at the conference. A souvenir booklet titled *Sadhan Basu—the man, scientist and teacher* containing a short biographical sketch of Professor Basu, a brief resumé of his contributions as a scientist and a teacher, a list of his publications *etc.* was brought out by the Celebration Committeeand was released during the inaugural ceremony of the National Conference on 5th December, 1986.

It is our proud privilege to convey on behalf of the *Professor Sadhan Basu 65th Birthday Celebration Committee* our heartiest thanks to the distinguished authors who graciously responded to our invitation and contributed articles at a short notice. The Celebration Committee is grateful to the Council of the Indian Chemical Society for accepting the proposal for the publication of this commemoration issue. We gratefully acknowledge the cooperation offerred in this endeavour by Professor M. M. Chakrabarty, Hony. Editor of the Journal (Physical and Industrial Chemistry Sections) and Mr. Prabir K. Gupta, Executive Editor for their kind cooperation in bringing out this issue.

Mihir Chowdhury
Convener

Sunil K. Talapatra
Hony. Secretary
The Indian Chemical Society
and
Convener

Animesh Chakravorty
Convener

Professor Sadhan Basu 65th Birthday Celebration Committee

INFORMATION FOR AUTHORS OF CONTRIBUTIONS AND PUBLISHERS OF BOOKS

1. **Manuscripts for publication** in the *Journal of the Indian Chemical Society* should be typed with double spacing on one side of good quality paper (Bond) with at least 3.5 cm margin on the left hand side and clear margin on all other sides ; ***the original and 2 carbon copies are to be submitted.*** **These should be addressed to the Honorary Editor, Indian Chemical Society, 92 Acharya Prafulla Chandra Road, Calcutta-700 009.**

On the top right hand corner of the title page of the manuscript, the **section** (viz. Inorganic Chemistry, Physical Chemistry, Organic Chemistry, Analytical Chemistry, Biochemistry, Industrial Chemistry/Chemical Engineering, *etc.*) for which the communication is to be considered **should be clearly indicated.**

On receipt of a paper the author sending the paper shall be duly intimated of the Society's registration number for the manuscript which must be quoted by the author in all future correspondence on it to the Society. *All such future correspondence should be addressed to the* **Executive Editor.**

2. **A paper will not be accepted for publication unless the author or at least one of the authors (in case of a contribution submitted jointly by more than one author) is a Fellow or a Member of the Indian Chemical Society of some category.**

3. Original contributions to new chemical knowledge, both experimental and theoretical, in all the areas of Chemistry, are accepted for publication in the *Journal of the Indian Chemical Society.* Two types of contributions are considered for publication : *Articles* and *Notes.* Both categories should have sufficient information to permit repetition of the experimental work.

Contributions which have been published or accepted for publication in another journal or in any other freely available printed work **will not be published** in the *Journal of the Indian Chemical Society.* **A declaration to that effect from the author must accompany a manuscript submitted for publication.**

Authors are solely responsible for the factual accuracy of their contribution.

4. A prospective contributor should consult recent issues of this journal to get acquainted with its *contents* and *style.* Definitive accounts of significant completed studies presenting new important data or providing a fresh approach to an established subject should be submitted as **articles.** The presentation should be in a logical manner consistent with accuracy, clarity and brevity. The text should be divided into the following sections : (a) Introduction ; (b) Experimental ; (c) Results and Discussion ; (d) References. Divisions within the sections should be indicated by sub-headings. **Extensive review and unnecessary details of earlier work should be avoided.** Well known or previously published procedures followed in the experimental work should only be referred to, omitting details. Important findings and results of much interest which may require priority in publication shall be considered for publication as **notes.**

Any portion of the text for which a special type of print is required must be indicated : **single underlining** for *italic* type and **double underlining** for ***bold black*** type.

The *title* of a contribution should tell accurately and clearly what the paper is about. The first letter of each noun and adjective in the title must be in *capital.* The title shall be followed by the names of the authors and their addresses. The name of the senior author to whom correspondence may be made about the paper must be marked by an asterisk (*). His present address, if different from that quoted as above, must be given in a foot-note.

Every article must be accompanied by an informative *abstract* that summarises the principal findings of the work presented in the paper. Normally it should not be over 3 per cent of the length of the paper and should not exceed 250 words. It should be in a form that it may be used directly for publication in abstracting periodicals. This abstract should be typed before the main text and indented *ca* 2 cm to the right of it. *No such abstract is necessary for notes.*

5. The charge carried by an ion should be indicated in the following manner : Na^+, Cu^{2+}, $Co(NH_3)_6^{3+}$, Cl^-, SO_4^{2-}, $Fe(CN)_6^{3-}$, *etc.* Standard abbreviations should be used throughout the experimental section e.g., m.p., b.p., sec, min, h, mg, g, kg, mm, cm, cps, tlc, uv, ir, nm, *etc.* Analytical results should be reported in the form : (Found : N,......; Cl, ... ; Ni,....... Calcd. for...... ; N,...... ; Cl,...... ; Ni,...... %).

6. *Literature citations* **should be numbered consecutively and these numbers are to appear as superscripts in appropriate positions in the text. Care must be exercised for uniformity in reference citations.** "Ibid", "Idem", "et al", *etc.* should not be used. *Abbreviations for titles of journals must ordinarily conform to those used by the "Chemical Abstracts" published by the American Chemical Society (vide : "List of Periodical Abstracted"). References to uncommon journals should also give corresponding references in Chemical Abstract.* **All the references must be typed in their serial order at the end of the text in the manuscript. The names (not surnames only) of all the authors should be given.** A few sample citations are given below :

P. C. RAY, *J. Indian Chem. Soc.*, 1924, **1**, 207.

R. J. KULA, D. T. SAWYER, S. I. CHAN and C. M. FINLEY, *J. Am. Chem. Soc.*, 1963, **85**, 2930.

C. S. GARNER and D. A. HOUSE in "Transition Metal Chemistry", ed. R. L. CARLIN, Marcel Dekker, New York, 1970, Vol. 6, p. 59.

Foot-notes must be referred to in the text with suitable symbols such as *, †, ‡, §, ‖, *etc.*

7. **Instructions for Diagrams and Figures** : The number of tables, diagrams and photographs should not be more than what is absolutely necessary, in view of the fact that the reproduction of such materials is very costly. **If these exceed 20% of the pages of the text, authors may have to pay for the excess cost.**

a. Figures should be numbered with Arabic numerals and mentioned consecutively in the text indicating their respective locations. *All Figures must have legends and these should be typed out separately on a sheet of paper at the end of the main text of the manuscript.* **Legends should not duplicate information in the text.**

b. One set of the drawings should be made with India ink on tracing paper or good quality white drawing paper. *Graph paper should not be used.* Lines should contrast sharply with the back-ground. **Most drawings should be planned for reproduction to a column width of 7.5 cm. Lettering should be large enough to be 1.5 mm high after reduction.** Large drawings should be simplified for submitting with the manuscript, in a size which is reducible to not more than 16 cm × 22 cm. For satisfactory reproduction all drawings should be approximately twice the size in which they are to appear in the print. Use of legends in the body of the diagram must be reduced to the minimum. Free-hand drawings and drawings unsuitable for block making cannot be accepted. If necessary the Editors may get the figures redrawn properly for which the actual cost is to be borne by the author(s). Structures and formulae which cannot be composed must also be submitted as suitable drawings for blockmaking.

c. If original tracings are not available, glossy prints of the tracings can be used if the back-ground is clear and the lines are distinct.

d. Photographs should be glossy black and white prints with sharp contrast. Paper clips mark the surface, and writing on the back of photos often punches through, spoiling the prints. **Photographs of equipment should be avoided.** Photomicrographs should be unmounted and should not be more than 7.5 cm wide.

8. *Reprints* shall be supplied only on receipt of payment of the usual charges, *i.e.*, 50 reprints @ Rs. 15/- (U. S. $ 5.00 for foreign) per page or part thereof, subject to a minimum charge of Rs. 35/- (U. S. $ 12.50 for foreign). 100 reprints of 1-2 pages @ Rs. 50/- and for subsequent 2 pages or part thereof @ Rs. 40/-, next 100 reprints or part thereof at half the original rate. For foreign, 100 reprints @ U. S. $ 8.00 per page or part thereof subject to a minimum of U. S. $ 20.00. Next 100 reprints or part thereof at half the original rate. *Additional postage is to be paid for Air Mail Charge. No free reprints are supplied and no such request can be entertained.* Reprint order form is sent to author with the proof.

9. **Books submitted for review** in the *Journal of the Indian Chemical Society* must be sent in **duplicate** to the Honorary Editor, Indian Chemical Society, 92 Acharya Prafulla Chandra Road, Calcutta-700 009, so that one copy may be retained in the Library of the Indian Chemical Society, while the other copy may be retained by the reviewer for his personal use.

In case of rejection of a paper, the opinion of the Honorary Editor shall ordinarily be treated as final.

Journal of the Indian Chemical Society

VOLUME LXIII | NUMBER 1 | JANUARY 1986

CONTENTS

CONTENTS

CONTENTS

AUTHOR INDEX

Journal of the Indian Chemical Society

VOLUME LXIII | NUMBER 2 | FEBRUARY 1986

CONTENTS

CONTENTS

CONTENTS

CONTENTS

Journal of the Indian Chemical Society

VOLUME LXIII NUMBER 3 MARCH 1986

CONTENTS

CONTENTS

CONTENTS

NOTES

CONTENTS

AUTHOR INDEX

NOTE : An asterisk in the heading of each paper indicates the author for correspondence.

Journal of the Indian Chemical Society

VOLUME LXIII NUMBER 4 APRIL 1986

CONTENTS

CONTENTS

CONTENTS

CONTENTS

Journal of the Indian Chemical Society

VOLUME LXIII NUMBER 5 MAY 1986

CONTENTS

CONTENTS

CONTENTS

CONTENTS

AUTHOR INDEX

Note: An asterisk in the heading of each paper indicates the author for correspondence.

Journal of the Indian Chemical Society

VOLUME LXIII | NUMBER 6 | JUNE 1986

CONTENTS

Zakir Husain ... Jamia ... M. I. ...

CONTENTS

NOTES

CONTENTS

AUTHOR INDEX

NOTE : An asterisk in the heading of each paper indicates the author for correspondence.

J. Indian Chem. Soc.,
Vol. LXIII, January 1986, pp. 1-9

Investigation of Solids and Surfaces by Photoacoustic Spectroscopy†

C. N. R. RAO*, P. GANGULY and T. SOMASUNDARAM

Solid State and Structural Chemistry Unit, Indian Institute of Science, Bangalore-560 012

After presenting the essentials of the principles and instrumentation involved in photoacoustic spectroscopy, a variety of studies of solids and surfaces carried out by this technique are reported. Some of the important aspects of the spectroscopy examined are signal saturation, intensity enhancement and fluorescence quenching. Applications to the study of amorphous solids, phase transitions and surfaces are discussed.

PHOTOACOUSTIC spectroscopy has emerged to become a very useful absorption spectroscopic technique in recent years. The technique is based on the photoacoustic effect discovered by Graham Bell[1] over a century ago. Photoacoustic effect in gases has been understood almost since its discovery, but it is only in the last few years that a proper theoretical treatment of photoacoustic effect in solids has been possible[2]. After the absorption of radiation by a solid sample, the excited state can decay radiatively or non-radiatively; if the radiation is modulated, the heat given out during non-radiative decay will also be modulated. The heat diffusion into the coupling fluid (ordinarily ambient air in the cell) produces pressure variation with the same frequency as the frequency of modulation (f) and this can be detected by a microphone. The direct correspondence between the light absorbed by the sample and the intensity of the sound signal picked up by the microphone makes photoacoustic spectroscopy a viable alternative to conventional optical spectroscopy. Photoacoustic spectroscopy has advantages over the optical technique in certain situations. For example, in the case of solids[3], scattering by powder samples does not impose limitations in photoacoustic spectroscopy (PAS). Furthermore, PAS is also a surface-sensitive technique[3], requiring hardly a monolayer coverage of the absorbing substance. In this article we shall discuss the principles and applications of photoacoustic spectroscopy with particular reference to solids and surfaces.

Theoretical model :

The model that has been most useful in understanding PAS of solids is the one due to Rosencwaig and Gersho[4] (RG). The RG model is based on a one-dimensional analysis of the production of a PA signal in a cylindrical cell and gives an exact equation for the magnitude and phase of the signal in terms of the thermal, optical and geometrical properties of cell, sample and the ambient gas. The sample of thickness, *l*, is mounted on a backing material as shown in Fig. 1. If the backing material and the gas are non-absorbing, the following thermal

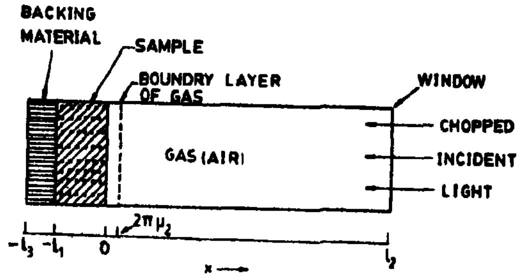


Fig. 1. Cross sectional view of the photoacoustic cell.

diffusion equation (where, the distance x changes from zero at the surface to negative values inside the solid) can be written

$$\frac{\partial^2 \theta}{\partial x^2} = \frac{1}{\alpha_1}\frac{\partial \theta}{\partial t} - A \exp(\beta x)\ [1+\exp(i\omega t)]$$

$$\text{where, } A = \frac{\beta I_0 \eta}{2K_1} \qquad (1)$$

The various terms in equation (1) are defined as follows: θ = temperature, I_0 = intensity of incident light, η = efficiency of conversion of light into heat, K_i = thermal conductivity (cal cm^{-1} s^{-1} K^{-1}), ρ_i = density (g cm^{-3}), C_i = heat capacity (cal g^{-1} K^{-1}), α_i = thermal diffusivity ($=K_i/\rho_i C_i$) (cm^2 s^{-1}), μ_i = $(1/a_i)$ = thermal diffusion length ($=(2\alpha_i/\omega)^{1/2}$) (cm), ω = chopping frequency ($=2\pi f$) (Hz).

The subscript i = 1, 2 and 3 refers to the solid, gas and backing, respectively. The real part of the solution of equation (1) represents the temperature-variation in the cell relative to the ambient. On applying the boundary conditions (*viz.* (i) cell walls are at the ambient temperature and (ii) there is continuity of temperature and flux at the surface) to the a.c. and d.c. components of the time-dependent spatial temperature variation, we obtain the time dependent and independent temperature distribution in the cell. The real part of the a.c. component gives the temperature variation in the gas,

$$T_{a.c}(x,t) = \exp(-a_2 x)[\theta' \cos(\omega t - a_2 x) - \theta'' \sin(\omega t - a_2 x)] \qquad (2)$$

† Dedicated to Professor Sadhan Basu on the occasion of his 65th birthday.
Contribution No. 820.

where, θ' and θ'' are the real and the imaginary parts of θ which determine the in-phase and quadratic components. The time-dependent temperature variation attenuates rapidly to zero at a distance $2\pi\mu_s$. The boundary layer of thickness $2\pi\mu_s$ responds thermally to temperature acting as an acoustic piston for the gas column.

The displacement of the boundary layer $\delta x(t)$ can be determined by knowing the average temperature within the boundary layer,

$$\delta x(t) = \frac{\theta\mu_s}{\sqrt{2}T_0} \exp\,[i(\omega t - \pi/4)] \tag{3}$$

where, T_0 is the sum of the ambient and d.c. temperatures at the surface. Assuming that the rest of the gas responds to the action of the acoustic piston adiabatically, the incremental pressure $\delta p(t)$ is given by,

$$\delta p(t) = Q \exp\,[i(\omega t - \pi/4)]$$

$$\text{where } Q = \frac{\gamma p_0 I_0}{\sqrt{2} l_s T_0 a_s} \tag{4}$$

γ being the ratio of specific heats. The actual pressure variation is given by the real part of equation (4),

$$Q = Q' + iQ'' \tag{5}$$

we thus see that Q represents the complex envelope of sinusoidal pressure variation

$$Q = \frac{\beta I_0 \gamma p_0}{\sqrt{2}2T_0 K_1 l_g a_g (\beta^2 - \sigma^2)} \cdot \frac{(r-1)(b+1)e^{\sigma l_1} - (r+1)(b-1)e^{-\sigma l_1} + 2(b-r)e^{-\beta l_1}}{(g+1)(b+1)e^{\sigma l_1} - (g-1)(b-1)e^{-\sigma l_1}} \tag{6}$$

where, $b = K_s a_s/K_1 a_1$; $g = K_g a_g/K_1 a_1$; $r = (1-i)\beta/a_1^2$ and $\sigma = (1+i)a_1$. Equation (6) can be employed to evaluate the magnitude and phase of the acoustic pressure wave in the cell.

Aamodt and others[5] have modified the RG model by applying the Navier-Stokes equation for heat conduction. McDonald and Wetsel[6] have included corrections for mechanical vibration of the sample at high modulation frequencies.

Instrumentation :

A photoacoustic spectrometer for the study of solids is not very different from the conventional optical spectrometer. It consists of a radiation source, a monochromator, a light modulator, a sample cell fitted with a microphone (detector) and the data collection and processing system (recorder, microprocessor *etc.*). Since photoacoustic detection involves the detection of sound rather than photons, care has to be exercised to minimise external noise.

The PA signal varies inversely with the gas volume, v, in the cell and one has to therefore minimise v, without damping the acoustic signal. Since only the boundary layer of the gas $2\pi\mu_s$ responds thermally, l_g should be greater than μ_s ; at the same time, l_g has to be kept small to minimise thermoviscous damping. The optimal value of l_g is 0.1-0.2 cm. The signal can be improved by employing low temperatures and high gas pressures ; use of gases with high thermal conductivity can also improve the signal. Signal enhancement has also been accomplished by using volatile liquids in the cell[7]. Noise can be reduced by using polished materials ; the signal to noise ratio is enhanced by the use of materials which undergo a small temperature rise for large heat input. Scattered light should be allowed to escape (by proper cell design) before it is absorbed by the walls, microphone *etc.* Acoustic isolation helps in avoiding spurious signals while vibration-free mounting is useful to avoid effects due to mechanical vibrations. The design of the cell depends on the physical nature of the sample. For variable temperature measurements, the microphone would have to be kept outside the sample chamber and connected by an acoustic-proof capillary. Fast cooling or heating adversely affects the microphone due to pressure surges ; condensation of water should be avoided.

Solids in the form of powders (or powder compacts) can be readily studied by PAS. Films deposited on quartz plates as well as smears can also be examined. Substances adsorbed on solid surfaces (from solution or some other means) can also be investigated.

An indigenous photoacoustic spectrometer for the uv-visible range : The block diagram of a spectrometer indigenously built in our laboratory[8] is shown in Fig. 2. Light from a high pressure xenon lamp is focussed onto a GM250 monochromator fitted

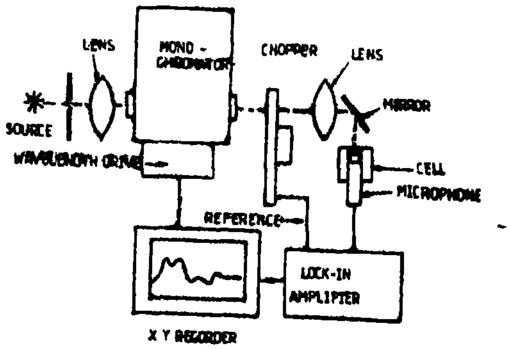


Fig. 2. Block diagram of the single-beam photoacoustic spectrometer fabricated by the authors.

with a Schoeffel holographic grating. A tungsten lamp would suffice if only the visible region is of interest. The light emerging from the monochromator passes through a chopper (PAR 194A) capable of providing frequencies in the 10-1 000 Hz range. The PA cell is an air-tight aluminium chamber which has been designed taking the various factors mentioned earlier into account. A condenser microphone (GR 1961) with a flat frequency

response in the range 10-2 000 Hz is attached to the rear side of the sample chamber with an air-tight sealing. The signals from the microphone and reference from the chopper are fed to a lock-in-amplifier (PAR 124A) and the output of the tuned amplifier gives the sound signal which is recorded as a function of the wavelength of light.

Variable temperature measurements can be carried out by employing cells described by Ganguly and Rao[8]. The cell for low-temperature measurements has been designed in such a way that the sample is surrounded by a cold finger which in turn is connected to liquid nitrogen reservoir, the whole system being kept under vacuum. A stainless steel capillary is welded to the sample holder to provide passage of the sound to the microphone while a 3-way stopcock provides the necessary equilibrium pressure during temperature changes. In the high-temperature cell, the microphone is kept away from the sample chamber but connected with a glass capillary. Temperature is sensed by a chromel-alumel thermocouple placed near the sample. Temperatures only upto 550 K could be attained since a teflon O-ring was used in the spectrometer.

Electronic spectra of solids :

Electronic absorption spectra of solid substances can be recorded by the PAS technique provided the transitions do not involve radiative decay. The substance can be crystalline or amorphous, single crystal or polycrystalline ; it can even be in the form of a gel. In Fig. 3 we show the unnormalised PA spectra of Nd_2O_3 and $NdAlO_3$ in the visible

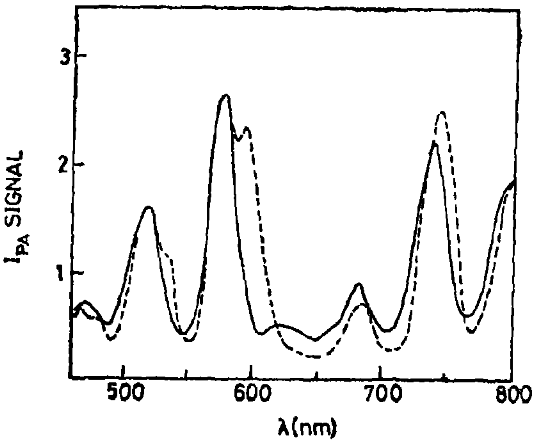


Fig. 3. Unnormalised spectra of Nd^{III} compounds : (- - -) Nd_2O_3 and (—) $NdAlO_3$; Δλ 10 nm, f 28 Hz.

region ; the slight differences arise from the different modes of de-excitation[8]. In Fig. 4 we show the spectra of single crystal and polycrystalline samples of $NaNO_2$ in the uv region ; we see little difference between the spectra as indeed expected. PAS is ideally suited to record the spectra of solids which are sparingly soluble in solvents. However, PAS has no particular advantage over transmission

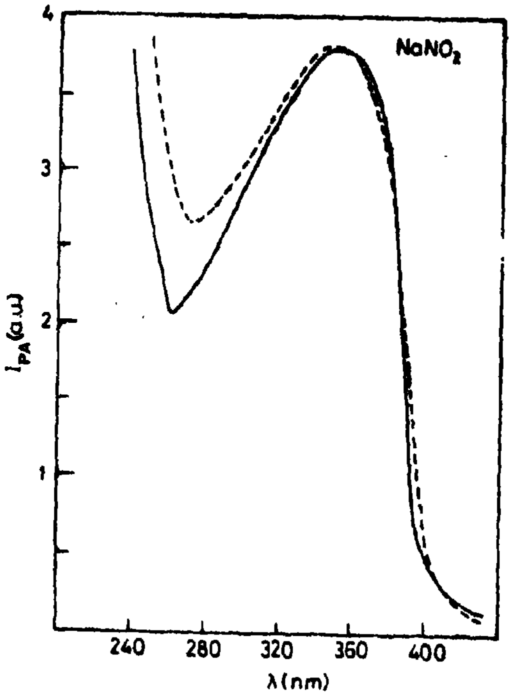


Fig. 4. Normalised spectra of $NaNO_2$ (intensities normalised to be equal at 360 nm) : (- - -) powdered sample and (—) single crystal ; Δλ 5 nm, f 40 Hz.

optical spectra (recorded with KBr pellets or oil mulls between quartz plates) and diffuse reflectance spectra.

Signal saturation :

The active layer in the solid responding thermally in PAS has a thickness of $2\pi\mu_1$. As the thermal oscillations, generated at a distance x from the surface, move towards the surface, their amplitude attenuate exponentially[6] as $\exp(-x/\mu_1)$. For $x = 2\pi\mu_1$, the attenuation becomes $\exp(-2\pi)$. If the sample thickness is greater than $2\pi\mu_1$ and the surface of the sample is in contact with the gas, the heat distribution is given by $\beta \exp(-\beta s)$, where, s is the distance from the surface and β is the absorption coefficient. The increase in the PA signal accompanying an increase in absorptivity can be attributed to the movement of the heat distribution into the active layer and closer to the surface ; this prevails till $\beta^{-1} = \mu_1$, when the heat distribution moves completely inside the active layer and saturation sets in (Fig. 5). Further increase in β will eventually lead to full saturation[8] when $10\,\beta^{-1} = \mu_1$.

According to the RG model, saturation can be avoided by changing the frequency of modulation such that $\mu_1 < \beta^{-1}$. This is not however suitable for materials with $\beta > 10^4$ cm^{-1} as one would require frequencies greater than 10^4 Hz to bring them out of the saturation regime ; use of such a high frequency also leads to enormous reduction of the signal to noise ratio. Proper sample preparation can avoid saturation[9] by bringing down the sample

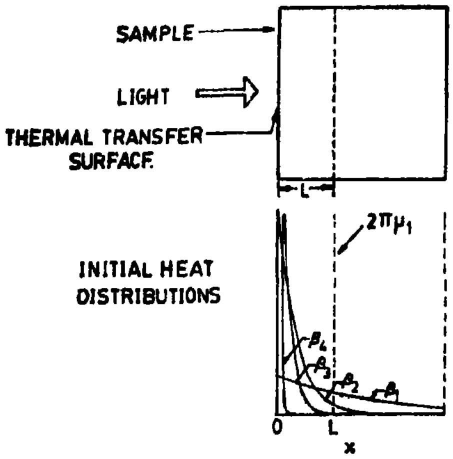


Fig. 5. Attenuation of heat distribution in the solid sample after light absorption for various β values[8]. The boundary layer ($2\pi\mu_1$) is indicated ($\beta_1<\beta_2<\beta_3<\beta_4$).

size to less than β. This can be done for example by dispersing the absorbing substance in a non-absorbing matrix or over the surface of a non-absorbing solid ; another possibility is to prepare a thin layer of the sample by vacuum or solution technique. In Fig. 6 we show the use of such techniques in the case of tetraphenylporphin[9].

Intensity enhancement :

Since PAS is specially useful in providing information on materials of low absorption coefficient or opaque substances, it would be particularly beneficial if the limits of detection can be extended by some means. The PA signal from solids can be enhanced several-fold by placing volatile liquids[7], such as diethyl ether or acetone in the cell ; the enhancement which is more marked for low β and high f depends upon the vapour pressure of the liquid. In order to hold the liquids, the PA cell sample holder is made of two concentric portions, the outer portion containing a non-absorbing solid (*e.g.* Al_2O_3) soaked in the liquid. In Fig. 7 we show the PA spectra of $Nd_2Al_6O_{12}$ in air and in the presence of diethyl ether to illustrate the intensity enhancement in the presence of a volatile liquid. The intensity enhancement is found to vary linearly with the vapour pressure. The enhancement is likely to be due to the desorption and adsorption of the adsorbed vapours on the solid surface, accompanying the thermal oscillations. The factors reponsible for the intensity enhancement are the efficient heat transfer arising from the reduction in the thermal diffusion length in the gas phase (μ_g) and the increase in the number of gas molecules in the gas phase due to desorption. PAS can also be employed to investigate liquid-liquid interfaces where again intensity enhancement by volatile liquids can be exploited.

Fluorescence quenching :

If the decay after optical absorption is through a radiative process such as fluorescence, one would expect the PA signal to have little or no intensity. Quenching of luminescent pathways would however give rise to PA signal as illustrated in the case of Ho_2O_3 and Ho_2O_3-Co, F (Fig. 8). The doped sample exhibits additional lines which arise from the known energy levels of Ho^{III} ; obviously, these extra lines were not present in the spectrum of pure Ho_2O_3 due to fluorescent decay[10].

Fluorescent quantum yields, η, of solid materials are difficult to determine compared to solutions because the number of quanta absorbed from a monochromatic radiation cannot be compared with the number of quanta of polychromatic radiation emitted due to geometrical problems associated with solid samples. Employing the PA saturation technique, η can be determined for solid luminescent

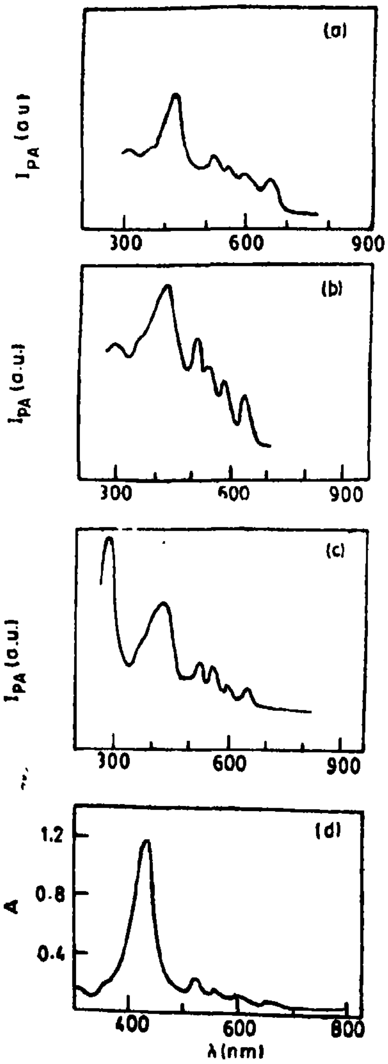


Fig. 6. Photoacoustic spectra of tetraphenylporphin[9] (TPP) : (a) 0.35 wt% of TPP mechanically dispersed in $BaSO_4$ by cogrinding, (b) 0.1 wt% of TPP chemically dispersed on $BaSO_4$ by slurry method, (c) 0.8 μg of TPP smear on quartz plate, and (d) optical spectrum of TPP.

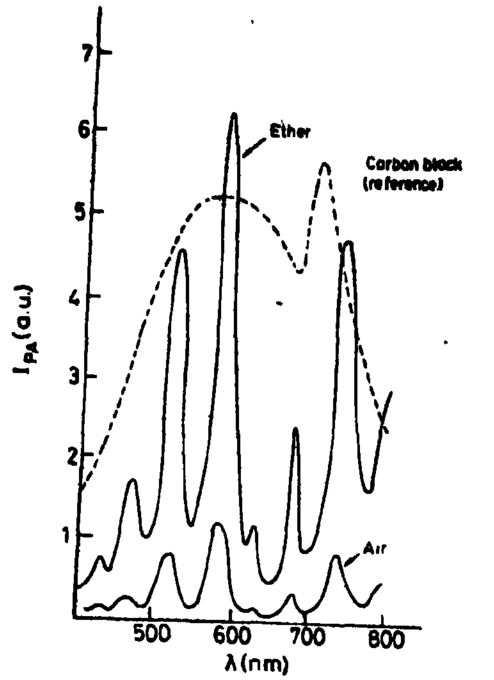


Fig. 7. PA spectrum of $Nd_2Al_6O_{12}$ in the presence of air (bottom curve) and ether (top curve). The reference spectrum of carbon black is also shown.

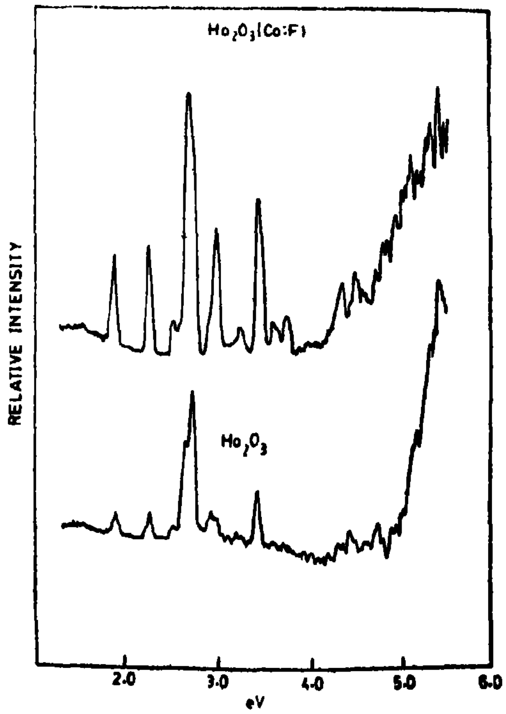


Fig. 8. PA spectra of pure and doped holmium oxides[10].

samples[11]. The PA signal characteristic of a fluorescent sample can be written as,

$$I_F = k_F p_F \left[1 - \eta + \eta\left(\frac{\nu_0 - \nu_F}{\nu_0}\right)\right] \quad (7)$$

where, k_F is a constant characteristic of the thermal properties of the sample and the instrumental characteristics, p_F is the power absorbed by the sample, and ν_0 and ν_F are the excitation and emission frequencies, respectively. For a non-fluorescent sample, the PA signal is given by,

$$I_{NF} = k_{NF}\, p_{NF} \quad (8)$$

we therefore obtain,

$$\frac{I_F}{I_{NF}} = \frac{k_F\, p_F}{k_{NF}\, p_{NF}} \left(1 - \frac{\lambda_0}{\lambda_F}\eta\right) \quad (9)$$

where, λ_0 and λ_F represent the excitation and emission wavelengths, respectively. For saturated signals, we can assume[11] that $p_F = p_{NF}$. Equation (9) then becomes,

$$\frac{I_F}{I_{NF}} = \frac{k_F}{k_{NF}} \left(1 - \eta\frac{\lambda_0}{\lambda_F}\right) \quad (10)$$

We can calculate η from the known values of λ_0 and λ_F and measured values of I_F and I_{NF}. It is obvious that a plot of I_F/I_{NF} against λ is nothing but the normalised spectrum using carbon black. Particle size seems to affect the value of η thus obtained[11]. PAS can however be fruitfully employed to determine η in solution media[12,13].

Solid state reactions :

Reactions of solids can be followed by PAS provided there are appropriate absorption bands of the reactants or/and products in the uv or visible region. Chance and Shand[14] have employed PAS to carry out photocalorimetry. They have made use of the fact that the heat due to light absorption as well as the heat liberated in the reaction are measured in PAS. Accordingly, in a polymerisation reaction, the time-dependence of the intensity of the PAS bands would depend on the heat of the reaction relative to the heat associated with photo-absorption ; the rate of polymerisation would determine the heat of polymerisation at a given time. In PAS, the intensity of a band depends on the power absorbed and the efficiency of conversion of light into heat, η, while in optical spectroscopy (OS) the intensity depends only on the power absorbed. For a substance with $\eta = 1$, therefore, a plot of (PAS)/(OS) *vs* wavelength should be a straight line with zero slope. If $\eta \neq 1$, the plot will give the wavelength dependence of the photo-reaction or the action spectrum. Such action spectra have been recorded for the polymerisation of diacetylenes[15].

Amorphous solids :

Optical spectroscopic characterisation of many of the amorphous solids by conventional techniques is rendered difficult due to the highly reflecting and absorbing nature of these materials. Optical studies on such solids are therefore made with thin films which are difficult to prepare. Ganguly and Rao[3] have shown that PAS is an effective tool for studying amorphous materials, since only the absorbed light is converted into heat (or the PA signal) and the scattered light does not pose any serious problem.

PA spectra of several arsenic chalcogenide glasses have been investigated in this laboratory[16]

and the study has provided absorption edges of these materials. The thermal coefficients of the absorption edges have been obtained by recording temperature-dependent PAS. In Fig. 9, we show the normalised PA spectra of amorphous and crystalline As_2S_3 and As_2Se_3. There is a steep rise in photo-absorption in the 500-600 nm region. The

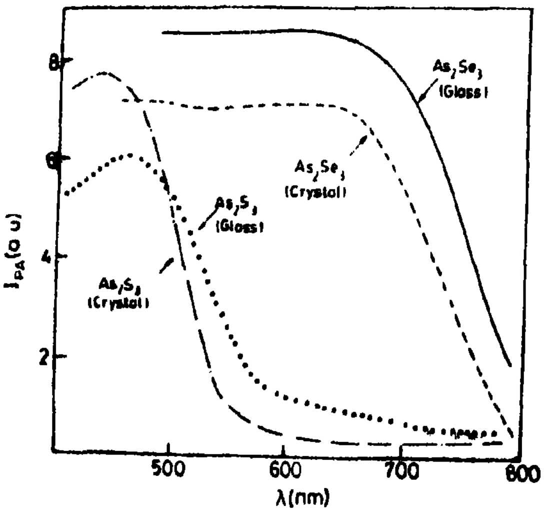


Fig. 9. Normalised PA spectrum of As_2S_3 and As_2Se_3.

absorption edges are rather smeared out in the case of amorphous materials. We have taken 90% maximum normalised intensities to represent the band energies and these values correspond well with the reported data. The edge energies for the crystalline phases are higher than for the glasses. This is because the greater spread of the non-bonding levels of the chalcogenides in the glassy state which constitute the top of the valence band. Temperature-dependent PA spectra of As_2S_3 glass indicate a red shift consistent with the earlier observation by Young[17]. The thermal coefficient of the band edge energy calculated from temperature-dependent PAS measurements gives a value 7.1×10^{-4} eVK^{-1} which is in good agreement with the reported value of 7.0×10^{-4} eVK^{-1}.

Phase transitions in solids :

PA effect depends not only on optical but also on thermal properties of the material. The thermal diffusion length, μ_1, which gives the distance from which heat can diffuse to the surface and produce a PA signal is given by,

$$\mu_1=\left(\frac{k_1}{\pi\rho_1 C_1 f}\right)^{1/2} \qquad (11)$$

During a phase transition the thermal properties change continuously or abruptly. These changes are manifested by a change in the PA amplitude. Monitoring the PA amplitude as a function of temperature should therefore provide information about the phase transition. We have investigated[18] several first and second order phase transitions in solids and compared our experimental results with the predictions of the RG model based on the known changes in specific heat and thermal diffusivity. The PA signal at a second order transition for a thermally thick material behaves as $C_1^{-1/2}$ or C_1^{-1} depending upon whether the material is optically opaque or not. This dependence is based on the assumption that k_1 does not change during a transition, and this does not always hold. We can derive an equation for α_1 considering the changes in k_1 and other factors[19],

$$\alpha_1=\frac{1}{3}\bar{v}_0\bar{l}_0 \qquad (12)$$

where $\bar{v}_0$ and $\bar{l}_0$ are the average sound velocity and average mean-free path of phonons, respectively in the solid. This equation indicates that a PA signal which depends on α_1 should be influenced by $\bar{v}_0$ and $\bar{l}_0$. Our studies have shown that changes in the PA amplitude are dominated by C_1 changes; α_1 also plays a decisive role.

Sodium nitrite undergoes a first order transition from a ferroelectric to an incommensurate antiferroelectric phase at 437 K followed by a second order transition to a paraelectric phase at 438 K. These phase transitions were followed at 360 and 400 nm with single crystal as well as polycrystalline samples. The transitions were clearly seen both while heating and cooling and were separated by 2° in the cooling run. After temperature and amplitude normalisation, the PA curves showed nearly the same behaviour (Fig. 10). Particle size of the material does not seem to affect the phase transition to any measurable extent.

Cobalt monoxide undergoes antiferromagnetic ordering at the Neel temperature of 290 K. We have followed this transition for powdered CoO using white light. There was no temperature hysteresis and the transition was clearly seen both while heating and cooling. Comparison of the PA amplitude with the actual changes[20] in C_1 and α_1 show that the curve fits well with an $\alpha_1^{1/2}$ behaviour (Fig. 11).

First order transitions have also been studied using the PA effect. The first order transition of of $CsNO_3$ has been followed by mixing it with carbon black and using white light. Comparison of the reported values with the experimental results show that the observed curve fits better with a $C_1^{-\frac{1}{2}}$ dependence (Fig. 12). Our studies show that there is no direct correlation between latent heat changes and PA amplitude changes accompanying phase transitions in solids.

Surface studies :

PAS can give information about the species adsorbed on solid surfaces provided the substrate is a non-absorbing substance, such as alumina or silica. A few monolayers of the chemisorbed species do not show saturation effects. We have exploited these

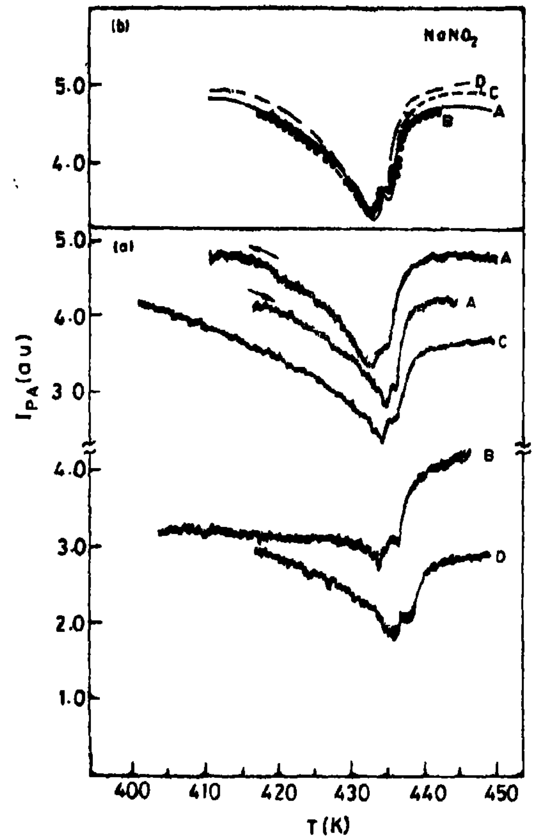


Fig. 10. I_{PA} *vs* T plots for $NaNO_2$ as obtained (a) without any corrections and (b) after corrections for temperature and amplitude changes : (A) single crystal at 360 nm, (B) single crystal at 400 nm, (C) powdered single crystal at 360 nm, and (D) commercial sample with carbon black and using white light.

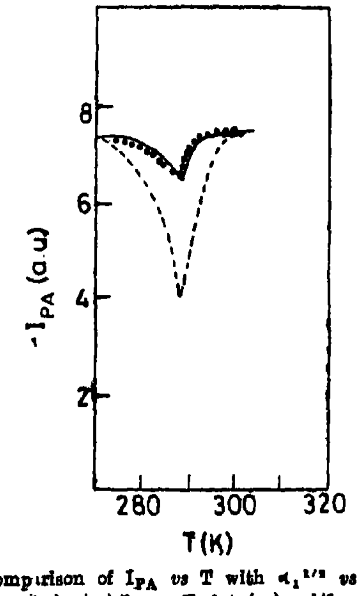


Fig. 11. Comparison of I_{PA} *vs* T with $\alpha_1^{1/2}$ *vs* T for CoO (powder) ; (—) I_{PA} *vs* T plot, (···) $\alpha_1^{1/2}$ *vs* T for data of Salamon *et al.*[30], and (- - -) $\alpha_1^{1/2}$ *vs* T for data of Zhuze *et al.*[19].

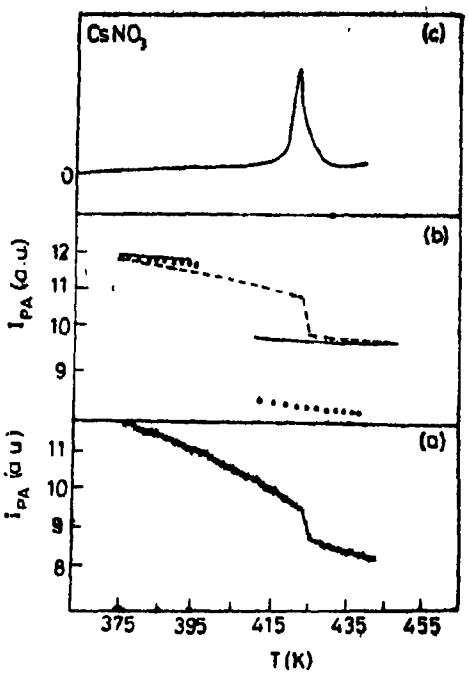


Fig. 12. (a) Plot of I_{PA} *vs* T for powdered $CsNO_3$, (b) Plot of I_{PA} T *vs* T for same sample (— — —) compared with C_1^{-1} *vs* T (···) and $C_1^{-1/2}$ *vs* T (—), and (c) differential scanning calorimeter trace of the same sample.

factors to investigate surface properties, such as surface area, surface acidity and metal states.

Adsorption of dyes on commercial activated alumina and chromatographic alumina (B.D.H.) possessing different surface areas has been examined[31] to show the surface sensitivity of PAS. Dye solutions of varying concentration were added to weighed quantities of the alumina samples and the solids filtered off after equilibration. The solid was transferred into a PA cell and the spectrum recorded. The normalised PA intensity at 580 nm per unit weight of the solid increased with increase in dye (crystal violet) concentration reaching a maximum constant value corresponding to a maximum coverage. The ratio of the intensity values for the two samples was 4.7. Visible absorption spectroscopy was employed to check whether the ratio represents the real surface area[8]. Thus, a decrease in the concentration of the supernatent dye solution after adsorption Δm and equilibrium concentration, m, could be fitted into a Langmuir equation,

$$\frac{m}{\Delta m} = \frac{m}{\Delta m_{max}} + \frac{m}{K \Delta m_{max}} \qquad (13)$$

from the plots of $(m/\Delta m)$ *vs* m, the amount adsorbed for complete monolayer coverage Δm_{max} and hence the surface area was calculated using a value of 90 Å^2 for the molecular area of the dye crystal violet. The estimated surface areas were 179 and 39 m^2 g^{-1} for activated and B.D.H. alumina,

respectively with a ratio 4.6, indicating that PAS intensity ratios are real and represent real surface area ratios (Fig. 13).

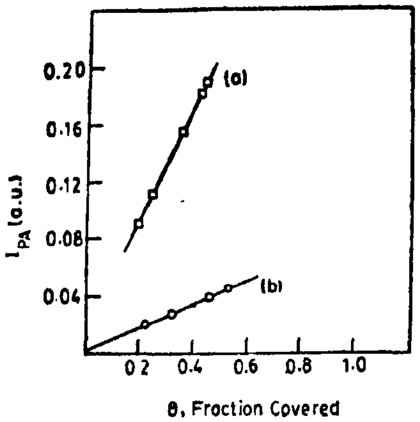


Fig. 13. Plot of I_{PA} *vs* fraction covered, *θ*, for two different alumina samples: (a) commercial alumina, and (b) chromatographic alumina.

In view of the surface sensitivity of PAS, we considered it valuable to investigate the possibility of using the technique for determining acidities of surfaces[23]. Experimentally, the procedure involves adding dry benzene (2 ml) to a pre-weighed (~0.2 g) amount of the catalyst followed by the addition of the indicator solution (0.5 ml) (in dry benzene). Solutions of n-butylamine in benzene were then added in varying amounts and equilibrated for 1 h with intermittent shaking. The spectra were recorded for the slurries in the PA cell. With bromocresol green indicator, there is only one band at 420 nm in 1% silica-alumina, whereas for 10% silica-alumina, there is one band at 550 nm corresponding to the acid form of the first titration range (lower pK_{HB+}). In the second titration range, we observe a band maximum at 600 nm corresponding to the base form whereas the band at 420 nm now corresponds to the acid form. The spectra at various titration ranges are shown in the Fig. 14. Using this procedure, we have carried out a systematic study of the acidity *distribution in a series of silica-alumina* samples by PAS and the results are shown in Fig. 15. These distributions correspond well with those found by other techniques.

We have also employed PAS for the study of surface metal states. Alumina samples impregnated with nickel nitrate solutions were heated separately at 110, 400, 600 and 800° and the PA spectra recorded at room temperature. The spectral data indicate that at 110° the sample resembles NiO, whereas other samples show a peak at 580 nm which progressively increases with the treatment temperature. This can be attributed to the increased Ni diffusion into the bulk. To check this, we have adsorbed dimethylglyoxime (DMG) over the surfaces. The Ni-DMG peak decreased to half its value at 400° (relative to 110°) indicating that only surface Ni can

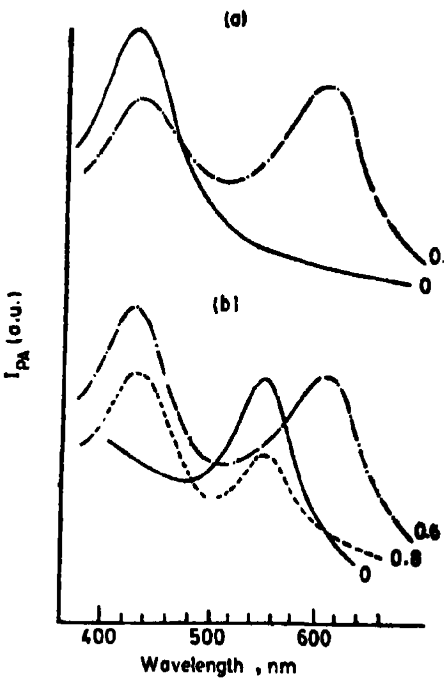


Fig. 14. Normalised PA spectra of bromocresol green adsorbed on (a) silica-alumina (1%), and (b) silica-alumina (10%) with different amounts of n-butylamine in mmol g^{-1} of the solid (indicated against each curve).

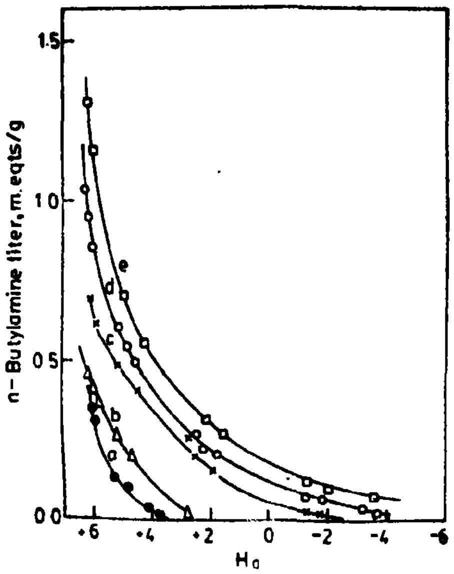


Fig. 15. Plots of the n-butylamine titre against the Hammett acidity function, H_0, for (a) silica, and (b) to (e) silica-alumina samples with different alumina contents: (b) 0.1; (c) 1.0; (d) 8.5 and (e) 10.0 wt%.

bond with DMG and their diffusion into bulk reduces the intensity of the Ni-DMG peak. The basicity of Na_2O-alumina samples have been determined[23] with the adsorption of phenolphthalein

indicator. These successes indicate the potential use of PAS for surface studies.

Acknowledgement

The authors thank the Indian National Science Academy, New Delhi, for support of this research which enabled them fabricate the photoacoustic spectrometer.

References

1. A. G. BELL, *Philos. Mag*, 1881, **11**, 510.
2. A. ROSENCWAIG, "Photoacoustics and Photoacoustic Spectroscopy", John Wiley, New York, 1980.
3. P. GANGULY and C. N. R. RAO, *Proc. Indian Acad. Sci. (Chem. Sci.)*, 1981, **90**, 153.
4. A. ROSENCWAIG and A. GERSHO, *J. Appl. Phys.*, 1976, **47**, 64.
5. L. C. AAMODT, J. C. MURPHY and J. G. PARKER, *J. Appl. Phys*, 1977, **48**, 927.
6. F. A. McDONALD and G. C. WETSEL, Jr., *J. Appl. Phys.*, 1978, **49**, 2313.
7. P. GANGULY and T. SOMASUNDARAM, *Appl. Phys. Lett.*, 1983, **43**, 160.
8. J. F. McCLELLAND and R. N. KNISELEY, *Appl. Phys. Lett.*, 1976, **28**, 467.
9. J. W. LIN and L. P. DUDEK, *Anal. Chem.*, 1979, **51**, 1627.
10. A. ROSENCWAIG, *Anal. Chem.*, 1975, **47**, 592A.
11. M. J. ADAMS, J. G. HIGHFIELD and G. F. KIRKBRIGHT, *Anal. Chem.*, 1980, **52**, 1260.
12. W. LEHMANN and H. J. LUDEWIG, *Chem. Phys. Lett.*, 1977, **45**, 177.
13. M. J. ADAMS, J. G. HIGHFIELD and G. F. KIRKBRIGHT, *Anal. Chem.*, 1977, **49**, 1850.
14. R. R. CHANCE and M. L. SHAND, *J. Chem. Phys.*, 1980, **72**, 948.
15. C. M. RAO and D. BALASUBRAMANIAN, *J. Phys. Chem.*, 1982, **86**, 989.
16. T. SOMASUNDARAM, P. GANGULY and K. J. RAO, *Proc. Indian Acad. Sci. (Chem. Sci.)*, 1983, **92**, 65.
17. P. A. YOUNG, *J. Phys. C. Solid State*, 1971, **4**, 93.
18. T. SOMASUNDARAM, P. GANGULY and C. N. R. RAO, *J. Phys. C. Solid State*, 1985, in the press.
19. V. P. ZHUZE, O. N. NOVRUZOV and I. SHELYKH, *Sov. Phys. Solid State (Engl. Transl.)*, 1969, **11**, 1044.
20. M. B. SALAMON, P. R. GARNIER, B. GOLDING and E. BUEHLER, *J. Phys. Chem. Solids*, 1974, **35**, 851.
21. K. JAGANNATHAN, P. GANGULY and C. N. R. RAO, *J. Mol. Struct.*, 1982, **79**, 173.
22. K. JAGANNATHAN, P. GANGULY and C. N. R. RAO, *J. Catal.*, 1982, **75**, 262.

J. Indian Chem. Soc.,
Vol. LXIII, January 1986, pp. 10-15

Laser Photoacoustic Spectroscopy of Azulene†

D. KUMAR, R. V. NAUMAN, T. L. MATHERS and S. P. MCGLYNN*

Chemistry Department, The Louisiana State University, Baton Rouge, LA 70803, U.S.A.

and

R. MOHANTY

Physics Department, Southern University, Baton Rouge, LA 70813, U.S.A.

The purpose of this work is to present a simple, inexpensive technique, one based on analog circuitry, which (i) corrects laser induced signals (photogalvanic, photoacoustic, fluorescence or whatever) on a pulse-by-pulse basis for the fluctuations of the individual excitation pulses and (ii) is applicable to both linear and non-linear processes. This technique is demonstrated by photoacoustic spectroscopic (PAS) investigations of azulene, it being thought that the numerous questions besetting the electronic spectroscopy of this molecule might yield to PAS probings. The O,O bands of the $S_1 \leftarrow S_0$ and $S_2 \leftarrow S_0$ transitions are presented at high resolution and the former is shown to contain four difference progressions. Comparision of PAS and absorption spectra (AS) suggests an onset of either photochemistry or luminescence upon excitation of the 1 484 cm^{-1} a_1 fundamental of the S_1 state. A new method for measuring fluorescence quantum yields is presented and discussed.

PHOTOACOUSTIC spectroscopy (PAS) is a sensitive monitor of non-radiative, energy-degradative pathways. Unfortunately, PAS technology has had to await the development of tunable lasers, sensitive microphones and piezoelectric transducers. With their advent, PAS has realised some of its potential, and various ways have been developed[1] for optimising the signals of gaseous, liquid and solid samples, as well as those of optically dense and/or scattering media.

Pulsed lasers, however, are characterised by high peak-powers and low duty-cycles. They also suffer from poor pulse-to-pulse power stability which, along with the low duty-cycle, can pose serious signal extraction problems. One may have to resort to box-car integrators with large effective time-constants and to extremely-slow scan speeds in order to extract the detailed spectroscopic structure. Alternatively, expensive, computer-based, digital data acquisition systems may be used to maximise the system resolution. The technique described here[2] is different in that it corrects the individual signals for laser power fluctuations, on a pulse-by-pulse basis, and is based on simple analog circuitry. It is a considerable improvement over conventional analog systems because it forces the duty-cycle towards unity. It is also applicable both to linear and non-linear spectroscopic measurements.

Azulene provides a sensitive test of spectrometer capabilities because of the many questions that beset its electronic spectroscopy. For example, azulene fluorescence is anomalous[3-5], being $S_2 \rightarrow S_0$ rather than $S_1 \rightarrow S_0$; few, if any, triplet states have been established with any certainty ; and, finally, the $S_2 \leftrightarrow S_0$ emissive/absorptive events do not exhibit the Lewschin mirror-image characteristic[6]. Despite extensive study[7-12], these problems remain largely unsettled.

It seemed that PAS, by virtue of its unique capabilities, could provide answer to some of the above questions. This inference is based on the following statements.

(i) The putative $S_1 \rightarrow S_0$ non-emissivity requires that, in the absence of any λ-dependent photochemistry, the $S_1 \leftrightarrow S_0$ absorption and PA spectra be identical.

(ii) The complexity of the $S_2 \leftarrow S_0$ absorption band has been attributed to a vibronic coupling of S_2 and S_4 states mediated by a_1 normal modes. If such be the case, the non-radiative energy transfer that occurs to the adjoining manifold of rovibronic states built on S_0, S_1, or T_4 states of lower or comparable energy from the pure S_2 states might be expected to differ from that arising in vibronically-contaminated S_2 states. That is, if the $S_2 \leftarrow S_0$ absorption band is as complicated as is supposed, transfer probabilities within it need not be uniform and one should see differences between the PAS and absorption spectra.

(iii) If, in fact, the $S_1 \rightarrow S_0$ quantum yield is zero, then the $S_2 \rightarrow S_0$ quantum yield (the value of which, $\phi_F \cong 0.03$, is both very low and quite uncertain[13]) should be independently determinable from $S_2 \leftarrow S_0$ and $S_1 \leftarrow S_0$ PAS data.

(iv) The origin band of the $S_1 \leftarrow S_0$ transition exhibits considerable hot band activity and it is difficult to analyse. The greater resolution of laser PAS should facilitate such an analysis.

† Dedicated to Professor Sadhan Basu on the occasion of his 65th birthday.

Thus, the purpose of this work is to describe a recently-constructed photoacoustic spectrometer and to examine its performance by addressing the electronic spectroscopy of the azulene molecule.

Experimental

The photoacoustic spectrometer[a] is shown schematically in Fig. 1. The excitation source is a Chromatix CMX-4 flash-lamp pumped, tunable dye laser of pulse width ~1 μs, peak power ~6-8 kW and band width ~3 cm^{-1} (without etalon) or 0.1-0.2 cm^{-1} (with etalon). The pulse generator produces a sequence of pairs of pulses R (reset) and T (trigger), both 10-15 μs wide, at some predetermined rate (upto 30 pairs/s). The R pulse resets the box-car integrator (PAR model 160, suitably modified by addition of an electronic switch to the integrator board) and the peak detector. The T pulse, positioned on the trailing edge of the R pulse, triggers the laser and the box-car integrator.

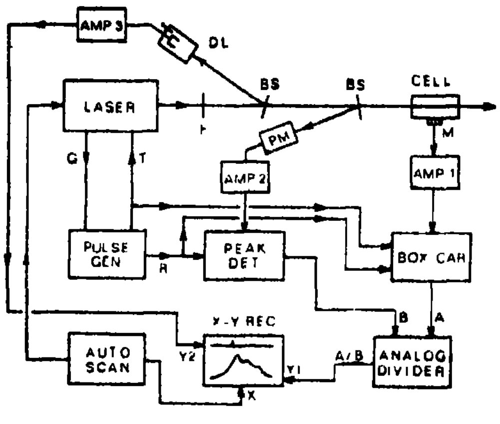


Fig. 1. Schematic of PA spectrometer: (G) CMX-4 internal gate signal, (R) reset pulse, (T) trigger pulse, (L) laser beam, (F) filter, (BS) beam-splitter, (M) microphone, (PM) photomultiplier tube, and (DL) hollow cathode discharge lamp. Amplifier 3 is followed by a rectifier and filter to convert AC into unidirectional signals. Amplifier 2 incorporates a simple RC integrator to give total pulse energy for each pulse.

The box-car, operated at very low time-constant, behaves much like a gated detector. The box-car gate is set on the first peak of the damped, acoustic ringing signal generated in the microphone. The peak-detector gets its reference signal from the photomultiplier tube, which is a wideband GaAs photocathode with nearly-flat response. Since the PA signal is proportional to laser pulse energy (*i.e.* not to peak intensity), the amplifier AMP2 contains an RC integrator (τ ~20 μs) which generates a pulse, the height of which is proportional to total pulse energy. Hence, for a given laser pulse, the box-car integrator, the peak detector and the analog divider generate signals A, B and A/B, respectively, all of which are held constant over the repetition time interval between the laser pulses (100 ms at 10 pps rate). Immediately prior to T-triggering of the next laser pulse, the R-pulse resets (*i.e.* 'zeroes') both the peak detector and the box-car so that they are conditioned for that laser pulse. This arrangement produces a sequence of normalised A/B signals at the analog divider output and maintains each of these signals constant over the time interval between pulses. That is, the effective duty cycle approaches unity. The resultant pulse train is averaged by an RC integrator, the smooth signal from which is then fed to one channel of a dual pen X-Y recorder. The second channel of the X-Y recorder displays the wavelength calibration markers that are generated by the photogalvanic effect in a neon hallow cathode discharge lamp. The AUTO-SCAN scans the laser at predetermined scan speeds (cm^{-1}/s) and also, through TTL control, activates the time-base and the pen-down mechanism of the X-Y recorder.

Excessively strong or weak pulses are eliminated from the A/B train by CMOS switches. These switches, activated by voltage comparators, monitor the over-voltage at A, B and A/B and the under-range at B. This procedure ensures that the analog divider operates in a linear range, with the result that smooth A/B output is obtained not only in the presence of large pulse fluctuations but even in the presence of 'misfires'. The voltage comparators also provide a visual indication of level-excess problems by activating a set of LED's. The non-radiative detection sensitivity of the apparatus is obtained from the absorbance data for azulene (assuming negligible $S_1 \rightarrow S_0$ emissivity) and is better than 10^{-9} J per pulse.

The advantage of this inexpensive equipment is its ability to normalise the signal, on a pulse-by-pulse basis. In addition, the improvement in duty-cycle and the ability to study non-linear processes (by replacing the analog divider module by an analog multi-function module capable of exponentiating voltages to arbitrary powers) can be matched only be expensive microprocessor-based, data-acquisition systems.

The sample cell, 1 mm thickness, is shown in Fig. 2. It is used at Brewster angles in order to minimise window reflection losses. The all-quartz construction reduces background to insignificant values. The dead space in the connecting tube is minimised in order to increase system sensitivity. Window deposition of condensible vapors is prevented by window temperatures that are slightly greater than that of the cell body. The contact gas, either argon or nitrogen, is held at atmospheric pressure. The cell is thoroughly purged with the contact gas prior to all measurements. The microphone is a Knowles Electronics BT 1759 with built-in pre-amplifier.

Azulene is purified by vacuum sublimation at temperature differentials of 25-30°. The process is slow but it produces long, thin, pure, wafer-like azulene crystals.

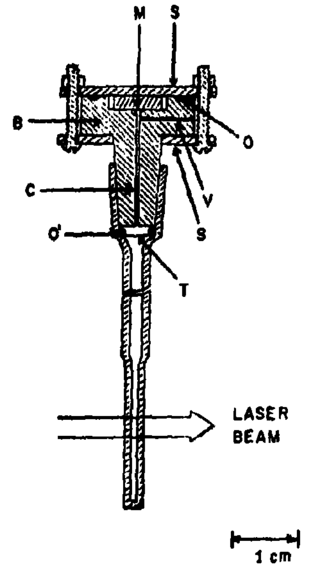


Fig. 2. Schematic of PA cell. A 2.5 cm diameter, 1 mm thick standard quartz absorption cell was fitted, as shown, with a 5 cm long quartz tube. The end of this tube was tapered to receive the microphone carriage. (M) microphone, (R) teflon block, (S) stainless steel plates, 1/16" thick, (O) O-ring seal for microphone cavity, (T) thin teflon diaphragm supported by O-ring, O', (C) thin channel, 0.2 mm diameter, and (V) vent hole.

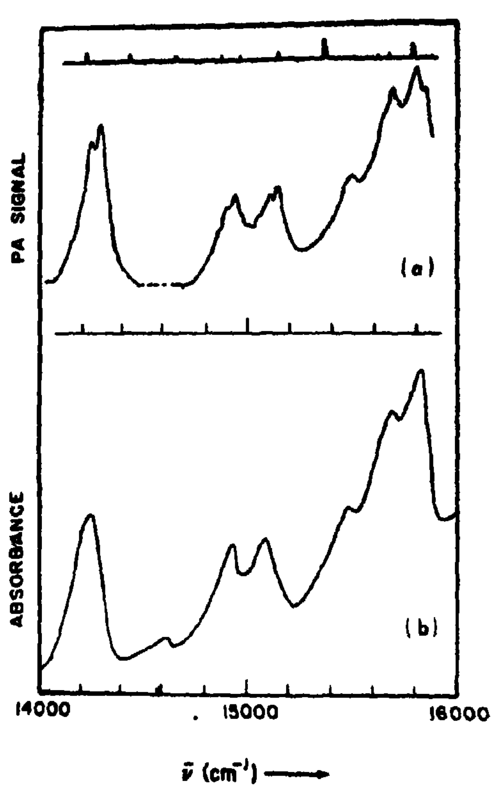


Fig. 3. (a) Partial gas-phase PA spectrum of azulene $S_1 \leftarrow S_0$; T=61°: N_2 'contact' gas; p=1 atm. The superposed vertical pips are the neon calibration markers; laser bandwidth=8 cm^{-1}, pulse repetition rate=10 pps, laser scan speed=1 cm^{-1}/s, time-constant for final averaging=1 s. Broken line indicates a gap in the spectrum due to low power of the laser dye in this wavelength region; (b) Partial gas-phase absorption spectrum of the $S_1 \leftarrow S_0$ transition of azulene. The PA spectrum is recorded on a linear scale whereas the absorption spectrum is on a logarithmic scale.

Results and Discussion

$S_1 \leftrightarrow S_0$ transition :

Sensitivity of PAS : PA and absorption spectra of the $S_1 \leftrightarrow S_0$ transition of gaseous azulene are shown in Fig. 3. The resolution of this spectrum in a 1 mm path is considerably better than that reported by Hunt and Ross[7] who used a 4 m absorption path length, higher concentrations of azulene and photographic plates. That is, the sensitivity of the PA spectrometer is some 10^6 times greater than that of the absorption system used by Ross and, additionally, it exhibits improved resolution. Modern spectrophotometers (*e.g.* Cary 217) cannot remotely approach this sensitivity even at one-tenth the resolution. That is, the PA technique has enormous analytic potential.

The origin band : The temperature dependence of the PA $S_1 \leftrightarrow S_0$ origin is shown in Fig. 4. Two sequence intervals had been reported previously[8]. However, the data of Fig. 4 suggest four such intervals. A good gaussian analysis is obtained by choosing the origin at 14 294.9 cm^{-1}, individual band half-widths of 8 cm^{-1} and four progressions of -7.4 (6 members), -50.1 (4 members), $+7.1$ (3 members) and $+28.2$ cm^{-1} (4 members), respectively.

Several attempts[7,9,11] to assign the normal modes of azulene in S_0 and S_1 states are available. The following considerations, then, are pertinent to the assignment of the sequences observed in the $S_1 \leftarrow S_0$ transitions.

(i) There is temptation to associate the -7.4 cm^{-1} sequence with the ninth a_1 mode (1 396 cm^{-1} in S_0) because of the general activity of this vibration in the $S_1 \leftarrow S_0$ transition. However, the S_0/S_1 decrement[7] in this mode in the gas phase is only 1 cm^{-1} and, besides, the rather high energy of 1 400 cm^{-1} is inconsistent with the extensive hot band activity of this sequence. The temperature dependency of this sequence suggests a low-energy mode, either one of the a_2 modes (189 and 331 cm^{-1} in S_0, respectively)[9] or one of the b_2 modes (240 and 304 cm^{-1} in S_0, respectively)[9].

(ii) The -50.1 cm^{-1} sequence could correspond to either the fourth or fifth a_1 normal modes (900 and 971 cm^{-1} in S_0, respectively) because these exhibit S_0/S_1 decrements of 41 and 59 cm^{-1}, respectively, in the gas phase[9]. However, the temperature dependency of the first sequence member suggests

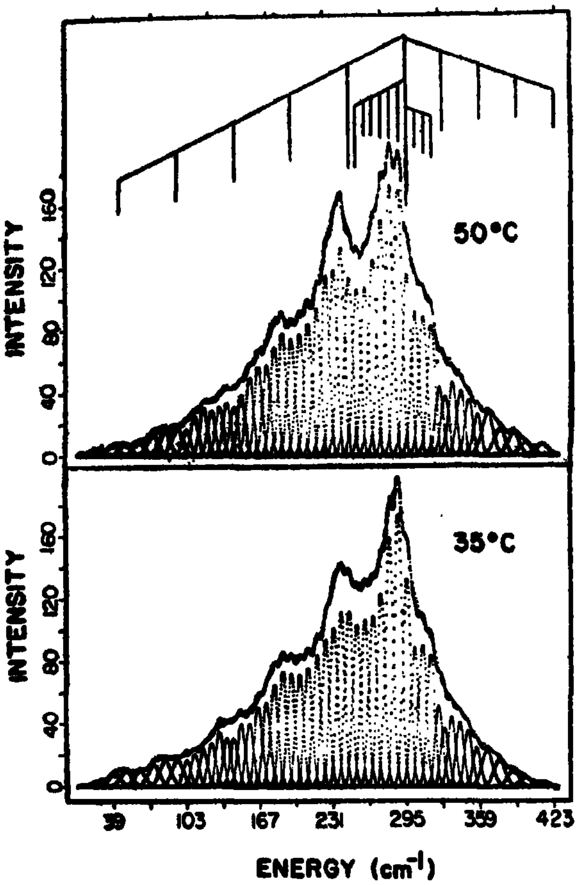


Fig. 4. Photoacoustic spectra of the $S_1 \leftarrow S_0$ origin band of azulene at 50 and 35°. The computer fit and the various series of vibrational difference bands are also shown. To add 14 000 cm^{-1} to each abscissal energy in order to get absolute energies.

a vibrational energy of 400-500 cm^{-1} and eliminates these possibilities. Nor does the first a_1 normal mode (406 cm^{-1} in S_0) suffice because this mode exhibits[9] an S_0/S_1 decrement of 22-24 cm^{-1}. Consequently, the best assignment for this sequence, given that 10% S_0/S_1 frequency decrements are not uncommon, is either the third a_1 or b_2 normal modes (542 and 562 cm^{-1} in S_0, respectively)[10].

(iii) The rapid increase with temperature of the 14 277 cm^{-1} band relative to the 14 285 cm^{-1} band is undoubtedly attributable to the 406 cm^{-1} (in S_0) vibrational mode discussed immediately above.

(iv) The sequences that lie at higher energy than the O,O band are the ones with the greater physical implications. The +7.1 and +28.2 cm^{-1} sequence energies correspond rather well with the S_0/S_1 increments of 8 and 23 cm^{-1} observed in gas-phase azulene for the two lowest-energy b_1 normal modes[9,11]. Furthermore, the energies of these normal modes are not inconsistent with observed temperature dependencies.

S_1 emissivity or photochemistry : The PAS and AS are compared in Fig. 3. On the whole, the AS and PAS of the $S_1 \leftarrow S_0$ transition are remarkably similar, a fact that suggests that the S_1 state is either largely non-emissive or emissive only from the O,O origin band.

There is, however, an anomaly at 1 580 cm^{-1} (*i.e.* in the 4th band of the $S_1 \leftarrow S_0$ transition). The relative decrease of intensity of this band in PAS suggests that energy absorbed in this band is converted into either luminescence or photochemical reaction. Since an infrared CH vibrational emission of azulene has been reported[14] following $S_1 \leftarrow S_0$ excitation, it is not unreasonable to suggest that the 1 580 cm^{-1} anomaly, pertaining as it does to a CH-active mode, is corroborative of the infrared emission. Furthermore, it is implied by these PA data that the quantum yields of this ir CH emission process are non-uniform throughout the $S_1 \leftarrow S_0$ absorption band.

$S_2 \leftrightarrow S_0$ transition :

Vibronic coupling : The $S_2 \leftarrow S_0$ origin band in the PA spectrum is shown in Fig. 5. Unlike $S_1 \leftarrow S_0$, no progessions on the higher frequency side of the assigned O–O band are observed. The lower resolution evident in this spectrum is attributable, in part

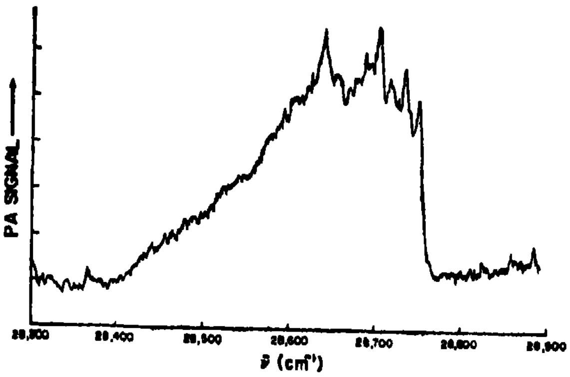


Fig. 5. Photoacoustic spectrum of the $S_2 \leftarrow S_0$ origin band of azulene at 50° in the presence of argon at 1 atm pressure.

at least, to the frequency doubling required for higher energies. A lack of synchrony between the scan rate of the doubling crystal and that of the laser fundamental caused a loss of power in the 2nd harmonic, with the result that the spectrum had to be 'patched-up' from short, isolated scans. By this means, most of the $S_2 \leftarrow S_0$ region was recorded. No discrepancies that would suggest any variation of quantum yield throughtout this excitation region were found. Thus, the near-identity of PA and absorption signals in the 28 000 to 33 000 cm^{-1} region of the $S_2 \leftarrow S_0$ excitation region indicates little or no effect of vibronic coupling on $S_2 \rightarrow S_1$ or $S_2 \rightarrow S_0$ degradative routes.

Quantum yields : An $S_1 \rightarrow S_0$ fluorescence has been reported[6] and an ir CH stretching luminescence following excitation in $S_1 \leftarrow S_0$ has been observed[14]. Regardless of the verity of either report, it is a fact that the total emission quantum yield after $S_1 \leftarrow S_0$ excitation is essentially zero. Given that such is true, it should be possible to estimate the $S_2 \rightarrow S_0$ quantum yield of fluorescence.

The fluorescence conversion efficiency may be expressed either in term of a fluorescence energy yield

$$\eta_E = \frac{\iint N_e \bar{\nu}_e \, d\bar{\nu}_e \, dt}{\iint N_a \bar{\nu}_a \, d\bar{\nu}_a \, dt}$$

or a fluorescence quantum yield

$$\phi_F = \frac{\int N_e \, dt}{\int N_a \, dt}$$

where, N is the number of photons, $\bar{\nu}$ is an energy unit, and the subscripts a and e indicate absorption and emission, respectively. For a narrow band excitation, the fluorescence quantum yield can be expressed as

$$\phi_F = \eta_E \, \bar{\nu}_a / \bar{\bar{\nu}}_e$$

where, $\bar{\nu}_a$ is the excitation frequency (cm^{-1}) and $\bar{\bar{\nu}}_e$ is the barycenter frequency (cm^{-1}) of the fluorescence band. The photoacoustic signal, on the other hand, depends upon the heat conversion efficiency η_H which, in the absence of any photochemistry, is given by $\eta_H = 1 - \eta_E$.

The estimation of $S_2 \rightarrow S_0$ fluorescence quantum yield is simplified by considering only single frequency excitation from S_0 to S_1 (and also S_2), time integrals being eliminated by considering total number of photons in the laser pulse. The null or nearly null quantum yield for $S_1 \rightarrow S_0$ emissivity enables us to write the photoacoustic signal PA_1 for $S_1 \leftarrow S_0$ excitation as

$$PA_1 = k \, N_1 \, h \, \nu_1 \, (1 - 10^{-A_1})$$

where, k is a constant that relates deposited thermal energy to acoustic signal, N_1 is the number of incident photons of frequency ν_1 in the laser pulse, and A_1 is the absorbance of the sample at this same frequency. The normalised photoacoustic signal PA_1^* generated by the spectrometer is defined as

$$PA_1^* = \frac{k \, N_1 \, h \, \nu_1 \, (1 - 10^{-A_1})}{S_1 \, R_1 \, N_1 \, h \, \nu_1} = \frac{k(1 - 10^{-A_1})}{S_1 \, R_1}$$

where, S_1 is the spectral responsivity of the photomultiplier tube at this wavelength, and R_1 is the polarisation dependent reflection coefficient of the beam splitter including, as needed, the additional attenuation required to reduce the reference beam intensity to measurable levels. Since the polarisation changes from horizontal to vertical when doubling crystals are used to generate the second harmonic for $S_2 \leftarrow S_0$ excitation, the value of R will also change by an amount which depends upon angle and various other known characteristics of the beam splitter. All of these additional attenuation factors in R need not be known if the system remains undisturbed from measurement to measurement.

The photoacoustic signal PA_2 for $S_2 \leftarrow S_0$ excitation is

$$PA_2 = k(N_{a2} \, h \, \nu_2 - N_{e2} \, h \, \bar{\nu}_{e2}) = k \, N_{a2} \, h \, \nu_2 \left(1 - \frac{\bar{\nu}_{e2}}{\nu_2} \phi_{F2}\right)$$

where, N_{a2} is the number of photons of frequency ν_2 absorbed from the laser pulse, N_{e2} is the number emitted at a mean frequency of $\bar{\nu}_{e2}$, and ϕ_{F2} is the quantum yield for $S_2 \rightarrow S_0$ fluorescence. The normalised photoacoustic signal PA_2^* is then given by

$$PA_2^* = \frac{k \, N_{a2} \, h \, \nu_2}{S_2 \, R_2 \, N_2 \, h \, \nu_2} \left(1 - \frac{\bar{\nu}_{e2}}{\nu_2} \phi_{F2}\right)$$

Since $N_{a2} = N_2 \, (1 - 10^{-A_2})$, where N_2 is the number of photons in the laser pulse at the $S_2 \leftarrow S_0$ excitation wavelength and the sample absorbance is A_2, we may write

$$PA_2^* = \frac{k}{S_2 \, R_2} \, (1 - 10^{-A_2}) \left(1 - \frac{\bar{\nu}_{e2}}{\nu_2} \phi_{F2}\right)$$

The quantity k can be eliminated by combining the expressions for PA_1^* and PA_2^*, to yield

$$\phi_{F2} = \left[1 - \frac{PA_2^* \, R_2 \, S_2 \, (1 - 10^{-A_1})}{PA_1^* \, R_1 \, S_1 \, (1 - 10^{-A_2})}\right] \frac{\nu_2}{\bar{\nu}_{e2}}$$

Thus, the $S_2 \rightarrow S_0$ fluorescence quantum yield can be obtained if the sample absorbances for the $S_1 \leftarrow S_0$ and $S_2 \leftarrow S_0$ excitations are known at the wavelengths used to excite PA_1^* and PA_2^*, respectively. The absorption spectra for the $S_1 \leftarrow S_0$ and $S_2 \leftarrow S_0$ transitions in the origin band regions of azulene vapor at 50° were recorded on a Cary 217 using 10 cm absorption cells. The mean $S_2 \rightarrow S_0$ fluorescence ($\bar{\nu}_{e2}$) was taken[6] to be 26 300 cm^{-1}. Some prominent peaks in the $S_2 \leftarrow S_0$ and $S_1 \leftarrow S_0$ origin bands were used to calculate ϕ_{F2} and its value was found to lie in the range 0 to 6%. The observed variation is largely attributable to spectral noise arising from the low value of A_1. Our results for the fluorescence quantum yield from S_2, while not very precise, agree with those obtained by more conventional means[18], indicating the absence of any appreciable photochemistry, at least for low energy excitations into either S_1 or S_2.

Photoacoustic spectroscopy has been used previously[15] to estimate fluorescence quantum yields. Our method differs in that the non-emissivity of S_1 of azulene provides an internal standard for system calibration. Should the quantum yield of the $S_1 \rightarrow S_0$ emission happen not to be exactly zero, the value of ϕ_{F2}, as obtained here, will constitute a minimum value. The analysis given here may be extended to the situation where both S_1 and S_2 are emissive and it can be shown that, in the absence of photochemistry and vibrational emissivity, a knowledge of the quantum yield of fluorescence from one state

can be used, *via* PA spectroscopy, to obtain that of the other. The method is particularly facile when one state is known not to emit because, in this instance, no photon yield measurements whatever are required. This latter appears to be the case for azulene.

In summary, the pulse-by-pulse signal normalisation technique described here is widely applicable. In addition, the extremely high sensitivity of the PA spectrometer permits the extraction of additional valuable information concerning azulene.

Acknowledgement

This work was supported by the U. S. Department of Energy.

References

1. "Optoacoustic Spectroscopy and Detection", ed. Y. H. PAO, Academic Press, New York, 1977; "Photoacoustics and Photoacoustic Spectroscopy", ed. A. ROSENCSWAIG, Wiley-Interscience, New York, 1980.
2. D. KUMAR, R. V. NAUMAN, R. MOHANTY, S. P. McGLYNN and G. L. FINDLEY, *Rev. Sci. Instrum.*, 1983, 54, 463.
3. M. BEER and H. C. LONGUET-HIGGINS, *J. Chem. Phys.*, 1955, 23, 1390.
4. G. VISWANATH and M. KASHA, *J. Chem. Phys.*, 1956, 24, 574.
5. An $S_1 \rightarrow S_0$ fluorescence has been reported but it has no independent confirmation. P. M. RENTZEPIS, *Chem. Phys. Lett.*, 1969, 3, 717; D. HUPPERT, J. JORTNER and P. M. RENTZEPIS, *J. Chem. Phys.*, 1972, 56, 4826.
6. J. W. SIDMAN and D. S. McCLURE, *J. Chem. Phys.*, 1956, 24, 757.
7. G. R. HUNT and I. G. ROSS, *J. Mol. Spectrosc.*, 1962, 9, 50.
8. A. R. LACEY, E. F. McCOY and I. G. ROSS, *Chem. Phys. Lett.*, 1973, 21, 233.
9. G. J. SMALL and S. KUSSEROW, *J. Chem. Phys.*, 1974, 60, 1558.
10. W. G. HERKSTROETER, *J. Am. Chem. Soc.*, 1975, 97, 4161.
11. R. S. CHAO and R. K. KHANNA, *Spectrochim. Acta, Part A*, 1977, 33 53.
12. D. BOULER, W. S. FELPS, J. LEWIS, R. V. NAUMAN and S. P. McGLYNN, *Chem. Phys. Lett.*, 1979, 67, 420.
13. S. MURATA, C. IWANAGA, T. TODA and H. KOKUBUN, *Ber. Bunsenges. Phys. Chem.*, 1972, 76, 1176.
14. G. P. SMITH and J. R. BARKER, *Chem. Phys. Lett.*, 1981, 78, 253; J. R. BARKER, *J. Phys. Chem.*, 1984, 88, 11.
15. See, for example, A. C. TAM in "Ultrasensitive Laser Spectroscopy", ed. D. S. KLIGER, Academic Press, New York, 1983.

J. Indian Chem. Soc.,
Vol. LXIII, January 1986, pp. 16-21

Fourier Transform Infrared Kinetic Study of the Thermal Decomposition of Tetramethyl-1-3-cyclobutanedione and Dimethylketene†

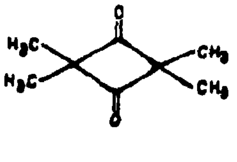
MARTIN VALA*, JOSEPH BAIARDO[a], DAVID LATHAM, RANAJIT MUKHERJEE[b] and STEFAN PASCYZ[c]

Department of Chemistry, University of Florida, Gainesville, Florida 32611

The vapor phase thermolysis of tetramethyl-1,3-cyclobutanedione (TMCBD) has been studied in the temperature range 383-430° by Fourier transform infrared spectroscopy. The first order decay constant is log $(k_1/s^{-1}) = 13.78 - (48\ 400$ cal mol^{-1}/2.303 RT). The decomposition of TMCBD leads exclusively to dimethylketene (DMK) whose buildup and subsequent decay were also followed kinetically. Studied at higher temperatures (450-520°), a first order decay constant of log $(k_2/s^{-1}) = 10.72 - (48\ 800$ mol^{-1}/2.303 RT) was determined for the thermal decomposition of DMK. Rates of decomposition of TMCBD and the corresponding cyclobutanone are compared and shown to be consistent with a twisted quasizwitterionic transition state. Long time (2 h) pyrolysis of TMCBD leads to *tetramethylethylene and isopropenyl isopropyl* ketone products but no DMK. These observations are rationalised by a scheme involving formation of tetramethylcyclopropanone (TMCP) from DMK and dimethylmethylene radicals, followed by decay of TMCP to the observed products.

THE thermolysis and photolysis of cyclobutanone and its alkylated derivatives have been the subjects of intense investigation[1,2]. The photolysis of cyclobutanedione and its derivatives has also been much studied[3-7], but little attention appears to have been given to the detailed study of the thermolysis of the cyclobutanediones. It has been of general knowledge[8] for many years that the thermal decomposition of 1,3-cyclobutanedione (CBD) leads to ketene products, but the kinetics of the process and the presence of other decomposition pathways have not been reported. In this paper we present results on the kinetics and products of the thermolysis of tetramethyl-1,3-cyclobutanedione (TMCBD).

Three primary routes for *photolytic* decay have been proposed[4,5] to account for the observations on TMCBD.


$+h\nu \longrightarrow (CH_3)_2C{=}C(CH_3)_2 + 2CO$ (1)


$+CO$ (2)

$\longrightarrow 2(CH_3)_2C{=}C{=}O$ (3)

It has been shown[5] that decomposition *via* the lowest triplet $n\pi^*$ state proceeds exclusively to dimethylketene (DMK, equation (3)), while decay *via* singlet $n\pi^*$ states yields tetramethylcyclopropanone (TMCP), CO (equation (2)) and DMK. The mechanism of production of tetramethylene (TME, equation (1)) is not completely understood but it appears not to be an important decomposition route[4].

The purpose of the present investigation was to determine the primary thermal decomposition products and thermolysis kinetics for TMCBD. We were interested in determining whether both TMCP and DMK were formed (as in the singlet state photolysis) or whether DMK was the sole product (as in the triplet state sensitised photolysis), or whether other decomposition routes were active. Preliminary results on long time (~2 h) pyrolyses of gaseous samples, followed by product recuperation and mass spectrometric analysis, indicated that only TMCP and TME were formed. To verify this result FTIR was used to monitor, *in situ*, the thermolysis of TMCBD. These studies showed that DMK was formed exclusively, a result seemingly contradictory to our preliminary studies. Thermolysis decay constants for TMCBD disappearance were measured in the temperature range 383 to 430° and Arrhenius activation parameters determined. In addition, the thermal decomposition of the primary product DMK was followed kinetically in the range 450-520° and its activation parameters obtained.

Experimental

Preliminary studies : Small quantities (~1 g) of solid TMCBD (Eastman Kodak, recrystallised)

† Dedicated to Professor Sadhan Basu on the occasion of his 65th birthday.

[a]Present address : Monsanto Corp., Research Labs., St. Louis, Mo. 63146.

[b]Department of Magnetism, Indian Association for the Cultivation of Science, Jadavpur, Calcutta-700 032.

[c]Department of Chemistry, Adam Mickiewicz University, Poznan, Poland.

were added to 20 cm long (2.0 cm ϕ) Pyrex tubes, attached to a vacuum line, evacuated and sealed off. The tubes were placed in a horizontal resistance-heated furnace and pyrolysed at 360° for 2 h. The tubes were opened in a glove-box under N_2 atmosphere and solvent (aniline or CCl_4) added. Gas chromatographic/mass spectrometric analyses were then performed on the solutions.

Reaction cell : A conventional 'static' vapor phase reaction cell was constructed from Pyrex tubing (25 × 10 cm) wrapped with asbestos tape and nichrome wire (1.63 Ω/ft). The end windows (KBr, International Crystal, 50 mm ϕ) were attached to the cell *via* O-ring seals. The central portion of the cell was heated separately from the end portions to preclude excessive heating of the O-rings and sample condensation on the windows. The temperature of each of the three sections of the cell was monitored individually by thermocouples located in the insulation but in contact with the glass. A small radius cell was also utilised in some initial experiments with no effect on the rates observed. Cell pressures were monitored by a Wallace Tiernan pressure gauge.

Solid TMCBD was admitted to the reaction cell *via* a special greaseless Teflon-glass stopcock, the rotatable portion of which had been hollowed out to contain the sample. Inserted in an upright manner, the stopcock allowed the cell to be evacuated prior to sample introduction. Once the desired reaction temperature was stabilised the insert was rotated 180°, allowing the sample to drop into the cell, vaporise and commence decomposition. Aging of the cell was accomplished by repeated thermal decomposition runs with TMCBD itself. Reaction temperatures ranged between 380 and 520°.

Infrared spectrometer : The decomposition of TMCBD was followed spectroscopically using a Nicolet 7199 Fourier transform infrared spectrometer. The reaction cell was positioned between the main optical bench and the gc-ir optical bench with glass tubing (sealed to the outside of the KBr sample windows with O-rings) connecting each bench to the cell to preserve the integrity of the purge (liquid N_2 boil-off) in both optical benches. The light pipe was also purged and kept at ambient temperature. A HgCdTe (77 K) detector was used in the gc-ir bench. A spectrometer mirror velocity of 0.88 cm/s was used throughout ; spectra of only 4 cm^{-1} resolution were collected to enable rapid collection sequences. Full aperature and the Happ-Genzel apodization function were utilised. The spectral range covered was 800-4 000 cm^{-1}, but only the 950-2 300 cm^{-1} region was examined in detail since the reactant and major products were known to have bands in this region.

Data acquisition and reduction : To monitor the thermal decomposition as a function of time with the FT-ir required that spectra be collected as rapidly as possible in the initial stages and less frequently as the reaction progressed. To accomplish this, a set of macros was written that allows one to program the collection of spectra at different rates during the course of the process being monitored. The temporal resolution was limited by our optical arrangement and detector (MCT-type A) to about 20 single scan interferograms (4 cm^{-1} resolution, full spectral range) per minute. One can choose the four available 'time windows' for example as (W1) 20 spectra per min (1 scan each) for 5 min, followed by (W2) 2 spectra per min for 10 min, and so on for the remaining two time windows. Signal averaging is done (typically 10 scans/spectrum) in all but the fastest regime. Starting the data collection a few seconds prior to sample introduction allows monitoring the buildup of TMCBD as it is vaporised.

For the particular case of TMCBD pyrolysis, 65 interferograms were collected in W1, 20 spectra at 22 s intervals in W2, 10 spectra every 4 min in W3 and 10 spectra at 10 min intervals in W4. The choice of program may be changed depending on the temperature of the run. In this way one is able to monitor the relatively fast decay of the dione reactant and the much slower decomposition of the dimethyl ketene intermediate.

At the end of data collection another macro is started which converts each of the data files to absorbance spectra, relative to a background which was collected immediately prior to sample introduction. Integration of up to 4 regions is then performed (with base-line correction, if desired) and the results printed along with the time at which data collection was initiated. Two strong bands, at 2 133 cm^{-1} (CO stretch of DMK[8]) and at 1 755 cm^{-1} (antisymmetric CO stretch of the dione[9]) were chosen. While the integration of the former band was straightforward (limits of 2 185 to 1 990 cm^{-1}), the integration of the latter was complicated by the appearance of a broader weak band on its low frequency tail. This interference was avoided by integrating from the high frequency limit (1 830 cm^{-1}) to the band maximum (1 755 cm^{-1}) and multiplying by two. This was possible because of the symmetric band shape of the TMCBD carbonyl stretch, as determined in separate experiments. Absorption due to CO was seen at higher resolution (1 cm^{-1}). The P branch of the CO absorption superimposes on the DMK C=O stretch ; however, it is weak and does not affect the results at 4 cm^{-1} resolution.

The integrated areas of the bands as a function of time were then fit *via* a linear least-squares program to suitable kinetic models and the rate constant for each temperature determined.

Results

Preliminary long-time pyrolysis : The gas chromatographic analysis of the decomposition product mixture showed three major peaks, two of which were readily identified by their mass spectro-

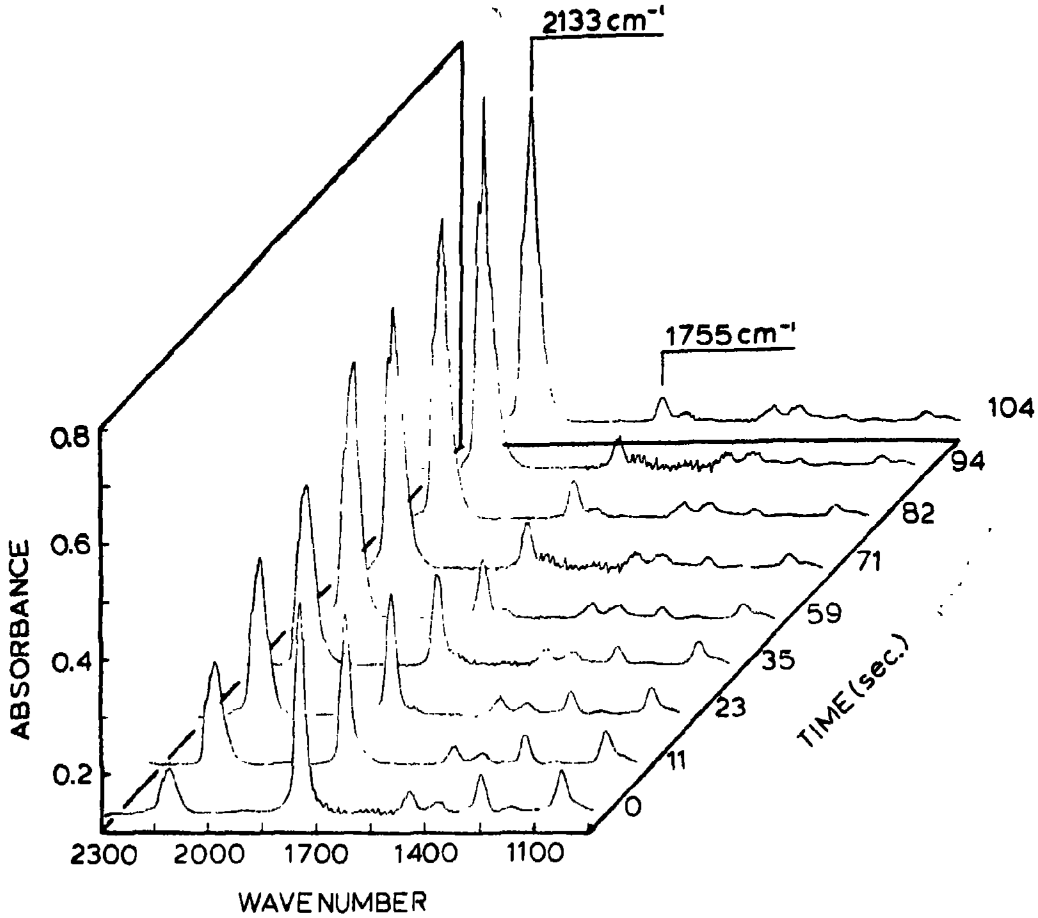


Fig. 1. Time evolution of the infrared band (1 100-2 800 cm^{-1} region) due to TMCBD decomposition (1 755 cm^{-1}) and DMK buildup and decay (2 133 cm^{-1}).

metric fragmentation patterns as undecomposed TMCBD parent and TME product. The third gc peak gave a parent mass peak of 112 and a fragmentation pattern which fits an isopropenyl isopropyl ketene (IPIPK) parent well.

Solution (CCl_4) infrared spectra were also run of the pyrolysed sample. No peak at 1 840 cm^{-1} (from TMCP[a]) was observed but a band at 1 810 cm^{-1} was apparent. Substituted vinyl groups are known[10] to absorb in the 1 750–1 810 cm^{-1} region. Thus, we conclude that the third gc peak is indeed due to the IPIPK product.

Decomposition rate constants: Fig. 1 shows the time evolution of a portion (first ~2 min) of the infrared spectra recorded. The band at 1 755 cm^{-1} (TMCBD) clearly decreases with time, whereas the band at 2 133 cm^{-1} (DMK) increases, reaches a maximum, and then decreases. No band at 1 840 cm^{-1} (TMCP) was observed at any time[11]. It may be noted that the first spectrum shown in Fig. 1 (at t=0) was not in fact the first recorded after introduction of the sample. A buildup of the TMCBD peak was observed due to its vaporisation ; thus our determination of the decay kinetics was not initiated until just after the TMCBD peak had reached a maximum. From these initial experiments the following mechanism was proposed,

$$\text{TMCBD} \xrightarrow{k_1} 2\ \text{DMK} \qquad (1)$$

$$\text{DMK} \xrightarrow{k_1} \text{Products} \qquad (2)$$

$$\text{TMCBD} \xrightarrow{k_3} \text{TMCP} + \text{CO} \qquad (3)$$

where the products of DMK decomposition are probably CO and dimethylmethylene radical (*vide infra*). The third step was included for two reasons. First, our preliminary experiments indicated the presence of TMCP (or more accurately, IPIPK) in the long-time pyrolysis reaction mixture. And, second, Frey and Hopf[1] observed that thermolysis of the analogous mono-carbonyl compound, tetramethylcyclobutanone led to two pathways of decomposition. The major one leads to isobutene and DMK while the minor one yields tetramethylcyclopropane and CO. (We show later that the

third pathway above (*cf.* (3)) is not observed under our reaction condition.)

The three reaction steps (1)-(3), lead to the following integrated reaction rate expressions,

$$D(t) = D(O)e^{-(k_1+k_2)t} = D(O)e^{-k'_1 t} \quad (4)$$

$$K(t) = \frac{2k'_1 D(O)}{k'_1 - k_2}\left[e^{-k_2 t} - e^{-k'_1 t}\right] \quad (5)$$

where, D(t) stands for TMCBD concentration at time t and K(t) for DMK concentration at time t, and $k'_1 = k_1 + k_2$. Since our dependent variable is infrared absorbance and not concentration, the Beer's law expressions $A_D(t) = \epsilon_D l D(t)$ and $A_K(t) = \epsilon_K l K(t)$, where ϵ_D, ϵ_K are the molar absorptivities of TMCBD and DMK and l is the cell pathlength, were substituted into (4) and (5). For first order decomposition of TMCBD, plots of *ln* $A_D(t)$ *vs* t should be linear. Indeed, good linear plots were found and from their slopes, values of k'_1 ($= k_1$, *vide infra*) determined. They are given in Table 1 as a function of temperature for the range 383-430°. Above ~430°, the TMCBD decay times were too rapid to follow with the present technique.

TABLE 1—RATE CONSTANTS (k_1) FOR THERMAL DECOMPOSITION OF TETRAMETHYLCYCLOBUTANEDIONE AS A FUNCTION OF TEMPERATURE

Temp. °C	$10^3\ k_1/s^{-1}$
383	0.383
390	0.801
401	1.12
412	2.02
420	3.33
423	3.65
430	5.14

From (5), it can be seen that if k'_1 either (i) becomes very large compared to k_2 (*e.g.* as at high temperatures), or (ii) the ketene concentrations are only sampled at long times (t very large, *i.e.* after the TMCBD concentration has dropped to essentially zero) this expression becomes (after the Beer's law substitutions),

$$A_K(t) = \frac{2A_D(O)k'_1}{k'_1 - k_2}\left(\frac{\epsilon_K}{\epsilon_D}\right)e^{-k_2 t} \quad (6)$$

Thus plots of *ln* $A_K(t)$ *vs* t, should be linear with slopes equal to $-k_2$ and intercepts equal to $\frac{2A_D(O)k'_1\epsilon_K}{(k'_1 - k_2)\epsilon_D}$. By using both long times and high temperatures, linear plots for the decomposition of DMK were found. The values determined for k_2 over the range 450-520° are given in Table 2. It may be noted that bands for both TMCBD and DMK decomposition were observed for the entire temperature range sampled (383-520°), but reliable kinetics for each were obtained only in the ranges quoted.

TABLE 2—RATE CONSTANTS (k_2) FOR THERMAL DECOMPOSITION OF DIMETHYLKETENE AS A FUNCTION OF TEMPERATURE

Temp. °C	$10^4\ k_2/s^{-1}$
450	0.106
462	1.63
468	2.06
480	3.25
490	5.12
500	8.60
520	20.09

It is of interest to determine the relative magnitudes of the extinction coefficients for the dione and the ketene. It can be seen, from (6), that the intercept of the plot of *ln* $A_K(t)$ *vs* t contains the desired ratio. The quantities $A_D(O)$ and k'_1 were found from the TMCBD decay, while k_2 was determined from the DMK decay. The results obtained for ϵ_K/ϵ_D are shown in Table 3. The values should of course be constant with temperature. The average is 1.3 ± 0.2 ($\pm\sigma$).

TABLE 3—RATIO OF EXTINCTION COEFFICIENTS (ϵ_K/ϵ_D) FOR THE DMK 2 133 cm^{-1} BAND AND THE TMCBD 1 755 cm^{-1} BAND

Temp. °C	ϵ_K/ϵ_D
383	1.26
390	1.035
401	1.22
412	1.34
420	1.55
423	1.35
430	1.57
450	1.67

Arrhenius parameters : Arrhenius plots for the data contained in Tables 1 and 2 are shown in Fig. 2. The Arrhenius equations describing these plots are given by

$$\log [k_1/s^{-1}] = 13.78 - (48\ 400\ \text{cal mol}^{-1}/2.303\ RT)$$

for the decomposition of TMCBD and

$$\log [k_2/s^{-1}] = 10.72 - (48\ 800\ \text{cal mol}^{-1}/2.303\ RT)$$

for the decomposition of DMK.

We have stated above that at no time in the vapor phase ir studies did we observe an infrared band at 1 840 cm^{-1} which would have indicated the presence of TMCP as a decomposition product. With the estimated lower limit[14] for TMCP of $\epsilon \sim 2.0 \times 10^4$ l mol^{-1} cm^{-2} about equal to the ϵ_{CO} for DMK[8], we estimate that if 5% or more of the decomposition of TMCBD had occurred *via* the TMCP pathway we could have observed it. A confirmation of the relative unimportance of this route can be gotten from the Arrhenius plots. If we assume for the moment that both k_1 and k_3 routes are important in the TMCBD decomposition, each

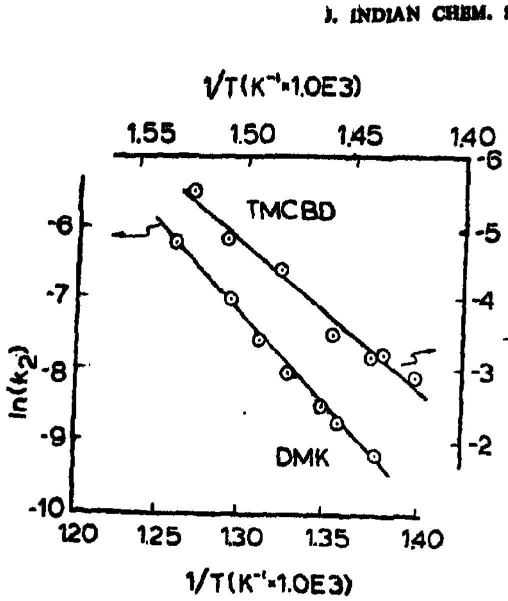


Fig. 2. Arrhenius plots for thermal decomposition of TMCBD (upper and right axes) and DMK (lower and left axes). Data from Tables 1 and 2.

rate will be described by its own Arrhenius equation and the observed rate by

$$k'_1 = k_1 + k_8 = A_1 e^{-\Delta E_1/kt} + A_8 e^{-\Delta E_8/kt}.$$

Plotting $ln\ k'_1$ *vs* T^{-1} will yield non-linear plots. However, if $k_1 \gg k_8$, plots of $ln\ k'_1$ *vs* T^{-1} will be linear. Since we observe a good linear plot of $ln\ k_1$ *vs* T^{-1} (*cf.* Fig. 2) this confirms that the k_8 route to TMCP is much slower (if not zero) compared to the k_1 route to DMK.

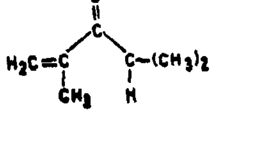
Discussion

TMCBD decomposition : From our results we have demonstrated that the only primary thermal decomposition product of TMCBD is DMK. The decay of TMCBD was followed spectroscopically in the ir simultaneously with the buildup and decay of DMK. No other major decomposition products from TMCBD were noted, although because of the low pressures used, trace amounts (< 5%) of other products could have been produced but not observed. If we accept that DMK is the sole primary thermolysis product, how can the appearance of isopropenylisopropylketone and tetramethylethylene in our long time pyrolysis studies be understood ? The most likely explanation seems to be that with such long pyrolysis times secondary reactions are occurring. We suggest the following scheme

$$\text{DMK} \rightarrow (CH_3)_2C: + CO \quad (4)$$

$$(CH_3)_2C: + \text{DMK} \rightarrow \text{TMCP} \quad (5)$$

$$\text{TMCP} \rightarrow (CH_3)_2C{=}C(CH_3)_2 + CO \quad (6)$$

TMCP→  (7)

Pathways (4) and (5) have previously been proposed by Haller and Srinivasan[7] as an alternate route for formation of the TMCP observed in photolysis decomposition products. Pathway (7) has been shown by Turro and coworkers[4] to occur upon heating in the vapor phase chromatographic analysis of a crude photolysis decomposition mixture. (The dimerisation of DMK to TMCBD is slow[13,14] and only becomes significant at pressures above 1 atm, so is of no importance here.) In this scheme the formation of TMCP is a bimolecular one but since the decomposition of TMCBD is fast relative to DMK, a large excess of DMK will be present in the reaction cell as the dimethylmethylene is formed. Thus the TMCP formation reaction will become increasingly more probable as the TMCBD and DMK decay reactions proceed. An alternate route to the TME product (instead of (6)) could be the bimolecular reaction of two dimethylmethylene radicals. This is considered less likely given the expected excess of DMK in the cell which will react with the dimethylmethylene to form TMCP and given the fact that both TME and IPIPK were observed to be major long-time pyrolysis products. In summary, it appears reasonable to conclude that the appearance of TME and IPIPK in our long-time thermolysis mixture results from secondary reactions occurring after the primary decay of TMCBD to DMK.

It is of interest to determine the effect on the reaction rate and activation energy of the addition of a carbonyl group to the cyclobutanone moeity. Frey and Hopf[1] have measured the thermolysis rate constant of 2,2,4,4-tetramethylcyclobutanone to be $\log k_1 = 14.859 - (55\,945 \text{ cal mol}^{-1}/2.303\ RT)$ for the major decomposition pathway to isobutene and DMK. For the minor (6%) pathway to tetramethylcyclopropane and CO, they found a similar though less favored rate, $\log k_2 = 14.867 - (59\,587 \text{ cal mol}^{-1}/2.303\ RT)$. The rate for the decomposition of TMCBD found here is $\log k = 13.78 - (48\,400 \text{ cal mol}^{-1}/2.303\ RT)$. Evaluating these rates at 400° (the middle of our range), the TMCBD decay rate constant is a factor of ~25 greater than the rate for the mono-ketone decay. This is an understandable rate increase within the twisted quasizwitterionic transition state model previously proposed by Frey[15] and Egger[16] for the thermal decomposition of cyclobutanes and cyclobutanones. A twisted transition state was suggested by Frey and coworker[15] to account for the effects of alkyl substituents in cyclobutane systems in an attempt to incorporate some of the ideas of orbital symmetry conservation into the problem. In this model, alkyl substituents on nonadjacent ring positions are expected to interfere sterically in the twisted transition state model and hence to decrease the rate of decomposition. The slower rate of decomposition of 2,2,4,4-tetramethylcyclobutanone compared to cyclobutanone is thus perfectly rationalised within this model. Egger[16] further suggested that there is a charge separation in the twisted transition state of cyclobutanones which becomes zwitterionic-like and

leads to larger decay rates for substituents in the 3-position than in the 2- or 4-positions. Within this model then we would expect that substitution of a carbonyl group in the 3-position of 2,2,4,4-tetramethylcyclobutanone would lead to an enhanced rate of decomposition for TMCBD. This is of course just what we observe. Similarly, a comparison of 1,3-cyclobutanedione (CBD) stability to TMCBD stability is predictable within this model. Since the major influence of the transannular methyl groups in TMCBD is a steric one tending to constrain the transition state geometry, the expectation is that the TMCBD should decompose more slowly than CBD. Although no kinetic data are available for CBD thermolysis, one report on its infrared spectroscopy remarks that it is an unstable compound[17]. On the other hand, TMCBD is known to be a relatively stable molecule.

DMK decomposition: The investigation of the kinetics of decomposition of the parent ketene has undergone an interesting evolution. In 1958, Young[18] studied the decomposition of ketene in the 780-860 K (100 torr) range and found that the reaction order was 2. Ten years later, Huda and Kuratani[19] used shock tube methods with a 1140-1530 K temperature range to study ketene's decay and found a reaction order of 1.5. Then, in 1971, Wagner and Zabel[20] also using shock tube methods (in the temperature range 1 300-2 000 K) determined the ketene decay reaction order to be 1 and the rate constant to be $k = 3.6 \times 10^{15} \exp(-59\,300 \pm 2\,000 \text{ cal mol}^{-1}/RT)\ l \text{ mol}^{-1} \text{ s}^{-1}$. Although not directly measured the latter measurement implied that the primary decomposition products were methylene radical and CO. To prove this point, Reineke and Strein[21] in an elegant molecular beam experiment expanded a gas mixture of ketene decomposition products and argon into a vacuum and mass spectrometrically analysed for the methylene species. Their measured ionisation potential is in excellent agreement with the spectroscopic value determined earlier by Herzberg[22].

In the result presented here no attempt was made to determine the reaction order. The detection of the dimethylmethylene radical in the ir would have been difficult if not impossible given the other species present in the reaction cell or produced from the TMCBD decomposition. As mentioned previously, CO was observed, its bands lying on the low frequency edge of the TMCBD carbonyl stretch. They could however not be used for quantitative measurement since they were resolution limited. A single run at 0.25 cm^{-1} revealed their vibrational/rotational pattern clearly. Nevertheless, the similarities in the reaction rates of the parent ketene and the dimethylated compound ($k_{DMK}/k_{KET} \sim 17$ at 475°) supports the conclusion made in the previous section that the primary decomposition route in DMK is to the dimethylmethylene radical and CO.

Acknowledgement

National Science Foundation is gratefully acknowledged for its support of this research. The authors also wish to thank the NATO organisation for partial support of this work, Dr. Roy King, University of Florida Chemistry Department for the gc/mass spectral analyses and Mr. William Griffith, now at Ohio State University, for the preliminary pyrolysis studies.

References

1. H. M. Frey and H. Hopf, *J. Chem. Soc., Perkin Trans.* 2, 1973, 2016 and references therein.
2. N. E. Lee and E. K. C. Lee, *J. Chem. Phys.*, 1969, 50, 2094 and references therein; J. Hemminger and E. K. C. Lee, *J. Chem. Phys.*, 1971, 54, 1405.
3. E. A. LaLancette and R. E. Benson, *J. Am. Chem. Soc.*, 1961, 83, 4867.
4. N. J. Turro, P. A. Leermakers, H. R. Wilson, D. C. Neckers, G. W. Byers and G. F. Vesley, *J. Am. Chem. Soc.*, 1965, 87, 2613 ; 1964, 86, 955, 4128.
5. I. Haller and R. Srinivasan, *Can. J. Chem.*, 1965, 43, 3165.
6. R. Spafford and M. Vala, *J. Photochem.*, 1978, 8, 61.
7. I. Haller and R. Srinivasan, *J. Am. Chem. Soc.*, 1965, 87, 1144.
8. W. E. Hanford and J. C. Sauer in "Organic Reactions", eds. R. Adams, W. Bachman, L. Fieser, J. Johnson and H. Snyder, Wiley. New York, 1946, Vol. 3.
9. F. O. Nicolaisen, O. F. Nielsen and M. Vala, *J. Mol. Struct.*, 1972, 13, 349.
10. R. Conley, "Infrared Spectroscopy", Allyn and Bacon, Boston, 1972.
11. Although the molar absorptivity of the carbonyl stretch in TMCP has not been reported, Haller and Srinivasan[5] have extrapolated from data of Burer and Gunthard[12] on cyclic alkanones that the lower limit of ϵ_{CO} for TMCP should be $\sim 2.0 \times 10^4\ l \text{ mol}^{-1} \text{ cm}^{-2}$. By comparison, ϵ_{CO} for DMK[8] is $1.9 \pm 0.3 \times 10^4\ l \text{ mol}^{-1} \text{ cm}^{-2}$.
12. T. Burer and H. H. Gunthard, *Helv. Chim. Acta*, 1956, 39, 356.
13. J. S. Chickos, D. E. Sherwood, Jr. and K. Jug, *J. Org. Chem.*, 1978, 43, 1146.
14. R. Huisgen and P. Otto, *J. Am. Chem. Soc.*, 1968, 90, 5342.
15. A. T. Cocks and H. M. Frey, *J. Chem. Soc. (A)*, 1969, 1671.
16. K. W. Egger, *J. Am. Chem. Soc.*, 1973, 95, 1745.
17. F. A. Miller, F. E. Kiviat and I. Matsubara, *Spectrochim. Acta, Part A*, 1968, 24, 1523.
18. J. R. Young, *J. Chem. Soc.*, 1958, 2909.
19. M. Tsuda and K. Kuratani, *Bull Chem. Soc. Jpn.*, 1968, 41, 53.
20. H. G. Wagner and F. Zabel, *Ber. Bun. Gesell.*, 1971, 75, 114.
21. W. Reineke and K. Strein, *Ber. Bun. Gesell.*, 1976, 80, 343.
22. G. Herzberg, *Proc. R. Soc. London, Ser. A*, 1961, 262 ; *Can. J. Phys.*, 1961, 39, 1511.

J. Indian Chem. Soc.,
Vol. LXIII, January 1986, pp. 22-28

Applications of High Resolution Infrared Diode Laser Spectroscopy†

V. B. KARTHA, V. A. JOB and P. K. CHAKRABORTI

Bhabha Atomic Research Centre, Trombay, Bombay-400 085

Tunable diode lasers for the infrared region are now available commercially and can be used for general high resolution spectroscopic studies as well as in special techniques, like study of supercooled molecular beams, trace and ultratrace analysis, precise frequency and intensity measurements *etc*. The present paper reviews the techniques and applications of TDL-s in some of these fields, with special reference to molecules like ammonia, sulfur hexafluoride and heavy water.

HIGH resolution infrared spectra of polyatomic molecules in the free state give information on vibration-rotation energy levels, molecular geometry, molecular force fields, dipole moments, vibration-rotation interaction, intermolecular potentials *etc*. Such studies have become of great importance recently because of the advances in theory of vibration-rotation interaction in terms of molecular structure and symmetry and also because of the availability of narrow line width (10^{-4} cm^{-1}) tunable diode lasers spanning the entire infrared region of 3-30 μm, which enable very fine interactions to be determined accurately. Recent high resolution diode laser studies on molecules like SF_6[1], isotopic ammonias[2,3] and substituted methanes[4-7], to take only a few examples, illustrate the insight one can get on the complex interactions present in seemingly simple molecules. The theoretical analysis of the spectra thus gives a clear understanding of the finer details of quantum mechanical interpretation of molecular structure.

The understanding of many chemical physics problems depend on the detection and characterisation of one or more molecular species, before, during, and after collision processes involving photons, electrons, atoms, or molecules. The initial state parameters will strongly influence the relevant cross section of interest. The evolution of the reaction will be reflected on the process of the microscopic conversion of the translational and internal states of the reactants into the translational and internal states of the products, through the states of the intermediate complexes. The decay processes after the collision determine the final products. High resolution diode laser infrared spectroscopy can provide unambiguous information on most of the steps considered above. Very often these studies are carried out under molecular beam[8-10] conditions, where the diode laser technique provides a very sensitive, non-destructive, non-perturbing probe[11-14].

A semiconductor diode laser spectrometer has been operational in our laboratory for the last few years. We have used this for several high resolution spectral studies, supercooled nozzle beam studies and applications in trace analysis[3,7,14-17]. The present paper reviews some of our results and also summarises some of the important results from other laboratories. For more information on applications of diode laser spectroscopy, the reader may refer to some of the excellent review articles available in literature[18-20].

Experimental

The spectrometer in our laboratory is shown schematically in Fig. 1. The tunable diode lasers (TDL) are mounted on a closed cycle refrigerator cold head. A maximum of four lasers can be mounted on a single cold head so that a sufficiently large spectral region can be covered in any experiment, by applying current to any one of the four

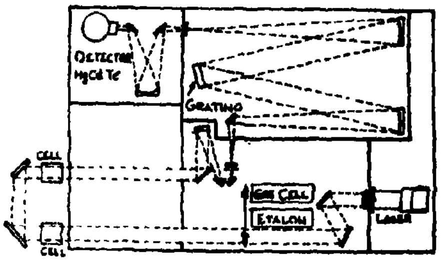


Fig. 1. Tunable diode laser (TDL) spectrometer, schematic.

lasers and positioning its output into the sample cell, using a collimating lens, mounted on a precision XYZ translational stage. The beam from the cell is then focussed at the entrance slit to a 1/2 m grating monochromator, where it can be chopped

† Dedicated to Professor Sadhan Basu on the occasion of his 65th birthday.

A part of the article was presented at the National Conference on Spectroscopy and Theoretical Chemistry held at Calcutta, December 5-7, 1985.

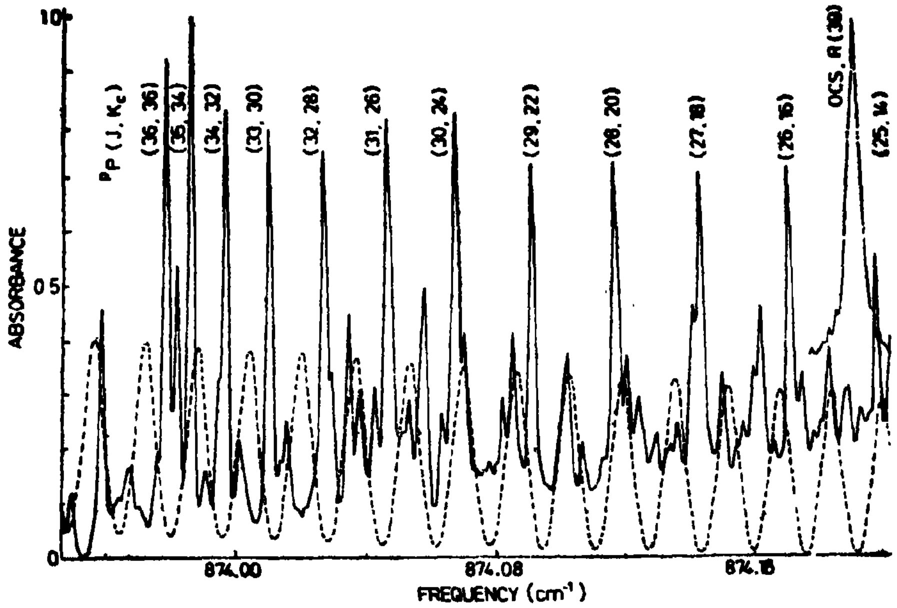


Fig. 2. TDL spectrum of a section of the ν_{14} band of s-tetrazine. OCS lines used for reference can be seen in the spectrum. Dotted curve shows interference fringes from the 7.5 cm Ge-etalon, used for calibration.

by a tuning fork chopper. The monochromator is used to select a single mode of the laser, since usually the TDL gives its output in two or three different modes, separated by 2-3 cm^{-1}. The radiation from the exit slit of the monochromator, is focussed on to a liquid N_2 cooled HgCdTe(MCT) detector. The signal from the detector is fed to a pre-amplifier and lock-in amplifier and used for recording the spectrum. Accurate calibration of the spectrum can be done by using a standard reference sample and fringes from a 3″ Ge-etalon. A typical spectrum is shown in Fig. 2.

For our supercooled nozzle beam experiments, the beam from the exit slit of the monochromator is recollimated and transported to the nozzle beam set up, a schematic of which is shown in Fig. 3. The TDL beam is then refocussed at the nozzle, its exact position along the molecular beam being precisely controlled by proper positioning of the focussing lens. After passing through the supercooled beam, the radiation is focussed on to the MCT detector by another lens, and spectrum recorded as before. For many spectral studies at low pressures and temperatures, and for trace analysis, we have used several types of long-path cells. In such experiments, the sample cells are kept outside the instrument, and the collimated laser beam transported along the required path and then returned to the monochromator entrance slit.

Results and Discussion

Molecular spectroscopy : As mentioned in the introduction, in this review we will illustrate some typical results of high resolution spectral studies which have given information on complex interactions as evinced from finer details of the spectrum.

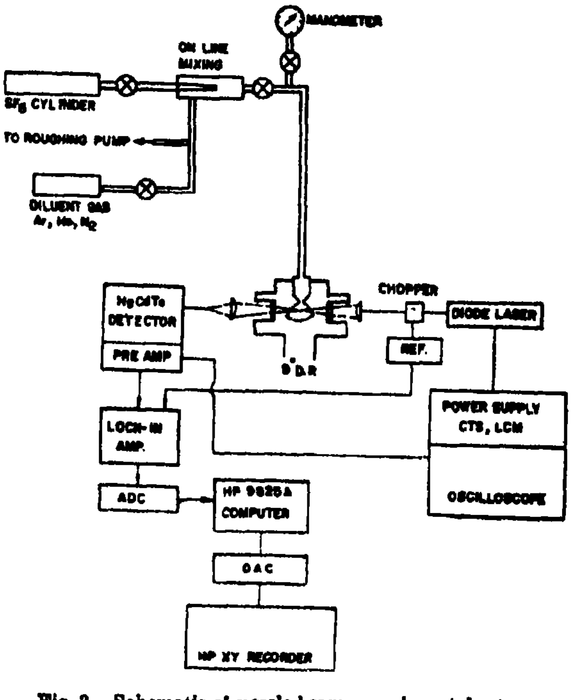


Fig. 3. Schematic of nozzle beam experimental set-up.

The ammonia molecule has always served as a good theoretical model for all vibration-rotation spectroscopy. It is well known that this molecule, in addition to its small amplitude vibrational

modes Q_1, Q_3 and Q_4 possesses the large amplitude inversion motion Q_2, which takes the place of the symmetric bending mode. This large amplitude motion is represented by the well known double minimum potential. Interaction between the small and large amplitude motions in this molecule gives rise to peculiar effects in the spectrum, some of which we have been able to observe in our high resolution studies. Similarly, deviations from the standard polynomial form of the energy levels of a symmetric rotor arising from perturbations due to $\Delta k = \pm 3n$ type interactions have also been observed in the isotopic ammonias. Such perturbations arise from near coincidences of symmetric and antisymmetric levels differing in K by 3 and the deviation observed from energy level calculation based on the polynomial expression give an idea of such interaction.

For the isotopic molecules $^{14}NH_3$ and $^{15}NH_3$, we have fitted more than 500 lines in the TDL spectrum of the ν_2 band (inversion mode), with an accuracy better than 0.0005 cm^{-1} (Ref. 3). In this fit, we started with the standard polynomial expression for the energy levels given by

$$E^{\circ}(J,K) = T_v + BJ(J+1) + (C-B)K^2 - \sum_{l=2}\sum_{m=0} (-1)^l D_{lm}\, J(J+1)^m K^{2(l-m)}$$

where l is the order of the term and m the power of $J(J+1)$. (For comparison with conventional energy expression[21] the quartic distortion constants D_J, D_{JK} and D_K are denoted by D_{22}, D_{21} and D_{20}). The $\Delta k = \pm 3n$ interactions modify this, and in the Nielsen-Dennison approximation[22], the corrected energy levels are given by

$$E'(J,3) = E^{\circ}(J,3) \mp (-1)^J f(J,3)\eta_3$$

$$E'(J,6) = E^{\circ}(J,6) \pm (-1)^J f(J,3) \times f(J,6)\eta_6$$

where

$$f(J,K) = [J(J+1) - K(K-1)]\,[J(J+1) - (K-1)(K-2)]\,[J(J+1) - (K-2)(K-3)]$$

and η_3 and η_6 are constants.

Belov *et al.*[23] have shown that higher order interaction terms have to be incorporated for the ν_2 state and have given appropriate interaction matrix, with the diagonal elements as given above ($E^{\circ}(J,K)$, or $E'(J,K)$ as the case may be) and appropriate off-diagonal elements for the interaction discussed above. We have fitted more than 500 lines of the TDL spectra for each of $^{14}NH_3$ and $^{15}NH_3$ and combining this data with data from pure inversion and inversion rotation spectra have calculated accurate spectroscopic constants for both isotopic molecules. The perturbation correction to some of the energy levels in the ν_2 state of $^{14}NH_3$ and $^{15}NH_3$, arising from the off-diagonal terms in the interaction matrix are given in Table 1. It can be seen that these corrections are quite significant, especially for higher J values, and unless they are included the observed spectra could never be reproduced by theoretical calculation. Other interesting aspects of the Ammonia spectra arising from inversion rotation interaction are discussed in more detail elsewhere[24,25].

TABLE 1—PERTURBATION CORRECTION IN THE ν_2 STATE OF AMMONIA ($cm^{-1} \times 10^5$)*

J	K	$^{14}NH_3$ a	$^{14}NH_3$ s	$^{15}NH_3$ a	$^{15}NH_3$ s
3	1	0	0	0	0
3	2	0	0	0	0
3	3	280	0	−22	0
5	3	−228	0	−164	0
6	3	7	−12	7	−13
6	4	−68	−20	−65	−20
6	5	−40	−17	−39	−17
6	6	−15	−7	−15	−7
15	1	9 408	−25 810	9 528	47 457
15	2	49 877	14 388	−23 482	14 246
15	3	−6 207	17 190	−5 662	17 095
15	15	−656	−506	−654	−508

* These are typical values for different J and K states. Correction for all levels of J≤16 are given in Ref. 8.

Several other examples are available in literature[26–30], which illustrate the application of high resolution TDL spectra in interpretation of finer interactions in molecular energy levels. Recently considerable interest has been aroused in the spectra of spherical top molecules of the type XY_6 with O_h symmetry, because of their use in laser multiphoton reaction and isotope enrichment. The spectra of spherical top molecules should be very simple in the harmonic oscillator-rigid rotator approximation because of the high degree of degeneracy of the spherical top wave function. But in reality, vibration-rotation and other interactions, remove the degeneracy, and extremely complicated energy level patterns result for such a system, giving rise to complex vibration-rotation spectra, observable by high resolution TDL spectroscopy techniques. Complete and correct interpretation of these spectra obviously will provide the confirmation of the theoretical models. Also, study of laser-induced processes in such systems require a precise knowledge of the frequencies and interactions.

In Fig. 4 we show a diode laser scan of sections of the P, Q and R branches of the ν_3 mode of SF_6 at 947 cm^{-1}. The spectra show the relatively simple structure of the low J transitions, the complex manifold structure for even moderately high J values (*e.g.* P-14) and the very complex band head structure of the Q-branch (see later). A complete analysis of this complicated spectrum has been done by several workers[1] and molecular parameters and interaction constants have been obtained, leading to considerable advance in the theory of spectra of spherical tops[31–36].

Diode laser spectroscopy of supersonic molecular beams : Supersonic nozzle-cooled beams are used in many molecular dynamics experiments, for spectroscopic studies of larger polyatomic molecules, production of weakly bound van der Waals molecules *etc.* Several spectroscopic techniques are available for study of such beams[16] and tunable diode laser spectroscopy forms a very convenient

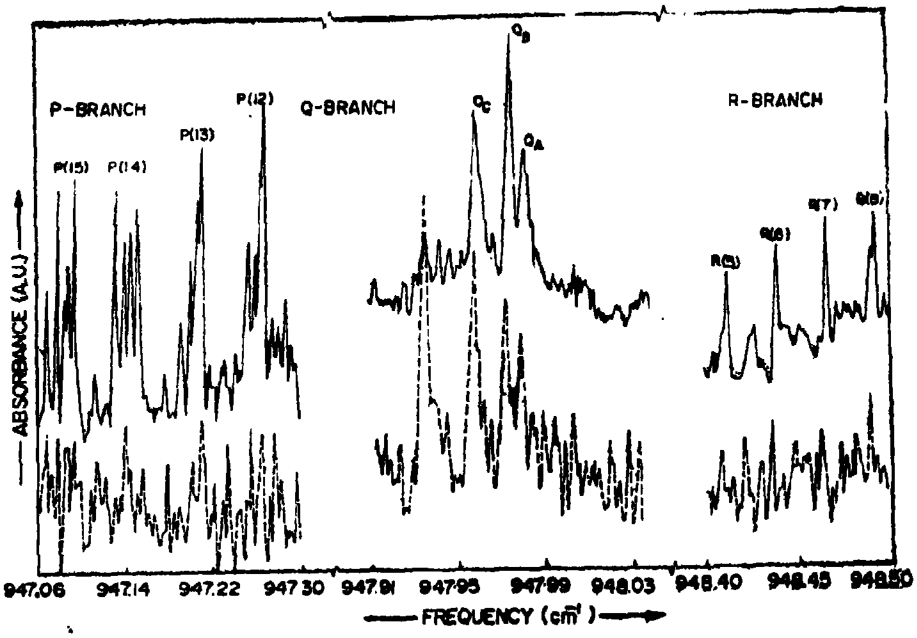


Fig. 4. A diode laser scan of parts of the P, Q and R branches of ν_3 mode of SF_6. Upper continuum curves are spectra of pure SF_6 expanding from a 75 μm nozzle at 300 K. Lower dashed curves represent corresponding regions of the spectra taken with a 10 cm cell at 300 K and 0.25 torr.

technique for getting information on the beam characteristics.

In a supersonic nozzle beam the gas under study (either alone, or mixed with an inert carrier gas, like He) is led into the system under high pressure (several hundreds to several thousands torr) where it is allowed to expand through a nozzle of 50-100 μm diameter into a vacuum chamber maintained at high vacuum. Under these conditions of isentropic expansion, the system cools down to very low temperatures without change of phase, attaining translational temperatures of the order of 1 K, with rotational temperatures closely following it. The vibrational temperatures are also reduced considerably, though not as low as the other two. The supercooled beam coming out of the nozzle thus provides a simple absorption spectrum, because of the depopulation of the higher rotational and vibrational levels. A study of such beam sources in itself is of great interest since the beams are in thermal non-equilibrium for many physical quantities, like translational and internal temperatures. The extremely low temperature baths of such beams also offer an ideal environment for very weak binding leading to the formation of van der Waals dimers[37,38], higher clusters[39,40] and ultimately to the massive onset of condensation *etc.*[11,13,39,41,42]. Information on all these processes can be obtained by TDL spectroscopic studies on the beam[11-14,16,39,42].

Typical scans for the absorption spectrum of SF_6 in the nozzle beam, are shown in Fig. 5, under various conditions of stagnation pressure and dilution. The spectra correspond to the Q-branch region of the ν_3 stretching mode. The most

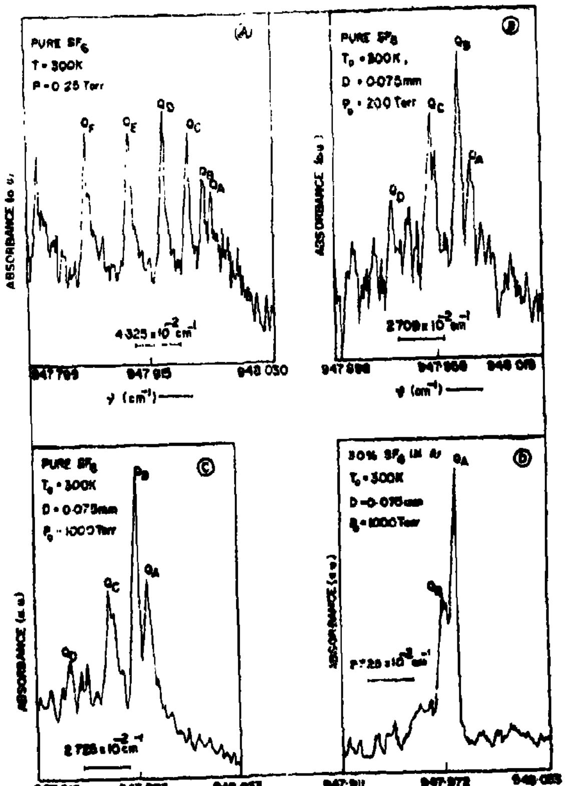


Fig. 5. Diode laser absorption spectra of Q-branch of ν_3 band of SF_6 : (A) in a 10 cm cell ; (B, C and D) of nozzle-cooled SF_6. Spectra were taken with a 75 μm nozzle under condition indicated at a distance of 7.5 mm from nozzle exit.

noticeable feature of this region is the series of sharp band heads spread over a region of only 0.25 cm^{-1}. McDowell and coworkers[1,20,34,38,39] have shown that these band heads arise from the octahedral splitting of the triply degenrate ν_3 level, the different heads being formed from different groups, at different J values. The appearance of the heads will therefore, depend upon the rotational population distribution, their intensity thus providing a sensitive measure of the rotational temperature of the beam[14,16]. It is clearly seen from Fig. 5 that higher stagnation pressures as well as greater dilution with an inert gas increase the cooling, leading to lower and lower rotational temperatures. Detailed information on the rotational relaxation in the beam can be obtained by just studying the diode laser spectrum under various conditions, at different points along the beam axis. Some of these results are illustrated in Fig. 6, where the rotational temperature is plotted as a function of distance on the beam axis and concentration of SF_6 in the gas stream. Analysis of the data from such studies will give parameters like fractional change in ϵ (mean random velocity per collision), γ (the average specific heat ratio), relaxation cross-section for internal degrees of freedom as a function of temperature, vibrational predissociation of van der Waals' molecules *etc*.

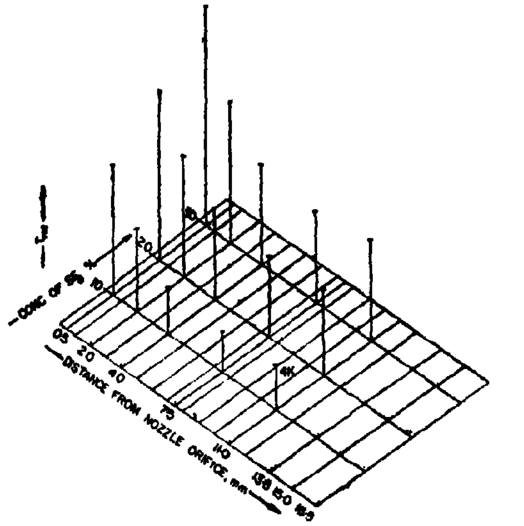


Fig. 6. Composite plot of rotational temperature of nozzle-cooled SF_6, against concentration of SF_6 and distance from nozzle exit.

Similar diode laser studies have been carried out in other systems[41,42] also, giving information on jet profile, cluster formation, condensation *etc*. Spectral changes occurring due to condensation in the nozzle beam, in the case of ammonia, are illustrated in Fig. 7.

Application of diode laser spectroscopy in trace analysis : Tunable diode laser spectroscopy has several advantages over conventional absorption techniques for trace and ultra trace analysis. The very high resolution available with the laser eliminates all interference from major components. Also, the peak intensity will be increased considerably compared to low resolution measurements, increasing sensitivity. The laser characteristics of high intensity and good collimation will allow the use of very long path lengths[43], of the order of several hundreds of meters, so that ultra trace components can be easily detected. Measurements of

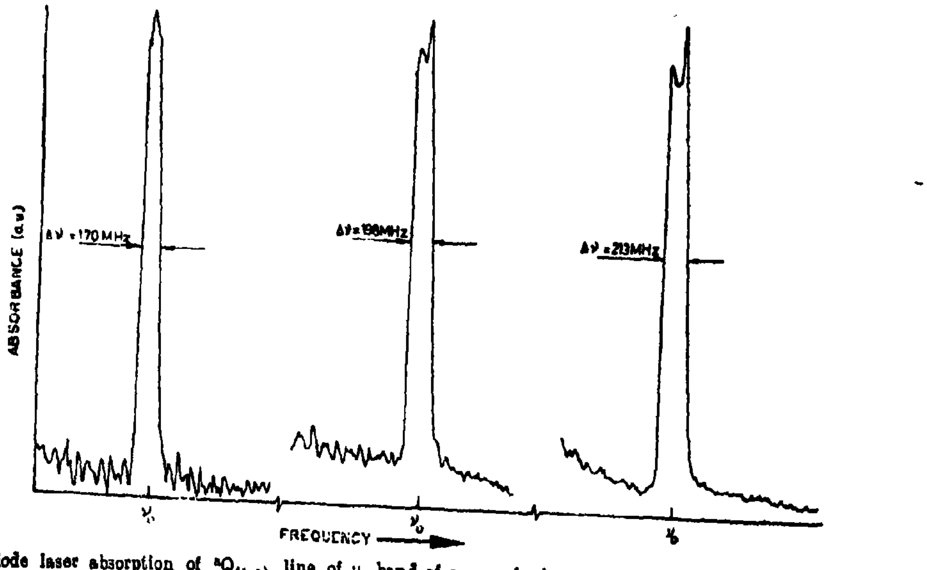


Fig. 7. Diode laser absorption of $^aQ_{(1,1)}$ line of ν_2 band of ammonia in a nozzle beam, at a location 1 mm from nozzle exit; stagnation temp., 300 K, stagnation pressure, (a) 500, (b) 1 000 and (c) 2 000 torr. Onset of massive condensation is depicted by appearance of a *dip* at ν_0 location, corresponding to jet axis. Red and blue shifted peaks are due to Doppler shifts in flanks of expansion beam. Measured line widths are considerably larger than room temperature Doppler width of ~80 MHz. (For further details, Ref. 42).

small quantities of absorption over large backgrounds can be easily made, and remote samples, transient species *etc.* can be studied without any difficulty. Several analytical methods have been developed using TDL techniques and we discuss one example below to illustrate the capabilities of the technique.

In the production of heavy water (D_2O) for nuclear reactors, the starting material is natural water, with deuterium concentration of about 0.015%. This deuterium is present as HDO, and analysis of the HDO concentration in the natural range is thus very useful in the early stages of enrichment. We have developed a TDL method for this analysis. The HDO line chosen, with the calibration curve is shown in Fig. 8. The total sample used in this analysis will be only about 5 mg.

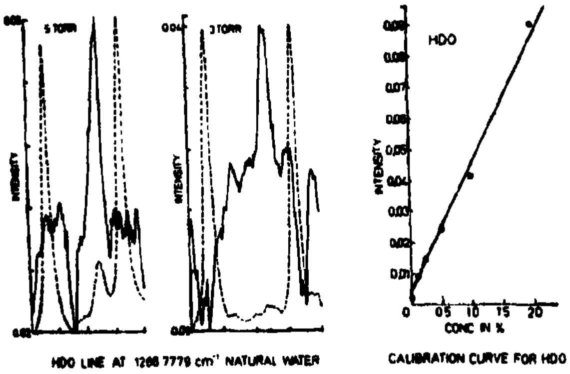


Fig. 8. HDO spectrum and calibration curve. Dashed lines are N_2O lines used for calibration.

This is very important, when we consider that same method can be used for analysis of reactor grade heavy water (99.8% D_2O), where conventional infrared spectroscopy requires a few grams of the sample. More details of trace and ultra trace analyses using diode laser techniques, may be found elsewhere[17,19,44].

References

1. J. P. Aldridge, H. Filip, H. Flicker, R. F. Holland, R. S. McDowell, N. G. Nereson and K. Fox, *J. Mol. Spectrosc.*, 1975, **58**, 165 ; R. S. McDowell, H. W. Galbraith, C. D. Cantrell, N. G. Nereson and E. D. Hinkley, *J. Mol. Spectrosc.*, 1977, **68**, 288.
2. S. Urban, V. Spirko, D. Papousek, R. S. McDowell, N. G. Nereson, S. Belov, L. I. Gershstein, A. V. Maslovskij, A. K. Krupnov, J. Curtis and K. N. Rao, *J. Mol. Spectrosc.*, 1980, **79**, 455.
3. V. A. Job, N. D. Patel, R. D'Cunha and V. B. Kartha, *J. Mol. Spectrosc.*, 1983, **101**, 48.
4. L. J. Radziemski, Jr., R. F. Begley, H. Flicker, N. G. Nereson and M. J. Reisfeld, *Opt. Lett.*, 1978, **3**, 241.
5. G. Restelli and F. Capellani, *J. Mol. Spectrosc.*, 1979, **78**, 161.
6. P. P. Das, V. M. Devi and K. N. Rao, *J. Mol. Spectrosc.*, 1980, **84**, 305.
7. P. K. Wahi, V. A. Job and V. B. Kartha, *J. Mol. Spectrosc.*, in the press.
8. M. A. D. Fluendy and K. P. Lawley, "Chemical Application of Molecular Beam Scattering", Chapman and Hall, London, 1973.
9. D. H. Levy, L. Wharton and R. E. Smalley in "Chemical and Biochemical Applications of Lasers", ed. C. B. Moore, Academic Press, New York, 1970, Vol. 2, Ch. 1.
10. R. B. Bernstein, 'Chemical Dynamics via Molecular Beam and Laser Techniques", Oxford University Press, New York, 1982.
11. S. S. Fisher, *Phys. Fluids*, 1971, **22**, 1261.
12. B. J. C. Wu and G. A. Laguna, *J. Chem. Phys.*, 1979, **71**, 2991.
13. G. Baldacchini, S. Marchetti and V. Montalitici. *Chem. Phys. Lett.*, 1982, **91**, 423.
14. P. K. Chakraborti, V. B. Kartha, R. K. Talukdar, P. N. Bajaj and A. Joshi, *Chem. Phys. Lett.*, 1983, **101**, 397.
15. K. B. Thakur, V. A. Job and V. B. Kartha, *J. Mol. Spectrosc.*, 1984, **107**, 373.
16. P. K. Chakraborti, R. Talukdar, P. N. Bajaj, A. Joshi and V. B. Kartha, *Chem. Phys.*, 1985, **95**, 145 ; P. N. Bajaj, R. K. Talukdar, V. B. Kartha and P. K. Chakraborti in "Lasers and Applications", eds. H. D. Bist and J. S. Goela, Tata McGraw-Hill, New Delhi, 1984, p. 171.
17. R. D'Cunha, V. A. Job, A. Joshi, V. B. Kartha, N. D. Patel, C. S. Somanathan and K. B. Thakur in "Trace Analysis and Technological Development", ed. M. Sankar Das, Wiley Eastern, New Delhi, 1983, p. 322.
18. K. W. Nill and F. A. Blum in "Laser Spectroscopy of Atoms and Molecules", ed. H. Walther, Springer-Verlag, Heidelberg, 1976, Ch. 2.
19. R. S. Eng, J. F. Butler and K. J. Linden, *Opt. Eng.*, 1980, **19**, 945.
20. R. S. McDowell in "Vibrational Spectra and Structure", ed. J. R. Durig, Elsevier, Amsterdam, 1981, Vol. 10, Ch. 1.
21. G. Herzberg, "Molecular Spectra and Molecular Structure. II. Infrared and Raman Spectra of Polyatomic Molecules", Van Nostrand, New York, 1945, p. 400.
22. H. H. Nielsen and D. M. Dennison, *Phys. Rev.*, 1947, **72**, 1101.
23. S. P. Belov, L. I. Gershstein, A. F. Krupnov, A. V. Maslovskij, S. Urban, V. Spirko and D. Papousek, *J. Mol. Spectrosc.*, 1980, **84**, 288.
24. V. Spirko, J. M. R. Stone and D. Papousek, *J. Mol. Spectrosc.*, 1976, **60**, 159.
25. V. A. Job, S. B. Kartha, K. B. Thakur and V. B. Kartha, communicated.
26. R. S. McDowell, L. J. Radziemski, H. Flicker, H. W. Galbraith, R. C. Kennedy, N. G. Nereson, B. J. Krohn, J. P. Aldridge and J. D. King, *J. Chem. Phys.*, 1978, **69**, 1513.
27. K. C. Kim, W. B. Person, D. Seitz and B. J. Krohn, *J. Mol. Spectrosc.*, 1979, **76**, 322.
28. C. W. Patterson, R. S. McDowell, N. G. Nereson, R. F. Begley, H. W. Galbraith and B. J. Krohn, *J. Mol. Spectrosc.*, 1980, **80**, 71.
29. J.-M. Flaud, C. Camy-Peyret, V. M. Devi, P. P. Das and K. N. Rao, *J. Mol. Spectrosc.*, 1980, **84**, 234.
30. G. Baldacchini, S. Marchetti and V. Mentelatici, *J. Mol. Spectrosc.*, 1984, **103**, 257.
31. W. G. Harter and C. W. Patterson, *Int. J. Quantum Chem.*, 1977, **11**, 479.
32. K. Fox and B. J. Krohn, *J. Comput. Phys.*, 1977, **25**, 386.
33. H. W. Galbraith, C. W. Patterson, B. J. Krohn and W. G. Harter, *J. Mol. Spectrosc.*, 1978, **73**, 475.
34. B. J. Krohn, *J. Mol. Spectrosc.*, 1978, **73**, 462.
35. E. G. Brock, B. J. Krohn, R. S. McDowell and C. W. Patterson, *J. Mol. Spectrosc.*, 1979, **76**, 301.
36. C. W. Patterson, H. W. Galbraith, B. J. Krohn and W. G. Harter, *J. Mol. Spectrosc.*, 1979, **77**, 457.
37. P. K. Chakraborti, *Pramana*, in the press.
38. A. Van Deursen, A. Van Lumig and J. Reuss, *Int. J. Mass Spectrom. Ion. Phys.*, 1975, **18**, 129.

39. T. E. Gough, D. G. Knight and G. Scoles, *Chem. Phys. Lett.*, 1983, **97**, 155.

40. R. E. Miller, R. O. Watts and A. Ding, *Chem. Phys.*, 1984, **83**, 155.

41. F. Vreken and J. Reuss, *Appl. Phys. B*, 1984, **34**, 149.

42. P. N. Bajaj, R. K. Talukdar, V. B. Kartha and P. K. Chakraborti, communicated.

43. K. C. Kim, E. Griggs and W. B. Person, *Appl. Opt.*, 1978, **17**, 2511.

44. V. R. Rose Mary, K. B. Thakur, C. S. Somanathan, V. A. Job and V. B. Kartha, Proc. Natl. Symp. Absorption Spectrometry, Indian Soc. Anal. Scientists, Feb. 13-15, 1984, Bombay.

J. Indian Chem. Soc.,
Vol. LXIII, January 1986, pp. 29-34

Photoassisted Solid-catalysed Reduction of N_2 by Water. Evidence for a Photostationary State and for Catalytic Activity of many Oxides†

NORMAN N. LICHTIN and KALAMBELLA M. VIJAYAKUMAR

Department of Chemistry, Boston University, Boston, Ma. 02215, U. S. A.

Yields of NH_3, produced when N_2 was contacted with bulk liquid water or water vapour over a number of metal oxides under illumination from xenon lamps, were measured under a range of conditions. Active catalysts included CoO, Co_3O_4, Co-Mo-Al-oxide, Co-Mo-Ti-oxide, Cr_2O_3, α-Fe_2O_3, MoO_3, Nd_2O_3, PbO, Pr_6O_{11}, TeO_2, $\overline{W}O_3$, Zn-Fe-oxide, La-Ni-oxide and La-Ti-oxide as well as a ferric ion-containing zeolite. System variables included period of reaction, short wavelength limit of light, temperature, flow-rate of gaseous reactant, weight of catalyst per unit volume of liquid water and concentration of initially added NH_3. It has been shown that at or below 30° in the presence of illuminated suspensions of α-Fe_2O_3 or Cr_2O_3 in water, NH_3 is both formed and decayed in the reaction cell so that a photostationary state is ultimately reached. A 40° or above, NH_3 can be swept out of the cell rapidly so that decay is negligible. Under the latter conditions, over α-Fe_2O_3, $E_{activation}$=46 kJ mol^{-1}. $E_{activation}$=19 kJ mol^{-1} over α-Fe_2O_3 in the absence of bulk water. In the presence of either water vapor or liquid water, both α-Fe_2O_3 and Cr_2O_3 maintained their catalytic activity for prolonged periods of time. The use of air did not alter the activity of Cr_2O_3 significantly. Several oxides with band-gap energies significantly smaller in magnitude than $E°$=1.23 V of the six-electron reduction of N_2 by H_2O to aqueous NH_4OH, are active catalysts. At least one step of the reaction must in these cases involve absorption of more than one photon per electron transferred.

THE sunlight-driven reduction of N_2 to ammonia by water is a potential route to fixation of nitrogen, the attractiveness of which lies in both avoidance of the high energy requirement of the Haber-Bosch process and in the possibility of generating ammonia at the locations of its use as an agricultural fertiliser. This paper reports results of an investigation of the photoassisted solid-catalysed reduction of N_2 by water and draws attention to some of the factors which affect efficiency of the process.

Photoassisted solid-catalysed reduction of N_2 by water was early described by Schrauzer and Guth[1]. Their report describes experiments involving illumination of semiconductors in the presence of gases with no bulk liquid phase present. Most of these experiments employed pure or iron-doped powdered TiO_2 which had been heated in air to 1 000° and then conditioned by exposure to the vapour pressure of water at room temperature. Illumination was usually with a 360 W mercury arc lamp through glass. Photodecomposition of water to H_2 and O_2 was observed when illumination took place under an argon atmosphere. Replacement of argon by N_2 inhibited production of H_2 completely and replaced it with NH_3 and 2-20 mol% of N_2H_4. Replacement of half the N_2 by H_2 or Ar gave the same results, indicating that the reduction of N_2 by water does not involve H_2 as a reactant. NH_3 was also photogenerated, although less efficiently, when air replaced pure N_2. Anatase was less active catalytically than rutile. Doping TiO_2 with Fe increased catalytic activity, as did doping with Co, Mo and Ni, but incorporation of a number of other metals (Pd, Pt, Ag, Au, V, Cr, Pb and Cu) did not increase activity. α-Fe_2O_3 catalysed formation of NH_3 from N_2 and H_2O but was less active than TiO_2. N_2 also inhibited the photoreduction of acetylene over water-equilibrated TiO_2 or iron-doped TiO_2 with concommitant production of NH_3. Neither quantum yields nor efficiencies of conversion of incident energies were measured. Related studies on photo-assisted catalysis of reduction of N_2 over various naturally-occuring sands were subsequently reported by Schrauzer and coworkers[2,3]. Reduction of N_2 to NH_3 upon bubbling N_2 through aqueous suspensions of powdered semiconductors under illumination through borosilicate glass with a high-pressure mercury lamp was studied by Miyama and coworkers[4]. They found that yields of NH_3 obtained under standard conditions with TiO_2, ZnO, $SrTiO_3$, CdS and GaP varied over a factor of about three, decreasing with increasing band-gap. The authors ascribed this trend to variation in the amount of light absorbed.

Somewhat larger-scale reduction of N_2 to NH_3 over a catalyst of Fe^{III}-doped TiO_2 supported on γ-Al_2O_3 under near-uv illumination with a

† Dedicated to Professor Sadhan Basu on the occasion of his 65th birthday.

high-pressure mercury vapor lamp was studied by Augugliaro and coworkers[5-8]. These workers employed a fluidised bed reactor at 80-120° with a feedstock consisting of N_2 and water vapour. They calculated that the observed yields of NH_3 corresponded to consumption of 0.8-1.6 layers of surface hydroxyl per hour and found no diminution in hourly yields for more than 24 h. This result provides a significant answer for their conditions to the doubts expressed by Van Damme and Hall[9] that the reactions observed by Schrauzer and Guth[1] were catalytic. Substantial increases in the photoefficiency of photoassisted reduction of N_2 by water by surface-loading of the rutile form of TiO_2 with iron clusters deposited by thermal decomposition of $(C_6H_5)_2Fe(CH_3)_2$ were reported by Radford and Francis[10]. Photoassisted reduction of N_2 to ammonia in suspensions of powdered TiO_2 in aqueous 1 *M* Na_2CO_3 has also been reported[11]. Photoassisted reduction of N_2 by a suspension in water of a zeolite which had been exchanged with Ti^{III} has also been reported[12,13]. However, this reaction apparently involves stoichiometric oxidation of Ti^{III} rather than oxidation of water.

Some of the results of our research on photoassisted solid-catalysed reduction by water of N_2 and mixtures of N_2 and CO_2 has been reported in the patent literature[14-16] and in abstracts of papers[17,18].

Experimental

Two sets of conditions were employed, experiments in which reactant gases were bubbled through illuminated suspensions of catalyst powders in bulk liquid water and experiments in which N_2 and water vapour were passed in the absence of bulk liquid water over illuminated thin films of finely-divided catalyst powders deposited on an interior face of the cell. Reactants included N_2 alone and air. Light sources were 150 W Osram xenon lamps. The cell was located 30 cm from the lamp. The collimated beam illuminated 11 cm^2 of the approximately 25 cm^2 area of solution or film which was normal to the beam. Unless otherwise indicated, conditions of illumination were maintained constant within each set of data. Illumination cells were of Pyrex so that only light at $\lambda \gtrsim 300$ nm was incident on the reactants. In many experiments, cut-off filters were used to exclude part or all of the ultraviolet. Reaction temperatures were controlled to $\pm 1°$. Integrating devices based on the electrical output of silicon solar cells ('Sunstations'[19]) were used to monitor incident light energy. Catalyst powders (finer than 200 mesh, ASTM) were typically conditioned for use by heating at 100-400° under 1 atm of flowing argon for 24 h. NH_3 was determined colorimetrically by Nessler's method. Linde PP grade N_2 was routinely used. Reactant air was supplied by Linde. Flow-rates of reactant gases were 50-100 $cm^3 min^{-1}$ unless otherwise indicated.

Films of catalyst for use in the absence of bulk water were prepared by dispersing catalyst powder in water or organic liquid and allowing the liquid to evaporate slowly while the powder deposited on the glass. Fresh films were dried in static air at 60-200° for 24 h and were then purged with flowing dry N_2 at 30° for 12 h before first use. Used films were similarly purged for 4-6 h between runs. Reactant N_2 was saturated with water vapor by bubbling it through liquid water. Figs. 1 and 2 are schematic diagrams of the apparatuses used, respectively, for

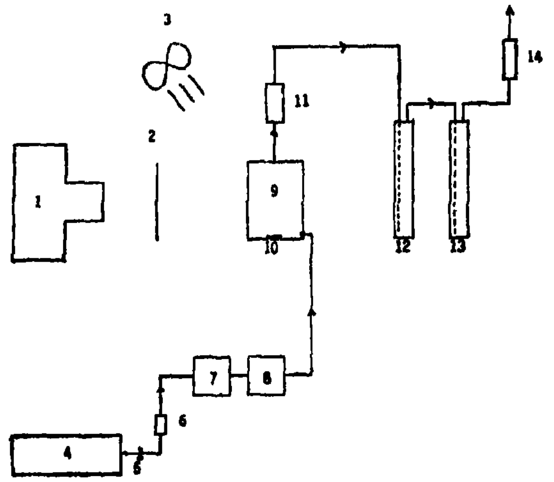


Fig. 1. Schematic of apparatus for reaction in presence of bulk liquid water: (1) light source: 150 W-Xe with quartz lenses, (2) glass filter, (3) blower, (4) gas cylinder, (5) needle valves, (6) flow meter, (7) chromous perchlorate deoxygenator, (8) water vapour saturator, (9) photochemical reactor, (10) magnetic stirrer, (11) condenser, (12) ice-cooled trap, (13) ice-cooled trap and (14) flow meter.

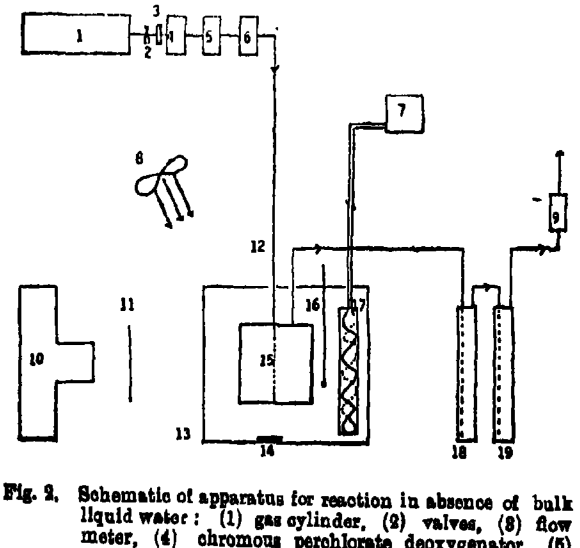


Fig. 2. Schematic of apparatus for reaction in absence of bulk liquid water: (1) gas cylinder, (2) valves, (3) flow meter, (4) chromous perchlorate deoxygenator, (5) water vapour saturator, (6) fritted glass vapor condenser, (7) thermostat, (8) blower, (9) flow meter, (10) light source: 150 W-Xe, (11) glass filter, (12) gas lines, (13) water bath, (14) magnetic stirrer, (15) reaction cell, (16) thermometer, (17) heat exchanger coils, (18) ice-cooled trap and (19) ice-cooled trap.

experiments in the presence and absence of bulk liquid water.

Results and Discussion

Reduction of N_2 in the presence of bulk liquid water : Ammonia was the only product observed in significant amounts when N_2 saturated with water vapor was bubbled through an illuminated dilute aqueous suspension of catalyst. At 30° or below, essentially all of this product remained in the reaction cell under reaction conditions. At 40° or above, most of the NH_3 was swept into the traps.

Tables 1 and 2 present data which indicate that with either α-Fe_2O_3 or Cr_2O_3 as catalyst, yields of ammonia approach limiting values. Each yield recorded in Table 1 was measured in a separate experiment, *i.e.* ammonia was only determined at the end of each experiment. A brief induction period is apparent in these data. With a constant proportion of catalyst, the yield of NH_3 then approaches a limiting value. The rate of approach to the plateau increases with the proportion of catalyst. Table 2 summarises data with Cr_2O_3 as a photocatalyst collected in the same way as the data of Table 1. Again, an approach to a limiting yield of NH_3 is apparent. Yields with air are essentially the same as with high-purity nitrogen. The limiting yield with Cr_2O_3 is approximately twice that observed with α-Fe_2O_3.

TABLE 1—REDUCTION OF N_2 OVER α-Fe_2O_3[a] AT 28° UNDER ILLUMINATION[b] AT $\lambda > 350$ nm IN PRESENCE OF BULK LIQUID WATER : EVIDENCE FOR LIMITING YIELDS OF NH_3

Proportion of catalyst w/v%	Reaction time h	Total yield of NH_3 mol
0.10	0.17	Trace
0.10	0.33	Trace
0.10	0.50	0.10
0.10	1.00	0.15
0.10	2.00	0.28
0.10	4.00	0.40
0.10	12.00	0.50
0.33	0.33	0.38
0.33	3.00	0.48
1.00	0.33	0.59
1.00	6.00	0.68

[a] Baker analysed reagent. [b] Xenon lamp with 350 nm cut-off filter.

The data of Table 3 present evidence for photo-assisted decay of ammonia in the presence of either α-Fe_2O_3 or Cr_2O_3. Each line of data in Table 3 represents a separate experiment at the end of which the yield of NH_3 was determined. It is apparent that with either α-Fe_2O_3 or Cr_2O_3 as catalyst, there is a smaller net increase in the amount of NH_3 under illumination in the presence of N_2 in solutions initially dosed with ammonia than with pure water. Net *decrease* in the amount of NH_3 was observed under illumination when the amount of NH_3 initially added was 5 mol whether N_2 or Ar was passed.

TABLE 2—REDUCTION OF N_2 OVER Cr_2O_3[a] AT 28° UNDER ILLUMINATION[b] AT $\lambda > 420$ nm IN PRESENCE OF BULK LIQUID WATER : EVIDENCE FOR LIMITING YIELDS OF NH_3

Proportion of catalyst w/v%	Reaction gas	Reaction time h	Total yield of NH_3 mol
0.10	N_2	0.5	0.57
0.10	N_2	1.0	0.94
0.10	N_2	4.0	1.10
0.10	N_2	19.0	0.88
0.10	Air	1.0	0.60
0.10	Air	3.0	1.10
0.10	Air	12 0	0.97
0.088	N_2	19.0	0.56
0.88	N_2	12.0	0 98
1.00	N_2	10.0	1.24
0.088	Air	11.0	0.54
0 165	Air	12.0	1.(1
0.38	Air	12.0	1.05

[a] Fisher. [b] Xenon lamp with 420 nm cut-off filter.

TABLE 3—EFFECT OF ADDED NH_3 ON YIELDS IN THE REDUCTION OF N_2 OVER α-Fe_2O_3[a] and Cr_2O_3[b] AT 27-28° UNDER ILLUMINATION[c] AT $\lambda > 420$ nm IN PRESENCE OF BULK LIQUID WATER : EVIDENCE FOR DECOMPOSITION OF NH_3

Catalyst	Atmosphere[d]	Reaction period h	Initially added	Amount of NH_3 after reaction mol	Difference
Fe_2O_3	N_2	3	none	0.87	+0.87
Fe_2O_3	N_2	1	0.10	0.21	+0.11
Fe_2O_3	N_2	7	2.0	2.4	+0.4
Fe_2O_3	Ar	20	5.0	2.8	−2.2
Fe_2O_3	Ar	22	5.1	3.3	−1.8
(Fe_2O_3 dark	Ar	20	5.0	4.6	−0 4)
Cr_2O_3	N_2	3	none	0.98	+0.98
Cr_2O_3	N_2	22	none	0.98	+0.98
Cr_2O_3	N_2	7	0.30	0.98	+(.68
Cr_2O_3	N_2	24	5.0	3 7	−1.3
(Cr_2O_3 dark	N_2	20	5.0	4.9	- 0.1)
Cr_2O_3	Ar	24	5.1	3.1	−2.0
(Cr_2O_3 dark	Ar	20	5.2	4.9	−0.3)

[a] 0.10 w/v% Baker, A.R. [b] 0.17 w/v% Baker, A.R. [c] Xenon lamp with 420 nm cut-off filter. [d] 1 atm., 2-5 ml min^{-1} flow-rate.

The decrease was about 60% larger with Ar than with N_2. The decrease under illumination with N_2 present or absent was several times larger than it was in the dark.

The data of Table 4 show little or no decay of the catalytic activity of α-Fe_2O_3 or Cr_2O_3 in, respectively, 44 or 38 h of use of their aqueous suspensions for reduction of N_2. Each line of data in Table 4 represents a separate experiment at the end of which the cell contents were centrifuged, the supernatant liquid removed and the yield of NH_3 determined. The recovered catalyst powder was then resuspended in an aliquot of pure water and passage of gas and illumination resumed. The whole reaction cycle was performed a total of five times after starting with fresh catalyst powder. With both pure N_2 over α-Fe_2O_3 and air over Cr_2O_3, the observed variation in the presumably limiting yield of NH_3 is relatively small and random.

TABLE 4—INFLUENCE OF RECYCLING α-Fe_2O_3[a] AND Cr_2O_3[a] ON YIELDS OF NH_3 IN THE REDUCTION OF N_2 AT 27-28° UNDER ILLUMINATION[b] AT $\lambda \geq$ 420 nm IN PRESENCE OF BULK LIQUID WATER : EVIDENCE FOR STABILITY OF CATALYTIC ACTION

Catalyst feedstock[c]	No. of times catal. reused	Period of illumn.[d] h	Yield of NH_3 mol
Fe_2O_3/N_2	0	3	0.87
Fe_2O_3/N_2	1	4	0.65
Fe_2O_3/N_2	2	5	0.91
Fe_2O_3/N_2	3	12	0.65
Fe_2O_3/N_2	4	20	0.58
Cr_2O_3/air	0	12	0.97
Cr_2O_3/air	1	8	0.84
Cr_2O_3/air	2	15	0.86
Cr_2O_3/air	3	4	0.68
Cr_2O_3/air	4	4	0.85

[a] 0.1 w/v% of Baker, A.R. catalyst. [b] Xenon lamp with 420 nm cut-off filter. [c] 30-40 ml min^{-1} flow-rate of gas. [d] In individual experiments.

Yields of NH_3 using catalysts with widely differing band-gap energies are summarised in Table 5. Since neither the wt/vol proportion of catalyst, nor period of illumination, nor lower wavelength limit is constant over the set of experiments, comparison must be made with caution. (It must be noted that in no case has the assumption that the action of the metal oxides is only catalytic been proved.) To the extent that the data represents photostationary state compositions, only the variation in the lower wavelength limit is significant. Comparison of the nine yields obtained with illumination at $\lambda \geq$ 420 nm (corresponding to photon energy $\leq$2.96 eV) which are underlined with solid lines in Table 5, reveals no consistent pattern of variation of plateau yields with band-gap energy.

TABLE 5—REDUCTION AT 30° OF N_2 BY AQEOUS SUSPENSIONS OF ILLUMINATED PHOTOCATALYSTS : BAND-GAP SEQUENCE

Catalyst w/v%	Cut-off[a] λ (nm)/ period of illumn. (b)	Band-gap energy[c] eV	Yield of NH_3 mol
La-Ni-oxide/0.17	420/16	0	0.32
Platinised La-Ni-oxide/0.17	420/36	0	1.7
La-Ti-oxide/0.33	320/24	0	2.9
CoO/0.33	320/15	0.8	3.6
Co_3O_4/0.10	420/12	0.9	1.7
Pr_6O_{11}/0.10	350/6	1.2	0.49
TeO_2/0.10	350/10	1.5	0.37
Cr_2O_3/0.33	420/12	1.9	0.96
α-Fe_2O_3/0.10	420/12	2.2	0.65
Nd_2O_3/0.17	420/14	2.2	1.1
WO_3/0.17	420/16	2.8	1.6
MoO_3/0.17	420/16	2.9	1.25
PbO/0.10	350/22	3.2	0.81
Fe^{III} in mol sieve[b]/0.10	420/5	–	1.9

[a] Illumination by xenon lamp. [b] Linde 5A molecular sieve exchanged with 1% aqueous BAR $FeCl_3$ and dried at 300°; illumination by a quartz halogen lamp. [c] Ref. 20.

Similarly, the three yields obtained with illumination at $\lambda \geq$ 350 nm (3.55 eV) which are underlined with dotted lines, do not vary systematically with band-gap energy. The two yields obtained with $\lambda \geq$320 nm (3.88 eV) are significantly higher than all the others but no conclusion can be drawn as to the reason for this observation. It is noteworthy that one of the catalysts, Fe^{III} in Linde molecular sieve 5A, is neither a semiconductor nor metallic. The significance of the effectiveness of catalysts with small band-gaps is taken up below at the end of next section, in connection with results obtained in the absence of bulk liquid water.

The formal activation energy for the formation of NH_3 in 0.1 %wt/vol aqueous suspensions of α-Fe_2O_3 (Baker, A.R.) illuminated at $\lambda \geq$ 420 nm with N_2 passing at 60 ml min^{-1} was determined in the usual way. Reaction periods for individual runs were 20-48 h and reaction temperatures were 40, 50, 60 and 70°. Under these conditions, negligible amounts of NH_3 remain in the reaction cell; essentially the entire product is collected in the traps. Decay of NH_3 does not complicate the picture under these conditions. The resulting apparent activation energy, 46 kJ mol^{-1}, is relatively large. This experiment has practical significance. It demonstrates that not only can decay of NH_3 be avoided by raising the reaction temperature high enough to drive it from solution, but the rate of conversion of N_2 to NH_3 can be substantially increased by raising the temperature.

Reduction of N_2 in absence of bulk liquid water : The data of Table 6 show that N_2 is reduced to NH_3 over illuminated α-Fe_2O_3 in the presence of water vapor and absence of bulk liquid water. Although there are a few unexplained substantial fluctuations in the rate of production of NH_3, no significant trend is apparent over the 225 h of exposure. The results of a similar experiment

TABLE 6—REDUCTION OF N_2[a] BY WATER OVER α-Fe_2O_3[b] AT 28° UNDER ILLUMINATION[c] AT $\lambda \geq$ 350 nm IN ABSENCE OF BULK LIQUID WATER : EVIDENCE FOR STABILITY OF CATALYTIC ACTION

Total reaction time h	Total NH_3 yield mol	Differential rate of formation of NH_3 mol h^{-1}
6	0.38	0.064
24	1.18	0.042
31	1.58	0.057
44	1.97	0.034
54	2.78	0.081
70	3.18	0.025
103	4.57	0.042
128	6.34	0.089
144	6.91	0.027
160	7.77	0.034
197	8.59	0.029
225	9.44	0.030

[a] Flowing at 30 ml min^{-1}. [b] Baker, A.R. deposited from isopropanol and conditioned by heating at 300° under flowing argon for 12 h. [c] Xenon lamp with cut-off filter.

using a film of Cr_2O_3 presented in Table 7, are similar except that the experiment was continued for 329 h ; differential rates were approximately half those obtained with α-Fe_2O_3 and there was an induction period. These experiments confirm that the activity of these catalysts is encouragingly stable. Since ammonia is rapidly swept into the collecting traps, the behavior of these 'dry' systems is not complicated by its decay.

A set of experiments employing a film of α-Fe_2O_3 illuminated at $\lambda \geqslant 420$ nm and 29° showed that the rate of formation of NH_3 increased by a factor of six as the flow-rate of N_2 increased from 2 to 100 ml min^{-1}. Further doubling of the flow-rate had a negligible effect on the rate. The formal activation energy for the formation of NH_3 over α-Fe_2O_3 under illumination at $\lambda \geqslant 420$ nm in the absence of bulk liquid water was determined in the usual way. Temperature was varied from 30 to 70° and the flow-rate of N_2 was 60 ml min^{-1}. The data correspond to an apparent activation energy of 19 kJ mol^{-1}, less than half the value observed in the presence of bulk liquid water. The efficiency of conversion of incident photons from a xenon lamp equipped with a 420 nm cut-off filter into energy stored in NH_3 was determined for the reaction in the absence of bulk liquid water at 30° by assuming that the photoreaction is the reverse of the combustion of NH_3,

$$NH_3(g)+3/4\ O_2(g) \rightarrow 1/2\ N_2(g)+3/2\ H_2O(g)$$
$$\Delta H = -75.68 \text{ kcal mol}^{-1}$$

Integrated incident light energy was measured with a 'Sunstation'[19]. This measurement yielded

$$\text{Engineering efficiency} = \frac{\text{Calculated stored energy}}{\text{Incident light energy}} \times 100 = 10^{-4}\%$$

for an experiment which produced 0.05 mol h^{-1} of NH_3 at a flow-rate of 50 ml min^{-1}.

The rate of formation of NH_3 observed under similar conditions using a film of Co_3O_4 (band-gap $=0.9$ eV) which had been deposited from water (Table 7) was more than two times that obtained with α-Fe_2O_3 which had been deposited from isopropanol. The rate of formation of NH_3 over a film of Co_3O_4 which had been deposited from aqueous isopropanol was more than five times that obtained with the latter α-Fe_2O_3 film. These results are consistent with the observations summarised in Table 5 which show that several low-band-gap materials are effective catalysts in the presence of bulk liquid water. $\Delta E°$ for the six-electron redox reaction, $1/2\ N_2(g)+5/2\ H_2O(l) \rightleftharpoons NH_4OH(aq)+3/4\ O_2(g)$, is -1.23 V[21]. Thus, if the catalytic mechanism explicitly involves electrons from conduction bands, the overall reduction of N_2 over semiconductors with band-gap energies substantially less than 1.23 V requires the promotion of more than one electron on the average per electron equivalent transferred in the reaction. Such behavior would be required of La-Ni-oxide, La-Ti-oxide, CoO and Co_3O_4. Elucidation of the chemical mechanism of such processes remains to be accomplished. Similarly, no mechanistic explanation of the catalytic effectiveness of zeolite 5A containing Fe^{III} can be offered at present.

TABLE 7—REDUCTION OF N_2[a] BY WATER OVER Cr_2O_3[b] AT 28° UNDER ILLUMINATION[c] AT $\lambda \geqslant 420$ nm IN ABSENCE OF BULK LIQUID WATER : EVIDENCE FOR STABILITY OF CATALYTIC ACTION

Total reaction time h	Total NH_3 yield mol	Differential rate of formation of NH_3 mol h^{-1}
18	0.02	0.001
46	0.59	0.020
68	0.94	0.016
91	1.22	0.018
116	1.72	0.020
140	2.26	0.022
164	2.78	0.020
188	2.93	0.008
214	3.79	0.033
238	4.81	0.042
266	5.28	0.017
286	5.57	0.015
313	5.89	0.012
329	6.56	0.042

[a] Flowing at 30 ml min^{-1}. [b] Fisher, deposited from isopropanol and conditioned by heating on flowing argon at 300° for 12 h. [c] Xenon lamp with 420 nm cut-off filter.

Films of several catalysts which had been shown[22] to be active in the photoassisted reduction of CO_2 by H_2 were found to also promote the reduction of N_2 by water vapour under illumination ($\lambda \geqslant 420$ nm) at rates similar to that observed with α-Fe_2O_3. These catalysts included Co-Mo-Al-oxide, Co-Mo-Ti-oxide, Zn-Fe-oxide and platinised La-Ni-oxide. Activity was followed for periods ranging from 48 to 146 h.

Acknowledgement

This work was supported by ARCO Solar, Inc.

References

1. G. N. SCHRAUZER and T. D. GUTH, *J. Am. Chem. Soc.*, 1977, 99, 7189.
2. G. N. SCHRAUZER, T. D. GUTH, M. R. PALMER and J. SALEHI in "Solar Energy : Chemical Conversion and Storage", eds. R. R. HAUTALA, R. B. KING and C. KUTAL, Humana Press, Clifton, 1979, p. 261.
3. H. MIYAMA, N. FUJII and Y. NAGAE, *Chem. Phys. Lett.*, 1980, 74, 523.
4. G. N. SCHRAUZER, N. STRAMPACH, L. N. HUI, M. R. PALMER and J. SALEHI, *Proc. Natl. Acad. Sci. USA*, 1983, 80, 3873.
5. V. AUGUGLIARO, A. LAURICELLA, L. RIZZUTI, M. SCHIAVELLO and A. SCLAFANI in "Hydrogen Energy Press", Proceedings 3rd World Hydrogen Energy Conference, Tokyo, June 1980, eds. T. N. VEZIROGLU, K. FUEKI and T. OHTA, pp. 2, 589.
6. V. AUGUGLIARO, A. LAURICELLO, L. RIZZUTI, M. SCHIAVELLO and A. SCLAFANI. *Int. J. Hydrogen Energy*, 1982, 7, 845.
7. V. AUGUGLIARO, F. D'ALBA, L. RIZZUTI, M. SCHIAVELLO and A. SCLAFANI, *Int. J. Hydrogen Energy*, 1982, 7, 851.

8. P. L. YUE, F. KHAN and L. RIZZUTI, *Chem. Eng. Sci.*, 1983, 38, 1893.
9. H. VAN DAMME and W. HALL, *J. Am. Chem. Soc.*, 1979, 101, 4373.
10. P. P. BADFORD and C. G. FRANCIS, *J. Chem. Soc., Chem. Commun.*, 1983, 1520.
11. D. MONHEIT, S. GRAYER, N. GODINGER, V. KATZIR and M. HALMANN, "Abstracts of the 5th International Conference on Photochemical Conversion and Storage of Solar Energy", Osaka 1984, p. 75.
12. F. KAHN, P.-L. YUE, L. RIZZUTI, V. AUGUGLIARO and M. SCHIAVELLO, *J. Chem. Soc., Chem. Commun.*, 1981, 1049.
13. F. KHAN, P. YUE, L. RIZZUTI, V. AUGUGLIARO and A. BRUCATO, *Ind. Eng. Chem. Prod. Res. Dev.*, 1983, 22, 238.
14. N. N. LICHTIN, U. S. Pat., 4 427 509/1984.
15. N. N. LICHTIN and K. M. VIJAYAKUMAR, U. S. Pat., 4 427 510/1984.
16. N. N. LICHTIN and E. BERMAN, U. S. Pat., 4 448 311/1984.
17. N. N. LICHTIN and K. M. VIJAYAKUMAR, "Abstracts of the 163rd Meeting of the Electrochemical Society", May 8-13, 1983, p. 782.
18. N. N. LICHTIN, K. M. VIJAYAKUMAR and M. M. KHADER, "Extended Abstracts of the 1985 Meeting of the International Solar Energy Society", 1985, p. 438.
19. E. BERMAN and D. BIRAN, *Solar Energy*, 1978, 20, 455.
20. O. V. KRYLOV, "Catalysis by Non-metals", Academic Press, New York, 1970.
21. Lange's Handbook of Chemistry, 12th ed., ed. J. A. DEAN, McGraw-Hill Book Co., New York, 1979, 9-1.
22. K. M. VIJAYAKUMAR and N. N. LICHTIN, *J. Catal.*, 1984 90, 173.

J. Indian Chem. Soc.,
Vol. LXIII, January 1986, pp. 35-42

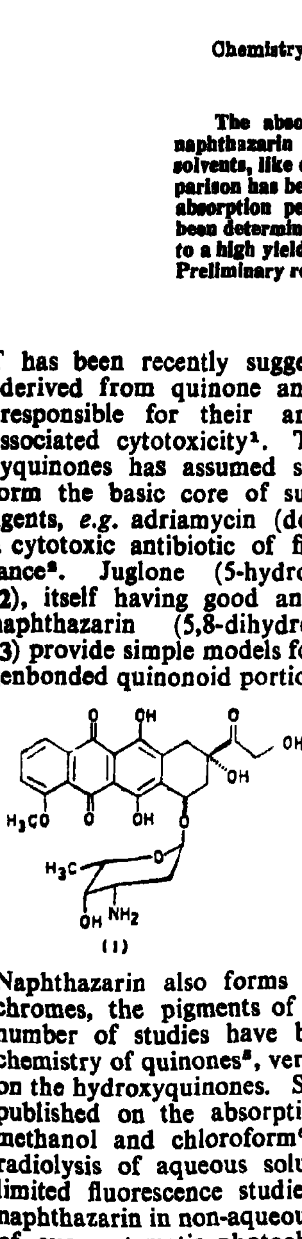
Photophysics and Laser Flash Photolysis of Hydroxyquinones. Studies on Juglone and Naphthazarin†

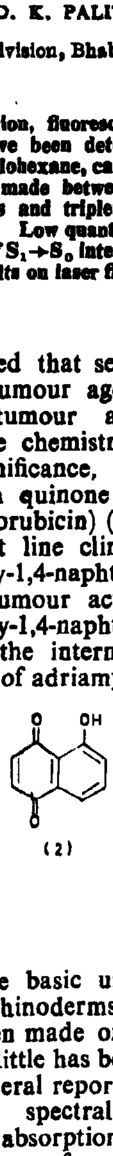
D. K. PALIT, T. MUKHERJEE and J. P. MITTAL*

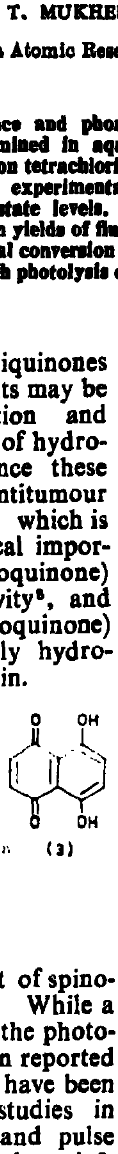
Chemistry Division, Bhabha Atomic Research Centre, Trombay, Bombay-400 085

The absorption, fluorescence and phosphorescence characteristics of juglone and naphthazarin have been determined in aqueous solutions of different pH, and other solvents, like cyclohexane, carbon tetrachloride, methanol, ethylene glycol *etc.* Comparison has been made between experimental and theoretically calculated values of absorption peaks and triplet state levels. Ground and excited state pK_a values have been determined. Low quantum yields of fluorescence and phosphorescence point out to a high yield of $S_1 \rightarrow S_0$ internal conversion process and possibility of photoenolisation. Preliminary results on laser flash photolysis of juglone are reported.

IT has been recently suggested that semiquinones derived from quinone antitumour agents may be responsible for their antitumour action and associated cytotoxicity[1]. The chemistry of hydroxyquinones has assumed significance, since these form the basic core of such quinone antitumour agents, *e.g.* adriamycin (doxorubicin) (**1**) which is a cytotoxic antibiotic of first line clinical importance[2]. Juglone (5-hydroxy-1,4-naphthoquinone) (**2**), itself having good antitumour activity[3], and naphthazarin (5,8-dihydroxy-1,4-naphthoquinone) (**3**) provide simple models for the internally hydrogenbonded quinonoid portion of adriamycin.


(1)


(2)


(3)

Naphthazarin also forms the basic unit of spinochromes, the pigments of echinoderms[4]. While a number of studies have been made on the photochemistry of quinones[5], very little has been reported on the hydroxyquinones. Several reports have been published on the absorption spectral studies in methanol and chloroform[6], absorption and pulse radiolysis of aqueous solutions of naphthazarin[7], limited fluorescence studies of reduced products of naphthazarin in non-aqueous media[8] *etc.* In course of our systematic photochemical studies on hydroxyquinones, we studied the absorption and luminiscence characteristics of juglone and naphthazarin in a number of solvents. We report here some of our principal observations and compare our data with some theoretically calculated values. We also report here some preliminary results on the laser flash photolysis of juglone.

Experimental

Absorption spectra were recorded on a Hitachi 330 microprocessor-controlled recording spectrophotometer. Fluorescence excitation and emission spectra were recorded in a AMINCO-Bowman 4-8202B spectrophotofluorometer fitted with a R-136 potted photomultiplier tube and a F-42C Riken Denshi X-Y/T recorder. For concentrated solutions a front surface accessory was used. Phosphorescence spectra were recorded at 77 K in quartz tubes (2 mm i.d.), using a suitable Dewar flask and a AMINCO-Keirs phosphoroscope. A laser kinetic spectrometer (Applied Photo Physics Ltd., London) operating with a KrF excimer laser (248 nm), in conjunction with a Gould Biomation 4500 transient digitiser and a PDP 11/23 microcomputer, was used for monitoring the transient absorption and decay kinetics. A Norsk Data ND-560 computer was used for theoretical calculations and data fit. A Orion 901 digital ionalyser was used for pH measurements.

Semi-empirical self-consistent multiconfigurational calculations using π-electron PPPCI method was used for both the compounds, both for the singlet and the triplet levels. The usual version of the PPP (Pariser-Parr-Pople) method was used[9,10]. Interactions between mono-excited configurations, formed by promotion of one electron from one of the six highest occupied π-molecular orbitals to one of the six lowest unoccupied π-molecular orbitals were considered. The systems studied were assumed to be planar and the rings were taken as regular hexagons. SCF molecular orbitals served as the basis for the CI calculations. Only resonance integrals between nearest neighbours were considered.

Fluorescence quantum yield was calculated with three different standards[11], (i) anthracene in cyclohexane (for $\lambda_{exc} = 260$ nm), $\phi = 0.36$; (ii) quinine bisulphate in 0.5 mol dm^{-3} H_2SO_4 (for $\lambda_{exc} = 300$

† Dedicated to Professor Sadhan Basu on the occasion of his 65th birthday.

A part of the article was presented at the National Conference on Spectroscopy and Theoretical Chemistry held at Calcutta, December 5-7, 1985.

310 nm), $\phi=0.55$; and (iii) rhodamine-B in ethanol (for $\lambda_{exc}=490$ nm), $\phi=0.97$.

The areas under the fluorescence curves of the standard and samples were compared. Necessary corrections were made due to the small difference in optical densities of the solution and due to variation of refractive index of the solvents, by using the formula[11],

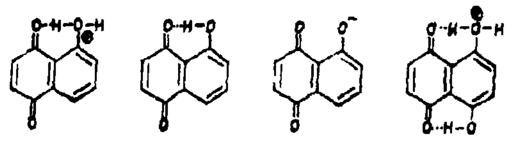
$$\frac{\phi_{sample}}{\phi_{standard}} = \frac{Area_{sample}}{Area_{standard}} \times \frac{OD_{standard}}{OD_{sample}} \times \frac{n_1^2}{n_2^2} \quad (1)$$

where, n_1 and n_2 are refractive index for the solvent used for the sample and the standard, respectively. In several cases where either the fluorescence was too weak or scattering overlap was significant, quantum yield determination was not attempted.

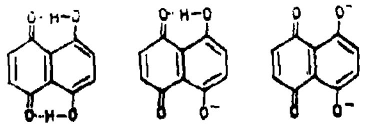
Juglone (Sigma) and naphthazarin (synthesised sample[12]) were recrystallised from alcohol and vacuum sublimed before use. Phosphate and borate buffers, perchloric acid and sodium hydroxide were all G.R. (Sarabhai) reagents. Solvents were all spectrograde (E. Merck or Fluka). Where necessary, solutions were deoxygenated by bubbling high purity argon (Indian Oxygen) for 30 min.

Results and Discussion

The hydroxyquinones can occur in a number of states of protonation due to the ionisation of their hydroxyl groups in aqueous solutions. Thus, juglone can be either cationic (4), neutral (5) or anionic (6) in aqueous solutions, depending on *p*H of the solution, while naphthazarine can be cationic (7), neutral (8), anionic (9) or dianionic (10).



JH_2^+ (4) JH (5) J^- (6) NzH_3^+ (7)



NzH_2 (8) NzH^- (9) Nz^{2-} (10)

Absorption studies: The absorption spectra of juglone in water, at *p*H values of 5 and 10.7 are shown in Fig. 1. The absorption spectra were shown to be identical throughout *p*H 1 to 7, showing that no ionisation took place within this range. With increasing *p*H (> 7), the visible peak at 420 nm gets red-shifted to 515 nm. The main uv peak at 248 nm gets slightly red-shifted to 258 nm. The spectra in 0.5 mol dm^{-3} H_2SO_4 also showed the same feature as at *p*H 5, showing that JH_2^+ probably exists only in very strong acid. The wavelengths of the absorption maxima and extinction coefficient values are shown in Table 1. The large shift in λ_{max}, compared to those in 1,4-naphthoquinone[5] is worth noting.

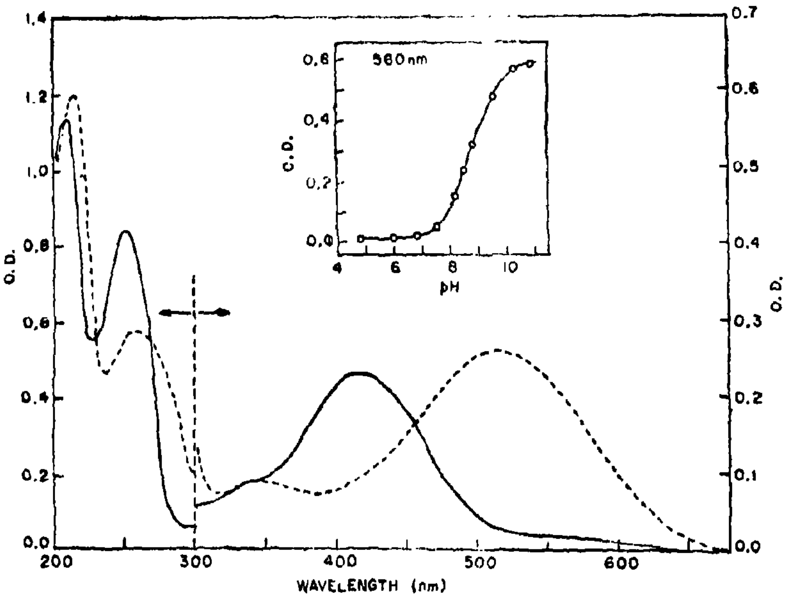


Fig. 1. Absorption spectra of juglone (~ 6.45×10^{-5} mol dm^{-3}) in water ; (–) *p*H 7 and (– –), *p*H 10.5. (Inset) Variation of optical density at 560 nm for juglone as a function of *p*H ; (O) experimental points and (–) computer best fit ; with $pK_a=8.85$.

TABLE 1—ABSORPTION CHARACTERISTICS OF JUGLONE AND NAPHTHAZARIN IN DIFFERENT SOLVENTS AND COMPARISON WITH SOME THEORETICALLY CALCULATED VALUES

Solvent	λ_{max}, nm (log ε)	
	Juglone	Naphthazarin
Water, neutral[a]	208(4.22), 248(4.13), 310(2.98), 420(3.56)	209(4.54), 266(3.89), 340(3.03), 482(3.72), 518(3.73), 556(3.47)
Anion[b]	215(4.26), 258(3.97), 350(3.17), 515(3.61)	211(4.76), 292(3.78), 528(sh)(3.64), 578(3.81), 610(3.76)
Di-anion[c]	—	308(3.73), 575(3.94), 613(4.06)
Methanol	248(4.11), 340(sh)(3.05), 407(sh)(3.55), 422(3.56)	265(3.86), 330(3.10), 483(3.71), 511(3.73), 552(sh)(3.49)
Cyclohexane	245(3.87), 320(3.14), 406(sh)(3.58), 428 (3.59)	264(4.01), 330(3.1), 486(3.67), 516(sh)(3.90), 524 (3.92), 544(3.74), 5.62(3.80)
Carbon tetrachloride	325(3.07), 412(sh)(3.57), 428(3.58)	334(3.05), 489(3.76), 524(3.83), 546(3.68), 564(3.65)
PPPOI (this work)*	208(0.0341), 233(0.1448), 265(0.4956), 328(0.1003), 333(0.0580)	211(0.0537), 285(0.0930), 265(0.4850), 331(0.0055) 341(0.1701)
PPPOI[d]*	233(0.08), 254(0.07), 264(0.38), 375(0.09), 418(0.10)	262(0.24), 268(0.13), 266(0.09), 402(0.0001), 417 (0.16)
CNDOCI[e]*	249(0.11), 262(0.001), 283(0.31), 316 (0.17), 440(0.16), 445(0.06)	—

[a] pH 5. [b] pH 10.7(J⁻), 9.1(NzH⁻). [c] pH ~ 13(Nz²⁻). [d] Refs, 9, 10. [e] Ref. 13. * Oscillator strength in parenthesis.

The absorbances at 420, 515 and 560 nm were measured as a function of pH over the range 5 to 11. Experimental absorbances, A_{obs}, were fitted to equation (2),

$$A_{obs} = \frac{A_1}{1+10^{pH-pK}} + \frac{A_2}{1+10^{pK-pH}} \quad (2)$$

where, A_1 and A_2 refer to absorbances attributed to the forms JH and J^-, respectively, and pK is the pK_a value of JH. The best computer fit between the experimental and computed absorbance was obtained with $pK_a = 8.85 \pm 0.05$. The result for 560 nm is shown in the inset to Fig. 1. Other wavelengths (*viz.* 420 and 515 nm) gave the same values of pK_a. It is clear that juglone is a stronger acid than phenol or α-hydroxynaphthalene ($pK_a \sim 10$), as expected from the greater potential for delocalisation in the anionic form. Similar experiments were performed with naphthazarin. The data were identical to those reported by one of us elsewhere[7] and are shown in Table 1. The pK_a of NzH_2 and NzH^- were 7.85 and 10.7, respectively[7].

Absorption spectra were also recorded in cyclohexane, carbon tetrachloride, methanol and ethylene glycol. The essential features of the absorption spectra of juglone do not change much from solvent to solvent. Fig. 2 shows few such spectra. However, naphthazarin spectra show a remarkable solvent dependence (Fig. 3). Table 1 lists all the absorption maxima and extinction coefficients for both juglone and naphthazarin. It also lists the calculated maxima by different methods. There is good agreement between the experimental λ_{max} values and the corresponding calculated ones.

Since these compounds contain both quinonoid and benzenoid rings, it is expected that there should be a strong peri-interaction between the two rings. Thus the hydroxy groups cause a pronounced red-shift of the benzenoid absorption. Similarly, the weak n π* quinonoid absorptions are inter-mixed with stronger π π* benzenoid absorptions. Intra-molecular hydrogen bonding also perturbs the expected absorbance values. In our calculated values (Table 1) we could not include the latter effect. It will be extremely interesting if appropriate perturbation functions for the intra-molecular H-bonding could be incorporated in the calculations. In some cases, certain calculated transitions do not show as maxima on the absorption curves because they are hidden under the envelopes of other main bands. More insight on the benzenoid and quinonoid nature of different bands could be made by our fluorescence studies.

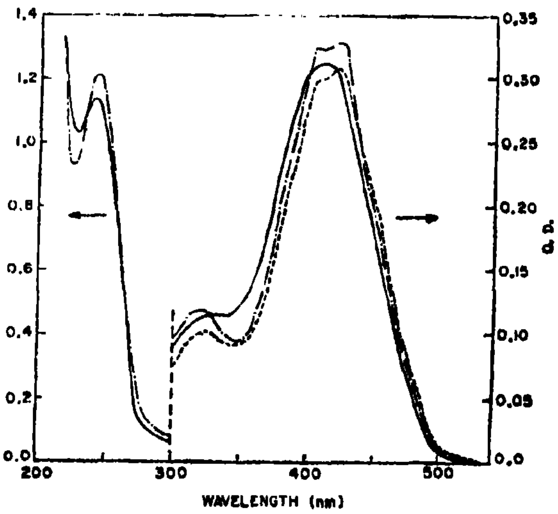


Fig. 2. Absorption spectra of juglone in some organic solvents: (—) methanol, (–·–) cyclohexane, (– –) carbon tetrachloride.

Fluorescence studies : Quinones are well known to have extremely weak fluorescence and a high

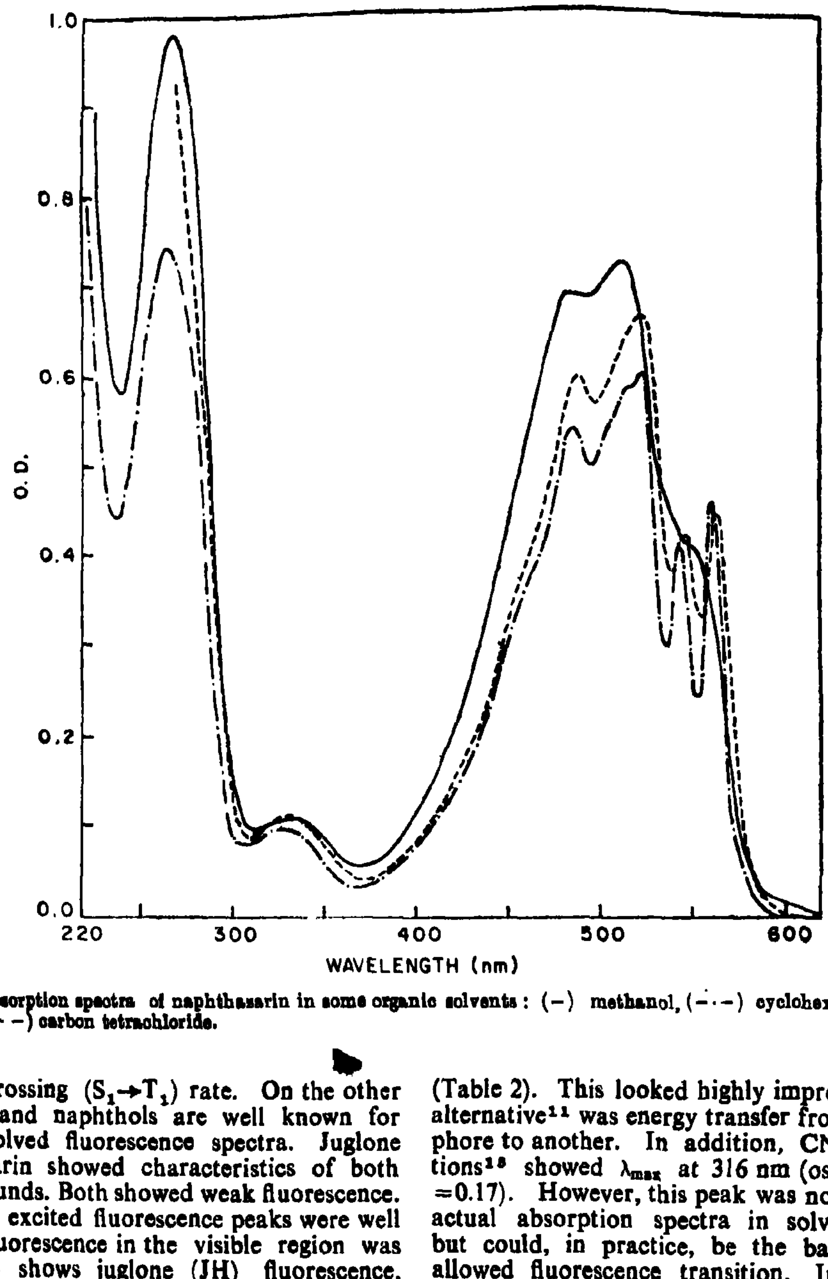


Fig. 8. Absorption spectra of naphthazarin in some organic solvents : (–) methanol, (–·–) cyclohexane, and (– –) carbon tetrachloride.

inter-system crossing ($S_1 \rightarrow T_1$) rate. On the other hand, phenols and naphthols are well known for their well resolved fluorescence spectra. Juglone and naphthazarin showed characteristics of both class of compounds. Both showed weak fluorescence. While the uv excited fluorescence peaks were well resolved, the fluorescence in the visible region was broad. Fig. 4 shows juglone (JH) fluorescence, when the spectra were recorded with different excitation wavelength. While JH absorption maximum in the uv is at 248 nm, the excitation maximum was found to be ~310 nm. In spite of repeated purification of the sample from different batches, there was no change in the excitation or fluorescence maxima. The position of fluorescence maxima was independent of $\lambda_{excitation}$ of either 248 or 310 nm. Tlc of all the samples (silica gel) showed no sign of any impurity present. Any re-sublimable impurity, therefore, has to be < 0.1% of the quinone. The fluorescence has thus to be very strong for this impurity, with estimated quantum yield ≫1 (Table 2). This looked highly improbable. Another alternative[11] was energy transfer from one chromophore to another. In addition, CNDOCI calculations[18] showed λ_{max} at 316 nm (oscillator strength =0.17). However, this peak was not detectable in actual absorption spectra in solvents (Table 1), but could, in practice, be the basis for a more allowed fluorescence transition. In the case of naphthazarin in water and alcohol solutions, an additional strong fluorescence was observed at ~450 nm, when excited witn 260 nm light (Fig. 5). The excitation spectrum for this 450 nm fluorescence gave a peak at ~400 nm in addition to 260 nm. However, the 400 nm region is only a shoulder in the absorption spectrum of naphthazarin and PPPCI calculations[18] showed an extremely weak peak at 402 nm and a strong one at 416 nm. We, therefore, conclude that the 400 nm transition represent a benzenoid transition.

The quantum yields of uv-excited fluorescence from both the compounds were small (Tables 2

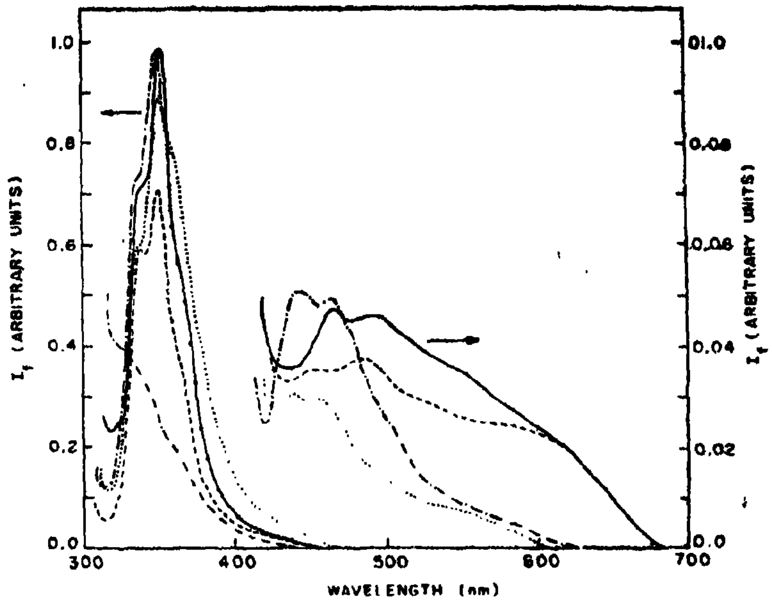


Fig. 4. Fluorescence spectra of juglone in different solvents : (–) ethylene glycol, (– –) methanol, (...) cyclohexane, (–.–) carbon tetrachloride and (– –.– –) water (pH 5); λ_{exc} for left-hand curves, 300 nm and for right-hand curves, 400 nm.

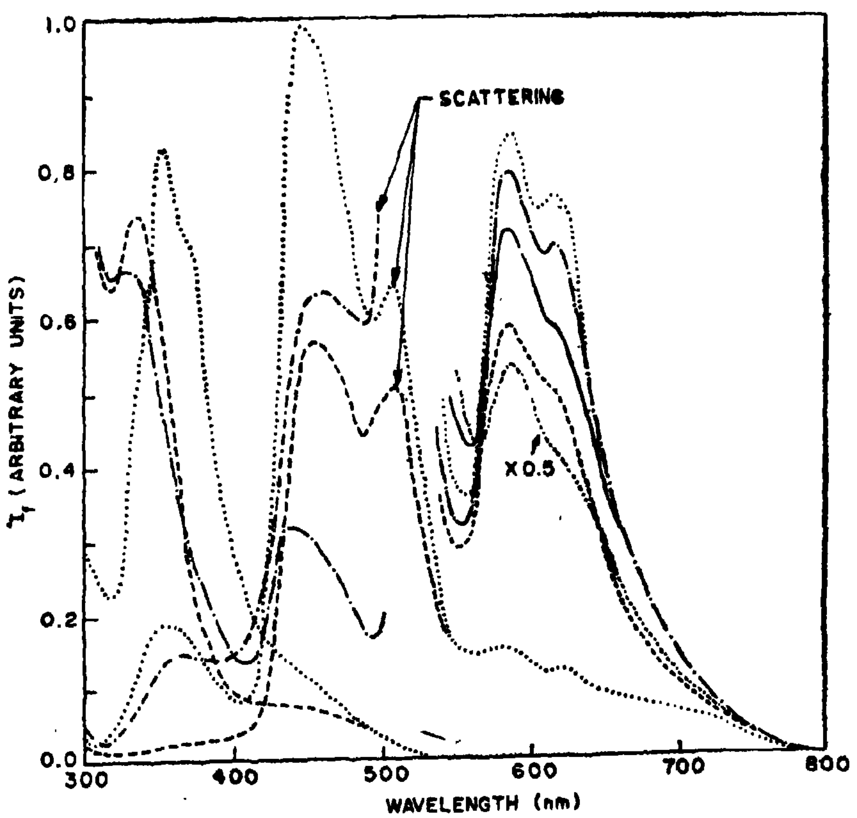


Fig. 5. Fluorescence spectra of naphthazarin in different solvents : (–) ethylene glycol, (– –) methanol, (···) cyclohexane, (–.–) carbon tetrachloride and (– –.– –) water (pH 5); λ_{exc} for left-hand curve, 300 nm ; for the middle curves, 360 nm ; and for the right-hand curves, 490 nm.

TABLE 2—FLUORESCENCE CHARACTERISTICS OF JUGLONE

Solvent	λ_{max} (fluor.) nm	E_S^* kJ mol^{-1}	ϕ_{fl}
Water (pH 5)	334 sh^a, 346^a	358.5^a	0.16^a
Methanol	336 sh^a, 348^a	356.4^a	0.085^a
	450 sh^b, 485^b	266.1^b	i
Ethylene glycol	336 sh^a, 348^a	356.4^a	0.17
	465^b, 493^b	257.5	i
Carbon tetrachloride	442^b, 463^b	270.9^b	i
Cyclohexane	336 sh^a, 348^a	356.4^a	0.077
	440^b, 456^b	272.1	i

* Determined from the shortest wavelength transition.

λ_{exc} = ^{a} 300, ^{b} 400 nm. ^{b} Used instead of 420 nm (exc. max.) to minimise scattering overlap. i = Indeterminate accurately due to scattering overlap.

and 3). The fluorescence induced by excitation due to absorption in the visible region had lower quantum yield in case of juglone (Table 2), but comparable in case of naphthazarin (Table 3). In completely aprotic solvents (*i.e.* CCl_4) the quantum yield was marginally increased, probably due to a decrease in $S_1 \rightarrow S_0$ internal conversion. The effect of viscosity was more significant in juglone than in naphthazarin, as shown by the use of ethylene glycol. In relatively concentrated solutions ($>10^{-4}$ mol dm^{-3}), front surface optics were always used to avoid distortion caused by self-absorption of emitted fluorescence in the visible region when usual perpendicular optics were used. A comparison of Tables 2 and 3 also shows that the visible bands have a mixed benzenoid *cum* quinonoid character, with naphthazarin having more benzenoid character than juglone.

TABLE 3—FLUORESCENCE CHARACTERISTICS OF NAPHTHAZARIN

Solvent	λ_{max} (fluor.) nm	E_S^* kJ mol^{-1}	ϕ_{fl}
Water (pH 5)	365^{a,b}, 460^{a,b}	328.1^{a,b}	i^{a,b}
	585^c, 612^c	204.7^c	0.022^c
Water (pH 9.1)	360^{a,b}, 420 sh^{a,b}	332.6^{a,b}	—
Water (pH 12.5)	~ 400^{a,b}	—	—
Methanol	455^a, 336^b	356.4^b	0.009^{a,c}
	585^c, 612 sh^c	204.7^c	i^b
Ethylene glycol	362^{a,b}, 452^a	330.8^{a,b}	0.009^a
	587^c, 618 sh^c	204.0^c	0.01^b, 0.011^c
Carbon tetrachloride	331^b, 588^c, 620^c	361.8^b, 203.6^c	i^b, 0.011^c
Cyclohexane	373 sh^{a,b}, 450^a	321.0^{a,b}	0.019^a,
	590^c, 620^c	203.0^c	0.062^b
			0.012^c

* Determined from the shortest wavelength transition.
λ_{exc} = ^{a} 260, ^{b} 300, ^{c}490 nm. ^{b} Used instead of 330 nm (exc. max.) to minimise scattering overlap. i = Indeterminate due to scattering overlap.

In aqueous solutions, we observed fluorescence from JH and NzH_2, very weak fluorescence from NzH^-, but none from J^- and Nz^{2-}. This shows that the molecules essentially behave like a phenol for fluorescence in aqueous solutions. Due to the absence of fluorescence from the ionic forms, only shift in absorption could be used to calculate the excited (S_1) state pK_a values, by using equation (3).

$$pK_a = pK_a^* - \frac{Nhc}{2.303RT}(\bar{\nu}_A - \bar{\nu}_B) \quad (3)$$

where, N = Avogadro number, h = Planck constant, c = velocity of light, R = universal gas constant, T = temperature (at 298 K), and $\bar{\nu}_A$, $\bar{\nu}_B$ = wave number of absorption peaks.

By putting in appropriate values of 420 and 515 nm for juglone and 514 and 610 nm for naphthazarin, and using pK_a (JH) = 8.85 (this work) and pK_1 (NzH_2) = 7.35 (Ref. 7), we could calculate pK^* (S_1) values equal to *ca* −0.4 for juglone and 1.4 for naphthazarin. This explains why juglone fluorescence characteristics do not change due to change in *p*H from 1 to 7 and naphthazarin between *p*H 4 to 7. In strongly acidic solution, however, naphthazarin fluorescence was somewhat different than at *p*H 5.

Phosphorescence and laser flash photolysis studies: Most quinones have a near unity triplet yield[8]. Weak fluorescence from both juglone and naphthazarin indicated possibility of a strong phosphorescence. However, phosphorescence spectra determined in ethanol-methanol (4 : 1), ethylene glycol-water (1 : 1), aqueous 0.5% glucose and 3-methylpentane matrices at 77 K was found to be very weak. The quantum yield could not be accurately determined due to this weak nature of the phosphorescence. The spectral characteristics are shown in Fig. 6 and tabulated in Table 4. The low quantum yield of both fluorescence and phosphorescence probably indicate that either one or

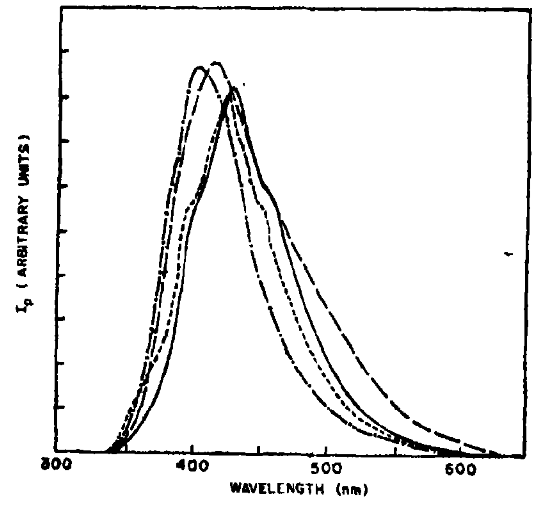


Fig. 6. Phosphorescence spectra of juglone (λ_{exc} = 350 nm) and naphthazarin (λ_{exc} = 260 nm) at 77 K in ethanol-methanol (4 : 1, v/v) : (–) juglone and (- - -) naphthazarin ; and in 3-methylpentane : juglone (– –) and naphthazarin (–.–).

both of $S_1 \rightarrow S_0$ internal conversion and $T_1 \rightarrow S_0$ inter-system crossing are predominant processes for such compounds. However, $T_1 \rightarrow S_0$ transition is

TABLE 4—PHOSPHORESCENCE CHARACTERISTICS AT 77 K OF JUGLONE AND NAPHTHAZARIN

Matrix used	Phosphorescence λ_{max} nm		E_T kJ mol^{-1}		Other bands nm	
	Juglone[a]	Naphthazarin[b]	Juglone	Naphthazarin	Juglone	Naphthazarin
Ethylene glycol-Water (1 : 1)	448	422	267.0	283.4	423, 478	408 sh, 434 sh
Ethanol-methanol (4 : 1)	428	424	279.4	282.1	402 sh, 454	399 sh, 452 sh
3-Methylpentane	415	404	288.2	296.0	—	384 sh, 418 sh
PPPCI calculation[c] (SCFCIO)	434	456	275.9	262.6	339, 476, 754	340, 476, 749

λ_{exc} = [a] 250, [b] 260 nm. [c]Refs. 9, 10.

spin-forbidden, while $S_1 \rightarrow S_0$ transition is highly allowed, especially due to the ground state symmetry of the parent molecules. Thus, in both juglone and naphthazarin, $S_1 \rightarrow S_0$ internal conversion could be the most predominant process. An alternative method was adopted to study the triplet characteristics. The transient absorption (Fig. 7) obtained in methanol solutions after 150 and 400 nanoseconds after the laser flash, in a laser kinetic spectrometer, showed two distinct peaks at 330 and 375 nm with a shoulder at ~360 nm. The 330 nm peak decayed faster than the 375 nm peak. Juglone semiquinone radicals have an absorption maximum[14] at ~375 nm, but none at 330 nm. The 330 nm absorption decayed by a first order kinetics ($k = 4.4 \times 10^6$ s^{-1}) whereas

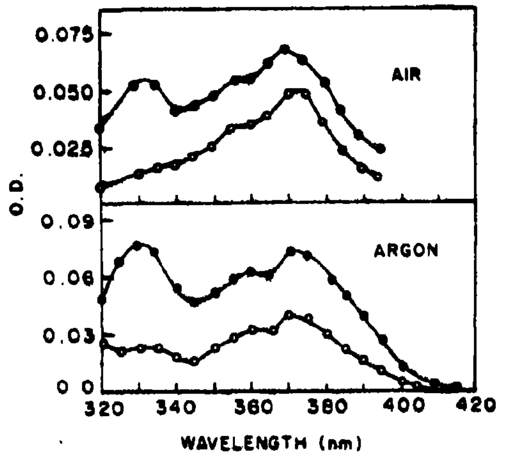
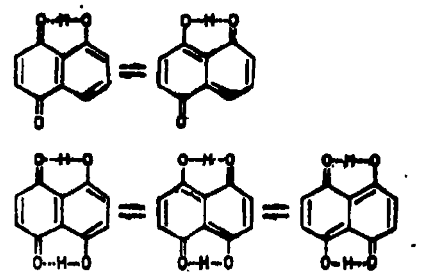


Fig. 7. Absorption spectra of the transients produced by laser flash photolysis of juglone in air-saturated and argon bubbled methanol solutions, after (●) 150 and (○) 400 ns of the laser flash.

the 375 nm peak decayed by a second order kinetics ($2k = 4.5 \times 10^7 \times \epsilon_{375}$ dm^3 mol^{-1} cm^{-1}). Our preliminary assumption is that the 330 nm peak belongs to a genuine T–T absorption, while the 375 nm peak is most likely the result of absorption by juglone semiquinone produced by hydrogen abstraction from methanol by the triplet state of juglone. This hypothesis is further strengthened by the fact that in aerated solutions, the decay of 330 nm peak is faster and that of 375 nm peak slower than in de-oxygenated solutions. In aerated solutions, juglone semiquinone undergos an equilibrium reaction with oxygen[14],

$$JH^{\cdot -} + O_2 \rightleftharpoons JH + O_2^{\cdot -} \quad (4)$$

The laser flash photolysis studies thus show that the triplet population must be significant and therefore, $T_1 \rightarrow S_0$ inter-system-crossing must be responsible for the weak phosphorescence observed. Alternatively, either the phosphorescence life-time could be very short (*ca* ≤ microsecond) to elude determination by a conventional phosphoroscope, or, $T_1 \rightarrow S_0$ deactivation could be caused due to the photoenolisation[15] in the excited state as follows,



Further support for our hypothesis could be obtained from the observations that excited quinizarin (1,4-dihydroxy-9,10-anthraquinone) was capable of abstracting hydrogen from different solvents[16] and that excited 1-hydroxy-9,10-anthraquinone undergoes fast radiationless decay in 3-methylpentane, but shows weak phosphorescence in diethyl ether-ethanol due to breaking of intra-molecular hydrogen bonds by the solvent[17]. We hope to resolve the exact nature of the transitions by our comprehensive laser flash photolysis studies with the hydroxyquinones[18].

Acknowledgement

The authors gratefully acknowledge the assistance of Dr. V. K. Kelkar in the computer calculations and thank Dr. R. M. Iyer, Head, Chemistry Division, for his interest in the work.

References

1. B. K. SINHA and C. F. CHIGNELL, *Chem. Biol. Interactions*, 1979, **28**, 301, and references therein.

Accession Number.
85821
Date 23.11.87

2. F. ARCAMONE in "Doxorubicin Anticancer Antibiotics", of Medicinal Chemistry Monographs, Academic Press, London, 1981, Vol. 17, and references therein.
3. J. R. BROWN in "Progress in Medicinal Chemistry", eds. G. P. ELLIS and G. B. WEST, North-Holland Publishing Co., Amsterdam, 1978, Vol. 15.
4. L. H. PIETTE, M. OKAMURA, G. P. RABOLD, R. T. OGATA, R. E. MOORE and P. J. SCHEUER, *J. Phys. Chem.*, 1967, 71, 29.
5. J. M. BRUCE in "Chemistry of Quinones and Quinonoid Compounds", ed. S. PATAI, J. Wiley, New York, 1972, Chapter 9.
6. I. SINGH, R. T. OGATA, R. E. MOORE, C. W. J. CHANG and P. J. SCHEUER, *Tetrahedron*, 1968, 24, 6053.
7. E. J. LAND, T. MUKHERJEE, A. J. SWALLOW and J. M. BRUCE, *J. Chem. Soc., Faraday Trans.*, 1, 1983, 79, 391.
8. J. G. VAN DAMME and R. E. DE NEVE, *J. Pharm. Sci.*, 1979, 68, 16.
9. R. PARISER and R. G. PARR, *J. Chem. Phys.*, 1953, 21, 466, 767.
10. J. A. POPLE, *Trans. Faraday Soc.*, 1953, 49, 1375.
11. C. A. PARKER in "Photoluminescence of Solutions", Elsevier, London, 1968, pp. 261-268.
12. H. E. FIERZ-DAVID and W. STOCKAR, *Helv. Chim. Acta*, 1943, 26, 92.
13. J. CASADO, J. PELETEIRO and M. A. RIOS, *Prog. Theo. Org. Chem.*, 1977, 2, 892.
14. T. MUKHERJEE, *Radiat. Phys. Chem.*, communicated.
15. J. N. PITTS, H. W. JOHNSON and T. KUWANA, *J. Phys. Chem.*, 1962, 66, 2456.
16. B. G. SOMERS, R. F. ZÜRCHER and H. LABHART, *Helv. Chim. Acta*, 1966, 49, 1980.
17. A. A. LAMOLA and L. J. SHARP, *J. Phys. Chem.*, 1966, 70, 2634.
18. D. K. PALIT, T. MUKHERJEE, L. J. MITTAL and J. P. MITTAL, unpublished.

J. Indian Chem. Soc.,
Vol. LXIII, January 1986, pp. 43-49

A Laser Flash Photolysis Study of Sydnone Triplets. Photophysical Behaviours and Singlet Oxygen Sensitisation†

K. BHATTACHARYYA[a], M. MUNEER[b], R. K. TIKARE[b], P. K. DAS*[a] and M. V. GEORGE*[a,b]

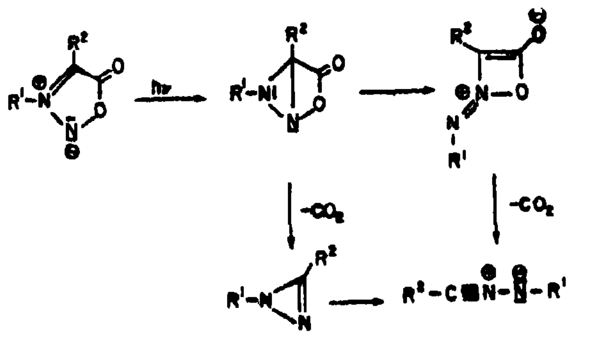
Chemistry Department and Radiation Laboratory, University of Notre Dame, Notre Dame, Indiana-46556

and

Department of Chemistry, Indian Institute of Technology, Kanpur-208 016

Under energy transfer sensitisation in fluid solutions, sydnones form triplets (λ_{max}^{T} = 380-400 nm) characterised by short lifetimes (0.2-2 μs). From kinetic studies using these compounds as triplet donors and acceptors, their triplet energies are estimated at 41-47 kcal mol^{-1}. Based on the lack of any residual absorbance change following the decay of triplets, it is claimed that they are not involved as precursors in the phototransformation of sydnones to nitrilimines. The oxygen quenching of sydnone triplets occurs predominantly by the energy transfer mechanism producing singlet oxygen in nearly quantitative yields.

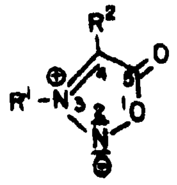
SUBJECT of many steady-state photochemical studies[1-7], sydnones (1,2,3-oxadiazol-5-ones) undergo facile photoelimination of carbon dioxide producing nitrilimines (Scheme 1). Only very



Scheme 1

limited information is available regarding the nature of the excited states participating in this photoreaction or the details of bond reorganisation leading to the overall transformation. The excited state properties of sydnones assume special significance because of their 'meso-ionic' nature[8] in the ground state. Although, for several related systems, the triplets of metastable zwitterionic species have been implicated[9] as distinct entities in the course of ring closures along triplet routes; to the best of our knowledge, no attempt has been made to characterise triplets directly photogenerated from stable dipolar substrates.

Employing time-resolved techniques, based on nanosecond laser flash photolysis and pulse radiolysis, we have investigated the spectral and kinetic behaviours of the triplets of a number of sydnones (Chart 1). It is shown that though short-lived,



(1) $R^1 = R^2 = C_6H_5$
(2) $R^1 = p\text{-}CH_3C_6H_4$; $R^2 = C_6H_5$
(3) $R^1 = CH_3$; $R^2 = C_6H_5$
(4) $R^1 = p\text{-}CH_3C_6H_4$; $R^2 = CH_3$
(5) $R^1 = C_6H_5$; $R^2 = H$
(6) $R^1 = p\text{-}CH_3C_6H_4$; $R^2 = H$

Chart 1

these triplets do not undergo CO_2 elimination to nitrilimines. In view of the reactivity[7] of sydnones with singlet oxygen ($^1O_2^*$, $^1\Delta_g$), the interaction of their triplets with ground-state oxygen ($^3O_2$, $^3\Sigma_g^-$) is of interest; in the latter case, one may expect direct 1,3-addition (spin-allowed) to compete favourably with energy transfer leading to $^1O_2^*$. In order to throw light on this aspect, we have measured the efficiency of $^1O_2^*$ production in the course of the quenching of sydnone triplets by $^3O_2$.

Experimental

The preparation of sydnones **1-6** (Chart 1) was carried out by literature methods referred to in earlier publications[5-8]. Benzene and acetonitrile,

† Dedicated to Professor Sadhan Basu on the occasion of his 65th birthday.
Document No. NDRL-2763 from the Notre Dame Radiation Laboratory.
[a]University of Notre Dame. [b]Indian Institute of Technology.

both from Aldrich, were of spectral grades. *N*-Methylthioacridone (NMTA) was prepared from *N*-methylacridone according to the procedure available in the literature[10,11]. Thiocoumarin was obtained as a gift (from Professor V. Ramamurthy). The other compounds and reagents used in this work were of best grades commercially available, and were purified by recrystallisation or by distillation under reduced pressure.

The ground-state absorption spectra were recorded in a Cary 219 spectrophotometer (1 nm band-pass). For laser flash photolysis, use was made of outputs from a Quanta-Ray Nd-YAG system coupled with a Quanta-Ray PDL-1 dye laser unit. The laser pulse excitation was carried out at 355 (third harmonic), 425 (stilbene 420 in methanol pumped at 355 nm) or 485 nm (coumarin 480 in methanol pumped at 355 nm); the intensities of the pulses (~6 ns) were kept in the range 4-10 mJ. The details of the kinetic spectrophotometer and the data collection system are given in previous publication[12,13]. The pulse radiolysis experiments were performed, employing 7 MeV electron pulses (5 ns) from Notre Dame ARCO-LP-7 linear accelerator; further details are available elsewhere[14]. Except for oxygen quenching, the solutions for both laser photolysis and pulse radiolysis were deoxygenated by bubbling high-purity argon through them (10-15 min).

Results

Quenching of sensitiser triplets by sydnones: Under direct laser excitation, none of the sydnones under study produces transients having properties characteristic of a triplet (see later). Thus, we took resort to the energy transfer sensitisation method for generating the triplets. For this purpose, it was necessary to know the approximate location of triplet energies (E_T) of these molecules. Since practically no phosphorescence is observed for the sydnones in glassy matrices at 77 K, their E_T's were estimated[15] in fluid solutions by measuring the rate constants (k_q^T) for the quenching of a series of sensitiser triplets with varying E_T's in the range 41-69 kcal mol^{-1}. Sydnones **1**, **3** and **5** were used as representative quenchers. k_q^T's were obtained from the linear plots based on the equation,

$$k_{obsd}^T = k_0^T + k_q^T \text{ [sydnone]}$$

where, k_{obsd}^T is the pseudo-first order rate constant for the decay of a sensitiser triplet and k_0^T is the rate constant for its decay in the absence of a quencher. Except for tris(bipyridine)ruthenium(II) complex, the sensitiser triplets were monitored by transient absorptions in benzene at or near the maxima at 460-700 nm; at these long wavelengths, absorptions due to the sydnone triplets (*i.e* products of energy transfer) were small (see later). The triplet decay kinetics in the case of the Ru^{II} complex in acetonitrile was followed in terms of its phosphorescence emission at 630 nm. In experiments where the sensitiser triplets were produced by direct laser excitation at 355 nm, the sydnone quenchers, particularly **1** at relatively high concentrations (1-2 m*M*), absorbed a significant fraction of laser photons; however, this was not a serious problem because the direct excitation of sydnones did not produce any transients having serious spectral or temporal overlap with the sensitiser triplet.

The data concerning k_q^T are presented in Table 1. In spite of some fluctuations in k_q^T's their trends with respect to sensitiser E_T's suggest fall-off regions at E_T=41-47 kcal mol^{-1}. In particular, k_q^T's for benz[*a*]anthracene (E_T=47 kcal mol^{-1}) and pyrene-1-aldehyde (E_T ~ 45 kcal mol^{-1}) indicate that while the triplet energy of sydnone **1** is lower than that of the aldehyde, that of **3** as well as **5** is slightly

TABLE 1—BIMOLECULAR RATE CONSTANTS FOR THE QUENCHING OF SENSITISER TRIPLETS BY SYDNONES IN BENZENE AT 296 K

Sensitiser	E_T[a] cal mol^{-1}	Laser excitation wavelength nm	Monitoring wavelength nm	k_q^T[b], 10^9 M^{-1} s^{-1}		
				1	3	5
Benzophenone	69	355	532	4.9	4.6	6.1
Phenanthrene[c]	62	355	490	4.8	5.2	6.4
Chrysene[c]	57	355	590	5.1	5.2	6.3
Fluorenone	53	425	645	2.9	5.1	3.7
Camphorquinone	52	485	700	2.6	5.2	2.8
Thiocoumarin	51	425	485	6.8	8.0	6.6
tris(Bipyridine) Ru^{II}[d]	48	485	630	2.4	0.8	1.2
Benz[*a*]anthracene[c]	47	355	490	4.0	3.2	4.4
Pyrene-1-aldehyde	~45	425	460	2.7	~0.6	≤0.1
N-Methylthioacridone[e]	45	485	520	3.6	1.1	4.1
9,10-Diphenylanthracene[f]	41	485	460	<0.1	<0.1	<0.1

[a] Ref. 22; S. L. Murov, "Handbook of Photochemistry", Marcel-Dekker, New York, 1973; H. Görner, *J. Phys. Chem.*, 1982, **86**, 2026; C. V. Kumar, S. K. Chattopadhyay and P. K. Das, *Photochem. Photobiol.*, 1983, 38, 141; S. K. Chattopadhyay, C. V. Kumar and P. K. Das, *Chem. Phys. Lett.*, 1983, **98**, 250; T. R. Evans and P. A. Leermakers, *J. Am. Chem. Soc.*, 1967, **89**, 4380. [b] ±15%. [c] Benzene containing 5% ethyl iodide was used for these aromatic hydrocarbons. [d] Phosphorescence was monitored for the complex in acetonitrile. [e] k_q^T's for NMTA triplet quenching by the other three sydnones are 3.8, 2.7 and 4.0×10^9 M^{-1} s^{-1} for 2, 4 and 6, respectively. [f] The triplet of 9,10-diphenylanthracene was produced *via* sensitisation by NMTA triplet (λ_{ex}=485 nm) in a solution saturated with the anthracene.

higher (*i.e.* at 45-47 kcal mol^{-1}). From the onsets of the lowest-energy absorption band-systems of sydnones in benzene (~ 400 nm for **1** and **2** and ~ 370 nm for **3**-**6**), their lowest singlet excited states, as seen in absorption, are estimated at 71 and 77 kcal mol^{-1} for **1**-**2** and **3**-**6**, respectively. Since the singlet-triplet energy separation[16] for a π,π^* state is typically of the order of 30 kcal mol^{-1}, E_T's of sydnones suggested by k_q^T's in Table 1 and by their ground-state absorption spectra are consistent with one another.

Triplet absorption spectra and decay kinetics : It is evident from the data in Table 1 that the triplets of camphorquinone (CQ ; $E_T = 52$ kcal mol^{-1}) and thiocoumarin ($E_T = 51$ kcal mol^{-1}) possess sufficiently high energies for exothermic excitation transfer to the sydnones. More importantly, these two sensitisers can be excited at laser wavelengths in the visible (specifically, 485 and 425 nm, respectively) where the sydnones do not absorb, thus permitting the use of high concentrations (20-50 m*M*) of the latter. Upon laser flash photolysis of CQ or thiocoumarin in the presence of sydnones, short-lived transients are observed. As shown in Figs. 1 and 2, these transients absorb primarily in the spectral region 380-450 nm and decay by clean first order kinetics. Similar transient absorption phenomena are also observed in the course of the pulse

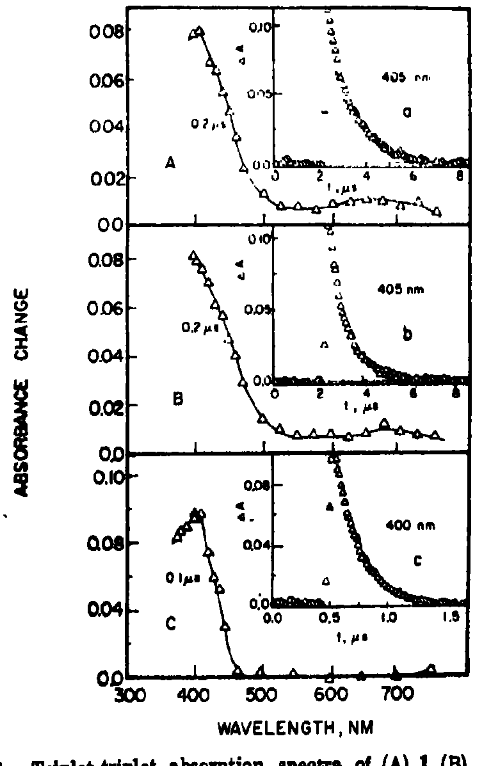


Fig. 1. Triplet-triplet absorption spectra of (A) **1**, (B) **2** and (C) **3** in benzene. The triplets were produced by sensitization by $^3CQ^*$ ($\lambda_{ex} = 485$ nm) in the presence of 20-30 m*M* sydnones. The insets show typical kinetic traces for triplet decay at or near the absorption maxima : (a) **1**, (b) **2** and (c) **3**.

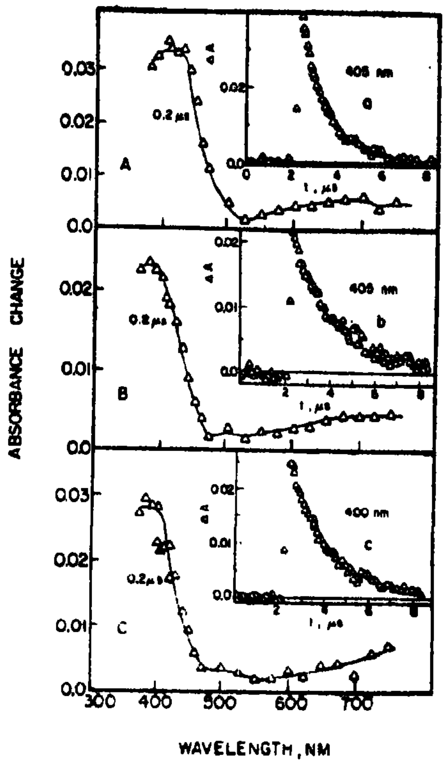


Fig. 2. Triplet-triplet absorption spectra of (A) **4**, (B) **5** and (C) **6** in benzene. These were observed under sensitization by $^3CQ^*$ ($\lambda_{ex} = 485$ nm) in the presence of 20-30 m*M* sydnones. Representative kinetic traces for triplet decay are shown in the insets : (a) **4**, (b) **5** and (c) **6**.

radiolysis[17] of 0.1 *M* biphenyl in the presence of 5-10 m*M* sydnones in benzene. In these experiments, biphenyl triplets ($E_T = 66$ kcal mol^{-1}), initially produced by energy transfer from pulse radiolytic solvent triplets, sensitise the formation of sydnone triplets (see equations 1-3, Bz ≡ benzene, Bp ≡ biphenyl and S ≡ sydnone). A few representative transient spectra are shown in Fig. 3.

$$Bz \xrightarrow{e^-} {}^1Bz^*, {}^3Bz^*, \text{ions} \quad (1)$$

$$^3Bz^* + Bp \rightarrow {}^3Bp^* + Bz \quad (2)$$

$$^3Bp^* + S \rightarrow {}^3S^* + Bp \quad (3)$$

The assignment of the observed transients as sydnone triplets is based on the following facts. First, they are formed under conditions in which triplet energy transfer to sydnones is feasible. Second, they are quenched by typical triplet quenchers, namely, oxygen, di-*tert*-butylnitroxy radical and ferrocene (see later). Third, when they are generated in the presence of ~ 0.5 m*M* all-*trans*-1,6-diphenyl-1,3,5-hexatriene ($E_T = 34$ kcal mol^{-1}), relatively slow formation of the triplet of the latter with characteristic, intense absorption spectrum at 400-450 nm ($\lambda_{max}^T = 426$ nm in benzene) is noted ;

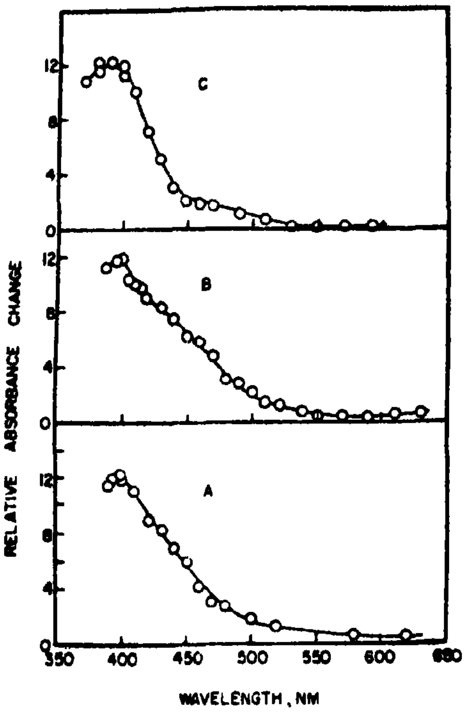


Fig. 3. Transient absorption spectra of the triplets of (A) **1**, (B) **2** and (C) **5** produced *via* sensitisation by pulse-radiolytic biphenyl triplet in benzene.

this establishes the triplet sensitising capability of the observed transients from sydnones.

Assuming that the quenching of $^3CQ^*$ by sydnones occurs entirely by energy transfer, we have determined their triplet-triplet extinction coefficients using the comparative technique. In this, the end-of-pulse absorbance change (ΔA_{CQ}^T) due to $^3CQ^*$ at 700 nm in the absence of a quencher is compared with that (ΔA_S^T) due to $^3S^*$ at 380-410 nm produced in the presence of high [S] so that the decay of $^3CQ^*$ occurs essentially by energy transfer to S (that is $k_q^T [S] \gg k_0^T$, see equations 4 and 5). Equation (6) was used to calculate sydnone triplet extinction coefficients (ϵ_S^T). For ϵ_{CQ}^T at 700 nm, a

$$^3CQ^* \xrightarrow{k_0^T} {}^1CQ \tag{4}$$

$$^3CQ^* + {}^1S \xrightarrow{k_q^T} {}^3S^* + {}^1CQ \tag{5}$$

$$\epsilon_S^T = \epsilon_{CQ}^T \cdot \frac{\Delta A_S^T}{\Delta A_{CQ}^T} \tag{6}$$

value of 900 M^{-1} cm^{-1} was used (as determined by the comparative method in which anthracene, $\epsilon^T = 4.5 \times 10^4$ M^{-1} cm^{-1} at 428 nm in benzene, was used as the acceptor). The triplet spectral data (λ_{max}^T and ϵ_{max}^T) and lifetimes (τ_T) for sydnones are summarised in Table 2.

It is noted (Table 1) that the sydnones quench *N*-methylthioacridone (NMTA) triplet ($E_T = 43$ kcal mol^{-1}) with rate constants significantly higher than those expected from the trends for the other sensitisers. For example, energy transfer from $^3NMTA^*$ to sydnone **5** would be endothermic although k_q^T in this case is close to the limit of diffusion control. In order to throw some light on the quenching mechanism, the efficiency (ϕ_{ET}) of energy transfer was obtained based on equation (7),

$$\phi_{ET} = \frac{\Delta A_S^T}{\Delta A_{NMTA}^T} \cdot \frac{\epsilon_{NMTA}^T}{\epsilon_S^T} \tag{7}$$

where, ΔA^T's are end-of-pulse triplet absorbance changes due to $^3NMTA^*$ at 520 nm (measured by 485 nm laser excitation of NMTA in the absence of a sydnone) and due to $^3S^*$ at 380-410 nm (measured by excitation of NMTA in the presence of ~50 mM sydnone) and ϵ^T's are the corresponding T – T extinction coefficients. The value[11] of 9.3×10^3 M^{-1} cm^{-1} was used for ϵ_{NMTA}^T. The ϕ_{ET} data given in Table 2 suggest interaction(s) other than energy transfer to be operative in the case of **3**-**6**. It should also be noted that the absorbance changes in the region (400-490 nm) of NMTA ground-state absorption following the decay of transients ($^3S^*$) show practically no permanent loss of the thioketone.

Quenching of sydnone triplets: The bimolecular rate constants (k_qT) for the quenching of sydnone triplets by oxygen, di-*tert*-butylnitroxy (DTBN, stable free radical) and ferrocene were obtained by measuring the observed rate constant (k_{obsd}^T) for

TABLE 2—SPECTRAL AND KINETIC PROPERTIES OF SYDNONE TRIPLETS IN BENZENE AT 296 K

Sydnone	λ_{max}^T [a]	ϵ_{max}^T [b]	τ_T [c]	ϕ_{ET} [d,e]	k_q^T, $10^9 M^{-1}s^{-1}$ [e]			ϕ_Δ^T [e]
					O_2	DTBN	Ferrocene	
1	≤400	6.8	1.2	1.0	2.0	0.061	1.6	0.78
2	≤400	6.4	1.0	1.0	1.9	0.039	1.6	0.88
3	400	7.8	0.22	0.57	1.8	0.052	2.3	
4	400	2.0	1.3	0.16	1.7	0.078	5.1	
5	380	1.4	2.0	0.19	1.9	0.16	6.7	0.80
6	380	1.7	2.3	0.33	1.8	0.12	5.7	0.38

[a] ±5 nm. [b] ±20%. [c] ±15%. [d] ϕ_{ET} denotes the efficiency of energy transfer in the quenching of NMTA triplet by sydnones (see text). [e] ±20%

the enhanced decay of their transient absorption (380-410 nm) as a function of quencher concentration. A few plots based on $k_{obsd}^T = \tau^{T-1} + k_q^T[Q]$ with ferrocene as the quencher are presented in Fig. 4. The k_q^T data are given in Table 2. Attempts to quench the triplets of **2**, **3** and **5** by dimethyl acetylenedicarboxylate (dipolarophile) and 2,5-dimethyl-2,4-hexadiene proved unrewarding (k_q^T's $\leq 1.5\times10^9$ M^{-1} s^{-1}). Also, azulene was found to be a poor quencher for the triplets of **1** and **2** ($k_q^T < 10^9$ M^{-1} s^{-1}).

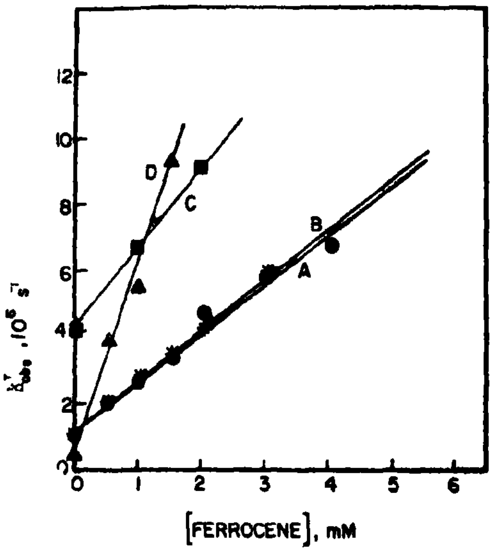


Fig. 4. Plots for the quenching of sydnone triplets by ferrocene : (A) **1**, (B) **2**, (C) **3** and (D) **6**.

Efficiency of singlet oxygen sensitisation by sydnone triplets : With **1**, **2**, **5** and **6**, the fractions (ϕ_Δ^T) of sydnone triplets (quenched by $^3O_2$) that lead to $^1O_2^*$ formation were measured. Two methods based on CQ and NMTA as the triplet sensitisers respectively were used under 485 nm laser excitation. For both, diphenylisobenzofuran (DPBF) was employed as $^1O_2^*$ monitor. The various steps leading to $^1O_2^*$ formation are as follows (Sens $\equiv$ sensitiser, *i.e.* CQ or NMTA, and D $\equiv$ DPBF).

$$^3Sens^* \rightarrow {}^1Sens \qquad (8)$$

$$^3Sens^* + {}^3O_2 \rightarrow {}^1Sens + {}^1O_2^* \qquad (9a)$$

$$\rightarrow {}^1Sens + {}^3O_2 \qquad (9b)$$

$$^3Sens^* + {}^1S \rightarrow {}^1Sens + {}^3S^* \qquad (10)$$

$$^3S^* \rightarrow {}^1S \qquad (11)$$

$$^3S^* + {}^3O_2 \rightarrow {}^1S + {}^1O_2^* \qquad (12a)$$

$$\rightarrow {}^1S + {}^3O_2 \qquad (12b)$$

$$\rightarrow \text{other reactions} \qquad (12c)$$

$$^1O_2^* \rightarrow {}^3O_2 \qquad (13)$$

$$^1O_2^* + D \rightarrow DO_2 \qquad (14)$$

The method based on NMTA as the sensitiser was applied to **1** and **2**, since ϕ_{ET} in these cases were unity (Table 2). Solutions of NMTA in aerated benzene (absorbance = 0.1 at 485 nm in 2 mm cell) containing 0.05 mM DPBF and varying concentrations of sydnones (0.0-5.0 mM) were flash photolysed at 485 nm and the negative absorbance changes (ΔA^D) due to DPBF ground-state depletion (equation 14) measured at 420 nm. From the dependence of ΔA^D on [S], it was possible to calculate ϕ_Δ^T for $^3S^*$ with respect to that for $^3NMTA^*$. The details of the method are given elsewhere[19]. The method based on CQ as the sensitiser was applied to **4** and **5** and required using high concentrations of sydnones so that $^3CQ^*$ was quenched entirely by energy transfer to them (may be noted that $^3CQ^*$ is quite long-lived even in aerated benzene, $\tau_T = 2.2$ μs). It was important that **4** and **5** in the ground-state were poor reactants[19] for $^1O_2^*$. Comparison of absorbance change (ΔA_{CQ}^T) due to $^3CQ^*$ at 700 nm in the absence of DPBF and sydnone with that due to DPBF bleaching at 420 nm observed in the presence of 0.05 mM DPBF and 10-30 mM sydnone led to the measurement of ϕ_Δ^T. Use was made of equation (15),

$$\phi_\Delta^T = \frac{\Delta A^D}{\Delta A_{CQ}^T} \cdot \frac{\epsilon_{CQ}^T}{\epsilon^D} \cdot \frac{k_{11} + k_{12}[^3O_2]}{k_{12}[^3O_2]} \cdot \frac{k_{13} + k_{14}[D]}{k_{14}[D]} \qquad (15)$$

where, the rate constants k_{11}, k_{13} and k_{14} refer to equations (11), (13) and (14), respectively and k_{12} represents the overall rate constant for sydnone triplet quenching by oxygen (equations 12a-c). k_{11} and k_{12} are the rate parameters measured in the present study (Table 2) and the values for k_{13} and k_{14} are available in the literature[20]. ϕ_Δ^T data (Table 2) obtained by the two methods suggest that the sydnone triplet quenching by oxygen is dominated by energy transfer (equation 12a).

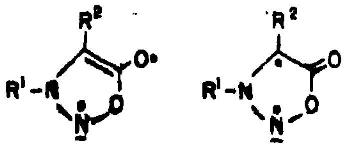
Discussion

Direct laser flash photolysis of sydnones **1** and **2** in benzene or methanol and **4-6** in methanol, produces long-lived transients ($\lambda_{max} = 360$-380 nm and τ's > 100 μs), characterised by oxygen-insensitive decay kinetics. These are best assigned as nitrilimines, spectral and kinetic behaviors of which will be described elsewhere. The decay of the sydnone triplets observed in the present study does not lead to any significant residual absorption attributable to nitrilimines. Thus, the phototransformation of sydnones to nitrilimines (Scheme 1) appears to be a reaction originating from the singlet state. Also, under 485 nm laser excitation of CQ in the presence of 0.5-1 mM sydnones, practically no depletion in the region of their ground-state absorption (320-340 nm) results from the triplet decay ; this suggests that photochemistry in the lowest triplet state of sydnones is negligible. Our findings differ sharply with the conclusions reached by Huseya *et al.*[4] for 3-cyclohexyl-4-phenylsydnone. Based on the marked quenching effect of 1,3-pentadiene on the photochemical reaction of 3-cyclohexyl-4-phenylsydnone,

the triplet state has been implicated as photoreactive for this system.

The k_q^T data (Table 2) with ferrocene ($E_T \sim 39$ kcal mol^{-1}) as the quencher give semiquantitative estimates for the energies of relaxed triplets of the sydnones at $\geqslant 40$ kcal mol^{-1}. For 4-6, k_q^T's are in the limit of diffusion-control and hence the relaxed triplet energies for these systems should be higher than E_T of ferrocene by at least 2-3 kcal mol^{-1}. A comparison of these estimates with E_T's arrived at from k_q^T's for the quenching of sensitiser triplets by sydnones (Table 1) points out that there is no substantial structural relaxation in the lowest triplet state of sydnones following their photoexcitation. This is not surprising in view of the geometric constraint and rigidity imposed by the five-membered ring.

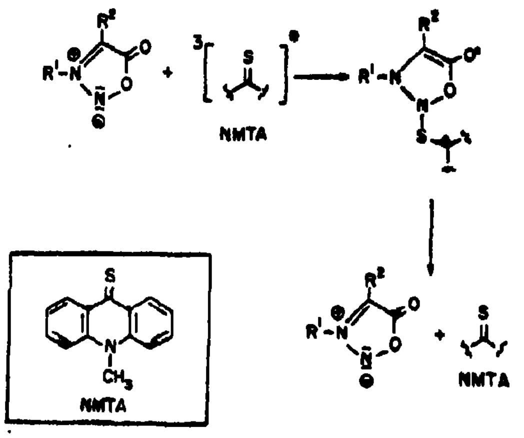
It seems plausible that the decay of sydnone triplets represents nearly vertical inter-system crossing from a biradicaloid triplet configuration 7 to the ground-state zwitterionic configuration. It is of interest to examine how the substituents at 3- and 4-positions affect the inter-system crossing rates. The lifetime (τ_T) data in Table 2 reveal the



(7) (8)

following trend : 5, 6 > 1, 2, 4 > 3. Thus, while the substitution of an aryl or an alkyl group at the 4-position results in the shortening of τ_T, the aryl substitution at the 3-position makes τ_T longer. It seems that an aryl or an alkyl group at the 4-position stabilises a radical center at this position (biradicaloid structure 8) and hence decreases the average distance between the two unpaired electrons. The latter in turn favours spin-orbit coupling[21] for inter-system crossing. On the other hand, an aryl group at the 3-position makes the lone pair of electrons on the nitrogen atom less available for mediating inter-system crossing. Hence, τ_T increases on going from 3 to 1 or 2.

The efficiency of energy transfer (ϕ_{ET}) in the course of the quenching of NMTA triplet ($E_T = 43$ kcal mol^{-1})[22] by a sydnone is determined by the relative location of the triplet energy of the latter with respect to NMTA; that is, by the exothermicity of the energy transfer process. Specifically, with 4-6 as quenchers, the energy transfer is decisively endothermic and, although the k_q^T's are high, a major portion of the quenching takes place by a non-energy-transfer mechanism. Since no loss of NMTA occurs as a result of the interaction, a permanent dipolarophilic 1,3-addition of the thioketone triplet to sydnones is ruled out. In analogy to the mechanism of quenching of thioketone triplets by olefins, the formation of an unstable diradical that reverts to ground states, may be invoked in the course of the interaction of ^{3}NMTA* and sydnones. This is shown in Scheme 2.



Scheme 2

The rate constants for the quenching of sydnone triplets by oxygen are all close to $1/9\ k_{diff}$, where k_{diff} is the rate constant for a fully diffusion-controlled process. This conforms to mechanism(s) of oxygen quenching in which the singlet configuration of the encounter complex between oxygen

$$^3S^* + {}^3O_2 \xrightleftharpoons{1/9\ k_{diff}} {}^1(S..O_2) \rightarrow {}^1S + {}^1O_2^* \quad (16a)$$

or other singlet products

$$\xrightleftharpoons{1/3\ k_{diff}} {}^3(S..O_2) \rightarrow {}^1S + {}^3O_2 \quad (16b)$$

$$\xrightleftharpoons{5/9\ k_{diff}} {}^5(S..O_2) \quad (16c)$$

and the triplet substrate plays the major role (equation 16a). The nearly quantitative efficiencies of $^1O_2^*$ photosensitisation (Table 2) point out to the dominance of energy transfer. Permanent 1,3-addition of $^3O_2$ to $^3S^*$, though spin-allowed, appears to be a negligible process (quantum efficiency<20%) compared to the energy transfer. This is supported by the fact that within our experimental errors, we do not observe any significant depletion of sydnone ground state absorption following the oxygen quenching of their triplets (sensitised by ^{3}CO* or ^{3}NMTA* in air-saturated benzene).

Acknowledgement

The work described herein was supported by the Office of Basic Energy Sciences, Department of Energy (U. S.) and the Department of Science and Technology, Government of India.

References

1. O. H. KRAUCH, J. KUHLS and H. PIEK, *J. Tetrahedron Lett.*, 1966, 4043.
2. M. MÄRKY, H. MEIER, A. WUNDERLI, H. HEIMGARTNER, H. SCHMID and H.-J. HANSEN, *Helv. Chim. Acta*, 1978, 61, 1477 ; M. MÄRKY, H.-J. HANSEN and H. SCHMID, *Helv. Chim. Acta*, 1971, 54, 1275.

3. H. GOTTHARDT and F. REITER, *Tetrahedron Lett.*, 1971, 2749 ; H. GOTTHARDT and F. REITER, *Tetrahedron Lett.*, 1976, 2331 ; H. GOTTHARDT and F. REITER, *Chem. Ber.*, 1979, **112**, 1206.
4. Y. HUSEYA, A. CHINONE and M. OHTA, *Bull. Chem. Soc. Jpn.*, 1972, **45**, 3202.
5. Y. HUSEYA, A. CHINONE and M. OHTA, *Bull. Chem. Soc. Jpn.*, 1971, **44**, 1667.
6. C. S. ANGADIYAVAR and M. V. GEORGE, *J. Org. Chem.*, 1971, **36**, 1589.
7. V. BHAT, V. M. DIXIT, B. G. UGARKAR, A. M. TROZZOLO and M. V. GEORGE, *J. Org. Chem.*, 1979, **44**, 2957.
8. W. D. OLLIS and C. A. RAMSDEN in "Advances in Heterocyclic Chemistry", eds. A. R. KATRITZKY and A. J. BOULTON, Academic Press, New York, 1976, Vol. 19, pp. 1-22 ; M. OHTA and H. KATO in "Nonbenzenoid Aromatics", ed. J. P. SNYDER, Academic Press, New York, 1969, pp. 117-248 ; F. H. C. STEWART, *Chem. Rev.*, 1964, **64**, 129.
9. E. W. FORSTER and K. H. GRELLMAN, *Chem. Phys. Lett.*, 1972, **14**, 536 ; K. H. GRELLMAN and V. SCHMITT, *J. Am. Chem. Soc.*, 1982, **104**, 6267 ; H. WELLER and K. H. GRELLMAN, *J. Am. Chem. Soc.*, 1983, **105**, 6268 ; E. ZADOR, J. M. WARMAN, L. H. LUTHJENS and A. HUMMEL, *J. Chem. Soc., Faraday Trans. 1*, 1974, 227 ; A. A. LEONE and P. S. MARIANO, *Rev. Chem. Intermediates*, 1981, **4**, 81.
10. F. ARNDT and L. LORENZ, *Chem. Ber.*, 1930, **63**, 3121.
11. C. V. KUMAR, H. F. DAVIS and P. K. DAS, *Chem. Phys. Lett.*, 1984, **109**, 184.
12. V. NAGARAJAN and R. W. FESSENDEN, *J. Phys. Chem.*, 1985, **89**, 2330.
13. P. K. DAS, M. V. ENCINAS, R. D. SMALL, JR. and J. C. SCAIANO, *J. Am. Chem. Soc.*, 1979, **101**, 6965, and references therein.
14. L. K. PATTERSON and J. LILIE, *Int. J. Radiat. Phys. Chem.*, 1974, **6**, 129 ; R. H. SCHULER and G. K. BUZZARD, *J. Am. Chem. Soc.*, 1976, **98**, 563.
15. K. SANDROS, *Acta Chim. Scand.*, 1964, **18**, 2355 ; W. G. HERKSTROETER and G. S. HAMMOND, *J. Am. Chem. Soc.*, 1966, **88**, 4769 ; W. G. HERKSTROETER, *J. Am. Chem. Soc.*, 1975, **97**, 4161.
16. S. P. MCGLYNN, T. AZUMI and M. KINOSHITA "Molecular Spectroscopy of the Triplet State", Prentice-Hall, Englewood Cliffs, 1969.
17. E. J. LAND, *Proc. R. Soc. London, Ser. A* 1968, **305**, 457 ; R. BENSASSON and E. J. LAND, *Trans. Faraday Soc.*, 1971, **67**, 1904.
18. K. BHATTACHARYYA and P. K. DAS, *Chem. Phys. Lett.*, 1985, **116**, 326.
19. K. BHATTACHARYYA, P. K. DAS and M. V. GEORGE, in preparation.
20. S. K. CHATTOPADHYAY, C. V. KUMAR and P. K. DAS, *J. Photochem.*, 1984, **24**, 1.
21. L. SALEM and C. ROWLAND, *Angew. Chim. Int. Ed. Engl.*, 1972, **11**, 92.
22. A. SAFARZADEH-AMIRI, R. E. VERRALL and R. P. STEER, *Can. J. Chem.*, 1983, **61**, 894.
23. V. RAMAMURTHY, *Org. Photochem.*, 1985, **7**, 231.

J. Indian Chem. Soc.,
Vol. LXIII, January 1986, pp. 50-55

Anthracene Sulphonates as Fluorescence Probes for Triton X-100 Micelles†

SUBHASH C. BHATTACHARYA and K. K. ROHATGI-MUKHERJEE

Physical Chemistry Laboratory, Jadavpur University, Calcutta-700 032

The emission properties of 1-anthracene sulphonate, 2-anthracene sulphonate, 1,5-anthracene disulphonate and 1,8-anthracene disulphonate have been studied in Triton X-100 micellar medium. The changes in the emission characteristics as a function of surfactant concentration have been used for locating the site of residence of the fluorescent probes in the micelles.

MICELLES, vesicles and liposomes are often used as membrane biomimetic agents[1-3]. The importance of membrane in biological systems lies in their capacity to provide a matrix for arranging the reaction sequentially for efficient interaction, that is, they help compartmentalisation of the reactants dynamically. Compartmentalisation concentrates and localises reactants for efficient interaction. The most commonly cited example is natural photosynthesis. The components of photosynthetic apparatus are dynamically arranged in the thylakoid membrane for light harvesting, charge separation, vectorial electron transfer, water oxidation and carbon dioxide fixation[3]. Micelles serve as suitable media for demonstrating the advantage of compartmentalisation on electron transfer[4-6] and energy transfer interactions[7-9].

Micelles may be considered as miniaturised cages of volume v which may be charged or neutral. The surface charges reflect the polarity of the head group. The micelles are uniformly distributed in the bulk phase and form a 'pseudophase'. These micellar assemblies are in dynamic equilibrium with the surfactant monomers. There are two time constants, (i) movement of single molecule of detergent in the micelle, mobile monomer-micelles equilibrium ($\tau \simeq \mu s$) and (ii) cooperative formation and dissolution of micelles as a whole ($\tau \simeq$ ms). The topological features of the interior of the micelles is determined by the nature of the surfactant. The substrate molecules may be sequestered and organised in the micellar interior or on the micellar boundary. The fluorescence probes have been used to provide information on the structure and dynamics of many systems[10,11]. The effective lifetime of fluorescence varies from 10^{-6} to 10^{-12} s and that of phosphorescence from 10^{1} to 10^{-6} s and hence, these luminescent probes allow scanning of dynamic properties within the time scale of tens of a second to picosecond. Much fundamental insight has been gained from fluorescence quenching experiments.

For quite sometimes past we have been interested in variously substituted anthracene sulphonates and subtle changes in their photophysical and photochemical properties dependent on the position of attachment of SO_3^- group. The introduction of SO_3^- group not only makes these compounds water soluble but also brings about changes in their excited state properties[12,13], such as emission characteristics, fluorescence lifetimes, excited state dipole moments and redox potentials[13]. The sulphonate groups affect the overall symmetry property of the anthracene moeity and also introduce negatively charged centres in the molecule. Thus these molecules develop regions of varied physical characteristics. The properties of four molecules, two monosulphonates, 1-anthracene sulphonates (1-AS) and 2-anthracene sulphonate (2-AS), and two disulphonates 1,5-anthracene disulphonate (1,5-AS) and 1,8-anthracene disulphonates (1,8-AS), have been well studied and were selected for further studies in miceller system.

The emission spectra of monosulphonates are sensitive to solvent. Specially 1-AS gives a completely structureless emission spectrum in aqueous solution which develops vibrational features on addition of ACN, EtOH, EG, THF *etc.* It appears that the interaction is very specific with H_2O. Evidences are that an exciplex with one or two water molecules is formed in the excited state. Fluorescence spectral studies in CTAB micelles[14] have established that 1-AS can be used as a probe for water pools in membranes and micelles. On the other hand, 1,5-AS exhibits regular vibrational features as obtained for anthracene in organic solvents. With two units of negative charge, on bulky SO_3^- groups they are expected to lie on the micellar surface. This property has been exploited and 1,5-AS has been used for studying ion flux across the membranes using fluorescence quenching technique[15]. These sulphonates do not interact with positively charged micelles of SDS.

† Dedicated to Professor Sadhan Basu on the occasion of his 65th birthday.

A Part of the article was presented at the National Conference on Spectroscopy and Theoretical Chemistry held at Calcutta, December 5-7, 1985.

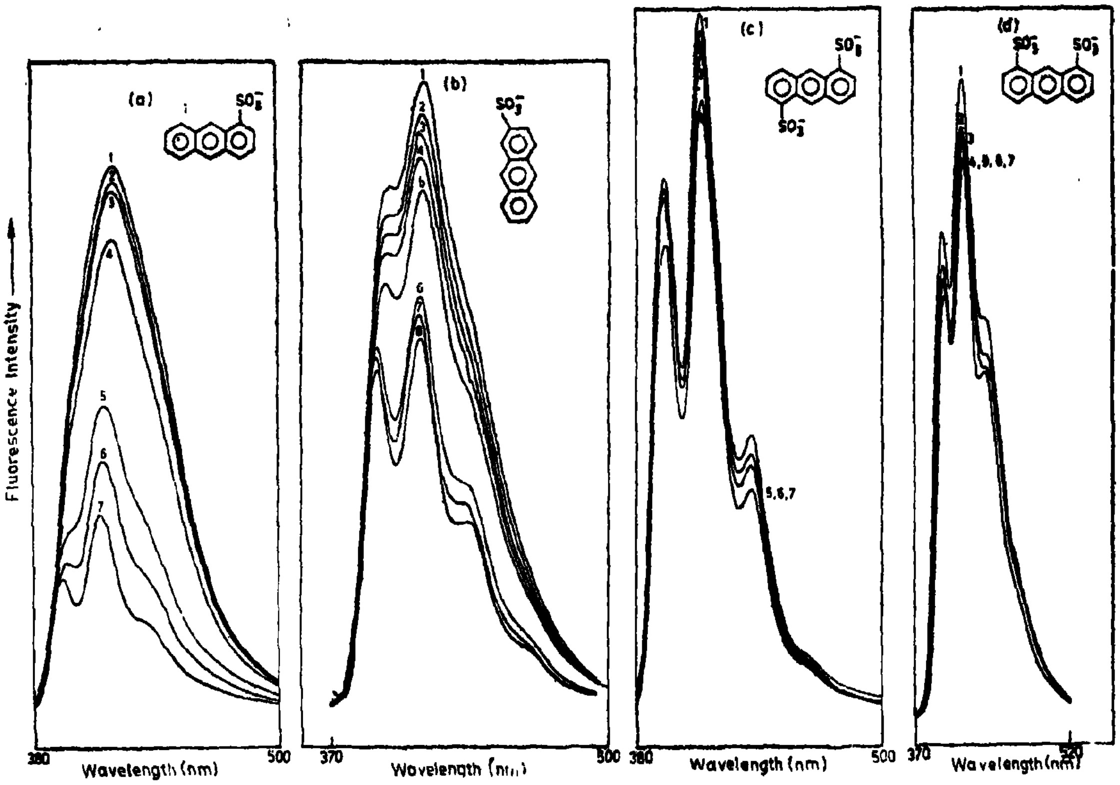


Fig. 1. Fluorescence spectra of anthracene sulphonates as a function of Triton X-100 concentrations : (a) anthracene 1-sulphonate, (b) anthracene 2-sulphonate, (c) anthracene 1,5-disulphonate and (d) anthracene 1,8-disulphonate ; concentration of Triton X-100 : (1) 0.0, (2) 5.0×10^{-5}, (3) 1.0×10^{-4}, (4) 5.0×10^{-4}, (5) 1.0×10^{-3}, (6) 5.0×10^{-3} and (7) 1.0×10^{-2} *M*.

For a better understanding of interaction between surfactants and the fluorophor a study of these anthracene sulphonates with the surfactant TX-100 has been taken up. The neutral surfactant Triton X-100 (octylphenoxypolyethoxyethanol) has no charged interface and can provide at least three distinct regions[16] : relatively polar polyether interface region, inner core hydrocarbon region and the potentially π-bonding aromatic region in the centre. The changes in the emission characteristics as a function of surfactant concentration have been used for locating the site of residence of the fluorescent probes in TX-100 micelles.

Experimental

Anthracene 1,2-monosulphonates and 1,5-, 1,8-disulphonates abbreviated as 1-AS, 2-AS, 1,5-AS and 1,8-AS, where prepared by reducing corresponding anthraquinones with Zn-dust and 20% NH_4OH for 4-6 h. The products were treated with active animal charcoal to remove traces of anthraquinones and other impurities, crystallised three to four times from water and obtained as the sodium salt. Triton X-100 (B.D.H.) was used as such.

Fluorescence spectra were recorded with a Perkin-Elmer MPF 44B spectrofluorimeter. The fluorescence spectra were measured for dilute solutions (10^{-5} to 10^{-6} *M*) of anthracene sulphonates with gradual addition of TX-100. Concentration of surfactant was varied from 10^{-5} to 10^{-2} *M*. All the solutions were deoxygenated prior to mixing.

Results and Discussion

The changes observed in the fluorescence spectra of these probe molecules as a function of Triton X-100 (TX-100) concentration are presented in Fig. 1. The spectra of disulphonates have sharp vibrational features which show slight changes on micellisation but monosulphonates, specially 1-AS show considerable variation in vibrational features as well as in fluorescence intensity. In Fig. 2 are plotted variation in fluorescence intensity as a function of TX-100 concentration expressed in terms of molar concentration of micelles. The literature values[16] of C.M.C. and aggregation number for TX-100 are 2.5×10^{-4} *M* and 140, respectively and were used to calculate the micelle concentration from the expression,

$$[M_n] = \frac{[TX\text{-}100] - C.M.C.}{140}$$

where, [TX-100] is the analytical concentration of the surfactant. Using fluorescence intensity as a

marker to probe molecules in the aqueous phase (F_w) and the micellar phase (F_m), a change in intensity is observed at C.M.C. (Fig. 2) which is sharp for 1-AS, but not so sharp for 2-AS and 1,5-AS. From these spectral data, it is possible to calculate the binding constant K for substrate-micelle interaction.

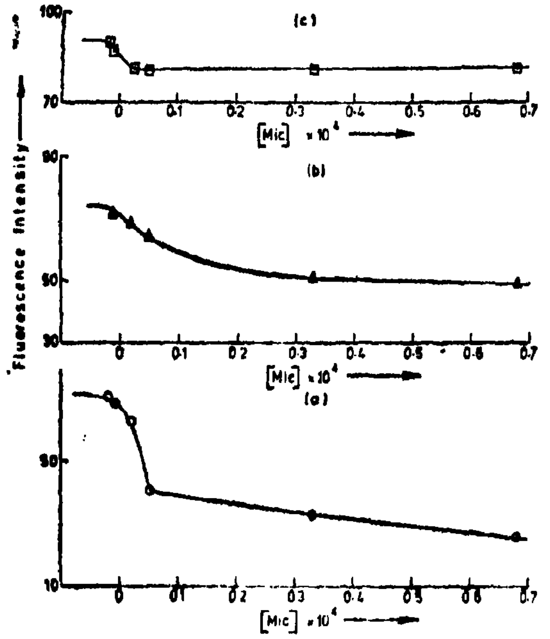


Fig. 2. Plot of fluorescence intensity (*F*) of (a) anthracene 1-sulphonate, (b) anthracene 2-sulphonate and (c) anthracene 1,5-disulphonate *vs* micellar concentration.

Determination of binding constant K: Since the fluorescence lifetimes of the substrate molecules are in the nanosecond range, the micelles may be considered as individual compartments and one can build up multiple equilibria model[11,12] for micellisation of solute. For a given concentration of the solute and the micelles, the solute will be distributed between the aqueous phase (w) and the micellar phase (m) in accordance with the mass law expression,

$$S_w + M_n \underset{k_b}{\overset{k_a}{\rightleftharpoons}} S_m \qquad (1)$$

where, k_a is the rate constant for the entry of the solute molecule within the micelle and k_b its exit rate constant, and $K = k_a/k_b$.

The binding constant K for solute-micelle interaction is similar to Michaelis constant for enzyme catalysed reaction and is given as

$$K = \frac{[S]_m}{[S]_w[M_n]} \quad \text{and} \quad K[M_n] = \frac{[S]_m}{[S]_w} \qquad (2)$$

where, $[S]_m$ and $[S]_w$ represent the concentration of the solutes in the micellar phase and the aqueous phase, respectively and $[M_n]$ is the concentration of micelles with aggregation number n. For a given $[M_n]$, $K[M_n]$ assumes the role of partition coefficient for the solute in the two phases. Assuming that the observed fluorescence F, of the solution is the sum of the fractional fluorescence of aqueous and micellar phase

$$F = \alpha F_m + (1-\alpha) F_w \qquad (3)$$

where, $\alpha = [S]_m/[S]_T$, fraction of solute in the micellar phase, $[S]_T$ being the total concentration of the solute,

$$[S]_T = [S]_m + [S]_w \qquad (4)$$

One can solve for α in equation (3) and express in terms of respective concentrations,

$$\alpha = \frac{F - F_w}{F_m - F_w} = \frac{[S]_m}{[S]_T} = \frac{K[S]_w[M_n]}{[S]_T}$$

The expression can be simplified,

$$\frac{F - F_w}{F_m - F_w} = \frac{K[S]_w[M_n]}{[S]_w + [S]_m} = \frac{K[M_n]}{1 + K[M_n]} \qquad (5)$$

and can be rearranged to give

$$\frac{1}{F - F_w} = \frac{1}{F_m - F_w}\left(1 + \frac{1}{K[M_n]}\right) \qquad (6)$$

By plotting $(F - F_w)^{-1}$ *vs* $[M_n]^{-1}$, the binding constant K can be evaluated from the ratio of intercept/slope. Very good linear plots were obtained (Fig. 3) for the three anthracene sulphonates when their

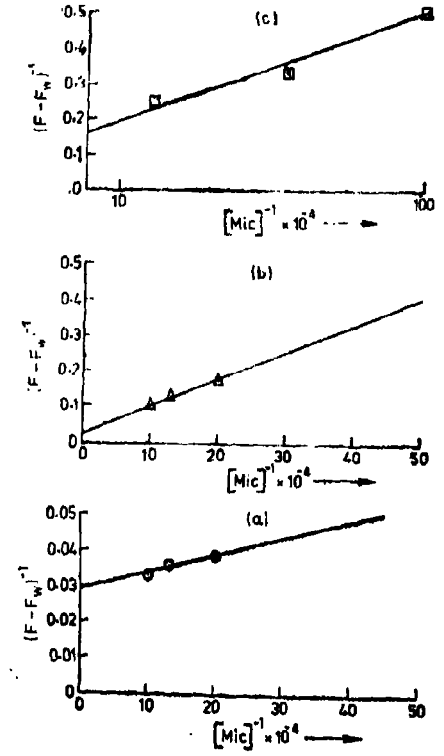


Fig. 3. Plot of $(F - F_w)^{-1}$ *vs* micellar concentration of (a) anthracene 1-sulphonate, (b) anthracene 2-sulphonate and (c) anthracene 1,5-disulphonate.

fluorescence was analysed in this way. The binding constants K for the three solutes, 1-AS, 2-AS and 1,5-AS are 6.7×10^{5}, 3.2×10^{4} and 4.7×10^{3} M^{-1}, respectively. Evidently the probes are bound fairly strongly in the order 1-AS > 2-AS > 1,5-AS, which is in the inverse order of their solubilities in water.

Distribution of solute molecules in micelles : It is now well established that statistical distribution of solute molecules in the micellar cages follows Poisson statistics[19,20]. The probability $P_{(n)}$ that *n* solute molecules will reside in a given micellar cage is given by

$$P_{(n)}=\frac{\langle s\rangle^{n}}{n!}e^{-\langle s\rangle} \qquad (7)$$

where, $\langle s\rangle$ is the average number of solubilised molecules per micelle and *n* is the occupancy number. For a concentration $[1\text{-AS}]=5.32\times10^{-6}M$ and $[M_n]$ ranging between 0.52×10^{-5} to $6.8\times10^{-5}M$, the percentage of micelles with 0, 1, 2, 3 solute molecules are calculated from equation (7) and presented in Table 1. The gross distribution of solute between

TABLE 1—DISTRIBUTION OF SOLUBILISED SOLUTE MOLECULES ACCORDING TO POISSON STATISTICS*

$[M_n]$	$<s>$	$P_{(0)}$	$P_{(1)}$	$P_{(2)}$	$P_{(3)}$	Occupied micelles
0.52×10^{-5}	1.02	36.1	36.1	18.8	6.4	57.6
1.6×10^{-5}	0.33	71.8	23.8	3.9	0.4	43.7
3.3×10^{-5}	0.16	85.3	1.4	1.1	—	15.0
6.8×10^{-5}	0.08	92.5	7.2	0.28	—	7.5

* All data reported as percentage of total micelles concentration.

the micellar and the aqueous phase, calculated from the simple expression $[S_m]/[S_w]=K[M]$, at different micellar concentrations for 1-AS at analytical concentration $5.32\times10^{-6}M$, are given in Table 2. The

TABLE 2—PARTITION OF SOLUTE ANTHRACENE 1-SULPHONATE IN MICELLAR PHASE AND AQUEOUS PHASE

Solution No.*	$[M_n]$	$[S_m]/[S_w]$
(5)	0.52×10^{-5}	3.5
(6)	3.3×10^{-5}	22.0
(7)	6.8×10^{-5}	45.3

* Solution number represent numbering of solution in Fig. 1 for 1-AS.

details are worked out only for 1-AS. The data indicate that for solution (7) total concentration of solute in the micellar phase is 45.3 times more than that in the aqueous phase and they occupy only 7.5% of the available micellar cages. That is, nearly 92.5% of micellar cages are empty. Calculations show that $[S_m]=5.2\times10^{-6}$, *i.e.* most of the 1-AS is within the micelle following the mass action law given by equation (1). Therefore, the emission spectrum obtained for solution (7) represents the emission of 1-AS totally bound to micelles.

The spectral changes observed on increase of micellar concentration are reminiscent of changes induced when increasing proportions of acetonitrile was added to an aqueous solution of 1-AS (Fig. 4a). From this observation one gets the impression that 1-AS molecules are gradually moving towards interior of the micellar core in the more hydrophobic region. The neutral detergent Triton X-100 has in effect four chemically different regions of polarity, CH_2OH head group at water micelle interface, region of polyoxyethylene chain of lower polarity, π-bonding phenyl group and the interior hydrocarbon core. But it can be established that the emission spectrum from solution (5) is a superposition of the emission from the solute in the aqueous phase and that in the micellar phase. There is a blue-shift of 5 nm when 1-AS enters the micellar phase ; λ_{max} in micelle = 415 and in water = 420 nm. The fraction of solutes in the micellar phase α is calculated to be 0.78 and therefore, $(1-\alpha)$ in aqueous phase is 0.22. Assuming that spectrum (7) in Fig. 1 is that for completely micellised 1-AS and spectrum (1) gives the intensity distribution in the aqueous phase, it is possible to construct the spectrum (5) by point by point calculation of fluorescence intensity at each wavelength. The spectrum could be reproduced within the experimental error. This confirms that the fluorescence spectra of solution at low micellar concentrations near C.M.C. are the summation spectra of those in aqueous and micellar phase, and do not truly represent the position of the probe molecules in the micelles.

Localisation of probe molecules in micellar phase : The localisation of the probe molecules in the micellar phase is normally attempted by comparing the observed spectral changes with those obtained for solvents of known polarity or viscosity or chemical structure. Of course there are more refined techniques, such as ^{1}H nmr or ^{13}C nmr studies. From ^{13}C nmr studies it has been established[17] that TX-100 has rigid structure near the phenyl ring but the flexibility increases as one goes towards the core or the interface region. The fluorescence spectra[14] of 1-AS in $ACN-H_2O$ mixed solvents and in glycerol at room temperature and 77 K are presented in Fig. 4. It is evident that the ratio of peak heights of 1-0 and 0-0 vibrational bands of 1-AS vary in a characteristic manner in different environments (Hamm effect). The effect has been well established for pyrene as a fluorescent probe of polarity[20,21]. The values are recorded in Table 3 for $ACN-H_2O$, $THF-H_2O$ and $EtOH-H_2O$ and dioxane$-H_2O$ systems as well as for glycerol at room temperature and 77 K. The peak height ratio observed for TX-100 is 1.50. This ratio is not observed for aprotic solvents, like ACN and THF, the ratios are higher for ethanol and increase further for dioxane. For glycerol, it has a ratio 1.43 at room temperature and 1.61 at 77 K. The latter values are near that for 1-AS in TX-100. From these observations, one can infer that 1-AS is

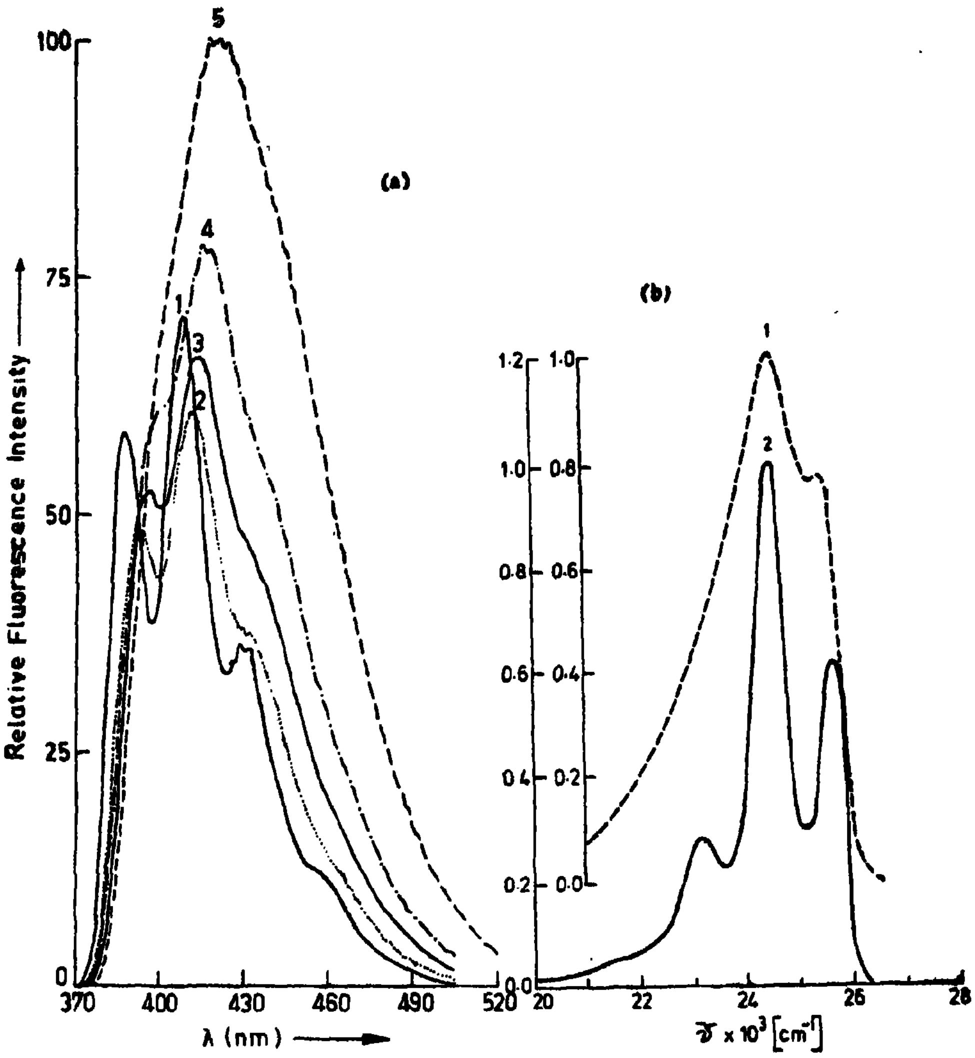


Fig. 4. Fluorescence spectra of 1-AS in (a) water-acetonitrile mixture (1 to 5) in 0, 80, 50, 80 and 100% water; (b) glycerol at (1) room temperature and (2) 77 K.

Table 8—Variation of the Ratio of Peak Height $F_{1\to0}/F_{0\to0}$ Vibrational Band of Fluorescence Spectra of 1-AS in Mixed Solvents

Cosolvent + H_2O	ACN	THF	EtOH	Dioxane	Glycerol RT*	Glycerol 77 K	TX-100
100 : 0	1.20	—	—	—	1.48	1.61	1.50
80 : 20	—	1.06	1.15	1.59	—	—	—
70 : 30	1.25	—	—	—	—	—	—
60 : 40	—	1.03	1.19	1.54	—	—	—
50 : 50	1.27	—	—	—	—	—	—
40 : 60	—	1.08	1.26	1.47	—	—	—
20 : 80	1.33	1.18	1.28	1.41	—	—	—

Fluorescence spectra in aqueous solution is devoid of any vibrational features. ACN = Acetonitrile, THF = tetrahydrofuran.
* Room temperature.

located in an environment of high concentration of ether groups and its motion is restricted. The most likely situation is for SO_3^- groups to reside near the CH_2OH head groups of the surfactant and for the hydrocarbon rings to be near the dioxan like oxyethylene chain. Since in 1-AS, long axis of the

anthracene skeleton is perpendicular to the SO_3^- group, the molecule will try to accomodate transversely and perturb the micellar structure. Its motion is hindered as in a viscous solvent, like glycerol at low temperatures. On the other hand, 2-AS can align along the surfactant chain creating less problem of accomodation. The disulphonates, 1,5-AS and 1,8-AS are too bulky to accomodate within the micelle and reside on the surface without much perturbation.

Acknowledgement

We thank Dr. Sekhar Basu for the fluorescence spectra in mixed solvents.

References

1. B. A. Lindig and M. A. J. Rodgers, *Photochem. Photobiol.*, 1980, **31**, 617.
2. M. Calvin, *Photochem. Photobiol.*, 1983, **37**, 349 ; *Acc. Chem. Res.*, 1978, **11**, 309.
3. C. A. Evans and J. R. Bolton, *Photochem. Photobiol.*, 1979, **30**, 697.
4. Y. Moroi, A. M. Braun and M. Grätzel, *J. Am. Chem. Soc.*, 1979, **101**, 567.
5. I. Wilner, W. E. Ford, J. W. Otvos and M. Calvin, *Nature (London)*, 1979, **280**, 823.
6. T. Matsuo, *Pure Appl. Chem.*, 1982, **54**, 1693.
7. J. Escabi-Perez, F. Nome and J. H. Fendler, *J. Am. Chem. Soc.*, 1977, **99**, 7749.
8. U. Samanta and K. K. Rohatgi-Mukherjee, *Indian Acad. Sci. Lett.*, 1978, **1**, 17.
9. H. Sato, Y. Kusumoto, N. Nakashima and K. Yoshihara, *Chem. Phys. Lett.*, 1980, **71**, 326.
10. N. J. Turro, M. Grätzel and A. M. Braun, *Angew. Chem. Int. Ed. Engl.*, 1980, **19**, 675, and references therein.
11. K. Kalyansundaram, *Chem. Soc. Rev.*, 1978, **4**, 453.
12. A. K. Gupta, S. Basu and K. K. Rohatgi-Mukherjee, *Can. J. Chem.*, 1980, **58**, 1046 ; S. Basu and K. K. Rohatgi-Mukherjee, *J. Lumin.*, 1984, **29**, 89, and references therein.
13. K. K. Rohatgi-Mukherjee and S. C. Bhattacharya, communicated.
14. S. K. Ash and K. K. Rohatgi-Mukherjee, *Indian J. Biochem. Biophys.*, 1979, **16**, 28.
15. W. R. Jeffrey, A. B. Sachs, D. J. Cash, R. B. Pasquale and G. P. Hess, *Anal. Biochem.*, 1983, **135**, 89.
16. R. J. Robson and E. A. Dennis, *J. Phys. Chem.*, 1977, **81**, 1075.
17. A. A. Robeiro and E. A. Dennis, *J. Phys. Chem.*, 1976, **80**, 1746.
18. L R. Fischer and D. G. Oakenfull, *Chem. Soc. Rev.*, 1977, **16**, 25.
19. S. Basu, Ph. D. Thesis, Jadavpur University, 1982.
20. A. Nakajima, *Bull. Chem. Soc. Jpn.*, 1971, **44**, 3272.
21. K. Kalyansundaram and J. K. Thomas, *J. Am. Chem. Soc.*, 1977, **99**, 2037.

J. Indian Chem. Soc.,
Vol. LXIII, January 1986, pp. 56-59

Studies on the Effect of Lifetime Variation on Magnetic Field Modulation of Exciplex Luminescence†

DEB NARAYAN NATH, SAMITA BASU and MIHIR CHOWDHURY

Department of Physical Chemistry, Indian Association for the Cultivation of Science, Jadavpur, Calcutta-700 032

The lifetime of the pyrene-N,N-dimethylaniline exciplex luminescence with a fixed concentration of donor and acceptor has been varied by adding quenchers and/or changing solvents. Its effect on the magnetic field modulation of the exciplex luminescence has been studied. The results are discussed in the light of electron hopping theory and possible environmental perturbation on the ISC process occuring on the bi-radical pair.

THE magnetic field modulation of radical pair (r.p.) recombination in solution has become a subject of interest in recent years[1-6]. The effect of magnetic field on inter-system crossing (ISC) has been extensively studied by probing the triplet state through delayed fluorescence[7-9] and direct triplet absorption[10-14] and also by probing the singlet state through exciplex luminescence[15,16]. The observation of the increase of the half-width of the magnetic field effect ($B_{1/2}$) with increase in donor concentration has initiated intense theoretical studies on the role of electron hopping in spin dynamics[17-19]. It is suggested that electron hopping between different donor and acceptor sites in solutions reduces the lifetime of a fixed nuclear environment and causes an uncertainty broadening of the energy levels which couples with hyperfine coupling and Zeeman interaction to increase the effective $B_{1/2}$[17,18]. In the above theoretical framework, the solvent has been assumed to affect only the diffusion kinetics of the process through its macroproperties, like viscosity, dielectric constant (ϵ) *etc.* and not the spin rephasing dynamics of the r.p. directly. In an earlier paper[16] based on our results with isotopically substituted solvent and 3-component mixed donor systems, we have suggested a more direct role of the non-bonded surrounding molecules in the spin evolution process. On replacing CH_3OH by CD_3OD we have observed a decrement of $B_{1/2}$ value for pyrene and *N,N*-dimethylaniline (Py-DMA) model exciplex system ([Py] = 10^{-4} *M*; [DMA] = 0.3×10^{-2} *M*) from 51 ± 2 to 45 ± 2 G. We have also found that addition of another donor DMT (having almost identical $B_{1/2}$ as DMA and with concentration same as that of DMA) in a Py-DMA exciplex system has the same effect on $B_{1/2}$ as that of doubling the DMA concentration although, the rate of exchange of electron between DMA and DMT is much lower compared to that between two DMA molecules[16]. These observations have led us to propose a tentative mechanism that the environment of the decaying exciplex can also modulate the ISC process through solvent hyperfine interaction (HFI). An alternative explanation of the results based on the level broadening due to environmental effect on lifetime of the exciplex is however conceivable. It may be argued that addition of a second donor might quench the exciplex luminescence and reduce the lifetime causing an uncertainty broadening of the energy levels and thus an increment in $B_{1/2}$. In this paper we have explored this possibility of correlation of $B_{1/2}$ with the lifetime (τ). The negative correlation reinforces our contention that probably the environmental perturbation occurs directly on the spin-rephasing process.

Experimental

The experimental arrangement is very similar to the one used in previous experiments[16]. A stable Wien bridge oscillator with synchronous output followed by a 60 W variable power amplifier has been used as the a.c. source. The photomultiplier was cooled to 0° to increase the signal to noise ratio. Commercially available compounds of the highest quality were purified by zone refining (pyrene) and vacuum distillation (DMA, propan-1-ol). Spectra grade CH_3OH (Aldrich) was used without further distillation. CsCl and KI (E. Merck) were purified through crystallisation.

The test solutions were 10^{-4} *M* in pyrene and 0.27×10^{-2} and 6×10^{-2} *M* in DMA. Quencher concentration was varied over 3×10^{-2} to 20×10^{-2} *M*. The mixed solvents were prepared by mixing CH_3OH and C_3H_7OH at different volume ratios. All samples were kept in closed sample cell through which nitrogen gas was bubbled for 40 min to deoxygenate. The sample characteristics remained steady throughout the experimental time. The lifetime (τ) of the exciplex luminescence was measured with a Applied Photophysics nanosecond spectrofluorometer based on time correlated single photon counting technique. The flash lamp was operated with 1 atm pressure of nitrogen and the

† Dedicated to Professor Sadhan Basu on the occasion of his 65th birthday.

Presented at the National Conference on Spectroscopy and Theoretical Chemistry held at Calcutta, December, 5-7, 1985.

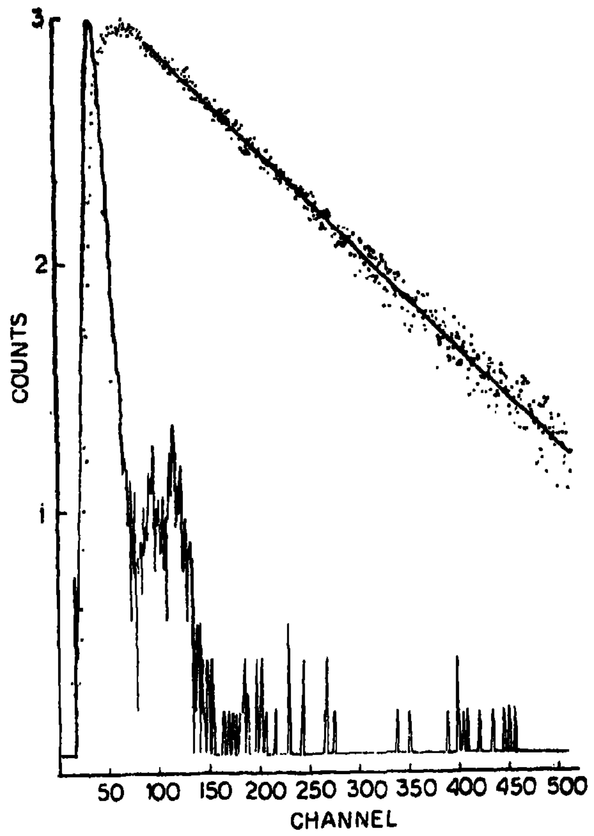


Fig. 1. Pump data, decay data and single exponential deconvolution fit for the system [Py]=0.1 m*M*, [DMA]=60 m*M* in the mixed solvent (methanol-propanol=2 : 1 (v/v), N_2 bubbled); Chisqr=1.08 ns/channel=0.164, τ=17.8ns.

TABLE 1—MEASURED $B_{1/2}$ VALUES (±2 G) AND $\Delta\phi/\phi$ VALUES FOR SYSTEMS WITH DIFFERENT LIFETIMES

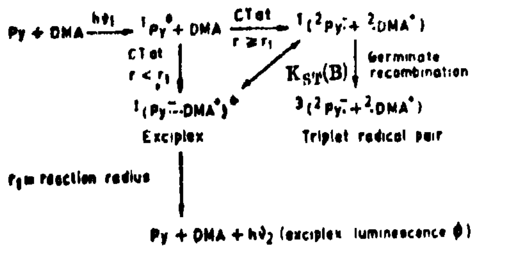
DMA concn. m*M*	Quencher concn. m*M*	Solvent	ϵ	τ ns	$B_{1/2}$ G	$\frac{\Delta\phi}{\phi}\times 100$
2.7		CH_3OH	33	25.9	50	1.60
60		CH_3OH	33	9.2	70	2.11
60	KI 60	CH_3OH	>33	6	65	0.84
60	CsCl 80	CH_3OH	>33	6	66	0.82
60	KI 200	CH_3OH	>33	4.7		0.25
60		CH_3OH+ C_3H_7OH (2 : 1)	28.6	17.8	69	2.24
60		CH_3OH with air (O_2)	33	6		0

FWHM of the pump function was 1.8 ns. The decay data was deconvoluted by the Applied Photophysics deconvolution program DECON1. The τ value was measured at wavelength 540 nm and the $B_{1/2}$ at 550 nm.

Results and Discussion

We have measured (i) the percentage change in luminescence intensity ($\Delta\phi/\phi$) on application of saturating magnetic field and (ii) the field at which the change in luminescence intensity is half of the value reached on saturation ($B_{1/2}$), as a function of the lifetime of the exciplex. The lifetime has been varied by two methods, (i) by adding quenchers which collisionally deactivate the exciplex and (ii) by changing the dielectric constant (ϵ) of the solvent which changes the ionisation rate or ionisation equilibrium of the exciplex, thus affecting its luminescence yield. A typical decay curve is shown in Fig. 1 and our results are displayed in a comprehensive manner in Table 1.

The complete ISC process is shown in Scheme 1. The magnetic field induced increment of the exciplex luminescence ($\Delta\phi$) originates from those



Scheme 1. ISC process in a biradical pair.

specimen of radical pairs which are initially uncaged ($r > r_1$) and form luminescent exciplex (caged r.p.) only after a diffusive excursion conserving the spin state. In the absence of the external magnetic field a portion of the uncaged radical pairs undergoes ISC through HFI during geminate recombination, while in its presence the degenarcy is lifted causing reduction in $K_{ST}(B)$, and the rate of back-formation of the caged r.p. is strengthened. For this reason, the magnetic field sensitivity ($\Delta\phi/\phi$) is high in case of triplet absorption[11] or delayed fluorescence studies[8] ($\approx$18%), but is very low in the present case of singlet luminescence ($\approx$2%). Quenchers cause a marked decrease in $\Delta\phi/\phi$, presumably because the collisional quenching is more effective in the case of uncaged radical pair in comparison with that in the caged ones, and hence, cause a faster decrease in the number of exciplex molecules formed by recombination of radical pairs (*i.e.* as measured by $\Delta\phi$) compared with the number of fluorescent exciplexes originally formed at $r < r_1$ (*i.e.* as measured by ϕ). This observation is in conformity with the previous qualitative observation that O_2 quenches the magnetic field effect faster than the luminescence (Table 1).

The dependence of exciplex luminescence ϕ and the relative magnetic field effect $\Delta\phi/\phi$ at a fixed strength (H = 240 G) on the dielectric constant ϵ is shown in Fig. 2. The data is similar to the case of Py-DEA exciplex system as reported by Petrov and others[15]. While ϕ decreases monotonically with increase in ϵ, $\Delta\phi/\phi$ shows a maxima at intermediate dielectric constant ($\epsilon\approx$30). As dielectric constant diminishes ($\epsilon < 30$) the r.p. tends to be more caged and the relative distance between them does not allow sufficient level degeneracy to cause ISC through HFI and hence, $\Delta\phi$ decreases. Whereas for increased ϵ, the formation of the caged luminescent exciplex from the uncaged r.p. decreases because of the increasing potential barrier (due to reorientation of the solvent molecule) and the lowering of the ion-pair dissociation limit[15]. This decrease is more rapid than that of the fluorescent exciplex which has formed directly ($r<r_1$) and so $\Delta\phi/\phi$ again decreases. Table 1 also shows a decrease in $\Delta\phi/\phi$ on decreasing donor concentration ; this is

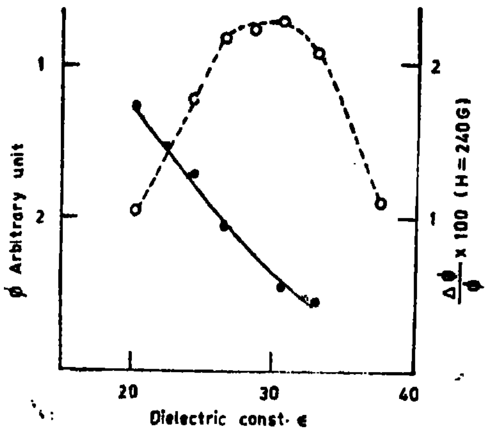


Fig. 2. Dependence of exciplex fluorescence yield ϕ and the relative magnetic field effect $\Delta\phi/\phi$ (broken curve) at a field strength H = 240 G on the dielectric constant of the solvent ϵ (in Debye); [Py] = 0.1 m*M*; [DMA] = 60 m*M*. Some of the points are obtained with single component solvents, propan-1-ol (ϵ = 20), methanol (ϵ = 33) and acetonitrile (ϵ = 37). Others are obtained in mixed solvent with methanol and propanol at different volume ratios.

more of an artifact than real, for at low donor concentration, the pyrene excimer luminescence accompanies the exciplex luminescence and hence the ϕ value is overestimated.

Table 1 clearly shows that the measured $B_{1/2}$ values have no relationship with the τ values, either in the case where a decrease in τ has been brought about by addition of quenchers or when τ is increased by choosing a solvent of lower dielectric constant. The observed τ values, of course, refers to caged luminescence exciplex but they can be assumed to run parallel to uncaged radical pair level broadening. A longer lived luminescent exciplex is analogous to a time window of longer delay, in which the magnetic field effect originates from the participation of radical pairs which have longer lifetime and hence less level broadening. This negative correlation significantly establishes the point that the increase of $B_{1/2}$ due to increase in DMA concentration as observed first by Weller and others[8] and that due to increase in DMT concentration as observed by us[16] cannot possibly be explained as caused by variation of the lifetime of exciplex or the radical pair. In the reported experiments with sampling time window at various delays the $B_{1/2}$ value for the system anthracene/DMA in CH_3CN has been observed to be increased from 58 to 67 G as the delay is decreased from 11 to 7 ns[11]. There are also reported data that at very short delay time the $B_{1/2}$ value increases rapidly and becomes almost independent of HFI[10,11]. These are very appropriately explained on the basis of the energy level broadening caused by the experimental constraint of selective sampling at short times. But this apparently is not responsible for the increase in $B_{1/2}$ with increase in donor

concentration which has been observed through both the transient triplet absorption and steady state singlet luminescence studies. The failure to obtain any direct correlation of lifetime of the exciplex (varied over identical range, 17 to 6 ns) with the observed $B_{1/2}$ values suggests that the change in $B_{1/2}$ on addition of excess DMT or DMA is probably brought about by direct environmental perturbation on spin rephasing rate rather than through the environmental nfluence on lifetime. The influence of environment on the nuclear hyperfine interaction through a perturbation of the electronic wavefunction has indeed been observed in Mössbauer spectroscopy of iron complexes, although the magnitude of perturbation is much less than that required in the present case. It may be pointed out, however, that in the present case the magnetic nucleii of the environment (*i.e.* protons) are also expected to be coupled 'directly' to the electronic wavefunction of the radical pair providing larger change in the 'total' average nuclear hyperfine interaction. Indeed, hyperfine coupling of ionic free radical wavefunction with magnetic unclei of non-bonded counter ion is known in epr spectroscopy[20].

Acknowledgement

This work has been supported by the SERC Grant (No. 23(IP-2)/81-STP-II) from the Department of Science and Technology, New Delhi.

References

1. A. L. Buchachenko, *Russ. Chem. Rev.* (*Engl. Transl.*), 1976, **45**, 761.
2. P. W. Atkins and T. P. Lambert, *Chem. Soc. Annu. Rep., Ser. A*, 1975, **72**, 67.
3. Y. Tanimoto, H. Hayashi, S. Nagakura, H. Sakuragi and K. Tokumaru, *Chem. Phys. Lett.*, 1976, **41**, 267.
4. N. J. Turro and B. Kraeutler, *J. Am. Chem. Soc.*, 1978, **100**, 7432.
5. N. J. Turro and B. Kraeutler, *J. Am. Chem. Soc.*, 1979, **101**, 7435.
6. B. Kraeutler and N. J. Turro, *Chem. Phys. Lett.*, 1980, **70**, 266.
7. H. J. Werner, H. Staerk and A. Weller, *J. Chem. Phys.*, 1978, **68**, 2419.
8. F. Nolting, H. Staerk and A. Weller, *Chem. Phys. Lett.*, 1982, **88**, 523.
9. A. Weller, F. Nolting and H. Staerk, *Chem. Phys. Lett.*, 1983, **96**, 24.
10. H. Staerk, R. Treichel and A. Weller, *Chem. Phys. Lett.*, 1983, **96**, 28.
11. H. W. Kruger, M. E. Michel-Beyerle and E. W. Knapp, *Chem. Phys.*, 1983, **74**, 205.
12. Y. Sakaguchi, S. Nagakura and H. Hayashi, *Chem. Phys. Lett.*, 1980, **72**, 420.
13. Y. Sakaguchi, S. Nagakura and H. Hayashi, *Chem. Phys. Lett.*, 1981, **82**, 213.
14. Y. Tanimoto and M. Itoh, *Chem. Phys. Lett.*, 1981, **83**, 626.
15. N. Kh. Petrov, A. I. Shushin and E. I. Frankevich, *Chem. Phys. Lett.*, 1981, **82**, 339.
16. D. N. Nath and M. Chowdhury, *Chem. Phys. Lett.*, 1984, **109**, 13.
17. K. Shulten and P. G. Wolynes, *J. Chem. Phys.*, 1978, **68**, 3292.
18. E. W. Knapp and K. Shulten, *J. Chem. Phys.*, 1979, **71**, 1878.
19. E. W. Knapp and W. Lersch, *Chem. Phys. Lett.*, 1984, **110**, 259.
20. H. Sharp and M. C. R. Symons in "Ions and Ion Pairs in Organic Reactions", ed. M. Swarc, Wiley-Interscience, New York, 1972, Vol. 1, Ch. 5.

J. Indian Chem. Soc.,
Vol. LXIII, January 1986, pp. 60-63

Solvent Effect on the Photochemistry of Anthraquinones†

J. CHOUDHURI, A. ROY and S. ADITYA

Department of Chemical Technology, University Colleges of Science & Technology, University of Calcutta, 92 A. P. C. Road, Calcutta-700 009

The spectral properties and the photochemical reactions of anthraquinone in ethanol, aqueous ethanol, formic acid, sulphuric acid, sulphuric acid-ethanol and formic acid have been studied. In ethanol, aqueous ethanol and formic acid, the lowest excited state of the quinone is $n-\pi^*$ and the only photochemical reaction that can be detected is photoreduction to semiquinone while in concentrated (98%) to aqueous 60% H_2SO_4 as well as ethanol-H_2SO_4, the lowest state has more $\pi-\pi^*$ character and the sole photochemical reaction is photo-substitution to produce hydroxyanthraquinone.

EXTENSIVE studies have been made on the photochemical reactions of *p*-quinones[1,2], particularly in alcoholic solution, because of their relevance to some important photosensitising effect, phototendering of cellulosic materials and photosensitised oxidation of various substrates. Recently, further interest has been aroused through the use of quinones in the field of solar energy storage as sensitisers as well as electron acceptors in photogalvanic cells[3] or as a photocatalyst in photo-oxidation of chloride ion to chlorine[3] or splitting of water[4]. Some quinones, such as 1,4-benzoquinone, 1,4-naphthaquinone, 9,10-anthraquinone, anthraquinone-2-sulphonate *etc.*, are photoreduced under appropriate conditions with unit efficiency, independent of wavelength of the exciting light. The excited state responsible for the reaction is proposed[5] to be the lowest triplet n-π^* state of the quinone, which in presence of H-donors, such as alcohols undergoes photoreduction to produce semiquinone radical and a hydroxyalkyl radical (from alcohol) which may disproportionate or further be oxidised to the corresponding aldehyde or ketone by the ground state quinone.

It was initially proposed[6] that photoreduction of carbonyls always proceeds through abstraction of hydrogen atom. Subsequent studies[7] have shown that at least with amines, sulphides *etc.* having low ionisation potentials, the photoreduction occurs through transfer of electron. However, some recent studies[8] have shown that even with alcohol, water and carboxylic acids, electron transfer is the primary step followed by proton depending on the equilibrium of semiquinone/semiquinolate ion.

Though photoreduction is a more common photochemical reactions with quinones, substitution products are also often obtained, in some cases as the only photochemical product. Thus, anthraquinone-2-sulphonate in aqueous medium, on irradiation, produces both the semiquinone and hydroxy derivatives[9], while 9,10-anthraquinone in concentrated sulphuric acid medium gives hydroxy derivative as the only photo-product[10]. Similarly, 1-methoxy-9,10-anthraquinone in aqueous acetonitrile containing ammonia gives 96% yield of 1-amino-9,10-anthraquinone, and 2-methoxy derivative gives 70% 1-amino-2-methoxyanthraquinone[11]. It is not clearly known whether the photoreduction and substitution occur from the same excited state or that substitution proceed through the initial step of photoreduction or not.

The present work has been carried out with anthraquinones to study its photoreduction and photo-substitution processes in different solvents with a view to correlating the different processes with the excited state precursors.

Experimental

Anthraquinone (U.S.S.R.) was recrystallised from benzene in dark and dried in a vacuum desiccator.

The light sources used were a medium pressure mercury vapour lamp T/MS/577, 80 W (Thermal Syndicate, U.K.) and a 100 W HBO lamp (Osram GmbH) mounted vertically on an optical bench. Monochromatic light of different wave-lengths were obtained by using a high radiance monochromator (Applied Photophysics). The solutions were photolysed in a 3 ml quartz cell, the temperature being maintained at 29 ± 0.1° by a thermostatic arrangement. The intensity of light incident on the cell was determined by ferrioxalate actinometry. Other experimental details are given elsewhere[9].

Anthrasemiquinone was detected and estimated from the absorption spectra, with absorption maximum at 380 nm ($\epsilon = 1.2 \times 10^4$ M^{-1} cm^{-1}). Semiquinone readily oxidised in presence of oxygen. The spectra of the photolysed solution under anaerobic medium and that after subsequent oxygenation was recorded with a Beckman DB spectrophotometer. The difference of the two after normalisation gave the spectra of the reduced

† Dedicated to Professor Sadhan Basu on the occasion of his 65th birthday.

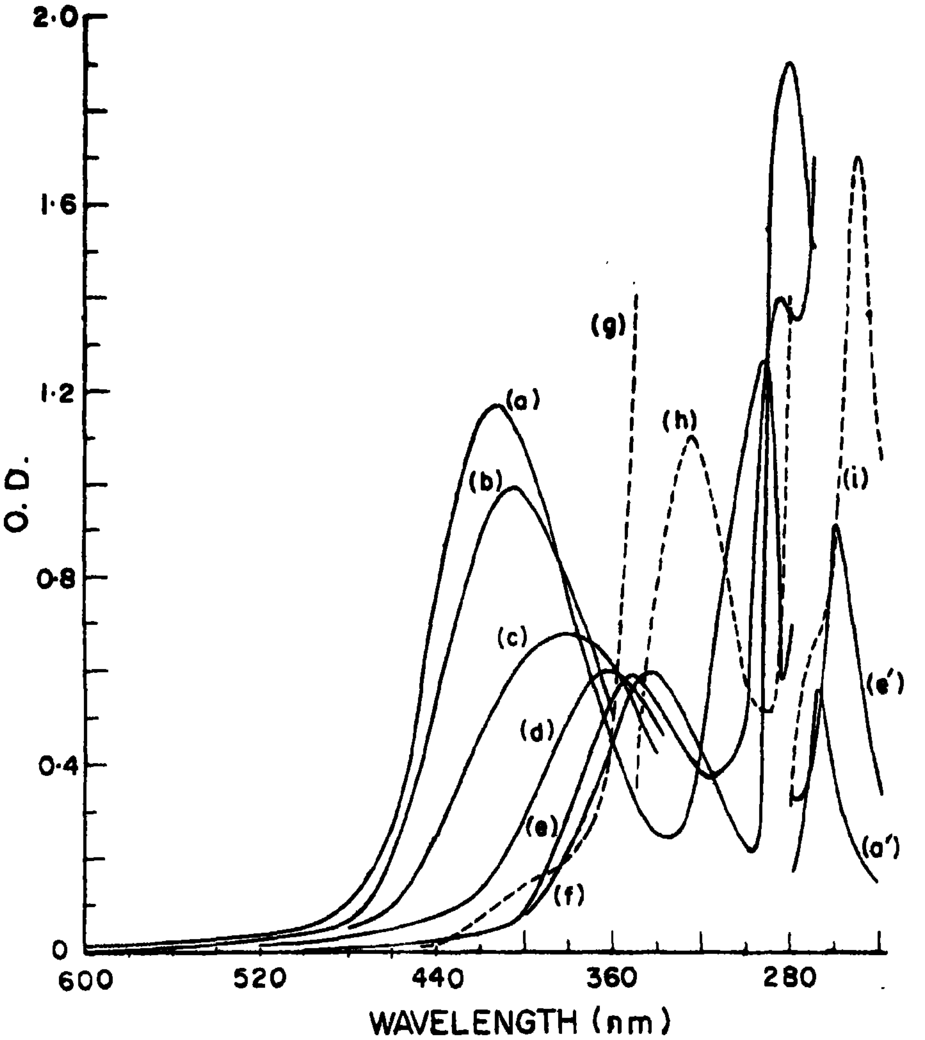


Fig. 1. Absorption spectra of anthraquinone in ethanol (– –) and (–) aqueous sulphuric acid of different compositions (% v/v) : (a) (a′) 98.0, (b) 88.2, (c) 78.4, (d) 68.6, (e) (e′) 58.8 and (f) 49.0% H_2SO_4, and [AQ] from (a) to (f) = 1×10^{-4} and (a′) to (e′) = 2.5×10^{-5} *M* ; (g) (h) (i) ethanol, and [AQ] for (g) = 1.3×10^{-5}, (h) = 2.6×10^{-4} and (i) = 4.0×10^{-5} *M*.

products. Hydroxy derivative was identified by the method described earlier[10].

Results and Discussion

Fig. 1 shows the absorption spectra of anthraquinone in ethanol and in different concentrations of aqueous sulphuric acid medium. In ethanol the absorption bands at 250, 265-275, 325 and 400 nm have been assigned to allowed π-π^*, forbidden π-π^* and n-π^* transitions, respectively[12]. Addition of water to ethanol solution does not alter the band-positions. But addition of sulphuric acid to ethanol (Fig. 1) or increase in sulphuric acid concentration in aqueous H_2SO_4 medium shifts all the bands to a considerable extent. Thus, the 250 nm band shifted to 268 nm, the 265-271 nm band to 310 nm and the 325 nm to 410 nm in concentrated sulphuric acid medium. The n-π^* band at 400 nm in ethanol could not be detected at higher H_2SO_4 concentrations, probably due to superimposition of the lower band. Substituent or solvent often switches the electronic configuration of T_1 and T_2 states of aryl carbonyls, *i.e.* n-π^* and π-π^* may flip-flop energetically as a result of change in solvent polarity. In ethanol or aqueous ethanol the lowest excited state of anthraquinone is of n-π^* character while with increasing H_2SO_4 proportion, the π-π^* state gradually shifted to longer wavelength and lowest state assumes more of π-π^* character. No thermal reaction occurs in concentrated sulphuric acid after keeping several hours in dark and even on heating[10]. Similar solvent dependent shift and switching of lowest excited state has been observed with acetophenone in cyclohexane and acetonitrile[13].

TABLE 1—QUANTUM YIELD OF SEMIQUINONE IN PHOTOLYSIS OF ANTHRAQUINONE IN ETHANOL AND AQUEOUS ETHANOL UNDER ANAEROBIC MEDIUM AT 313 nm

Anthraquinone concn. $= 2.5 \times 10^{-4}$ *M*, Time of irradiation = 10 min, Radiation source = Medium pressure Hg vapour lamp

Proportion of ethanol-water	Number of quanta absorbed at 313 nm	Number of molecules formed	Quantum yield
10 : 0	3.798×10^{17}	14.565×10^{16}	0.38
9 : 1	3.816×10^{17}	13.893×10^{16}	0.36
8 : 2	3.171×10^{17}	11.977×10^{16}	0.38
7 : 3	3.572×10^{17}	12.744×10^{16}	0.36
6 : 4	3.505×10^{16}	13.415×10^{16}	0.38

TABLE 2—QUANTUM YIELD OF SEMIQUINONE IN PHOTOLYSIS OF ANTHRAQUINONE IN ALKALINE ETHANOL UNDER ANAEROBIC MEDIUM AT 313 nm

Anthraquinone concn. $= 2.5 \times 10^{-4}$ *M*, Sodium hydroxide solution = 0.1 *N*, Time of irradiation = 10 min.

Proportions of ethanol-NaOH	Number of quanta absorbed at 313 nm	Number of molecules formed	Quantum yield
9 : 1	0.960×10^{17}	0.909×10^{17}	0.95
8 : 2	0.846×10^{17}	0.822×10^{17}	0.97
7 : 3	0.846×10^{17}	0.794×10^{17}	0.94
6 : 4	0.836×10^{17}	0.794×10^{17}	0.95

Photolysis of anthraquinone in ethanol under anaerobic medium produces semiquinone with oxidation of ethanol to aldehyde, as also reported earlier[6]. Table 1 shows the quantum yield values of semiquinone in ethanol and aqueous ethanol media. Addition of water upto 6 : 4 (ethanol-water) does not alter the quantum yield. Moreover, no other product could be observed. It may be mentioned here that with anthraquinone-2-sulphonate, photolysis in 1 : 1 aqueous ethanol medium produces semiquinone as well as hydroxy derivative of the quinone. In alkaline medium, with anthraquinone-2-sulphonate, the yield of semiquinone (semiquinolate ion) as well as hydroxy derivative increases sharply with the increase in alkali concentration[6]. With anthraquinone, the quantum yield of semiquinolate ion is higher in alkaline medium, but it does not increase with increase in alkali concentration (Table 2). No hydroxy product is observed even at highest alkali concentration.

Fig. 2 shows the absorption spectra of anthraquinone in different proportion of H_2SO_4-water after photolysis. The product formed has been identified to be a hydroxy derivative. Irradiation under anaerobic condition also produces hydroxy product but no semiquinone can be detected even in 6 : 4 H_2SO_4-water medium. It is apparent from the spectra that the maximum yield of the hydroxy derivative is obtained at 4 : 1 H_2SO_4-water medium.

While in 1 : 1 ethanol-water medium, the sole photochemical product is semiquinone (quantum yield 0.38) no semiquinone is photochemically produced even in 1 : 2 H_2SO_4-ethanol medium, the only product being hydroxy derivative. The above results indicate that while in ethanol or aqueous ethanol the lowest n-π^* state is responsible for photoreduction, in H_2SO_4-water or H_2SO_4-ethanol the π-π^* state shifts to longer wavelength and becomes the lowest state and no photoreduction

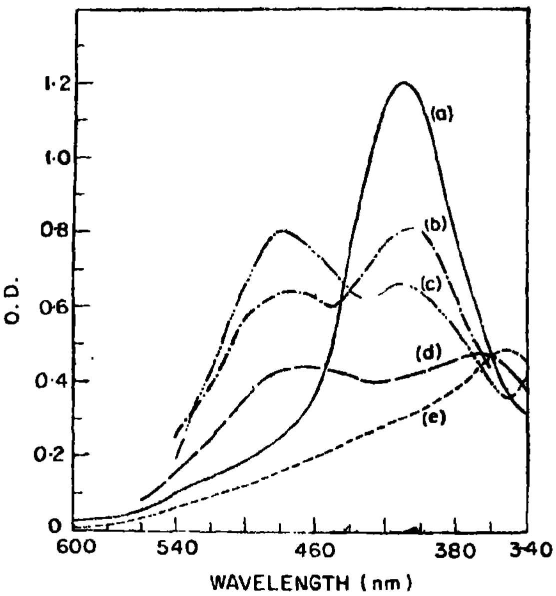


Fig. 2. Absorption spectra of anthraquinone in aqueous sulphuric acid of different compositions after irradiation at 366 nm for 1 h : (a) 98.0, (b) 88.2, (c) 78.4, (d) 68.6 and (e) 58.8% H_2SO_4.

product is observed. It has also been noted that with anthraquinone-2-sodium sulphonate, similar shift in absorption bands occurs in H_2SO_4 medium compared to that in aqueous or aqueous ethanol media and photolysis in concentrated H_2SO_4 under anaerobic condition yields only hydroxy product, while in aqueous or aqueous ethanol medium (even upto 1 *M* H_2SO_4 solution), anaerobic irradiation produces both semiquinone and hydroxy derivative as stated earlier.

Use of formic acid instead of sulphuric acid, however, does not shift the band position from that

Table 3—Quantum Yield of Semiquinone in Photolysis of Anthraquinone in Formic Acid-Water under Anaerobic Medium at 313 nm

Proportion of formic acid-water	Time of irradiation h	Number of quanta absorbed at 313 nm	Number of molecules formed	Quantum yield
10 : 0	2	14.158×10^{17}	0.388×10^{16}	0.0027
9 : 1	2	14.357×10^{17}	0.670×10^{16}	0.0046
8 : 2	2	13.496×10^{17}	1.724×10^{16}	0.013
7 : 3	2	14.159×10^{17}	2.688×10^{16}	0.019

in ethanol and photolysis under anaerobic medium produces semiquinone only, though with a lower yield. Increase in water proportion increases the semiquinone yield (Table 3).

Flash photolysis[8] of anthraquinone in ethanol or aqueous ethanol produces a transient absorbing at 490 nm. The transient has been assigned to be the semiquinolate ion, formed by abstraction of electron by the excited quinone. No such transient is observed with anthraquinone in concentrated H_2SO_4 or aqueous H_2SO_4, further confirming that in sulphuric acid medium the initial step is different from that in ethanol or aqueous ethanol media, where an electron is abstracted by the excited molecule.

Similar shift in absorption bands also occurs on the introduction of substituents, like hydroxy, methoxy or halogens, to quinones and in many cases photoreduction efficiency becomes extremely low[14].

Acknowledgement

The authors are thankful to U.G.C., New Delhi, for financial assistance.

References

1. A. V. El'tsov, O. P. Studzinskii and K. V. M. Grebenkina, *Russ. Chem. Rev.* (*Engl. Transl.*), 1977, **46**, 93.
2. A. Roy and S. Aditya, *Int. J. Hydrogen Energy*, 1983, **8**, 91.
3. H. R. Scharf and R. Weitz, *Tetrahedron*, 1979, **35**, 2255.
4. I. Okura and N. Kim Thuan, *Chem. Lett.*, 1980, 1569.
5. S. A. Carlson and D. M. Hercules, *J. Am. Chem. Soc.*, 1971, **93**, 5611.
6. C. F. Wells, *Trans. Faraday Soc.*, 1961, **57**, 1703, 1719.
7. P. J. Wagner, *Top. Curr. Chem.*, 1976, **66**, 1; N. J. Turro and C. G. Lee, *Mol. Photochem.*, 1972, **4**, 427.
8. J. Choudhuri, A. Roy and S. Aditya, communicated.
9. A. Roy, D. Bhattacharyya and S. Aditya, *J. Indian Chem. Soc.*, 1982, **59**, 585.
10. G. G. Mihai, P. G. Tarassov and N. Filipescu, *J. Chem. Soc., Perkin Trans. 1*, 1975, **14**, 1374.
11. J. Griffiths and C. Hawkins, *Chem. Commun.*, 1973, 111.
12. A. Kuboyama, *Bull. Chem. Soc. Jpn.*, 1960, **33**, 1027.
13. H. Lutz, E. Breheret and L. Lindqvist, *J. Phys. Chem.*, 1973, **77**, 1758.
14. J. M. Bruce in "The Chemistry of Quinonoid Compounds", ed. S. Patai, Wiley, New York, 1974.

J. Indian Chem. Soc.,
Vol. LXIII, January 1986, pp. 64-68

Chemical Physics with Quistors†

PRADIP K. GHOSH

Department of Chemistry, Indian Institute of Technology Kanpur, Kanpur-208 016

A brief review of the present status of applications of Quistors to mass spectrometry, study of ion-molecule reactions, precision hyperfine spectroscopy and molecular ion spectroscopy is presented.

THE objective of this review is to present briefly the current status of applications of the Quistor (Quadrupole Ion Store or Radiofrequency Ion Trap) in the area of chemical physics.

Principle of operation of the device : While the two-dimensional quadrupole mass filter uses four rods of hyperbolic cross section, and with a field diameter $2r_o$, opposite electrodes shorted together, a voltage of $U+V\cos\omega t$ applied across the adjacent electrodes the single particle ion motion is given by the following two Mathieu equations,

$$\frac{d^2x}{d\zeta^2}+(a+2q\cos 2\zeta)\,x=0$$

$$\frac{d^2y}{d\zeta^2}-(a+2q\cos 2\zeta)\,y=0$$

where, $a=\frac{8eU}{mr_0^2\omega^2}$, $q=\frac{4eV}{mr_0^2\omega^2}$, and $\zeta=\frac{\omega t}{2}$.

The radiofrequency *ion trap structure* (Fig. 1) involves a three-dimensional force field, generated by a voltage $U-V\cos\omega t$ applied between an

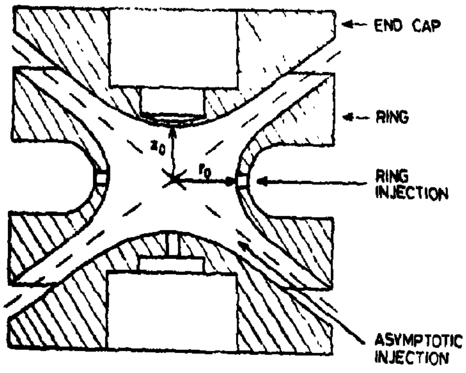


Fig. 1. Quadrupole radiofrequency ion trap (Quistor).

annular ring electrode with hyperbolic profile and oriented along the xy plane, and two end-cap electrodes that are hyperboloids of revolution about the z-axis. The ion motion in the latter case is expressed by the following Mathieu equations,

$$\frac{d^2z}{d\zeta^2}+(a_z-2q_z\cos 2\zeta)\,z=0$$

$$\frac{d^2r}{d\zeta^2}+(a_r-2q_r\cos 2\zeta)\,r=0$$

where, $a_z=-2a_r=-\frac{4eU}{mz_0^2\omega^2}$, $q_z=2q_r=-\frac{2eV}{mz_0^2\omega^2}$,

$\zeta=\frac{\omega t}{2}$, $r_0^2=2z_0^2$ and r represents either x or y.

Mathieu equations have stable or unstable solutions depending on the values of the parameters a and q ; the aq plane, therefore, is divided into stable and unstable zones. Unlike the two-dimensional quadrupole, the stability diagram for the quistor is asymmetric with respect to the q-axis (dashed line in Fig. 2 ; the enclosed region is the stable zone), and usually the lower part of the diagram is used. For a mass selective operation, the voltages applied are such that only a small range of $\Delta m/z$ ions is stable. While the stable condition in a two-dimensional quadrupole means that the ion is confined along the x- and y-direction and it moves with constant velocity along the z-direction, in the three-dimensional force field, a stable motion along the x-, y-, and z-directions means that the ion is 'trapped' inside the structure. The dashed line of Fig. 2 is the theoretical stability diagram corresponding to the single particle ion motion. The solid lines represent experimentally obtained[5] stability diagrams for various *m/z* ions and probably include space charge effects. Principles and early applications have been reviewed in detail in Refs. 1 and 2 ; several aspects of recent applications are presented in Refs. 3 and 4.*

Mass spectrometry : The first obvious application has been to mass spectrometry where it could serve as both a sensitive and a miniature mass spectrometer. In the method of resonance detection[1], besides the rf voltage $V\cos\omega t$, an additional ω_{ac} is applied between the end-cap electrodes. When the stored ions have their fundamental

* This review considers only the rf trap (Quistor) which has also been called the 'Paul trap' (after the inventors of the device, W. Paul and coworkers). The 'Penning traps' have the Quistor structure, but for ion confinement, use, instead of the rf field, an electric potential and a magnetic field. Using special ion cooling techniques, nearly Doppler-free spectroscopy has been possible using this device (for example, Ref. 4). A couple of other recent achievements using such traps are, determination of positron/electron g-factor ratio of high accuracy, and a measurement of positron/electron mass ratio which is at least two orders of magnitude more accurate than any previous data (P. B. SCHWINBERG, R. S. VAN DYCK, JR. and H. G. DEHMELT, *Phys. Rev. Lett.*, 1981, 47, 1679 ; P. B. SCHWINBERG, R. S. VAN DYCK, JR. and H. G. DEHMELT, *Phys. Lett., A*, 1981, 81, 119).

† Dedicated to Professor Sadhan Basu on the occasion of his 65th birthday.

A part of the article was presented at the National Conference on Spectroscopy and Theoretical Chemistry held at Calcutta, December 5-7, 1985.

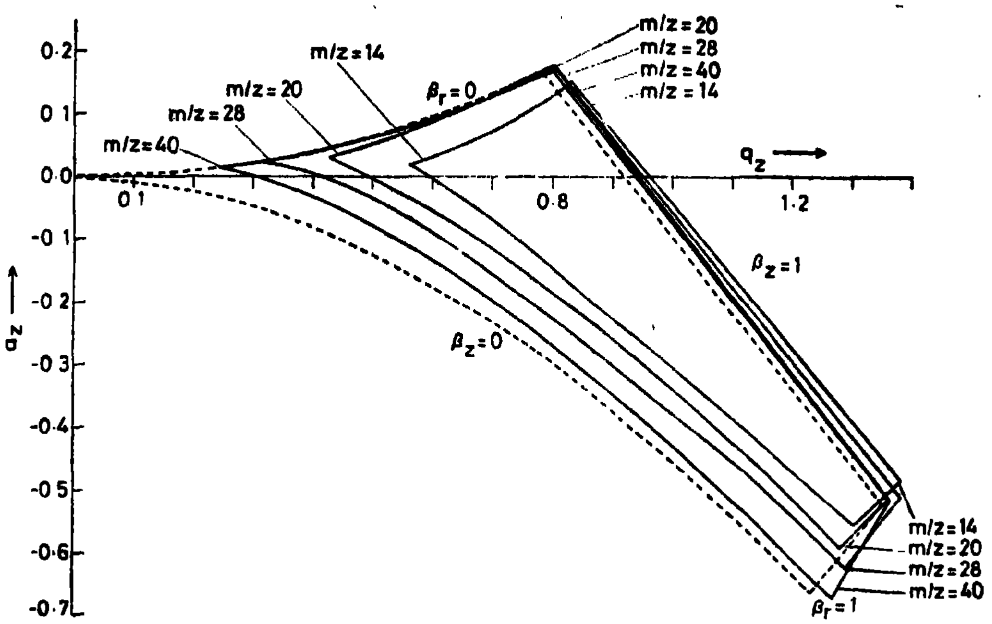


Fig. 2. Stability diagrams of the Quistor. The dashed line represents the single particle theoretical stability diagram. The solid lines represent mass dependent stability diagrams obtained from experiments[4]. Areas enclosed by the lines represent the stable zones for ions.

frequency of motion ω_z in the axial direction same as ω_{se}, ions are collected at the end-cap electrodes, and this current could be detected. In another method[6] that is commonly used, the quistor is set for a specific m/z and the ion concentration is allowed to build. After an adequate build-up, the ions are pulsed out of the trap to a detector through an aperture on one of the end-caps. In a recent application[7] using a mass selective instability mode, the trapping voltage applied is such that initially a range of m/z ions are stable and all of them are trapped. The U(dc) or the V cos ωt(rf) voltages are then scanned in a manner such that successively different m/z ions become unstable, they pass out through the field structure, and are detected, leading to a mass spectrum. Using this mode of operation at high background pressures of about 10^{-3} torr of helium or hydrogen—the external gases damping the ion motion-significantly enhanced mass resolution, sensitivity and detection limit have been obtained.

Study of ion-molecule reactions : Ion-molecule reactions have been studied by employing quistors. In the quistor-quadrupole combination instruments[8] the quistor is used in place of the conventional ion source with the quadrupole acting as the ion detector. In pulsed operation of such experiments, the first pulse results electron impact ionisation of the parent gas inside the confinement region and generates the primary reactant ion. Between two such consecutive ion creation pulses, ion-molecule reactions take place. The ions of interest, primary or secondary, are selectively confined in the trap, and after a variable time period ejected into the quadrupole and detected. Results are consistent with other techniques, and indicate ion kinetic energy in the range 1-3 eV. Recently ionic multi-photon dissociation processes have been studied[9] by using quistors, and reaction pathways have been examined by selective removal of possible precursors.

Microwave spectroscopy and atomic hyperfine structure : In the late sixties Schuessler and co-workers[10] first applied the quistor to the study of hyperfine structure of $^3He^+$ by an exchange collision technique. In this interesting experiment, $^3He^+$ ions are first generated by electron impact and kept trapped in the confinement region. A beam of spin polarised Cs atoms is then passed through the $^3He^+$ ion cloud. The polarised Cs beam acts in two ways. First, by spin exchange, it transfers its polarisation to the stored $^3He^+$ ions itself losing polarisation,

$$Cs\uparrow + He^+\downarrow \rightarrow Cs\downarrow + He^+\uparrow$$
$$Cs\uparrow + He^+\uparrow \rightarrow Cs\uparrow + He^+\uparrow$$

In a simultaneous second process, charge exchange with He^+ takes place. This charge exchange process proceeds through two different channels, the fast singlet channel,

$$Cs\uparrow + He^+\downarrow \rightarrow He^*(\uparrow\downarrow - \downarrow\uparrow) + Cs^+ + \Delta E_1$$

and the slow triplet channels,

$$Cs\uparrow + He^+\uparrow \rightarrow He^*\uparrow\uparrow + Cs^+ + \Delta E_3$$
$$Cs\uparrow + He^+\downarrow \rightarrow He^*(\uparrow\downarrow + \downarrow\uparrow) + Cs^+ + \Delta E_3$$

ΔE_1 and ΔE_3 are respectively the ionisation energy differences for the singlet and triplet charge-exchange reactions.

The charge-exchange cross section depends on the energy defect ΔE, relative velocity of Cs and He^+, and the ionisation energies of the ground state Cs and excited He^* atoms. In the case of Cs and He, $\Delta E_1 = 0.08$ eV and $\Delta E_3 = -0.26$ eV, and the singlet charge-exchange cross section is estimated to be about 20 times larger than that of the triplet state. The spin-exchange cross section is much faster than even the singlet charge-exchange cross section ; so the trapped ions assume the same polarisation as the Cs atoms in a time interval that is short compared to the neutralisation time. The quistor remains immersed in a magnetic field for the purpose of the microwave spectroscopic experiment. In the third step, when the microwave radiation of the right frequency is shone, the optical transition, $He^+\uparrow \rightarrow He^+\downarrow$ takes place. When this transition occurs, additional $He^+\downarrow$ ions are generated but they lose their charge fast by the singlet channel and hence are lost rapidly from the trap. So if the number of helium ions stored in the trap is monitored as the microwave frequency is swept, the precise frequency of transition is recorded by a rapid loss of ions from the trap. All possible hfs structure of $^3He^+$ were measured by Schuessler and coworkers using the ion-storage exchange collision technique. This study has been followed by hfs determination of $^{199}Hg^+$ by other workers[11-13] using the ion trap.

A recent application of microwave spectroscopy has been to the determination of ground state hyperfine splitting of $^{137}Ba^+$ by using tunable lasers[14]. The use of tunable lasers opens up more general applications in the spectroscopy of stored ions ; it also has the advantage of improved signal to noise ratio. In this particular experiment, schematically shown in Fig. 3, the $6S_{1/2}$ state (F – 2) ions created by surface ionisation are pumped by a pulsed tunable laser at 493.4 nm. The excited P state has a decay mode to the $5D_{3/2}$ state with a branching ratio of 2.8 and a fluorescence wavelength 649.6 nm. As the microwave output frequency is swept across the hyperfine transition, the fluorescence count rate at 649.6 nm records the occurrence of the hyperfine transition. By application of this method the ground state hyperfine splitting of $^{137}Ba^+$ has been measured with a precision of 4.6×10^{-11}.

Experiments are underway for storing low energy highly charged ions and also radioactive ions, produced on-line from a nuclear accelerator, for the purpose of atomic spectroscopy[15].

Molecular spectroscopy : Laser induced fluorescence spectra of molecular ions is another area where rf ion traps have been employed.

In the study of fluorescence spectra of $BrCN^+$ ions[16], the ion trap used was of cylindrical geometry, a variant of the quistor using hyperbolic geometry. In this experiment, the ions are first created by pulsed electron beam bombardment of the parent neutral gas. Any excited electronic states that are created then relax radiatively, and mass selection in the trap takes place. Following this delay, a 10 ns 1 cm^{-1} bandwidth laser pulse—dye laser pumped by a nitrogen laser—passes through the ion cloud, and any subsequent fluorescence is then monitored at right angles to the exciting radiation. By varying the dye laser frequency the entire spectrum is obtained. Besides other information, the C – Br stretching frequencies of the molecular ion have been derived using this technique.

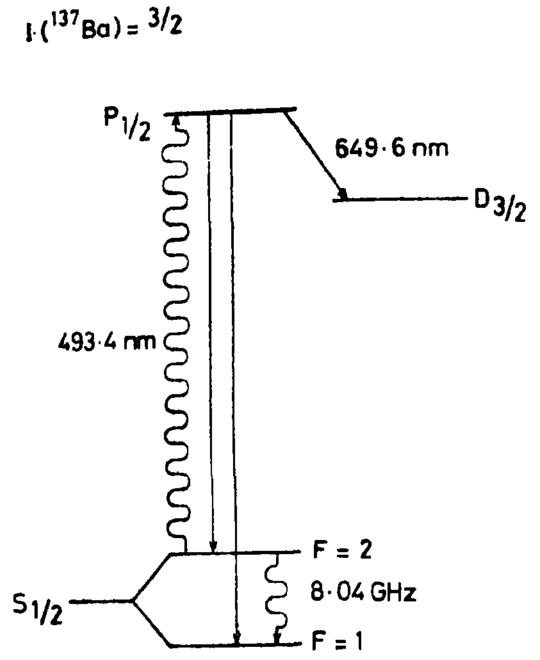


Fig. 3. Schematic diagram showing the transitions involved in ground state hfs determination of $^{137}Ba^+$ using the Quistor and laser fluorescence[14].

In another experiment, by monitoring laser induced fluorescence spectra, charge transfer reactions of N_2^+ with Ar and that with N_2 have been studied[17]. Ion-molecule reactions alter the internal energy distribution of the trapped N_2^+ ; by monitoring these changes charge transfer cross sections for individual initial vibrational states have been estimated.

Yet in another study[18], radiative lifetimes of excited electronic states of molecular ions have been measured using the ion trap. The storage times used were such that allowed only electronic relaxation. In this experiment, ions which are in the ground electronic state, or in an optically metastable state, are excited with a laser pulse, and the time dependence of the resulting fluorescence is monitored ; from this the radiative lifetimes of the upper states could be determined. These studies have included the $N_2^+ B^2\Sigma_u^+$ state, $CO^+ A^2\Pi$ state, and for the ions CH^+ and CD^+, obtained from fragmentation of CH_4, the $A^1\Pi$ state.

Ion stabilities from theory : The involvement of our laboratory in this area has been in theoretical

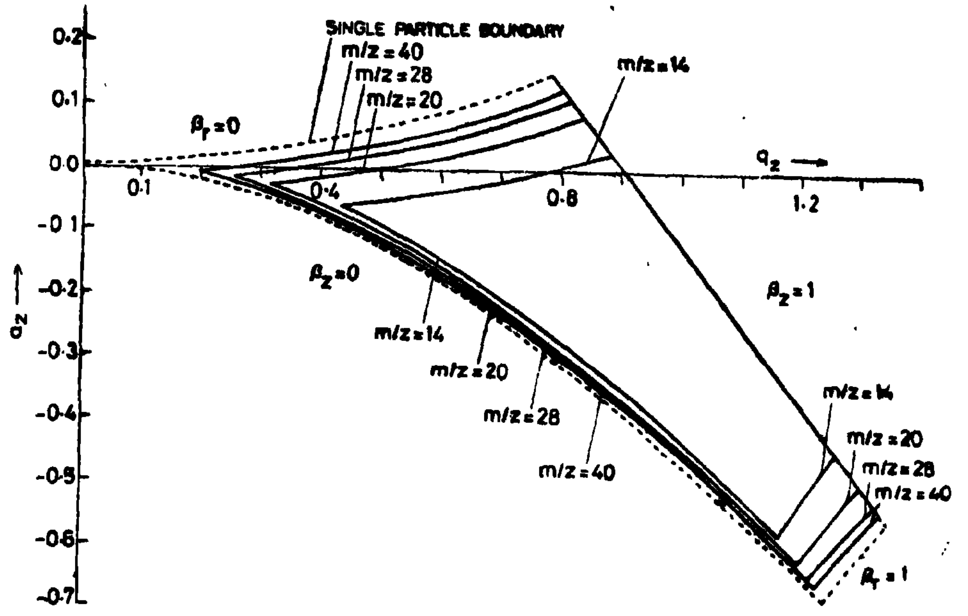


Fig. 4. Theoretical stability diagrams from a many-particle calculation showing mass dependence.

examination of the quistor operation ; this includes exploring ways by which an external injection could be effected for ions which could not be generated inside the trap, and attempting theoretical prediction of stability properties that takes into account space charge effects. Early work on ion stability properties from theory, is presented in Ref. 2. We first examined[19] ion path lengths which would have influence on overall collision probability. We then initiated a study[20] of asymptotic (Fig. 1) pulsed injection of ions. This was examined by Todd and coworkers[21] using the phase space dynamics method. Later this was extensively studied by O and Schuessler[22] which included other injection modes, such as ring injection. We then initiated *ab initio* studies of many-particle systems in an attempt to evolve stability diagrams that include space charge effects. We first examined[23] a conical injection mode around the z-axis and a concentric ring injection ; both of these, difficult to execute experimentally, though pertained to many-particle systems, reduced to single particle calculations because of special geometries. Recently, we have made calculations[24] on realistic modes using only a few particles but considering all electrostatic and electromagnetic forces besides the Mathieu forces. In the initial study it predicted correctly the nature of shifts of two stability lines. In a recent study[25], assuming thermalisation of ions, it has qualitatively predicted correctly the mass dependence (Fig. 4) as observed in experiments[5] (Fig. 1).

References

1. W. PAUL and H. STEINWEDEL, *Z. Naturforsch., Teil A*, 1953, 8, 448 ; U. S. Pat. 2 939 952/1960.
2. "Quadrupole Mass Spectrometry and its Applications", ed. P. H. DAWSON, Elsevier, Amsterdam, 1976.
3. J. F. J. TODD, *Int. J. Mass Spectrom. Ion Proc.*, 1984, 60, 3.
4. G. WERTH, *Contemp. Phys.*, 1985, 26, 241.
5. J. F. J. TODD, R. M. WALDREN and R. E. MATHER, *Int. J. Mass Spectrom. Ion Phys.*, 1980, 34, 325.
6. P. H. DAWSON and N. R. WHETTEN, *J. Vac. Sci. Technol.*, 1968, 5, 11.
7. G. C. STAFFORD, JR., P. E. KELLY, J. E. P. SYKA, W. E. REYNOLDS and J. F. J. TODD, *Int. J. Mass Spectrom. Ion Proc.*, 1984, 60, 85.
8. G. LAWSON, R. F. BONNER, R. E. MATHER, J. F. J. TODD and R. E. MARCH, *J. Chem. Soc. Faraday Trans. 1*, 1976, 545.
9. R. J. HUGHES, R. E. MARCH and A. B. YOUNG, *Int. J. Mass Spectrom. Ion Phys.*, 1982, 42, 255.
10. H. A. SCHUESSLER, E. N. FORTSON and H. G. DEHMELT, *Phys. Rev.*, 1969, 187, 5.
11. F. G. MAJOR and G. WERTH, *Phys. Rev. Lett.*, 1973, 30, 1155.
12. M. D. MCGUIRE, R. PETSCH and G. WERTH, *Phys. Rev., A*, 1978, 17, 1999.
13. M. JARDINO, M. DESAINT FUSCIEN, R. BARILLET, J. VIENNET, P. PETIT and C. AUDOI, *Appl. Phys.*, 1981, 24, 107.
14. R. BLATT and G. WERTH, *Phys. Rev., A*, 1982, 25, 1476.
15. H. A. SCHUESSLER, International Symposium on Hyperfine Interactions, IIT Kanpur, 1984.
16. F. J. GRIEMAN, B. H. MAHAN and A. O'KEEFE, *J. Chem. Phys.*, 1981, 74, 857.
17. B. H. MAHAN, C. MARTNER and A. O'KEEFE, *J. Chem. Phys.*, 1982, 76, 4433.
18. B. H. MAHAN and A. O'KEEFE, *Astrophys. J.*, 1981, 248, 1209.
19. P. K. GHOSH, A. S. ARORA and L. NARAYAN, *Int. J. Mass Spectrom. Ion Phys.*, 1977, 23, 237.

20. M. NANDKISHORE and P. K. GHOSH, *Int. J. Mass Spectrom. Ion Phys.*, 1979, **29**, 345.

21. J. F. J. TODD, D. A. FREER and R. M. WALDREN, *Int. J. Mass Spectrom. Ion Phys.*, 1980, **36**, 371.

22. C. S. O and H. A. SCHUESSLER, *Appl. Phys., B*, 1982, **27**, 129 ; *J. Appl. Phys.*, 1981, **52**, 1157 ; *Int. J. Mass Spectrom. Ion Phys.*, 1981, **40**, 67.

23. R. CHATTOPADHYAYA and P. K. GHOSH, *Int. J. Mass Spectrom. Ion Phys.*, 1980, **36**, 365 ; 1981, **41**, 1.

24. A. P. CHATTOPADHYAY and P. K. GHOSH, *Int. J. Mass Spectrom. Ion Phys.*, 1983, **46**, 75 ; 1983, **49**, 253.

25. A. HARIHARAN and P. K. GHOSH, unpublished (to be presented in the 10th International Conference on Mass Spectrometry, Swansea, 1985).

J. Indian Chem. Soc.,
Vol. LXIII, January 1986, pp. 69-72

Electronic States of Isomeric Hydroxybenzoic Acids and their Mono- and Di-anionic Species†

DHARAM V. S. JAIN*, FATEH S. NANDEL**, PREM SINGLA and DAMAN JIT KAUR

Department of Chemistry, Panjab University, Chandigarh-160 014

Absorption and emission spectra of isomeric hydroxybenzoic acids in different solvents and at different pH values have been studied. The results have been supplemented by CNDO/S calculations. Their electronic states have been characterised. The acid-base equilibria in the ground and excited states have also been discussed.

THE photochemistry and photobiology of substituted benzenes has attracted attention of many groups of workers[1-6]. For better understanding of their photochemical behaviour it is imperative that electronic states of these molecules are well characterised. No systematic and complete study[7-9] has been reported so far on hydroxybenzoic acids. Here, we present in some details the electronic spectra of hydroxybenzoic acids under different experimental conditions as a part of our program[10-12] of systematic study of the electronic spectra of disubstituted benzenes. The concentration of benzoic acids have been so chosen as to avoid the formation of dimeric species which can lead to complication in the interpretation of the spectra.

Experimental

Solutions of hydroxybenzoic acids (B.D.H., AnalaR) in warm ethanol were treated with activated charcoal, filtered, cooled and kept aside to obtain hydroxybenzoic acids as crystalline solids. The crystals were washed with cold ethanol and dried under vacuum. Absolute ethanol for use as solvent, was twice distilled over sodium metal and stored over molecular sieves. Cyclohexane and methylcyclohexane[13] were stirred with sulphuric acid, washed with water and dried over fused calcium chloride, and distilled twice over sodium metal. Acetonitrile was distilled over phosphorous pentoxide, and its middle fraction (b.p. 354 K) was used. Methanol (A.R. grade) was used as such. Water was triple-distilled over potassium dichromate and potassium permanganate solutions.

Absorption spectra were taken on a UV VIS-NIR Hitachi spectrophotometer. Oscillator strength f is calculated by using the relationship,

$$f = 4.32 \times 10^{-9}\, \epsilon_{max}\, \Delta\bar{\nu}$$

where, ϵ_{max} is the experimental extinction coefficient at band maximum and $\Delta\bar{\nu}$ is the half band width (in wave numbers). The fluorescence measurements were made on a Perkin-Elmer MPF-44B spectrofluorimeter. Calculations were carried in the CNDO/S approximation of Del Bene and Jaffe[14,15], using the quantum chemistry program exchange (QCPE 174). Bond lengths and bond angles used in these calculations were taken from literature[16]. The molecular axes and number of atoms are designated in Fig. 1. The excited states were generated from the ground state occupied and virtual orbitals through a configuration interaction procedure between the forty lowest energy singly excited states. The characterisation of electronic

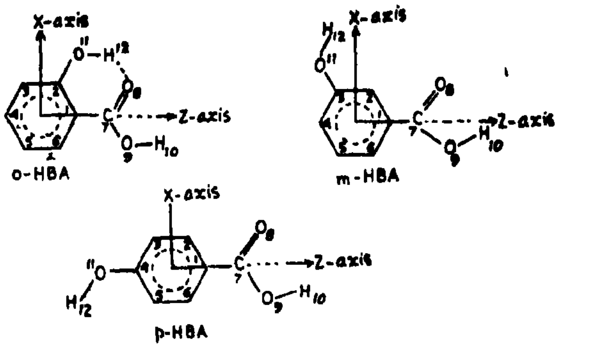


Fig. 1. Molecular axes designations of hydroxybenzoic acids, Y-axis is out of plane.

states have been made on the basis of configurational analysis. In order to study the intramolecular charge transfer in these states it is convenient to divide each hydroxybenzoic acid into the sub-systems $-OH$, $-C_6H_4-$ and $-COOH$. The charge on the various sub-systems have been obtained from the knowledge of electron densities on various atoms in the group. The electron densities on various atoms in the excited state j are given by.

$$^j\rho_A = \rho_A^0 + \sum_m^{CI} \sum_{\mu}^{A} C_{jm}^2 (C_{\mu r}^2 - C_{\mu i}^2)$$

† Dedicated to Professor Sadhan Basu on the occasion of his 65th birthday.
** Present address: Department of Biophysics, Panjab University, Chandigarh-160 014.

TABLE 1—ABSORPTION MAXIMA ($\bar{\nu}$, kK) OF ISOMERIC HYDROXYBENZOIC ACIDS IN VARIOUS SOLVENTS

Cyclohexane	Methylcyclohexane	Acetonitrile		Methanol		Ethanol	
$\bar{\nu}$	$\bar{\nu}$	$\bar{\nu}$	f	$\bar{\nu}$	f	$\bar{\nu}$	f
		o-Hydroxybenzoate Acid					
32.05 41.67 46.30	32.47 42.02	32.79 42.37	0.535 0.338	33.00 42.55 47.61	0.257 0.369 0.508	32.89 42.55 47.40	0.189 0.404 0.386
		m-Hydroxybenzoic Acid					
33.00 42.74 47.39	33.11	33.89 42.73	0.055 0.140	33.67 42.55 47.89	0.090 0.246 0.561	33.67 42.74 46.51	0.119 0.372 0.515
		p-Hydroxybenzoic Acid					
		35.21 39.68	0.008 0.789	33.33 39.37 48.54	Shoulder 0.408 0.340	33.33 39.22 47.17	0.012 0.687 0.874

TABLE 2—ABSORPTION MAXIMA ($\bar{\nu}$, kK) OF ISOMERIC HYDROXYBENZOIC ACIDS AT DIFFERENT pH VALUES

pH 1 (neutral)		pH 7 (monoanion)		pH >10 (dianion)	
$\bar{\nu}$	f	$\bar{\nu}$	f	$\bar{\nu}$	f
		o-Hydroxybenzoic Acid			
32.79 42.02 49.02	0.106 0.157 0.981	34.01 43.48	0.371 0.499	32.36* 41.49 43.86	0.102 0.171 0.133
		m-Hydroxybenzoic Acid			
33.76 42.02 48.08	0.087 0.148 0.574	34.64 43.48	0.126 0.467	31.95 41.15 45.87	0.061 0.162 0.520
		p-Hydroxybenzoic Acid			
39.06 46.81	0.657 0.421	35.46 40.65	0.043 0.443	35.46 46.08	0.490 0.168

* In 5 *N* KOH.

in which ρ_A^0 is the ground electron density on atom A and C_{jm} being the coefficient of the m th configuration contributing to the j th state. C_{pi} and C_{pi} are the orbital coefficients of the final and initial MO involved in the m th configuration. All calculations have been done on DEC 2050 machine.

Results and Discussion

Absorption spectra :

Neutral molecules : The absorption spectra of isomeric hydroxybenzoic acids were determined in various solvents. The $\bar{\nu}_{max}$ (in kK) values together with the oscillator strength (f) for these compounds are given in Tables 1 and 2. Due to the poor solubility of *p*-hydroxybenzoic acid in cyclohexane and methylcyclohexane the spectra could not be recorded even for the saturated solutions. The low energy absorption bands are blue-shifted with increase in the dielectric constant of polar solvents. However, this band is blue-shifted in methanol with respect to the spectra in acetonitrile for *o*-hydroxybenzoic acid whereas for *m*- and *p*-hydroxybenzoic acid a small red-shift is observed in going from acetonitrile to methanol. In aqueous solutions the spectra were recorded at pH~1 to ensure that the acids are present mainly in neutral form.

Monoanions : In water the carboxylic group of these molecules gets deprotonated. It has been found that between pH 7 and 8 the absorption spectra (Table 2) correspond to the species $HOC_6H_4COO^-$. All the bands are shifted to higher frequency in the benzoate ions.

Dianions : At still higher pH the phenolic group also dissociates to give the anion $\bar{O}C_6H_4CO\bar{O}$. For hydroxybenzoic acid, the dianion exists only in highly alkaline media (5 *M* KOH). The absorption spectra shift towards lower frequency side of the corresponding neutral molecules. This is possibly due to the participation of the lone pairs on hydroxyl oxygen and the carboxyl oxygens with the π-electron system of the benzene ring in the same plane.

TABLE 3—FLUORESCENCE MAXIMA ($\bar{\nu}$, kK) OF ISOMERIC HYDROXYBENZOIC ACIDS IN DIFFERENT SOLVENTS AND AT DIFFERENT *p*H VALUES

Hydroxybenzoic acid	Cyclohexane	Methylcyclohexane	Ethanol	Water		
				*p*H=1	*p*H=7	*p*H>11
ortho-	26.74-27.03	23.64	22.42-22.72	23.51-23.81 (23.66)	23.9	24.6*
meta-	30.67-31.45	30.03	26.74-28.90	27.80	24.60	24.6
para-	35.21-36.23	—	32.05-32.47	31.06-31.45 (31.25)	No fluorescence	29.9

* In 5 *N* KOH.

Emission spectra :

The emission bands for the hydroxybenzoic acids in different solvents and at different *p*H values are given in Table 3. It is apparent from Table 3 that significant red-shift in fluorescence occurs as the solvent polarity increases when compared to the spectrum in cyclohexane. This is indicative of increase in the dipole moment upon excitation. The behaviour of *o*-hydroxybenzoic acid is quite different from the *m*- and *p*-hydroxybenzoic acids. Due to close vicinity of OH and COOH groups and decrease in the *p*K of OH dissociation and increase in *p*K of COOH dissociation, the formation of zwitterion[17] in the excited state is possible.

Table 2 reveals that the mono- and di-anions of *meta*-isomer fluoresce at the same wavelength whereas the monoanion of *p*-HBA is non-fluorescent and the dianion of all isomers are strongly fluorescent. All the hydroxybenzoic acids show phosphorescence. The lowest triplet in EPA as solvent is observed at 24.55 in *ortho*-, 23.53 in *meta*- and 24.85 kK in case of *para*-hydroxybenzoic acids.

TABLE 4—ELECTRONIC STATE OF HYDROXYBENZOIC ACIDS

Experimental ν kK	Theoretical $\bar{\nu}$ kK	Theoretical f	Type
	o-Hydroxybenzoic Acid		
	24.53	0	S_1 $n\pi^*$
32.05	35.26	0.040	S_2 $\pi\pi^*$
	40.16	0	S_3 mix
	41.16	0	S_4 $n\pi^*$
41.67	43.30	0.042	S_5 $\pi\pi^*$
46.30	50.47	0.436	S_6 mix
	m-Hydroxybenzoic Acid		
	25.12	0	S_1 $n\pi^*$
33.00	35.67	0.019	S_2 $\pi\pi^*$
	41.03	0	S_3 $n\pi^*$
42.74	44.97	0	S_4 mix
47.39	50.36	0.502	S_5 $\pi\pi^*$
	p-Hydroxybenzoic Acid		
	25.68	0	S_1 $n\pi^*$
33.33*	35.96	0.006	S_2 mix
	41.22	0	S_3 $\pi\pi^*$
	42.47	0	S_4 $\pi\pi^*$
39.37*	48.21	0.169	S_5 mix
48.54*	51.54	0.407	S_6 mix

* In methanol.

Theoretical results and their correlation with experimental data :

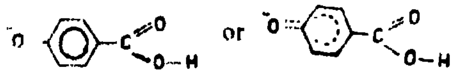
The theoretical values (after configuration interaction) are compared with the experimental results in cyclohexane (in methanol in the case of *p*-HBA) in Table 4. A number of theoretically predicted transitions for which oscilator strength is zero or small are not observed experimentally. The $S_0 \rightarrow S_2$ transition in all the isomeric hydroxybenzoic acids (mainly polarised along the short axis) has been assigned to the lowest observed band. The second experimentally observed band have been assigned to the theoretically predicted $S_0 \rightarrow S_5$ in *o*- and *p*-hydroxybenzoic acids and to $S_0 \rightarrow S_4$ in the case of *m*-hydroxybenzoic acid, which are polarised along the long axis of the benzene. The strongest absorption band at 46.30 kK in *o*-HBA and at 47.39 kK in *m*-HBA have been assigned to the $S_0 \rightarrow S_6$ and $S_0 \rightarrow S_5$ transitions, respectively. The agreement between the experimental and theoretical values of transition energies and other quantities seem to confirm the assignments.

Nature of the lowest excited state :

In benzoic acid and the lowest excited state is of $n\pi^*$ nature, however, in hydroxybenzoic acids the lone pair on oxygen of hydroxyl group is in conjugation with the π-electrons of benzene and this extended conjugation may lead to the energy of $\pi\pi^*$ transition nearly equal to or slightly lower than $n\pi^*$ transition energy. This is supported experimentally by the facts, (i) that the extinction coefficient of all the bands are quite large which cannot be due to $n\pi^*$ transition, (ii) that at room temperature fluorescence is generally observed if S_1 is a $\pi^* \rightarrow \pi$, and phosphorescence if S_1 is $\pi^* \rightarrow n$ and (iii) that the observed solvent effect also support the nature of the transition to be $\pi\pi^*$. It is possible that the $n\pi^*$ transition ($S_0 \rightarrow S_1$) may be burried under the strong $\pi\pi^*$ band.

The fluorescence properties (Table 3) of the various anionic species are quite interesting. In the case of *o*-HBA both the mono- and di- anionic forms fluoresce and the $\bar{\nu}_{max}$ are well separated. For the *m*-HBA, both the mono- and di-anionic forms fluoresce at the same $\bar{\nu}_{max}$ value whereas the monoanionic form in the case of *para*-isomer is non-fluorescent and the dianionic form is fluorescent. This could be explained as follows :

It is well known that the acidity of the phenolic[1,8,16] group increases tremendously in the singlet excited state. Thus, in the excited state the monoanion of *m*-HBA is converted into the dianion and the fluorescence data even at *p*H 7 correspond to that of dianions. This is further supported by the fluorescence data in the alkaline media. As mentioned earlier, the monoanion of *p*-HBA does not fluoresce whereas the dianion does. This clearly indicates the different behaviour of monoanions of *m*- and *p*-HBAs in the excited state, *i.e.* in the excited state monoanion of *m*-HBA is converted into the dianion and the monoanion of *p*-HBA is not converted into the dianion as the dianionic form is fluorescent. Possibly in the excited state, the phenolic hydrogen is transferred to the carboxylate ion inter-molecularly or intra-molecularly giving the

species 

which might be having the lowest singlet state of $n\pi^*$ nature and is thus non-fluorescent. It is worth mentioning here that the determination of gaseous phase acidity of these molecules by Kabrle[20] indicate that for *p*-HBA in the gaseous state it is the phenolic hydrogen which dissociates first, preferentially over the carboxylic hydrogen. The theoretical INDO calculations[21] on these molecules are also in agreement with our observations.

Acid-base equilibria :

The excited state pK_a values pK_a^* at room temperature for the equilibrium (I) and (II).

$$HO\phi COOH \rightleftharpoons HO\phi COO^- + H^+ \qquad (I)$$

$$HO\phi COO^- \rightleftharpoons {}^-O\phi COO^- + H^+ \qquad (II)$$

were calculated the Forster[22] cycle method, *i.e.* $pK_a - pK_a^* = 2.3\times10^{-3} (\bar{\nu}_{HA} - \nu_A)$, where ν_{HA} and $\bar{\nu}_A$ are the band maxima (cm^{-1}) of the acid and the conjugate base, respectively. The ground state pK_a values for the equilibrium (I) determined potentiometrically for the *o*-, *m*-, *p*-HBAs are respectively 3.00, 4.08 and 4.07, and the corresponding excited state pK_a^* (I) values calculated using the absoption data are found to be 5.56 and 6.31, respectively for the *o*- and *m*-HBA. The pK^* (I) and also pK^* (II) values for the *para*-isomer could not be calculated as the mono- and di-anionic species absorb at the same wavelength. The ground state pK_a (II) values for *o*-, *m*- and *p*-HBAs 10.82, 9.80 and 9.46 respectively, and the corresponding value for pK^* (II) are 10.35 and 3.73 for *o*- and *m*-HBAs. The pK^* values for equilibrium (I) are large compared to pK (I) and for equilibrium (II), pK^* (II) values are lower compared to pK_a (II) in the ground state. These are in agreement with the pK^* values reported for these type of equilibrium[18,19]. For the pure $\pi\pi^*$ singlet state the electronic charge density on the carboxylic group (q_{COOH}) increases and a qualitative correlation exists between q_{COOH} and pK^* (I) (Table 5). The fluorescence data cannot be used for the determination of pK^* (I) and pK^* (II) for the reasons explained above.

TABLE 5 – GROUND AND EXCITED STATE CHARGE DENSITIES IN HYDROXYBENZOIC ACIDS

Compound	Sub-system	Sate		Remarks
		S_0	^1L_b	
o-HBA	–OH	–0.106	0.033	$\pi\pi^*$
	–COOH	–0.001	–0.048	
	–ϕ–	–0.011	–0.166	
m HBA	–OH	–0.061	0.012	$\pi\pi^*$
	–COOH	–0.046	–0.106	
	–ϕ–	–0.015	–0.080	
p-HBA	–OH	–0.059	0.010	Mixed
	–COOH	–0.059	0.087	
	–ϕ–	–0.006	–0.056	

References

1. J. T. PINHEY and R. D. G. BIGBY, *Tetrahedron Lett.*, 1969, 1267.
2. J. T. PINHEY and R. D. G. BIGBY, *Tetrahedron Lett.*, 1969, 1271.
3. T. MATSUURA and OMURA K, *Bull. Chem. Soc. Jpn.*, 1966, **39**, 944.
4. J. A. BARLTROP, A. THOMSON and N. J. BUNCE, *J. Chem. Soc.* (C), 1967, 1142.
5. D. R. ARNOLD and P. C. WONG, *J. Am. Chem. Soc.*, 1967, **99**, 3861.
6. A. MARTIN, *Indian J. Chem., Sect. A*, 1977, **15**, 1093.
7. O. F. BEZUKOV, M. F. VUKS, V. L. RAPOPORT, L. V. SHURUPORA and A. A. MALEVSKII, *Mol. Fis. Biofis. Vodn. Sist.*, 1974, 2, 85.
8. W. L. PAUL and S. G. SCHULMAN, *Anal. Chim. Acta*, 1974, **69**, 195.
9. V. K. GORCHAKOVSKII and A. V. FINKEL'SHTEIN, *Zh. Fis. Khim.*, 1972, **46**, 496.
10. D. V. S. JAIN, F. S. NANDEL and P. L. SINGLA, *Indian J. Chem, Sect. A*, 1982, **21**, 559.
11. D. V. S. JAIN, F. S. NANDEL and P. L. SINGLA, *Indian J. Chem*, *Sect. A*, 1984, **23**, 451, 546.
12. D. V. S. JAIN, F. S. NANDEL, P. L. SINGLA and D. KAUR, *Indian J. Chem*, *Sect. A*, in the press.
13. J. A. RIDDICK and W. B. BUNGER, "Organic Solvents Physical Properties and Method of Purification", Wiley-Interscience, New York, 1970.
14. J. DELBENE and H. H. JAFFE, *J. Chem. Phys.*, 1968, **48**, 1807.
15. "QCPE 174 Quantum Chemistry Program Exchange", Indian University, Bloomington.
16. L. E. SALTON, *Chem. Soc. Spec. Publ.*, 1965, 18.
17. J. CATALAN and F. TOMAS, *Adv. Mol. Relaxation Processes*, 1976, **8**, 87.
18. W. BARTOK, P. J. LUCCHESI and N. S. SNIDER, *J. Am. Chem. Soc.*, 1962, **84**, 1842.
19. G. JACKSON and G. PORTER, *Proc. R. Soc. London, Ser. A*, 1961, **260**, 13.
20. T. B. MCMAHON and P. KEBARLE, *J. Am. Chem. Soc.*, 1977, **99**, 2222.
21. J. CATALAN and A. MACIAS, *J. Chem. Soc., Perkin Trans. 1*, 1979, 1632.
22. TH. FORSTER, *Z. Electrochem.*, 1950, **34**, 531.

J. Indian Chem. Soc.,
Vol. LXIII, January 1986, pp. 73-79

Lanthanide(III) f-f Transition Probabilities†

STEPHEN F. MASON

Chemistry Department, King's College, University of London, Strand, London WC2R 2LS, England

The dynamic coupling mechanism for f – f transition probabilities in lanthanide(III) complexes is extended to include the polarisability-anisotropy of the ligands, with applications to complexes with D_3 and D_4 coordination polyhedra. The ligand-polarisation and the crystal-field mechanisms for f – f transition probabilities are found to be complementary, applying primarily to the lower and the higher even 2^{λ}-pole transitions, respectively.

THE f-f transitions of lanthanide and actinide coordination compounds belong to the general class, $\Delta l=0$, which includes the d-d excitation of transition metal complexes and the p-p promotions of heteroatoms in organic chromophores. The probabilities of $\Delta l=0$ transitions are sensitive to the particular stereochemistry and to the polarisability of the ligand groups in the molecular environment of the chromophore, whether an open-shell metal ion or an organic heteroatom. Over a series of compounds containing a common chromophore, the oscillator strength of a given $\Delta l=0$ transition is found to cover a range of more than two orders of magnitude, dependent upon the symmetry of the ligand array and the electronic softness of the ligand groups. The intensity range is common to the organic p-p type[1], the d-d class in transition metal complexes[2], and to the quadrupolar f-f transitions of lanthanide coordination compounds[3,4]. For chiral stereochemistries, the rotational strengths of the $\Delta l=0$ transitions are even more sensitive to the particular location and to the polarisability of the ligand groups in the molecular environment of the chromophore[5].

Localised-system mechanisms :

The localised-system model for electronic transition probabilities, where electron exchange between the chromophore and the ligands is neglected, was developed in two directions during the 1930s, in connection with the theory of optical activity. The one-electron theory[6] postulated the mixing of the $\Delta l=0$ with $\Delta l=\pm 1$ electronic transitions of the chromophore under a static dissymmetric field due to the ligand groups. In contrast, the dynamic coupling theory[7] proposed that the leading electric multipole moment of the chromophore transition induces, and couples to, a secondary electric transition dipole in each ligand group.

Both of the localised-systems mechanisms were applied to the p-p type excitations of organic chromophores, notably the $n\rightarrow\pi^*$ carbonyl transition of chiral ketones. Following the early studies[6,8,9] the static coupling model was developed[10,11] on the basis that, at the oxygen atom, the $2p_y\rightarrow 2p_x$ component of the carbonyl $n\rightarrow\pi^*$ transition near 300 nm mixes with the corresponding Rydberg excitation, $2p_y\rightarrow 3d_{yz}$, under the Coulombic field of the incompletely-screened nuclei of the substituent atoms. In the corresponding development of the dynamic coupling model, it was proposed[12] that the leading electric moment of the carbonyl $n\rightarrow\pi^*$ transition, the xy-component of a quadrupole at the oxygen atom, induces a secondary electric dipole transition moment in a substituent group, dependent upon the polarisability of the group and its location in the molecular frame of the carbonyl chromophore. The electric dipole induced in the substituent group and the zero-order magnetic dipole moment have a scalar product which gives the carbonyl $n\rightarrow\pi^*$ transition a rotational strength conforming to the empirical octant rule[12], while the corresponding dipole strength becomes enhanced[13].

The parallel development of the localised-systems model for the f-f and the d-d transition probabilities in the lanthanide and transition metal coordination compounds was confined largely to the static-coupling mechanism, due to the general success of the crystal-field interpretation of the observed Stark-splittings of the corresponding transition energies. Following the pioneer applications[14-16], the static coupling mechanism for the Laporte-forbidden[17] transition probabilities was placed upon a quantitative basis for both the transition metal[18,19] and the lanthanide[20,21] coordination compounds.

The oscillator strengths of the d-d excitations in octahedral transition metal complexes are accommodated by the vibronic form of the static coupling mechanism[18], whereas the values calculated for the corresponding electronic transitions in analgous tetrahedral complexes are too small by some two orders of magnitude[19]. A further anomaly became apparent from studies of the temperature dependence of the d-d absorption intensities. The d-d oscillator strengths of octahedral transition metal complexes are found to increase as the temperature is raised, in accord with the vibronic static coupling mechanism. The intensity enhancement is due to the larger excursions from O_h symmetry with increasing tem-

† Dedicated to Professor Sadhan Basu on the occasion of his 65th birthday.

perature, owing to the increasing population of the higher vibrational levels of the non-totally symmetric modes in the electronic ground state of the complex[28]. A similar trend is expected for tetrahedral complexes, but the contrary behaviour is observed[28].

Stereochemical ligand hypersensitivity :

In the parallel application of the static coupling mechanism and its vibronic extension to the f-f transition probabilities of lanthanide coordination compounds[30,31], an exceptional set of hypersensitive f-f excitations was identified, following the selection rules for electric quadrupole transitions[3]. The oscillator strength of a hypersensitive f-f excitation, such as the $^4I_{9/2} \rightarrow {}^4G_{5/2}$ transition of a Nd^{III} complex near 590 nm, covers a range of some three magnitude orders, dependent upon the stereochemical symmetry of the ligand set, the polarisability of the ligands, and the metal-ligand bond lengths[4]. At the lower end of the range, exemplified by Nd^{III} as a guest ion in the LaF_3 host lattice, static coupling estimates give the 590 nm transition an intensity compatible with experiment[34], but the corresponding estimates for other Nd^{III} complexes are too small, particularly for the trihalides NdX_3 in the vapour phase at the higher end of the range[36].

In the initial survey of the possible sources of f-f hypersensitivity, an inhomogeneous dielectric mechanism was suggested, based upon the quasi-diatomic model of a lanthanide ion coordinated to a ligand with a polarisability larger than that of the surrounding medium[3]. The ligand increases the spatial gradient of the electric field vactor of the radiation across the lanthanide ion, and so enhances the f-f electric quadrupole transition probability[3]. Although intensity data were available for a number of lanthanide coordination compounds, the inhomogeneous dielectric mechanism was applied to no specific cases, and its potential as a dynamic coupling alternative to the standard static crystal field mechanism was not fully appreciated until recently[36,37].

Isotropic ligand polarisation :

The productive applications of the complementary dynamic coupling mechanism for the estimation of dipole and rotational strengths to the p-p excitations of chiral ketones[14,15] prompted an extension of the mechanism to d-d and f-f transition probabilities in open-shell metal ion coordination compounds. The extension provided a quantitative analysis for the d-d rotational strengths[38] of the chiral tris-diamine complexes of cobalt(III), and for the relatively large d-d dipole strengths[39] and the singular negative temperature coefficient of those strengths[40] in the tetrahedral halide-ion complexes of cobalt(II). In addition, the d-d Faraday transition probabilities determined from the magnetically-induced circular dichroism spectra of tetrahedral cobalt(II) complexes, while anomalous in sign according to static-coupling crystal field theory[41-43], are accommodated by the dynamic-coupling mechanism[44,45]. Applied initially to investigate the large oscillator strengths of the $^4I_{9/2} \rightarrow {}^4G_{5/2}$ f-f transition of neodymium(III) in the gaseous trihalides[46], the dynamic ligand polarisation mechanism is found to account for a wide range of hypersensitive f-f intensities[47,48], including the dipole strengths vibronically-induced in centrosymmetric lanthanide coordination compounds[49].

The Laporte-forbidden $\Delta l=0$ electronic promotions, according to the ligand-polarisation model, acquire a first order electric dipole probability from the correlated resultant of electric dipoles induced in the individual ligands by an allowed even-multipole electric moment of the metal ion excitation. The allowed electric 2^λ-pole moments of a $\Delta l=0$ transition lie in the range, $2<\lambda<2l$, that is, a quadrupole only for p-p promotions, the 2^2- and the 2^4-pole for d-d excitations, and the 2^6-pole additionally in the case of f-f transitions. Owing to the dependence of the potential between an electric 2^λ-pole and a dipole on $R_L^{-\lambda-2}$, where R_L is the metal-ligand bond length, the dynamic polarisation mechanism is the most effective for transitions with an electric quadrupole as the leading moment.

For isotropic ligands, such as the halide ions, or with ligands taken to have the mean polarisability $\bar{\alpha}_L(\nu_{om})$ at the metal ion transition frequency, the first order electric dipole moment, μ^γ_{om}, of the metal ion excitation, $M_o \rightarrow M_m$, with the electric quadrupole component, $\theta^{\alpha\beta}_{om}$, as its leading moment is given by the relation,

$$\mu^\gamma_{om} = -\sum_L \theta^{\alpha\beta}_{om}\, G^L_{\alpha\beta\gamma}\, \bar{\alpha}_L(\nu_{om}) \qquad (1)$$

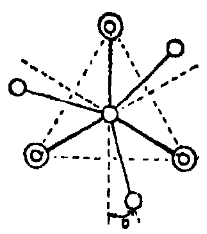
where, the sum is taken over the ligands, L. The geometric tensor $G^L_{\alpha\beta\gamma}$ represents the radial and angular terms governing the potential between the electric quadrupole component, $\theta^{\alpha\beta}_{om}$, centred on the metal ion, and the induced dipole, with γ-polarisation, located in the ligand, L. The Greek suffixes (α, β, γ) denote cartesian components (x, y or z) in the coordinate frame of the metal complex.

The development of equation (1) for a given $|f^NJ\rangle \rightarrow |f^NJ'\rangle$ quadrupolar transition of the metal ion in a complex with a single set of symmetry-related ligands affords an expression for the dipole strength of the transition as a function of the L–M–L bond angle, with a constant M–L bond length[48,50]. Relative to a unit dipole strength for the corresponding monocoordinate diatomic M–L case, a trigonal ML_3 complex has a ligand polarisation dipole strength which varies with the cosine of the L–M–L bond angle, c, according to the function, $3[1-3c+5c^2]$, over the stereochemical range from D_{3h} to C_{3v}. For trigonal complexes ML_3, notably, the lanthanide trihalides in the vapour phase, the dipole strength is an optimum for the bond angle of 117°, but the ligand polarisation intensity is only 1% smaller at the D_{3h} equilibrium nuclear configuration. The corresponding expression for the regular four-coordinate complexes over the general D_{2d} range, $\{-60[c+c^2+c^3]\}$, shows that the ligand polarisation dipole strength is optimum

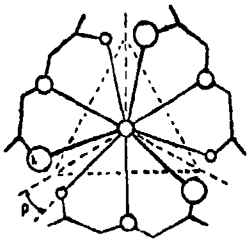
for an exact tetrahedral stereochemistry. The singular temperature-decrease in the dipole strengths of the quadrupole-allowed d-d transitions of the cobalt(II) tetrahalides is due to the large vibrational excursions from regular T_d symmetry with an increase in temperature[30,31].

Anisotropic ligand polarisation :

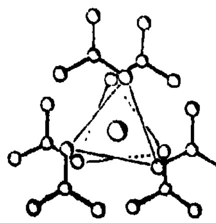
New features of the dynamic polarisation mechanism emerged from the analyses of the single crystal polarised spectra of the trigonal europium(III) complexes, $[Eu(H_2O)_9](EtSO_4)_3$ (I), $Na_3[Eu(ODA)_3].NaClO_4.6H_2O$ (II), and $Gd(Eu)Al_3(BO_3)_4$ (III). The $[EuO_9]$ cluster in each of the complexes (I) and (II) is made up of two ligand sets, a trigonal planar $[ML_3]$ group and a superimposed trigonal prism $[ML_6]$ group, the latter being regular (D_{3h}) in the nonahydrate (I), but distorted (D_3) in the complex (II), where each tridentate ODA ligand consists of the dianion of oxy-diacetic acid $[O(CH_2CO_2)_2]^{2-}$. The two D_{3h} ligand sets in the nonahydrate (I) are displaced by a small angle, *ca.* 5°, from the staggered configuration, so that the $[EuO_9]$ chromophore has C_{3h} symmetry overall. The six-coordinate $[EuO_6]$ cluster of the borate (III) has the D_3 distorted trigonal prism symmetry[40].



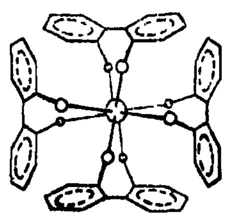
(I) $C_{3h}[Ln(H_2O)_9]^{3+}$ in $[Ln(H_2O)_9](EtSO_4)_3$



(II) D_3 9-coordinate $[Ln(ODA)_3]^{3-}$ in $Na_3[Ln\{O(CH_2CO_2)_2\}_3]$. $NaClO_4.6H_2O$



(III) D_3 6-coordinate $[Ln(BO_3)_6]^{3-}$ in $Gd(Ln)Al_3(BO_3)_4$



(IV) D_4 8-coordinate $[Ln(bpyO_2)_4]^{3+}$ in [Ln(bipyridine-*N,N'*-dioxide)$_4$]$(ClO_4)_3$

The application of equation (1) to the $\Delta M_J = \pm 2$ component of the $^7F_0 \rightarrow {}^5D_2$ f-f transition of Eu^{III} at a trigonal site, where the (xy) and (x^2-y^2) components of an electric quadrupole are the leading transition moments, shows that the contribution of both the $[ML_3]$ and the $[ML_6]$ ligand set to the first order electric dipole transition moment is substantial. The two contributions are out of phase, however, so that the net resultant is small in the complexes (I) and (II). With only the $[ML_6]$ trigonal prism ligand set, the complex (III) has a $\Delta M_J = \pm 2$ dipole strength larger by an order of magnitude than the corresponding strength of either the complex (I) or (II) (Table 1). In contrast, the pure magnetic-dipole transition $^7F_0 \rightarrow {}^5D_1$, is ligand-insensitive, and has a similar dipole strength in each of the Eu^{III} complexes[40] (Fig. 1, Table 1).

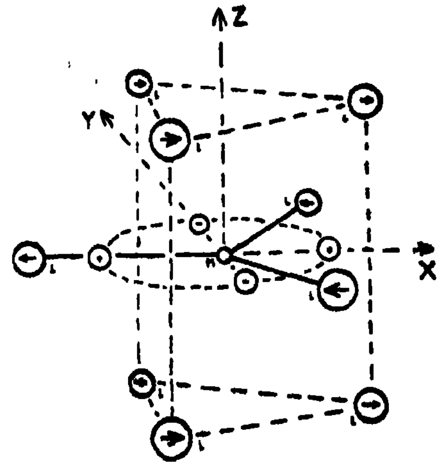


Fig. 1. The electric dipole moments induced in the ligands of a 9-coordinate trigonal Ln^{III} complex by the (x^2-y^2) component of the electric quadrupole f-f transition moment of the metal ion, showing the negative interference between the resultant induced dipole of the equatorial $[ML_3]$ ligand set and that of the $[ML_6]$ trigonal prism ligand set.

The treatment of the $\Delta M_J = \pm 1$ component of the $^7F_0 \rightarrow {}^5D_2$ f-f transition of Eu^{III}, with the (yz) and (zx) components of an electric quadrupole as the leading moments at a trigonal site, requires a consideration of the anisotropy of the ligand polarisability. The $\Delta M_J = \pm 1$ component is observed in the spectra of the D_3 complexes (II) and (III), but not in that of the C_{3h} nonahydrate (I), as expected on group-theoretical grounds. The mean polarisability approximation of the dynamic coupling mechanism (equation 1) fails to account for the observed $\Delta M_J = \pm 1$ dipole strengths. These are accommodated by the inclusion of the ligand anisotropy through the relation,

$$\langle 0 \mid \mu_\gamma^{(1)} \mid m \rangle = -\langle 0 \mid \theta^{(2)}_{\alpha\beta} \mid m \rangle \sum_L [\alpha_{\gamma\delta} G^{(3)}_{\alpha\beta\delta}]_L^{(2)} \quad (2)$$

where, $\alpha^L_{\gamma\delta}$ refers to the $\gamma\delta$-component of the polarisability tensor of the ligand L in the global coordinate frame of the complex at the transition frequency. The electric dipole polarisability tensor of a ligand is made up of the three irreducible sets, $\alpha^{(0)}$, $\alpha^{(1)}$, and $\alpha^{(2)}$. The scalar mean polarisability, $\alpha^{(0)}$, enters into equation (1), whereas the five symmetric polarisability components, forming an irreducible second rank tensor, $\alpha^{(2)}$, are of primary concern in equation (2).

Recent theoretical analysis of the dynamic coupling mechanism[41,42], and an earlier study of crystal field and general one-electron mechanisms for f-f transition probabilities[43], show that the

TABLE 1—EUROPIUM(III) COORDINATION COMPLEXES

Frequency $\tilde{\nu}$ (cm^{-1}) and dipole strength D_{om} ($10^{-66}C^2m^2$) of the zero-order magnetic dipole $^7F_0 \rightarrow {^5D_1}$ and electric quadrupole $^7F_0 \rightarrow {^5D_2}$ f - f transition of Eu^{III} observed in the axial (ax) and in the polarised (π parallel, σ perpendicular) *ortho*-axial single crystal spectra of (I) $[Eu(H_2O)_9](EtSO_4)_3$, (II) $Na_3[Eu(ODA)_3].2NaClO_4.6H_2O$, (III) $Gd(Eu)Al_3(BO_3)_4$, and the spectrum of (IV) $[Eu(bpyO_2)_4](ClO_4)$ in acetonitrile solution

Transition component (polarisation)	I (C_{3h}) $\tilde{\nu}$	I (C_{3h}) D_{om}	II (D_3) $\tilde{\nu}$	II (D_3) D_{om}	III (D_3) $\tilde{\nu}$	III (D_3) D_{om}	IV (D_4) $\tilde{\nu}$	IV (D_4) D_{om}
$^7F_0 \rightarrow {^5D_1}$								
$\Delta M = \pm 1$ (π+ax)	19 020	30	18 981	31	18 966	38	18 990	28
$\Delta M = 0$ (σ)	19 024	26	18 965	24	18 995	23		
$^7F_0 \rightarrow {^5D_2}$								
$\Delta M = \pm 2$ (σ+ax)	21 490	10	21 433	14	21 419	230	*a*	*a*
$\Delta M = \pm 1$ (σ+ax)	*a*	*a*	21 484	62	21 491	220	21 470	680

a = Absent.

introduction of the polarisability anisotropy of the ligands increases the scope of the dynamic mechanism by widening the range of the allowed ranks (t) of the ligand-dependent tensor, $[\alpha_{\gamma\delta}\, G^{(s)}_{\alpha\beta\delta}]_L^{(t)}$ in equation (2). If the polarisability of the ligand group is contracted to the scalar mean value, the tensor overall is limited to rank-3, the rank of the geometric component, $G^{(3)}_{\alpha\beta\delta}$. The rank restriction is not necessarily lifted on taking the polarisability anisotropy of the ligands into account, notably, for the higher coordination symmetries, such as C_{3h}, D_{3h} or T_d, where the point group operations limit the coordinated ligand groups to an effectively cylindrical form around a metal-ligand bond axis.

More generally, the representation of the ligand polarisability element, $\alpha^L_{\gamma\delta}$, by one of the five components of the symmetric second rank polarisability tensor of the ligand group requires, in equation (2), an introduction of the direction cosines referring to the orientation of the ligand bonds considered in the overall frame of the coordination polyhedron[18]. Thereby, the element, $\alpha^L_{\gamma\delta}$, is transformed into the local diagonal form in terms of the anisotropy invariant, $\beta_L = (\alpha_\parallel - \alpha_\perp)_L$, on the assumption of an effectively cylindrical ligand bond symmetry. Each set of direction cosines forms a tensor of rank-2 and contraction extends the range of allowed ranks (t) of the ligand dependent tensor, $[\alpha_{\gamma\delta}\, G^{(s)}_{\alpha\beta\delta}]_L^{(t)}$ in equation (2), to first and second, in addition to the third-rank tensor alone required in the corresponding scalar mean-polarisability approximation (equation 1).

The even, second-rank, ligand-dependent tensors are unique to the anisotropic ligand polarisation mechanism for quadrupolar $\Delta l = 0$ electronic transitions. The corresponding ligand-dependent terms of the crystal field mechanism, A^t_p, are necessarily odd, with t = 1, 3 for quadrupolar electronic promotions, and they imply cylindrically symmetric metal-ligand interaction. Local $C_{\infty v}$ symmetry around each metal-ligand bond is precluded in coordination polyhedra with dihedral symmetry and, for the quadrupolar metal ion excitations, only the rank-2 ligand dependent tensors survive in a D_4 coordination cluster[41,42]. The rank-2 tensor mediates solely the $\Delta M_J = \pm 1$ quadrupolar transition component in a D_4 complex, as in the D_3 cases of $[Eu(ODA)_3]^{3-}$ and $Gd(Eu)Al_3(BO_3)_4$ where, additionally, a rank-3 ligand-dependent tensor governs both the anisotropic and the mean isotropic polarisability contributions of the ligand groups to the probability of the corresponding $\Delta M_J = \pm 2$ transition component[40,44] (Fig. 2).

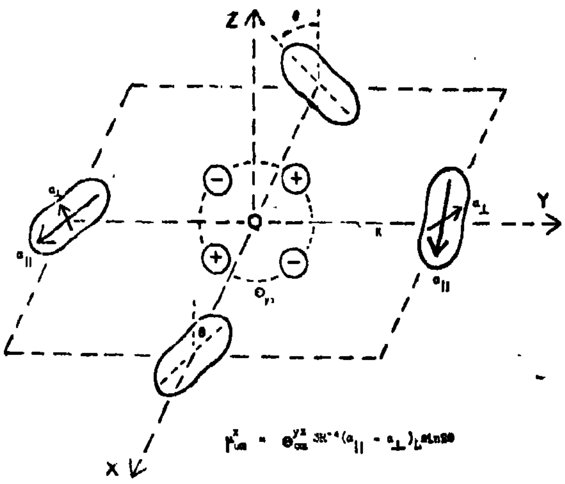


Fig. 2. Only a second rank field polarisation tensor, dependent on the ligand polarisability anisotropy, survives for electric quadrupole transitions of D_4 complexes, restricted to the yz- and the degenerate zx- component of the quadrupole transition moment.

The eight-coordinate tetrakis(2,2'-bipyridine-*N*,*N'*-dioxide)lanthanum perchlorate crystal structure[45] indicates that the complex cation has D_4 symmetry, and the spectrum of the analogue, $[Eu(bpyO_2)_4](ClO_4)_3$ (IV), in the region of the $^7F_0 \rightarrow {^5D_2}$ absorption shows only the $\Delta M_J = \pm 1$ component, assigned from a comparison of its frequency with that of the corresponding component for the D_3 analogues (II) and (III) (Table 1). The dipole

strength of the component for the complex (IV) is consistent, through equation (2), with the measured polarisability anisotropies of the ligand bonds, including that of the *N*-oxide bond[44], which makes the major intensity contribution[44]. While the $\Delta M_J = \pm 1$ component of the $^7F_0 \rightarrow {}^5D_2$ transition in the D_3 analogues (II) and (III) has an electric dipole probability governed similarly by a unique rank-2 polarisation tensor, the upper state has E symmetry in D_3, like the upper state of the corresponding $\Delta M_J = \pm 2$ component, and M_J-mixing cannot be ruled out in the D_3 cases. A corresponding M_J-mixing is not feasible in the complex (IV), since states with B_1 and B_2 symmetry result from the $\Delta M_J = \pm 2$ component and only the upper state of the $\Delta M_J = \pm 1$ component has E symmetry in the D_4 group of (IV). Thus both the crystal field and the isotropic ligand polarisation intensity mechanism are ruled out for the D_4 complex (IV), leaving anisotropic ligand polarisation as the sole localised-systems mechanism consistent with the observed dipole strength[44].

Complementary static and dynamic coupling intensity contribution :

The theory of f-f transition probabilities due to Judd[20] and Ofelt[21] provides, for a given lanthanide coordination compound, a set of three dipole strength parameters, Ω_λ ($\lambda = 2$, 4 or 6), which may be compared with the corresponding observed quantities. Although the Judd-Ofelt theory was formulated on the electrostatic crystal field basis[20,21], the intensity parameterisation is general for all one-electron mechanisms[48]. The empirical intensity parameters are obtained from the manifold of $J \rightarrow J'$ bands, each with the dipole strength $D_{JJ'}$, observed in the f-f spectrum of the Ln^{III} complex through the relation,

$$D_{JJ'} = (2J+1)^{-1} \sum_\lambda \Omega_\lambda \,|\, (J' \| U^{(\lambda)} \| J) \,|^2 \qquad (3)$$

The reduced matrix elements in equation (3), $(J' \| U^{(\lambda)} \| J)$, refer to the unit tensor $U^{(\lambda)}$ operating within the $4f^N$ configuration and express the fractional even 2^λ-pole moment of the $J \rightarrow J'$ transition. The corresponding dipole strength parameters, Ω_λ, represent the square modulus of the first order electric dipole moment of the f-f excitation, whether of a crystal field or another origin, associated with the zero-order electric 2^λ-pole moment ($\lambda = 2$, 4 or 6) of the transition. With a set of the reduced matrix elements of $U^{(\lambda)}$, a least-squares analysis of the manifold of $J \rightarrow J'$ intensities in the spectrum of a given Ln^{III} complex provides the three empirical Ω_λ(obs) parameters[47,48].

The crystal field and the ligand polarisation mechanisms for f-f transition probabilities are independent within the localised-systems model, and the first order electric dipole moments given by the two mechanisms for a particular excitation are vectorially additive. The expression for the total dipole strength parameter, Ω_λ(tot), of the $J \rightarrow J'$ manifold exhibited by a particular Ln^{III} complex contains terms corresponding, not only to the square modulus of each first order electric dipole moment, Ω_λ(CF) for the crystal field contribution and Ω_λ(LP) for the ligand polarisation contribution, but also to a pseudoscalar cross term, Ω_λ(CT), between the static and the dynamic component of the first order electric-dipole transition moment,

$$\Omega_\lambda(\text{tot}) = \Omega_\lambda(\text{CF}) + \Omega_\lambda(\text{LP}) + \Omega_\lambda(\text{CT}) \qquad (4)$$

The cross term, Ω_λ(CT), is non-vanishing for a first order static field and dynamic coupling electric dipole moment with the same polarisation, connected with a common component of a given zero-order electric 2^λ-pole moment of the metal ion transition[49-51].

The ligand polarisation dipole strength parameter, Ω_λ(LP), represents essentially the square modulus of the first order electric-dipole transition moment of equations (1) and (2) and the analogous expressions for the corresponding zero-order electric 2^4- and 2^6-pole moments of the metal ion transition. The crystal field dipole strength parameter, Ω_λ(CF), is made up of two principal terms, one dependent solely on the metal ion, $P_{\lambda t}$, which expresses the mixing of a f-f transition possessing a leading 2^λ-pole moment with a dipolar $4f \rightarrow 5d$ or $4f \rightarrow ng$ transition, and the other dependent only on the ligands, A_p^t, representing the odd-parity electrostatic crystal field experienced by the metal ion,

$$\Omega_\lambda(\text{CF}) = (2\lambda+1) \sum_{t=1}^{7} \sum_{m=-t}^{+t} \,|\, P_{\lambda t} A_p^t \,|^2 (2t+1)^{-1} \qquad (5)$$

The order (t) of the crystal field parameter A_p^t is restricted to the values, $t = (\lambda \pm 1)$, with $\lambda = 2$, 4 or 6.

Estimates of the crystal field and the ligand polarisation contributions to the overall dipole strength of particular $J \rightarrow J'$ f-electron transitions in the complexes $[Ln(H_2O)_9]^{3+}$ (I) and $[Ln(ODA)_3]^{3-}$ (II), for the Ln^{III} cases of Pr, Eu, Tb and Ho, indicate that the crystal field contribution is generally dominant, the ligand polarisation contribution being of comparable significance only for the hypersensitive quadrupolar transitions[49,50]. In complexes of the structural types (I) and (II), the ligand polarisation contribution to the first order electric-dipole transition moment is minimised by negative interference, due to the out-of-phase relation between the individual contributions of the $[ML_3]$ and the $[ML_6]$ ligand sets[40]. Moreover, for D_3 and higher dihedral coordination polyhedra, such as the complex (II), only the anisotropic polarisability contributions (equation 2) are non-zero for $\Delta M_J = \pm 1$ transitions[40,44], and these contributions were not taken into account in the estimates[49,50].

The eight-coordinate tetrakis(dithiocarbamate)-Ln^{III} complexes, $Na[Ln(Et_2dtc)_4]$, provide a more comprehensive comparison of the relative crystal field and ligand polarisation contributions to the overall dipole strength parameters, Ω_λ (equation 4), for the majority of the lanthanides[51]. Crystals of

the coordination compounds, $Na[Ln(Et_2dtc)_4]$, are isomorphous over the lanthanide range La to Yb, and the crystal structure of the La^{III} complex shows that the $[LaS_8]$ cluster has the stereochemical form of a distorted dodecahedron, in which the four CS_2 chelate groups are arranged at the vertices of a quasi-tetrahedron[19]. The transition frequencies and the dipole strengths over the generally accessible f-f manifold have been determined for the majority of the $Na[Ln(Et_2dtc)_4]$ complexes[32], allowing an extraction of the three dipole strength parameters, Ω_λ with $\lambda=2$, 4 or 6, for each member of the series.

The calculated estimates of the total dipole strength parameters, $\Omega_\lambda(tot)$, for the series of $[Ln(Et_2dtc)_4]^-$ complexes are in fair agreement with the corresponding empirical values $\Omega_\lambda(obs)$ for $\lambda=4$ and 6 directly and for $\Omega_2(tot)$ with an allowance for the screening of the 4f electrons by the outer $5s^25p^6$ shell[28], partly compensated by nephelauxetic effects. In principle[24], the Hartree-Fock radial expectation values for the 4f electrons of the Ln^{III} ion, $\langle r^\lambda\rangle_{HF}$, require scaling by a screening, σ_λ, and an antiscreening, τ_λ, factor to give the effective value, $\langle r^\lambda\rangle_{eff}$, where,

$$\langle r^\lambda\rangle_{eff}/\langle r^\lambda\rangle_{HF}=(1-\sigma_\lambda)/\tau_\lambda \qquad (6)$$

For the series of $[Ln(Et_2dtc)_4]^-$ complexes, the comparison of the $\Omega_\lambda(tot)$ estimates with the corresponding $\Omega_\lambda(obs)$ values indicates[28] that the screening/antiscreening ratio (equation 6), while approximating to unity for $\lambda=4$, 6, has a value, in the case of $\lambda=2$, of *ca.* 0.8 for the heavier lanthanides and decreases over the lighter lanthanides to *ca.* 0.5 for Pr^{III}. Calculated values[24] of the screening constants σ_4 and σ_6 are small, but the values obtained for σ_2 are 0.675 for Tm^{III} and as large as 0.825 for Pr^{III}. These theoretical σ_2 values indicate that the antiscreening constant τ_2 approximates to 0.4, due largely to nephelauxetic and Ln^{3+} charge-reduction effects[28] (Fig. 3).

Overall the calculated dipole strength parameters (equation 4) show that the dynamic polarisation mechanism is important mainly for the hypersensitive quadrupolar f-f transitions, as originally envisaged[18,28] from the dependence of $\Omega_\lambda(LP)$ upon $R_L^{-2\lambda-4}$. There are no major differences between the relative crystal-field and ligand-polarisation contributions to the $\Omega_\lambda(tot)$ values across the series of $Na[Ln(Et_2dtc)_4]$ complexes from Pr to Yb. On an average over the series, the ligand polarisation contribution to $\Omega_\lambda(tot)$ decreases from 66 to 17 and to 0.1% for $\lambda=2$, 4, 6, respectively, while the corresponding crystal field contribution increases from 5 to 57 and 98.5%, respectively. The remaining pseudoscalar cross term component, $\Omega_\lambda(CT)$ in equation (4), is significant for $\lambda=2$ and 4, contributing the respective average of 29 and 25%, respectively[31,32].

Conclusion :

Within the general independent-systems model, the static and the dynamic coupling mechanisms provide complementary first order perturbation treatments of $\Delta l=0$ electronic transition probabilities. The multiplet-to-multiplet f-f intensities of the excitations with an electric 2^6-pole as the leading moment are governed predominantly by the crystal field mechanism in the $[Ln(Et_2dtc)_4]^-$ complexes, and probably in all lanthanide coordination compounds. The dynamic polarisation mechanism has its salient applications to the probabilities of $\Delta l=0$ transitions with an electric quadrupole or, to a lesser degree, an electric hexadecapole as the leading moment in noncentric compounds with a single set of polarisable ligands, which are symmetry-related, or approximately so. Where there are multiple sets of ligands with a small polarisability, as in the case of the Ln^{III} guest ions in the LaF_3 host lattice, both the crystal field[24] and the ligand polarisation[37] treatments account individually for the observed quadrupolar f-f intensities, and the two mechanisms are not distinguished.

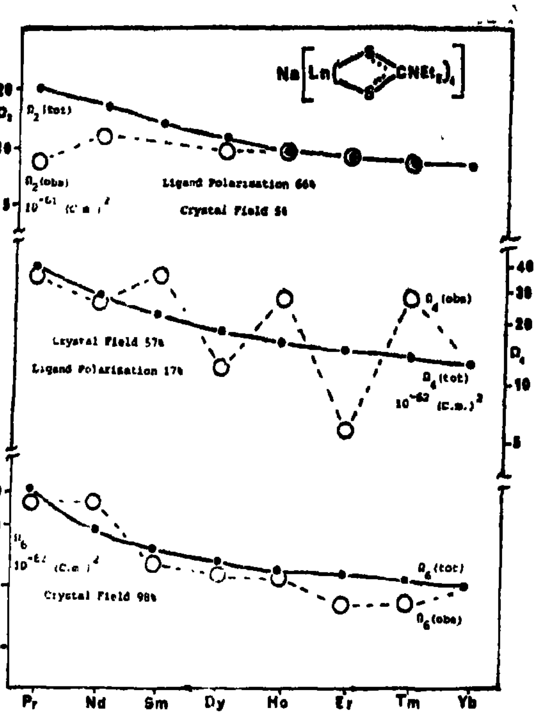


Fig. 3. The relationship across the series of lanthanide coordination compounds, $Na[Ln(Et_2dtc)_4]$, between the observed, Ω_λ (obs), and the total calculated dipole strength parameter, Ω_λ (tot) (equation 4), with a screening/antiscreening ratio (equation 6) of unity for $\lambda=4$, 6 and with the value of 0.8 for $\lambda=2$.

A distinction between the two mechanisms may by drawn from the restriction of the ligand-dependent crystal field parameters, A_t^s (equation 5) to the odd values, $t=(\lambda\pm1)$, with $\lambda=2$, 4 or 6, depending upon the leading electric 2^λ-pole of the metal ion transition. A group-theoretical treatment of the electric dipole intensity parameters for f-f transitions shows that the range is restrictive, the even value, $t=\lambda$, being allowed additionally for more

general one-electron mechanisms[49]. The corresponding dynamic coupling ligand-dependent parameters, including the components of the symmetric second-rank polarisability tensor of the ligands, $[\alpha^{(2)}G^{(\lambda+1)}]^{(t)}$, have the range of ranks $t=\lambda$, $(\lambda\pm1)$, required group-theoretically[40–44]. The even-rank value, $t=\lambda$, is particular to the dynamic coupling mechanism and, for quadrupolar $\Delta l=0$ transitions in coordination compounds with D_4 and higher dihedral symmetry, such as (IV), the only non-zero dynamic polarisation intensity parameters are second rank, like those of the $\Delta M_J=\pm1$ quadrupolar transitions in the D_3 complexes (II) and (III).

References

1. S. F. MASON, *Quart. Rev. Chem. Soc.*, 1961 **15** 287; 1963. **17**, 20.
2. C. K. JORGENSEN. *Adv. Chem. Phys.*, 1963, **5**, 33.
3. C. K. JORGENSEN and B. R. JUDD, *Mol. Phys.*, 1964, **8**, 281.
4. R. D. PEACOCK, *Struct. Bonding*. 1975, **22**, 83.
5. S. F. MASON, "Molecular Optical Activity and the Chiral Discriminations", Cambridge University Press, 1982, pp. 38 ff, 103, ff.
6. E. U. CONDON, W. ALTAR and H. EYRING, *J. Chem. Phys.*, 1937, **5**, 753.
7. J. G. KIRKWOOD, *J. Chem. Phys.*, 1937, **5**, 479.
8. W. J. KAUZMAN, J. E. WALTER and H. EYRING, *Chem. Rev.*, 1940, **26**, 339.
9. A. MOSCOWITZ, *Adv. Chem. Phys.*, 1962, **4**, 67.
10. T. WATANABE and H EYRING, *J. Chem. Phys.*, 1964, **40**, 3411.
11. T. D. BOUMAN and A. MOSCOWITZ, *J. Chem. Phys.*, 1968 **48**, 3115.
12. E. G. HORN and C. E. WEIGANG, JR., *J. Am. Chem Soc.*, 1966, **88**, 3673; *J. Chem. Phys.*, 1968, **48**, 1127.
13. G. M. ROBINSON and C. E. WEIGANG, JR., *J. Am Chem Soc.*, 1969, **91**, 3709.
14. J. H. VAN VLECK, *J. Phys. Chem*., 1937, **41**, 67.
15. L. J. F. BROER, C. J. GORTER and J. HOOGSCHAGEN, *Physica*, 1945, **11**, 231.
16. Y. TANABE and S. SUGANO, *J. Phys. Soc. Jpn.*, 1954, **9**, 753, 766.
17. O. LAPORTE, *Z. Phys.*, 1924, **51**, 512.
18. A. D. LIEHR and C. J. BALLHAUSEN, *Phys. Rev.*, 1957, **106**, 1161.
19. C. J. BALLHAUSEN and A. D. LIEHR, *J. Mol. Spectrosc.*, 1958, **2**, 342; 1960, **4**, 190.
20. B. R. JUDD, *Phys. Rev.*, 1962, **127**. 750.
21. G. S OFELT, *J. Chem. Phys.*, 1962, **37**, 1962.
22. C. HOLMES and D. S. McCLURE, *J. Chem. Phys.*, 1957, **26**, 1686.
23. D. M. GRUEN and R. L. McBETH, *Pure Appl. Chem.*, 1963, **6**, 23.
24. R. P. LEAVITT and C. A. MORRISON, *J. Chem. Phys.*, 1980, **73**, 749.
25. D. M. GRUEN and C. W. DE KOCK, *J. Chem. Phys.*, 1966, **45**, 455.
26. B. R. JUDD, *J. Chem. Phys.*, 1979, **70**, 4830.
27. B. R. JUDD, *ACS Symposium Series*, 1980, **131**, 267.
28. S. F. MASON and R. H. SEAL, *Mol. Phys.*, 1976, **31**, 755.
29. R. GALE, R. E. GODFREY, S. F. MASON, R. D. PEACOCK and B. STEWART, *J. Chem. Soc., Chem. Comm.*, 1975, 329.
30. R. GALE, R. E. GODFREY and S. F. MASON, *Chem. Phys. Lett.*, 1976, **38**, 441.
31. P. J. STEPHENS, *J. Chem. Phys.*, 1965, **43**, 444.
32. R. G. DENNING, *J. Chem. Phys.*, 1966, **45**, 1307.
33. R. G. DENNING and J. A. SPENCER, *Symp. Faraday Soc.*, 1969, **3**, 84.
34. R. GALE, R. E GODFREY and S. F. MASON, *Chem. Phys. Lett.*, 1976, **38**, 446.
35. S. F. MASON, *Struct. Bonding*, 1980, 39, 43.
36. S. F. MASON. R. D. PEACOCK and B. STEWART, *Mol. Phys.*, 1975, **30**, 1829.
37. R. D. PEACOCK, *J. Mol. Struct.*, 1978, **46**, 203.
38. A. F. KIRBY and R. A. PALMER, *Inorg. Chem.*, 1981, **20**, 1030.
39. T. R. FAULKNER and F. S. RICHARDSON, *Mol. Phys.*, 1978, **35**, 1141; 1979, **36**, 193.
40. R. KURODA, S. F. MASON and C. ROSINI, *Chem. Phys. Lett.*, 1980, **11**, 11; *J. Chem. Soc., Faraday Trans. 2*, 1981, 2125.
41. B. STEWART, *Mol. Phys.*, 1983, **50**, 161.
42. M. F. REID and F. S. RICHARDSON, *J. Chem. Phys.*, 1983, **79**, 5735.
43. D. J. NEWMAN and G. BALASUBRAMANIAM, *J. Phys., C*, 1975, **8**, 37.
44. S. F. MASON, and B. STEWART, *Mol. Phys*, 1985, **55**, 611.
45. A. R. AL-KARAGHOULI, R. O. DAY and J. S. WOOD, *Inorg. Chem.*, 1978, **17**, 3701.
46. R. S. ARMSTRONG, M. J. ARONEY, K. E. CALDERBANK and R. K. PIERENS, *Aust. J. Chem.*, 1977, **30**, 1411.
47. W. T. CARNALL, P. R. FIELDS and B. G. WYBOURNE, *J. Chem. Phys.*, 1965, **42**, 3797.
48. W. T. CARNALL, P. R. FIELDS and K. RAJNAK, *J. Chem Phys.*, 1968, **49**, 4412, 4424, 4443, 4447, 4450.
49. F. S. RICHARDSON, J D. SAXE, S. A. DAVIS and T. R. FAULKNER, *Mol. Phys.* 1981, **42**, 1401
50. F. S. RICHARDSON, *Chem. Phys. Lett.*, 1982, **86**, 47.
51. S. F. MASON and G. E. TRANTER, *Chem. Phys. Lett.*, 1983, **94**, 29.
52. M. CIAMPOLINI, N. NARDI, P. C LAMARINO and P. ORIOLI, *J. Chem. Soc., Dalton Trans.*, 1977, 879.
53. S. F. MASON, *Inorg. Chim. Acta*, 1984, **94**, 313.
54. P. ERDOS and J. H. KANG, *Phys. Rev.*, 1972, **6**, 3393.

J. Indian Chem. Soc.,
Vol. LXIII, January 1986, pp. 80-84

Multicomponent Phosphorescence Spectrum of Triphenylamine and its Separation by MIDP Spectroscopy†

T. N. MISRA

Optics Department, Indian Association for the Cultivation of Science, Calcutta-700 032

and

NORIKO IWASAKI and MINORU KINOSHITA

The Institute for Solid State Physics, The University of Tokyo, Roppongi, Minato-ku, Tokyo 106, Japan

The phosphorescence spectra of triphenylamine have been measured in various matrices at 1.4 K. In the neat crystal, the O,O band is most intense, while in the other matrices, the bands around at 0-100 cm⁻¹, which is assigned to the movement of the ensemble of three benzene rings, appear very strongly. The dependence of the spectra on matrices is interpreted by difference in molecular conformation.

INTEREST in the study of aromatic amines stems from the fact that the phosphorescence to the fluorescence quantum yield ratio is large and the mean phosphorescence life time is short in these molecules compared to those in aromatic hydrocarbons. This enhancement of spin-orbit coupling in aromatic amines is very sensitive to the twisting of the lone-pair orbital (*l*-orbital) axis of the nitrogen atom relative to the attached ring planes[1,2]. In addition to this fact, in aromatic amines which have more than two benzene rings, the interaction between rings plays an important role in the optical properties. The MO calculations have shown that the electron-transfer interaction between the two benzene rings of diphenylamine[3] is important in interpreting the absorption spectrum of the molecule. Due to these facts we can expect the radiative properties of aromatic amines depend very much on the molecular geometry and therefore, on matrices.

In this paper we report the phosphorescence spectra of triphenylamine in a neat crystal and in some other matrices at liquid helium temperature. In the neat crystal, the phosphorescence spectrum is very sharp, while in other matrices, it is very broad and is separated into the spectra of several components with the aid of MIDP (microwave induced delayed phosphorescence) spectroscopy. The dependence of spectra on matrices is interpreted by difference in molecular geometry.

Experimental

Triphenylamine (Tokyo Kasei Co.) was purified by recrystallisation from ethanol, vacuum sublimation and finally by zone-refining (more than 100 passes). The substances used as matrices were purified by the same procedure. Neat and mixed crystals were grown by Bridgman method.

The samples were excited by an Ushio 250 W high pressure Hg lamp through Toshiba UV-D33S filter. An 8 bits, 64 kbytes microcomputer 20 IF800 (Oki Denki Co., Ltd.) controlled the experimental equipment consisting of excitation and detection shutters, microwave sweep oscillators (Hewlett Packard 8620A and Weinshell 221), a Jobin-Yvon HR1000 monochromator and a Biomation 805 waveform recorder. Simultaneously the microcomputer treated the signals from the waveform recorder by appropriate procedure and accumulated the data.

The MIDP spectroscopy was applied for separating a multicomponent emission into a set of spectra of individual components. This method was originally used for obtaining a set of sub-level spectra[4]. However, the method utilising a lock-in amplifier is sometimes subject to difficulty in determining an uniform baseline over a whole spectral region. Especially, the difficulty arises when it is applied to multicomponent emission and strongly emitting components do not respond to the applied microwaves resonant to a particular component. The use of a microcomputer makes it possible to compensate the background even in such a case. A CRT display of the initial setting for taking an MIDP spectrum is shown in Fig. 1. The phosphorescence decay curves with and without microwaves are alternately measured at a certain wavelength and shown here as a superposition. In this particular example, two zero-field microwave transitions are observed ; one is weak at 2.19 GHz and the other is strong at 2.25 GHz. The vertical lines are input from the computer console to separate the regions of the dark level and the transitions. The dark level in the region I is used commonly to correct the intensity in the regions II and III.

The integrated intensity of the MIDP signal in the region II, for instance, at the wavelength

† Dedicated to Professor Sadhan Basu on the occasion of his 65th birthday.
A part of the article was presented at the National Conference on Spectroscopy and Theoretical Chemistry held at Calcutta, December 5-7, 1985.

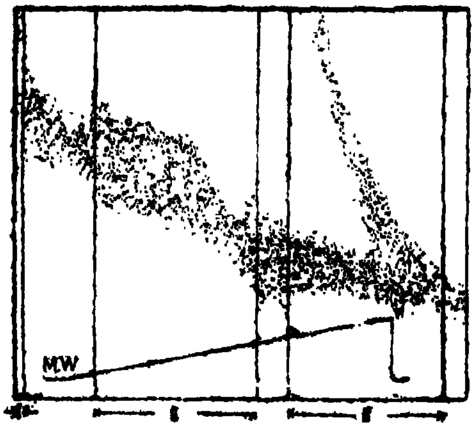


Fig. 1. A hard copy of the CRT display showing the initial setting for obtaining MIDP spectra. There are two MIDP signals which are separated by the vertical lines as the regions II and III. The region I determines the dark level. The microwave transitions occur at 2.19 and 2.25 GHz. The output of ramp voltage for microwave sweep is indicated by an inset denoted by M.W.

λ, $I_{II,\lambda}$, is given by

$$I_{II,\lambda} = \sum_{\substack{t_i \\ \text{(region II)}}} \{I_M(t_i) - I_O(t_i)\}_\lambda,$$

where, $I_M(t_i)$ and $I_O(t_i)$ are the intensity of the decay with and without microwaves at time t_i, respectively. The summation runs over the whole time region of II. For a weak signal, the intensity data may be accumulated to improve S/N ratio, and then the spectrometer is scanned to the next wavelength successively. In this way, the MIDP spectrum of the component responding to the microwaves of 2.19 GHz is obtained. The spectrum for the species resonant to the microwaves of 2.25 GHz corresponding to the region III is also stored simultaneously in the computer. The MIDP spectra shown in Fig. 5 were obtained in this way.

Results

Neat crystal : The phosphorescence spectrum of the triphenylamine neat crystal at 1.4 K is shown in Fig. 2. The lower spectrum was measured with 10 μm entrance and exit slit widths and the upper one was recorded with 70 μm slit widths in order to magnify relatively weak vibrational band structure. The O, O band is very strong and very sharp. Only one species seems to contribute to the phosphorescence in the neat crystal. Indeed, no emission from any other traps is observed even when the temperature is elevated to 4.2 K.

Several weak but sharp vibrational bands are observed at 0-100, 0-288, 0-718 and 0-1 593 cm^{-1}. The assignments of the vibrational bands in the spectrum have been performed on the basis of the vibrational analysis of ir and Raman spectra of related aromatic amines[6] and on refering to a few ir and Raman data previously reported for tri-

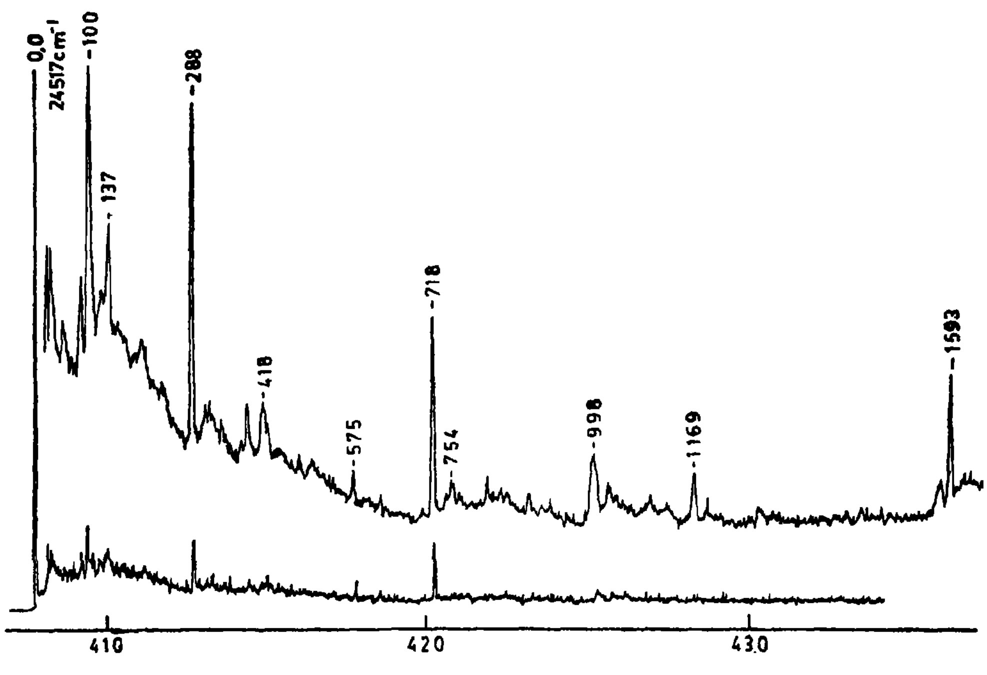


Fig. 2. The phosphorescence spectrum of the triphenylamine neat crystal at 1.4 K. The upper trace is a magnification with wider slitwidths.

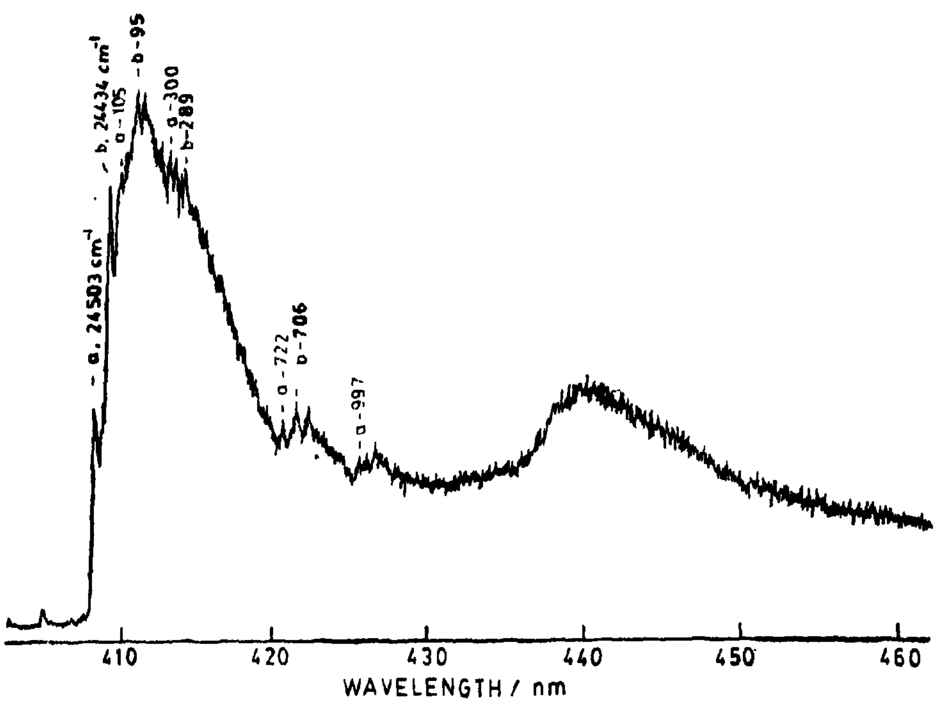


Fig. 3. The phosphorescence spectrum of triphenylamine in diphenylamine at 1.4 K.

phenylamine[6,7]. The band at 0-100 cm^{-1} is attributed to the ensemble movement of the three benzene rings. The band at 0-288 cm^{-1} would be due to the C–N–C deformation. The band at 0-718 cm^{-1} would be assigned to the vibrational mode of benzene rings of which the frequency changes very much with substituents attached to N in aromatic amines. These vibrations which are related to the nitrogen atom appear relatively strongly among the vibronic bands observed in the phosphorescence spectrum. On the other hand, the following vibrations which are mainly distributed on the benzene moiety appear very weak. These vibrations are 418, 754, 998 and 1 169 cm^{-1} and are assigned to the vibrations originating from ν_{18}, ν_{11}, ν_1 and ν_6 of benzene, respectively. Only the band at 0-1 593 cm^{-1} also originating from benzene ν_8, appears relatively strongly.

The phosphorescence decay of the triphenylamine neat crystal is exponential even at 1.4 K with the lifetime of 270 ms. The spin-lattice relaxation is not suppressed and no microwave transitions are observed in the neat crystal.

In diphenylamine: The phosphorescence spectrum of triphenylamine in diphenylamine is shown in Fig. 3. The spectrum becomes very broad, but there are some very weak vibrational bands superimposed on it. The vibrational analysis of these bands indicates the presence of at least two emitting species as denoted by *a* and *b* in the spectrum in addition to the species giving rise to the broad spectrum. The vibrational frequencies of the bands correspond well to those observed in the neat crystal. The MIDP signals are observed around 2.24 and 1.96 GHz. A similar spectrum of triphenylamine is also observed in the bis(4-bromophenyl) ether host.

In methylcyclohexane (MCH): The phosphorescence spectrum of triphenylamine in MCH shows somewhat complicated behaviour. The spectra partly shown in Fig. 4 indicate that there is a concentration dependence. At a concentration higher than 10^{-4} mol dm^{-3} the spectrum shows the maximum at 407.5 nm. When the concentration is lower than 10^{-5} mol dm^{-3} the maximum position shifts to 409.5 nm and the very sharp band appears at 405.6 nm.

The MIDP signals are observed at 2.19, 2.25, 2.31 and 2.33 GHz. The decay rate constants for the fast decaying components are commonly found to be about 4.5 s^{-1} and those for the slowly decaying components about 0.5 s^{-1}. The relative intensities of these signals also show a concentration dependence. The signals are very weak at 10^{-3} mol dm^{-3}. At 10^{-4} mol dm^{-3}, the signals at 2.25, 2.31 and 2.33 GHz are strong, but the signal at 2.19 GHz is weak. At 10^{-5} mol dm^{-3}, on the contrary, the signal at 2.19 GHz is strong, but the others become weak.

To see the relation between the phosphorescence spectrum and the microwave transitions, the MIDP spectra are measured around the O,O band at 1.4 K. The emission spectra from the components, those responded to the microwaves of 2.33, 2.31, 2.25 and 2.19 GHz, are shown in Fig. 5. The MIDP spectra

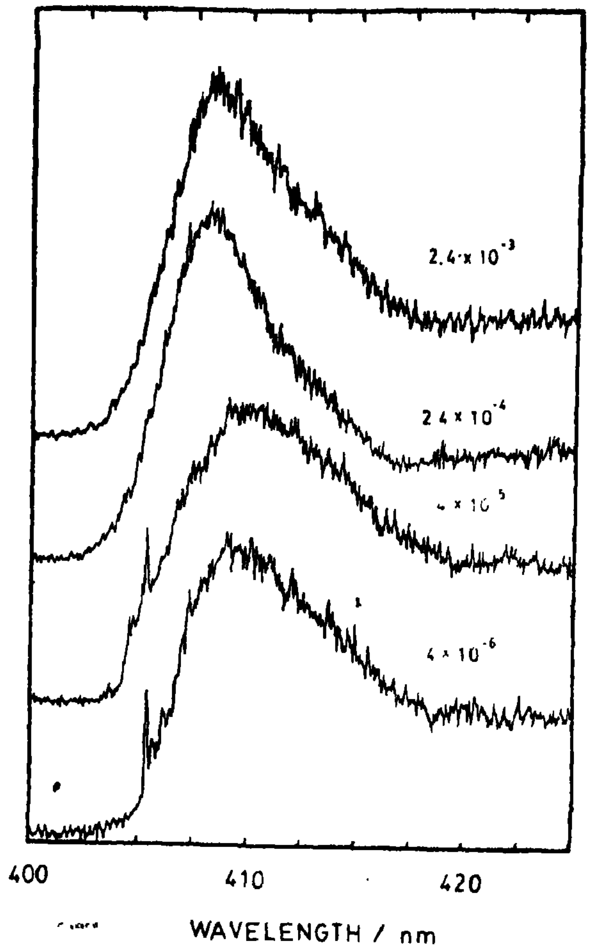


Fig. 4. The phosphorescence spectra of triphenylamine in methylcyclohexane at various concentrations and at 1.4 K.

observed at 2.33, 2.31 and 2.25 GHz are shifted from each other, but the spectral shapes are almost identical with each other having a shoulder band separated by about 110 cm^{-1} from the main peak. This wavenumber corresponds well to the vibration assigned to the ensemble motion of the phenyl groups. Thus, these three spectra could be ascribed to triphenylamine embedded in different environments in MCH.

The MIDP spectrum obtained at 2.19 GHz, is broad in comparison with the others and seems to consist of several components. This might mean that the signal at 2.19 GHz includes the counterparts of the other signals originally belonging to degenerate transitions and consists of three or more components. We have tried EEDOR (electron-electron double resonance) experiments to find any correlation among these signals, but without any success. We have also tried to further decompose the MIDP signal at 2.19 GHz into any components by narrowing the sweep width of the microwaves, but have not succeeded in obtaining any definite result. From these observations, it seems to be probable that the four signals belong to different species of triphenylamine.

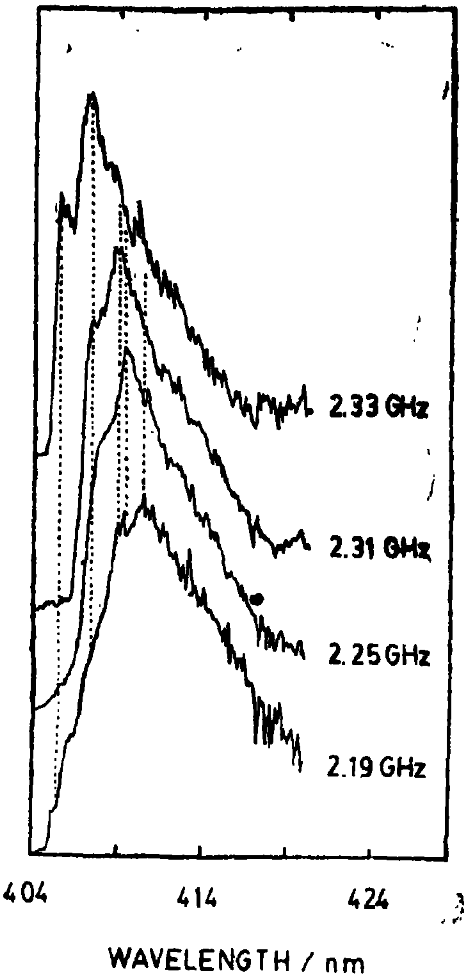


Fig. 5. The MIDP spectra of triphenylamine in methylcyclohexane (10^{-4} mol dm^{-3}) around the 0,0 band at 1.4 K. The multicomponent emission is separated into four components by the microwave transitions at the frequencies indicated.

Discussion

The phosphorescence spectrum of triphenylamine changes markedly depending on matrices. This finding is just in accordance with the expectation we made in the introductory section. As the spin-orbit coupling in aromatic amines is dependent on the relative orientation of the *l*-orbital and the benzene ring planes, the radiative properties of triphenylamine would be sensitively determined by the twist angle of phenyl groups to a pyramidal plane and the C–N–C angle.

These angles are expected to be susceptible to the environmental effect and the molecular conformation would be determined by the environment of the molecule embedded. In the gas phase, the

electron diffraction studies[9] have shown that triphenylamine has the C_s symmetry and the twist angle and the C–N–C angle are 47±5 and 116°, respectively. In a benzene solution, the C–N–C angle has been estimated to be 110-107° from the measurements of electric dipole moment[10]. On the other hand, the analysis of the crystal structure of triphenylamine has not yet been completed ; it has been terminated at the stage that there are either two or four molecules in the asymmetric unit[11]. However, the molecular structure in a crystal may be inferred from the structure of triphenylphosphin. In a crystal, triphenylphosphin has no C_s symmetry and the angles of three benzene ring planes relative to the pyramidal planes are not equal[12]. This is explained by the repulsion due to inter-molecular forces rather than the repulsion of the hydrogen atoms within the molecule. Probably this result would also apply to triphenylamine and this susceptivity to the environmental effect on molecular conformation would explain the difference observed in the phosphorescence spectra of this compound.

In the neat crystal, most of the phosphorescence intensity is concentrated on the well-defined O,O band and the vibrations mainly associated with the benzene rings carry the intensity only slightly. This suggests that the density of the two unpaired electrons comprising the triplet state is comparatively high in the proximity of the central nitrogen atom, although the results of photoelectron spectroscopy[8] indicate that the highest occupied molecular orbital of triphenylamine is the π-orbital which is spread over the benzene rings. In MCH, on the other hand, the vibronic bands at 0-110 and around 0-1 500 cm^{-1} which are related to the vibrations in the benzene moiety become very strong, indicating that the two electrons have higher probability to reside on the benzene rings. Therefore, in the neat crystal, triphenylamine seems to take a conformation favorable for admixture of the (l, π^*) state into the lowest triplet state, whereas in MCH it takes conformations less favorable for admixture. Since it is the (l, π^*) state that is most responsible for the spin-orbit coupling, even a slight change in the degree of its admixture would have rather large effect on the radiative properties of such a molecule as triphenylamine which is liable to the environmental perturbations. In other words, the phosphorescence spectrum of triphenylamine is subject to a marked change depending on matrices, even though the molecular conformations in different matrices are varying only slightly from each other.

In methylcyclohexane, the spectra show the concentration dependence. The reason for this is not clear at this stage. There may exist molecular aggregates at higher concentration, or there may also be a possibility that methylcyclohexane takes different structures depending on the concentration of triphenylamine.

References

1. M. KASHA and H. R. RAWLS, *Photochem. Photobiol.*, 1968, **7**, 561.
2. E. C. LIM and M. KEDZIERSKI, *Chem. Phys. Lett.*, 1973, **20**, 242.
3. T. HINOHARA, S. OHO and T. MORITA, *Bull. Chem. Soc. Jpn.*, 1971, **44**, 629.
4. E. KANEZAKI, N. NISHI, M. KINOSHITA and K. NIIMORI, *Chem. Phys. Lett.*, 1974, **29**, 529.
5. A. PERRIER-DATIN and J.-M. LEBAS, *J. Chem. Physico-chim. Biol.*, 1972, **69**, 591.
6. R. T. C. BROWNLEE, R. E. J. HUTCHINSON, A. R. KATRITZKY, T. T. TIDWELL and R. D. TOPSOM, *J. Am. Chem. Soc.*, 1968, **90**, 1757.
7. S. HIGUCHI, H. TSUYAMA, S. TANAKA and H. KAMADA, *Spectrochim. Acta, Part A*, 1973, **30**, 463.
8. T. P. DEBIES and J. W. RABALAIS, *Inorg. Chem.*, 1974, **13**, 308.
9. Y. SASAKI, K. KIMURA and M. KUBO, *J. Chem. Phys.*, 1959, **31**, 477.
10. C. W. N. CUMPER and A. P. THURSTON, *J. Chem. Soc.* (*B*), 1971, 422.
11. E. R. HOWELLS, F. M. LOVELL, D. ROGERS and A. J. C. WILSON, *Acta Cryst.*, 1954, **7**, 298.
12. J. J. DALY, *Z. Krist.*, 1963, **118**, 332 ; J. J. DALY, *J. Chem. Soc.*, 1964, 3799.

J. Indian Chem. Soc.,
Vol. LXIII, January 1986, pp. 85-90

X-Ray Edge Absorption Coefficients and Covalency of Bonding†

K. J. RAO

Solid State and Structural Chemistry Unit, Indian Institute of Science, Bangalore-560 012

A method has been suggested for measurement of covalency of bonding using X-ray edge absorption coefficients. Expressions have been derived which emphasise the role of screening by electrons involved in covalent bonding. Usefulness of the method in understanding bonding in a few glasses has been illustrated. Use of higher initial quantum states in edge absorption studies has been shown to give rise to higher sensitivity of absorption coefficients to covalency effect.

COHESION in solids arises from different types of bonding[1]. Among these ionic covalent and metallic types of bonding give rise to large cohesive energies compared to van der Waals and hydrogen bond types. In many solids, cohesion arises from more than one type of bonding. The structure and stability of solids are determined by the details of such bonding. Thus, close packed structures are common in metals and large coordinations occur in ionic solids. Similarly, more open low coordination structure of covalent solids is a consequence of directionality of bonding in them. Melting and solid state polymorphism can also be directly related to the nature of interaction potentials in these materials[2]. Hence, one of the primary concerns of physical chemistry is to understand the nature of bonding in solids in sufficient detail.

The need to understand the nature of bonding becomes even more acute in amorphous solids because here, one finds very often the same chemical compound existing with and without long-range order. With the loss of long-range order, the temperature ranges of stability of the glasses decrease to almost two-thirds or less[3] (the glass transition temperature, T_g is approximately equal to two-thirds of the melting temperature, T_m). Further, the specific volumes of glasses are also generally higher than those of corresponding crystalline solids. Combined with the observation that covalently bonded materials are usually good glass formers[3], the above features make it appear quite probable that the bonding in glasses is more covalent. Increase in covalency introduces a directionality in bonding and reduction in the coordination number. Increased covalency is often associated with a shrinkage in the inter-atomic distances which increases the cohesive energy arising from the near-neighbour interactions[4,5]. This conditioning of the nature of bonding in amorphous solids is an important subject to study in order to understand the glassy state.

This work is confined to a consideration of the ionic-covalent bond duality which pervades a very large part of inorganic solids. Many attempts have been made to relate quantitatively the extent of ionicity of a bond to chemical parameters, like electronegativity differences, *etc.*[6,7]. But ionicity estimates are very difficult to obtain experimentally. Several methods have been discussed in the literature[8-10]. But the applicability of these methods become quite restricted since they are generally based on measurement of magnetic properties or optical transitions arising in transition-metal ions. It has now been found that a suitable experimental method is provided by X-ray absorption spectroscopy (XAS). Materials with ionic-covalent mixed types of bonding may be investigated by an analysis of the absorption coefficients of the edges in XAS. This paper describes briefly an analysis of covalency effect using absorption coefficients in XAS. Some examples from the author's investigations are presented where the method appears quite promising.

Covalency also causes chemical shifts in edge energies[11,12]. But the analysis of chemical shifts can be quite complicated[13] and is unsuitable when covalency effects are marginal.

Principles of XAS :

X-ray spectroscopy consists of measuring X-ray absorption coefficients as a function of proton energy. Sudden jumps in absorption coefficients occur at the absorption edges (Fig. 1) due to the excitation of core electrons. Well above the edge, the absorption coefficients decay and is associated with intensity modulations described as Extended X-ray Absorption Fine Structure (EXAFS)[14]. This region consists of valuable structural information which, however, is not discussed in this article. Absorption coefficient variations are also present at the edges also upto ~ 30 eV above the edge and are described as X-ray Absorption Near Edge Structure (XANES).

† Dedicated to Professor Sadhan Basu on the occasion of his 65th birthday.

Communication No. 327 from Solid State and Structural Chemistry Unit.

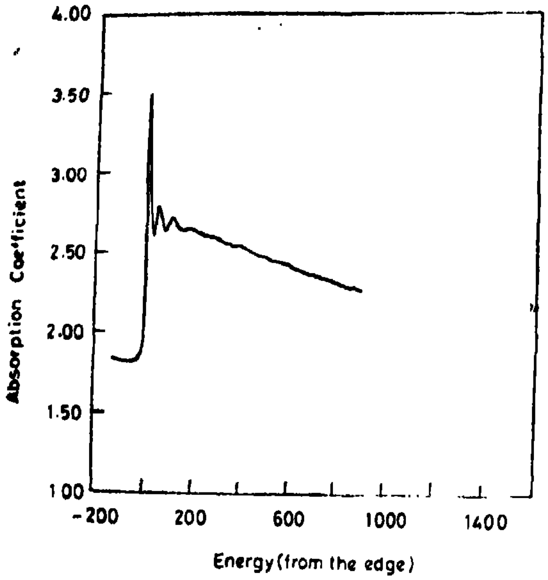


Fig. 1. A typical *X*-ray absorption spectrum associated with the L_3-edge of Th in crystalline ThF_4. The spectrum is unnormalised.

The origin of XANES is quite simply excitation of core electrons to available unoccupied energy levels which may have atomic or molecular character[3,16]. Unoccupied final states of very high energies (well above the bonding states) often correspond to extended states and electrons in such levels undergo multiple scattering from neighbouring atoms which affects the spectral features. Such effects are both complicated and poorly understood[17]. The features closely associated with the absorption edge are a result of excitations to localised bound states and may, therefore, be treated as core electron spectrum. Excitations are governed by the selection rules of atomic and molecular spectroscopy. With conventional *X*-ray sources edge spectra can be obtained quite easily at energies corresponding to K-edges of elements like Ti and above. But with the advent of synchrotron radiation, sufficiently good spectra can be obtained even for edges requiring photons of 7-8 A wavelength. It enables study of K-edges of elements such as aluminium and silicon. With heavier elements (such as silver and beyond), it is convenient to study the L-edge spectra Rare-earth L-edges are particularly suitable for investigation with most *X*-ray sources. Though much less has been reported in the literature on M-edge spectra, M-edges of heavier elements, like thallium, bismuth, lead, *etc.* should in principle be easy to investigate. *X*-ray spectra are recorded straight as absorption coefficients in synchrotron based work which are further normalised using experimental edge jumps[14].

Absorption coefficients and effect of covalency :

In general, the absorption coefficient corresponding to such an edge is given by[18]

$$\mu=\frac{4\pi e^2}{n\hbar c}\,|\,M_{if}\,|^2.\delta(E_i-E_f-\hbar\omega) \qquad (1)$$

where, n is the refractive index, E_i and E_f are the energies of the initial and final states, respectively, ω is the circular frequency of the photon, δ is Kroneckers delta and M_{if} is the dipole matrix element (defined further later). The expression is derived on the basis of one electron approximation and Koopman suddenness criterion. In further discussions, we assume the applicability of equation (1). M_{if} is given by the expression,

$$M_{if}=\langle i\,|\,r_a\,|\,f\rangle \qquad (2)$$

where, $\langle i\,|$ and $|\,f\rangle$ are the initial and final state wave functions, respectively. One can, therefore, theoretically evaluate the absorption coefficients, provided suitable wave functions are available. In the present context where we investigate the variation of bonding nature, approximate wave functions, such as Slater orbitals may be employed without serious prejudice to the basic objective.

Absorption coefficients are affected significantly when the final state wave functions are affected as may be easily seen from equations (1) and (2). The final states are affected when the nature of bonding is altered because such changes remove or reinforce electron density in the final state. When the final state is a valence state directly involved in bonding, the effect is quite obvious. But when the final state is a vacant orbital not involved in bonding, the variation in electron density in the bonding orbital alters the screening of the final state which in turn affects M_{if}. The first situation is illustrated by some transition metal complexes where the bonding states are themselves final states in $L_{2,3}$-edge spectra. The absorption coefficients are determined by vacancies in the d-orbitals which vary according to the nature of ligands. But the situation arising from screening of the final states is particularly valuable in the study of bond-ionicity variations which we exploit further in the following.

Let us consider a completely ionic complex with an M^{a+} .. A^{b-} bond. Further, that the valence levels involved in the M ... L bonding are ns and np (n is the principal quantum number). The associated $L_{2,3}$-spectra make use of vaccant nd levels for $|\,f\rangle$ When A is substituted by a less electronegative ligand A′, the M-A′ bond becomes slightly covalent. As a consequence of this a small electron density may be considered to have been brought back to ns, np levels of M. This alters the screening of nd levels which affects $|\,f\rangle$ and M_{if}. Let us suppose ν electrons are added back to ns, np levels by covalency. We can estimate the effect of this on M_{if} by using appropriately screened wave func-

tion for $|f\rangle$ (and also for $|i\rangle$) in the form,

$$|f\rangle,\ (|i\rangle) = (r^{n_f^*-1}) \exp[(z-s_f)]\, r/n_f^*] \quad (3)$$

$$(\mu_{cov}/\mu_{ion}) = |M_{if}|^2_{cov} / |M_{if}|^2_{ion} \quad (4)$$

where, μ_{ion} and μ_{cov} are absorption coefficients corresponding to purely ionic and partially covalent situations, respectively.

$$|M_{if}|_{ion} = \int_0^\infty [r^{n_f^*-1}\, e^{(z-s_f)r/n_f^*}] \,.\, r \,.\, [r^{n_i^*-1}\, e^{(z-s_i)r/n_i^*}]\, dr \quad (5)$$

with a similar expression for $|M_{if}|_{cov}$. The quantities in equation (5) can be simplified with the following substitutions,

$$\left.\begin{aligned} (n_f^*+n_i^*-1) &= n_e \\ z(1/n_f^*+1/n_i^*) &= Z_e \\ (s_f/n_f^*+s_i/n_i^*) &= S_e \end{aligned}\right\} \quad (6)$$

Equation (5) may now be written as

$$|M_{if}|_{ion} = \int_0^\infty r^{n_e} \,.\, e^{(Z_e - S_e)r}\, dr$$

and

$$|M_{if}|_{cov} = \int_0^\infty r^{n_e} \,.\, e^{(Z - S'_e)r}\, dr \quad (7)$$

Hence,

$$\frac{|M_{if}|^2_{cov}}{|M_{if}|^2_{ion}} = \frac{|\Gamma(n_e+1)/(Z_e-S'_e)^{n_e+1}|^2_{cov}}{|\Gamma(n_e+1)/(Z_e-S_e)^{n_e+1}|^2_{ion}} = \left(\frac{Z_e-S_e}{Z_e-S'_e}\right)^{2n_e+2} \quad (8)$$

where, $\Gamma(x)$ are Gamma functions. S'_e is higher than S_e because of the screening caused by the electrons responsible for covalent bonding. S_e and S'_e are related as

$$S'_e = S_e + \frac{\nu \times 0.35}{n_f^*}$$

where, ν is the number of covalency electrons added to ns, np levels. Hence, equation (8) becomes

$$\frac{|M_{if}|^2_{cov}}{|M_{if}|^2_{ion}} = \left(\frac{Z_e-S_e}{Z_e-S_e-0.35\nu/n_f^*}\right)^{2n_e+2} \quad (9)$$

Since $(Z_e - S_e) \gg 0.35\ \nu/n_f^*$ the relation for absorption coefficient ratio becomes

$$\frac{\mu_{cov}}{\mu_{ion}} = \frac{|M_{if}|^2_{cov}}{|M_{if}|^2_{ion}} = 1 + \frac{0.35\ \nu(2n_e+2)}{(Z_e-S_e)\,n_f^*} \quad (10)$$

Equation (9) and (10) very clearly establish that when a bond becomes less ionic (or more covalent) the edge absorption coefficient should also increase. In fact, equation (9) could be generalised as

$$\frac{\mu_{cov}}{\mu_{ion}} = \frac{Z_e-S_e-S_0}{Z_e-S_e-S} \quad (11)$$

where, S_0 like S is the screening factor (screening divided by n_f^*) arising due to known covalency of M–L bond in a standard whose edge absorption coefficient is μ_{ion}. S_0 is zero for ideally ionic M–L bond. The degeneracies of the final states, however, do not affect equation (11) or other previous expressions. It may further be noted from equations (6) and (9) that $Z_e - S_e$ is systematically smaller for initial states of lower quantum number n_i^*. This further suggests that the effect of covalency on absorption coefficient ratio get amplified by the choice of higher energy initial states, M-edge spectra being more sensitive to covalency than L-edge spectra and being still more sensitive than K-edge spectra.

Two important results of this simple analysis are as follows: (i) increase in bond covalency always brings about an enhancement in the edge absorption intensities and (ii) this effect is more pronounced for initial states of higher quantum numbers. It is therefore possible to use edge spectroscopy to determine covalency of bonding by investigating the absorption coefficients. Before discussing some of the examples, we may wish to note that irrespective of the nature of wavefunctions employed in the analysis, a direct correlation exists between the edge absorption coefficients and the covalency of bonding. Since $|f\rangle$ is essentially atomic in character the measurements monitor the covalency effect using spectroscopic property of the central atom only. Also, the changes occurring in μ measures the totality of the covalency effect of all the ligands. The information obtained from the measurements reflect an average covalency of the M–L bonds. This feature has both advantages and disadvantages. The method does not provide information about covalencies of each individual types of bonds when several types of ligands are present around the central atom. For the same reason it could be advantageous in amorphous materials where only such average bond ionicity information is meaningful.

Some case studies :

We shall briefly consider some examples from studies in glasses. In crystalline NdF_3, Nd^{III} ion is coordinated to nine fluoride ions and bonding of neodymium to fluorine is considered to be completely ionic. However, when NdF_3 is added to BeF_2 glass neodymium cannot be expected to maintain its large coordination number. A lower coordination number is very likely for neodymium in the glasses. But the value should still be higher than that of beryllium (equal to four) since Nd^{III} ions are unlikely to substitute for Be^{II} ions in the glass. EXAFS studies[18] have confirmed these features indicating that neodymium has a coordination number of seven in these glasses. The decreased coordination is also associated with a small decrease in the Nd–F

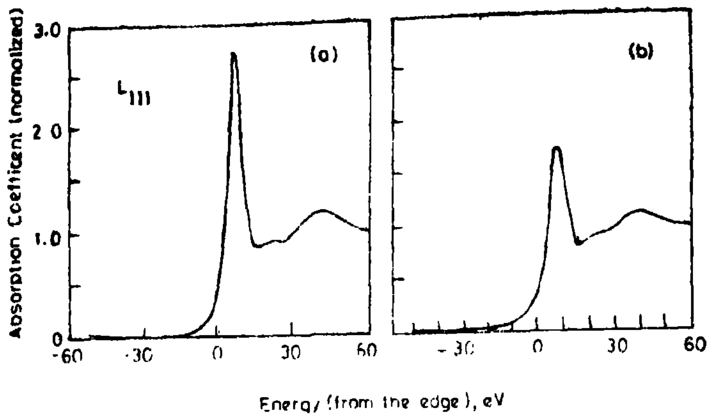


Fig. 2. Normalised L_3-edge spectrum of Nd^{III} : (a) in glass (NdF_3-BeF_2) and (b) in crystalline NdF_3 (normalisation procedure may be seen in Ref. 18).

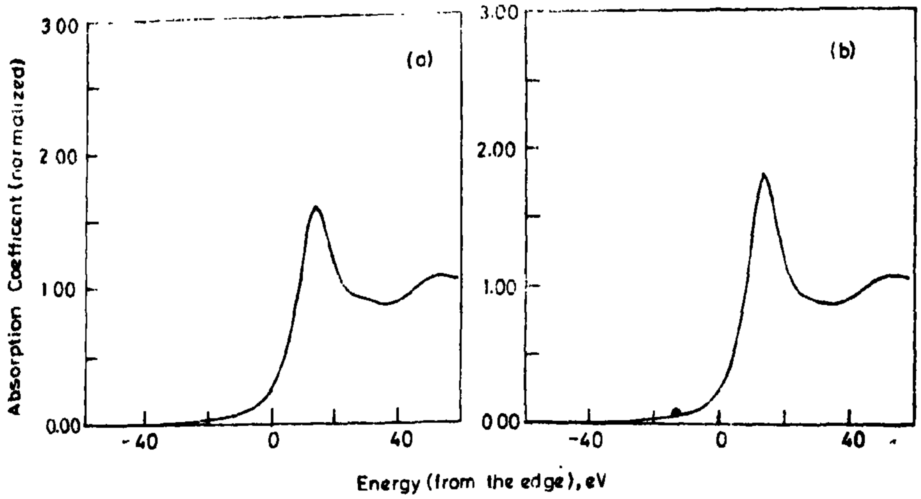


Fig. 3. Normalised L_3-edge spectra of Th^{IV} : (a) in crystalline ThF_4 and (b) in ThF_4-HfF_4 glass.

distance which again indicates enhanced covalency of Nd - F bonding. One should, therefore, expect this increase to be reflected in the edge absorption coefficients of neodymium in $NdF_3 - BeF_2$ glass.

Neodymium L_3-edge spectra is shown in Fig. 2. For both crystalline NdF_3 and $NdF_3 - BeF_2$ glass, L_3-edge arises from 2p→5d ($^2P_{3/2} \rightarrow {}^2D_{5/2}$) transition in neodymium at an edge energy of 6208.0 eV. When Nd - F bonds become covalent it corresponds to a reverse transfer of charge from fluorine to neodymium which puts back electron density in the 4f levels of neodymium. Such 4f electrons screen the 5d level (the final state for the L_3-edge) and hence, the absorption coefficient increases (Fig. 2). Using appropriate values of screening constants in equation (8) the intensity ratio can be expressed as $\mu_g/\mu_c = 1 + 0.105\,\delta$, where δ is the number of electrons involved in covalency. Covalent electrons amounts to $(\delta/3) \times 100\%$ covalency (assuming that all the three electrons of neodymium are involved in covalent bonding for 100% covalency). Experimental value of $(\mu_{glass}/\mu_{crystal})$ is equal to 1.15 (evaluated on the basis of the areas under the normalised absorption coefficient peaks) and it may be easily seen that the covalency should be of the order of 50% in the glass (perhaps a high estimate). The significant point of this analysis is that bonding in glass definitely becomes considerably more covalent.

A similar analysis has been performed in $ThF_4 - HfF_4$ glasses[16]. The L_3-edge absorption coefficient of thorium at 16.3 keV in the glass (composition : 0.33 ThF_4, 0.67 HfF_4) and in crystalline ThF_4 are shown in Fig. 3. A significant feature of this glass is that the coordination numbers of thorium in the glass and in the crystal are equal, and equal to eight. The absorption coefficient ratios were found to be about 1.06 which suggest that Th - F bond is about 30% more covalent in the glasses.

Another example which is illustrative of the use of the absorption coefficient analysis in bonding studies is provided by the lead oxyhalide glass

$PbO.PbX_2$ (X=F, Cl). L_3-edge absorption of lead has been used to demonstrate that the average ionicity of lead-ligand bond decreases in the oxyhalide glasses as a function of PbX_2 concentration. On the basis of other structural investigations it was established that lead is always bonded to two oxygens and four halide[40-42] ions in the entire glass-forming compositions. It is to be expected, however, that PbX_2-rich compositions should be more ionic because PbF_2 and $PbCl_2$ are typically ionic materials while PbO is a highly covalent compound[43]. Such a change in the covalency of the average lead-ligand bond has immediate consequences on the geometry of $[PbO_2X_4]$ units. In fact, we have shown elsewhere[42] that the symmetry of the $[PbO_2F_4]$ octahedra changes all the way from $C_s \rightarrow C_{2v} \rightarrow D_{4h}$ as PbF_2 concentration in the glass is increased. The more symmetrical arrangement of the ligands require a pronounced increase in the ionicity of the lead-ligand bond. Completely covalently bonded $[PbO_2F_4]$ unit corresponds to the presence of ten electrons in the bonding orbitals of which we assume five electrons would be involved in shielding the final d states of the L_3-edge absorption. In the purely ionic compositions there would be only two electrons in lead valence level corresponding to Pd^{II} ion. The extremes of ionicity (0% and 100%) therefore corresponds to shielding by five and two electrons respectively in the (6s, 6p) valence shell of lead. The absorption coefficient, μ_{L_3} is given by

$$\mu_{L_3} = (K\omega_{L_3}\, a^2)/[b+cg]^{1.2.4} \qquad (12)$$

where, K, a, b and c are constants, $K=(4\pi e^2/nc)$, $a=\Gamma(6.2)=169.41$, $b=39.622$ and $c=0.313$, and g is the number of electrons involved in covalency which varies between 0 and 3. Variation of μ_{L_3} is shown as a function of g in Fig. 4a, where μ is given in units of K. In Fig. 4b variation of the absorption coefficients of the L_3-edge is also shown for comparison. The trends appear quite satisfactory. No absolute comparisons have, however, been made.

Concluding remarks :

A case has been made here to show that covalency effect can be monitored through the absorption coefficient measurements associated with X-ray edge absorptions. The advantage of such a method is that ligand properties do not enter the analysis. Ionicity is quantified through a direct evaluation of the effective electron density causing additional screening. Electrons involved in covalent bonding do not affect the formal valence state of the atom. In a more systematic study, it should be possible to generate plots of absorption coefficients *versus* percentage covalencies of bonding for a given atom in its different formal valence states. Covalencies of unknown bonding situations may then in principle be determined through interpolation. Bonding in pure metal (preferably in vapour state) and in free ions (perferably in dilute solutions in indifferent solvents) may be used to generate the extreme points on such a plot. Covalencies determined by interpolation in such plots can be much more reliable than estimates obtained from simple electronegativity differences. Further, determination of edge absorption coefficients should also be quite simple particularly with the availability of intense and highly polarised light sources at synchrotron facilities.

Equation (11) can be cast into a more elegant form, if we consider μ_{ion} as the edge absorption coefficient of the free ions (or as suggested before, absorption coefficients in dilute solutions of inert

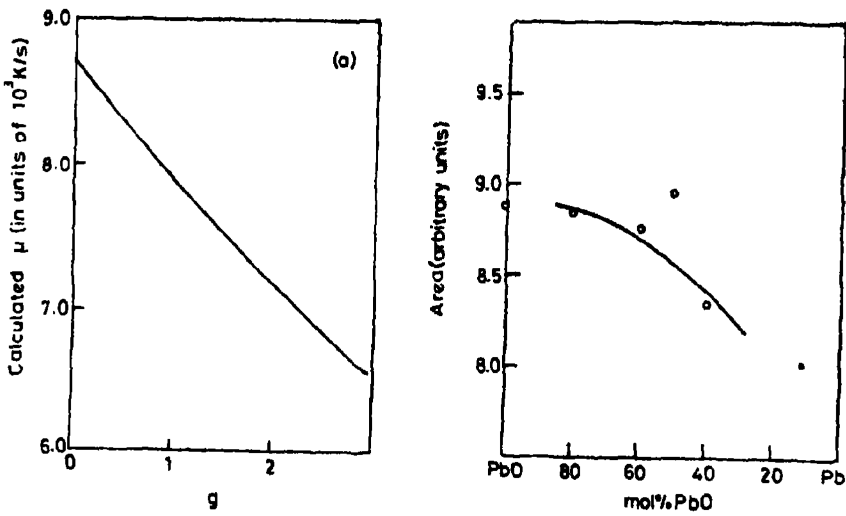


Fig. 4. (a) Variation of L_3-edge absorption coefficient of Pb^{II} as a function of the number of covalent electrons. (b) Variation of the experimental L_3-edge absorption coefficients of Pb^{II} in PbO-PbF_2 glasses as a function of PbF_2 concentration.

solvents). If we substitute $a=(Z_s-S_s)$ in equation (11),

$$(\mu_{cov}/\mu_{ion})=a/(a-S) \quad (13)$$

Equation (13) can be further simplified by taking logarithims and expanding $\ln(1\pm z)\simeq\pm z$ so that

$$\ln(\mu_{cov}/\mu_{ion})\simeq S/a$$

or more simply,

$$\mu_{cov}=\mu_{ion}\exp(S/a) \quad (14)$$

Thus, a log linear relation exists between additional screening by the covalent electrons and the edge absorption coefficients. Further, the slope 1/a is characteristic of the quantum number of initial states and is higher for higher values of n_i. 1/a may be considered as an amplification parameter. Measurements of *X*-ray edge absorption coefficients may thus provide a veritable tool to study covalency effects in bonding.

Acknowledgement

Thanks are due to Professor C. N. R. Rao, for his kind encouragement, and to Mr. U. Selvaraj, for his help in preparing the manuscript.

References

1. M. O'Keeffe and A. Navrotsky, "Structure and Bonding in Crystals", Academic Press, New York, 1981, Vols. I and II.
2. C. N. R. Rao and K. J. Rao, "Phase Transitions in Solids", McGraw-Hill, New York, 1979.
3. "Introduction to Glass Science", eds. L. D. Pye, H. J. Stevens and W. C. Lacourse, Plenum, New York, 1972.
4. J. E. Huheey, "Inorganic Chemistry", Harper, London, 1978.
5. R. D. Shannon and H. Vincent, *Struct. Bonding*, 1974, 19, 1.
6. L. Pauling, "The Nature of the Chemical Bond", Cornell University Press, Ithaca, 1960.
7. T. V. Ramakrishnan in "Solid State Chemistry", ed. C. N. R. Rao, Marcel Dekker, New York, 1974, p. 187.
8. B. C. Tofield, *Prog. Inorg. Chem.*, 1976, 20, 153.
9. M. Gerloch, and J. R. Miller, *Prog. Inorg. Chem.*, 1968, 10, 1.
10. J. Owen and J. H. M. Thornley, *Rep. Prog. Phys.*, 1966, 29, 675.
11. U. C. Srivastava and H. L. Nigam, *Coord. Chem. Rev.*, 1973, 9, 275.
12. C. N. R. Rao, P. R. Sarode, R. Parthasarathy and K. J. Rao, *Phil. Mag.*, 1980, 41, 581.
13. K. J. Rao, J. Wong and M. J. Weber, *J. Chem. Phys.*, 1983, 78, 6228.
14. J. Wong in "Topics in Applied Physics", eds. H. J. Gientherodt and H. Beck, 1980, Vol. 46, Ch. 4.
15. L. A. Grunes, *Phys. Rev.*, *B*, 1983, 27, 2111.
16. T. K. Sham, *Phys. Rev.*, *B*, 1985, 31, 888.
17. P. A. Lee, P. Citrin, P. Eisenberger and B. Kincaid, *Rev. Mod. Phys.*, 1981, 53, 769.
18. F. C. Brown in "Synchrotron Radiation Research", eds. H. Winik and S. Doniach, Plenum, New York, 1980.
19. K. J. Rao, J. Wong and M. W. Shafer, *J. Solid State Chem.*, 1984, 55, 110.
20. B. G. Rao and K. J. Rao, *Phys. Chem. Glasses*, 1984, 25, 11.
21. K. J. Rao, J. Wong and B. G. Rao, *Phys. Chem. Glasses*, 1984, 25, 57.
22. B. G. Rao, H. G. K. Sundar and K. J. Rao, *J. Chem. Soc., Faraday Trans. 1*, 1984, 3491.
23. K. J. Rao and J. Wong, *J. Chem. Phys.*, 1984, 81, 4832.
24. K. J. Rao, B. G. Rao and J. Wong, *J. Chem. Phys.*, communicated.

J. Indian Chem. Soc.,
Vol. LXIII, January 1986, pp. 91-94

Electron Spin-Lattice Relaxation of Toluene and *p*-Xylene Anions†

RANJAN DAS and BALU VENKATARAMAN

Tata Institute of Fundamental Research, Homi Bhabha Road, Bombay-400 005

Electron spin-lattice relaxation times (T_{1e}) of toluene and *p*-xylene anions have been determined by the pulsed saturation recovery technique. Toluene anion exhibits short and nearly temperature independent T_{1e} (1.8 ± 0.4 μs) in the temperature range studied (188 to 205 K). This is in agreement with the fact that toluene anion has a close lying excited orbital state at about 500 cm^{-1} and the temperature behaviour follows closely that observed earlier for T_{1e} of benzene anion (orbitally degenerate system) in CW saturation studies. *p*-Xylene anion exhibits larger T_{1e}'s (9.5 μs at 205 K) and is a linear function of (η/T) with zero intercept. *p*-Xylene anion has been estimated to have its first electronic excited state at 1 500 cm^{-1}. It is proposed that Orbach type mechanisms arising from a closely lying excited electronic level are dominant for spin-lattice relaxation in toluene anion. In *p*-xylene anion, however, spin rotation interaction is believed to play the dominant role with Orbach type processes being insignificant since 1 500 cm^{-1} >> kT.

THE alkyl substituted benzene anion radicals are known to have low lying excited orbital states and have been the subject of intense studies by electron spin resonance (esr) for several years. One of the most important consequences of the orbital degeneracy is the short electron spin-lattice relaxation time[1-6], T_{1e}, and large esr linewidth[7-9] (short electron spin-spin relaxation time, T_{2e}) for benzene anion radical. It is expected that vibronic interaction would lift this degeneracy even in benzene anion. Different alkyl substitutions will lift the degeneracy to different extents. The magnitude of the splitting has been estimated theoretically[10] and experimentally[11,12].

Measurements of T_{1e} of benzene and substituted benzene anions utilising the continuous-wave (CW) saturation technique have been made[1,2,5,6]. It is well known that such estimates of T_{1e} by CW saturation technique suffer from unreliability in view of the difficulty in measuring true linewidths and the amplitude of the microwave magnetic field, H_1. Greater would be the ambiguity when one faces inhomogeneous broadening which is bound to occur in the case of hydrocarbon anions due to their interaction with counter ions. A fair amount of effort has been made to estimate such effects and apply corrections to T_{1e}'s measured by the CW saturation technique[2]. However, it has been our experience that T_{1e}'s measured in this way have not always been reliable[13]. Such examples will be pointed out even in this paper.

The most direct way of measuring T_{1e} is the pulsed saturation recovery technique which has been applied for several years to free radicals in solution in our laboratory and a few other laboratories[13-18]. With the recent availability in our laboratory of a computer controlled time domain pulsed esr spectrometer capable of extensive signal averaging[19], we have been able to extend our sensitivity to measure T_{1e}'s of radicals at very low concentrations, $\sim 5 \times 10^{-6}$ *M*, for a single esr line of width about 0.5 G. Alkyl substituted benzene anions are known to be obtained by alkali metal reduction process only in these concentration ranges (10^{-4} to 10^{-6} *M*) and hence, our spectrometer is eminently suitable for studying such systems.

The mechanism of spin-lattice relaxation of free radicals in solutions have been established fairly well except in those cases where orbital degeneracy exists[20]. In such cases, it is believed[21] that an Orbach type of mechanism is dominant when the splitting between the two electronic states is less than 6 kT, where k is the Boltzmann constant. However, there is controversy regarding the exact nature of the mechanism and many models have been proposed[21-25]. It is believed that measurements of T_{1e}'s of several alkyl substituted benzene anions in different solvents over different ranges of temperature would throw light on the mechanisms based on the Orbach model. We present here a preliminary report on our measurements of T_{1e}'s, by the pulsed saturation recovery technique, of toluene and *p*-xylene anions in dimethoxyethane (DME) solution.

Experimental

Pulsed esr spectrometer : The pulsed esr spectrometer is a home-built homodyne X-band spectro-

† Dedicated to Professor Sadhan Basu on the occasion of his 65th birthday.

A Part of the article was Presented at the National Conference on Spectroscopy and Theoretical Chemistry held at Calcutta, December 5-7, 1985.

meter[16] similar to the one described by Fessenden and coworkers[18]. There is a facility to change independently the microwave pump power and the 'observe' power and to change the phase of the pump power by 180° between alternate experiments in order to separate free induction decay signal and the saturation recovery signal from the observed M_y component of the magnetisation as has been suggested by Percival and Hyde[19]. The magnetic field and microwave frequency interlock ensures that the resonance condition for any desired position of the esr line is maintained for any length of time, allowing extensive signal averaging.

The temperature of the sample was varied by flowing precooled nitrogen gas through a quartz Dewar inserted into the microwave cavity. The temperature of the nitrogen gas was controlled using a Varian 4540 temperature control accessory. The sample temperature was monitored with a POWERTEK digital thermometer using a chromel-alumel thermocouple. The temperature was maintained constant to ±1 K.

Chemicals : Toluene and *p*-xylene (S.M. and Fluka, respectively) were used without further purification. The DME (Aldrich) solvent was distilled from sodium and dehydrated by lithium aluminium hydride. It was then distilled under vacuum into a storage vessel containing sodium mirror and anthracene. The formation of deep green anthracene dianion showed that the solvent was free from oxygen or any other paramagnetic impurity.

Sample preparation : The anion radicals were prepared by the well known alkali metal reduction process using potassium under high vacuum. At temperatures below 230 K, both the radicals gave blue colour indicating their presence. The concentration of the radicals were estimated by comparison with a standard sample of a nitroxide as described elsewhere[20].

Measurements of saturation recovery signal : The measurement of the saturation recovery signal involved a cycle of 4 experiments. In order to suppress the transients arising from the microwave pulses, a signal, obtained when the magnetic field was off resonance, was subtracted from the signal when it was at resonance. It was repeated for the other phase of the pump power. The whole cycle was repeated a desired number of times to improve the signal to noise ratio so that weak signals could be studied.

Results

In a typical experiment, the observed saturation recovery signal is shown in Fig. 1(a) and 1(b) for toluene and *p*-xylene anions, respectively. The electron spin-lattice relaxation times are estimated by the least-square fit of the curves to a single exponential. We did not find any discernible free induction decay signal from either of the systems,

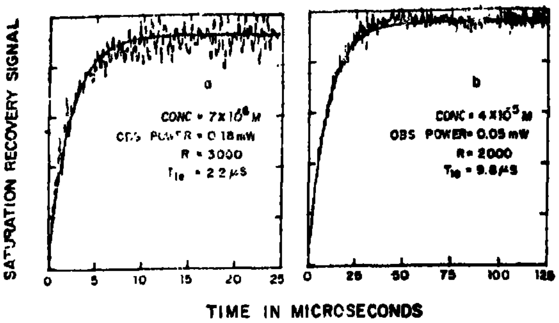


Fig. 1. Saturation recovery curves for (a) toluene anion and (b) *p*-xylene anion in DME at 200 K and 195 K, respectively. The noisy traces are the averaged signal after R experiments and the smooth curves are fits to single exponentials with denoted T_{1e}'s.

indicating very short effective spin-spin relaxation times for both cases.

Toluene anion : Fig. 2 shows the second derivative esr spectrum of toluene anion in DME at 196 K. The measurements of T_{1e} were carried out not at the central line but at the line indicated by the arrow since at the centre there are two closely spaced lines. For off-resonance, the field was placed at the position marked 'A' in the Fig. The range of temperature variation has been limited because of

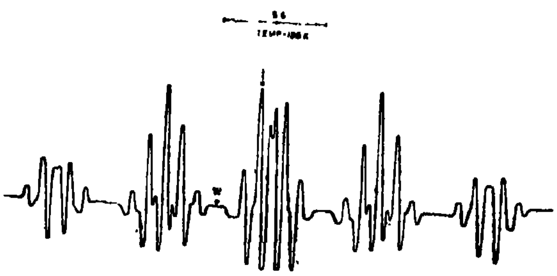


Fig. 2. Second derivative esr spectrum of toluene anion at 196 K. The T_{1e}'s were measured by observing the saturation recovery for the line marked with the arrow.

the considerable increase in linewidths at temperatures higher than 210 K. The large number of hyperfine lines also places a limit on the sensitivity for toluene anion. However, it is noted that in the temperature range of measurement, *viz.* 185 to 210 K, there is no discernible temperature dependence of T_{1e} within experimental error (Fig. 3).

It was found that at 'observe' power greater than even 0.2 mW, the saturation recovery traces had non-exponential shapes as predicted by the Bloch equations[18]. It was, therefore, necessary to observe the saturation recovery at 'observe' powers between 0.1 and 0.02 mW. At these power levels, the traces were nearly exponential, but with poor signal to noise ratio even after taking averages of 20 000 experiments. The T_{1e} determined under these conditions were nearly the same for the two. In

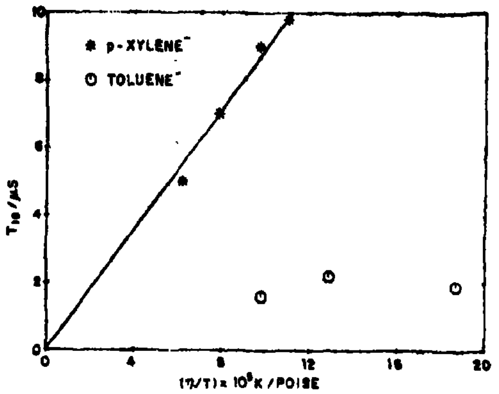


Fig. 3. Plot of T_{1e}'s of p-xylene and toluene anions as a function of η/T. The concentrations of the radicals are given in Fig. 1. η values are taken from Ref. 28.

view of the above difficulties, the values of T_{1e} reported here are accurate to about 20%.

p-*Xylene anion :* Since *p*-xylene anion has a smaller number of hyperfine lines, the signal to noise ratio for its esr signal is better than that of toluene anion for similar radical concentrations. The relaxation of the central line was studied and for off-resonance the field was placed between it and the neighbouring line.

In contrast to toluene anion, the exponential nature of the saturation recovery signal was seen to be valid upto 2.0 mW of 'observe' power. Since T_{1e} determined in this way is dependent upon the amplitude of the 'observe' microwave power, the true T_{1e} was determined from the limiting value at zero observing power, from a $1/T_{1e}$ *vs* ('observe' power) plot[27]. A typical plot of such measurements is shown in Fig. 4.

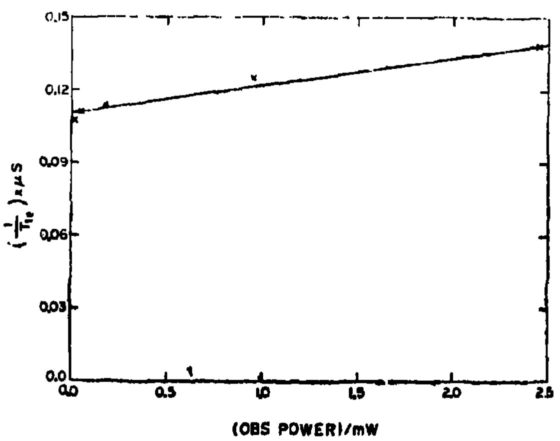


Fig. 4. Plot of $1/T_{1e}$ *vs* 'observe' microwave power for *p*-xylene anion at 205 K.

In the temperature ranging from 185 to 225 K, the T_{1e} for *p*-xylene anion changes from 9.5 to 5.0 μs with an accuracy of better than 10%.

Discussion

From analysis of proton hyperfine splitting constants[11,18] and theoretical studies[10], it has been estimated that the separation between the ground state and the lowest excited electronic state is about 500 cm^{-1} in toluene anion and about 1 500 cm^{-1} in *p*-xylene anion. Thus, one would expect Orbach type of mechanisms to be more important for relaxations in toluene anion. Since 1 500 cm^{-1} is greater than 6 kT (~834 cm^{-1} at 200 K), it is expected that the major relaxation mechanisms for *p*-xylene anion would be processes other than the Orbach mechanisms.

If the equation (74) of Kivelson[8(b)] is right we should expect for toluene anion, T_{1e} to be comparable to that calculated by him for benzene anion assuming an energy separation (δ) of 500 cm^{-1}. With parameters of Table 1 in his paper for benzene anion, the equation predicts about 1 μs for T_{1e} with $\delta = 500$ cm^{-1} at 200 K. However, the temperature dependence of τ_c in his equation is left vague. From the analysis of the data of Jones and coworkers[1,8] on benzene anion, it is noted that no clear temperature dependence is established within experimental errors. For the temperature range in their experiments (154 to 200 K) T_{1e} should have increased by a factor of 3 at lower temperatures if τ_c is assumed to be temperature independent and $\delta = 500$ cm^{-1} in the Kivelson equation. This temperature dependence will decrease drastically if one assumes a smaller δ (*e.g.* the ratio of T_{1e}'s is only 1.23 for $\delta = 100$ cm^{-1}). For the temperature range of our measurements for toluene anion (188 to 205 K) assuming τ_c to be nearly temperature independent, the T_{1e}'s should vary in the ratio of 1.4 for $\delta = 500$ cm^{-1} and our data (Fig. 3) exhibits no temperature dependence within the limits of experimental error. This behaviour is similar to that of benzene anion, a clear case of nearly orbitally degenerate system[1,8]. From all these evidences we infer that as in benzene anion, Orbach mechanisms arising from a closely lying excited electronic level are the major contribution to spin-lattice relaxation in toluene anion. Without more refined data it would not be possible to comment meaningfully on the validity of Kivelson mechanism[8] or of other mechanisms based on Orbach type processes[21,26].

Fig. 3 depicts the dependence of T_1 on η/T for *p*-xylene anion also. The linear relationship is well demonstrated and the intercept is zero. Such a behaviour is followed in cases where spin-rotation interaction is dominant[18,15]. This behaviour is in great contrast to what is observed in toluene anion. The contribution from modulation of g-anisotropy and hyperfine anisotropy is expected to be very small since no marked line width variation among hyperfine components is observed. Further, in both toluene and *p*-xylene anions, exchange interactions are expected to be insignificant at these concentrations. However, a more careful investigation is yet to be carried out.

Freed and coworkers[6] have determined T_{1e} of *p*-xylene anion to be 1.94 μs at 203 K by CW saturation technique. This is to be compared with our value of 9.5 ± 0.5 μs at 205 K. The most probable error in the earlier measurement must have been the unreliability in determining T_s in the presence of unresolved hyperfine splitting.

The study of electron spin-lattice relaxation of radicals in solution with close lying excited electronic states by the saturation recovery technique has demonstrated the effect of Orbach mechanisms on T_{1e}'s. It is noted that these effects dominate when the energy separation is less than 6 kT and for separation of the order of 400 cm^{-1}, T_{1e}'s are nearly temperature independent. A systematic study of several alkyl substituted anions with different energy separations is expected to throw light on the details of the relaxation mechanisms operating in nearly degenerate systems.

References

1. R. D. Bataiczk and M. T. Jones, *J. Chem. Phys.*, 1972, **56**, 3898.
2. M. T. Jones and M. Komarynsky, *J. Chem. Phys.*, 1972, **56**, 4404.
3. G. Bignol and W. Müller-Warmuth, *Phys. Lett.*, 1964, **11**, 292.
4. M. T. Jones, *J. Chem. Phys.*, 1965, **42**, 4054.
5. R. G. Kooser, W. V. Volland and J. H. Freed, *J. Chem. Phys.*, 1969, **50**, 5243.
6. M. R. Das, S. B. Wagner and J. H. Freed, *J. Chem. Phys.*, 1970, **52**, 5404.
7. M. G. Townsend and S. I. Weissman, *J. Chem. Phys.*, 1960, **32**, 309.
8. J. L. Sommerdijk, E. de Boer, F. W. Pijpus and H. van Willigen, *Z. Phys. Chem.* (Frankfurt am Main), 1969, **63**, 183.
9. B. G. Segal, M. Kaplan and G. K. Fraenkel, *J. Chem. Phys.*, 1965, **43**, 4191.
10. W. D. Hobey *J. Chem. Phys.*, 1965, **43**, 2187.
11. M. T. Jones, *J. Phys. Chem.*, 1978, **82**, 1138.
12. M. T. Jones, S. Metz and T. C. Kuechler, *Mol. Phys.*, 1977, **33**, 717.
13. S. K. Rengan, M. P. Khakhar, B. S. Prabhananda and B. Venkataraman, *Pramana*, 1974, **3**, 95.
14. K. V. Lingam, P. G. Nair and B. Venkataraman, *Proc. Indian Acad. Sci., Sect. A*, 1972, **76**, 207.
15. S. K. Rengan, M. P. Khakhar, B. S. Prabhananda and B. Venkataraman, *J. Magn. Reson.*, 1974, **16**, 35.
16. P. W. Percival and J. S. Hyde, *Rev. Sci. Inst.*, 1975, **46**, 1522, and references therein.
17. P. W. Percival and J. S. Hyde, *J. Mag. Reson.*, 1976, **23**, 249.
18. R. W. Fessenden, J. P. Hornak and B. Venkataraman, *J. Chem. Phys.*, 1981, **74**, 3694.
19. R. Das and B. Venkataraman, communicated.
20. References in Ref. 13.
21. J. H. Freed and R. G. Kooser, *J. Chem. Phys.*, 1968, **49**, 4715.
22. D. Kivelson, *J. Chem. Phys.*, 1966, **45**, (a) 751, (b) 1324.
23. H. M. McConnell and A. D. McLachlan, *J. Chem. Phys.*, 1961, **34**, 1.
24. H. M. McConnell, *J. Chem Phys.*, 1961, **34**, 13.
25. J. H. Freed, *J. Chem. Phys.*, 1968, **49**, 376.
26. R. Das and B. Venkataraman, *Proc. Indian Acad. Sci.* (*Chem. Sci.*), 1985, **95**, 117.
27. P. W. Atkins, K A. McLauchlan and P. W. Percival, *Mol. Phys.*, 1973, **25**, 281.
28. C. Carvajal, K. J. Tölle, J. Smid and M. Szwarc, *J. Am. Chem. Soc.*, 1965, **87**, 5548.

J. Indian Chem. Soc.,
Vol. LXIII, January 1986, pp. 95-100

Hyperfine and Exchange Interactions in Tetraethylammoniumbis(maleonitriledithiolato)cuprate(II), $[NEt_4]_2[Cu(mnt)_2]$†

P. KUPPUSAMY and P. T. MANOHARAN*

Department of Chemistry, Indian Institute of Technology, Madras-600 036

Single crystal epr study on $[NEt_4]_2[Cu(mnt)_2]$ diluted into the diamagnetic Ni^{II} analog shows the *g* and *A* tensors to be axially symmetric and to be having coincident principal axes. The pure Cu^{II} salt shows a single exchange narrowed epr line. The anisotropic line widths have been analysed to obtain a value of $1\,700 \pm 300$ G for *J* in this system. The estimate of *J* has been further confirmed by computing and comparing the Fourier components of the spin correlation functions using Blume-Hubbard and Anderson-Weiss theoretical models.

THE metal dithiolene complexes of the type $[MS_4C_4R_4]^{n-}$, where M = Cu and Ni group metals; and R = H, CH_3, CF_3, C_6H_5, CN, *etc.*, have been of considerable interest to chemists as well as physicists for more than two decades. The continued interest stems from the fact that these materials possess unusual structural, magnetic and conducting properties as is evident from the large number of reviews[1-3] and research publications. Of greater significance is the magnetic properties of maleonitriledithiolato (R = CN, mnt) complexes of Cu^{II} and Ni^{III} ions[4-7]. In the past few years, we have been actively involved in the study of such systems using *X*-ray crystal structure, epr, magnetic susceptibility and optical measurements[8-16]. In this article, we report the exchange and hyperfine interactions in a Cu^{II} complex, namely, tetraethylammoniumbis(maleonitriledithiolato)cuprate(II), $[NEt_4]_2[Cu(mnt)_2]$.

The compound $[NEt_4]_2[Cu(mnt)_2]$ is interesting in that it behaves as a semiconductor having a large negative temperature coefficient of resistivity[6]. The resistivity above 300 K is comparable to those of some of the better known wide-band-gap inorganic semiconductors. Magnetic susceptibility measurements show the exchange interaction in this system is too weak to be measured accurately. We have employed epr technique, which is known to be a better tool to study weaker and finer interactions, and demonstrated nicely the effect of exchange modulation on the broadening effects, such as hyperfine and dipolar interactions apart from getting a reasonable estimate for the isotropic exchange coupling constant. The magnetic parameters of the 'isolated' molecule needed for the present work were obtained by diluting the Cu^{II} compound into the isomorphous Ni^{II} analog and these results are also presented in this article, though measurements of this kind have been made by Maki *et al.*[17]. However, the present emphasis is to measure these parameters very accurately. Furthermore, we decided to have a look into the direction cosines of the magnetic parameters since the crystal structures of the host and paramagnetic part have been known subsequent to the earlier work of Maki *et al.*[17].

Experimental

Both the Cu^{II} and Ni^{II} complexes were synthesised separately according to the published procedure[18]. Large red-brown crystals of $[NEt_4]_2[Cu(mnt)_2]$ were obtained by slow evaporation of a solution of the 'pure' compound in ethanol-water (1 : 1, v/v) mixture. In the case of Ni^{II} compound, large deep-red plates with well developed faces were obtained from acetone-isopropyl alcohol (3 : 1, v/v) solutions of $[NEt_4]_2[Ni(mnt)_2]$ containing 0.5% by weight of the Cu^{II} analog by slow evaporation at 10°.

The isomorphous nature of the lattices was established by measuring the unit cell constants using Enraf-Nonius CAD-4 diffractometer. The morphologies of the crystals were determined by optical goniometer. Though the two systems were isomorphous they were found to grow with different morphologies in the respective solvents.

Single crystal epr measurements were carried out with a Varian E-112 spectrometer operating at X- (~9.5 GHz) and Q-band (~35 GHz) frequencies using 100 kHz field modulation. The crystals were mounted at the end of a quartz rod having an L-shaped wedge using APIEZON-N grease. Rotation of the crystal was done with the use of a goniometer. The spectra were recorded for 10° intervals. DPPH (diphenylpicrylhydrazyl) was used as a *g*-calibrant. The magnetic field was earlier calibrated. All the epr measurements were made at room temperature. The line widths reported in this paper are peak-to-

† Dedicated to Professor Sadhan Basu on the occasion of his 65th birthday.

A part of the article was presented at the National Conference on Spectroscopy and Theoretical Chemistry held at Calcutta, December 6-7, 1985.

peak width of the derivative spectrum, ΔB_{pp}. The error in line width measurement is $\pm$ 2 G and that in *g*-factor is $\pm$ 0.002.

Results and Discussion

Crystal structure : The unit cell parameters of the Cu^{II} and Ni^{II} compounds are collected in Table 1. It is evident from a comparison of the two sets of values that the two lattices are isomorphous to each other. The crystal structure of the Cu^{II} salt has been reported to be done but it is yet to be published[19]. The structure of the Ni^{II} compound has been solved recently in this laboratory[20].

TABLE 1 – UNIT CELL PARAMETERS OF $[NEt_4]_2[Cu(mnt)_2]$ AND $[NEt_4]_2[Ni(mnt)_2]$

	$[NEt_4]_2[Cu(mnt)_2]$	$[NEt_4]_2[Ni(mnt)_2]$
a	7.595 (8) Å	7.5608 (7) Å
b	8.601 (3) Å	8.7017 (9) Å
c	13.111 (5) Å	12.626 (3) Å
α	94.6 (1)°	93.78 (1)°
β	108.1 (1)°	104.27 (1)°
γ	75.6 (1)°	75.257 (9)°
V	789 Å³	779 Å³
Z	1	1
space group	P1̄	P1̄

The structure consists of monomeric anionic units stacked along *a*-axis of the unit cell. A projection of the packing onto *ab* plane of the unit cell is shown in Fig. 1. The Ni atom of the anion has an approximate square planar configuration with all the four Ni – S distances equal within experimental error. The whole anion unit is planar to within 0.047 Å. The shortest metal-metal contact is along the stack axis, *a* (~7.6 Å).

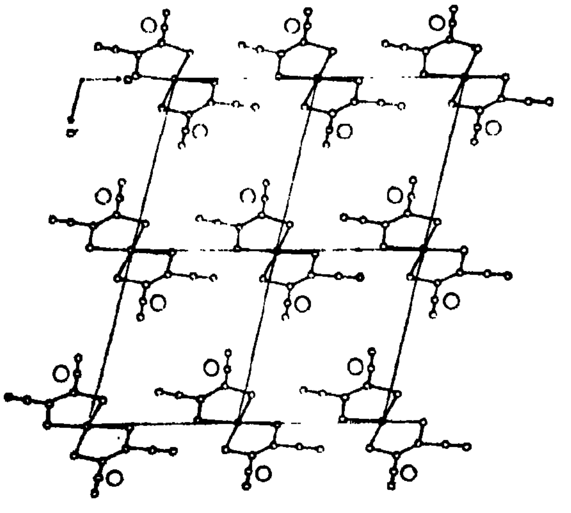


Fig. 1. Projection of the structure of $[NEt_4]_2[Ni(mnt)_2]$ onto *ab* plane. The circles refer to $[NEt_4]^+$ ions.

By virtue of the triclinic space group P1̄ with $Z = 1$, we have only one set of magnetically equivalent site in this lattice.

Epr of Cu^{II} diluted in $[NEt_4]_2[Ni(mnt)_2]$: The single crystal X-band epr measurements were made by rotating the crystal, in a fixed magnetic field vector, with respect to three orthogonal axes X, Y and Z. At all orientations one could observe two sets of four sharp lines ; the two sets due to the presence of the two isotopes of copper, namely, ^{63}Cu (69.09%) and ^{65}Cu (30.91%) and four lines in each set due to $I = 3/2$ of both the isotopes. A typical single crystal spectrum is shown in Fig. 2. It must be noted that since the magnetic moments of the two isotopes of copper are nearly equal (+2.226 and +2.385 B.M. for ^{63}Cu and ^{65}Cu, respectively) usually either the lines will be overlapping with each other making the analysis difficult or

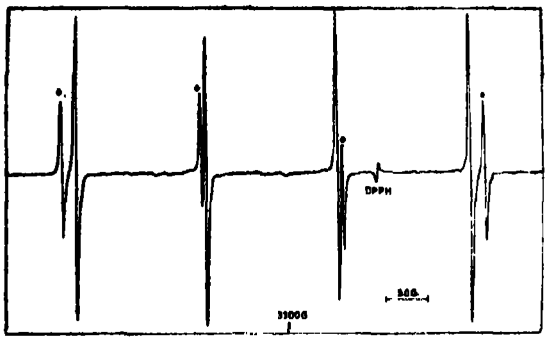


Fig. 2. X-band epr spectrum with $B \parallel g_z$. The lines marked with • are those of ^{65}Cu isotope (30.91%).

the lines due to the less abundant ^{65}Cu will be ignored in the interpretation of the spectra. However, in the present case, the resonances were very sharp such that the two sets of lines could be very clearly resolved without any overlap between them, particularly the outer most ones.

The angular variations of the *g*-factor in XY, YZ and ZX planes are shown in Fig. 3. The measured *g*-values were used to construct the

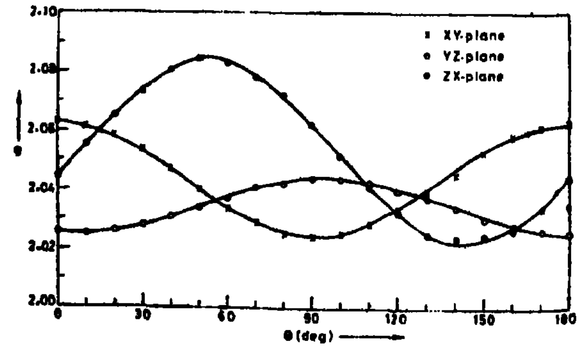


Fig. 3. Angular variation of *g* in (×) XY-, (○) YZ- and (●) ZX- planes. The solid curves are the least-squares fit to the experimental points in the respective planes.

g^2-matrix using a least squares minimisation procedure and this matrix was then diagonalised by Jacobi's method to get the principal values of g-tensor and their direction cosines with respect to the laboratory frame work X, Y and Z. The principal values and their direction cosines are listed in Table 2. The g-tensor can be considered as almost axially symmetric, though there is a slight rhombicity. These values agree well with those reported for Cu^{II} diluted in $[NBu_4]_2Ni(mnt)_2$ by Maki *et al.*[17].

TABLE 2—PRINCIPAL g AND A VALUES* AND THEIR DIRECTION COSINES

Parameter	Direction cosines X	Y	Z
$g_x = 2.022$	0.681	−0.410	0.742
$g_y = 2.026$	0.257	0.912	0.320
$g_z = 2.085$	0.808	−0.021	−0.589
$A_{\parallel}(^{63}Cu) = 162$	0.795	−0.013	−0.607
$A_{\perp}(^{63}Cu) = 39$	—	—	—
$A_{\parallel}(^{65}Cu) = 174$	0.799	−0.013	−0.601
$A_{\perp}(^{65}Cu) = 42$	—	—	—

* A values in 10^{-4} cm^{-1} ; error in g-factor measurements $= \pm 0.002$; error in A values $= \pm 1 \times 10^{-4}$ cm^{-1}.

The angular variations of $A(^{63}Cu)$ and $A(^{65}Cu)$ in YZ, ZX and XY planes are given in Figs. 4, 5 and 6, respectively. Comparison of the g- and A-variations in the respective planes shows that the two tensors have coinciding principal axes directions, within experimental error (± 3°). To the first order, the transition energies for a system with axial g- and hyperfine splitting tensors would be

$$h\nu(\theta) = \beta g(\theta)[B_0 + K(\theta)m] \quad (1)$$

where, $h\nu$ is the transition energy in ergs, B_0 is the strength of the applied magnetic field, θ is the angle that B_0 makes with g_z, and m is the allowed values of I. $K(\theta)$ is the angle dependent hyperfine splitting parameter in Gauss given by

$$g(\theta)^4 g(\theta)^2 = A_{\parallel}^2 g_{\parallel}^4 \cos^2\theta + A_{\perp}^2 g_{\perp}^4 \sin^2\theta \quad (2)$$

The values of $g(\theta)^4$ $K(\theta)^2$ were used in the same manner as with $g^2(\theta)$ to get the principal values of

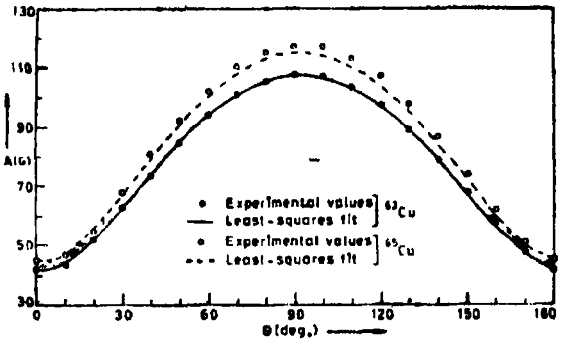


Fig. 4. Angular variation of A for (●) ^{63}Cu and (○) ^{65}Cu isotopes in YZ-plane.

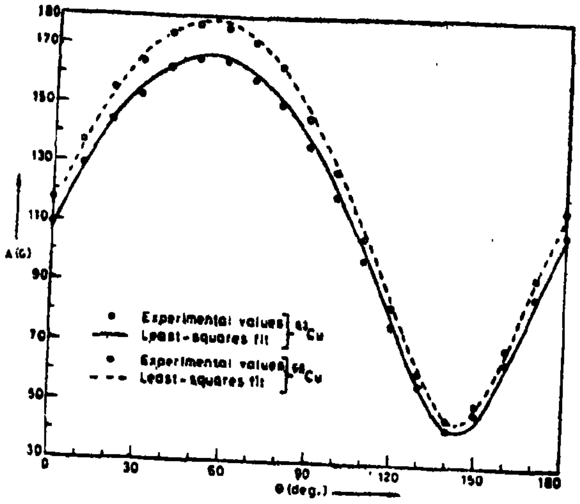


Fig. 5. Angular variation of A for (●) ^{63}Cu and (○) ^{65}Cu isotopes in ZX-plane.

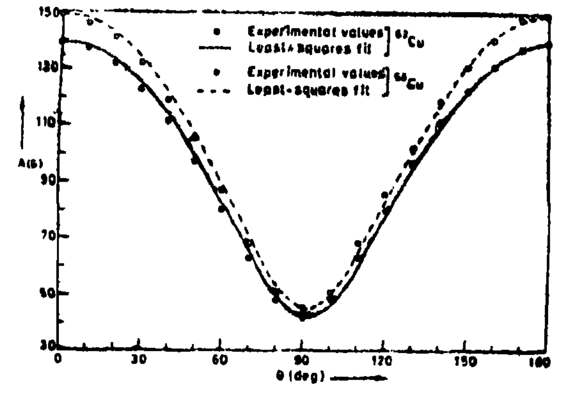


Fig. 6. Angular variation of A for (●) ^{63}Cu and (○) ^{65}Cu isotopes in XY-plane.

(g^4K^2) tensor and hence the A-tensor. The results are given in Table 2. It must be mentioned that we could get identical direction cosines for the z-components of g and A. In the case of X-Y(⊥) components due to the axially symmetric nature of A we could not get any meaningful direction cosines.

The relative values of A for the two isotopes $A_{\parallel}(^{65}Cu)/A_{\parallel}(^{63}Cu)$ (1.072) and $A_{\perp}(^{65}Cu)/A_{\perp}(^{63}Cu)$ (1.070) are in excellent agreement with the ratio of their magnetic moments, $\mu(^{65}Cu)/\mu(^{63}Cu)$ (1.071). To our knowledge, this is the first case of this type of systems where the hyperfine tensor for the less abundant ^{65}Cu nucleus is reported. In earlier studies, either ^{65}Cu splitting has been ignored due to poor resolution[17] or studies have been done with ^{65}Cu enriched sample[8].

Another interesting aspect of the present study is the observation of 'spin-flip' and 'forbidden' transitions, the latter being due to the quadrupolar nature of the Cu nuclei. However, analysis of these features are not discussed herein.

Epr of pure $[NEt_4]_2[Cu(mnt)_2]$:

g-tensor : A single exchange narrowed epr line with nearly Lorentzian shape was observed at all orientations and at both X- and Q-band frequencies. The observed g values in the three orthogonal planes were used to set up the g^2-matrix by a least-squares procedure. This matrix on diagonalisation yielded the principal g values and their direction cosines with respect to the rotation axes b, a^* and c^* defined as follows,

$$b = b$$
$$c^* = b \times a$$
$$a^* = b \times c^*$$

The results along with direction cosines calculated from the crystal structure are given in Table 3 for comparison. The agreement between the experimental and calculated direction cosines is very good.

TABLE 3—PRINCIPAL g VALUES AND THEIR DIRECTION COSINES FOR $[NEt_4]_2[Cu(mnt)_2]$

Principal g values	Direction cosines					
	Observed			Calculated		
	b	a^*	c^*	b	a^*	c^*
g_x=2.019	0.591	0.804	−0.058	0.619	0.785	−0.095
g_y=2.021	0.410	−0.858	−0.889	0.424	−0.861	−0.881
g_z=2.086	−0.695	0.475	−0.540	−0.661	0.508	−0.556

Line width : The angular variations of the peak-to-peak derivative line width (ΔB_{pp}) in the three planes at X-band are shown in Fig. 7. No significant difference in line width was observed at Q-band frequency. This along with the fact that magnetic susceptibility measurements[9] show weakly

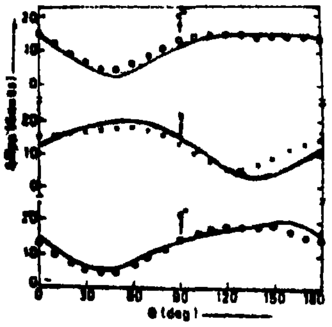


Fig. 7. Angular variation of the experimental line width in (○) a^*c^*, (×) c^*b and (●) ba^* planes. The solid lines are the simulated variations in the respective planes using equation (3) with J = 1 700 G.

coupled spins suggests that the exchange interaction is weak and smaller than the two Zeeman frequencies. Hence, the relative magnitude of the various interactions are given as

$$\mathscr{H}_z^Q > \mathscr{H}_z^X > \mathscr{H}_{ex} > \mathscr{H}_{hyp} > \mathscr{H}_{dip}$$

Though $\mathscr{H}_{ex}$ is smaller, it is still sufficiently larger to modulate the broadening effects of hyperfine and dipolar interactions, resulting in a single and sharp resonance.

The line widths are, however, temperature dependent and decrease smoothly as the crystal is cooled[9].

Line width analysis : For strong exchange narrowing cases, the observed line width is related to the isotropic exchange coupling constant J by Van Vleck's[21] expression as

$$\sqrt{3}/2\ \Delta B_{pp} = M_2^t/J \tag{3}$$

where M_2^t is, in general, the sum of the secular and non-secular second moments of hyperfine and dipolar interactions. The full second moment is used when $\mathscr{H}_{ex} > \mathscr{H}_z$ while only the secular moments will be effective in contributing to the observed line width when $\mathscr{H}_{ex} < \mathscr{H}_z$. In the intermediate case $\mathscr{H}_z^X < \mathscr{H}_{ex} < \mathscr{H}_z^Q$, one would observe frequency dependent non-secular contribution and hence width.

In the present case we have to consider only the secular part of the second moments and hence we write

$$M_2^t = M_2^{hyp}\ (\text{sec.}) + M_2^{dip}\ (\text{sec.}) \tag{4}$$

The secular part of the dipolar second moment for $S = 1/2$ is given by

$$M_2^{dip}\ (\text{sec.}) = \frac{9\bar{g}^4\,\beta^4}{16h^2} \sum_{i \neq j} (3\cos^2\psi_{ij} - 1)^2\, r_{ij}^{-6} \tag{5}$$

where, $\bar{g}^2 = (g_\parallel^2 + 2g_\perp^2)/3$, and ψ_{ij} is the angle between r_{ij} (the vector connecting the dipolar coupled spins) and the effective field $g.B_0$. For an orientation (θ, ϕ) of B_0, the effective field angles (ψ, ϕ) are

$$\cos\psi = [g_\parallel/g\ (\theta)]\cos\theta \tag{6}$$

The hyperfine second moment for $I = 3/2$ is given by

$$M_2^{hyp}\ (\text{sec.}) = \frac{5}{4}\, K^2\ (\theta)/g^2\ (\theta) \tag{7}$$

$$\text{where, } g^2\ (\theta) = g_\parallel^2 \cos^2\theta + g_\perp^2 \sin^2\theta \tag{8}$$

$$K^2\ (\theta) = A_\parallel^2\, g_\parallel^2 \cos^2\theta + A_\perp^2\, g_\perp^2 \sin^2\theta \tag{9}$$

The dipolar and hyperfine second moments were computed for each orientation from a knowledge of the atomic coordinates given by the crystal structure[20] and by using the molecular principal values of g- and A-tensors obtained from doped single crystal studies (*vide infra*). For computational simplicity axial symmetry was assumed in the case of g-tensor and only the ^{63}Cu hyperfine tensor was used. The computed second moments were then fitted with the experimental line widths by using equation (3) to obtain a value of 1 700±300 G for J. The agreement between the simulated line widths for J=1 700 G and the experimental values is remarkably good as is seen in Fig. 7. Though in principle J can be obtained from a single measurement, it is gratifying to note that the estimate holds good for all orientations and in all the three planes with a fair degree of precision.

Fourier components :

The hyperfine coupling involves two-spin correlation functions of the form,

$$C_{ij}(t)=[3/S(S+1)]\langle S_i^z(S_j^z(0)\rangle \quad (10)$$

where, i and j refer to various sites in the lattice and its contribution to line width, Γ_h (half width at half height) is given by

$$\Gamma_h=\int_0^\infty (a^{(0)}+a^{(1)}\cos\omega_0 t)\, C(t)\, dt \quad (11)$$

In the above expression, $a^{(0)}$ and $a^{(1)}$ are the secular ($\Delta m=0$) and non-secular ($\Delta m=\pm 1$) hyperfine second moments, respectively while ω_0 is the Zeeman frequency. $C(t)$ is the autocorrelation function for $i=j$. In the high temperature limit, Γ_h is given by

$$\Gamma_h=a^{(0)}\, g(0)+a^{(1)}\, g(\omega_0) \quad (12)$$

where, $g(\omega)$ are the Fourier components of the autocorrelation function $C(t)$ given by

$$2g(\omega)=\int_{-\infty}^{+\infty} C(t)\exp(i\omega t)dt \quad (13)$$

The dipolar interactions, on the other hand, leads to four-spin correlation functions given by

$$C_{ijkl}(t)=[3/2\; S(S+1)]^2\langle S_i^+(t)S_j^+(t)\; S_k^-(0)\, S_l^-(0)\rangle \quad (14)$$

where, i, j, k and l refer to the sites in the lattice with $i\neq j$ and $k\neq l$. Taking only the diagonal correlation and further using strong decoupling approximation we get

$$C_{ijkl}(t)\propto\langle S_i^+(t)\, S_i^-(0)\rangle^2\propto C^2(t) \quad (15)$$

The dipolar contribution to the observed line width, Γ_d is given as

$$\Gamma_d=M_2^{(0)}f(0)+M_2^{(1)}f(\omega_0)+M_2^{(2)}f(2\omega_0) \quad (16)$$

where, $M_2^{(0)}$, $M_2^{(1)}$ and $M_2^{(2)}$ are respectively the secular ($\Delta m=0$) and non-secular ($\Delta m=\pm 1,\ \pm 2$) dipolar second moments while $f(\omega)$ are the Fourier components of $C^2(t)$ given by

$$2f(\omega)=\int_{-\infty}^{+\infty} C^2(t)\exp(i\omega t)dt \quad (17)$$

Now the total contribution to the observed peak-to-peak derivative width, ΔB_{pp} is given as

$$\Gamma_{total}=\frac{\sqrt{3}}{2}\Delta B_{pp}=\Gamma_h+\Gamma_d \quad (18)$$

In the present case, since $\mathscr{H}_{ex}\langle\mathscr{H}_s$, one can ignore the non-secular broadenings and hence, equation (18) becomes

$$\frac{\sqrt{3}}{2}\Delta B_{pp}=a^{(0)}\, g(0)+M_2^{(0)}f(0) \quad (19)$$

Since the spin correlations arising from $\mathscr{H}_{ex}$ are isotropic the angular dependent line widths provide enough equations to obtain the individual Fourier components.

The ΔB_{pp} values in the a^*c^* plane were fitted into the expression by a least-squares procedure to get

$$g(0)=0.60\pm 0.05\times 10^{-8}\ G^{-1} \text{ and}$$

$$f(0)=0.70\pm 0.10\times 10^{-8}\ G^{-1}.$$

The agreement between the least-squares curve and the experimental values is shown in Fig. 8.

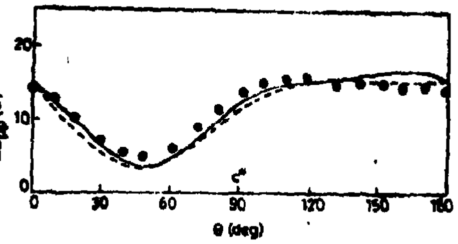


Fig. 8. Experimental and theoretical line width variation in the a^*c^*-plane : (●) experimental points ; (———) least squares fit to the experimental points in the evaluation of $g(0)$ and $f(0)$ and (– – –) line width variation based on B – H model with $g(0)=0.89\times 10^{-8}$ G^{-1} and $f(0)=0.42\times 10^{-8}\ G^{-1}$.

The Fourier components of the secular part of the spin correlation functions can be computed from theoretical models like Blume-Hubbard[22] and Anderson-Weiss[23]. The Blume-Hubbard high temperature approximation of $C(t)$ for $S=1/2$ is

$$C_{BH}(t)=\cos h^{-2}(\tfrac{1}{2}\hat{J}t) \quad (20)$$

where, $\hat{J}$ is the root-mean-square exchange ($\hat{J}=\sqrt{2}J$). The Fourier components of $C(t)$ and $C^2(t)$ are

$$g_{BH}(0)\ =\ 2/\hat{J}$$

$$f_{BH}(0)\ =\ 4/3\hat{J}$$

The Anderson-Weiss proposal of Gaussian $C(t)$ for exchange narrowing is

$$C_G(t)\ =\ \exp[-\tfrac{1}{2}\pi\,\omega_e^2 t^2] \quad (21)$$

with $\omega_e=J$. This leads to the following expressions for $g(0)$ and $f(0)$

$$g_G(0)\ =\ \frac{1}{\omega_e}$$

$$f_G(0)\ =\ \frac{1}{\sqrt{2}\,\omega_e}$$

The computed Fourier components for $J=1\,700$ G, obtained from epr line width analysis (*vide infra*), are given in Table 4. These values compare reasonably well with the experimental values. We find that $g(0)$ is slightly over estimated by B – H *model* while $f(0)$ is underestimated by both the models.

TABLE 4—FOURIER COMPONENTS OF SECULAR SPIN CORRELATION FUNCTIONS

Fourier component	Experimental	B – H model ($\hat{J}=2\,400$ G)	A – W model ($J=1\,700$ G)
$g(0)\times 10^8 G$	0.60±0.05	0.88	0.59
$f(0)\times 10^8 G$	0.70±0.10	0.55	0.42

However, it may be worth noting that we could analyse the results and estimate a reasonable value for the isotropic exchange coupling constant from the single crystal epr data. Also, we have successfully compared and confirmed this value using theoretical models of exchange narrowing phenomena.

References

1. J. A. McCleverty, *Prog. Inorg. Chem.*, 1968, **10**, 49.
2. J. S. Miller and E. J. Epstein, *Prog. Inorg. Chem.*, 1976, **20**, 1.
3. R. P. Burns and C. A. McAuliffe, *Adv. Inorg. Radiochem.* 1979, **22**, 303.
4. J. F. Weiher, L. R. Melby and R. E. Benson, *J. Am. Chem. Soc.*, 1964, **86**, 4329.
5. K. W. Plumlee, B. M. Hoffman, J. A. Ibers and Z. G. Soos, *J. Chem. Phys.*, 1975, **63**, 1926.
6. K. W. Plumlee, B. M. Hoffman, M. T. Ratajack and C. R. Kannewurf, *Solid State Comm.*, 1974, **15**, 1651.
7. D. Snaathorst, H. M. Doesburg, J. A. A. J. Perenboom and C. P. Keijzers, *Inorg. Chem.*, 1981, **20**, 2526.
8. P. T. Manoharan, J. H. Noordik, E. de Boer and C. P. Keijzers *J. Chem. Phys.*, 1981, **74**, 1980.
9. B. L. Ramakrishna and P. T. Manoharan, *Inorg. Chem.*, 1983, **22**, 2113.
10. P. Kuppusamy, B. L. Ramakrishna and P. T. Manoharan, *Proc. Indian Acad. Sci.* (*Chem. Sci.*), 1984, **93**, 977.
11. P. Kuppusamy, B. L. Ramakrishna and P. T. Manoharan, *Inorg. Chem.*, 1984, **23**, 3886.
12. B. L. Ramakrishna and P. T. Manoharan, *J. Phys.*, 1983, **44**, C1405.
13. B. L. Ramakrishna, P. Kuppusamy, P. T. Manoharan and M. Hunziker, *J. Phys.*, 1983, **44**, C1419.
14. P. Kuppusamy and P. T. Manoharan, *Inorg. Chem.*, 1985, **24**, 3053.
15. P. Kuppusamy, C. Mahadevan, M. Seshasayee and P. T. Manoharan, *J. Cryst. Spect. Res.*, 1985, **15**, 359.
16. P. Kuppusamy, N. Venkatalakshmi and P. T. Manoharan, *J. Cryst. Spect. Res.*, 1985, **15**, 629.
17. A. H. Maki, N. Edelstein, A. Davison and R. H. Holm, *J. Am. Chem. Soc.*, 1964, **86**, 1580.
18. A. Davison and R. H. Holm, *Inorg. Synth*, 1971, **10**, 8.
19. K. W. Plumlee, M. T. Ratajack, B. M. Hoffman, C. R. Kannewurf and J. A. Ibers, unpublished work.
20. C. Mahadevan, C. H. Subramaniam, A. Radha, M. Seshasayee and P. T. Manoharan, *Acta Crystallogr.*, *C*, 1984, **40**, 2032.
21. J. H. Van Vleck, *Phys Rev.*, 1948, **74**, 1168.
22. M. Blume and J. Hubbard, *Phys. Rev.*, *B*, 1970, **1**, 3815.
23. P. W. Anderson and P. R. Weiss, *Rev. Mod. Phys.*, 1953, **25**, 269.

J. Indian Chem. Soc.,
Vol. LXIII, January 1986, pp. 101-104

High-resolution Proton Resonance Spectra of Dihalobis(2-(arylazo)pyridine)-ruthenium(II) and -osmium(II)†

A. K. MAHAPATRA, B. K. GHOSH, S. GOSWAMI and A. CHAKRAVORTY*

Department of Inorganic Chemistry, Indian Association for the Cultivation of Science, Calcutta-700 032

The high-resolution ^1H nmr spectra of several isomeric 2-(arylazo)pyridine(L) complexes of type ML_2X_2 (M = Ru, Os ; X = Cl, Br) are reported and completely assigned. Spectral features diagnoistic of geometric structures are delineated and applied to isomers of new complexes.

STRUCTURE and reactivity studies in ruthenium and osmium chemistry of 2-(arylazo)pyridine(L) have received recent attention[1-10]. Interesting cases of geometrical isomerism occur[1,2] in the pseudo-octahedral dihalo species ML_2X_2 (X = Cl, Br). In the present work, we describe the high-resolution ^1H nmr spectra of selected ML_2X_2 complexes including some hitherto unreported species. Complete assignment of spectra is achieved in several cases and features diagnoistic of geometric structure are identified.

Experimental

^1H nmr spectra were measured at 270 MHz (Brucker) or 360 MHz (Jeol) in $CDCl_3$. All chemical shifts are referenced to tetramethylsilane.

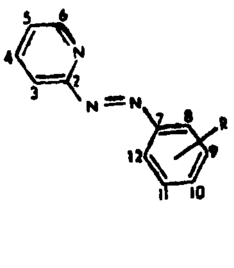
The isomers of $Ru(pap)_2Cl_2$, $Ru(tap)_2Cl_2$ and $Os(tap)_2Br_2$ studied in this work were prepared following reported procedures[1,2,6-8] (pap = 2-(phenylazo)pyridine ; tap = 2-(*m*-tolylazo)pyridine). The ligand dap (2-(*p*-*N*,*N*-dimethylaminophenylazo)-pyridine) was prepared[11] by condensing 2-aminopyridine with *p*-nitrosodimethylaniline in dry toluene in the presence of sodium.

Preparation and separation of two isomers of $Ru(dap)_2Cl_2$: Dinitrogen was passed through a stirred solution of dap (600 mg, 2.68 mmol) in methanol (30 ml) for 15 min. A solution of ruthenium trichloride trihydrate (350 mg, 1.34 mmol) in methanol (20 ml) was added to it. The mixture was heated to reflux for 6 h. A violet solution was obtained which was dried in vacuum. The solid violet mass was subjected to chromatography on a silica gel (B.D.H., 60-120 mesh) column (30 × 1 cm). Dichloromethane eluted a small green band and from the eluent the tt isomer was isolated (6%) by removal of solvent. A major blue-violet band was then eluted with acetonitrile. The solid mass obtained by removal of solvent in vacuum was suspended in xylene (boiling range 137-142°) (75 ml) and heated to reflux for 9 h in order to convert any tt isomer present to the tc isomer. The pure tc complex (50%) was obtained by removing the solvent ; tt isomer (Found : C, 49.82 ; H, 4.44 ; N, 17.97), cc isomer (Found : C, 50.00 ; H, 4.45 ; N, 17.92. $RuC_{26}Cl_2H_{28}N_8$ calcd. for : C, 49.99 ; H, 4.49 ; N, 17.95%).

Preparation of tc-$Os(dap)_2Cl_2$: Dinitrogen was passed through a solution of dap (100 mg, 0.442 mmol) in 2-methoxyethanol (30 ml), and $(NH_4)_2$-$OsCl_6$ (100 mg, 0.227 mmol) was added. The mixture was heated to reflux for 4 h. The solvent was then evaporated to dryness in vacuum. The violet solid thus obtained was subjected to chromatography on silica gel (B.D.H., 60-120 mesh) column (20 × 1 cm) using benzene-acetonitrile (9 : 1) as the eluent. A violet band was eluted out and from it the required complex (59%) was obtained by removal of solvent in vacuum (Found : C, 43.70 ; H, 3.95 ; N, 15.71. $OsC_{26}Cl_2H_{28}N_8$ calcd for : C, 43.75 ; H, 3.93 ; N, 15.70%).

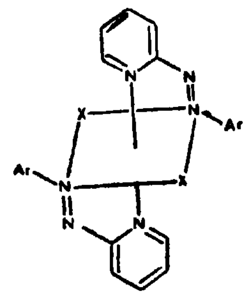
Results and Discussion

Isomerism of ML_2X_2 species : The azopyridines(L) of interest and their abbreviations are shown in structure (1). The pseudo-octahedral



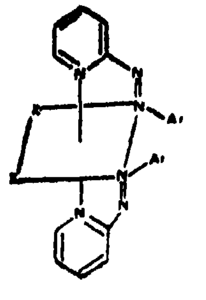
(1)

B = H, pap
B = 9-Me, tap
B = 10-NMe$_2$, dap

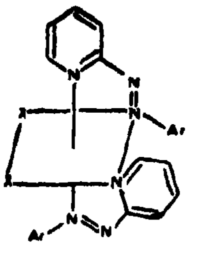


(2)

† Dedicated to Professor Sadhan Basu on the occasion of his 65th birthday.



(3)



(4)

ML_2X_2 species can in principle occur in five geometrically isomeric forms[1,8] – two and three of these respectively have the MX_2 group in *trans*- and *cis*-geometries. Of the five possible isomers, a maximum of three have been observed in practice. The geometries of N(pyridine), N(pyridine) and N(azo), N(azo) pairs in the observed isomers are *trans-trans* tt (2), *trans-cis* tc (3) and *cis-cis* cc (4).

While $Ru(pap)_2Cl_2$ and $Ru(tap)_2Cl_2$ occur in tt, tc and cc forms[6], only the tc and cc varieties are observed in the corresponding osmium compounds[6,7]. The structures of tc- and cc-$Ru(pap)_2Cl_2$[18] as well as tc- and cc-$Os(tap)_2Cl_2$[7,13] are accurately known from X-ray work.

The $Ru(dap)_2Cl_2$ and $Os(dap)_2Cl_2$ complexes are reported here for the first time. The ruthenium complex occurs in only two isomeric forms, one green and the other blue-violet. On the other hand, $Os(dap)_2Cl_2$ is found to exist exclusively in one form. Geometrical assignments of these species were achieved on the basis of ir, uv-vis and electrochemical data[14] and more importantly on ^1H nmr data. The latter will be considered in this work.

Spectra of tt and tc isomers of pap and tap complexes: All the complexes display highly resolved ^1H nmr spectra (a representative case in Fig. 1). Chemical shift and spin-spin splitting (among nearest neighbour protons only) data are in Table 1. Interspectral correlations are displayed schematically in Fig. 2.

The signals from protons of the pyridine rings are readily assigned on the basis[15] of chemical shifts and spin-spin splittings. Thus, the 6-H is a doublet with a relatively low J value (~5 Hz). The phenyl ring protons are assigned on a similar basis using substituent-induced change in splitting patterns and chemical shifts as additional indicators. For example, 8-H and 12-H are coincident doublets in pap isomers whereas the 8-H signals appear as separate singlet in the corresponding tap isomers. Further, the 8-H signals are very significantly shifted to higher fields in going from a pap isomer to the corresponding tap isomer in accord with the electron releasing character of the methyl substituent[16].

We now consider the consequence of going from the tt to the tc isomer for a given ligand. The major effects are seen in the protons closest to the metal atom. The 6-H is shifted downfield by δ ~0.4 and the 8-H and 12-H are shifted upfield by δ ~0.7 in going from tt to tc configuration. The two chelate rings are approximately coplaner and orthogonal in the tt and tc isomers, respectively. The larger mutual shielding deshielding effects and higher spectral spread in the tc isomer is thus qualitatively understandable. An important result is that the 6-H and 8-H, 12-H chemical shifts in tt and tc isomers are of diagnoistic value for identification of geometry of the ruthenium complexes: tt isomer: 6-H, δ 8.9; 8-H, 12-H, 7.3-7.6; and tc isomer: 6-H, 9.4; 8-H, 12-H, 6.5-6.8. This result is utilised below for characterisation of the $Ru(dap)_2Cl_2$ isomers.

Isomeric structure of the dap complexes: The green isomer of $Ru(dap)_2Cl_2$ has the 6-H signal at

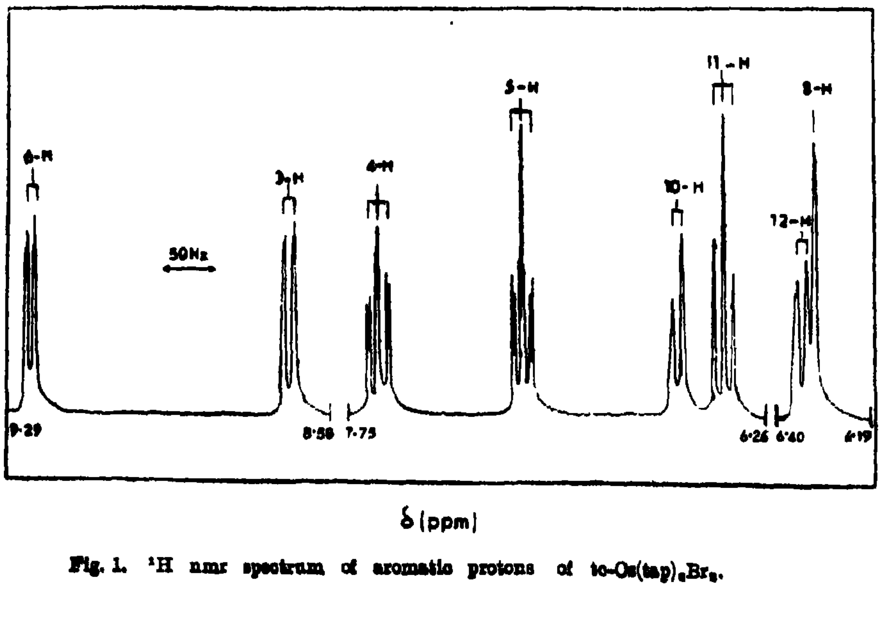


Fig. 1. ^1H nmr spectrum of aromatic protons of tc-$Os(tap)_2Br_2$.

Table 1 — ^{1}H nmr Spectral Data in $CDCl_3$

Compd.	δ/(J)										
	6-H	3-H	4-H	5-H	8-H	9-H	10-H	11-H	12-H	9-Me	10-NMe_2
tt-Ru(pap)$_2$Cl$_2$	8.92 (4.4)	8.60 (7.2)	8.19 (7.6)	7.82 (6.3)	7.54 (8.5)	6.98 (7.8)	7.18 (7.2)	6.98 (7.8)	7.54 (8.5)	—	—
tt-Ru(tap)$_2$Cl$_2$	8.91 (4.4)	8.58 (8.3)	8.17 (7.9)	7.79 (5.9)	7.34	—	6.97 (7.8)	6.97 (7.5)	7.40 (7.5)	2.19	—
tc-Ru(pap)$_2$Cl$_2$	9.86 (5.4)	8.52 (8.8)	7.99 (7.7)	7.52 (6.6)	6.82 (8.5)	7.11 (7.6)	7.28 (6.8)	7.11 (7.8)	6.82 (8.5)	—	—
tc-Ru(tap)$_2$Cl$_2$	9.37 (5.9)	8.52 (7.8)	8.00 (7.8)	7.52 (6.4)	6.60	—	7.08 (7.8)	6.98 (7.6)	6.58 (9.2)	2.14	—
tc-Os(tap)$_2$Br$_2$	9.24 (5.9)	8.66 (8.2)	7.68 (7.8)	7.87 (6.6)	6.81	—	6.93 (7.7)	6.85 (7.3)	7.08 (7.6)	2.18	—
tt-Ru(dap)$_2$Cl$_2$	8.94 (5.5)	8.48 (8.1)	8.06 (7.9)	7.62 (8.9)	7.60 (9.6)	6.20 (9.2)	—	6.20 (9.2)	7.60 (9.6)	—	3.09
tc-Ru(dap)$_2$Cl$_2$	9.51 (5.1)	8.36 (7.8)	7.92 (7.8)	7.44 (6.8)	6.82 (9.3)	6.24 (9.3)	—	6.24 (9.8)	6.82 (9.8)	—	3.04
tc-Os(dap)$_2$Cl$_2$	9.11 (6.0)	8.49 (8.0)	7.64 (7.4)	7.38 (6.2)	6.56 (9.1)	6.21 (9.2)	—	6.21 (9.2)	6.56 (9.1)	—	3.02

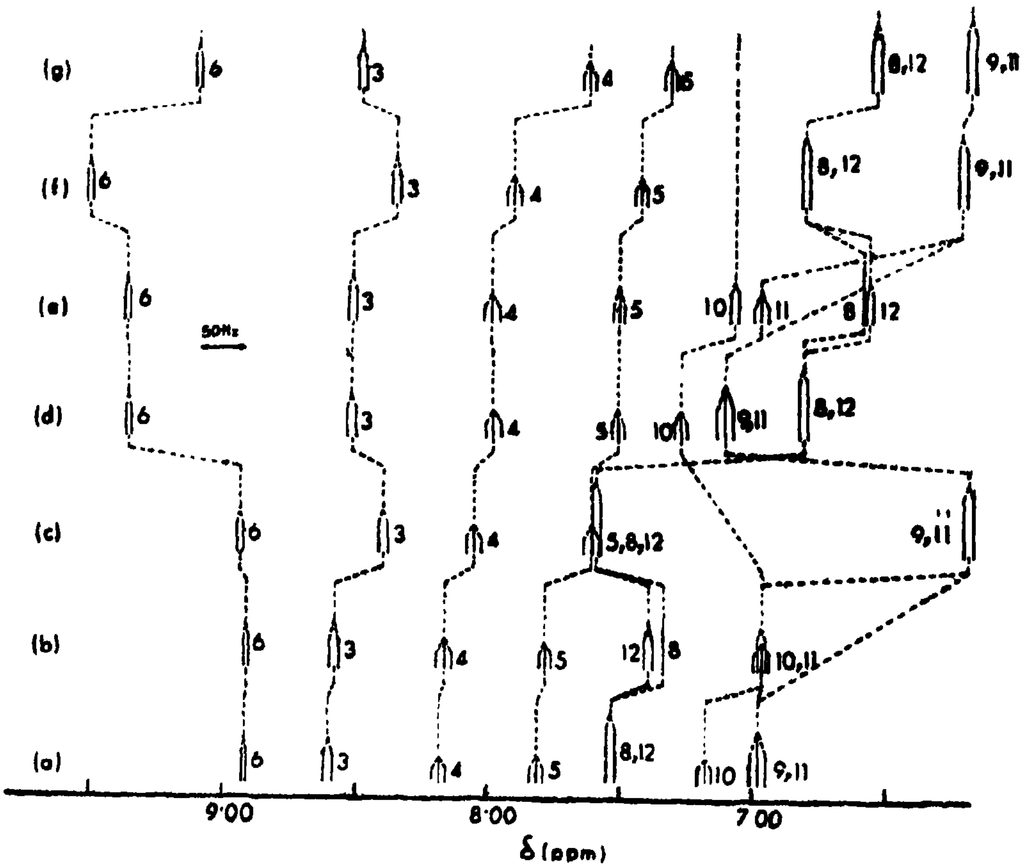


Fig. 2. Schematic ^{1}H nmr spectra of complexes: (a) tt-Ru(pap)$_2$Cl$_2$, (b) tt-Ru(tap)$_2$Cl$_2$, (c) tt-Ru(dap)$_2$Cl$_2$, (d) tc-Ru(pap)$_2$Cl$_2$, (e) tc-Ru(tap)$_2$Cl$_2$, (f) tc-Ru(dap)$_2$Cl$_2$ and (g) tc-Os(dap)$_2$Cl$_2$. Numbers in the figure indicate the proton number.

δ 8.94 while the 8-H, 12-H doublet occur at 7.60. On the other hand, the corresponding signals in the blue-violet isomer occur at δ 9.51 and 6.82, respectively. Clearly the green isomer has the tt configuration while the blue-violet form is tc. All other properties of the two isomers are in accord[14] with this geometric assignment. Similarly, the only observed isomer Os(dap)$_2$Cl$_2$ has tc geometry. We note the large (δ ~0.8) upfield shift of 9-H, 11-H signal in going from a pap to the corresponding dap isomer. The strong electron releasing character of the NMe_2 is no doubt responsible.

Spectra of cc isomers : In tt and tc isomers the chelate rings are equivalent due to the presence of two-fold symmetry. The cc isomer is devoid of such symmetry. The nmr spectra of cc complexes are indeed much more complex than those of tt and tc isomers. We shall not consider the details of such spectra any further here since complete and unambiguous assignment of aromatic signals have not been achieved so far. Among $Ru(tap)_2Cl_2$ isomers, tt and tc display a single 9-Me signal (Table 1) while cc has two such signals (δ 2.21 and 2.41) as expected. Similarly both the observed isomers of $Ru(dap)_2Cl_2$ have single NMe_2 signal (Table 1).

Acknowledgement

Financial assistance received from the Department of Science and Technology and Council of Scientific and Industrial Research, New Delhi, is gratefully acknowledged.

References

1. S. Goswami, A. R. Chakravarty and A. Chakravorty, *Inorg. Chem.*, 1981, 20, 2246.
2. S. Goswami, A. R. Chakravarty and A. Chakravorty, *Inorg. Chem.*, 1982, 21, 2737.
3. S. Goswami, A. R. Chakravarty and A. Chakravorty, *J. Chem. Soc., Chem. Commun.*, 1982, 1288.
4. S. Goswami, A. R. Chakravarty and A. Chakravorty, *Inorg. Chem.*, 1983, 22, 602.
5. S. Goswami, R. N. Mukherjee and A. Chakravorty, *Inorg. Chem.*, 1983, 22, 2825.
6. B. K. Ghosh, S. Goswami and A. Chakravorty, *Inorg. Chem.*, 1983, 22, 3358.
7. B. K. Ghosh, A. Mukhopadhyay, S. Goswami and A. Chakravorty, *Inorg. Chem.*, 1984, 23, 4633.
8. R. A. Krause and K. Krause, *Inorg. Chem.*, 1980, 19, 2600.
9. R. A. Krause and K. Krause, *Inorg. Chem.*, 1982, 21, 1714.
10. S. Wolfgang, T. C. Strekas, H. D. Gafney, R. A. Krause and K. Krause, *Inorg. Chem.*, 1984, 23, 2650.
11. R. W. Faessinger and E. V. Brown, *J. Am. Chem. Soc.*, 1951, 73, 4606.
12. A. Seal and S. Ray, *Acta Crystallogr., C*, 1984, 40, 929.
13. A. Mukhopadhyay and S. Ray, unpublished results.
14. A. Mahapatra, B. K. Ghosh, S. Goswami and A. Chakravorty, unpublished results.
15. B. Pesce, "Nuclear Magnetic Resonance in Chemistry", Academic Press, New York, 1965, p. 174.
16. H. Gunther, "NMR Spectroscopy—An Introduction", Wiley, Chichester, 1980, p. 65.

J. Indian Chem. Soc.,
Vol. LXIII, January 1986, pp. 105-107

Nuclear Quadrupole Resonance Studies on some Donor-Acceptor Type Complexes†

RAMA BASU

Department of Chemistry, University College of Science University of Calcutta, Calcutta-700 009

A Townes and Dailey's analysis was carried out on the nqr data published so far by the author with some unpublished ones and also on some other existing literature data reported earlier. The results tally with the theoretical interpretation in many cases. The discrepancy observed in some cases may be due to higher multipolar interactions.

ELECTRON donor-acceptor type complexes show significant nqr frequency shift with respect to the frequency of the initial component molecules having the same probe. Direct connection between nqr coupling constant and charge distribution leads to the expectation that nqr should be a sensitive device for the study of inter-molecular charge transfer in solid state.

Weiss's suggestion[1] that nqr frequency should shift due to molecular complex formation through charge transfer interaction has been well demonstrated with molecules having quadrupolar nucleus either in acceptors or in donors or in both the donors and acceptors at the same time[2-8]. As expected, a linear relation between nqr shift and the charge transfer interaction energy $h\nu_{op}$ or the ionisation energy of the donor was obtained in all these cases. However, Maksyutin[9] while studying the interaction of picryl chloride with substituted aromatic hydrocarbons proposed from theoretical consideration that if ^{35}Cl be on the donor molecule, $\Delta\nu$ should be negative and if ^{35}Cl be on the acceptor molecule $\Delta\nu$ should be positive, although his experimental results even donot always follow his proposition. The present author[2-4] also showed in earlier communications that although a linear relation between the nqr shift ($\Delta\nu$) and the donor ionisation potential or $h\nu_{op}$ was obtained in all cases, Maksyutin's idea of negative shift with respect to donor or positive shift with respect to acceptor was not always corroborated with. However, according to Maksyutin, geometrical factors would also be of significant importance for the nqr shift in case of disubstituted-benzenes. According to Douglass[10], the crystal field effect frequently shift quadrupole resonance frequencies by ± 200 kHz. In order to determine any shift arising from charge transfer, these crystal field effect as well as geometrical factors would have to be eliminated. Unfortunately, these extranaeous effects are not obtainable at present either from experiments or calculations. Although electronic factor possesses a systematic character, the other two factors, namely, geometrical factors and crystal field effect to a certain degree possess an accidental character, hence superposition of all these factors leads to the absence of any definite regularity in the nqr frequency shifts.

Frequency changes in these molecular complexes may be due primarily to change in electron density in the π- and σ-orbitals of the Cl atom. Maksyutin's analysis takes into account only π-orbital changes. However, in most cases it is the ^{35}Cl nqr signal that has been recorded when Cl atom is introduced as a substituent in the donor or acceptor. In these compounds, charge transfer takes place between the π-molecular orbital of the donor and acceptor, and the Cl atom does not participate in the electron exchange directly, the only effect that the electron transfer can have is on the nature of the character of the C – Cl bond. So in all probability, frequency changes would have contribution from the changes in electron density of σ-orbitals of the Cl atom as well. With this contention, we have calculated the change in ionicity of the C – Cl bond present in the donor or acceptor or in both following Townes and Dailey, with the nqr frequency reported earlier by the present author as well as by others.

Theory :

Townes and Dailey's model[11] analyses the nqr signal in molecules in terms of field gradient at the quadrupolar nucleus. The covalency of C – Cl bond is calculated following Townes and Dailey theory by the relation,

$$\left(\frac{eq\,Q}{h}\right)_{exp} = (1-i)\left(\frac{eq\,Q}{h}\right)_{atom}$$

where, i is the ionic character of the bond and therefore (1 – i) is the covalent character of the bond, $(eq\,Q/h)_{atom}$ is the nqr frequency for the atomic chlorine which is 109.7 MHz. In resonance terms following Townes and Dailey, bonding in these complexes may be described as a hybrid of a

† Dedicated to Professor Sadhan Basu on the occasion of his 65th birthday.

A part of the article was presented at the National Conference on Spectroscopy and Theoretical Chemistry held at Calcutta. December 5-7, 1985.

pure covalent bond and a pure ionic bond,

$$Q = (1 - i)(R - Cl) + i(R^{+} - Cl^{-})$$

where, i is the fractional ionic character of the bond. Calculation of i, therefore, amounts to estimating the extent of electron density change of Cl atom in a R – Cl bond.

Results and Discussion

We have calculated the ionicity of R – Cl bond of a large number of molecular complexes. The results are shown in Table 1. The nqr frequency change and ionicity of C – Cl bond in molecular complexes of *p*-chloronitrobenzene and *o*-chloronitrobenzene with different hydrocarbons are reported in the 8th International Symposium on NQR held at Darmstadt, Germany.

From Table 1 it may be observed that the ionicity of the C – Cl bond changes appreciably as it enters into complexation. Townes and Dailey's analysis suggests that the dipole moment of the C – Cl bond in the donor molecule will increase and that in the acceptor decrease on charge transfer complex formation. As expected, the data for chloranilic acid, tetrachlorophthalic anhydride and chloranil (acceptors) show that the ionicity decreases as these go into complexation. Same is true for *p*-dichlorobenzene, *p*-chloroaniline and *p*-chlorophenol, the ionicity increases as they go for complexation with DDQ, chloranil, tetrachlorophthalic anhydride, chloranilic acid and *p*-chloronitrobenzene as donors, whereas a few others show opposite effect. Thus, a perfect generality cannot be claimed. The discrepancy may arise due to the presence of dipolar and multipolar interaction in

TABLE 1—IONICITIES OF DONORS, ACCEPTORS AND THE ELECTRON DONOR-ACCEPTOR COMPLEXES

Aceeptors	Donors	Ionicity of the C-Cl bond in the complex from nqr data
Chloranilic acid ionicity = 0.6554	Benzene	0.6547
	Naphthalene	0.6549
	Triphenylene	0.6528
	Pyrene	0.6522
	Anthracene	0.6512
Tetrachlorophthalic anhydride ionicity = 0.6552	Benzene	0.6541
	Naphthalene	0.6534
	Pyrene	0.6499
	Anthracene	0.6489
Chloranil ionicity = 0.6591	Benzene	0.6566
	Naphthalene	0.6559
	Triphenylene	0.6528
	Pyrene	0.6528
	Anthracene	0.6512
p-Chloronitrobenzene ionicity = 0.6639	Naphthalene	0.6606
	Anthracene	0.6582
	Pyrene	0.6589
	Chrysene	0.6596
	Biphenyl	0.6624
o-Chloronitrobenzene ionicity = 0.6667	Naphthalene	0.6639
	Anthracene	0.6589
	Chrysene	0.6617
	Biphenyl	0.6660
Picryl chloride ionicity = 0.6410	Benzene	0.6392
	Fluorobenzene	0.6383
	Chlorobenzene	0.6358
	Bromobenzene	0.6354
	Toluene	0.6347 (anti.)
		0.6388 (syn.)
	Iodobenzene	0.6381
	Phenol	0.6304
	Nitrobenzene	0.6402
	p-Xylene	0.6406
	p-Iodotoluene	0.6406
	p-Cresol	0.6399
	p-Bromotoluene	0.6390
	p-Chlorotoluene	0.6340 (anti.)
		0.6362 (syn.)
		0.6824 (^{35}Cl *p*-chlorotoluene)
		0.6837 (^{35}Cl *p*-chlorotoluene)
	p-Fluorotoluene	0.6350
	Mesitylene	0.6318
	Durene	0.6356
	Pentamethylbenzene	0.6330
	Naphthalene	0.6360
	Anthracene	0.6372
	Phenanthrene	0.6361

(Table 1 contd.)

		Donor	Acceptor
p-Dichlorobenzene ionicity = 0.6818	DDQ ionicity = 0.6627	0.6840	0.6518
	Chloranil ionicity = 0.6591	0.6871	0.6567
	Tetrachlorophthalic anhydride ionicity = 0.6552	0.6909	0.6620
	Chloranilic acid ionicity = 0.6554	0.6917	0.6627
	p-Chloronitrobenzene ionicity = 0.6689	0.6904	0.6749
p-Chloroaniline ionicity = 0.6896	DDQ ionicity = 0.6627	0.6901	0.6569
	Chloranil ionicity = 0.6591	0.6917	0.6566
	Tetrachlorophthalic anhydride ionicity = 0.6552	0.6970	0.6548
	Chloranilic acid ionicity = 0.6554	0.6976	0.6591
	p-Chloronitrobenzene ionicity = 0.6689	0.6991	0.6704
p-Chlorophenol ionicity = 0.6813	DDQ ionicity = 0.6627	0.6888	0.6529
	Chloranil ionicity = 0.6591	0.6852	0.6548
	Tetrachlorophthalic anhydride ionicity = 0.6552	0.6886	0.6566
	Chloranilic acid ionicity = 0.6554	0.6898	0.6585
	p-Chloronitrobenzene ionicity = 0.6689	0.6905	0.6715

the crystals of charge transfer complexes. This will considerably affect the bond character of C – Cl bond because of the change in potential gradient at Cl atom. This arises also from dipole-induced dipole interaction. Also, while calculating, the dipole moment geometry of the complexes should play a dominant role as well.

References

1. A. Weiss, "Nuclear Quadrupole Resonance in Topics in Current Chemistry", Springer-Verlag, Berlin, 1972, p. 1.
2. R. Basu and M. Ghosh, *J. Chem. Phys.*, 1978, **68**, 2510.
3. R. Basu and M. Ghosh, *Indian J. Chem., Sec. A*, 1979, **17**, 399.
4. A. K. Das and R. Basu, *Indian J. Chem., Sect. A*, 1983, **22**, 914.
5. H. O. Hooper, *J. Chem. Phys.*, 1964, **41**, 599.
6. D. F. R. Gilson and C. T. O'Konski, *J. Chem. Phys.*, 1968, **48**, 2767.
7. R. A. Bennet and H. O. Hooper, *J. Chem. Phys.*, 1967, **47**, 4855.
8. C. H. Fleming and W. M. Hanna, *J. Am. Chem. Soc.*, 1971, **93**, 5030.
9. Y. K. Maksyutin, T. A. Babushkin, Ye. N. Guryanova and G. K. Semin, *Theor. Chim. Acta*, 1969, **14**, 48.
10. D. C. Douglass, *J. Chem. Phys.*, 1960, **32**, 1882.
11. C. H. Townes and B. P. Dailey, *J. Chem. Phys.*, 1949, **17**, 782.

J. Indian Chem. Soc.,
Vol. LXIII, January 1986, pp. 108-112

Some Applications of Mössbauer Spectroscopy†‡

C. K. MAJUMDAR

Magnetism Department, Indian Association for the Cultivation of Science, Jadavpur, Calcutta-700 032

Mössbauer spectra of iron-containing inorganic and organometallic compounds provide important information. *The products of corrosion of mild steel in dilute saline and acidic medium have been identified and the diffusion constant that gives the rate of the corrosion reaction has been measured.* Iron bearing minerals of eastern India are being systematically explored for geochemical information. Radiation damage *in steel with iron* has also been studied to learn about defects formed in the process.

THE Mössbauer effect is the analog of atomic resonance fluorescence in nuclei. It is based on Mössbauer's discovery that the nuclear recoil during gamma emission or absorption could be reduced essentially to zero if the emitting or absorbing nucleus was embedded in a solid. The available energy E is used in nuclear excitation as well as excitation of phonons in the solid. There will be always emission or absorption of gamma rays without phonons being involved. The recoilless zero-phonon line is the Mössbauer line. It is extremely sharp.

Much has been done with the Mössbauer effect using many isotopes[1]. The most useful isotope is ^{57}Fe which we too have been using in our work. The relevant data are well known. The 14.4 keV Mössbauer line is due to a transition from a spin 3/2 excited state to the spin 1/2 ground state. The magnetic moments of the ground and excited states are 0.091 and −0.15 nm, respectively. The excited state has a quadrupole moment of 0.21 b.

If the source emitting a sharp Mössbauer line is deliberately moved with a velocity v, the energy of the line is altered by $\Delta E = (v/c)$ E. For the 14.4 keV gamma ray of ^{57}Fe a velocity 1 mm s^{-1} is equivalent to $\Delta E = 4.808 \times 10^{-8}$ eV.

A standard Mössbauer apparatus consists of (i) a drive, usually electromechanical, capable of moving the sources, (ii) an absorber which may be cooled when necessary, (*iii*) a detector, normally a proportional counter, and (iv) the associated electronics including a multichannel analyser. The apparatus we have is an ECIL MBS 35 Mössbauer spectrometer. The multichannel apparatus has been constructed following the design developed at the Tata Institute of Fundamental Research (T.I.F.R.). The single channel of MBS 35 spectrometer is used as a window to select the 14.4 keV radiation. The cryostat useful down to liquid nitrogen temperature has been fabricated by us.

Basic data of ^{57}Fe Mössbauer work :

The following facts are necessary for the interpretation and understanding of the work using the Mössbauer isotope ^{57}Fe.

(i) If the absorbing ^{57}Fe nucleus is in a magnetic medium, for instance α-Fe below the Curie temperature, it will feel the enormously high internal field of the magnetic state (~330 kOe for α-Fe). The Zeeman splitting of the nuclear levels in such a field will give rise to a six-line absorption pattern (Fig. 1).

(*ii*) If the absorbing ^{57}Fe nucleus is in a nonmagnetic, non-cubic environment, the quadrupole moment of the excited state gives rise to a doublet (Fig. 2). Generally, the quadrupole splitting due to a Fe^{II} ion is much larger than that due to a Fe^{III} ion. If the environment is magnetic, the line spacings of the six-finger pattern are not uniform.

(*iii*) The finite size of the nucleus and the electron density at the nucleus, which is susceptible to changes in the chemical environment, cause a shift of the centroid of the lines. The shift is called the isomer shift and is now measured from the standard sodium nitroprusside absorber.

Some typical results :

We shall describe some of the data collected by us and their interpretation. Without large material preparation and characterisation facilities we mostly use naturally occurring minerals and compounds or study phenomena where sample preparation is trivial. Occasionally we get samples from chemists engaged in synthesis of chemicals.

Chemical information : The valence state Fe^{II} or Fe^{III} can be identified easily by the quadrupole splitting. Very often overlapping narrow doublets are seen, showing the presence of Fe^{III} ions in *inequivalent sites*; this fact can be combined with structural data usefully. Interesting information

† Dedicated to Professor Sadhan Basu on the occasion of his 65th birthday.

Experimental work in Mössbauer spectroscopy was started in the Physics department of Calcutta University in 1980. The field had already been explored for more than twenty years, and any meaningful work was possible only in interdisciplinary areas involving several departments. Professor Sadhan Basu, as Palit Professor of Chemistry and later as Director of the Indian Association for the Cultivation of Science, encouraged the research activities.

‡ A part of the article was presented at the National Conference on Spectroscopy and Theoretical Chemistry held at Calcutta, December 5-7, 1985.

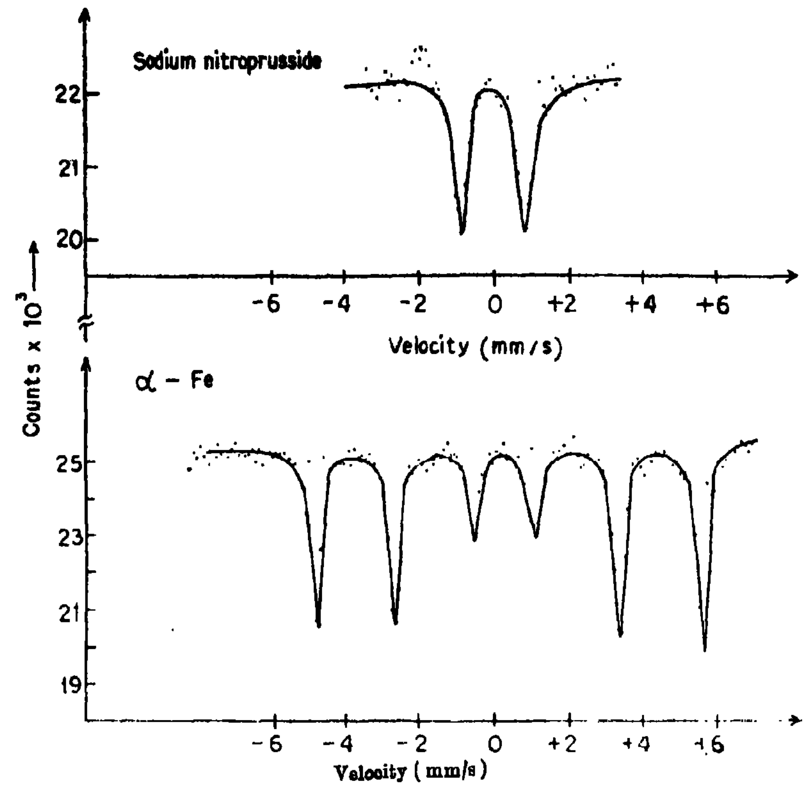


Fig. 1. Mössbauer spectra of sodium nitroprusside and α-Fe (these are required for calibrating the apparatus and the isomer shift measurements).

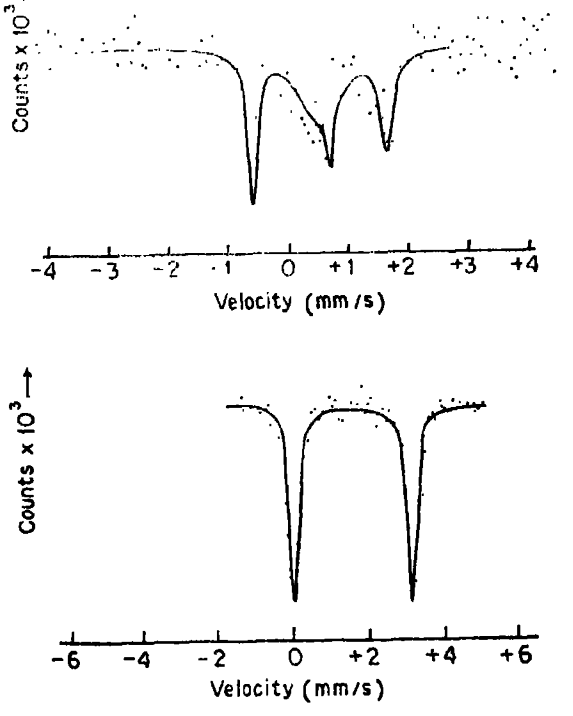


Fig. 2. Spectrum of $FeSO_4.7H_2O$ (below; the wide quadrupole separation due to the Fe^{II} ion may be noted). The upper part is the spectrum of an organometallic compound showing overlapping doublets (courtesy: G. Mukherjee, and S. N. Poddar, unpublished).

about the functioning of haemoglobin or organometallic insecticides can be found. Coupled with susceptibility measurements, the spin state of iron can be identified. Magnetic phase transformations have been monitored and the critical indices measured from Mössbauer experiments.

Fig. 2 shows the spectrum of $FeSO_4.7H_2O$, where the wide quadrupole splitting is typical of the Fe^{II} state. It also shows the spectrum of an organometallic complex with two overlapping doublets. The iron ion appears to be in the Fe^{III} state. The measured isomer shift and quadrupole splitting can be compared, respectively, with detailed theoretical calculations of the s-electron density at the iron nucleus and the electric field gradient at the iron nucleus.

Corrosion : Corrosion[2] of iron or rusting is an electrochemical process which occurs in diverse forms under different circumstances[3]. One form we have investigated to know the nature and composition of the oxides and oxyhydroxides and the rate of corrosion[4]. Rusting is prevented by using inhibitors and surfactants and the change in the rate of corrosion with these can be domonstrated with the Mössbauer effect.

Four oxyhydroxides of iron, α-, β-, γ- and δ-FeOOH as well as two oxides, α- and γ-Fe_2O_3 are known. If the oxygen supply is restricted, the mixed oxide Fe_3O_4 (magnetite) may form.

The Mössbauer spectrum of the corrosion products of a sample of mild steel exposed to 0.1 *N*

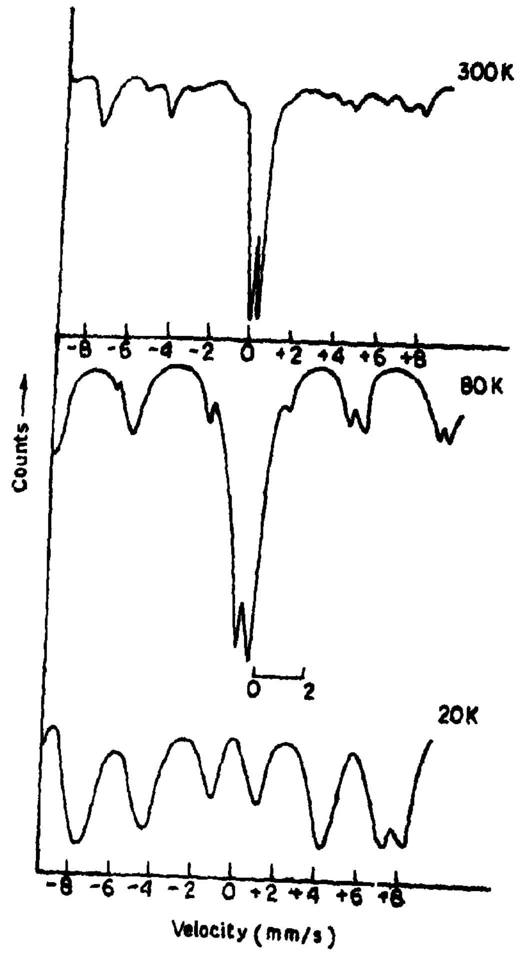


Fig. 3. Spectra of corrosion products[4,6]. The spectrum at 20 K was taken by S. Mishra and H. G. Devare of T. I. F. R. on the same sample (courtesy : J. Ray).

HCl solution for about five months shows a central doublet with weak satellite lines. The isomer shifts and quadrupole splitting of the central doublet are characteristic of trivalent oxyhydroxides. For more precise identification we note the widely different Néel temperatures T_N of the products : 950 for α-Fe_2O_3, 403 for α-FeOOH 295 for β-FeOOH and 73 K for γ-FeOOH. The *six-finger* patterns are expected for the α-form well above the room temperature, for the β-form just below the room temperature and for the γ-form just below the liquid nitrogen temperature.

The situation is complicated by superparamagnetism. Although the temperature is *below* T_N, the long range order does not set in and the internal field does not manifest itself in the spectrum as long as the sample size is less than a *critical size*. This critical size turns out to be about 15 to 17 nm and the corrosion products are usually in fine *microcrystallites* of size smaller than this critical size. Hence, the spectrum will not have six-finger pattern but will show only the doublet with quadrupole splitting as it would in a paramagnetic medium. Well below the transition temperature, the internal field builds up sufficiently and the six-finger pattern appears. If α-Fe_2O_3 is formed, its six-line pattern would show up at room temperature. If α-FeOOH is formed, at room temperature the pattern due to the internal field may or may not be seen, the critical size dictating the situation. With β-FeOOH, the internal field can be seen at liquid nitrogen temperature where α-FeOOH will also be seen definitely. For γ-FeOOH, the doublet alone is seen down to liquid nitrogen temperature, but will split at liquid hydrogen or helium temperature. Thus, measurements at room temperature, liquid nitrogen and liquid hydrogen or helium temperature would identify the products easily.

Fig. 3 shows the Mössbauer spectrum of a mild steel sample exposed to 0.1 *N* HCl solution. The top curve at room temperature shows the central doublet due to γ-FeOOH and weak lines due to α-Fe_2O_3 and α-FeOOH. The identification is done by taking the spectrum of pure α-Fe_2O_3 and α-FeOOH. The middle curve at liquid nitrogen temperature shows no further splitting hence, the β-form is not present. The central doublet splits in the spectrum taken at 20 K, thus showing that it is γ-FeOOH. In this particular case, the amounts of γ-FeOOH, α-Fe_2O_3 and α-FeOOH are 52, 33 and 15%, respectively.

The transmission Mössbauer geometry is not convenient for the study of corrosion rate as the product must form a thick layer and then be scraped off the sample for taking the spectrum. In the initial stages of the reaction the products form a thin layer. The rate is, therefore, better studied by a surface sensitive tool and the electron reemission Mössbauer (ERM) study is more suitable.

The ERM counter has been made at the Bhabha Atomic Research Centre, Bombay[6], and the experiment was done by exposing mild steel sample to 0.1 *N* HCl solution for 5, 10, 20, 30, 60 *etc.* minutes and taking the spectrum. The central doublet due to corrosion product grows steadily while the iron lines disappear. The reaction is an inhomogeneous one at the solution-solid interface and controlled by diffusion. Our data are consistent with the parabolic law[8] characteristic of the process, that is, the thickness of the corrosion layer grows as $t^{1/2}$, where t is the time of exposure to the corroding agent. The diffusion constant is 1.4×10^{-18} cm^2 s^{-1}, corresponding to a growth of about 300 nm thickness in one hour.

Unsaturated organic compounds and compounds containing sulphur act as *inhibitors*. Thiourea is a typical inhibitor. Surfactants usually contain a long aliphatic hydrocarbon chain with one or more polar functional sites, such as NH_2, OH, HSO_3, or COOH. They form lamellar micelles or other aggregates on the metallic surface affecting the cathodic or anodic reaction. We have shown that the slowing down of corrosion can be measured and that there are

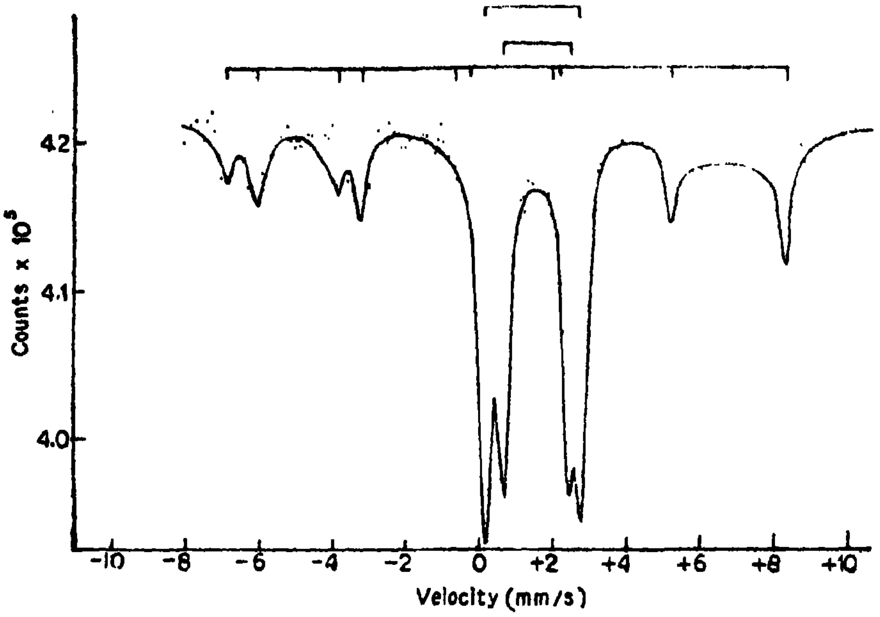


Fig. 4. Spectra of a greenshale rock (work with D. Das, M. K. Bose and M. Chakraborti, unpublished). The narrow doublet is due to $FeCO_3$, the wider doublet is due to chlorite, and the other lines are of magnetite.

several mechanisms of inhibition. Further studies on the efficiency of inhibitors and surfactants would be interesting.

Study of iron-bearing rocks and minerals in eastern India : By Mössbauer spectroscopy one can determine in a rock the nature and content of the iron compounds—oxide, silicate, sulphate, oxyhydroxide, carbonate or any other form. The most dramatic use of the technique was made on lunar rocks[7].

The eastern part of India abounds in iron ores. By a systematic study of the ores from a region one can learn a lot about the geophysical and geochemical history of the region. The total iron content can be measured, this depends on the known isotopic abundance of ^{57}Fe, the source strength, sample preparation and thickness and chemical composition. Usually the Mössbauer results on total iron content are lower than those due to chemical analysis, but at least a lower bound on iron content can be found. The ferrous-ferric ratio is much more easily determined and tells us much about the geochemistry of the minerals. Some of the compounds available in pure form exhibit interesting phenomena : siderite $FeCO_3$ has a metamagnetic transformation at 38 K ; the disulphide FeS_2 shows a structural transformation between two forms, pyrite and marcasite ; and so on.

Fig. 4 shows the Mössbauer spectrum at room temperature of the middle section of a greenshale rock. The rock had a greenish side exposed to atomosphere ; this part was identified as mostly chlorite, hydrated magnesium ferrous aluminosilicate. The middle section had evidence of ferrous carbonate and magnetite. The magnetite lines are easily identified in the Figure. The inner doublet is due to $FeCO_3$, while the strong outer doublet is due to chlorite.

The Mössbauer information of a pure compound, say haematite α-Fe_2O_3, will always be the same, but where the stoichiometry or the ferrous-ferric ratio can change with geological environment (as in magnetite or ferrites) the spectra differ and provide information. We have seen magnetite spectra with six-lines ; then x in $Fe_{3-x}O_4$ is nearly 0.3.

Radiation damage studies : The study of radiation damage of metal has become important for information required in operating nuclear reactors and space vehicles. Radiation can create point defects, interstitials and dislocations, and occasionally melts the metal which then recrystallises. The potentiality of the technique can be seen from a work of Verbiest and Pattyn[8]. This is an integration of heavy ion physics and Mössbauer spectroscopy at low temperature, radioactive ^{57}Co is directly implanted into aluminium at liquid helium temperature. The sample is annealed at higher temperature to get ^{57}Co at proper sites and then bombarded with aluminium atoms to produce damage. The Mössbauer spectra taken in such samples reveal information on interstitials, clusters and vacancies of various types.

In the Variable Energy Cyclotron Centre (V.E.C.C.) at Calcutta we have been exposing several stacks of stainless steel foils to alpha-beams of energy 30 MeV and taking their Mössbauer spectra. A stack of eight 25μ foils was exposed. The full width at half the maximum (FWHM) has increased by 50% (Fig. 5). Actually two foils got fused in the heat generated in the bombardment and a large part of the broadening is due to increase in

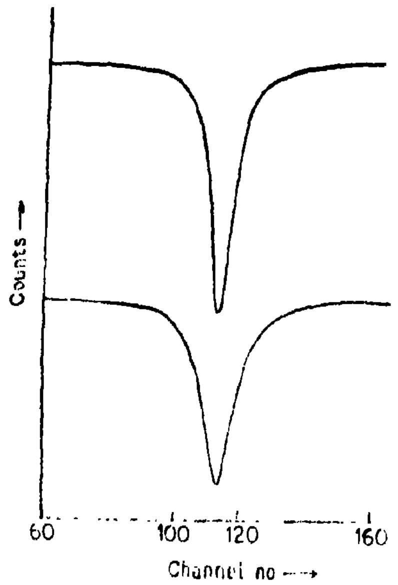


Fig. 5. Broadening of Mössbauer line of iron in steel due to α-bombardment at V.E.C.C. (work with G. Mukhopadhyay *et al.*). Only part of the broadening is due to radiation damage.

thickness. The alpha-particle bombardment destroys the cubic symmetry around the ^{57}Fe nucleus at some sites and the resulting quadrupole splitting broadens the line. Several stacks exposed at V.E.C.C. are being analysed.

Acknowledgement

The work is being carried out with the help of K. Choudhury, D. Das, G. Mukhopadhyay and B. K. Das. The author thanks Dr. R. Nagarajan, Dr. K. G. Prasad and Prof. R. P. Sharma of T.I.F.R., for help in construscting the multichannel apparatus, and Dr. J. Ray, Mr. S. N. Mishra and Prof. H. G. Devare for the spectrum taken at 20 K. Thanks are due to Dr. K. R. P. M. Rao of B.A.R.C., for collaborating with us for the ERM work and to Prof. M. K. Bose and Mr. M. Chakrabarti of Presidency College for supplying the geological specimens. The work on corrosion was partially supported by a grant from U.G.C., New Delhi.

References

1. H. Frauenfelder, "The Mössbauer Effect", W. A. Benjamin, New York, 1962; G. K. Werthlim, "Mössbauer Effect: Principles and Applications", Academic Press, New York, 1964; V. G. Bhide, "Mössbauer Effect and its Applications", Tata McGraw-Hill, New Delhi, 1973.
2. U. R. Evans, "The Corrosion and Oxidation of Metals: Scientific Principles and Practical Applications", Edward Arnold, London, 1977.
3. K. Choudhury, B. K. Das, C. K. Majumdar and M. Adhikari, *Phys. Stat. Solidi*, 1982, **74**, K 27.
4. K. Choudhury, D. Das, C. K. Majumdar, K. R. P. M. Rao and M. Adhikari, *Phys. Stat. Solidi*, 1985, **91**, 29.
5. N. K. Jaggi, K. R. P. M. Rao and Y. D. Dande, "Nucl. Phys. Solid State Phys. Symp.", Bombay, 1981-82, p. 557; N. K. Jaggi, K. R. P. M. Rao, Y. D. Dande, P. K. Chauhan and H. S. Gadkyar, "Proc. International Conference on the Applications of Mössbauer Effect", Jaipur, 1982, p. 317.
6. N. F. Mott, *Trans. Faraday Soc.*, 1939, **35**, 1175; 1940, **36**, 472; 1947, **43**, 429.
7. A. B. Muir, Jr. in "Mössbauer Effect Methodology", ed. I. J. Gruverman, Plenum Press, New York, 1968, Vol. 4, p. 75; S. S. Hafner, in Mössbauer Spectroscopy, "Topics in Applied Physics", ed. U. Gonser, Springer-Verlag, Berlin, 1975, Vol. 5, pp. 167-99.
8. E. Verbiest and H. Pattyn, *Phys. Rev., B*, 1982, 2 , 5097.

J. Indian Chem. Soc.,
Vol. LXIII, January 1986, pp. 113-117

Molecular Basis for Specificity in Protein-Nucleic Acid Interactions†

GIRJESH GOVIL

Chemical Physics Group, Tata Institute of Fundamental Research, Homi Bhabha Road, Bombay-400 005

In most biological processes, the information transfer is controlled by specific protein-nucleic acid interactions. The rules for such interactions are not clearly understood. The specificity of interaction may be in the nature of inter-molecular forces or in the three dimensional structures of the two classes of biopolymers or in both. In this review of the work from our laboratories, an attempt has been made to answer the important question as to how proteins read the language of nucleic acids. The approach is based on theoretical calculations of inter-molecular interaction energies and 2D nmr investigations of the secondary structure of some protein binding sequences of oligonucleotides, such as GGATCC GGATCC (Bam HI recognition sites), GAATTC GAATTC (ECORI recognition sites) and GAATTCCCGAATTC (repair enzymes binding sites).

PROTEIN-nucleic acid interactions play a crucial role in biological processes[1,2]. Non-specific binding between these two linear polymers can occur wherever there is a possibility of inter-molecular forces which are strong enough to bind the two molecules together. Such an interaction may then be governed only by the adaptability of proteins and nucleic acids in the sense of stereochemical constraints and may not depend critically on the nature of base or amino acid sequence. One example of non-specific interaction is the binding of histones or polyamines to DNA, a process which plays an important role in the packing and stabilisation of the structure of chromatin. However, from the view of biological control, a more important phenomenon is the selective recognition where by specific base sequences in nucleic acids can be recognised by particular proteins. Such a selective recognition is important in information transfer during replication, transcription, translation, repressor mechanisms and differentiation. Among the important examples of specific recognition of base sequences by proteins are the functional properties of restriction endonucleases, ribosomal proteins, RNA polymerases, repressors *etc*. In many cases, a length of about 3-7 nucleotide units in a long segment of nucleic acid containing 70 to 1000 bases can be selectively recognised by proteins. Thus, in these cases, the binding constant for the specific site differs by a factor of 10^4 to 10^6 from that corresponding to the non-specific sites. Certain proteins have structural rather than base specificity. For example, proteins involved in DNA repair, replication and recombination bind strongly to single stranded regions.

Our knowledge about the molecular events involved in the recognition of nucleic acids by proteins is rather sketchy. In our laboratories, we have been involved in answering some of the basic questions pertaining to molecular mechanisms in specific protein-nucleic acid interactions. This review is mainly based on our own modest contributions to an explosive and interesting field. A more extensive review has been published recently by Helene and Lancelot[1]. The question we have asked in this paper is: 'How do proteins recognise specific sequences of nucleotides in long chains of nucleic acid'? The related question as to how 'nucleic acids recognise proteins', is less attractive from biological viewpoint.

Inter-molecular forces in protein-nucleic acid interaction :

The rules for nucleic acid-nucleic acid recognition were enunciated about a quarter of century ago in terms of G : C and A : T(U) base pairing through hydrogen bonding[3]. The complexity of problems in protein-nucleic acid interaction becomes obvious when one realises that here one has to consider a possible combination of at least six different classes of bases (two base pairs G : C and A : T(U) in double stranded systems and four bases for single-stranded systems) with twenty two amino acid residues. In addition, the negatively charged phosphate groups in the nucleic acid backbone and the amide moiety in the peptide backbone provide ideal sites for electrostatic and hydrogen-bonding interactions, respectively.

An understanding of the relative strength of the various types of inter-molecular interactions can be reached through quantum chemical approach. In our laboratories, we have used an approach based on second order pertubation theory[4] where one expresses the binding energy (E_b) between two

† Dedicated to Professor Sadhan Basu on the occasion of his 65th birthday.

A part of the article was presented at the National Conference on Spectroscopy and Theoretical Chemistry held at Calcutta, December 5-7, 1985.

molecules as a sum of electrostatic (E_e), polarization (E_p), dispersion (E_d) and repulsion (E_r) terms,

$$E_b = E_e + E_p + E_d + E_r \qquad (1)$$

The electrostatic interaction is estimated by expressing the molecular charge distribution in terms of multicenter-multipole expansion and then retaining monopole-monopole, monopole-dipole and dipole-dipole terms. The value of E_p is obtained through the use of bond polarisability while E_d and E_r are estimated using Kitaigorodskii potential functions[5].

As is the case with many other molecular systems, proteins and nucleic acids combine with each other through a set of relatively weak non-bonded interactions. Formation of covalent linkages in recognition processes are rare though not entirely absent. The inter-molecular forces involved include electrostatic, stacking and hydrogen bonding. These interactions may be further stabilised by hydrophobic interactions, metal ions and water bridges. The amino acid residues can thus be classified according to the type of interactions by which they bind to nucleic acids.

Interaction of basic amino acid residues : Positively charged amino acid residues, Lys, Arg and under certain *p*H conditions His, can interact with the negatively charged phosphate groups in nucleic acid backbone through Coulombic interactions. The binding energies of such interactions are of the same order as that for ionic bonds in inorganic solids[6,7] (Table 1). The term E_e in equation (1) makes almost 90% contribution to E_b.

Although Coulombic interactions involving point charges are radial in nature, a directional nature to such interactions is imparted by the fact that the charges on the nucleic acid backbone and the protein side chains are highly delocalised. Further, the position and the orientation of the charged groups are governed by the three-dimensional structure of nucleic acids and proteins. It is therefore not surprising that we observe a certain amount of structural specificity even at the sub-molecular level at which the above calculations have been made. Lys^+ and His^+ have a greater affinity for RNA rather than A- or B-DNA. On the other hand, Arg^+ shows a preferential affinity to A-DNA as compared to RNA. The relative affinities of the three basic amino acid residues follow the order $Lys^+ > His^+ > Arg^+$. In general, A-DNA forms more stable complexes with basic amino acids than the B-DNA. Conformational variations on the DNA backbone can lead to sites with differential affinity for proteins. Thus, sequence dependent geometrical variations can be recognised by the basic amino acid residues. Secondly, interactions with basic amino acid residue may induce a conformational change in DNA or RNA, thus making it possible for functional groups in proteins to interact at additional sites in nucleic acids.

Arg^+ can also interact rather strongly with guanine, cytosine and G : C base-pairs of nucleic acids[8] Here, the proton donor and acceptor groups in the two moieties are involved, leading to two hydrogen bonds. However, the binding energy of 36-39 kcal mol^{-1} (Table 1) is much higher than what one expects on the basis of two hydrogen bonds. In fact, a careful analysis of the various contributions to interaction energies reveal that a large fraction arises from electrostatic interation between atoms not involved directly in hydrogen bonding. Clearly, such an interaction can selectively recognise G, C regions in double stranded nucleic acids and G and C in single strands.

Interaction with acidic amino acids : A convenient mode of interaction between the two biopolymers can be through hydrogen bonding. Since the hydrogen bonds are directional, such interactions can be highly specific, especially when a particular functional group is involved in two hydrogen bonds. The anionic forms of glutamic acid and aspartic acid can form a pair of hydrogen bonds with guanine in single stranded nucleic acids[8]. There are two interesting aspects of this interaction. First,

TABLE 1—INTER-MOLECULAR INTERACTIONS BETWEEN FUNCTIONAL GROUPS IN PROTEINS AND NUCLEIC ACID

Functional group in protein	Functional group in nucleic acid	Nature of interaction	Binding energy kcal mol	Selectivity of interaction, if any
Arg^+, Lys^+, His^+	Backbone (PO_4^-)	Electrostatic	90-180	Preference for RNA and A-DNA
Arg^+	G, C and G : C	Electrostatic and H bonding	36-39	Highly selective to G and C in both single and double stranded regions
Glu^-, Asp^-	G	Electrostatic and H bonding	23-25	Selective to G in single stranded regions
Trp, Tyr, Phe, His	Bases and base-pairs	Stacking	6-18	Preference to single stranded regions or kinked structure. G, C rich regions are preferred
Asp, Glu, Asn, Gln	Bases and base-pairs	Hydrogen bonding	6-15	Greater binding energy for G, C rich region
Peptide back bone	Bases and base-pairs	Hydrogen bonding	1-10	Highly dependent on the long range adaptability of protein structure-preference for double stranded regions
Hydrophobic amino acids	Hydrophobic regions	Van der Waal and hydrophobic	<3	Non selective

the interaction energies (23-25 kcal mol^{-1}) are a factor of two higher than that expected from purely hydrogen bonding considerations. Again, a large contribution to the binding energy in these cases comes from electrostatic interactions involving atoms not directly involved in hydrogen bonding interactions. Secondly, since the interaction for these residues is limited to G in single stranded-nucleic acids, the recognition process can be highly selective.

Hydrogen bonding with neutral amino acid residues : A number of bonding schemes involving two or more hydrogen bonds between Asp, Glu, Asn and Gln on one hand and G, C, T, A and U on the other, are theoretically possible[8]. The binding energies for these complexes vary between 6-15 kcal mol^{-1} (Table 1) and follow the following order,

$$G:X > C:X > A:X > U(T):X$$

where, X=Glu, Asp, Gln or Asn. The bases generally prefer binding with Gln and Asn. Thus, single stranded nucleic acid can bind to protein sequences containing above residues in a variety of ways.

A more interesting aspect is the possibility of the binding of above amino acid residues with double helical nucleic acids. With A : U or A : T base pairs, hydrogen bonding with Asn, Gln, Asp and Glu can occur only in the major groove of B-DNA. With G : C base pairs, interaction can occur both in the major groove and in the minor groove but complexes in the major groove are more stable by almost 3-4 kcal mol^{-1}. Glu and Asp have a higher affinity for G : C base pairs while Gln and Asn can bind to G : C and A : U(T) base pairs with equal case.

A large contribution (almost 90%) to the total binding energies in these cases arises from electrostatic term.

Aromatic amino acids : Aromatic amino acid residues Tap, Tyr, Phe and His can bind to nucleic acid bases and base-pairs through stacking interactions[9-11]. The predominant contribution to the total binding energy for these complexes comes from the dispersion term. Due to a favourable contribution from hydrophobic effects, stacking can assume an even greater importance in aqueous solutions. Energy minimisation show that a vertical separation of 3.2 to 3.4 Å between the aromatic residues of proteins and bases of nucleic acids leads to the most stable configuration. Such an interaction will lead to a partial ordering of single stranded nucleic acids such that the bases on adjoining nucleotide overlap with the aromatic amino acids on either side leading to an inter-nucleotide separation of 6-7 Å. However, in the case of double stranded nucleic acids in A, B or Z form, the base-pairs are already stacked with vertical separation of 2.8-3.4 Å and the intercalation of aromatic amino acids is sterically prohibited. The nucleic acid may, therefore, have to unfold locally to allow the amino acid residue to get in. A more interesting possibility is that the protein binding regions have kink structures[12] where the inter-nucleotide distances are ideally suited for an aromatic residue to interleave between adjoining base-pairs. An analysis of the geometrical pattern of base-aromatic amino acid interaction shows that the heteroatom of the bases overlap with the aromatic part of the amino acids. Further, the aromatic moieties of the two components overlap only partially supporting the selective book mark hypothesis[13,14] which states that the nucleotide sequences can be recognised by amino acid chain acting like book-marks.

In general, it is found that G among the purines and C among the pyrimidines, have higher binding energies. Thus, in actual protein-nucleic acid interactions G, C rich regions will be preferred both in single and double stranded nucleic acids.

Hydrogen bonding involving peptide backbone : An interesting mode of interaction of proteins with nucleic acids is the involvement of the amide-NH and C=O groups in the peptide backbone with nucleic acid bases and base-pairs[15-17]. Such an interaction is not critically dependent on the amino acid sequence and can occur in bridge-region of two other amino acids involved in interaction through one of the mechanisms described above. The major groove in double stranded nucleic acids is preferred for such interaction.

Other interactions : In addition to the interaction schemes listed above, the protein nucleic acid interactions can be stabilised by van der Waal and hydrophobic interactions. These interactions are weak and non-directional. Hence, they are not likely to be important in specific recognition though they may make an additional contribution to a scheme otherwise stabilised by stronger inter-molecular forces. Metal bridges, *e.g.* PO_4^-...Mg^{2+}...Asp^- are possible and these can make substantial contribution to binding energy. However, it is not clear how such interactions on their own can lead to specificity. Finally, formation of covalent linkage between peptide and nucleotide fragments can lead to the formation of nucleoproteins. Again, such interactions are not involved in recognition processes.

Role of secondary structure of nucleic acids :

While the mechanisms described in the previous section lead to a certain degree of specificity both in terms of sequence and structure, it is not clear whether the protein binding regions of nucleic acids are structured in a way so as to achieve a highly specific binding or whether such a shape is induced by the protein so as to reach optimum interaction by the functional group.

The structure of nucleic acid has attracted renewed interest in recent years following the results of potential energy calculations, nmr and *X*-ray crystallography on small molecules which indicated considerable conformational flexibility[3,18].

Our group has made substantial contribution in delineating conformational preferences of polynucleotides[19–23]. These results indicate that the proposed structure of B-DNA may be an oversimplification for the conformation of natural DNAs. In fact, by careful control of experimental conditions, at least three different forms have been characterised for polynucleotides. These are A, B and Z. Other imaginative models have been proposed but at the moment there are no experimental proofs to support them. The characteristic of these structures are as follows.

(i) B-DNA forms a helix of 10.5 base-pairs per turn of 34 Å height and has a diameter of 20 Å. The corresponding numbers are 12, 44.6 Å and 18 Å for Z-DNA and 11, 25 Å and 25 Å for A-DNA.

(ii) The repeating unit is mononucleotide for A- and B-DNA and the base conformation is *anti*. The important difference in the two structure is that deoxyribose ring has a C3′ *endo* geometry in the former and C2′ *endo* geometry in the latter. In Z-DNA the repeating unit is a dinucleotide with bases in the alternating *syn* and *anti* conformation and generally, the sugar geometry alternates between C2′ *endo* and C3′ *endo*.

Under physiological condition, all evidences point to B-DNA as the most dominant structure[18]. However, there can be local conditions or steric constraints which may cause localised variations in the structure. Such microheterogeneities in the structure may then become hot points for recognition. We have recently worked out solution conformations of a number of protein-binding sequences which support such a hypothesis. The technique used for this purpose is the recently developed 2D FT nmr. The main advantage of nmr is that it can provide structural information in solutions[8] unlike the conventional technique of *X*-ray crystallography which is applicable to solid state. The two dimensional *J*-correlated spectra (COSY[24], COSS[25], SUPERCOSY[26] *etc.*) provide information on the *J* couplings which in fact can be correlated with dihedral angles along the various chemical bonds[8]. The NOESY spectra provide information on all the short interproton distances (<5 Å) in the molecule. These two pieces of information can be combined with chemical shifts to detect conformational heterogeneity in structure of nucleic acids.

Structure of GGATCC GGATCC : This sequence has two binding sites for Bam HI endonuclease. The unit recognised by this enzyme is GGATCC. In a double helical system, the nucleic acid segment is cleaved as indicated by arrows,

```
 ↓           ↓
1 2 3 4 5 6  7 8 9 10 11 12
G G A T C C  G G A T  C  C
C C T A G G  C C T A  G  G
          ↑              ↑
```

Using 2D nmr, we find[27,28] that at ambient temperature, the overall conformation is a right-handed B-DNA with most of the deoxyribose units acquiring a conformation close to C2′ *endo*. However, the sugars attached to GI and G7 adopt a C3′ *endo* conformation leading to C2′ *endo* -C3′ *endo* junctions. Such structure have been seen earlier in complexes of short segments of DNA with drugs, and have been named as kinks[18]. The kink structure has the unique feature that the base-pairs are separated by more than 6 Å making it feasible for Bam HI to detect and interact at these site through an aromatic amino acid.

GAATTCGAATTC : This dodecamer has two specific recognition sites for ECOR I restriction endonuclease indicated by arrows,

```
 ↓           ↓
1 2 3 4 5 6  7 8 9 10 11 12
G A A T T C  G A A T  T  C
C T T A A G  C T T A  A  G
          ↑              ↑
```

The unit recognised is GAATTC. Also, the T-C-G segment is significant since the enzyme DNAase-I is known to cut DNA preferentially at TCG sites. Our studies[29] on this double helical system shows that while the molecule attains a right-handed structure it is different from either A or B DNA since the sugar acquire a O1′ *endo* conformation. Moreover, the cytosine at position 6 in the sequence slips away from T5 and acquire a backbone conformation which is different from the rest of the molecule.

GAATTCCCGAATTC : This molecule[30] has the same sequence as the previous one except that there are two additional cytosine residues, C7 and C8 which do not have

```
1 2 3 4 5 6 7 8 9 10 11 12 13 14
G A A T T C C C G A  T  T  C
C T T A A G C C C T  T  A  A  G
```

complementary guanines. Such mismatches are significant for recognition by repair enzymes, synthetase and polymerase. We observe that the geometry of the oligonucleotide diffees significantly in the mismatch region with C6, C7 looping out on either side.

CGCGCGCGCGCG : This oligonucleotide is interesting since at high salt concentration the molecule undergoes a transition from B to Z form[31]. Such transitions have been well characterised in CG-series and are brought about by high concentration of cations. It is possible that the cationic interaction at the phosphate sites induces a C3′ *endo*-C2′ *endo* sugar pucker variation in the backbone. One of the questions we hope to answer is whether such a transition are to be brought about locally by specific binding with basic amino acids Lys^+ or Arg^+.

The examples discussed above are indicative that the molecular conformation of DNA may play a vital role in specific recognition.

Acknowledgement

Our reverend *Guru* Prof. Sadhan Basu has been a guiding force and a source of inspiration to all involved with various aspects of Molecular Sciences in India. Certainly, the author and his colleagues have drawn continuous inspiration from his work.

The author is grateful to a number of his colleagues whose work is cited here, and make particular mention of Drs. H. T. Miles, A. Saran, N. V. Kumar, R. V. Hosur, K. V. R. Chary, Shri M. Ravi Kumar and Ms. Anu Sheth. The research work described here has been made possible by the D. S. T., New Delhi, supported 500 MHz FT NMR National Facility and the CDC-Cyber at Tata Institute of Fundamental Research.

References

1. C. Helene and G. Lancelot, *Prog. Biophys. Mol. Biol.*, 1982, **39**, 168.
2. G. Govil and R. V. Hosur, "Conformation of Biological Molecules", Springer-Verlag, New York, 1982.
3. J. D. Watson and F. H. C. Crick, *Nature* (*London*), 1953, **171**, 737.
4. P. Claverie in "Intermolecular Interactions; From Diatomics to Biopolymers", ed. B. Pullman, Wiley, New York, 1978.
5. J. Caillet and P. Claverie, *Acta Crystallogr.*, *A*, 1975, **31**, 448.
6. N. V. Kumar and G. Govil, *Biopolymers*, 1984, **23**, 1979.
7. G. Govil, N. V. Kumar, M. Ravi Kumar, R. V. Hosur, K. B. Roy and H. T. Miles, *J. Biosci.*, 1985, **52** 645.
8. N. V. Kumar and G. Govil, *Biopolymers*, 1984, **23**, 1995.
9. N. V. Kumar and G. Govil in "Conformation in Biology", eds. R. Srinivasan and R. H. Sarma, Adenine Press, 1982.
10. N. V. Kumar and G. Govil, *Biopolymers*, 1984, **23**, 2009.
11. N. V. Kumar and G. Govil in "Molecular Basis of Cancer", ed. R. Rein, Alan R. Liss, New York, 1985.
12. H. M. Sobell in "Biological Macromolecules and Assemblies", eds. F. A. Jurnak and A. McPherson, Wiley, 1985, Vol. 2.
13. P. E. Brown, *Biochem. Biophys. Acta*, 1970, **213**, 282.
14. E. J. Gabbay, K. Sanford and C. S. Baxter, *Biochemistry*, 1972, **11**, 3429.
15. R. V. Hosur, *Curr. Sci.*, 1980, **49**, 928.
16. R. V. Hosur, N. V. Kumar and G. Govil, *Int. J. Quantum Chem.*, 1981, **20**, 23.
17. R. V. Hosur and A. Pohorille, *Int. J. Quantum Chem.*, 1981, **20**, 33.
18. W. Saenger, "Principles of Nucleic Acid Structure", Springer-Verlag, New York, 1984.
19. G. Govil and A. Saran, *J. Theor. Biol.*, 1971, **30**, 621.
20. G. Govil and A. Saran, *J. Theor. Biol.*, 1971, **33**, 399.
21. A. Saran and G. Govil, *J. Theor. Biol.*, 1971, **33**, 407.
22. R. Tewari, R. K. Nanda and G. Govil, *Biopolymers*, 1974, **13**, 2015.
23. G. Govil, *Biopolymers*, 1976, **15**, 2303.
24. W. P. Aue, E. Bertholdi and R. R. Ernst, *J. Chem. Phys.*, 1982, **64**, 2229.
25. R. V. Hosur, M. Ravi Kumar and A. Sheth, *J. Magn. Reson.*, 1985, in the press.
26. R. V. Hosur, K. V. R. Chary, A. Kumar and G. Govil, *J. Magn. Reson.*, 1985, **62**, 123.
27. R. V. Hosur, M. Ravi Kumar, K. B. Roy, Tan Zu-Kun, H. T. Miles and G. Govil in "Magnetic Resonance in Biology and Medicine", eds. G. Govil, C. L. Khetrapal and A. Saran, Tata McGraw-Hill, New Delhi, 1985.
28. M. Ravi Kumar, R. V. Hosur, K. B. Roy, H. T. Miles and G. Govil, *Biochemistry*, 1985, **24**, 7703.
29. K. V. R. Chary, R. V. Hosur, G. Govil, Tan Zu-Kun and H. T. Miles, communicated.
30. R. V. Hosur, M. Ravi Kumar, K. V. R. Chary, A. Sheth, G. Govil and H. T. Miles, unpublished.
31. A. Sheth, M. Ravi Kumar, R. V. Hosur, G. Govil and H. T. Miles, unpublished.

J. Indian Chem. Soc.,
Vol. LXIII, January 1986, pp. 118-122

Cation Complexation and Conformational Changes of Crown Ether Complexes of Bovine Serum Albumin†

D. DASGUPTA, V. THANABAL and V. KRISHNAN*

Department of Inorganic and Physical Chemistry, Indian Institute of Science, Bangalore-560 012

Macrocyclic polyethers, benzo-15-crown-5 and dibenzo-18-crown-6 have been coupled to bovine serum albumin (bsa) *via* diazolinkage in order to elucidate the changes in conformation of the protein upon (i) conjugate formation and (ii) addition of Na^+, K^+ and Ca^{2+} to the crown ether moieties of the conjugate. Gel filtration studies of the coupled complex reveal the homogeneity and the presence of cross linkage in the conjugate of *cis* and *trans* dibenzo-18-crown-6. Optical absorbance, fluorescence and pmr spectroscopic studies indicate that the tyrosine moieties of the protein to be the sites of appendage of the crown ethers. Circular dichroic (CD) spectra of the bsa conjugates have shown a decrease in the ordered conformation of the protein upon conjugation and the loss in conformation follows the order, *trans*-conjugate > *cis*-conjugate > benzo-15-crown-5 conjugate. It is further pointed out that the addition of K^+ and Ca^{2+} leads to a decrease in α-helical content of *cis*-conjugate, while Na^+ has no preceptible effect, as observed on the addition of Na^+ ions. The significance of these results *vis-a-vis* the role of proteins in the ion transport in presence of an ionophore is discussed.

THE crown ethers, first reported by Pederson[1], are known to selectively sequestrate alkali and alkaline earth cations from aqueous environments and solubilise the complexes formed in the lipid fraction of the cell membrane[2,3]. This knowledge has triggered considerable research interest for using them as membrane-active complexones. The effect of these ionophores on the ion-transport in the respirating rat liver mitochondria has shown that the uptake of crown ether by mitochondria is related to the cation complexing ability of the ionophore[4,5]. Despite this, information regarding the behaviour of crown ether in membrane which is a two dimensional solution of globular integral proteins dispersed in a fluid lipid matrix, are wanting[6]. The crown ether in such matrix can also interact with proteins. The importance of proteins is clearly brought about in a demonstration of the change in conformational feature of a protein during ion-transport process. Our interest has been in the development of macrocyclic entities in general, and crown ethers in particular, as ionophores to understand the mode of uptake and delivery of cations across a membrane. Earlier we investigated the ionophoric behaviour of several metallo crown porphyrins and demonstrated metal dependent uncoupling of mitochondrial energy potential[7]. Here, we examine the cation complexation properties and accompanying conformational changes of crown ether conjugates of a protein.

This report deals with the coupling reaction of two crown ethers, benzo-15-crown-5 (1) and dibenzo-18-crown-6 (2) with a representative protein, bovine serum alumin (bsa) and a study of the changes in conformation of the protein resulting from (i) the appendage of the crown ether followed by (ii) the encapsulation of the metal ion by the crown ether moiety. The choice of bsa as the protein, in spite of it being a serum protein, is that it has been characterised well and its properties well documented. Apart from this, these conjugates afford a bsa-hapten conjugate to raise antibody of crown ethers in order to study its immunological properties[8]. Such possibilities are even more important in view of the limited pharmacological study of these crown ethers[9].

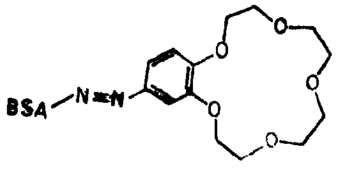
Experimental

bsa and tris-HCl buffer were obtained from Sigma Chemicals, USA. The column materials, Sephadex G-200 and Sepharose 4B used for gel chromatography were from Pharmacia Fine Chemicals, Sweden. All other reagents used were of analytical grade. Water used in the preparation of buffers was double-distilled and deionised by passing through Chelex-100 resin.

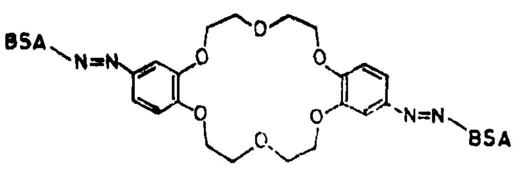
The 4'-aminobenzo-15-crown-5, *cis*- and *trans*-diaminodibenzo-18-crown-6 were synthesised and diazotised using the procedure described earlier[10]. The coupling of the arenediazonium ethers to bsa was accomplished by adopting a procedure similar to the one employed for *p*-aminobenzoic acid to bsa[8]. A *p*H of 9-9.5 was maintained during the coupling reaction at 0-5°. The reaction mixture was dialysed extensively at 0° until the dialysate was free from any unreacted diazonium salts as apparent from the absence of any absorbance at 400 nm. It was then lyophilised and stored below

† Dedicated to Professor Sadhan Basu on the occasion of his 65th birthday.

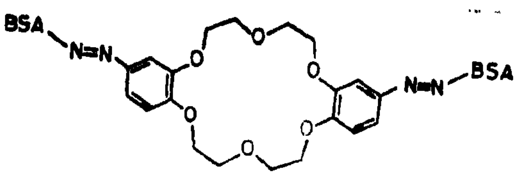
0° for subsequent use. The spectrometers employed were Beckman 26 (for absorption), Perkin-Elmer fluorescence spectrometer and Bruker FT. 270 MHz nmr spectrometer. The CD spectra were recorded on a Jasco 10 spectropolarimeter calibrated with camphor-d-10-sulphonic acid[10]. Cells of the path lengths of 1 mm and 0.5 mm were employed for recording the spectra in the far-uv region, 210-250 nm.



Benzo-15-crown-5(1)-conjugate



trans-Dibenzo-18-crown-6(2) conjugate



cis-Dibenzo-18-crown-6(2)-conjugate

Results and Discussion

The facile completion of the diazo coupling reaction is evidenced from the color of lyophilised product. The structural integrity of the products was established using gel filtration, optical absorption, fluorescence, and ^{1}H nmr spectral methods.

A comparison of the elution profile of bsa and 1-conjugate of bsa employing Sephadex G-200 (Fig. 1a) shows the homogeneity of the protein as indicated by the appearance of single peak. The elution profile for the 1-conjugate suggests a marginal net increase in the molecular weight which results from the appendage of the crown ether to the protein. The intactness of the 17-disulphide bridges of the protein in the conjugate is apparent from the elution profile of the conjugate which is eluted in a single peak and has no other peak to the right of that single peak. Similar experiments for *cis*-2 and *trans*-2 appended bsa revealed that the eluate comes within the void volume of Sephadex G-200 indicating a molecular weight of 20 k daltons (Fig. 1b) for these conjugates. This could arise because of the extensive cross linking in the protein due to the presence two diazo groups in the crown ethers. However, the homogeneity of these products are seen from the single elution peak when Sepharose 4B is employed.

Apart from the elution profile of the conjugates as mentioned above, the absorption spectra in both uv and visible regions also indicate the presence of the covalently coupled crown ether in the protein. Fig. 2a shows the uv spectra of the bsa and the coupled crown ether conjugates. The relative enhancement in the 280 nm band as observed for

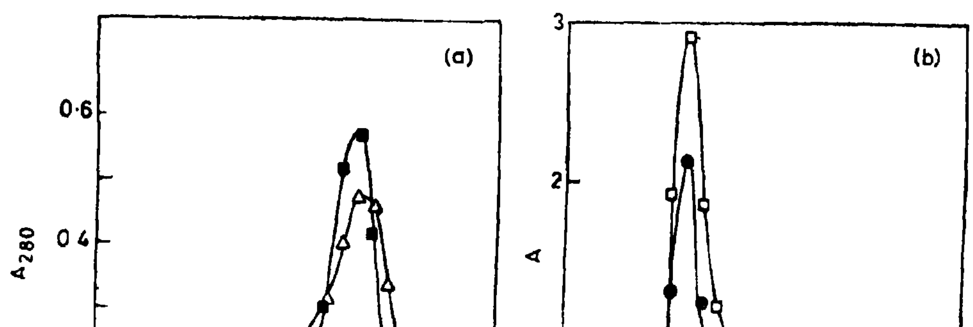


Fig. 1. (a) The elution profile of (■) bsa and (Δ) benzo-15- crown-5-conjugate through a Sephadex G-200 column (34 cm × 1 cm) at a flow rate of 8 ml h⁻¹. The eluent was double-distilled deionised water at pH 7.0. The optical density of the fractions had been measured at 280 nm. (b) The elution profile of (●) *cis*- and (□) *trans*-dibenzo 18-crown-6 through the same column as mentioned above under the identical conditions. The optical density of the fractions had been measured at 370 nm. The arrows indicate the void volume as measured by means of blue dextran.

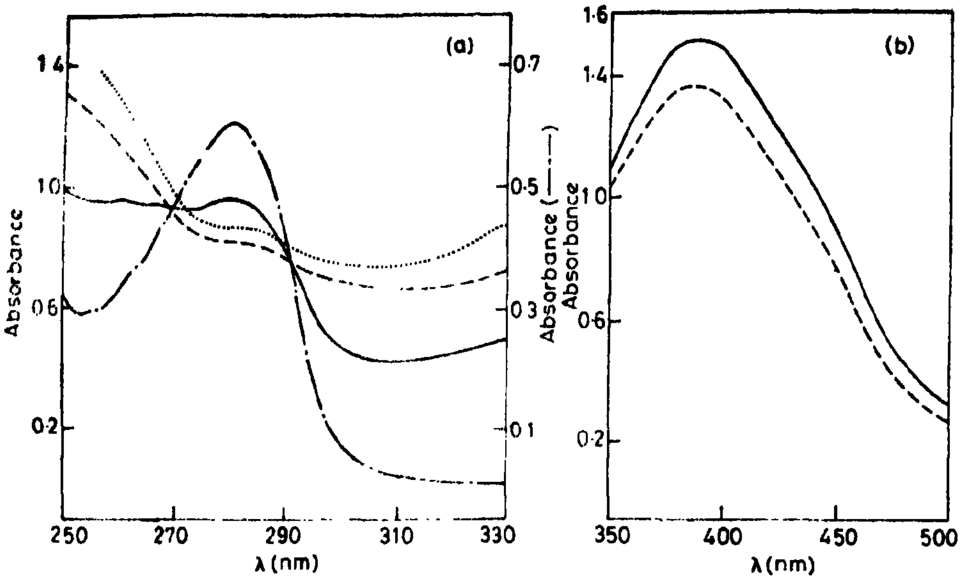


Fig. 2. (a) Uv spectra of (———) bovine serum albumin, (- - -) benzo-15-crown-5-conjugate, (- - -) *cis*-dibenzo-18-crown-6-conjugate and (—.—) *trans*-dibenzo-18-crown-6-conjugate at pH 7.0 and 20°. The concentrations of all are 1 mg ml^{-1}. (b) The visible spectra of (———) *cis*-dibenzo-18-crown-6-conjugate and (- - -) *trans*-dibenzo-18-crown-6 at pH 7.0 and 20°. The concentration of both are 0.5 mg ml^{-1}.

the conjugates, is traced to the presence of additional aromatic groups from the appended crown ether part. In addition, the broad band in the visible spectra of the complex conjugates (Fig. 2b) provides sufficient proof for the presence of diazo chromophore. The interesting question as to which of the possible amino acid residues in bsa, the crown ethers are attached is worthy of consideration. Among the number of amino acid (aa) residues in bsa, tyr, his, trp, lys and arg are the possible sites that can be covalently linked to diazo groups. Of these tyrosine has the highest affinity for such diazo coupling reaction[9]. The site of coupling can be judged from the ratio of the number of moles of arenediazonium salt and bsa (in terms of amino acid residues) employed for the coupling reaction. It is worthy to mention at this point that there are 19 tyrosine residues in bsa and an employ of 20 moles of arenediazonium salt as used in the present study would essentially couple all the tyrosine residues.

The site of binding of crown moiety to bsa is sought from fluorescence studies. It is observed that there is a marked decrease in the fluorescence intensity of the crown ether conjugates when excited at 278 nm corresponding to tyrosine absorption as compared to the bsa alone (Fig. 3). The quenching can be ascribed to the energy transfer between tyr and the coupled crown ethers containing the aryl rings. The examples of such energy transfer leading to fluorescence quenching of the proteins (enzyme, like carboxypeptidase) in presence of bound dansyl group as observed in enzyme(carboxypeptidase)-substrate complex have been reported

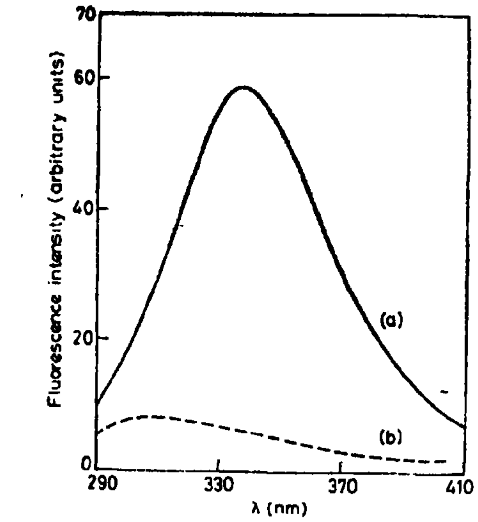


Fig. 3. Fluorescence emission spectrum of (a) bsa (0.2 mg ml^{-1}) and (b) benzo-15-crown-5-conjugate (0.2 mg ml^{-1}) excited at 278 nm at pH 7.0 and 25°.

earlier[11]. That the coupling has taken place predominautly to the tyr residues of the bsa is further shown from the ^1H nmr spectrum of 1-conjugate of the protein. The observed line broadening of the aryl protein signals (at δ 7-8) of the conjugates supports the presence of the coupled tyr residues.

The above spectroscopic studies apart from showing the homogeneous nature of the conjugates, also reveal the tyrosine residues as the sites of

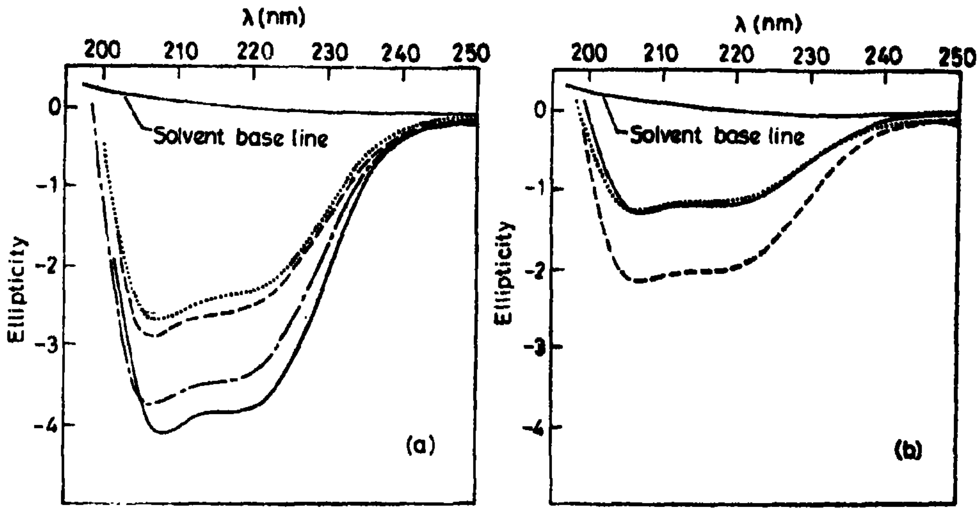


Fig. 4. (a) Far-uv CD spectra of (———) bsa, (– – –) benzo-15-crown-5-conjugate, (– – –) *cis*-dibenzo-18-crown-6-conjugate, and (–.–) *trans*-dibenzo-18-crown-6-conjugate at pH 7.0 and 20°. The ordinate represents the observed dichrograph record unconverted into the molar ellipticity scale since the concentrations of all the solutions were maintained at 5 mg ml^{-1} and the path length of the cell was kept fixed. (b) The CD spectra of *cis*-dibenzo-18-crown-6 conjugate (5 mg ml^{-1}) in presence of (– – –) NaCl (100 *M*), (—) KCl (100 m*M*) and (–.–) $CaCl_2$ (100 m*M*) at *p*H 7.0 and 20°.

attachments for the crown ethers. However, the possibility of binding to other amino acids which appears very remote from stoichiometric considerations can not be totally eliminated from these studies. It is of interest to study by means of CD spectroscopy the cation complexation properties of the appended crown ethers and investigate the conformational features arising from the backbone structure of the protein.

The far-uv CD spectra of the bsa along with those of the crown ether conjugates in the region 210-250 nm (Fig. 4a) reveal a change in the conformation of bsa. The spectra as depicted are not converted into molar ellipticity scale since the concentrations of all the solutions are maintained at 5 mg ml^{-1} and the path length of the cell has been kept fixed at 0.5 mm. The lower dichroic values (θ_{221}) in the conjugates represent less α-helical content in the bsa[13]. Thus, the α-helicity of the protein, bsa, decreases with the nature of the appended ether and follows the order *trans*-**2** > *cis*-**2** > **1**. Along with the above observed changes in the dichroic absorption in the far-uv region, there is a feeble dichroic band observed around the 350-450 nm region corresponding to the diazo chromophore. Since this band is very small in magnitude, it was not studied in detail. However, the presence of such a band lends further support to the coupling of crown ether to the protein.

With the two-fold objectives of studying the capacity of appended crown ethers to encapsulate the cations and the changes in conformation of the protein that ensues the ion encapsulation, we examined the CD spectra of crown ether conjugate proteins in presence of varying amounts of different cations K^+, Na^+ and Ca^{2+}. The effects that may arise from any non-specific absorption of cations by bsa alone is discounted by running the spectrum of bsa under similar conditions. Addition of cations, Na^+, K^+ and Ca^{2+} to **1**-, and *trans*-**2**-conjugates does not produce any appreciable changes in the ellipticity (θ_{221}) values (Fig. 5). Interestingly, considerable decrease in the dichroic value was observed for the *cis*-**2**-complex (Fig. 4b). The decrease in α-helical content of *cis*-**2**-conjugate on addition of K^+ is more pronounced than that of Na^+, paralleling increased stability of K^+-**2** complex compared to that of Na^+-**2** complex. Similar trend is also observed for the *trans*-**2**-conjugate though the change in the magnitude of (θ_{221}) value is small. It is worthwhile to note that with the addition of K^+ and Ca^{2+}, there was approximately 50% decrease in the value of ellipticity (θ_{221}), indicating a dramatic loss in α-helicity on cation complexation (Figs. 4b and 5).

An explanation as to the further loss in α-helical content of the conjugate protein on cation complexation can be viewed from the repulsions set up by the cations encapsulated in the appended crown ethers. This becomes more obvious due to clustering of tyr residues in domains I and II (Fig. 6). The cross linking that occurs in *cis*- and *trans*-**2**-conjugates, in fact, should promote random orientation of the ether moieties and hence, disordered cation occupation. We expect the decrease in α-helical content to be the same in both the conjugates. However, the reason for the different behaviour remains uncertain.

The aforementioned result point out that (i) there is a net change in the conformation of bovine

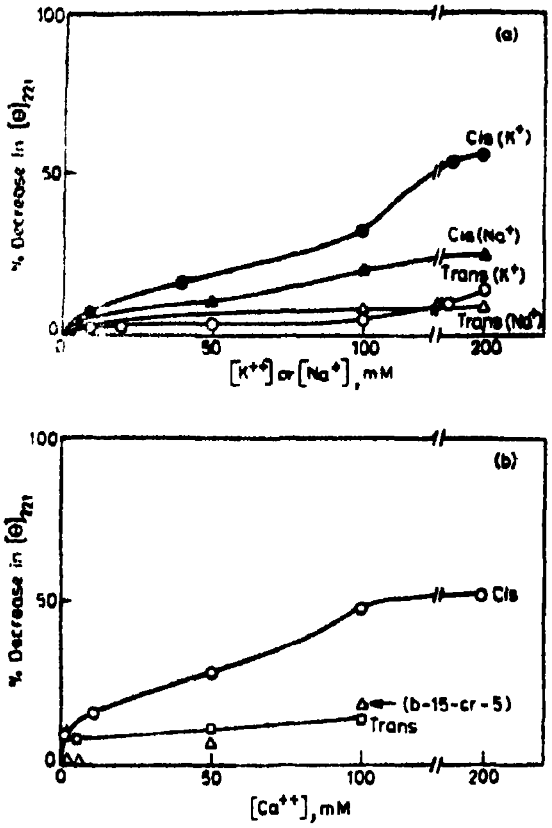


Fig. 5. Percentage decrease in the mean residual molar ellipticity value (at 221 nm) of benzo-15-crown-5-conjugate, *cis*- and *trans*-dibenzo-18-crown-conjugates as a function of the changes in the concentrations of metal ions. The mean residual molar ellipticity has been calculated from the relation : $\theta]_{221} = D_{1cm} \times \bar{M}/10 \times 3300$ (K cm² dmol⁻¹), where D and $\bar{M}$ denotes the observed dichrograph record and the mean residue weight of the amino acids in the protein, respectively.

serum albumin due to coupling with the crown ethers ; the extent of change depends upon the nature of crown ethers and (ii) the encapsulation of cations by certain crown ethers changes the protein conformation, the extent of change that results, depends also upon the nature of cation.

The ionophoric activity of these crown ethers have so far been understood only in terms of the solubility of their cation complexes in the lipid bilayer leading to the eventual transport of the cations across the membrane. Notwithstanding the limitation that bsa is a serum protein, the present observations are significant from the point of view underlying the possible role of proteins during the ion transport even in presence of the ionophore, crown ether.

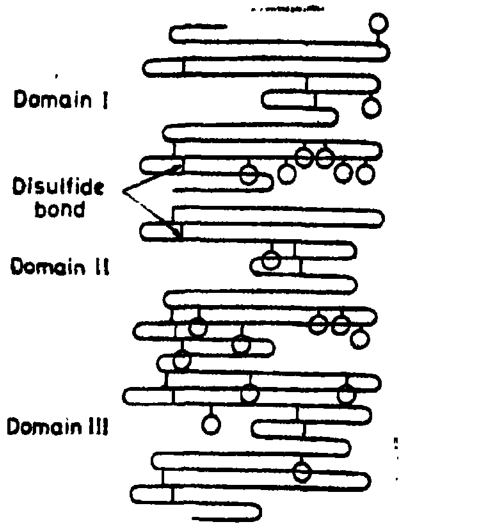


Fig. 6. The relative positions of the tyrosine residues in the primary sequence of bsa (primary sequence of bsa taken from J. R. Brown, F.E.B.S , 11th Meeting, Copenhagen, 1977, 50).

Acknowledgement

The work is supported by Department of Science and Technology, Government of India. One of the authors (V.T.) is thankful to Department of Atomic Energy, Government of India, for the award of a Senior Research Fellowship.

References

1. C. J. PEDERSON, *J. Am. Chem. Soc.*, 1967, **89**, 2495, 7017.
2. G. EISENMAN, S. M. CIANNI and G. SZABO, *Fed. Proc.*, 1968, 27, 1289.
3. Y. A. OVCHINIKOV, V. T. IVANOV and A. M. SHKROB in "Membrane-Active Complexones", Elsevier, Amsterdam, 1974, pp. 56-66, 263-396.
4. G. EISENMAN, *Fed. Proc.*, 1968, 27, 1249 ; D. C. TOSTESON, *Fed. Proc.*, 1968, **27**, 1269 ; H. LARDY, *Fed. Proc.*, 1968, 27, 1278.
5. E. J. HARRIS, B. ZABA, M. R. TRUTER, D. G. PARSONS and J. N. WINGFIELD, *Arch. Biochem. Biophys.*, 1977, **182**, 311.
6. S. J. SINGER, *Ann. Rev. Biochem.*, 1974, **43**, 805 ; J. KYTE, *Nature (London)*, 1981, **292**, 201.
7. D. DASGUPTA, V. THANABAL and V. KRISHNAN, *Biochem. Biophys. Res. Commun.*, 1982, **104**, 1427.
8. A. NISONOFF in "Methods in Immunology and Immunocytochemistry", eds. C. A. WILLIAMS and M. W. CHASE, Academic Press 1976, p. 120 ; D. SHANKARANARAYAN, C. GOPALAKRISHNAN, S. K. NAZIMUDDIN, S. VISWANATHAN, L. KAMESWARAN and V. KRISHNAN, *Curr. Sci.*, 1979, **48**, 682, and related references therein.
9. V. THANABAL and V. KRISHNAN, *Synth. React. Inorg. Metal-Org. Chem.*, 1981, **11**, 659.
10. H. A. SOBERS, "CRC Handbook in Biochemistry and Selected Data for Molecular Biology", CRC Press, Cleveland, 1970.
11. D. S. AULD in "Bioorganic Chemistry", ed. E. E. VAN TAMELIN, Academic Press, New York, 1977, p. 1, and related references therein.
12. Y. H. CHEN and J. T. YANG, *Biochem. Biophys. Res. Commun.*, 1971, **44**, 1285.

J. Indian Chem. Soc.,
Vol. LXIII, January 1986, pp. 123-136

Cell Surface Carbohydrate mediated Processes. Chemical Model for Cell-Cell and Cell-Lectin Interaction†

P. LALIT KUMAR SINGH, K. VIJAYALAKSHMI and S. K. PODDER*

Department of Biochemistry, Indian Institute of Science, Bangalore-560 012

THE carbohydrate moieties of cell surface present either as glycoproteins or glycolipids (together termed glycoconjugates) are implicated to play roles in a variety of biochemical phenomena namely, binding of bacteria to intestinal epithelium[1], aggregation of slime mold and sponge cells[2], yeast mating[3], sperm-egg binding[4], and interaction between cells in immune response[5]. It can function as receptors to a variety of ligands, like glycoprotein hormones, bacterial toxins (CT and DT) during their entry into cells[6]. Their presence as a class of marker molecules in plasma membrane in blood group typing, cellular differentiation and oncogenesis make their study even more interesting with specific reference to their isolation, characterisation and biosynthesis[7]. The underlying principle in all these processes is that surface glycoconjugates present in one cell bind to a complementary carbohydrate binding protein on another, resulting in specific adhesion. Alternatively, a multivalent carbohydrate binding protein, like plant lectin can cross-link carbohydrate moiety on adjacent cells. Examples of both types are known. Although functional importance of such molecules are well documented, molecules themselves have been isolated in few cases[8]. Even the actual mechanism of the process at the molecular level is not understood, mainly because of difficulties in experimentation with intact cells. There are even problems associated with the isolation of adhesion molecules using *in vitro* cell-cell interaction.

To circumvelent the problem suitable cell surface analogue has been developed. The inert plastic surface derivatised with chemically defined carbohydrate ligands has been developed in detecting and isolating specific cell adhesion molecules. This has been reviewed recently[9]. On the other hand, the liposomal system with specific carbohydrate marker has been developed to study molecular mechanism of complex carbohydrate ligand interaction at the cell surface as well as to examine its possible use in the development of organ specific delivery system. The article will briefly summerise (i) the properties of a few lectins and their specificity towards simple and complex carbohydrate at the surface and problem relating to the complexity of lectin induced agglutination reaction and (ii) the use of liposomal system towards understanding molecular mechanism of lectin mediated agglutination.

Carbohydrate specificity of lectins towards simple sugar :

The lectin-group of plant proteins present in large amount in seed extracts having a remarkable ability to agglutinate erythrocytes has been known long before the host of interesting chemical and biological properties have been discovered[10,11]. Its property to agglutinate erythrocytes in some cases with high specificity has been used in typing human blood and in the study of chemical nature of blood group substances. A surge in lectin research came primarily because of the increased agglutinability of transformed cells by plant lectins and discovery of hepatic lectin that is responsible for the maintainance of glycoconjugate level in serum. Since then studies on biochemical properties of lectins of various origin and their application in isolation of glycoproteins of functional importance became wide-spread. This is mainly because of the carbohydrate recognising properties of lectins. Tables 1 and 2 summarises carbohydrate specificity of some well studied lectins.

It is seen from Table 1 that the affinity (K_a) of sugar binding site on lectin for appropriate monosachharide is of the order of 10^3-10^4 M^{-1}. In going from monosachharide to disachharide, K_a increases marginally. In both cases, the binding is non-cooperative. The measured association rate constant k_f is about 10^4-10^5 M^{-1} s^{-1} which is about a factor of 100 less than that of enzyme substrate reaction and is too small for a diffusion controlled reaction. In contrast, its binding to cell is cooperative nature and occurs with $t_{1/2}$ equal to 1 to 2 min. The calculated forward rate constant k_f is 10^5-10^6 M^{-1} s^{-1} which is higher than that found for simple sugar[12]. The lectin induced agglutination of cell occurs much slowly as can be seen from Fig. 1, where the average size of lectin induced cluster is plotted against time (t) for myeloma cell line. The slower rate of agglutination is rather expected but the higher value for k_f than that of simple sugar is rather surprising.

The observed higher affinity for binding of lectin to cell surface carbohydrate by 100-1 000 fold

Abbreviations: CT = Cholera toxin, DT = diphtheria toxin, DPPC = dipalmitoyl phosphatidyl choline, WGA = wheat germ agglutinin, GD_{1a} = disialoganglioside.

† Dedicated to Professor Sadhan Basu on the occasion of his 65th birthday.

TABLE 1—PHYSICOCHEMICAL PROPERTIES OF LECTIN BINDING TO CARBOHYDRATE

Lectin	Carbohydrate	k_f $M^{-1}s^{-1}$	k_d s^{-1}	K_{eq} M^{-1}
RCA	p-Nitrophenyl-β-Dgal[a]	4.5×10^5	30 ± 3	1.5×10^4
	Galactose[b]	—	—	1.2×10^3
	Lactose[c]	—	—	1.5×10^4
PNA	Methyl-β-D-galactoside[d]	3.7×10^4	39.4	0.94×10^3
	Methyl-β-D-lactoside[e]	4.0×10^4	29.0	1.4×10^3
	Dgal-β(1-3)-DgalNAc[f]	—	—	2.8×10^4
	Methyl-Umb-Dgal-β(1-3)-DgalNAc[g]	7.1×10^3	0.24	2.9×10^4
WGA	Methyl-Umb-glcNAcp[h]	3.0×10^6	1.8×10^2	1.7×10^4
	Methyl-Umb-(glcNAcp)$_2$[i]	1.0×10^7	2.0×10^2	5.0×10^4
ConA	p-Nitro-α-Dmannoside[i]	5.4×10^4	6.2	8.7×10^3
	Methyl-Umb-(manp)$_2$[j]	—	—	$13.9\pm0.5\times10^4$
SBA	Methyl-Umb-β-galNAc[k]	1.1×10^4	0.36	8.0×10^4

[a] Ref. 18. [b] Ref. 15. [c] Olsnes *et al.*, *J. Biol. Chem.*, 1974, **249**, 803. [d] Neurohr *et al.*, *Biochem.*, 1981, **20**, 3499. [e] Neurohr *et al.*, *Biochem.*, 1982, **21**, 498. [f] Neurohr *et al.*, *Eur. J. Biochem.*, 1982, **123**, 305. [g] Lootiens *et al.*, *FEBS Lett.*, 1983, **162**, 193. [h] Lootiens *et al.*, *J. Biosci.*, 1983, **5**, (suppl. 1), 105. [i] Ref. 8. [j] Lewis *et al.*, *Arch. Biochem. Biophys.*, 1976, **172**, 689. [k] De Boeck *et al.*, *J. Biol. Chem.*, 1984, **259**, 7067.

TABLE 2—AFFINITY PARAMETERS FOR LECTIN BINDING TO CELLS

Lectin	Cell type	K_a M^{-1}
RCAI[a]	Normal calf thymocyte	4.8×10^7
WGA[a]	Normal calf thymocyte	2.6×10^6
ConA[b]	Mouse normal thymocyte	1.9×10^6
SBA[c]	Mouse normal spleen	2.0×10^6
PNA[d]	Human erythrocyte (NT)	
	A type	1.2×10^7
	B type	2.7×10^7

[a] R. Kornfeld and Siimons, *J. Biol. Chem.*, 1974, **249**, 1295. [b] D. Stobo], A. S. Rosenthal and W. E. Paul, *J. Immunol.*, 1972, **108**, 1. [c] A. Novogrodsky *et al.*, *Proc. Natl. Acad. Sci. USA*, 1973, **70**, 2515. [d] Sharon *et al.*, *Arch. Biochem. Biophys.*, 1977, **180**, 570.

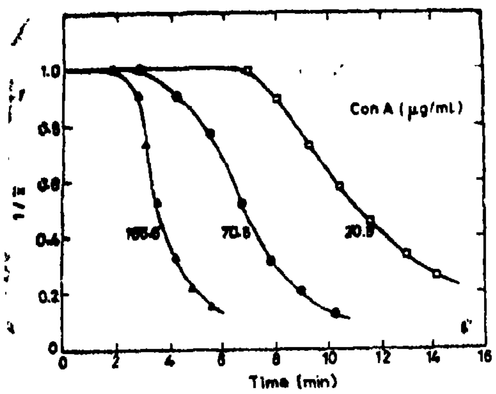


Fig. 1. Kinetics of conA-induced agglutination of sarcoma 180 ascite cells. $\bar{X}$ represents the average number of cells per clump and calculated from the absorbance changes at 546 nm of suspension of cells when different amounts of conA (μg ml^{-1}) added to it ($\bar{X}$ is calculated according to W. A. M. Linnemans *et al.*, *Expt. Cell Res.*, 1976, **101**, 191; from the spectral data of K. M. Hwang *et al.*, *Cancer Res.*, 1974, **34**, 3396).

can be rationalised in the following way. Lectin may have extended binding site for a chain of two or more specific sugar in appropriate linkage giving rise to a high affinity. Alternatively, lectin may bind simultaneously two or more receptors so that observed affinity is equal to the product of separate association constants for simple sugar as it is known to be the case in the binding of monosialoganglioside GM_1 to cholera toxin[13]. The cell surface has a variety of glycolipid and glycoprotein receptors, their relative proportion as well as their chemical nature are known to change upon oncogenic transformation which in turn will control the complex pattern of interaction with lectins and hence, their agglutinability as shown in Fig. 2. Further complexity would arise due to the involvement of cytoskeletal elements. It is evident that

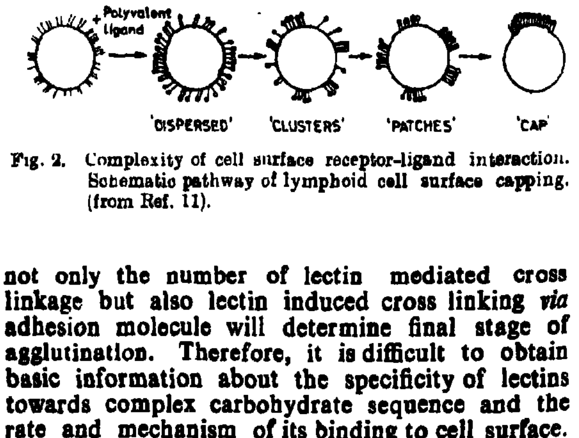


Fig. 2. Complexity of cell surface receptor-ligand interaction. Schematic pathway of lymphoid cell surface capping. (from Ref. 11).

not only the number of lectin mediated cross linkage but also lectin induced cross linking *via* adhesion molecule will determine final stage of agglutination. Therefore, it is difficult to obtain basic information about the specificity of lectins towards complex carbohydrate sequence and the rate and mechanism of its binding to cell surface. On the other hand, glycoconjugate embedded liposome can be used as a chemical model for the study of mechanism of cell surface receptor mediated reaction in general. The advances that have been made from studies on model liposomal systems have been recently reviewed[14]. We would like to focuss our attention particularly to the kinetic complexity of the reaction between lipsome bearing glycoconjugate and lectin.

Lectin binding to liposome bearing glycoconjugate :

Earlier, it has been shown that interaction between conA and carbohydrate moiety of glycoprotein lectin RCA_1 from castor bean leads to the precipitin reaction with characteristic time constant observed for the binding of lectins to cells and the precipitin complexes dissociate slowly in the presence of sugar, specific to conA. The calculated rate constant of the formation of the 1 : 1 RCA_1 : conA and its dissociation from the measurement of time dependent appearance and disappearance of turbidity in the presence of hapten sugar is found to be $3\times10^{3}\ M^{-1}\ s^{-1}$ and $7\times10^{-5}\ s^{-1}$, respectively[15]. Their ratio yields a value $4.3\times10^{7}\ M^{-1}$ for the interaction specificity of conA towards complex carbohydrate sequence of agglutinin, RCA_1. This value is of comparable magnitude for other conA complex carbohydrate system[16]. This finding prompted us to develop liposome bearing glycoconjugate particularly with glycospingolipid gangliosides because of its implicated functions listed in Table 3.

TABLE 3—FUNCTION OF GLYCOSPHINGOLIPID*

1. Constitutive component of outer leaflet of lipid bilayer confering rigidity.
2. Cell surface marker and antigens.
3. Cell-cell interaction and recognition.
   (i) Cell contact response and contact inhibition.
   (ii) Neuroglia interaction.
   (iii) Retinolectal recognition.
   (iv) Neuro-muscular recognition.
4. Differentiation marker.
   (i) Early embryo and teratocarcinoma.
   (ii) Crypt to villus cell differentiation.
   (iii) Erythrocyte differentiation.
   (iv) Myogenic differentiation.
   (v) Neuroblastoma.
   (vi) Lymphoid cell differentiation and mitogenesis.
5. Cell growth regulation and oncogenesis.
6. Interaction with bio-active factors : bacterial toxins, glycoprotein hormones and viruses-implication as receptor.

* S. Hakamori, *Annu. Rev. Biochem.*, 1981, **50**, 733.

Glycospingolipid forms micelles at small concentrations and its C.M.C. lies in micromolar-nanomolar range depending on the nature of the carbohydrate sequence and charge[17]. Thus, its carbohydrate moiety is not easily accessible to even glycosidases and lectins. The accessibility, however, increases when they are embedded in liposome as well as in mixed micellar system, *i.e.* deoxycholate-lecithin. It has also been found that the addition of a divalent lectin RCA_1 to a vesicle containing GM_1 (5-20%) results in the increase of turbidity due to aggregation of vesicles as shown Fig. 3. In the case of bivalent lectin, SL-SL vesicles are held together by two lectin sugar bonds. The number of cross links increases as valency increases. Since initial binding (Step 1) is likely to contribute very little to the observed turbidity as lectin is added to the solution of vesicle bearing gangliosides, the initial rate of change of turbidity is given by equation (1).

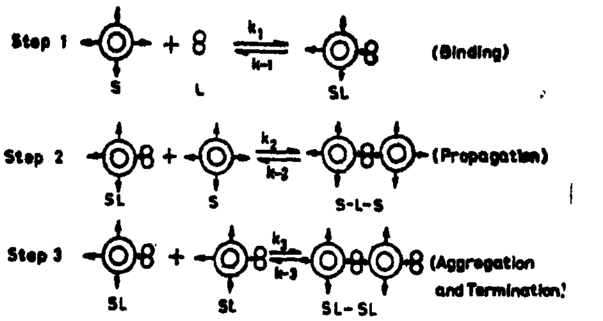


Fig. 3. Mechanism of lectin (L) induced vesicle (S) aggregation through the carbohydrate moiety of glycolipid/glycoprotein embedded into the vesicles : (8) a bivalent lectin *e.g.* RCA_1, (→) expanded sugar residues, (S) vesicle containing glycoconjugates, (L) a bivalent lectin, and (SL) lectin-vesicle complex.

$$\frac{dA}{dt}=k_2[SL].[S] \tag{1}$$

since $t\to0$, $[SL]\ll[S]$.

Under steady state condition, *i.e.*

$\frac{d[SL]}{dt}=0$, [SL] is given by the equation (2).

$$[SL]=\frac{k_1[S][L]}{k_2[S]+k_{-1}} \tag{2}$$

Substituting (2) in (1), one obtains equation (3)

$$(dA/dt)_{t\to0}=\frac{k_2k_1[S]^2[L]}{k_2[S]+k_{-1}} \tag{3}$$

Case 1. when $k_2[S]\ll k_{-1}$, equation (3) becomes,

$$(dA/dt)_{t\to0}=\frac{k_1}{k_{-1}}\times k_2[S]^2[L] \tag{4}$$

Case 2. when $k_2[S]\gg k_{-1}$,

$$(dA/dt)_{t\to0}=k_1[S][L] \tag{5}$$

When $\frac{k_1}{k_{-1}}=K_{eq}$, the equillibrium constant of binding, [L] and [S] represent concentrations of lectin and surface carbohydrate, respectively. Values for k_1 and k_{-1} for the binding of lectins to soluble sugar is $1\text{-}6\times10^{4}\ M^{-1}\ s^{-1}$ and 20-30 s^{-1} (Tables 1 and 2). The vesicle aggregation is found to occur when [L] and [S] are in the micromolar range, the assumption $k_2[S]\ll k_{-1}$ is more satisfactory. Under these conditions, the initial rate of the vesicle aggregation is proportional to the lectin concentration as well as to the square of the concentration of available carbohydrate on the surface of vesicle as expected for a bimolecular aggregation step. Under conditions $k_2[S]\gg k_{-1}$, though difficult to achieve experimentally, rate of precipitin reaction is first order with respect to lectin and sugar. This first order dependence on lectin can be used to determine the specificity of a

soluble sugar (hapten) from experimentally observed decrease in the initial rate of vesicle aggregation. When the hapten is present in large excess, the fraction of lectin molecule available for the reaction is given by equation (6),

$$(1-\theta)=\frac{1}{1+K_a[H]} \quad (6)$$

where, θ is the fraction of lectin site saturated with hapten and K_a is the affinity constant of the hapten-lectin system. Since the initial velocity is proportional to the concentration of the free lectin, it is possible to calculate K_a from the slope of the plot of v_t/v_0 against [H] where v_t and v_0 are the initial velocity in the presence and absence of hapten[18]. This simple method is equally applicable to water soluble complex carbohydrate.

In view of the kinetic complexity, the apparent forward rate constant of aggregation of vesicles can be estimated from the $t_{1/2}$ value (*i.e.* time for 50% change in turbidity when lectin is added to a solution of liposome bearing glycoconjugate) assuming the rate of vesicle aggregation is given by

$$\frac{dA}{dt}=k_2c^2\theta(1-\theta) \quad (7)$$

where, c is the concentration of surface carbohydrate and θ is the fraction occupied by the lectin. The apparent $t_{1/2}$ depends on c and pass through a minimum as $\theta\rightarrow1$. This has been verified experimentally[19].

The dissociation complex of the type S – L – S took place slowly in the presence of soluble hapten and follows first order rate law. The calculated first order rate constant depends on the concentration of hapten and its chemical nature as found in the case of sugar induced dissociation of RCA_1 – conA complex[14]. Hence, k_{-2} can be estimated similarly from the time dependent change in turbidity of the precipitin complex in the presence of soluble sugar. The k_2 thus can be estimated from the relation (8),

$$k_2=k_{-2}\times K_{eq}, \quad (8)$$

where, K_{eq} (M^{-1}) is the association constant which can be determined from the measurement of relative rate of aggregation in the presence of varying amounts of soluble hapten sugar[17].

This kinetic method has advantages over that involving separation of the precipitin complex because it is simple and less time consuming[20]. It also offers to estimate the contribution of factors that are often indicated to account for the increased agglutinability of transformed cells, *viz.* (i) receptor density, (ii) membrane fluidity (determined by the composition of lipid matrix), (iii) steric accessibility (*i.e.* influence of one on the other when two different types of glycoconjugates are present) and (iv) effect of head group. It is evident that the understanding of the molecular basis of these factors is, however, necessary in order to examine more critically the involvement of the cytoskeletal element. It may be emphasised here that few quantitative study has so far been made to establish the rate law of such complex process[21]. Nevertheless, the effect of receptor denisty, chemical nature of head group of phospholipid, carbohydrate sequence, cholesterol content on the agglutinability of vesicles bearing glycoconjugate have been examined either in terms of initial rate of change in turbidity or normalised first order rate constant when lectin is present in excess in various lectin liposomal systems.

The most important observation reported from the studies of vesicles containing GM_1 was that in the range of receptor concentration 2-10 mol% agglutination by lectin RCA_1 was extremely sensitive to receptor density (*i.e.* concentration in the plane of membrane). Thus, the rate of vesicle agglutination increased 20-fold when the mole ratio of GM_1 was from 1 : 123 to 1 : 55. A 4-fold increase in the rate is, however, expected for bimolecular aggregation. The apparent rate of vesicle agglutination was found to be sensitive to the cholesterol content of the vesicle[18]. In contrast, the apparent specificity of binding remains unchanged[22]. Apart from the concept of receptor density

TABLE 4—LIPOSOME BEARING GLYCOCONJUGATE AS MODEL FOR LECTIN-RECEPTOR INTERACTION AT CELL SURFACE

Lectin	Receptor	K_f $M^{-1}s^{-1}$	K_a M^{-1}
	1. Glycolipids		
RCA_1	GM_1[a]	—	2.2×10^{6}
	Lactosyl ceramide[b]	1.4×10^{4}	8.7×10^{5}
	Gal-s. space gr c-cholesterol[c]	—	—
WGA	GM_1 and GM_3[d]	—	—
	GM_3[b]	5.8×10^{3}	1.9×10^{5}
ConA	glc-fatty acid[e]	—	—
	2. Glycoproteins		
ConA	Band-3[f]	—	10^{5}—10^{6}
Succinyl conA	Band-3[g]	—	2.1×10^{6}
WGA	glycophorin[h]	—	2.5×10^{5}

[a] Surolia *et al.*, *Nature (London)*, 1975, 257, 802. [b] S. K. Podder, Annual Report of CSIR project on 'Receptor-ligand interaction and transmembrane signalling', 1984. [c] Slama *et al.*, *Biochem.*, 1980, 19, 4595. [d] Redwood *et al.*, *Biochem. Biophys. Acta*, 1976, 455, 681. [e] Hampton *et al.*, *J. Biol. Chem.*, 1980, 255, 6766. [f] Ketis *et al.*, *Biochem. Biophys. Acta*, 1982, 689, 194. [g] Chicken *et al.*, *Biochem. Biophys. Acta*, 1983, 729, 200. [h] Ketis *et al.*, *Biochem. Biophys. Acta*, 1983, 685, 347.

several other important concepts emerged from such studies listed in the Table 4. Rando and Bongerter[23] established the concept of threshold concentration from the observation that the agglutination takes off dramatically at some 5 mol% receptor density. In addition, they were able to show that the agglutinability of a poor hapten can be improved by increasing length of spacer arm within certain limit[24]. The latter is, however, remeniscent of the striking difference in agglutinability of vesicle bearing galactose ceramide and lactosyl ceramide[25]. Others have shown that the accessibility of sugar group is controlled by the effective size of polar head group of phospholipid and introduced the concept of steric accessibility from the observation that the replacement of phosphatidyl choline by phosphatidyl ethanolamine confers agglutinability of glycolipid with a four-spacer arm embedded in zwitterionic PL (phosphatidyl choline) vesicles. In contrast, the agglutinability of PL vesicle containing glyco lipid ten-spacer arm remains unaffected[26,27].

Various studies on model membrane system indicated that vesicle size and its storage stability and transmembrane assymetry is governed not only by the method of preparation but by its phospholipid composition and cholesterol content. Thus, it is rather difficult to make comment on the molecular mechanism leading to the observed variation of agglutinability of vesicles. Evidently transmembrane assymetry (*i.e.* in plane distribution of embedded receptor) and surface potential and finally metastability of mixed vesicle system leading to alteration of vesicle size will most likely be important parameter to control the agglutinability of model membrane system (*i.e.* rate and extent of the precipitin reaction) in addition to the specificity, length of sugar sequence, anomericity of the α-carbon atom[28]. The magnitude of specificity is determined not only by the chain length of sugar sequence and number of sugar residues that are accomodated in the cleft of binding site and finally, whether or not more than one site of lectin in the plane of membrane are involved in binding step as shown in the Fig. 3.

During the past several years efforts have been made in this laboratory to assess the individual contribution of the above mentioned various factors influencing the reactivity of glycoconjugates embedded in liposome and their corelation with the variations of agglutinability of liposome bearing glycoconjugates and of transformed cells.

We have, however, restricted ourselves to the study of glycoconjugate specially glycosphingolipid in the lipid vesicles with respect to their size, stability, transmembrane distribution and surface potential using various chemical probes, namely, monovalent neuraminidase, acridine orange and galactose specific lectins[28]. The major emphasis has been to examine their possible receptor function towards lectin and toxin. Some of the interesting informations obtained are summarised here.

The transbilayer distribution of GD_{1a} in sonicated GD_{1a}-DPPC vesicles becomes increasingly assymetric in favour of outer layer with increasing mole fraction of ganglioside (X_G) upto 0.5 and then levels off with 100% GD_{1a} in the outer surface. The surface charge density as monitored by metachromatic spectral shift of acridine orange in the presence of liposome bearing various mole percent of GD_{1a} also shows the same behaviour. The rate of desialation of GD_{1a} in the outer surface of lecithin matrix by neuraminidase when corrected for transbilayer distribution shows changes resembling composition dependent phase behaviour. This suggests that neuraminidase can be used as a probe for the study of the phase behaviour of lecithin-ganglioside system. The affinity and catalytic rate for desialation are inversely related suggesting the formation of non-productive enzyme-substrate complex ES at low X_G values presumably because of non-specific interaction between neuraminidase and liposome. In contrast, liposome bearing mixed ganglioside are unstable as reflected in the rate and amplitude of the precipitin reaction with WGA. They can be stabilised either by adding Ca^{2+} or incorporating lactosyl ceramide which then become cryptic towards RCA_1. Thus, surface potential seems to play an important role in controlling the reactivity and stability of liposome bearing gangliosides.

In view of this interesting finding, liposome bearing asialo-GM_1 is now being investigated to study specificity of well characterised galactose specific plant lectins, namely, peanut agglutinin (PNA), RCA_1 and plant toxin ricin. Fig. 4 shows the initial rate and amplitude of the precipitin reaction between vesicle containing asialo-GM_1 (2.9 μM) by PNA, RCA_1, and ricin (RCA_2) at the same concentration of 2.26 μM. It is seen that the initial rate of the reaction with PNA is lower than that of ricin and agglutinin, however, the final amplitude is found to be much higher in the case of PNA. Ricin reacts faster with a higher amplitude than agglutinin. This shows that the overall rate and mechanism of the pricipitin reaction of vesicles by lectins is not solely determined by the valency of lectin. Other factors still to be identified are important as well.

Fig. 5 shows the corresponding dissociation curve of the precipitin complex in the presence of lactose. In the case of ricin and agglutinin, there is a very fast phase which can not be resolved. However, in the case of peanut lectin the very fast phase seems to be absent. The dissociation of both agglutinin- and ricin-asialo GM_1 system occur in μM range of lactose concentration while that of PNA in the mM range.

Tables 5-7 summerise some of the preliminary data collected in this laboratory (*i.e.* the initial rate and amplitude of precipitin reaction of vesicles containing asialo-GM_1 with lectins, the $t_{1/2}$ values and their dependence of the concentration of sugar). The K_a (M^{-1}) and k_d values determined

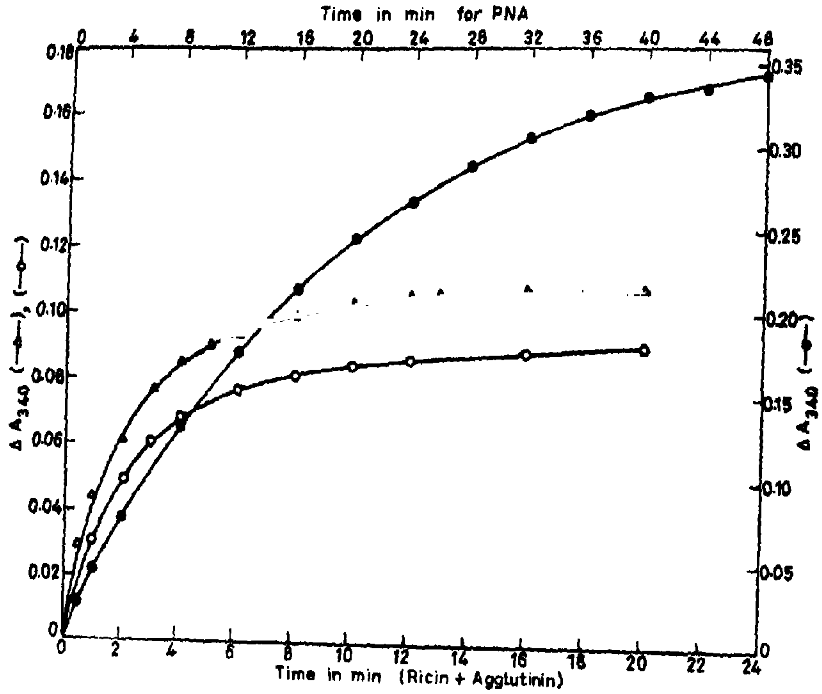


Fig. 4. Kinetics of precipitin reaction of vesicles containing asialo GM_1 (5% mole ratio of asialo GM_1 to DML, dimyristoyl lecithin) by PNA, RCA_1 and RCA_2 (concn. of asialo GM_1 in vesicles $= 2.9\times10^{-6}$ M) : (Δ) RCA_1, (●) PNA and (○) RCA_2 ; all 2.26×10^{-6} M.

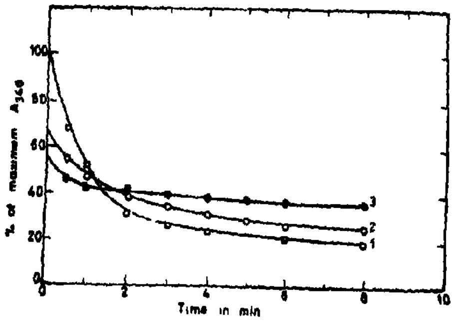


Fig. 5. Kinetics of sugar (lactose) induced dissociation of the precipitin complex formed between vesicles containing asialo GM_1 and lectins (lactose concn. in parenthesis) : (□) PNA-asialo GM_1 (28.8 mM), (○) RCA_1-asialo GM_1 (27.8 μM) and (●) RCA_2-asialo GM_1 (54.64 μM) : protein $= 2.26\times10^{-6}$ M, asialo $GM_1 = 2.9\times10^{-6}$ M.

TABLE 5—INITIAL RATE AND AMPLITUDE OF PRECIPITIN REACTION BETWEEN LECTIN AND LIPOSOME BEARING ASIALO GM_1

Lectin concn. μM	Concn. of asialo GM_1 μM	Initial rate (A_{340}) $\times10^{-3}M^{-1}s^{-1}$	Amplitude (A_{340} at 12 min)
PNA (2.26)	2.9	1.77	0.176
RCA_1 (2.26)	2.9	1.28	0.105
RCA_2 (2.26)	2.9	3.2	0.086

TABLE 6—DEPENDENCE OF $t_{1/2}$ OF DISSOCIATION OF PRECIPITIN COMPLEX FORMED BETWEEN LECTIN AND LIPOSOME BEARING ASIALO GM_1 ON THE CONCENTRATION OF LACTOSE

Concn. of lectin μM	Concn. of asialo GM_1 μM	Lactose concn. μM	$t_{1/2}$ s
PNA (2.26)	2.9	(a) 28.8*	48.0
		(b) 38*	28.8
		(c) 47.6*	24.0
RCA_1 (2.26)	2.9	(a) 17.7	17.5
		(b) 27.8	14.4
		(c) 45.45	10.4
RCA_2 (2.26)	2.9	(a) 20	30.0
		(b) 40	18.0
		(c) 54.54	12.0

* mM.

from concentration dependence of $t_{1/2}$ on lactose as described here is also included in Table 7.

Conclusion :

It is clear from the above discussion that binding of lectin to liposome bearing simple glycosphingolipid is rather a complex process. The accessibility of exposed carbohydrate is controlled by a variety of factors, namely, surface charge, nature of polar head group of the lipid matrix and can be quantitatively expressed in terms of rate and extent of precipitin reaction. The specificity of

TABLE 7—BINDING PARAMETERS OF VARIOUS LECTINS TO ASIALO-GM_1

Lectin concn. μM	Asialo GM_1 in vesicle μM	k_d* s^{-1}	K_a** M^{-1}
Ricin (RCA_2) (2.26)	2.9	0.89	5.06×10^4 (4.65×10^4)
Agglutinin (RCA_1) (2.26)	2.9	0.07	2.9×10^5
PNA (2.26)	2.9	4.5×10^{-4}	1.5×10^7

* Average value calculated from $t_{1/2}$ values given in Table 5 using the relation,

$$k_d = \frac{0.69}{t_{1/2} \times C_s \times K_{eq(s)}}$$

where, C_s is the concentration of sugar hapten and $K_{eq(s)}$ is the equilibrium constant for hapten to lectin.

** $K_a(M^{-1})$ was calculated using the relation,

$$K_a\ (\text{complex}) = \frac{k_d\ (\text{simple})}{k_d\ (\text{complex})} \times K_{eq}\ (\text{simple})$$

The value in paranthesis is obtained independantly from the inhibition experiment of ricin.

binding of accessible carbohydrate to lectin is, however, comparable to those found for cell-lectin interaction. The results from these studies would also indicate existence of higher order complexity in the binding of lectin with model membrane bearing intrinsic membrane bound glycoproteins because not only the presence of multiple carbohydrate chain but also of their complex sugar sequence. Further complexity could arise from the variation of lipid-protein interaction which in turn may determine accessibility and orientation of carbohydrate. Grant and Sharon made pioneering studies on liposome bearing Band-3 protein (conA receptor) and glycophorin (WGA receptor) of human erythrocytes[89-91]. The Band-3 protein is a folded polypeptide chain of approximately 96 000 D molecular weight with a single large N-linked carbohydrate chain. In contrast, glycophorin has a small polypeptide backbond (molecular weight of 12 000 D) which transverse only once and bears 16 short carbohydrate chains of which 15 are O-linked[92-94]. In both cases, binding of conA and WGA to the reconstituted glycoprotein was only observable in the presence of 3 mg ml^{-1} albumin. The binding exhibits characteristics of co-operativity. This has been imposed a greater difficulty in the quantitation of binding. Recently it has been shown that conA reacts with surface of phospholipid-liposomes through two distinct classes of binding sites, a relatively small number of high affinity sites and a much larger number of low affinity sites. Addition of bovine serum albumin induces extensively additional binding of conA to liposomal membrane and this binding is saturable and specific, *i.e.* methyl mannosidc inhibitable. In contrast, divalent succinyl conA shows little tendency to binding to liposome either in the presence or absence of albumin[95].

Either dramatic the conformation changes in conA due to succinylation or the repulsive barrier is too large for the nucleation of binding or a combination of both could lead to such observation. For ligand induced vesicle agglutination as discussed here as well as cellular adhesion to occur there exists the repulsive barrier which need to be overcome. This can, however, be achieved in many different ways, namely, by increasing of number of non-covalent interaction, *viz.* hydrogen bonding by way of increasing receptor density, valency of the ligand and decreasing in surface charge density of the same sign. Among these the effect of receptor density and its distribution in the plane of membrane which is likely to be very sensitive to the host matrix composition has also been documented in other studies on model membrane bearing glycolipid hapten, *viz.* antibody binding and complement fixation and *in vivo* and *in vitro* cell-liposome interaction. The latter has, however, been investigated with regard to the development of organ specific delivery system[96]. Finally, it may be emphasised once again that kinetics of the precipitin reaction between lectin and liposome bearing glycolipid and its dissociation in the presence of hapten sugar is extremely complex, however, gave interesting information. That it exhibits many features of complex agglutination reaction, *viz.* multiple type of binding, co-operativity even in the case of simple system, like GM_1-DPPC vesicles seem to suggest that involvement of factors, like membrane fluidity and cytoskeletal elements in giving rise to increased agglutinability of transformed cells has so far been over-emphasised. The exact molecular mechanism leading to such complex pattern in model system is not yet fully understood. It could partly be due to heterogeneity of vesicle sizes in the case of the GM_1-liposome-RCA_1 system. The observed co-operativity could also be due to unique conformation changes in lectin that might have been resulted from the binding of complex carbohydrate sequence at the liposome surface. It is known that binding simple sugar to lectin occurs in one step and is of non-cooperative

in nature. In contrast, the binding of lectin to carbohydrate sequence at the liposomal surface is co-operative in nature in some cases. If this be the case, the binding characteristics of simple saccharides does not seem to have much relevance in understanding lectin mediated phenomena. It is evident that further insight into the molecular mechanism of lectin mediated phenomena is likely to be obtained from the further indepth studies of precipitin reaction hitherto described. Work in this direction is in progress in the laboratory.

Acknowledgement

This work is financially supported by C.S.I.R. and D.S.T., New Delhi.

References

1. N. Firon, I. Ofek and N. Sharon, *Carbohydr. Res.*, 1983, **120**, 235.
2. J. Ray and R. A. Lerner, *Cell*, 1982, **28**, 91.
3. D. Burke, L. Mendoca-Prediato and C. E. Ballou, *Proc. Natl. Acad. Sci. USA*, 1980, **77**, 318.
4. V. D. Vacquier and G. D. Moy, *Proc. Natl. Acad. Sci. USA*, 1977, **74**, 2456.
5. N. Sharon, *Immunol. Today*, 1984, **5**, 143.
6. "Molecular Action of Toxins and Viruses", eds. P. Cohen and S. Von Heningen, 1982, Vol. 2.
7. E. A. Kabat, "Blood Group Substances, Their Chemistry and Immunochemistry", Academic Press, New York, 1956.
8. G. Edelman, *Annu. Rev. Biochem.*, 1985.
9. R. L. Schnaar, *Anal. Biochem.*, 1984, **143**, 1.
10. G. L. Nicholson, *Int. Rev. Cytol.*, 1974, **39**, 89.
11. G. L. Nicholson, *Biochem. Biophys. Acta*, 1976, **457**, 57.
12. P. Cuatrecasses, *Biochem.*, 1973, **12**, 1312.
13. J. D. Dwyer and V. A. Bloomfield, *Biochem.*, 1982, **21**, 3231.
14. C. W. M. Grant and M. W. Peters, *Biochim. Biophys. Acta*, 1984, **779**, 403.
15. S. K. Podder, A. Surolia and B. K. Bachhawat, *Eur. J. Biochem.*, 1974, **44**, 151.
16. Barzinger and D. J. Firth, *J. Biol. Chem.*, 1979, **254**, 2400.
17. S. Formisano, *Biochem.*, 1979, **18**, 1119.
18. S. K. Podder, A. Surolia and B. K. Bachhawat, *FEBS, Lett.*, 1978, **85**, 313.
19. S. K. Podder, A. Surolia and B. K. Bachhawat, *Indian J. Biochem. and Biophys.*, 1981, **18**, 322.
20. A. Surolia, B. K. Bachhawat and S. K. Podder, *Nature (London)*, 1975, **257**, 802.
21. G. C. Goodwin, K. Hammond, I. G. Lyle and M. N. Jones, *Biochim. Biophys. Acta*, 1982, **689**, 80.
22. A. Surolia and B. K. Bachhawat, *Biochem. Biophys. Res. Commun.*, 1978, **83**, 779.
23. R. R. Rando and F. W. Bongerter, *J. Supramol. Struct.*, 1979, **11**, 295.
24. J. S. Slama and R. R. Rando, *Biochem.*, 1980, **19**, 4595.
25. W. Curatolo, A. O. Yau, D. M. Small and B. Sears, *Biochem.*, 1978, **17**, 5740.
26. R. Sundler, *Biochim. Biophys. Acta*, 1984, **771**, 59.
27. I. J. Goldstein and C. E. Hayes, "Advances in Carbohydrate Chemistry and Biochemistry", 1978, Vol. 35, pp. 128-334.
28. S. K. Podder, DST project report on "Development of drug carrier and enzyme therapy : Factors affecting rates and mechanism of uptake of liposome entrapped materials of therapeutic potential', 1982 ; P. D. Thomas, Ph.D. Thesis, 1982.
29. D. G. Barratt, F. J. Sharom, A. E. Thade and C. W. M. Grant, *Biochim. Biophys. Acta*, 1977, **465**, 191.
30. F. J. Sharom, D. G. Barratt and C. W. M. Grant, *Proc. Natl. Acad. Sci. USA*, 1977, **74**, 2751.
31. N. V. Ketis, J. Girdlestone and C. W. M. Grant, *Proc. Natl. Acad. Sci. USA*, 1980, **77**, 3788.
32. T. L. Steck, *J. Supramol. Struct.*, 1978, **8**, 311.
33. T. Tsuji, T. Irimura and T. Osawa, *Biochem. J.*, 1980, **187**, 677.
34. J. Jarnefelt, J. Rush, Y. Li and R. A. Laine, *J. Biol. Chem.*, 1981, **253**, 8006.
35. C. A. Chicken and J. Sharon, *Can. J. Biochem. Cell Biol.*, 1985, **63**, 65.
36. B. K. Bachhawat and P. Das Gupta, Proceeding of the International Conference on Medical Application of Liposomes, Japan, Dec. 14-17, 1984.

J. Indian Chem. Soc.,
Vol. LXIII, January 1986, pp. 131-137

Conformation of Mammalian Lens Proteins : Photoinduced Changes in Relation to Cataract Formation†

BIRESWAR CHAKRABARTI*, SWAPAN K. BOSE** and KRISHNAGOPAL MANDAL

Eye Research Institute and Harvard Medical School, 20 Staniford Street, Boston, Mass. 02114, U.S.A.

Although the secondary structures of all lens crystallins are more or less similar, their tertiary structures are remarkably different as manifested in their near-uv circular dichroic and intrinsic or extrinsic fluorescence spectra. Methylene blue-sensitised photooxidation causes a change in the tertiary structure of lens crystallins but in each case subtle differences exist in the nature of the changes. Photoinduced changes in the conformation of lens protein are discussed in terms of destabilisation of the protein structure during cataractogenesis.

FUNCTIONALLY, the lens of the eye must be transparent and highly refractive. The mammalian lens is composed largely of soluble proteins, commonly known as crystallins ; three classes α, β, and γ, are distinguished on the basis of chemical characteristics, such as molecular weight (MW) and electrophoretic mobility[1]. β-Crystallins can be further separated by gel chromatography into two components[2] of differing molecular weight, β_H (high) and β_L (low), and γ by ion-exchange chromatography into several fractions[3], the major ones being γ-II, γ-III and γ-IV.

The lens contains about 35% (by weight) structural proteins. This high crystallin concentration imparts to the lens its uniformly high refractive index, yet leaves it completely transparent in the normal tissue[4]. Lens transparency may depend on conformation, inter-moleculer interactions, and long-range ordering of the densely packed crystallins[5,6].

Simply defined, a cataract is a lens opacity that results in loss of transparency and that occurs mainly in the central (nucleus) rather than the peripheral (cortex) region of the tissue. Cataract formation is a slow but irreversible process. Among the physicochemical changes that human lens crystallins undergo during aging and cataractogenesis are increased protein-protein aggregation and formation of insoluble proteins, increased pigmentation in the nucleus, and formation of blue fluorescent products[7-11]. The aggregation is stabilised either by disulphide bonds formed by oxidation of sulphydryl groups of cysteine residues or by unknown covalent non-disulphide crosslinks or possibly by non-covalent associations[9,10,12].

Considerable progress has been made in elucidation of the chemical (primary) structure of crystallins[2,13-15] and the chemical changes in aging and cataractogenesis. However, little is known of the conformation, the interactions between different segments of the amino acid chains, and the spatial orientation of groups susceptible to chemical change, and the changes of these features during aging and cataractogenesis.

The conformation of a protein is usually described by its secondary and tertiary structures. Because of the interactions between various amino acid side chains and the relative degree of interaction with water, proteins are rarely fully extended, linear chains ; instead they fold to form complex, three-dimensional structures. Frequently, monomeric units at some position along the chain engage in specific interactions (mainly hydrogen bonds) with other units close by or at some distance along the linear sequence and form an identifiable substructure called the secondary structure ; alpha-helices and beta-sheets in proteins are common examples. Secondary structure carries little, if any, information about spatial orientations. Tertiary structure carries no identifiable features, but it provides information about orientation and describes all of the interactions of all atoms of the protein in three-dimensional space. The interactions, obviously, are related to the spatial distribution of atoms or groups of atoms and their microenvironments.

The three-dimensional structure of γ-II crystallin has been determined in great detail from X-ray analysis by Blundel and coworkers[16-17]. The protein's stability was ascribed to its high degree of internal symmetry. γ-III and γ-IV also have internal structural symmetry, with predominantly beta-sheet structure folded into domains[18]. Spectroscopic analysis of the secondary and tertiary structure of α-, β-, and γ-crystallins[19-22] have provided data on the conformation of lens protein in solution. We have noted changes in tertiary structure in the presence of sugar molecules[23] and in aging[24].

† Dedicated to Professor Sadhan Basu on the occasion of his 65th birthday.

** On leave of absence from the Department of Chemistry, University of Calcutta.

The possible role of light in the etiology of human cataract is of intense research interest[26-31], because the eye is a major photoreceptor organ of the body and because photooxidation of tryptophan (Trp) (amino acid residue abundant in lens protein) yields pigmented and fluorescent oxidation products, some of which are present in mature or cataractous lens. Photochemical damage to the lens protein involves formation of covalent disulphide and non-disulphide crosslinks[26,28,30].

We have undertaken[32-35] a systematic investigation of the light-induced conformational changes of lens crystallins using various spectroscopic techniques—absorption, fluorescence, and circular dichroism (CD). The present paper briefly outlines the structural aspects of lens crystallins, reports results of our studies of photoinduced conformational changes of crystallins, particularly β- and γ-, and discusses the mechanism of such processes.

Experimental

The cortex (70-80% of lens volume) was removed from lenses (0.9-1.0 g) from 1- to 2-week-old calves, and the water-soluble proteins were extracted and fractionated by gel and ion-exchange chromatography[33,34]. The ultra-pure chemicals used were bought commercially. Protein solutions were dialysed at 4° against respective buffers, just prior to spectroscopic analysis. Protein concentration was determined with a standard absorption value at 280 nm[33] or by the Lowry method[36]. β- and γ-Crystallins used for photochemical studies were unfractionated samples; β- contained both β'_H and β_L, and γ- was a mixture of its subfractions, γ-I to γ-IV.

Fluorescence was measured on a Perkin-Elmer MPF-44A spectrofluorometer and CD spectra on a AVIV 60 DS CD spectropolarimeter modified as described previously[19,32]. Absorption was recorded on a Beckman DU-8 spectrophotometer. The protein sample in the presence of methylene blue (MB) was irradiated in a set-up described previously[32].

Results

The near-uv spectra of all crystallins and the far-uv spectra of β- (which represents other crystallins also) are shown in Figs. 1-4. The far-uv CD of all crystallins are similar, but not identical[19,31,32]; all show a minimum around 216 nm (Fig. 3, inset), which is characteristic of beta-sheet conformation. Further information on the secondary structure was obtained from curve-fitting methods[37-39] of CD spectra and X-ray[15] analysis (Table 1). The near-uv CD of the crystallins are *not* similar: intensity, peak, and shoulder positions vary. γ-Crystallins, in addition, show intense rotational strength around 235 nm; among γ-crystallins distinct differences exist in the 225-250 and 280-320 nm regions (Fig. 1). Vibrational progressions of phenylalanine (Phe) are prominent in α-; thus, the CD between 250-280 nm is more structured than that of β- and γ-. Based on absorption, pH difference absorption, and pH difference CD spectra[19,32], we have assigned the near-uv CD bands of all crystallins (Table 2).

The quantum yield and emission maxima for native and denatured crystallins are given in Table 3. In the native form, emission maxima (excited at 280-295 nm) of all crystallins were shifted to a wavelength shorter than that of free Trp, which emits at 350 nm. γ-II showed a maximum blue

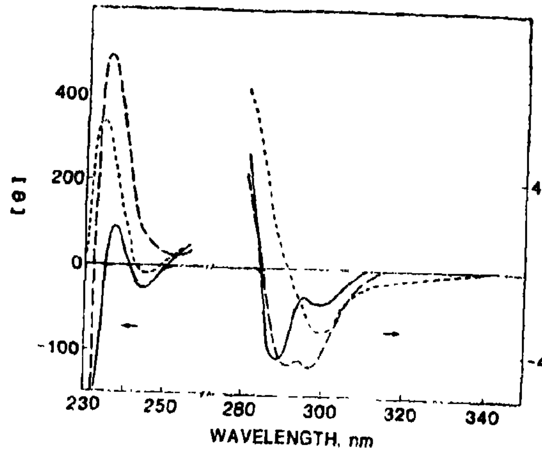


Fig. 1. Near-uv CD spectra of γ-crystallin in 20 m*M* phosphate buffer (pH 7.0): (—) γ-II, (— —) γ-III and (- - -) γ-IV.

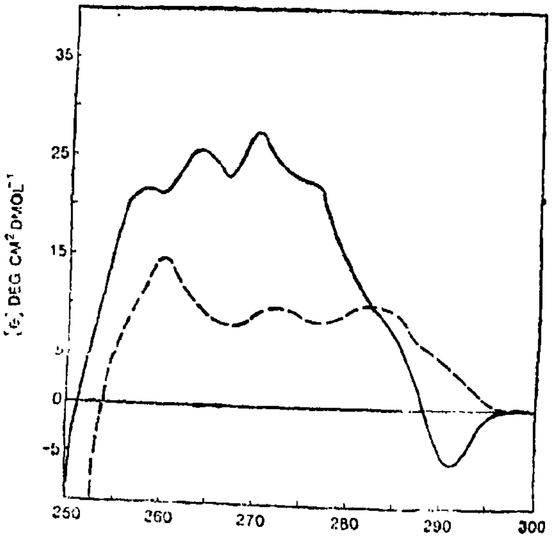


Fig. 2. Near-uv CD spectra of α-crystallin: (—) control and (- - -) irradiated in daylight at 37° for 1.5 h. Reaction mixture for photolysis contains 2.4 mg ml^{-1} of protein and 10^{-5} *M* MB in 0.1 *M* phosphate buffer (pH 7.4).

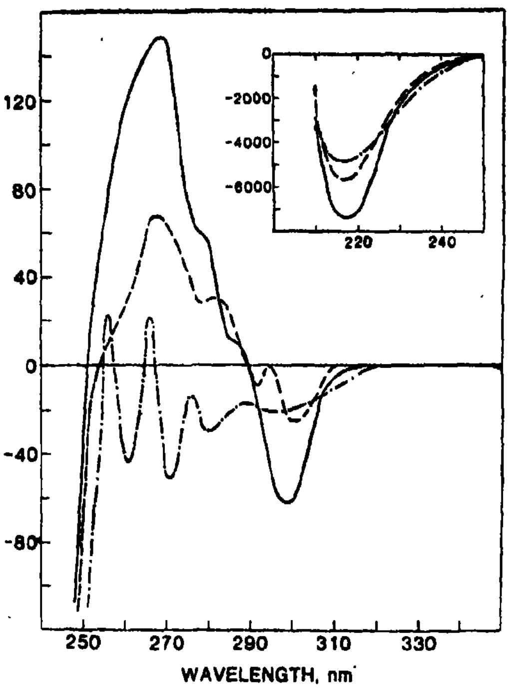


Fig. 3. Near-uv and far-uv (inset) CD spectra of β-crystallin : (—) control ; irradiated at 37° in daylight for (– – –) 1.5 and (· .—) 6 h. Reaction mixture for photolysis contains 1 mg ml^{-1} of protein and 10^{-5} *M* MB in 0.1 *M* phosphate buffer (pH 7.4).

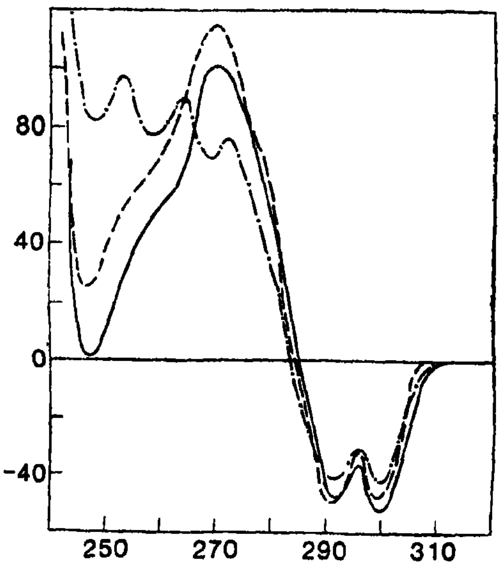


Fig. 4. Near-uv CD spectra of γ-crystallin : (—) control, (– – –) control labeled with iodoacetamide and (–. –) iodoacetamide-labeled control irradiated for 0.5 h. Experimental conditions same as in Fig. 3.

shift to 324 nm, and α-crystallin showed the least shift, to 336 nm. In the presence of a protein denaturant, 6 *M* guanidine hydrochloride or 8 *M*

TABLE 1—SECONDARY STRUCTURE ESTIMATES FROM FAR-UV CD SPECTRA (200-240 nm) OF LENS PROTEINS†

Curve-fitting method or other	Protein (crystallin)	Percentage α-helix	β-sheet	Random coil	β-turn
Brahms and Brahms[a]	α	0	45	37	18
	β_H	0	51	42	7
	β_L	8	48	40	4
	γ-II	0	61	28	11
	γ-III	0	58	29	13
	γ-IV	0	52	31	17
Hennessey and Johnson[b]	α	3	53	28	16
	β_H	0	60	22	18
	β_L	7	70	19	4
	γ-II	5	56	24	15
	γ-III	5	46	31	18
	γ-IV	5	45	30	20
X-ray crystallography[c]	γ-II	25*	49	←—26—→ (undefined)	

† Compiled from Refs. 16, 21, and 22 and from unpublished data.

* These are not true alpha-helix, as all are distorted and short. Calculation is strictly on the basis of ϕ/Ψ bond angles.

[a] Refs. 37 and 38. [b] Ref. 39. [c] Ref. 16.

urea, the emission maxima shift to longer wavelengths. A shoulder around 305 nm (not shown) due to tyrosine (Tyr) emission can be seen in some crystallins when they are denatured[16].

In the MB-sensitised reactions, the near-uv CD spectra of all crystallins change (Figs. 2-4). In the far-uv CD, the CD minimum at 216 nm for both α-[34] and β- remain unaltered even after 6 h of irradiation ; however, the decrease in intensity (Fig. 3, inset) indicates a slight decrease in the beta-sheet content. Although the photodynamic actions on α-crystallin have been studied in detail by using 300 nm radiation[32] and in the presence of MB[33,34] or riboflavin[35] (RF), for comparison we have shown a near-uv spectrum of α-crystallin after 1.5 h irradiation. Between α- and β-, there are distinct differences in the near-uv spectra of 1.5 h irradiated samples ; for example, for α- the 0-0 ^1L_a Trp band at 295 nm disappears, but for β- the band exists even after 6 h of irradiation. It appears that for α-, both ^1L_a and ^1L_b Trp band are equally affected, whereas for β- the ^1L_a Trp band changes significantly. After 6h of irradiation, predominantly the Phe vibrational structure is visible for α-[34], whereas the spectrum of β-tends to become negative. In addition, 0-0 ^1L_b Tyr, 0+850 cm^{-1} Tyr, ^1L_b Trp, and vibronic Phe are still identifiable for β-.

Both α- and β-crystallin solutions remained clear over a long period of irradiation. However, γ-solution became turbid during irradiation, the onset of turbidity depending upon the protein concentration. Assuming that the turbidity arises from the disulphide crosslinks, SH groups of β-crystallin were labeled with iodoacetamide[40]. Upon irradiation of such a sample (0.06 mg ml^{-1}), no turbidity was observed even on 6 h irradiation, whereas the unlabelled protein became turbid in 2 h. However,

TABLE 2—ASSIGNMENTS OF NEAR-UV CD BANDS

α	β_H	β_L	γ-II	γ-III	γ-IV
−294 (0−0 ^1L_b Trp)*	−297 (0−0 ^1L_b Trp)	−295 (0−0 ^1L_b Trp)	−299 (0−0 ^1L_b Trp)	−298 (0−0 ^1L_b Trp)	−300 (0−0 ^1L_b Trp)
−286 (0+~950 cm^{-1} ^1L_b Trp)	+286 (superimposed 0+~950 cm^{-1} ^1L_b Trp and ^1L_b Tyr)	+283 (superimposed 0+~950 cm^{-1} ^1L_b Trp and ^1L_b Tyr)	−288 (superimposed 0+~950 cm^{-1}+ 0−0 ^1L_b Tyr negative)	−289 (superimposed 0+950 cm^{-1}+ 0−0 ^1L_b Tyr negative)	+288 (0−0 ^1L_b Tyr positive)
+281 (0−0 ^1L_b Tyr)	—	—	—	—	—
+272 (0+~800 cm^{-1} ^1L_b Tyr)	+276 (0+~800 cm^{-1} ^1L_b Tyr)	+275 (0+~800 cm^{-1} ^1L_b Tyr)	+270 (0+800 cm^{-1} ^1L_b Tyr)	+270 (0+800 cm^{-1} ^1L_b Tyr)	+275 (0+~800 cm^{-1} ^1L_b Tyr)
+266 (superimposed ^1L_a Trp+Phe)**	+267 (superimposed ^1L_a Trp+Phe)	+265 (superimposed ^1L_a Trp+Phe)	+250 to 266 region (superimposed ^1L_a Trp+Phe)	+250 to 266 region (superimposed ^1L_a Trp+Phe)	+250 to 266 region (superimposed ^1L_a Trp+Phe)
+258 (superimposed Phe+^1L_a Trp)	+261 (superimposed ^1L_a Trp+Phe)	+254 (superimposed ^1L_a Trp+Phe)	−245 and +235 (exciton bands of ^1L_a Tyr)	+235 (exciton bands of ^1L_a Tyr)	+235 and −245 (exciton bands of ^1L_a Tyr)
+255 (superimposed Phe+^1L_a Trp)	+253 (superimposed ^1L_a Trp+Phe)	—	—	—	—

Based on absorption, and difference (pH 6-11.5) CD and absorption spectra ; for details Refs. 19 and 22 may be seen.
* −294 indicates negative CD band (or shoulder) at 294 nm ; band assignments are given in the parenthesis.
** ^1L_a Trp is actually a broad structureless band located at the 250 to 280 nm region.

TABLE 3—FLUORESCENCE PARAMETERS OF LENS CRYSTALLINS†

Crystallin	Native		Denatured in guanidine hydrochloride	
	λ_{max}	φ Trp*	λ_{max}**	φ Trp
α	336	0.180	350 (350)	0.118
β_H	334	0.102	350 (350)	0.128
β_L	334	0.106	350 (350)	0.121
γ-II	324	0.065	344 (336)	(mixtures
γ-III	329	0.105	350 (336)	of the
γ-IV	334	0.121	350 (336)	three, 0.142)

† Compiled from Refs. 19 and 22.
* Quantum yields, φ, were obtained by excitation at 295 nm.
** Values in parentheses, in urea.

a concentrated solution (1 mg ml^{-1}) of the labeled protein became turbid upon irradiation for 1 h or less, indicating that non-disulphide aggregation is also involved. For CD measurements, we used 1 mg ml^{-1} of this protein solution and irradiated for 0.5 h. Even though no appreciable turbidity was observed, the solution was filtered through a 0.22 μm Millipore filter prior to measurement.

Labeling with iodoacetamide does not alter the near-uv CD of γ-crystallin significantly, but labeled γ-, upon MB-sensitised irradiation for 0.5 h, shows a change (Fig. 5) that is similar to that of α-crystallin[24] irradiated for the same time. An increase in the 250 nm band with distinct vibrational peaks of Phe is seen. This has been attributed to a sign reversal of Phe transitions from negative to positive by the generated $^1O_2$ and the sensitiser[24] ; in the normal near-uv CD of all crystallins we assigned the dichroic bands of Phe as negative[19]. In the case of β-, however, Phe bands still remain negative after 6 h of irradiation.

Fig. 5 shows a red shift (4-5 nm) of Trp emission of β-crystallin after sensitised irradiation.

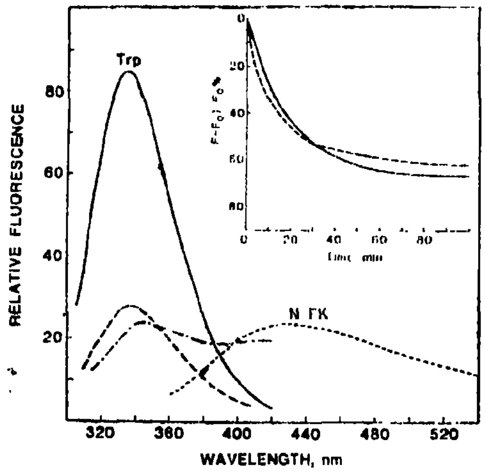


Fig. 5. Trp fluorescence (λ_{ex} 295 nm) of a reaction mixture same as in Fig. 3 : (—) control ; (— —) irradiated for 1.5 h and (—.--) irradiated for 6 h. Irradiation conditions same as in Fig. 3. Intensity scale for 6 h is 10 times that of the control. (- - -) Non-Trp (N-FK type) fluorescence (λ_{ex} 320 nm) after 6 h of irradiation with sensitivity scale 10 times that of control for Trp fluorescence. (Inset) Time course in percent loss of Trp fluorescence : (—) β-crystallin (1 mg ml^{-1}) and (- - -) γ-crystallin (0.06 mg ml^{-1}). Experimental conditions same as in Fig. 3.

The inset shows the kinetics of Trp photooxidation for β- and γ-. However, no significant shift (as was observed[24] for α-crystallin) in the steady-state emission in MIANS (6-[4'-maleimidylanilino]naphthalene-2-sulphonic acid)-labeled β-crystallin was observed, presumably because thiol groups of β- are already in a polar environment[20].

Discussion

Our studies of lens proteins have two objectives, (i) to elucidate the structural features of the individual crystallins that endow them with stability and the interactions between them that give rise to a highly ordered, transparent structure, and (ii) to understand the cause and mechanism by which these proteins aggregate and the lens loses transparency during cataractogenesis.

Although three-dimensional structural analyses have suggested that all the γ-crystallins, and possibly β-, have the same highly symmetrical, two-domain, antiparallel, beta-sheet backbone structure as described for γ-II[14-17], considerable differences have been noted in the spectral properties of α-, β- and γ- crystallins, and also of γ-II, γ-III and γ-IV[19-22].

The assessments from curve-fitting methods of far-uv CD spectra support the notion that all crystallins have very similar secondary structures, namely, 50% or more beta-sheet (presumably all antiparallel) and little or no alpha-helix. Yet subtle differences exist in the shape of the far-uv CD spectra[21,22].

The tertiary structure of a protein in solution can be conveniently assessed from its near-uv CD and fluorescence spectra, provided the protein contains aromatic acid residues, particularly Trp and Tyr. Lens proteins are generally rich in such residues, and thus their tertiary structures may be important with respect to stability[41]. The theoretical aspects of the near-uv CD and its relevance to a protein's tertiary structure have been extensively reviewed[42]. The aromatic rings of Phe, Tyr, and Trp gain their near-uv CD through interactions with each other or even with the peptide backbone. The mechanisms of interaction by which an unsymmetric environment (of aromatic residues) may induce CD bands are either one electron, or μ-m, and/or μ-μ coupling. The position, intensity, and sign of the near-uv CD bands are not only dependent on these interaction parameters but are also strongly influenced by the microenvironment of the aromatic side chains, *e.g.* hydrogen bonding, polar or charged groups, and polarisability. Most importantly, some aromatic side chains may be on the surface and exposed mainly to water but still have contact with other moieties. Buried chains may exist in a variety of environments ranging from non-polar (hydrophobic) to polar (hydrophilic). Both near-uv CD and fluorescence spectroscopy can provide information on the microenvironments of the aromatic residues, and the two techniques have been combined to detail the tertiary structure of lens crystallins in solution[19-24].

In contrast to secondary structure, the tertiary structures of lens crystallins differ considerably, as manifested in their near-uv CDs (Figs. 1-4) and fluorescence properties (Table 3). This is mostly due to the fact that the microenvironments of Trp, Tyr, and Cys residues are not the same in each crystallin[20,22]. For example, Trp residues in γ-crystallins are buried in the hydrophobic interior of the protein, and α- and β-crystallins they are presumably in more polar evironments; from emission maxima and quantum yield values it has been suggested that the hydrophobicity of Trp environments decreases in the order, γ-II > γ-III > γ-IV > β > α. The order is more or less reversed[20] in the case of Cys residues as is evident from the fluorescent parameters of MIANS-labeled SH groups of Cys. Differences in the microenvironments of these residues indicate that their spatial arragements, reactivities, or accessibilities to reactants are not similar.

The remarkable differences in the tertiary structures of lens crystallins may well account for the low-temperature aggregation[43] of γ-crystallin, loss of solubility of α-crystallin with aging[1,9], and ease of disulphide formation in β-crystallin[1]. Although lens crystallins have very symmetrical structures that may confer stability in the normal healthy lens, any change, metabolic or environmental (light), could disrupt the arrangements of these reactive groups (Trp, Tyr, or Cys) and alter their interaction properties, leading to loss of transparency[10].

We have previously shown[23] that irradiation of α-crystallin by 300 nm light causes cosiderable photooxidation of Trp residues with the formation of N-formylkynurenine (N-FK)-type products. Since N-FK is an effective sensitiser[44], the observed conformational change is essentially a sensitiser-induced process. α-Crystallin also undergoes a major conformational change in a dye-sensitised (MB or RF) reaction[24,25]. In general, a photosensitiser in the presence of an oxidisable substrate (*e.g.* amino acid or protein) follows two major pathways[45] upon excitation, as illustrated below.

$$\text{Sens} \xrightarrow{h\nu} {}^1\text{Sens} \xrightarrow[\text{crossing}]{\text{inter-system}} {}^3\text{Sens}$$

Type I :

$${}^3\text{Sens} \xrightarrow{\text{substrate}} \text{Radicals} \xrightarrow{O_2,\ H_2O}$$

(by H atom or electron transfer)

$$\text{Active species of oxygen (eg. } O_2^{-\cdot},\ {}^{\cdot}OH,\ H_2O_2) \xrightarrow{\text{substrate}} \text{Oxygenated products}$$

Type II :

$${}^3\text{Sens} \xrightarrow[\text{energy transfer}]{O_2} {}^1O_2 \xrightarrow{\text{substrate}} \text{Oxygenated products}$$

Using inhibitors specific for the active species of oxygen, it has been shown[24] that, in the MB-sensitised reaction, singlet oxygen $^1O_2$ (type II) and

sensitiser itself play a major role in the conformational change of α-crystallin. In contrast, the RF-[35] or N-FK[33,34]-sensitised reaction, a type II process, is less significant, and in the case of N-FK, conformational change is not as drastic as with MB or RF.

The secondary structure of β- following photosensitisation remains virtually unaltered as manifested in the far-uv CD whereas the near-uv CD (tertiary structure) and fluorescence change drastically. A red shift in the Trp emission indicates that some residues that were buried in the non-polar regions of the protein are now exposed. This is supported by the fact that the rate of Trp photooxidation is significantly faster in the MB-sensitised reaction (Fig. 5, inset) than upon irradiation by 300 nm light[33].

γ-Crystallin behaves very differently from β- and α- in that the protein solution becomes turbid upon irradiation for 1 h in the presence of MB. Since we observe a significant change in the near-uv CD of γ-crystallin irradiated for 0.5 h (Fig. 4), the turbidity is very likely preceded by conformational change.

In this study, we have demonstrated that MB-sensitised photooxidation reaction causes a change in tertiary structure of lens crystallins but in each case subtle differences exist in the nature of the changes. In a sensitised reaction, only Cys, methionine, histidine, Trp, and Tyr reridues of a protein are vulnerable to photooxidation[45]. The ease and extent of oxidation of these residues are dependent on their sequence, spatial orientation and micro-enviornments, and these in turn reflect the tertiary structure of the protein. Thus, it is the difference in tertiary structure observed among the crystallins[16,20] that is responsible for the variations in the nature of the photoinduced conformational changes.

There is enough evidence to indicate that disruption in the protein structure can be caused by a photosensitised reaction that could eventually lead to cataract formation. However, normal lens contains inhibitors—superoxide dismutase, ascorbate, catalase, and glutathione—that scavenge the superoxide anion (O_2^-.), ·OH, H_2O_2, and quench $^1O_2$ and triplet sensitiser. Lack of these protective mechanisms will favour photoinduced changes in the protein structure, particularly when the sensitisers riboflavin (vitamin B) and N-FK have been identified in the lens[28].

Acknowledgement

The work was supported by U.S. National Institutes of Health grants R0 1 EY04161 and T32 EY07074. The authors are grateful to Ms. Marie Messmer who provided skilled technical help.

References

1. J. J. Harding and K. J. Dilley, *Exp. Eye Res.*, 1976, **22**, 1.
2. H. Bloemendal and P. Herbrink, *Ophthalmic Res.*, 1974, **6**, 81.
3. I. Björk, *Exp. Eye Res.*, 1964, **3**, 254.
4. W. W. De Jong in "Molecular and Cellular Biology of the Eye Lens", ed. H. Bloemendal, Wiley, New York, 1981, p. 221.
5. G. B. Benedek, *Appl. Opt.*, 1971, **10**, 459.
6. M. Delaye and A. Tardieu, *Nature* (*London*), 1983, **302**, 415.
7. J. A. Jedziniak, J. H. Kinoshita, E. M. Yates and G. B. Benedek, *Exp. Eye Res.*, 1975, **20**, 367.
8. D. Roy and A. Spector, *Proc. Natl. Acad. Sci. USA*, 1976, **73**, 3484.
9. H. J. Hoenders and H. Bloemendal in "Molecular and Cellular Biology of the Eye Lens", ed. H. Bloemendal, Wiley, New York, 1981, p. 279.
10. J. J. Harding in "Molecular and Cellular Biology of the Eye Lens", ed. H. Bloemendal, Wiley, New York, 1981, p. 327.
11. R. C. Augusteyn, *Ophthalmic Res.*, 1975, **7**, 217.
12. Z. Dische and H. Zil, *Am. J. Ophthalmol.*, 1951, **34**, 104.
13. L. Croft, *Biochem. J.*, 1972, **128**, 961.
14. H. P. C. Driessen, P. Herbrink, H. Bloemendal and W. W. De Jong, *Eur. J. Biochem.*, 1981, **121**, 83.
15. G. Wistow, B. Turnell, L. Summers, C. Slingsby, D. Moss, L. Miller, P. Lindley and T. Blundell, *J. Mol. Biol.*, 1983, **170**, 175.
16. T. Blundell, P. Lindley, L. Miller, D. Moss, C. Slingsby, I. Tickle, B. Turnell and G. Wistow, *Nature* (*London*), 1981, **289**, 771.
17. L. Summers, G. Wistow, M. Narebor, D. Moss, P. Lindley, C. Slingsby, T. Blundell, H. Bartunik and K. Bartels in "Peptide and Protein Reviews", ed. M. T. W. Hearn, 1984, Vol. 3, p. 147.
18. Y. N. Chirgadze, Y. V. Sergeev, N. P. Fomenkova and V. D. Oreshin, *FEBS Lett.*, 1981, **131**, 81.
19. J. N. Liang and B. Chakrabarti, *Biochemistry*, 1982, **21**, 1847.
20. U. P. Andley, J. N. Liang and B. Chakrabarti, *Biochemistry*, 1982, **21**, 1853.
21. R. J. Siezen and P. Argos, *Biochim. Biophys. Acta*, 1983, **748**, 56.
22. K. Mandal, S. K. Bose, B. Chakrabarti and R. J. Siezen, *Biochim. Biophys. Acta*, 1985, **832**, 156.
23. J. Liang and B. Chakrabarti, *Biochem. Biophys. Res. Commun.*, 1981, **102**, 180.
24. J. N. Liang, S. K. Bose and B. Chakrabarti, *Exp. Eye Res.*, 1985, **40**, 461.
25. A. Pirie, *Biochem J.*, 1971, **125**, 203.
26. S. Zigman, *Photochem. Photobiol.*, 1977, **26**, 437.
27. S. Lerman and R. Borkman, *Acta Ophthalmol.*, 1978, **56**, 139.
28. J. D. Goosey, J. S. Zigler, Jr. and J. H. Kinoshita, *Science*, 1980, **208**, 1278.
29. S. Lerman, "Radiant Energy and the Eye", Macmillan, New York, 1980, p. 146.
30. J. S. Zigler, Jr. and J. D. Goosey, *Photochem. Photobiol.*, 1981, **33**, 869.
31. J. Dillon, *Curr. Eye Res.*, 1984, **3**, 145.
32. U. P. Andley, P. Sutherland, J. N. Liang and B. Chakrabarti, *Photochem. Photobiol.*, 1984, **40**, 343.
33. S. K. Bose, K. Mandal and B. Chakrabarti, *Biochem. Biophys. Res. Commun.*, 1985, **128**, 1322.
34. K. Mandal, S. K. Bose and B. Chakrabarti, *Photochem. Photobiol.*, 1986, in the press.
35. S. K. Bose, K. Mandal and B. Chakrabarti, *Photochem. Photobiol.*, 1986, in the press.
36. O. L. Lowry, N. J. Rosenbrough, A. L. Farr and R. J. Randall, *J. Biol. Chem.*, 1951, **193**, 265.
37. S. Brahms and J. G. Brahms, *J. Chim. Phys.*, 1979, **76**, 841.
38. S. Brahms and J. G. Brahms, *J. Mol. Biol.*, 1980, **138**, 149.

39. J. P. HENNESSEY, JR. and W. C. JOHNSON, JR., *Biochemistry*, 1981, **20**, 1085.

40. R. J. SIEZEN, F. G. M. COENDERS and H. J. HOENDERS, *Biochim. Biophys. Acta*, 1978, **537**, 456.

41. S. K. BURLEY and G. A. PETSKO, *Science*, 1985, **229**, 23.

42. E. H. STRICKLAND, *CRC Crit. Rev. Biochem.*, 1974, **2**, 113.

43. R. J. SIEZEN, M. R. FISCH, C. SLINGSBY and G. B. BENEDEK, *Proc. Natl. Acad. Sci. USA*, 1985, **82**, 1701.

44. P. WALRANT and R. SANTUS, *Photochem. Photobiol.*, 1974, **20**, 455.

45. C. S. FOOTE, *Acc. Chem. Res.*, 1968, **1**, 104.

J. Indian Chem. Soc.,
Vol. LXIII, January 1986, pp. 138-143

Characterisation of the Tal Fruit (*Borassus flabellifer*) Polysaccharide. Its Induction of Metachromasia and Circular Dichroism with Pinacyanol†

ASHOKE KUMAR BHATTACHARYYA and MEDINI KANTA PAL*

Department of Biochemistry and Biophysics, Kalyani University, Kalyani-741 235

and

AMALENDU DAS

Department of Chemistry, Jadavpur University, Calcutta-700 032

Aqueous extract of the mesocarp of ripe palmyra palm (*Borassus flabellifer*, local name ; *Tal* fruit) furnished a polysaccharide material (BF-A) which on saponification gave polysaccharide material (BF-B) containing GalA (53), Glc (25) Gal (3.16), Ara (2.66), Xyl (2.24), and Rha (1.5%). The results of pectinase treatment and periodate oxidation indicate that BF-B is essentially a polygalacturonan strongly associated with a glucan which is different from starch. The unsaponified BF-A has an equivalent weight (average weight containing one anionic group) of 825 (as K-salt) and does not induce metachromatic spectral shift of toluidine blue (TB). The corresponding saponified product BF-B has an equivalent weight of 338 (as K-salt), and induces metachromatic spectral shift of the dyes TB and pinacyanol chloride (PCYN), thereby indicating that many of the carboxylic groups in BF-A are esterified. The stoichiometry of the compound of BF-B and TB shows that TB binds surprisingly to alternate carboxyl groups of BF-B, the other carboxyl groups of the polygalacturonan chain appear to be masked in being associated with the glucan portion. From the strong CD (in the visible region) of the compound of the dye PCYN and BF-B, it is postulated that the polygalacturonan portion of BF-B has an extended helical structure encasing or associating the glucan component.

BORASSUS flabellifer is one of the four species of the family *palmae* and belongs to the genus *Borassus*. It is a native of tropical Africa and is found in India, Burma and Ceylone.

The black trunk of the plam tree attains a height of 12-18 m (even more) and girth of 1-2 m. It bears terminal crown of large fan like leaves 1-1.5 m in width. The spathes begin to appear in November-December. Male and female flowers are borne on different trees. The fruits, when ripe, are large having brownish black skin and weigh 1-2.5 kg a piece. Just below the thin skin, the body of the ripe fruit is covered with fibres which hold a soft yellow edible viscous mass (mesocarp) encasing 1-3 hard seeds or nuts[1]. The fruit has several medicinal uses[2]. The green fruits have large tender nuts which contain a colourless soft sweet and essentially carbohydrate material that is much relished in the summer. A galactomannan[3] and a mannan[4] have been characterised from this source.

In this communication, we report the average carbohydrate composition, polyelectrolytic and chromotropic properties of the saponified polysaccharide material obtained by water extraction of the yellow pulp.

Experimental

Descending paper chromatography (pc) was performed on Whatman No. 1 MM papers using the solvent systems (v/v) : (A) ethyl acetate-pyridine-water (8 : 2 : 1), (B) 1-butanol-ethanol-water (4 : 1 : 1) and (C) 1-butanol-acetic acid-water (3 : 1 : 1). Staining reagents were (*a*) alkaline silver nitrate and (*b*) benzidine-periodate.

Hexuronic acids were estimated by the carbazole method[5] and neutral sugars by the phenol sulphuric acid method[6]. Absorbances were measured with a Beckman DB spectrophotometer ; metachromatic spectra were read with a Toshniwal CL 10-A_2 vis-spectrophotometer or Cary 17D spectrophotometer. Circular dichroism (CD) were recorded with a JASCO J-500C spectropolarimeter using 1.00 cm circular cuvettes. Conductimetric titrations were carried out with a Toshniwal CLO 1.02 A conductivity bridge. All evaporations were carried out below 40° under reduced pressure.

Glc was performed with a glass column (6 mm × 1.83 m) containing 3% of ECNSS-M on Gas Chrom Q(100-120 mesh) at 190° for alditol acetates of neutral sugars using the same instrument as reported[7]. Pectinase (polygalacturonase ; poly-

† Dedicated to Professor Sadhan Basu on the occasion of his 65th birthday.

α-1,4-galacturonide glycuronohydrolase ; E.C.No. 3.2.1.15 ; from *Aspergillus niger*, Sigma) was used in this investigation. Ir spectrum was taken as KBr pellets using a Perkin-Elmer 297 instrument. Specific rotation values were recorded with a Jasco DIP-181 digital polarimeter.

Isolation of the Tal polysaccharide (BFA) : The outer skin of the Tal fruit (2 kg) was carefully removed and the edible gummy yellow pulp (the mesocarp) was extracted by pressed-sieving. It (750 g) was suspended in a double-walled nylon-cloth bag. A yellowish viscous juice (100 ml) gradually oozed out and collected in a container below. It was diluted with water (100 ml) and filtered under suction. To the filtrate KOAc (7 g) was added. From the resulting solution the polysaccharide material was precipitated by gradual addition of ethanol. The first turbidity (a gray precipitate) appearing on addition of ethanol (125 ml) was centrifuged (7000 r.p.m., 45 min, 25°) out. To the supernatant liquor more ethanol (275 ml) was added and the mixture allowed to stand overnight. The precipitate (BF-A, 3.1 g, yellowish) was collected by centrifugation and dried by solvent (ethanol, acetone) exchange.

Saponification of BF-A : BF-A (2.6 g) dissolved in KOH (0.1 *M*) was flushed with nitrogen and left overnight under nitrogen at room temperature (25°). The solution was centrifuged and the supernatant liquor neutralised (*p*H ~8) with cold AcOH and dialysed (24 h) against water. The bag content was centrifuged (7000 r.p.m., 30 min, 25°) and a small precipitate appearing was rejected. To the supernatant liquor, KOAc (7 g) was added and the polysaccharide precipitated by gradual addition of ethanol (2.5 vol). The precipitate (BF-B ; 1.5 g, yellowish) was collected in the usual way.

Identification of the monosaccharide components of BF-B : BF-B (12.92 mg) was hydrolysed with sulphuric acid (0.5 *M*, 4 ml) in a sealed tube at 100° for 16 h. The hydrolysate was neutralised with prewashed $BaCO_3$, centrifuged and filtered. The filtrate was decationised (Dowex-50, H^+) and concentrated to syrup. Pc of the syrup (solvents A, B and C, staining reagent *a*) gave two prominent spots corresponding to Glc and GalA. There were trace amounts of Gal, Ara, Xyl and Rha.

Another weight of BF-B (4.58 mg) was mixed with myo-inositol (1032 μg) and hydrolysed with sulphuric acid (0.5 *M*, 3 ml) as described earlier. The hydrolysate was neutralised ($BaCO_3$), decationised (Dowex-50, H^+) and Dowex-1 (formate) and the neutral monosaccharides were converted[8] into the alditol acetate mixture. The glc of the product furnished Glc, Gal, Xyl, Ara and Rha in the molar ratios of ~15 : 2 : 2 : 2 : 1.

Enzymic hydrolysis of BF-B : To a solution of BF-B (18.95 mg) in NaOAc buffer (5 ml, *p*H 4.0), pectinase (2.93 mg) was added and incubated at 33.5° under a drop of toluene for 16 h. The reaction mixture was then heated to 100° for 20 min, cooled, centrifuged and filtered. The filtrate was decationised (Dowex-50, H^+) and the solution was concentrated (~2 ml) and examined by pc (solvent A, stain *a*). This furnished a single spot corresponding to GalA.

The above solution was passed through a Dowex-1 (formate) column (1×30 cm) and the mixture of neutral monosaccharides (monitored by Molisch[9] test) was eluted with water (200 ml). It was concentrated to syrup and subjected to pc (solvent A, stains *a* and *b*). It revealed the presence of Gal, Ara, Xyl and Rha ; along with, there were some carbohydrate materials staying at the base line. The syrup was diluted (~2 ml) and extensively dialysed. The bag content was concentrated and the polysaccharide (~1.2 mg) precipitated with ethanol (2 vol). The precipitate (0.8 mg) was hydrolysed (0.5 *M* H_2SO_4, 1 ml, 100°, 16 h), and the hydrolysate after neutralisation and usual work up was examined by pc. It furnished a single spot corresponding to Glc.

The uronic acid portion retained by the Dowex-1 (formate) column was eluted with formic acid (0.3 *M*, 60 ml) and the effluent evaporated to dryness. Pc of the residue (~4 mg) gave a single spot corresponding to 'GalA'. The residue was dried over P_2O_5, and the acid converted[10] into methyl ester methyl glycoside by refluxing with dry methanolic HCl (1%, 5 ml, 10 h). The solvent was evaporated and the residue treated with Dowex-1 (formate) resin in cold water and filtered. The filtrate was concentrated (~2 ml) by lyophilisation. To it KBH_4 (50 mg) was added and left for 20 h at 10°. The excess of KBH_4 was decomposed with Dowex-50 (H^+) resin and filtered. The filtrate was evaporated to dryness and boric acid was removed as methyl borate. The residue was hydrolysed with sulphuric acid (0.5 *M*, 3 ml, 100°, 16 h). The hydrolysate was neutralised ($BaCO_3$), centrifuged, filtered and the filtrate decationised (Dowex-50, H^+) and lyophilised. The residue was converted into the alditol acetate and subjected to glc when only one peak corresponding to Gal was obtained.

Oxidation of BF-B with periodic acid : Solutions of BF-B (21.7 mg) in water (10 ml) and periodic acid (0.1 *M*, 10 ml) were separately cooled (4°) and mixed together. The mixture was kept in the dark under stirring condition. Aliquotes (0.1 ml) were taken out at intervals and titrated for formic acid with standard NaOH (0.01 *M*) using methyl red indicator. In 72 h, the liberation of formic acid became constant. The reaction mixture was then treated with $Ba(OH)_2$ (0.1 *M*) and the precipitate was removed by centrifugation. Excess $Ba(OH)_2$ was precipitated by bubbling CO_2 and the precipitate centrifuged out. The resulting solution was concentrated (2 ml) and a small amount of precipitate appearing at this stage was filtered off. The filtrate was reduced with KBH_4 (~50 mg) for overnight at room temperature. Excess borohydride was decomposed by acidifying (cold AcOH,

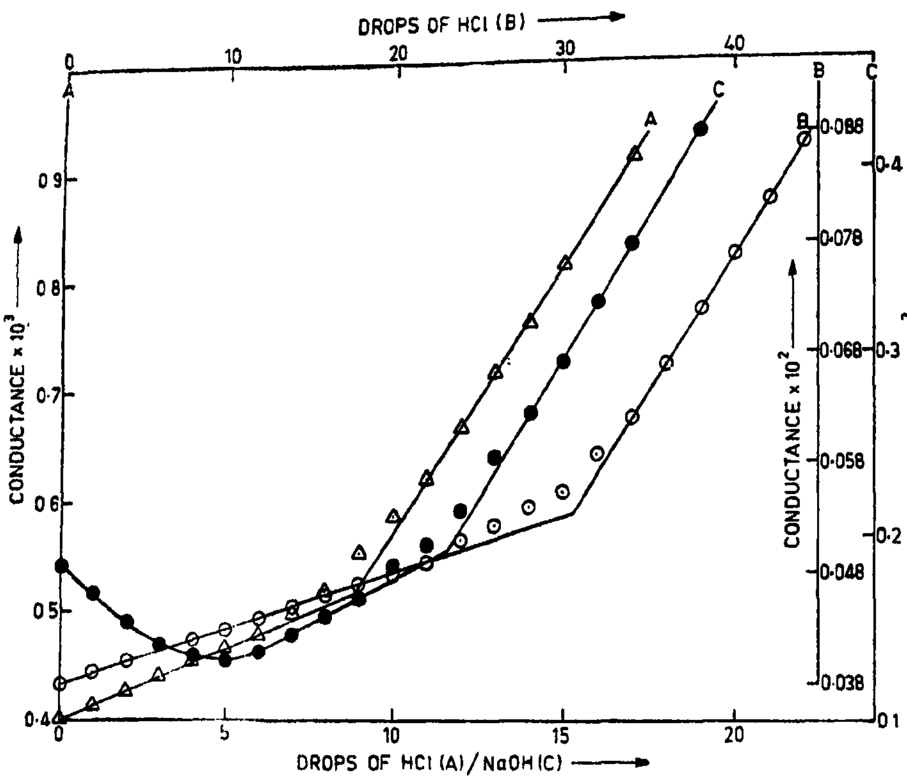


Fig. 1. Conductimetric titration of (A) BF-A (26.3 mg) by 0.084 *N* HCl, (B) BF-B (36.9 mg) by 0.084 *N* HCl and (C) BF-B (17.0 mg) in the acid form by 0.103 *N* NaOH.

4 *N*) to *p*H ~5 and boric acid was removed as methyl borate. The resulting solution was decationised (Dowex-50, H^+), concentrated (1 ml) and examined by pc (solvent A, staining reagents *a* and *b*). In both the cases there was an immobile white patch at the base line and a spot corresponding to GalA.

The reaction mixture was slowly passed through a Dowex-1 (formate) column (1×15 cm). The column was washed with water and the effluent concentrated. Pc (solvent A, stains *a* and *b*) indicated the same white patch at the base line and there was no monosaccharide spot. The solution was evaporated and a part of the solid (~2.8 mg) was hydrolysed with H_2SO_4 as described earlier. The hydrolysate was worked up in the usual way and examined by pc (solvents A and B, stain *a*) when a single spot corresponding to Glc was obtained. The Dowex-1 (formate) column was then eluted with formic acid (0.3 *M*, 10 ml) and the effluent evaporated. The residue was hydrolysed with trifluoroacetic acid (1 ml, 50% solution) for 12 h at 100°. The acid was evaporated and the residue examined by pc (solvent A, stain *a*), which revealed the presence of GalA, glycerol and threic acid. There was no Glc spot.

Equivalent weight of BF-A and BF-B : Equivalent weight (average weight containing one anionic group) of BF-A (26.3 mg) was determined by direct conductimetric titration of its solution with standard HCl (0.084 *N*) and found to be 827. A similar titration of BF-B (36.9 mg) gave an equivalent weight 338. Equivalent weight of BF-B was also determined by converting it (17.0 mg) to the acid form by treatment with Dowex-50 (H^+) followed by conductimetric titration[11] against standard NaOH (0.103 *N*) and found to be 335 (Fig. 1).

Stoichiometry of the compound formed between toluidine Blue (T.B) and BF-B : Portions (10 ml) of $1.64\times10^{-4}M$ TB in $1.00\times10^{-3}M$ NaCl containing different amounts of BF-B in a series of stoppered test tubes were shaken with petroleum ether (b.p. 60-80°) (2 ml). The compound between TB and BF-B was thus removed from the aqueous phase[12,13]. The excess dye remaining in the aqueous phase in each case was estimated from Beer's law and the dye removed as compound with BF-B was calculated by difference. From the plot of μ-mol of dye removed *vs* μ-mol of BF-B added, the stoichiometry of TB—BF-B came to be 1 : 2.

Results and Discussion

The polysaccharide material present in the juice of ripe Tal fruit was isolated by precipitation with ethanol in presence of KOAc. The product BF-A being considerably esterified as evidenced[14] by ν_{max} at 1 735 and 1 260 cm^{-1}, was saponified with

KOH into a polyanion of higher charge density (hence low equivalent weight); the saponified product BF-B, as well as the unsaponified product BF-A were isolated as their potassium salts. Conductimetric titration results (Fig. 1) gave equivalent weights (average weight containing one anionic group) 825 ± 3 and 338 ± 3, respectively for BF-A and BF-B. Hydrolysis of BF-B furnished mainly GalA (53%) and Glc (25%) along with minor components, like Gal (3.16%), Ara (2.66%), Xyl (2.24%) and Rha (1.53%). This composition suggested that BF-B (or the original product BF-A) was likely to be pectic substance. The presence of considerable amount of glucose was interesting as it indicated the possibility of an associated starch like component. But neither BF-A nor BF-B gave any colour with iodine.

Pc of the pectinase hydrolysate of BF-B detected considerable amount of GalA and the neutral fraction obtained from the hydrolysate gave faint spots of Gal, Ara, Xyl and Rha. The presence of these four minor components was also corroborated by glc. It was significant to note that Glc constituting 25% of BF-B was not detectable in the above hydrolysate even in the concentrated state. It has been found[15] before that the crude pectinase used in the present investigation is a non-specific enzyme capable of complete depolymerisation of pectic substances (irrespective of their having insertions[15] or substitutions of neutral monosaccharide residues) as well as the accompanying galactans and arabinans. It has also been found that any starch like component alone or associated with such pectic substances was also depolymerised. But in the present case, the glucan portion remains unaffected by the pectinase and stayed as a white patch at the base line in the pc of the pectinase hydrolysate.

The above hydrolysate was dialysed when the bag content retained the glucan portion and the dialysate contained the rest of the monosaccharides as evidenced by pc and glc. No Glc could be detected even in the concentrated dialysate. This finding clearly indicated that BF-B was essentially a polygalacturonan (pectic substance) associated with the glucan component. The absence of any aldobiuronic acid in the acid hydrolysate of BF-B was also consistent with this conclusion.

Since there is no reliable existing method for the separation of such a polymer mixture, further evidence for such a model was sought from the results of Smith degradation. BF-B was oxidised with periodic acid[16] in dark at 4°, the liberation of formic acid became constant in 72 h. The oxidised product was reduced and the inorganic ions were removed. Pc of the resulting product showed an immobile patch at the base line and some GalA. Apparently some GalA residues survived the oxidation and were released during the subsequent operations. The acidic components (oxidised or unoxidised) were held on a Dowex-1 (formate) column and the effluent was worked up to solid. Hydrolysis of the solid followed by pc and glc, identified it to be the pure glucan. Thus, isolation of the pure glucan portion once again substantiated the earlier contention that the glucan was a separate entity and the other (very minor quantity) monosaccharides were some how attached with the pectic acid portion.

The acidic portion was eluted from the Dowex-1 (formate) column and hydrolysed. Pc of the hydrolysate furnished GalA, glycerol and threic acid. As complete oxidation of pectic acid is rather difficult, therefore, occurrence of some GalA was quite expected[17]. The formation of threic acid, the results of enzymic reaction and the high specific rotation value of BF-B, $[\alpha]_{589.5}^{+}$ 165° (c 0.275, H_2O) confirmed the structure of the pectic acid as of the conventional type, *i.e.* essentially a (1→4)-α-D-galacturonan. Failure of the accompanying glucan to develop any colour with iodine and its resistance to periodate indicated that in all probability the glucan was not a starch like polymer.

An attempt was made to determine the relative mode of distribution of the major sugar residues (GalA and Glc) in BF-B from some spectral measurements. Broad metachromatic spectra of BF-B-toluidine blue system (Fig. 2) showed that BF-B was rather a weak chromotrope. This would be a bit unbecoming of a polygalacturonan having an anionic site on every monosaccharide residue[18,19]. In the present case, this requires either (i) GalA residues to be interpersed by the glucosyl residues in the same chain or (ii) there should be blocking of the alternate anionic sites of

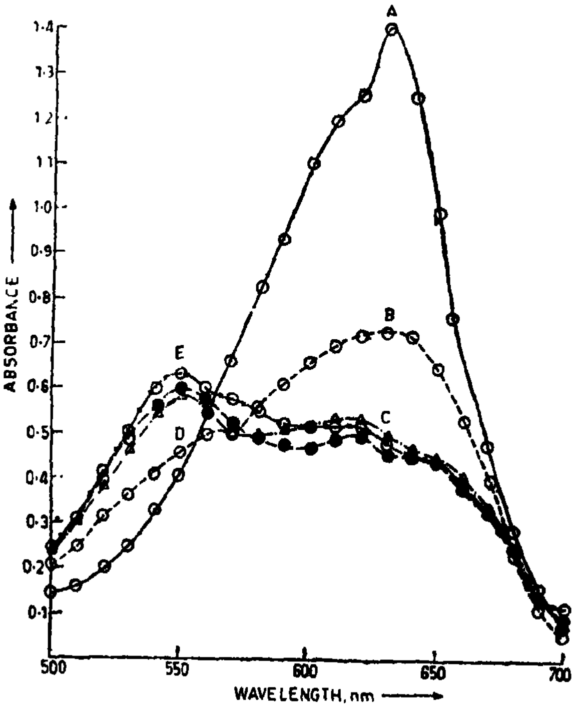


Fig. 2. Absorption spectra of 5.2×10^{-5} M toluidine blue in water (A); in presence of BF-B in the polymer-dye mol ratio of (B) 1.1, (C) 3.3, (D) 5.5, and (E) 11.0.

the pectic acid because of its having a special type of helicity due to its association with the glucan. While the first possibility is untenable because of the hydrolysis products of BF-B, the second one receives the strong support from the study of stoichiometry of TB–BF-B compound by the 'shaking with immiscible organic solvent' method[12]. Fig. 3 gives the stoichiometry of TB–BF-B compound to be 1 : 2 indicating that the dye cations are bound at alternate anionic sites of polygalacturonate in BF-B and every alternate COO^- group is engaged in forming strong association with the glucan component and hence, is not available for the dye binding.

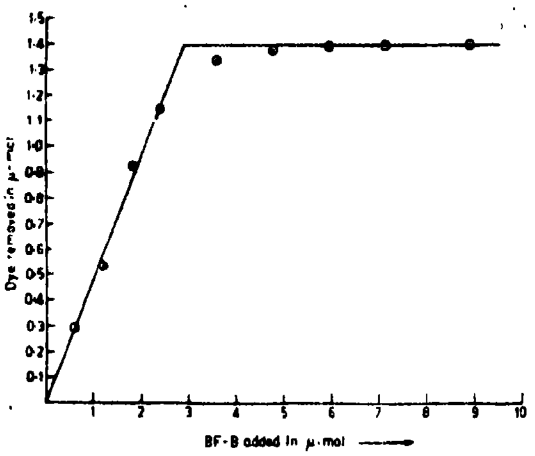


Fig. 3. Stoichiometry of BF-B—toluidine blue compound. Removal of BF-B — toluidine blue (TB) compound from aqueous phase by shaking with petroleum ether. 10 ml portions of 1.64×10^{-4} *M* TB containing various amounts of BF-B as indicated were shaken with petroleum ether and the dye left in the aqueous layer estimated.

The possibility of a helical structure in BF-B might be inferred from a parallel study of its metachromasia and circular dichroism (CD) of the BF-B–pinacyanol (PCYN) system in the visible range as depicted in Figs. 4 and 5, respectively. PCYN is a cyanine dye, and the shape of the metachromatic spectrum of this dye strongly depends on the nature of the polyanions inducing the spectral change[20,21]. Apparently BF-B induced sharp but multiple banded spectral change in PCYN (Fig. 4) having metachromatic bands at 485 and 590 nm with a minor band around 635 nm. The shape of the metachromatic spectrum was rather insensitive to polymer/dye ratio at least upto 33. Fig. 5 depicts the strong CD exhibited by BF-B–PCYN system in the visible region. PCYN or its aggregate does not have any chirality and metachromatic compound of PCYN and polyanion like Na-polyacrylate does not exhibit CD[22]. However, compound of PCYN with poly (L-glutamic acid) at both acidic and neutral *p*H exhibits dichroism in the visible absorption range of the dye, the shapes of the metachromatic and CD spectra characteristically

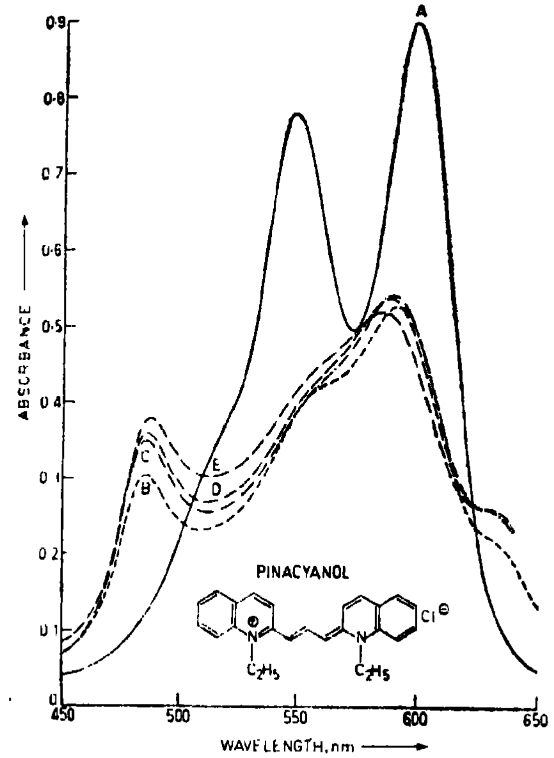


Fig. 4. Absorption spectra of 1.16×10^{-5} *M* pinacyanol in water (A); in the presence of BF-B at polymer-dye mol ratio of (B) 1.52, (C) 3.79, (D) 11.38, and (E) 33.37.

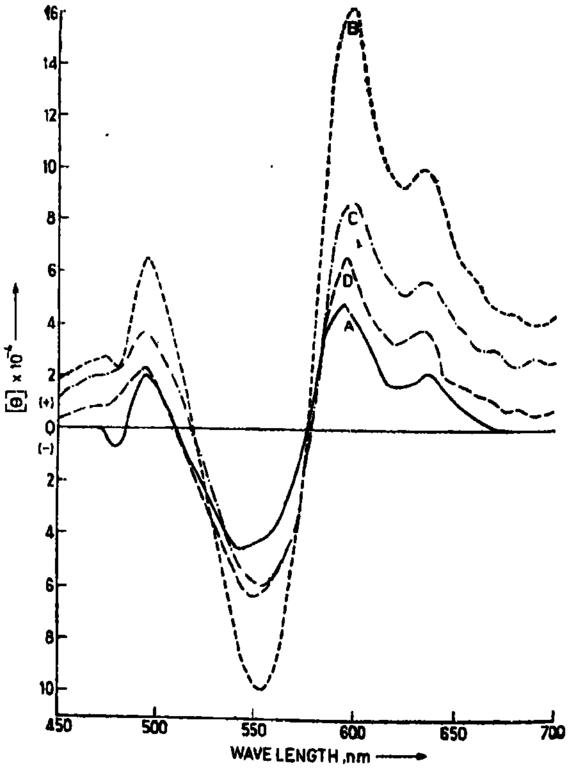


Fig. 5. CD spectra of 1.16×10^{-5} *M* pinacyanol in the presence of BF-B in water at polymer-dye mol ratio of (A) 1.52, (B) 3.79, (C) 11.38, and (D) 33.37.

depend on the conformation of the polyglutamic acid[23]. The importance of chromophore-chromophore interaction in metachromasia and extrinsic dichroism of dye-polyanion complexes has been pointed out[24-26]. The extrinsic optical activity of a symmetric chromophore bound on the side chains of a helical polyanion could be[27] (i) strong chromophore-chromophore interaction, the polyanion serving only to fix the relative geometry with transition dipoles of the chromophores coupled in a chiral arrangement; (ii) local interaction between the chromophore and the dissymmetric field of the helix; and (iii) perturbation of the chromophore by the dissymmetric field of the chiral atom in the polyanion. The exhibition of CD by BF-B – PCYN system indicated strong chromophore-chromophore interaction[28], and high [θ] values observed for the system suggested that mechanism (i) played the predominant role; lower [θ] values would be expected for other two mechanisms[29]. Considering the similarities between the CD spectra of PCYN induced by BF-B (Fig. 5) and by Na-poly (L-glutamate)[28], it could reasonably be suggested that poly GalA in BF-B, like Na-polyglutamate[30], had an extended helical conformation around the glucan component; the alternate possibility of a double helix involving both glucan and galacturonan could not be ruled out on the basis of the present data, though the proportions of GalA and Glc (molar ratio 2 : 1) supported the former model. PCYN cations were, therefore, bound around the BF-B extended helix with their transition moments coupled in a chiral arrangement, either helical or with systematic constraints, to exhibit circular dichroism.

Acknowledgement

The authors are thankful to Prof. M. Chaudhuri, I.A.C.S., Calcutta, for putting the spectropolarimeter at their disposal and to (Miss) Rina Ghosh, research scholar of the Chemistry Department, Jadavpur University, for various assistance.

References

1. "The Wealth of India, A Dictionary of Indian Raw Materials and Industrial Products", C. S. I. R., New Delhi, 1952, Vol. 1, pp. 203-206.
2. K. R. Kirtikar and B. D. Basu, "Indian Medicinal Plants", 2nd ed., Basu, Allahabad, 1975, Vol. IV, pp. 2571-2575.
3. A. K. Mukherjee, D. Choudhury and P. Bagchi, *Can. J. Chem.*, 1961, 39, 1408.
4. C. V. N. Rao and A. K. Mukherjee, *J. Indian Chem. Soc.*, 1962, 39, 711.
5. Z. Dische, *J. Biol. Chem.*, 1947, 167, 189.
6. M. Dubois, K. A. Gilles, J. K. Hamilton, P. A. Rebers and F. Smith. *Anal. Chem.*, 1956, 28, 350.
7. S. K. Sikder and A. Das, *Carbohydr. Res.*, 1979, 71, 273.
8. U. Lindahl, *Biochem. J.*, 1970, 116, 27.
9. D. Glick, *Methods Biochem. Anal.*, 1955, 2, 320.
10. A. Das and M. Heidelberger, *Carbohydr. Res.*, 1976, 48, 304.
11. M. K. Pal and M. Chaudhuri, *Makromol. Chem.*, 1970, 133, 151.
12. F. C. A. Macintosh, *Biochem. J.*, 1941, 35, 776.
13. M. K. Pal and M. Schubert, *J. Histochem. Cytochem.*, 1961, 9, 673.
14. R. M. Silverstein and G. C. Bassler. "Spectrometric Identification of Organic Compounds", 2nd ed., Wiley, New York, 1967, pp. 91-92; L. J. Bellamy, "The Infrared Spectra of Complex Molecules", 2nd ed., Wiley, New York, 1958, p. 179.
15. A. Das, unpublished data.
16. J. E. Scott, *Biochim. Biophys. Acta*, 1968, 170, 471.
17. A. F. Abdel-Fallah and A. A. Khaireldin, *J. Chem., U. A. R.*, 1970, 13, 27; A. F. Abdel-Fallah and M. Edress, *J. Sci. Food Agric.*, 1972, 23, 871.
18. M. K. Pal, *Makromol. Chem.*, 1958, 28, 91.
19. K. W. Walton and C. R. Ricketts, *Brit. J. Exp. Pathol.*, 1954, 35, 227.
20. W. West and S. Pearce, *J. Phys. Chem.*, 1965, 69, 1894.
21. M. K. Pal and B. K. Ghosh, *Makromol. Chem.*, 1979, 180, 959.
22. M. K. Pal, unpublished data.
23. M. K. Pal and M. Mandel, *Biopolymers*, 1979, 18, 2267.
24. M. K. Pal and M. Mandel, *Biopolymers*, 1977, 16, 33.
25. L. Stryer and E. R. Blout, *J. Am. Chem. Soc.*, 1961, 83, 1411.
26. A. L. Stone and H. Moss, *Biochim. Biophys. Acta*, 1967, 136, 56.
27. M. H. Loucheux and C. Duflot, *Biopolymers*, 1973, 12, 121.
28. M. K. Pal and M. Schubert, *J. Am. Chem. Soc.*, 1962, 84, 4384.
29. H. Nomori, N. Tsuchikasi, S. Takagi and M. Hatano, *Bull. Chem. Soc. Jpn.*, 1973, 48, 2522.
30. S. Krimm and L. Tiffany, *Isr. J. Chem.*, 1974, 12, 189.

J. Indian Chem. Soc.,
Vol. LXIII, January 1986, pp. 144-148

Kinetics of Adsorption of Ionic Surfactants at Alumina-Water Interface†

L. GHOSH, K. P. DAS** and D. K. CHATTORAJ*

Department of Food Technology and Biochemical Engineering, Jadavpur University, Calcutta-700 032

Adsorption of ionic surfactants from solution on the alumina-water surface has been studied as a function of time. Adsorption seems to be almost complete in about 20 minutes. Attempt has been made to understand the mechanism of the adsorption process. Adsorption being diffusion controlled, the diffusion coefficient of the surfactant micelles were determined from the kinetic data. Diffusion coefficient values were found to increase systematically with increase in the chain length of the surfactants. An empirical equation has also been proposed which fits the kinetic data well.

THERE has long been a growing interest in understanding the physicochemical aspects of adsorption of surfactants, proteins, lipids, bile salts *etc.* at various types of interfaces[1-5]. Adsorption of ionic surfactants from solution is generally time-dependent even when highly purified adsorbing materials are used. Garner and Mina[6] have shown that the surface diffusion coefficient of the surfactants is dependent upon the number of carbon atoms present in the amphiphiles. Very recently Graham and Phillips[7] have shown that the rate of change of surface concentration of the protein at the air-water interface is diffusion controlled but at higher surface coverages there exists an energy barrier.

Although large number of studies have been reported on the adsorption of ionic surfactants at the interfaces, no systematic study of adsorption kinetics has been done to throw light on the mechanism of the adsorption process. In the present paper, an attempt has been made to study the kinetics of adsorption of cationic and anionic surfactants at the alumina-water interface. Attempts have been made to understand the role of diffusion in the adsorption process and to calculate the diffusion coefficients of the surfactant micelles from the kinetic data. An empirical equation that fits the kinetic data has also been proposed.

Experimental

Alumina powder (E. Merck) used was of chromatographic grade of high purity. It was thoroughly washed with deionised water and dried overnight in air-oven at 100-105° to a constant weight before the experiment.

Highly purified surfactants, *viz.* sodium dodecyl sulphate (SDS), cetyl trimethyl ammonium bromide (CTAB), myristyl trimethyl ammonium bromide (MTAB) and dodecyl trimethyl ammonium bromide (DTAB) were used, which were obtained as gifts from Dr. K. S. Birdi of the Danish Technical University. The curves indicating variation of the surface tension of water in the presence of increasing concentrations of the surfactants did not exhibit any minima. CMC's of the surfactants measured from conductivity experiments were in agreement with the values reported in literature[8]. Water used throughout the experiment was deionised and distilled from alkaline potassium permanganate solution. The aqueous media used were phosphate buffers of ionic strength 0.125 for *p*H 6.0 and 8.0, whereas acetate buffer of ionic strength 0.125 was used for *p*H 4.0. All inorganic salts used were of analytical grade.

Determination of surface area of adsorbent : The surface area of the adsorbent alumina powder was determined by measuring the adsorption of palmitic acid from benzene solution on the adsorbent. The method was same as described elsewhere[9] and the value was found to be 61.62 ± 0.38 $m^2 g^{-1}$.

Measurement of adsorption kinetics : A stock quantity of buffer or salt solution of definite *p*H and ionic strength was prepared, which was treated as a solvent for the preparation of the solution of surfactant. Then the solutions of the respective surfactants near the CMC values were prepared with this solution by the appropriate dilution in a standard joint wide-mouth bottle of capacity 200 ml. Alumina powder (4-5 g) was weighed accurately and poured into the solution bottle and immediately the whole solution was shaken carefully avoiding the formation of foam and the stopwatch was started. The solution (2.0 ml) was then withdrawn after 2 min interval and stored in test tubes. After each withdrawal, the system was shaken thoroughly for a few seconds and then the powder was allowed to settle. Solutions were withdrawn after complete settling of alumina

† Dedicated to Prof. Sadhan Basu on the occasion of his 65th birthday.

** Present Address : Guest Scientist, Physical Chemistry 1, Chemical Center, University of Lund, Sweden.

(complete within ~1 min) so that only clear supernatant was withdrawn. The whole set of experiment was carried out in a water-bath at 30.0 ± 0.2°.

The collected surfactant solutions after proper dilution were analysed by the dye-partition technique[10]. For this, a dye methylene blue in 0.01 *N* HCl or a vinyl disulphine blue in 0.01 *N* H_2SO_4 were used to form cationic and anionic dye-surfactant complexes respectively. The concentration of the dye was usually kept 100 mg dm^3. Partition was carried out between an aqueous electrolyte solution and an organic chloroform layer for the extraction of dye-amine complex. A definite volume of the coloured solution was taken in a Klett tube with the help of a long needle glass syringe and the absorbancy of the amine-bound dye in chloroform layer was measured in a Klett Summerson colorimeter using red filter. The extraction of the dye-bound surfactant with chloroform was done at constant temperature by keeping the bottles inside a thermostatic bath. From the comparison of this absorbancy with those of the blank containing known concentrations of the surfactant, the concentration of the surfactant was estimated within 3-4% error.

Calculation of amount adsorbed as a function of time : If C_i be the initial concentration and V_i be the initial volume of the surfactant solution, then considering the mass balance with respect to surfactant, one can write,

$$\frac{C_iV_i}{1000}=\frac{C_1(V_1+V_w)}{1000}+\Gamma_R^1.W \qquad (1)$$

where, C_1 = final molar concentration of the solution after time t_1, V_w = volume of solution (ml) withdrawn. V_1 = volume of solution (ml) left after time t_1, Γ_R^1 = amount (mole) adsorbed per gram after time t_1, and W = weight of the alumina powder taken in gram.

After a second step of withdrawal of some volume V_w from the solution at time t_2, one can write,

$$\frac{C_iV_i}{1000}=\frac{C_1(V_1+V_w)}{1000}+\Gamma_R^1.W$$
$$=\frac{C_2(V_2+V_w)}{1000}+\frac{C_1V_w}{1000}+\Gamma_R^2.W \qquad (2)$$

where, C_2 = final molar concentration of the solution after time t_2, V_2 = volume of solution (ml) left after time t_2 and Γ_R^2 = amount (mole) adsorbed per gram after time t_2.

Thus, after n times withdrawal at time t_n, are can write,

$$\frac{C_iV_i}{1000}=\frac{C_1(V_1+V_w)}{1000}+\Gamma_R^1.W$$
$$=\frac{C_2(V_2+V_w)}{1000}+\frac{C_1V_w}{1000}+\Gamma_R^2.W$$
$$=\frac{C_n(V_n+V_w)}{1000}+\frac{C_{n-1}V_w}{1000}+\frac{C_{n-2}V_w}{1000}+\dots$$
$$+\frac{C_2V_w}{1000}+\frac{C_1V_w}{1000}+\Gamma_R^n.W \qquad (3)$$

$$\Gamma_R^n=\frac{C_iV_i}{1000\,w}-\frac{C_nV_n}{1000\,w}-\frac{V_w}{1000\,w}(C_1+C_2+C_3+\dots+C_n)$$
$$=\frac{1}{1000\,w}\left[(C_iV_i-C_nV_n)-V_w\sum^{n}C\right]\ \text{mol g}^{-1} \qquad (4)$$

Hence, the amount adsorbed per gram at any time t was calculated with the help of equation (4). From the knowledge of surface area of the alumina powder and utilising equation (4) the amount Γ_R^n (equal to Γ_R) of a surfactant adsorbed in millimole per square meter of alumina was calculated.

Results and Discussion

The extents of adsorption, Γ_R of the cationic and anionic surfactants at the alumina-water interface as a function of time are shown in Figs. 1 and 2. Fig. 1 shows the time variation of Γ_R for cationic surfactants at *p*H 6.0 and anionic surfactant SDS at *p*H 4.0. It is found from the Figs. that for DTAB, MTAB and SDS, the adsorption is

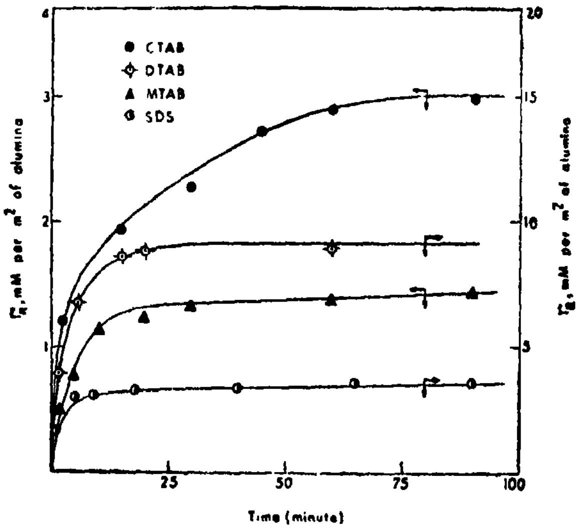


Fig. 1. Plot of Γ_R *vs* t for CTAB, DTAB, MTAB (phosphate buffer, *p*H 6.0) and SDS (acetate buffer, *p*H 4.0) at 30° ; μ=0.125 (NaCl).

almost complete within 20 min. For CTAB with an initial concentration of 10×10^{-4} mol dm^3, the completion of adsorption requires about 1 h. The different values of Γ_R at the state of completion of this kind is of course a function of final equilibrium concentration of the surfactant in the bulk. At *p*H 8.0 (Fig. 2), adsorption is almost complete within 30 min for all the cationic surfactants.

The rate of adsorption of a solute from solution at an interface usually depends on several factors. The adsorption of ionic surfactants at the alumina-water interface depends primarily on the rate of arrival of the surfactant molecules at the interface. The surfactant molecules approach the interface from the bulk through diffusion and get adsorbed

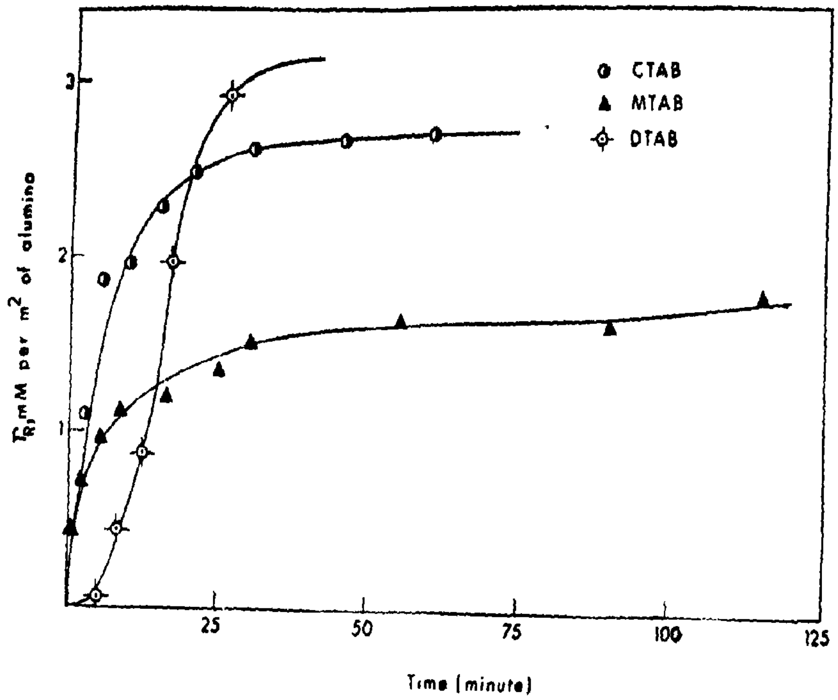


Fig. 2 Plot of Γ_R *vs* t for CTAB, MTAB and DTAB (phosphate buffer, *p*H 8.0) at 30° ; μ=0.125.

at the interface. Hence, such adsorption, at least the initial stage of adsorption will be diffusion controlled. The concentrations of the surfactants used for the kinetic study were higher than the respective CMC of the surfactants. So the rate of adsorption will be dependent on the rate of diffusion of micelles at the interface.

At the initial stage of adsorption, the energy barrier for the approach of the micelle or surfactant molecule towards the interface is zero, *i.e.* the activation energy to the adsorption at the surface is zero. The amount adsorbed at the interface is then related to the diffusion coefficient D and time t by the equation[11,12]

$$\Gamma_R = 2C_R\left(\frac{Dt}{3.142}\right)^{\frac{1}{2}} \tag{5}$$

where, C_R is the substrate surfactant concentration. It is further assumed that C_R remains essentially constant during the adsorption process and t is the time of adsorption.

The present kinetic data has been well fitted to this equation by plotting Γ_R against $t^{1/2}$. Such plots are shown in Figs. 3 and 4. It is seen from these figures that Γ_R bears a linear relationship with $t^{1/2}$ upto certain time after which it deviates from linearity. Such deviations were also observed for the kinetics of adsorption of proteins at interfaces[7]. The deviation is possibly due to the fact that as more and more surfactants get adsorbed, the substrate concentration C_R decreases and cannot be considered constant. From the linear portion of the plots, diffusin coefficient of the surfactant micelles have been calculated from the slopes of the curve. The values of the diffusion coefficients of ionic surfactants at different *p*H are shown in Table 1.

The diffusion coefficient values, as seen from Table 1, are of the order of 10^{-9} to 10^{-12} m^2 s^{-1}. These orders are in good agreement with micellar diffusion coefficient values reported in literature[14]. It is also known that the migration velocity of the adsorbable molecules or ions is a function of the number of carbon atoms. Usually the surface diffusion coefficient value increases rapidly with an increase in the number of carbon atoms. The overall adsorption rate is a function of chain length only and not of the nature or the position of the hydrophilic end group[15]. In our results too (Table 1), we find the same trend. For DTAB, at *p*H 8.0, D is of the order of 10^{-12}, for MTAB 10^{-11} and for CTAB 10^{-9}. Similarly at *p*H 6.0, diffusion coefficients is least for DTAB bearing of the order of 10^{-11}. For MTAB, it is of the order of 10^{-10} and for CTAB 10^{-9}. For SDS, micellar diffusion coefficient is of the order of 10^{-10} m^2 s^{-1} at *p*H 4.0. Thus we see that the overall adsorption rate is a function of chain length, a conclusion similar to that made earlier by Shinoda *et al.*[6].

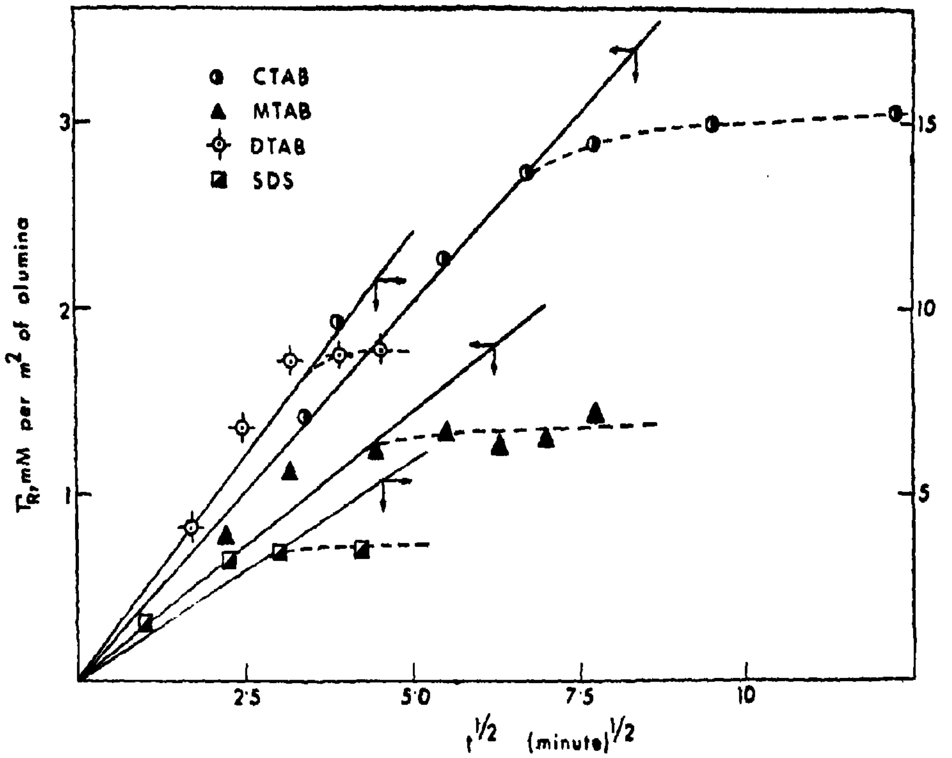


Fig. 3. Plot of Γ_R vs $t^{1/2}$ for CTAB ($\Gamma_R = 1\times10^4$), MTAB ($\Gamma_R = 1\times10^5$), DTAB ($\Gamma_R = 1\times10^5$), (phosphate buffer, pH 6.0) and SDS ($\Gamma_R = 1\times10^3$; acetate buffer, pH 4.0) at 30° ; $\mu = 0.125$.

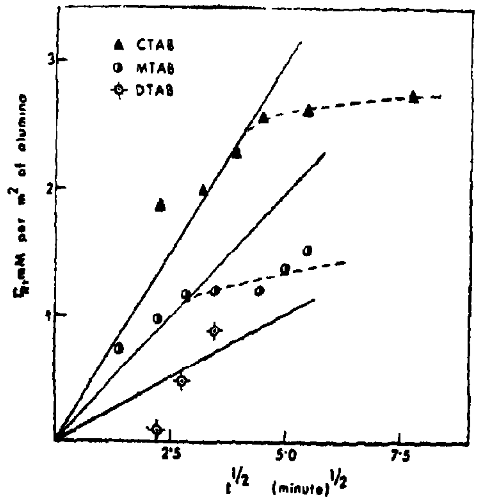


Fig. 4. Plot of Γ_R vs $t^{1/2}$ for CTAB ($\Gamma_R = 1\times10^4$), MTAB ($\Gamma_R = 1\times10^5$) and DTAB ($\Gamma_R = 1\times10^3$), (phosphate buffer, pH 8.0) at 30° ; $\mu = 0.125$.

It is also interesting to note that the adsorption kinetic data were fitted in good agreement in an empirical type of equation,

$$\frac{dC_R}{dt} = k(C_R)^n \quad (6)$$

TABLE 1—VALUES OF DIFFUSION COEFFICIENTS (D) OF IONIC SURFACTANTS

Surfactants	pH 4.0 (μ=0.125) D $m^2 s^{-1}$	pH 6.0 (μ=0.125) D $m^2 s^{-1}$	pH 8.0 (μ=0.125) D $m^2 s^{-1}$
SDS	1.00×10^{-10}	—	—
CTAB	—	2.16×10^{-9}	4.71×10^{-9}
MTAB	—	2.86×10^{-10}	8.13×10^{-11}
DTAB	—	8.88×10^{-11}	6.11×10^{-13}

where, k and n are two constants. This equation demands a linear plot of log dC_R/dt against log C_R. Such plots are shown in Figs. 5 and 6. From the slope and intercept of these plots, the empirical constants n and k has been found out and reported in Table 2.

TABLE 2—VALUES OF n and k FOR IONIC SURFACTANTS AT DIFFERENT pH

Surfactants	pH 4.0		pH 6.0		pH 8.0	
	n	k	n	k	n	k
SDS	1.3	0.11	—	—	—	—
CTAB	—	—	1.4	1.8	1.7	10.1
MTAB	—	—	1.3	0.11	1.4	0.41
DTAB	—	—	4.0	120000	5.0	50000

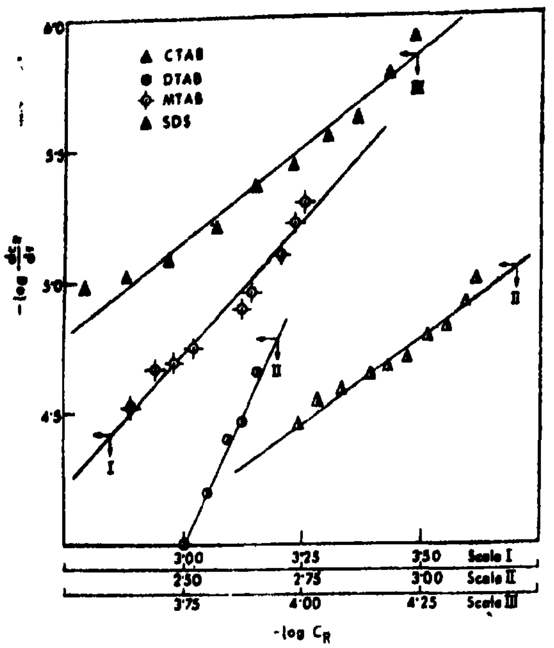


Fig. 5. Plot of log dC_R/dt *vs* log C_R for CTAB, DTAB, MTAB (phosphate buffer, *p*H 6 0; and SDS (acetate buffer, *p*H 4 0) at 30° ; μ=0.125.

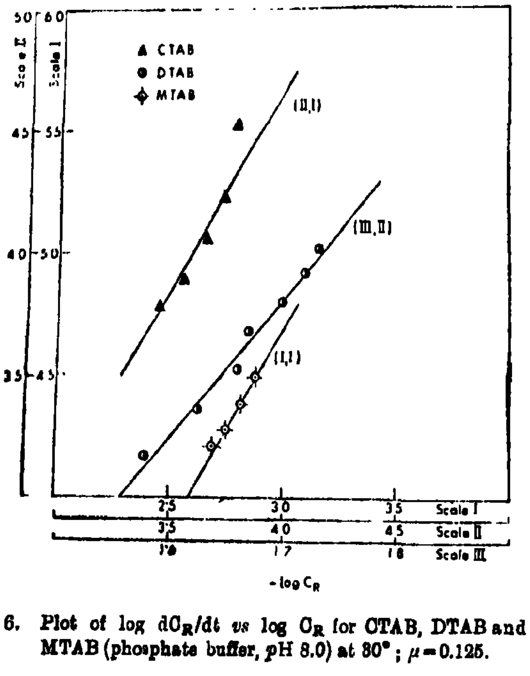


Fig. 6. Plot of log dC_R/dt *vs* log C_R for CTAB, DTAB and MTAB (phosphate buffer, *p*H 8.0) at 30° ; μ=0.125.

References

1. "Solution Behavior of Surfactants", eds. K. L. MITTAL a E. J. FENDLER, Plenum Press, New York, 1982, Vol.

2. W. NORDE, Ph. D. Thesis, Agricultural Universi Wageningen, The Netherlands, 1976.

3. D. K. CHATTORAJ and K. S. BIRDI, "Adsorption and t Gibbs Surface Excess", Plenum Press, New York, 1984.

4. G. L. GAINES, "Insoluble Monolayers at Liquid G Interface", Interscience, New York, 1966.

5. K. SHINODA, T. NAKAGAWA, B. TAMAMUSHI and ISEMURA in "Colloidal Surfactants", Academic Pre New York, 1963.

6. F. H. GARNER and P. MINA, *Trans. Faraday Soc.*, 19 **55**, 1016, 1067.

7. D. E. GRAHAM and M. C. PHILLIPS, *J. Colloid. Interfa Sci.*, 1979, **70**, 403.

8. P. MUKHERJEE and K. J. MYSELS, "Critical Micelle Co centration of Aqueous Surfactant System", N. S. R. D. 1971.

9. A. SAMANTA and D. K. CHATTORAJ, *Prog. Colloid ar Polym. Sci.*, 1983, **68**, 144.

10. P. MUKHERJEE, *Anal. Chem.*, 1956, **28**, 870.

11. I. LANGMUIR and V. J. SCHAEFOR, *J. Am. Chem. Soc* 1937, **59**, 2100.

12. F. MACRITCHIE and A. E. ALEXANDER, *J. Colloid Sci* 1963, **18**, 453.

13. J. G PETROW and R. MILLER, *Colloid Polym. Sci.*, 197 **255**, 669.

14. K. SHINODA, T. NAKAGAWA, B. TAMAMUSHI and ISEMURA in 'Colloidal Surfactants", Academic Pres New York, 1963, p. 117.

15. K. SHINODA, T. NAKAGAWA, B. TAMAMUSHI and I ISEMURA in "Colloidal Surfactants", Academic Pres New York, 1963, p. 186.

J. Indian Chem. Soc.,
Vol. LXIII, January 1986, pp. 149-156

Some Recent Advances in Separation Processes in Polymeric Media†

R. A. MASHELKAR

Chemical Engineering Division, National Chemical Laboratory, Pune-411 008

Some recent advances in separation techniques involving polymeric systems have been discussed. The areas that have emerged predominantly over the past ten years, Such as polymeric mechanochemical devices, of separations, polymeric adsorbents, stress induced polymer separations, separations of protein or polymer solutions through size selective water absorbing polymer gels *etc.*, have been focussed. Some contributions from the National Chemical Laboratory have been cited.

IN the field of separation technology, a number of cases where separations involve polymeric systems in one form or the other have been emerging in a very dominant way. The first case naturally relates to areas where polymers themselves act as separators (for instance, membrane processes). The second one relates to those where separations in polymeric media are conducted. Stripping of polymeric melts containing trace impurities of monomers (as in ethylene/molten polyethylene case) could be cited as a specific example. The purpose of this brief review is to provide a rather broad calssification of these processes and then dwell on some of the more exciting findings in recent years. Wherever possible, a reference will be made to the contributions from the polymer science and engineering school at National Chemical Laboratory.

The area where polymers themselves are used as separators comprise polymeric membranes, polymeric ion-exchange resins, polymer flocculants *etc.* As regards the separation processes in polymeric systems, a number of areas can be cited. These include solvent or monomer stripping from molten polymers, concentration of polymeric or protein solutions through the use of new water absorbing polymers, separation of macromolecules by using finite stress fields *etc.* It is impossible to provide an exhaustive coverage of systems falling in both the above categories. Therefore, we will focus rather sharply on the following areas only, where some exciting advances have been made in recent years.

(i) New developments in polymeric mechanochemical devices, which act as chemical valves for affecting separations.

(ii) Some recent advances in polymeric adsorbents.

(iii) Separations of dilute protein or polymer solutions through size selective water absorbing polymeric gels.

(iv) Stress induced polymer separations.

It is believed that although the field of separation processes in polymeric media has been exhaustively studied, the above areas have emerged predominantly over the past five to ten years, and no comprehensive coverage of these exciting developments is to be found in the literature.

Membrane separations—a quick overview :

Before dealing specifically with mechanochemical membranes, it might be useful to take a quick bird's eye view of the area of membrane separations in general.

By contrast with the widely used methods of distillation, freezing *etc.*, the separation of mixtures by membrane techniques does not involve phase conversions of the components being separated. The operations are normally carried out at ambient temperatures. Consequently, membrane methods are very economical and have low energy requirements. For example, in desalination of water by reverse osmosis, the consumption of thermal energy is significantly less than that for running a distillation system. Similarly, the energy consumption for obtaining oxygen enriched air by membrane methods could be up to 50% less than that in the cryogenic methods. The unit capital investment for the construction of membrane type separating devices is comparatively small and the period of recoupment is short too. In some cases, particularly in microbiological and medical preparations, satisfactory separation of mixtures with a change in the properties of the components may be found to be impossible except by membrane methods. The drawbacks of the membrane type separation methods includes the need for preliminary purification of the system being separated in order to avoid contamination by particles in suspension. Furthermore, there are no all purpose membranes and membranes of different compositions and morphology will be required for separation of different systems.

† Dedicated to Professor Sadhan Basu on the occasion of his 65th birthday.

It is not intended to provide a complete review of the membrane separation processes and such reviews already exist in the literature[1-4]. For a given separation process, there is a bewildering range of membranes. For instance, numerous kinds of polymers in combination with solvent and other additives are used for preparation of membranes for specific purposes in reverse osmosis. For example, composite membranes have become very popular. Table 1 shows a broad classification of membrane separation processes and Table 2 shows some examples of polymers used for preparation of reverse osmosis membranes. Membrane technology has made extensive inroads into various fields. Table 3 shows some of the industrial applications of membrane processes. In a given process, there may be number of alternatives and these could depend very much upon the operating conditions, raw materials and desired separation products.

TABLE 1—MEMBRANE SEPARATION TECHNIQUES

Reverse osmosis Dialysis Electrodialysis Piezodialysis Gas permeation Pervaporation	*Dense membrane*
Ultrafiltration Microfiltration	*Porous membrane*
Extraction	*Liquid membrane*
Enzymatic reaction Facilitated transport Detection of chemicals	*Chemically active membrane*

TABLE 2—MATERIALS FOR MEMBRANE

Reverse Osmosis

Asymmetric Membrane

Cellulose acetate
Aromatic polyamide
Polybenzimidazole
Aromatic polyhydrazide
Polyamidimide
Sulphonated polyphenylene oxide
Polyhydantoin
Polymidazopyrrolone

Composite Membrane

(Polyethylenimine+TDI)/polysulphone (NS-100)
Furfuryl alcohol/polysulphone
(Polyethylenimine+isophthaloyl chloride)/polysulphone
(Epichlorohydrin+ethylenediamine+isophthaloyl chloride)/polysulphone
Furan resin/polysulphone
Sulphonated polyfurfuryl alcohol

The use of a membrane technology involves the solution of a whole complex range of scientific, technological and design problems. These include the study of mechanism of kinetics and transport of liquids and gases in membranes and the development of the corresponding quantitative theories, the development of and modification of new types of polymeric materials, development of new techniques and equipment for production of commercially usable membrane systems, *etc.* It could also involve the development and organisation of production of auxiliary materials for separating elements and equipment and also of special pumps, compressors, filters *etc.* for preliminary purification of systems, monitoring and measuring devices and automation facility, the designing of final membrane modules *etc.* It is thus evident that a mere synthesis of polymeric membrane material in the laboratory is not just adequate and a total integrated effort has to be launched.

Mechanochemical polymeric devices :

Some exciting developments have been reported in the past few years, which relate to permselective membranes in which the mechanochemical contractile forces exhibited within the membranes enlarge the pore size isothermally and lead to a marked increase in water permeability and improved performance of macromolecular separations.

TABLE 3—SEPARATION TECHNOLOGY AND INDUSTRIAL APPLICATIONS

	Reverse osmosis	Dialysis	Electro-dialysis	Ultrafil-tration	Microfil-tration	Gas perme-ation
Desalination	++	–	++	–	–	–
Ultrapurification of water	++	–	–	+	++	–
Treatment of waste water	++	–	+	++	++	–
Recovery of reusable materials	++	++	++	++	–	++
Salt production	–	–	++	–	–	–
Purification of foods industries	++	++	++	++	++	--
Purification in pharmaceutical industries	–	+	+	+	++	–
Production of chemicals	–	–	++	–	–	++
Medical equipment	+	++	–	++	++	++

+ ≡ Less preferred. ++ ≡ More preferred.

The novel mechanochemical system converts chemical into mechanical energy by polymer-polymer complexation between complementary polymers[5,6]. Such dilations and contractions in these systems are related to the drastic conformational shrinkages of a three-dimensional network consisting of polymethacrylic acid (PMAA) due to a reversible complexation with solved polyethylene glycol (PEG). Osada and Takeuchi[7] have demonstrated that in the presence of a small amount of PEG, PMAA membrane loaded with 100 times the weight of the dry membrane could contract and dilate many times to over 90% of its length. The work done per contraction by one gram of contractile substance was 5×10^{-8} cal, and the membrane exhibited more than 2 000 g cm^{-2} of stress when the contraction was performed under constants membrane dimensions, *i.e.* under conditions of isomeric contraction.

A natural corollary of the above observation is that if the mechanochemical contraction is developed isothermally, the contractile stress appearing in the membrane should expand the pore through which the water and macromolecular solute permeates. Thus conceptually it is possible to obtain ultrafiltration membranes having mechanochemically expanding and contracting pores. Fig. 1 shows the effect of a mechanochemical contraction of the PMAA membrane on water permeability when a small amount of PEG with a molecular weight of 3 000 was subsequently added to water. It was seen that the PMAA membrane exhibited a marked increase in water permeation as soon as the membrane was contacted with the PEG solution. Once the PMAA membrane is treated with PEG, the water permeates the membrane with a high velocity. On the other hand when the membrane is rinsed with alkali (*p*H 8) to dissociate the complex and remove PEG, the membrane recovers the initial low water permeability.

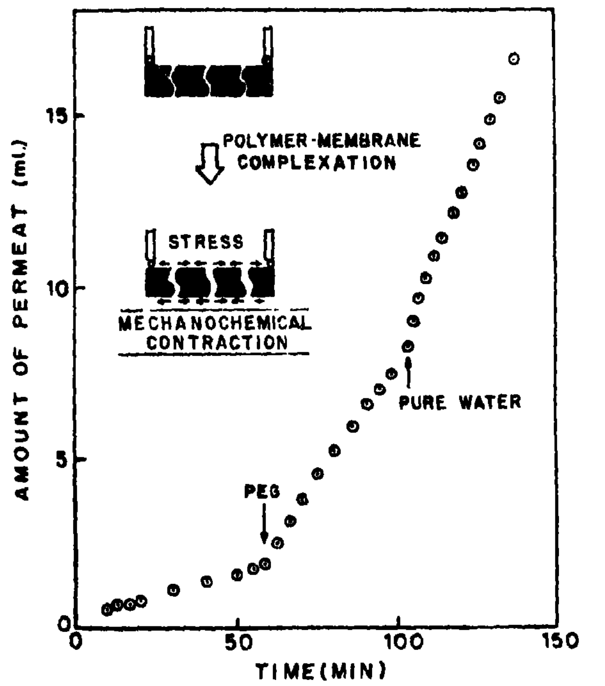


Fig. 1. Effect of mechanochemical contraction of the PMMA membrane on water permeability when PEG is added to water.

The increased water permeation in the presence of PEG is due to the expansion of pores because the water permeability bears the same relation to the molecular weight of PEG as the work done by the contractile membrane or the stress generated under isometric contraction. This is demonstrated in Fig. 2, which shows the dependence of water permeability (1), relative contraction (2), and stress (3) of PMAA membrane on the molecular weight of PEG. K_0 and K denote the permeability constant for PMAA membrane treated and untreated with PEG, respectively. The presence of a maxima, when PEG reaches a molecular weight of 3 000 in every curve in Fig. 2, indicates that the membrane-PEG complexation takes place not only on the surface, but inside the wall membrane as a result of the penetration of PEG molecules through the expanded pore channel. Osada and Takeuchi[7] observed that water soluble polymers other than PEG capable of forming complexes with PMAA, such as polyvinyl pyrollidone, polymethyl vinyl ether, polyvinyl alcohol *etc.* could neither contract the membrane nor increase the water permeation.

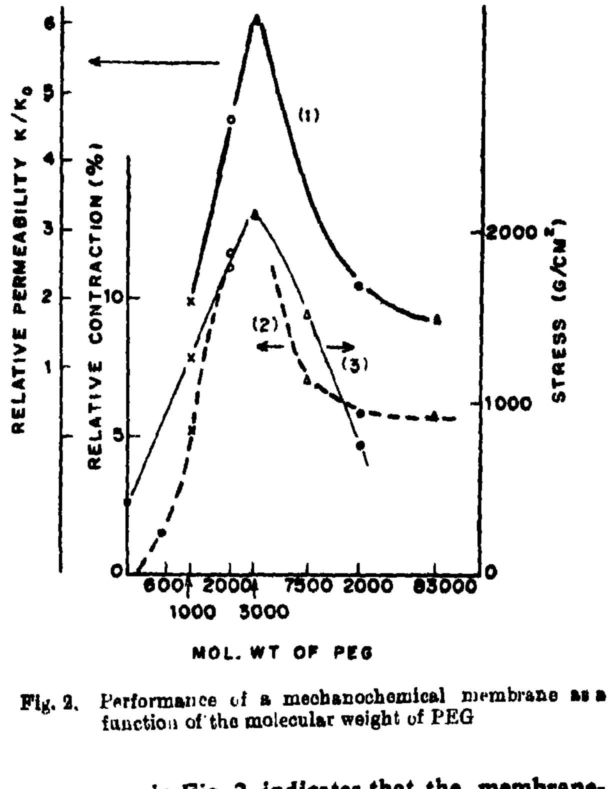


Fig. 2. Performance of a mechanochemical membrane as a function of the molecular weight of PEG

Thus, the mechanochemical PMAA membrane can behave as a 'chemical valve'.

As regards the tests of such mechanochemical devices with haemoglobin and albumin solutions, some data are presented in Fig. 3. It is seen that both protein solutions can permeate the membrane without decreasing the high permeation velocity for pure water released by the PEG, whereas in the case of a PMAA membrane treated with PEG the protein clogged the membrane rapidly thereby reducing the permeability. Osada and Takeuchi[7] observed that the mechanochemical membrane could improve the performance of protein separation by about 240 times for albumin and 55 times for haemoglobin in comparison with PMAA membrane which was not treated with PEG.

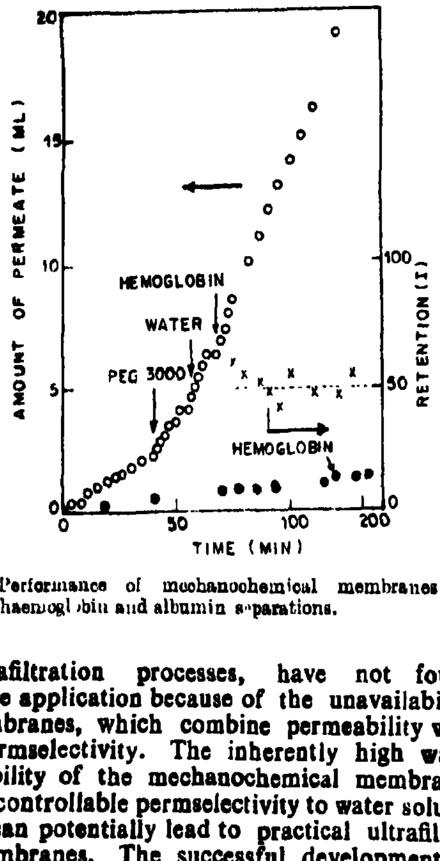


Fig. 3. Performance of mechanochemical membranes for haemoglobin and albumin separations.

Ultrafiltration processes, have not found extensive application because of the unavailability of membranes, which combine permeability with high permselectivity. The inherently high water permeability of the mechanochemical membranes plus its controllable permselectivity to water soluble solutes can potentially lead to practical ultrafiltration membranes. The successful development of such 'chemical valves' may therefore open up a new area of separation.

Polymer adsorbents :

Synthetic polymers are being increasingly used to remove organic species from an aqueous medium by physicochemical adsorption and also for extraction of metals. They apparently offer some major advantages in both these processes. Indeed novel polymers which coordinate to metals are likely to offer the possibility of providing the basis for the next major phase of development of extraction and separation processes. In some cases, they may even offer an advantage over conventional solvent extraction and ion-exchange processes for separating metals. For instance, solvent extraction, in which a metal is extracted into an organic phase, is particularly used for the concentration above 200 ppm whereas ion-exchange is useful below 100 ppm. Polymers with metal coordinating ability could be useful over the entire concentration range that is from trace concentration upwards. Moreover, the polymers can be designed to be extremely selective to precious or base metals in many conditions of concentration, *p*H or temperature. The utilisation of these polymers has led to the developments which have a commercial potential. Their use as scavengers of precious metals cetainly appears to be promising.

When focussing on separation of organic molecules by polymeric adsorbents, it has to be emphasised that the binding energies of synthetic polymers are lower than those of activated carbon for the same organic molecules. These lower binding energies help in providing easy recovery of polymeric adsorbents by regeneration[8,9]. Whenever the economics of solvent or chemical regeneration of adsorbent is favourable, the use of polymeric adsorbent could be advocated. An additional advantage of polymeric resins is that they have durable matrices as compared to conventional adsorbents, such as activated carbon.

Polymeric adsorbents find a special use in the adsorption of many organic pollutants from the waste water. A comprehensive summary has been provided[10]. The choice of these adsorbents will depend upon the factors such as the nature of the organic components, presence of electrolytes in waste water, *p*H of the solution *etc*. Systematic studies on polymeric adsorption have appeared in the literature[11,12]. Such adsorbents can be regenerated by changing the *p*H or by using a solvent. The reagent used should be such that the sorbate can be easily recovered or the sorbate regenerant mixtures can be recycled to the main process. To regenerate an adsorbent resin loaded with the solute, a solvent system should be chosen such that the solvating forces of the solvent for the solute will overcome the adsorbent resin attractive forces. The solute can then migrate to the solvent phase. We shall now discuss some of the specific applications of polymeric adsorbents.

For adsorption of phenol from various waste waters, cross linked polymethylacrylate resin, crosslinked polystyrene and vinyl pyridine-divinyl benzene copolymer can be used for adsorption of phenol from various waste waters[9]. Kowabata and Ohira[13] found that if porous copolymers of vinylpyridine and divinylbenzene with large areas can be used then the adsorbent capacity of the resin can be further increased. *p*-Nitrophenol, chlorinated phenols and other phenolics can also be separated by using polymeric adsorbents[9].

In the area of recovery of metals by using polymeric adsorbents, a number of advances are continuing. An interesting one was reported by Husband and Rowley[14] recently. They observed that fulvic acid, which is one of the humic components of soil is an important natural chelator of metals and as such implicated in the mobilisation of metals in soils and in natural waters. They further observed that maleic anhydride can be polymerised in the presence of either tertiary phosphines or tertiary amines and the polymer produced by initiation with pyridine was very similar both spectroscopically and in many of its other properties to fulvic acid. By binding poly (maleic anhydride) to polystyrene, they undertook experiments on lead recovery. Laboratory scale experiments showed that it had an excellent capacity for Pb^{II} and could adsorb it upto 0.42 mmol g^{-1} of adsorbent, while adsorbing Mg^{II}, Zn^{II} and Cd^{II} in trace quantities. The adsorbent could be easily regenerated for reuse by treatment with 2 *M* nitric acid. Given the potential of the material as a lead scavanger and current concern about lead toxicity, the polymer may prove useful in practical water treatment applications.

Some polymeric resins have also been used for uranium recovery from sea water. The oceans contain 4.5×10^9 tons of uranium and it is conceived that about 10^8 tons in the upper 100 m of the ocean is immediately accessible for recovery. Number of studies on large scale feasibility of uranium recovery from see water by synthetic polymer adsorption, especially of the acrylonitrile-divinyl benzene-copolymeric amidoxime resin have been attempted. They appear to show good promise. The concentration of urarnium in the sea water is quite low (3 g dm^{-3}) and therefore, the economics of such processes has not been found to be viable so far. However, new innovations in adsorbent synthesis could change the picture dramatically.

Polymeric gels as size-selective separators :

The problem of separation processes focussing around concentration of dilute solutions of organic or biological materials is becoming increasingly important. Specific examples include the removal of water from starch and cheese whey, the concentration of antibiotics in fermentation broths and the recovery of protein products of genetically engineered microorganisms. Various methods have been used for concentrating dilute solutions of macromolecules. Electrophoretic and ultrafiltration techniques *etc.* have been commonly used on laboratory scale. Interestingly, a new concept of using crosslinked gels to concentrate solutions of high molecular weight solutes has emerged recently. Such gels are size-selective and they can concentrate solutes whose size exceeds a certain minimum. The resulting separation process provides an interesting alternative to ultrafiltration. In ultrafiltration, a polymer membrane separates a solution at high pressure from a solvent at low pressure. Solvent is forced through the membrane from high to low pressure, while the solute is retained and thus concentrated. This one step process is conceptually simpler than the polymeric gel process to be described later. However, it has the disadvantage that the concentration polarisation near the membrane implies large pressure drops and expensive equipment. Additionally, the possibility of the macromolecules, such as proteins and DNA being subjected to harmful shearing stresses[15] is quite real.

Two concrete efforts on concentrating dilute solutions of macromolecular systems will be described here. The first effort at National Chemical Laboratory uses a crosslinked acrylate gel, whereas the one from the Minnesota (U.S.A.) school relates to using a hydrolysed crosslinked polyacrylamide bead, which is produced commercially as a packing for gel permeation chromatography. These studies, which almost appeared at the same time in the open literature, indicate the powerful potential of the techniques.

Vartak *et al.*[16] synthesised crosslinked acrylate gels which had a capacity to pick up water to the extent of 150 g g^{-1}. The polymerisation was carried out in glass tubes and after polymerisation the gel sticks were used as such for concentration of macromolecules. Proteins having a wide range of molecular weights (10 000-450 000) were concentrated using the gel sticks. About ten-fold concentration of different proteins was attained and the recoveries were also rather high (Table 4). They found that the gel sticks could be effectively used for concentrating other high molecular weight substances also such as starch, carboxymethyl cellulose, DNA *etc.* Vartak *et al.* found that low molecular weight compounds, such as glucose, sucrose, acetic acid, methanol and other inorganic solutes did not concentrate. It was postulated that this property of the gel could be made use of to eliminate product inhibition in some of the enzyeme catalysed reactions which are inhibited by low molecular weight products. Vartak *et al.* also focussed their attention on the process of cellulose hydrolysis and looked at the problems of recovery and reuse of cellulase from the hydrolysis reactor, since the economics of solution hydrolysis could presumably be improved by improving the separation techniques. As is well known, the separation of enzymes from the soluble products, such as glucose from the cellulose hydrolysates presents a problem. They performed experiments on concentration of cellulase and the recovery of glucose from a mixture of cellulase and glucose. They found that the enzymes could be concentrated to 30-fold with about 90% recovery. The recovery of glucose was about 75%. Such a method, if found technologically successful, could provide an imnportant direction to the recovery of cellulase and glucose from the cellulose hydrolysates.

Cussler *et al.*[17] went a step further in providing a technologically viable scheme for using cross-

TABLE 4—CONCENTRATION OF MACROMOLECULES USING DRY GEL STICKS*

Macromolecule	M_r	pI	Experimental pH	Concentration mg ml^{-1} Initial	Concentration mg ml^{-1} Final	Recovery %
Subtilisin inhibitor	10 000	5.9	7.5	800[a]	6 200[a]	85
Cytochrome c	12 500	10.8	12.8	0.1	0.8	80
Myoglobin	17 000	7.2	9.8	0.5	3.7	81
Soybean trypsin inhibitor	21 000	4.5	7.5	0.25	2.0	80
Bovine serum albumin	68 000	4.9	7.8	0.5	4.1	90
Ferritin	450 000	4 6	7.5	0.05	0.05	90.4
CM cellulose	—	—	6.0	10.0	82.0	90
Starch	—	—	6.0	5.0	41.0	84
DNA	—	—	7.5	0.02	0.16	80

* Ref. 16. [a] Concentrations of subtilisin inhibitor expressed in units/ml.

TABLE 5—CONCENTRATION OF DILUTE AQUEOUS SOLUTION USING HYDROLYSED POLYACRYLAMIDE GELS*

Mol. wt. solute	Dalton	Solute size nm	Feed conc.	Raffinate conc.	Efficiency**
Polystyrene latex	—	990	0.21	0.35	85
Bovine serum albumin	66 000	7.2	0.082	0.183	93
Heamoglobin	64 500	6.2	0.78	1.26	91
Polyethylene glycol	8 000-8 700	8.8	0.56	1.09	91
Sucrose	342	0.84	1.00	1.09	6
Urea	60	0.58	3.00	3.00	0

* Ref. 17. ** Defined as (measured increase in concentration) × (raffinate volume)(initial solution volume).

linked gels as size-selective extraction solvents. Observing that swelling characteristic of the gels is a strong function of the pH of the surrounding solution, they designed an elegant regeneration step. Small gel spheres are added to a dilute solution containing macromolecules. As the spheres swell they absorb the low molecular weight solvent but exclude high molecular weight solutes. The rafinate, now concentrated in the high molecular weight solutes, can then be separated from the swelling gels by filtration. Using gels whose swelling is a very strong function of pH, addition of an acid would collapse the gel volume and release much of adsorbed solvent. The collapsed gel is then separated from the released solvent by filtration and added to a small amount of base, gel can then be added to a fresh solution where it will swell again. Some of the results on concentration of dilute solutions using such polymeric gels obtained by Cussler *et al.* are shown in Table 5. It is readily seen that excellent efficiency of separation is achieved especially for higher molecular weight solutes. In particular, it was seen that solutions which are greater that 3 nm in diameter could be concentrated with an efficiency of at least 80%. These efficiencies are reduced by weak solute absorption on the surface of the gel spheres. For example, for the 34.6 nm polystyrene latex, some latex adhered weakly to the gel surface. When this latex was removed by washing, the reported extraction efficiency was 97%. In this sense, the el extractions are similar to freeze concentration echniques used in the food industry, where solutes an adhere to ice crystals. For such techniques to be technologically viable, repeated use of the gels should be possible. Cussler *et al.* have provided data which show that for upto 12 cycles of regeneration there was practically no change in the latex concentration efficiences. They noticed that there was a little cumulative loss due to the latex adsorption on the gel. This adsorption, which is responsible for inefficiencies, is apparently most significant for the first cycle and is less important as the gel is reused. There is an obvious limitation on the cut-off point with respect to the solute-size. However, the work at National Chemical Laboratory indicates that by increasing the density of crosslinks in the polymeric gels it should be possible to shift this point. If the gel interacts equally with water and with the protein solute, it will still absorb only the water, because the protein is too large to diffuse between the gels crosslinks. As a result, gels would be like extraction solvents whose selectivity will depend on differences in rates of diffusion. The development of these gels could open up a new era of separation technology. Cosiderable research for lowering the cut-off point for separation appears to be necessary.

The disadvantage of solute loss due to adsorption essentially occurs due to the direct contact between the water absorbing gel and the solute. Besides, the batch made of operation has an inherent disadvantage. Recently, Kulkarni *et al.*[18] have developed an improved separation process, which eliminates these drawbacks. Fluxes of the order of 0.8-1.4 kg/m^2 h atm have been reached, such devices show a considerable promise for future developments.

Stress induced separations :

There is a growing awareness now that macromolecules tend to migrate whenever there is a variation of shear rate in a following medium. More precisely stated, in any non-homogeneous deformation field it is impossible to maintain a uniform polymer concentration for a sufficiently long length of time. A number of possible mechanists explanations for such changes have been reported in the literature and we shall summarise some of these. What is important to appreciate is the possible role that such phenomena might play in practical separation systems.

Some suggestions attributing the phenomena of polymer migration to the changes in entropy arising out of the deformation of the molecule had appeared in the sixties[19,20]. The essence of the proposed hypothesis was that in a deforming liquid, the macromolecules would stretch and thus create free energy differences in different positions within the fluid. More specially, in a non-uniform flow field, the entropy and free energy would become position dependent. In order to compensate for such free energy changes, concentration gradients would be induced. The end result is that polymer molecules would migrate towards regions of low stress level. If a polymer solution was to flow through a capillary then a polymer depleted low viscosity layer will be formed adjacent to the wall through which the high viscosity liquid might appear to slip through.

Recently, several researchers[21-24] have laid major stress on developing a quantitative description of such hypothesis. Metzner[25] developed the following expression for the concentration difference adjoining a stagnant region (2) and flowing region (1) of a dilute polymer solution,

$$\ln \frac{C_2}{C_1} = \frac{\operatorname{tr} \underline{\underline{\tau}}}{2\, RT\, C_1}$$

where, C is the concentration, R is the gas constant, T is the absolute temperature and $\underline{\underline{\tau}}$ is the deviatoric stress. Since tr $\underline{\underline{\tau}}$ is always positive, the above equation suggests that with an increasing intensity of stress field, the concentration in the stagnant region is increasingly higher when compared to that in the flowing liquid. The above development has a very important consequence in a number of areas and some of these are summarised below.

Secondary oil recovery :

The most important field in which the phenomenon of polymer migration may have a major influence is the flow through a porous medium. Oil recovery, for exampe, employs water soluble polymers as mobility control agents for the flowing liquid used to drive out the oil trapped within the porous reservoir structure. Among various other complexities associated with polymer flow through porous media, polymer retention is a critical factor affecting the oil recovery. Although retention can be due to noncontinuum effects, like adsorption and pore blockage, separation due to polymer migration from the flowing stream to the relatively stagnant dead end pores is quite possible. In fact, the observation by petroleum technologists in the case of flow of a polysaccharide and polyacrylamide solutions through different porous media shows evidence of such polymer separation and retention[27].

Size exclusion chromatography :

Size exclusion chromatography involves flow of polymer solutions through packed columns wherein the fluid is subjected to an ill-defined non-uniform flow field. The resulting macromolecular migration and consequent separation therefore significantly alters the elution characteristics. The flow rate dependent elution characteristics reported exhaustively by Aubert and Tirrell[28,29] confirm this behaviour.

Polymer fractionation :

If the argument about entropy induced changes leading to polymer molecule separations is correct then such a mechanism should tend to a fractionation of polymer molecule with respect to molecular weight along the radius of a capillary. The possibility of molecular fractionation was experimentally studied by Shreiber and Storey[30] using polyethylene melt extruded through a capillary and a microtonic procedure to obtain peripherial layer of the polymer. They observed as high as 40% reduction in molecular weight of this outer layer as compared to that of the whole extrudate. Whitlok and Porter[30] undertook similar measurement of capillary extrusion of polystyrene and again obtained differences in molecular weight. However, the influence of stress induced polymer fractionation was somewhat negligible. It is quite possible that the flow lengths used by Whitlock and Porter were insufficient. The degradation effects might also complicate the situation further.

An exciting shear field flow fractionation technique (shear FFF) has been described recently by Giddings and Brantley[31]. The configuration of the device is a concentric cylinder system with the inner cylinder rotating. The axial motion is superposed on the rotational motion. Simplified analysis indicates that a molecular fractionation with very high selectivity can be attained rather easily. In fact maximum selectivity factors of 3 could be achieved, which are better than all other separation techniques, such as sedimentation FFF(1), thermal and flow FFF(0.5), steric FFF(0.30) and size exclusion chromatography (0.05 to 0.22).

Concluding remarks :

In the foregoing, we have summarised some of the recent advances in separation techniques that have emerged over the past few years. A number of these prove the 'scientific feasibility' of the concepts, but we are sure that with continued

research efforts, these could prove to be 'technologically viable' and open up a new era of separation processes.

References

1. S. L Matson, J. Lopez and J. A. Quinn, *Chem. Eng. Sci*, 1983, **38**, 503.
2. S. A. Stern and H. L. Frisch, *Ann. Rev. Mat. Sci.*, 1981, **11**, 523.
3. H. K. Lonsdale, *J. Membrane Sci.*, 1982, **10**, 81.
4. D. R Paul and G. Morel, *Encyclopedia of Chemical Technology*, 1981, **15**, 92.
5. Y. Osada, *J. Polym. Sci. Polym Lett Ed.*, 1980, **18**, 281.
6. Y. Osada and M. Sato, *Polymer*, 1980, **21**, 1057.
7. Y. Osada and Y. Takeuchi, *J. Polym. Sci.*, 1981, **19**, 303.
8. C R. Fox, *Hydrocarbon Processing*, 1975, **54**, 109.
9. C. R. Fox, *Hydrocarbon Processing*, 1978, **57**, 269
10. S. J. Parulekar, M. M Sharma, J. B. Joshi and Y. T. Shah, *J. Sep Proc. Technol.*, 198?, **3**, 2.
11. T. Furusawa and J. M. Smith, *AIChE J.*, 1974, **20**, 88.
12. H. Komiyama and J. M. Smith, *AIChE J.*, 1974, **20**, 728.
13. N. Kowabata and K. Ohira, *Environ. Sci. Technol*, 1979, **13**, 1396.
14. F. M. Husband and A. G. Rowley, *Chem. Ind. (London)*, 1932, 118.
15. T. J. Narendranathan and P. Dunhill, *Biotechnol. Bioeng.*, 1982, **24**, 2103.
16. H. G. Vartak, M. V. Rele, M. Rao and V. V. Deshpande, *Anal. Biochem.*, 1983, **133**, 2?0.
17. E. L. Cussler, M. R Stokar and J. E. Varberg, *AIChE J.*, 1984, **30**, 578.
18. J. H. Aubert and M. Tirrell, *Sep. Sci. Technol.*, 1980, **15**, 123.
19. W F. Busse, *J Polym. Sci., Part A*, 1967, **2**, 1261.
20. H. P. Shreiber and S. H. Storey, *J. Polym. Sci, Part B*, 1965, **3**, 723.
21. A. Dutta and R. A. Mashelkar, *J. Polym. Sci.*, 1982, **27**, 2739.
22. A. Dutta and R. A. Mashelkar, *Rheol. Acta*, 1982, **21**, 52.
23. A. Dutta and R. A. Mashelkar, *J. Non-Newt. Fluid Mech.*, 1984, **16**, 279.
24. Y. Cohen and A B. Metzner, *J. Rheol.*, 1985, **29**, 67.
25. Y. Cohen and A. B. Metzner, *AIChE Symp. Ser.*, 1982, **212**, 78, 77.
26. A B. Metzner in "Improved Oil Recovery by Surfactant and Polymer Flooding", eds. D. O. Shah and R. S. Schechter, Academic Press, New York, 1977, p. 439.
27. J. M Maerker, *J. Pet. Technol.*, 1973, **25**, 1307.
28. J. H. Aubert and M. Tirrell, *Sep. Sci. Technol.*, 1980, **15**, 123.
29. J. H. Aubert and M Tirrell, *J. Liq. Chromatogr.*, 1983, **6**, 219.
30. L. R. Whitlock and R. S. Porter, *J. Polym. Sci., Part A*, 1972, **2**, 877.
31. J. C. Giddings and S. L. Brantley, *Sep. Sci. Technol.*, 1984, **19**, 631.

J. Indian Chem. Soc.,
Vol. LXIII, January 1986, pp. 157-160

Poly(vinyl propionate) and Poly(ethyl acrylate)—A Miscible Polymer Pair†

C. BHATTACHARYYA, S. N. BHATTACHARYYA and B. M. MANDAL*

Department of Physical Chemistry, Indian Association for the Cultivation of Science, Jadavpur, Calcutta-700 032

A new miscible polymer pair, *viz.* poly(vinyl propionate) (PVPr) and poly(ethyl acrylate) (PEA) is reported. Blends of these polymers form clear films, clear solutions in common solvents and have single glass transition temperatures. Miscibility of these two polymers in binary combinations with poly(methyl acrylate) (PMA) or poly(vinyl acetate) (PVA) was also examined. Differential scanning calorimetry (D.S.C.) reveals that PVPr+PVA, PEA+PVA, PMA+PVPr and PMA+PEA are immiscible, although the first three pairs form clear films.

ISCIBLE blends of polymers are of rare occurrence[1,2]. This situation arises because mixing of molecules of similar chemical nature is ısually associated with small positive heat of mixing. n the case of small molecules this positive heat of nixing does not pose a problem towards homogeneous mixing because its unfavourable effect is out-eighed by the combinatorial entropy of mixing which is positive. For polymer-polymer mixtures, he value of the latter per unit volume is exceedingly small in comparison to that for mixtures of small nolecules due to the much smaller number of molecules involved in the former systems. The heat of nixing per unit volume, on the other hand, is a unction of the number of segmental contacts which emains nearly constant with increase in molecular ize. The result is that for polymer-polymer mixures, the heat of mixing becomes the determining actor for miscibility.

An additional unfavourable factor arises from he difference in the free volumes of the components which results in a positive non-combinatorial free nergy of mixing[3]. Thus, unless the components of binary polymer mixture are so similar in chemical roperties that the heat of mixing is zero or very ear to it and also unless they are similar in physical roperties, is homogeneous mixing of like polymers chieved. However, unlike the polymer pairs which ave complimentary similarity, those having complimentary dissimilarity are miscible because the nixing is exothermic in such cases due to the resence of strong specific interactions between iem[4]. The latter may be regarded as a manifestaon of the existence of complimentary dissimilarity etween polymer pairs.

Nevertheless, there exist few examples of pairs f like polymers which are miscible. Recently, we ave reported that the like polymer pair PVA, $-CH_2-CH(OCOCH_3)-$, and PMA, $-CH_2-CH(COOCH_3)-$, is miscible and their miscibility is not ue to the existence of any complimentary dissiilarity between them[5]. This system must therefore be associated with an exceedingly small heat of mixing. This is not unlikely as the repeating unit of the two polymer molecules differ only in the orientation of the COO group as would be evident from their chemical structures shown above. They also do not differ much in physical properties[6]. Their T_g values differ by about 30° (T_g of PVA is 32° and that of PMA is 3°)[7]. It occurred to us that the higher homologues of these two polymers having the same number of carbon atoms in their respective repeating units might be miscible. We hypothesised that the next higher homologues, *viz.* PVPr, $-CH_2-CH(OCOCH_2CH_3)-$ and PEA, $-CH_2-CH(COOCH_2CH_3)-$, stand in better stead than the PVA+PMA system with regard to the similarity in chemical properties inasmuch as their hydrogenated monomers are identical, being ethyl propionate for both. If the hydrogenated monomers are approximated as polymer segments[8], the heat of mixing, due to exchange interaction, should be approximately zero and smaller than that for PVA+PMA systems for which the hydrogenated monomers, although very similar, are not identical. Also, the difference in the T_g values of PVPr and PEA is about 34° which is similar to that for PVA and PMA system (T_g of PVPr is 10° and that of PEA is −24°)[6]. Hence, the difference in free volumes of the components in this blend will also be of the same order as between PMA and PVA. We report here a preliminary study of the miscibility of PVPr and PEA.

It would be also of interest to examine whether the other binary blends obtainable from the four polymers PMA, PEA, PVA and PVPr are miscible. This paper reports also the results of preliminary investigations on the miscibility of these blends.

Experimental

The solvents were of reagent grade. They were dried and distilled before use. Ethyl acrylate monomer was an I.P.C.L. product.

† Dedicated to Professor Sadhan Basu on the occasion of his 65th birthday.

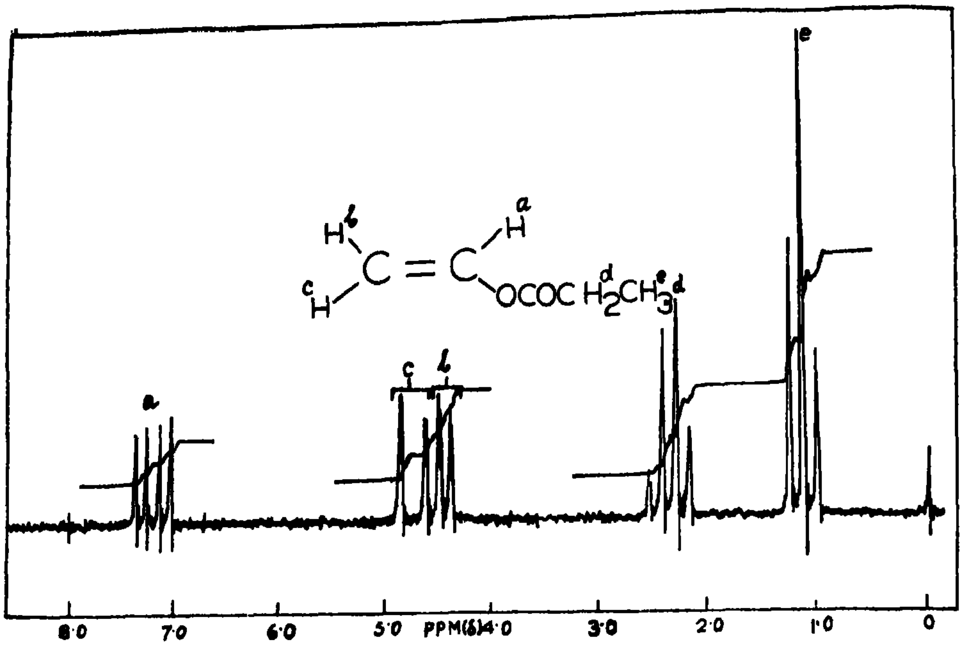


Fig. 1. The ^{1}H nmr spectra of vinyl propionate in CCl_4 with TMS as internal standard

Vinyl propionate was synthesised from vinyl acetate and propionic acid by the vinyl interchange reaction following Adelman[9]. Anhydrous propionic acid was obtained from L.R. grade propionic acid (Loba) by fractional distillation using a column (1 m long) packed with porcelain rings (3 mm). Vinyl acetate (L.R.) was dried over $CaCl_2$ and distilled under reduced pressure. Vinyl acetate (25 mol), mercuric acetate (11.5 g), concentrated H_2SO_4 (3 g) and copper acetate (0.5 g) were mixed in a 5 liter 3-necked flask provided with a mercury-seal stirrer. The flask was cooled to 20°. Anhydrous propionic acid (4 mol) was added slowly while stirring. Stirring was continued for 2 h after which it was stopped and the reaction mixture in the stoppered flask was allowed to stand at 30° for 72 h. The reaction was stopped by the addition of sodium acetate (12 g) and the mixture was fractionally distilled at reduced pressure using the same column as described above. The fraction boiling in the range 48-52° at 16.5-17.2 cm Hg pressure, was collected and refractionated under reduced pressure using propionic acid as a chaser and copper acetate (0.2 g) as polymerisation inhibitor. Pure vinyl propionate was obtained in 30% yield. The ^{1}H nmr spectra of the material (Fig. 1) recorded using a Varian T-60 instrument at room temperature showed it to be pure. The resonances due to the various protons are indicated in the figure.

PEA ($\bar{M}_n$ = 773 000) was prepared by the solution polymerisation of the monomer in benzene (20%, v/v) at 60° under a nitrogen atmosphere using 2,2'-azobisisobutyronitrile (AIBN) as initiator (0.1%, w/v). The polymerisation was carried to 20% conversion and the polymer was isolated by precipitating into petroleum ether (b.p. 40-60°). The polymer was purified by dissolution in benzene and precipitation into petroleum ether.

PVPr ($\bar{M}_n$ = 34 700) was prepared by polymerising vinyl propionate in bulk using AIBN initiator (0.1%, w/v) at 60° in an ampoule which was provided with a vacuum stopcock and a teflon coated stirring bar. The monomer was thoroughly degassed in a high vacuum line to 2×10^{-6} torr using the standard freeze-thaw technique. Polymerisation was continued for a pre-determined time (1.5 h) to keep the conversion low (*ca.* 15%) in order to minimise branching. After polymerisation the monomer was distilled off the polymerised solution in the high vacuum line into a similar ampoule in which a calculated amount of initiator was previously introduced. The monomer was again degassed and the polymerisation conducted at 60° as before. This procedure was repeated 6 times. Increasingly lesser time was required to achieve similar conversion as the recovery and polymerisation cycle progressed. In this way 30 g polymer was obtained from 55 g monomer and 15 g monomer still remained. The polymer was isolated by dissolving it in benzene and precipitating into petroleum ether. All the 6 batches of polymers were mixed and purified by dissolving in benzene and precipitating into petroleum ether. All polymer samples were finally dried in a vacuum-oven at 100° for 3 days. The preparation of the blends was already described[6]. PMA was a fractionated sample ($\bar{M}_v$ = 705 940) described earlier[5]. PVA was a whole polymer (AYAF-419) ($\bar{M}_v$ = 98 000) obtained from Union Carbide Corporation (U.S.A.).

Casting film of polymer blends : A 2% solution of the two polymers in the desired ratio was poured in a Petri dish which was then kept in a desiccator over $CaCl_2$. The desiccator was provided with a small opening for the evaporation of the solvent. The clarity of the film was examined visually. The blend was isolated by wetting the film with water and dried in a vacuum-oven at 100° for 3 days and used for T_g measurements.

Determination of miscibility of blends in common solvent : Required amounts of polymer blends of known compositions and solvents were weighed into 6 mm glass tubes (Corning). The tubes were sealed and the clarity of the solutions was examined after an equilibration period of 96 h.

Determination of glass transition temperature (T_g) *:* The T_g's were measured using a Perkin-Elmer DSC-2C or a DSC-2 differential scanning calorimeter (D.S.C.) calibrated with indium, water and n-octane. The blends were held at 373 K in the D.S.C. apparatus for 15 min and then quenched to 200 K where they were held for 5 min. The samples were then scanned at the heating rate of 20 K min^{-1} for the PEA+PVPr blends and 10 K min^{-1} for others from 200 to 373 K. T_g values were taken as the onset of the change of slope in the heat capacity plot determined by extrapolating both slopes to the point of intersection.

Molecular weight determinations : Intrinsic viscosity was determined in benzene at 30°. The following equations was used to obtain $\bar{M}_n$; for poly(ethyl acrylate),

$$[\eta] = 27.7 \times 10^{-5}\ M_n^{0.67}$$

and for poly(vinyl propionate) Buselli *et al.*[10] used the equation for poly(vinyl acetate) given by Nakajima[11],

$$[\eta] = 8.91 \times 10^{-8}\ \bar{P}_n^{0.62}$$

Results and Discussion

In order to determine the miscibility of the two polymers PVPr and PEA, the clarity of the films of their blends was first examined. For this purpose the films were cast from four different solvents, *viz.* toluene, 1,2-dichloroethane (DCE), ethyl acetate (EtOAc) and acetone which represent four different chemical classes, *viz.* aromatic hydrocarbon, chlorinated aliphatic hydrocarbon, aliphatic ester and aliphatic ketone, respectively. Three blend compositions, *e.g.* PVPr : PEA = 3 : 1, 1 : 1 and 1 : 3 by weight were tested ; films of each blend composition being cast from all the four solvents. All the films turned out to be clear providing the first evidence that the polymer pair is miscible.

It should however be noted that the film clarity test alone does not provide unequivocal proof that a polymer pair is miscible. An immiscible pair may yield clear films if the refractive indices of the polymers are closely matched. On the other hand, a miscible polymer blend may yield an opaque film if it is cast from a solvent, the strengths of interaction of which with the two polymers differ greatly[12].

A further test for the miscibility of the two polymers is to check the clarity of the solutions of the blends in common solvents. Clear solutions at all compositions are indicative of miscible polymer-polymer systems. However, a cloudy solution does not necessarily prove that the polymers are immiscible. For example, Patterson *et al.* showed theoretically as well as experimentally that a miscible polymer pair may yield a cloudy solution in a common solvent if the strengths of interaction of the solvents with the two polymers differ from each other, the maximum tolerable difference in the values of the χ parameters for obtaining clear solution depends on the molecular weights of the two polymers and the value of the thermodynamic interaction parameter between the miscible polymer pairs[12-14]. The polymer pair PEA+PVPr gives clear solutions at room temperature at all compositions in the two solvents tested, *viz.* acetone and toluene. This observation indicates that the two polymers are miscible at least at room temperature (*ca.* 32°).

Finally, the ultimate evidence in support of the homogeneity of the polymer blends is available from T_g studies. The differential scanning calorimetry (D.S.C.) traces of the polymer blends of PVPr+PEA at 7 different compositions along with those of the pure polymers are shown in Fig. 2. It is evident from the figure that each blend is characterised by a single T_g. The T_g's of the blends lie in between the T_g values of the pure components.

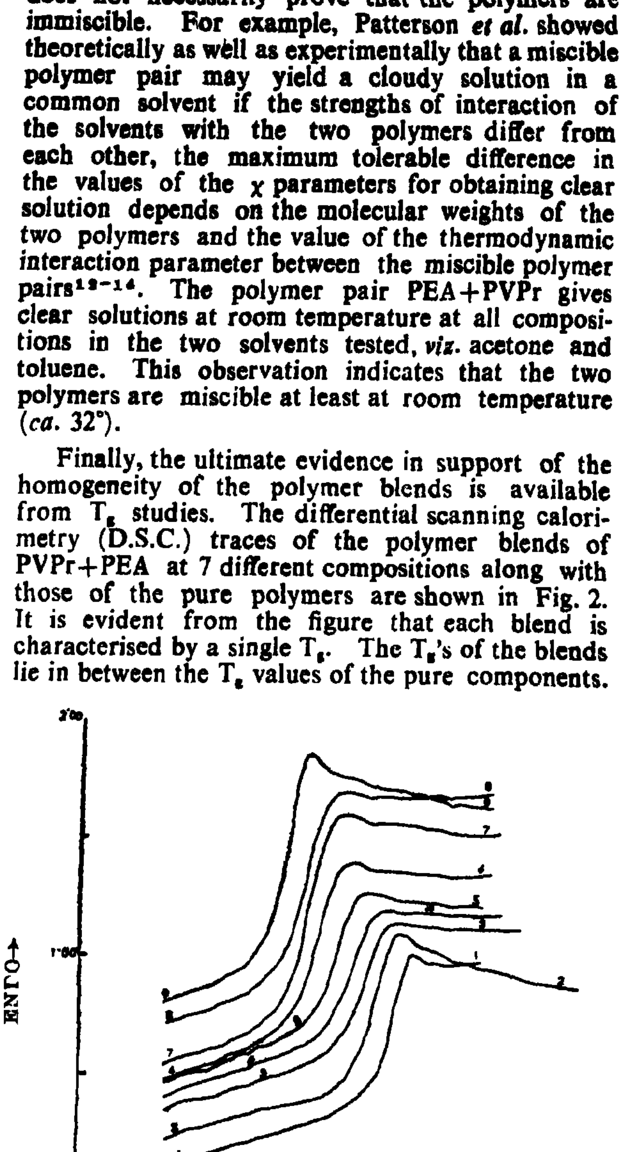


Fig. 2 The differential scanning calorimetry traces of the pure polymers PVPr and PEA and their blends. The weight fractions of PVPr in the blends for curves 1 through 9 are 1, 0.88, 0.75, 0.66, 0.50, 0.38, 0.25, 0.16 and 0, respectively.

From the above observations we conclude that PVPr and PEA are miscible in all proportions.

Thus, our expectation regarding their miscibility turns out to be correct. Further investigations with regard to construction of phase diagrams, determination of thermodynamic interaction parameter (χ_{23}) *etc.* between the components of this polymer pair are in progress in our laboratory.

Regarding the miscibility of the other blends obtainable from the four polymers PMA, PEA, PVA and PVPr, we note that six binary combinations are possible from these four polymers. These are PMA+PVA, PEA+PVPr, PMA+PEA, PVA +PVPr, PMA+PVPr and PEA+PVA. Of these we have shown here and earlier that the first two yield miscible blends[5]. The literature reports that solutions of PMA and PEA phase separate in many solvents and hence they are immiscible[15]. In agreement with this observation we have found that the blends of these two polymers form opaque films. All the remaining three pairs (at 1 : 1 w/w composition) form clear films when cast from benzene, toluene or acetone. However, the D.S.C. traces reproduced in Fig. 3 show that each of the two pairs, *viz.* PVA+PVPr and PEA+PVA exhibits two T_g's indicating that these combinations

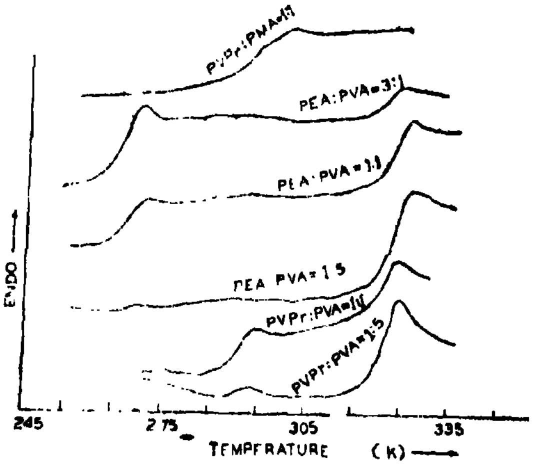


Fig. 3. D.S.C. traces of the polymer blends indicated in the figure.

make immiscible blends even though they give clear films. In the literature PEA and PVA have been stated to be compatible without, of course, any proof[16]. The T_g results just described do not support this view. The miscibility of the remaining pair PMA+PVPr could not be clearly established by D.S.C. because the T_g's of the component polymers are too close to permit satisfactory resolution even though their exist two T_g's. A D.S.C. trace for the 1 : 1 blend is included in Fig. 3. A shoulder is of course, noticed half way the D.S.C. trace for the 1 : 1 blend. From this observation and also from the immiscibility of the other pairs for which the carbon numbers of the repeating units are not equal, it is reasonable to conclude that PMA and PVPr are not miscible.

It may be concluded from this study that there exist good chances to find miscible binary blends from the combination of a polyvinyl ester and a polyacrylate when the carbon numbers of the repeating units are equal. This conclusion follows from the observation that PMA+PVA, and PEA+PVPr are miscible and from the arguments set forth in the introduction section.

Acknowledgement

The authors would like to express their sincere thanks to Mr. S. K. Ray, Department of Chemistry, McGill University, Montreal, Canada, for kindly performing the differential scanning calorimetry of the PEA+PVPr polymer blends using a Perkin-Elmer DSC-2C instrument. Thanks are also due to I.P.C.L., Baroda, and to Union Carbide Corporation, U.S.A., for gift samples of ethyl acrylate and PVA, respectively.

References

1. A. Dobry and F. Boyer-Kawenoki, *J. Polym. Sci.*, 1947, **2**, 90.
2. R. L. Scott, *J. Chem. Phys.*, 1949, **17**, 279.
3. D. Patterson, *Macromolecules*, 1969 **2**, 672.
4. O. Olabisi, *Macromolecules* 1975, **8**, 316.
5. A. K. Nandi, B. M Mandal and S. N. Bhattacharyya, *Macromolecules*, 1985, **18**, 1454.
6. "Polymer Hand Book", eds. J Bandrup and E. H. Immergut, 2nd ed., Wiley, New York, 1975, Chap. III.
7. E. H. Riddle, "Monomeric Acrylic Esters", Reinhold, New York, 1954, p. 60.
8. R L. Adelman, *J. Org. Chem.*, 1949, **14**, 1057.
9. H. Sumitomo and Y. Hachihama, *Kobunshi Kogaku*, 1955, **12**, 479
10. A. J. Buselli, M. K. Lindemann and C. E. Blades, *J. Polym. Sci.*, 1958, **28**, 485.
11. A. Nakajima, *Kobunshi Kogaku*, 1949, **6**, 451 (*Chem. Abstr.*, 1951, **46**, 1294).
12. A. Robard, D. Patterson and G. Delmas, *Macromolecules*, 1977, **10**, 706.
13. A. Robard, Ph. D. Thesis, McGill University, Montreal, 1978.
14. L. Zeman and D. Patterson, *Macromolecules*, 1972, **5**, 513.
15. S. Krause in "Polymer Blends", eds. D. R. Paul and S. Newman, Academic Press, New York, 1978, Vol. 1, p. 79, and references therein.
16. J. F. H. Van Eijnsbergen, *Chim. Peintures*, 1941, **4**, 253. (quoted in Ref 15, p. 72).

J. Indian Chem. Soc.,
Vol. LXIII, January 1986, pp. 161-167

A Statistical, Quantum Mechanical and Acoustic Study of Liquids†

R. V. GOPALA RAO

Department of Physical Chemistry, Jadavpur University, Calcutta-700 032

Modern liquid state theories deal with various aspects of liquids and solutions. Some of the methods used in tackling the problems that confront the chemist have been described in this short review, which incidentally give the tremendous progress made in the application of these theories to liquids and solutions. This paper reviews the progress made in this field including some of the contributions made by the author and his group.

CHEMISTS deal extensively with liquids and solutions. The application of equilibrium and non-equilibrium statistical mechanics to liquids[1-8], solutions[9], liquid metals[10-15], alloys[16-20] fused salts[21-25] and to such complex mixtures like emulsions[26,27] is a strong proof of the importance of this discipline in the investigations of chemical problems. The primary object of these studies is to obtain both equilibrium and non-equilibrium properties of liquids in terms of inter-molecular forces.

The earlier theories are partly phenomenological in character. Thus, the surface tension and compressibility is connected by a two parametric equation and can be written as[108-110]

$$Y=\left(\frac{A}{\beta_T}\right)^{\tau} \tag{1}$$

where, A and τ are found to be general constants nearly equal to 0.021 atm^{-1} (erg s^{-2})$^{\tau}$ and 1.624, respectively.

Further, $C_1 = \left[\frac{\partial}{\partial p}(1/\beta_T)\right]_T$ first used by Born and was extensively investigated by Rao and his group, its connection to various potential parameters and intermolecular force constants. Thus for the potential function,

$$U(r)=A\ r^{-n}-B\ a^{-m}-C\ a^{-p} \tag{2}$$

C_1 is given by[111]

$$C_1=\frac{1}{3}\,\frac{[Rm(n-m)(n+m+6)+p(n-p)(n+p+6)]}{Rm(n-m)+p(n-p)} \tag{3}$$

where, R is the gas constant.

Further, the molecular diameter, σ, is related to C_1 through the δ parameter as [112-115]

$$\frac{(3C_1-1)}{2}=\delta \tag{4}$$

and

$$\sigma=(\delta-1)\delta^{-1}\ V^{1/3}\ N^{-1/3} \tag{5}$$

It is also connected to the velocity of sound, U_1, at various pressures as [46]

$$U_1=Cp^{\lambda} \tag{6}$$

where,

$$\lambda=\frac{C_1-1}{2} \tag{7}$$

Similarly, assuming a polynomial to represent the pressure of a fluid as

$$P=\frac{RT}{V}+\frac{B_2}{V^2}+\frac{B_3}{V^3}+\frac{B_4}{V^4} \tag{8}$$

one can obtain a relation between the compressibility and vapour pressure fluid as[117]

$$\frac{\beta_T RT}{V_1}\left[6\ \ln\left(\frac{RT}{pV_1}\right)-11\right]=1 \tag{9}$$

where V_1 is the molar volume of the liquid, β_T is the isothermal compressibility and p is the vapour pressure at temperature T.

However, the thermodynamic and other equilibrium properties, according to modern statistical mechanical theories can be simply obtained through the use of the structure factor (SF)[16-27] or its Fourier transformation (FT), namely the radial distribution function (RDF)[1,2]. It is possible to obtain through purturbation theories equation of state[28-31], through which equilibrium properties can be obtained. Further, the static SF and RDF can be used to obtain the transport properties[32-36], thus pointing to the fact that one can obtain all properties of liquids through a unified approach.

Significant structure theory :

Much of the work done on significant structure theory is based on a large number of parameters and hence, has been criticised and is not used now. However, the theory can be utilised to predict the properties of liquids[37-42] even though it may be considered empirical.

Distribution function theories :

The most notable contribution in the study of liquids is the analytical solution for the direct corre-

† Dedicated to Professor Sadhan Basu on the occasion of his 65th birthday.

lation function (DCF) obtained with the hard sphere potential function for the non-linear Percus-Yevick integral equation by Wertheim[43] and Thiele[44]. The DCF is defined through the equation known as the Ornstein-Zernike's equation written as

$$h(r_{12}) = C(r_{12}) + \rho\int c(r_{23}) \cdot h(r_{23})d\vec{r}_3 \qquad (10)$$

where, $h(r_{12})$ is the total correlation function and is equal to $[g(r)-1]$ and $C(r_{12})$ is the DCF.

Atomic liquids :

Through the use of the mean spherical model approximation (MSMA) the structure function can be obtained. The MSMA is defined as

$$C(r) = C_{ref}(r) \quad r \leqslant \sigma \qquad (11)$$

$$= \frac{u(r)}{K_BT} \quad r > \sigma \qquad (12)$$

where, $C_{ref}(r)$ is the reference DCF which is generally taken as the hard sphere system and $u(r)$ is the potential function. Extensive work done by the author and his students has shown that in the case of metals the square-well potential is an appropriate potential[1,3,45-51]. Even in the case of non-metallic liquids the square-well potential gives reasonably good results. The SF defined in the case of atomic liquids can be written as

$$S(k) = \frac{1}{1-\rho\tilde{C}(k)} \qquad (13)$$

where, $\tilde{C}(k)$ is the FT of C(r), the DCF.

The structure factor in the improved MSMA requires that the DCF outside the core is given by

$$C(r) = -\beta u_1(r)\, g_0(r) + \tfrac{1}{2}\beta^2 u_1^2\, g_0(r) \qquad (14)$$

instead of that given in equation (12), where $u_1(r)$ is the perturbing potential and $g_0(r)$ is the reference hard sphere RDF. Extensive calculations in the evaluation of SF of several metals have been made by Rao and Sen[18] and Rao and Joardar[19] with this approximation.

In the long wave limit the SF is related to compressibility as

$$S(o) = \rho k_B T \beta_T \qquad (15)$$

where, β_T is the isothermal compressibility and the rest of symbols have their usual significance. From equation (15) it is possible to formulate the equation of state through the random phase approximation (RPA) and one can then obtain various thermodynamic properties[18,28-31,46]. In addition, it is possible to obtain from the SF the potential function of the molecules[47-50]. Besides, the DCF can also be obtained from the SF through the use of the following equation

$$C(r) = \frac{1}{2\pi^2\rho r}\int_0^\infty \frac{k[S(k)-1]}{S(k)} \sin kr\, dr \qquad (16)$$

From the DCF it is possible to obtain potential parameters. Such calculation have been made for methane by Rao and Murty[51].

Higher order structural correlation functions :

The pressure derivative of the SF is related to higher order correlation functions[52-54]. Rao and Murty[52] and Rao and Sen[54,53] calculated these pressure coefficients in the $\rho^{-1/3}$ model in the MSMA. Expressions for the higher order SF's in the long wave limit are also derived[52-54].

Self consistent approximation and evaluation of the virial coefficients :

The RDF at the medium concentrations can be expressed in a power series as a function of density, ρ, as

$$g(r) = e^{-\beta u(r)}[1 + \rho g_1(r) + \rho^2 g_2(r) + \ldots] \qquad (17)$$

where the $g_1(r)$ are connected to various virial coefficients of the fluid. These $g_1(r)$ can be computed topologically, and using the self consistent requirement of the pressure and compressibility equations of state one can calculate the virial coefficients[55-60].

Partial structure factors (PSF) *in alloys :*

It is not always possible to obtain PSF's of alloys from experiment. Hence, model potential calculations become imperative. Further, it is found that the potential parameters obtained for pure liquid metals can be used lucratively for obtaining the PSF's[16-20]. From these partials one can obtain the Bhatia-Thornton partial structures which are related to the thermodynamic activities of the constituents of the alloy. Even when compound formation is there the PSF's and also the *total* SF can be obtained. We give in Figs. 1-4 the partials and the total structure factors of Gold-Caesium alloy which forms a compound and considerable volume contraction[61] takes place in the compound formation. The agreement even in this case is quite satisfactory.

Triplet correlation functions in alloys can be calculated with model potentials. Such calculations of triplet correlation functions were performed in Na – K alloy by Rao and Murty[119].

Fused salts :

From a consideration of the various forms of $C_{ij}(r)$, Rao and Pal[21-24] postulated that even for charged hard spheres of unequal diameter the form of $C_{ij}(r)$ remains the same inside the core as for charged hard spheres

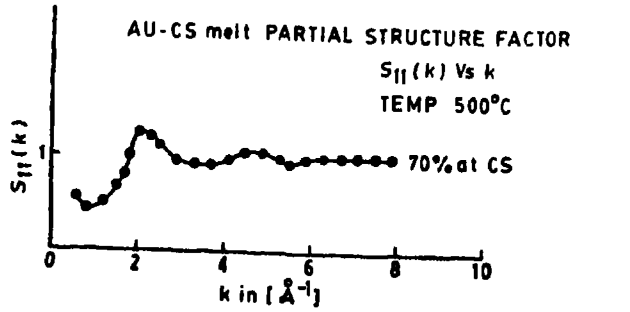


Fig. 1. Gold-caesium alloy-gold-gold partial structure at 500°, 70% at Cs.

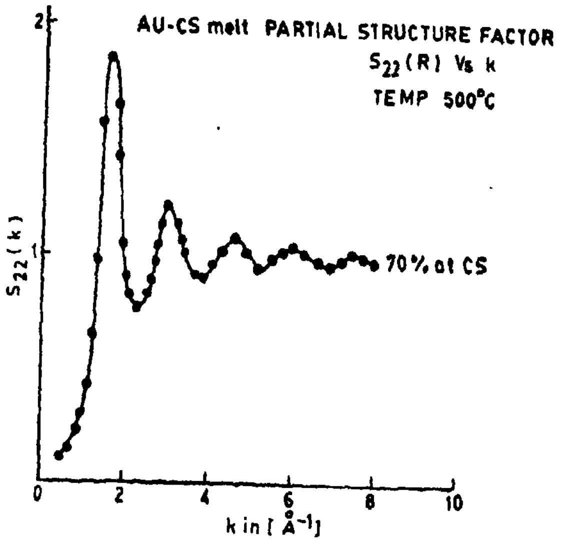


Fig. 2. Gold-caesium alloy-caesium-caesium partial structure at 500°.

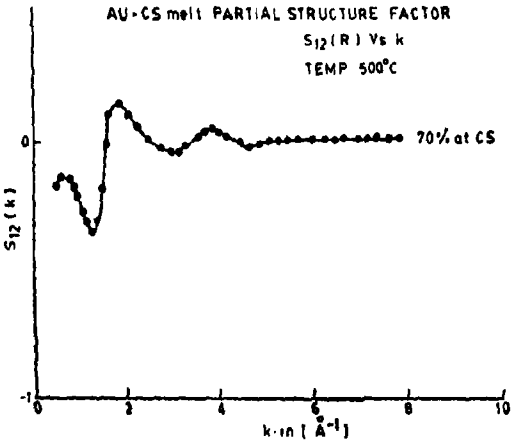


Fig. 3. Gold-caesium alloy-gold-caesium partial structures at 500°, 70% at Cs.

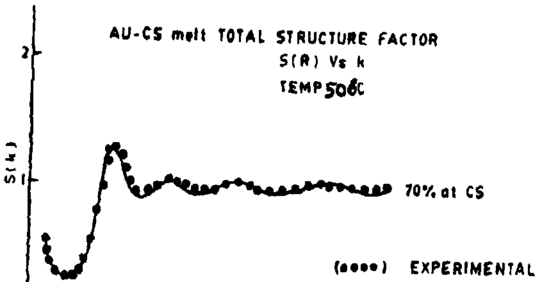


Fig. 4. Gold-caesium alloy-total structure factor at 500°.

of equal diameter. The latter have the same form as neutral and hard spheres. Thus, they concluded that the DCF of charged hard spheres should have the form as

$$C_{ij}(r)=\alpha^1+\beta^1 r+\gamma^1 r^3 \tag{18}$$

where, α^1, β^1 and γ^1 are functions of packing fraction and charge on the spheres and the details of these parameters are explained in the original papers[21-24]. Thus by suitably choosing σ and hence, $\eta=\left(\frac{\pi\rho\sigma^3}{6}\right)$ it is possible to generate $S_{ij}(k)$ the partial SF's in good agreement with experiment. We give below in Figs. 5 and 6 the partial structures and their corresponding RDF's of NaI[48]. We give

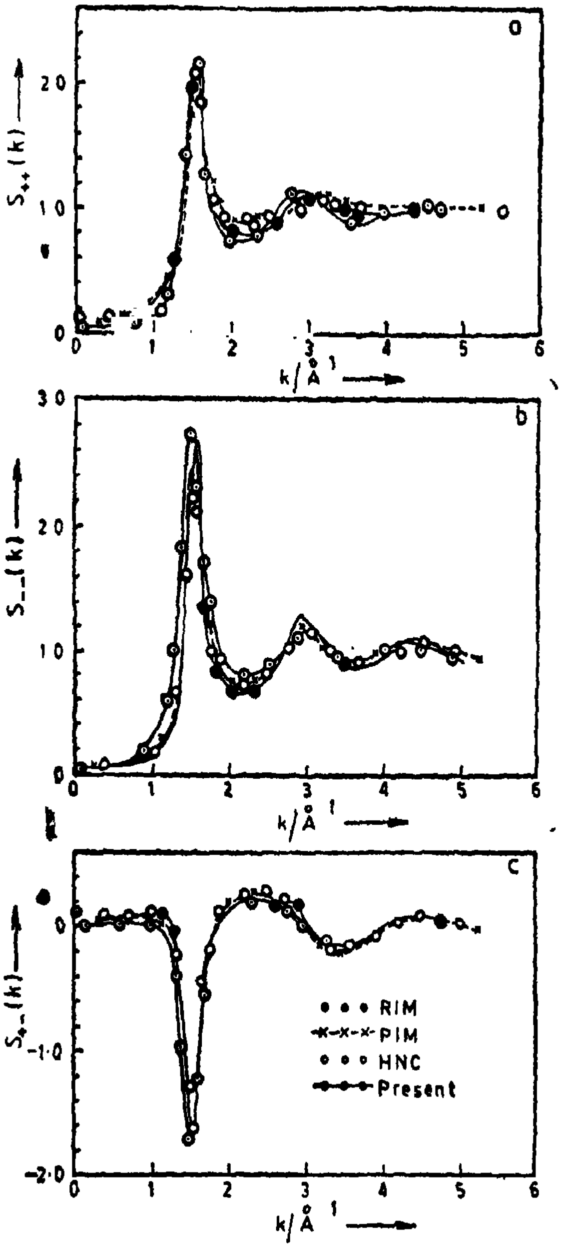


Fig. 5. Partial structure factors, S_{ij} (k) of molten NaI.

in Fig. 7 the FT of the partial direct correlation function of KCl[66].

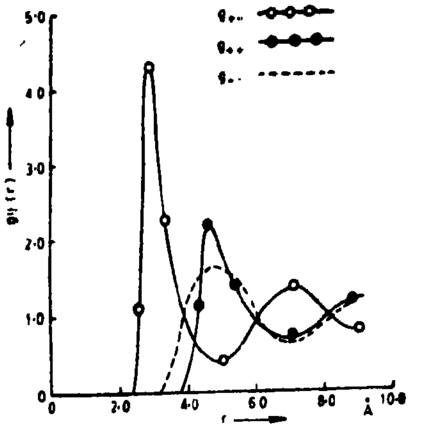


Fig. 6. Partial radial distribution function g_{ij} (r) of molten NaI.

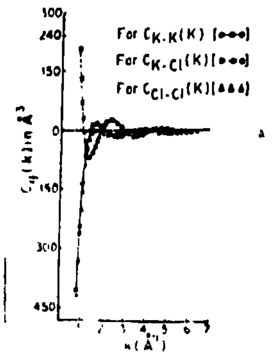


Fig. 7. Direct correlation function C_{ij} (k) for molten KCl.

Charged hard sphere model :

The charged hard sphere model can be used to calculate in the one component plasma approximation the SF's of metals with the DCF obtained by Palmer and Weeks[108] who perturbed the charged hard spheres with a coloumb potential. For accurate description of electron correlation one has to take into consideration the k dependent dielectric constant and the so-called linear screening optimisation approximation. Detailed calculations have been performed for the evaluation of the SF of noble metals[109]. These calculations can be extended for the evaluation of like charge SF's in the case of molten salts[110].

Molecular liquids :

The study of molecular liquids is rather involved because of the orientation problem of the atoms. Both intra- and inter-molecular interactions have to be considered. In the begining, the orientation model approach was used[68-69] but recently the so-called reference interaction site model (RISM) approach[70-72] and its various modification are being applied. Cummings and Stell[73] gave an excellent description of the various interaction site models for molecular liquids.

Pseudo-potential (Ps) study of liqud metals :

Gibbs-Bogoliubov's inequality principle in the thermodynamic perturbation method allows the determination of the equilibrium properties with the use of an appropriate pseudopotential[73-75]. The SF can also be generated[76,77]. However, the method is computer time consuming as the diameters have to be determined by a variation technique and does not yield accurate results.

Light scattering and frequency-dependent SF in the hydrodynamic limit :

Mountain[78] developed a single relaxation time mechanism for the evaluation of spectral distribution of scattered light. This method fails when absorption occurs by more than one mechanism. The single relaxation mechanism has been applied to toluene to obtain the intensity spectrum. From these calculations, the Brillouin shifts and phonon velocity can also be calculated[79].

Turbidity and light-scattering :

The application of statistical mechanics to emulsions, colloidal solutions and macromolecules is fast gaining momentum. The hard sphere model and the MSMA perturbation version are being used to obtain turbidity and the SF and other associated properties in these solutions. Using the compressibility data of the emulsions one can obtain the potential energy parameter[80]. The partial structures as well as turbidities[80-82] can then be predicted. When we are dealing with globular protein solutions the predictions can be very accurate. The recent studies of colloids and emulsions with the help of neutron and *X*-ray diffraction studies give structural correlation and form factors of these solutions containing macromolecules[82]. The intensities and the various structural features of the micelle at different concentrations can be predicted[82].

Acoustic aspects of the study of liquids :

Visco-elastic properties of liquids : Schofield[83] in an important paper obtained expressions for the elastic moduli of liquids through the method of fluctuation. It was shown that C_{11}, C_{12} and C_{44} are related to the I_1 and I_2 integrals, defined by

$$I_1 = \frac{\rho}{2k_BT}\int g(r)r \frac{du(r)}{dr} \vec{dr} \tag{19}$$

$$I_2 = \frac{\rho}{2k_BT}\int g(r)r^2 \frac{d^2u(r)}{dr^2} \vec{dr} \tag{20}$$

These equations were applied assuming a square-well potential for several types of liquids[84]. These I_1 and I_2 integrals coupled with Zwanzing and Mountain's equations[85] along with Lennard-Jonh 6-12 potential was applied to boron trioxide[86] to arrive at the high frequency moduli. Collins and Raffel[87] derived expressions for the shear and bulk

viscosities which can also be casted in terms of I_1 and I_2 integrals. The viscosities of B_2O_3 with a L-J 6-12 potential at various temperature[88] and also several other square-well fluids were computed[89].

The I_1 and I_2 integrals can also be applied to molten salts and the viscosities η_S and η_B and high frequency moduli, namely G_∞ and K_∞ can be obtained[89]. The Collin-Raffels equations for viscosities can be usefully applied through the use of RDF and its derivative[84,90,91].

Collins and Raffel from hydrodynamic considerations derived an expression for the friction coefficient[97], which is given by

$$\gamma^2 = \frac{\rho}{3m} \int \Delta^2 u(r)\, g(r)\, dr \tag{21}$$

Through the use of an effective mass concept first introduced by Egelstaff[92], the diffusion coefficients for the square-well and hard sphere fluids can be calculated[84,91].

Non-linear acoustics : The measurement of ultrasonic propagation constants become unreliable when sound waves of finite amplitude pass through the fluids because of non-linear effects, like acoustic streaming and distortion of wave form due to attenuation of high frequency components, since attenuation is proportional to f^2. The non-linear terms B, A and C can be obtained through the pressure derivative of sound velocity and they can be evaluated through the use of Rao-Keer constant[93], $C_1 = \left[\frac{\partial}{\partial P}\left(1/\beta_T\right)\right]_T$. These acoustic parameters have been evaluated for square-well fluids and compared with experiment[94].

Shear and structural relaxation times in liquids : Through the use of Caranhan and Starlings equation of state and Zwanzig-Mountains equation for G_∞ and K_∞ the high frequency shear and bulk moduli respectively, one can derive expressions for the shear relaxation times[95-97]. When the liquid possesses a permanent dipole moment one has to use a modified form of the equation of state in the evaluation of high frequency bulk modulus[98].

Some applications of the liquid state equations to solids :

The resemblance between liquids and solids is very similar. Extensive applications of solid state theories to derive liquid state properties is in long use[99-103]. The present equations of liquids state even though crudely assumes isotropy is solids as is true in liquids will be highly interesting to apply and find out what type of results are obtained. Assuming a hard sphere model, extensive calculations have been done by Rao and Das Gupta[104] in the evaluation of SOE's for a variety of solids. Also, the pressure derivatives of SOE's can be calculated through the pressure derivatives of I_1 and I_2 integrals.

An expression has been arrived at for C_{111} in terms of packing fraction η and S(o) the long wave limit of SF. Thus, one can calculate C_{111} through equation (22).

$$C_{111} = -\left[5 + \frac{4(1-\eta)^2\,(2+\eta)\eta}{S(o)\,(1+2\eta)^2}\right] C_{11} \tag{22}$$

All these calculated values compare favourably with the experiment.

Space limitations do not permit the author to describe the detailed applications of modern liquid state theories to electrochemical[105] and various other physicochemical problems[106,107] that one confronts in liquid state.

Acknowledgement

The author wishes to thank C.S.I.R., U.G.C., I.N.S.A. and D.S.T., New Delhi, for financial assistance to some of the authors' works described in this review.

References

1. R. V. Gopala Rao, *Proc. Indian Acad. Sci.*, 1984, **93**, 459.
2. R. V. Gopala Rao, *Curr. Sci.*, 1982, **51**, 869.
3. R. V. Gopala Rao and K. V. S. Syamasundar, *Indian J. Phys.*, 1974, **48**, 286.
4. R. V. Gopala Rao and A. K. Murty, *Phys. Stat. Sol.* (b), 1974, **66**, 703.
5. R. V. Gopala Rao and A. K. Murty, *Chem. Phys. Lett.*, 1975, **31**, 605.
6. R. V. Gopala Rao and A. K. Murty, *Z. Naturforsch.*, 1975, **30**, 619.
7. R. V. Gopala Rao and T. Nammalvar, *Pramana*, 1976, **6**, 284.
8. R. V. Gopala Rao and R. N. Joardar, *Indian J. Phys.*, *Sect. A*, 1977, **51**, 317.
9. I. R. McDonald, "Equilibrium Theory of Liquid Mixtures", Statistical Mechanics Specialist Periodic Report, K. Singer, Senior Reporter, Chemical Society, London, 1973, Vol. 1, pp. 134-64.
10. R. V. Gopala Rao and A. K. Murty, *Phys. Lett.*, *A*, 1975, **51**, 9.
11. R. V. Gopala Rao and D. Sen, *Indian J. Pure Appl. Phys.*, 1976, **11**, 135.
12. R. V. Gopala Rao and D. Sen, *Chem. Phys. Lett.*, 1976, **43**, 455.
13. R. V. Gopala Rao and R. N. Joardar, *Can. J. Phys.*, 1978, **56**, 721.
14. R. V. Gopala Rao and D. Sen, *Indian J. Phys.*, *Sect. A*, 1977, **51**, 587.
15. R. V. Gopala Rao and D. Sen, *Indian J. Pure Appl. Phys.*, 1978, **16**, 25.
16. R. V. Gopala Rao and A. K. Murty, *Indian J. Phys*, 1976, **50**, 856.
17. R. V. Gopala Rao and D. Sen, *Proc. Indian Natl. Sci. Acad.*, 1979, **45**, 10.
18. R. V. Gopala Rao and B. Das Gupta, *Phys. Rev.*, communicated.
19. R. V. Gopala Rao and B. M. Satpathy, *Phys. Stat. Sol.* (b), 1982, **110**, 273.
20. S. R. Palchaudhuri, R. N. Joardar and R. V. Gopala Rao, *Phys Stat. Sol* (b), 1984, **126**, 443.
21. R. V. Gopala Rao and S. K. Pal, *Pramana*, 1984, **22**, 529.
22. R. V. Gopala Rao and S. K. Pal, *Indian J. Pure Appl. Phys*, 1984, **22**, 696.
23. R. V. Gopala Rao and S. K. Pal, *Phys. Stat. Sol.* (a), 1984, **84**, 43.
24. R. V. Gopala Rao and S. K. Pal, *Phys. Stat. Sol.* (a), 1984, **83**, 529.
25. R. V. Gopala Rao and B. Das Gupta, unpublished.

26. M. C. S. REDDY and A. K. MURTY, *J. Mol. Struct.*, 1982, **90**, 127.
27. J. B. HAYTER, *Faraday Discuss. Chem. Soc.*, 1983, **76**, 7.
28. R. V. GOPALA RAO and T. NAMMALVAR, *Indian J. Pure Appl. Phys.*, 1976, **14**, 99.
29. R. V. GOPALA RAO and R. N. JOARDAR, *Indian J. Pure Appl. Phys.*, 1976, **14**, 905.
30. R. V. GOPALA RAO and R. N. JOARDAR, *Indian J. Pure Appl. Phys.*, 1977, **15**, 599.
31. R. V. GOPALA RAO and S. K. DATTA, *Z. Phys Chem.*, 1983, **264**, 771.
32. R. V. GOPALA RAO, *Indian J. Pure Appl. Phys.*, 1975, **13**, 459.
33. R. V. GOPALA RAO and T. NAMMALVAR, *Indian J. Phys.*, 1977, **51**, 132.
34. R. V. GOPALA RAO, R. K. CHAKRABORTY and R. BHATTACHARYA, *Indian J. Phys., Sect. A*, 1977, **51**, 145.
35. R. V. GOPALA RAO and B M. SATPATHY, *Z. Phys. Chem.*, 1983, **264**, 991.
36. R. V. GOPALA RAO and A. K. MURTY, *Pramana*, 1977, **9**, 587.
37. R. V. GOPALA RAO and K. N. SWAMY, *Z. Phys. Chem.*, 1974, **255**, 237, 299.
38. R. V. GOPALA RAO and T. NAMMALVAR, *Z. Phys. Chem., N. F.*, 1972, **78**, 64.
39. R. V. GOPALA RAO and K. N. SWAMY, *Z. Phys. Chem.*, 1970, **71**, 218 ; 1970, **72**, 241 ; 1971, **73**, 215.
40. R. V. GOAPALA RAO and T. NAMMALVAR, *Z. Phys. Chem.*, 1971, **75**, 77.
41. R. V. GOPALA RAO and T NAMMALVAR, *Indian J. Phys.*, 1970, **44**, 445.
42. R. V. GOPALA RAO and K. N. SWAMY, *Indian J. Pure Appl. Phys.*, 1970, **8**, 451, 601.
43. M. WERTHEIM, *Phys. Rev. Lett.*, 1963, **8**, 321.
44. E. THIELE, *J. Chem Phys.*, 1963, **39**, 474.
45. R V. GOPALA RAO and A. K. MURTY, *Indian J. Pure Appl. Phys*, 1975, **13**, 158.
46. R. V. GOPALA RAO and D. SEN, *Indian J. Pure Appl. Phys.*, 1981, **19**, 213.
47. R. V. GOPALA RAO and R. N. JOARDAR, *Phys. Lett., A*, 1978, **67**, 71.
48. R. V. GOPALA RAO and B. M. SATPATHY, *Indian J. Pure Appl. Phys*, 1981, **19**, 976.
49. R. V. GOPALA RAO and R. N, JOARDAR, *J. Phys. C*, 1979, **12**, 4129.
50. R. V. GOPALA RAO and D. SEN, *Proc. Indian Nat. Sci. Acad, A*, 1980, **46**, 822.
51. R. V. GOPALA RAO and A. K. MURTY, *J. Phys. C*, 1974, **7**, 2219.
52. R. V. GOPALA RAO and A. K. MURTY, *Indian J. Phys.*, 1976, **50**, 812.
53. R. V. GOPALA RAO and D. SEN, *Indian J. Phys. Sect. B*, 1978, **52**, 128.
54. R. V. GOPALA RAO and D. SEN, *Indian J. Pure Appl. Phys.*, 1978, **16**, 901.
55. R. V. GOPALA RAO and K. N. SWAMY, *Indian J. Pure Appl. Phys.*, 1972, **10**, 10.
56. R. V. GOPALA RAO and K. N. SWAMY, *Physica*, 1972, **58**, 129.
57. R. V. GOPALA RAO and K. N. SWAMY, *J. Phys. A*, 1972, **5**, 499.
58. R. V. GOPALA RAO, T. NAMMALVAR and K. N. SWAMY, *Indian J. Pure Appl. Phys.*, 1974, **12**, 47.
59. R. V. GOPALA RAO and K. N. SWAMY, *Aust. J. Phys.*, 1973, **26**, 675.
60. R. V. GOPALA RAO and T. NAMMALVAR, *Z. Naturforsch., Teil A*, 1976, **31**, 81.
61. R. V. GOPALA RAO and M. S. BHATTACHARYA, unpublished.
62. R. V. GOPALA RAO and B. DAS GUPTA, unpublished.
63. R. V. GOPALA RAO and R. N. JOARDAR, *Phys. Lett., A*, 1978, **67**, 71.
64. R. V. GOPALA RAO and R. N. JOARDAR, *J. Phys. C*, 1979, **12**, 4129.
65. R. V. GOPALA RAO and R. N. JOARDAR, *Mol. Phys.*, 1980, **40**, 309.
66. R. V. GOPALA RAO and R. N. JOARDAR, *Proc. Indian Sci Acad.*, 1981, **90**, 43.
67. R. V. GOPALA RAO and B. M. SATPATHY, *Proc. Indian Natl. Sci. Acad.*, 1982, **48**, 599.
68. R. V. GOPALA RAO and B. M. SATPATHY, *Proc. Indian Acad. Sci*, 1982, **91**, 267.
69. R. V. GOPALA RAO and R. N. JOARDAR, *J. Phys. C*, 1981, **14**, 4745.
70. R. V. GOPALA RAO and B. M. SATPATHY, *Indian J. Pure Appl. Phys.*, 1983, **21**, 92.
71. R V. GOPALA RAO and B. M. SATPATHY, *Proc. Indian Natl. Sci. Acad.*, 1984, **50**, 1262.
72. P. T. CUMMINGS and G. STELL, *Mol. Phys.*, 1982, **46**, 383.
73. R. N. JOARDAR and R. V. GOPALA RAO, *Phys. Stat. Sol. (b)*, 1982, **109**, 137.
74. R. N. JOARDAR, PALCHAUDHURI and R. V. GOPALA RAO, *Phys Stat. Sol. (b)*, 1984, **125**, k83.
75. R. N. JOARDAR, PALCHAUDHURI and R. V. GOPALA RAO, *Phys. Rev. B*, 1984, **30**, 4417.
76. R N. JOARDAR, PALCHAUDHURI and R. V. GOPALA RAO, *Indian J. Pure Appl. Phys.*, 1983, **21**, 151.
77. R. N. JOARDAR, PALCHAUDHURI and R. V. GOPALA RAO, *Acustica*, 1984, **55**, 57.
78. R. D MOUNTAIN, *J. Natl. Bur. Stand. (Washington) A*, 1966, **70**, 207.
79. R V. GOPALA RAO and R. DAS, unpublished.
80. M. C. S. REDDY, *J. Mol. Liq.*, 1985, **30**, 57.
81. E. A. NIEUWENHUIS and A. VRIJ, *J. Colloid Interface Sci.*, 1979, **71**, 321.
82. *Faraday Discuss. Chem. Soc.*, 1983, **76**.
83. P. SCHOFIELD, *Proc. Phys. Soc.*, 1966, **88**, 149.
84. R. V. GOPALA RAO and B. DAS GUPTA, *Acustica*, 1984, **55**, 241.
85. R. ZWANZIG and R. D. MOUNTAIN, *J. Chem. Phys.*, 1965, **43**, 4464.
86. R. V. GOPALA RAO and B. DAS GUPTA *Acustica*, 1985, **57**, 44.
87. F. C. COLLINS and H. RAFFEL, *J. Chem. Phys.*, 1958, **29**, 699.
88. R. V. GOPALA RAO and B. DAS GUPTA, *Acustica*, 1983, **54**, 112.
89. R. V. GOPALA RAO and B. DAS GUPTA, *Acustica Lett.*, in the press.
90. R V. GOPALA RAO, P. CHAKRABORTY and BHATTACHARYA, *Indian J. Pure Appl. Phys.*, 1977, **15**, 826.
91. R. V. GOPALA RAO and D. SEN, *Indian J. Phys., Sect. A*, 1977, **51**, 382.
92. P. A. EGELSTAFF, 'An Introduction to Liquid State", Academic Press, 1967, p. 126.
93. H. V. KEHR, *Z. Phys. Chem. (Liepsig)*, 1972, **251**, 23.
94. R. V. GOPALA RAO and R. N. JOARDAR, *Indian J. Pure Appl. Phys.*, 1979, **17**, 430.
95. R. V. GOPALA RAO and T. NAMMALVAR, *Acustica*, 1975, **34**, 51.
96. R V. GOPALA RAO and T. NAMMALVAR, *Acustica*, 1975, **34**, 88.
97. V. VENKATA-SESHAIAH, S. PANDURANGA RAO and R. V. GOPALA RAO, *Z. Phys. Chem., N. F.*, 1974, **88**, 109.
98. R. V. GOPALA RAO and R. N. JOARDAR, *Acustica*, 1978, **40**, 126.
99. E. A. MOELWYN-HUGHES, *J. Phys. Chem.*, 1957, **55**, 1246.
100. LENNARD-JONES and EEVONSHIRE, *Proc. R. Soc. London, Ser. A*, 1937, **163**, 58.
101. Z. W. SALSBURG and W. S. WOOD, *J. Chem. Phys.*, 1960, **33**, 1439.
102. B. J. ALDER and T. E. WAINWRIGHT, *Phys. Rev.*, 1962, **127**, 359.
103. A. RAHAMAN, *Phys. Rev. A*, 1964, **136**, 405.
104. R. V. GOPALA RAO and B. DAS GUPTA, unpublished.
105. C. W. OUTHWAITE, "Specialist Periodic Report Statistical Mechanics", Senior Reporter, K. SINGER, Chemical Society, London, 1975, Vol. 2.
106. D. A. MCQUARRIER, "Statistical Mechanics", Harper and Row, London, 1978.
107. A. MUNSTER, "Statistical Thermodynamics", Springer-Verlag, Berlin, 1974, Vol. II.
108. R. V. GOPALA RAO and V. V. SUBBA RAO, *Z. Phys. Chem.*, 1962, **221**, 357.

109. A. V. GROSSE, German Town Laboratires (A Report), 1970, 1970-14, NYO-4176-4.
110. A. V. GROSSE, *Nature* (*London*), 1971, **232**, 170.
111. R. V. GOPALA RAO and H. V. KEER *Z. Phys. Chem.*, 1962, **219**, 321.
112. R. V. GOPALA RAO and K. N. SWAMY, *Indian J. Pure Appl. Phys.*, 1970, **8**, 604.
113. R. V. GOPALA RAO, *Indian J. Pure Appl. Phys.*, 1967, **5**, 857.
114. R. V. GOPALA RAO, V. V. SESHAIAH, R. G. KRISHNA and K. N. SWAMY, *J. Sci. Ind. Res.*, 1970, **29**, 66.
115. R. V. GOPALA RAO and V. VENKATA SESHIAH, *Indian J. Phys.*, 1969, **43**, 424.
116. R. V. GOPALA RAO and B. S. M. RAO, *Trans. Faraday Soc.*, 1966, **62**, 2704.
117. R V. GOPALA RAO and J. C. M. LI, *Z. Phys. Chem.*, 1960, **213**, 166.
118. R. V. GOPALA RAO and A. K. MURTY, *Chem. Phys. Lett.*, 1976, **38**, 197.
119. R. V. GOPALA RAO and R. DAS, *Indian J. Phys.*, in the press.
120. R. V. GOPALA RAO and R. DAS, unpublished.
121. R. G. PALMER and J. D. WEEKS, *J. Chem. Phys.*, 1973, **58**, 4171.

J. Indian Chem. Soc.,
Vol. LXIII, January 1986, pp. 168-178

Effect of Non-equilibrium Solvation Dynamics on Photochemical Reactions in Solution†

BIMAN BAGCHI

Solid State and Structural Chemistry Unit, Indian Institute of Science, Bangalore-560 012

In many photochemical (or photophysical) reactions in solution, the electronic relaxation rate is of the same order of magnitude as the solvent relaxation rate. In such a situation the electronic relaxation rate may depend critically on the details of the solvent relaxation. Recent picosecond laser spectroscopy experiments have unambiguously showed the importance of such solvation dynamics and have revealed qualitatively several new aspects of solvent effects. Some of these effects cannot be explained by the traditional transition state theories which assume that solvent is at equilibrium with the reactive motion at every stage of the reaction. Recent experiments have also indicated an apparent breakdown of Kramers' theory for the viscosity dependence of rates of these ultrafast processes. In this article, we present new theoretical calculations to explore the effects of the non-equilibrium solvation dynamics on the reaction rates of these processes. We also consider the effect of 'memory' of solvent forces on reaction rates. These 'memory effects' may play an important role in the breakdown of Kramers' theory.

MOST known chemical reactions take place in the liquid phase. The various effects of solvent on chemical reactions have been studied extensively over the years[1-5]. Recent advances in picosecond laser spectroscopy have added a new dimension to this field[6,7]. It is now possible to study ultrafast processes where reaction rates lie in the picosecond or in the subpicosecond regime. This allows one to study the role of solvent forces on short time scales. Recent experimental studies have concentrated on understanding the role of solvent viscosity on reaction rate[8-15] and also on the effect of solute-solvent interactions on the reaction potential energy surface[8,11]. On the theoretical side, attempts have been made to extend and generalise the stochastic theories of reaction rate[16-24] with various degrees of success in explaining the experimental results.

In this paper we consider two aspects of the solvent effects. Firstly, we consider the non-Markovian effects on chemical reactions in solution. Secondly, we study the effects of non-equilibrium solvation dynamics on chemical reactions.

The motivation for the study of the non-Markovian effects comes from recent experimental results[9,10] which reveal an apparent failure of the well known Kramers' theory to explain the viscosity dependence of isomerisation reactions in solution. The experiments of Velsko *et al.*[9,10] and of others[8] reveal a significantly smaller effect of viscosity on rates at high viscosities than that predicted by Kramers' theory. It has been argued that the experimentally observed partial saturation of the viscoisty effects arise from the frequency dependence of the frictional forces that inhibit barrier crossings[9,24]. For sharp barriers the *effective* friction in the barrier region can be much smaller than its zero frequency value at high viscosities. In this paper we present a treatment of these non-Markovian effects in a form which is somewhat different from what exists in the literature[24].

The second topic addressed in this paper is the effect of non-equilibrium solvation dynamics on reaction rate in solution. The central idea here is that for ultrafast reactions, the solvent molecules may not be able to follow the reaction and as a result, the reaction may occur from a state of incomplete equilibration with the solvent. The non-equilibrium solvation may play an important role in those chemical reactions which occur in polar media and where significant change in the value of the permanant dipole moment occurs in the course of the reaction. Since the polar forces are long ranged, they are usually slow to respond to the changes in the polar character of the reacting molecule. This may lead to significant non-equilibrium effects which are not treated in the standard transition state based theories.

The organisation of the rest of the paper is as follows : the general ideas and the concepts, consideration of the non-Markovian effects, the non-equilibrium solvature dynamics considered at length, and concludes with a brief discussion.

General considerations :

In this section we briefly discuss the theories and the concepts that are used to describe chemical reactions in the liquid phase.

† Dedicated to Professor Sadhan Basu on the occasion of his 65th birthday.
Contribution No. 317 from the Solid State and Structural Chemistry Unit.
A part of the article was presented at the National Conference on Spectroscopy and Theoretical Chemistry held at Calcutta, December 5-7, 1985.

Transition state theory: The transition state theory (TST) is the earliest theory for chemical reactions in solution. The transition state is identified with an imaginary 'dividing surface' separating the reactant and the product states in the configuration space. For a one-dimensional potential surface, the transition state is usually chosen to be the state with the maximum energy in the barrier region. The basic assumption of TST is that once the reacting system crosses the transition state, it *never* returns to the same state again. It can be shown that when TST is not exact, it *overestimates* the exact, equilibrium rate constant[25,28].

The general expression for the TST rate constant is given in terms of partition functions of the transition state, the reactants and the products[1-4]. However, for chemical reactions in solution this general expression is of little use because of the difficulties in evaluating the partition functions. The usual procedure is to express the rate constant in terms of thermodynamic functions which are accessible experimentally. The following well known expression was derived by Wynne-Jones and Eyring[8],

$$k^{TST} = \frac{k_B T}{h}\, e^{\Delta S^{\neq}/k}\, e^{-\Delta H^{\neq}/k_B T} \tag{1}$$

where, $\Delta S^{\neq}$ and $\Delta H^{\neq}$ are the entropy of aetivation and the enthalpy of activation per molecule, k_B is the Boltzmann constant, h is the Planck's constant and T the temperature. It is a standard procedure to relate $\Delta H^{\neq}$ to energy of activation. For many practical purposes $\Delta H^{\neq}$ can be taken equal to $\Delta E^{\neq}$ (Refs. 1-4).

Equation (1) has the advantage that the effects of solvent on the reaction potential surface can be incorporated, at least in principle, through $\Delta S^{\neq}$ and $\Delta H^{\neq}$. However, one must then make the additional assumption that the solvent molecules are in equilibrium with the reacting system at all times during the reaction. For a fast reaction involving movement of polar or ionic groups in a polar solvent, the above assumption of complete equilibrium at all stages of the reaction may breakdown. This is because for a fast reaction, the solvent molecules will not be able to rearrange sufficiently rapidly to follow its equilibrium path. There will be some degree of non-equilibrium solvation in the transition state or its neighbourhood.

We can make the above discussion more quantitative by defining (somewhat arbitrarily) an average life-time $\tau^{\neq}$ of the transition state. In a one dimensional model, $\tau^{\neq}$ can be defined by the following relation[1],

$$\tau^{\neq} = \frac{\Delta l}{v} \tag{2}$$

where, Δl is the length of a segment of reaction coordinate in the neighbourhood of the transition state—this length defines a 'transition state like' complex (Fig. 1), and v is the velocity of the reacting

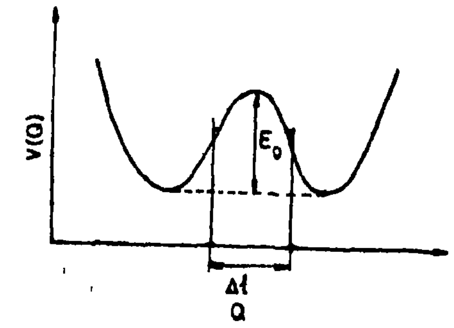


Fig. 1. Curve of a one-dimensional potential energy surface plotted against the reaction coordinate (Q). The length Δl denotes a neighbourhood of the transition state.

system across the barrier. We want to compare $\tau^{\neq}$ with the solvent relaxation time τ defined through

$$\tau = \mu_{solv}/\zeta \tag{3}$$

where, μ_{solv} is the effective mass of the solvent relaxation and ζ is the relevant friction parameter. An estimate of v can be obtained from kinetic theory,

$$v = (2k_B T/\mu)^{1/2} \tag{4}$$

where, μ is the effective mass of the reaction. For an isomerisation reaction $\mu \simeq 100$ amu, so $v \simeq 2 \times 10^4$ cm s^{-1} at 300 K. Estimation of Δl is tricky. Approximately this can be set equal to the interval between the points where the barrier height is half of its maximum. Assuming that the barrier is an inverted parabola with barrier frequency 10^{13} s^{-1} and barrier height 5 kcal mol, we obtain $\Delta l \simeq 10^{-8}$ cm. This gives $\tau^{\neq} \simeq 5 \times 10^{-13}$ s. This value of $\tau^{\neq}$ is comparable to the value of τ for many liquids. This implies that a clear separation of time scales may not exist between $\tau^{\neq}$ and τ and as a result, the assumption of complete solvation at every stage of the reaction may breakdown making the TST expression for the rate constant (equation (1)) unreliable.

In the *Non-equilibrium solvation dynamics* section we shall consider the effects of non-equilibrium solvation on photochemical reactions in more detail.

Kramers' theory: It is known that rates of many chemical reactions depend strongly on viscosity of the solvent. This is especially true for those reactions which involve a spatial rearrangement of molecular groups as the rate determing step of the reaction. The transition state theory, however, totally ignores this dynamical aspect of solvent forces. In solution phase reactions the main assumption of TST, that no trajectory crosses the dividing surface more than once, breaks down. The frictional forces exerted by the solvent induce recrossings of the trajectories and reduce the rate below the TST value. The most well known theory of viscosity dependence of rate is due to Kramers[16]. In the following we briefly review Kramers' theory.

In order to study the effects of solvent frictional forces on the rate of a chemical reaction in solution,

Kramers' modelled the reactive motion as the passage of a Brownian particle over a one-dimensional potential barrier. Kramers' assumed that the motion along the reaction coordinate is given by the following ordinary Langevin equation[1,6,17],

$$\mu\frac{dv}{dt}=F(x)-\zeta v(t)+f(t) \tag{5}$$

where, μ and v are respectively the effective mass and the velocity along the reaction coordinate, F(x) is the force arising from the potential in the barrier region, ζ is the zero-frequency friction parameter and f(t) is the delta-correlated white noise. ζ and f(t) are related by the fluctuation-dissipation theorem[17],

$$\langle f(o)f(t)\rangle = k_BT\delta(t) \tag{6}$$

Equation (6) is known as the white-noise approximation for the random force. F(x) is assumed to arise from a static potential which is an inverted parabola

$$F=\mu\omega_b^2\,x \tag{7}$$

The details of Kramers' analysis is easily available; here, we quote the final expression for the rate constant given by

$$k=\frac{\omega_R}{2\pi\omega_b}\left[\left(\frac{\zeta^2}{4}+\omega_b^2\right)^{1/2}-\frac{\zeta}{2}\right]e^{-E_0/k_BT} \tag{8}$$

where, ω_R is the frequency of the (assumed harmonic) reactant well and E_0 is the molecular activation energy of the one dimensional potential surface. Equation (8) has two important limiting properties. If $2\omega_b \gg \zeta$, then one obtains the TST result of this model with a rate constant independent of the friction parameter ζ. In the opposite limit, when $2\omega_b \ll \zeta$, then equation (8) predicts a rate constant inversely proportional to the friction,

$$k\equiv k^{SL}=\frac{\omega_R\,\omega_b}{2\pi\,\zeta}\,e^{-E_0/k_BT} \tag{9}$$

This limit is known as the Smoluchowski limit. In the next section we shall examine the validity of this limit.

Kramers' theory provides us with a simple and elegant expression for the frictional dependence of the rate. Unfortunately, this theory has some drawbacks which limit its applicability. In the following we briefly mention the two most important limitations of the Kramers' theory.

(i) Kramers' treatment is one-dimensional. For reactions in large molecules, there may be several non-reactive modes that interact strongly with the reactive mode.

(ii) The assumption that the solvent forces on the reactive motion are delta-correlated (equation (6)) in time is subject to suspect for sharp barriers for which ω_b^{-1} is smaller than the bath correlation time at high viscosities. In this limit, the reactant may not stay long enough at the barrier top to probe all the solvent motions. The zero-frequency friction then *overestimates* the solvent drag on the reactive motion and one must take into account the frequency dependence of the friction. That is, equation (6) is to be discarded and retention of the 'memory' of solvent forces is necessary to obtain a consistent description.

In the next section we consider the effects of the frequency dependence of friction on the reaction rate. We shall see that the memory- or the non-Markovian effects can alter the viscosity dependence of the rate constant qualitatively.

Non-Markovian effects :

Recent experimental studies[8-11] on photochemical isomerisation of several large organic molecules in solution, have indicated an apparent breakdown of the well known Kramers' theory[16]. The most important result of these investigations is that Kramers' theory does not have the correct *curvature* to describe the viscosity dependence of the rate at both high and low viscosities. Velsko *et al.*[10] found that their results could be fitted very well to a viscosity dependence of the following form,

$$k=A_0\eta^{-\alpha}\exp(-E_0/k_BT) \tag{10}$$

where, A_0 is a viscosity independent constant, E_0 is the *isoviscous* activation energy and η is the zero-frequency shear viscosity. The value of the exponent α lies in the range $1 \geq \alpha \geq 0.1$ with $\alpha=0.26$ for the ground state DODCI and $\alpha=0.43$ for the excited state DODCI[10]. For the excited state diphenyl butadiene (DPB), $\alpha=0.59$ fits the experimental data well[9]. At the viscosities studied in the above experiments, Kramers' theory predicts $\alpha=1$, *i.e.* the attainment of the Smoluchowski limit[17]. This non-attainment of the Smoluchowski limit is remarkable and is the subject of the present discussion.

The precise reason for the breakdown of Kramers' theory at high viscosities is still far from understood. There are two different explanations that have been put forward. The first explanation is based on the experimental fact, that the magnitude of the exponent α correlates well with the frequency ω_b of the potential barrier. If ω_b is small, then $\alpha \simeq 1$, but if ω_b is large (which implies a sharp barrier), then α is much less than unity. Since ω_b^{-1} is a measure of the 'residence time' τ^*, near the barrier top, it appears that the frequency dependence of solvent friction may play an important role in the breakdown of Kramers' theory[9,10]. A different explanation that has been advocated[8] for the breakdown of Kramers' theory is based on multidimensional nature of the potential surface. In a large molecule, there are many degrees of freedom that can be coupled with the reactive degree of motion. Since Kramers' theory is a one-dimensional theory, this multidimensionality of the potential surface can significantly modify the predictions of Kramers' theory. In fact, it can be shown that an adiabatic coupling between the reactive mode and other non-reactive modes of the reacting molecule is essentially equivalent to a frequency dependent friction in a one-dimensional picture. The form of the frequency dependent friction is, however, different in this case[23,26].

The effects of the frequency dependence of friction on the rates of chemical reactions in solution have been investigated by various authors in recent years[31-38]. We mention the work of Bagchi and Oxtoby[34] who showed, by using the hydrodynamic expression of Zwanzing and Bixon[39], that the non-Markovian theory of Grote and Hynes[31] can qualitatively explain the experimental results of Velsko *et al.*[9,10]. Bagchi and Oxtoby[34] observed that the breakdown of Kramers' theory occurs because the *effective* friction in the barrier region is much smaller than its zero-frequency value at high viscosities for sharp barriers. These authors argued that if the barrier is too high and sharp, frequency dependence of friction will play an important role and the Smoluchowski limit may never be realised, in total breakdown of Kramers' theory. However, this conclusion of Bagchi and Oxtoby[34] is perplexing and contradicts the traditional belief. One serious limitation of the argument of these authors is that it depends heavily on the Maxwell forms for the frequency dependence of viscosity assumed in their work. Another problem is that the conclusion is based on numerical solution of Grote-Hynes theory. In this section we shall reexamine this problem by using a different approach.

We start with the following expression for the rate constant, k, for a one-dimensional reaction[31],

$$k = k^{TST}(\lambda_r/\omega_b) \qquad (11)$$

where, k^{TST} is the transition state rate constant given by

$$k^{TST} = \frac{\omega_R}{2\pi} \exp(-E_0/k_BT) \qquad (12)$$

where, ω_R is frequency of motion in the reactant well and ω_b is the barrier frequency. λ_r is given by the following self-consistent relation[31],

$$\lambda_r = \frac{\omega_b^2}{\lambda_r + \hat{\zeta}(\lambda_r)/\mu} \qquad (13)$$

where, μ is the effective mass of reactive motion. $\hat{\zeta}(\lambda_r)$ is the Laplace transform of the time dependent friction ζ (t),

$$\hat{\zeta}(\lambda_r) = \int_0^\infty dt\, e^{-\lambda_r t} \zeta(t) \qquad (14)$$

Equation (13) predicts the transition state result for very weak friction ($\lambda_r \sim \omega_b$) and the Kramers' result for low barrier frequency, *i.e.*, $\omega_b \to 0$, so that $\hat{\zeta}(\lambda_r)$ may be replaced by $\hat{\zeta}(0)$. If the barrier frequency is large ($\omega_b > 10^{13}\ s^{-1}$) then the situation is not so straightforward and one must solve equation (13) to obtain λ_r. Bagchi and Oxtoby[34] used the Zwanzig-Bixon expression[39] for $\hat{\zeta}(\lambda_r)$. The expression is rather cumbersome, so we write it symbolically as

$$\hat{\zeta}(p) = F(p, \eta_s(p), \eta_v(p), c, \rho_0, R, \beta) \qquad (15)$$

The functional form of F (in Laplace plane) is given elsewhere[34]. In equation (15), $\eta_s(P)$ and $\eta_v(P)$ are the frequency dependent shear and bulk viscosities, respectively, ρ_0 is the solvent density, c is the velocity of sound, β is the slip parameter, zero for pure slip and infinity for stick boundary conditions, and R is the hydrodynamic radius of the reactive moiety. For isomerisation reactions, the reactive motion is a twisting motion of a part of the organic molecule around a molecule-fixed axis.

Bagchi and Oxtoby[34] assumed simple Maxwell forms for $\eta_s(p)$ and $\eta_v(p)$

$$\eta_s(p) = \frac{\eta_s^0}{1 + p\tau_s} \qquad (16a)$$

$$\eta_v(p) = \frac{\eta_v^0}{1 + p\tau_v} \qquad (16b)$$

where, η_s^0 and η_v^0 are respectively the zero frequency shear and bulk viscosities. The viscoelastic relaxation constants τ_s and τ_v are given by[40]

$$\tau_s = \frac{\eta_s^0}{G_\infty}; \quad \tau_v = \frac{\eta_v^0}{K_r} \qquad (17)$$

where, G_∞ is the infinite frequency shear viscosity and K_r is the relaxation part of the bulk modulus[40]. Subsequent analysis of the viscosity dependence of the rate constant, especially of the non-attainment of the Smoluchowski limit at high viscosity for sharp potential barriers, depend crucially on the functional relations between $\eta_s(p)$, η_s^0 and τ_s (for details, Ref. 24). Therefore, the conclusions derived are also valid only to the extent these relations are reliable.

In this section we present an alternative analysis based on an asymtotic form of $\hat{\zeta}(p)$. Here, it is possible to obtain an analytic expression for k without using the Maxwell forms and the relations (17).

For simplicity we assume that the reactive motion is translation of a sphere of radius R and mass m in a liquid of density ρ_0. We consider the fluid to be incompressible, *i.e.* the sound velocity c. In this limit the expression for $\hat{\zeta}(p)$ simplifies and is given by[41]

$$\hat{\zeta}(p) = \frac{9M\nu}{2R^2}\left[1 + R\left(\frac{p}{\nu}\right)^{1/2} + \frac{pR^2}{9\nu}\right] \qquad (18)$$

where, ν is the kinetic viscosity and M is the mass of the displaced fluid. ν and M are given by

$$\nu = \frac{\eta}{\rho_0}; \quad M = \frac{4\pi}{3} R^3 \rho_0 \qquad (19)$$

Next, we substitute equation (18) into the self-consistent condition (equation (13)) to obtain the following equation,

$$A\lambda_r^2 + B\nu^{1/2}\lambda_r^{3/2} + C\nu\lambda_r = \omega_b^2 \qquad (20)$$

where,

$$A = 1 + M/2\mu \qquad (21a)$$

$$B = \frac{9M}{2\mu R} \qquad (21b)$$

$$C = \frac{9M}{2\mu R^2} \qquad (21c)$$

Equation (20) has several interesting features. Firstly, in the limit $\nu \to 0$, we find $\lambda_r = \frac{1}{\sqrt{A}} \omega_b$, *i.e.* a 'transition state type' result (for k is equal to k^{TST} only when $\lambda_r = \omega_b$). A is of the order of unity, so the difference is small. The reason for the non-attainment of the TST result is that for incompressible fluid, the initial condition for the velocity correlation function exhibits a lack of continuity. The discrepency is eliminated if compressibility is taken into account. This discrepency definitely affects quantitative result but has no influence on the qualitative conclusions of this section.

In the limit of large viscosity (*i.e.* $\nu \to \infty$), we recover the Smoluchowski limit

$$k \to \frac{\omega_b}{C\nu} k^{TST}, \qquad (22)$$

i.e. rate is inversely proportional to the macroscopic viscosity. This result seems to indicate that the earlier conclusion of Bagchi and Oxtoby[34] on the non-attainment of the Smoluchowski limit for sharp barriers is limited to liquids obeying Maxwell forms for viscoelastic relaxations.

The most interesting feature of equation (20) is, however, manifested in the intermediate regime of viscosity. In this regime, equation (20) exhibits a non-analytic dependence of the rate on the viscosity parameter ν. What is more important is the range over which the non-analytic dependence holds. In order to study this aspect, we use the following estimates, which are taken to mimic isomerisation of DPB, $\rho_0 = 1$ g cm^{-3}, $R = 3 \times 10^{-8}$ cm, $M = 3.4 \times 10^{-22}$ g and $\mu = 1.6 \times 10^{-23}$ g, to obtain the following equation,

$$2.05\, x^2 + (\nu')^{1/2} x^{3/2} + 0.1 \nu' x = 1 \qquad (23)$$

where,

$$x = \lambda_r / \omega_b \qquad (24a)$$

$$\nu' = B^2 \nu / \omega_b \qquad (24b)$$

There is a slight approximation involved in using equation (23) to study the effects of viscosity because we have fixed the solvent density yet varying the viscosity. If viscosity is changed by varying temperature then the solvent density will not be much affected whereas viscosity is a strong function of temperature. This justifies the use of equation (23). It may be note that the prefactor of the term linear in ν' in equation (23) is small. Therefore, one may have to reach a very large value of ν' before the Smoluchowski behaviour is obtained.

We have plotted the solution of equation (23) in Fig. 2. The dependence of the rate parameter x on viscosity parameter ν' is surprisingly similar to the results obtained earlier[34]. The graph has a viscosity dependence which is qualitatively similar to the experimental results of Velsko *et al.* [9,10]. However, a quantitative comparison between theory and experiment is meaningless at this stage because of the approximations that are involved in deriving equation (20) and the uncertainity in the values of the potential parameters.

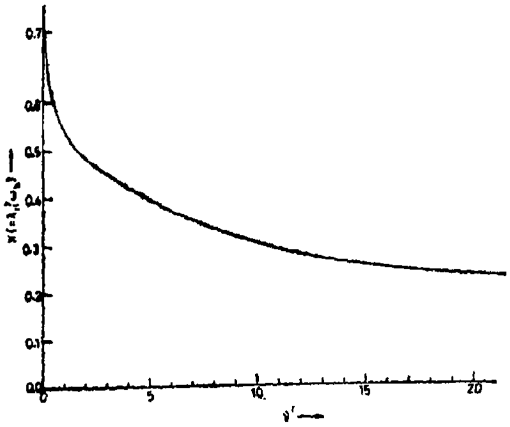


Fig. 2. The rate parameter $x(=\lambda_r/\omega_b)$ is plotted against the reduced viscosity parameter ν', as obtained by solving equation (28) of the text.

As mentioned earlier, equation (20) predicts Smoluchowski behaviour for large values of ν. For the values of parameters chosen in obtaining equation (23), it is possible to obtain a rough estimate of the value of ν required to produce Smoluchowski limit. From equation (23), SL is obtained around $\nu' \simeq 100$. For $\omega_b = 10^{13}$ s^{-1}, we get $\eta \simeq 1$ cp which is too small a value to obtain SL. Clearly equation (23) is not reliable for quantitative purposes. This point deserves further study. It is surprising that compressibility (or acoustic dissipation) would play such an important role.

Non-equilibrium solvation dynamics :

The non-Markovian effect discussed in the last section focuses on the failure of the solvent motions to 'track' the fast reactive motion at the barrier. This effect can be termed 'dynamical non-equilibrium' effect. The assumption made is that the barrier height and the barrier shape remain unchanged within a homologous series of solvents. Another related assumption is that the reacting molecule is fully solvated at each point along the reaction coordinate so that the potential surface is time independent. In the following we briefly discuss the range of validity of the last assumption.

If the solute-solvent interactions are dominated by short-range forces, then the equilibrium solvation hypothesis may be reliable. The situation changes drastically if the solute molecule possesses a large dipole moment and the solvent is highly polar. In many experimentally studied cases, the dipole moment of the solute molecule is different in the excited state from its value in the ground state[43]. Therefore, a solvent reorganisation follows the excitation. Since the polar interactions are long ranged, the time of solvent reorganisation towards the new equilibrium may be comparable to the time scale of the reacting event. In such a situation,

which is quite common in experiments, the equilibrium solvation hypothesis will break down.

In order to understand the non-equilibrium solvation effects on photochemical reactions, we shall consider the following two situations. (A) The reacting event is a rediationless 'jump' from a minimum in the excited state surface to a maximum on the ground state surface (Fig. 3). In the terminology of photochemistry, this is a 'diabatic' photoreaction[43,44]. The reactive motion is the motion on the excited potential surface from the initial position to the reactive region. The reactive motion is controlled by the potential surface and the solvent viscous forces. We consider the case where the permanant dipole moment of the molecule changes significantly on excitation. (B) The reactive motion involves a thermally assisted crossing of an activation barrier on the excited state potential surface (Fig. 4). The activation barrier height E_0 is such that $E_0/k_BT \geq 5$.

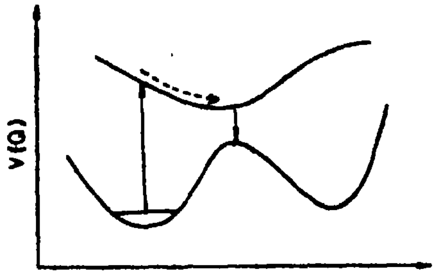


Fig. 3. A typical potential energy diagram for a photochemical reaction which occurs without the intervention of an activation barrier. The solid arrows indicate the positions of the excitation and the 'jump'. The dashed line denotes the reactive motion on the excited surface.

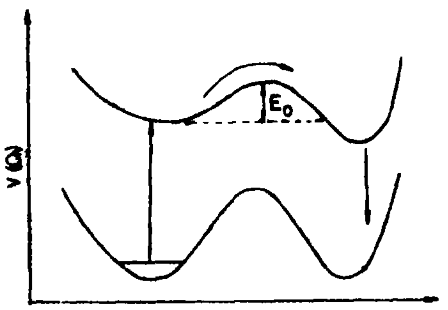


Fig. 4. A typical potential energy diagram for an 'adiabatic' photoreaction where the rate limiting step is a thermally assisted crossing of an activation barrier.

Recent experiments on triphenylmethane (TPM) molecules[14,15] and on dimethylaminogenzonitrile (DMABN)[8] have revealed the effects of solvent polarity on photochemical reactions in solution. These experiments showed that the solvent polarity can modify the reaction potential surface to the extent that a crossover from the zero barrier (case (i)) to a finite activation barrier (case (ii)) can take place. We shall discuss the mechanism of such a crossover after our discussion of the two cases.

Case (A) : Reaction in the absence of a barrier On excitation to higher electronic states, both the magnitude and the direction of the permanant dipole moment can undergo significant changes. Since the process of optical excitation and emission are much faster than any relaxation processes involved, we model the change in dipole moment on excitation and fluorescence by Heaviside functions

$$\underline{\mu}^{(b)}(t) = \underline{\mu}_g^{(b)} + H(t=0)[\underline{\mu}_e^{(b)} - \underline{\mu}_g^{(b)}] + H(t=t_1)[\underline{\mu}_g^{(b)} - \underline{\mu}_e^{(b)}] \qquad (25)$$

where, $\underline{\mu}_g^{(b)}$ and $\underline{\mu}_e^{(b)}$ are the dipole moments in the body-fixed frame to the solute molecule in the ground and excited states, respectively. H(t) is a Heaviside function. Equation (25) is simply a statement of the fact that the molecule is excited from its ground electronic state at time $t=0$ and it fluorences back at time $t=t_1$. The time t_1 will, however, be determined by the interaction within the system (solute+solvent). The average of t_1 is essentially the time-constant which we want to calculate.

It may be noted that the dipole moments $\underline{\mu}_g^{(b)}$ and $\underline{\mu}_e^{(b)}$ are given in the body-fixed frame. In a photochemical reaction, the reactive motion may involve a rotational or torsional motion of a part of the reacting molecule with respect to the rest. In such a situation the reactive motion may be coupled to the rotational motion of the dipole moment in the space-fixed frame. Let us briefly consider this point. The origin of rotational motion is random collisions with other solvent molecules. In the liquid phase, the rotational motion will hardly experience any systematic potential, expect the reaction-field of the dipole moment itself in polar liquids. However, the effect of this reaction-field does not qualitatively change the nature of the diffusion process. The reactive motion, on the other hand, may involve some particular rearrangements of molecular groups and will usually experience a restoring force. The reactive motion will also experience random collisions with the solvent molecules so the reactive motion is sort of a diffusion in a force-field. Let us consider a specific example, *p*-dimethylaminonitrile. In the excited state this molecule develops a charge separation between the phenyl and the amino group, thereby generating a large change in dipole moment[8]. The reactive motion (shown by an arrow in Fig. 5) hardly changes the direction of the dipole moment, although the magnitude of the excited state dipole moment may change significantly. In this case, the dipolar motion is not *explicitly* coupled to the reactive motion, although the potential surface for reactive motion may depend on dipolar motion. First, we consider the effect of dipolar motion on the photochemical reaction by neglecting the direct coupling between the rotational motion of the dipole and the reactive motion. Because of this approximation, the effects of

dipolar interactions enter only in the average, time dependent, stabilisation energy of the excited state potential surface.

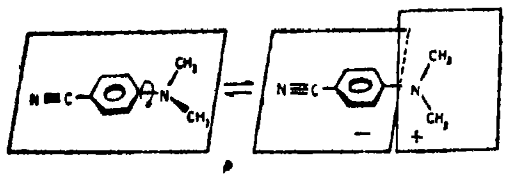


Fig. 5. The reactive motion in the excited *p*-dimethylaminonitrile is shown by an arrow. The motion leads to a significate separation of charge density as indicated in the figure.

Let $\langle E_s \rangle^g_{eq}$ and $\langle E_s \rangle^e_{eq}$ denote the average stabilisation energies due to dipolar interactions in the ground and excited states of the solute molecule in equilibrium with the polar solvent. $\langle E_F \rangle^e_g$ is the interaction energy when the excited molecule is in the Franck-Condon state of the ground-state solvent configuration and $\langle E_F \rangle^g_e$ denotes the reverse situation. Let $\langle E_s(t) \rangle^e$ denote the time-dependent stabilisation energy when the molecule is in the excited state at a time t after the optical excitation. Obviously $\langle E_s(t \to \infty) \rangle^e = \langle E_s \rangle^e_{eq}$. If Q denotes the reaction coordinate, then the energy difference between the excited and the ground surface is given by

$$\Delta E_{eg}(t, Q) = \langle E_s(t, Q) \rangle^e - \langle E_F(t, Q) \rangle^g_e \qquad (26)$$

Later in this section we shall give an explicit expression for ΔE_{eg} (t, Q) from dielectric continum theory. Let us now study the limiting properties of equation (26). In the limit $t \to \infty$, we have the equilibrium solvation of the excited state and $\langle E_F(t, Q) \rangle^g_e$ becomes equal to $\langle E_F \rangle^g_e$ so that equation (26) becomes

$$\Delta E_{eg}(\infty) = \langle E_s \rangle^e_{eq} - \langle E_F \rangle^g_e. \qquad (27)$$

In equation (27) and hereafter we have dropped Q for convenience. In the limit $t \to 0$, equation (26) reduces to

$$\Delta E_{eg}(0) = \langle E_F \rangle^e_g - \langle E_s \rangle^g_{eq} \qquad (28)$$

If the reaction is slow or the solvent relaxation is fast, then the reaction probes only the contribution ΔE_{eg} (∞), and this effect is well-studied. However, interesting things may happen when the reaction competes with ΔE_{eg} (t). This is the regime what we call non-equilibrium solvation regime. Before we develop a mathematical formulation of this problem, let us consider the following there regimes. (i) Solvent is frozen. Then relaxation occurs from the same environment to which it is initially excited. (ii) Solvent relaxation is much faster than the reaction. In this case equilibrium solvation is an adequate representation. (iii) Solvent relaxation and reaction rate are comparable to each other. This is the non-equilibrium solvation regime.

A clear evidence of the existence of non-equilibrium solvation dynamics comes from the experimentally observed time evolution of fluorescence Stokes shift of polar molecules in polar solvents[45,46]. In many cases, the maximum of the fluorescence spectra changes from a significant blue shift at short times to a red shift at longer times where the shifts are measured with respect to the fluorescence in non-polar solvents. The time evolution of these shifts can be explained in terms of the stabilisation energies of the ground and the excited states[47]. We shall show below that these same stabilisation energies play a crucial role in determining the rate of a photochemical reaction, and in some cases, may even alter the course of the reaction.

Let us briefly discuss the essence of the solvent effects. Let the dipole moment of the excited state has a large magnitude but retains the same direction (*i.e.* $|\mu_e| > |\mu_g|$ and $\hat{\mu}_e \parallel \hat{\mu}_g$). Then the following relations hold,

$$\Delta E_{eg}(0) < 0$$
$$\Delta E_{eg}(\infty) < 0 \qquad (29)$$
$$\text{and } \Delta E_{eg}(\infty) < \Delta E_{eg}(0)$$

i.e. the long time energy difference between the two states is less than the initial difference. The situation is illustrated pictorially in Fig. 6. Now the time evolution of $\Delta E_{eg}(t)$ enters into the dynamics of the photochemical reaction in the following

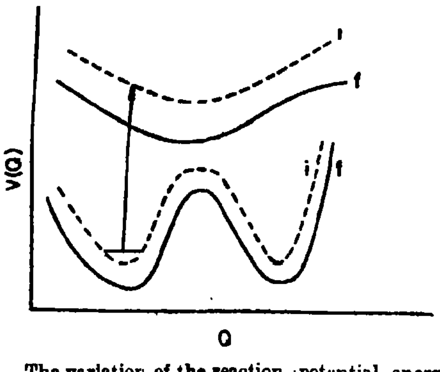


Fig. 6. The variation of the reaction potential energy surface as a result of solvation of a dipolar molecule in a polar solvent. The legends 'i' and 'f' denote the initial and final states, respectively.

manner. The rate of 'jump' or internal conversion from the excited surface to the ground surface is an exponential function of the energy gap[48]. We write this dependence in the following form,

$$k_{nr}(x, t) = k_0 S(x) \exp[-\alpha \Delta E_{eg}(t)] \qquad (30)$$

where, k_0 is the rate of radiation-less transition from the minimum of the excited state potential surface (where the rate is maximum) in non-polar solvents, S(x) is the sink function which gives the position dependence of the decay (Ref. 31 may be seen for a discussion on the sink function S(x)) and α is a constant which, like k_0, is a molecular property. The important thing to note is the exponential dependence of the rate on $\Delta E_{eg}(t)$. If the dipole moment of the excited surface changes by a significant amount or undergoes a significant rotation, then k_{nr} may change sufficiently rapidly with time to compete with the overall decay rate

of the excited state population. Next we proceed to calculate this population decay rate.

In the present case, there is no high barrier for the reactive motion so one must solve for the time dependent probability of the system remaining on the excited state surface. In our model, the radiationless relaxation is represented by a position dependent sink. The motion along the potential surface is governed by the force from the potential (approximated as harmonic) and the viscous drag of the solvent. We model all these competing factors by a modified Smoluchowski equation of the following form[31],

$$\frac{\partial P}{\partial t}(x, t) = A\,\frac{\partial^2 P}{\partial x^2}(x, t) + B\,\frac{\partial}{\partial x}\,xP(x, t) - k_{nr}(x, t)\,P(x, t) \qquad (31)$$

where, $A = k_B T/\zeta$ and $B = \omega^2\mu/\zeta$, ω being the frequency of motion on the excited surface, ζ the relevant friction coefficient, μ the reduced mass of the reactive motion. $k_{nr}(x, t)$ is given by equation (30).

Several choices of the sink function were considered in Ref. 31. Here, we assume a Gaussian form centred at the minimum of the excited state potential surface

$$S(x) = e^{-x^2/a^2} \qquad (32)$$

where, a is related to the width of the sink. The Gaussian sink is quite realistic because the energy difference between two harmonic surfaces is a quadratic function of x, and so the exponential energy gap law predicts a shifted Gaussian probability distribution for the transition probability between two surfaces.

With the choice of sink function (equation 32), it has not been possible to solve equation (31) analytically. Instead, it may be solved by a series expansion. We define and operator $\mathcal{L}$ by

$$\mathcal{L} = B\,\frac{\partial}{\partial x}\left(\frac{A}{B}\frac{\partial}{\partial x} + x\right) \qquad (33)$$

We expand P(x, t) in the eigenfunctions of the Fokker-Planck operator $\mathcal{L}$

$$P(x, t) = \sum_{n=0}^{\infty} \sigma_n(t)\, b_n(x) \qquad (34)$$

where $b_n(x)$ is the n-th eigenfunction of $\mathcal{L}$ (Ref. 31),

$$\mathcal{L}\, b_n = -n\,B\,b_n \qquad (35)$$

$$b_n(x) = A_n^{1/2} \exp\left(-\frac{x^2}{2V^2}\right) H_n\left(\frac{x}{\sqrt{2}V}\right) \qquad (36)$$

where, H_n is the Hermite polynomial of order n, $V = (A/B)^{1/2}$ and the normalisation constant A_n is given by

$$A_n = (V\,n!\,2^n\sqrt{2\pi})^{-1} \qquad (37)$$

The conjugate eigenfunction b_n^+ is defined through[31],

$$b_n^+\,\mathcal{L} = -n\,B\,b_n^+ \qquad (38a)$$

$$b_n^+ = A_n^{1/2}\,H_n\left(\frac{x}{\sqrt{2}V}\right) \qquad (38b)$$

b_n and b_n^+ are orthonormal. Following the usual procedure, we obtain the following system of equations for $\sigma_m(t)$,

$$\sigma_m(t) = -m\,B\,\sigma_m(t) - k_0 \exp[-\alpha\,\Delta E_{eg}(t)] \sum_{n=0}^{\infty} (A_n A_m)^{1/2}\, I_{m,n}\, \sigma_n(t) \qquad (39)$$

where,

$$I_{m,n} = (-1)^{\frac{m+n}{2}}\, 2^{m+n+\frac{1}{2}}\, V\left(1 + \frac{a^2}{2V^2}\right)^{-\frac{m+n}{2}} \otimes \left(\frac{a^2}{a^2+2V^2}\right)^{1/2} \Gamma\left(\frac{m+n+1}{2}\right) {}_2F_1\left(-m, -n; \frac{1-m-n}{2}; \frac{a^2+2V^2}{4V^2}\right), \quad (m+n) \text{ even} \qquad (40)$$

where, ${}_2F_1$ is an ordinary hypergeometric function[46] defined as

$${}_2F_1(a, b, c; Z) = \sum_{l=0}^{\infty} \frac{(a)_l\,(b)_l}{(c)_l}\,\frac{Z^l}{l!} \qquad (41)$$

$(Y)_l$ is Pochhamer's symbol[46]. In the present case, both a and b are either negative integers on zero, so ${}_2F_1$ is a polynomial with the upper limit of the sum (equation (41)) at min (m, n).

Equation (39) can be solved numberially to obtain the time dependent probability distribution P(t). However, we need an expression for $\Delta E_{eg}(t)$ for such a calculation. Next, we present an expression for $\Delta E_{eg}(t)$.

Expression for $\Delta E_{eg}(t)$: We assume that the dominant contribution to $E_{eg}(t)$ comes from dipolar interaction energy which we write in the following form[47],

$$\Delta E(t) = -\tfrac{1}{3}(\epsilon_c + 2)\,\underline{\mu}(t) \cdot \int_{-\infty}^{t} dt'\, r(t-t')\,\underline{\mu}(t') \qquad (42)$$

where, r(t) is given, in the Debye approximation, by the following expression,

$$r(t) = \frac{2}{3R^3\,\epsilon_c\,\tau_D}\left[(\epsilon_c+2)/(2\epsilon_\infty+\epsilon_c)\right] \times \left[\epsilon_0 - \epsilon_\infty + \frac{(\epsilon_0-\epsilon_\infty)(\epsilon_c+2\epsilon_0)}{\epsilon_0+2\epsilon_\infty}\right] e^{-t/\tau_L} = \frac{3}{\epsilon_0+2}\,F\,e^{-t/\tau_L} \qquad (43)$$

where,

$$\tau_L = \frac{\epsilon_c + 2\epsilon_\infty}{\epsilon_0 + 2\epsilon_0}\,\tau_D \qquad (44)$$

where, F is defined by equation (43), ϵ_0 and ϵ_∞ are respectively the zero frequency and infinite frequency dielectric constants of the polar solvent, τ_D is the Debye relaxation time constant of the medium, ϵ_c and R are the infinite frequency dielectric constant and the radius of the solute particle (approximated by a sphere), respectively.

Two comments on equations (42-44) are in order. Firstly, these expressions are derived with the assumption that the solvent is a dielectric continuum and that the response function of the solvent is given adequately by a frequency dependent dielectric constant. Secondly, a simple Debye relaxation form[49],

$$\epsilon(\omega)=\epsilon_\infty+\frac{\epsilon_0-\epsilon_\infty}{1-i\,\omega\,\tau_D} \qquad (45)$$

is assumed for $\epsilon(\omega)$. This is obviously a simplifying approximation and can be easily improved[48] by using a more realistic form for $\epsilon(\omega)$. The spherical shape assumption for the solute particle is also not realistic, but this assumption is not expected to affect the qualitative or semi-quantitative conclusions of this work.

Using the above expressions, some straightforward manipulations lead to the following expression for $\Delta E_{eg}(t)$[47],

$$\Delta E_{eg}(t)=F\,\tau_r(\mu_e\mu_g\cos\psi-\mu_e^2)(1-e^{-t/\tau_r})$$
$$+F\,\tau_r(\mu_g^2-\mu_e\mu_g\cos\psi)e^{-t/\tau_r} \qquad (45)$$

where, $\tau_r^{-1}=\tau_L^{-1}+2D$, and ψ is the angle of rotation of the dipole upon excitation, measured in the body-fixed frame, and D is the rotational diffusion coefficient of the solute molecule.

Equation (39) can now be solved numerically to obtain P(t). A similar calculation was carried out elsewhere[31]. Equation (39) is a straightforward generalisation of the above mentioned work to consider non-equilibrium solvation dynamics.

A detailed numerical solution of equation (39), with $\Delta E_{eg}(t)$ given by equation (46), will be presented elsewhere. However, several interesting qualitative features of the solvent effect on the reaction rate can be drawn from the analytic structure of the above equations and are given below.

(i) If the reaction rate is much faster than the solvent relaxation rate (both k_0 and ω are large so that rate of decay is larger than solvent relaxation rate), then the electronic relaxation occurs from the excited state which is Franck-Condon state of the ground state. It the dipole moment (in the body-fixed frame) rotates by more than $\pi/2$ but less than $3\pi/2$ on excitation, then the excited Franck-Condon state can have significantly larger separation from the ground state than what would be present when both the states are in equilibrium with the surrounding solvent. This effect would tend to reduce the rate of reaction. On the other hand, if the rotation of the dipole moment is such that $\pi/2 \geqslant \psi \geqslant -\pi/2$ then the reaction rate can increase because of this non-equilibrium effect.

(ii) It the reaction rate is much slower than the solvent relaxation then the reaction would occur from the excited state in equilibrium with the surrounding solvent. In this case the theory of equilibrium solvation is applicable.

(iii) In the general case where no such separation of time scales exists, we expect the non-equilibrium solvation dynamics to influence the rate of the reaction significantly. In this case the decay function P(t) will show departure from the decay function evaluated at solvent equilibrium at the initial and the intermediate times. There are several scenerios that are possible. If the excited molecule finds the initial environment unfavourable, then the initial decay would be slower than the equilibrium decay. A schematic representation of the decay behaviour is shown in Fig. 7.

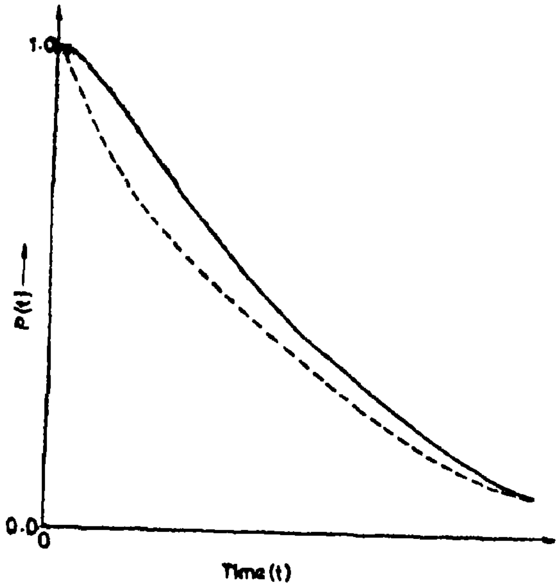


Fig. 7. The time evolution of the excited state population P(t). The dashed line is result from Ref. 31. The solid line includes the effect of non-equilibrium solvation.

There may be an interesting side-effect of this slow initial decay of the excited state from an unfavourable solvent environment. It may lead to an adiabatic reaction with a finite non-zero activation barrier. A crossover behaviour of this type has been observed recently by Sundstron and Gillbro[14] in their experiments on solvent dependence of electronic relaxation of TPM dyes.

Case (B) : Reaction in the presence of a barrier : In this case the non-equilibrium solvation dynamics can affect the rate and even the course of the reaction if the reaction coordinate is coupled to solvent relaxation. One simple way in which this coupling can occur is the following. It may be considered that the reactive motion is a twist of one part of the solute molecule around the other. Such a twisting motion can lead to a change in the magnitude and in the direction of the dipole moment. Depending on the state of solvent polarisation around the solute molecule, the activated complex may be stabilised or destabilised. In the former case, the activation barrier that would be probed by the reactive motion would be less than that in a

non-polar solvent, and the reverse is true if the activated complex is destabilised.

One recently studied example is the isomerisation of dimethylaminobenzonitrile (DMABN) in polar media[8]. In the excited state, this molecule undergoes a rotation of the dimethylamino group about the amino-phenyl bond. The motion results in a charge separation and the twisted form develops a large dipole moment. The reaction is shown in Fig. 5, where the reactive motion is shown by an arrow. In this case, experiments seem to indicate that the dipole moment changes by a rapid jump near the product well followed by solvent stabilisation. Obviously, several other scenerios are also possible. In the case of DMABN, the potential parameters of the reaction change with the polarity of the solvent. If the reaction is faster than solvent relaxation (which may be true in an associated liquid) then the effect of non-equilibrium solvation dynamics may become important.

At present, there is no reliable theoretical calculation for these non-equilibrium effects. van der Zwan and Hynes[29,30] have carried out some model calculations to show the importance of these non-equilibrium effects, but their model is not very realistic. Further work on this field would certainly be worthwhile.

Discussion

It is evident from the preceding analysis that non-equilibrium solvation dynamics can profoundly affect the kinetics of a chemical reaction in solution. In order to enable experimental study of the novel effects discussed in this paper, the reacting system (reactant(s)+solvent) must satisfy the following conditions. (i) The rate of the chemical reaction must be comparable to the relevant solvent relaxation rate. (ii) The reactive event must involve a change in a molecular property which can alter the reaction potential energy surface *via* coupling of this property to the surrounding solvent. Obviously dipole moment is such a molecular property whose change in a polar solvent can have a significant effect on the potential energy surface.

It is obvious that photochemical isomerisation reactions in polar solvents are good candidates for the study of the non-equilibrium solvation effects. These effects are likely to be important in picosecond or in subpicosecond regime. Further theoretical and experimental studies to understand the role of non-equilibrium solvation processes in chemical reactions in solution will certainly be worthwhile.

References

1. S. G. Entelis and R. P. Tiger, "Reaction Kinetics in the Liquid Phase", Wiley, New York, 1976.
2. E. A. Moelwyn-Hughes, "The Kinetics of Reaction in Solution", Claredon, Oxford, 1947.
3. S. Glasstone, K. J. Laidler and H. Eyring, "The Theory of Rate Processes", McGraw-Hill, New York, 1941.
4. K. Laidler, "Theories of Chemical Reaction Rates", McGraw-Hill, New York, 1969.
5. E. S. Amis, "Solvent Effects on Reaction Rates and Mechanisms", Macmillan, New York, 1966.
6. R. M. Hochstrasser in "Picosecond Phenomena", eds. C. V. Shank, R. M. Hochstrasser and V. Kaiser, Springer, Berlin, 1980, Vol. II.
7. G. R. Fleming, S. Velsko and D. Waldeck in "Picosecond Phenomena", eds. K. B. Eisenthal *et al.*, Springer, Berlin, 1982, Vol. III.
8. J. Hicks, M. Vandersall, Z. Barbarogic and K. B. Eisenthal, *Chem. Phys. Lett.*, 1985, **116**, 18.
9. S. P. Velsko and G. R. Fleming, *J. Chem. Phys.*, 1982, **76**, 3553.
10. S. P. Velsko, D. H. Waldeck and G. R. Fleming, *J. Chem. Phys.*, 1983, **78**, 249.
11. K. M. Keery and G. R. Fleming, *Chem. Phys. Lett.*, 1984, **93**, 322.
12. S. Russo and P. J. Thistlethwaite, *Chem. Phys. Lett.*, 1984, **91**, 106.
13. V. Sundström and T. Gillbro, *Chem. Phys. Lett.*, 1984, **109**, 538.
14. V. Sundström and T. Gillbro, *Chem. Phys. Lett.*, 1984, **110**, 303.
15. V. Sundström and T. Gillbro, *J. Chem. Phys.*, 1984, **81**, 3463.
16. H. A. Kramers, *Physica*, 1940, **7**, 284.
17. S. Chandrasekhar, *Rev. Mod. Phys.*, 1943, **1**, 15.
18. J. L. Skinner and P. J. Wolynes, *J. Chem. Phys.*, 1978, **69**, 2143 ; 1980, **72**, 4913.
19. S. H. Northrup and J. T. Hynes, *J. Chem. Phys.*, 1980, **73**, 2700.
20. J. A. Montgomery, D. Chandler and B. J. Berne, *J. Chem. Phys.*, 1979, **70**, 4056.
21. R. F. Grote and J. T. Hynes, *J. Chem. Phys.*, 1980, **73**, 2715.
22. R. F. Grote and J. T. Hynes, *J. Chem. Phys.*, 1982, **77**, 3736.
23. R. F. Grote and J. T. Hynes, *J. Chem. Phys.*, 1981, **74**, 4465 ; 1981, **75**, 2191.
24. B. Bagchi and D. W. Oxtoby, *J. Chem. Phys.*, 1983, **78**, 2735.
25. B. Carmeli and A. Nitzan, *Phys. Rev. Lett.*, 1983, **49**, 423 ; 1983, **51**, 233.
26. B. Carmeli and A. Nitzan, *J. Chem. Phys.*, 1984, **80**, 3596.
27. D. K. Garrity and J. L. Skinner, *Chem. Phys. Lett.*, 1983, **95**, 46.
28. B. M. Ladanyi and G. T. Evans, *J. Chem. Phys.*, 1983, **79**, 944.
29. G. van der Zwan and J. T. Hynes, *J. Chem. Phys.*, 1982, **76**, 2993.
30. G. van der Zwan and J. T. Hynes, *Chem. Phys. Lett.*, 1984, **90**.
31. B. Bagchi, G. R. Fleming and D. W. Oxtoby, *J. Chem. Phys.*, 1983, **78**.
32. B. Bagchi, S. Singer and D. W. Oxtoby, *Chem. Phys. Lett.*, 1983, **99**, 225.
33. J. T. Hynes in "The Theory of Chemical Reaction", ed. M. Baer, Chemical Rubber, Boca Raton, (in the press).
34. B. Bagchi, *Int. Revs. Phys. Chem.*, in the press.
35. E. Wigner, *J. Chem. Phys.*, 1937, **5**, 720.
36. P. Pechukas, *Ann. Rev. Phys. Chem.*, 1985, **32**, 159.
37. R. Kubo, *Rep. Prog. Phys.*, 1966, **29**, 255.
38. A. G. Zawadzki and J. T. Hynes, *Chem. Phys. Lett.*, 1985, **113**, 476.
39. R. Zwanzig and M. Bixon, *Phys. Rev. A*, 1970, **2**, 2005.
40. K. F. Herzfeld and T. A. Litovitz, "Absorption and Dispersion of Ultrasonic Waves", Academic, New York, 1959.
41. R. Zwanzig and M. Bixon, *J. Fluid Mech.*, 1975, **69**, 21.
42. W. Liptay in "Excited States", ed. E. C. Lim, Academic, New York, 1984, Vol. 1.
43. N. J. Turro, "Modern Molecular Photochemistry", Benjamin/Cummings, Menlo Park, 1978.

44. W. G. DAUBEN, E. L. MCINNIS and D. M. MICHNO in "Rearrangements in Ground and Excited States", ed. P. DE MAYO, Academic, New York, 1980.
45. T. OKAMURA, M. SUMITANI and K. YOSHIHARA, *Chem. Phys. Lett.*, 1983, **94**, 339.
46. L. A. HALLIDAY and M. R. TOPP, *J. Phys. Chem.*, 1978, **82**, 2415.
47. B. BACCHI, D. W. OXTOBY and G. R. FLEMING, *Chem. Phys.*, 1984, **86**, 257.
48. M. ABRAMOWITZ and L. A. STEGUN, "Handbook of Mathematical Functions", Dover, New York, 1972.
49. C. J. F. BOTTCHER, "Theory of Electric Polarization", Elsevier, Amsterdam, 1978, Vol. 2.

J. Indian Chem. Soc.,
Vol. LXIII, January 1986, pp. 179-185

Thermodynamic Theories of Precipitation, Dissolution, Freezing and Melting Potentials†

R. P. RASTOGI, P. C. PANDEY and A. K. TRIPATHI

Department of Chemistry, Banaras Hindu University, Varanasi-221 005

THE precipitation and dissolution potentials are a novel class of phenomena which have been extensively studied during recent years[1-7]. Thermodynamic theories of precipitation and dissolution potentials have also been developed[8,9]. The purpose of the present paper is to develop an improved model and the corresponding theory of this phenomena. It is also intended to examine to what extent the new theory agrees with new data on precipitation potential using micro electrode[10] and dissolution potential using rotating electrode[8], and to develop corresponding theories of freezing potential[11-15] and melting potential[16] in order to explain the experimental results.

The model used earlier is based on the postulate that precipitation potentials essentially arise due to a difference in the rate of attachment of cations and anions during crystallisation or to a difference in detachment rate during dissolution in addition to other factors. In this model, the crucial site is supposed to be crystal(α)-solution(β) interface. On the solution side of the interface, ions are supposed to exist as bare ions. So long as the crystallisation or dissolution proceeds, both the regions are in non-equilibrium. However, when the crystal of an electrolyte is in contact with its saturated solution for a long time, equilibrium is established. The free energy change in the electrical process is equivalent to the free energy change during transfer of bare ions from the β-phase to α-phase.

The precipitation potential[8] has been conceptually defined as follows. 'The precipitation potential difference arising from an electrical double layer developed at a liquid-crystal interface by the ion migration from the liquid phase. The algebraic sign of the precipitation potential is the same as the electrostatic polarity (+) or (−), of the end of the dipolar double layer on the crystal side of the interface'. Similarly, the conceptual definition[8] of dissolution potential is as follows. 'The dissolution potentials is the potential difference arising from an electrical double layer developed at a liquid crystal interface by the process of crystal dissolution (ion migration) into the liquid phase. The algebraic sign of the dissolution potential is the same as the electrostatic polarity (+) or (−), of the end of the dipolar double layer on the crystal side of the interface'.

When precipitation takes place, the bare ions from the interface after being stripped of hydrated water molecules get attached in the lattice. The stripping occurs in the adjacent liquid phase just before entering the crystal lattice. The essential reaction occurring at the interface is

$$A^+ + B^- \rightleftharpoons AB\,(\alpha)$$

Similarly, when dissolution takes place, the bare ions detach from the lattice and plunge into the medium and the basic reaction occurring at the interface is

$$AB(\alpha) \rightleftharpoons A^+ + B^-$$

Phase potential and diffusion potential or similar potential are usually superimposed in the potentials observed during dissolution and precipitation of electrolytes by the techniques described earlier. The double layer in both the cases consist of bare cation and anion.

Precipitation potential : Based on the above considerations, Rastogi and Khan obtained the following expression for the precipitation potential[8] for uni-univalent electrolyte,

$$-F(\Delta\phi)^{\alpha,\beta} = t_1^a[\mu_1^{0\alpha} + RT \ln a_1^\alpha - \mu_1^{0\beta} - RT \ln a_1^\beta]$$
$$- t_2^a[\mu_2^{0\alpha} + RT \ln a_2^\alpha - \mu_2^{0\beta} - RT \ln a_2^\beta] \qquad (1)$$

where, F = Faraday and $(\Delta\phi)^{\alpha,\beta}$ = potential between α- and β-phase.
Further,

$$t_1^a = \frac{U_1^a}{U_1^a + U_2^a}\ ;\ t_2^a = \frac{U_2^a}{U_1^a + U_2^a} \qquad (2)$$

where, U_1^a and U_2^a are the speeds of attachment of cations and anions. $\mu_i^{0\alpha}$ and $\mu_i^{0\beta}$ are the standard chemical potential of the ion i in α- and β-phase, respectively.

Equation (1) can be written as

$$-F(\Delta\phi)^{\alpha,\beta} = t_1^a[(\mu_1^{0\alpha} - \mu_1^{0\beta})] - t_2^a[(\mu_2^{0\alpha} - \mu_2^{0\beta})]$$
$$+ \left[(t_1^a - t_2^a)\, RT \ln \frac{a^\alpha}{a^\beta}\right] \qquad (3)$$

when it is assumed that

$$\frac{a_1^\alpha}{a_1^\beta} = \frac{a_2^\alpha}{a_2^\beta} = \frac{a^\alpha}{a^\beta}$$

† Dedicated to Professor Sadhan Basu on the occasion of his 65th birthday.

A part of the article was presented at the National Conference on Spectroscopy and Theoretical Chemistry held at Calcutta, December 5-7, 1985.

Equation (3) can be rearranged as

$$-F(\Delta\phi)^{\alpha,\beta}=t_1^a[\mu_1^{o\alpha}-\mu_1^{o\beta}-RT\ln a_1^{sat}]$$
$$-t_2^a[\mu_2^{o\alpha}-\mu_2^{o\beta}-RT\ln a_2^{sat}]+RT\,(t_1^a-t_2^a)\ln\frac{a^{\alpha}\,a^{sat}}{a^{\beta}} \quad (4)$$

Putting,

$$t_1^a[\mu_1^{o\alpha}-RT\ln a_1^{sat}]-t_2^a[\mu_2^{o\alpha}-\mu_2^{o\beta}-RT\ln a_2^{sat}]=-F(\Delta\phi)^{*}_{phase}$$

we have

$$-F(\Delta\phi)^{\alpha,\beta}=-F(\Delta\phi)^{*}_{phase}+RT\left(\frac{U_1^a-U_2^a}{U_1^a+U_2^a}\right)\ln\frac{a^{\alpha}\,a^{sat}}{a^{\beta}} \quad (5)$$

which can be rewritten as follows when a^{α} is taken to be unity,

$$(\Delta\phi)^{\alpha,\beta}=(\Delta\phi)^{*}_{phase}+\frac{RT}{F}\left(\frac{U_1^a-U_2^a}{U_1^a+U_2^a}\right)\ln\frac{a^{\beta}}{a^{sat}} \quad (6)$$

The quantity $(\Delta\phi)^{*}_{phase}$ is difficult to measure or estimate theoretically. However, when $t\to\infty$, this is equal to phase potential, so that when $t\to\infty$, $a^{\beta}\to a^{sat}$ and

$$(\Delta\phi)^{\alpha,\beta}_{t\to\infty}=(\Delta\phi)_{phase} \quad (7)$$

Again, to a first approximation for the non-equilibrium case,

$$d\ln\frac{a^{\alpha}}{a^{\beta}}=\left[\frac{H^{\alpha}-H^{\beta}}{RT^2}\right]dT \quad (8)$$

which can be written as

$$\ln\frac{a^{\alpha}}{a^{\beta}}=+\frac{(H^{\alpha}-H^{\beta})}{RT^2_{av}}\,\Delta T$$

$$i.e., \ln\frac{a^{\alpha}}{a^{\beta}}-\ln\frac{a^{\alpha sat}}{a^{\beta sat}}=+\frac{(H^{\alpha}-H^{\beta})}{RT^2_{av}}(T_c-T_s)$$
$$=-\frac{(H^{\alpha}-H^{\beta})}{RT^2_{av}}\,\Delta T \quad (9)$$

where, $T_{av}=\frac{T_s+T_c}{2}$ and $a^{\beta sat}$ denotes the activity of ions in saturated solution in non-equilibrium. Here, T_s = saturation temperature.

$\Delta T=T_s-T_c$, where T_c is the crystallization temperature. $\Delta H^{\alpha,\beta}=H^{\alpha}-H^{\beta}$ is the net enthalpy change of the processes

$$A^{+(\beta)}+B^{-(\beta)}\longrightarrow AB\ (\alpha)$$

Accordingly, we can write,

$$(\Delta\phi)^{\alpha,\beta}=(\Delta\phi)^{*}_{phase}+\frac{1}{F}\left(\frac{U_1^a-U_2^a}{U_1^a+U_2^a}\right)\frac{\Delta H^{\alpha,\beta}\,.\,\Delta T}{T_s} \quad (10)$$

The magnitudes of $(\Delta\phi)_{phase}$ and $(\Delta\phi)^{*}_{phase}$ are likely to be similar. Further, diffusion potential will have a negligible magnitude when measurement are made with the microelectrode.

Dissolution potential: We recall that dissolution process is a non-equilibrium process. During dissolution, the region of interest is again the liquid interface just adjacent to the solid. It should be noted that both solid and liquid regions near the interface are in non-equilibrium so long as dissolution takes place. Bare ions get detached from the crystal lattice which jump into the liquid phase and get solvated at once. Amongst other factors, the sign and magnitude of the potential is supposed to depend on the relative speed of detachment of ions.

We consider the dissolution in a slightly undersaturated solution and that a certain amount of crystals adhere to the electrode when $t\to\infty$. We assume that diffusion potential is eliminated in the experiments. Following the treatment of Rastogi and Khan**, we get

$$-(\Delta\phi^{\alpha,\beta}+\Delta\phi^{\beta,\delta})=\frac{t_1^d}{e_1}\,\Delta\mu_1^{\alpha,\beta}+\frac{t_2^d}{e_2}\,\Delta\mu_2^{\alpha,\beta}$$
$$+\frac{t_1}{e_1}\,\Delta\mu_1^{\beta,\delta}+\frac{t_2}{e_2}\,\Delta\mu_2^{\beta,\delta} \quad (11)$$

$$\text{where, } t_1^d=\frac{U_1^d}{U_1^d+U_2^d}\ \text{ and }\ t_2^d=\frac{U_2^d}{U_1^d+U_2^d} \quad (12)$$

and U_1^d and U_2^d are speeds of detachment of unhydrated (bare) cations and anions, respectively. Further, t_1 and t_2 are effective transport numbers of cation and anion at the β/δ interface**.

$$-(\Delta\phi)^{\alpha,\beta}=\left(\frac{t_1^d}{e_1}\,\Delta\mu_1^{\alpha,\beta}+\frac{t_2^d}{e_2}\,\Delta\mu_2^{\alpha,\beta}\right) \quad (13)$$

$$-(\Delta\phi)^{\beta,\delta}=\left(\frac{t_1}{e_1}\,\Delta\mu_1^{\beta,\delta}+\frac{t_2}{e_2}\,\Delta\mu_2^{\beta,\delta}\right) \quad (14)$$

Further,

$$(\Delta\phi)^{\beta,\delta}=-\frac{RT}{F}\left(\frac{U_1-U_2}{U_1+U_2}\right)\ln\frac{a^{\beta}}{a^{\delta}} \quad (15)$$

when we suppose that

$$\frac{a_1^{\beta}}{a_1^{\delta}}=\frac{a_2^{\beta}}{a_2^{\delta}}=\frac{a^{\beta}}{a^{\delta}} \quad (16)$$

for uni-univalent electrolytes.

Equation (13) can be rewritten as

$$-(\Delta\phi)^{\alpha,\beta}=\frac{t_1^d}{F}(\mu_1^{\alpha}-\mu_1^{\beta})-\frac{t_2^d}{F}(\mu_2^{\alpha}-\mu_2^{\beta}) \quad (17)$$

$$\text{where, } e_1=-e_2=F \quad (18)$$

The chemical potential in α and β phases are given by

$$\mu_i^{\alpha}=\mu_i^{o\alpha}+RT\ln a_i^{\alpha}\ (i=1,2) \quad (19)$$

$$\mu_i^{\beta}=\mu_i^{o\beta}+RT\ln a_i^{\beta}\ (i=1,2) \quad (20)$$

* It was stated[9] that the mobilities of the cations and anions at the crystal interface would be equivalent to ionic mobilities. This is a gross oversimplification. Further, there is a mistake of sign in equations (45) and (46) in the manuscript. Further, in equation (84), $(\Delta\phi)II=-(\Delta\phi)_{diff}$ so that $(\Delta\phi)_{diff}=-RT/F.$ $(t_1-t_2)\ln a^{\beta}/a$. Again, t_i may not necessarily be equal to conventional transport number since the transport across the interface β/δ has to be considered.

** The lower limit of second integral on the right hand side of equation (16) in Ref. 9 should be read as μ^{β} instead μ(sat).

where, $\mu_i^{0\alpha}$ and $\mu_i^{0\beta}$ are the standard chemical potentials of species i in α- and β-phases, respectively. Hence, equation (17) can be written as

$$-F(\Delta\phi)^{\alpha,\beta}=t_1^d[\mu_1^{0\alpha}-\mu_1^{0\beta}-RT\ln a_1^{sat}]$$
$$-t_2^d[\mu_2^{0\alpha}-\mu_2^{0\beta}-RT\ln a_2^{sat}]$$
$$-t_1^d\ln\frac{a_1^{\alpha}\cdot a_1^{sat}}{a_1^{\beta}}-t_2^d\ln\frac{a_2^{\alpha}\cdot a^{sat}}{a_2^{\beta}} \quad (21)$$

where, a_1^{sat} and a_2^{sat} denote the activities of ions 1 and 2 in the saturated solution. If $(\Delta\phi)_{phase}$ denotes the phase potential, it can be easily shown that

$$\mu_1^{0\alpha}-\mu_1^{0sat}-RT\ln a_1^{sat}=-F(\Delta\phi)_{phase} \quad (22)$$

$$\mu_1^{0\alpha}-\mu_2^{0sat}-RT\ln a_2^{sat}=+F(\Delta\phi)_{phase} \quad (23)$$

where, μ_1^{0sat} and μ_2^{0sat} are the corresponding standard chemical potentials in saturated solution. Thus $\mu_1^{0\beta}$ and μ_i^{0sat} need not be equal. Hence, using equations (22), and (23) we get,

$$-F(\Delta\phi)^{\alpha,\beta}=-F(\Delta\phi)^*_{phase}-RT(t_1^d-t_2^d)\ln\frac{a^{\beta}}{a^{sat}\ a^{\alpha}} \quad (24)$$

where, $(\Delta\phi)^*_{phase}$ may be called as non-equilibrium phase potentials which would be equal to $(\Delta\phi)_{phase}$ in equilibrium.

In writing equation (24) we have supposed that

$$\frac{a_1^{sat}\ a_1^{\alpha}}{a_1^{\beta}}=\frac{a_2^{sat}\ a_2^{\alpha}}{a_2^{\beta}}=\frac{a^{sat}\ a^{\alpha}}{a^{\beta}}$$

Thus, equation (24) can be written as

$$-F(\Delta\phi)^{\alpha,\beta}=-F(\Delta\phi)^*_{phase}$$
$$-\frac{RT}{F}\left(\frac{U_1^d-U_2^d}{U_1^d+U_2^d}\right)\ln\frac{a^{\beta}}{a^{\alpha}\cdot a^{sat}} \quad (25)$$

Assuming that $a^{\alpha}=1$ for solid, we have,

$$(\Delta\phi)^{\alpha,\beta}=(\Delta\phi)^*_{phase}+\frac{RT}{F}\left(\frac{U_1^d-U_2^d}{U_1^d+U_2^d}\right)\ln\frac{a^{\beta}}{a^{sat}} \quad (26)$$

when $t\rightarrow\infty$ and solid still adheres to the electrode, $a^{\alpha}=a^{sat}$ and $(\Delta\phi)^*_{phase}=(\Delta\phi)_{phase}$.

Comparison of equations (6) and (26) shows that since $(\Delta\phi)^*$ would have the same value at a fixed temperature for both the cases, $(\Delta\phi)_{diss}$ and $(\Delta\phi)_{ppt}$ will have the same sign and their ratio (θ) at a fixed temperature would be given by,

$$\frac{(\Delta\phi)_{diss}}{(\Delta\phi)_{ppt}}\approx 1 \quad (27)$$

since

$$\frac{U_1^a-U_2^a}{U_1^a+U_2^a}\approx\frac{U_1^d-U_2^d}{U_a^d+U_2^d}$$

if it is assumed that

$$U_i^a\propto\frac{1}{r_i}\ ;\ U_i^d\propto\frac{1}{r_i}$$

Thermodynamic theory of freezing and melting potential : The freezing and melting potentials have been conceptually defined as follows. 'The freezing potential is the potential difference arising from an electrical double layer developed at the in/solution interface by the ion-migration from the liquid phase. The algebraic sign of the freezing potential is the same as the electrostatic polarity (+) or (−), of the end of the dipolar double layer on the lattice side of the interface'. Similarly, the 'melting potential is the potential difference arising from an electrical double layer developed at a liquid/crystal interface by the process of melting (ion-migration) into the liquid phase. The algebraic sign of the melting potential is the same as the electrostatic polarity (+) or (−), of the end of the dipolar double layer on the lattice side of the interface'.

Both freezing and melting processes are non-equilibrium processes. Just at the solid/liquid interface, both phases are in non-equilibrium. This interface contains bare hydro nium and hydroxyl ions which get attached to the crystal lattice during freezing. Similarly, when ions get detached from the lattice along with free H_2O molecule and clusters of hydrogen bonded H_2O molecules but only the ions contribute to the generation of electric potential. At the melting interface, there is a layer of free unhydrated ions.

We assume that H_3O^+ and OH^- are dissolved in a large mass of H_2O molecules. We denote the solid phase by α, non-equilibrium solid/liquid interface by β and bulk liquid phase by δ.

Following the procedure of Rastogi and Khan, we get the expression for the freezing potential $(\Delta\phi)^{\alpha,\beta}$,

$$-F(\Delta\phi)^{\alpha,\beta}=t_1^a[\mu_1^{0\alpha}+RT\ln a_1^{\alpha}-\mu_1^{0\beta}-RT\ln a_1^{\beta}]$$
$$-t_2^a[\mu_2^{0\alpha}+RT\ln a_2^{\alpha}-\mu_2^{0\beta}-RT\ln a_2^{\beta}] \quad (28)$$

where, F = Faraday, $(\Delta\phi)^{\alpha,\beta}$ = potential difference between α and β phases and $\mu_i^{0\alpha}$ and $\mu_i^{0\beta}$ are the standard chemical potential of i th species in α and β phases, respectively. Further t_1^a and t_2^a are the transport number of attachment of hydronium and hydroxyl ion to growing ice lattice which can be expressed as

$$t_1^a=\frac{U_1^a}{U_1^a+U_2^a}\ ;\qquad t_2^a=\frac{U_2^a}{U_1^a+U_2^a} \quad (29)$$

Equation (1) can be written as

$$-F(\Delta\phi)^{\alpha,\beta}=t_1^a[\mu_1^{0\alpha}-\mu_1^{0\beta}-t_2^a[\mu_2^{0\alpha}-\mu_2^{0\beta}]$$
$$+(t_1^a-t_2^a)\ RT\ln\frac{a^{\alpha}}{a^{\beta}} \quad (30)$$

where, it is assumed as

$$\frac{a_1^{\alpha}}{a_1^{\beta}}=\frac{a_2^{\alpha}}{a_2^{\beta}}=\frac{a^{\alpha}}{a^{\beta}}$$

Equation (30) can be rearranged as

$$-F(\Delta\phi)^{\alpha,\beta}=t_1^a[\mu_1^{0\alpha}-\mu_1^{0\beta}-RT\ln a_1^{\delta}]$$
$$-t_2^a[\mu_2^{0\alpha}-\mu_2^{0\beta}-RT\ln a_2^{\delta}]+RT\ (t_1^a-t_2^a)\ln\frac{a^{\alpha}.a^{\delta}}{a^{\beta}} \quad (31)$$

where, a^{δ} represents the normal liquid phase where the ions are hydrated.

We can write from equation (31),

$$-t_1^a[\mu_1^{o\alpha}-\mu_1^{o\beta}-RT\ln a_1^\beta]-t_2^a[\mu_2^{o\alpha}-\mu_2^{o\beta}-RT\ln a_2^\beta] = -(\Delta\phi)^*_{phase} \quad (32)$$

Since,

$$-F(\Delta\phi)^{\alpha,\beta} \cdot F(\Delta\phi)^*_{phase}+RT\left(\frac{U_1^a-U_2^a}{U_1^a+U_2^a}\right)\ln\frac{a^\delta}{a^\beta} \quad (33)$$

where, we have assumed that a^α is the unity and $(\Delta\phi)^*_{phase}$ is the non-equilibrium phase potential which is difficult to measure or estimate theoretically.

Further, equation (33) can be written as

$$(\Delta\phi)^{\alpha,\beta}=(\Delta\phi)^*_{phase}+\frac{RT}{F}\left(\frac{U_1^a-U_2^a}{U_1^a+U_2^a}\right)\ln\frac{a^\beta}{a^\delta} \quad (34)$$

where $t\rightarrow\infty$, $a^\beta\rightarrow a^\delta$ and $(\Delta\phi)^{\alpha,\beta}_{t\rightarrow\infty}=(\Delta\phi)_{phase}$.

We can write from equation (34),

$$(\Delta\phi)_{freez}=\frac{RT}{F}\left(\frac{U_1^a-U_2^a}{U_1^a+U_2^a}\right)\ln\frac{a^\beta}{a^\delta} \quad (35)$$

where, $(\Delta\phi)_{freez}$ represents the freezing potential.

We can derive an analogous equation for melting potential in the following manner. Using the procedure of Rastogi and Khan, we obtain the expression,

$$-F(\Delta\phi)^{\alpha,\beta}=\frac{t_1^d}{e_1}(\Delta\mu_1^{\alpha,\beta})+\frac{t_2^d}{e_2}(\Delta\mu_2^{\alpha,\beta}) \quad (36)$$

where, t_1^d and t_2^d are the transport number of detachment of hydronium and hydroxyl ions. This can be expressed as

$$t_1^d=\frac{U_1^d}{U_1^d+U_2^d}\,;\quad t_2^d=\frac{U_2^d}{U_1^d+U_2^d}$$

where, U_1^d and U_2^d are respectively the speed of detachment of hydronium and hydroxyl ions. Equation (37) can be rearranged as

$$-F(\Delta\phi)^{\alpha,\beta}=\frac{t_1^d}{e_1}(\mu_1^\alpha-\mu_1^\beta)-\frac{t_2^d}{e_2}(\mu_2^\alpha-\mu_2^\beta) \quad (37)$$

where, $e_1=-e_2$ and μ_i^α and μ_i^β are the chemical potential in α- and β-phases, respectively. The chemical potential of ith species in α- and β-phases can be given by equations (38),

$$\mu_i^\alpha=\mu_i^{o\alpha}+RT\ln a_i^\alpha\ (i=1,2)$$
$$\mu_i^\beta=\mu_i^{o\beta}+RT\ln a_i^\beta\ (i=1,2) \quad (38)$$

where, $\mu_i^{o\alpha}$ and $\mu_i^{o\beta}$ are the chemical potential of species i in α- and β-phases, respectively. Hence equation (38) can be written as

$$-F(\Delta\phi)^{\alpha,\beta}=t_1^d[\mu_1^{o\alpha}+RT\ln a_1^\alpha-\mu_1^{o\beta}\ \ RT\ln a_1^\beta]-t_2^d[\mu_2^{o\alpha}+RT\ln a_2^\alpha-\mu_2^{o\beta}-RT\ln a_2^\beta]$$

or,

$$-F(\Delta\phi)^{\alpha,\beta}=t_1^d[\mu_1^{o\alpha}-\mu_1^{o\beta}-RT\ln a_1^\beta]-t_2^d[\mu_2^{o\alpha}-\mu_2^{o\beta}-RT\ln a_2^\beta]-(t_1^d-t_2^d)RT\ln\frac{a^\alpha a^\delta}{a^\beta} \quad (39)$$

where it is assumed that

$$\frac{a_1^\alpha.a_1^\delta}{a_1^\beta}=\frac{a_2^\alpha.a_2^\delta}{a_2^\beta}=\frac{a^\alpha.a^\delta}{a^\beta}$$

where δ represents the bulk of solution and a_i^α is assumed to be unity, a_i^δ is the activity of ith species in bulk of solution.

We can write from equation (39),

$$-F(\Delta\phi)_{1\ phase}=\mu_1^{o\alpha}-\mu_1^{o\delta}-RT\ln a_1^\delta \quad (40)$$
$$+F(\Delta\phi)_{2\ phase}=\mu_2^{o\alpha}-\mu_2^{o\delta}-RT\ln a_2^\delta \quad (41)$$

where, μ_i^0 is the corresponding standard chemical potential in liquid phase when the ions are hydrated. It should be noted that $\mu_i^{o\beta}$ need not be equal to μ_i^0. Using equations (39), (40) and (41), it can be easily shown that

$$-F(\Delta\phi)^{\alpha,\beta}=-F(\Delta\phi)^*_{phase}-RT(t_1^d-t_2^d)\ln\frac{a^\beta}{a^\delta a^\alpha} \quad (42)$$

where, $(\Delta\phi)^*_{phase}$ may be called as non-equilibrium phase potential which would be equal to $(\Delta\phi)_{phase}$ at equilibrium.

Equation (42) can be written as

$$-F(\Delta\phi)^{\alpha,\beta}=-F(\Delta\phi)^*_{phase}-RT\left(\frac{U_1^d-U_2^d}{U_1^d+U_2^d}\right)\ln\frac{a^\beta}{a^\delta} \quad (43)$$

where, a^α is assumed unity and when $t\rightarrow\infty$, $a^\beta\rightarrow a^\delta$ and $(\Delta\phi)^*_{phase}=(\Delta\phi)_{phase}$.

From equation (43) we can get,

$$(\Delta\phi)_{melt}=\frac{RT}{F}\left(\frac{U_1^d-U_2^d}{U_1^d+U_2^d}\right)\ln\frac{a^\beta}{a^\delta} \quad (44)$$

where, $(\Delta\phi)_{melt}$ represents the maximum value of melting potential.

On comparison of equations (35) and (44), we find that provided the activity of α-phase remains unchanged during freezing and melting, the freezing and melting potential would be related by the expression,

$$(\Delta\phi)_{melt}/(\Delta\phi)_{freez}=\left(\frac{U_1^d-U_2^d}{U_1^d+U_2^d}\right)\Big/\left(\frac{U_1^a-U_2^a}{U_1^a+U_2^a}\right)\frac{T_m}{T_f} \quad (45)$$

Results

The data on precipitation potential using microelectrode and dissolution potential using rotating electrode have been recorded in Table 1. The comparison between experimental and the theoretical values of precipitation potential has been made in Table 2. Similarly, the comparison between experimental and theoretical values of dissolution potential has been made in Table 3. The experimental results on freezing potential and melting potential have been recorded in Table 4.

TABLE 1—PRECIPITATION POTENTIAL USING (MICRO-ELECTRODE) AND DISSOLUTION POTENTIAL USING (ROTATING-ELECTRODE) OF ELECTROLYTES

Electrolyte	Precipitation potential* mV	Dissolution potential** mV	$\frac{(\Delta\phi)_{diss}}{(\Delta\phi)_{ppt}}$	θ
NaCl	−33 ± 2 (−54)	−22	0.67	0.9742
KCl	−44 ± 1 (−56)	−25	0.57	0.9742
KI	−48	−35	0.73	0.9742
KBr	−37 ± 3	−31	0.84	0.9742
$BaSO_4.4H_2O$	50 ± 1	38	0.76	0.9742
$BeCl_2.2H_2O$	—	−37[a]	—	—
$CuSO_4.5H_2O$	31 ± 4	20	0.65	0.9742
Cu_2Cl_2	—	−152[a]	—	—
$NiSO_4.6H_2O$	—	43	—	—
$NiSO_4.7H_2O$	—	44	—	—
$(C_2H_5)_4NI$	−30 ± 2	23	0.77	0.9742
$K_4Fe(CN)_6$	−71 ± 3	−124	1.74	0.9742
$BaCl_2.2H_2O$	—	−218	—	—
NH_4Cl	—	−161	—	—

* $\Delta T = 12°$, $T_s = 323$ K figure in parenthesis denotes values obtained with large platinum electrode.

** T = 303 K. [a] Ref. 5.

Discussion

The values of $\theta = T_d/T_p \frac{(\Delta\phi)_{diss}}{(\Delta\phi)_{ppt}}$ calculated using equation (27) have been compared in Table 1. The agreement is satisfactory as can be expected. The case of $K_4Fe(CN)_6$ is a little anomalous, but, since in the precipitation process four K^+ along with one $Fe(CN)_6^{4-}$ have to get attached to the crystal lattice, $(U_1^a - U_2^a)$ is expected to be much smaller than $(U_1^d - U_2^d)$ since the detachment of four K^+ from the lattice would be easier process.

Exact experimental tests of equations (6) and (10) is difficult. However, these can be used to compute approximate values of precipitation potentials. This can be done provided the values of a^{sat} and a^{β} ; ΔH ; and U_1^a and U_2^a are known. For NaCl, KCl, KBr and KI, values of $(a^{sat}; d)$ are available. (a^{β}) for the unhydrated ions can be estimated from the following relation between activity coefficient $f_{\pm}$ and an assumed concentration C,

$$\log f_{\pm} = -\frac{a_0 \sqrt{C}}{1+\beta a_0 \sqrt{C}} \quad (46)$$

and

$$a_{\pm} = f_{\pm} . C$$

where, a_0 denotes the ion size parameter for bare ion. Similarly, ΔH can be estimated from crystal energy. Values of U_1^a and U_2^a are not known. However, we may suppose that

$$U_1^a = \frac{k_1}{r_1} \text{ and } U_2^a = \frac{k_2}{r_2} \quad (47)$$

since the speed of attachment of ions is likely to be inversely proportional to ionic radii. For sake of simplicity we put, $k_1 = k_2$, thus,

$$\frac{U_1^a - U_2^a}{U_1^a + U_2^a} \approx \frac{r_2 - r_1}{r_1 + r_2} \quad (48)$$

Substituting the values of the quantities a^{sat}, a^{β}, ΔH and $(U_1^a - U_2^a)/(U_1^a + U_2^a)$ obtained in the above manner in equations (10) and (6), values af $(\Delta\phi)_{ppt}$ have been computed for NaCl, KCl, KBr and KI. These are compared in Table 2 with the experimental values. The agreement is fair considering the uncertainties involved.

Equation (26) can also be examined in a similar manner. U_1^d and U_2^d would be inversely proportional to ionic radii of the bare ions so that an equation

TABLE 2—COMPARISON OF EXPERIMENTAL AND THEORETICAL VALUES OF PRECIPITATION POTENTIAL COMPUTED BY EQUATIONS (6) AND (10)

Electrolyte	r_2 Å	r_1 Å	$f_{\pm}^{sat}$	a^{sat}	$\log (a^{\beta})$*	ΔH kcal mol^{-1}	T_s K	$(\Delta\phi)_{ppt}^{**}$ mV	$(\Delta\phi)_{ppt}^{\dagger}$ mV	$(\Delta\phi)_{ppt}$ (exp.) mV
NaCl	1.81	0.95	0.986	7.179	0.428	−181	323	−9	−92	−33 ± 2
KCl	1.81	1.33	0.590	3.369	0.357	−163	323	−4	−40	−44 ± 1
KBr	1.95	1.33	0.636	4.034	0.447	−160	323	−2	−49	−37 ± 3
KI	2.16	1.33	0.683	6.368	0.619	−151	323	−4	−77	−48

* The values of a^{β} calculated from equation (46). ** $(\Delta\phi)_{ppt}$ calculated from equation (6). † $(\Delta\phi)_{ppt}$ calculated from equation (10).

TABLE 3—COMPARISON OF EXPERIMENTAL AND THEORETICAL VALUES (COMPUTED BY EQUATION (26)) OF DISSOLUTION POTENTIAL OF ELECTROLYTES

Electrolyte	log f	$\log (a^{\beta})$†	f^{sat}	a^{sat}	h^+	h^-	$\frac{r_2 - r_1}{r_2 + r_1}$	$\frac{r_2h_1 - r_1h_2}{r_2h_1 + r_1h_2}$	$\Delta\phi$* mV	$\Delta\phi$** mV	$\Delta\phi$ (exp.) mV
NaCl	−0.393	0.396	0.986	6.064	6	1	0.316	0.985	−7	−23	−22
KCl	−0.349	0.347	0.590	2.927	6	1	0.152	0.978	−1	−7	−25
KBr	−0.346	0.427	0.636	3.772	6	0	0.190	0.1	−2	−11	−31
KI	−0.346	0.640	0.683	6.270	6	0	0.315	1	−4	−13	−35

† Values of a^{β} calculated by equation (46). * $(\Delta\phi)_{diss}$ calculated using values of equation (48). ** $(\Delta\phi)_{diss}$ calculated using values of equation (50).

TABLE 4—FREEZING AND MELTING POTENTIAL OF WATER CONTAINING IMPURITIES

Impurity	Concn.	$(\Delta\phi)_{freez}$[a]	$(\Delta\phi)_{melt}$[b]	θ^*
NaCl	2.5×10^{-5}	-183 ± 13	-210 ± 15 (-220 ± 18)	1.14
NaCl + Urea (10^{-4})	2.5×10^{-5}	-237 ± 10	-215 ± 17	0.91
NaCl + Sucrose (10^{-4})	2.5×10^{-5}	-59 ± 11	-2.8 ± 8	8.69
KCl	2.5×10^{-3}	-75 ± 7	-85 ± 7 (-92 ± 10)	1.08
KCl	2.5×10^{-4}	-250 ± 10	-245 ± 20	0.98
KCl + Urea (10^{-4})	2.5×10^{-4}	-275 ± 11	-259 ± 10	0.95
KCl + Sucrose (10^{-4})	2.5×10^{-4}	-88 ± 8	-240 ± 18	2.73
CsCl	2.5×10^{-3}	-125 ± 10	-160 ± 10	1.24
CsCl	2.5×10^{-4}	-225 ± 10	-290 ± 15	1.28
CsCl	2.5×10^{-5}	-200 ± 12	-225 ± 18	1.13
CsCl	2.5×10^{-6}	-125 ± 10	-150 ± 11	1.20
KI	2.5×10^{-4}	-285 ± 10	-300 ± 15	1.05
NH_4Cl	5×10^{-5}	218 ± 10	300 ± 12 (320 ± 15)	1.88
NH_4Cl + Urea (10^{-4})	5×10^{-5}	283 ± 13	315 ± 10 (325 ± 17)	1.12
NH_4Cl + Sucrose (10^{-4})	5×10^{-5}	88 ± 7	325 ± 10 (338 ± 12)	1.38
$(NH_4)_2CO_3$	5×10^{-5}	295 ± 13	350 ± 17 (335 ± 20)	1.18
$(C_2H_5)_4NI.H_2O$	10^{-4}	-50 ± 5	-75 ± 7	1.5
Urea	1×10^{-4}	230 ± 12	-200 ± 18 (-220 ± 15)	-0.86

[a] Measurements made with microelectrode. [b] Most of the measurements made with stationary electrode; however values of $(\Delta\phi)_{melt}$ in parenthesis in column 4 denotes, observed melting potential using rotating electrode.

identical to equation (48) can be used, *viz.*

$$U_1^d = \frac{k_1^1 h_1}{r_2}\ ;\ U_2^d = \frac{k_2^1 h_2}{r_1} \qquad (49)$$

since the speed of detachment would be more if ions have greater affinity for the solvent as measured by the hydration number. In equation (49), h_1 and h_2 represent the hydration number of cation and anion, respectively. If we again assume that $k_1^1 = k_2^1$,

$$\frac{U_1^d - U_2^d}{U_1^d + U_2^d} = \frac{r_2 h_1 - r_1 h_2}{r_1 h_2 + r_2 h_1} \qquad (50)$$

Thus, $(\Delta\phi)_{diff}$ can be computed using equations (26) and (49) or (50). The values are reported in Table 3. Again the agreement is reasonably satisfactory considering the approximation involved in estimating the values of parameters. The agreement is better when equation (50) is used.

We can make a semi-quantitative comparison between theory and experiment at least in the case of freezing and melting potential of aqueous solution of alkali halides, NH_4Cl and $(NH_4)_2CO_3$. In these cases, ions seggregating at the interface during freezing and melting would be the same. Therefore, U_1^a may be expected to be equal to U_1^d and $U_2^a = U_2^d$ so that

$$\left(\frac{U_1^a - U_2^a}{U_1^a + U_2^a}\right) \approx \left(\frac{U_1^d - U_2^d}{U_1^d + U_2^d}\right) \qquad (51)$$

Using equations (45) and (51), we can obtain,

$$(\Delta\phi)_{melt}/(\Delta\phi)_{freez} = T_m/T_f \qquad (52)$$

Since, $T_m > T_f$, it follows that

$$(\Delta\phi)_{melt}/(\Delta\phi)_{freez} > 1 \qquad (53)$$

Experimental results recorded in Table 4 show that this expectation is in agreement with the experimental data.

The results on freezing and melting potentials of aqueous solution of urea are anomalous so far as the sign is concerned. In case of freezing, the speed of attachment of H_3O^+ would be greater than OH^- in view of the chain mechanism, so that

$$U_1^a > U_2^a \qquad (54)$$

hence, the sign of the freezing potential is positive. On the other hand, in case of melting since the size of OH^- is smaller than that of H_3O^+,

$$U_2^d > U_1^d \qquad (55)$$

hence, the sign of melting potential is negative. It should be noted that in both the cases, a^β/a^δ is positive and greater than unity.

The influence of urea and sucrose on the magnitude of freezing potential of aqueous solution of electrolyte can also be explained on the basis of equation (34) and (44), where urea is added a^α would decreases while it would increase when sucrose is added. The values of a^β would be the same for the case of freezing and melting potential since the crystal/solution interface would be unaffected by the addition of urea or sucrose. Hence, the magnitudes of $(\Delta\phi)_{freez}$ would increase on the addition of urea and the same would decrease on the addition of sucrose as is experimentally observed.

The ratio of $(\Delta\phi)_{melt}/(\Delta\phi)_{freez}$ for aqueous solution of electrolyte and sucrose in a number of cases lies between 2 and 4. The anomaly seems to be due to the following reason.

During melting, the β-phase in the immediate vicinity of solid phase α has unhydrated ions in more or less a destructured environment, however, on freezing the β-phase would have such ions in a structured environment. Hence, the activity of H_2O in the two cases would be markedly different

and $(\Delta\phi)_{melt}$ would be much greater than $(\Delta\phi)_{free}$.

Acknowledgement

Thanks are due to the Department of Science and Technology, New Delhi, for financial support.

References

1. R. P. Rastogi, R. K. Dass and B. P. Batra, *Nature (London)*, 1961, **191**, 765.
2. R. P. Rastogi and R. D. Shukla, *J. Appl. Phys.*, 1970, **41**, 2787.
3. R. P. Rastogi, R. D. Shukla and S. Bhagat, *J. Electrochem. Soc.*, 1974, **121**, 1564.
4. R. P. Rastogi, P. C. Pandey and A. K. Tripathi, *J. Electrochem. Soc.*, communicated.
5. R. P. Rastogi and P. C. Pandey, *Indian J. Chem., Sect. A*, 1985, **24**, 449.
6. N. Ibl, W. Richarz and H. Wedekekehr, *Z. Phys. Chem.*, 1975, **985**, 123.
7. H. L. Girdhar and R. P. Matta, *J. Electroanal. Chem.*, 1979, **89**, 407.
8. R. P. Rastogi and S. A. Khan, *J. Electrochem. Soc.*, 1983, **130**, 1327.
9. R. P. Rastogi and S. A. Khan, *J. Electrochem. Soc*, 1980, **127**, 1989.
10. B. Scharifker and G. Hills, *J. Electroanal. Chem.*, 1981, **130**, 81.
11. R. P. Rastogi and A. K. Tripathi, *J. Chem. Phys.*, 1985, **83**, 1404.
12. E. J. Workman and S. E. Reynolds, *Phys. Rev.*, 1950, **78**, 254.
13. A. W. Cobb and G. W. Gross, *J. Electrochem. Soc.*, 1969, **116**, 796.
14. H. R. Pruppacher, E. H. Steinberger and T. L. Wang, *J. Geophys. Res.*, 1968, **73**, 571.
15. J. M. Caranti and A. J. Illingworth, *J. Geophys. Res.*, 1983, **88**, 8483.
16. V. Lefebre, *J. Colloid Interface Sci*, 1983, 33, 572.

ERRATA

Vol, LXIII, January 1986

Page 48, line 32 : *for* $^3(S\cdots O_4)$ *read* $^3(S\cdots O_2)$

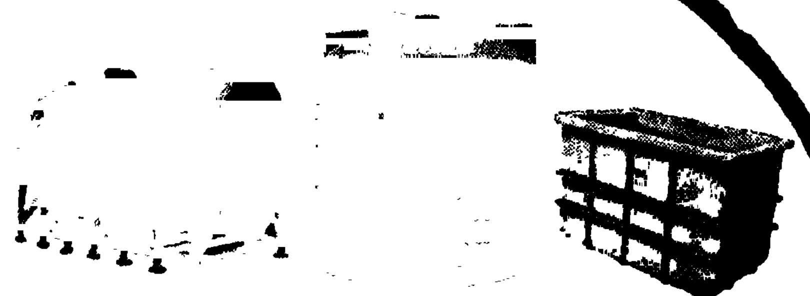
line 56 : *for* H. Pirk, *J. Tetrahedron*

read H. J. Pirk, *Tetrahedron*

J. Indian Chem. Soc.,
Vol. LXIII, January 1986.

Sintex

The Readymade Solution to problems of storage, processing and mixing of acids, alkalies, chemicals and liquid food stuffs.



Horizontal Tanks – upto 10,000 Lits. Vertical Tanks – upto 20,000 Lits. Rectangular Tanks – upto 2,500 Lits

SINTEX – the first and the only large sized one piece polyethylene mouldings in India, offer the ideal and instant solution to the problems of storage, handling processing and mixing of chemicals. Apart from excellent resistance to most acids, alkalies and chemicals, SINTEX have many exclusive features:

Wide range:
Available in various sizes and shapes from 200 lits. to 20,000 lits

Easy Installation:
Sintex tanks are extremely light in weight and can be installed conveniently.

Option of welded fittings:
While adaptor checknut system is standard with Sintex tanks, welded fittings can be given if required.

Easy repairability:
In case of accidental damage Sintex Tanks can be repaired easily at site by hot air welding, using a hot air gun with or without built in compressor.

Unique design:
Sintex Vertical Tanks with closed mouths are made in special corrugated construction for extra mechanical strength. These tanks have a moulded-in platform for inspection.

Excellent After Sales Service:
There is A SINTEX distributor close to you and he is well equipped to offer technical and other assistance to keep Sintex Tanks safe and functional

FDA Approved for Food processing:
Sintex tanks are made out of FDA approved grades of polyethylene and are ideally suited for processing and handling of food products.

Proven Durability:
Sintex Tanks are in use in scores of industries for storing,processing, mixing and handling of a variety of chemicals, and liquid food stuffs. The fact that Sintex Tanks have been performing faultlessly for the last ten years is a testimony to the durability and trouble free performance of SINTEX Tanks

For further information, contact:

SINTER PLAST CONTAINERS
Plastics Division,
THE BHARAT VIJAY MILLS LTD.
KALOL (N. GUJARAT) 382 721 Gram. SINTEX
Phone. 2687 – 2244 Telex: 0121-296 BVM IN

Ahmedabad : 179, New Cloth Market Ahmedabad-380 002. Phone 362976, 361046.
Bombay : 18, World Trade Centre Cuffe Parade, Colaba, Bombay 400 005 Phone: 211653, 217869.
Calcutta : 10, Middleton Street, Calcutta-700 071. Phone 214028
Madras : 123, Angappa Naiken Street, (3rd floor) Madras-600 001.
New Delhi : GF-3 Osian Building, 12, Nehru Place, New Delhi 110019. Phone 681188

Sidhan-SP-90

J. Indian Chem. Soc.,
Vol. LXIII, February 1986, pp. 187-190

Fluorine containing Bioactive Heterocycles†

KRISHNA C. JOSHI*

Department of Chemistry, University of Rajasthan, Jaipur-302 004

In recent decades, there has been considerable interest in medical applications and biochemistry of organic compounds containing fluorine. The discovery of 5-fluorouracil in the fifties is a classical example of a heterocyclic compound where the replacement of even one hydrogen by a fluorine atom led to great modification in biological activity of the parent non-fluorinated heterocycle. This presentation gives a background to this exciting new area in organic chemistry and briefly describes some of the recent work in the author's laboratory.

ALTHOUGH fluorine was discovered by Moissan in 1886, the biochemical aspects of compounds containing carbon-fluorine bond received greater attention only since the late 1940s when Rudolph Peters elucidated the mechanism of the toxic action of fluoro acetate and established the concept of 'lethal synthesis'[1]. However, during the decades since the 1950s, a tremendous development has taken place in the clinical applications of fluorinated compounds and many new heterocycles are in actual use in clinical medicine and as agricultural chemicals. This remarkable progress is due to several characteristic features of the fluorocarbon chemistry system[2]. Fluorine does not behave as a 'true halogen' due to its position in the Periodic Table. The nine protons in the nucleus of the element strongly interact with a similar number of electrons since all of them occupy inner shells. Thus, the Van der Waal's radius of fluorine (1.35 Å) is contracted to such an extent that it closely resembles that of a hydrogen atom (1.2 Å). It is the only element which can replace hydrogen without notable steric consequences and is also the most electronegative element. This close resemblance with bioactive hydrogen analogs with respect to steric requirements at enzyme receptor sites may lead to pitfalls such as a 'lethal synthesis'.

TABLE 1

	Covalent radii Å	Bond lengths Å	Van der Waal's radii Å
H	0.37	H_3C—H 1.11	H 1.2
F	0.72	H_3C—F 1.39	F 1.35
Cl	0.98	H_3C—Cl 1.78	Cl 1.8

For similar reasons, there are several interesting features of a carbon-fluorine bond, *viz.* (i) the C—F bond distance is less than C—C bond distance (1.54 Å), (ii) the C—F bond strength increases; chemically, it leads to the fact that a CF_3 group is unusually stable and will remain unchanged under very rigorous reaction conditions, and (iii) the ionic character of the bond increases with fluorination (C—F, 43; C—Cl, 12; C—Br, 7; C—I, 2%).

The accumulation of fluorine on carbon leads to increased oxidative and thermal stability, and many organofluorine compounds are thus useful due to their being metabolically non-degradable (*viz.* inhalation anesthetics, synthetic blood *etc.*).

TABLE 2—COMPARATIVE BOND ENERGIES

Bond	Energy kcal mol^{-1}
C—H	98
C—F	108-116
C—Cl	81
C—Br	68
C—I	57

Yet another important feature of these compounds is that incorporation of fluorine may lead to increased lipid solubility, thereby enhancing rates of absorption and transport of drugs *in vivo*. In fact, the CF_3 group is one of the most lipophilic of all substituents. This explains the introduction of CF_3 (and $SO_2.CF_3$) in many heterocycles used as drugs, dyes, herbicides *etc.*

This change in properties may confer on the molecule unusual physical and biological properties, and this knowledge has been quickly translated into useful applications in the field of medicinal chemistry. The similarity of steric bulk and the dissimilarity of chemical behaviour enable many fluorinated compounds to act as antimetabolites with respect to their corresponding halogen-free compounds. A typical example is that of fluoroacetic acid. Thousands of cattle die every year mainly in South Africa, Australia and other parts of Southern Hemisphere after eating plants like gifblaar (*Dichapotalum cynosum*), box poison (*Oxylo-*

† Acharya P. C. Ray Memorial Lecture (1982) delivered under the auspices of the Indian Chemical Society on November 5, 1985 at Raipur.

blum perviflroum) and heart lead poison (*Gastrolobium bilobum*). The toxicity of these plants is due to the presence of fluoroacetic acid whose concentration may exceed 1% of the dry weight of leaves or seeds. When fluoroacetic acid (or a precursor) is ingested, it mimics acetic acid so well that it can intrude into the tricarboxylic acid cycle (Krebs-Martius-Knoop cycle), and replaces the natural metabolite and combines with the oxalylacetic acid to give α-fluorocitric acid. The metabolic cycle is then blocked, the fluorocitric acid can neither be eliminated, nor 'digested' and the biomolecular key-units are paralysed by this 'lethal synthesis'[1].

Once the principle of 'antimetabolite formation by introduction of fluorine' was recognised, it was tempting to apply it to chemotherapy, and during recent decades, some notable successes have been achieved in heterocyclic chemistry. It will suffice here just to give one well known example which shows how even the replacement of one hydrogen by a fluorine atom can greatly modify the biological activity of the parent non-fluorinated compound. This is the monofluorination of uracil to give 5-fluorouracil (5-FU) which was synthesised by Heidelberger *et al.*[3,4] with this idea in mind. 5-Fluorouracil, a potent anticancer drug, and its derivatives have been the subject of many recent publications. It was found to be incorporated in place of uracil into RNA of bacterial and mammalian cells as well as that of some viruses. Subsequently, it was revealed that 5-fluoro-2′-deoxyuridine (5-FUDR) is even more effective and less toxic than 5-FU itself. Both of these substances are anabolised to 5-fluoro-2′-deoxyuridylic acid (5-FUDRP), a potent competitive inhibitor of thymidylate synthetase, the enzyme which normally converts 2′-deoxyuridylic acid to thimidylic acid, an essential component of DNA. This is due to the presence, at the critical C-5 position, of fluorine which blocks the essential addition of formate. Since 5-FU and its anabolites are concentrated in cancer cells, this enzymetic blockade inhibits tumour growth by causing 'thymineless death' of neoplastic cells[5].

New fluorine containing heterocycles :

During the last two decades, the research group of the author has given considerable attention to the synthesis of fluorine containing bioactive molecules. Recently, fluorinated 1,3-diketones have been employed as reaction intermediates for synthesis of different types of bioactive heterocycles. Thus, we have been able to incorporate perfluoroalkyl groups, like CF_3, C_2F_5 into heterocycles by indirect methods. Such compounds include the various pyrazoles[6], isoxazoles[7], pyrazolo[1,5-*a*]pyrimidines[8], 1,2,4-triazolo[4,3-*b*]pyridazines[9], 1*H*-pyrazolo[3,4-*b*]pyridines[10], various 1,4-diazepines[11], 1, 5-benzodiazepines[12], pyrazolo[5, 1-*c*]1, 2, 4-triazines[13], *etc.* Some of these compounds have shown promising CNS depressant, antiobesity and anticholinergic activites.

Our more recent interest has been in fluorine containing indoles[14] and particularly spiro-indoles[15] and a number of novel heterocyclic systems have been reported. It is not possible to review all the work done but some of our recent work in the field of pyrazole and indole chemistry are briefly narrated here.

Fluorine containing pyrazoles and their derivatives :

The pyrazolopyridine nucleus has aroused great interest in recent years due to a wide variety of biological activities associated with it. Antiinflammatory, antipyretic, analgesic, bactericidal, vasodilating, respiration stimulating, bronchodilating and hypotensive activities of this system have been reported in the literature. The first synthesis of 1*H*-pyrazolo[3,4-*b*]pyridine nucleus was reported by Bulow[16]. However, its fluorine containing derivatives have not received attention. We have employed fluorinated 1,3-diketones, prepared by us earlier, to introduce fluorinated moieties into the system. A number of new 1*H*-pyrazolo[3,4-*b*]pyridines have been reported[10]. An interesting observation was the fact that when instead of 1-(4′-fluorophenyl)-4,4,4-trifluorobutane-1,3-dione, 1-(4′-fluorophenyl)butane-1,3-dione was used, two isomeric products were obtained which could be separated by column chromatography and the second product was identified as pyrazolo[1,5-*a*]pyrimidine.

The chemistry and biological activities of pyrazolo[3,4-*e*][1,4]thiazepines have received little attention. Only a few references can be found in the literature concerning the antiinflammatory activity of pyrazolothiazepines. We have reinvestigated the reaction of 5-aminopyrazole with aldehydes and characterised the identity of the intermediate leading to pyrazolo[3,4-*e*][1,4]thiazepines about which there was some ambiguity in the literature[17].

In view of the interesting psychopharmacological properties associated with previous compounds, the system has been further investigated[18]. The pyrazolothiazepin-7-ones have been reduced by $LiAlH_4$ to pyrazolo[3,4-*e*][1,4]thiazepines and converted into pyrazolo[3,4-*e*][1,4]thiazepin-7-thiones by phosphorus pentasulphide, and such conversions are being reported for the first time in such systems. Very recently[19], we have employed α-ketohydrazonyl halides (1) as versatile reaction intermediates for synthesis of various categories of heterocycles

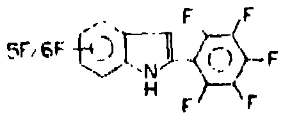
$$\underset{\displaystyle\text{Br}}{\text{Ar.CO.}\overset{}{\underset{|}{\text{C}}}} = \text{N.NH.Ar}'$$

(1)

including pyrazolo[5,1-*a*]imidazoles[20] and 3-aroyl-4-acetyl/benzoyl-5-methyl-1-phenylpyrazoles[21].

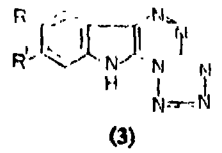
Fluorine containing indoles :

The indole nucleus is well known for its psychopharmacological activity. Oxypertine and diindolylmethane derivatives are potent CNS depressants. Medmain and methylmedmain have shown antiserotonin and hypotensive activities. Introduction of substituents at 5- or 6-position of the indole ring is expected to prevent enzymatic hydroxylation and conjugation. It has been observed that incorporation of fluorine atom into the indole ring would tend to increase drug persistence by increasing its solubility in lipid material and fat deposits in the body. Encouraged by these observations, we have undertaken a comprehensive programme for developing new fluorine containing indoles as possible psychopharmacological agents. Amongst the types investigated are 5/6-substituted-2-aryl-indoles and bis-indolylmethanes[22,23] as possible antidepressants and antifertility agents, indolyl glyoxamides and tryptamines[24,25], indole-2,3-dione derivatives[26] *etc.* Only two compounds are mentioned here. We have recently reported the synthesis of 2-pentafluorophenyl-5/6-fluoroindoles (2) and their various derivatives which are likely to possess novel biological properties[27].



(2)

Another novel heterocyclic system synthesised by us is 10*H*-tetrazolo[5',1' : 3,4][1,2,4]triazino-[5,6-*b*]indole (3) which we could obtain while investigating the reactions of 3-hydrazino-1,2,4-triazino[5,6-*b*]indole[28].



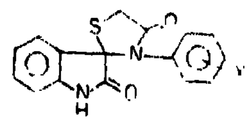
(3)

Various fluorinated derivatives obtained from 3-hydrazino-5*H*-1,2,4-triazino[5,6-*b*]indole have also been prepared[29].

Indoles with C-3 as spiro atom :

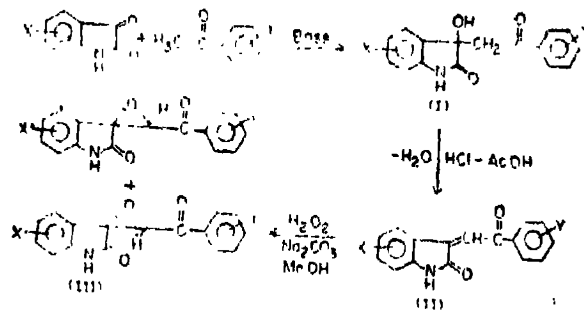
More recently, spiro-indoles have been associated with various biological activities[18]. While exploring the subject, we found the lack of literature on their fluoroanalogs, synthetic and spectral details *etc.* We have, therefore, given a good deal of attention to fluoro-analogs of indoles with C-3 as spiro atom and incidentally synthesised some new heterocyclic systems.

The first system investigated was spiro[3*H*-indole-3,2'-thiazolidine]-2,4'(1*H*)-diones (4) which was prepared by a modified convenient synthesis[30] without isolating the intermediate isatin-3-anils. There were only two references in the literature for such compounds of which one was a patent and other did not report any yields or spectral data.



(4)

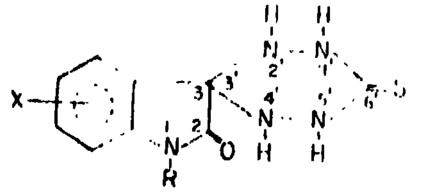
In another study, fluorinated isatins have been subjected to different reactions which include their conversion to 3-aroylmethyleneindol-2-ones and the reactions of the latter with hydrazine yielding spiro-[indole-3,3'-pyrazol]-2-ones[31]. Further, the reaction of 3-aroylmethyleneindol-2-ones with hydrogen peroxide has been reinvestigated as it was felt that theoretically, the product should exist in the form of two isomers differing in the stereochemical arrangement of the hydrogen atom of oxirane ring. No such report was cited in the literature. Also, the mass fragmentation studies of such compounds have not been reported earlier. We have been able to isolate the two geometrical isomers by preparative tlc over silica gel G using benzene-ethyl acetate (1 : 1) under ultraviolet lamp[32]. The two compounds were found to give identical mass spectrum, although in the pmr spectrum, the peak due to C*H* was at a slightly different position in the two cases (Scheme 1).



Scheme 1. [1 : 1 isomeric mixture of III ; separated by preparative tlc over silica gel G using benzene-ethyl acetate (1 : 1)]. Identical ir and mass spectra ; in pmr, peaks due to C*H* slightly different δ 5.1 (IIIa) and 5.2 (IIIb). Epoxidation : Disappearance of II (C*H*) resonance signal at δ 7.15 ; ir 1 050 cm^{-1} (oxirane ring).

We have also investigated the reactions of fluorinated isatins and *N*-acetylisatins with thiocarbohydrazide[33,34]. A literature survey revealed various interesting reactions of thiocarbohydrazide with cyclic ketones, cyclic *ortho*-diketones and isatin. On reinvestigating the reaction, we found that isatin, when treated with thiocarbohydrazide in aqueous ethanolic medium, gave a novel spiro compound 2-oxo-1',2',4',5'-tetrahydrospiro[3*H*-indole-3,3'-1,2,4,5-tetrazine]-6'-thione (5) in 65-70% yield whereas

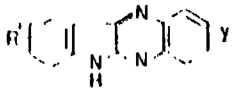
N-acetylisatin on similar treatment, afforded only a thiocarbohydrazone.



(5)

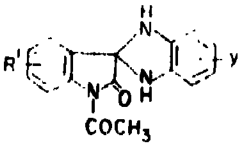
ir 1 700 (C=O) (isatin: 1 730 and 1 680) and −NH peaks 3 400, 3280, 3 200, 3 100 cm^{-1} (NH); pmr $N^{1'}H$ and $N^{8'}H$ (2H, δ 11.1), $N^{4'}H$ (1H, δ 14.15, downfield due to H bonding), $N^{1}H$ (δ 12.45) and NH of indole (δ 8.3); mass (R=H) M^+ m/e 235 (65%), and M^+-CO 207 (100%)

Earlier, we also investigated the reactions of isatin and *N*-acetylisatin with fluorinated 1,2-phenylene diamines and 2,3-diaminopyridine[24] in different media. The reactions are solvent dependent and while in glacial acetic acid, indole-2,3-diones afford exclusively indolo[2,3-*b*]quinoxalines (6); the same



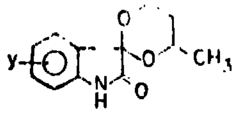
(6)

reactants, with 1-acetylindole-2,3-diones gave a spiro derivative, which was characterized as 1′-acetyl-1,3-dihydrospiro[2*H*-benzimidazole-2,3′-[3*H*]indol]-2′(1′*H*)-ones (7).



(7)

Yet another new spiro system bearing an indolone moiety was obtained during the oxalic acid-catalysed ketalisation of fluorinated indole-2,3-diones with alkanediols[26]. Butan-1,3-diol, under such conditions, yielded 4-methylspiro[1,3-dioxane-2,3′-[3*H*]indole-2′(1′*H*)one (8).



(8)

Acknowledgement

The author would like to sincerely thank a large number of his former and present students without whose devoted work, he could not have achieved much. It is not possible for to mention the names of all his students here but this particular presentation is based mainly on the contributions of Dr. Vijai N. Pathak, Dr. Kalpana Dubey, Dr. Pramila Arya, Dr. Sushma Bhargava, Dr. Renuka Jain, Dr. Pooran Chand, Dr. Urmila Garg, Dr. Vineeta Grover, Dr. Anshu Dandia, Dr. Saroj Garg, Dr. Vandana Sharma, Dr. Sharda Sharma and Dr. R. K. Chaturvedi.

References

1. R. A. PETERS, *Proc. R. Soc., Ser. B*, 1952, **139**, 143.
2. R. E. BANKS, "Organofluorine Chemicals and their Industrial Applications", Ellis Horwood, 1979.
3. C. HEIDELBERGER, *Nature, (London)*, 1957, **179**, 663.
4. R. DUSCHINSKY, E. PLEVEN and C. HEIDELBERGER, *J. Am. Chem. Soc.*, 1957, **79**, 4599.
5. K. C. JOSHI, Proceedings of the 1st ASPAC Congress, Singapore, 1981, pp. 242-260.
6. K. C. JOSHI and V. N. PATHAK, *Indian J. Chem.*, 1973, **11**, 389.
7. K. C. JOSHI, V. N. PATHAK and V. GROVER, *Pharmazie*, 1979, **34**, 68.
8. K. C. JOSHI and K. DUBEY, *J. Pract. Chem.*, 1979, **321**, 341.
9. K. C. JOSHI and K. DUBEY, *Pharmazie*, 1979, **34**, 801.
10. K. C. JOSHI, V. N. PATHAK and U. GARG, *J. Heterocycl. Chem.*, 1979, **16**, 1141.
11. K. C. JOSHI, V. N. PATHAK and S. BHARGAVA, *Indian J. Chem., Sect. B*, 1976, **14**, 1004.
12. K. C. JOSHI, V. N. PATHAK, P. ARYA and P. CHAND, *Pharmazie*, 1979, **34**, 718.
13. K. C. JOSHI and K. DUBEY, *Indian J. Chem., Sect. B*, 1979, **17**, 52.
14. K. C. JOSHI and P. CHAND, *Pharmazie*, 1982, **37**, 1.
15. K. C. JOSHI, R. JAIN and P. CHAND, *Heterocycles*, 1985, **27**, 957.
16. C. BULOW, *Chem. Ber.*, 1910, **43**, 3401.
17. K. C. JOSHI, *J. Heterocycl. Chem.*, 1980, **17**, 789.
18. K. C. JOSHI and P. CHAND, *Heterocycles*, 1981, **16**, 71.
19. K. C. JOSHI, V. N. PATHAK and S. SHARMA, *O.P.P.I. Briefs*, 1985, **17**, 146.
20. K. C. JOSHI, V. N. PATHAK and S. SHARMA, *Indian J. Chem., Sect. B*, 1985, **24**, 124.
21. K. C. JOSHI, V. N. PATHAK and S. SHARMA, *J. Heterocycl. Chem.*, 1985, in the press.
22. K. C. JOSHI, V. N. PATHAK and P. CHAND, *J. Prakt. Chem.*, 1978, **320**, 701.
23. K. C. JOSHI, V. N. PATHAK and P. CHAND, *Indian J. Chem., Sect. B*, 1978, **16**, 933.
24. K. C. JOSHI, V. N. PATHAK and P. ARYA, *Agric. Biol. Chem.*, 1979, **43**, 171.
25. K. C. JOSHI, V. N. PATHAK and P. CHAND, *Agric. Biol. Chem.*, 1978, **42**, 1723.
26. K. C. JOSHI, R. PATNI, P. CHAND, V. SHARMA, S. K. BHATTACHARYA and Y. V. RAO, *Pharmazie*, 1984, **39**, 153.
27. K. C. JOSHI, V. N. PATHAK and R. K. CHATURVEDI, Abstracts, XIth International Symposium on Fluorine Chemistry, East Berlin, 1985.
28. K. C. JOSHI and P. CHAND, *J. Heterocycl. Chem.*, 1980, **17**, 1783.
29. K. C. JOSHI and P. CHAND, *Heterocycles*, 1981, **16**, 43.
30. K. C. JOSHI, R. PATNI and P. CHAND, *Heterocycles*, 1981, **16**, 1555.
31. K. C. JOSHI, R. JAIN and S. GARG, *Pharmazie*, 1985, **40**, 21.
32. K. C. JOSHI, R. JAIN and S. GARG, *J. Heterocycl. Chem.*, 1984, **21**, 977.
33. K. C. JOSHI, Abstracts, IXth International Congress of Heterocyclic Chemistry, Tokyo, 1983, p. 316.
34. K. C. JOSHI, R. JAIN, A. DANDIA and V. SHARMA, *J. Heterocycl. Chem.*, 1985, in the press.
35. K. C. JOSHI, A. DANDIA and P. CHAND, *Indian J. Chem., Sect. B*, 1984, **23**, 743.
36. K. C. JOSHI, R. JAIN, P. CHAND and V. SHARMA, *Indian J. Chem., Sect. B*, 1984, **23**, 386.

J. Indian Chem. Soc.,
Vol. LXIII, February 1986, pp. 191-194

Studies on Coordination Polymers of Fumaryl-bis-*N*-phenylhydroxamic Acid and Fumaryl-bis-*N*-*m*-tolylhydroxamic Acid with some Group III Elements

(Mrs.) V. DURGA KUMARI and K. N. MUNSHI*

Chemistry Department, Nagpur University, Nagpur-440 010

Manuscript received 4 June 1983, revised 22 June 1984, accepted 15 November 1985

Coordination polymers of fumaryl-bis-*N*-phenylhydroxamic acid (FPHA) and fumaryl-bis-*N*-m-tolylhydroxamic acid (FTHA) with some group III metals were synthesised. These coordination polymers have been characterised by their elemental analysis, ir and reflectance spectral data, conductance and DTA measurements.

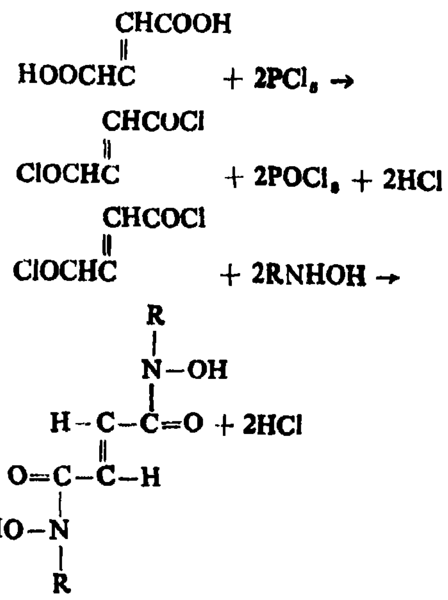
THE survey of literature available on coordination polymers shows that most of the work which is synthetic in nature centres around the transition metal ions. These metals have been used with their oxidation number two with different bis-ligands. The simultaneous fulfilment of the coordination number as well as the oxidation number resulted into neutral highly insoluble co-ordination polymers. The work on group III elements, particularly with oxidation number three, has not been attempted in detail as a simple bis-ligand is not able to yield the polymers of desired nature. In such cases, however, the use of primary comparatively less stable complex is made and ultimately the product is a mixed ligand coordination polymer or complex.

Coordination polymers of a number of bis-hydroxamic acids with transition metals have been reported by Kharche[1]. However, coordination polymers of bis-hydroxamic acids with group III elements are rarely studied. Fumaryl-bis-*N*-phenyl- and fumaryl-bis-*N*-m-tolyl-hydroxamic acids have been synthesised for the first time in these laboratories[2]. Present investigation includes synthesis and characterisation of coordination polymers of FPHA and FTHA.

Experimental

The chemicals used were all of AnalaR or chemically pure grade.

Preparation of ligands : The general methods employed in the synthesis of *N*-arylhydroxamic acids are outlined in the literature [3,4]. Freshly prepared *N*-arylhydroxylamine and vacuum-distilled acid chloride in stoichiometric proportions were reacted at low temperatures (0° or lower). Dicarboxic acid (*i.e.* fumaric acid) was used for the synthesis of FPHA and FTHA. Firstly, the acid dichloride was prepared and then it was condensed with two moles of *N*-phenylhydroxylamine and *N*-m-tolylhydroxylamine separately which were obtained by controlled reduction of nitrobenzene and *m*-nitrotoluene.



bis-hydroxamic acid

where, $R=C_6H_5$ or $CH_3.C_6H_4$.

Synthesis of coordination polymers : Coordination polymers were prepared by the reaction of metal acetylacetonates/metal oxinates and bis-ligands employing suitable solvent medium under proper set of conditions ; which includes first the preparation of primary complexes either *β*-diketonates or oxinates.

Preparation of simple complexes or primary complexes : Methods previously employed[5,6] for the preparation of *β*-diketonates involve the addition of sodium or ammonium *β*-diketone to the metal salt solution. In the case of oxinates, 8-hydroxyquinoline dissolved in dilute acetic acid was added to the metal salt solution and *p*H was adjusted with dilute ammonia.

Preparation of mixed ligand coordination polymers : Coordination polymers of FPHA and FTHA with group III metals were prepared by heating and then digesting the mixture containing ligand (0.005 mol) and metal acetylacetonates (0.005 mol) or metal oxinates (0.005 mol) on water-bath. Table 1 shows different solvent ratios that were taken. For a series, the conditions were same but to increase the yield and to overcome the solubility difficulties of the reactants, different ratios of the solvents were taken. All the polymers were bright-yellow in colour and insoluble in all common organic solvents. Hence, the products were purified by repeated washings with the solvents employed for their preparation.

TABLE 1—PREPARATIVE CONDITIONS OF POLYMERS OF FPHA AND FTHA WITH GROUP III METAL IONS

Polymer	Solvent DMF-EtOH ratio (v/v)	Remarks
Al^{III}-acac-FPHA	1 : 4	Amorphous
Al^{III}-oxine-FPHA	2 : 3	Amorphous
Sc^{III}-acac-FPHA	2 : 3	Crystalline
Y^{III}-acac-FPHA	3 : 2	Crystalline
La^{III}-acac-FPHA	4 : 1	Crystalline
Al^{III}-acac-FTHA	1 : 4	Amorphous
Sc^{III}-acac-FTHA	2 : 3	Crystalline
Y^{III}-acac-FTHA	3 : 2	Crystalline
La^{III}-acac-FTHA	4 : 1	Amorphous

TABLE 2—CHARACTERISATION DATA OF COORDINATION POLYMERS OF FPHA AND FTHA WITH GROUP III METAL IONS

Sl. no.	Polymer (assigned composition)	Analysis % : Found/(Calcd.) C	H	N	M	Decomp. temp. °C	Specific resistance Ω cm
(a)	FPHA (L) polymers :						
1.	$\{[Al\text{-}L\text{-}acac].3H_2O\}_n$	53.10 (52.85)	4.95 (5.25)	6.10 (5.88)	6.30 (5.65)	410	7.0×10^7
2.	$\{[Al\text{-}L\text{-}oxine].3H_2O\}_n$	56.45 (57.59)	4.78 (4.60)	7.31 (8.06)	6.02 (5.16)	355	1.0×10^8
3.	$\{[Sc\text{-}L\text{-}acac].H_2O\}_n$	56.30 (55.03)	4.62 (4.58)	6.95 (6.11)	8.75 (9.81)	320	8.8×10^7
4.	$\{[Y\text{-}L\text{-}acac].3H_2O\}_n$	43.20 (42 43)	4.69 (4.64)	6.17 (5.20)	15.98 (16.50)	300	9.1×10^7
5.	$\{[La\text{-}L\text{-}acac].3H_2O\}_n$	41.30 (42.76)	3.95 (4.25)	5.02 (4.76)	24.90 (23.6)	295	4.4×10^8
(b)	FTHA (L′) polymers :						
1.	$\{[Al\text{-}L'\text{-}acac].2H_2O\}_n$	57.70 (56.86)	5.13 (5.55)	5.01 (5.76)	4.82 (5.53)	305	1.1×10^7
2.	$[Sc\text{-}L'\text{-}acac]_n$	58.60 (58.19)	5.32 (4.91)	6.12 (5.98)	8.60 (9.59)	285	4.1×10^7
3.	$\{[Y\text{-}L'\text{-}acac].3H_2O\}_n$	47.60 (48.77)	4.76 (5.12)	4.41 (4.94)	16.90 (15.7)	326	6.3×10^7
4.	$\{[La\text{-}L'\text{-}acac].3H_2O\}_n$	42.91 (44.81)	4.16 (4.70)	4.14 (4 54)	25.00 (26.90)	270	4.9×10^7

Physical measurements : The D.T.A. apparatus fabricated at I.I.T., Bombay was used for recording thermograms of the compounds in air. The infrared spectra (400-4 000 cm^{-1}) were obtained using a Specord-75 spectrophotometer in nujol. A single beam Karl-Zeiss VSU-2-p spectrophotometer was used for recording reflectance spectra. A Beltronix million megohm meter MM 500 (India) was used to measure the conductance. Magnetic susceptibility was determined by Gouy's method[1].

Results and Discussion

The analytical data of polymers (Table 2) suggest general formula $(M\text{-}acac\text{-}FPHA)_n$, $(M\text{-}oxine\text{-}FPHA)_n$ and $(M\text{-}acac\text{-}FTHA)_n$. Most of these polymers were found to contain some water molecules as water of crystallisation.

The ir spectra of a number of coordination polymers of bis-hydroxamic acids have been investigated and reported by Kharche[1] and Gandhi[6]. Ir spectra of FPHA and FTHA show the presence of OH stretching band around 3 100 cm^{-1} (OH) which disappears in polymers indicating coordination to the central metal ion *via* deprotonation. The three consecutive bands 1 625, 1 600 and 1 570 cm^{-1} of FPHA and 1 650, 1 630 and 1 600 cm^{-1} of FTHA which exist due to various resonating structures of R—N (C=O)—OH in these ligands, shifted towards lower frequency side in these polymers indicating the coordination through carbonyl group forming a C=O ..M linkage.

The N—O stretching vibrations are found at 965 and 950 cm^{-1} in FPHA and FTHA. This particular band is reported to be shifted towards higher frequency side with an increase in intensity[7]. However, in the polymers of hydroxamic acids with

TABLE 3—INFRARED SPECTRAL BONDS* (CM^{-1}) OF FPHA AND FTHA POLYMERS WITH GROUP III METAL IONS

(a) FPHA polymers :

FPHA	acac	oxine	Al^{III}-acac	Al^{III}-oxine	Sc^{III}-acac	Y^{III}-acac	La^{III}-acac	Assignments
—	—	—	3 200-3 500 b	3 200-3 500 b	3 200-3 500 b	3 200-3 500 b	3 200-3 500 b	H–O–H
3 100 mb	—	3 300-3 500 b	—	—	—	—	—	OH of oxine and FPHA
—	—	1 577	—	1 575 sh	—	—	—	C=N of oxine
1 640 sh			1 660 sm	1 660 sh	1 650 s	1 650 sm	1 650 sh	C–O of FPHA and acetylacetone
1 625 sh	1 709	—	1 620 sm	1 560 sh	1 560 sh	1 600 sh	1 560 sh	
1 600 sh			1 580 sm					
1 570 sh			1 540 sh	1 540 sm	1 530 sm	1 530 sh	1 540 s	
—	—	—	—	1 105 sm	—	—	—	C–O of oxine at C–O...M site
965 s	—	—	950 sm	950 sm	950 sm	950 sm	950 sm	N–O stretch of FPHA

(b) FTHA polymers :

FTHA	acac	Al^{III}-acac	Sc^{III}-acac	Y^{III}-acac	La^{III}-acac	Assignments
—	—	3 200-3 500 b	—	3 200-3 500 b	3 200-3 500 b	H–O–H
3 100 b	—	—	—	—	—	OH of FTHA
1 650 sh		1 650 sh	1 650 sh	1 650 s	1 650 sh	C=O of FTHA and acetylacetone
1 630 sm	1 709	1 590 sm	1 590 sh	1 590 s	1 575 sh	
1 600 sh		1 525 sm	1 520 sm	1 520 b	1 530 b	
950 s	—	950 sm	950 sm	950 sm	950 sm	N–O stretch of FTHA

*b ≡ broad, sh ≡ shoulder, sm ≡ strong medium, s ≡ strong, m ≡ medium

several transition metal ions prepared in these laboratories the shifting of this band is found towards lower frequency side as well as higher frequency isde. This band is shifted towards lower frequency side in FPHA polymers and there is no change in its position in FTHApolymers.

The presence of band at 3 500-3 400 cm^{-1} indicates lattice water in these polymers except in the case of Sc^{III}-acac-FTHA. In the case of polymers prepared using metal acetylacetonate combination, the C=O stretch of treacetylacetone at 1 707 cm^{-1} is shifted towards lower frequency side and appeared in the region 1 650-1 575 cm^{-1} suggesting coordination of acetylacetone also to the central metal ion. In the same way, the coordination of oxine to the central metal ion is shown by the shifting of 1 577 cm^{-1} of C=N stretch to 1 575 cm^{-1} and another band around 1 100 cm^{-1} due to C–O stretch at C–O ..M site (Table 3).

The study of reflectance spectra showed that the maximum absorbance is at 350 nm for both the ligands. Polymers showed an absorption maxima in the region 370 to 420 nm and the complexation shift is towards higher frequency side. The spectra obtained are due to charge transfer.

Magnetic moments of FPHA and FTHA polymers showed that all the polymers are diamagnetic.

Thermal studies of coordination polymers of bis-hydroxamic acids have been reported[1]. All these polymers show a sharp exotherm besides the larger one at temperatures range 125-300°. It has been observed in case of few polymers that the small exothermic peak is not associated with weight loss. This is reported as due to solid-solid phase transition, probably a structural change occuring after the removal of water of crystallisation or otherwise[8].

On the basis of above grounds D.T.A. of FPHA and FTHA polymers have been studied. These polymers are of the same nature as discussed above and the only difference is the presence of a primary ligand and its contribution towards the heat stability. Decomposition temperatures are reported on the basis of D.T.A. (Table 2). The second exothermic peak being very large, the temperature corresponding to its starting point is taken as the decomposition temperature. A sharp exothermic peak (160-300°) is followed by the larger one (270-410°) in these compounds, and the larger one is associated with the major weight loss. As the TGA is not carried out for these polymers, a detailed discussion is not possible.

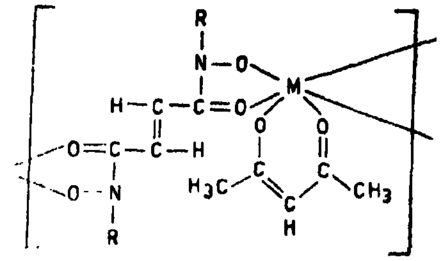
From decomposition temperatures supported by specific resistance date for FPHA and FTHA polymers it has been found that in the case of Al^{III}-, Sc^{III}-, Y^{III}- and La^{III}-acac-FPHA polymers, thermal stability decreases from Al^{III} to La^{III}. In the case of FTHA polymers Al^{III}, Sc^{III}, Y^{III}, and La^{III}, thermal stability decreases from Al^{III} to La^{III}. However, Y^{III}-acac-FTHA polymer is thermally more stable than Sc^{III}-acac-FTHA polymer which may be due to difference in the degree of polymerisation. Of all the polymers, Al^{III}-acac-FPHA polymer has the highest heat stability.

TABLE 4—PROPOSED STRUCTURE OF THE POLYMERIC UNIT

Metal-acac-FPHA ($R = C_6H_5$)

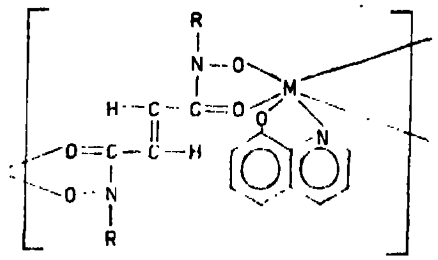
Metal-acac-FTHA ($R = CH_2C_6H_5$)

M = Al^{III}, Sc^{III}, Y^{III}, La^{III}



Metal-oxine-FPHA ($R = C_6H_5$)

M = Al^{III}



The specific resistance of FPHA and FTHA polymers are given in Table 2.

Proposed structures: The confirmation and characterisation of the compounds prepared in the present course of investigations are no doubt difficult because of their insolubility and intractibility. Their formation as polymers from steric considerations and establishing the structures on the basis of elemental analysis are therefore tentative (Table 4).

The composition has been suggested on the basis of elemental analysis (Table 2) which is also explained by ir spectra. Observations of the composition of some of the compounds lead to the conclusion that they should be simple polynuclear complexes, but their extreme insolubility makes one to believe in their polymeric nature with more complex features present.

References

1. V. W. KHARCHE, Ph.D. Thesis, University of Nagpur, 1979.
2. N. R. GANDHI, Ph.D. Thesis, University of Nagpur, 1982.
3. Y. L. YALE, *Chem. Rev.*, 1943, 33, 209.
4. U. PRIYADARSHINI and S. G. TONDEN, *J. Chem. Eng. Data*, 1967, 12, 143.
5. W. BILTZ, *Ann.*, 1904, 33, 334.
6. T. MOELLER and ULRICH, *J. Inorg. Nucl. Chem.*, 1956, 2, 164.
7. N. N. GHOSH and S. K. MUKHOPADHYAY, *J. Indian Chem. Soc.*, 1973, 50, 553.
8. W. W. WENDLANDT, *Thermochim. Acta*, 1974, 9, 101.

J. Indian Chem. Soc.,
Vol. LXIII, February 1986, pp. 195-197

Coordination Compounds of Uranium(IV) and Dioxouranium(VI) with Nitrogen-containing Heterocyclic Ligands

S. C. JAIN*, M. S. GILL and G. S. RAO

Chemistry Division, Bhabha Atomic Research Centre, Trombay, Bombay 400 085

Manuscript received 6 August 1984, revised 4 July 1985, accepted 15 November 1985

Synthesis and characterisation of the complexes of uranium(IV) and dioxouranium(VI) with imidazole (Imz) pyrazole (Pyz) and trimethylsilane imidazole (Tmi) have been described. Compounds of different stoichiometries are obtained depending on the uranium salt and the ligand used. The infrared spectral studies (4 000-200 cm^{-1}) established that in all the complexes, the coordination of the ligand to the metal ion is through the pyridine nitrogen in preference to the amine nitrogen. Possible structures of some of the compounds have been discussed in the light of the ir results.

IMIDAZOLE and pyrazole molecules fall in the class of aromatic heterocyclic compounds and the unique structural feature involving pyrrole nitrogen and pyridine nitrogen make them interesting ligands. Though the pyridine nitrogen of these ligands is normally considered to be the coordination site, coordination *via* pyrrole nitrogen has been reported recently[1]. The present work describes the preparation and characterisation of the complexes of uranium(IV) and dioxouranium(VI) with imidazole, pyrazole and trimethylsilane imidazole.

Experimental

The uranium salts were prepared and purified by suitable methods[2]. The ligands (Aldrich) were used as such without further purification. The compounds, in general, were prepared[3] by dissolving a known weight of the uranium salts in a suitable solvent and adding to it the required amount of the ligand followed by the isolation of the complex as a precipitate. In the case of uranium(IV) chloride, the preparations were carried out in tetrahydrofuran and handling of the complexes were carried out in a dry-box.

The uranium and chlorine contents in the compounds were determined by gravimetric method as U_3O_8 and AgCl. Carbon, hydrogen or nitrogen contents were determined by micro analysis. The analytical results are given in Table 1. The infrared spectra of the compounds were recorded on a Perkin-Elmer 577 spectrophotometer in nujol using caesium iodide optics.

Results and Discussion

The analytical results (Table 1) show that under similar conditions, uranium(IV) chloride forms 1 : 2 complexes with pyrazole and trimethylsilane imidazole whereas with imidazole a 1 : 3 compound is formed. While uranyl nitrate forms 1 : 2 compounds, with Pyz, uranyl oxalate and sulphate gave 1 : 1 type of complexes. All the complexes are insoluble in most of the common organic solvents. The compounds decompose turning black before melting.

TABLE 1—ANALYTICAL RESULTS

Sl. no.	Complex	Colour	M.p.* °C	Analysis % : Found/(Calcd.) U%	Cl%	C%	H%	N%
1.	UCl_4.3Imz	Greenish grey	~195	40.8 (40.76)	23.5 (24.28)	17.8 (18.50)	2.2 (2.05)	13.6 (14.39)
2.	UCl_4.4Pyz	Green	~255	46.6 (46.14)	28.8 (27.49)	13.1 (13.96)	1.9 (1.55)	11.1 (10.86)
3.	UCl_4.2Tmi	Greenish grey	~170	38.3 (36.16)	21.1 (21.48)	21.6 (21.81)	4.1 (3.69)	8.2 (8.48)
4.	$UO_2(NO_3)_2$.2Imz	Yellow	~150	43.7 (44.91)	—	—	—	15.3 (15.85)
5.	$UO_2(NO_3)_2$.2Pyz	Yellow	~148	45.3 (44.91)	—	13.9 (13.58)	1.8 (1.51)	16.02 (15.85)
6.	$UO_2(C_2O_4)$.Imz	Yellow	~290	56.7 (55.87)	—	13.2 (14.09)	1.2 (0.93)	7.3 (6.57)
7.	$UO_2(C_2O_4)$.Pyz	Yellow	~290	56.0 (55.87)	—	13.8 (14.08)	1.8 (0.93)	6.9 (6.57)
8.	$UO_2(SO_4)$.Pyz	Yellow	~300	54.4 (54.84)	—	8.6 (8.29)	1.7 (0.92)	6.0 (6.45)

* Decomposed turning black.

A comparison of the spectra of the complexes with those of the respective ligands (Tables 2 and 3) bring out interesting features. A positive shift in the ν_{N-H} for the bands at 3 280 and 3 066 cm^{-1} in the case of pyrazole, and 3 200 and 3 060 cm^{-1} for imidazole clearly indicate the non-involvement of the pyrrole nitrogen in bonding to the uranium atom. The ring stretching vibrations due to $\nu_{C=C}$ and $\nu_{C=N}$ in the region 1 540-1 324 cm^{-1} for the two ligands also show a general trend of moving to higher frequency region for the complexes. The ring vibrations for the trimethylsilane imidazole complex are identical to imidazole complex. This observation confirms that coordination in all the cases involves pyridine nitrogen[4] and the electrons on pyrrole nitrogen form part of the aromatic sextet and therefore, are not available for coordination[5]. Other ligand bands, such as C–H in-plane and out-of-plane bending, ring breathing and ring deformation modes do not show any significant change as a result of coordination.

TABLE 2—INFRARED DATA FOR IMIDAZOLE AND ITS COMPLEXES (cm^{-1})

Imz	UCl_4.3Imz	$UO_2(C_2O_4)$.Imz	$UO_2(NO_3)_2$.Imz	Assignments
3 200 s	3 300 sb	3 380 s	3 480 sh	ν_{N-H}
3 060 s	3 230 s	3 180 s	3 300 s	
			3 160 sb	
1 540 s	1 575 s	1 575 sh	1 585 s	Ring stretching
1 485 sh	1 515 s	1 510 m	1 510 sh	
1 446 s	1 440 s	1 445 s	1 450 sb	
1 324 s	1 350 sb	1 350 s	1 335 sb	

s≡Strong, sh≡shoulder, b≡broad, m≡medium.

TABLE 3—INFRARED DATA FOR PYRAZOLE AND ITS COMPLEXES (cm^{-1})

Pyz	UCl_4.2Pyz	$UO_2C_2O_4$.Pyz	UO_2SO_4.Pyz	$UO_2(NO_3)_2$.2Pyz	Assignments
3 280 s	3 300 sh	3 450 s	3 400 sh	3 425 s	ν_{N-H}
				3 310 s	
3 066 s	3 230 s	3 390 s	3 140 s	3 100 s	
1 525 m	1 538 s	1 540 sh	—	1 540 s	Ring stretching
1 485 s	1 510 sh	1 505 w	1 515 w	1 520 s	
1 385 s	1 408 m	1 405 m	1 405 m	1 400 s	
1 345 s	1 350 sh	1 354 sh	1 350 sh	1 350 s	

s≡Strong, sh≡shoulder, m≡ medium, w≡weak.

Though pyrazole and imidazole are isomers having pyridine nitrogen as the coordination site, UCl_4 formed 1 : 2 adduct with Pyz and 1 : 3 adduct with Imz (Table 1). Similar adducts have been reported to be ionic in nature[3]. In such cases, uranium atom can be assumed to have coordination number of six and eight. Due to insoluble nature of these compounds it was not possible to determine their molar conductance. New strong and broad bands in the far-infrared region 255-240 cm^{-1} arise due to the ν_{U-Cl} and are in good agreement with the literature values[3].

In the case of $UO_2(NO_3)_2$.2Pyz and $UO_2(NO_3)_2$.2Imz, the separation of 205 and 225 cm^{-1} in the ν_1 (N–O stretch) and ν_4(NO_2 asym), respectively (Table 4), are of the same order as reported

TABLE 4—NITRATE INFRARED ABSORPTION BANDS (cm^{-1})

NO_3-C_{2v}	$UO_2(NO_3)_2$.2Imz	$UO_2(NO_3)_2$.2Pyz
ν_1 1 485 vs	1 520 s	1 505 s
ν_2 1 030 vs	1 040 vs	1 040 s
ν_3 748 m	755 ms	758 ms
ν_4 1 288 s	1 295 s	1 300 sh
ν_5 723 w	735 m	720 m
ν_6 812 m	815 s	825 s
$\nu_2+\nu_3$ 1 773 w	1 775 w	1 750 m,b
$\nu_2+\nu_5$ 1 730 w	1 650 m	1 650 m,b
$\nu_2+\nu_1$ 2 540 w	2 500 m	2 520 ms
$\nu_2+\nu_4$ 2 296 w	2 350 m	2 360 w

s≡Strong, vs≡very strong, m≡medium, w≡weak, ms≡medium strong, b≡broad, sh≡shoulder.

in our earlier work[3] for bidentate NO_3 groups having C_{2v} symmetry. In view of the fact that the NO_3 groups in these compounds act as bidentate and the ligands as monodentate, the central uranium atom in these adducts can be assumed to be octa-coordinated with two (o,o) bidentate nitrate groups and two ligand (L) molecules in equatorial plane and the two oxygen of UO_2 in the axial direction.

The strong bands in the region 1 650-1 350 cm^{-1} are assigned to carboxylic stretching frequencies in the case of the oxalato-complexes. The bands at 1 490, 1 360, 1 328, 795 and 498 cm^{-1} for UO_2-(C_2O_4).Imz and at 1 505, 1 335, 1 310, 804 and 485 cm^{-1} for $UO_2(C_2O_4)$.Pyz are characteristic for coordinated oxalato group[6]. This suggests that in the complex, the planar symmetrical configuration of the oxalate groups where they act as bridges between two UO_2 ions in polymeric form, is retained[7].

The presence of coordinated sulphate in the case of UO_2SO_4.Pyz is indicated by the splitting into triplet of ν_3 (1 255, 1 130, 1 010 cm^{-1}) and ν_4 (635, 602, 590 cm^{-1}). Further, the appearance at 1 000 cm^{-1} of ν_1 mode which is infrared forbidden in uncoordinated SO_4 also support the chelating nature of SO_4 in the compound[8].

In the cases of both the compounds UO_2-(C_2O_4).L and UO_2SO_4.L, the central uranium atom can be assumed to be seven-coordinate with pentagonal bipyramidal arrangement of the donor atoms.

The $\nu_{as}(UO_2)$ and $\nu_{sym}(UO_2)$ vibrations appear at 940 and 830 cm^{-1}, respectively. In the far-infrared spectra new bands in the region 380-340 cm^{-1} assigned to ν_{U-N} modes are in good agreement to those reported in literature[9]. The bands at ~ 220 and 420-400 cm^{-1} have been assigned to δ_{O-U-O} and ν_{U-O}, respectively.

Acknowledgement

The authors thank Dr. R. M. Iyer, Head, Chemistry Division, for his keen interest.

References

1. B. S. Tovrog and R. S. Drago, *J. Am. Chem. Soc.*, 1977, 99, 2203.
2. G. Brauer, "Handbook of Preparative Inorg. Chemistry", 2nd. ed., Academic Press, London, 1965, Vol. 2.
3. S. C. Jain, M. S. Gill and G. S. Rao, *J. Indian Chem. Soc.*, 1981, 58, 210.
4. S. C. Jain, *J. Inorg. Nucl. Chem.*, 1973, 35, 505.
5. R. J. Sundberg and R. Bruchmartin, *Chem. Rev.*, 1974, 74, 471.
6. G. Condorbellt, I. Fragala and S. Giuffrida, *J. Inorg. Nucl. Chem.*, 1975, 37, 1177.
7. G. S. Rao, S. C. Jain and M. S. Gill, *Indian J. Chem., Sect. A*, 1982, 21, 526.
8. K. Nakamoto, J. Fujila, S. Tanaka and M. Kulayashi, *J. Am. Chem. Soc.*, 1959, 79, 4904.
9. H. W. Turner, R. A. Anderson, A. Zalkin and D. H. Templeton, *Inorg. Chem.*, 1979, 18, 1221.

J. Indian Chem. Soc.,
Vol. LXIII, February 1986, pp. 198-200

Cobalt(II), Nickel(II), Copper(II), Zinc(II), Cadmium(II), Dioxouranium(VI) and Oxovanadium(IV) Complexes with 2-(N-α-Benzyl-2-hydroxybenzylidineimino)-ethane Sulphonic Acid

ASHOK GAHLOT, (Miss) SHOBHA SHARMA and R. K. MEHTA*

Chemistry Department, University of Jodhpur, Jodhpur-342 001

Manuscript received 6 March 1985, revised 31 July 1985, accepted 2 December 1985

The dissociation constants of 2-(N-α-benzyl-2-hydroxybenzylidineimino)ethane sulphonic acid (H_2BE) and stability constants of its chelates with Co^{II}, Ni^{II}, Cu^{II}, Zn^{II}, Cd^{II}, $U^{VI}O_2$ and $V^{IV}O$ have been determined in aqueous medium ($\mu = 0.1\ M$) at 25, 35 and 45° using Calvin's extension of Bjerrum's method. Values of $\Delta G°$, $\Delta H°$ and $\Delta S°$ of the chelates have been evaluated. Elemental analysis, molecular weight, electronic and ir spectra, magnetic moments and conductance of the solid complexes indicate an octahedral stereochemistry for these chelates except those of the Zn^{II} and Cd^{II} which possesses a tetrahedral geometry.

THE stability constants of the chelates of 2-(N-α-benzyl-2-hydroxybenzylidineimino)ethane sulphonic acid (H_2BE) with Co^{II}, Ni^{II}, Cu^{II}, Zn^{II}, Cd^{II}, $U^{VI}O_2$ and $V^{IV}O$ have been evaluated using Calvin's extension of Bjerrum's method[1,2].

Experimental

2-(N-α-Benzyl-2-hydroxybenzylidineimino)ethane sulphonic acid (H_2BE) was synthesised by the method reported earlier[3], m.p. 180° (Found ; C, 58.90 ; H, 4.19 ; N, 4.56 ; S, 10.42. $C_{16}H_{17}NSO_4$ calcd. for : C, 59.40 ; H, 4.29 ; N, 4.62 ; S, 10.56%).

The following mixtures (total volume 40 ml) were prepared and titrated against carbonate-free 0.1*M* sodium hydroxide solution at 25, 35 and 45° in nitrogen atmosphere and the titration curves are found to be of the usual shapes : (A) 10.0 ml 0.01*M* H_2BE+4.0ml 1.0*M* $NaClO_4$+26.0ml water ; (B) 10.0 ml 0.01*M* H_2BE+4.0 ml 1.0*M* $NaClO_4$+10.0 ml 0.01*M* metal ion solution+16.0 ml water ; (C) 20.0 ml 0.01*M* H_2BE+4.0 ml 1.0*M* $NaClO_4$+10.0 ml 0.01*M* metal ion solution +6.0 ml water.

Results and Discussion

The pK_1 and pK_2 values of the H_2BE are found to be 7.92 and 10.02 at 25°, 7.40 and 9.74 at 35°, and 6.95 and 9.21 at 45°, respectively. These values suggest that H_2BE is a biprotic ligand. The metal-ligand stability constants are read from the formation curves drawn by plotting $\bar{n}$ *vs* $-\log$ [A^-]. The refinement is done by the computational methods[4] and the values obtained by different methods are in agreement and their average values are summarised in Table 1. The order of stability found, $V^{IV}O > U^{VI}O_2 > Cu^{II} > Ni^{II} > Co^{II} > Zn^{II} > Cd^{II}$, is in accordance with Irving-Williams rule[5].

Thermodynamic functions : The values of overall changes in free energy ($\Delta G°$), enthalpy ($\Delta H°$) and entropy ($\Delta S°$) have been evaluated using Gibbs-Helmholtz equation[6] (Table 1). $\Delta G°$ values of all the chelates are more negative at 45° than at lower temperature. It is further observed that $\Delta H°$ is positive in all cases, which suggests endothermic nature of reactions. The positive values of $\Delta S°$ indicate that entropy term is favourable for their formation.

Solid chelates :

Preparation : The solid metal chelates were synthesised by refluxing a mixture of metal nitrate (0.01*M* in 15 to 20 ml 75% ethanol) and H_2BE (0.01*M* in 25 to 50 ml 75% ethanol) for 2-3 h in nitrogen atmoshphere. On concentrating the mixture, the coloured precipitate obtained was filtered, washed with ethanol and dried (~70%). All the metal chelates were synthesised by this method.

The solid metal chelates do not possess sharp melting points, and decompose on heating between 250 to 280°. These compounds were analysed for C, H, N, S, metal and water (Table 2). Their molecular weights were determined ebulliometrically. From these data it is evident that the metal chelates exist as monomer in the solid state and possess 1 : 1 (metal-ligand) stoichiometry.

The solid Co^{II}, Ni^{II}, Cu^{II}, and $V^{IV}O$ chelates are found paramagnetic (Table 1) and the rest diamagnetic. On crystallisation, the composition of the metal chelates remains unaltered.

TABLE 1—AVERAGE STABILITY CONSTANTS, THERMODYNAMIC FUNCTIONS AND MAGNETIC MOMENTS OF METAL CHELATES OF 2-(N-α-BENZYL-2-HYDROXYBENZYLIDINEIMINO)ETHANE SULPHONIC ACID (H_2BB)

Metal ion		Stability constant			$-\Delta G°$ kJ mol^{-1}			$\Delta H°$ kJ mol^{-1} at 35°	$\Delta S°$ JK^{-1} mol^{-1} at 35°	μ_{eff} at 303 K B.M.
		25°	35°	45°	25°	35°	45°			
Co^{II}	log K_1	5.80	6.35	7.48	64.87	70.23	73.43	62.60	24.77	4.45
	log K_2	3.95	4.95	5.30						
Ni^{II}	log K_1	6.30	7.05	8.15	71.49	76.01	80.98	69.85	20.00	2.93
	log K_2	4.65	5.50	6.45						
Cu^{II}	log K_1	7.10	7.65	8.18	79.02	32.44	86.89	38.10	14.39	1.88
	log K_2	5.15	6.10	6.85						
Zn^{II}	log K_1	4.38	5.95	7.10	33.03	35.32	37.14	28.12	23.37	—
	log K_2	—	—	—						
Cd^{II}	log K_1	3.75	4.95	6.35	30.07	31.55	33.42	19.93	37.66	—
	log K_2	—	—	—						
$U^{VI}O_2$	log K_1	7.32	8.15	8.50	81.42	88.16	92.24	79.83	27.04	—
	log K_2	5.80	6.65	7.15						
$V^{IV}O$	log K_1	8.10	8.65	9.13	85.36	92.53	96.81	85.28	23.53	1.69
	log K_2	6.35	6.95	7.70						

TABLE 2—YIELD, MOLECULAR WEIGHT, ELEMENTAL ANALYSIS AND CONDUCTANCE OF H_2BB AND ITS HYDRATED METAL CHELATES

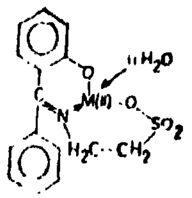
Compd.	Yield %	Molecular weight	Analysis % : Found/(Calcd.) C	H	N	S	Metal	Water	ΔM Ω^{-1} cm^{-2} mol^{-1}
$[Co(C_{15}H_{13}NSO_4)(H_2O)_3]$	67	409 (416)	3.56 (3.60)	4.40 (4.56)	3.31 (3.36)	7.61 (7.69)	14.11 (14.18)	12.95 (12.98)	3.0
$[Ni(C_{15}H_{13}NSO_4)(H_2O)_3]$	72	406 (415)	3.58 (3.61)	4.51 (4.57)	3.29 (3.37)	7.68 (7.71)	13.91 (13.79)	12.93 (13.01)	4.7
$[Cu(C_{15}H_{13}NSO_4)(H_2O)_3]$	81	411 (420)	3.50 (3.57)	4.48 (4.52)	3.31 (3.33)	7.53 (7.63)	14.88 (15.00)	12.83 (12.85)	6.0
$[Zn(C_{15}H_{13}NSO_4)(H_2O)]$	68	376 (386)	3.76 (3.88)	3.70 (3.88)	3.53 (3.62)	8.19 (8.29)	16.79 (16.83)	4.56 (4.66)	3.7
$[Cd(C_{15}H_{13}NSO_4)(H_2O)]$	76	427 (433)	3.40 (3.46)	3.42 (3.46)	3.17 (3.23)	7.29 (7.39)	25.76 (25.86)	4.07 (4.15)	3.8
$[UO_2(C_{15}H_{13}NSO_4)(H_2O)]$	72	583 (591)	2.51 (2.53)	2.49 (2.53)	2.28 (2.36)	5.33 (5.41)	40.21 (40.27)	3.02 (3.04)	6.7
$[VO(C_{15}H_{13}NSO_4)(H_2O)_2]$	63	398 (406)	3.58 (3.69)	4.10 (4.18)	3.39 (3.44)	7.78 (7.88)	12.49 (12.56)	8.80 (8.86)	8.6

* Calculated values in parenthesis.

Electronic spectra : The electronic spectra in benzene of the Co^{II} chelate consist of two bands at 8 650 and 22 000 cm^{-1} which can be assigned to the transitions $^4T_{1g}$ (F)→$^4T_{2g}$ (F) and $^4T_{1g}$ (F)→ $^4T_{1g}$ (P), respectively. These bands suggest an octahedral stereochemistry for the Co^{II} chelate. The spectra for the Ni^{II} chelate show two bands at 13 650 and 26 400 cm^{-1} assignable to the transitions $^3A_{2g}$ → $^3T_{1g}$ (F) and $^3A_{2g}$ → $^3T_{1g}$ (P), respectively. These bands suggest an octahedral stereochemistry around Ni^{II} ion[7,8]. In the case of Cu^{II} chelate, a broad absorption band at 12 810 cm^{-1} is observed which may be due to the transition ^2E_g → $^2T_{2g}$. It suggests an octahedral stereochemistry for Cu^{II} chelate. The $V^{IV}O$ chelate shows two bands at 11 570 and 18 700 cm^{-1} assignable to the transitions $d_{xy} \rightarrow d_{xz}$, d_{yz} and $d_{xy} \rightarrow d_{x^2-y^2}$ respectively in an octahedral environment of VO^{2+}.

Ir spectra : Ir spectra of H_2BB show bands at 3 260, 1 610 and 1 190 cm^{-1} assignable to ν_{OH}, ν_{CN} and ν_{SO_2OH}, respectively. ν_{CN} of H_2BB around 1 610 cm^{-1} is shifted to lower frequency side on complexation, indicating participation of the azomethine nitrogen in coordination. In the metal chelates, two new bands in the ranges 400-420 and 580-600 cm^{-1} suggest the formation of M—N and M—O bonds in them. All the complexes give one broad band in the region 3 200-3 230 cm^{-1} due to ν_{OH} of the water molecule. The loss of water molecules at relatively high temperature (>180°) indicates that these are coordinated and not lattice field.

It appears that due to steric factors, 1 : 2 (metal-ligand) stoichiometry is not attended. In view of the experimental evidences received, Co^{II}, Ni^{II}, Cu^{II}, $U^{VI}O_2$ ane $V^{IV}O$ chelates may be assigned an octahedral stereochemistry, whereas Zn^{II} and Cd^{II} chelates are tetrahedral as is common with these ions. These structures are represented in Fig. 1.



When n = 1, M(II) = Zn, Cd or UO_2.
n = 2, M(II) = VO
n = 3, M(II) = Co, Ni or Cu.

Fig. 1. Bivalent metal chelate of 2-(*N*-α-benzyl-2-hydroxybenzylidineimino)ethane sulphonic acid (H_2BE).

References

1. M. CALVIN and K. W. WILSON, *J. Am. Chem. Soc.*, 1945, 67, 2003.
2. J. BJERRUM, "Metal Amine Formation in Aqueous Solution", P. Haase and Sons, Copenhagen, 1941.
3. P. MEHTA and R. K. MEHTA, *Proc. Indian Natl. Sci. Acad., Sect. A*, 1984, 50, 69.
4. H. IRVING and H. S. ROSSOTI, *J. Chem. Soc.*, 1958, 3397.
5. H. IRVING and R. J. P. WILLIAMS, *J. Chem. Soc.*, 1953, 3192.
6. K. B. YATSIMIRSKII and V. P. VASILEB, "Instability Constant of Complex Compounds", Van Nostrand, New Yoik, 1960, p. 63.
7. M. C. DAY and J. SELVIN, "Theoretical Inorganic Chemistry", Reinhold, New York, 1962, p. 325.
8. A. B. P. LEVER, "Inorganic Electronic Spectroscopy", Elsevier, New York, 1968, p. 333.
9. J. SELVIN, *Chem. Rev.*, 1965, 65, 165.

J. Indian Chem. Soc.,
Vol. LXIII, February 1986, pp. 201-202

Study of Stability Constants of Complexes of some Divalent Metal Ions and Rare Earth Metal Ions with 5-Benzal-3-phenyl-2-thioxo-4-imidazolidinone

PRITAM S. VARMA, (Miss) CELINE D'SOUZA and N. B. LAXMESHWAR*

Physical Chemistry Laboratory, Institute of Science, Bombay-400 032

Manuscript received 26 December 1984, revised 7 October 1985, accepted 2 December 1985

The stepwise stability constants of complexes of 5-benzal-3-phenyl-2-thioxo-4-imidazolidinone with Cu^{II}, Zn^{II}, Ni^{II} and Cd^{II} as transition metal ions and Sm^{III}, Gd^{III} and Dy^{III} as rare earth metal ions are determined by Calvin-Bjerrum potentiometric titration method. The study was conducted in 3 : 1 (v/v) dioxane-water medium at ionic strength 0.1 μ and temperature 27 ± 1°. The order of the stability constants is found to be in agreement with the order reported by earlier workers. In case of rare earth metal ions, the stability constants observed are slightly lower as compared to the divalent metal ions studied, thereby indicating lesser ionic character.

STOICHIOMETRIC stability constants of 5-membered ring compounds containing sulphur with different metal ions in solution have been extensively studied. 2-Thioxo-4-imidazolidinone also called 2-thiohydantoin belongs to this class of 5-membered heterocyclic compounds. The determination of stoichiometric stability constants of 2-thioxo-4-imidazolidinone, its 3-*N*-substituted derivatives and 5,5-dimethyl-3-*N*-substituted derivatives have been carried out[1]. The present investigation is aimed at determining the stoichiometric stability constant of 5-benzal-3-phenyl-2-thioxo-4-imidazolidinone (1) also called 5-benzal-3-phenyl-2-thiohydantoin with some transition and rare earth metal ions.

N-1 position in the compound is not substituted, thus giving rise to the tautomeric form N=C–SH from where the proton dissociates and the metal ion forms a complex. This is confirmed by ir spectral studies[2] of 2-thioxo-4-imidazolidinone and its 3-*N*-derivatives which give vibrations, characteristic of SH and C=N in dioxane medium and vibrations characteristic of C=S in KBr matrix.

Experimental

5-Benzal-3-phenyl-2-thioxo-4-imidazolidinone was prepared by standard methods[3]. The ligand being sparingly soluble in water, a medium of 3 : 1 (v/v) dioxane-water was used. Metal ions used were in the form of metal perchlorates prepared from A. R. grade metal oxides. The concentrations of the metal perchlorate solutions were determined dy EDTA titrations. The *p*H readings were taken on a Phillips PR 950M with glass-calomel electrode assembly at 27±1°. Nitrogen atmosphere is maintained throughout the titration. The free acid, free acid plus ligand, free acid plus ligand plus metal ion are titrated separately against carbonate-free standard sodium hydroxide solution (1.0601 1*M*). Sodium perchlorate was added to maintain constant ionic strength.

Results and Discussion

Due to basic N at 1-position, the protonation takes place, hence the graph of B against volume of alkali added showed back curves in case of acid plus ligand plus metal ion titration. New graphs

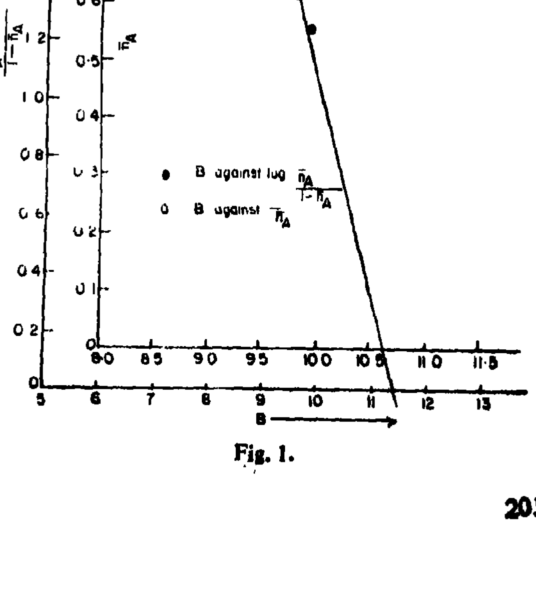


Fig. 1.

were obtained by shifting the curves with equivalent amount of alkali for the protons absorbed. $\bar{n}_A$ values were obtained by Irving and Rossotti equations and then pK values for the reagent are calculated. This value was confirmed by the plots of (i) B *vs* $\bar{n}_A$ and (ii) B *vs* log $\bar{n}_A/(1-\bar{n}_A)$ (Fig. 1).

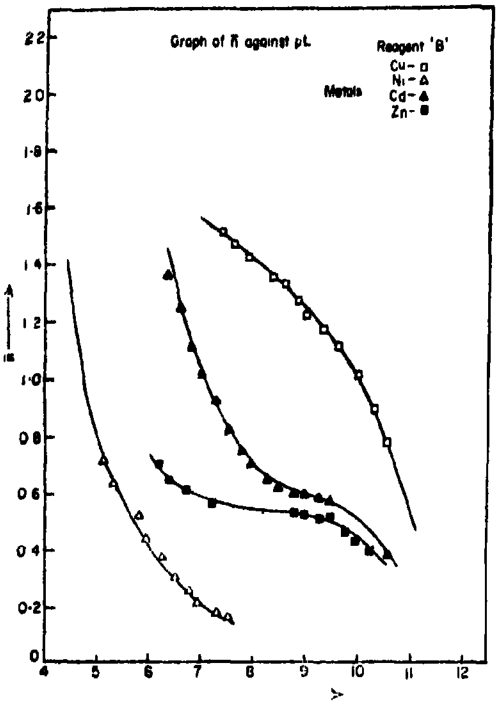


Fig. 2.

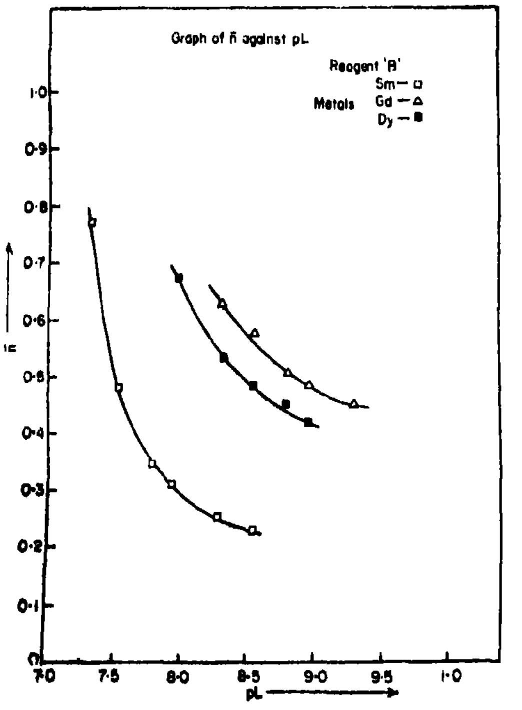


Fig. 3.

As per Irving and Rossotti method, $\bar{n}$ values were calculated and plotted against the corresponding calculated pL values to obtain the formation curves of the metal complexation equilibria (Figs. 2 and 3). These formation curves were used to determine log k_1 and log k_2 by half-integral method. In some cases log k_2 values are obtained by extrapolating the graphs. The curves obtained are fairly symmetrical in nature in all the cases. Limits of error and the standard deviation for k values were applied and the most representative values are recorded in Table 1. The order of stability constants in case of divalent transition metal ions studied is found to be Cu>Cd>Zn>Ni.

TABLE 1—STEPWISE STABILITY CONSTANTS OF COMPLEXES

Temp. = 27±1°, μ = 0.1

Metal ion	Cu^{II}	Zn^{II}	Ni^{II}	Cd^{II}	Sm^{III}	Gd^{III}	Dy^{III}
log k_1	11.025	9.350	5.700	10.000	7.50	8.12	8.40
log k_2	7.40	—	4.425	6.25	—	—	—

The observed order is in agreement with the order given by Irving and Williams. The observed order Cd>Zn is in agreement with the observations made earlier with few exceptions[4,5]. This order is further supported by the exceptions based on, increase in ionisation potential and reciprocal ionic radius on passing from cadmium to zinc. However, the observed order Zn>Ni contradicts the order Cu>Ni>Zn given by Mellor and Maley[6] but is supported by many other workers[7-9]. The reversal of this order is attributed to stearic factors.

As regards complexes of rare earth metal ions, the stability constants were slightly lower as compared to the divalent metal ions, thereby indicating lesser ionic character. In order to find the detailed stability order, the study of the whole series of lanthanides is under investigation.

Acknowledgement

The authors are highly grateful to Dr. D. G. Vartak, B. A. R. C. and Dr. M. S. Mydeo, Ruia College, Bombay, for their valuable suggestions.

References

1. M. T. COMPANYWALLA, M.Sc. Thesis, Bombay University, 1976.
2. P. V. KAMAT, N. B. LAXMESHWAR and M. G. DATAR, *J. Indian Chem. Soc.*, 1971, **48**, 199.
3. T. N. GHOSH, *J. Indian Chem. Soc.*, 1934, **11**, 31.
4. K. J. PEDERSON, *Acc. Chem. Scand.*, 1969, **23**, 676.
5. A. E. MARTALL and M. CALVIN, "Chemistry of Metal Chelate Compounds", Prantice Hall, New York, 1952, p. 551.
6. D. P. MELLOR and L. A. MALEY, *Nature (London)*, 1947, **159**, 370; 1948, **161**, 436.
7. W. D. JOHNSTON and H. FREISER, *J. Am. Chem. Soc.*, 1952, **74**, 5239; *Anal. Chim. Acta*, 1954, **11**, 201.
8. R. G. CHARLES and H. FREISER, *Anal. Chim. Acta*, 1954, 11. 1, 101.
9. V. T. ATHAVALE, L. H. PRABHU and D. G. VARTAK, *J. Inorg. Nucl. Chem.*, 1966, **28**, 1237.

J. Indian Chem. Soc.,
Vol. LXIII, February 1986, pp. 203-205

Thermodynamic and Structural Studies of Chelates of 2-Hydroxyphenyl-4-benzamidothiosemicarbazide with Cerium(IV) and Uranium(VI)

SHREESH BHARDWAJ*, M. N. ANSARI, M. C. JAIN and W. U. MALIK†

Department of Chemistry, S. D. College, Muzaffarnagar-251 001

Manuscript received 10 January 1985, revised 19 August 1985, accepted 15 November 1985

Interaction between Ce^{IV} and U^{VI} with 2-hydroxyphenyl-4-benzamidothiosemicarbazide has been studied. Spectrophotometric, electrometric and chemical analysis give 1 : 2 metal-ligand ratio. Stepwise stability constants have been calculated *p*H-metrically at different ionic strengths and at different temperatures. Thermodynamic parameters have been calculated which reveal exothermic interaction between metal and ligand and support the formation of stable complexes. The complexes have been characterised by ir studies.

EXTENSIVE stoichiometric and structural studies of Cr^{III}, Mn^{II}, Fe^{III}, Co^{II}, Ni^{II}, Cu^{II} and Ag^{II} complexes of 2-hydroxyphenyl-4-benzamidothiosemicarbazide have been reported earlier[1,2]. In this communication, characterisation and thermodynamic parameters of Ce^{IV} and U^{VI} complexes of this ligand have been reported.

Experimental

Fresh solution of 2-hydroxyphenyl-4-benzamidothiosemicarbazide (OH-BTSC) was used. Stock solutions of ceric ammonium nitrate and uranyl acetate were prepared in CO_2-free double-distilled water and their strengths were calculated by the usual methods. All the chemicals were of AnalaR and B.P. grade. Optical measurements were made on a Bausch and Lomb Spectronic–20 spectrophotometer. The *p*H titrations at different temperatures and amperometric titrations at –0.4 V (selected from the plateaux of OH-BTSC) *vs* SCE were carried out as reported earlier[1,3]. The *p*H-values were corrected[4] for mixed solvents.

Equimolar solutions of ceric ammonium nitrate and OH-BTSC were mixed with stirring in a 1 : 2 stoichiometric ratio. *p*H of the solution was raised to about 9.0 for separation of the complex. The cerium(IV) complex was centrifuged, washed with water and finally recrystallised from acetone and dried in vacuum desiccator. Uranium(VI) complex, being highly soluble in water, was isolated by mixing equimolar solutions of metal ions and ligand in acetone-ethanol mixture (90 : 10, v/v) at $pH \simeq 9.5$. The complex was recrystallised from acetone.

The solid complexes were analysed for elements to ascertain their composition. Uranium was estimated gravimetrically as U_3O_8 and cerium(IV) was estimated volumetrically by titration with standard iron(II) solution. Nitrogen was estimated microanalytically by Dumas method and sulphur as $BaSO_4$. The results of chemical analysis are given in Table 1. Ir spectra of ligand and metal complexes were recorded in KBr medium on a Beckman–20 spectrophotometer. Magnetic measurements of the complexes were made on the Gouy's magnetic balance at 30°.

TABLE 1—ANALYTICAL DATA

Compd.	Analysis % Found/(Calcd.)		
	Metal	N	S
$(C_{16}H_{22}N_8O_8S_2)U$	31.35	14.75	8.55
	(31.47)	(14.81)	(8 48)
$(C_{16}H_{22}N_8O_7S_2)Ce$	21.78	17.65	10.56
	(21.81)	(17.43)	(9.98)

Results and Discussion

Preliminary studies reveal that metal salt solutions when mixed with OH-BTSC gave dark brownish orange and orange coloured solutions with Ce^{IV} and U^{VI}, respectively. Conductivity measurements for the uranium complex in non-polar solvents show its ionic nature while Ce^{IV} complex is non-ionic.

Vosburgh-Cooper's curves[5] indicated complexation as the λ_{max} values 385 nm and 445 nm, occurring in the absorption spectra of Ce^{IV} and U^{VI} metal ions were shifted to 370 nm and uv region, respectively in the presence of ligand. Wavelength

Present address : * Department of Chemistry, Indo-Soviet Friendship Pharmacy College, Moga, Punjab.
† Department of Chemistry, University of Roorkee, Roorkee-247 672.

region 480-520 nm was chosen for absorption measurements since in this region, the complexes absorb appreciably high as compared to the reactants. Normal Job's[6] and slope-ratio[7] curves were obtained. Job's curves peaked at 0.33 mole fraction corresponding to 1 : 2 M-L ratio and the slope of curves 1, 2 and 3, 4 for Ce^{IV} and U^{VI}, respectively (Fig. 1) further showed 1 : 2 M-L ratio for both the complexes. Amperometric studies also confirmed 1 : 2 stoichiometry for these complexes.

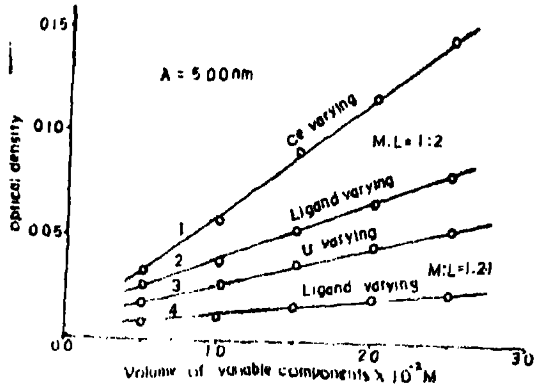


Fig. 1

The pK values of OH-BTSC were determined pH-metrically at 26 and 32° at different ionic strengths. These values did not differ appreciably and were found to be almost the same, 8.5 and 10.2. Maximum lowering in case of 1 : 2 metal-OH-BTSC mixture and inflection corresponding to 4 moles of KOH : 1 mole of metal indicated 1 : 2 metal-ligand ratio in the complexes.

At 26 and 32°, pH-titrations of OH-BTSC alone and in presence of different concentrations of metal ions, at different ionic strengths (only in the case of uranium, constant ionic strength could be maintained), were performed according to Calvin and Melchior[8], gave normal titration curves when titrated against 0.1 M KOH; and from these the formation curves were constructed. The pL values at $\bar{n}$=0.5 and 1.5 gave the values of stepwise stability constants, log K_1 and log K_2, and of overall stability constant, log K (Table 2). In the case of uranium complex, overall stability constants were calculated graphically at zero ionic strength (Fig. 2, curves 1, 2; Table 2). For cerium complex, the apparent average values of log K are 29.46 and 29.02 at 26 and 32°, respectively.

TABLE 2

Temp. °C	Values of log K at different ionic strengths for U^{VI} complex			
	0.067 M	0.133 M	0.200 M	0.00 M
26	18.94	19.20	19.39	18.77
32	18.78	18.97	19.23	18.50

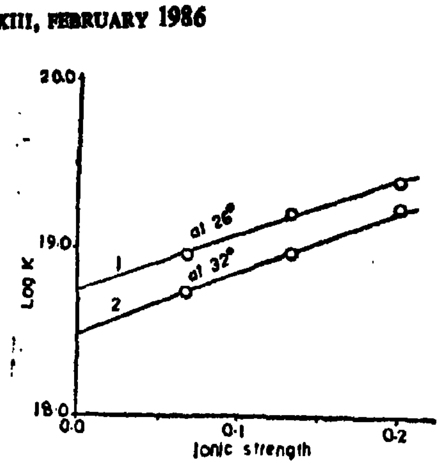


Fig. 2

From the knowledge of overall stability constants, thermodynamic parameters, *viz.* $\Delta H°$, $\Delta G°$, $\Delta S°$ were calculated at 26° (Table 3). It is clear from the pH data that $\bar{n}$ increases with the increase in pH values upto $\bar{n}$=2, showing thereby that the ionic form of the ligand takes part in the reaction and further proves 1 : 2 metal-ligand ratio in the complexes. Furthermore, the reaction between metal ion and OH-BTSC is exothermic and proceeds spontaneously as indicated by the respective negative values of $\Delta H°$ and $\Delta G°$. Positive values of $\Delta S°$ confirm the formation of stable complexes.

TABLE 3—THERMODYNAMIC PARAMETERS AT 26°

Compd.	G° kJ mol⁻¹	H° kJ mol⁻¹	S° JK⁻¹ mol⁻¹
$(C_{16}H_{16}N_6O_4S_2)U$	−107.458	−78.575	+96.60
$(C_{16}H_{16}N_6O_2S_2)Ce$	−168.658	−125.139	+145.50

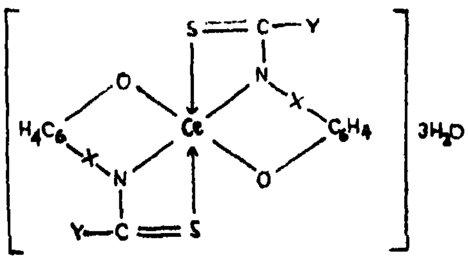
A sharp band at 3 555 cm⁻¹ in the ir spectrum of OH-BTSC has been assigned to the phenolic group, which disappeared in the spectra of the metal chelates, suggesting the loss of phenolic hydrogen on complexation, establishing a bond between metal and phenolic oxygen in these complexes. The sharp band at 1 610 cm⁻¹ observed in OH-BTSC spectrum is due to the bending vibrations of amino and amide groups. This band is shifted to 1 620 cm⁻¹ in both the complexes, suggesting the non-involvement of amido nitrogen in complex formation. However, the decrease in the intensity and lowering of absorption band from 1 200 to 1 160 cm⁻¹ due to N−C−S bending plus NH_2 rocking and NH_2 deformation in these complexes, support the metal-nitrogen (attached to imido nitrogen atom) bonding. The sharp absorption bands in OH-BTSC occurring at 3 300, 3 285 and 3 200 cm⁻¹ are due to the NH and NH_2 stretching frequencies. These vibrations in the Ce^{IV} comlpex have been broadened in the region 3 200-3 480 cm⁻¹, and two broad bands in the region 3 400-3 520 and 3 200-3 320 cm⁻¹ for U^{VI} complex are observed. The shifting of the NH−NH_2 vibrations to the higher wavelengths suggests the non-

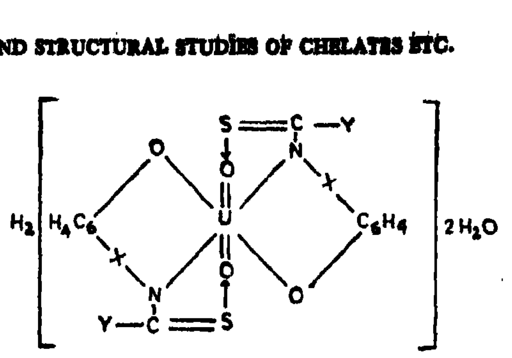
participation of hydrazine group in complex formation[9,10]. However, their broadness indicates the presence of lattice water. Loss in weight as well as fading of colour observed when the complexes are put over concentrated H_2SO_4 in vacuum desiccator, further support the presence of water of crystallisation. The sharp bands in OH-BTSC at 1 325, 1 300, 1 075, 710 and 690 cm^{-1} were assigned to the C=S stretching frequencies. Similar assignment has been made for thioacetamides, thiosemicarbazide and other thio-compounds[11-15]. The intensities of these vibrations decreased and shifted to lower wavelength region at 1 310, no band, 1 040, 690, 660 cm^{-1} in Ce^{IV} complex, and 1 300, no band, 1 040, 685 and 635 cm^{-1} in U^{VI} complex, showing that sulphur is involved in the bonding. In the spectra of uranium complex, two new bands at 900 and 790 cm^{-1} are assigned to UO_2^{2+} ion. Usually two characteristic frequencies in the regions 950-890 and 830-820 cm^{-1} were reported for UO_2^{2+} in the metal chelates[16]. Lowering of these frequencies in the uranium complex is a clear indication for the involvement of oxygen of UO_2^{2+} in bonding.

Both the complexes are found to be diamagnetic. On the basis of the above findings, the following reactions and structures have been given to these complexes.

$$Ce(NO_3)_4 + 2C_6H_4(OH)CONHNHC(=S)-NHNH_2 \rightarrow Ce[C_6H_4(O)CONHNC(=S)-NHNH_2]_2 + 4HNO_3$$

$$UO_2(CH_3COO)_2 + 2C_6H_4(OH)CONHNHC(=S)-NHNH_2 \rightarrow H_2[UO_2\{C_6H_4(O)CONHNC(=S)-NHNH_2\}_2] + 2CH_3COOH$$





X = CONH ; Y = $NHNH_2$

References

1. S. BHARDWAJ, M. N. ANSARI, R. D. KAUSHIK and M. C. JAIN, *J. Indian Chem. Soc.*, 1984, 61, 484.
2. S. BHARDWAJ, M. N. ANSARI, M. C. JAIN and W. U. MALIK, *J. Indian Chem. Soc.*, communicated.
3. S. BHARDWAJ, M. N. ANSARI, M. C. JAIN and W. U. MALIK, *Indian J. Chem.*, communicated
4. L. G. VAN UITERT and C. G. HASS, *J. Am. Chem. Soc.*, 1953, 75, 451.
5. W. C. VOSBURGH and G. R. COOPER, *J. Am. Chem. Soc.*, 1941, 63, 437.
6. P. JOB, *Ann. Chim. (Paris)*, 1928, 9, 113.
7. A. E. HARVEY and D. L. MANNING, *J. Am. Chem. Soc.*, 1950, 72, 4488 ; 1952, 74, 4744.
8. M. CALVIN and N. C. MELCHIOR, *J. Am. Chem. Soc.*, 1948, 70, 3270.
9. B. A. CIMGRASS, R. L. SOMORJAU and C. H. BALEY, *Can. J. Chem.*, 1961, 39, 957.
10. K. NAKAMOTO, "Infrared Spectra of Inorganic and Coordination Compounds", John Wiley, New York, 1963.
11. L. J. BELLAMY and P. E. ROGARSCH, *J. Chem. Soc.*, 1960, 2218.
12. I. SUZUKI, *Bull. Chem. Soc. Jpn.*, 1926, 35, 1286.
13. I. SUZUKI, *Bull. Chem. Soc. Jpn.*, 1926, 35, 1449.
14. I. SUZUKI, *Bull. Chem. Soc. Jpn.*, 1926, 35, 1456.
15. L. H. LITTLE, G. W. POLLING and J. LEIJA, *Can. J. Chem.*, 1961, 39, 754.
16. J. SELBIN, *Angew Chem.*, 1966, 5, 712.

J. Indian Chem. Soc.,
Vol. LXIII, February 1986, pp. 206-209

Ion-exchange Behaviour of Stannic Tungstophosphate towards Bivalent Metal Ions

A. P. GUPTA*

Chemistry Department, Delhi College of Engineering, Kashmere Gate, Delhi-110 006

and

M. QURESHI, V. SHARMA, R. C. KAUSHIK and H. O. GUPTA

Chemical Laboratories, Z. H. College of Engineering and Technology, Aligarh Muslim University, Aligarh-202 001

Manuscript received 19 September 1984, revised 16 August 1985, accepted 29 October 1985

Sn^{IV} tungstophosphate (Sn-W-P) was prepared by adding 0.1 *M* Sn^{IV} chloride solution to 0.1 *M* tungstophosphoric acid solution in different volume ratios. The dried gel of Sn-W-P was refluxed in 6 *M* phosphoric acid for 100 h before breaking down into small granules. Its ion-exchange capacity, chemical composition (Sn-W-P, 2 : 1 : 3.2), chemical dissolution, *p*H titration, heat treatment, ir spectra and distribution coefficients for 11 bivalent metal ions in various media have been studied. The quantitative separation of Zn^{II}-Cd^{II} and Hg^{II}-Cu^{II} were also achieved on its columns.

THE present considerable status of the synthetic inorganic ion-exchange materials is due to their growing application potentiality in energy resources recovery, pollution abatement and in achieving metal ion separation of analytical scope.

The insoluble salts of hetero-polyacids with polyvalent metals are preferred to other ion-exchangers as they exhibit selective ion-exchange behaviour. Therefore, now-a-days the investigation of these salts has become a field of interest. Besides the sizable studies on simple salts, Qureshi *et al.* have published their findings on crystalline Sn^{IV}-vanadophosphate[1], (Sn-v-p)[1], Sn^{IV}-molybdroarsenate[2], Sn^{IV}-tungstoarsenate[3,4] and hydrous antimony sulphide[5]. The present report summarises the synthesis, characterisation and ion-exchange behaviour of Sn^{IV}-tungstophosphate (Sn-W-P).

Experimental

Tin(IV) chloride pentahydrate (Poland) and phosphotungstic acid (U.S.A.) were used. All other reagents used were of analytical grade.

A Elico LI-10 *p*H meter, a Bausch & Lomb Spectronic-20 colorimeter, and a Perkin-Elmer spectrophotometer were used for potentiometric, spectrophotometric and ir absorption measurements. The shaking was performed in a SICO temperature controlled shaker.

Synthesis of Sn^{IV}-tungstophosphate (Sn-W-P): Sn(IV) tungstophosphate was prepared by adding 0.1 *M* tin(IV) chloride solution to 0.1 *M* tungstophosphoric acid (PWA) solution in different volume ratios (Table 1). The mixture was heated to boiling and then adjusted to the desired *p*H value. The resulting precipitate was allowed to stand for 24 h at room temperature. It was filtered and washed with 1 *M* HCl followed by demineralised water (dmw). The gel was dried at 40°. The dried product was broken down into small granules by immersing it in water. These granules were dried, and were subjected to refluxing in 6 *M* H_3PO_4 for 100 h. The resulting material was washed with dmw and converted into the H^+-form by treatment with 1 *M* HNO_3 in the usual manner.

Ion-exchange capacity: The ion-exchange capacity of various samples of Sn-W-P was determined by the usual column method (Table 1).

Chemical composition: The exchanger (200 mg) was dissolved in concentrated sulphuric acid and hydrochloric acid mixture (2 : 1). Tungsten was determined with α-benzoin oxime gravimetrically as tungsten(VI) oxide[6]. In the filtrate Sn^{IV} was reduced with lead, and then determined by the potassium dichromate method[6]. Phosphate was determined by the ammonium molybdate method[6]. The mole ratio of Sn^{IV}-tungstophosphate was found to be 2 : 1 : 3.2 (Sn-W-P).

Chemical dissolution: A sample (100 mg) of the exchanger was taken in a flask with the solution (50 ml) concerned. After shaking for 6 h, the undissolved portion of the exchanger was filtered off. Tin, tungsten and phosphorus were determined spectrophotometrically in the filtrate. The results are given in Table 2.

pH-titrations: *p*H titrations were carried out by the method of Topp and Pepper[7]. The results are plotted in Fig. 1.

Heat treatment: Sample S_A was heated at different temperatures in muffle furnance for 1 h. The ion-exchange capacity of the heated samples was determined. The effect of temperature upon ion-exchange capacity is shown in Fig. 2.

Measurement of ir spectra: Ir spectra of samples (S_A and S_B) of Sn^{IV}-tungstophosphate and of phosphotungstic acid in H^+-form dried at 40°, were taken by the KBr disc technique. The results are presented in Fig. 3 and Table 3.

Distribution coefficient determination: The distribution coefficient (K_d) for metal ions was determined on Sn^{IV}-tungstophosphate (sample S_A) in different solutions. The cation-exchange loading for the system was less than 3% of the apparant ion-exchange capacity. The following equation was used for calculation,

$$K_d = \frac{I-F}{F} \times \frac{50}{0.50}$$

where, I is the volume of EDTA solution (5 m*M*) used to titrate the original cation solution, F is the volume of EDTA solution (5 m*M*) used to titrate the cation solution after equilibrium.

The total solution was 50 ml and the amount of exchanger 0.50 g. The results are given in Table 4.

Column operation: For separation studies, a column (30×0.3 cm dia) was used, and exchanger (0.50 g) was kept in the column with glass wool support. The rate of flow was 9 to 10 drops min^{-1}. The effluent was titrated with EDTA solution (5 m*M*). Quantitative separations of Zn^{II}-Cd^{II} and of Hg^{II}-Cu^{II} were achieved on these columns.

Results and Discussion

The various samples of Sn^{IV}-tungstophosphate have been prepared at different *p*H values. It is clear from Table 1 that at *p*H 3 it shows ion-exchange capacity as well as mechanical stability. The synthesised samples A and B show the same ion exchange-capacity and same apparent stability. The unrefluxed (UR) samples show less ion-exchange capacity than the refluxed one. The refluxing of the material in 6 *M* phosphoric acid solution for 100 h increases the ion-exchange capacity. It hints to the possibility that the refluxing develops some new additional exchange sites in the molecule of Sn^{IV}-tungstophosphate.

A comparative study of stannic tungstophosphate with tungstoarsenate (Sn-W-As) and molybdoarsenate (Sn-Mo-As) (Table 2) shows that the material under study is more stable than the tungstoarsenate and molybdoarsenate. It has been reported earlier that almost all the inorganic ion-exchangers get dissolved in alkaline medium completely but tin(IV)-tungstophosphate exhibits significant chemical stability in 10^{-3} *M* NaOH solution. It gets dissolved negligibly in 0.1 *M* NaOH. Thus, this ion-exchange material possess salient features for performance studies in alkaline medium.

TABLE 1—CONDITIONS OF SYNTHESIS AND ION-EXCHANGE CAPACITY OF Sn^{IV}-TUNGSTO PHOSPHATE

Reagent: 0.1 *M* Stannic chloride + 0.1 *M* tungstophosphoric acid

Sl. no.	*p*H of mixture	Mixing ratio	I.E.C. for Na^+ (meq/g)		Remarks
			UR	R	
1.	0	2 : 1	0	0	
2.	1	2 : 1	1.04	—	Unstable
3.	3	2 : 1 (S_A)	1.61	1.22	Stable
4.	3	2 : 1 (S_B)	0.66	1.20	Stable

S_A = Stannic tungsto phosphate prepared by using phospho tungstic acid synthesised in the laboratory. S_B = Stannic tungsto phosphate prepared by using imported phosphotungstic acid. UR = Unrefluxed sample. R = Refluxed sample.

The *p*H-titration curves (Fig. 1) show the monofunctional characteristics of the samples and their ion-exchange capacity to be 2.50 meq g^{-1}, while its apparent ion-exchange capacity is 1.20 meq g^{-1}. It means that the apparent ion-exchange capacity is only about 48% of the calculated one.

The ion-exchange capacity of Sn^{IV}-tungstophosphate decreases on drying in air with increase in temperature. It is quite stable upto 500°. The curves (Fig. 2) indicate that all the three materials can be used as ion-exchanger upto 600°. The order of their thermal stabilities regarding the loss in ion-exchange capacity upon drying is as follows: tungstoarsenate > tungstophosphate > molybdoarsenate.

The ir spectra (Table 3) reveal that the absorption maxima at 3 500-3 100 and 1 700-1 600 cm^{-1} are mainly common in all the three spectra, which means that the designated constituents and their mode of presence is common. The maxima at 1 200-900 cm^{-1} is shown by the samples S_A and S_B while PWA absorbs at 1 080 cm^{-1}, but these two peaks correspond to the same designation. The shift in band frequency may be due to difference in the crystal structures of these two materials, *i.e.* stannic tungstophosphate and phosphotungstic acid. In the lower frequency range, ir radiations are absorbed by PWA only. The designations to these peaks are given in Table 3. The ir study hints that stannic tungstophosphate and phosphotungstic acid are quite different from each other regarding their structures.

TABLE 2—CHEMICAL DISSOLUTION (mg/50 ml) OF STANNIC TUNGSTOPHOSPHATE, TUNGSTOARSENATE AND MOLYBDOARSENATE

Sl. no.	Solvent	Sn-W-P Sn	Sn-W-P W	Sn-W-P P	Sn-W-As Sn	Sn-W-As W	Sn-W-As As	Sn-Mo-As Sn	Sn-Mo-As Mo	Sn-Mo-As As
1.	Water	0.0	0.0	0.02	0.65	1.0	1.8	0.0	6.6	3.8
2.	4 M HNO_3	1.12	0.0	0.0	8.0	0.6	1.0	3.6	20.0	17.5
3.	0.1 M NH_4NO_3	0.0	0.0	0.0	0.63	2.0	1.6	*	*	*
4.	0.1 M NaOH	2.8	7.5	0.3	*	*	*	*	*	*
5.	0.01 M NaOH	0.9	0.5	0.4	*	*	*	*	*	*
6.	n-Butanol	–	0.0	0.01	0.09	0.0	0.18	0.0	0.0	0.0

* Dissolve completely.

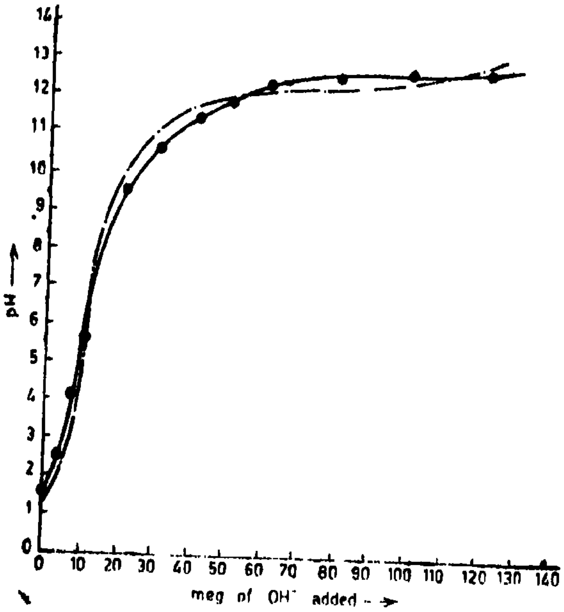


Fig. 1. pH-titration curves of stannic tungstophosphate: (—.—) S_A and (●) S_B.

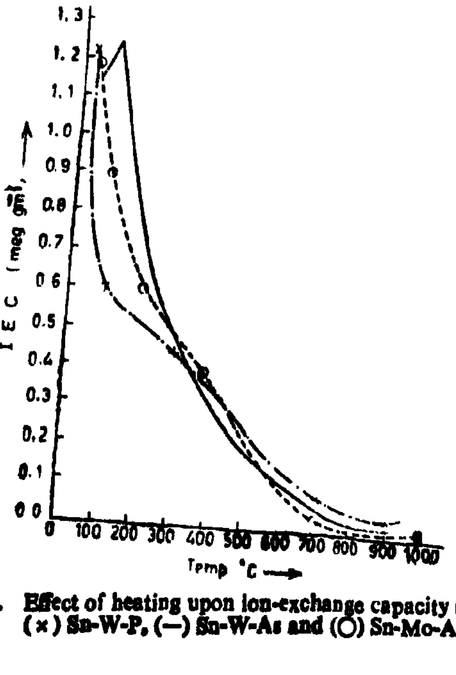


Fig. 2. Effect of heating upon ion-exchange capacity (IEC): (×) Sn-W-P, (—) Sn-W-As and (O) Sn-Mo-As.

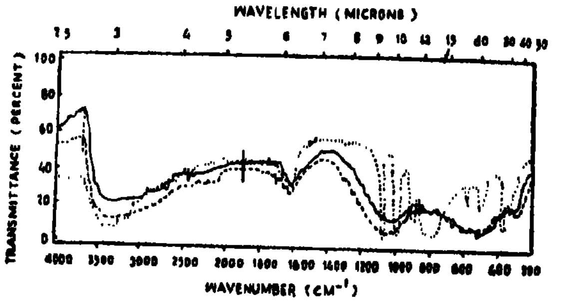


Fig. 3. Ir spectra: (– –) stannic tungstophosphate, (–) Sn-W-P and (...) phosphotungstic acid.

TABLE 3—IR SPECTRA OF STANNIC TUNGSTOPHOSPHATE SAMPLES (S_A AND S_B) AND PHOSPHOTUNGSTIC ACID (PWA)

ν_{max} (cm^{-1})	Peak appeared in	Designation
3 500-3 100 br	S_A, S_B, PWA	ν_1(OH)
2 420 s	PWA	$\delta_1(H_2O)$ coord.
1 700-1 600 m	S_A, S_B, PWA	$\delta_2(H_2O)_t$
1 200-1 900 br	S_A, S_B, PWA	δ_2(M - OH), $(H_2O)_{int.}$
1080		and ν_1 (P–O)
1 000-975 s	PWA	Superposition of
900-880 s	PWA	ν_3(P–O), (W–O) and
850-750 m	PWA	aqua wagging twist and rock
570 s	PWA	Interatomic ν_6(O–P–O)
520 s	PWA	
390-360 m	PWA	Interatomic ν_4(O–W–O)
320 s	PWA	

Our experience shows that absorption of an ion is different upon different ion-exchangers. It reveals the selectivity of inorganic ion-exchangers. The uptake sequence (Table 4) for some bivalent metal ions on Sn^{IV}-tungstophosphate at different pH values is given below.

pH 1 : Ni>Hg>Co>Cu>Mg>Sr>Ba>Ca=Zn=Cd=Mn

pH 3 : Co>Ni>Hg>Ca>Ba>Mg>Sr>Zn>Cd>Mn>Cu

pH 11 : Sr>Ba>Zn>Ca>Co>Cu>Hg>Mn>Ni>Mg>Cd

It is clear from Table 4 that there is a large difference in the K_d values of Zn^{II}, Cd^{II}, Cu^{II} and Hg^{II}. The quantitative separations of Zn^{II} from Cd^{II}, and Cu^{II} from Hg^{II} were successively

TABLE 4—K_d VALUES (ml g^{-1}) OF METAL(II) IONS ON Sn^{IV}-TUNGSTOPHOSPHATE SAMPLE DRIED AT 40°

Ion	pH 1 (0.1 M HNO_3)	pH 3 (0.001 M HNO_3)	pH 11 (0.001 M NaOH)
Mg	57	936	672
Ca	0	3 787	3 413
Sr	9	844	21 625
Ba	3	1 590	20 000
Zn	0	755	3 520
Cd	0	580	13
Mn	0	500	750
Cu	181	280	1 750
Hg	3 250	5 850	827
Ni	7 206	7 536	730
Co	208	13500	2500

achieved on a small column of Sn^{IV}-tungstophosphate. The least adsorbed Cd^{II} was eluted with 1 mM NaOH, Zn^{II} and Cu^{II} were eluted with 0.1 M HNO_3, and Hg^{II} was eluted with 1.5 M HNO_3 in 0.5 M NH_4NO_3 solution.

References

1. M. QURESHI and R. C. KAUSHIK, *Anal. Chem.*, 1977, **49**, 1965.
2. M. QURESHI, R. KUMAR and R. C. KAUSHIK, *Sep. Sci. Technol.*, 1978, **130**, 185.
3. M. QURESHI, R. KUMAR, V. SHARMA and T. KHAN, *J. Chromatogr.*, 1976, **118**, 175.
4. M. QURESHI, V. SHARMA, R. C. KAUSHIK and T. KHAN, *J. Chromatogr.*, 1976, **128**, 149.
5. A. P. GUPTA, M. QURESHI and Y. SUNANDA, *Indian J. Chem., Sect. A*, 1983, **22**, 721.
6. A. I. VOGEL, "A Text Book of Quantitative Inorganic Analysis", Longmans, New York, 1978, pp. 399, 424, 499.
7. N. E. TOPP and K. W. PEPPER, *J. Chem. Soc.*, 1949, 3299.

J. Indian Chem. Soc.,
Vol. LXIII, February 1986, pp. 210-215

Reaction of Polymerisation Initiators with Metal Salts and Metal Complexes in Solutions. Interaction of Potassium Monopersulphate with Copper(II) Salts and Copper(II)/Hydroquinone Couple

PRAFULLA K. SAHOO, SUDARSHAN SEND, HIMANSU S. SAMANTARAY, SAKTI P. BHATTACHARJEE and RAJANI K. SAMAL*

Macromolecular Research Laboratory, Department of Chemistry, Ravenshaw College, Cuttack-753 003

Manuscript received 21 September 1984, revised 16 August 1985, accepted 15 November 1985

The catalytic decomposition of $KHSO_5$ in presence of Cu^{II} ions and Cu^{II}/phenol couples in aqueous medium (25-50°) is facile and follows first order kinetics ($k_{d_{Cu^{II}}} = 0.192 \times 10^{-5} s^{-1}$, $k_{d_{HQ}} = 0.46 \times 10^{-5} s^{-1}$ and $k_{d_{Cu^{II}/HQ}} = 8.29 \times 10^{-4} s^{-1}$).

$CuSO_4$/hydroquinone couple catalyses $KHSO_5$ decomposition, the rate obeying the following equation,

$$-\frac{d[KHSO_5]}{dt} = \beta k_d [Cu^{II}]^{0.49} [HQ]^{0.98} [KHSO_5]^{1.16}$$

The catalytic efficiency of Cu^{II}, HQ and Cu^{II}/HQ couple has been established from kinetic and spectrophotometric data. The mechanism of $KHSO_5$ decomposition has been proposed and the activation energy and other thermodynamic parameters have been calculated.

THE peroxygen compounds, like organic peroxides, hydroperoxides and inorganic peroxo salts are known to undergo facile homolysis of the peroxo-linkage in the presence of a trace of metal salt impurities to yield free radicals[1-7], thereby finding wide applications as free radical initiators and/or curing agents for polymer and resin industries. Sheldon and Koohi[8] noticed that the participation of a given metal ion in a free radical process is strongly influenced by factors such as the kind of ligand bound to the metal ion and the presence of complexing agents in the reaction systems. Barton *et al.*[9-11] observed that the rate of cumene hydroperoxide (CHP) decomposition by Cu^{II}-acetate was strongly affected by the addition of complexing agents such as amino alcohols. Indicator and Sahani[12,13] found that the rate of t-butyl hydroperoxide (t-BHP) decomposition was greatly accelerated by metal acetylacetonates and such reactions caused high rate of initiation in vinyl and diene polymerisation.

However, no such studies have been reported on the influence of metal salts, comlexing agents and metal salt/complexing agent couples on the free-radical decomposition of potassium monopersulphate excepting a few preliminary reports from our group[14-17]. Kenedy and Stock[18] used potassium monopersulphate for oxidation of a multitude of organic substrates for preparative purpose. Recently, we have been examining the influence of various metal salts, complexing agents and metal salt/complexing agent couples on the rate of decomposition of $KHSO_5$ in order to evaluate the condition of its decomposition for a high rate of initiation in vinyl polymerisation and graft copolymerisation. Present report is one aspect of these studies.

Experimental

Potassium monopersulphate (99.8%) was gifted by Du Pont Co., U.S.A., and was used as such. Acrylonitrile, sulphuric acid, $CuSO_4$, $Cu(NO_3)_2$, $Cu(OAc)_2$, $CuCl_2$, phenol, nitrophenols, cresols, *o*-chlorophenol, catechol, hydroquinone, resorcinol, pyrogallol, α-naphthol, β-naphthol and phenanthroline were of AnalaR grade.

Methods: Acrylonitrile (AN) was purified by standard method[19]. $KHSO_5$ solution (0.129 *M*) was prepared in triple-distilled water and was stored in a refrigerator. Visible spectra were taken in a Beckmann 25 spectrophotometer at 25±0.5°. Experiments were carried out in coloured stoppered reaction vessels. Cu^{II} salts of appropriate concentration were separately taken and thermostated at the desired temperature for 1 h, after which the $KHSO_5$ solution of appropriate concentration was added to each reaction vessel. The course of the initiator decomposition was followed by cerimetry using ferroin as indicator. The experiment was repeated for different concentrations of Cu^{II} salts

and of $KHSO_5$ for different temperatures. The studies were repeated for each phenol. The nature of the decomposition process was also studied by adding acrylonitrile (0.754 *M*) to the reference and the actual experimental systems separately before adding the initiator. Precipitates of polyacrylonitrile obtained was estimated gravimetrically and by average molecular weight determination from intrinsic viscosity data.

$$[\eta]=3.335\times10^{-4}\times\overline{M}_w^{0.75}\ \mathrm{dl\ g^{-1}}$$

Results and Discussion

Decomposition of potassium monopersulphate ($KHSO_5$, 2.58×10^{-2} *M*) with various Cu^{II} salts, like $Cu(OAc)_2$, $CuCl_2$, $Cu(NO_3)_2$ and $CuSO_4$ (2.5×10^{-3} *M*) at 30° follows first order kinetics with rate constants (30°) 0.232×10^{-5}, 0.202×10^{-5}, 0.195×10^{-5} and $0.192\times10^{-5}s^{-1}$, respectively, showing no significant effect of the anions. Hence, detailed examination was carried out with $CuSO_4$ to determine the most efficient conditions for its use. Rate dependence on $CuSO_4$ concentration and temperature at constant [$KHSO_5$] are given in Figs 2 and 3, respectively, and on $KHSO_5$ concentration and temperatures at constant [$CuSO_4$] can be seen in Figs. 4 and 3, respectively. The increasing value of k_{obs} with increasing [Cu^{II}] is due to the increase in concentration of complex ion formed by interaction of the vacant d^9-orbital of Cu^{II} ion with the bridged peroxo orbital of $KHSO_5^{2\sigma-24}$, which disproportionates readily. This complex formation between Cu^{II} and $KHSO_5$ can also be seen from the visible spectra (Fig. 1).

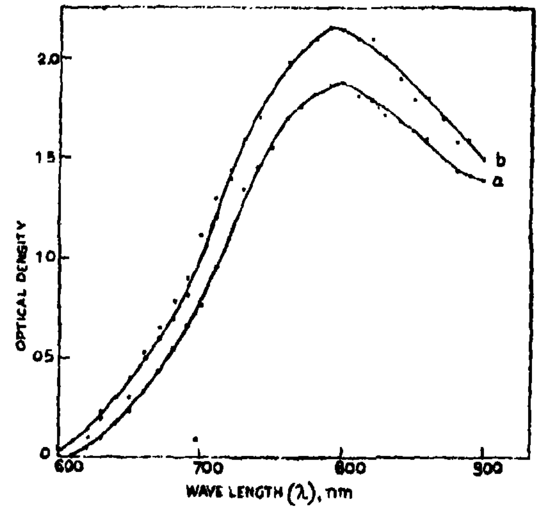


Fig. 1. Visible spectra of (a) [$CuSO_4$] = 0.02 *M* and (b) [$CuSO_4$] = 0.02 *M* + [$KHSO_5$] = 0.0129 *M* or [$CuSO_4$] = 0.02 *M* + [HQ] = 0.02 *M*.

Increase of temperature increases the rate of interaction of Cu^{II} with $KHSO_5$ followed by fast homolysis as shown by the k_{obs} value. From the Arrhenius plot (Fig. 3), the energy of activation (ΔE) and other thermodynamic parameters were

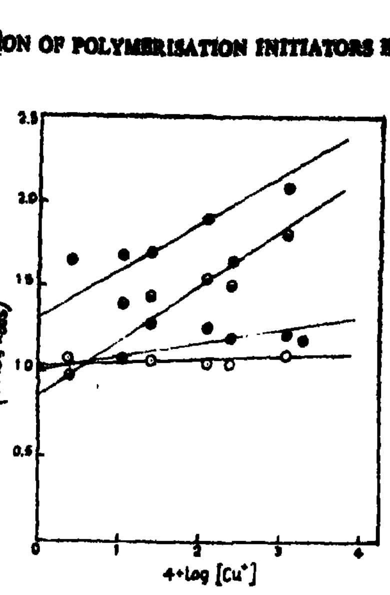


Fig. 2. Plot of log k_{obs} *vs* log [Cu^{II}] at various temperatures in decomposition of $KHSO_5$, catalysed by $CuSO_4$; [$KHSO_5$] = 0.0129 *M* and [Cu^{II}] = 0.25-125 × 10^{-3} *M*: (◎) 25, (●) 30, (⊖) 40 and (⊕) 50°.

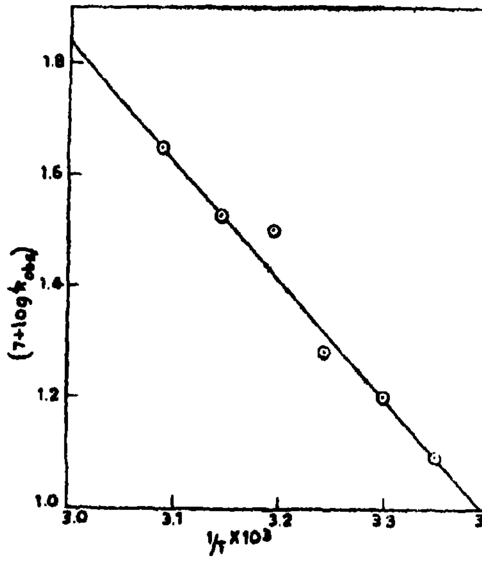


Fig. 3. Arrhenius plot of log k_{obs} *vs* 1/T in decomposition of $KHSO_5$ catalysed by $CuSO_4$; [$KHSO_5$] = 0.0129 *M* and [Cu^{II}] = 25 × 10^{-3} *M*.

computed as ΔE=41.0 kJ mol^{-1}, $\Delta S^{\neq}$=−227.19 J mol^{-1} K^{-1}, $\Delta H^{\neq}$=43.59 kJ mol^{-1}, $\Delta G^{\neq}$=114.68 kJ mol^{-1}, log β=−19.13 and log A = 0.38. The decrease of k_{obs} with increasing [$KHSO_5$] (Fig. 4) may be attributed to (i) formation of stable complex of Cu^{II} with $KHSO_5$ thus resisting subsequent disintegration, (ii) the arrest of Cu^{II} ions by the anions of monopersulphate. The activity of Cu^{II} ion to interact with the orbital of the peroxo-bridge is, therefore, reduced and hence the rate of decomposition of $KHSO_5$ decreases.

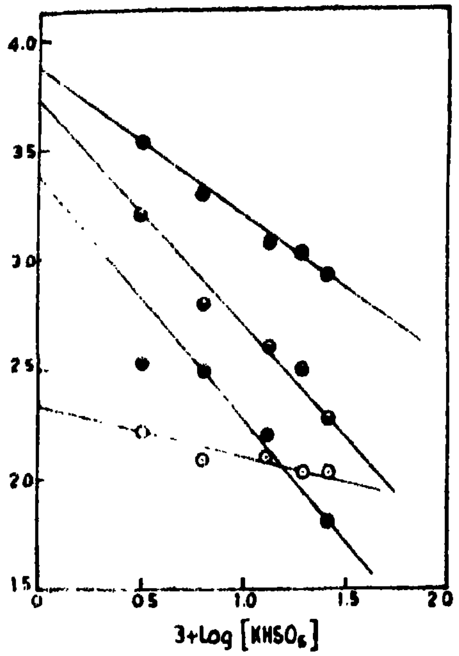


Fig. 4. Plots of log k_{obs} *vs* log $[KHSO_5]$ at various temperatures in decomposition of $KHSO_5$ catalysed by $CuSO_4$; $[CuSO_4] = 125 \times 10^{-4} M$ and $[KHSO_5] = 3.235 - 25.8 \times 10^{-3} M$: (◎) 25, (●) 30, (⊖) 40 and (⊕) 50°.

Catalysis by Cu^{II}/phenolic couples: The effect of some complex forming phenols, like pyrogallol, α-naphthol, salicylaldehyde and hydroquinone ($2 \times 10^{-3} M$) on the first order rate constant (k_{obs}) of $KHSO_5$ ($2.58 \times 10^{-3} M$) decomposition were studied and rate constants were found to be 2.58×10^{-5}, 3.22×10^{-5}, 0.15×10^{-5} and 0.46×10^{-5} and $0.15 \times 10^{-5} s^{-1}$, respectively. Further, the initiator $KHSO_5$ was subjected to the action of the above phenolics in the presence of $CuSO_4$ ($2.5 \times 10^{-3} M$) at 30° and the rate constants were found to be 8.31×10^{-5}, 8.29×10^{-5}, 7.29×10^{-5} and $0.35 \times 10^{-5} s^{-1}$ for the couples Cu^{II}/α-naphthol, Cu^{II}/hydroquinone, Cu^{II}/pyrogallol and Cu^{II}/salicylaldehyde, respectively.

Comparison of the rate data indicates that addition of $CuSO_4$ solution ($2.5 \times 10^{-3} M$) to the reaction mixture containing HQ and $KHSO_5$ enhances the rate of decomposition of $KHSO_5$ by a factor of 18 and the rate is also nearly 40 times higher than that for $CuSO_4$ alone. With salicylaldehyde, pyrogallol and α-naphthol, the addition of $CuSO_4$ does not enhance the rate remarkably. It has, therefore been established that $CuSO_4$/HQ couple is the most efficient in causing decomposition of $KHSO_5$. The catalytic decomposition of $KHSO_5$ by Cu^{II} is almost independent of the nature of anions, even in the presence of hydroquinone. The rate constants (30°) for the decomposition of $KHSO_5$ ($2.58 \times 10^{-3} M$) by various Cu^{II} salts ($2.5 \times 10^{-3} M$)/HQ ($2 \times 10^{-3} M$) couple were found to be 8.59×10^{-5}, 9.04×10^{-5}, 9.24×10^{-5} and $8.76 \times 10^{-5} s^{-1}$ for $CuSO_4$, $CuCl_2$, $Cu(OAc)_2$ and $Cu(NO_3)_2$, respectively.

Effect of hydroquinone concentration (0.5×10^{-3}-$3.0 \times 10^{-3} M$) on the rate (30°) is depicted by the plot of log k_{obs} *vs* log [HQ] in Fig. 5 which is a linear with unit (0.98) slope indicating first order-dependence of the rate on [HQ]. The enhancement of the rate may be due to the increase in the concentration of Cu^{II}/HQ complex, which catalyses $KHSO_5$ decomposition. The effect of $[CuSO_4]$ (0.25×10^{-3}-$75.0 \times 10^{-3} M$) (30°) is exhibited by the plot of log k_{obs} *vs* log $[Cu^{II}]$ in Fig. 5 which is linear with slope of 0.5 indicating half order dependence of the rate on $[CuSO_4]$. The decreasing rate at high $[Cu^{II}]$ (beyond 12.5 *M*) might be attributed to the formation of adduct between Cu^{II} ion and HSO_5^- anion, which is not affected by the Cu^{II}/HQ complex.

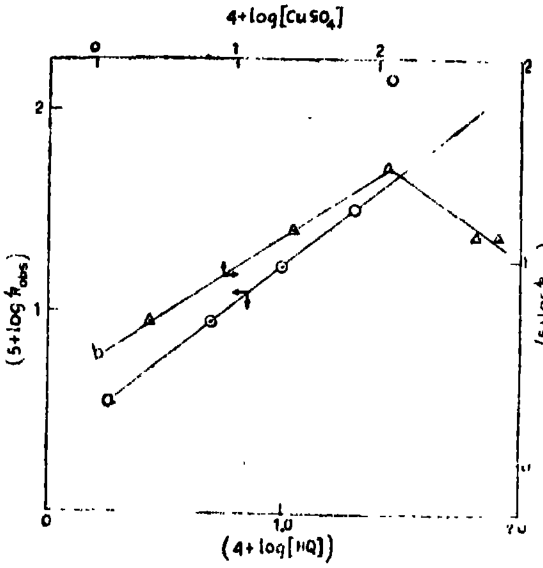


Fig. 5. (a, ◎) Plot of log k_{obs} *vs* log [HQ] at 30°, in decomposition of $KHSO_5$ catalysed by Cu^{II}/HQ; $[Cu^{II}] = 25 \times 10^{-3} M$, $[KHSO_5] = 0.0258 M$ and $[HQ] = 0.5 - 3.0 \times 10^{-3} M$. (b, △) Plot of log k_{obs} *vs* log $[CuSO_4]$ at 30° in decomposition of $KHSO_5$ catalysed Cu^{II}/HQ; $[HQ] = 2.0 \times 10^{-3} M$, $[KHSO_5] = 0.0258 M$, $[CuSO_4] = 0.25 - 75.0 \times 10^{-3} M$.

Effect of $[KHSO_5]$ (0.322×10^{-3}-$2.58 \times 10^{-3} M$) on the rate (30°) is given by Fig. 6 which is a linear plot of log k_{obs} *vs* log $[KHSO_5]$ with slope equal to unity (0.91) for the $KHSO_5$ range (0.322×10^{-3}-$0.645 \times 10^{-3} M$) indicating first order dependence of the rate on $[KHSO_5]$ upto $0.645 \times 10^{-3} M$, beyond which the rate decreases. Further, the rate (k_{obs}) was found to increase (8.06×10^{-5} to $17.37 \times 10^{-5} s^{-1}$) on increasing temperature from 25 to 40° at a given ($[Cu^{II}]$ ($2.5 \times 10^{-3} M$), $[KHSO_5]$) ($2.58 \times 10^{-3} M$) and [HQ] ($2.0 \times 10^{-3} M$). From the Arrhenius plot (Fig. 7), the energy of activation (ΔE) and hence other thermodynamic parameters were

computed as $\Delta E=40.33$ kJ mol^{-1}, $\Delta S^{*}=-196.64$ J mol^{-1} K^{-1}, $\Delta H^{*}=42.92$ kJ mol^{-1}, $\Delta G^{*}=104.5$ kJ mol^{-1}, $\log \beta=-17.44$ and $\log A=2.97$.

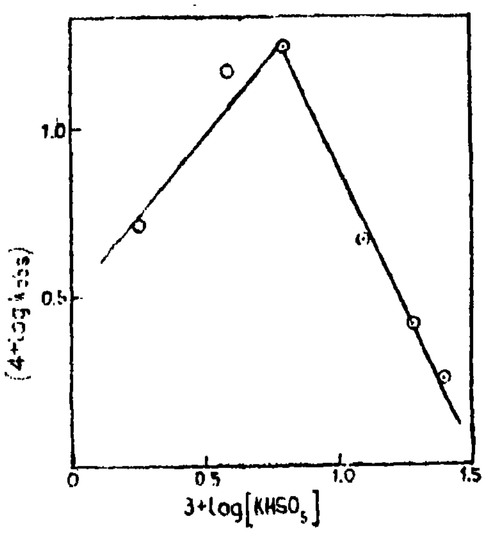


Fig. 6. Plot of log k_{obs} vs log [$KHSO_5$] at 30° in decomposition of $KHSO_5$ catalysed by Cu^{II}/HQ; [$CuSO_4$] = 2.5×10^{-3} M, [HQ] = 2.0×10^{-3} M and [$KHSO_5$] = 0.322 − 2.58 × 10^{-2} M.

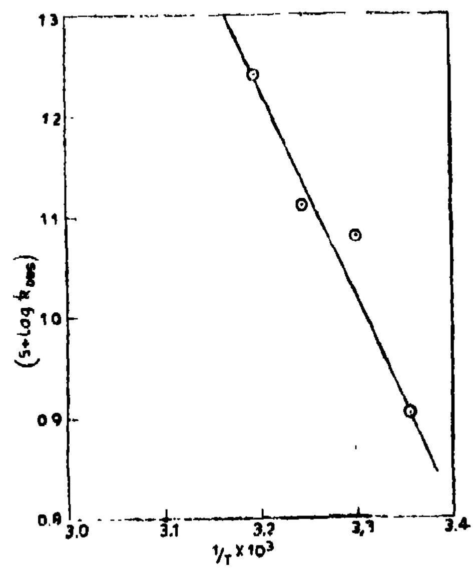


Fig. 7

Fig. 7. Arrhenius plot of log k_{obs} vs 1/T in decomposition of $KHSO_5$ catalysed by $CuSO_4$/HQ; [$CuSO_4$] = 2.5×10^{-3} M, [$KHSO_5$] = 0.0258 M and [HQ] = 2.0×10^{-3} M.

Reaction mechanism :

Catalytic effect of Cu^{II} ions : The decomposition of $KHSO_5$ by Cu^{II} salts can be considered to proceed through the intermediate Cu^{II}-monopersulphate complex (Fig. 1) which subsequently decomposes and produces free radicals in subsequent steps. The order of decomposition reaction of $KHSO_5$ depends upon its concentration and the temperature, and lies between 0.07 to 0.67. At 40° in the range of 0.25×10^{-3} to 200×10^{-3} M of [Cu^{II}], the observed order is 0.33 (Fig. 2). This inhibition with increasing $KHSO_5$ concentration (Fig. 4) indicates increasing salt formation with Cu^{II} ions, thus preventing interaction with Cu D° orbital.

The free radical nature of the reaction is evident from acrylonitrile polymerisation to polyacrylonitrile, with average molecular weight ($\bar{M}_w$), 8.5×10^4.

The following reaction mechanism has been proposed to interpret the above results,

(i) $Cu^{2+}+HSO_5^- \overset{\beta}{\rightleftharpoons} \text{Complex} \overset{k_d}{\longrightarrow}$

$$Cu^{2+}+\dot{O}H+SO_4^{2-} \overset{k_d}{\longrightarrow} Cu^{2+} + O\bar{H} + S\bar{O}_4$$

(ii) $Cu^{2+}+HSO_5^- \overset{\beta}{\rightleftharpoons} \text{Complex} \overset{k_d}{\longrightarrow} Cu^{I}$-complex $+ H^+ + S\bar{O}_5$

$S\bar{O}_5+Cu^{I}$-complex $\longrightarrow S\bar{O}_4 + O_2 + HSO_4^-$

(iii) $S\bar{O}_4 + H_2O \longrightarrow HSO_4^- + \dot{O}H$

(iv) $2\dot{O}H \longrightarrow H_2O + \frac{1}{2}O_2$

(v) $HS\bar{O}_4 + H^+ \longrightarrow H_2SO_4$

The rate of $KHSO_5$ decomposition can be expressed as follows,

$$-\frac{d\,[KHSO_5]}{dt} = k_d\,\beta\,[Cu^{II}]_0^x\,[KHSO_5]_0^y \,, \quad (1)$$

$x : y = 1 : 2 = 0.5 : 1$

$$-\frac{d\,[KHSO_5]}{dt} = k_d\,\beta\,[Cu^{II}]^{0.5}\,[KHSO_5]^{1.0} \quad (2)$$

The rate equation (2) holds good at moderate $CuSO_4$ and $KHSO_5$ concentrations.

Catalysis by Cu^{II}/HQ couple : It is noticed that $CuSO_4$/HQ couple is an efficient catalyst for $KHSO_5$ decomposition, although the maximum activity is concentration dependent and also prone to thermal action. Further, in the three-component reaction, $CuSO_4$/HQ/$KHSO_5$, the rate with respect to the reacting components has been observed to be 0.49, 0.98 and 1.2, respectively. This results can be interpreted by considering an intermediate formation of an unstable complex between $[Cu(H_2O)_6]^{2+}$ species, existing in aqueous solution with HQ and $KHSO_5$ by successive displacement of water molecules. The formation of complex between Cu^{II} and phenols have been identified[22-27].

$$[Cu(H_2O)_6]^{2+}+2HQ \overset{\beta_1}{\rightleftharpoons} [Cu(H_2O)_4\ (HQ)_2]^{2+}$$

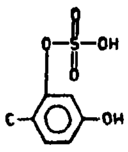
$$[Cu(H_2O)_4\ (HQ)_2]^{2+}+2KHSO_5 \overset{\beta_2}{\rightleftharpoons} [Cu(HQ)_2(KHSO_5)_2(H_2O)_2]_{2+}$$

Complex-I

The addition of further ligand to complex-I is difficult, because of Jahn-Teller effect. The complex then disintegrates into various products where one $KHSO_5$ molecule and HQ on one side of the plane are active to react.

$$\text{Complex-I} \xrightarrow{k_d} \text{Products}$$

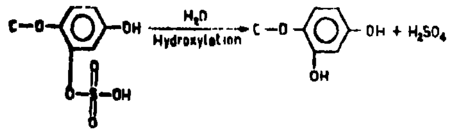
$$\text{Complex-I} \xrightarrow{k_d} SO_4^{\bar{\cdot}}+\dot{O}H+$$



Cu^{I}-complex

$$SO_4^{\bar{\cdot}} + H_2O \longrightarrow HSO_4^- + \dot{O}H$$

$$2\dot{O}H \longrightarrow H_2O + \tfrac{1}{2}O_2$$



All the above processes lead to the following rate expression,

$$-\frac{d\,[KHSO_5]}{dt} = (\beta_1+\beta_2)\ k_d\ [Cu^{II}]^{1/2}\ [KHSO_5]^{1.0}\ [HQ]^{1.0} \qquad (3)$$

According to our observed rate and taking $(\beta_1+\beta_2=\beta)$, equation (1) is changed to

$$-\frac{d\,[KHSO_5]}{dt} = \beta\ k_d\ [Cu^{II}]^{0.49}\ [HQ]^{0.98}\ [KHSO_5]^{1.16} \qquad (4)$$

Equations (3) and (4) are the same, taking into account the experimental and graphical errors.

We can, therefore, conclude that in the reaction of a polymerisation initiator, potassium monopersulphate, with Cu^{II} salts and their phenol complexes especially hydroquinone, the peroxo salt undergoes ready decomposition to free radicals through the intermediate formation of unstable complexes. Similar reactions to free radicals not involving intermediate complex, also holds good in its reaction with phenols. But neither Cu^{II} nor the phenols alone are significantly effective for $KHSO_5$ decomposition. However, Cu^{II}/HQ couple in all molar proportions is quite effective catalyst to cause facile decomposition and the rates of decomposition sharply increase by increasing their molar ratios. Hence, Cu^{II}/HQ is a first catalyst for $KHSO_5$-decomposition to free radicals, that enhances the rate of initiation in vinyl polymerisation leading to polymers of high kinetic chain length. The novelty of the complex catalysed peroxide decomposition leading to high rate of initiation makes a compromise that chemical entities which are long since been recognised as retarders and/or inhibitor[18,19] of radical addition reactions change their characteristics to accelerate such reactions when brought together in solution at appropriate molar ratios.

Acknowledgement

The authors express their indebtedness to Prof. Y. Ikada, Research Centre for Medical Polymers and Biomaterials, Kyoto University, Japan, for his continuous inspiration and fruitful suggestions. One of the authors (R.K.S.) is thankful to C.S.I.R., New Delhi, for financial support.

References

1. E. T. DENISON and N. M. EMANUEL, *Usp. Khim.*, 1960, **29**, 1409.
2. R. HIATT, K. C. IRWIN and C. W. GOULD, *J. Org. Chem.*, 1968, 33, 1430.
3. N. M. EMANUEL, Z. K. MAIZUS and I. P. SKIBIDA, *Angew. Chem.*, 1969, **81**, 91.
4. W. H. RICHARDSON, *J. Org. Chem.*, 1965, **30**, 2804.
5. Y. KAMIYA and K. U. INGOLD, *Can. J. Chem.*, 1964, **42**, 1027.
6. Z. K. MAIZUS, I. P. SKIBIDA and N. M. AMENUEL, *Dokl. Akad. Nauk. SSSR*, 1965, **164**, 374.
7. C. S. SHEPPARD and U. R. KAMATH, *Polym. Eng. Sci.*, 1979, **19**, 597.
8. R. A. SHELDON and J. K. KOCHI, *Oxid. Combust. Rev.*, 1973, **5**, 135.
9. J. BARTON and V. HORANSKA, *Makromol. Chem.*, 1974, **175**, 1861.
10. J. BARTON and V. HORANSKA, *Makromol. Chem.*, 1972, **157**, 87.
11. J. BARTON, V. HORANSKA and I. LEBOC, *Makromol. Chem.*, 1975, **176**, 1743.
12. N. INDICATOR and C. J. SAHANI, *Macromolecules*, 1975, **8**, 935.
13. N. INDICATOR and C. J. SAHANI, *J. Polym. Sci., Polym. Chem. Ed.*, 1978, **16**, 2683, 2997.
14. R. K. SAMAL, R. R. DAS, M. C. NAYAK, G. V. SURYANARAYANA and D. P. DAS, *J. Polym. Sci., Polym. Chem. Ed.*, 1981, **19**, 2751.
15. R. K. SAMAL, M. C. NAYAK and D. P. DAS, *Eur. Polym. J.*, 1981, **18**, 313.
16. R. K. SAMAL, S. C. SATRUSALLYA and B. L. NAYAK, *J. Polym. Sci., Polym. Chem. Ed.*, 1982, **20**, 409.
17. R. K. SAMAL, S. C. SATRUSALLYA and B. L. NAYAK, *J. Macromol. Sci. Chem.*, 1983, **19**, 475.
18. R. J. KENNEDY and A. M. STOCK, *J. Org. Chem.*, 1960, **25**, 1901.

19. C. H. BAMFORD, A. D. JANKINS and R. JOHNSTON, *Proc. R. Soc. London, Ser. A*, 1957, 239, 214.
20. A. P. BHARGAVA, R. SWAROOP and Y. K. GUPTA, *J. Chem. Soc., A*, 1970, 2783.
21. R. SWAROOP and Y. K. GUPTA, *Indian J. Chem.*, 1971, 9, 361.
22. M. KIMURA, *J. Phys. Chem.*, 1973, 77, 1265.
23. L. M. BHARADWAJ, D. N. SHARMA and Y. K. GUPTA, *Inorg. Chem.*, 1978, 17, 246.
24. N. M. EMANUEL, Z. K. MAIZUS and I. P. SKIBIDA, *Angew. Chem*, 1969, 81, 91.
25. M. BOTELSKY, C. HEITNEV and K. R. S. ASCHEL, *Bull. Soc. Chim. Fr.*, 1952, 943.
26. P. V. KAMAT, N. B. LAXMESHWAR and M. G. DATAR, *J. Chem. Soc.*, 1969, 345.
27. S. N. DUBEY and R. C. MEHROTRA, *J. Indian Chem. Soc.*, 1966, 43, 73.
28. M. P. GODSAY, G. A. HARPELL and K. E. RUSSEL, *J. Polym. Sci.*, 1962, 57, 641.
29. W. I. BENGOUH and W. H. FAIR SERVCE, *Proc. R. Soc.*, 1965, 1206.

J. Indian Chem. Soc.,
Vol. LXIII, February 1986, pp. 216-218

Nuclear Magnetic Resonance. Part-I. Dynamic ^1H nmr Spectral Studies on Indole-1-carboxaldehydes

K. M. BISWAS*, R. N. DHARA, (Mrs.) HAIMANTI MALLIK and (Miss) SUMITA ROY

Department of Chemistry, University College of Science, University of Calcutta, 92 A. P. C. Road, Calcutta-700 009

Manuscript received 7 May 1984, revised 27 March 1985, accepted 2 December 1985

3-Ethylindole-1-carboxaldehyde (1) and 3-phenylindole-1-carboxaldehyde (2) are shown to exist in (E) and (Z) conformations by dynamic ^1H nmr spectral studies. The coalescence temperature of the two rotamers of 2 is 23° and that in the case of 1 is 50°. This difference is probably due to the effect of the electron withdrawing phenyl group of the former and the electron donating ethyl group of the latter. The spectrum of the weighted average of the two rotamers of each of 1 and 2 is observed at elevated temperature (90°). The aldehyde proton of the (E) rotamers and H-7 of the (Z) rotamers resonate at higher frequencies than the corresponding protons of the other rotamers because of the deshielding effect of the benzene ring on the former and of the magnetic anisotropy of the carbonyl group on the latter. The barriers to internal rotation about the N—C bond of the (E) and (Z) onfigurations of 1 have been determined and discussed in terms of electronic effect.

ELGUERO *et al.*[1] demonstrated restricted rotation in a number of indole-1-carboxaldehydes and anisotropy effect of their carbonyl group by elegant dynamic ^1H nmr spectral studies. In continuation of our work in this area[2,3], we now report the results of our variable temperature ^1H nmr spectral studies on the indole-1-carboxaldehydes (1, 2 and 3), which were prepared for other purposes[4-6].



(E) (Z)

(1) $R = R^2 = H$, $R^1 = Et$
(2) $R = R^2 = H$, $R^1 = Ph$
(3) $R = R^1 = Ph$, $R^2 = Me$

The ^1H nmr data concerning the (E) and (Z) rotamers of 1 and 2 are described in Tables 1 and 2, and the populations of the two rotamers of 1 and the values of the barriers to their internal rotation in Tables 3 and 4.

At −5°, the aldehyde proton of 1 gave rise to two sharp singlets and H-2 and H-7 of its (Z) rotamer resonated as a sharp singlet and a clean multiplet, respectively, and the signals for these two protons of its (E) conformer probably merged with those of the other aromatic protons. As the temperature was raised, their signals gradually became broad and finally coalesced to a sharp singlet and a clean multiplet as a result of increased rate of rotation about the N—C bond and the observed spectrum was only that of the weighted average of the two conformers. The signal for H-2 of 1 could not be observed in DMSO-d_6 either at 23° or at 90° as it probably merged with those of the other aromatic protons. The methyl protons of 1 also appeared as a double triplet at −5° confirming the existence of two conformers at this temperature. This signal changed to a clean triplet at elevated temperatures.

Each of the signals for the aldehyde proton and H-7 of 2 in $CDCl_3$ appeared as a hump at 23°, presumably due to the fact that its two conformers were in a state of coalescence at this temperature (Table 2). In DMSO-d_6 at 23°, these signals as well as that of H-2 appeared as a hump, a broad singlet and a sharp singlet, respectively. However, at 90° the first two signals changed to a sharp singlet and a clean multiplet for the same reason as mentioned in the case of 1.

The electron donating inductive effect of the ethyl group at position 3 of 1 enhances the double bond character of the N—C bond by increasing electron density on the nitrogen atom. This results in the increase of the barrier to rotation about its N—C bond in comparison to that of 2 whose phenyl group at position 3 cannot increase electron density on the nitrogen atom as effectively as the ethyl group of 1, possibly the phenyl group rather decreases electron density on the nitrogen atom by its electron withdrawing effect[5,6].

The barriers to internal rotation at coalescence temperature of 1 were determined using the equation established by Shanan-Atidi and Bar-Eli[1,7,8],

TABLE 1—^{1}H Nmr SPECTRAL DATA OF 3-ETHYLINDOLE-1-CARBOXALDEHYDE (1) AT VARIABLE TEMPERATURE

Solvent	Temp. °C	Conformer	Chemical shifts (δ), multiplicities and coupling constants (Hz)					
			H-2	H-7	Other Ar-*H*	*CHO*	CH_2	CH_3
$CDCl_3$	-5	Z	7.05,s	8.32-8.43,m	7.2-7.7,m	9.03,s	2.70,q (8)	1.3, 2×t (8)
		E		7.2-7.7,m		9.35,s	2.70,q (8)	1.3, 2×t (8)
$CDCl_3$	23	Z	6.92-7.15,h	8.2-8.5,h	7.23-7.60,m	8.92-9.18,h	2.69,q (8)	1.3,t (8)
		E		7.23-7.60,m		9.22-9.48,h	2.69,q (8)	1.3,t (8)
$CDCl_3$	35	Z	6.85-7.05,h	8.25-8.52,h	7.23-7.60,m	8.85-9.05,h	2.69,q (8)	1.3,t (8)
		E		7.23-7.60,m		9.10-9.35,h	2.69,q (8)	1.3,t (8)
$CDCl_3$	50	Coalesced form	7.20-7.60,m	8.10-8.47,h	7.20-7.60,m	9.00-9.33,h	2.69,q (8)	1.3,t (8)
DMSO-d_6	23	Z	7.3-7.7,m	8.2-8.5,h	7.3-7.7,m	9.20-9.35,h	2.69,q (8)	1.3,t (8)
		E		7.3-7.7,m		9.5-9.7,h	2.69,q (8)	1.3,t (8)
DMSO-d_6	90	Coalesced form	7.3-7.7,m	8.18-8.29,m	7.3-7.7,m	9.40,s	2.69,q (8)	1.3,t (8)

TABLE 2—^{1}H Nmr SPECTRAL DATA OF 3-PHENYLINDOLE-1-CARBOXALDEHYDE (2) AT VARIABLE TEMPERATURE

Solvent	Temp. °C	Chemical shifts (δ) and multiplicities			
		H-2	H-7	Other Ar-*H*	*CHO*
$CDCl_3$	23	7.2-7.7,m	8.2-8.55,h	7.20-7.70,m	9.00-9.43,h
DMSO-d_6	23	8.15,s	8.40,bs	7.40-8.00,m	9.45-9.8,h
DMSO-d_6	90	8.15,s	8.35-8.48,m	7.55-8.05,m	9.60,s

TABLE 3—POPULATION OF CONFORMERS (Z AND E) OF 1 AT VARIABLE TEMPERATURE IN DIFFERENT SOLVENTS

Solvent	Temp. °C	Conformer	Percentage
$CDCl_3$	-5	Z	55
		E	45
$CDCl_3$	23	Z	64
		E	36
$CDCl_3$	35	Z	72
		E	28
DMSO-d_6	23	Z	70
		E	30
DMSO-d_6	90	Coalesced form	100

as the rotamers (E) and (Z) of 1 were not equally populated. However, the calculations were based on the values of X corresponding to ΔP published recently[9], which are reported to provide more accurate results[9] than the graphic procedure of the former workers. The higher barrier to internal rotation for 1 compared to those of indole-1-carboxaldehyde[1] (*viz.* 61.5 and 63.1 kJ mol^{-1}) can also be explained in terms of electronic effect (*vide supra*), and this is supported by the fact that the values of the barrier to internal rotation of 1 compare favourably with those of 3-methylindole-1-carboxaldehyde[1] (*viz.* 68.1 and 70.0 kJ mol^{-1}). The rate constants k_A and k_B were calculated using the equation of Shanan-Atidi and Bar-Eli[7] but the values of X corresponding to Δp[9] were used. The values of k tally well with those of *p*-methoxy-*N*,*N*-dimethylthiobenzamide[10].

The spectrum of 5-methyl-2,3-diphenylindole-1-carboxaldehyde (3) did not show any change on rerecording[8] at lower temperature (23°, DMSO-d_6) or at higher temperature (90°, DMSO-d_6), probably

TABLE 4—BARRIERS TO INTERNAL ROTATION IN 3-ETHYLINDOLE-1-CARBOXALDEHYDE (1)

Solvent	Rotamer (E) population %	Signal observed	T_c K	$\Delta\nu$ Hz	τ	k_A s^{-1}	k_B s^{-1}	ΔG_c^* kJ mol^{-1}
$CDCl_3$	45	CHO	323	28.8	9.446 ×10^{-3}	48	58	E→Z 68.3±0.5 Z→E 68.9±0.5

because the coalescence temperature of its two rotamers lies below 23°.

Experimental

Nmr spectra were recorded on a Perkin-Elmer R-32 spectrometer equipped with a variable temperature controller. The temperature could be measured accurately to ±0.5°. The chemical shifts are given in ppm relative either to TMS or DSS as internal reference; coupling constants are given in Hz, and the $\triangle Gc^{*}$ values in kJ mol^{-1}. The preparation of the compounds (1-3) has been recorded elsewhere[a].

Acknowledgement

The authors like to thank Professor A. H. Jackson, University College, Cardiff, U.K., for recording the spectrum of 1 (at −5 and 50°) and Professor A. Chatterjee of this Department, for her interest in the work.

References

1. J. Elguero, C. Marzin and M. E. Peek, *Org. Magn. Reson.*, 1975, **6**, 445.
2. K. M. Biswas and A. Chatterjee, *J. Org. Chem.*, 1973, **38**, 4002.
3. K. M. Biswas and R. N. Dhara, *Indian J. Chem., Sect. B*, 1982, **21**, 632.
4. K. M. Biswas and H. Mallik, *Indian J. Chem., Sect. B*, 1983, **22**, 927.
5. K. M. Biswas, R. N. Dhara, H. Mallik and S. Roy, *Tetrahedron*, 1984, **40**, 4351.
6. W. A. Remers and R. K. Brown in "The Chemistry of Heterocyclic Compounds", ed. W. J. Houlihan, Wiley-Interscience, New York, 1972, Vol. 25, Part I, p. 116.
7. H. Shanan-Atidi and K. H. Bar-Eli, *J. Phys. Chem.*, 1970, **74**, 961.
8. H. S. Gutowsky, "Dynamic Nuclear Magnetic Resonance Spectroscopy", eds. L. M. Jackman and F. A. Cotton, Academic Press, New York, 1975.
9. J. Sandström, "Dynamic NMR Spectroscopy", Academic Press, New York, 1982, pp. 81-2.
10. Reference 9, p. 155.

J. Indian Chem. Soc.,
Vol. LXIII, February 1986, pp. 219-220

Pyridine Sulphenyl Halides. Part I

Y. D. KULKARNI* and R. V. SINGH

Department of Chemistry, Lucknow University, Lucknow-226 007

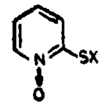
Manuscript received 12 February 1982, accepted 2 December 1985

N-Oxide-2-pyridine sulphenyl bromide has been found to be more stable as compared to known ones. It undergoes nucleophilic reaction with amines yielding sulphenamides. Several compounds possessing high antimicrobial activity were obtained in the course of these synthesis.

IN our studies to develop newer blocking agents in peptide synthesis, the use of pyridine sulphenyl halides as α-amino blocking agent was considered. So far pyridine sulphenyl halides have been little studied[1], apart from tetrafluoro-4-pyridine sulphenyl chloride[2], tetrachloro-4-pyridine sulphenyl chloride[3], tetrachloro-2-pyridine sulphenyl chloride[4] and 5-nitro-2-pyridine sulphenyl chloride[5]. However, these sulphenyl chlorides were so unstable that they existed only in anhydrous conditions and quickly decomposed in open air to their respective disulphides.

Matsueda and Aiba[6] have reported the synthesis of 3-nitro-2-pyridine sulphenyl chloride and found it sufficiently stable to be preserved for long periods at 0°. The stability of 3-nitro-2-pyridine sulphenyl chloride could be attributed to the neighbouring nitro group *ortho* to sulphenyl chloride which produced strong resonance stabilisation to the molecule owing to the decrease in the basic character of nitrogen atom of the pyridine ring and also due to a specific non-bonding attractive interaction between sulphur and oxygen atom. It was, therefore, considered worthwhile to synthesise *N*-oxide-2-pyridine sulphenyl halides, which possess both of these structural features, *viz*. decrease in the basic character of the nitrogen atom of the pyridine ring due to *N*-oxide group and also a non-bonding attractive interaction between the neighbouring oxygen and sulphur atoms. In actual practice, these considerations were found to be sufficiently valid and *N*-oxide-2-pyridine sulphenyl bromide, prepared by the action of bromine on *N*-oxide-2-pyridine disulphide (1) was found to be fairly stable. It could be stored in a desiccator for several days without any decomposition.

N-Oxide-2 pyridine sulphenyl bromide reacted with amines to give sulphenamides (Table 1) in high yields. Compounds 1, 3 and 4 were selected and screened[7] against different strains of bacterial and fungal infections, of which *N*-oxide-2-pyridine disulphide (1) was found to be most active (Table 2).



2 : X = Br
3-13 : X = Amine

Experimental

All melting points are uncorrected. Ir spectra (KBr) were recorded on a Perkin-Elmer 157 spectrophotometer. Nmr spectra were run on a Varian A 0D instrument using TMS as the internal reference (chemical shift in τ scale). Uv spectra (MeOH) were recorded on a Perkin-Elmer 202 spectrophotometer. Mass spectra were recorded on JMS D300 JEOL instrument.

N-Oxide-2-chloropyridine, *N*-oxide-2-pyridinethiol and *N*-oxide-2-pyridine disulphide (1) were prepared according to the known procedures[8,9].

N-*Oxide-2-pyridine sulphenyl bromide* (2) : Bromine (0.48 g, 0.003 mol) was carefully added to a mechanically stirred solution of *N*-oxide-2-pyridine disulphide (1 ; 0.252 g, 0.001 mol) in dry dichloromethane (5 ml) at 0° and stirred for 1 h. The resultant solid (2) was filtered, washed with CH_2Cl_2 (to remove traces of disulphide) and dried *in vacuo*, yield quantitative, m.p. 125-6° (Found S, 11.08 ; Br, 55.0. $C_5H_4Br_3NOS$ requires : S, 11.17 ; Br, 55.8%). It was found to be stable for long periods in anhydrous conditions but was slowly reconverted into disulphide (1) when exposed to air, in contact with water and also in hydroxylic solvents.

N-*Oxide-2-pyridine sulphenamides* (3-13) : *N*-Oxide-2-pyridine sulphenyl bromide (2 ; 0.001 mol) was added in small portions to a srirred solution of an amine (0.001 mol) and triethylamine (0.003 mol) in dichloromethane (10 ml) at 10-20°. The compounds (Table 1) were recrystallised from

TABLE 1—*N*-OXIDE-2-PYRIDINE SULPHENAMIDES

Compd. no.	X	M. p. °C	Solvent of recrystallisation*	Molecular formula	Analysis % : Found/(Calcd.) C	H	N	S
3	piperidino	95	a	$C_{10}H_{14}N_2OS$	56.93 (57.14)	6.32 (6.66)	13.10 (13.33)	14.98 (15.23)
4	morpolino	136	a	$C_9H_{12}N_2O_2S$	50.73 (50.94)	5.42 (5.66)	13.02 (13.20)	14.90 (15.09)
5	pyrrolidino	134	a	$C_9H_{12}N_2OS$	55.01 (55.10)	5.87 (6.12)	14.06 (14.28)	16.15 (16.32)
6**	diethylamino	163d	a	$C_{10}H_{17}IN_2OS$	35.11 (35.29)	4.81 (5.00)	8.02 (8.23)	9.21 (9.41)
7**	*N*-methylpiperizino	200d	a	$C_{12}H_{21}I_2N_3OS$	28.06 (28.29)	3.98 (4.12)	8.02 (8.25)	5.98 (6.28)
8**	*N*-phenylpiperazino	138d	a	$C_{17}H_{23}I_2N_3OS$	35.41 (35.72)	3.97 (4.02)	7.10 (7.35)	5.37 (5.60)
9	4′-carbethoxyanilino	179	a	$C_{14}H_{14}N_2O_3S$	57.70 (57.92)	4.63 (4.82)	9.33 (9.65)	10.91 (11.03)
10	4′-nitroanilino	189	b	$C_{11}H_9N_3O_3S$	50.01 (50.19)	3.20 (3.42)	15.83 (15.96)	11.95 (12.16)
11	4′-bromoanilino	180	b	$C_{11}H_9BrN_2OS$	44.14 (44.44)	2.87 (3.03)	9.13 (9.42)	10.51 (10.77)
12	4′-chloroanilino	184	b	$C_{11}H_9ClN_2OS$	52.11 (52.27)	3.24 (3.56)	10.87 (11.08)	12.51 (12.67)
13	2′,4′-dichloroanilino	178	b	$C_{11}H_8Cl_2N_2OS$	45.76 (45.99)	2.58 (2.78)	9.39 (9.75)	11.01 (11.14)

*aBenzene-petroleum ether, bdichloromethane. **Separated as methiodide salts.

TABLE 2—ANTIMICROBIAL SCREENING

Sl. no.	Infections	MIC* (μg ml⁻¹) 1	3	4
	Bacterial			
1.	*Streptococcus faecalis*	12.5	50.0	50.0
2.	*Klebsiella pneumonae*	12.5	25.0	25.0
3.	*Escherichia coli*	12.5	25.0	25.0
4.	*Pseudomonas aeruginosa*	25.0	12.5	12.5
5.	*Streptococcus aureus*	12.5	12.5	12.5
	Fungal			
1.	*Candida albicans*	12.5	nil**	nil
2.	*Cryptococcus neoformans*	12.5	nil**	nil
3.	*Sporotrichum schenelii*	12.5	25.0	25.0
4.	*Trichophyton mentagrophks*	12.5	25.0	50.0
5.	*Aspergillus fumigatus*	50.0	50.0	50 0

*Minimum inhibitory concentration (MIC) was expressed in terms of micrograms per millilitre at which growth of the test organism was completely inhibited.

**Found to be inactive at test concentration (50 μg ml⁻¹).

appropriate solvent in yields 50-70%. Compound 6-8 were isolated in the form of their methiodides.

N-*Oxide-2-pyridine sulphenyl piperidine* (3) : It showed strong ir bands at 2 950 (methylene), 1 600 (aromatic) and 1 220 cm⁻¹ (N→O). Uv (MeOH) absorption at λ_{max} 242 nm (ϵ_{max} 20 000) and 320 nm (2 600) confirmed the presence of pyridine ring. Piperidino protons in pmr spectra were observed at τ 8.42 (6H, m) and 7.01 (4H, m) and pyridine protons were found at τ 2.61 (2H), 2.36 (1H) and 1.89 (1H). In its mass spectrum M^+ was observed at *m/e* 210 (mol. formula $C_{10}H_{14}N_2OS$) and base peak at *m/e* 84 (*M*-126) for piperidine nucleus, lent further support for its structure.

N-*Oxide-2-pyridine-sulphenyl morpholine* (4) : It showed strong ir bands at 2 950, 1 600 and 1 225 cm⁻¹. In its mass spectrum M^+ was observed at *m/e* 212 and the base peak at *m/e* 86 (*M*-126) for morpholine.

Acknowledgement

The authors wish to thank Professor V.S. Misra, for the departmental facilities and Dr. R. S. Kapil of C.D.R.I., Lucknow, for his keen interest.

References

1. H. L. YALE in "Pyridine and its Derivatives", ed. E. KLINGSBERG, Interscience, New York. 1964, Part IV, Ch. 15.
2. R. E. BANKS, R. N. HASZELCHINE, D. R. KARSA, F. E. RICKETT and I. M. YOUNG, *J. Chem. Soc.* (*C*), 1969, 1660.
3. E. AGER, B. IDDON and H. SUSCHITZKY, *J. Chem Soc.* (*C*), 1970, 1530.
4. B. IDDON, H. SUSCHITZKY, A. W. THOMPSON and E. AGER, *J. Chem. Soc., Perkin Trans.* 1, 1974, 2300.
5. H. FOX, B. FROHNAU and P. DIEDRICH, U. S. Pat. 2 476 655/1949.
6. R. MATSUEDA and K. AIBA, *Chem. Lett.* (*Jpn.*), 1978, 951.
7. M. L. DHAR, M. M. DHAR, B. N. DHAWAN, B. N. MEHROTRA and C. ROY, *Indian J. Exptl. Biol.*, 1968, 6, 232.
8. E. SHAW, J. BENSTEIN, K. LOOSE and W. A. LOTT, *J. Am. Chem. Soc.*, 1950, 72, 4362.
9. J. BENSTEIN and K. A. LOOSE, Ger. Pat., 1224744/1966 (*Chem. Abstr.*, 1967, 66, 10853).

J. Indian Chem. Soc.,
Vol. LXIII, February 1986, pp. 221-222

Synthesis and Biological Activity of some Pyrido-2-carboxamido-pyrazoline and -isoxazoline Derivatives

N. K. MANDAL, R. SINHA and K. P. BANERJEE*

P. G. Department of Chemistry, Bhagalpur University, Bhagalpur-812 007

Manuscript received 1 July 1985, accepted 2 December 1985

2-Acetoacetamidopyridine on condensation with aromatic aldehydes yielded the corresponding pyrido-2-carboxamido-α,β-unsaturated ketones which on heating with hydrazine hydrate/phenylhydrazine and hydroxylamine hydrochloride gave the corresponding pyrido-2-carboxamido pyrazoline and isoxazoline derivatives. The biological activity of some representative compounds were tested.

ACETAMIDO derivatives, in general, have been found to possess fungicidal[1], herbicidal[2] and schistosomicidal activities. Substituted amides in which amido-H has been substituted with heterocyclic moiety[3], have been claimed as potential local anaesthetics. A perusal of the above finding reveals that a heterocyclo-carboxamido group may be of significant importance, the presence of which makes a compound biologically active. Again, pyrazoline/isoxazoline derivatives[4-7] have also been claimed as potential biologically active compounds. Hence, it was thought that a heterocyclo-carboxamido group, if introduced to pyrazoline/isoxazoline moiety, the resulting compound may have considerable potency. Considering all these factors it was thought worthwhile to synthesise a few pyrido-2-carboxamido pyrazoline/isoxazoline derivatives (Scheme 1) and test their biological action.

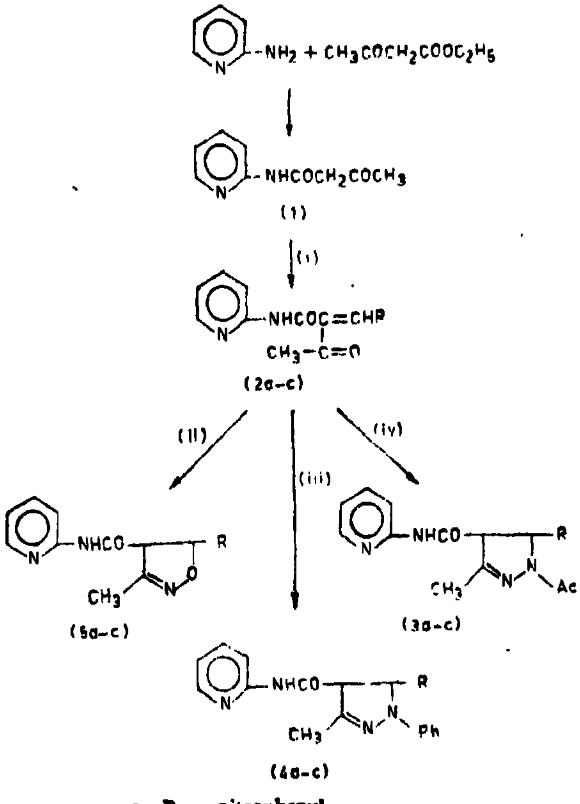
Experimental

All melting points are uncorrected ir spectra (KBr) were recorded on a Beckmann IR-20 spectrophotometer.

2-Acetoacetamido pyridine[8] (1): A mixture of 2-aminopyridine (0.01 mol) and ethylacetoacetate (0.01 mol) was heated at 155° for 1.5 h. On cooling, the colourless crystals of 1 were separated. It was filtered off and then recrystallised from ethanol, (25%), m.p. 112°.

3-(Pyrido-2-carboxamido)-4-aryl-but-3-en-2-one (2): A mixture of 1 (0.01 mol) and an aromatic aldehyde (0.01 mol) was fused for 10 min and the resulting mass was cooled and crystallised from ethanol to yield 2. The results are incorporated in Table 1.

N-*Acetyl-3-methyl-4-(pyrido-2-carboxamido)-5-arylpyrazoline* (3): A mixture of 2 (0.005 mol), hydrazine hydrate (0.035 mol), ethanol (50 ml) and glacial acetic acid (10 ml) was refluxed for 9 h.



a ; R = *p*-nitrophenyl
b ; R = *m*-nitrophenyl
c ; R = 4-methoxy-3-hydroxyphenyl

Scheme 1. *Reagents*: (i) R.CHO ; (ii) $NH_2OH.HCl$; (iii) $Ph.NH_2NH_2$; (iv) $NH_2NH_2.H_2O$, AcOH.

The resulting solution was concentrated, cooled and poured over ice-water when a yellow product was separated which was filtered off and then crystallised from ethanol to yield 3. The results are incorporated in Table 1.

N-Phenyl-3-methyl-4-(pyrido-2-carboxamido)-5-arylpyrazoline (**4**) : A mixture of **2** (0.005 mol), phenyl hydrazine (0.005 mol), ethanol (50 ml) and piperidine (1 ml) was refluxed for 10 h. The resulting mixture was concentrated, cooled and then poured into acidified ice-cold water when coloured compounds were separated which were filtered off and crystallised from ethanol to yield **4**. The results are incorporated in Table 1.

3-Methyl-4-(pyrido-2-carboxamido)-5-aryl-isoxazoline (**5**) : A mixture of **2** (0.005 mol), hydroxylamine hydrochloride (0.005 mol), ethanol (50 ml) and KOH (0.005 mol) was refluxed for 12 h. The resulting mixture was concentrated, cooled and poured into ice-water. The yellow compound obtained was filtered off and crystallised from ethanol to yield **5**. The results are incorporated in Table 1.

TABLE 1

Compd. no.	R	M.p.	Colour	Yield %
2a	p-NO_2-C_6H_4	233	White	68
2b	m-NO_2-C_6H_4	216	White	61
2c	4-OCH_3-3-OH-C_6H_3	142d	White	57
3a	p-NO_2-C_6H_4	184	Yellow	62
3b	m-NO_2-C_6H_4	178	Yellow	89
3c	4-OCH_3-3-OH-C_6H_3	132d	Yellow	59
4a	p-NO_2-C_6H_4	157d	Yellow	71
4b	m-NO_2-C_6H_4	145	Yellow	52
4c	4-OCH_3-3-OH-C_6H_3	195	Yellow	64
5a	p-NO_2-C_6H_4	165	Yellow	58
5b	m-NO_2-C_6H_4	238	Yellow	72
5c	4-OCH_3-3-OH-C_6H_3	260	Yellow	45

Biological screening : Biological screening of some pyrazoline/isoxazoline derivatives was made[9] and the results are incorporated in Table 2.

TABLE 2—BIOLOGICAL SCREENING DATA*

Compd. no.	*B. Subtalis*	*E. coli*	*Xanthromonus citrii*	*B. pumilis*
3a	+	–	–	+
3b	–	+	–	–
4a	+	–	–	+
4c	–	+	–	–
5a	–	–	–	+
5b	–	+	–	–
Tetracycline	+ + +	+ + + + +	+ + +	+ + +

*Zone size . + ≅ 6-12 mm, + + ≅ 12-18 mm, + + + ≅ 18-24 mm, + + + + ≅ 24-30 mm, + + + + + ≅ > 30 mm. – ≅ No inhibition.

Results and Discussion

Pyrido-2-carboxamido-α,β-unsaturated ketones (**2**), prepared by the condensation of 2-acetoacetamidopyridine with aromatic aldehydes showed absorption bands at 1 700 (conjugated C=O), 1 620 (C=C), and 3 400 cm^{-1} (NH). These derivatives of unsaturated ketones (**2**), when heated with hydrazine hydrate and phenyl hydrazine, the corresponding pyridocarboxamidopyrazolines (**3**) and (**4**) respectively were obtained, obviously *via* the initial formation of hydrazone and phenylhydrazone derivatives which cyclised under the experimental conditions. The formation of these pyrazolines was confirmed by their positive Knorr's colour test[10], a characteristic test for arylpyrazolines. The structures of **3** and **4** were fully corroborated by ir spectral results which showed absorption at 1 685 (C=O), 1 635 (C=N), 1 225 (C–N) and 3 420 cm^{-1} (NH). Similarly, **2** on heating with hydroxylamine hydrochloride yielded the corresponding pyrido-2-carboxamido-isoxazoline (**5**) which showed ir bands at 1 660 (C=O), 1 605 (C=N) and 3 420 cm^{-1}(NH).

The biological activity of some representative compounds was initially tested and it was found that all the compounds exhibit some antibacterial activity against one or the other bacteria but none of the compounds was found to possess any significant biological activity.

Acknowledgement

The authors wish to thank Prof. K. D. Banerji, Head of the Department of Chemistry, Bhagalpur University, for providing facilities. The authors are also thankful to Dr. Y. D. Kulkarni of Lucknow University, for the screening results.

References

1. W. BRANDES, W. DAUM and P. KRAUS, *Chem. Abstr.*, 1978, **88**, 120822.
2. G. O'DOHERTY, U. S. Pat. 7 524 517/1975.
3. F. A. FRENCH and B. L. FREEDLONDER, *Concen. Res.*, 1958, 1920.
4. K. SEMPUKU, *Chem. Abstr.*, 1982, **97**, 110251.
5. Z. BRZOZOWSKI and E. POMARNACKA, *Chem. Abstr.*, 1981, **95**, 80807.
6. R. JAIN, R. N. GOYAL, S. TYAGI and S. AGARWAL, *Chem. Abstr.*, 1981, **95**, 80805.
7. MASUMI ITO and AKIRA SUGIWARA, *Chem. Abstr.*, 1967, **67**, 3015.
8. A. S. TOMCUFCIK and L. N. STARKER in "Pyridine and its Derivatives", ed. E. KLINGSBERG, Interscience, New York, 1962, Part III, p. 20.
9. R. S. VARMA and W. L. NOBLES, *J. Pharm. Sci.*, 1968, **57**, 1301.
10. V. KNORR, *Ann.*, 1887, **231**, 200.

J. Indian Chem. Soc.,
Vol. LXIII, February 1986, pp. 223-225

Synthesis and Physiological Activity of Thiazolidinyl-benzoxazines

C. SUDHAKAR, V. SURYACHANDER and K. RAJAMOHAN*

Department of Chemistry, Nizam College, Hyderabad-500 001

Manuscript received 29 October 1984, revised 26 April 1985, accepted 2 December 1985

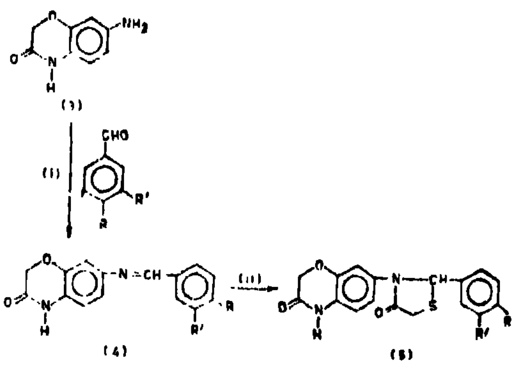
Some 7-(2-aryl-4-oxo-3-thiazolidinyl)-3,4-dihydro-2*H*-1,4-benzoxazine-3-ones (5) were prepared by addition, condensation of mercaptoacetic acid to arylidene-3,4-dihydro-2*H*-1,4-benzoxazine-3-one (4). Compounds 4 and 5 were compared with Dithane M-45 for their antifungal activity against *Heliminthosporium oryzae* and *Cephalosporium sacchari*, and correlated with structural features.

THIAZOLIDINONES were found to exhibit wide spectrum pharmacological activities. Thiazolidinones possess antitubercular, anaesthetic, antifungal and hypnotic activity[1-4]. Some of the 2*H*-1,4-benzoxazines have attracted attention as antispasmodics[5]. These reports prompted us to synthesise the title compounds as potential antifungal agents.

7-Nitro-3,4-dihydro-2*H*-1,4-benzoxazine-3-one (2), a key intermediate compound, was prepared[6] by nitration of 3,4-dihydro-2*H*-1,4-benzoxazine-3-one (1) and its corresponding 7-amino compound following the reported procedure[7].

7-Amino-3,4-dihydro-2*H*-1,4-benzoxazine-3-one (3) on condensation with substituted aromatic aldehydes resulted in Schiff bases (4). 7-Arylidene-3,4-dihydro-2*H*-1,4-benzoxazine-3-ones (4) on cyclocondensation with mercaptoacetic acid in dry benzene yielded 7-(2-aryl-4-oxo-3-thiazolidinyl)-3,4-dihydro-2*H*-1,4-benzoxazine-3-ones (5) (Scheme 1). The products 4 and 5 have been characterised by analytical and spectral (ir, pmr) data. A signal at δ 8.35 in pmr spectrum was characteristic of azomethine (4) proton and a sharp band at 1 625 cm^{-1} in ir spectrum was characteristic of C=N stretching. I.r. spectrum of 5 showed absorptions at 1 645 (lactam C=O) and 1 690 cm^{-1} (tertiary amide C=O).

Melting points were determined in open capillaries. Ir spectra (KBr) were taken on a Perkin-Elmer 237 spectrophotometer, and pmr spectra on a Varian EM-390 instrument using TMS as internal standard.



a ; R = H, R' = H
b ; R = CH_3, R' = H
c ; R = Cl, R' = H
d ; R = NO_2, R' = H
e ; R = OCH_3, R' = H
f ; R = Cl, R' = Cl
g ; R = OCH_3, R' = OH

Scheme 1. *Reagents* : (i) EtOH, 2 drops piperidine ; (ii) HS-CH_2COOH/dry C_6H_6.

Experimental

Arylidene-3,4-dihydro-2H-1,4-benzoxazine-3-one (4) : A mixture of 7-amino-3,4-dihydro-2*H*-1,4-benzoxazine-3-one (3) (1.65 g, 0.01 mol) and aryl aldehyde (1 g, 0.01 mol) was refluxed in 96% ethanol (16 ml) for 4 h in the presence of two drops of piperidine. The contents were concentrated and cooled to give Schiff bases (4) in 90% yield and recrystallised from 96% ethanol ; **4a** ν_{max} 1 680 (C=O), 1 625 (C=N) and 3 200 (NH) cm^{-1} ; δ($CDCl_3$) 4.54 (2H, s, CH_2), 7.41 (1H, d, *J* 7Hz, C_5-H), 7.74 (2H, m, C_6-C_8-H) and 8.34 (1H, s, azomethine proton).

7-(2-Aryl-4-oxo-3-thiazolidinyl)-3,4-dihydro-2H-1,4-benzoxazine-3-ones (5) : Mercaptoacetic acid (0.015 mol) was added to a well stirred solution of Schiff bases (4) (0.01 mol) in dry benzene and refluxed for 20 h using Dean and Stark trap. Solvent was removed by vacuum distillation and the residue treated with 1% $NaHCO_3$ solution, extracted with ether, dried with Na_2SO_4 and ether distilled off to give thiazolidinones (5) in 80% yield and recrystal-

TABLE 1—PHYSICAL DATA OF SCHIFF BASES AND THIAZOLIDINYLBENZOXAZINES*

Compd. no.	R	R′	M.p. °C	Yield %	Mol. formula	Analysis % : Found/(Calcd.) C	H	N
4a	H	H	176	90	$C_{15}H_{12}N_2O_2$	70.96 (71.42)	4.39 (4.76)	10.88 (11.10)
b	CH_3	H	196	75	$C_{16}H_{14}N_2O_2$	72.33 (72.18)	5.07 (5.26)	10.48 (10.52)
c	Cl	H	179	75	$C_{15}H_{11}ClN_2O_2$	62.69 (62.82)	3.84 (3.83)	9.80 (9.77)
d	NO_2	H	209	80	$C_{15}H_{14}N_3O_4$	60.12 (60.60)	3.52 (3.70)	14.16 (14.14)
e	OCH_3	H	260	80	$C_{16}H_{14}N_2O_3$	68.49 (68.08)	4.44 (4.96)	9.93 (9.92)
f	Cl	Cl	222	65	$C_{15}H_{10}Cl_2N_2O_2$	54.80 (56.07)	3.19 (3.11)	8.74 (8.72)
g	OCH_3	OH	168	60	$C_{16}H_{14}N_2O_4$	64.91 (64.42)	4.41 (4.69)	9.33 (9.30)
5a	H	H	142	85	$C_{17}H_{14}N_2SO_3$	62.05 (62.57)	4.03 (4.29)	8.54 (8.58)
b	CH_3	H	270	55	$C_{18}H_{16}N_2SO_3$	63.64 (63.52)	4.36 (4.70)	8.20 (8.23)
c	Cl	H	265	60	$C_{17}H_{13}ClN_2SO_3$	56.92 (56.58)	3.32 (3.60)	7.76 (7.76)
d	NO_2	H	273	45	$C_{17}H_{13}N_3SO_5$	54.17 (54.98)	3.49 (3.50)	11.26 (11.32)
e	OCH_3	H	205	48	$C_{18}H_{16}N_2SO_4$	59.66 (60.67)	4.40 (4.49)	7.81 (7.86)
f	Cl	Cl	234	65	$C_{17}H_{12}Cl_2N_2SO_3$	51.59 (51.64)	2.96 (3.03)	7.04 (7.08)
g	OCH_3	OH	282	50	$C_{18}H_{16}N_2SO_3$	63.66 (63.52)	4.91 (4.70)	8.20 (8.23)

*All compounds crystallised from ethanol.

TABLE 2—ANTIFUNGAL SCREENING DATA OF COMPOUNDS 4 AND 5

Average percent inhibition after 96 h.

Compd. no.	R	R′	*C. oryzae* 1 000 ppm	100 ppm	10 ppm	*C. sacchari* 1 000 ppm	100 ppm	10 ppm
4a	H	H	48	29	16	51	26	14
b	CH_3	H	36	27	12	45	19	9
c	NO_2	H	39	21	10	36	17	8
d	Cl	H	58	31	20	70	38	30
e	OCH_3	H	64	37	26	65	31	19
f	OCH_3	OH	67	37	22	64	29	17
g	Cl	Cl	71	33	28	75	40	30
5a	H	H	42	20	8	53	34	17
b	CH_3	H	35	18	6	33	19	8
c	NO_2	H	43	26	11	40	23	13
d	Cl	H	60	33	19	55	29	20
e	OCH_3	H	58	28	14	58	39	17
f	OCH_3	OH	61	32	15	60	37	22
g	Cl	Cl	66	31	16	63	40	28
Dithane M-45			100	89	72	100	90	74

lised from 96% ethanol; 5a ν_{max} 3 230 (NH), 1 645 (lactam C=O) and 1 965 cm^{-1} (tertiary amide C=O); δ (DMSO-d_6) 8.63 (1H, s, tertiary proton), 10.75 (1H, bs, NH), 7.5-7.9 (8H, m, Ar-H) and 4.45-4.59 (4H, d, J 12Hz, oxazine and thiazolidinone methylene protons).

The physical data of compounds 4 and 5 are given in Table 1.

Antifungal screening: The antifungal activity of the compounds 4 and 5 was evaluated against *H. oryzae* and *C. sacchari* by usual agar-plate technique[6] at 1 000, 100 and 10 ppm concentrations. A commercial fungicide Dithane M-15 was also tested under similar conditions for comparing the results (Table 2).

All the tested compounds of 4 and 5 were toxic to both the test fungi at 1 000 ppm and not so spectacular at lower concentrations, 100 ppm and 10 ppm. In general, compounds 4 were more potent than thiazolidinyl benzoxazines (5). Compounds having halogens or methoxyl group were found to show higher antifungal activity over those having hydrogen or methyl group.

Acknowledgement

The authors are thankful to the Prof. and Head of the Department of Chemistry, Nizam College, for providing facilities, and to Dr. K. Subhash Reddy, Department of Microbiology, Agricultural University, Rajendernagar, for screening the compounds. We are also thankful to B.H.E.L., for getting nmr and carbon and hydrogen analyses.

References

1. N. M. Turkevich, L. Y. Ladnaya, I. V. Pleshnev and O. L. Grom, *Khim. Issled. Farm.*, 1970, 64.
2. H. D. Troutmann and L. M. Long, *J. Am. Chem. Soc.*, 1948, 70, 3436.
3. J. Kinngawa and K. Nagase, *Chem. Abstr.*, 1965, 63, 5653.
4. W. J. Doran and H. A. Shonle, *J. Org. Chem.*, 1938, 3, 193.
5. U. S. Pat. 1 951 807 (*Chem. Abstr.*, 1934, 28, 3528).
6. K. Raja Mohan and N. V. Subba Rao, *Indian J. Chem.*, 1973, 11, 1076
7. D. H. R Barton, W. H. Linell and N. Senior, *J. Chem. Soc.*, 1945, 437.
8. J. G. Horsefall, *Bot. Rev.*, 1945, 11, 357.

J. Indian Chem. Soc.,
Vol. LXIII, February 1986, pp. 226-227

Scutellarein-7-*O*-β-D-Glucopyranosyl(1 → 4)-*O*-α-L-rhamnopyranoside from the Stems of *Thymus serpyllum* Linn.

J. S. WASHINGTION and V. K. SAXENA*

Chemistry Department, University of Saugar, Sagar-470 003

Manuscript received 4 April 1984, revised 26 April 1985, accepted 2 December 1985

Phytochemical examination of the stems of *Thymus serpyllum* resulted in the isolation and identification of a glycoside, scutellarein-7-*O*-β-D-glucopyranosyl(1→4)-*O*-α-L-rhamnopyranoside.

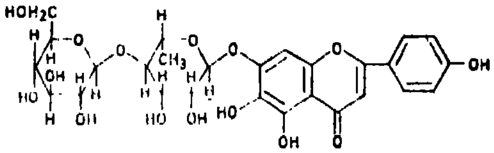
THYMUS serpyllum (N. O. Labiatae) is reputed for medicinal importance[1,2]. Since no work has been done on its stem, hence the chemical examination of the plant was undertaken.

Results and Discussion

The water soluble fraction of the ethanolic extract was successively extracted with different organic solvents. The methanol soluble fraction afforded the above reported glycoside. It was purified as cream-coloured compound (1.6 g). Acid hydrolysis (7%ethanolic H_2SO_4) yielded an aglycone $C_{15}H_{10}O_6$, m p 348°, and two sugars which were characterised as rhamnose and glucose by co-chromatography with authentic samples. The aglycone was identified as scutellarein by its sepecific colour reactions, m.p., spectral analysis, degradation studies and co-chromatography with an authentic sample.

Periodate oxidation of the glycoside consumed 3.2 moles of periodate with the production of 1.3 moles of formic acid per mole of the glycoside, suggesting the presence of a disaccharide having both the units in pyranose form. The position of the sugar linkage in the glycoside was determined by comparing the properties of the glycoside with those of the aglycone. The aglycone gave red colour when spotted on filter paper sprayed with *p*-toluene sulphonic acid and subsequent heating, a reaction specific for C_7—OH group, whereas the glycoside did not. Thereby confirming the position of glycosylation at C-7. A bathochromic shift of 7 nm in band II with sodium acetate ir, uv spectrum further confirmed the attachment of sugar at C_7 position[3,4].

The aqueous hydrolysate obtained by partial hydrolysis of the glycoside with 2% H_2SO_4 showed first the appearance of glucose, suggesting it to occupy the terminal position in the sugar moiety and rhamnose is linked glycosidically with the aglycone at position-7.



Thus keeping all the facts together the structure to the glycoside has been assigned as scutellarein-7-*O*-β-D-glucopyranosyl(1→4)-*O*-α-L-rhamnopyranoside.

Experimental

The air dried stems (3 kg) of *Thymus serpyllum* Linn. obtained from Himalayan Range Drug Field (Simla), were extracted with ethanol and the extract concentrated under reduced pressure and the concentrated extract was poured into excess of distilled water with continuous stirring. The water soluble part was concentrated to a dry viscous mass and extracted with ethyl acetate, followed by methanol. The methanol soluble part gave positive test for flavonoidal glycoside[5,6], and tlc examination showed two spots, indicating the presence of two compounds, which were separated by column chromatography over silica gel and eluted with ethyl acetate-methanol in the ratios of 1 : 1, 1 : 2 and 1 : 3. The eluates from methyl acetate-methanol (1 : 2) were of same R_f values and so were combined, and evaporation of the solvent yielded a cream coloured compound (420mg), crystallised from methanol, m.p. 238-39° (Found : C, 54.53 ; H, 5. 4. $C_{27}H_{30}O_{15}$ calcd. C, 54.54 ; H, 5.5%), M^+ 594 ; λ_{max} (MeOH) 277 and 333 , NaOEt Δ+54, $AlCl_3$ Δ+ 26 nm, no shift with NaOAc and $AlCl_3$; ν_{max} (KBr) 3 400, 1 680, 1 640, 1 560, 1 500, 1 280 and 821 cm^{-1}.

It gave +ve colour reactions for flavonoidal glycoside. ν_{max} at 3 400 indicated the presence of OH groups in it. Acetylation of the glycoside (50 mg) with Ac_2O/pyridine yielded nono-*O*-acetyl derivative, m. p. 164-66° (Found : C, 55.54 ; H,

4.8. $C_{45}H_{48}O_{24}$ calcd. C, 55.55 ; H, 4.9%), M^+ 927, thereby confirming the presence of nine hydroxy groups. Hydrolysis of the glycoside with 7% ethanolic H_2SO_4, yielded an aglycone, m.p. 348°, (Found : C, 61.96 ; H, 4.2. $C_{15}H_{10}O_6$ calcd. C, 62.94 ; H, 4.2%), M^+ 286. The aqueous hydrolysate was found to contain two sugars, glucose rhamnose (paper chromatography, R_f).

The aglycone showed bands : λ_{max} 277 and 333 ; +NaOEt Δ54 nm, + $AlCl_3$ Δ+ 26, NaOAc Δ+35 nm ; ν_{max} (KBr) 3 400, 2 940, 1 725, 1 640, 1 560, 1 500, 1 280 and 821 cm^{-1}. A peak at ν_{max} 3 400, indicates the presence of OH groups in it. On alkaline fusion. the aglycone (50 mg) yielded *p*-hydroxybenzoic acid and 1,2,3,5-tetrahydroxybenzene, m.p. 165°, confirmed by m.m.p., co-pc and co-tlc. Thus indicating the aglycone as 4,5,6,7-tetrahydroxyflavone which was further confirmed by its ^1H nmr and mass spectral studies. The important peaks obtained in the spectrum of the tetra-*O*-acetyl derivative of the aglycone : δ 6.51 (s, C_3-H), 6.73 (s, C_8-H) ; 7.56 (d, *J* 8.4 HZ, $C_{2'}$-H and $C_{6'}$-H), 6.89 (d, *J* 8, 2HZ, $C_{3'}$-H and $C_{5'}$-H), 2.45 (s, $C_{4'}$-OAc), 2.58 (s, C_5-OAc), 2.52 (s, C_6-OAc) and 2.54 (s, C_7-OAc) ; *m/z* 286 m+, 258, 257, 169, 158, 140 and 118.

The glycoside (50 mg) was hydrolysed by refluxing with 2% sulphuric acid. Aliquots at different interval were examined by paper chromatography. Glucose showed its appearance first, followed by rhamnose. The glycoside on permethylation[7] followed by hydrolysis, yielded 2 : 3 di-*O*-methyl-L-rhamnose and 2,3,4,6-tetra-*O*-methyl-D-glucose (confirmed by co-pc and co-tlc) clearly indicating the linkage between the two sugars through 1→4. The glycoside (20 mg) was dissolved in 25 ml of ethanol and was treated with 0.1*N* solution (25 ml) of sodium metaperiodate. The periodate consumed 3.2 moles and formic acid and liberated 1.3 moles were titrated by the trimetric method[8]. Enzymatic hydrolysis[9] of the glycoside indicated β-linkage between the sugars and α-linkage between L-rham nose and the aglycone.

Based on the above facts when kept together, the glycoside was assigned the structure as scutellarein-7-*O*-β-D-glucopyranosyl(1→4)-*O*-α-L-rhamnopyranoside, which was finally confirmed by ^1H nmr spectrum[10,11] of the nona-*O*-actyl derivative : δ 6.51 (H, s, C_3-H), 6.73 (1H, s, C_8-H), 7.56 (d, *J* 8.4 Hz, $C_{2'}$-H, $C_{6'}$-H), 6.89 (2H, d, *J* 8 2Hz, $C_{3'}$-H, $C_{5'}$-H), 2.45 (s, $C_{4'}$-OAc) ; 2.58 (3H, s, C_5-OAc), 2.52 (3H, s, C_6-OAc), 2.08 (3H, s, $C_{2''}$-OAc) ; 2.12 (3H, s, $C_{3''}$-OAc), 2.05 (3H, s, $C_{2'''}$-OAc), 2.04 (3H, s, $C_{3'''}$-OAc), 2.02 (3H, s, $C_{4'''}$-OAc), 2.0 (3H, s, $C_{6'''}$-OAc), 4.75 (1H, d, *J* 7.8 Hz, $C_{1''}$-H), 5.47 (1H, d, *J* 2Hz, $C_{1'''}$-H), 3.75-4.30 (m, 6 glucosoly protons) and 4.66-4.82 (4H, m, rhamnosyl protons).

References

1. The Wealth of India", C.S.I.R., New Delhi, 1942, Vol. X p. 235.
2. K. R. Kirtikar and B. D. Basu, "Indian Medicinal Plants", Indian Press, Allahabad, 1935, Vol. III, pp. 1988-89.
3. J. B. Harbone, J. J. Mabry and H. Mabry, "The Flavonoids", Chapman and Hall, London, 1970, pp. 62-75.
4. L. Jurd and R. M. Horowitz, *J. Org. Chem.*, 1957, 22 1618.
5. E. L. Hirst and J. K. N. Jones, *J. Chem. Soc.*, 1949, 1959.
6. L. H. Brigga and R. N. Locker, *J. Chem. Soc.*, 1951, 3136.
7. R. Khun, H. Trichamanu and I. Low, *Angew. Chem.*, 1953, 67, 32.
8. L. Jurd, in "Chemistry of the Flavonoid Compounds", ed. T. A. Geissman, Pergamon Press, London, 1962, pp. 107-155.
9. F. G. Manm and B. C. Soonders, "Practical Organic Chemistry", Landmann, New York, 1936, p. 365.
10. N. T. Barbara, M. Rudiger, J. J. Mabry and A. M. Powell, *Phytochemistry*, 1979, 18, 1855.
11. K. R. Markhan and J. J. Mabry, in "The Flavonoid", eds. J. B. Harborne, T. J. Mabry and H. Mabry, Chapman and Hall, London, 1975.

J. Indian Chem. Soc.,
Vol. LXIII, February 1986, pp. 228-229

Chemical Characterisation of *Eucalyptus kirtoniana* Seed Oil

B. MANDAL

Chemistry Department, B. N. Mahavidyalaya, Itachuna, Hooghly

and

B. ROY and S. GHOSH MAJUMDAR*

Chemistry Department, Burdwan University, Burdwan-713 104

and

C. R. MAITY

Biochemistry Department, Burdwan Medical College, Burdwan

Manuscript received 9 April 1984, revised 15 July 1985, accepted 2 December 1985

Seed oil from *Eucalyptus kirtoniana* was analysed for physico-chemical characteristics and fatty acid composition. The seed oil was rich in oleic acid and no unusual fatty acid was found.

LOCALISED shortages of traditional edible oils[1] have focused attention on the unconventional non-edible oils for their useful exploitation in recent times[2]. These minor non-edible oils, however, need to be investigated chemically prior to their exploitation. A number of studies on chemical characterisation of these minor non-edible oils have recently been reported[3-11]. In our laboratory, we have also started a systematic study on the chemical characterisation of these minor oils. As a part of our investigation, seed oil from *Eucalyptus kirtoniana* was analysed for physico-chemical characteristics and fatty acid composition.

Experimental

The mature fruits of *Eucalyptus kirtoniana* (Myrtaceae) were collected from the local forests of Burdwan and the seeds were removed from air-dried fruits. The seeds were powdered and the oil was extracted in a soxhlet apparatus using n-hexane. Physicochemical constants were determined according to the reported methods[12]. The seed oil was saponified at 110° for 12 h in ethanolic potassium hydroxide solution and unsaponifiable matters were extracted from the soap solution with ether. Saponified fatty acids were acidified, extracted with ether and the free fatty acids were then converted into their methyl esters with diazomethane. The mixture of methyl esters were applied to a 150 g diethylene glycol succinate (DEGS)/kg chromosorb WHMDS column of a Perkin-Elmer F11 gas liquid chromatograph for fatty acid analysis. The conditions employed were : column length 4 m, column temperature 200°, injection temperature 300°, attenuation 32×100, carrier gas nitrogen, speed of the carrier gas 2.6 kg/h and chart speed 60 cm/h. The peaks were identified using the reference compounds under the same conditions. The peak area percentages were considered as weight percentage.

Results and Discussion

The physicochemical characteristics of the seed oil and its fatty acid composition are presented in Table 1. It is seen that the seeds contained 29% oil. So this seed is worth commercial exploitation.

TABLE 1—PHYSICOCHEMICAL CHARACTERISTIC AND FATTY ACID COMPOSITION OF *Eucalyptus kirtoniana* SEED OIL*

Oil content of the seed	29%
Colour	dark red
Unsaponifiable matter	3.2%
Saponification value	197
Iodine value (Wij's)	102
Acid value	9.5%
Fatty acids (glc, DEGS column, %)	
Lauric (12 : 0)	0.7
Myristic (14 : 0)	3.4
Palmitic (16 : 0)	4.3
Stearic (18 : 0)	13.4
Arachidic (20 : 0)	2.1
Behenic (22 : 0)	4.5
Oleic (18 : 1)	50.4
Linoleic (18 : 2)	14.8
Linolenic (18 : 3)	6.4

*Average of four readings.

In our earlier studies, it has been shown that this deoiled seed cake is fairly good source of protein and may be used in animal feed formulations after ascertaining its non-toxicity[13-15]. The seed oil

contained no oxygenated fatty acids, such as epoxy, keto or hydroxy acids as revealed by glc. The high unsaponifiable matter, the high acid value and dark visible colour are some of the undesirable factors which can be easily removed by bleaching, deodourisation and refining.

The glc analysis showed the presence of only usual fatty acids in the seed oil. The seed oil is rich in oleic acid and contained significant proportion of linoleic acid. Thus, this seed oil appears promising for exploitation as a source of oleic acid-rich oil for use in the manufacture of soap and fatty acids. The seed oil may also be used for edible purposes after ascertaining its non-toxicity. Processing and biological testing of this seed oil are in progress in our laboratory.

Acknowledgement

The authors thank Dr. Pinaki Banerjee, Chemistry Department, North Bengal University, for his assistance. The work was conducted with grant-in-aid from C.S.I.R. and I.N.S.A., New Delhi.

References

1. *J. Am. Oil. Chem. Soc.*, 1980, **57**, 585A.
2. O. P. Vimal and K. T. Naphade, *J. Sci. Ind. Res.*, 1980, **39**, 197.
3. C. Rukmini, M. Vijayaraghavan and P. G. Tulpule, *J. Am. Oil. Chem. Soc.*, 1982, **59**, 415.
4. M. H. Kittur, C. S. Mahajanshetti, T. N. B. Kaimal and G. Lakshminarayana, *J. Oil. Technol. Assoc. (India)*, 1983, **15**, 43.
5. S. M. Osman and F. Ahmad in "Forest Oilseeds in New Sources of Fats and Oils", J. Am. Oil Chem. Soc. Monograph No. 9, eds. E. H. Piyde, L. H. Princen and K. D. Mukherjee, American Oil Chemists' Society, Champaign, 1980.
6. S. M. Ahmad, I. Ahmad, F. Ahmad and Osman, *J. Oil Technol. Assoc. (India)*, 1983, **15**, 80.
7. M. M. Siddiqui, I. Ahmad, F. Ahmad and S.M. Osman, *J. Oil Technol. Assoc. (India)*, 1983, **15**, 82.
8. A. Mannan, M. M. Siddiqui, R. Ahmad, I. Ahmad and M. Asif, *J. Oil Technol. Assoc. (India)*, 1983, **15**, 92.
9. K. Sundar Rao, A. J. Pantulu and G. Lakshminarayana, *J. Am. Oil Chem. Soc.*, 1983, **60**, 1259.
10. B. Mandal, S. Ghosh Majumdar and C. R. Maity, *J. Am. Oil Chem. Soc.*, 1984, **61**, 1447.
11. B. Mandal, S. Ghosh Majumdar and C. R. Maity, *Acta Alimentaria*, 1985, **14**, 3.
12. "Official Standarized and Recommended Methods", 2nd. ed., Society of Analytical Chemists, A.O.A.C., London, 1973, p. 675.
13. B. Mandal, S. Ghosh Majumdar and C. R. Maity, *Indian J. Physiol. Allied Sci.*, 1980, **34**, 114.
14. B. Mandal, S. Ghosh Majumdar and C. R. Maity, *Proc. Indian Natl. Sci. Acad., Sect. B*, 1982, **48**, 596.
15. B. Mandal, S. Ghosh Majumdar and C. R. Maity, *J. Food Sci. Technol.*, 1984, **21**, 307.

J. Indian Chem. Soc.,
Vol. LXIII, February 1986, pp. 230-232

Application of some Hydroxamic Acids for Spectrophotometric Determination of Palladium(II)

Y. K. AGRAWAL* and P. C. PAREKH

Analytical Laboratory, Pharmacy Department, Faculty of Technology and Engineering, M. S. University of Baroda, Baroda-390 001

Manuscript received 17 December 1984, revised 29 October 1985, accepted 15 November 1985

A sensitive and selective method for extraction spectrophotometric determination of Pd^{II} as a binary complex with *N-m*-chlorophenyl-*p*-methoxybenzohydroxamic acid (*m*-CMBHA), extracted from aqueous phase at *p*H 3.0 and ternary complex of PAN in isoamyl alcohol has been described. The binary and ternary complexes have the molar absorptivities 4.7×10^3 (λ_{max} 400 nm) and 1.2×10^4 (λ_{max} 620 nm) $dm^3\ mol^{-1}\ cm^{-1}$, respectively. Palladium was determined in the standard samples.

PALLADIUM is used as a catalyst for hydrogenation and dehydrogenation in liquid and gas phase reactions, most important use of palladium is in low current electrical contacts. There are several organic reagents used for the extraction and spectrophotometric determination of palladium[1-6]. However, they are less sensitive, time consuming, tedious and several metal ions, *viz.* Pt^{IV}, Ir^{III}, Ru^{III}, Rh^{III} *etc.* interfere[7-14]. Hydroxamic acids are potential analytical reagents and have been reported for the estimation of various metal ions[15-19]. No data are available for the extraction and a spectrophotometric determination of palladium, except *N*-phenylbenzohydroxamic acid (PBHA) and *N-p*-chlorophenylbenzohydroxamic acid[20,21]. In the present investigation, *N-m*-chlorophenyl-*p*-substituted-benzohydroxamic acids are studied for the extraction and spectrophotometric determination of palladium. *N-m*-Chlorophenyl-*p*-methoxybenzohydroxamic acid is found to be the most sensitive reagent amongst the hydroxamic acids and hence, the detailed studies are reported. The present system is comparable in sensitivity and its selectivity with commonly used reagents, like dithiazone and that its selectivity can be increased by the use of suitable marking agents.

Experimental

All the chemicals used were of AnalaR and G.R. grades, unless otherwise specified. Hydroxamic acids used for the extraction were synthesised as described elsewhere[22], and were recrystallised from a mixture of benzene and petroleum ether (b.p. 60-80°) before use. The purity of the hydroxamic acids were checked by m.p. uv and ir spectra. A 0.1% (w/v) solution of the reagent was prepared in isoamyl alcohol for extraction purposes.

A 0.1% (w/v) solution of 1-(2-pyridylazo)-2-naphthol (PAN) in 95% ethanol was prepared for ternary complex study. A standard palladium solution was prepared by dissolving a requisite amount of palladium chloride (Johnson Matthey) in 0.1 *M* HCl ; its final concentration was determined gravimetrically[23].

The spectral measurements were made on a VSU 2-P spectrophotometer with 1.0 cm quartz cells. The *p*H measurements were made with a Systronics digital *p*H meter.

Procedure : An aliquot of Pd^{II} solution (85.32 μg) was taken in a 60 ml separatory funnel, and the *p*H adjusted to 3.0 with 0.1 *M* HCl and 0.1 *M* NH_4OH. A 0.1% (w/v) solution (10 ml) of reagent in the isoamyl alcohol was then added and shaken for 15 min, the phases allowed to separate and the organic phase was transferred to a 25 ml volumetric flask after drying over anhydrous sodium sulphate. The extraction was repeated with the reagent solution (2×2.5 ml) and the extract collected to the mark with isoamyl alcohol and the absorbance measured at 400 nm against the blank.

For the ternary complex, 0.1% (w/v) PAN in 95% ethanol (2 ml) was added into the binary complex extract and diluted to 25 ml with isoamyl alcohol. The absorbance of the green coloured complex was measured after 20 min at 620 nm against a reagent blank.

Results and Discussion

The spectral characteristics of binary complexes of the palladium with the *N*-arylhydroxamic acids are given in Table 1.

TABLE 1—SPECTRAL CHARACTERISTIC OF PALLADIUM-HYDROXAMIC ACID COMPLEXES

Palladium = 3.4 ppm; pH = 3.0, Path length = 1 cm
Reagent = 0.1% (10 ml); Solvent = Isoamyl alcohol

Hydroxamic acids	Abrorbance	λ_{max} nm	molar absorptivity $\times 10^{3}$ dm^{3} mol^{-1} cm^{-1}
N-*m*-Chlorophenylbenzo	0.120	420	3.7
N-*m*-Chlorophenyl-*p*-Tolylbenzo	0.125	400	3.9
N-*m*-Chlorophenyl-*p*-Methoxybenzo	0.150	400	4.7
N-*m*-Chlorophenyl-*p*-Chlorobenzo	0.100	410	3.1
N-*m*-Chlorophenyl-*p*-Bromobenzo	0.100	410	3.1
N-*m*-Chlorophenyl-*p*-Fluorobenzo	0.100	410	3.1

To enhance the sensitivity of the method PAN was added as a chromogenic reagent. The green ternary complex has absorbance maximum at 620 nm. The spectral characteristics of the ternary systems are given in Table 2. Among the hydroxamic acids used here *N*-*m*-chlorophenyl-*p*-methoxybenzohydroxamic acid (*m*-CMBHA) was found to be the most sensitive reagent for palladium.

TABLE 2—SPECTRAL CHARACTERISTIC OF PALLADIUM-HYDROXAMIC ACID-PAN COMPLEXES

Palladium = 3.4 ppm; λ_{max} = 620 nm, Path length = 1 cm
Reagent = 0.1% (10 ml); pH = 3.0
Solvent = Isoamyl alcohol; PAN = 0.1% (2 ml) in ethanol

Hydroxamic acids	Absorbance	Colour	Molar absorptivity $\times 10^{4}$ dm^{3} mol^{-1} cm^{-1}
N-*m*-Chlorophenylbenzo	0.320	Green	1.0
N-*m*-Chlorophenyl-*p*-Tolylbenzo	0.350	Green	1.1
N-*m*-Chlorophenyl-*p*-Methoxybenzo	0.390	Green	1.2
N-*m*-Chlorophenyl-*p*-Chlorobenzo	0.288	Green	0.9
N-*m*-Chlorophenyl-*p*-Bromobenzo	0.288	Green	0.9
N-*m*-Chlorophenyl-*p*-Fluorobenzo	0.288	Green	0.9

Effect of p*H* : A set of experiment was carried out in order to study the influence of *p*H on extraction of Pd with *m*-CMBHA complex. The final *p*H of each aqueous solution was measured before extraction. The results (Table 3) show that the maximum extraction (100%) is obtained at the *p*H range 2.8-3.4 ; below and above this the extraction decreases and hence, the optimum *p*H 3.0 is selected for the present investigation.

Effect of reagent concentration : The extraction of Pd^{II} (85.32 μg/25 ml) was carried out with varying amounts of 0.1% (w/v) *N*-*m*-chlorophenyl-*p*-methoxybenzohydroxamic acid in isoamyl alcohol. It was observed that 10 ml of 0.1% (v/v) *m*-CMBHA was quite sufficient for the quantitative extraction of palladium. Excess of the reagent can be used without any difficulty.

TABLE 3—EFFECT OF *p*H ON EXTRACTION OF PALLADIUM WITH *N*-*m*-CHLOROPHENYL-*p*-METHOXYBENZOHYDROXAMIC ACID (*m*-CMBHA)

Palladium = 3.4 ppm; PAN = 0.1% (2 ml) in ethanol
Reagent = 0.1% (10 ml) CMBHA; Solvent = Isoamyl alcohol

*p*H	Extraction %	Pd-*m*-CMBHA λ_{max} 400 nm Colour	Molar absorptivity dm^{3} mol^{-1} cm^{-1}	Pd-*m*-CMBHA-PAN λ_{max} 620 nm Colour	Molar absorptivity dm^{3} mol^{-1} cm^{-1}
1.0	3	LY	1.4×10^{2}	Y	3.6×10^{2}
2.0	15	LY	7.0×10^{2}	Y	1.1×10^{3}
2.5	64	Y	3.0×10^{3}	GY	7.7×10^{3}
2.8	100	Y	4.7×10^{3}	G	1.2×10^{4}
3.0	100	Y	4.7×10^{3}	G	1.2×10^{4}
3.2	100	Y	4.7×10^{3}	G	1.2×10^{4}
3.4	100	Y	4.7×10^{3}	G	1.2×10^{4}
4.0	8	LY	3.7×10^{2}	Y	9.6×10^{2}
5.0	3	LY	1.4×10^{2}	Y	3.6×10^{2}

LY ≡ Light yellow. Y ≡ Yellow. GY ≡ Greenish yellow. G ≡ Green.

Effect of PAN concentration : Various chromogenic reagents, *viz.* PAR, brilliant green, crystal violet, xylenol orange, 1,10-phenanthroline, PAN, arsenazo III were tried for ternary complexes and for increasing the sensitivity of the method. PAN was found to be the most suitable for the spectrophotometric determination (Table 4).

TABLE 4 - EFFECT OF PAN CONCENTRATION

Palladium = 3.4 ppm; λ_{max} = 620 nm, Path length = 1 cm
Reagent = 0.1% (10 ml) CMBHA; *p*H = 3.0
Solvent = Isoamyl alcohol

Sl. no.	0.1% PAN ml	Absorbance	Colour	Molar absorptivity $\times 10^{4}$ dm^{3} mol^{-1} cm^{-1}
1.	0.5	0.350	Green	1.1
2.	1.0	0.390	Green	1.2
3.	2.0	0.390	Green	1.2
4.	3.0	0.390	Green	1.2
5.	4.0	0.370	Green	1.1

For maximum colour development 2 ml of 0.1% (w/v) PAN (in 95% ethanol) was enough. Lower concentration of the reagent gave incomplete complexation while the large excess increased the blank intensity.

Extraction time and stability of complex : Optimum time for the extraction was found to be 15 min though higher shaking time did not have any adverse effect on the extraction. The binary and ternary complexes are stable for 24 and 12 h, respectively.

Validity of Beer's law: The yellow binary complex of Pd^{II}-*N*-*m*-chlorophenyl-*p*-methoxybenzohydroxamic acid has maximum absorbance at 400 nm with a molar absorptivity 4.7×10^{3} dm^{3} mol^{-1} cm^{-1}. Pd-*N*-*m*-chlorophenyl-*p*-methoxybenzohydroxamic acid-PAN ternary complex has maximum absorbance at 620 nm having molar absorptivity 1.2×10^{4} dm^{3} mol^{-1} cm^{-1}. The binary and ternary systems obey Beer's law in the range 12-130 and 0.5-13.0 ppm, respectively.

Effect of diverse ions: In order to examine the utility of this method in the presence of other ions, their interference were studied Table 5. Pd is extracted in presence of diverse ions with *m*-CMBHA and then the colour developed by PAN. The several ions associated with palladium do not interfere. Fe^{III}, Ti^{IV}, Co^{II}, Ni^{II} and V^{V} are interfere in the determination of Pd. However, the interferences of Fe^{III} and V^{V}, Ti^{IV} and Co^{II} and Ni^{II} are eliminated by masking with ascorbic acid, fluoride and 1,10-phenanthroline, respectively.

TABLE 5 – EFFECT OF DIVERSE IONS

Palladium = 3.4 ppm; λ_{max} = 620 nm
Reagent = 0.1% (10 ml); Path length = 1 cm
Solvent = Isoamyl alcohol; *p*H = 3.0
PAN = 0.1% (2 ml) in Ethanol; Absorbance = 0.390

Ions	Added as	Amount mg	Absorbance
Mg^{II}	$MgSO_4$	60	0.390
Be^{II}	$Be(NO_3)_2$	40	0.390
Ba^{II}	$BaCl_2$	60	0.391
Pb^{II}	$Pb(NO_3)_2$	60	0.389
Cu^{II}	$CuCl_2$	40	0.389
Bi^{III}	$Bi(NO_3)_3$	30	0.391
Mo^{VI}	Na_2MoO_4	50	0.391
Ca^{II}	$CaCl_2$	40	0.390
Hg^{II}	$Hg(NO_3)_2$	50	0.390
U^{VI}	$UO_2(NO_3)_2$	40	0.389
$Ti^{IV\,a}$	$TiOCl_2$	30	0.391
$Fe^{III\,b}$	$FeCl_3$	40	0.391
$Ni^{II\,c}$	$NiSO_4$	40	0.390
$V^{V\,a}$	NH_4VO_3	60	0.391
$Co^{II\,c}$	$CoCl_2$	60	0.390

Masked with: [a]fluoride, [b]ascorbic acid, [c]1,10-phenanthroline.

Analysis of palladium in standard samples: A weighed quantity of the catalyst sample (Fluka) was digested with a mixture of perchloric and nitric acids and centrifuged. The filtrate was concentrated by heating and diluted to 100 ml with 0.05 *M* HCl. An aliquot of this solution was used for extraction of Pd. The method proposed has been applied to the determination of palladium in $Pd/CaCO_3$ catalyst and in other samples (Table 6). Results obtained are in agreement with those quoted.

TABLE 6—DETERMINATION OF PALLADIUM IN HYDROGENATION CATALYSTS

Catalyst	Standard value %	Palladium found, % AAS	Palladium found, % Present method*
Pd/Charcoal	5	4.93	4.98
Pd/Asbestos	5	4.98	5.01
$Pd/BaSO_4$	10	9.98	9.97
Pd/Charcoal	10	10.01	9.98
Pd/Carbonate	6	5.99	6.01

*Average of five values.

Acknowledgement

One of the authors (P.C.P.) is grateful to C.S.I.R., New Delhi, for the award of Junior Research Fellowship.

References

1. F. E. BEAMISH and W. A. E. MCBRYDE, *Anal. Chim. Acta*, 1953, 9, 349.
2. O. MENIS and T. C. RAINS, *Anal. Chem.*, 1955, 27, 1932.
3. M. OYOMO, *Anal. Chem. Acta*, 1980, 116, 161.
4. W. D. JACOBS, *Anal. Chem.*, 1961, 33, 2179.
5. K. L. CHENG, *Anal. Chem.*, 1954, 26, 1844.
6. R. B. SINGH, B. S. GARG and R. P. SINGH, *Talanta*, 1979, 26, 425.
7. V. K. GUSTIN and T. R. SWEET, *Anal. Chem.*, 1963, 35, 44.
8. M. IZQUIERDO, Thesis, Universidad Autonomade-Barcelona, 1982.
9. E. R. MARHENKE and E. B. SANDELL, *Anal. Chim. Acta*, 1963, 28, 259.
10. R. S. YOUNG, *Analyst*, 1951, 76, 49.
11. O. MENIS and T. C. RAINS, *Anal. Chem.*, 1955, 27, 1932.
12. K. L. CHENG and B. L. GOYDISH, *Microchem. J.*, 1966, 10, 158.
13. Z. MARCZENKO and M. JAROSZ, *Talanta*, 1981, 28, 561.
14. V. M. IVANOV, *Zh. Anal. Khim.*, 1967, 22, 763.
15. Y. K. AGRAWAL, *Rev. Anal. Chem.*, 1980, 5, 3.
16. Y. K. AGRAWAL and S. A. PATEL, *Rev. Anal. Chem.*, 1980, 4, 230.
17. Y. K. AGRAWAL and R. K. JAIN, *Rev. Anal. Chem.*, 1982, 6, 50.
18. R. PANDE and S. G. TANDON, *J. Indian Chem. Soc.*, 1977, 54, 990.
19. M. I. SHTOKAL, M. I. OSTROVSKAYA, V. L RYZHENKO and V. N. TOLOK, *Zh. Anal. Khim.*, 1978, 33, 2383.
20. A. D. SHENDRIKAR, *Talanta*, 1969, 16, 51.
21. Y. K. AGRAWAL and S. P. CHUDASAMA, *Bull. Soc. Chim. Belg.*, 1981, 90, 1033.
22. Y. K. AGRAWAL and S. G. TANDON, *J. Chem. Eng. Data*, 1977, 16, 371, 495.
23. A. I. VOGEL, "Textbook of Quantitative Inorganic Analysis Including Elementary Instrumental Analysis", 4th. ed., E.L.B.S., London, 1978, p. 474.

J. Indian Chem. Soc.,
Vol. LXIII, February 1986, pp. 233-235

Separation of Vanadium and Uranium by Liquid Anion-exchanger

SUPRA BANDYOPADHYAY and ARABINDA K. DAS*

Depatrment of Chemistry, Burdwan University, Burdwan-713 104

Manuscript received 8 February 1985, revised 30 August 1985, accepted 15 November 1985

A rapid and selective method for the extraction of vanadium as $VO_2(C_4H_4O_6)_2^{3-}$ and uranium as $UO_2(NO_3)_3^-$ with liquid anion-exchanger, Aliquat 336 (nitrate form) in chloroform and n-butanol medium respectively have been proposed. The effects of different variables on extraction have been investigated. The nature of the extracted species has been discussed. On the basis of the extraction data, mutual separat on of vanadium and uranium also separations from other commonly associated elements have been carried out.

HIGH molecular weight amines have been used extensively for the extraction of various metal ions as anionic complexes[1]. It may be used as a promising technique in industries and atomic energy programmes[2]. Not much work has been reported on the extraotion of either vanadium[3-5] or uranium[6,7] alone or on the separation of the two[8] using liquid anion exchangers. The present communication reports the extraction behaviour of vanadium as $VO_2(C_4H_4O_6)_2^{3-}$ and uranium as $UO_2(NO_3)_3^-$ with Aliquat 336 liquid anion-exchanger in nitrate form, $R_4N^+NO_3^-$ in suitable solvent. The effects of variables, such as *p*H of the aqueous phase, organic solvent, concentration of the extraction, equilibration time and various foreign ions, *etc.* have been investigated. On the basis of the extraction data, the mutual separation of vanadium and uranium has been made efficiently.

Experiemental

Aliquat 336 (Fluka, A.G.) was practical grade material. The nitrate form of the liquid-exchanger was obtained by treatment with 2 *M* HNO_3. Standard solutions of vanadium and uranium were prepared by dissolving NH_4VO_3 (E. Merck, G. R.) and $UO_2(NO_3)_2.6H_2O$ (AnalaR). All other chemicals used were of analytical grade.

Absorbance was recorded on a Shimadzu 190 double beam uv-visible spectrophotometer. The *p*H values were measured with a Systronics 331 expanded *p*H meter.

General extraction procedure for vanadium : The general extraction procedure is based upon solvent extraction technique. The aqueous phase was made up from a solution (5 ml) containing 300 μg of vanadium. A 5% potassium tartarate solution (1 ml) was then added, *p*H of the resulting solution adjusted to 5.0 and finally phthalate buffer (2 ml) was added. The aqueous phase was made up to 10 ml and equilibrated in a separatory funnel with 5% v/v liquid-exchanger solution (10 ml) in chloroform for 5 min. The two layers were allowed to settle for about 10 min. The organic phase was then separated carefully to another separatory funnel. To remove the organic solvent entrained in the separated aqueous phase, the latter was washed with chloroform (5 ml). The resulting chloroform extract was mixed with the earlier separated organic phase. The amount of vanadium present in the aqueous phase was estimated by spectrophotometric method[9]. The *p*H of the aqueous medium was adjusted to 4.0, then extracted with 0.1% oxine solution (2×5 ml) in chloroform. The absorbance of the extracted solution was measured at 550 nm against a reagent blank. Finally, the concentration of vanadium was determined from a calibration curve. Then, 10 ml of 0.01 *M* KOH solution was added to the organic phase in the separatory funnel and the mixture was shaken for 5 min. The two phases were allowed to settle. The aqueous phase was carefully withdrawn and again washed with chloroform (5 ml) to remove any entrained solvent present in the separated aqueous phase. The amount of vanadium extracted in that phase was estimated as in the case of aqueous phase.

General extraction procedure for uranium : 250 μg of uranium in a 30% potassium nitrate solution (5 ml) was taken, *p*H was adjusted to 8.5 and tris(hydroxymethyl)aminomethane buffer (2 ml) was added. The total volume of the aqueous phase was made upto 10 ml was taken in a separatory funnel and was shaken with 5% liquid-exchanger solution (10 ml) in n-butanol for 5 mins. The two layers were allowed to settle for about 10 min. Two phases were then separated carefully as in the case of vanadium separation and the uranium content was estimated in the two phases by spectrophotometric method[10]. In this method *p*H of the aqueous medium was adjusted to 8.8, then extracted

with 1.0% oxine solution (2×10 ml) in chloroform. The absorbance of the extracted solution was measured at 400 nm against a reagent blank. Finally, the concentration of uranium was determined from a calibration curve.

Separation procedure for vanadium and uranium: To the aqueous solution containing 300 μg of vanadium and 250 μg of uranium after adding 30% nitrate solution (5 ml), *p*H was adjusted to 8.5 and tris-buffer (2 ml) was added. It was then equilibrated with 5% liquid-exchanger (10 ml) in n-butanol. The two layers were allowed to settle and were separated carefully. As described in general extraction procedure, to remove the organic solvent entrained in the separated aqueous phase, the latter was washed with chloroform (5 ml). Finally, the uranium content of the organic phase was taken in 2 *M* nitric acid (10 ml) and then estimated by spectrophotometric method[10].

To the aqueous phase remaining after the separation of uranium, 5% tartarate solution (5 ml) was added, *p*H adjusted to 5.0 and phthalate-buffer (2 ml) was added. It was equilibrated with 5% liquid-exchanger (10 ml) in chloroform. Two layers were allowed to settle and separated as usual. Finally, as described in general extraction procedure, the vanadium content of the organic phase was taken in 0.01 *M* KOH solution (10 ml) and then estimated by spectrophotometric method[9].

Results and Discussion

Effect of pH: The extraction behaviour of the two metals with liquid-exchanger at different *p*H is given in Fig. 1. The working *p*H ranges for quantitative extraction of vanadium and uranium are respectively 4.4-5.9 and 8.0-9.6.

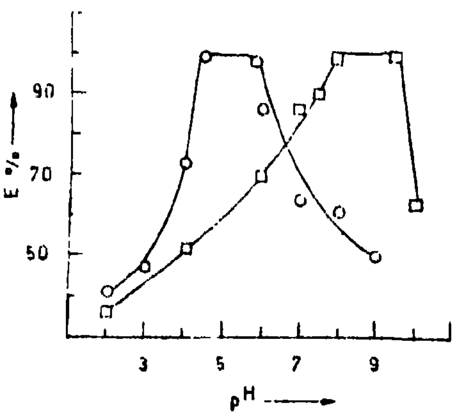


Fig. 1. Dependance of pH: (O) for vanadium and (□) for uranium.

Effect of solvents: The extraction behaviour of each of the metal was studied from aqueous solution having a definite *p*H into various organic solvents containing liquid-exchanger. The results indicate that most quantitative extraction of vanadium occurs with chloroform, the percentage of extraction being 98.75. Extraction with other solvents shows 78.75% in toluene, 70.0% in n-butanol and 46.25% in 1,2-dichloroethane. With nitrobenzene and isobutyl methyl ketone, emulsion formation was noted. Similarly, for uranium, n-butanol is most effective with percentage of extraction being 98.49. The results with other solvents are as follows: chloroform, 94.02%; benzene, 93.80%; toluene, 92.90%; 1,2-dichroethane, 88.95%; and isobutyl methyl ketone, 84.44%. With nitrobenzene an emulsion was formed.

Liquid-exchanger concentration: The effect of extractant concentration was studied by varying the concentration of liquid-exchanger from 0.2% to 10% using the diluents, chloroform for vanadium and n-butanol for uranium. It was found that the extraction increased with increasing extractant concentration and was complete at 5% liquid-exchanger.

Equilibration times: The contact time was varied from 30 s to 10 min. The extraction time was quantitative within 1 min and back-extraction was complete within 2 min. Contact and stripping time was kept 5 min all experiments.

Effect of foreign ions: The effect of diverse ions on the quantitative extraction of vanadium and uranium were studied separately by the general extraction procedure. For 30 ppm vanadium and 25 ppm uranium, tolerance limits (within an error of ± 2%) for various ions are given in Table 1.

TABLE 1—EFFECT OF DIVERSE IONS

Diverse ions	Tolerance limits (in ppm) For vanadium	For uranium
Ca^{II}	400	350
Sr^{II}	400	350
Ba^{II}	400	350
Mg^{II}	500	400
Mn^{II}	200	160
Ni^{II}	200	80
Co^{II}	200	80
Al^{III}	250	120
Cr^{III}	250	100
$Fe^{III\,a}$	100	100
$Cu^{II\,b}$	200	200
$Zn^{II\,a}$	250	200
$Ti^{IV\,c}$	350	300
Tungstate	150	150
Molybdate	100	80
Sulphate	200	100
Thiosulphate	300	260
Phosphate	400	320
Bromide	400	300
Iodide	400	300

In presence of: [a]phosphate, [b]thiosulphate, [c]fluoride.

Separation of vanadium and uranium: On the basis of the extraction data it has been possible to achieve the typical separation of the two metals in different synthetic mixtures following the procedure given under heading 'Separation procedure for vanadium and uranium'. The results are presented

in Table 2. The method may very well be suggested for the recovery of UO_2^{2+} from various uranium containing ores, like carnotite and uranite, and for the recovery of VO_3^- from the waste from uranium extractions.

TABLE 2—SEPARATION OF VANADIUM AND URANIUM

Sample No.	Composition (Amounts in μg)	Metals extracted, %	
		Vanadium	Uranium
1	$V^{5+}(300)+U^{6+}(250)$	99.5	100.0
2	$V^{5+}(300)+U^{6+}(250)+Ca^{2+}(100)+Mg^{2+}(100)+Ba^{2+}(100)$	102.0	98.4
3	$V^{5+}(300)+U^{6+}(250)+Al^{3+}(50)+Cr^{3+}(40)+Co^{2+}(40)$	98.8	101.0
4	$V^{5+}(300)+U^{6+}(250)+SO_4^{2-}(50)+PO_4^{3-}(50)+Br^-(50)$	98.5	99.5

Nature of the extracted species: The molar concentration of the liquid anion-exchanger was determined by stripping the chloride by sodium hydroxide solution and then titrating the chloride with standard $AgNO_3$ solution using K_2CrO_4 as an indicator.

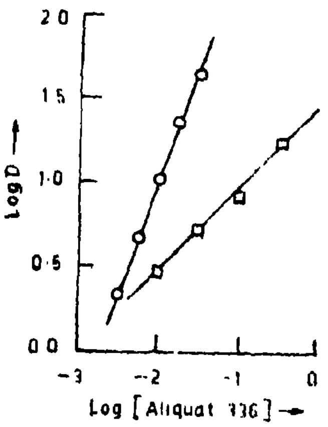


Fig. 2. Plot of log D against log [Aliquat 336]: (O) for vanadium and (□) for uranium.

In strong acid solutions, vanadate forms VO_2^+. V^{5+} forms negatively charged complexes with tartaric acid and potassium tartarate (concentration range 2-10%)[11]. On this basis, the separation may be accomplished by the liquid anion-exchanger. At a definite concentration of vanadium, the extraction of its tartarate complex as a function of liquid anion-exchanger concentration in chloroform was carried out. The extraction of VO_2^+ is quantitative provided the Aliquat 336-vanadium mole ratio is $\geqslant 3$. Plot (Fig. 2) of log D against log [Aliquat 336] provides a straight line with slope around 3. Thus the extraction mechanism of VO_2^+ may be given as,

$$3[R_4N^+]_o+[VO_2(C_4H_4O_6)_2^{3-}]_a \rightleftharpoons [(R_4N)_3VO_2(C_4H_4O_6)_2]_o$$

where, o is organic phase and a is aqueous phase.

The nitrate form of the liquid-exchang[er] obtained by treatment of Aliquat 336 with 2 [M] HNO_3 was taken in n-butanol and treated wi[th] the solution of UO_2^{2+} in 30% nitrate solution. T[he] extraction is quantitative when Aliquat 336-uraniu[m] mole ratio is $\geqslant 1$. Plot (Fig. 2) of log D again[st] log[Aliquat 336] produces a straight line with slo[pe] approximately 1. Hence, the extraction mechanis[m] of UO_2^{2+} similar to reported earlier[12] may be give[n] as

$$[R_4N^+NO_3^-]_o+[UO_2^{2+}+2NO_3^-]_a \rightleftharpoons [(R_4N)UO_2(NO_3)_3]_o$$

Acknowledgement

The authors are grateful to U.G.C., New Delh[i] for the equipment assistance.

References

1. H. GREEN, *Talanta*, 1973, **20**, 139.
2. A. K. DE, U. S. RAY and N. PARHI, *J. Indian Chem Soc.*, 1982, **59**, 1334.
3. T. KOLOINI, R. MODIC and B. GRAENER, *Hem. Ind.* 1975, **29**, 519.
4. A. DELEON, Bauxite. Alumina. Alum., Proc. Int. Symp ICSOBA, 2nd. 1969, **3**, 359 (Pub. 1979); (*Chem Abstr.*, 1973, **78**, 162473).
5. P. H. TEDESCO and J. A. G. QUINTANA, *Afinidad*, 1963 **20**, 226.
6. A. SATO and M. NOZAKI, *Japan*, 1960, 15757; (*Chem Abstr.*, 1962, **56**, 11295).
7. E. JUENGER and E. R. SCHMID, *Monatsh. Chem.*, 1974, **105**, 148.
8. C. J. LEWIS, *Chem. Eng.*, 1965, **72**, 101.
9. F. D. SNELL, C.T. SNELL, and C. A. SNELL, 'Colorimetric Methods of Analysis Including Photometric Methods', Vol. IIA, D. Van Nostrand, Princeton, 1959, p. 348.
10. J. BASSETT, R. C. DENNEY, G. H. JEFFERY an[d] J. MENDHAM, 'Vogel's Textbook of Quantitativ[e] Inorganic Analysis Including Elementary Instrumental Analysis', ELBS, London, 1978, p. 163.
11. M. QURESHI, H. S. RATHORE and R. C. KANSHIK, *Anal. Chem.*, 1975, **47**, 1710.
12. V. B. SHEVCHENKO, V. S. SHMIDT and E. A. NENAROKOMOV, *Zh. Neorg. Khim.*, 1960, **5**, 2354.

J. Indian Chem. Soc.,
Vol. LXIII, February 1986, pp. 236-237

Extraction Spectrophotometric Determination of Cobalt with β-Mercaptopropanoic Acid Anilide and its Applications

CHANDRIMA RAY and JYOTIRMOY DAS*

Department of Chemistry, University of Burdwan, Burdwan-713 104

Manuscript received 10 May 1984, revised 18 October 1985, accepted 15 November 1985

Small quantities (11-68 μg) of cobalt have been extracted into chloroform as the 1 : 3 complex with β-mercaptopropanoic acid anilide from solutions of *p*H 5.3-10.5 containing γ-picoline. The molar absorptivity of the red complex, measured at 480 nm is 1.33×10^4 dm^3 mol^{-1} cm^{-1}. Cobalt has been determined in the extract with a relative standard deviation of ±1.6%. The complex is stable upto two months, and sufficient amounts of Zn^{II}, Mg^{II}, Mn^{II}, Ba^{II}, Ca^{II}, Sr^{II}, V^{V}, Ce^{III}, Mo^{VI}, W^{VI}, Na, K, chloride or nitrate are tolerated. However, the separation from Be^{II}, Cu^{II}, Hg^{II}, Cd^{II}, Pb^{II}, Sn^{II}, Al^{III}, Cr^{III}, Fe^{III}, Bi^{III}, As^{III}, Th^{IV}, or U^{VI} has been effected using suitable masking agents. For the determination of the composition of the complex, solid complex has been isolated and elemental analysis, magnetic measurements and ir spectral studies have been performed. The method has been used to determine cobalt in ores, alloys and medicinal samples.

THIOGLYCOLIC acid[1,2] and its anilides[3,4] have been used for the spectrophotometric determination of cobalt. But the stability as well as the range of the metal determined in case thioglycolic acid is low. In the present work, β-mercaptopropanoic acid anilide has been used for the spectrophotometric determination of cobalt. This method permits the determination of cobalt in the presence of ten-fold excess of nickel.

Experimental

β-Mercaptopropanoic acid anilide : The reagent was prepared by refluxing a mixture of β-mercaptopropanoic acid (A.R., Fluka) and freshly distilled aniline in 1 : 1 proportion on a hot oil-bath (115-125°) for 3.5 h under an air condenser. The reagent was solidified by evaporation. When recrystallised from aqueous ethanol the compound was obtained as white crystalline needles, m.p. 80° (Found : N, 7.7 ; C, 59.38 ; H, 6.1 ; S, 17.75. Calcd. for : N, 7.73 ; C, 59.66 ; H, 6.07 ; S, 16.67%) ; ν_{max} 3 300 (NH) and 1 660 cm^{-1}(C=O).

Standard cobalt(II) solution : Cobalt sulphate (AnalaR) was dissolved in dilute sulphuric acid. The cobalt content of the solution was determined gravimetrically with α-nitroso-β-naphthol[5]. Finally, the solution was suitably diluted (~$10^{-4}M$).

All other chemicals used were of analytical grade.

γ-Picoline : A 10% stock solution of γ-picoline (AnalaR) was prepared by dissolving γ-picoline in aqueous ethanol.

Procedure for cobalt(II) : A known amount of a standard solution containing 11-68 μg of cobalt was taken and the reagent solution (2 ml) followed by 10% γ-picoline (2 ml) were added. The *P*H of the solution was adjusted to 6.2 by the addition of aqueous ammonia. The cobalt complex was extracted with chloroform (2×5 ml). The two organic layers were taken in a 10 ml volumetric flask, the volume adjusted to mark with a few drops of chloroform and dehydrated with anhydrous sodium sulphate. The absorbance of the red extract was measured at 480 nm using solvent blank.

Procedure for the determination of cobalt in ore, alloy and vitamin samples : The ore (limonite) and the alloy were decomposed by following standard methods[6]. The ore (0.9-1.2 g) was decomposed by nitric acid and potassium chlorate. The solution was taken in 100 ml measuring flask and ammonium fluoride (0.2 g) was added. Finally, the volume was made upto mark with dilute hydrochloric acid and an aliquot of 5 ml of the solution was used for the determination of cobalt. The alloy (0.9-1.0 g) was decomposed by nitric acid and hydrochloric acid (1 : 3) mixture. Tartaric acid (~0.15 g) was added to the resulting solution and the volume was made to 100 ml in a measuring flusk. 1 ml portion of a ten-fold diluted solution was used for the determination of cobalt. Two ampules (2×2 ml) of Macraberin Forte injection (Glaxo Lab., Bombay) were decomposed in a covered beaker with nitric acid following a standard procedure[6] for such samples by heating first at low temperature to avoid violent reaction. The mixture was cooled when reaction subsided and heated again with further nitric acid. The temperature was gradually raised

and finally the residue was heated to about 400° on a hot-plate. The ash was dissolved in dilute nitric acid (1 : 1) and evaporated slowly (1-2 h) on a steam-bath. Finally, the residue was taken in 25 ml water to which nitric acid was added in 0.25 ml portions until a clear solution was obtained on gentle heating. The cobalt content of this solution was determined by the procedure described above.

The results of analysis of samples of limonite (containing 0.5-0.6% Co) were within 1.5-2.0% While in case of alloys (Co, 5.3%) the error was 0.4%. The results were within 1.4% in case of the medicinal sample.

Results and Discussion

The absorbance values of several extracts containing varying amount of cobalt were recorded on a Beckmann DB 4500 spectrophotometer against solvent blank as the reagent has no absorbance above 290 nm. The curves indicate that λ_{max} of cobalt complex was at 480 nm. The λ_{max} for the reagent was at 245 nm.

Chloroform was found to be the most suitable solvent as 96% of the complex was extracted in the first step. The extent of extraction of the complex in isoamyl alcohol or isobutyl methyl ketone was very low and almost nil in benzene and carbon disulphide. The colour of the chloroform extract was found to be stable for more than 2 months. The experimental results showed that the extraction was complete in the range *p*H 5.3-10.5. Above *p*H 10.5 an emulsion was formed during extraction. It was observed that 5 mg reagent was sufficient for the quantitative complexation in aqueous layers. However, a ten-fold excess of the reagent had no adverse effect on the determination of cobalt. It was observed that complete extraction was possible in the presence of γ-picoline.

Optimum concentration range and absorptivity : On plotting the absorbance values of the extracts against concentration of cobalt, a straight line was obtained for 1.1-6.8 ppm of cobalt in chloroform. The optimum range[7] for the determination was 0.9-5.3 ppm and the Sandell sensitivity[7] 4.4×10^{-3} $\mu g\ cm^{-2}$. The molar absorptivity was 1.338×10^4 $dm^3\ mol^{-1} cm^{-1}$.

Effect of diverse ions : The tolerance limits for different foreign ions in the determination of cobalt were studied. The results indicate that most of the ions are tolerated upto 2 to 5 mg. However, fluoride had to be used to mask Be^{II}, Fe^{III} and Al^{III} while Mg-EDTA masked As^{III}, Sb^{III}, Bi^{III}, Th^{IV}, Pb^{II} and Cd^{II}. For Cr^{III}, in addition to Mg-EDTA, hot condition was necessary. The tolerance limit of Zn^{II} in the presence of ammonium chloride and UO_2^{II} in the presence of tartarate was studied. The tolerance limits of Sn^{II} in presence of sulphosalycilic acid, Hg^{II} in presence of iodide were studied ; in both the cases higher *p*H within the limit is recommended. For Cu^{II}, potassium cyanide was used to mask it. The determination of nickel and cobalt was possible in the same solution. The nickel complex was first extracted into chloroform from solutions adjusted to *p*H below 1 and measured at 450 nm. Subsequently, cobalt was extracted from the aqueous layer by the addition of 2 ml more of reagent solution and adjusting the *p*H to 6.8 with γ-picoline.

Effect of masking agent : The determination of cobalt was feasible in the presence of 200 mg of each of ammonium fluoride, tartrate, acetate, citrate, sulphosalycilate, ascorbate or iodide and 2 ml of 0.01 *M* Mg-EDTA. However, thioglycollic acid and EDTA were found to interfere.

Precision and accuracy : The relative standard deviation for 10 determinations of cobalt was ±1.6%. The confidence range[8] (95%) was calculated to be 3.47 ± 0.04 $\mu g\ ml^{-1}$.

Acknowledgement

The authors are indebted to the Geochemistry Division of Geological Survey of India, Calcutta, and Tata Iron and Steel Company, Jamshedpur, for the supply of analysed samples of the ore and alloy, respectively.

References

1. V. D. Anand, G. S. Deshmukh and C. M. Pandey, *Anal. Chem.*, 1961, 7, 1933.
2. L. P. Pandey, P. Das Gupta and A. Ghosh, *N. M. L. Tech. J.*, 1976, **18**, 39 (*Chem. Abstr.*, 1977, **87**, 161172).
3. N. Alexandru, N. Didine and A. Maria, *Chem. Anal.*, 1971, 3, 181 (*Chem. Abstr.*, 1972, 76, 148406).
4. C. Ray and J. Das, *Indian J. Chem., Sect. A*, 1985, 24, 40.
5. A. I. Vogel, 'A Text Book of Quantitative Inorganic Analysis', 4th ed., Longmans, London, 1978, p. 269.
6. K. Kodama, "Methods of Quantitative Inorganic Analysis", Interscience, New York, 1963, pp. 263, 269.
7. E. B. Sandel, "Colorimetric Determination of Trace Metals", 3rd ed., Interscience, New York, 1959, pp. 83, 97, 435.
8. W. J. Blaedel and V. W. Meloche, "Elementary Quantitative Analysis", 2nd ed., Harper and Row, New York, 1963, p. 621.

J. Indian Chem. Soc.,
Vol. LXIII, February 1986, pp. 238-240

A Simple Extractive Colourimetric Determination of Pyrocyclidine Hydrochloride from Pharmaceutical Preparation using Food Colours

G. S. SADANA and P. S. KUNHIPURAYIL

Department of Chemistry, G. N. Khalsa College, Matunga, Bombay-400 019

and

R. T. SANE

Department of Chemistry, Ramnarain Ruia College, Matunga, Bombay-400 019

Manuscript received 26 February 1985, accepted 15 November 1985

A simple colorimetric method for the estimation of procyclidine hydrochloride from its pharmaceutical formulations is described. The method is based on the formation of coloured complexes by the drug with reagents, like sunset yellow, Carmoisine-S and Fast Red-E in acidic medium. The coloured ion-pair complexes formed are quantitatively extracted under the experimental conditions. The method is statistically evaluated and is found to be precise and accurate.

PROCYCLIDINE hydrochloride is a parasympatholytic drug used in the treatment of the Parkinsonian syndrome. The B.P.[1] describes a non-aqueous titration method for the drug with perchloric acid as the titrant and crystal violet as the indicator. The U.S.P.[2] also describes a non-aqueous titration method but the end-point is determined potentiometrically.

For the determination of procyclidine hydrochloride from tablets, the B.P.[3] describes a volumetric method, using sodium dodecyl sulphate as titrant and dimethyl yellow-oracet blue-B as the indicator. In the U.S.P.[4], an extractive colourimetric method is described. The drug from the tablet is reacted with bromocresol purple in acetic acid solution to form a complex, which is extracted with chloroform. The absorbance is read at 405 nm. In the literature, gc[5], ir[6] and uv[7] spectrophotometric and extractive colorimetric[8] methods are described for the determination of procyclidine hydrochloride.

In the present communication, an extractive colourimetric method for the determination of procyclidine hydrochloride using food colours is described for the first time.

Experimental

Solutions of reagents were prepared in distilled water (w/v): Fast Red-E (2.0%), Carmoisine-S (0.2%) and Sunset yellow (0.5%). Potassium bipthalate buffer solution of *p*H 3 was prepared in distilled water for Fast Red-E and Sunset yellow. Potassium chloride-HCl buffer solution of *p*H 1 was prepared in distilled water for Carmoisine-S. Working standard solutions of procyclidine hydrochloride were prepared: in case of (i) Fast Red-E, 10 mg drug diluted to 100 ml (*i.e.* 100 μg ml^{-1}), (ii) Carmoisine-S, 20 mg drug diluted to 100 ml (*i.e.* 200 μg ml^{-1}) and (iii) Sunset Yellow 10 mg drug diluted to 250 ml (*i.e.* 40 μg ml^{-1}).

Sample solution: Twenty tablets of procyclidine hydrochloride after determining the average weight were powdered. Powder equivalent to the strength of the standard procyclidine hydrochloride solution was weighed and dissolved in distilled water and diluted upto the mark.

A Spekol CZ spectrocolorimeter with 1 cm matched glass cells was used.

Procedure: Appropriate amount of the standard drug solution was pipetted out into a series of separating funnels. To each flask, buffer and dye solutions were added as mentioned in Table 1. 10 ml chloroform (A.R.) was added to each funnel, and in the case of Carmoisine-S, 25 ml was used. The solutions were shaken for thorough mixing of the two phases and allowed to stand for a clear separation of the layers. The absorbance value of the chloroform layer was measured against the reagent blank at λ_{max}. A graph of the absorbance values against the corresponding concentration of procyclidine hydrochloride (μg ml^{-1}) was plotted. The sample solution was treated in a similar manner and the absorbance values measured. The amount of the drug present in the sample was computed from the calibration graph.

To study the recovery and accuracy of the proposed method for the determination of procyclidine hydrochloride a statistical study was done. A

TABLE 1—RESULTS OF THE PROPOSED METHOD FOR PROCYCLIDINE HYDROCHLORIDE

Sl. no.	Reagent (10 ml)	Amount of drug soln. prepared $\mu g\ ml^{-1}$	pH of buffer soln. (5.0 ml)	λ_{max} nm	Beer's law range $\mu g\ ml^{-1}$	Molar absorptivity $\times 10^{-3}$ $dm^3\ mol^{-1}\ cm^{-1}$	Stated amount of procyclidine HCl per tablet mg/tab.	Recovery %	Standard deviation	Coefficient of variation %
1.	Fast Red-E	100	3.0	517	5-20	12.9	5.0	99.72	0.09	0.73
							2.5	100.83	0.08	0.61
2.	Carmoisine-S	200	1.0	520	8-24	8.9	5.0	98.67	0.21	1.72
							2.5	101.72	0.15	1.22
3.	Sunset Yellow	40	3.0	485	4-20	12.9	5.0	102.95	0.14	1.65
							2.5	102.35	0.12	1.40

fixed volume of the sample solution was taken and three different volumes of the standard drug solution were added. Each level was carried out seven times. The total amount of the drug present in the sample was determined by the proposed method. The percentage recovery was calculated by the equation :

$$\% \text{ Recovery} = \frac{N(\Sigma XY)-(\Sigma X)(\Sigma Y)}{N(\Sigma X^2)-(\Sigma X)^2} \times 100$$

where, X = amount of drug added and Y = amount of the drug found per ml of the sample, and N = total number of observations.

The amount of the drug per ml of the sample by the proposed method was plotted against the amount of the drug added. The intercept represents the amount of drug per ml of the sample.

Stability study of procyclidine hydrochloride tablets by the proposed method : Accelerated stability study of the tablets were carried out by keeping the tablets in their packing at 50° for a period of 3 months (the three months period at 50° being equivalent to the condition of tablets at 2 years shelf-life). The samples from the pack were drawn at 1, 2, and 3 month period and its assay carried out by the proposed method.

It was observed that the procyclidine hydrochloride content in the tablet remained nearly constant, thus indicating that the product is stable for 2 years on shelf that has been studied. The results are given in Table 2.

Results and Discussion

The proposed method is simple, fast and accurate. It does not suffer any interference due to common excipients, like starch, talc, *etc*. The values of molar absorptivity obtained indicate that the reagents used are sensitive. The B.P.[1,8] and U.S.P.[3] methods require large quantities of the drug as compared to the proposed method, where relatively small quantities are used. The values of percentage recovery are within the pharmacopoeial limits. The values of standard deviation and coefficient of variations are low indicating high accuracy and reproducibility of the method.

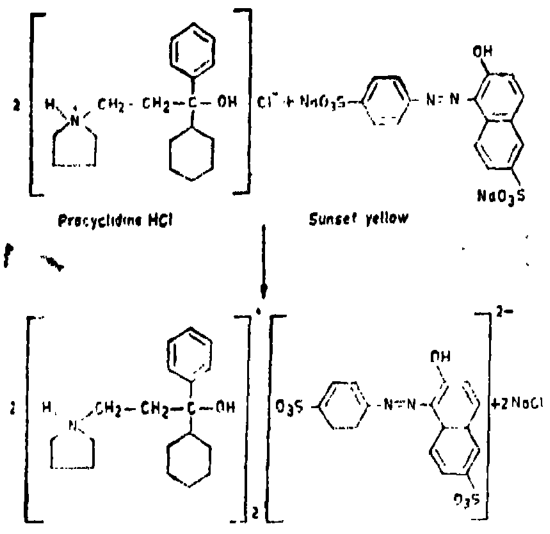
TABLE 2—RESULTS OF STABILITY STUDY OF PROCYCLIDINE HYDROCHLORIDE BY THE PROPOSED METHOD

Sl. no.	Months kept at 50°	Reagent	Stated amount of procyclidine HCl per tablet mg/tab.	Amount of drug found by the proposed method %
1.	1	Fast Red-E	5.0	100.66
	2			99.56
	3			98.14
2.	1	Fast Red-E	2.5	101.00
	2			99.80
	3			99.20
3.	1	Carmoisine-S	5.0	100.00
	2			99.62
	3			98.37
4.	1	Carmoisine-S	2.5	100.00
	2			98.75
	3			98.00
5.	1	Sunset Yellow	5.0	102.50
	2			102.50
	3			102.25
6.	1	Sunset Yellow	2.5	102.17
	2			102.20
	3			102.17

It is relatively more convenient to measure absorbance values at 515 to 520 nm on a spectrocolourimeter. This is because in the case of many yellow coloured ion-pair complexes the absorbance extends into the far-uv region and the exact determination of λ_{max} on a spectrocolorimeter become difficult. Again, the reagent blank in many cases have considerable absorbance in the region 410 nm and hence the absorbance have to be read at slightly higher wave length than the λ_{max}. From this point of view, dyes reported here have a definite advantage over the bromocresol purple reported in the U.S.P.[4] method.

The colour of the complex obtained is very stable over a period of 30 min and hence the method is practicable for routine analytical purpose and for studying the stability of the product.

The drug-dye complex was separated. From the ir and nmr studies we propose the reaction mechanism as shown



Ion-pair complex extracted in chloroform (λ_{max} = 485 nm)

Hence, a strong recommendation is made for the proposed method in the determination of procyclidine hydrochloride from its formulation, *viz.* tablets.

References

1. British Pharmacopoeia, Her Majesty's Stationary Office, London, 1980, p. 370.
2. The United States Pharmacopoeia, XX, Mack Publishing Co., Easton, 1980, p. 665.
3. British Pharmacopoeia, Her Majesty's Stationary Office, London, 1980, p. 812.
4. The United States Pharmacopoeia, XX, Mack Publishing Co., Easton, 1980, p. 666.
5. A. W. MISSEN, S. J. DICKSON and W. T. Cleary, *J. Anal. Toxicol.*, 1978, **2**, 238.
6. L. G. CHATTACH and L. A. DOAN, *J. Pharm. Sci.*, 1966, **55**, 372.
7. J. KRAEMAR and J. KRAEMAROUA, *Eslka Farm.*, 1966, **15**, 16.
8. R. T. SANE and S. V. SAWANT, *Indian Drugs*, 1982, **19**, 493.

Notes

Spectral Studies on Bis(β-naphthylidine-O-aminophenolate) Chelates of Cerium(III), Samarium(III), Gadolinium(III), Dysprosium(III), Cobalt(II) and Chromium(III)

P. SINGH and (Miss) VINITA RANI*

Department of Chemistry, S. S. V. College, Hapur-245 101

Manuscript received 13 October 1980, accepted 29 October 1985

Ce^{III}, Sm^{III}, Gd^{III}, Dy^{III}, Co^{II} and Cr^{III} complexes of tridentate Schiff base derived from the condensation of *o*-aminophenol and β-naphthylglyoxal have been prepared and studied by spectrophotometry and infrared spectroscopy. The stoichiometry of the complexes is established by spectrophotometric methods of analysis and elemental analysis. The binding of the functional groups of the ligand to metal on complexation have been confirmed by infrared spectral study.

Experimental

The ligand β-naphthylidine-*O*-aminophenol was prepared by refluxing equimolar quantities of both glyoxal and amine in ethanolic medium in the presence of a few drops of acetic acid. The contents were refluxed for 2 h and then poured into distilled water and filtered. Finally it was washed with ethanol.

The complexes were prepared by refluxing the metal salt and ligand solutions in dimethylformamide in the ratio of 1 : 2 for 2 h and after keeping it for 2 or 3 days to concentrate the volume, the crystals of the complexes were recovered and washed. The composition of the complexes was ascertained by elemental analysis. The infrared spectra(200-4 000 cm^{-1}) of the complexes were taken in KBr on a Perkin-Elmer Infra-Cord spectrophotometer.

The colour and melting point of the complexes are given in Table 1.

Results and Discussion

For the determination of stoichiometry, Vosburgh and Cooper's method was applied to determine the number of the complexes formed by the interaction of ligand and metal in the system. Equimolar solutions of metal and ligand were prepared and different sets were prepared in the ratios 1 : 1, 1 : 2, 1 : 3 and 1 : 4. The optical density of the mixture was measured by a Bauch & Lomb Spectronic 20. In the optical density *vs* wavelength plot, the maxima of curves show the number of the complexes formed in the system. The wavelength at which the maxima occurs is suitable for further study and this method was applied to select the wavelength for each system. Molar-ratio method was applied to determine the composition of the complexes. The curves were plotted between optical density and volume of variant (Fig. 1) and break in the curves shows the stoichiometry of all the complexes.

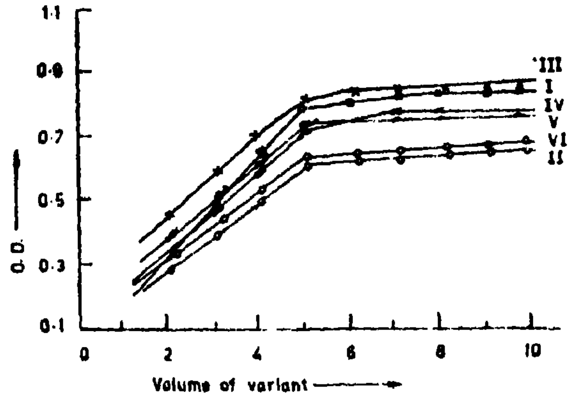


Fig. 1

Stability constant K_s has been evaluated by molar ratio method by the formula $K_s = (1-\alpha)/4\alpha^3 c^2$ where, α is the degree of dissociation and C is the total concentration of the complex in mol dm^3.

Free energy ΔF of complex formation has been

TABLE 1—COLOUR, M.P., STABILITY CONSTANT AND ANALYTICAL DATA OF COMPLEXES

Compd.	Colour	M.p. °C	Analysis % : Found/(Calcd.) C	H	N	Metal	K_s	ΔF
$Ce(C_{18}H_{12}O_2N)_2Cl$	Light brown	200	59.59 (59.00)	3.58 (3.47)	3.86 (3 80)	19.31 (19.28)	1.285×10^{11}	−15.476
$Dy(C_{18}H_{12}O_2N)_2NO_3$	Brown	215	55.98) (55.50)	3.10 (3.00)	5.44 (5.40)	20.98 (20.86)	1.568×10^{11}	−15.622
$Gd(C_{18}H_{12}O_2N)_2NO_3$	Dark brown	205	56.32 (56.20)	3.13 (3.07)	5.48 (5.35)	20.47 (20.40)	2.007×10^{12}	−17.169
$Sm(C_{18}H_{12}O_2N)_2NO_3$	Dark brown	217	56.84 (56.70)	3.16 (3.06)	5.53 (5.38)	19.73 (19.66)	6.621×10^{10}	−15.095
$Cr(C_{18}H_{12}O_2N)_2Cl$	Brown	220	68.03 (67.90)	3.78 (3.59)	4.41 (4.48)	8.19 (8.22)	2.717×10^{11}	−15.958
$Co(C_{18}H_{12}O_2N)_2$	Brown	230	71.29 (71.04)	3.96 (3.80)	4.62 (4.85)	9.57 (9.62)	1.783×10^{11}	−15.702

evaluated by the equation,
$-\Delta F = -2.303\ RT \log K_s$. Stability constant and free energy of the complexes are given in Table 1.

Ir spectral studies: The point of attachment of the ligand with the metal ion has been confirmed by studying the infrared spectrum of the ligand and the isolated chelates.

The strong bond appearing at 1 700 cm^{-1} (C=O) in the ligand is shifted to lower frequency at 1 680-1 690 cm^{-1} on complexation in all the systems, suggesting the formation of C—O—M bonding. The strong bond at 1 630 cm^{-1} in the ligand was assigned to azomethine group. On complexation, this gets lowered to 1 590-1 610 cm^{-1} indicating the formation of M—N bond. Hence, it is concluded that coordination occurs through CH=N and C=O group. A peak observed at 3 400 cm^{-1} (OH) in the ligand vanishes on complexation; therefore, it is concluded that the third point of attachment of metal to ligand occurs through the oxygen atom of OH group of the ligand.

References

1. A. N. SUNDAR RAM and C. P. PRABHABHARAN, *Indian J. Chem., Sect A*, 1976, **14**, 536.
2. OM PRAKASH, R. C. GUPTA and S. P. MUSHRAN, *Indian J. Chem., Sect. A*, 1979, **18**, 534.
3. P. K. SHARMA and P. ACHARYA, *J. Indian Chem., Soc.*, 1979, **56**, 961.
4. G. S. MANKU and A. N. BHAT, *Indian J. Chem., Sect. A*, 1977, **15**, 138.
5. M. MOHAN, *Indian J. Chem., Sect. A*, 1977, **15**,247.
6. B. SEN and R. DOSTEN, *J. Inorg. Nucl. Chem*, 1970, **32** 2707

Isolation of Halogeno and Complex-halogeno Anions as Salts of Oxinate Chelates of Bis(cyclopentadienyl)-titanium(IV) and -zirconium(IV)

ANAND K. SHARMA and N. K. KAUSHIK*

Department of Chemistry, University of Delhi, Delhi-110 007

Manuscript received 6 May 1983, revised 16 May 1984, accepted 15 November 1985

DOYLE and Tobias[1] pointed out that coordination of four oxygen atoms by strong covalent bonds to Cp_2M^{2+}(IV) moiety (M=Ti, V) would lead to weakening of the metal-ring bonds. In order to investigate, whether or not the coordination of two nitrogen and two oxygen atoms around the titanium(IV)/zirconium(IV) ion would produce a similar weakening of the metal-ring bonds, we studied the interaction of Cp_2TiCl_2/CP_2ZrCl_2 with 8-quinolinol in aqueous medium. We failed to isolate derivatives in which two 8-quinolinate groups coordinated to the Cp_2M^{2+} ($M=Ti^{IV}$, Zr^{IV}). However, ionic complexes of the type, $[Cp_2M$-(8-quinolinol)$]^+$ Cl^- in which only one bidentate 8-quinolinate group is coordinated to the titanium(IV)/zirconium(IV) ion are readily obtained. A number of halogeno and complex-halogeno salts of these complexes of the type $[Cp_2M$(8-quinolinol)$]^+X^-$ (M=Ti or Zr; $X^-=Br^-$, I^-, $CuCl_3^-$, $ZnCl_3(H_2O)^-$, $CdCl_4^{2-}$, $HgCl_3^-$) have been isolated in aqueous medium and characterised.

Experimental

All reagents used were of analytical grade. Nitrogen and halogens were determined by standard gravimetric methods[2]. Conductance measurements were made in nitrobenzene at 30±0.05° with a Systronic 304 digital direct reading conductivity meter. Infrared spectra (KBr) were recorded in the region 4 000-200 cm^{-1} with a Perkin-Elmer 621 grating spectrophotometer. ^1H nmr spectra were recorded in deuterated acetone at a sweep width of 900 Hz with a Perkin-Elmer R-32 spectrophotometer. Chemical shifts are expressed relative to an internal reference of TMS (1% by volume).

Preparation of complexes: An aqueous solution of $[Cp_2Ti$(8-quinolinol)$]^+Cl^-/[Cp_2Zr$(8-quinolinol)$]^+$ Cl^- was obtained by stirring an aqueous solution of Cp_2TiCl_2/Cp_2ZrCl_2 with an excess of solid 8-quinolinol for about 1 h. The solution was filtered and the filtrate added separately to a hot solution of KBr, KI, $CuCl_2$, $ZnCl_2$, $CdCl_2$ and $HgCl_2$. The solution was digested over water-bath for 4 h. Ionic complexes of the type, $[(Cp_2Ti$-(8-quinolinol)$]^+X^-$ and $[Cp_2Zr$(8-quinolinol)$]^+X^-$ ($X=Br^-$, I^-, $CuCl_3^-$, $ZnCl_3^-$, $CdCl_4^{2-}$ and $HgCl_3^-$, respectively) were precipitated. These were filtered and washed with petroleum ether.

Results and discussion

Table 1 lists the analytical data and physical characteristics of the complexes. The complexes are thermally stable and decompose at higher temperatures without melting. They are soluble in acetone and THF, and partially soluble in chloroform and dichloromethane. With $ZnCl_2$, an aquotrichlorozincate(II) anion, $[Cp_2M$(8-quinolinol)$]^+$, $ZnCl_3(H_2O)^-$ is precipitated. The presence of coordinated water is identified by its intense infrared absorption at ~3 450 cm^{-1}. Conductivity measurements show that all the complexes except $CdCl_4^-$ salts are 1 : 1 electrolytes in nitrobenzene. However, in case of $CdCl_4^{2-}$ salts, the results are consistent with those of 1 : 2 electrolytes, indicating that the dinegative anions are precipitated.

Infrared spectra: No halide bridging is observed in halide and complexhalo anion salts. The frequencies at 350-370 cm^{-1} region for complex-halogeno salts are characteristic of complex chloro anions[2,3]. A strong band at 1 500 cm^{-1} in the free 8-hydroxyquinoline may be assigned to C=N bond. In complexes, this band is shifted to lower wavenumber at ~1 330 cm^{-1} indicating the coordination of nitrogen atom of 8-hydroquinoline ligand to the metal[4]. Further, in the spectra of complexes,

Table 1—Analytical Data and Physical Characteristics

Sl. no.	Compd.	Colour	Dec. temp. °C	Conductance* $\Omega^{-1}cm^2mol^{-1}$	Analysis % : Found/(Calcd.) N	Halogen
1.	$[Cp_2Ti(8\text{-quinolinol})]^+Br^-$	Yellow	215-216	29.8	3.32 (3.48)	19.93 (19.89)
2.	$[Cp_2Ti(8\text{-quinolinol})]^+I^-$	Yellow	185-187	28.6	3.10 (3.12)	28.22 (28.28)
3.	$[Cp_2Ti(8\text{-quinolinol})]^+CuCl_2^-$	Green	98-100	30.2	2.80 (2.85)	21.61 (21.65)
4.	$[Cp_2Ti(8\text{-quinolinol})]^+ZnCl_3(H_2O)^-$	Greenish yellow	210-212	30.4	2.56 (2.74)	20.64 (20.81)
5.	$[Cp_2Ti(8\text{-quinolinol})]_2^+CdCl_4^{2-}$	Yellow	278-280	50.2	2.60 (2.77)	14.20 (14.05)
6.	$[Cp_2Ti(8\text{-quinolinol})]^+HgCl_3^-$	Yellow	140-142	30.0	2.08 (2.23)	16.80 (16.93)
7.	$[Cp_2Zr(8\text{-quinolinol})]^+Br^-$	Green	280-282	28.8	3.01 (3.15)	17.82 (17.95)
8.	$[Cp_2Zr(8\text{-quinolinol})]^+I^-$	Green	216-218	28.6	2.68 (2.84)	25.82 (25.79)
9.	$Cp_2Zr(8\text{-quinolinol})]^+CuCl_2^-$	Yellowish green	158-160	30.2	2.50 (2.62)	19.86 (19.90)
10.	$[Cp_2Zr(8\text{-quinolinol})]^+ZnCl_3(H_2O)^-$	Green	218-220	31.2	2.41 (2.53)	19.12 (19.25)
11.	$[Cp_2Zr(8\text{-quinolinol})]_2^+CdCl_4^-$	Yellowish green	146-150	50.6	2.49 (2.66)	13.32 (13.47)
12.	$[Cp_2Zr(8\text{-quinolinol})]^+HgCl_3^-$	Yellowish green	176-178	28.8	2.01 (2.08)	15.71 (15.84)

*0.50×10^{3} *M*.

disappearance of the broad ν_{O-H} at 3 600-3 560 cm^{-1} and appearance of a medium intensity band at 520 cm^{-1} due to ν_{M-O} show the deprotonation of phenolic OH group and bonding of the 8-hydroxyquinoline ligand to the metal through phenolic oxygen[5].

The bands occurring consistantly around 3 080 (C—H stretch), 1 430 (asymmetric ring breathing), 1 080 (C—H deformation of C_5H_5 ring) and 815 cm^{-1} (C—H bending out-of-plane deformation) in all the complexes suggest the presence of η^5-cyclopentadienyl ring[6]. An additional band near 440 cm^{-1} may be assigned to M-C_5H_5 vibrations[7].

Pmr spectra : ^{1}H nmr spectra of the complexes were recorded in deuterated acetone. The spectra of free oxine show the signals at δ 7.31 (4H, m), 8.05 (1H, q, *J* 9.0 and 2.5 Hz) and 8.73 (1H, q, *J* 4.0 and 1.6 Hz) due to the $C_{3,5,6,7}$, C_4 and C_2 protons, respectively. In the metal complexes, however, the former two signals (due to the $C_{3,5,6,7}$ and C_4) are not separately identifiable and resulting in a complex multiplet in the region δ 7.4-8.2. The resonance due to the C_2 protons is at δ 9.06 (q, *J* 4.0 and 1.8 Hz). The fact that it is shifted downfield with respect to the free oxine, supports the conclusion that the oxinate ligand is chelating. The spectra of the $ZnCl_3(H_2O)^-$ salts show an additional resonance signal due to the presence of a coordinated water molecules at δ 4.18. The resonance signals due to C_5H_5 group is observed as a singlet at δ 6.7.

Acknowledgement

The authors thank C.S.I.R., New Delhi, for the award of Senior Research Fellowship to one of them (A.K.S.).

References

1. G. Doyle and R. S. Tobias, *Inorg. Chem.*, 1967, **6**, 1111; 1968, **7**, 2484.
2. A. I. Vogel, "A Text Book of Quantitative Inorganic Analysis", Longmans, London, 1968.
3. K. Chandra, R. K. Sharma, B. S. Garg and R. P. Singh, *Transition Met. Chem.*, 1979, **4**, 367.
4. A. K. Sharma, G. S. Sodhi and N. K. Kaushik, *Bull. Soc. Chim. Fr.*, 1983, 152.
5. A. K. Sharma and N. K. Kaushik, *Synth. React. Inorg. Metal-Org. Chem.*, 1983, **12**, 827.
6. H. P. Fritz, *Adv. Organomet. Chem.*, 1964, **1**, 279.
7. R. S. P. Coutts and P. C. Wailes, *J. Organometal. Chem.*, 1975, **84**, 57.

Five- and Six-coordinate Low-spin Iron(III) Complexes

B. K. KANUNGO, B. PRADHAN
and
D. V. RAMANA RAO*

Department of Chemistry, Regional Engineering College, Rourkela-769 008

Manuscript received 13 September 1984, revised 7 October 1985, accepted 15 November 1985

IRON(III) is known to form high-spin, (S=5/2) low-spin (S=1/2) and intermediate-spin (S=3/2) complexes under the influence of different ligand fields. Spin-crossover phenomenon is usually observed with the iron(III) compounds. Examples of high-spin and spin-crossover compounds of iron(III) are numerous. However, there exists limited examples of low-spin iron(III) complexes. In continuation to our studies on iron(III)[1], we report in

the present communication, some simple anionic iron(III) complexes which are found to have low-spin states.

Experimental

All the chemicals used were of AnalaR grade. Suspension of tetramethylammoniumtetrachloroferrate(III) in ethanol was reacted with 2-benzazine/3,5-dimethylpyridine/3-methylpyridine / 1,3-diazole/2-methyl-1,3-benzodiazole / 4,5-diazaphenanthrene/1,2-diaminoethane in appropriate molar ratio, refluxed for a few minutes and cooled. The separated compounds were filtered through a sintered glass crucible, washed with ethanol followed by ether and dried *in vacuo* over anhydrous calcium chloride.

The composition of the complexes was established through elemental analyses carried out by standard methods. The conductance measurements in methanol medium were carried out using a Systronics 303 direct reading conductivity meter. The magnetic susceptibility was measured at room temperature with a Gouy balance and calculation was made computing diamagnetic corrections from Pascal's constant[2]. The ir spectra of the compounds were recorded in the region 4 000-400 cm^{-1} using a Perkin-Elmer 337 spectrophotometer with KBr optics. The electronic spectra of the solution in methanol medium were obtained using a Unicam SP-500 spectrophotometer. The molecular weight of the complexes was determined by Rast's method using diphenyl and C, H analyses were done by a Systems Control Semiautomatic instrument. The analytical data are returned in Table 1.

Results and Discussion

The compounds reported in the present communication belong to five- and six-coordinated categories. The coordination number and probable stereochemistry of these compounds have been suggested on the basis of their analytical data, infrared and electronic spectra, electrical conductivity, room temperature magnetic susceptibility and molecular weight determination. The values of Λ_m obtained between 112 and 169 Ω-1 (Table 1) in methanol medium indicate that the compounds are 1 : 1 electrolytes[3]. The low-spin compounds give rise to the $^2T_{2g}$ term, and the temperature-dependent magnetic moment is a function of spin-coupling parameter. The magnetic moment value is expected to be above spin-only value (1.73 B.M.) and less than about 2.5 B.M[4]. The observed values range 1.34-2.21 B.M. for hexacoordinated and 2.43-2.98 B.M. for pentacoordinated complexes. The μ_{eff} values for the latter are intermediate between spin-free and spin-paired complexes and can be attributed due to the spin-crossover system[5-7]. The molecular weight determination indicates that the complexes are monomeric.

Infrared spectra : The relevant infrared absorption bands due to the coordinated chelate of the complexes are discussed below. Bands due to tetramethylammonium ion[8] were obtained at 700-800 and 935-980 cm^{-1}. The ν_{C-H} band observed at ~ 3 000 cm^{-1} and $\nu_{C-C} + \nu_{C-N}$ bands at ~ 1 600 and 1 560 cm^{-1} indicate the coordination of the substituted pyridine[9,10]. In the spectra of the 1,3-diazole complexes, the N—H bending and stretching frequencies which occur at ~1 465 and ~3 300 cm^{-1}, respectively, clearly indicate that 1,3-diazole and its derivative are coordinated through the tertiary nitrogen atom as confirmed by the reported *X*-ray structural studies[11]. 1,2-Diaminoethane shows two bands at 1 700-1 500 and 950-850 cm^{-1} due to NH_2 stretching and CH_2 rocking[12]. In the present investigation, the former band is observed at 1 580 cm^{-1} whereas the latter is overlapped with the

TABLE 1—PHYSICAL AND ANALYTICAL DATA OF SOME ANIONIC IRON(III) COMPLEXES

Sl. no.	Compd.	Colour	M.p. °C	Λ_m $\Omega^{-1}cm^{-1}mol^{-1}$	Analysis % : Found/(Calcd.) Fe	Cl	C	H	μ_{eff} B.M.	Mol. wt.* Found/(Calcd.)
1.	$[C_4H_{12}N][FeCl_4(\beta\text{-pic})]$	Yellow	252	142.6	15.30 (14.60)	38.8 (37.2)	32.8 (32.9)	5.1 (5.2)	2.46	320.4 (364.98)
2.	$[C_4H_{12}N][FeCl_4(\beta\text{-pic})_2]$	Dark yellow	246	169.0	12.1 (13.1)	31.0 (33.3)	40.3 (41.9)	5.6 (5.7)	2.21	430.2 (458.11)
3.	$[C_4H_{12}N][FeCl_4(iq)]$	Yellow	249	159.6	13.9 (14.0)	35.4 (34.9)	38.3 (38.9)	1.7 (4.7)	2.98	376.4 (401.01)
4.	$[C_4H_{12}N][FeCl_4(iq)_2]$	Dark yellow	235	112 2	10.5 (10.9)	26.7 (27.2)	48.9 (49.8)	4.3 (4.9)	2 05	502.6 (530.17)
5.	$[C_4H_{12}N][FeCl_4(lu)]$	Reddish yellow	223	139.2	14.7 (13.9)	37.4 (37.1)	35.0 (34.8)	4.9 (5.5)	2.43	330.4 (378.85)
6.	$[C_4H_{12}N][FeCl_4(lu)_2]$	Reddish yellow	195	145.8	11.4 (11.3)	29.2 (30.2)	44.5 (44.5)	6.0 6.2)	1.94	445.8 (485.85)
7.	$[C_4H_{12}N[FeCl_4(iz)]$	Orange	248	120.2	16.4 (16.5)	41.7 (40.3)	24.6 (24.7)	(4.3 (4.7)	2.49	300.1 (339.85)
8.	$[C_4H_{12}N][FeCl_4(me\ biz)]$	Orange	255	126.3	13.8 (14.1)	35.1 (34.9)	35.3 (35.6)	4.8 (4.9)	2.57	400.8 (403.85)
9.	$[C_4H_{12}N][FeCl_4(en)]$	Yellow	203	120.5	15.8 (15.8)	40.3 (40.1)	20.9 (21.6)	5.9 (6.0)	2.12	307.6 (331.85)
10.	$[C_4H_{12}N][FeCl_4(o\text{-phen})]$	Dark	252	118.5	15.3 (12.1)	31.4 (29.8)	40.6 (42.5)	4.1 (4.4)	1.99	410.5 (451.85)

*Values calculated for 1 : 1 electrolytic complexes.

band of $(CH_3)_4N^+$ ion at 935 cm^{-1}. The ν_{C-H} at 1 580 cm^{-1} and δ_{C-H} at 760 cm^{-1} indicate the bidentate nature of 4,5-diazaphenanthrene coordinating through both the nitrogen atoms[13-15]. The absence of band at 3 200-3 500 cm^{-1} in the complexes attributable to coordinated water molecules indicate that water is not coordinated to the metal ion even in the pentacoordinated species[16].

In the electronic spectra of the octahedral complexes, bands were obtained at ~660, ~550 and ~412 nm, which may be assigned to $^3T_2 \rightarrow {}^3E_1$, $^3T_2 \rightarrow {}^3T_1$ and $^3T_2 \rightarrow {}^4T_1$ transitions. The values are consistent with the earlier observations[17].

References

1. B. K. Kanungo, B. Pradhan and D. V. Ramana Rao, *J. Indian Chem. Soc.*, 1982, **54**, 329.
2. P. W. Selwood, "Magnetochemistry", 2nd ed., 1956, pp. 78, 92, 93.
3. R. L. Dutta, Inorganic Chemistry, 2nd. edn., 1980.
4. B. N. Figgis and J. Lewis, *Prog. Inorg. Chem.*, 1964, **6**, 167.
5. P. C. H. Mitchell and D. A. Parker, *J. Chem. Soc., Dalton Trans.*, 1976, 1821.
6. R. R. Eley and N. V. Duffan, *J. Inorg. Nucl. Chem.*, 1972, **34**, 3681.
7. B. N. Figgis and J. Lewis, *Prog. Inorg. Chem.*, 1964, **6**, 171.
8. A. K. Das and D. V. Ramana Rao, *J. Indian Chem. Soc.*, 1971, **48**, 823.
9. J. D. Curry and D. H. Busch, *J. Am. Chem. Soc.*, 1964, **86**, 598.
10. B. Pradhan and D. V. Ramana Rao, *J. Indian Chem. Soc.*, 1979, **56**, 455.
11. B. K. S. Lundberg, *Acta Crystallogr.*, 1966, **21**, 901.
12. K. Nakamoto, "Infrared Spectra of Inorganic and Coordination Compounds", John Wiley, New York, 1970, pp. 225.
13. A. A. Schilt and R. C. Tailor, *J. Inorg. Nucl. Chem.*, 1959, **9**, 211.
14. R. G. Inskep, *J. Inorg. Nucl. Chem.*, 1962, **24**, 769.
15. N. P. Crawford and G. A. Nelson, *J. Chem. Soc., A*, 1969, 427.
16. K. Nakamoto, "Infrared Spectra of Inorganic and Coordination Compound", John Wiley, New York, 1970.
17. A. H. Awaid, B. L. Martin, E. Inn and A. H. White, *Inorg. Chem.*, 1969, **8**.

Studies on Water Decomposition Product of Iron(III) Peroxychromate by Ion-exchange Resins

(Miss) NEELAM MISHRA and B. M. L. TIWARI*

Chemistry Department, Government Science College, Rewa-486 001

Manuscript received 4 February 1985, revised 6 September 1985, accepted 2 December 1985

Several peroxychromates have earlier been reported[1-5] but not iron peroxychromate. Hence, to ascertain the composition of iron(III) peroxychromate the study of its water decomposition product has been undertaken.

* 11/28, Near Bichhiya Hospital, Rewa-486 001.

Experimental

Ice-cold solid Fe^{III} chromate[4] (1 g) and anhydrous H_2O_2 (2.5%, 20 ml) extracted in ethyl acetate, were mixed together, shaken occasionally and cooled in a freezing mixture for 30 min. Bluish violet iron(III) peroxychromate, soluble in ethyl acetate, was separated as in other cases[1-5]. The oxidising power of the peroxychromate was determined by Na_3AsO_3 and $KMnO_4$ methods[1,5] (Table 1).

Many sets of water decomposition product were prepared by decomposing the peroxychromate (20 ml) in contact with water (50 ml). The colourless organic layer was removed and the yellow aqueous layer was exchanged[6-8] with Dowex-50 (Na) and Amberlite-120 (Na) resins.

The presence of Fe^{III} in elutriant and of $Cr_2O_7^{2-}$ in effluent was established by usual qualitative tests, R_f values[9] (elutriant, 0.720; effluent, 0.319; $FeCl_3$, 0.725; $K_2Cr_2O_7$, 0.312), absorption (aqueous) and ir (KBr) spectra (effluent and $Na_2Cr_2O_7$: λ_{max} at 233, 315 and 350 nm; sharp absorptions at 950, 890 and 770 cm^{-1}). The concentration of Fe^{III} and Cr^{VI} in elutriant and effluent was estimated by colorimetric[10] and gravimetric[11] methods (Table 1).

TABLE 1—ANALYTICAL DATA

Fe^{III} peroxychromate = 20 ml.

Average amount (g) of			Ratio		
Fe^{III}	Cr^{VI}	Peroxy O_2^{2-}	a :	b :	c
0.00112	0.00315	0.00156	1 :	2.81 :	1.39
Calcd. :					
$Fe_2(Cr_2O_{10})_3 \xrightarrow{+H_2O} Fe_2(Cr_2O_7)_3 + 9O$			1 :	2.79 :	1.28

μ_{eff} at 304 K of elutriant – oxinate = 5.936 B.M.

The changes in pH (4.75-4.85) of a set of water decomposition product, on dilution with measured volumes (25-300 ml) of water, were found almost similar to dichromate solutions[6-7].

Results and Discussion

The above findings confirm that the water decomposition product of iron(III) peroxychromate is composed of Fe^{III} and $Cr_2O_7^{2-}$ in the ratio of 1 : 3. Further, the average amounts of the consttituents (Table 1) indicate that a very low percentage of iron(III) chromate is converted to peroxy compound. However, the experimental results and inferences are in agreement with the formulation[1-5,6-7] of iron(III) peroxychromate as $Fe_2(Cr_2O_{10})_3$.

Acknowledgement

The authors are thankful to Professor S. S. Sandhu, G. N. D. University, Amritsar, and Professor H. B. Saxena, Science College, Rewa, for suggestions and facilities.

References

1. H. J. EMELEUS and A. G. SHARPE, *Adv. Inorg. Chem. Radiochem.*, 1964, 6, 282, 300, 326.
2. S. P. S. JADON and D. S. RATHOR, *J. Indian Chem. Soc.*, 1976, 53, 527.
3. S. P. S. JADON, *Rev. Roum. Chim.*, 1981, 26, 1107.
4. A. BONNIN and A. LECERF, *Compt. rend.*, 1966, 262, 1782; 1968, 267, 1137.
5. I. M. KOLTHOFF and E. B. SANDELL, "Text Book of Quantitative Inorganic Analysis", 3rd. ed., MacMillan, London, 1955, p. 575.
6. B. UPADHYAY and S. C. TRIPATHI, *Chem. Pharm. Bull. Jpn.*, 1977, 25, 1.
7. N. MISHRA, S. TIWARI and B. M. L. TIWARI, *Vijnana Anusandhan Patrika*, 1984, 27, 46.
8. O. SAMUELSON, "Ion-Exchangers in Analytical Chemistry", John Wiley, New York, 1956, pp. 78-87, 133-39.
9. E. LEDERER and M. LEDERER, "Chromatography", Elsevier, New York, 1954, pp. 482-85.
10. F. D. SNELL and C. T. SNELL, "Colorimetric Methods of Analysis", Van Nostrand, New York, 1957, Vol. II, pp. 272-73, 307-10.
11. A. I. VOGEL, "A Text Book of Inorganic Quantitative Analysis", Longmans, London, 1959, pp. 456, 480.

Disproportionation of 4-Hydroxyazobenzene and Interaction with Copper(I)

P. N. GUPTA* and ANJU RAINA

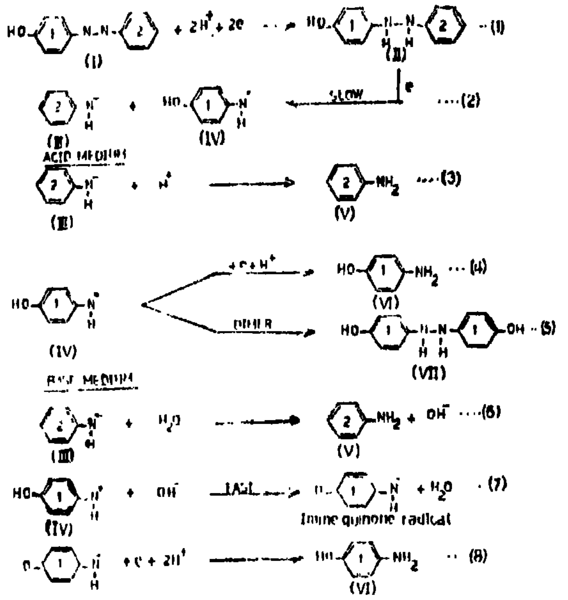
Department of Chemistry, University of Kashmir, Srinagar-190 006

Manuscript received 15 July 1985, accepted 17 January 1986

THE reduction of 4-hydroxyazobenzene at low concentration (for obvious reasons of maintaining the monomeric form[1] of the dye in solution) in Clark and Lubs (KH_2PO_4 and NaOH) buffer of pH 5.8-8.0 containing 1 M KCl at the dme gave a single well defined diffusion-controlled wave. The acidic ionisation constant of the compound was 6.7×10^{-8} under the experimental conditions and varies very slightly (pK_a 7.17 to 7.16) over the concentration range of 0.1-1.0 mM. The $E_{1/2}$ values shifted linearly with the change in pH according to the following equation,

$$E_{1/2}=0.08-0.07\,p\text{H}$$

The determined value of potential, $E^{0'}$ was -0.332 V at pH 6.5 which differed from the calculated value by -0.043 V, providing information that the reduction was not reversible. The substituent constants ($\rho=0.14$ and $\Sigma\sigma=-0.37$) were in confirmation with the work of various authors[2,3]. Several mechanistic pathways have been highlighted earlier[4,5] for the reduction of azo compounds. The proposed scheme (Scheme 1) of simultaneous protonation and electron transfer process, followed by slow electron attack to form radical (IV) and anion (III) is attributed to disproportionation reaction, presumably due to the strong electron attracting tendency of —OH in the moiety. Depending on the medium, the different set of products would be obtained, *e.g.* in acid, aniline (V) and 4-hydroxyaniline (VI), while in base, the latter is the only product. The possibility of remote reaction cannot be ruled out resulting in 4,4′-dihydroxyhydrazobenzene (VII) and aniline (V) in acid and base media respectively.



Scheme 1. Reduction scheme of 4-hydroxyazobenzene.

The addition of Cu^{I} (stock solution 0.75 mM) in dye solution (0.1 mM) was made in five steps ranging from 0.125 to 0.25 mM resulted in the following changes in the polarograms: (i) The wave height increased, (ii) $E_{1/2}$ shifted towards more negative potential and (iii) wave shape altered. The procedure was reversed with metal ion in cell while the adequate quantities of 4-hydroxyazobenzene was added. The polarograms showed dissimilar characteristics in the sense that a single composite anodic-cathodic wave[6] crossing base line at -0.24 V was noticed. This corresponds to the $E_{1/2}$ of the cathodic wave of Cu^{II} in this medium. The height of cathodic and anodic waves being equal favour disproportionation reaction at the dme. The log plot revealed linearity with a slope + 56 mV which indicates irreversible wave nature of Cu^{I} in this medium. The calculated $E_{3/4}-E_{1/4}$ resulted in $\propto n=0.923$, confirming irreversibility. The above observations indicate complexation.

Disproportionation[7] of Cu^{I} to Cu^{0} and Cu^{II} possessing high free energy change is a thermodynamically favourable reaction. This would certainly be induced by ligand which itself is capable of disproportionation. Stability parameters of complexes of Cu^{I} with the ligand in terms of changes in diffusion coefficient were evaluated by the method developed by Crow[8], which incorporates the change in diffusion current due to complexation in terms of ligand number, *i.e.*

$$\Delta i_d \propto \bar{n}.$$

The technique is applicable to reversible and irreversible processes alike. The difference in i_d values can be measured more accurately, therefore, it is advantageous over the methods which involve $E_{1/2}$ term.

The concentration of ligand bound to metal can be obtained from Bjerrum's treatment[9] (Table 1),

$$\bar{n}=(C_x-[x])/C_M$$

C_x, C_M and [x] are the total ligand, metal and free ligand concentrations, respectively. Calculations from the following expression,

$$\bar{n}=(1-\bar{n})\ \beta_1\ [x]+(2-\bar{n})\ \beta_2\ [x]^2$$

(by graphical method) gave stability constant β's in terms of $\bar{n}$ values as $\beta_1=15$, $\beta_2=1\times10^3$, $\beta_3=1.6\times10^5$ and $\beta_4=3.03\times10^6$. Similarly, the plots of $\bar{n}$ *vs* log [x] is in accordance with Fronaeus integral results in Fo [x] functions. Using these functions the following values of stability constants were obtained, $\beta_1=15.1$, $\beta_2=1.02\times10^3$, $\beta_3=1.59\times10^5$ and $\beta_4=3.01\times10^6$. In terms of equilibrium constant of each step it is found

$$\beta_1=K_1=15.1$$
$$\beta_2=K_1\ K_2=1.02\times10^3$$
$$\beta_3=K_1\ K_2\ K_3=1.59\times10^5$$
$$\beta_4=K_1\ K_2\ K_3\ K_4=3.01\times10^6$$

So that $K_2=67.5$, $K_3=155.8$ and $K_4=18.8$, indicating strong complexation in general. Comparing the two methods, the latter set of values seems more precise because of the involvement of exact integral functions. A clear cut inflection in the formation curve at $n\simeq4$ is probably due to Jahn-Teller effect, owing to which first 4 complexes of Cu are more stable. Further, Bjerrum method of corresponding

TABLE 1—LIGAND CONCENTRATION AND FORMATION FUNCTION

$C_x.10^4$	$[x].10^4$	$\bar{n}$	$\bar{n}/[x]$
1.0	0.75	0.025	500
3.0	1.50	0.014	933
5.0	2.5	0.270	1080
7.0	3.0	0.420	1400
10.0	3.8	0.590	1552
20.0	4.5	1.550	3444
30	8.75	2.120	2423
50	19.0	3.100	1613
100	63	3.70	587
200	165	3.95	239
300	260	4.00	154
400	360	4.125	114

solutions is suitable rather for less stable complexes. The hard ligand (−N=N−) can suitably interact with hard base Cu to justify high stability constant. The overall stability constant comes out characteristically as 7.37×10^{15} and is quite appropriate considering the type of the system under discussion. The free radical and the anion generated according to step 2 (Scheme 1) would initially be so reactive to interact with metal to present so called acid-base type neutrality. Evidently it would be likely that instead of four stepwise constants, only one β value could be ascertained. In other words, had there been fast electron attack, the above observation could be envisaged, however, it is not the case. This step could then be designated as slow step. Slow uptake of electron by hydrazo derivative has been depicted earlier[10] to proceed *via* radical ion formation only in alkaline medium, seems not well founded instead it should be independent of the medium as shown it Scheme 1. Parshall[11] during the course of study of metallation of azobenzenes, observed that substituent effect has direct relation with the complex formation reaction and that *para*-substituted molecules are more reactive otherwise as has been observed in this study.

Calculation of free energy changes and other thermodynamic parameters (Table 2) depict that absolute value of ΔF is increased from 1.546 to 9.059 kcal mol^{-1}, when the ligand number varied from 1 to 4. Complex formation in solution phase reaction favours such observation. Constancy in ΔH values indicates no effect of temperature during complexation (Table 2). Substantial changes in ΔS for the stepwise equilibrium is evident, resulting in $(\Delta S_3-\Delta S_2)>(\Delta S_2-\Delta S_1)$, which denotes that the stability constant in a series increases with the ligand number. However, $(\Delta S_4-\Delta S_3)$ is smaller than either of the two to provide information that further addition of ligand does not affect the equilibrium any more.

TABLE 2—CALCULATED THERMODYNAMIC PARAMETERS

Temp. °C	β_n	$-\Delta F$ kcal mol^{-1}	$-\Delta H$ (Graphically) kcal mol^{-1}	ΔS cal K^{-1} mol^{-1}
25	β_1 15.1	1.619		− 7.10
30	β_1 13.6	1.577		− 7.15
35	β_1 12.3	1.546	3.743	− 7.13
25	β_2 1020	4.130		+ 1.00
30	β_2 918	4.135		+ 1.015
35	β_2 826	4.138	3.827	+ 1.01
25	β_3 159000	7.138		+10.41
30	β_3 142000	7.190		+10.41
35	β_3 127000	7.240	4.035	+10.41
25	β_4 3010000	8.892		+16.85
30	β_4 2700000	8.975		+16.85
35	β_4 2430000	9.059	3.868	+16.85

A further probe into the complexation nature was worked out from the function[12], $f[x]=\bar{n}/[x]$ (Table 1). The function related to the stability constants by

$$\frac{\bar{n}}{[x]}=\beta_1+(2\beta_2-\beta_1^2)\,[x]+(3\beta_3-3\beta_1\,\beta_2+\beta_1^3)\,[x]^2$$

gives a maximum at about $[x]=4.5\times10^{-4}\,Ml^{-1}$ showing $2\beta_2>\beta_1^2$ (similarly, $\beta_3>\beta_1\,\beta_2-\beta_1^3/3$). An inference to this effect is that a relationship, $2K_2>K_1$ should exist between the formation constants of the first and second complex. The present study proves this beyond doubt. The increase in K_2 value is due to disproportionation step prior to complexation.

In order to describe complexation qualitatively a plot of log K_n *vs* f(n̄ − 1) has been drawn (Fig. 1). The higher values of K_1 and K_2 compared with

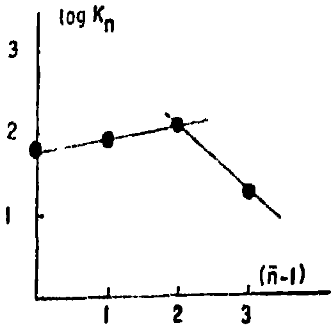


Fig. 1. Plot of log K_n *vs* (n̄ 1).

K_1 primarily reflects the presence of two possible structures, competing with each other. The tendency to form more stable structure (*i.e.* tetrahedral ones) is evident at *ca.* n̄=3 (Fig. 1). A sudden break indicates the conversion of stabler form into less stable structure which could have been observed at higher coordination number.

References

1. W. U. MALIK and P. N. GUPTA, *J. Electroanal. Chem. Interfacial Electrochem.*, 1975, **62**, 441 ; *Indian J. Chem., Sect. A*, 1977, **15**, 273.
2. T. M. FLORENCE, *J. Electroanal. Chem. Interfacial Electrochem.*, 1974, **52**, 115.
3. P. N. GUPTA and A. RAINA, *J. Indian Chem. Soc.*, 1985, **62**, 363.
4. W. U. MALIK and P. N. GUPTA, *J. Electroanal. Chem. Interfacial Electrochem.*, 1974, **54**, 417.
5. P. N. GUPTA, C. N. KACHRU and S. A. BHAT, *J. Electrochem. Soc. Jpn*, 1978, **46**, 92.
6. D. C. OLSON and J. VESILEVSKIS, *Inorg. Chem.*, 1971, **10**, 463.
7. J. K. SENNE, *Anal. Chem.*, 1971, **43**, 79 ; 1972, **44**, 585.
8. D. R. CROW, *J. Electroanal. Chem. Interfacial Electrochem.*, 1968, **16**, 137.
9. J. BJERRUM, *Chem. Rev.*, 1950, **46**, 381.
10. M. M. BAIZER, "Organic Electrochemistry", Dekker, New York, 1972, p. 336.
11. G. W. PARSHALL, *Acc. Chem. Res.*, 1970, **3**, 139.
12. B. LENARCIK, B. BARSZCZ and J. KULIG, *Rocz. Chemii*, 1977, **51**, 1315.

Effect of Ionic Surfactants on the Chromatographic Separation of Phenols

J. P. RAWAT* and ONKAR SINGH

Department of Chemistry, Aligarh Muslim University, Aligarh-202 001

Manuscript received 5 December 1983, revised 11 April 1985, accepted 2 December 1985

RECENTLY, the use of micellar systems in analytical techniques have been reviewed[1]. However, the use of surfactants has not been tried so far to study the movement of phenols on chromatographic papers. In this study we have made use of aqueous micellar (normal micellar) systems of different charge type in the separation of phenols. It is well known that the properties of micelles are drastically changed by the change of environment, hence the effect of alcohols and salts has been studied on the separation of phenols in the presence of such additives in the micellar systems.

This paper deals with the paper chromatography of 28 phenols of different types in aqueous sodium dodecyl sulphate (SDS) and cetyl trimethyl ammonium bromide (CTAB) systems. The effect of addition of propanol and electrolytes (NaCl and KBr) is also studied. The important separations, practically achieved, are reported.

Experimental

Chromatography was performed on Whatman No. 3 paper strips of size 15 × 3 cm using 20 × 5 cm glass jars.

Chemicals and solvents were of analytical grade. Sodium dodecyl sulphate (SDS) and cetyl trimethyl ammonium bromide (CTAB) were B.D.H. (England) products, which were further purified by repeated crystallisation from 95% ethanol followed by prolonged extraction from chloroform (100 h) and petroleum ether (60 h) to ensure the complete removal of traces of unreacted alcohol. It was then filtered and dried overnight in an hot air-oven to a constant weight. The purity of the surfactants was ensured from the absence of minimum in the surface tension *vs* concentration plots. The spotting solutions of phenols were prepared in ethanol. For the detection of various phenols, ferric chloride solution (0.1 *M*), sodium hydroxide solution (0.1 *M*) and 1% phosphomolybdic acid solution were used.

Procedure : Phenols were spotted with the help of fine glass capillaries on the strips. The paper was conditioned for 15 min and solvent was then allowed to ascend 11 cm in every case. The R_f values were calculated as usual.

Results

Detection : Phenols were easily detected on chromatograms. For the detection of various phenols, ferric chloride sodium hydroxide and phosphomolybdic acids were used. The variety of colours obtained with various types of phenols are as follows.

Phloroglucinol, catechol, xylenol, bromothymol blue, di(2-hydroxyphenylimino)ethane gave blue coloured spots.

In certain cases the use of sodium hydroxide spray was also made just after spraying ferric chloride to achieve clear detection. The colours observed with known phenols are as follows. *m*-Cresol and *p*-cresol gave brown spots. Resorcinol and gallic acid gave violet spots. 1-Nitroso-2-naphthol gave green spot. Pyrogallol gave blue spot.

8-Hydroxy-7-iodoquinoline-5-sulphonic acid and phenyl fluorone (9-phenyl-2,3,7-trihydroxy-6-fluorone) gave wine-red spots. *o*-Nitrophenol and picric acid gave yellow spots. Trihydroxy-6-fluorone and bromocresol green gave blue spots. Phenolphthalien gave pink spot. However, with some phenols where ferric chloride did not give satisfactory detection, the use of phosphomolybdic acid was made. The use of sodium hydroxide spray was also made just after spraying phosphomolybdic acid to achieve clear and quick detection. α-Naphthol, β-naphthol, *p*-nitrophenol, 2,4-dinitrophenol, 1,2,5,8-anthroxyanthraquinone, 4-chlorophenol and phenol gave blue spots. Quinol gave brown spots.

Chromatography: R_f values of the following 28 phenols in water and different concentrations of SDS and CTAB were calculated. Phenols studied were phlorogluoinol, α-naphthol, β-naphthol, 2,4-dinitrophenol, *p*-nitrophenol, catechol, *m*-cresol, *p*-cresol, phenol, resorcinol, gallic acid, *o*-nitrophenol, 1-nitroso-2-naphthol, xylenol, quinol, picric acid, vanilline, pyrogallol, bromothymol blue, 1,2,5,8-anthroxyanthraquinone, 4-(4-nitrophenyl)azoresorcinol, di(2-hydroxyphenylimino)ethane, 8-hydroxy-7-iodoquinoline-5-sulphonic acid, phenylfluorone (9-phenyl-2,3,7-trihydroxy-6-fluorone), trihydroxy-6-fluorone, 4-chlorophenol, bromocresol green, phenolphthelien.

The various solvent systems were (i) aqueous SDS system: 2, 4, 6, 8 and 10 mML^{-1} SDS; (ii) aqueous CTAB system: 0.1, 0.5, 0.7, 1.0 and 1.5 mML^{-1} CTAB; (iii) 2, 4, 6 and 8% propanol with SDS systems: 2, 4, 6, 8 and 10 mML^{-1} SDS; (iv) 2, 4, 6 and 8% propanol with CTAB systems: 0.1, 0.5, 0.7, 1.0 and 1.5 mML^{-1} CTAB; (v) 0.25, 0.05, 0.1 and 0.2 *M* NaCl with SDS systems: 2, 4, 6, 8 and 10 mML^{-1} SDS, (vi) 0.025, 0.05, 0.1 and 0.2 *M* KBr with CTAB systems: 0.1, 0.5, 0.7, 1.0 and 1.5 mML^{-1} CTAB.

The effect of propanol was studied on the movement of phenols in SDS and CTAB systems. The solutions of SDS and CTAB were prepared in propanol + water.

It is well known that the addition of electrolytes in the aqueous surfactant solution affects their properties. Aqueous micellar systems as such and in the presence of additives may influence the movement of phenols during the separation, hence various concentrations of sodium chloride and potassium bromide were added in the SDS and CTAB solution, respectively. These electrolytes were taken just as the representatives of the normal salts.

Separation: On the basis of difference in R_f values of phenols some analytically important separations were tried and those achieved practically are categorised as binary and ternary separations. The R_f values are given in paranthesis.

Binary separations of phenols achieved in 8% propanol with 8 mML^{-1} SDS are as follows: (i) phloroglucinol (0.91) from α-naphthol (0.46); β-naphthol (0.50), 2,4-dinitrophenol (0.46), *o*-nitrophenol (0.16), 1-nitroso-2-naphthol (0.58), vanilline (0.71), 1, 2, 5, 8-anthroxyanthraquinone (0.00), pyrogallol (0.67), di(2-hydroxyphenylimino)ethane (0.11), phenylfluorone (9-phenyl-2, 3, 7-trihydroxy-6-fluorone) (0.00); (ii) α-naphthol (0.46) from *p*-nitrophenol (0.71), catechol (0.95), *m*-cresol (0.95), *p*-cresol (0.78), phenol (0.89), resorcinol (0.65), gallic acid (0.73), quinol (0.72), picric acid (0.76), 4-chlorophenol (0.71), pyrogallol (0.67); (iii) β-naphthol (0.50) from *p*-nitrophenol (0.71), catechol, (0.95), *m*-cresol (0.95), *p*-cresol (0.78), phenol (0.89), xylenol (0.95), picric acid (0.76), thymol blue (0.98), phenolphthelien (0.78); (iv) 2,4-dinitrophenol (0.46) from catechol (0.95), *p*-nitrophenol (0.71), phenol (0.89), xylenol (0.95), picric acid (0.76), bromothymol blue (0.98), bromocresol green (0.92); (v) *p*-nitrophenol (0.71) from *o*-nitrophenol (0.16), xylenol (0.95), 4,4-nitrophenylazoresorcinol (0.80), bromocresol green (0.92); (vi) catechol (0.95) from *o*-nitrophenol (0.16), 1-nitroso-2-naphthol (0.58), 4-(4-nitrophenyl)azoresorcinol (0.08); (vii) *m*-cresol (0.95) from *o*-nitrophenol (0.16), 1-nitroso-2-naphthol (0.58); (viii) *p*-cresol (0.78) from *o*-nitrophenol (0.16), di(2-hydroxyphenylimino)ethane (0.11); (ix) phenol (0.89) from vanilline(0.71), *o*-nitrophenol (0.16); (x) resorcinol (0.65) from bromothymol blue (0.98), di(2-hydroxyphenylimino)ethane (0.11); (xi) gallic acid (0.73) from xylenol (0.95); (xii) *o*-nitrophenol (0.16) from quinol (0.72), picric acid (0.76), pyrogallol (0.67); (xiii) 1-nitroso-2-naphthol (0.58) from picric acid (0.76); (xiv) xylenol (0.95) from vanilline (0.71), quinol (0.72); (xv) picric acid (0.76) from 1,2,5,8-anthroxyanthraquinone (0.00), 4-(4-nitrophenyl)azoresorcinol (0.08); (xvi) vanilline (0.71) from bromothymol blue (0.98); (xvii) 4-chlorophenol (0.71) from bromocresol green (0.92).

Ternary separations of phenols achieved in 8% propanol with 8 mML^{-1} SDS are as follows: (i) phloroglucinol (0.91) and β-naphthol (0.50) from *p*-nitrophenol; (ii) 2,4-dinitrophenol (0.46) and *p*-nitrophenol (0.71) from *o*-nitrophenol (0.16); (iii) picric acid (0.76) and *o*-nitrohenol (0.16) from 2,4-dinitrophenol (0.46); (iv) *m*-cresol (0.95) and gallic acid (0.73) from 1, 2, 5, 8-anthroxyanthraquinone; (v) phenol (0.89) and α-naphthol (0.46) from 4-(4-nitrophenyl)azoresorcinol (0.08); (vi) *p*-nitrophenol (0.71) and *o*-nitrophenol (0.16) from 4-(4-nitrophenylazoresorcinol (0.08).

Discussion

The results of this study reveal that the nature of the solvent system differs considerably for the movement of various phenol. Use has been made of different solvent systems with variation in concentration and ratio of surfactants as well as that of the electrolytes. The results reveals that the R_f values of phenols are not much more affected by the higher concentration of added electrolytes (Fig. 1).

However, the selectivity is increased by the addition of surfactants.

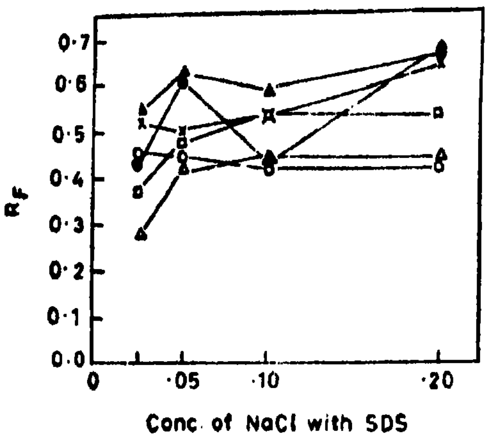


Fig. 1. Effect of SDS concentration on R_f value of α-naphthol in various concentration of NaCl : (○) NaCl ; (△) 2, (□) 4, (×) 6, (●) 8 and (▲)10 mM L^{-1} SDS.

The chromatography of phenol in these systems show differential selectivity which gives the differentiation of the R_f values, as a result the separation of isomeric phenols, *e.g.* *o*-nitrophenol from *p*-nitrophenol has been achieved. Various other important separations (binary and ternary) have been achieved in about 0.5 h using 8% propanol with 8 mML^{-1} SDS system as mobile phase.

The separations are quick and distinct zones are obtained on the paper (Fig. 2). The results show that a variety of aqueous micellar systems can be applied as mobile phase for interested separations.

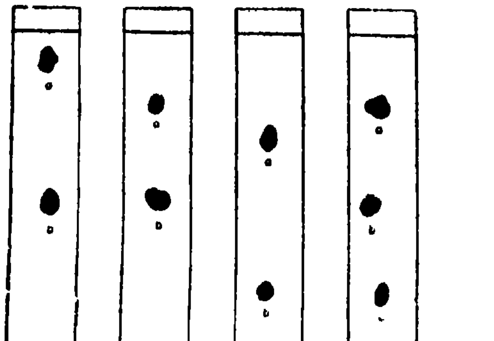


Fig. 2. Separations achieved in 8 mML^{-1} SDS : (Ia) phloroglucinol, (Ib) α-naphthol, (IIa) picric acid, (IIb) 2,4-dinitrophenol, (IIIa) *p*-nitrophenol, (IIIb) *o*-nitrophenol, (IVa) picric acid, (IVb) 2,4-dinitrophenol and (IVc) *o*-nitrophenol.

Acknowledgement

Financial support of U.G.C., New Delhi, is gratefully acknowledged. Thanks are also due to Professor W. Rahman, for facilities.

Reference

1. W. L. HINZE in "Solution Chemistry of Surfactants", ed. K. L. MITTAL, Plenum Press, New York, 1979, Vol. 1, p. 79.

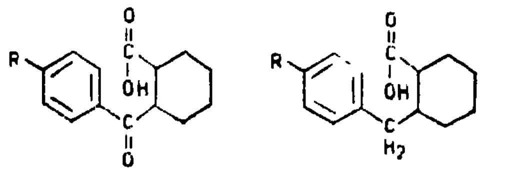
Cycloalkanes. Part-IV. Friedel-Crafts Condensation of *cis*-Cyclohexane-1,2-dicarboxylic Acid Anhydride with Aromatic Compounds and Synthesis of Simple and Substituted 2,3-Tetramethylene-5,6-benzcyclohexanes

K. C. MATHUR* and (Mrs.) LAJWANTI BHARGAVA

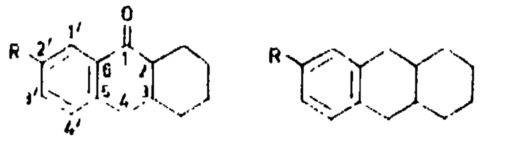
Department of Organic Chemistry, University of Jodhpur, Jodhpur-342 001

Manuscript received 23 October 1979, revised 15 December 1980, accepted 2 December 1985

THE Friedel and Crafts condensation between phthalic anhydride and simple, substituted and polynuclear aromatic hydrocarbons has been reported[1,2] in a bid to synthesise anthracene derivatives. However, no attempts have so far been made to condense *cis*-cyclohexane-1,2-dicarboxylic acid anhydride with aromatic hydrocarbons under Friedel-Crafts reaction conditions. We now report here the synthesis of simple and substituted 2,3-tetramethylene-5,6-benzcyclohexanes. The anhydride of *cis*-cyclohexane-1,2-dicarboxylic acid was



(1) (2)



(3) (4)

(a) R = H, (b) R = CH_3, (c) R = OCH_3

condensed separately with benzene, toluene and anisole in presence of anhydrous aluminium chloride to give the corresponding 2-aroylcyclohexane-1-carboxylic acids (1a-c) which were characterised by ir and tlc. These acids when reduced by Wolff-Kishner method[3] gave the corresponding 2-arylcyclohexane-1-carboxylic acids (2a-c) which were then converted into their chlorides by reaction with thionyl chloride. These acid chlorides when subjected to internal Friedel-Crafts reaction[4] furnished the corresponding cyclic ketones (3a-c) which on subsequent Wolff-Kishner reduction yielded the desired hydrocarbons (4a-c) (Table 1).

TABLE 1

Compd. no.	Aroyl	M.p. °C	Yield %	2,4-DNP M.p., °C	Mol. formula	ν_{max} cm^{-1}	Analysis % : Found (Calcd.) C	H
2-Aroylcyclohexane-1-carboxylic acid								
1a	Benzoyl	131-2	91.0	162	$C_{14}H_{16}O_3$	1 705 (C=O) 1 695 (C=O) 3 400–2 900 (OH)	72.60 (72.41)	7.24 (6.90)
1b	4′-Methylbenzoyl	103-4	91.8	145	$C_{15}H_{18}O_3$	1 700 (C=O) 1 690 (C=O) 3 300–2 850 (OH)	73.50 (73.17)	7.36 (7.32)
1c	4′-Methoxybenzoyl	105	54.7	100	$C_{15}H_{18}O_4$	1 700 (C=O) 1 685 (C=O) 3 400–2 850 (OH)	68.46 (68.70)	6.51 (6.87)
2-Arylcyclohexane-1-carboxylic acid								
2a	Benzyl	97	60.9		$C_{14}H_{18}O_2$	1 705 (C=O) 3 400–2 900 (OH)	77.42 (77.06)	8.51 (8.26)
2b	4′-Methylbenzyl	122	60.7		$C_{15}H_{20}O_2$	1 700 (C=O) 3 300–2 850 (OH)	77.66 (77.59)	8.58 (8.62)
2c	4′-Methoxybenzyl	195	60.8		$C_{15}H_{20}O_3$	1 700 (C=O) 3 400–2 800 (OH)	72.78 (72.58)	8.16 (8.06)
2,3-Tetramethylene-substitued-5,6-benzcyclohexan-1-one								
3a	–	80	88.2	92	$C_{14}H_{16}O$	1 700	84.39 (84.00)	8.25 (8.00)
3b	2′-Methyl	86	84.3	115	$C_{15}H_{18}O$	1 690	84.36 (84.11)	8.40 (8.41)
3c	2′-Methoxy	90	83.3	119-20	$C_{15}H_{18}O_2$	1 690	78.43 (78.26)	7.56 (7.83)
2,3-Tetramethylene-substituted-5,6-benzcyclohexane								
4a	–	59-60	90.5		$C_{14}H_{18}$		90.54 (90.32)	9.45 (9.68)
4b	2′-Methyl	126	90.3		$C_{15}H_{20}$		90.05 (90.00)	9.94 (10.00)
4c	2′-Methoxy	77-8	79.1		$C_{15}H_{20}O$		83.64 (83.33)	9.55 (9.26)

It was further observed that the condensation of *cis*-cyclohexane-1,2-dicarboxylic acid anhydride with benzene and toluene was carried out using the same medium as solvent and the keto acids (1a and b) were obtained in about 91% yield. When anisole was condensed under similar conditions poor yields of the keto acid was obtained. However, the keto acid (1c) was obtained in improved yields when anisole was condensed with the anhydride using nitrobenzene as the medium.

Experimental

All melting points are uncorrected. Infra-red spectra (nujol) were recorded on a Carl Zeiss, Jena Specord IR-75 spectrophotometer.

General procedure :

2-Aroylcyclohexane-1-carboxylic acid : *cis*-Cyclohexane-1,2-dicarboxylic acid anhydride (0.064 mol) was dissolved in dry aromatic hydrocarbon (42 ml) and powdered anhydrous aluminium chloride (0.128 mol) was added in small lots with frequent shaking. After storing the red coloured solution overnight, the complex was decomposed with ice-cold hydrochloric acid. Excess of the aromatic hydrocarbon was removed by steam distillation, the product extracted with ether, washed, dried and ether recovered. Pure keto acid was obtained on crystallisation from benzene.

2-Arylcyclohexane-1-carboxylic acid : The keto acid (0.02 mol) was dissolved in diethylene glycol (40 ml), potassium hydroxide (0.08 mol) and hydrazine hydrate (3.7 ml, 80%) were added and the mixture refluxed at 130-140° for 1 h. The condenser was then removed and the internal temperature was slowly raised to 190-5°. The condenser was replaced and the mixture refluxed for further 3 h at this temperature. The contents were then cooled, acidified with hydrochloric acid, extracted with ether, washed, dried and ether recovered. 2-Arylcyclohexane-1-carboxylic acid was obtained on crystallisation from benzene.

2,3-Tetramethylene-substituted-5,6-benzcyclohexane-1-one : To dry benzene (48 ml) reduced acid (0.018 mol) and thionyl chloride (9.6 ml) were added and the mixture refluxed for 3 h. After

removal of excess of thionyl chloride and benzene under reduced pressure, carbon disulphide (48 ml) and powdered anhydrous aluminium chloride (0.018 mol) were added to the residue and the mixture refluxed for further 3 h and then stored overnight at room temperature. Carbon disulphide was then removed and the complex hydrolysed with ice-cold hydrochloric acid. The product was then extracted with chloroform. The chloroform extract was successively washed with water, dilute hydrochloric acid, sodium bicarbonate solution (5%) and finally with water, dried and chloroform recovered. Pure cyclic ketone was obtained on crystallisation from benzene-petroleum ether.

2,3-Tetramethylene-substituted-5,6-benzcyclohexane: A mixture of cyclic ketone (0.012 mol), diethylene glycol (20 ml), potassium hydroxide (0.048 mol) and hydrazine hydrate (1.7 ml, 80%) was refluxed for 1 h at 130-140°. The condenser was then removed and the internal temperature was slowly raised to 190-5°. The condenser was replaced again and the mixture refluxed for further 3 h. The contents were cooled, acidified with hydrochloric acid, extracted with ether, washed, dried and ether recovered. The residue gave pure hydrocarbon on crystallisation from benzene-petroleum ether.

References

1. M. S. NEWMAN and C. D. MCCLEARY, *J. Am. Chem. Soc.*, 1941, 63, 1540.
2. B. B. BARNET and N. R. CAMPBELL, *J. Chem. Soc.*, 1935, 1031.
3. HUANG-MINLON, *J. Am. Chem. Soc.*, 1946, 68, 2487.
4. D. GINSBURG, *J. Chem. Soc.*, 1954, 2361.

Preparation of Arylazo-bis-acetoximes

NIZAMUDDIN

Department of Chemistry, B. N. College, Udaipur-313 001

and

D. N. PUROHIT*

Department of Chemistry, College of Science, Sukhadia University, Udaipur-313 001

Manuscript received 27 January 1984, revised 15 October 1985, accepted 2 December 1985

IN an earlier communication, the preparation of ten new hydroxytriazenes was reported by the authors[1], in view of the importance of this class of reagents in analytical chemistry. The arylazo-bis-acetoximes also have the same chelating moiety as hydroxytriazenes.

Mai[2] discovered a group of substances conveniently called as arylazo-bis-oximes by coupling diazonium salts (1 mol) with ald- or ket-oximes (2 mol). Bamberger[3] proved that arylazo-bis-oxime have the hydroxytriazene skeleton. Elkins and Hunter[4] reported preparation of six arylazo-bis-oximes and preparation of their nickel, cobalt, copper and iron complexes. Subsequently, Bhargawa and Sogani[5] reported the preparation of four arylazo-bis-oximes and screened for their utility in gravimetric analysis of copper and nickel.

The present communication describes the preparation of fourteen arylazo-bis-acetoximes and some of their physical properties. Qualitative spot test with α-naphthylamine has also been developed.

Experimental

Freshly prepared acetoxime (2 mol) was dissolved in 10% sodium hydroxide solution and then cooled to 0° by adding some crushed ice to it and kept in ice-bath. A diazotised salt solution of the substituted anilines (1 mol) was then added slowly under mechanical stirring to this solution. The *p*H was always maintained at ~ 10 and the temperature during the entire course of addition being kept at 0°. The crude compounds obtained are mostly dark coloured. The crude product in each case was washed twice with petroleum ether (b.p. 40-60°) to remove the coloured impurities, and recrystallised from ethanol-water mixture. The physical characteristics of the compounds are summarised in Table 1.

Two methods for the spot test detection of hydroxytriazenes were reported by Purohit[6]. The basis of the first test is the formation of pink colour when an acetic acid solution of α-naphthylamine is added to an acetic acid solution of hydroxytriazenes. In the second method, addition of 2 to 5 drops of a saturated ethanolic solution of picric acid to either a pinch of solid hydroxytriazene or a drop of its ethanolic solution gives a pink or red colour or precipitate. Spot test detection of arylazo-bis-acetoxime series of compounds with α-naphthylamine has been developed for the first time. However, with picric acid these have failed to respond to the test.

One drop of arylazo-bis-acetoxime solution in acetic acid (0.001%, w/v) was treated in a small test tube with a drops of acetic acid solution (0.01%, w/v) of α-naphthylamine. Pink or reddish brown colour developed immediately. Gentle warming of the test solution further intensified the colour. The test was performed with seventeen arylazo-bis-acetoxime compound. The results of the test are given in Table 1.

Discussion

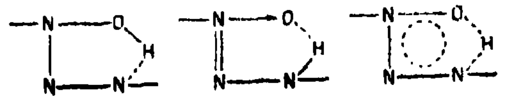
Hydroxytriazenes are reported to exist in intramolecular hydrogen bonded form (III). This group of compounds have also been named as triazene-oxide on the basis of possible existence of its tautomeric form (II).

TABLE 1—ARYLAZO-BIS-ACETOXIME COMPOUNDS

Sl. no.	Aryl	Colour, shape of crystals	M.p.	Analysis % : Found/(Calcd.)* C	H	N	Colour with α-naphthylamine
1.	*m*-Methylphenyl	Reddish brown, tiny	119°	59.10 (59.07)	7.48 (7.63)	20.63 (21.19)	Reddish brown colour on warming and then cooling
2.	*o*-Carboxyphenyl	White silky, flakes	102°	53.32 (53.05)	6.03 (6 16)	18.76 (19.03)	No action. Test not given
3.	*m*-Carboxyphenyl	Light reddish brown, tiny	174°	52 88 (53.05)	6.10 (6.16)	18.91 (19.03)	No change in colour. Test not given
4.	*p*-Carboxyphenyl	Light brown, fine	140°	53.17 (53.05)	5.90 (6.16)	18.68 (19.03)	No change in colour. Test not given
5.	*o*-Nitrophenyl	Yellow, large rectangular	48°	48 64 (48.80)	5.66 (5.80)	23.61 (23.72)	Light pink colour on gentle warming
6.	*m*-Nitrophenyl	Light brown, needless	50°	48.69 (48.80)	5.72 (5.80)	23.60 (23.72)	Pink colour on warming
7.	*p*-Nitrophenyl	Yellow, needless	69°	48.94 (48.80)	5.69 (5.80)	23.43 (23.72)	Pink colour on warming
8.	*o*-Chlorophenyl[a]	Brown, fine	111°	51.18 (50.62)	5.95 (6.02)	19.40 (19.68)	Violet red colour on slight warming
9.	*m*-Chlorophenyl[b]	Dark violet red, small	111°	50.41 (50.62)	5.98 (6.02)	19.52 (19.68)	Immediate pink colour in cold, intensified on heating
10.	*p*-Chlorophenyl[c]	Black, needles	113°	50.13 (50.61)	5.99 (6.02)	19.21 (19.68)	Immediate pink colour in cold, intensified on heating.
11.	*p*-Bromophenyl[d]	Yellow, needles	144°	43.61 (43.78)	5.39 (5.20)	17.61 (17.02)	Red colour on slight warming
12.	*o*-Methoxyphenyl	Violet, tiny	98°	55.89 (55.70)	7.28 (7.19)	19.66 (19.99)	Reddish brown colour on warming
13.	*m*-Methoxyphenyl	Blackish brown, fine	103°	55.56 (55.70)	6.87 (7.19)	19.63 (19.99)	Reddish brown colour on warming
14.	*p*-Methoxyphenyl	Shining brown, tiny	139°	55.81 (55.70)	7.02 (7.19)	19.75 (19.99)	Reddish brown colour on warming

*Halogen % : [a]Cl, 12.04 (12.44) ; [b]Cl, 12.67 (12.44) ; [c]Cl, 12.13 (12.44) ; [d]Br, 23.82 (24.27).

It has been observed that arylazo-bis-acetoximes do not give spot tests with picric acid but give a positive spot test with α-naphthylamine. This may be indicative of a greater contribution of hydroxy-triazene form (I) towards the final structure. The negative picric acid test can also be interpreted to mean that the contribution of triazene-oxide form (II) is either altogether absent or is negligible and that arylazo-*bis*-acetoximes might be existing predominantly in form I.



(I) (II) (III)

Acknowledgement

The authors are thankful to U.G.C., New Delhi, for the award of Teacher Research Fellowship to one of them (N.).

References

1. D. N. PUROHIT and NIZAMUDDIN, *J. Indian Chem. Soc.*, 1983, 60, 712.
2. J. MAI, *Chem. Ber.*, 1892, 25, 1685.
3. E. BAMBERGER, *Chem. Ber.*, 1896, 29, 104; 1897, 30, 2280; 1899, 32, 1677; 1900, 30, 3510; 1899, 33, 1546.
4. M. ELKINS and L. HUNTER, *J. Chem. Soc.*, 1940, 653.
5. S. P. BHARGAVA and N. C. SOGANI, *J. Indian Chem. Soc.*, 1971, 48, 1113.
6. D. N. PUROHIT, *Anal. Chim. Acta*, 1973, 63, 493; 1973, 66, 468.

Raney Nickel Desulphuration of Cyclic Nitrogen and Sulphur containing Compounds. Desulphuration of 1,2,4-Thiadiazolidines

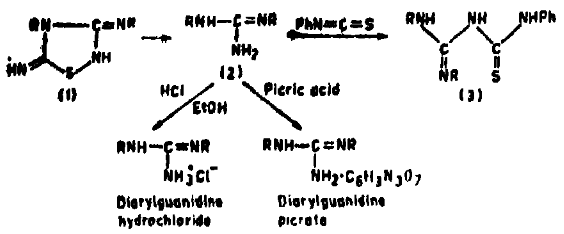
M. UMAR ALI and M. G. PARANJPE*

Department of Chemistry, Nagpur University, Nagpur-440 010

Manuscript received 28 December 1983, revised 16 April 1985, accepted 2 December 1985

RECENTLY, we have carried out the desulphuration studies of certain acyclic thioamido group containing compounds[1,2] in the presence of Raney nickel (W-2). The present paper describes the Raney nickel desulphuration of certain cyclic thioamido group containing system.

When 5-imino-4-phenyl-3-phenylimino-1,2,4-thiadiazolidine (1a) was desulphurated in boiling ethanolic medium in the presence of Raney nickel (W-2), a pale yellow solution was produced. This on removing the solvent, afforded a solid crystallised from ethanol, m. p. 150°. This product neither reduced Fehling's solution nor Tollen's reagent. It formed a hydrochloride, m.p. 137° and a picrate, m.p. 170° by its interaction with cold concentrated HCl and aqueous picric acid, respectively. On reaction with phenyl isothiocyanate it produced 1-(*N*, *N'*-diphenyl)formamidino-3-phenylthiourea (3a), m. p. 165-66° (Scheme 1).



where, R = a, phenyl ; b, *p*-tolyl ; c, *o*-tolyl ; d, *m*-tolyl ; e, *p*-chlorophenyl ; f, *m*-chlorophenyl ; and g, *p*-anisyl.

Scheme 1

On the basis of all the above facts, the product with m.p. 150° was identified as 1,3-diphenylguanidine (2). Its identify was also confirmed through its undepressed m.m.p. with authentic sample and superimposable ir spectra. The desulphuration of 1a in boiling benzene medium also afforded 1,3-diphenylguanidine (2a).

All the other 4-aryl-3-arylimino-5-imino-1,2,4-thiadiazolidines (1b-g) on Raney nickel desulphuration in both ethanolic and benzene media afforded the corresponding 1,3-diarylguanidines (2b-g) and the latter on reaction with phenyl isothiocyanate produced 1-(*N,N'*-diaryl)formamidino-3-phenylthioureas (3a-g) (Table 2).

Experimental

Raney nickel was prepared as usual[3]. The required phenyl isothiocyanate was prepared by the oxidative decomposition of ammonium phenyldithiocarbamate[4] in the presence of lead nitrate. 1-Arylthioureas were prepared by the interaction of ammonium thiocyanate and arylamine hydrochloride[5]. The so-called Hector's bases were prepared according to the procedure described earlier[6], *viz.* by the oxidation of an appropriate arylthioureas with hydrogen peroxide followed by basification with dilute ammonium hydroxide.

Desulphuration of 1,2,4-thiadiazolidines (1). *Formation of 1,3-diarylguanidines* (2) : Details of a typical desulphuration reaction of the 1,2,4-thiadiazolidine (1a) are as follows. A suspension of 1a (5.4 g, 0.02 mol) in ethanol (50.0 ml) was added to a

Table 1—4-Aryl-3-arylimino-5-imino-1,2,4-thiadiazolidines (1)

Compd. no.	1-Arylthiourea (g)	1 (g) m.p. °C	Analy : % Found/(Calcd.) N	S
1a	Phenyl (7.6)	4-Phenyl-3-phenylimino (4.7), 182	21.23 (20.89)	11.72 (11.94)
b	*p*-Tolyl (8.3)	4-*p*-Tolyl-3-*p*-tolylimino (5.4), 132	19.19 (18.91)	10.63 (10.81)
c	*o*-Tolyl (8.3)	4-*o*-Tolyl-3-*o*-tolylimino (5.0), 175	19.32 (18.91)	10.38 (10.81)
d*	*m*-Tolyl (8.3)	4-*m*-Tolyl-3-*m*-tolylimino (4.8), 110	19.25 (18.91)	10.57 (10.81)
e*	*p*-Chlorophenyl (9.3)	4-*p*-Chlorophenyl-3-*p*-chloropnenylimino (5.6), 159	17.05 (16.61)	9.27 (9.49)
f*	*m*-Chlorophenyl (9.3)	4-*m*-Chlorophenyl-3-*m*-chlorophenylimino (5.5), 172	16.82 (16.61)	9.16 (9.49)
g*	*p*-Anisyl (9.1)	4-*p*-Anisyl-3-*p*-anisylimino (4.5), 75	17.28 (17.07)	9.43 (9.76)

* Prepared for the first time.

Table 2—Raney Nickel Desulphuration of some 4-Aryl-3-arylimino-5-imino-1,2,4-thiadiazolidines (1)

Sl. no.	Aryl substituent	1,2,4-Thiadiazolidine (1) (g)*	Product: Diarylguanidine (2) (g)	M.p. °C	Yield %	N% : Found/(Calcd.)	Hydrochloride M.p. °C	Picrate M.p. °C	Amidinothiourea (3) M.p. °C	Analysis % : Found/(Calcd.) N	S
1.	Phenyl	1a (5.4)	2a (3.4)	150	80	19.65 (19.90)	138	170	3a 165	16.35 (16.18)	9.05 (9.25)
2.	*p*-Tolyl	1b (5.9)	2b (3.9)	173	81	17.28 (17.57)	100	155	3b 137	14.49 (14.97)	8.23 (8.55)
3.	*o*-Tolyl	1c (5.9)	2c (3.7)	179	78	17.72 (17.57)	184	167	3c 175	14.72 (14.97)	8.33 (8.55)
4.	*m*-Tolyl	1d (5.9)	2d (3.6)	110	76	17.09 (17.57)	160	185	3d 139	15.05 (14.97)	8.07 (8.55)
5.	*p*-Chlorophenyl	1e (6.7)	2e (4.5)	138	80	14.46 (15.00)	180	214	3e 137	13.52 (13.49)	7.58 (7.71)
6.	*m*-Chlorophenyl	1f (6.7)	2f (4.3)	141	76	15.23 (15.00)	200	180	3f 135	13.42 (13.49)	7.29 (7.71)
7.	*p*-Anisyl	1g (6.6)	2g (4.1)	158	75	15.49 (15.50)	195	112	3g 132	13.97 (13.79)	7.53 (7.88)

*1 and Raney nickel taken in 1 : 5 ratio. Satisfactory C and H analyses obtained in all cases.

suspension of Raney nickel (W-2 ; 27.0 g) in ethanol (100.0 ml) and the resulting mixture was refluxed with constant stirring for 150 min. The used-up Raney nickel was removed by hot filtration. The solvent was distilled out from the filtrate, and the resulting solid was crystallised from ethanol to yield the product (2a) (3.4 g, 80%), m.p. 150° (Found : N, 19.65. Reqd. for $C_{13}H_{12}N_3$: N, 19.90%) ; ν_{max} 3 375 (NH), 1 635 (C=N), 1 372 (Ar), 1 295 (C—N) and 1 070 cm^{-1} (Ar—Cl)[7-9] ; δ 7.05-7.40 (ArH) ; 2a afforded a hydrochloride when treated with concentrated hydrochloric acid, m.p. 138° (Found : Eq. wt., 240.8. Reqd. for $C_{13}H_{12}N_3$. HCl : Eq. wt, 247.5) ; its ethanolic solution when mixed with aqueous picric acid gave a picrate, m.p. 170° (Found : N, 19.39. Reqd. for $C_{13}H_{13}N_3 \cdot C_6H_3N_3O_7$: N, 19.09%).

Formation of 3a : To a solution of 2a (0.5 g) in ethanol (25.0 ml) phenyl isothiocyanate (0.5 ml) was added, and the mixture refluxed for 150 min. The solvent was then removed by distillation and 1 - (*N, N'*-diphenyl) formamidino-3-phenylthiourea (3a) crystallised from ethanol (0.7 g), m.p. 165° (Found : N, 16.35 ; S, 9.05. Reqd. for $C_{20}H_{18}N_4S$: N, 6.18 ; S, 9.25%) ; ν_{max} 3 370 (NH), 1 550 (C=N) 1 370 (Ar) and 1 300 cm^{-1} (C—N) ; δ 6.69-6.93 (ArH).

Acknowledgement

One of the authors (M.U.A.) wishes to express thanks to Prof. K. N. Munshi for providing facilities and to the Ministry of Education, Government of India, for the award of a scholarship.

References

1. M. Umar Ali and M. G. Paranjpe, *J. Indian Chem. Soc.*, 1985, 62, 666.
2. M. Umar Ali and M. G. Paranjpe, *Indian J. Chem., Sect. B*, 1984, 23, 573.
3. R. Mozingo, *Org. Synth.*, 1965, 3, 181 ; 1941, 21, 15.
4. A. I. Vogel, "A Text Book of Practical Organic Chemistry", 4th ed., Longmans, London, 1978, p. 736.
5. H. Krall and R. D. Gupta, *J. Indian Chem. Soc.*, 1935, 12, 629.
6. D. S. Hector, *Ber. Dtsch. Chem. Ges.*, 1889, 22, 1176 ; K. B. Lal and H. Kral, *J. Indian Chem. Soc.*, 1939, 16, 31 ; C. P. Joshua, V. K. Verma and K. S. Suresh, *Tetrahedron Lett.*, 1961, 19, 663.
7. A. D. Cross and R. A. Jones, "An Introduction to Practical Infrared Spectroscopy", Plenum, New York, 1969.
8. R. M. Silverstein and G. C. Bassler, "Spectrometric Identification of Organic Compounds", John Wiley, New York, 1963.
9. N. B. Colthup, L. H. Daly and S. B. Wiberley, "Introduction to Infrared and Raman Spectroscopy", Academic Press, New York, 1964.

Isolation of 16-Hentriacontanone, Alcohols and Sterols from the Leaves of *Annona squamosa*

MUKAT BEHARI* and RAJESH KUMAR SHARMA

Research Laboratories, S. V. College, Aligarh-202 001

Manuscript received 17 May 1983, revised 14 November 1983, accepted 9 March 1984

THE leaves of *Annona squamosa* (Annonaceae) commonly known as Sarifah, are widely used as anthelmintic and also for other ailments[1]. They contain an acrid principle fatal to insects[2] and used to kill lice[3]. The alcoholic extract of the leaves is reported to have anticancer[4] activity. The survey of literature revealed that no other work except the isolation of alkaloids[4,5] and essential oils[6] from the leaves has so far been carried out. The present note deals with the chemical examination of petroleum ether extractives of the leaves of this plant.

The air dried leaves of *A. squamosa* collected from the surroundings of Aligarh were extracted with petroleum ether (b.p. 60-80°). The unsaponifiable fraction on column chromatography over silica gel was separated into three fractions.

Ketone : This fraction was obtained on elution of the column with petroleum ether-benzene (1 : and purified with methanol as white amorphous powder, m.p. 83-84° ; R_f 0.90 and ν_{max} 1 700 cm^{-1} (ketone). Gc-mass over OV-17 showed the single peak having molecular ion peak at *m/e* 450 and other peaks at *m/e* 254 and 239. It was identified 16-hentriacontanone on the above basis and by preparing its oxime, m.p. 57-58°.

Alcohols : This fraction was obtained on elution of the column with petroleum ether-benzene (2 : and purification from methanol as white solid, m. 85-86° ; R_f 0.40 ; ν_{max} 1 070 and 3 200 cm^{-1}. Glc analysis over SE-30 represented it to be mixture a homologous series of aliphatic alcohols with maximum participation of n-hexacosanol (C_{26}, 39%), n-octacosanol (C_{28}, 36%) and n-triacontanol (C_{30}, 19%) along with other homologues in small quantities. Even-carbon number alkanols[7] were dominated.

Sterols : This fraction was obtained on further elution of the column with benzene and purified with methanol. It gave positive Liebermann Burchard test and R_f 0.15. Its acetyl derivative was found to be a mixture of 24-methylcholest-5-ene-3β-ol (campesterol), 24-ethylcholesta-5, 22-diene-3β-ol (stigmasterol) and 24-ethylcholest-5-ene-3β-ol (β-sitosterol) identified as acetate on the basis of co-argentation tlc. The major product, sitosteryl acetate was separated from the plate and was identified on the basis of co-tlc and m. m. p. The acetyl derivative on glc analysis over OV-17 confirmed the presence of campesterol (RRt=1.31, 28.6%), stigmasterol (RRt=1.42, 4.6%) and β-sitosterol (RRt=

1.62, 66.7%). RRt of sterol acetates were given relative to cholesterol.

The interesting observations reported earlier that alkanols[8] possess antiinflammatory activity comparable with β-methasone and β-sitosterol[9] possesses antiinflammatory activity, similar to hydrocortisone and oxyphenabutazone and antipyretic activity similar to acetyl salicylic acid, suggest that the presence of sterols and alkanols in the leaves of this plant might be responsible for its medicinal value.

Tlc (silica gel) plates were developed with carbon tetrachloride-ethyl acetate (95 : 5) for determining R_f values, whereas argentation tlc plates (silica gel-20% silver nitrate) were developed five times with methylene chloride-carbontetrachloride (1 : 5, v/v) for separation of acetyl derivatives of sterols.

Acknowledgement

The authors are grateful to Dr. S. C. Gupta, Principal, S. V. College, Aligarh, for providing facilities. Thanks are due to Prof. T. Matsumoto, Japan, for glc analysis, Dr. I. S. Ahuja for ir spectra and C.S.I.R., New Delhi, for the award of Junior Research Fellowship to one of the authors (R.K.S.).

References

1. G. V. SATYAVATI, "Medicinal Plants of India", I.C.M.R., New Delhi, 1976, Vol. 1, pp. 75-76.
2. R. N. CHOPRA, "Indigenous Drugs of India", Calcutta, 1958, p. 577.
3. K. R. KIRTIKAR and B. D. BASU, "Indian Medicinal Plants", Delhi, 1975, Vol. 1, p. 67.
4. D. S. BHAKUNI, *Phytochemistry*, 1976, 18, 1584.
5. H. WANGE, M. REITER and W. FERSTL, *Planta Medica*, 1960, 40, 75.
6. R. N. CHOPRA, "Supplement of Glossary of Indian Medicinal Plants", C.S.I.R., New Delhi, 1974, p. 6.
7. M. BEHARI, C. K. ANDHIWAL and M. STREIBL, *Coll. Czech. Chem. Commun.*, 1977, 42, 1385.
8. K. BASU, B. DASGUPTA, S. K. BHATTACHARYA, R. LAL and P. K. DAS, *Curr. Sci.*, 1971, 40, 86.
9. M. B. GUPTA, R. NATH, N. SHRIVASTAVA, K. SHANKER, K. KISHORE and K. P. BHARGAVA, *Planta Medica*, 1980, 39, 157.

Spectrophotometric Studies on Bisulphite-salicyldehyde Compound

S. P. CHATTOPADHYAY and ARABINDA K. DAS*

Department of Chemistry, University of Burdwan, Burdwan-713 104

Manuscript received 12 September 1983, revised 28 June 1985, accepted 2 December 1985

THE addition compound between carbonyl group and bisulphite ion has an importance since it is a basis for the determination of many aldehydes and ketones[1]. A series of aldehyde-bisulphite compounds have been studied and their dissociation constants were determined by Kerp and Bauer[2]. Regarding spectrophotometric studies, a furfural-bisulphite complex have been described earlier[3].

The present method may be used for the estimation of microgram quantities of bisulphite ion. The spectrophotometric studies can also be used to obtain quantitative information of aldehyde-sulphite equilibria.

Experimental

A 0.095 *M* stock solution of salicyldehyde (B.D.H., England) in ethanol-water (40%, v/v) was used. A 0.0034 *M* sulphite solution was prepared by dissolving reagent grade $Na_2S_2O_5$ (E. Merck, G.R.) in double-distilled water. All other chemicals used were reagent grade. All aqueous solutions were made by using double-distilled water.

Absorbance measurements were made on a Beckman 26 double beam uv-visible spectrophotometer equipped with 1 cm quartz cells. A Systronics 331 expanded scale *p*H meter equipped with glass electrode was used for *p*H measurements.

Procedure for the determination of sulphite : To an aliquot (0.5-2.0 ml) of the salicyldehyde solution (9.54×10^{-4} *M*) were added various amounts (0.5-6.0 ml) of a solution containing 50.0 to 550.0 μg sulphite. *p*H of the solution was adjusted between 3.5 to 6.0 followed by addition of sodium dihydrogen phosphate buffer (1.0 ml). The volume of the resulting mixture was brought up to the mark in a 10 ml volumetric flask. The absorbance was measured at 256 nm after 30 min against the reagent blank.

Results and Discussion

Absorbance spectra : The absorbance value of salicyldehyde was found to decrease due to the formation of a complex with bisulphite ion. Fig. 1 shows typical absorption curves (λ_{max} =256 nm) for salicyldehyde and bisulphite-salicyldehyde complex.

Working range : The absorbance values of several salicyldehyde solutions containing known amounts of sulphite were taken. In all cases, blanks were used as references. It was found that the absorbance values gradually decreased with the addition of sulphite. It is seen from Fig. 2 that such a decrease occurs linearly upto 55.0 ppm sulphite, and further addition of sulphite causes deviation from linearity. Thus, the working range for the determination of sulphite by using salicyldehyde has been found to be upto 55.0 ppm with the detection limit[4] of 2.4 ppm.

Effect of pH and diverse ions : The absorbance values of solutions were sensitive to *p*H. Below *p*H 3.5, no appreciable[5] absorbance difference between bisulphite ion and salicyldehyde was detectable. Above this *p*H, with the formation of higher amounts of bisulphite-salicyldehyde complex, the absorbance difference ($\bar{D}$) remained the same until

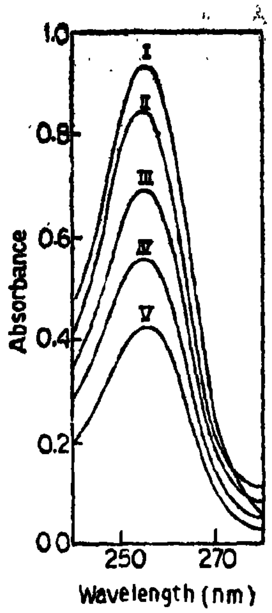


Fig. 1. Absorbance spectra: (I) salicyldehyde solution only; in presence of (II) 20.5, (III) 44.0, (IV) 88.0 and (v) 147.0 ppm sulphite.

The tolerance limits of diverse ions (within an error of ± 2%) were studied. The results indicated that for determination of 27.6 ppm sulphite, no interference was caused by 500 ppm of chloride (as NaCl), nitrate (as $NaNO_3$), sulphate (as Na_2SO_4); 200 ppm of fluoride (as NaF), tartarate (as Na-K-tartarate), EDTA (as Na-EDTA); 100 ppm of Mn^{II} (as $MnSO_4$), Cd^{II} (as $CdSO_4$), Zn^{II} (as Zn-acetate). Fe^{III}, iodide, thiosulphate and thiocyanate ions have been found to interfere.

Nature of the compound: The Job's method of continuous variations[6] was applied by mixing varying proportions of equimolar solutions of salicyldehyde and sulphite. The difference ($\bar{D}$) between the absorbance of each mixture and the value which would have been obtained had no reaction with bisulphite occurred, was calculated. This was plotted against the ratio (R) of the sulphite concentration to the total concentration of sulphite and salicyldehyde. A representative result for solutions with total molarity of 1.18×10^{-4} *M* for sulphite plus salicyldehyde at *p*H 5 and temperature 34° are shown in Fig. 3. The minimum indicates that a

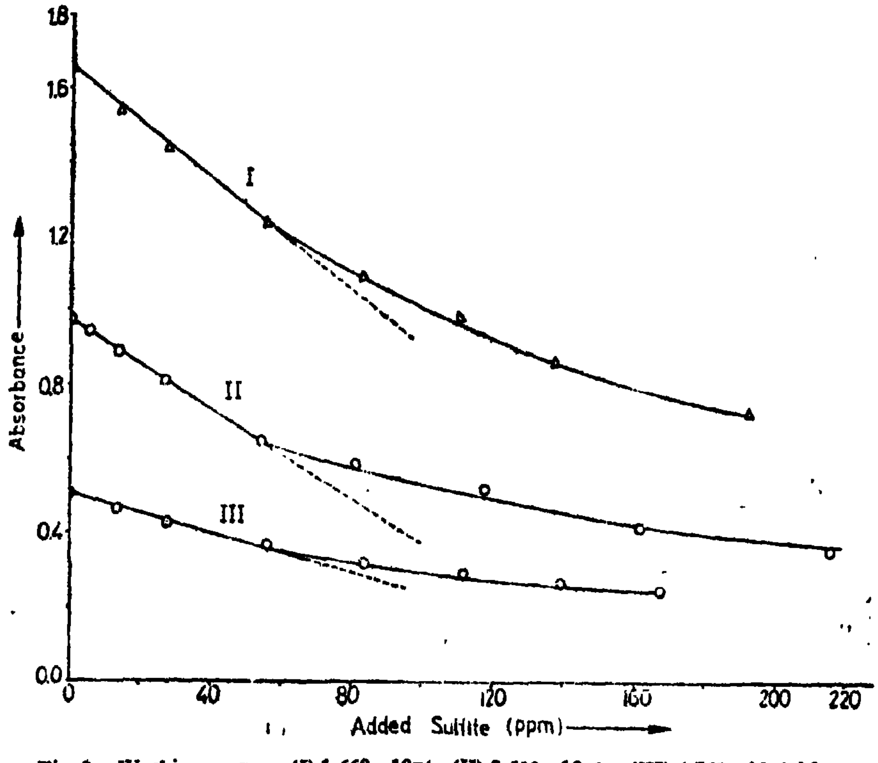


Fig. 2. Working range: (I) 1.669×10^{-4}, (II) 9.539×10^{-5}, (III) 4.769×10^{-5} *M* salicyldehyde.

*p*H 6.0 was reached. Above *p*H 6.0, with the less availability of HSO_3^-, the concentration of the bisulphite-salicyldehyde compound decreased, as a result the absorbance value would again be nearer to pure salicyldehyde solution.

complex containing busulphite and salicyldehyde is formed in a 1 : 1 ratio. Job's curve of similar nature can also be formed in some other cases[7,8]. However, these results show that maximum reaction occurs at equal concentrations of sulphite and

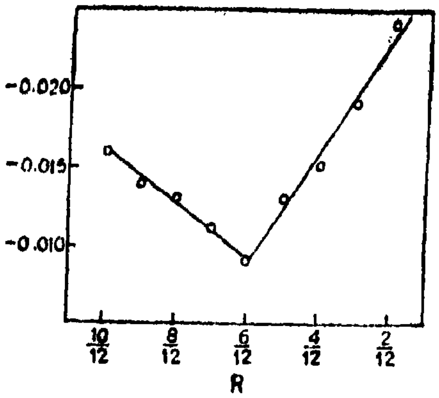
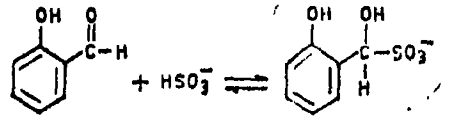


Fig. 3. Job's plot [D – absorbance of sulphite salicydehyde mixture – absorbance of salicyldehyde solution ; R – sulphite concentration/total concentration of sulphite + salicyldehyde].

salicyldehyde and that the complex is of the following type[9],



The addition compound thus formed is an *o*-hydroxy sulphonic acid or its salt which splits to a certain degree into its components in aqueous solution. The formation of such hydroxy compound has also been reported in connection with formaldehyde-bisulphite addition complex[9]. Nevertheless, the extent of this decomposition depends upon the stength of the union between the components (which is a function of the temperature), the concentration and *p*H of the solution[1].

Molar absorptivity and formation constant : The negative values of D for a complex indicate that accurate evaluation of molar absorptivity and formation constant is a tricky one[10]. Rose Drago[11,12] formulated a most generalised equation (equation 1) to determine equilibrium constant spectrophotometrically. This equation (1) contains two unknowns : K and ϵ_C, respectively the equilibrium constant and molar absorptivity of the complex. A straightforward, convenient graphical method, based on the consideration of two linear plots, for solving the Rose-Drago equation has been reported by Seal *et al.*[13]

$$K^{-1} = \frac{C_D^0 C_A^0(\epsilon_C - \epsilon_A)}{d - d_A^0} - C_D^0 - C_A^0 + \frac{d - d_A^0}{\epsilon_C - \epsilon_A} \quad (1)$$

were, C_D^0 and C_A^0 are the initial concentrations of the donor and acceptor, respectively, ϵ_A is the molar absorptivity of the acceptor, d_A^0 is the absorbance of the initial concentration of the acceptor, and d corresponds to the total absorbance at any given wavelength for a cell of 1 cm path length. Equation (1) can be written in the form :

$$y = A + BC - B^2x \quad (2)$$

$$\text{where, } y = \frac{C_A^0 C_D^0}{d - d_A^0}, \; C = C_A^0 + C_D^0, \; x = d - d_A^0,$$

$$A = K^{-1}/(\epsilon_C - \epsilon_A) \text{ and } B = 1/(\epsilon_C - \epsilon_A).$$

Now, x is a linear function of C_C, the equilibrium concentration of the complex and equation (2) gives a linear plot of y *vs* x with slope, $s = -B^2$ and intercept, $i = A + BC$. Finally, $K = B/A$ and $\epsilon_C = 1/B + \epsilon_A$ may be calculated.

Using the above graphical procedure, the equilibrium constant and molar absorptivity values of salicyldehyde-bisulphite system have been calculated. A representative linear plot of y *vs* x for this system is shown in Fig. 4. The calculated values of ϵ_C and K are respectively -172 dm^3 mol^{-1} cm^{-1} and 5.29×10^5 dm^3 mol^{-1}. The negative ϵ_C values for other systems, though not common, have been reported earlier[14]. The value of K obtained by the present method is comparable to K values for other aldehyde-sulphite compounds determined previously by other method[8].

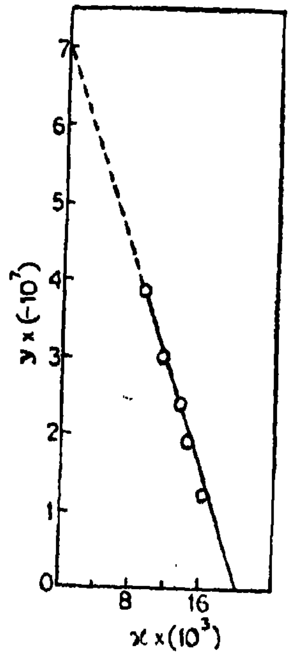


Fig. 4. Plot of y *vs* x (equation 2).

Acknowledgement

The authors wish to thank Dr. B. K. Seal, Professor of Chemistry, Burdwan University, for suggestions and helpful discussions.

References

1. I. M. KOLTHOFF and V. A. STENGER, "Volumetric Analysis", 2nd. ed., Interscience, New York, 1942, Vol. 1, 213.
2. W. KERP and E. BAUER, *Arb. Kaiserl. Gesundh.*, 1907, 26, 231.
3. J. F. HARRIS and L. L. LOCH, *Anal. Chem.*, 1962, 34, 201

4. J. BASSETT, R. C. DENNEY, G. H. JEFFERY and J. MENDHAM, "Vogel's Text book of Quantitative Inorganic Analysis including Elementary Instrumental Analysis", 4th ed., E.L.B.S., London 1982, p. 834.
5. H. W. SCOGGINS, *Anal. Chem.*, 1970, **42**, 1091.
6. P. JOB, *Anal. Chim.*, 1936, 11, 97.
7. R. K. NANDA and S. ADITYA, *J. Indian Chem. Soc.*, 1963, **40**, 660.
8. R. C. DAS, R. K. NANDA and S. ADITYA, *J. Indian Chem. Soc.*, 1963, **40**, 739.
9. P. K. DASGUPTA, K. DECESARE and J. C. ULLREY, *Anal. Chem.*, 1980, **52**, 1912.
10. M. B. LASATER and R. C. ANDERSON, *J. Am. Chem. Soc.*, 1952, **74**, 1429.
11. N. J. ROSE and R. S. DRAGO, *J. Am. Chem. Soc.*, 1959, **81**, 6138.
12. R. S. DRAGO and N. J. ROSE, *J. Am. Chem. Soc.*, 1969, **81**, 6141.
13. B. K. SEAL, A. K. MUKHERJEE and D. C. MUKHERJEE, *Bull. Chem. Soc. Jpn.*, 1979, **52**, 2088.
14. R. L. MIDDAUGH, R. S. DRAGO and R. J. NIEDZIELSKI, *J. Am. Chem. Soc.*, 1964, **86**, 388.

Determination of Zinc in Milk Samples using 1-(2-Quinolylazo)-2,4,5-trihydroxybenzene as Spectrophotometric Reagent

ISHWAR SINGH* and (Mrs.) POONAM

Department of Chemistry, Maharshi Dayananda University, Rohtak-124 001

Manuscript received 22 February 1985, revised 6 September 1985, accepted 15 November 1985

ZINC is an essential metal in biological system and its essentiality for human being was recognised only recently. Zinc has been found considerably in milk samples and in this paper the trace amounts of the metal has been determined spectrophotometrically by 1-(2-quinolylazo)-2,4,5-trihydroxybenzene (QATB)[1]. The method is simple and rapid.

Experimental

Synthesis of QATB: Stoichiometric amounts of 2-hydrazinoquinoline[2] (1.59 g, 0.01 mol, dissolved in the minimum amount of dilute hydrochloric acid) and 2,5-dihydroxy-1,4-benzoquinone[3] (1.4 g, 0.01 mol in ethanol) were mixed and refluxed for 30 min. The solution was then cooled and made ammoniacal. Excess of ammonia was boiled off and the solution was allowed to stand overnight. The dark red precipitate obtained was recrystallised from ethanol and dried over phosphorus pentoxide. The purity of the compound was checked by thin layer chromatography and elemental analysis (Found: C, 64.2; H, 3.8; N, 15.1. $C_{15}H_{11}N_3O_3$ requires: C, 64.05; H, 3.91; N, 14.95%). A $1\times10^{-3}M$ reagent solution was prepared. Reagent solutions were discarded when a week old.

Preparation of solutions: A $1\times10^{-3}M$ stock solution of zinc was prepared by dissolving appropriate amount of analytical grade zinc(II) sulphate heptahydrate in water, standardised complexometrically with EDTA[4], and further diluted as required for working standards. A fresh 1% solution was prepared and kept in amber-coloured bottle. A 0.5 *N* NaOH solution was prepared.

Standard calibration curve for zinc: To a suitable aliquot containing zinc (2.8-9.0 μg) were added 1% ascorbic acid (0.5 ml) and $1\times10^{-3}M$ QATB (1 ml). A 0.5 *N* NaOH solution (2.0 ml) was then added and diluted to 10 ml keeping the final concentration of ethanol to 40% (v/v). The absorbance was measured at 560 nm against a reagent blank.

Results and Discussion

Addition of an ethanolic solution of QATB to a very dilute solution of zinc(II), in a medium containing not less than 30% (v/v) ethanol (otherwise a precipitate was obtained), resulted in a dark brown colour in alkaline solution having λ_{max} at 560 nm. The colour intensity was shown maximum and constant at 0.05-0.25 *N* NaOH, and 25 molar excess of reagent was required for complete complexation. Beer's law validity range with optimum concentration range in ppm is 0.0-1.37 and 0.28-0.9, respectively. Sandell's sensitivity and molar absorptivity are 0.0012 μg Zn/cm^2 and 5.4×10^4 dm^3 mol^{-1} cm^{-1}, respectively. The composition (M : L) determined by Job's method is 1 : 2. The method is highly sensitive as well as selective for zinc, and the transition metals either donot form complex with QATB in high alkaline medium or if formed by a few, are masked by cyanide except manganese. In absence of manganese(II), zinc ions which are also masked by cyanide, are demasked by adding formaldehyde solution, and this procedure was applied to find out trace levels of zinc in milk samples.

Effect of foreign ions: Effect of diverse ions on the colour development of zinc complex with QATB was studied by taking 0.65 μg ml^{-1} of zinc(II), adding varying amounts of diverse ions and following the recommended procedure. It was observed that fluoride, nitrate, nitrite, sulphate, sulphite, alkaline earths, lanthanides, aluminium(III), indium(III), antimony(III), bismuth(III), chromium(III), platinum metals (except palladium) and thorium(IV) did not interfere at all. However, sulphide and manganese(II) interfered seriously. Cyanide also interfered but a 150-fold cyanide concentration is tolerated in presence of 1% formaldehyde solution. This is due to instability of tetracyanozincate ions in presence of formaldehyde[5] and zinc ions are again free to interact with the reagent. Results of tolerance limits, in parts per million (given in parenthesis) of various ions in solution that caused a deviation smaller than $\pm$ 2% in absorbance are as follows: chlroide (600), bromide (600), iodide (100), thiosulphate (100), phosphate (50), bromate (20), thiocyanate (40), citrate (40), tartarate (40), oxalate (20), EDTA (25), Fe^{II} (56, masked by 1%

CN^-), Ni^{II} (25, masked by 1% CN^-), Co^{II} (25, masked by 1% CN^-), Cu^{II} (20, masked by 1% CN^-), Pb^{II} (10, masked by EDTA), Mo^{VI} (40), W^{VI} (40), $U^{VI}O_2$ (20), V^V (20, masked by 1% CN^-), Cd^{II} (20), Hg^{II} (20) and Ag^I (10, masked by EDTA).

Determination of zinc in milk samples: Dry ashing method[6] was used in determining the zinc contents of milk. Milk (25 ml) was added dropwise to a heated crucible to evaporate without forthing and after removal of moisture it was heated strongly to 450-500°. Concentrated nitric acid (1 ml) was added after cooling. It was then evaporated to dryness and ignited again at 450-500° for ~ 1h. Care was taken to avoid loss by sputtering. The resulting white ash was dissolved in the minimum amount of dilute nitric acid and made up to 25 ml in a standard flask. To the aliquot (1 or 2 ml), was added 0.1% KCN solution (0.5 ml) to mask the interfering metals and then 1% formaldehyde (1 ml) was added and zinc was determined by the recommended procedure.

Recovery of zinc from milk samples: The standard milk samples were spiked by adding known amounts of zinc and the total zinc was determined with the reagent. Table 1 reports the recovery data obtained with QATB and confirms the precision of the method. It was noted that zinc contents were variable in samples taken from different animal and breed, as well as time of the lactation process. Another factor of variation might be dependent upon the feed, age and health of the animal. It was also noticed that milk samples kept overnight in galvanised utensils have slightly higher zinc contents, which may be due to contamination of zinc during pasteurisation.

TABLE 1—RESULTS AND RECOVERY DATA FOR ZINC IN VARIOUS MILK SAMPLES WITH QATB AS REAGENT*

Milk samples	Zn^{II} found $\mu g\ ml^{-1}$	Zn^{II} added $\mu g\ ml^{-1}$	Zn^{II} recovered $\mu g\ ml^{-1}$	Range of % recovery
Cow	3.67, 3.52, 3.81, 4.07	2.8	6.67, 6.12, 6.48, 6.80	96.83 – 103.09
Buffalo	2.98, 3.28, 3.06, 3.25	2.8	5.90, 6.05, 5.63, 5.83	96.08 – 102.99
Goat	3.84, 4.09, 3.57, 4.02	2.8	6.86, 7.02, 6.45, 6.72	98.97 – 103.31
Govt. supply (skimmed milk)	4.15, 3.90, 4.20, 4.08	2.8	6.70, 6.93, 6.80, 6.98	96.40 – 103.42

* Number of analyses = 4.

Acknowledgement

One of the authors (P.) is thankful to C.S.I.R., New Delhi, for financial assistance.

References

1. I. SINGH and POONAM, *Talanta*, 1984, 31, 109.
2. W. H. PERKIN and R. ROBINSON, *J. Chem. Soc.*, 1913, 1078.
3. R. G. JONES and H. A. SHONLE, *J. Am. Chem. Soc.*, 1945, 67, 1034.
4. A. I. VOGEL, "A Text Book of Quantitative Inorganic Analysis", 4th ed., Longmans, London, 1978.
5. S. SHIBATA, in "Chelates in Analytical Chemistry", eds. H. A. FLASCHKA and A. J. BARNARD, JR., Marcel Dekker, New York, 1972, Vol. 4.
6. A. A. SCHILT and P. J. TAYLOR, *Anal. Chem.*, 1970, 42, 220.

Rapid Method for the Determination of Coking Value of some Carbonaceous Materials

ARUNKANTI CHAUDHURI, A. K. SETH, SISIR KR. RAY* and P. N. MUKHERJEE

Central Fuel Research Institute, P.R.I.-828 108, Dhanbad

Manuscript received 28 April 1983, revised 27 May 1985, accepted 17 January 1986

THE coking value is a measure of the amount of carbon (coke) left on heating a sample of carbonaceous materials, like tar, pitch and similar products, under specified conditions. The coking value is generally determined by Conradson carbon method[1]. A simple, convenient and elegant method has been developed by the authors in this laboratory.

Experimental

The apparatus very similar to that used for proximate analysis of coal can be employed in the present method. The muffle furnace in addition to having rapid heat regaining capacity, should have an arrangement to exclude air circulation inside the furnace during the experiment. It is worth mentioning that heating may be done either by gas or electricity. A steady temperature of 570±5° should be maintained and sample heated for 7 min for the determination of coking value.

Accurately weighed sample (0.5-2.0 g) is taken in the silica crucible (specifications in Table 1). To

TABLE 1—SPECIFICATIONS OF THE SILICA CRUCIBLE* (DIMENSIONS IN mm)

	Crucible	Lid
1.	Hight : 38	Internal dia. : 27
2.	External dia. : 25	Dia. of well : 21
3.	Internal dia. : 22	Depth of the well : 4
4.	Combined weight of the crucible and lid should be between 12-14 gms.	
5.	Maximum clearance between crucible and lid, at the top edge of the crucible should be 0.5 mm.	

*Crucible must be cylindrical, translucent, with a lid of capsule type.

this accurately weighed inert material (2-3 g), *i.e.* sand of specified grade (Table 2), is mixed.

Table 2—Specifications of Standard Sand

The essential characteristics of the sand suitable for use in the determination of coking value should be as follows.

1. It should be completely inert and be of pure silica and should be free from impurities, such as clay, chalk and iron carbonates.
2. It should pass a 30 mesh IS sieve (BS-52) and be retained on 20 mesh IS sieve (BS-72).
3. It should not contain more than 5% oversize and or 10% undersize.
4. On heating for 3 h at 920°, the undersize produced by disintegration should not exceed 2.5%.
5. Its solubility in hot dilute hydrochloric acid should not exceed 0.5%.

Travancore sand as well as coke powder may be used as inert material. However, in this method, Travancore sand is chosen instead of coke powder because the latter may increase the percentage of coking value of the sample under test by coke/tar/volatile interaction[8]. The quantity of sample to be taken for the determination of coking value is indicated in Table 3.

Table 3 - Quantity of Sample Required for Coking Value Determination

Sl. no.	Coking value %	Quantity of sample required g
1.	≤10	1.5 -2.0
2.	10-30	1.0 -1.5
3.	≥30	0.50-1.0

Fourteen samples having coking values 1.50 to 62.77% were subjected to the tests at four different temperatures, namely, 570, 620, 670 and 730°. From the results of the experiments (Table 4) it is seen that 570±5° is the ideal temperature for carrying out the investigation.

Regarding the repeatibility of the tests, duplicate determinations were carried out for a number of samples (Table 5). In all the determinations, the results of successive tests were well within 2.4% of the average of the two tests.

Table 5—Repeatability of Duplicate Determinations of the Modified Method*

Sl. no.	I determination	II determination	Average	± % Deviation from average
1.	64.42	63.58	64.00	0.70
2.	52.04	52.34	52.19	0.20
3.	51.86	51.90	51.88	0.04
4.	51.60	51.30	51.45	0.30
5.	53.56	53.58	53.57	0.01
6.	72.90	71.66	72.28	0.86
7.	33.20	33.34	33.27	0.20
8.	29.45	28.31	28.88	2.00
9.	7.19	7.18	7.185	0.00
10.	20.13	20.91	20.52	1.80
11.	1.83	1.65	1.74	5.20
12.	1.71	1.62	1.66	2.40

* % variation of each determination from the average result.

Discussion

For the determination of coking value as described above, only common equipments which are necessary for proximate analysis of coal and coke are required. In the present method there is drastic reduction in time for the determination of coking value (Conradson method, ~ 1 h ; present method, ~ 0.5 h).

In Conradson method heating is done by gas of calorific value of ~ 500 btu/ft[3] which is sometimes difficult to generate in many laboratories ; moreover, the rate of heating is controlled mainly by regulating the inflow of the gas in the burner, which involves personal error. Further, in Conradson carbon method, a time period of 30 ± 2 min must be observed even it is necessary to use different burner or gas to do so. It is to be noted, however,

Table 4 - Results of Coking Values at Different Temperatures and their Difference from Conradson Carbon

Sl. no.	Conradson carbon (A) % (w/w)	730° (B) % (w/w)	Diff. (A-B) % (w/w)	670° (C) % (w/w)	Diff. (A-C) % (w/w)	620° (D) % (w/w)	Diff. (A-D) % (w/w)	570° (E) % (w/w)	Diff. (A-E) % (w/w)
1.	62.77							64.00	-1.23
2.	58.16	50.52	-7.64	54.06	-4.10	54.46	-3.70	58.04	+0.12
3.	55.28	47.48	-7.80	50.26	-5.02	50.91	-4.37	53.57	+1.71
4.	52.75	44.13	-8.62	47.55	-5.20	47.32	-5.43	51.45	+1.30
5.	52.51	44.30	-8.21	48.41	-4.10	47.47	-5.03	51.88	+0.63
6.	52.14	45.09	-7.05	47.47	-4.67	48.18	-3.96	52.19	-0.05
7.	48.56	41.50	-7.06	43.40	-5.16	44.48	-4.08	48.64	-0.08
8.	34.32							33.27	+1.05
9.	32.21	29.25	-2.95	29.69	-2.51	31.67	-0.53	32.28	-0.08
10.	30.08							28.88	+1.20
11.	22.00	19.60	-3.04	23.60	-1.64	21.01	-0.99	20.52	+1.48
12.	11.61	9.31	-2.28	9.00	-2.61	10.12	-1.49	10.35	+1.26
13.	1.70							1.66	+0.04
14.	1.50							1.74	-0.24

TABLE 6—COKING VALUES OF SAMPLES DETERMINED BY CONRADSON CARBON METHOD USING DIFFERENT BURNERS AND GASES

Sl. no.	Burner	Gas	Sample No. 1 wt. %	Sample No. 2 wt. %	Sample No. 3 wt. %	Sample No. 5 wt. %	Sample Tar wt. %
1.	Gansen Burner	Cokeoven gas	86.00	89.80	80.37	78.30	56.10
		Cal gas (L.P.G.)	60.23	63.98	52.38	43.46	27.38
2.	Bunsen Burner	Cokeoven gas	55.52	57.21	48.86	42.10	25.05
		Cal gas (L.P.G.)	57.03	58.87	49.75	42.62	26.12
3.	Meker Burner	Cokeoven gas	55.60	58.67	50.05	42.40	25.51
		Cal gas (L.P.G.)	56.23	59.05	50.54	41.92	26.63

Coke oven gas – C.V. = ~500 Btu/fit[3].
Cal gas (L.P.G.) – C.V. = ~1 150 Btu/fit[3].

that the tolerence of variation of calorific value of the gas to be used as a heating medium, has not been mentioned in Conradson carbon method. In India, light petroleum gas (LPG) having high calorific value (~ 1150 Btu/ft[3]) is generally used as heating medium in different laboratories.

With a view to study the effect of using different gases having wide variation in calorific values as well as that of different burners, namely bunsen, meker, gansen (the new type of burner meant for LPG which is in use in India) *etc.* several experiments have been conducted for the determination of coking values of different pitch and tar samples by Conradson method using different burners and gases. The results of the experiments are shown in Table 6. There is definite limitation on the use of different types of burners as well as gases of different calorific values by the Conradson carbon method as is evident from the Table 6. The present method does not impose such stipulation either on the use of gas or on burners since the experiment is conducted at a particular coking temperature which may be achieved either by using gas or electricity.

It is interesting to observe that total time required for the determination of coking value is hardly 0.5 h for the present method. In contrast, coking value determination by Conradson method requires at least 1h. Apart from the simplicity of apparatus and method of heating, this is an important parameter in industry since it helps determination of more samples in short period. The other methods employed for coking value determinations are Ramsbottom[4], Norske and modified Norske[5]. Ransbottom method is suitable for lubricating oils and distillate fuel oils. In Norske method, the time required for one determination is 6-7 h. Moreover, this method has not been tried for samples other than pitch having coking values ranging 40 to 50%.

Thus, it is evident from the foregoing discussion that the present method can be conveniently adopted for the determination of coking value of all types of carbonaceous materials since it has got several advantages.

References

1. "Standard methods for Testing Tar and its products", 5th. ed., published by Standardization of Tar Products Tests Committee, Gomersal, 1962.
2. N. N. DAS GUPTA, *I. S. I. Bull.*, 1956, 8, 90.
3. B. K. MAZUMDAR and N. N. CHATTERJEE, "Year Book of the Cokeoven Managers' Association", COMA, 1971, pp. 322-342.
4. J. S. S. BRAME and J. G. KING, "Fuel, Solid, Liquid and Gases", 5th ed., Edward Arnold, London, 1961, p. 494.
5. L. P. CHARETTE and L. GIROLAMI, *Fuel*, 1958, 4, 382.

J. Indian Chem. Soc.,
Vol. LXIII, February 1986, pp. 263-265

Book Reviews

Introduction to Nuclear Science, M. N. Sastri, Affiliated East West Press Private Limited, New Delhi, 1984, pp. 169, Rs. 17.00.

THE book has been divided into ten chapters. It starts with historical introduction beginning from the discovery of radioactivity culminating in projecting the future of nuclear fusion.

Any discussion on nuclear science should be preceded by an up-to-date information of nuclear structure. Thus chapter 2 is dedicated to this, where various nuclear models are depicted qualitatively. Chapter 3 deals with radioactive decay laws which have been explained thoroughly by taking various examples. Chapter 4 concerns with nuclear reactions where compound nucleus mechanism as well as various types of nuclear processes are discussed briefly. Chapter 5 is devoted to a qualitative discussion of some features of α-, β- and γ-decay processes.

Chapters 6 and 7 deal with basic processes in the interaction of radiation with matter and the principles involved in the detection and measurement of nuclear radiations. Chapter 8 is devoted to a discussion of some important features of nuclear fission. In this chapter, reference has also been made to nuclear reactors and their use in power generation. An up-to-date account of developments in India in this field has been indicated.

Chemical and biological effects of radiation which constitute two different subjects by themselves have been dealt with in chapter 9. Only some basic features have been discussed. Radionuclides now-a-days find applications in various fields. Chapter 10 deals with this aspect touching on tracer methods, activation analysis, dating techniques, tracer applications in chemistry, biology, medicine, agriculture, *etc.*

The book is very well put together. However, the chapter on nuclear reactions should have been preceded by the chapter on radioactive decay processes and followed by the chapter on nuclear fission. This book has been written in a very popular fashion. It is noteworthy that the author has given in the appendix a list of important events in the development of nuclear science in chronological order. The book has been made more attractive by the fact that pictures of illustrious scientists in the field of nuclear science have been presented in appropriate places in the text. All considered, the book will largely appeal as a popular reading material to a wide audience of nuclear scientists and technologists.

S. N. Bhattacharyya

Fluid Mechanics and Its Applications, Vijay Gupta and Santosh K. Gupta, Wiley Eastern Limited, New Delhi, 1984, pp. xii+536, Rs. 43.00, ISBN 0 85226 342 2.

THIS book is designed to meet the requirements for undergraduate students in engineering from all disciplines. It is presented in a very readable form enabling one to understand the basic principles of the subject quite easily. The level of mathematics is kept as low as possible so that a student can pay more attention on the complexities of fluid flow phenomenon and its engineering applications.

The text presumes that the student has covered calculus, statics and dynamics, and thermodynamics. It is systematically organised in sixteen chapters. The first seven chapters cover materials needed for basic understanding of the subject.

After an introduction in chapter 1, fluid statics is covered in chapter 2. From chapter 3, the various aspects of fluid flow phenomena encountered are dealt with. Control volume approach is first introduced in chapter 3 and it is then applied to different practical problems in subsequent chapters. Equation for conservation of mass, momentum theorems and equation of motion are introduced in chapters 4, 5 and 6. Chapter 7 deals with energy equations based on application of first law of thermodynamics to steady-flow processes. Engineering application of fluid mechanics is covered in chapters 8, 10 and 14, where the relations derived in earlier chapters are applied directly. Chapter 14 also outlines the topic on fluidics which utilises the properties of fluid logic very similar to electronic logic gates. In modern day engineering practice, a design engineer must resort to some form of model test programme before taking any decision at the design stage of a project. This type of scaled-model testing and similarity analysis for engineering design are presented in chapter 9. Chapter 11 contains an introduction on different simplifying assumptions and approximations required in some fluid mechanics problems for which closed form analytical solutions are seldom obtained. Inviscid flow, boundary layer theory, effects of compressibility, and turbulent flow are then covered in chapters 12, 13, 15 and 16.

A short bibliographical note is appended at the end of the text to guide the reader to some standard books on fluid-flow phenomena. Those books may be consulted along with the present book for more rigorous and detailed study. The appendix includes some common units and conversion factors, some useful formulae, dimensional analysis and properties of fluids.

The book contains numerous practical examples as an aid to understand the theory. A variety of problems are also included at the end of each chapter. Answers to problems are also given. It should prove very useful to the students.

S. K. Bhattacharyya

Organic Synthesis : Concepts, Methods, Starting Materials, Jurgen Fuhrhop and Gustav Penzlin, Verlag Chemie, Weinheim, 1983, pp. 153, DM 78.

ORGANIC synthesis had a colourful start some hundred years ago with the synthesis of two important colouring matters, alizarin and indigo almost at the time Le Bel and Van't Hoff formulated their famous theory of tetrahedral carbon. Since then it has progressed steadily, sometimes with phenomenal stride, and at present, appears to reach its apex. Intellectually, no other branch of chemistry is so much challenging and, if the goal is achieved, so much satisfying than an elegant synthesis of an intricate molecule. As pointed out by Professor Woodward, there is excitement, adventure, and challenge and there can be great art in organic synthesis. There is very little left to chance. Mainly due to collaborative efforts of organic and inorganic chemists, today a synthetic chemist has in his reportoire a plethora of novel reagents, new reactions, bizarre reaction conditions, and even new thought processes which enable him to embark on a complex synthesis with more confidence and higher chance of success. Three things are of paramount importance in modern synthesis : concepts, methods and starting materials, and it is exactly the three which form the subject matter of the book 'Organic Synthesis'.

The book has been divided into four chapters : synthons in the synthesis of carbon chains and carbocycles, selective functional group interconversions (FGI), retro-synthetic analysis of simple organic compounds, and methods in the construction of complex molecules. The first chapter describes the synthesis of different types of mono- and bi-functional compounds through the application of reactions of various donor and acceptor synthons. The features of diverse synthons have been presented with numerous illustrations. The reader will find brief but useful discussion on regiospecific enolate formation, umpolung, Wittig, Horner, and Peterson reactions. Among others, it also contains synthetic procedures for different carbocycles including some bridged ones. Throughout this chapter, the authors have admirably pointed out the application of acceptor and donor synthons.

The second chapter deals with selective functional group interconversions (FGI). The purpose and the various aspects of FGI, *viz*, regioselectivity, selective reagents, enantioselectivity, and heterocyclic synthesis have been nicely classified in the brief introduction. Two elaborate sections on reduction and oxidation describe various methods available and their applicability on different substrates, due emphasis being given on the selectivity of the reagents. Sections on olefin synthesis and synthesis of carboxylic acid derivatives are brief but do not fail to cite the more important and generally useful methods. The three tables containing respectively the reactivity of reducing agents, some selective oxidation reactions, and selective elimination reactions for olefin synthesis have been nicely compiled. The section on the synthesis of nitrogen heterocycles, though brief, reflects the systematic approach that characterises the entire book. The last section of this chapter describes the protection of different functional groups in organic synthesis.

In the third chapter, *viz*. retro-synthetic analysis of simple organic compounds, attempts have been made to provide an introduction to the planning of simple target molecules (employing mainly elementary reactions) based on the synthon approach of E. J. Corey and functional group interconversions discussed in the earlier two chapters. The concept of retro-synthetic analysis (antithesis) has been very elegantly clarified. Syntheses of simple acyclic, cyclic, and bridged polycyclic target molecules have been illustrated with occassionally alternative modes of disconnections leading to different synthons. One striking feature of the chapter is the inclusion of a long list of relatively inexpensive starting materials (compounds with diverse functional groups) with their approximate prices. The purpose of this rather unusual feature is to help the uninitiated chemist in designing synthesis using simple precursors so that he can develop his originality in planning and applying functional group interconversions. The reviewers agree with the authors that this would clearly enhance the industrial and therefore social impact on academic research in synthesis.

The final chapter, *viz*. methods in the construction of complex molecules illustrates how the knowledge acquired in the earlier three chapters has been and can be applied in the synthesis of complex molecules. Fairly comprehensive treatment of synthesis of various natural products, *e.g*. oligonucleotides, peptides, macroheterocycles, porphyrins, prostaglandins, steroids, alkaloids has been made. A section illustrating the use of inexpensive carbohydrates, *e.g*. sugar derivatives as chiral precursors of different natural products has been given which demonstrates how simple sugar chemistry can be involved in intricate syntheses. A few industrially useful partial syntheses and some typical academic total syntheses of complex antibiotics are described. Finally, there is an interesting section on the synthesis of esoteric

polycyclic hydrocarbons, such as cyclobutadienes, tetrahedranes, prismanes and dodecahedranes.

The book is lucidly written and very systematically organised. References are quite recent and cover almost all major work in synthetic chemistry. It is a pleasure going through the book and sharing the experience of *tour de force* of the great synthetic chemists of our time with some wholesome chemistry in the bargain.

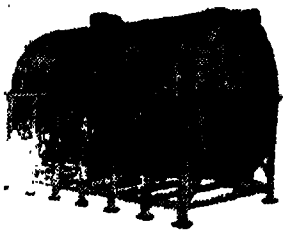
D. Nasipuri

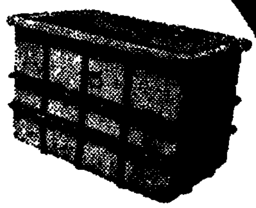
and

Anup Bhattacharya

Sintex

The Readymade Solution to problems of storage, processing and mixing of acids, alkalies, chemicals and liquid food stuffs.





Horizontal Tanks – upto 10,000 Lts. Vertical Tanks – upto 20,000 Lts. Rectangular Tanks – upto 2,800 Lts

SINTEX – the first and the only large sized one piece polyethylene mouldings in India, offer the ideal and instant solution to the problems of storage, handling, processing and mixing of chemicals. Apart from excellent resistance to most acids, alkalies and chemicals, SINTEX have many exclusive features;

Wide range:
Available in various sizes and shapes from 200 lits. to 20,000 lits

Easy installation:
Sintex tanks are extremely light in weight and can be installed conveniently.

Option of welded fittings:
While adaptor checknut system is standard with Sintex tanks, welded fittings can be given if required.

Easy repairability:
In case of accidental damage Sintex Tanks can be repaired easily at site by hot air welding, using a hot air gun with or without built in compressor.

Unique design:
Sintex Vertical Tanks with closed mouths are made in special corrugated construction for extra mechanical strength. These tanks have a moulded-in platform for inspection.

Excellent After Sales Service:
There is A SINTEX distributor close to you and he is well equipped to offer technical and other assistance to keep Sintex Tanks safe and functional

FDA Approved for Food processing:
Sintex tanks are made out of FDA approved grades of polyethylene and are ideally suited for processing and handling of food products.

Proven Durability:
Sintex Tanks are in use in scores of industries for storing, processing, mixing and handling of a variety of chemicals, and liquid food stuffs. The fact that Sintex Tanks have been performing faultlessly for the last ten years is a testimony to the durability and trouble free performance of SINTEX Tanks.

For further information, contact:
SINTER PLAST CONTAINERS
Plastics Division,
THE BHARAT VIJAY MILLS LTD.
KALOL (N. GUJARAT) 382 721 Gram: SINTEX
Phone: 2687–2244 Telex: 0121-296 BVM IN

Ahmedabad : 179, New Cloth Market, Ahmedabad-380 002, Phone: 362976, 361046.
Bombay : 18, World Trade Centre Cuffe Parade, Colaba, Bombay 400 005 Phone: 211653, 217869.
Calcutta : 10, Middleton Street, Calcutta-700 071, Phone: 214028
Madras : 123, Angappa Naiken Street, (3rd floor) Madras-600 001.
New Delhi : GF-3 Oplan Building, 12, Nehru Place, New Delhi 110019, Phone: 681188

J. Indian Chem. Soc.,
Vol. LXIII, March 1986, pp. 267-269

Preparation and Characterisation of Chromium(III) Complexes of Maleanilic and Phthalanilic Acids

C. L. SHARMA*, R. S. ARYA and S. S. NARVI

Department of Chemistry, University of Roorkee, Roorkee-247 667

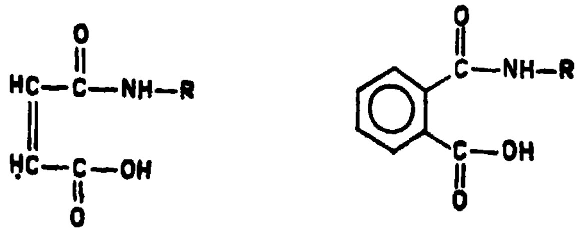
Manuscript received 7 January 1984, revised 12 December 1984, accepted 31 July 1985

The complexes of the type $[Cr(A\text{-}A)_3]$, where A-A = maleanilic and phthalanilic acids, and their 4-methyl, 4-chloro, 4-nitro and 1-naphthyl derivatives have been prepared. The magnetic, conductance, ir and electronic spectral studies indicate their octahedral structure.

ANILIC acids are very useful from analytical[1-3] and biochemical point of view[4-6]. Their complexes with calcium, aluminium and thorium ions have also been found of great industrial and biochemical importance[7,8], chromium(III) compounds in general occurring in brewers, yeast and other foods were found to be of outstanding biological activity. Keeping these facts in view, we are reporting in this communication the preparations and characterisation of chromium(III) complexes of maleanilic acid and its 4-methyl, 4-chloro, 4-nitro and 1-naphthyl derivatives and phthalanilic acid and its 4-methyl, 4-chloro, 4-nitro and 1-naphthyl derivatives. These complexes are also expected to be of biochemical and analytical importance.

Experimental

All the reagents used were of AnalaR grade. Maleanilic acid (m.p. 205°) was prepared[9] by treating the solution of maleic anhydride, and aniline in solvent ether at 15-20°. 4-Methyl (m.p. 201°), 4-chloro (m.p. 198°), 4-nitro (m.p. 194°) and 1-naphthyl (m.p. 200°) maleanilic acids were similarly prepared by taking the different substituted primary aromatic amines in place of aniline. Phthalanilic acid (m.p 107°) was prepared by treating the solution of phthalic anhydride with aniline in benzene at room temperature[10], 4-methyl (m.p. 201°), 4-chloro (m.p. 199°), 4-nitro (m.p. 197°) and 1-naphthyl (m.p. 186°) phthalanilic acids were also similarly obtained by using different substituted primary aromatic amines. All these compounds were recrystallised from alcohol.



Maleanilic acids   Phthalanilic acids

R = Phenyl, 4-tolyl, 4-nitrophenyl, 4-chlorophenyl and 1-naphthyl

The techniques, apparatus and method of calculations were the same as reported earlier[11].

Preparation of complexes : Chromium hydroxide, freshly prepared by the addition of potassium hydroxide in the solution of chromium chloride, was mixed with anilic acids in the ratio of 1 : 4. Alcohol was then added to bring the mixture in suspended form which was refluxed on water-bath for ~6 h. The precipitates formed were filtered, washed several times with alcohol and then dried in a desiccator over anhydrous sulphuric acid.

The results of chemical analysis, conductances in methanol and the values of magnetic moment at room temperature are given in Table 1.

Results and Discussion

Ir spectral studies : The main characteristic features of the ir spectra of the complexes are as follows. The N—H stretching frequency occurs at around 3 150 cm^{-1} which was present at around 3 350 cm^{-1} in the spectra of free anilic acids. The carbonyl stretching frequency of the secondary amide fall within the range 1 660-1 680 cm^{-1} which is well removed from 1 700 cm^{-1} band in free secondary amide. Although C=O does not take part in coordination, the shift towards lower side may be due to the mass effect of heavy metal ion linked to nitrogen[12] and thus weakening of C=O linkage[13]. The stretching bands at around 1 470 cm^{-1} (C—N) in the spectra of anilic acids shifted to about 1 480 cm^{-1} in the spectra of their complexes. The bands obtained in the region 1 600-1 620 and 1 365-1 400

* 134/3, Vikas Nagar, U. O. R., Roorkee-247 667.

TABLE 1—ANALYTICAL DATA OF COMPLEXES

Sl. no.	Compd.*	Analysis % : Found/(Calcd.) M	C	H	N	μ_{eff} B.M.	Molar conductances Ω^{-1} cm^2 mol^{-1}
1.	[Cr(P)$_3$]	6.80 (6.74)	65.90 (65.34)	3.90 (3.92)	5.40 (5.44)	3.74	7.25
2.	[Cr(4-methyl P)$_3$]	6.35 (6.39)	66.00 (66.39)	4.45 (4.46)	5.20 (5.16)	3.78	5.00
3.	[Cr(4-nitro P)$_3$]	5.70 (5.73)	55.10 (55.61)	2.98 (3.00)	9.30 (9.27)	3.72	8.50
4.	[Cr(4-chloro P)$_3$]	5.90 (5.94)	58.20 (57.62)	3.08 (3.11)	4.75 (4.80)	3.75	4.80
5.	[Cr(1-naphthyl P)$_3$]	5.55 (5.51)	68.10 (68.77)	3.88 (3.85)	4.50 (4.46)	3.79	9.25
6.	[Cr(M)$_3$]	8.40 (8.36)	58.50 (57.93)	3.92 (3.89)	6.80 (6.76)	3.75	8.00
7.	[Cr(4-methyl M)$_3$]	7.80 (7.83)	59.15 (59.69)	4.52 (4.55)	6.30 (6.33)	3.73	4.20
8.	[Cr(4-nitro M)$_3$]	6.90 (6.87)	48.20 (47.60)	2.82 (2.80)	11.15 (11.10)	3.72	3.60
9.	[Cr(4-chloro M)$_3$]	7.20 (7.17)	49.00 (49.66)	2.90 (2.91)	5.75 (5.79)	3.74	6.30
10.	[Cr(1-naphthyl M)$_3$]	6.60 (6.56)	63.05 (63.61)	3.83 (3.81)	5.27 (5.30)	3.76	6.50

*P = Phthalanilic acid, M = maleanilic acid (both contain deprotonated carboxylic acid group).

TABLE 2—ELECTRONIC SPECTRAL DATA AND CALCULATED TRANSITION ENERGY (cm^{-1})

Compd. no.*	Expt. of calculation	$^4A_{2g}\rightarrow{}^4T_{2g}$ (ν_1)	$^4A_{2g}\rightarrow{}^4T_{1g}$(F) ($\nu_2$)	$^4A_{2g}\rightarrow{}^4T_{1g}$(P)	B	β_{35}	$\lvert\delta\nu\rvert$ cm^{-1}	$\lvert\delta\nu\rvert$ %	LFSE k cal mol^{-1}
1	Expt.	16 200	22 500	36 300	–	–	–	–	231.85
	(c)	10 Dq	22 916	35 884	680	0.74	±416	1.49	
2	Expt.	16 500	22 800	36 500	–	–	–	–	236.75
	(c)	10 Dq	23 047	36 247	653	0.71	±247 −253	0.88	
3	Expt.	16 800	23 000	37 000	–	–	–	–	241.05
	(c)	10 Dq	23 276	36 724	640	0.70	±276	0.97	
4	Expt.	16 700	22 900	36 800	–	–	–	–	239.60
	(c)	10 Dq	23 167	36 533	640	0.70	±267	0.94	
5	Expt.	17 200	23 500	37 600	–	–	–	–	246.77
	(c)	10 Dq	23 655	37 440	633	0.69	−160 +155	0.54	
6	Expt.	16 000	22 200	36 100	–	–	–	–	229.57
	(c)	10 Dq	22 743	35 562	687	0.75	−538 +543	1.95	
7	Expt.	16 300	22 500	36 300	–	–	–	–	233.84
	(c)	10 Dq	22 880	35 920	600	0.72	±380	1.36	
8	Expt.	16 600	22 800	36 800	–	–	–	–	238.17
	(c)	10 Dq	23 157	36 438	653	0.71	−362 +357	1.26	
9	Expt.	16 400	22 600	36 500	–	–	–	–	235.29
	(c)	10 Dq	22 990	36 110	660	0.72	+390	0.89	
10	Expt.	17 000	23 000	37 500	–	–	–	–	243.89
	(c)	10 Dq	23 438	37 057	633	0.69	−443 +438	1.52	

* Corresponding to Sl. no. in Table 1.

cm^{-1} indicated the coordination through carboxylate[14]. The bands due to M–N and M–O were obtained at ≈ 410 and ≈ 350 cm^{-1}, respectively.

Electronic spectral studies : The values of molar conductances (Table 1) in the range 4.8-9.25 Ω^{-1} cm^2 mol^{-1} indicated the non-electrolytic nature of the complexes. The values of magnetic moments are close enough to spin-only value for octahedral complexes. The deviations $|\delta\nu_{2,3}|$ between the calculated and experimental values (Table 2) also indicated an octahedral geometry for these complexes. Table 2 also contains experimental absorption band energies, the values of 10 Dq, B, β_{35} and ligand field stabilisation energies.

The value of first spin-allowed band was directly taken as 10 Dq. The values of ν_2 and ν_3 were calculated using the standard equations which include configuration interactions[15]. The value of Racah's inter-electronic repulsion parameter B has been calculated by three different methods as

discussed by Konig[15]. It is interesting to note that the calculated values of B and nephelauxetic ratio (β_{35}=B in complex/B in free ion) depend significantly on the method adopted for their calculation. The calculated transition energy according to procedures (a), (b) and (c) is of the order of a few percent and decreases according to $|\delta\nu$ (b)$| > |\delta\nu$ (a)$| > |\delta\nu$ (c)$|$. Thus, the values obtained by the method (c) only which provided the best fit for the transitions ν_2 and ν_3 are given in Table 2.

The reflectance spectra of the complexes also gave nearly the same bands as were obtained in their electronic spectra in solution indicating thereby no dissociation of the complexes in solution.

References

1. S. K. DATTA, *Z. Anal. Chem.*, 1955, **148**, 267.
2. S. K. DATTA, *Z. Anal. Chem.*, 1955, **148**, 259.
3. S. K. DATTA, *Z. Anal. Chem.*, 1955, **148**, 334.
4. K. N. VONKAULLA, *Bibliotheca Haematol.*, 1962, **19**, 174.
5. S. MALCOLM and D. PRESSMAN, *J. Am. Chem. Soc.*, 1954 **76**, 2863.
6. S. H. UNGER and C. HANSCH, *Proc. Phys. Org. Chem.*, 1976, **12**, 111.
7. UPJOHN, *Brit.*, 1956, **27**, 751.
8. S. HASTING and T. HENRY, 1949, **45**, 2490.
9. M. P. CAVA, A. A. DEANA, K. MUTH and M. J. MITCHELL, *Org. Synth.*, 1973, **5**, 944.
10. M. V. SUBBA RAO and C. V. RATNAM, *J. Sci. Ind. Res.*, 1962, **47**, 218.
11. C. L. SHARMA and T. K. DE, *J. Indian Chem. Soc.*, 1981, **58**, 119.
12. G. NARAIN, *J. Inorg. Nucl. Chem.*, 1966, **28**, 2403.
13. G. NARAIN, P. SHUKLA and L. N. SRIVASTAVA, *J. Prakt. Chem.*, 1966, **31**, 123.
14. C. L. SHARMA, T. K. DE and P. K. JAIN, *Chem. Scr.*, 1981, **18**, 79.
15. E. KONIG, *Struct. Bonding*, 1971, **9**, 175.

J. Indian Chem. Soc.,
Vol. LXIII, March 1986, pp. 270-272

Cobalt(II) Complexes of Tridentate Schiff Bases

C. K. BHASKARE*

Department of Chemistry, Shivaji University, Kolhapur-416 004

and

P. G. MORE

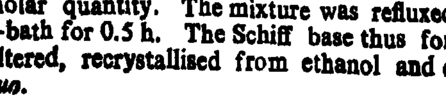
Shivraj College of Science, Gadhinglaj-416 502

Manuscript received 18 December 1984, revised 20 August 1985, accepted 17 January 1986

Cobalt(II) complexes of type ML_2, where M is Co^{II}, and L is Schiff base formed by condensation of 4-aryl-2-aminothiazole and β-hydroxy-α-naphthaldehyde or salicylaldehyde derivatives (R' = 5-methyl and 5-chloro) have been prepared and characterised by elemental analysis, magnetic and spectroscopic measurements. Elemental analysis suggests the stoichiometry to be 1 : 2 (metal-ligand). Magnetic susceptibility data coupled with electronic spectra suggest an octahedral structure for the complexes. Infrared spectra of the complexes agree with the coordination to the central metal atom through two nitrogen atoms and bonding through oxygen of the hydroxyl group. Conductance measurements suggest the non-electrolytic nature of the complexes.

METAL complexes of Schiff bases are studied extensively due to synthetic flexibility of these compounds and their selectivity as well as sensitivity towards the central metal atom. A number of reviews have been devoted to coordination chemistry of Schiff base metal complexes[1-7].

In the present study, a series of new Schiff bases have been synthesised using substituted salicylaldehydes (R'=5-methyl and 5-chloro) or β-hydroxy-α-naphthaldehyde and 4-aryl-2-aminothiazoles. These tridentate, monoprotic ligands form 1 : 2 complexes with cobalt(II) ion. The octahedral complexes are non-ionic, monomeric with bonding through oxygen of the hydroxyl group and coordination through two nitrogen atoms.



R = H, CH_3, OCH_3 or Cl
R' = CH_3 and Cl

Experimental

Synthesis of tridentate Schiff bases : A solution of *o*-hydroxy aldehyde in ethanol was added to the ethanolic solution of 4-aryl-2-aminothiazole[8] in equimolar quantity. The mixture was refluxed on water-bath for 0.5 h. The Schiff base thus formed was filtered, recrystallised from ethanol and dried *in vacuo*.

Preparation of Co^{II} complexes : An ethanolic solution of cobalt acetate (0.01 mol) (Albright and Wilson) was added to the ethanolic solution of the Schiff base (0.02 mol) The reaction mixture was refluxed on water-bath for 30 min. The brown red crystals separated, were filtered, washed with ethanol and dried *in vacuo*.

Physical measurements : Ultraviolet and visible spectra were recorded in chloroform solution on a Beckman DU-2 spectrophotometer. Infrared spectra in KBr pellets were recorded on a Beckman IR-20 spectrophotometer in the 4 000-250 cm^{-1} region. Electrical conductivity of the complexes in nitrobenzene solution were measured with a Philips PR 9500 conductivity bridge with a dip type cell PV 9055. Magnetic susceptibility measurements were carried out by Gouy method at room temperature. Diamagnetic corrections were applied by using Pascal's constants[9].

Results and Discussion

All the cobalt(II) complexes are found to be sparingly soluble in chloroform, benzene or nitrobenzene. The complexes are crystalline, reddish brown in colour and melt with decomposition above 250°. Elemental analysis data (Table 1) suggest that the complexes have 1 : 2 (metal-ligand) stoichiometry. The molecular weight determination suggests the monomeric nature of the complexes. Very low conductivity in nitrobenzene solution showed that the complexes are non-electrolytic in nature.

Electronic spectra : Three bands are observed in the electronic spectra of the Co^{II} complexes which are due to spin-allowed transitions. A strong and intense band at ~26 000 cm^{-1} ($\epsilon \approx 1000$ dm^3

TABLE 1—ELEMENTAL ANALYSIS AND MAGNETIC SUSCEPTIBILITY DATA OF Co^{II} COMPLEXES

R	R′	Analysis % : Found/(Calcd.)						μ_{eff}
		C	H	N	S	Co	Mole	B.M.
Complexes of Schiff bases derived from substituted-salicylaldehyde								
H	CH_3	63.00 (63.27)	4.20 (4.03)	8.71 (8.68)	9.80 (9.92)	9.00 (9.13)	620 (645)	4.90
CH_3	CH_3	64.44 (64.19)	4.65 (4.45)	8.21 (8.32)	9.43 (9.31)	8.50 (8.75)	638 (673)	4.93
OCH_3	CH_3	61.10 (61.28)	4.20 (4.26)	7.70 (7.94)	9.20 (9.07)	8.20 (8.36)	665 (705)	4.98
Cl	CH_3	57.00 (57.14)	3.24 (3.36)	7.60 (7.84)	8.80 (8.96)	7.95 (8.26)	669 (714)	4.86
H	Cl	55.88 (55.97)	2.81 (2.91)	8.03 (8.16)	9.70 (9.32)	8.46 (8.60)	650 (686)	4.92
CH_3	Cl	57.30 (57.14)	3.24 (3.36)	7.60 (7.84)	8.70 (8.96)	8.13 (8.26)	680 (714)	4.98
OCH_3	Cl	54.50 (54.69)	3.00 (3.21)	7.30 (7.50)	8.40 (8.57)	7.70 (7.90)	701 (746)	5.08
Cl	Cl	50.70 (50.86)	2.21 (2.38)	7.50 (7.41)	8.53 (8.47)	7.80 (7.31)	711 (755)	4.89
Complexes of Schiff bases derived from β-hydroxy-α-naphthaldehyde								
H	—	66.60 (66.94)	3.50 (3.62)	7.60 (7.81)	8.70 (8.92)	7.80 (8.11)	600 (717)	5.10
CH_3	—	67.40 (67.55)	3.86 (4.02)	7.36 (7.51)	8.71 (8.59)	7.40 (7.91)	695 (745)	4.96
OCH_3	—	64.60 (64.86)	3.70 (3.86)	7.01 (7.20)	8.08 (8.23)	7.31 (7.59)	720 (777)	4.88
Cl	—	61.30 (61.01)	2.89 (3.05)	7.03 (7.12)	8.01 (8.14)	7.20 (7.50)	725 (786)	5.03

TABLE 2—SPECTRAL DATA OF Co^{II} COMPLEXES (cm^{-1})

R	R′	Method[a]	ν_1	ν_2	ν_3	10 Dq	B	β_{35}
H	CH_3	Expt	8 600	18 000	20 000	—	—	—
		(a)	Fitted	Fitted	14 174	9 400	425	0.437
		(b)	Fitted	18 351	Fitted	9 752	837	0.861
		(c)	8 423	Fitted	Fitted	9 576	848	0.873
		(d)	8 280	17 680	Fitted	9 400	813	0.837
H	Cl	Expt	8 500	18 200	19 600	—	—	—
		(a)	Fitted	Fitted	21 070	9 700	918	0.945
		(b)	Fitted	18 137	Fitted	9 637	815	0.839
		(c)	8 533	Fitted	Fitted	9 667	813	0.837
		(d)	8 555	18 255	Fitted	9 700	820	0.844
H	—	Expt	8 560	18 200	19 750	—	—	—
		(a)	Fitted	Fitted	18 371	9 640	726	0.747
		(b)	Fitted	18 262	Fitted	9 700	822	0.846
		(c)	8 528	Fitted	Fitted	9 672	824	0.848
		(d)	8 501	18 141	Fitted	9 640	818	0.842

[a]Ref. 10.

mol^{-1} cm^{-1}) may be due to the ligand→metal charge transfer.

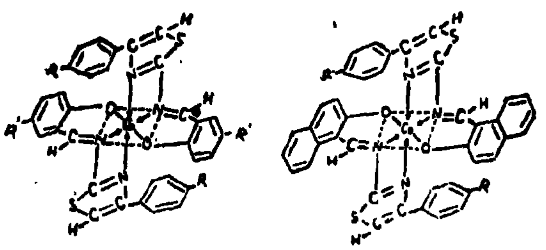
$$^4T_{2g} \leftarrow {}^4T_{1g}\ (\nu_1) \sim 8\,600\ cm^{-1}$$
$$^4A_{2g} \leftarrow {}^4T_{1g}\ (\nu_2) \sim 18\,000\ cm^{-1}$$
$$^4T_{1g} \leftarrow {}^4T_{1g}\ (\nu_3) \sim 20\,000\ cm^{-1}$$

The experimental values of the absorption bands in the electronic spectra are treated by using the numerical methods as given by Konig[10] to obtain corrected values of the band energies ν_1, ν_2 and ν_3. It is observed that the consistent values of the band energies are obtained by the methods b, c and d. The values of 10 Dq, B and β_{35} [11] for the methods b, c and d are also quite consistent. The values for a set of the three representative complexes are given in Table 2. All the values calculated as above show a quite well mutual agreement. The values of B for the complexes lie in the range 800-870 cm^{-1} and β_{35} values lie in the range 0.8 to 0.9 supporting the octahedral geometry for the complexes.

Magnetic susceptibility : The magnetic moments of the complexes lie in the range 4.8-5.2 B.M. (Table 1). This supports the octahedral geometry for the complexes[12].

Infrared spectra : The infrared spectra of the ligands show a broad weak band at ~ 2 900 cm^{-1} instead of a strong band at ~ 3 100 cm^{-1} due to the phenolic OH group. This may be due to the intra-molecular hydrogen bonding between hydroxyl hydrogen and nitrogen of the azomethine group forming a stable six-membered ring[13]. The complexes also do not show the OH group frequency thereby indicating that the OH group of the Schiff base is utilised in the formation of Co—O bond. This is further supported by the shift of C-O frequency from 1 280 cm^{-1} (in the ligands) to the higher frequency at ~ 1 330 cm^{-1} in the complexes[13,14]. The spectra of the ligands show a sharp band of high intensity at ~ 1 630 cm^{-1} (C=N). The shifting of this $\nu_{C=N}$ to a lower value at ~1 580 cm^{-1} in the complexes suggests the coordination to the central metal atom through the nitrogen of the azomethine group[13,14]. A broad weak band observed between 400 to 475 cm^{-1} may be either due to ν_{M-O} or ν_{M-N} [15].

In the light of the above discussion, an octahedral geometry is proposed for the complexes. Coordination to the central metal atom takes place through the oxygen of the hydroxyl group, nitrogen of the azomethine group and nitrogen of the thiazole ring as shown below,



Acknowledgement

One of the authors (P.G.M.) is thankful to the U.G.C., New Delhi, for the award of a Research Fellowship.

References

1. R. H. HOLM, G. W. EVERETT, Jr. and A. CHAKRAVORTY, *Prog. Inorg. Chem.*, 1966, 7, 83.
2. S. YAMADA, *Coord. Chem. Rev.*, 1966, 1, 415.
3. S. YAMADA, *Coord. Chem. Rev.*, 1967, 2, 83.
4. R. H. HOLM and M. J. O'CONNOR, *Prog. Inorg Chem.*, 1971, 14, 241.
5. M. A. ALI and S. E. LIVINGSTONE, *Coord. Chem. Rev.*, 1974, 13, 101.
6. V. CASELLATO, M. VIDALI and P. A. VIGATO, *Coord. Chem. Rev.*, 1977, 23, 31.
7. M. C. GOLONKA and A. BARTECKI, *Coord. Chem. Rev.*, 1979, 31, 251.
8. B. DASH and M. K. ROUT, *J. Indian Chem. Soc.*, 1955, 32, 663.
9. B. N. FIGGIS and J. LEWIS, "Modern Coordination Chemistry", Interscience, New York, 1960, p. 415.
10. E. KONIG, *Struct. Bonding*, 1971, 9, 175.
11. A. B. P. LEVER, "Inorganic Electronic Spectroscopy", Elsevier, Amsterdam, 1968, p. 212.
12. R. L. CARLIN, "Transition Metal Chemistry", Marcel Dekker, New York, 1965, Vol. 1, p. 1.
13. J. E. KOVACIC, *Spectrochim. Acta, Part A*, 1967, 23, 183.
14. P. TEYSSIE and J. J. CHARETTE, *Spectrochim. Acta*, 1963, 19, 1407.
15. D. M. ADAMS, "Metal-ligand and Related Vibrations," Edward Arnold, London, 1967.

J. Indian Chem. Soc.,
Vol. LXIII, March 1986, pp. 273-275

Copper(II) Complexes of 3-*N*-Aryl Substitute Thioquinazolones

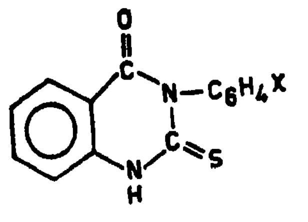
L. D. DAVE*, CHERIAN MATHEW and VARUGHESE OOMMEN

University Department of Chemistry, Bhavnagar University, Bhavnagar-364 002

Manuscript received 18 March 1985, accepted 2 December 1985

Cu^{II} complexes and their pyridine adducts of 3-phenyl/*p*-tolyl/*p*-methoxyphenyl/*p*-ethoxyphenyl/*p*-chlorophenyl/*p*-bromophenyl-quinazoline-2-thione-4-one (HL) are prepared. Elemental analysis, magnetic and spectral data show that the copper complexes without pyridine have square-planar structure and the pyridine adducts have tetragonal structure.

QUINAZOLINE-2-thione-4-one exhibits diverse coordinating behaviour[1] towards different metal ions. In some complexes, it is reported to behave as a monodentate ligand with sulphur or oxygen as the coordinating atom and in some other complexes as bidentate, coordinating through sulphur and tertiary nitrogen atoms. Even though a large number of related ligands are reported, the complexing behaviour of the title ligands are not much studied; only a few are reported[2-5]. In the present communication, we report Cu^{II} complexes formed with several 3-*N*-arylquinazoline-2-thione-4-one (HL) and pyridine adducts. The 3-*N*-aryl substituents on quinazoline-2-thione-4-one used are: 3-phenyl (HPQT), 3-*p*-tolyl (HTQT), 3-*p*-methoxyphenyl (HMPQT), 3-*p*-ethoxyphenyl (HEPQT), 3-*p*-chlorophenyl (HCPQT) and 3-*p*-bromophenyl (HBPQT).



(HL)

X = H/CH_3/OCH_3/OC_2H_5/Cl/Br

Experimental

Analytical grade reagents and pure distilled solvents were used throughout the work.

p-Substituted-phenyl isothiocyanates were prepared as given in the literature[6]. These *p*-substituted-phenyl isothiocyanates and anthranilic acid in equimolar quantities were condensed in presence of glacial acetic acid to get the corresponding ligands[7]. The ligands were found soluble in acetone, dioxane and partially soluble in methanol.

Copper complexes were prepared by mixing 0.1 *M* solution of cupric nitrate in distilled water and 0.1 *M* solution of the ligands in dioxane. The buff coloured precipitates immediately formed on mixing the solutions were digested on a water-bath for 30 min. The solids which separated were filtered, washed with hot water and acetone to remove excess metal ions and unreacted ligands, respectively. The complexes were found to be insoluble in common organic solvents except DMF.

The pyridine adducts of the above copper complexes were prepared by heating the latter in excess pyridine at 110° till a pasty mass was obtained. Excess pyridine present was pumped out at room temperature in vacuum, when the dry pyridine adducts were obtained. All the complexes were found to be insoluble in common organic solvents including DMF.

Nitrogen was estimated by Kjeldhal's[8] method. Copper and sulphur were estimated gravimetrically by weighing as cupric oxide[9] and barium sulphate[10]. The conductivity of the complexes which were soluble was determined using a Toshniwal conductivity bridge. Room temperature magnetic susceptibility was determined by Gouy method. The values are given in Table 1. Electronic spectra of the soluble complexes were recorded on a Beckman Du 7 high speed spectrophotometer in DMF. Ir spectra of the ligands and complexes were recorded on a Beckman spectrophotometer in the form of KBr pellets, at a range 4 000-200 cm^{-1}. Epr measurements were carried out on a Varian E9 spectrometer at room temperature and liquid N_2 temperature in polycrystalline state and in solution. Various epr parameters are given in Table 2.

TABLE 1—ANALYTICAL DATA

Sl. no.	Compd.	Analysis % : Found/(Calcd.) N	S	Cu	Molar conductance Ω^{-1} cm^2 mol^{-1}	Magnetic moment B.M.
1.	$Cu(TQT)_2$	9.58 (9.83)	11.31 (11.27)	11.17 (11.15)	9.8	2.16
2.	$Cu(MPQT)_2$	8.4 (8.9)	10.32 (10.17)	10.3 (10.1)	10.2	2.19
3.	$Cu(EPQT)_2$	8.96 (8.52)	9.5 (9.73)	9.65 (9.66)	10.9	2.08
4.	$Cu(CPQT)_2$	8.32 (8.77)	10.31 (10.02)	9.7 (9.9)	9.6	2.05
5.	$Cu(BPQT)_2$	7.4 (7.7)	8.4 (8.8)	8.6 (8.7)	10.5	2.03
6.	$Cu(PQT)_2$ 2py	11.48 (11.55)	8.6 (8.8)	8.78 (8.73)	–	2.05
7.	$Cu(TQT)_2$ 2py	11.2 (11.12)	8.32 (8.47)	8.25 (8.41)	–	1.97
8.	$Cu(MPQT)_2$	10.45 (10 67)	8.02 (8.13)	8.16 (8.06)	–	1.91
9.	$Cu(EPQT)_2$ 2py	10.15 (10 3)	7.78 (7.85)	7.81 (7.79)	–	1.95
10.	$Cu(CPQT)_2$ 2py	10.48 (10.55)	7.95 (8.04)	7.87 (7.97)	–	1.90
11.	$Cu(BPQT)_2$ 2py	9.38 (9.49)	7.28 (7.23)	7.2 (7.17)	–	1.98

TABLE 2—EPR PARAMETERS

Sl. no.	Compd.	Polycrystalline state RT[a]		LNT[b]		Solution state RT[a]		LNT[b]			$G_{average} = \frac{g_{\parallel}-2}{g_{\perp}-2}$
		$g_{\parallel}$	$g_{\perp}$	$g_{\parallel}$	$g_{\perp}$	g_{iso}	$g_{\parallel}$	$g_{\perp}$	$A_{\parallel}$	$g_{\parallel}/A_{\parallel}$ $\times 10^{-4}$	
1.	$Cu(TQT)_2$	2.16	2.04	2.15	2.04	2.07	2.2	2.05	170.5	129	4.0
2.	$Cu(MPQT)_2$	2.18	2.04	2.16	2.05	2.15	2.2	2.05	170	129	3.90
3.	$Cu(EPQT)_2$	2.12	2.03	2.12	2.03	2.10	2.24	2.05	172.5	130	4.3
4.	$Cu(CPQT)_2$	2.15	2.04	2.17	2.04	2.05	2.22	2.06	167	133	3.9
5.	$Cu(BPQT)_2$	2.15	2.04	2.15	2.04	2.12	2.25	2.06	165	136	4.0
6.	$Cu(PQT)_2$ 2py	2.25	2.07	2.32	2.08	2.10	2.21	2 05	165	134	4.0
7.	$Cu(TQT)_2$ 2py	2.16	2.04	2.19	2.05	2.10	2.21	2.05	168	132	4.0
8.	$Cu(MPQT)_2$ 2py	2.15	2.04	2.12	2.03	2.08	2 23	2.06	171.5	130	3.9
9.	$Cu(EPQT)_2$ 2py	2.18	2.05	2.21	2.05	2.12	2.22	2.05	170.5	130	4.1
10.	$Cu(CPQT)_2$ 2py	2.17	2.04	2.27	2.07	2 15	2.20	2 05	168	131	4.0
11.	$Cu(BPQT)_2$ 2py	2.19	2.05	2.25	2.06	2 15	2 23	2.06	169	132	4.0

[a]RT ≡ Room temperature, [b]LNT ≡ liquid N_2 temperature.

Results and Discussion

From the elemental analyses it was found that the non-pyridine copper complexes have 1 : 2 M-L stoichiometry and the pyridine adducts have 1 : 2 : 2 M-L-py stoichiometry. So the ligands behave as bidentate chelating agents. Molar conductances of the non-pyridine copper complexes were measured in DMF and have a very low value, suggesting the covalent nature of the complexes.

The values of the magnetic moment of the complexes were found to be 1.9-2.2 B.M., suggesting the presence of one unpaired electron. The excess over the value for one unpaired electron (1.73 B.M.) found for the complexes can be attributed to spin-orbit coupling[11,12]. Pyridine molecules give rise to a six-coordinate complex.

It has been proved from the ir spectra that quinazoline-2-thione-4-one exists as thione in solid state, although it may change to thiol form in solution[13]. This is known to be the case in many such thiones[14]. In this case also the ir spectra show that the compounds exist as thiones. Since nitrogen atom at position 3 bears a substituent, there is only one NH group in the ligands. The band observed at 3 100 cm^{-1} is assigned to ν_{N-H} (nitrogen at position 1) in the spectra of the ligands. It is not observed in the spectra of all the complexes. Hence, we conclude that the nitrogen atom at position 1 is taking part in coordination to metal ion. The band observed at about 1 685 cm^{-1} in all the ligands is considered to be due to $\nu_{C=O}$. It is observed with little change in the spectra of the complexes. So we conclude that the carbonyl

oxygen is not taking part in complex formation. In the spectra of the complexes, we observe two new bands at 690 (C—S) and 1 610 cm^{-1} (C=N). The change from $\nu_{C=S}$ to ν_{C-S} shows that the mercapto form of the ligands binds itself to the metal. Hence, we assume that binding of the copper atom to the ligand is taking place through the nitrogen atom at position 1 and the negative sulphur of the thiol group. This is further supported by the far-ir studies which give evidence for M—N and M—S bonds. The bands due to these are observed at 480 and 310 cm^{-1}, respectively. In the case of pyridine adducts, we observe the band due to pyridine in addition to the bands observed for Cu^{II} complexes. The complexes were quite stable at room temperature even though they contain a four-membered ring including the metal ion and sulphur. Such a stable system was reported earlier[15].

The electronic spectra of the non-pyridine complexes were recorded in DMF. They show three weak bands at 555, 640 and 670 nm, which can be assigned to the transitions[16], $^2E_g \leftarrow {^2B_{1g}}$, $^2B_{2g} \leftarrow {^2B_{1g}}$ and $^2A_{1g} \leftarrow {^2B_{1g}}$, on the assumption of a square-planar structure for these complexes. The pyridine adducts are insoluble even in DMF and hence their spectra in solution could not be studied.

Epr spectra of these complexes were recorded in solid state and in solution at room temperature and at liquid N_2 temperature. For non-pyridine complexes the DMF solution and for the pyridine adducts a mixture of pyridine and acetone solution, were used. Polycrystalline epr spectra of these complexes are of general shape[17] from which the values of $g_{\parallel}$ and $g_{\perp}$ tensors were calculated. The spectra do not show any resolution at the $g_{\perp}$ region. So it can be assumed that g_x and g_y are the same or nearly the same. We do not observe any $\Delta M_s = \pm 2$ transition at half-field at room temperature, thus ruling out any Cu—Cu interaction. Further, the G values, where $G=(g_{\parallel}-2)/(g_{\perp}-2)$, calculated for these complexes are four or nearly equal to four suggesting very low Cu—Cu interaction[18].

From the room temperature solution spectra, g_{iso} and A_{iso} values were obtained. The g_{iso} values calculated from the room temperature polycrystalline as well as liquid N_2 temp rature solution are in fair agreement with the above g_{iso} values. The liquid N_2 temperature solution spectra show four clear bands in the $g_{\parallel}$ region, expected for Cu^{II} complexes. Hyperfine splitting constants $|A_{\parallel}|$ of copper calculated from the spectra are typical of square-planar copper complexes[19]. The fine structure in the $g_{\perp}$ region may be due to the further splitting of the copper $g_{\perp}$ band by nitrogen atoms. The superhyperfine splitting is found to be ≈ 13 G which is of the usual order due to nitrogen. The values of $g_{\parallel}$ and $g_{\perp}$ calculated at different conditions, are typical of copper(II) complexes with axial symmetry[18,20]. In all the cases $g_{\parallel} > g_{\perp}$, suggesting that the molecules are elongated tetragonal or square-planar with unpaired electron in the $d_{x^2-y^2}$ orbital[17], the ground state term being $^2B_{1g}$. The $g_{\parallel}/A_{\parallel}$ ratio is in the range of square-planar CuN_2S_2 complexes[19].

Acknowledgement

Two of the authors (C.M. and V.O.) are thankful to C.S.I.R., New Delhi, and Bhavnagar University, respectively, for financial assistance.

References

1. B. Singh, R. N. Pandey, D. K. Sharma, U. S. Sharma and Uday Bhanu, *Indian J. Chem., Sect. A*, 1981, 20, 1097.
2. T. N. Ghosh, *J. Indian Chem. Soc*, 1930, 7, 981.
3. G. R. Dave, G. C. Mewada and G. C. Amin, *Colora e*, 1969, 16, 49 (*Chem. Abstr*, 1969, 71, 97983).
4. S. K. Sengupta and Nizzamuddin, *Indian J. Chem., Sect. A*, 1982, 21, 426.
5. L. D. Dave, C. Mathew and V. Oommen, *Indian. J. Chem., Sect. A*, 1983, 22, 420.
6. A. I. Vogel, "Practical Organic Chemistry", 3rd ed., Longmans, London, 1956, p. 644.
7. C. Parkanyi and A. Vystrail, *Chem. Listy*, 1956, 50, 666 (*Chem. Abstr.*, 1956, 50, 8657).
8. A. I. Vogel, "A Textbook of Quantitative Inorganic Analysis", Longmans, London, 1975, p. 529.
9. Cuming and Key, "Quantitative Chemical Analysis", Oliver & Boyd, London, 1956, p. 257.
10. A. I. Vogel, "Elementary Practical Organic Chemistry", Longman, London, 1961, part III, p. 660.
11. J. Lewis and R. G. Wilkins, "Modern Coordination Chemistry", Interscience, New York, 1960, p. 427.
12. A. Earnshaw, "Introduction to Magnetochemistry", Academic Press, New York, 1966, p. 34.
13. B. Singh, M. M. P. Rukhaiyar and R. J. Sinha, *J. Inorg. Nucl. Chem.*, 1977, 39, 29.
14. C. N. R. Rao, R. Venkataraghavan and T. R. Kasthuri, *Can. J. Chem.*, 1964 42, 36.
15. B. A. Cartwright, D. O. Langguth, Jr. and A. C. Skapski, *Acta Cry tallogr. B*, 1979, 35, 63.
16. A. B. P. Lever, "Inorganic Electronic Spectroscopy", Elsevier, New York, 1968, p. 355.
17. F. K. Kneubul, *J. Chem. Phys*, 1960, 33, 1074.
18. B. J. Hathway and D. E. Billing, *Coord. Chem. Rev.*, 1970, 5, 143.
19. U. Sakaguchi and A. W. Addison, *J. Chem. Soc., Dalton Trans.*, 1979 600.
20. A. D. Toy, S. H. H. Cheston, J. R. Pilbrow and T. D. Smith, *Inorg. Chem.*, 1971, 10, 2219.

J. Indian Chem. Soc.,
Vol. LXIII, March 1986, pp. 276-277

Reactions of Copper(II) Salts with Benzoylacetone and γ-Picoline or Imidazole

C. M. DANI

Research and Control Laboratory, Rourkela Steel Plant, Rourkela-769 011

and

A. K. DAS*

Department of Chemistry, Government College, Rourkela-769 004

Manuscript received 2 February 1984, accepted 6 February 1986

Six mixed ligand complexes of the type $[Cu(bzac)L_2]X$ and $[Cu(bzac)L_2 ClO_4]$, where bzacH = benzoyl acetone, L = γ-picoline or imidazole and X = Cl^- or NO_3^- have been synthesised by reacting the cupric salts with benzoylacetone and γ-picoline or imidazole in 1 : 1 : 2 molar ratio in ethanol medium. The analytical, conductance, magnetic susceptibility, infrared and electronic spectral data reveal that the complexes of the first and second categories are square-planar and pentacoordinated, respectively.

THERE has been considerable interest in recent years, in the study of mixed ligand complexes of metal β-diketonates with ligands containing different donor atoms of varying electronegativities, in view of their significance and diverse uses. Some mixed ligand complexes of copper(II) containing dibenzoylmethane and nitrogen donor ligands have been reported[1] in an earlier communication. In continuation of our studies[2] on mixed ligand complexes of Cu^{II} and Ni^{II} containing acetylacetonate, trichloroacetate and N, S or O donors, we report in the present communication, the results of the reactions of Cu^{II} salts with benzoylacetone and γ-picoline or imidazole in 1 : 1 : 2 stoichiometric ratio in ethanol medium.

Experimental

All the chemicals used were of BDH AnalaR quality.

Preparation of complexes : The complexes were prepared by refluxing ethanolic solutions of Cu^{II} salts, benzoylacetone and γ-picoline or imidazole in 1 : 1 : 2 molar ratio for about 30 min and then keeping the resulting solutions overnight. The complexes were filtered, washed with absolute ethanol several times followed by ether and dried *in vacuo*.

Analyses and physical measurements : Analyses of copper and chloride were carried out by standard methods. Carbon and hydrogen were determined microanalytically. Magnetic measurements of the complexes were conducted at room temperature by Gouy method. Molar conductances of the complexes in DMF were measured using a Systronic 303 direct reading conductivity meter. Ir spectra were recorded on a Perkin-Elmer 577 spectrophotometer in the range 4 000-200 cm^{-1} and electronic spectra of the complexes in chloroform medium were recorded using Hitachi 320 spectrophotometer.

Results and Discussion

Analytical data and some of the physicochemical properties of the complexes (Table 1) are consistent with the proposed formulations. The room temperature magnetic moment values of 1.84-1.97 B.M. suggest the paramagnetic nature of the Cu^{II} complexes containing one unpaired electron. The complexes are fairly soluble in methanol, chloroform and dimethylformamide. Chloride and nitrate complexes have Λ_M values in the range, 43.2-51.7 Ω^{-1} cm^2 mol^{-1} suggesting 1 : 1 electrolytic nature of the complexes. The molar conductance values 6.2-7.0 Ω^{-1} cm^2 mol^{-1} of the perchlorato complexes indicate their non-electrolytic nature.

Ir spectra : Some important ir bands of diagnostic importance are discussed. In the present complexes, the occurrence of bands due to $\nu_{C=O}$ and $\gamma_{C=C}$ around 1 610-1 582 and 1 545-1 540 cm^{-1}, respectively reveals[1,2] the presence of coordinated β-diketone group of benzoylacetone. The $\gamma_{C=C}$ + $\nu_{C=N}$ bands of γ-picoline observed at 1 610, 1 570 and 1 498 cm^{-1} are shifted to 1 615, 1 5 2 and 1 508 cm^{-1}, respectively in the γ-picoline complexes indicating[4-6] coordination of the ligand through the nitrogen atom. The absorption band centering at 3 165 cm^{-1} in the ir spectrum of imidazole is attributed to ν_{N-H} and is shifted 10-15 cm^{-1} to

* Present address : Bonaigarh College, Bonaigarh, Dt. Sundargarh, Orissa.

TABLE 1—ANALYTICAL DATA OF THE MIXED LIGAND COMPLEXES OF COPPER(II)

Compd.	Colour	M.p. °C	Analysis % : Found/(Calcd.) Cu	Cl	C	H	Λ_M Ω^{-1} cm^2 mol^{-1}	μ_{eff} B.M.
[Cu(bzac)(γ-pic)$_2$]Cl	Shining green	155.0	14.28 (14.24)	7.14 (7.95)	59.6 (59.19)	4.98 (5.15)	50.4	1.84
[Cu(bzac)(Iz)$_2$]Cl	Light blue	182.0	15.95 (16.03)	8.48 (8.95)	48.26 (48.46)	4.01 (4.29)	46.8	1 89
[Cu(bzac)(γ-pic)$_2$]NO$_3$	Green	172.0	13.91 (13.44)		55.21 (55.86)	5.11 (4.86)	51.7	1.92
[Cu(bzac)(Iz)$_2$]NO$_3$	Green	190.0	14.48 (15.03)		44.94 (45.42)	3.89 (4.02)	43.2	1.97
[Cu(bzac)(γ-pic)$_2$ClO$_4$]	Shining green	132.0	12.10 (12.45)		50.96 (51.76)	4.21 (4.50)	6.2	1.85
[Cu(bzac)(Iz)$_2$ClO$_4$]	Shining green	188.0	14.40 (13.80)		41.10 (41.72)	3.10 (3.69)	7.0	1.84

lower frequencies in the imidazole complexes. A shift in $\nu_{C=N}$ from 1 582 to ~ 1 560 cm^{-1} and the presence of ν_{N-H} in the spectra of these complexes suggest the involvement of tertiary nitrogen of imidazole in coordination. The nitrate complexes, [Cu(bzac)L$_2$] NO$_3$ show a strong N—O stretching mode around 1 350 cm^{-1} (ν_3) region and two ir active deformation modes around 850 (ν_2) and 760 cm^{-1} (ν_4). These indicate ionic nature of the nitrate ion having D_{3h} symmetry[8-10]. The perchlorato complexes display three sharp bands at ~ 1 100, ~ 1 080 and ~ 1 070 cm^{-1}, and another band at ~ 920 cm^{-1} suggesting the coordinated behaviour of ClO_4^- ion[11-14]. Further, monodentate behaviour of ClO_4^- is supported by the absence of ν_{ClO_3} band around 1 270-1 245 cm^{-1}. The non-ligand bands occuring around 428-418 cm^{-1} and 322-300 cm^{-1} regions may tentatively be assigned to ν_{Cu-O} and ν_{Cu-N} modes, respectively.

Electronic spectra : The electronic spectra of chloride and nitrate complexes show two absorption bands at ~ 540 and 660 nm which may be assigned to $^2B_{1g} \rightarrow {}^2E_g$ and $^2B_{1g} \rightarrow {}^2B_{2g}$ transitions, respectively for a square-planar stereochemistry[15,16] around copper(II). The observed spectra further eliminate[17] the possibility of tetrahedral or pseudo-tetrahedral structure for the complexes. The presence of a broad electronic spectral band at ~ 640 nm in the perchlorate complexes, favours pentacoordination around copper(II)[18-20]. However, *X*-ray studies alone can reveal the exact stereochemistry of these pentacoordinated complexes.

Acknowledgement

The authors wish to thank Prof. D. V. Ramana Rao, for encouragement, the management of Rourkela Steel Plant, for providing facilities, and the R.S.I.C. at C.D.R.I., Lucknow, for running the spectra of the complexes.

References

1. K. M. PUROHIT and D. V. RAMANA RAO, *Indian J. Chem., Sect. A*, 1982, 21, 437.
2. C. M. DANI and A. K. DAS, *J. Indian Chem. Soc.*, 1984, 61, 381.
3. S. N. DAS and K. C. DASH, *J. Indian Chem. Soc.*, 1979, 56, 459.
4. R. C. PAUL and S. L. CHADHA, *Spectrochim Acta*, 1966, 22, 615.
5. R. C. PAUL and S. L. CHADHA, *Indian J. Chem.*, 1968, 6, 272.
6. D. FORSTER and D. M. L. GOODGAME, *J. Chem. Soc.*, 1964, 2790.
7. A. K. DAS and D. V. RAMANA RAO, *Indian J. Chem.*, 1971, 9, 481.
8. N. F. CURTIS and Y. M. CURTIS, *Inorg. Chem.*, 1965, 4 804.
9. C. C. ADDISON and D. F. SUTTON, *Prog. Inorg. Chem.*, 1967, 8, 1169.
10. B. M. GATEHOUSE, S. E. LIVINGSTONE and R. S. NYHOLM, *J. Chem Soc.*, 1957, 4227.
11. L. E. MOORE, R. B. GAYHERT and W. E. BULL, *J. Inorg. Nucl Chem.*, 1964, 24, 898.
12. K. NAKAMATO, "Infrared Spectra of Inorganic and Coordination Compounds", John Wiley, New York, 1970, p. 175.
13. G. DYER, J. G. HARTLEY and L. M. VENANZI, *J. Chem. Soc.*, 1965, 3091.
14. I. M. PROCTOR, B. J. HATHAWAY and P. J. NICHOLLS, *J. Chem. Soc.*, 1968, 1678.
15. L. SACCONI and M. J. CIAMPOLINI, *J. Chem. Soc.*, 1964, 276.
16. J. BJERRUM, C. J. BALHAUSEN and C. K. JOGENSEN, *Acta Chem. Scand.*, 1954, 8, 1275.
17. A. B. P. LEVER, "Inorganic Electronic Spectroscopy", Elsevier, Amsterdam, 1968, p. 359.
18. T. SHIGEMATSU, M. TABUSHI, M. MATSUI and M. MUNAKATA, *Bull Chem. Soc. Jpn.*, 1968, 41, 2656.
19. P. E. RAKITA, S. KOPPERL and J. P. PACKLER, JR. *J. Inorg. Nucl. Chem.*, 1968, 30, 2139.
20. R. D. GILLARD and G. WILKINSON, *J. Chem. Soc. (A)*, 1963, 359.

J. Indian Chem. Soc.,
Vol. LXIII, March 1986, pp. 278-280

Coordination Polymers of some First Row Transition Metals

M. N. PATEL* and B. N. JANI

Department of Chemistry, Sardar Patel University, Vallabh Vidyanagar-388 120

Manuscript received 16 August 1984, revised 3 June 1985, accepted 24 December 1985

This paper describes the synthesis and characterisation of some new coordination polymers derived from poly Schiff base (PSB) and first row transition metal ions. Ir study showed that the metal ions are coordinated through oxygen of hydroxy group and nitrogen of adjacent azomethine group. The decomposition temperatures of the polymeric chelates were found to be in the order : Ni > Co > Cu > Mn and the thermal activation energy in the order, Ni > Cu > Co > Mn. Probable structures of these compounds have been proposed on the basis of elemental analyses, electronic spectra, ir spectra, and TG analysis.

THE first row transition metals are characterized by their ability to form a wide range of coordination complexes in which the octahedral, tetrahedral and square-planar stereochemistry predominate. This inspired us to prepare a polymeric ligand which would be able to form complexes with a variety of transition metals. This communication describes the preparation and characterisation of chelates prepared from PSB derived from 4,4'-dihydroxy-3,3'-dipropyl biphenyl with *o*-dianisidine. The stereochemistry of the polychelates has been studied by electronic spectra, ir, magnetic moment, TG analysis and elemental analysis.

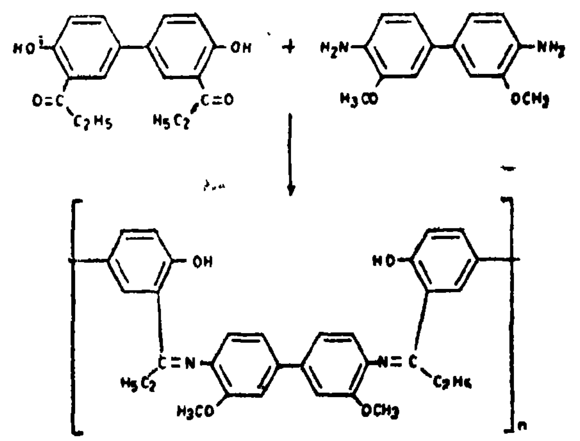
Experimental

All the metal acetates used in the present work were of A.R. Grade. All the solvents were used after double-distillation.

C and H analyses were made on a Coleman C—H—N analyser. The metal content was determined by EDTA titration technique after decomposition of the polychelates. The magnetic susceptibility was measured by Gouy method at room temperature. The ir spectra in KBr phase in the range 3 600-450 cm^{-1} were recorded on a Carl Zeiss Jena UR-10 spectrophotometer. Electronic spectra were recorded on a Beckman DU spectrophotometer. The TG analysis was carried out on Linseis thermogravimetric analyser.

Preparation of PSB : The ligand (PSB) was prepared from hydroxy ketone 4,4'-dihydroxy-3,3'-dipropyl bipehnyl (DDPBP) and *o*-dianisidine as described below.

DDPBP and *o*-dianisidine were dissolved separately in ethanol in stoichiometric proportion and were mixed and refluxed for 8 h. It was cooled and a dark yellow coloured PSB was separated out. It was filtered, washed with ethanol and dried. It was insoluble in common organic solvents but found soluble in DMF, DMSO and H_2SO_4. The reaction path way is shown below,



Preparation of chelates : Equimolar quantities of metal acetates and PSB were dissolved separately in DMF and mixed. The reaction mixture was refluxed for 6 h. The hot solution was poured into crushed ice. The precipitates were allowed to settle down, filtered, washed with hot water and dried. They were purified by soxhlet extraction in methanol to remove impurities and dried.

Results and Discussion

The polychelates are insoluble in common organic solvents and are dark in colour. Elemental data are given in Table 1. From the data, it is revealed that all the polychelates have general formula $[ML]_n$.

Infrared spectra : On comparison of infrared spectra of ligand and its polychelates, it is inferred that they are virtually identical with each other. However, they show important differences. Strong band of C=N in the ligand at 1 620 cm^{-1} shows

TABLE 1—ANALYTICAL DATA, COLOUR AND DECOMPOSITION TEMPERATURE

Sl. no.	Compd.	Colour	Decomp. temp. °C	Analysis % : Found/(Calcd.) C	H	M
1.	PSB	Dark yellow	320	75.20 (75.88)	6.12 (5.92)	—
2.	[Cu PSB].$2H_2O$	Brick red	250	64.10 (63.62)	5.90 (5.30)	10.12 (10.52)
3.	[Ni PSB.$2H_2O$]	Brown	290	64.70 (64.13)	5.10 (5.34)	9.60 (9.80)
4.	[Co PSB].$2H_2O$	Brown	270	63.82 (64.11)	5.68 (5.34)	9.40 (9.83)
5.	[Mn PSB.$2H_2O$]	Brick red	240	64.05 (64.54)	4.98 (5.37)	9.55 (9.23)

TABLE 2—TG, ELECTRONIC SPECTRAL AND MAGNETIC DATA OF PSB AND POLYCHELATES

Sl. no.	% Weight loss at temp. (°C) 100	200	300	400	500	600	Energy (cm^{-1}) Found / (Calcd.)		μ_{eff} B.M.	E_a kcal mol^{-1}	B_{35}	β_{35}	LFSE kcal mol^{-1}
1.	0.0	0.0	0.5	10.0	32.0	44.5	—	—	—	16.35	—	—	—
2.	1.5	7.5	23.0	58.0	71.0	79.5	15 750 18 350 24 390	— — —	1.89	13.50	—	—	—
3.	0.5	6.0	23.5	61.5	80.0	83.5	9 615 (9 615) 16 665 (15 253) 23 095 (24 507)	— — — — — —	2.64	15.47	727.66	0.673	33.0
4.	4.0	11.5	40.0	81.0	85.5	88.0	— (4 181) 9 045 (9 567) 16 805 (16 281)	— — — — — —	3.58	9.85	887.07	0.792	14.34
5.	0.0	4.5	24.5	65.0	82.0	88.0	14 400 16 600 20 000	— — —	5.25	5.22	—	—	—

either a positive shift[1] or a negative shift[3] in polychelates. In Cu^{II} an Co^{II} polychelates, it is shifted to higher frequency, *i.e.* at 1 630 and 1 625 cm^{-1}, respectively. While in Ni^{II} and Mn^{II} polychelates, it is shifted to lower frequency, *i.e.* at 1 595 and 1 590 cm^{-1}, respectively. The observable shift obtained in C=N stretch after complexing confirms the formation of a coordinate bond from imine nitrogen to the metal ion. The medium band observed at 1 270 cm^{-1} in the ligand is ascribed the phenolic C—O stretching vibration and on complexation does not show marked shift indicating that this frequency is not so sensitive to the chelation[3]. The spectrum of the ligand shows a broad and weak band in the region 2 710-2 830 cm^{-1} and is assigned to the intra-molecular hydrogen bonded OH group. On complexation, this band disappears indicating metal-oxygen bond formation in the polychelates[3]. Weak band in PSB and polychelates observed around 2 890 cm^{-1} is assigned to C—H stretching vibration. All the complexes contain weak to medium intensity broad band in the region 3 300-3 600 cm^{-1}, and a weak band around 790 cm^{-1}. These bands are assigned to ν_{OH} of water. Nature of water molecules (coordinated or lattice) is confirmed by TG analysis. In all the polychleates, the observed band in the neighbourhood of 500 cm^{-1} may be identified as M—N stretching frequency[4].

Thermal study : Thermal decomposition studies (Table 2) were made by heating the compound (~50 mg) at various temperatures in a furnace starting from 20°. The temperature was allowed to increase at a rate of 10° min^{-1}. Thermal stability studies of the polymeric metal chelates up to the decomposition point indicate that they are thermally stable. The weight losses of Ni^{II} and Mn^{II} polychelates at 200-225° are 6.00 and 6.5%, respectively. These weight losses correspond to two coordinated water molecules per repeating unit of polychelate. The Cu^{II} and Co^{II} polychelates show weight losses at 125-150° equal to 6.0 and 7.0%, respectively. These weight losses correspond to two lattice water molecules. The decomposition temperature of the PSB and its polychelates decreases in the order,

PSB(320°) > Ni(290°) > Co(270°) >
Cu(250°) > Mn(240°)

Goodwin and Bailar[5] observed the given thermal stability order for the polychelates as Ni > Cu > Co which is in agreement with the observation reported by Marvel and Torkoy[6]. We have observed the same order at 200° which does not remain unchanged up to 600° as Mn > Ni > Cu > Co. The thermal activation energy was calculated by employing the Broido method and values are summarised in Table 2.

Electronic and magnetic study: The diffuse electronic spectrum of the Cu^{II} polychelate shows three bands at 15 750, 18 350 and 24 390 cm^{-1}, the first two bands may be due to the d-d transition which suggests the square-planar stereochemistry[7]. Intense band at 24 390 cm^{-1} may be assigned to charge transfer or intra-ligand transition[8]. The room temperature magnetic moment of Cu^{II} polychelate is 1.89 B.M. which also supports the square-planar geometry[9]. Ni^{II} polychelate exhibits three bands at 9 615, 16 665 and 21 095 cm^{-1}. The position of these bands are consistant with those of an octahedral, essentially distorted structure[10]. These bands can be assigned to the transitions $^3A_{2g}$ (F) → $^3T_{2g}$ (F), → $^3T_{1g}$ (F) and → $^3T_{1g}$ (P), respectively. The magnetic moment value is 2.64 B.M. Subnormal magnetic moment value may be indicative of polymeric structure of the complex[11]. The diffuse reflectance spectrum of Co^{II} polychelate shows two bands at 9 045 and 16 805 cm^{-1}. These bands may be assigned to $^4A_2$ → $^4T_1$ (F) and → $^4T_1$ (P) transition, indicative of tetrahedral geometry of the chelate[12]. The magnetic moment is 3.58 B.M. This low value of magnetic moment is indicative of mixture of low-spin square-planar and high-spin tetrahedral stereochemistry[13]. The Mn^{II} polychelate exhibits the transition sextet → quartet. The ground term is $^6A_1$ (S) and exhibits three weak absorption maxima, one at 14 400 cm^{-1} which may arise due to $^6A_{1g}$ → $^4T_{1g}$ (^{4}G), another at 16 600 cm^{-1}, assigned to $^6A_{1g}$ → $^4T_{2g}$ (^{4}G) and the third at 20 000 cm^{-1}, assigned to $^6A_{1g}$ → ^4E_g $^4A_{1g}$ (^{4}G) for Mn^{II} ion in octahedral environment[14]. The magnetic moment is 5.25 B.M., lower than that generally observed for spin-free d^5 system. Lower magnetic moment may be due to aerial oxidation of Mn^{II} → Mn^{III} during the preparation of the complex[14].

From the elemental, magnetic, reflectance and infrared studies, it is concluded that the mental ion is coordinated to positions on two (or more) neighbouring ligand chains indicating the polymeric structure.

Acknowledgement

The authors are thankful to Professor R. P. Patel, Head, Department of Chemistry, for facilities. Financial assistance from U. G. C., New Delhi, to one of the authors (B. N. J.) is also gratefully acknowledged.

References

1. D. H. BUSH and J. C. BAILAR, JR., *J. Am. Chem. Soc.*, 1956, 78, 1137.
2. K. LAL, J. SINGH and S. P. GUPTA, *J. Inorg. Nucl. Chem.*, 1978, 40, 359.
3. N. S. BIRADAR and V. H. KULKARNI, *J. Inorg. Nucl. Chem.*, 1971, 33, 3781.
4. K. NAKAMOTO, "Infrared Spectra of Inorganic and Coordination Compounds", Wiley-Interscience, New York, 1970.
5. H. A. GOODWIN and J. C. BAILAR, JR., *J. Am. Chem. Soc.*, 1961, 83, 2467.
6. C. S. MARVEL and N. TORKOY, *J. Am. Chem. Soc.*, 1958, 80, 832.
7. L. D. DAVE, H. K. KOTHARI and P. SUDHAMSHUMOULI, *Indian J. Chem.*, 1974, 12, 771.
8. J. MALAVIYA, P. R. SHUKLA and L. N. SRIVASTAVA, *J. Inorg. Nucl. Chem.*, 1973, 35, 1706.
9. A. KAPAHI, K. B. PANDEYA and R. P. SINGH, *Indian J. Chem., Sect. A*, 1976, 14, 444.
10. D. K. RASTOGI and K. C. SHARMA, *J. Inorg. Nucl. Chem.*, 1974, 36, 2219.
11. V. K. ARORA, K. B. PANDEYA and R. P. SINGH, *J. Indian Chem. Soc.*, 1979, 56, 656.
12. M. N. PATEL and S. H. PATIL, *J. Macromol. Sci., Chem.*, 1982, 17, 675.
13. M. CALVIN and C. H. BARKLEW, *J. Am. Chem. Soc.*, 1946, 68, 2267.
14. K. DAY, *J. Indian. Chem. Soc.*, 1971, 48, 641.

J. Indian Chem. Soc.,
Vol. LXIII, March 1986, pp. 281-283

Copper(II), Nickel(II), Cobalt(II), Manganese(II), Iron(II), Zinc (II), Chromium(III), Oxovanadium(II) and Dioxo-uranium(II) Complexes of 4-Benzoylsemicarbazone-1-phenyl-3-methyl-2-pyrazolin-5-one

A. K. RANA and J. R. SHAH*

Department of Chemistry, Sardar Patel University, Vallabh Vidyanagar-388 120

Manuscript received 19 February 1985, revised 30 December 1985, accepted 17 January 1986

There is an extensive and interesting study on the extraction of metal complexes of 4-benzoyl-1-phenyl-3-methyl-2-pyrazolin-5-one. However, there is no report on the study of metal complexes of the 4-benzoylsemicarbazone-1-phenyl-3-methyl-2-pyrazoline-5-one (BscPMPO) and therefore, we report here the preparation and characterisation of its complexes with Cu^{II}, Ni^{II}, Co^{II}, Mn^{II}, Fe^{II}, Zn^{II}, Cr^{III}, $V^{IV}O$ and $U^{VI}O_2$.

ALL the solvents and reagents used were guaranteed reagents. BscPMPO (m p. 179°) was prepared by the usual method Metal nitrates were used in the preparation of Cu^{II}, Ni^{II}, Co^{II}, Mn^{II}, Zn^{II}, Cr^{III} and $U^{VI}O_2$ complexes. Ferrous ammonium sulphate and vanadyl sulphate were used in the preparation of Fe^{II} and $V^{IV}O$ complexes, respectively. In the preparation of all the complexes, the following general procedure was used. A stoichiometric quantities of the hot ethanolic solutions of metal salt and ligand were mixed with continuous stirring. To the resulting solution, sodium acetate (1 g) was added and refluxed for 1 h. The reaction mixture was then concentrated to half of its original volume. The product, thus obtained was then filtered and washed with hot water and finally with ethanol. The product was then dried in air. Aqueous metal solutions were used in the preparation of Fe^{II} and $V^{IV}O$ complexes.

All physicochemical measurements were made as described earlier[1].

Results and Discussion

Elemental analyses (Table 1) indicate metal-ligand ratio of 1 : 3 for Fe^{III} and Cr^{III} complexes and 1 : 2 for all other complexes. The conductivity measurements suggest non-ionic behaviour of the complexes in ethanol.

The ligand shows bands at 3 000, 3 230 and 3 350 cm^{-1} which may be assigned to the ν_{N-H} and ν_{O-H}[2]. The bands at 1 690, 1 610, 1 585 and 1 210 cm^{-1} may be assigned to amide I (and mainly due to ring $\nu_{C=O}$), $\nu_{C=N}$ (azomethine), amide II ($\nu_{CN}+\nu_{NH}$) and amide III (δ_{NH}), respectively[3]. The infrared spectra of complexes record a downward shift (~10 cm^{-1}), for the $\nu_{C=N}$ (azomethine) and in some complexes it is further shifted until completely masked by a broad band. This suggests the participation of the azomethine nitrogen in the coordination. All complexes show the absence of amide I, II and III bands and instead show new bands at 1 595 and 1 350 cm^{-1}. They may have their origin in vibration at mode of conjugated C=N—N=C grouping, suggesting destruction of keto group through enolisation[4,5] and participation of enolic oxygen in coordination. Infrared spectra of the Cu^{II}, Ni^{II}, Co^{II}, Mn^{II}, Zn^{II} and $V^{IV}O$ complexes show a broad band in the region 3 500-3 000 cm^{-1}. The broad nature of the band might be due to the mixing up of symmetric and antisymmetric ν_{OH} with that of ν_{N-H}. This suggests the presence of coordinated water molecules in the complexes. To account for the octahedral stereochemistry for the complexes, association of the two molecules of water might be there. In addition, rocking mode of vibration of coordinated water molecules is observed in the range 780-790 cm^{-1} for all these complexes. A strong and broad band at 945 cm^{-1} observed in the $V^{IV}O$ complex may be assigned to the $\nu_{V=O}$[6]. $U^{VI}O_2$ complex shows a broad band at 910 cm^{-1} which may be ascribed to the asymmetric stretching vibration of linear O—U—O[7].

The diffuse reflectance spectrum of the Cu^{II} complex consists of two bands at 14 600 and 20 830 cm^{-1}. Absence of any band below 10 000 cm^{-1} excludes the possibility for the tetra-

TABLE 1—ANALYTICAL AND CONDUCTIVITY DATA OF COMPLEXES

Compd.	Analysis % : Found/(Calcd.)			Λ_M^* $\Omega^{-1}cm^2mol^{-1}$
	M	C	H	
Cu(BscPMPO)$_2$(H$_2$O)$_2$	8.56 (8.25)	56.70 (56.10)	4.00 (4.90)	5.10
Ni(BscPMPO)$_2$(H$_2$O)$_2$	7.27 (7.67)	57.10 (56.43)	4.90 (5.00)	2.00
Co(BscPMPO)$_2$(H$_2$O)$_2$	7.40 (7.70)	57.60 (56.50)	5.70 (5.00)	2.05
Cr(BcPMPO)$_3$	5.04 (4.91)	60.50 (61.30)	5.00 (4.80)	1.00
Mn(BscPMPO)$_2$(H$_2$O)$_2$	7.96 (8.30)	57.00 (56.70)	4.78 (5.00)	8.30
Fe(BscPMPO)$_2$	5.10 (5.25)	61.70 (60.96)	4.40 (4.80)	3.55
VO(BscPMPO)$_2$(H$_2$O)	7.31 (6.90)	56.50 (57.10)	4.35 (4.90)	3.46
UO$_2$(BscPMPO)$_2$	25.60 (25.30)	46.80 (46.00)	4.25 (3.65)	2.35
Zn(BscPMPO)$_2$(H$_2$O)$_2$	9.30 (8.40)	56.93 (56.00)	5.27 (4.96)	10.40

*In EtOH.

hedral structure. For the complex with D_{4h} symmetry, following three transitions are possible, $^2B_{1g} \rightarrow {}^2A_{1g}$ (ν_1), $^2B_{1g} \rightarrow {}^2B_{2g}$ (ν_2) and $^2B_{1g} \rightarrow {}^2E_g$ (ν_3). Here, it may be assumed that because of the tetragonal distortion, the energy of the $^2B_{2g}$ state would have been very close to that of the $^2A_{1g}$ and as a result instead of three bands only two bands are observed. An approximate value of 10 Dq (6 275 cm^{-1}) have been determined[8]. The magnetic moment of the complex (2.19 B.M. is in the required range.

The Ni^{II} complex has a magnetic moment of 3.20 B.M., which is in the range required for six-coordinate spin-free octahedral complex. Its diffuse reflectance spectrum shows bands at 10 989, 16 949 and 23 810 cm^{-1} which are in the range required for the octahedral structure[9]. Values of B=519 cm^{-1} have been obtained using diagonal sum rule[9]. β is found to be 0.480. Low values of the $\bar{B}$ and β suggest the appreciable amount of the covalent character in the metal-ligand bond. The first two bands are broad and unsymmetrical. They also show splitting into two components (ν_1 at 10 989 and 10 416 cm^{-1} ; ν_2 at 16 949 and 16 129 cm^{-1}). It is possible to calculate Dt=65 cm^{-1}, Ds=451 cm^{-1}, Dq^{XY}=1 099 cm^{-1} and Dq^{z}=984 cm^{-1} from these splittings. The results suggest the higher field strength in the XY-plane.

The Co^{II} complex exhibits a broad band around 9 009 cm^{-1} which may be assigned to the $^4T_{1g}(F) \rightarrow {}^4T_{2g}$ transition (ν_1). The two shoulders at 19 230 and 20 410 cm^{-1} probably on the tail of the charge transfer band have been observed. The former may be assigned to $^4T_{1g}(F) \rightarrow {}^4T_{1g}$ (P) transition (ν_3) and the latter to the tetragonal distortion[10]. Using Ballhausen equation[11], 10 Dq= 10 140 cm^{-1}, B=757 cm^{-1} and β=0.676 have been calculated. The magnetic moment of the Co^{II} complex (4.43 B.M.) is close to the value required for octahedral structure. However, slightly low value is due to the lower symmetry of the complex.

The diffuse reflectance spectrum of the Mn^{II} complex shows bands at 12 660, 8 180 and 22 730 cm^{-1}, which suggest hexacoordinated structure for the complex[12]. The magnetic moment (5.80 B.M.) of the complex indicates high-spin octahedral environment.

Elemental analysis, magnetic and electronic spectral studies of the Fe^{II} complex suggest that it has been oxidised to Fe^{III} during its preparation. The magnetic moment (6.40 B.M.) of the complex is more than a spin-only value, indicating the presence of ferromagnetic impurity in the complex. The bands observed at 18 520, 19 610, 22 220 and 23 280 cm^{-1} may be assigned to the $^6A_{1g} \rightarrow {}^4T_{1g}$, $^6A_{1g} \rightarrow {}^4T_{2g}$, $^6A_{1g} \rightarrow {}^4E_g$ (G), $^4A_{1g}$ (G) and $^6A_{1g} \rightarrow {}^4T_{2g}$ (D) transitions, respectively[13].

Two bands have been observed for the Cr^{III} complex at 17 860 and 25 970 cm^{-1}. These may be assigned to the $^4A_{2g} \rightarrow {}^4T_{2g}$ and $^4A_{2g} \rightarrow {}^4T_{1g}$ transitions, respectively. The presence of shoulder at 16 950 cm^{-1} may be due to the lower symmetry of the complex. In tetragonal field, these may be assigned to the $^4B_1 \rightarrow {}^4B_2$ (17 860 cm^{-1}) and $^4B_1 \rightarrow {}^4E$ (16 950 cm^{-1}) transitions. Using ligand field theory of spin-allowed transitions for octahedral complex, B=853 cm^{-1} and β=0.927 have been obtained[14]. The $^4B_1 \rightarrow {}^4B_2$ transition equals to 10 Dq^{XY} and the separation energy between $^4B_1 \rightarrow {}^4E$ and $^4B_1 \rightarrow {}^4B_2$ is (35/4) Dt. Using Dt (104 cm^{-1}) and Dq^{XY} (1 786 cm^{-1}), Dq^{z}=1 604 cm^{-1} can be evaluated[15]. These values suggest nearly identical

field strength in the XY-plane and along Z-axis. The magnetic moment (3.45 B.M.) of the complex is less than that required for three unpaired electrons[16].

The $V^{IV}O$ complex shows bands at 12 350 and 17 240 cm^{-1} and a weak shoulder at 22 220 cm^{-1}. These may be assigned to $^2B_2 \rightarrow ^2E$, $^2B_2 \rightarrow ^2B_1$ and $^2B_2 \rightarrow ^2A_1$ transitions, respectively. The magnetic moment (2.10 B.M.) is higher than a spin-only value.

The spectra of $U^{VI}O_2$ complex generally show well defined vibronic structure between 21 280 and 30 300 cm^{-1} (Ref. 17). In the present study, the dimagnetic $U^{VI}O_2$ complex shows two bands at 26 315 and 20 000 cm^{-1}. The latter band might be due to metal → ligand charge transfer processes[17]. The Zn^{II} complex is dimagnetic and may have octahedral structure.

Acknowledgement

The authors are thankful to Professor R. P. Patel, Head of Chemistry Department, for his active interest. One of the authors (A.K.R.) is grateful to U.G.C., New Delhi, for financial assistance.

References

1. A. K. Rana and J. R. Shah, *Indian J. Chem., Sect. A*, 1981, 20, 924.
2. V. K. Arora, K. B. Pandeya and R. P. Singh, *J. Indian. Chem. Soc.*, 1979, 56, 656.
3. S. Chandra, B. B. Kaul, K. B. Pandeya and R. P. Singh, *J. Inorg. Nucl. Chem.*, 1977, 39, 2079.
4. R. C. Aggarwal and T. R. Rao, *J. Inorg. Nucl. Chem.*, 1978, 40, 171.
5. M. F. Iskander, L. El-Sayed and M. A. Kasheem, *Inorg. Chim. Acta*, 1976, 16, 147.
6. J. Selbin, *Coord. Chem. Rev.*, 1966, 1, 293.
7. J. I. Bullock and F. W. Parret, *Can. J. Chem.*, 1970 48, 3095.
8. D. E. Billing and A. E. Underhill, *J. Inorg. Nucl. Chem.*, 1968, 30, 2147.
9. D. K. Rastogi and K. C. Sharma, *J. Inorg. Nucl. Chem.*, 1974, 36, 2219.
10. B. Singh, Lakshmi and U. Agrawal, *Inorg. Chem.*, 1969, 8, 2341.
11. A. B. P. Lever and D. Ogden, *J. Chem. Soc. (A)*, 1967, 2041.
12. N. M. Karayannis, L. L. Pytlewski and M. M. Labes, *Inorg. Chim. Acta*, 1969, 3, 415.
13. A. K. Srivastava, V. B. Rana and Madan Mohan, *J. Inorg. Nucl. Chem.*, 1974, 36, 3864.
14. B. N. Figgis, "Introduction to Ligand Fields", Inter-Science, New York, 1967, p. 222.
15. A. B. P. Lever, *Coord. Chem. Rev.*, 1968, 3, 119.
16. B. C. Guha, *Proc. R. Soc. London, Ser. A*, 1951, 206, 353.
17. G. C. Pappalardo and A. Seminara, *J. Inorg. Nucl. Chem.*, 1976, 38, 1993.

J. Indian Chem. Soc.,
Vol. LXIII, March 1986, pp. 284-285

Tri-heteropoly Molybdo-Vanado Tellurate

S. K. ROY* and B. N. GHOSH

Department of Postgraduate Studies & Research in Chemistry, Ranchi University, Ranchi-834 008

Manuscript received 1 December 1984, revised 10 October 1985, accepted 17 January 1986

Synthesis of sodium, potassium and ammonium salts of heteropoly-5-molybdo-1-vanado tellurate anion $[TeVMo_5O_{24}]^{7-}$ are reported. They are characterised by chemical analysis, ir and uv spectra. Thermal stability of the compounds has been examined by DTA and TGA studies. The average molecular weight of sodium 5-molybdo-1-vanadotellurate has been determined by cryoscopy in $Na_2SO_4.10H_2O$-$Na_2SO_4.H_2O$ system and further been confirmed by Weissenberg X ray crystal diffraction meth d.

THE reportings[1-3] of mixed heteropoly complexes of molybdenum and tungsten are of much interest. Matjavic and coworkers[4] synthesised 6-heteropoly anion of general formula $[NiMo_{6-n}W_nO_{24}H_6]^{4-}$. Tsigdinos prepared and characterised a number of mixed 12-heteropoly anion of phosphomolybdovanadate[5] and phosphomolybdoniobates. Heteropoly anion of general formula $[XYW_{11}O_{40}H_2]^{n-}$, where X=Si, Ge, or P and Y=Co^{II}, Co^{III} or Ni^{II} has been prepared[6]. Similar substitution[7,8] has also been extended in dimeric phosphotungstate anion $[P_2W_{18}O_{62}]^{6-}$. Malik[9] reported that Mn^{II}, Zn^{II} and Fe^{III} can also replace molybdenum in 12-molybdosilicic acid to form a mixed heteropoly anion of the type $[SiYMo_{11}O_{40}H_2]^{n-}$. In view of the above literature survey, we have investigated the replacement of molybdenum by vanadium in the well characterised 6-heteropoly anion[10] $[TeMo_6O_{24}]^{6-}$.

Experimental

Sodium 5-molybdo-1-vanadotellurate : Sodium molybdate (10.73 g) dissolved in water (150 ml) and telluric acid (1.84 g) dissolved in water (100 ml), were mixed with each other with constant stirring followed by the addition of glacial acetic acid to maintain the *p*H at 2.5. To this mixture, freshly prepared sodium metavanadate (0.989 g), dissolved in water (100 ml) was added with stirring keeping the *p*H constant at 2.5 by acetate buffer solution. It was refluxed for 6 h at 60°, then evaporated and left for crystallisation. After 6 days bright yellow crystals were collected, recrystallised, washed with ethanol and hexane, and then analysed (Found : Na, 10.15 ; Te, 8.05 ; V, 2.95 ; Mo, 30.80 ; H_2O 23.76. Calcd. for $Na_7[TeVMo_5O_{24}].18H_2O$: Na, 10.53 ; Te, 8.37 ; V, 3.33 ; Mo, 31.41 ; H_2O, 21.20 %). The formulation of the compound was based on the views suggested by Evans[10] for heteropoly anion $[TeMo_6O_{24}]^{6-}$.

Potassium 5-molybdo-1-vanadotellurate : It was synthesised by refluxing a mixture of aqueous solution of potassium molybdate, potassium metavanadate and telluric acid in 5 : 1 : 1 ratio of 2.5-2.6 *p*H at a controlled temperature of 80° for 8 h. The needle shaped light yellow glassy crystals were collected and analysed (Found : K, 18.32 ; Te, 9.10 ; V, 4.70 ; Mo, 31.85 ; H_2O, 18.23. Calcd. for $K_7[TeVMo_5O_{24}].14H_2O$: K, 17.41 ; Te, 8.23 ; V, 3.31 ; Mo, 31.25 ; H_2O, 12.55 %).

Ammonium 5-molybdo-1-vanadotellurate : It was synthesised using ammonium molybdate, ammonium metavanadate and telluric acid. Following the same procedure as above, light orange transparent prismatic crystals were collected after 10 days (Found : N, 6.95 ; Te, 9.11 ; V, 4.10 ; Mo, 33.45 ; H_2O, 20.65. Calcd. for $(NH_4)_7[TeVMo_5O_{24}].16H_2O$: N, 6 72 ; Te, 8.78 ; V, 3.50 ; Mo, 32.85 ; H_2O, 19.76%).

Results and Discussion

Infrared spectra : The ir spectra of the three compounds were taken on a Perkin Elmer 577 spectrophotometer and the results are given in Table 1.

TABLE 1—IR SPECTRA OF HETEROPOLY MOLYBDATE

Compd.	ν_{max} cm^{-1}
$Na_7[TeVMo_5O_{24}].18H_2O$	3 360s, 1 560s, 955m, 935s, 800s, 760m, 960s, 325m
$K_7[TeVMo_5O_{24}].14H_2O$	3 300s, 1 625s, 950s, 925m, 805s, 750m, 685s, 330s
$(NH_4)_7[TeVMo_5O_{24}].16H_2O$	3 420s, 1 620s, 1 405s 960m, 930s, 800s, 760m, 690s, 325m

s = Strong, m = medium.

The peaks in the region 960-775 cm^{-1} correspond to Mo—O and V—O bridging[1] whereas those

TABLE 2 - THERMAL BEHAVIOUR OF HETEROPOLY MOLYBDATES

Compd.	Temp. (°C) of static heating experiments[a] Number of moles of water/ammonia lost						DTA data[b] (°C)	
	100	150	200	250	300	350	Endo	Exo
$Na_7[TeVMo_5O_{24}].18H_2O$	5 Stable	6 Stable	7 Stable	Stable	Unstable	–	30–80 110–140 160–195	270–290
$K_7[TeVMo_5O_{24}].14H_2O$	4 Stable	5 Stable	3 Stable	2 Stable	Almost stable	Unstable	30–85 105–130 185–215	320–345
$(NH_4)_7[TeVMo_5O_{24}].16H_2O$	6 Stable	9 Stable	8 Stable	Partly stable	Unstable	–	30–75 110–135 160–185	265–285

[a]1-2 g sample used for static heating ; stability ascertained by stirring heated sample in 50 ml of water 0.5 h, degree of insolubility of sample taken as a measure of stability. [b]Only endothermic and exothermic peaks upto the decomposition of compound given ; exotherms correspond to complete degradation of heteropoly cage.

in the range 325-330 cm^{-1} are attributed to Te—O octahedron[11]. The lattice water absorptions are observed at higher frequency region of 3 460 to 3 300 cm^{-1}, medium frequency range of 1 600 cm^{-1} and at lower frequency range of 690 cm^{-1} approximately[11].

Electronic spectra : Solution of $K_7[TeVMo_5O_{24}].14H_2O$ were examined spectrophotometrically in various buffer solutions. The compound in 0.1F K_2SO_4-0.2F $KHSO_4$ buffer solution (*p*H 2,5) showed the characteristic λ_{max} at 385 nm (ϵ 2.50×10^3). This λ_{max} remained almost the same when the spectra of the compound are taken in 0.1F $KOOCCH_3$ – 0.1F $HOOCCH_3$ (*p*H ~4.5). Thus, it appeared that the compound was stable at *p*H 2.5-4.5.

Thermal stability : All DTA and TGA experiments were performed under nitrogen at a heating rate of 5° min^{-1}. The thermal behaviour of the heteropoly compounds are given in Table 2. The dehydrated salts exist upto 350° when they are completely decomposed except the K-salt which decomposes near 400°. The endothermic peaks between 30 to 240° correspond to dehydration. Complete degradation of the heteropoly cage at a particular temperature is confirmed by exothermic peaks near that temperature and by chemical analysis, which indicates the existence of mixed oxides of the metal atoms. Insolubility in water, of the heated samples, also confirms the decomposition of the heteropoly salts.

Molecular weight : The molecular weight of $Na_7[TeVMo_5O_{24}].18H_2O$ was determined cryoscopically in $Na_2SO_4.10H_2O$-$Na_2SO_4.H_2O$ system by the method as has been applied by Thilo and Krüger[12] and recently by Flynn and Pope[13]. The cryoscopic constant was taken[13] as 1.8±.1 kg of water per mole. The derived apparent molecular weight was found to be 1283±250.

X-Ray diffraction : The compound $Na_7[TeVMo_5O_{24}].18H_2O$ was recrystallised from hot water and used for *X*-ray studies. The unit cell dimensions were determined using rotation and Weissenberg photographs. Crystal data : M_{obs}=1975 against M_{cal}=1968 ; a=14.62, b=12.48, c=11.52Å, $\alpha=\beta=\gamma=90°$, V=2186.13 Å^3, Z=2, D=3.0 g cm^{-3}.

Acknowledgement

The authors express their deep sense of gratitudes to the authorities of Planning and Development, Sindri, for *X*-ray, Central Fuel Research Institute, Dhanbad, for high temperature analyses and C.D.R.I., Lucknow, for spectral and elemental analyses

References

1. G. A. TSIGDINOS, *Top. Curr. Chem.*, 1978, **76**, 53.
2. T. J. R. WEAKLEY, *Struct. Bonding*, 1974, **18**, 131.
3. M. T. POPE, "Inorganic Chemistry Concept", Springer Verlag, Berlin, 1983, Vol. 8.
4. E. MATEJEVIC, M. KERKER, H. BEYER and F. THEUBERT, *Inorg. Chem.*, 1963, **2**, 581.
5. G. A. TSIGDINOS and C. J. HALLADA, *Inorg. Chem.*, 1968, **7**, 437 ; "Electrochemical Properties of Heteropoly Molybdates", Climax Molybdenum Company Bulletin, Cdb. 15, May, 1971.
6. L. C. W. BAKER and J. S. FIGGIS, *J. Am. Chem. Soc.*, 1970, **92**, 3794.
7. T. J. R. WEAKLEY and S. A. MALIK, *J. Inorg. Nucl. Chem.*, 1967, **29**, 2935.
8. T. J. R. WEAKLEY, *J. Chem. Soc., Dalton Trans.*, 1973, 341.
9. S. A. MALIK, *J. Inorg. Nucl. Chem.*, 1976, **38**, 879.
10. H. T. EVANS, JR., *J. Am. Chem. Soc.*, 1968, **90**, 3275.
11. K. NAKAMOTO, "Infrared Spectra of Inorganic and Coordination Compounds", John Wiley, 1963, pp. 107, 217.
12. E. THILO and G. KRÜGER, *Z. Electrochem.*, 1957, **61**, 24.
13. C. M. FLYNN and M. T. POPE, *Inorg. Chem.*, 1971, **10**, 2526.

J. Indian Chem. Soc.,
Vol. LXIII, March 1986, pp. 286-287

Complex Formation with some Bidentate Ligands. I. Solution Equilibria in the Complex Formation of Bivalent Metal Ions with some *vic*-Hydroxy Aldehydes

C. K. BHASKARE* and P. P. HANKARE

Department of Chemistry, Shivaji University, Kolhapur-416 004

and

R. S. RAMPURE

Department of Chemistry, Sangameshwar College, Solapur-413 003

Manuscript received 14 May 1982, revised 17 May 1983, accepted 3 March 1986

The proton-ligand stability constants of salicylaldehyde, 3-methylsalicylaldehyde, 4-methylsalicylaldehyde, 5-methylsalicylaldehyde and 5-bromosalicylaldehyde, and stability constants of their complexes with Cu^{II}, Co^{II}, Ni^{II}, Mn^{II}, Zn^{II}, Cd^{II} and Mg^{II} have been determined in ethanol-water medium (50% v/v) at μ = 0.1 *M* ($NaClO_4$) and 25° by the Calvin-Bjerrum *p*H-titration technique as modified by Irving and Rossotti. The order of the stability constants has been found to be Cu>Co>Ni> Mn > Zn > Cd > Mg, which is in agreement with the Irving-Williams order of stability of bivalent metal complexes.

MUCH work has been so far done on isolation of solid complexes of *vic*-hydroxy aldehydes and their derivatives and their characterisation. Equally important contributions are expected for complex formation in solutions. *vic*-Hydroxy aldehydes give interesting analytical reagents like oximes, thiosemicarbazones, semicarbazones, and versatile ligands like Schiff bases and anils. Present series aims at a detailed comparative study of these ligands.

Salicylaldehyde (SA), 3-methylsalicylaldehyde (3-MSA), 4-methylsalicylaldehyde (4-MSA), 5-methylsalicylaldehyde (5-MSA) and 5-bromosalicylaldehyde (5-BSA) from chelates with many metals. The present paper deals with the formation constants of the complexes of Cu^{II}, Co^{II}, Ni^{II}, Mn^{II}, Zn^{II}, Cd^{II} and Mg^{II} with SA, 3-MSA, 5-MSA and 5-BSA using Calvin-Bjerrum technique as modified by Irving and Rossotti. The studies were carried out in 50% (v/v) ethanol-water medium maintaining a constant ionic strength, μ=0.1 *M* ($NaClO_4$) at 25° (±0.1°).

Experimental

Potentiometric titrations were carried out by using Radiometer M-4 *p*H meter (calibrated with phthalate buffer). The readings of *p*H meter in 50% ethanol were corrected for solvent effect as previously reported[1-3].

Salicylaldehyde (AnalaR) was used as such. Other *vic*-hydroxy aldehydes were prepared by using standard procedures[4,5]. Carbonate-free sodium hydroxide (AnalaR) solution (0.98 *M*) was prepared according to the method of Serjeant[6]. Solutions of the ligands (0.04 *M*) were prepared by dissolving the requisite quantity of the compound in ethanol. Metal perchlorate solutions were prepared by treating 2 *M* $HClO_4$ (20 ml) with excess of the oxide or carbonate of A.R. grade and suitably diluting the resulting neutral solutions to 100 ml of 0.2 *M* (approximately). The metal contents were determined by standard procedures[7].

Titration procedure: Following solutions were titrated against standard sodium hydroxide (0.98 *M*) free from CO_2 : (i) 4 ml 0.2 *M* $HClO_4$+0.78 ml 4 *M* $NaClO_4$ + 20 ml ethanol + 15.22 ml distilled water, (ii) 4 ml 0.2 *M* $HClO_4$ + 0 78 ml 4 *M* $NaClO_4$ + 10 ml 0.04 *M* reagent + 10 ml ethanol + 15.22 ml distilled water and (iii) 2 ml 0.2 *M* $HClO_4$ + 2 ml 0.02 *M* metal perchlorate solution containing 0.2 *M* $HClO_4$ + 0.77 ml 4 *M* $NaClO_4$ + 10 ml 0.4 *M* reagent + 10 ml ethanol + 15.23 ml distilled water.

Results and Discussion

Salicylaldehyde, a representative *vic*-hydroxy aromatic aldehyde possesses favourable features for the formation of a stable five-membered chelate

ing with metal ions. The proton-ligand stability constants and the metal-ligand stability constants were calculated by using half-integral and graphical methods. The pK values of methyl substituted salicylaldehydes and 5-BSA are in the order, 4-MSA > 3-MSA > 5-MSA > SA > 5-BSA. Because of methyl group, there will be higher electron density around carbonyl oxygen compared with that of SA. Hence, there will be stronger hydrogen bond formation with C=O and hence phenolic proton will have higher ionisation energy[8]. The CH_3 group has positive inductive effect (+I) and there is increase in electron density at the oxygen atom of C=O group. This facilitates the formation of stronger hydrogen bonding as compared to SA. Increased hydrogen bonding hampers the ionisation of phenolic OH and leads to higher pK value. In 5-MSA, the methyl group is in *para* position to the OH group, and the former can donate electrons easily to the latter *via* hyperconjugation making 5-MSA more difficult to ionise as compared to SA. 4-MSA shows a very high pK value. The plot of Hammett σ^- values for the methyl substituent in *ortho*, *meta* and *para* positions to OH group against pK values gives a straight line plot. However, 4-MSA shows a deviation. The three of them decidedly have higher log K_1^H values as the effect of the CH_3-substituent. The behaviour of the substituent in *ortho* position is somewhat anomalous[9-11]. The proton-ligand stability constants are fairly in agreement with calculated values (except 4-MSA).

Electron repelling character of the substituents group is in increasing order, Br > H > m-CH_3 > o-CH_3 > p-CH_3. However, the pK values do not follow this order strictly and the o- and m-CH_3 substituents show strong difference from expected order.

The observed orders for the five ligands are SA, Cu > Ni > Mn > Zn > Cd > Mg ; 3-MSA, Co > Ni > Mn > Zn > Cd > Mg ; 4-MSA, Cu > Mn > Zn > Cd > Mg ; 5-MSA, Cu > Co > Mn > Zn > Cd > Mg ; 5-BSA, Ni > Mn > Zn > Cd. This is in agreement with earlier reports[9,12-14].

TABLE 1—FORMATION CONSTANTS FOR PROTON-LIGAND AND METAL-LIGAND SYSTEMS OF SA AND ITS SUBSTITUTED DERIVATIVES

Cations	Constant	SA	3-MSA	4-MSA	5-MSA	5-BSA
H^+	$-\log K_{OH}^{H}$	9.05	10.40	12.25	9.55	8 2
Cu^{II}	$-\log K_1$	6.60	–	9.11	7.23	–
Co^{II}	$-\log K_1$	–	5.86	–	6.04	–
Ni^{II}	$-\log K_1$	5.90	5.66	–	–	5.90
Mn^{II}	$-\log K_1$	5.32	5.09	8.14	5.35	5.33
Zn^{II}	$-\log K_1$	5.10	5.01	7.92	5.16	5.24
Cd^{II}	$-\log K_1$	4.37	3.96	6.66	4.35	4.41
Mg^{II}	$-\log K_1$	3.18	2.82	3.88	3.15	–

Acknowledgement

One of the authors (R.S.P.) is thankful to Prin. K. Bhogishayana, Sangameshwar College, Solapur, for encouragement and the other (P.P.H.) to U.G.C., New Delhi, for the award of a Junior Research Fellowship.

References

1. B. GUTBEZAHL, *J. Am. Chem. Soc.*, 1953, 75, 565.
2. R. G. BATES and G. SCHWARZENBACH, *Helv. Chim. Acta*, 1955, 38, 699.
3. R. G. BATES, "Determination of pH", John Wiley, New York, 1954, p 223.
4. J. C. DUFF, *J. Chem. Soc.*, 1941, 547.
5. C. M. BREWSTER and L. H. MILLAM, *J. Am. Chem. Soc.*, 1933, 55, 763.
6. E. P. SERJEANT and A. ALBERT, "Determination of Ionisations Constants", 2nd. ed., Chapman and Hall, London, 1971.
7. A. I. VOGEL, "The Text Book of Quantitative Inorganic Analysis", Longmans Green, London, 1961.
8. S. K. SRIVASTAVA, *Indian J. Chem., Sect. A*, 1978, 16, 88.
9. K. E. JABALPURWALA, K. A. VENKATACHALAM and M. B. KABADI, *J. Inorg. Nucl. Chem.*, 1964, 26, 1027.
10. C. JR. POSTMUS, A. K. IRVING, C. A. CRAIG and R. S. MATTHEWIS, *J. Org. Chem*, 1964, 29, 2693.
11. P. V. KAMAT, N. B. LAXMESHWAR and M. G. DATAR, *J. Indian Chem. Soc.*, 1969, 46, 345.
12. H. IRVING and R. J. P. WILLIAM, *Nature (London)*, 1948, 162, 746.
13. L. E. MALEY and D. P. MELLOR, *Nature (London)*, 1948, 161, 346.
14. R. G. PEARSON and F. BASOLO, "Mechanism of Inorganic Reactions - Study of Complexes in Solution", John Wiley, New York, 1958, p. 16.
15. H. IRVING and H. S. ROSSOTTI, *J. Chem. Soc.*, 1953, 3397.

J. Indian Chem. Soc.,
Vol. LXIII, March 1986, pp. 288-290

Application of Hard and Soft Acid-Base Theory in the Study of Mixed Ligand Thiocyanate-8-hydroxyquinoline Complexes of Bivalent Metal Ions of 3d-Transitional Series

(Miss) KANTI MISHRA and M. C. SAXENA*

Department of Chemistry, Dr. Harisingh Gour Vishwavidyalaya, Sagar-470 003

Manuscript received 21 June 1985, accepted 17 January 1986

Hard and soft acid-base theory has been applied in the study of mixed ligand complexes of the type $[M(II)(NCS)_2(HQ)_2]$, where M(II) = Mn^{II}, Fe^{II}, Co^{II}, Ni^{II}, Cu^{II} or Zn^{II}; HQ = 8-hydroxyquinoline. The values of 'matching' for the N-end and S-end of thiocyanate have been calculated; higher values of matching obtained for the N-end indicate that thiocyanate is bonded to these metal ions (border line cases between hard and soft acids) through its N-end. Another parameter, 'matching constant' determined for these complexes, appears to be useful for showing relative metal-ligand bond strength. Its values lie in the sequence Mn < Fe < Co < Ni < Cu > Zn.

Correlations of 'matching constant' with atomic number, sum of the first two ionisation potentials, standard oxidation potentials and charge-size ratio of the metal ions have also been studied.

THIOCYANATE is an ambidentate ligand; it may coordinate to a metal ion through nitrogen, or through sulphur, or through nitrogen and sulphur both by means of bridging. The class 'a' metal ions (or, hard acids) are generally bonded to its nitrogen atom, whereas the class 'b' (or, soft acids) are bonded to the sulphur atom. A number of metal mixed ligand thiocyanate complexes with various nitrogen donors, such as nitro- or methylphenanthroline[1], pyridine, picolines and isoquinoline[2-8] have been investigated. It appears that the mode of metal-thiocyanate bonding depends on the nature of metal ion and the substituent group present in the ligand, availability of d-orbitals in the ligand for back donation and steric requirements of the ligand.

Recently[9,10] quantitative 'softness values' (defined latter in the text) of metal ions and donor atoms of ligands have been used as supporting evidence for establishing the structure of some thiocyanate complexes. The present work describes the application of quantitative aspects of hard and soft acid-base (H.S.A.B.) theory[11] in establishing the mode of metal-thiocyanate linkage in the mixed ligand thiocyanate-8-hydroxyquinoline (oxine, HQ) complexes of Mn^{II}, Fe^{II}, Co^{II}, Ni^{II}, Cu^{II} and Zn^{II}.

Experimental

The metal nitrates/sulphates (AnalaR) were vacuum-dried before use. Potassium thiocyanate used was E. Merck (G.R.) reagent. 8-Hydroxyquinoline was recrystallised from ethanol, and the solvent was completely removed by drying.

Synthesis of mixed ligand thiocyanate-oxine complexes: The following general procedure was followed for preparing the complexes. The metal nitrate (sulphate in the case of Fe^{II} and Cu^{II}) and potassium thiocyanate were mixed in ethanolic solution in 1 : 2 mmol proportion. After stirring the reaction mixture for 2-2.5 h, the separated potassium nitrate (or sulphate) was filtered off and the filtrate was slowly evaporated to dryness under reduced pressure to obtain the metal thiocyanate. Subsequently, an excess of oxine solution in acetone was mixed with a freshly prepared solution of the metal thiocyanate (5 mmol). A colour change appeared initially; stirring for upto ~4 h resulted in the separation of solid mixed ligand complex which was filtered, washed and vacuum-dried.

The characterisation of the mixed ligand complexes on the basis of elemental analysis, molar conductance and magnetic measurements, and infrared and electronic spectral studies, has already been communicated[12]. The present work describes the application of H.S.A.B. principles in establishing the metal-thiocyanate mode of linkage and certain correlations of the 'matching constant' (defined latter in the text) with the metal ion characteristics.

The quantitative 'softness values' of the metal ion (Lewis acid), $E_n^{\dagger}$, and ligand (Lewis base), $E_m^{\dagger}$, have been calculated for the various metal ions

studied, NCS(N-end), SCN (S-end) and oxine by using Klopman's equations[13],

$$\overset{+}{E}_n^{\ddagger} = IP_n - b^2(IP_n - EA_n) - \frac{X_s(C_s^n)^2\,(1-1/e)}{R_s}\,[q_s - 2b^2X_s(C_s^n)^2] \quad (1)$$

$$\overset{+}{E}_m^{\ddagger} = IP_m - a^2(IP_m - EA_m) - \frac{X_r(C_r^m)^2\,(1-1/e)}{R_r}\,[q_r + 2b^2X_r(C_r^m)^2] \quad (2)$$

The terms used in equations (1) and (2) are, R_s and $R_r = (r+0.82)$, where r = ionic radius (Pauling) of Lewis acid and base, respectively; $b^2 = 1/4$; $a^2 = 3/4$; $(C_s^n)^2 = (C_r^m)^2 = 1$; e = dielectric constant of the solvent; $X_s = q_s\,(q_s-1)\sqrt{K}$; $X_r = q_r\,(q_r-1)\sqrt{K}$; $k = 0.75$, and q_s and q_r are the charges on the Lewis acid and base, respectively; IP_n = ionisation potential and EA_n = electron affinity of the Lewis acid; IP_m = ionisation potential and EA_m = electron affinity of the Lewis base; R_r and R_s = atomic radius of the Lewis acid and base (atom), respectively. The values of IP, EA and R have been evaluated for an atom as a neutral species by simple modifications in known methods[14-16]: These 'softness values' have been used for calculating a quantity 'total softness', $T\overset{+}{E}_{nm}^{\ddagger}$ defined by the expression,

$$T\overset{+}{E}_{nm}^{\ddagger} = \overset{+}{E}_n^{\ddagger}(M) + \Sigma\,\overset{+}{E}_m^{\ddagger}(NCS) + \Sigma\,\overset{+}{E}_m^{\ddagger}(L) \quad (3)$$

where, $\overset{+}{E}_n^{\ddagger}(M)$ = (total) softness of the metal ion, $\Sigma\,\overset{+}{E}_m^{\ddagger}$ (NCS) = total softness of NCS (N-end), $\Sigma\,\overset{+}{E}_m^{\ddagger}(L)$ = total softness of the ligand (HQ). A soft base is characterised by a higher value of $\overset{+}{E}_m^{\ddagger}$ and a soft acid by a lower value of $\overset{+}{E}_n^{\ddagger}$. Since the 'softness values' of Lewis acids and bases increase in reverse directions, a better match for metal-ligand interaction will be expected by higher values of absolute difference between $\overset{+}{E}_n^{\ddagger}$ and $\overset{+}{E}_m^{\ddagger}$. Thus, 'matching' $\overset{+}{E}_{nm}^{\ddagger}$ and another related parameter 'matching constant', $\Delta\overset{+}{E}_{nm}^{\ddagger}$ may be defined as,

$$\text{Matching} = \overset{+}{E}_{nm}^{\ddagger} = |\,\overset{+}{E}_n^{\ddagger} - \overset{+}{E}_m^{\ddagger}\,| \quad (4)$$

$$\text{Matching constant} = \Delta\overset{+}{E}_{nm}^{\ddagger} = |\,\overset{+}{E}_n^{\ddagger} - \overset{+}{E}_m^{\ddagger}\,| + \text{c.f.s.e.} \quad (5)$$

where, c.f.s.e. = crystal field stabilisation energy. The 'matching' and 'matching constant' values of the mixed complexes have been calculated from equations (4) and (5), respectively and used to predict the possibility of thiocyanate to link up with the metal ions (M) through nitrogen end (M-NCS) or through sulphur end (M-SCN).

Results and Discussion

The calculated values of 'matching' of N-end (M-NCS) and S-end (M-SCN) of the thiocyanate ion; total 'softness values', c.f.s.e., and 'matching constant' of the mixed ligand complexes are reported in Table 1.

The analytical and spectral studies have revealed[13] that the mixed ligand complexes are of the type $[M(II)(NCS)_2(HQ)_2]$, *i.e.* diisothiocyanato-bisoxinato-metal(II). The metal thiocyanate bonding is through the N-end of thiocyanate in these complexes. The positions of electronic spectral bands have been used also to calculate the c.f.s.e. values (Table 1).

A reference to Table 1 shows that the 'matching' values for M-NCS interaction are consistently greater than those for M-SCN for all the metal ions under study. It may, therefore, be concluded on the basis of a better match that these metal ions, which are borderline cases in terms of HSAB scale, prefer to link to the thiocyanate ion through its N-end. This is in full agreement with the conclusions drawn from the infrared spectral studies[13]. The total 'softness values' for the complexes show a general decrease from Mn^{II} to Cu^{II} and then an increase at Zn^{II}. The 'matching constant', however, appears to be a useful parameter of the strength of the metal-ligand bond as suggested by other workers[10]. The 'matching constant' values lie in the sequence Mn < Fe < Co < Ni < Cu > Zn, which is incidentally the natural order of stability (Irving-Williams series) of the complexes of these metal ions. The values of 'matching constants' may be correlated with metal ion characteristics. Plots of 'matching constants', $\Delta\overset{+}{E}_{nm}^{\ddagger}$ of diisothiocyanato-bisoxinato-metal(II) complexes with the atomic numbers(Z), sum of the first two ionisation potentials (ΣI), standard oxidation potentials (E_H^0) and

TABLE 1—MATCHING OF THIOCYANATE ION, TOTAL SOFTNESS VALUES, C. F. S. E. AND MATCHING CONSTANTS OF THE COMPLEXES $[M(II)(NCS)_2(HQ)_2]$

Metal	Matching of thiocyanate ion		Total softness value ($T\overset{+}{E}_{nm}^{\ddagger}$)	c. f. s. e. eV	Matching constant ($\Delta\overset{+}{E}_{nm}^{\ddagger}$)
	NCS (N-end)	SCN (S-end)			
Mn	8.76	5.86	57.36	0	11.61
Fe	8.69	5.79	57.29	1.81	13.35
Co	7.40	4.50	56.00	4.26	14.51
Ni	8.39	5.49	56.99	5.83	16.07
Cu	7.55	4.65	56.15	9.82	20.22
Zn	7.07	4.17	55.67	0	9.92

charge/size ratios (q/r) of the metal ions are shown in Fig. 1. Increase in 'matching constants' is

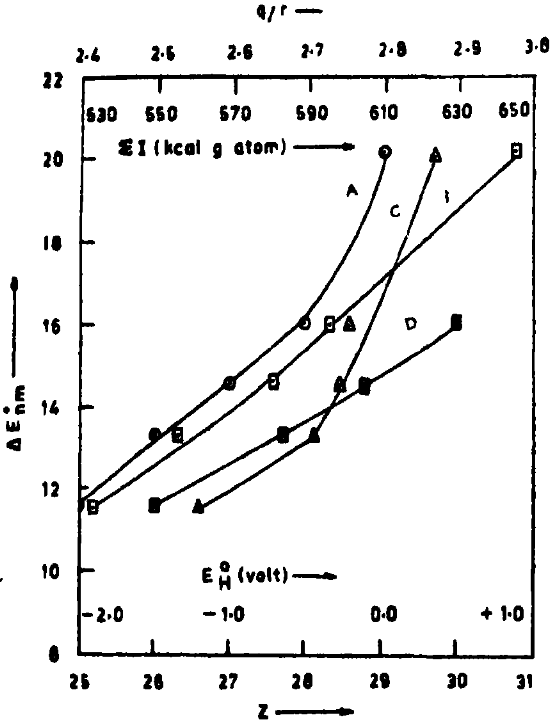


Fig. 1. Variation of matching constant ($\Delta E^{\ddagger}_{nm}$) with (A) atomic number (Z), (B) sum of the first two ionisation potentials (ΣI), (C) standard oxidation potentials (E^{0}_{H}) and (D) charge/size ratio (q/r) of the 3d-metal ions.

associated with an increase in the values of these properties. These plots clearly indicate the utility of 'matching constants' in expressing the metal-ligand bond strength of complexes and compare very well with similar correlations between the formation constants of complexes in solution and the above metal ion characteristics.

Acknowledgement

The authors are thankful to the Head, Department of Chemistry, Dr. Harisingh Gour Vishwavidyalaya, for facilities, and to Prof. P. P. Singh, Avadh University, for encouragement.

References

1. A. Sabatini and I Bertini, *Inorg. Chem.*, 1966, 5, 1025.
2. M. A. Porai-Koshits and A. S. Anishhshkiya, *Krystallografia*, 1958, 3, 676.
3. H. C. A. King, B. Koros and S. M. Nelson, *J. Chem. Soc*, 1963, 5449; 1964, 4832
4. M. A. Porai-Koshits and G. N. Tischenko, *Krystallografia*, 1959, 4, 239.
5. S. M. Nelson and T. M. Shepherd, *Inorg. Chem.*, 1965, 4, 813.
6. A. Turco and C. Pecile, *Nature (London)*, 1961, 191, 66.
7. S. Guru, B. B. Mahapatra and B. Paul, *J. Indian Chem. Soc.*, 1977, 54, 337.
8. B. K. Mohapatra, *J. Indian Chem. Soc.*, 1974, 51, 705.
9. P. P. Singh and A. K. Gupta, *Inorg. Chem.*, 1978, 17, 1.
10. P. P. Singh, S. K. Shrivastava and A. K. Shrivastava, *J. Inorg. Nucl. Chem.*, 1980, 42, 521, 533.
11. R. G. Pearson, *J. Chem. Educt.*, 1968, 45, 581, 643.
12. K. Mishra and M. C. Saxena, *J. Indian Chem. Soc.*, communicated.
13. G. Klopman, *J. Am. Chem. Soc.*, 1968, 90, 223.
14. M. J. S. Dewar and T. F. Martia, *J. Am. Chem. Soc.*, 1968, 91, 796.
15. R. T. Sanderson, "Chemical Bond and Bond Energy", Academic Press, New York, 1971, p. 1920.
16. J. E. Huheey, 'Inorganic Chemistry', Harper and Row, New York, 1972, pp. 71, 72.

J. Indian Chem. Soc.,
Vol LXIII, March 1986, pp. 291-294

Kinetics and Mechanism of Osmium Tetroxide Catalysed Oxidation of Benzoin and its Derivatives by Alkaline Hexacyanoferrate(III)

PRANATI MISRA, R. C. MOHAPATRA and N. C. KHANDUAL*

Department of chemistry, Ravenshaw College, Cuttack-753 003

Manuscript received 13 September 1984, revised 8 October 1985, accepted 6 February 1986

The kinetics of oxidation of benzoin and four substituted benzoins by alkaline hexacyanoferrate(III) in the presence of osmium tetroxide as catalyst have been investigated in t-butanol-water mixture at constant ionic strength. The rates of the reactions are found to be first order in [substrate], [alkali] and [catalyst], but zero order in [hexacyanoferrate(III)]. The rates of the reactions decrease with the decrease in the dielectric constant and increase with the increase in ionic strength of the medium. The mechanism involves the formation of an intermediate complex betwween the enolate and osmium tetroxide, which rapidly decomposes followed by a fast reaction between the reduced osmium species and hexacyanoferrate(III). This is consistent with the results obtained.

IN continuation of our earlier work on the kinetics of oxidation of aromatic ketones[1], pyridinium salts[2] and chalkones[3] by alkaline hexacyanoferrate(III), we report the kinetics of osmium tetroxide catalysed oxidation of benzoins (keto alcohol) by alkaline hexacyanoferrate(III). The mechanism of oxidation depends on the catalyst, osmium tetroxide and the exact role of the osmium tetroxide in the oxidation of benzoins has not yet been shown, and this prompted us to investigate the osmium tetroxide catalysed oxidation of benzoins by alkaline hexacyanoferrate(III). In the absence of the catalyst, the reaction is extremely slow or does not proceed at all.

Experimental

Benzoins were prepared and purified by the reported[4] method. Ethanol, potassium hexacyanoferrate(III), potassium chloride and potassium hydroxide were of AnalaR reagents. A 0.004 *M* solution of osmium tetroxide (Johnson Mathey) was prepared by dissolving a known weight of the sample in KOH solution (0.05 *M*). Dilution was made with triple-distilled water and the ionic strength adjusted with potassium chloride.

Kinetic measurement : The progress of the reaction in aqueous ethanol at the desired temperature was followed by withdrawing aliquots of the reaction mixture at known intervals of time and estimating the amount of he acyanoferrate(II) formed during the reaction by titrating against standard solution of ceric salt using ferrion as indicator. The standard zero order rate constants (k_0) reported are the average values of duplicate runs. Oxidation of the solvent did not occur under the conditions employed.

Stoichiometry : The reaction was carried out using a known excess of hexacyanoferrate(III) at 30° and the unconsumed oxidant determined as described above. The results showed that 1 mol of benzoin required 2 mol of hexacyanoferrate(III) indicating the stoichiometry to be 1 : 2. Benzil was found to be the product of oxidation. The pure product was characterised (ir, m.m.p.) as benzil, m.p. 96°.

Rate laws : The reaction is zero order in [hexacyanoferrate(III)] as shown by the constant values of k_0 over a ten-fold variation of [hexacyanoferrate(III)] (Table 1). The rate of the reaction increases with the increase in [benzoin] (Table 2), indicating the first order reaction with respect to benzoin. The oxidation rate of benzoin is directly proportional to [alkali] (Table 3) and hence the order in latter is unity. The rate constant increases with the increase in [catalyst]. The values of k_0 [OsO_4] show fairly concordant values of all concentrations of the catalyst (Table 4)

TABLE 1—DEPENDENCE OF RATE ON [HEXACYANOFERRATE(III)]

[Benzoin] = 0.05 *M* ; [OH^-] = 0.01 *M* ; [OsO_4] = 2.5 × 10^{-5} *M* ;
μ = 0.3 *M* ; Solvent : 30% t-butanol (v/v) ;
Temp. = 30°

[Hexacyanoterrate(III)] × 10^{3} *M*	k_0 × 10_6 mol dm^{-3} min^{-1}
1.0	19.20
2.0	19.20
4.0	19.00
6.0	19.00
8.0	18.78
10.0	18.50

TABLE 2—DEPENDENCE OF RATE ON [BENZOIN]

[Hexacyanoferrate(III)] = 0.002 *M*; $[OsO_4]$ = 2.5 × 10^{-5} *M*; $[OH^-]$ = 0.01 *M*; μ = 0.3 *M*; Solvent: 30% t-butanol (v/v); Temp. = 30°

[Benzoin] × 10^3 *M*	k_0 × 10^5 mol dm^{-3} min^{-1}	k_0, min^{-1} / [Benzoin]
1.0	3.85	0.385
2.0	7.60	0.380
4.0	15.25	0.386
5.0	19.20	0.384
8.0	30.50	0.381
10.0	38.50	0.385

TABLE 3—DEPENDENCE OF RATE ON $[OH^-]$

[Hexacyanoferrate(III)] = 0.002 *M*; [Benzoin] = 0.02 *M*; $[OsO_4]$ = 2.5 × 10^{-5} *M*; μ = 0.3 *M*; Solvent: 30% t-butanol (v/v); Temp. = 35°

$[OH^-]$ × 10^3 *M*	k_0 × 10^5 mol dm^{-3} min^{-1}	k_0, min / $[OH^{-1}]$
1.0	7.60	0.76
2.0	15.40	0.77
4.0	31.20	0.78
6.0	46.20	0.77
8.0	60.00	0.75
10.0	77.00	0.77

TABLE 4—DEPENDENCE OF RATE ON $[OsO_4]$

[Hexacyanoferrate(III)] = 0.002 *M*; [Benzoin] = 0.02 *M*; $[OH^{-1}]$ = 0.01 *M*; μ = 0.3 *M*; Solvent: t-butanol (v/v); Temp. = 30°

$[OsO_4]$ × 10^5 *M*	k_0 × 10^5 mol dm^{-3} min^{-1}	k_0, × 10^{-3} min^{-1} / $[OsO_4]$
1.0	2.8	0.28
1.5	4.35	0.29
2.5	7.60	0.30
3.5	10.85	0.31
5.0	15.10	0.31
6.0	19.20	0.32
7.0	23.80	0.34
10.0	33.00	0.33
12.0	38.40	0.32
14.0	42.00	0.30
15.0	45.00	0.30

Effect of ionic strength: The rate of reaction increases with the increase in ionic strength of the medium and a plot of log k_0 *vs* $\sqrt{\mu}$ is linear, indicating an ion-ion interaction. Added ferrocyanide showed no effect on the rate of oxidation.

Solvent effect: The decrease in the dielectric constant of the medium decreases the rate constant. The plot of log k_0 *vs* reciprocal of the dielectric constant of the medium is linear, which provides an additional evidence in favour of ion-ion reaction.

Effect of substituents on rate: The rate data of substituted benzoins at different temperatures have also been recorded in Table 5. Arrhenius equation has been found to be valid within the temperature range studied. The observed reactivity of the substituted benzoins confirms to thefollowing order,

$$4\text{-}OCH_3 > 4\text{-}CH_3 > H > 4\text{-}Cl > 2,2'\text{-Dinitro}$$

It is evident from the order of reactivity that the rate increases by the electron-releasing substituents on the benzene nucleus directly attached to the keto group and retarded by the electron-attracting groups. The logarithm of the rate constants at 35° correlate well with σ^+ values[5]. The value of ρ^+ is −1.15. A similar correlation between log k_0 and σ^+ has been observed earlier[6] for the dichromate oxidation of benzoins. The above order of reactivity is in agreement with the negative value of ρ^+. A common mechanism is envisaged for the substituted benzoins as the free energy of activation values are of same order of magnitude.

Isokinetic relationship: A linear relationship between the entropy of activation ($\Delta S^{\neq}$) and the enthalpy of activation ($\Delta H^{\neq}$) has been observed for the oxidation of benzoin[7]. The data can be fitted in the equation,

$$\Delta H^{\neq} = \Delta H_0^{\neq} + \beta \Delta S^{\neq}$$

where, $\Delta H^{\neq}$ = 21.15 kcal mol^{-1} and β = 330 K. The linear relationship shown by the majority of the substituted benzoins indicates that the same mechanism operates in all the cases[8].

Mechanism: The osmium tetroxide catalysed oxidation of benzoins by alkaline hexacyanoferrate(III) is characterised by the following: (i) the reaction rate is independent of initial concentration of hexacyanoferrate(III) but proportional to the concentration of benzoin, alkali and osmium tetroxide, (ii) the reaction rate decreases with the decrease in dielectric constant of the solvent but increases with the increase in ionic strength of the medium, (iii) the entropy of activation is found to be negative and a negative ρ^+ value

TABLE 5—REACTION RATES AND ARRHENIUS PARAMETERS FOR ALKALINE HEXACYANOFERRATE(III) OXIDATION OF BENZOIN IN t-BUTANOL-WATER MIXTURE

[Hexacyanoferrate(III)] = 0.002 *M*; [Substrate] = 0.02 *M*; $[OH^-]$ = 0.01 *M*; $[OsO_4]$ = 2.5 × 10^{-5} *M*; μ = 0.3 *M*; Solvent: 30% t-butanol (v/v); Temp. = 30°

Substrate	k_0, × 10^5 mol dm^{-3} min^{-1}			E kcal mol^{-1}	$-\Delta S^{\neq}$ e.u.	$\Delta H^{\neq}$ kcal mol^{-1}
	30°	35°	40°			
$4\text{-}OCH_3$	15.50	25.80	36.70	16.50	14.31	15.88
$4\text{-}CH_3$	12.80	21.70	32.50	17.40	11.71	16.78
H	7.60	12.80	20.50	18.20	10.17	17.58
4-Cl	6.20	10.60	16.30	19.20	7.29	18.58
2,2′-dinitro	5.50	8.80	12.80	19.80	5.71	19.18

is obtained, and (iv) benzil has been isolated as the product of oxidation with a stoichiometry of Δ hexacyanoferrate(III)/Δbenzoin, 2 : 1.

Thus under the above conditions, a probable rate law might be given as

$$\frac{-d[Fe(CN)_6^{3-}]}{dt} = k[\text{benzoin}][OH^-][OsO_4]$$

Benzoin is a keto alcohol. A ketone may react directly or through its enol form in oxidation reactions. Direct oxidations[9-11] by cobaltic, manganic and ceric salts have been shown to involve one-electron change and seem to have a free radical mechanism. In the present oxidation, no induced polymerisation of acrylonitrile or reduction of $HgCl_2$ has been seen. Hence, a free radical mechanism is ruled out. But on the other hand the reaction is alkali dependent, shows positive salt effect, sensitive to dielectric constant of the solvent composition and the entropy of activation is negative. The reaction probably proceeds through an ionic mechanism involving enolate intermediate.

Benzoin is easily oxidised to benzil by chromium(VI)[6,12]. The redox potential of $\rightarrow Cr^{VI}\ Cr^{III}$ couple is 1.36 V which is high enough to oxidise the substrate. The oxidation of the same substrate by alkaline hexacyanoferrate(III) on the other hand, donot proceed in the absence of the catalyst. This is possibly because the oxidation potential of hexacyanoferrate(III)$\rightarrow$hexacyanoferrate(II) couple is very low (−0.36 V), would not differ appreciably from that of benzoin$\rightarrow$benzil couple, the data for which is lacking in the literature. However, the oxidising or reducing capacity of a substance can be altered by diminishing the activity of the oxidised or the reduced form of the redox couple and this can be achieved by the addition of a suitable catalyst. The catalyst osmium tetroxide, would possibly play part in lowering the redox potential of benzoin$\rightarrow$benzil couple.

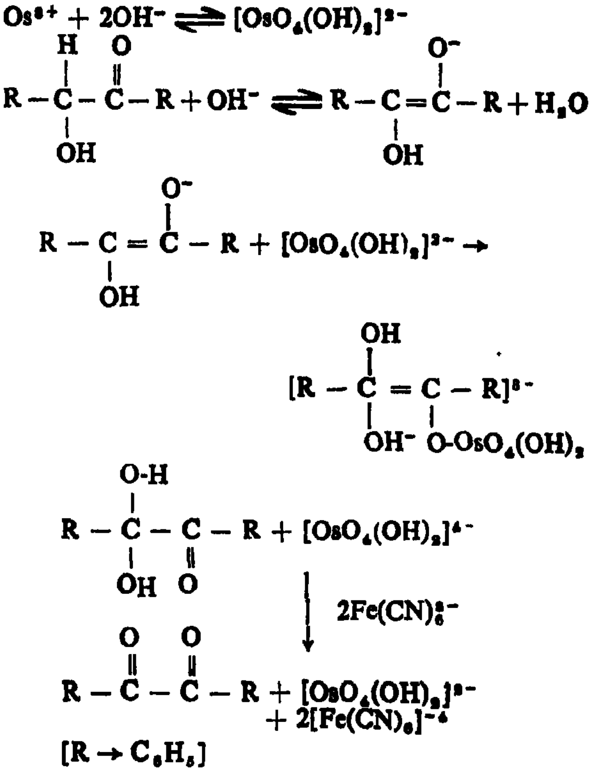
From the experimental observation it is worthwhile to mention that if only benzoin and OsO_4 are taken in alkaline medium the colour of the osmium tetroxide immediately disappears and if it is acidified and titrated against a standard solution of ceric sulphate, then two moles of ceric are used for one mole of OsO_4. This conclusively proves that it is the reduced osmium which is first oxidised to its original octavalent state by alkaline hexacyanoferrate(III). It has already been pointed out that the oxidation of benzoin with ceric sulphate is not appreciable under these conditions and hence it is possibly the Os^{VI} which reacts rapidly with hexacyanoferrate(III) ion.

The alkali dependence of oxidation process involved, clearly indicates the oxidation of benzoin takes place through an intermediate anion of the reducing substrate formed with hydroxyl ion. Since the uncatalysed oxidation does not proceed at all and hexacyanoferrate(III) is consumed without taking part in the rate law, it is assumed that hexacyanoferrate(III) does not react directly until after the rate determining step. It is the reduced osmium which is first oxidised to its original octavalent state.

A mechanism based on formation of a soluble complex between enolate ion and Os^{VIII} is suggested. We have isolated benzil as the product of oxidation and from the reaction sequence it has been observed that the electron-donating groups enhance the reaction rate and electron-attracting groups retard it. Further, according to the proposed rate law, the rate determining step involves the interaction between two negatively charged ions or between a negatively charged ion and a polar molecule and thus should correspond to a negative entropy change[13,14].

For the reaction involving interaction between similarly charged ions, the plots of log k_o *vs* reciprocal of dielectric constant should be a straight line having a negative slope. In the present investigations, similar results have also been obtained.

The mechanism proposed involves formation of complex between enolate ion and Os^{VIII}. This complex then decomposes to give benzil and Os^{VI} ion, and subsequently Os^{VIII} ion is then regenerated by the oxidation of Os^{VI} by two molecules of hexacyanoferrate(III) ion.



The same benzil has been isolated by Ramataatnan and Varadarajan[12] by the chromic acid oxidation of benzoin.

Acknowledgement

The authors are grateful to U.G.C., New Delhi, for financial assistance.

References

1. A. K. KASHYAP, R. C. MOHAPATRA and N. C. KHANDUAL, *J. Indian Chem. Soc.*, 1979, 56, 748.
2. R. C. MOHAPATRA and N. C. KHANDUAL, *Indian J. Chem., Sect. A*, 1982, 21, 517.
3. R. C. MOHAPATRA and N. C. KHANDUAL, *Indian J. Chem., Sect. A*, 1982, 21, 167.
4. S. B. MOHANTY, R. C. ACHARYA, C. N. NANDA and M. K. ROUT, *Indian J. Chem., Sect. A*, 1976, 14, 42.
5. H. C. BROWN and Y. OKAMOTO, *J. Am. Chem. Soc.*, 1957, 79, 1913; 1968, 80, 4980.
6. N. N. DAS, N. K. SARAN and R. C. ACHARYA, *J. Indian Chem. Soc.*, 1979, 56, 1208.
7. J. E. LEFFLER and E. GRUNWALD, "Rates and Equilibria in Organic Chemistry", Wiley, New York, 1963, p. 171.
8. P. L. NAYAK and M. K. ROUT, *J. Indian Chem. Soc.*, 1970, 47, 807; K. BOWDEN, N. B. CHAPMAN and J. SHORTER, *J. Chem. Soc.*, 1964, 337.
9. J. S. LITTLER, *J. Chem. Soc.*, 1962, 827, 832.
10. K. K. BANARJEE, P. NATH and G. V. BAKORE, *Bull. Chem. Soc. Jpn.*, 1970, 43, 2027.
11. V. VENKATKRISHNAN and M. SANTAPPA, *Z. Phys. Chem. (Frankfurt am Main)*, 1958, 16, 73.
12. S. RAMATATNAN and R. VARADARAJAN, *Indian J. Chem.*, 1972, 10, 237.
13. K. S. SHUKLA, P. C. MATHUR and O. P. BANSARL, *J. Inorg. Nucl. Chem.*, 1973, 35, 1301.
14. U. LAL, V. N. SINGH, H. N. SINGH and M. P. SINGH, *Indian J. Chem.*, 1972, 10, 329.

J. Indian Chem. Soc.,
Vol. LXIII, March 1986, pp. 295-298

The Catalytic Effect of Aluminium Ions added to Cupric Oxide Catalyst during Propan-2-ol Decomposition

E. A. HASSAN, A. A. SAID and K. M. ABD EL-SALAAM*

Chemistry Department, Faculty of Science, Assiut University, Assiut, Egypt

Manuscript received 17 July 1985, accepted 17 January 1986

The acid-base solid, $CuO-Al_2O_3$ was examined as a potential catalyst for decomposition of propan-2-ol. The high dehydrogenation activity occured for pure CuO at lower calcination temperature is related to the presence of basic active chemisorbed oxygen. Addition of Al^{III} ions in lower concentrations causes variation of either Fermi level and/or the oxidation-reduction state of the copper ions. At higher Al^{III} ions concentration, the solid solution formed varies the specificity of the surface towards the dehydrogenation-dehydration processes.

Cupric oxide has attracted considerable attention due to its industrial applications[1,2] and for fundamental understanding of catalyst activation[3]. Chemisorption of oxygen on copper oxide was studied and the process was visualised as an expansion of the lattice to incorporate the adsorbed oxygen creating vacancies[4]. Hence, a localised layer of negative charge is generated on the catalyst surface. Catalytic interaction of organic substances over its surface was carried out effectively. An increase of methanol conversion rate was produced over supported CuO where it was suggested that CuO was dispersed over the Al_2O_3 support[5]. XRD investigations of such material reveals the presence of Cu_2O peak as a second phase[6]. This is also was a result of the work carried out using copper containing zeolite by TPR[7].

This article examines the catalytic influence of Al^{III} ions either doped or mixed with CuO catalyst. Study of propan-2-ol decomposition was selected as a test reaction for the surface acid-base properties change over the surface.

Experimental

Catalysts were prepared by impregnating copper carbonate (A.R.) with $Al(NO_3)_3.9H_2O$ solution in molar ratios of 0.5 upto 50 mol %. The parent materials were dried at 110° and subsequently calcined at different temperatures from 200 upto 700° in a flow of dry air.

The decomposition of propan-2-ol was performed in a convential flow apparatus operated at atmospheric pressure. The apparatus used in this study was described previously[8]. For most runs, 0.5 g of catalyst was used diluted with quartz grains of uniform size. The total flow of N_2 gas was 400 ml (NTP) min^{-1} charged with 2.2% reactant of alcohol. Analysis were carried out with a PYE Unicam 104 flame ionisation detector (FID). The column (1/8" o.d. × 1.5 m) was PEG 20% filled with 60-80 mesh celite. In the exit-feed, acetone and propylene were detected as the only products of the catalytic experiments together with the unreacted alcohol. The accuracy of the analytical procedure used was within 5% on the basis of carbon material balance. The experimental results presented are not influenced by heat transport or diffusion limitation effects.

Results

Typical experimental results obtained with CuO calcined at 400° for 2 h at different reaction temperatures are given in Fig. 1. The catalyst flow rate ratio was 0.467 g cat/mol/l/h. Based on these data, two main processes taking place over the catalyst surface were (a) the dehydrogenation reaction where acetone was produced with a high % yield at low catalytic reaction temperature and (b) increasing the catalytic temperature, the dehydration process commenced at 200° and reached its maximum at 300° Also, it appears that the total conversion was 60% at 200° while it decreases monotoneously reaching a minimum at 400°. Noticing the variation of % conversion with the catalytic reaction temperature, it appears that from 200 upto 400° it is only 10% less. Consequently, it can be predicted that the dehydration reaction takes place at the expense of the dehydrogenation process.

The lattice nature of the solid catalysts was tested measuring its catalytic activity parameters against the calcination temperature. Fig. 2 indicates the surface property variation. At 300 and 400°, it seems that the surface has catalytic capacity towards dehydrogenation as well as dehydration

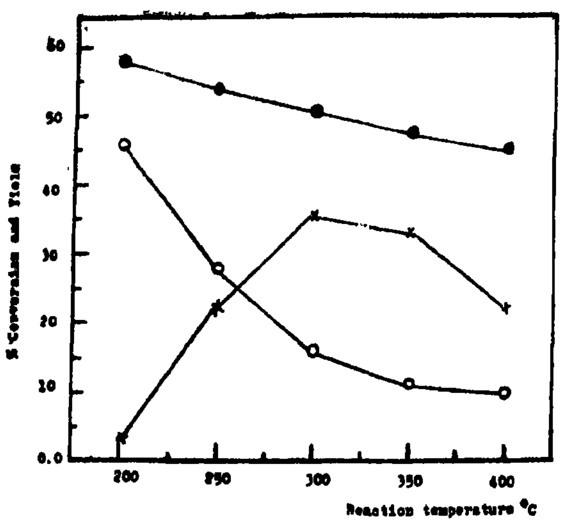


Fig. 1. Decomposition activity of CuO catalyst for propan-2-ol at different reaction temperatures: (●) conversion of propan-2-ol, (O) yield of acetone and (×) yield of propylene.

processes. After that temperatures, a large deviation occurred. The catalyst calcined at 700° has mainly dehydrogenation activity. These data indicate that different active sites are playing role over the surface as the calcination temperature developes.

The nature of the pores was tested for catalyst calcined at 400° using Wheeler's treatment[9] where effectiveness of the pores was calculated and showed no retardation effect on the catalytic process, *i.e.* the decomposition reaction is only influenced by the surface property.

Table 1 gives the experimental results of W/F values as a function of % conversion. It appears that on increasing W/F value the conversion increases.

The presence of Al^{III} ions in CuO matrix was studied under the same experimental conditions as in case of the pure catalyst. Fig. 3. describes the variation of % conversion yield of either acetone or propylene. At 0.5 mole % Al^{III} ions, the % conversion decreases. Adopting mechanism of

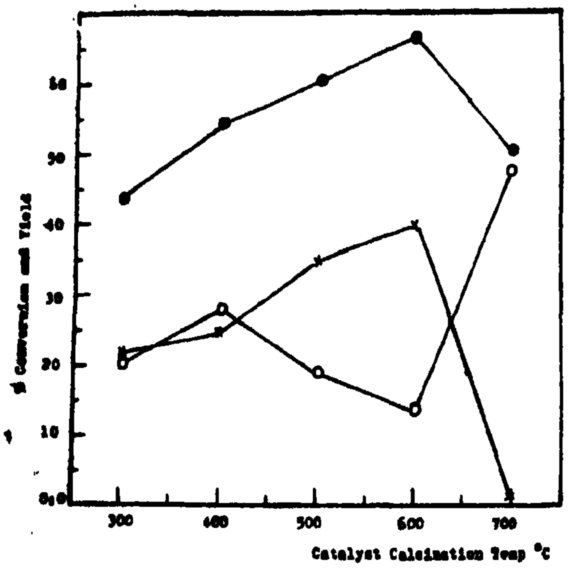


Fig. 2. Activity of CuO catalysts for propan-2-ol decomposition calcined at different temperatures for 2 h: (●) conversion of propan-2-ol, (O) yield of acetone and (×) yield of propylene.

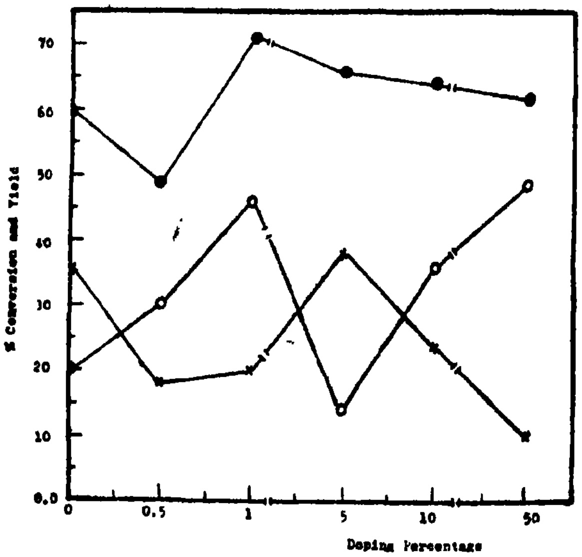


Fig. 3. Effect of Al^{III} ions doped and mixed with CuO catalyst calcined at 500° for 2 h for propan-2-ol decomposition: (●) conversion of propan-2-ol, (O) yield of acetone and (×) yield of propylene.

Table 1—% Conversion, Yield and Selectivity on CuO Catalyst Calcined at 400° for 2 h for Decomposition of Propan-2-ol

W/F	% Conv.	% Yield		% Selectivity	
		Acetone	Propylene	Acetone	Propylene
0.093	28.68	11.30	10.00	39.40	34.87
0.280	45.74	22.38	17.63	48.93	38.54
0.467	54.67	28.79	22.70	52.66	41.52
0.653	58.14	32.50	24.73	55.90	42.54
0.933	61.22	34.50	26.50	56.35	43.29

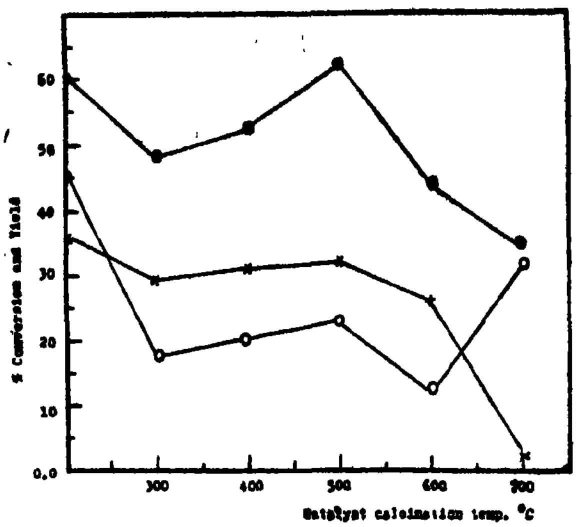


Fig. 4. Decomposition of propan-2-ol over CuO doped with 0.5 mol % Al^{III} calcined at different temperatures for 2 h: (●) conversion of propan-2-ol, (O) yield of acetone and (×) yield of propylene.

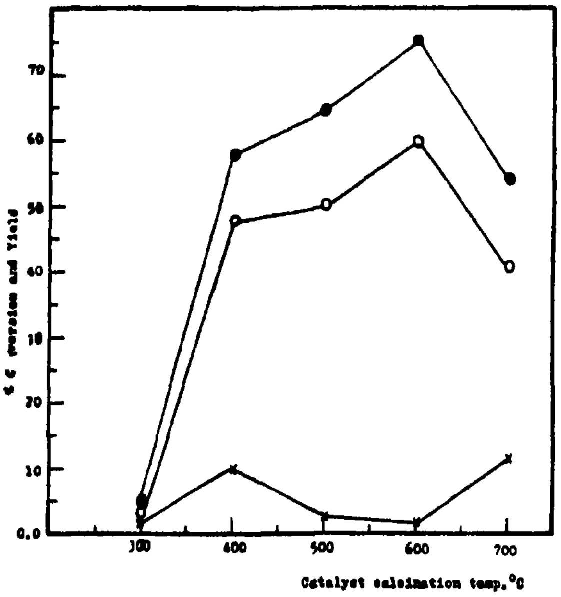


Fig. 5. Decomposition of propan-2-ol over CuO mixed with 50 mol % Al^{III} calcined at different temperatures: (●) conversion of propan-2-ol, (O) yield of acetone and (×) yield of propylene.

doping, as will be discussed later, consumption of the available active sites for propan-2-ol chemisorption decreases leading to low % conversion. Increasing Al^{III} ion concentration, the conversion increases reaching a maximum at 1 mol % and then gradually decreases. Further increase to 5 mol %, lead to a sudden drop for % acetone and an increase of % propylene. This phenomenon could be attributed to the increase of defects upto 1 mol %. At 5 mol %, the commencement of solid solution of copper aluminate starts, its property seems to be different than those of the individual oxides. Further formation of spinel structure leading to an enhancement of the dehydrogenation which occurs at the expense of the dehydration process.

The catalytic experiments conducted using catalysts contain either 0.5 or 50 mol % Al^{III} ions, were carried out to determine the difference between doping effect and solid solution formation over the catalyst surface. Figs. 4 and 5 illustrate these differences. A pronounced effect was found using CuO + 0.5 mol % Al^{III} ions where both processes are taking place, while with CuO + 50 mol % Al^{III} ion catalyst, the surface has entirely dehydrogenation activity.

Discussion

The results show that when the kinetics of a catalytic reaction are complex or unknown, the catalysts studied have to be compared at similar W/F values otherwise interpretation of the experimental results may be misleading.

One of the factors to control the activity in the decomposition of alcohols is the acid-base properties of the catalyst surface[10]. With acidic catalysts, the dehydrogenation predominantly takes place, while, over basic catalysts the dehydration reaction proceeds. Changes in their rate ratios will consequently attribute to the change in the acidic and basic centers activity.

For pure CuO catalyst, the most predominent change in the activity occurred at 200°, where the catalyst will tend to catalyse the dehydrogenation process. At higher catalytic temperature both reactions proceeded. This can be visualised on the basis of the experimental results of Gunningham *et al.*[11], that at 200°, more basic centers exist due to the oxygen chemisorption, adopting the following mechanism,

$$O_{2(g)} \rightarrow 2 \mid Cu \mid'' + 4 \mid e \mid^{\cdot} + Cu_2O$$

The change in the catalytic centers over the surface is illustrated in Fig. 2, where the effect of the catalyst backing temperature varied. A promiscuousness nature of the surface appeared at calcination temperature of 300°. At 600° calcination temperature, a wide variation occurs where propylene will be produced at the expense of acetone yield Previous work[12] has detected surface chemisorbed oxygen for catalysts calcined at lower rather higher temperatures. This phenomenon can support the idea that the oxygen chemisorbed can act as a dehydrogenation center specially for catalysts calcined at lower temperature and used at lower catalytic reaction temperatures.

Admission of Al_2O_3 into CuO matrix affects CuO catalytic properties in such a way that when Al^{III} ion has low concentration, the surface acts as dehydrogenation and dehydration catalyst. While, when Al^{III} ion reaches 50 mol %, the

activity polarises mainly to dehydrogenation reaction. It is obvious that there are several parameters that influence the catalytic activity. One of the most important factors, is the position of the Fermi level at the surface of the metal oxide[13,14] by which the charge transfer between the surface and alcohol molecules plays the dominant rate determining step; also, the oxidation-reduction reaction of metal oxide surface and the relative position and availability of the reaction sites on the surface where propan-2-ol dehydrogenation is structure sensitive.

Therefore, it could believe that Al^{III} ions in lower concentrations can cause the variation of either the Fermi level and the oxidation-reduction state of the surface *via* the following mechanism,

$$Al_2O_3 \rightarrow 2\ Al \mid Cu \mid' + Cu_2O + O_2 + 2e$$

This mechanism will hinder the amount of propan-2-ol chemisorbed and is in accordance with the experimental results of CuO catalyst doped with 0.5 mol % Al^{III} ions. On increasing of Al^{III} ion concentrations, the acidic nature of the surface increases due to the Lewis acid sites induction. This in its turn affects the % conversion where a maximum was obtained when 1 mol % Al^{III} ion was admitted. More Al^{III} ion will form $CuAl_2O_4$, its concentration will affect either the % conversion of the specificity of the surface towards the reaction process type.

References

1. R. G. Herman, K. Klier, G. W. Simmons, B. P. Finn and S. B. Bulko, *J. Catal.*, 1979, **56**, 407.
2. "Imperial Chemical Industries Catalyst Hand-book", Springer Verlag, New York, 1970.
3. W. N. Hurst, S. J. Gentry and A. Jones, *J. Catal.*, *Rev. Sci. Eng.*, 1982, **24**, 233.
4. W. E. Garner, T. J. Gray and F. S. Stone, *Proc. R. Soc. London, Ser. A*, 1949, **197**, 294.
5. H. Hvoge and L. T. Atkins, *J. Catal.*, 1962, **1**, 171.
6. P. B. Himelfarb, F. E. Wawner, Jr., A. Bieser and S. A. Vines, *J. Catal.*, 198?, **83**, 469.
7. S. J. Gentry, N. W. Hurst and A. J. Jones, *J. Chem. Soc., Faraday Trans.* 1, 1979, 1688.
8. K. M. Abd El-Salaam, E. A. Hassan and A. A. Said, *J. Surface Technol.*, 1983, **21**, 327.
9. A. Wheeler, *Adv. Catal.*, 1951, **3**, 249.
10. V. Krylov, "Catalysis by Non-metals", Academic Press, New York, 1970.
11. J. Gunningham, B. K. Hodnett, M. Ihyas, J. Tobin, E. L. Leahy and J. L. G. Fierro, *Faraday Discuss. Chem. Soc.*, 1981, **72**, 283.
12. K. M. Abd El-Salaam, A. A. Said and E. A. Hassan *J. Surface Technol.*, in the press.
13. P. Wolkenstein, *Kinet. Katal.*, 1955, **8**, 202.
14. K. Hauffe, *Adv. Catal.*, 1955, **7**, 213.

J. Indian Chem. Soc.,
Vol. LXIII, March 1986, pp. 299-300

Anodization of Zircaloy-4 in 0.1*M* KOH in Presence of Halide Ions

A. PANASA REDDY and K. S. SASTRY*

Department of Chemistry, University College of Science, Osmania University, Hyderabad-500 007

Manuscript received 27 May 1985, accepted 17 January 1986

The effect of halide ions on the kinetics of anodisation of zircaloy-4 in 0.1 *M* KOH have been studied at a constant current density of 4 mA cm^{-2} and at room temperature. At higher concentrations of halide ions (⩾ 0.1 *M*), there is no film formation and deleterious effects are observed. However, there is film formation and the kinetics of film formation are well studied at lower concentrations of halide ions. However, in the presence of iodide ions, there is a remarkable change in the kinetics of film formation.

ANODISATION of zirconium in various electrolytes have been studied by Young[1], Charlesby[2], Wilkins[3] and also by us[4-6]. In the present work, an attempt is made to study the effect of halide ions, mainly iodide ions, on the kinetics of anodisation of zircaloy-4 in 0.1 *M* KOH.

Experimental

Zircaloy-4 specimens (0.150 mm thick) used were a gift sample from Nuclear Fuel Complex, Hyderabad. The nominal analysis (%) given was Sn (1.44), Fe (0.23), Cr (0.07) and Zr (98.26). The procedures for the preparation of the specimens and chemical polishing was given in our earlier paper[6]. Anodisations were carried out in 0.1 *M* KOH in the presence of various proportions of halide ions at a constant current density of 4 mA cm^{-2}. Thickness of the film formed was estimated by capacitance measurements. The density and dielectric constant of ZrO_2 were taken as 5.7 g ml^{-1} and 24.7, respectively[7].

The constant current generator used was stabilised power supply, built by instruments Techniques Pvt. Ltd., Hyderabad. A digital LCR meter VLCR6 supplied by Vasavi Electronics, Hyderabad, was used for the capacitance measurements.

Results and Discussion

The chemically polished zircaloy-4 specimens were anodised in the electrolyte 0.1 *M* KOH in the presence and absence of halide ions in various proportions at a constant current density of 4 mA cm^{-2} and at room temperature.

In pure KOH the plots of formation voltage *vs* time and reciprocal capacitance *vs* time, and reciprocal capacitance *vs* formation voltage, were found to be linear upto 95 ± 5 V and the corresponding thickness was estimated to be 240 ± 10 nm. The current efficiency and the differential field of formation were found to be 41.36% and 5.062 MV cm^{-1}, respectively. Beyond this thickness (240 ± 10 nm) the current efficiency was found to fall gradually whilst the differential field decreased to 4.04 MV cm^{-1}.

There was no film formation when the ratio of [KOH] : [halide ion] < 10 : 1. and deleterious effects are observed, such as pitting and precipitation. However, there was film formation when the ratio was 100 : 1. It is found that there is an increase in the current efficiency and the differential field of formation in the presence of halide ions in 0.1 *M* KOH and it is shown in Table 1.

TABLE 1—ANODIC FILMS FORMED IN 0.1 *M* KOH IN PRESENCE AND ABSENCE OF HALIDE IONS

[KOH] : [X⁻]*	X⁻*	Current efficiency (η) %	Differential field, (F_D) MV cm^{-1}
100 : 1	F^-	74.68	5.46
100 : 1	Cl^-	55.71	5.24
100 : 1	Br^-	49.78	3.69
100 : 1	I^-	81.12	5.50
10 : 1	I^-	56.00	5.25
1 : 1	I^-	49.00	5.10
0.1 *M* KOH	–	41.36	5.06

*X^- ≡ Halide ion.

Addition of iodide ions to 0.1 *M* KOH showed that there was film formation when the ratio of [KOH] : [halide ion] ⩾ 1 : 1. The current efficiency and differential field were found to be increased with the decrease in the proportion of iodide ion in 0.1 *M* KOH. However, when the concentration

of iodide ions was > 0.1 *M*, there was no film formation and liberation of iodine was observed. The linearity of the plots of formation voltage *vs* time was increased in the presence of iodide ions and this was shown in Fig. 1.

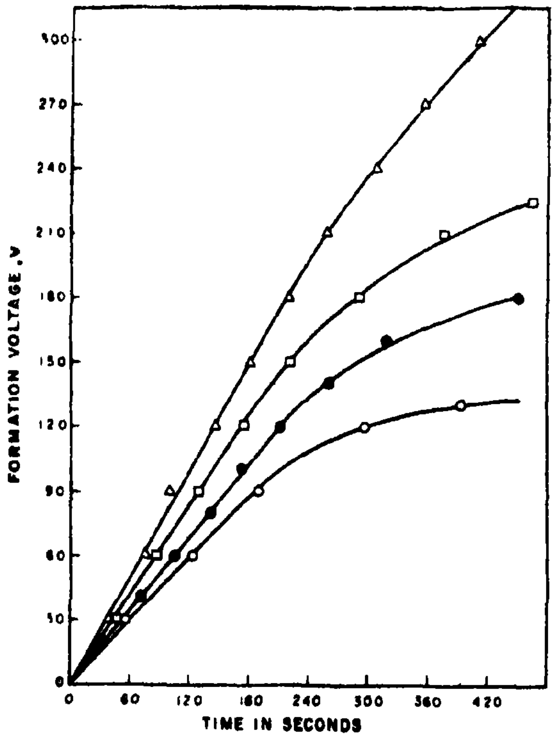


Fig. 1. Formation voltage *vs* time for anodisation of zircaloy-4 in 0.1 *M* KOH + various proportions of halide ions: (○) 0.0, (●) 0.1, (□) 0.01 and (△) 0.001 *M* I^-.

Sastry[4] and Sastry and Draper[8] studied the effect of anion impurities in 0.1 *M* KOH on the kinetics of anodic film formation on zirconium at a constant current density of 4.1 mA cm^{-2} and observed that the current efficiency and the differential field of formation were increased in the presence of anion impurities. They attributed these results to the incorporation of anion impurities into the anodic film and it was confirmed by radio-tracer techniques[6,8]. Hence, an increase in the current efficiency and the differential field with the addition of halide ions to 0.1 *M* KOH in the present work may be attributed to the incorporation of halide ions into the anodic film.

Acknowledgement

The authors wish to thank Prof. M. L. N. Reddy, Head, Department of Chemistry and Prof. T. Navaneeth Rao, Rector, Osmania University, for their keen interest and encouragement. One of the authors (A.P.R) expresses his gratitude to C.S.I.R., New Delhi, for the award of Senior Research Fellowship.

References

1. L. YOUNG, *Trans. Faraday Soc.*, 1959, **55**, 632.
2. A. CHARLESBY, *Acta Met.*, 1953, **1**, 340, 348.
3. N. J. M. WILKINS, *J. Electrochem. Soc.*, 1962, **109**, 998.
4. K. S. SASTRY, *J. Electrochem. Soc. India*, 1973, **22**, 161.
5. A. N. CHARY, Ph.D. Thesis, Osmania University, 1984.
6. A. PANASA REDDY, A. N. CHARY, CH. ANJANEYULU and K. S. SASTRY, *J. Electrochem. Soc. India*, 1984, **33**, 31.
7. L. YOUNG, Anodic Oxide Films, Academic Press, London, 1961.
8. K. S. SASTRY and P. H. G. DRAPER, *J. Electrochem. Soc. India*, 1975, **24**, 173.

J. Indian Chem. Soc.,
Vol. LXIII, March 1986, pp. 301-305

Partial Molal Volumes and Expansibilities of Sodium Salts of some Fatty Acids in Water at Various Temperatures†

RAJANI KANTA MOHANTY*, INDRANARAYAN BASUMALLICK, ARUN KUMAR DAS
and
SAKTIBRATA BHOWMIK

Department of Chemistry, Visva-Bharati University, Santiniketan-731 235

Manuscript received 12 April 1983, revised 3 September 1984, accepted 6 February 1986

The partial molal volumes ($\phi^{\circ}_{v} \equiv \bar{V}^{\circ}_{2}$) of the sodium salts of formic acid, acetic acid, propionic acid, n-butyric acid and n-valeric acid have been obtained from density measurements (pycnometrically) at 25, 35, 45 and 55°. The partial molal expansibilities (E°) have also been calculated from the temperature dependence of partial molal volumes. Both partial molal volumes and expansibilities have been dissected into ionic contributions using the additivity principle. The partial molal volumes of the hydrophobic anions have been found to vary in the order, n-valerate > n-butyrate > propionate > acetate > formate, and the expansibilities vary in the same order.

The partial molal volumes at different temperatures do not present a clear picture about the structure altering properties of these solutes, but the expansibilities do.

APPARENT and partial molal volumes of both electrolytes and non-electrolytes in water have been demonstrated to provide useful information about solute-solute, solute-solvent, and solvent-solvent interactions in solutions[1,2]. The existing literature[1,2] shows that extensive work on partial molal volumes of both electrolytes[1] and non-electrolytes[2] has been done. However, the temperature dependence work on partial molal volumes particularly of hydrophobic solutes is not that exhaustive and further work in this line is essential, since such temperature dependence studies are likely to provide[3,4] detailed insight into important aspects of solute-water interactions.

Sodium salts of fatty acids of a homologous series are a set of interesting solutes for studies of hydrophobic hydration. These salts have been studied by a number of techniques[5,6] but such studies are made mostly at a single temperature only. Hence, for the better understanding of the interaction of these salts with water, the present study has been taken up. It describes the results of density measurements of five homologous fatty acid salt solutions in water at four different temperatures (25, 35, 45 and 55°). The partial molal volumes and expansibilities have been obtained by processing the density data, by usual methods.

Experimental

Sodium formate, sodium acetate-trihydrate (both G.R., Merck), sodium propionate (Boehringer, analytical grade) were used without further purification. Sodium n-butyrate (SD) was recrystallised from ethanol-water (1 : 1) mixture. Sodium salt of n-valeric acid was prepared by neutralising n-valeric acid (Merck) with sodium bicarbonate (A.R., B.D.H.). The resulting salt was washed first with acetone and then with ether and recrystallised[7] from absolute ethanol. All these salts except sodium acetate trihydrate were oven-dried at 110° for 8 h and were kept in vacuum desiccators for 48 h before use.

Solutions of different molalities were made by weight-dilution method from the concentrated stock solutions in clean standard joint stoppered bottles. Triple-distilled water used, was prepared by redistilling the double-distilled water obtained by alkaline $KMnO_4$ distillation of deionised water in an all-glass apparatus.

Densities of aqueous solutions were measured with Ostwald-Sprengel type pycnometers (70 ml) which were previously calibrated at 25, 35, 45 and 55° using the same water. Six different pycnometers were used simultaneously. The pycnometers with the solutions were thermostated in a water-bath (temperature control within ± 0.05°) for 1 h for equilibration. After equilibration and adjustment of the menisci to fiducial marks they were allowed to stand for 1 h at room temperature and then weighed accurately to fifth place of decimal.

† Presented in part at the Annual Convention of Chemists at Madras, December 26-31, 1981.

The average uncertainties in the density determination were within $\pm 1\times10^{-5}$ g cm^{-3} which brings the uncertainties in the ϕ_v^0 values within 0.01-0.1 ml mol^{-1} in the temp erature range studied here..

Results and Discussion

From the measured density data at different temperatures, the apparent molal volumes (ϕ_v) of these salts were calculated using the following equation[8],

$$\phi_v = \frac{M}{d} - \frac{1000(d-d^0)}{mdd^0} \qquad (1)$$

where, M is the molecular weight of the solute, d is the density of solution, d^0 is the density of pure water (the values at different temperatures taken from Ref. 22) and m is the molality of the solution. Partial molal volumes (ϕ_v^0)# were obtained by plotting the calculated ϕ_v values against $m^{1/2}$ according to the Masson[9] equation,

$$\phi_v = \phi_v^0 + S_v^* m^{\frac{1}{2}} \qquad (2)$$

where, S_v^* is the experimental limiting slope. An illustrative plot of (ϕ_v) values against $m^{1/2}$ for these salts at 35° is shown in Fig. 1.

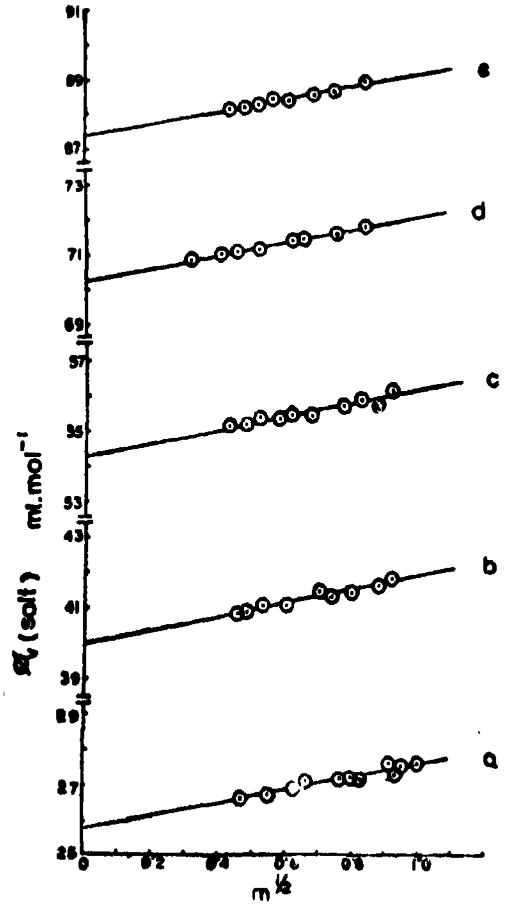


Fig. 1. Apparent molal volumes of sodium salts of fatty acids in water against square-root of molal concentration at 35° : (a) sodium formate, (b) sodium acetate, (c) sodium propionate, (d) sodium n-butyrate and (e) sodium n-valerate.

The ϕ_v^0 values of these salts at different temperatures are shown in Table 1. The partial molal volume of NaCl at 45° determined by us (ϕ_v^0 NaCl = 17.50 cm^3 mol^{-1}) agreed well with that of Millero[10] (ϕ_v^0 NaCl = 17.59 cm^3 mol^{-1}) confirming the validity of the present procedure.

The ionic partial molal volumes in water at different temperatures have been obtained from the partial molal volumes of the respective salts at 25, 35, 45° and 55° by making use of the partial molal volume of sodium ion in water (Table 2) following the additivity principle†,

$$\phi_v^0\,(RCOO^-) = \phi_v^0\,(RCOONa) - \phi_v^0\,(Na^+) \qquad (3)$$

The ionic partial molal volumes and the expansibilities of the anions are shown in Tables 3 and 4, respectively.

TABLE 1—PARTIAL MOLAL VOLUMES (ϕ_v^0, ml mol^{-1}) OF SODIUM SALTS OF FATTY ACIDS IN WATER AT DIFFERENT TEMPERATURES (°C)

Salt	ϕ_v^0, ml mol^{-1}			
	25°	35°	45°	55°
Sodium formate	25.05[a]	25.70 (1.92)	26.12 (1.74)	26.40 (1.56)
Sodium acetate	39.22[a]	39.99 (1.79)	40.51 (1.65)	40.90 (1.53)
Sodium propionate	53.38 (1.79)	54.30 (1.73)	55.27 (1.60)	55.75 (1.52)
Sodium n-butyrate	69.18[a]	70.26 (1.65)	71.45 (1.54)	72.16 (1.48)
Sodium n-valerate	86.20 (1.64)	87.42 (1.58)	88.74 (1.52)	89.56 (1.40)

[a]Ref. 5.

Values in parentheses represent the experimental limiting slopes.

TABLE 2—PARTIAL MOLAL VOLUMES OF SODIUM ION IN WATER AT VARIOUS TEMPERATURES (°C)

	25°	35°	45°	55°
ϕ_v^0 (Sodium ion) ml mol^{-1}	-6.9, -7.0[a]	-6.5	-6.3	-6.1

[a]Ref. 21.

-CH_2-group contribution : The -CH_2- group contribution to the partial molal volume (Table 5) is calculated from the partial molal volumes of two

The limiting apparent molal volume, ϕ_v^0 has been referred to as the partial molal volume ($\bar{V}_2^0$) throughout this paper, as they are same (Ref. 4b)

† Partial molal volumes of NaCl (Ref. 10) and that of Cl^- (Ref. 11) were plotted against temperature separately and the values at the temperatures required were found out from the graph and finally ϕ_v^0 Na^+ was obtained using the additivity principle.

TABLE 3—IONIC PARTIAL MOLAL VOLUMES (ϕ_v^o (ion), ml mol^{-1}) OF ACID ANIONS OF SODIUM SALTS OF FATTY ACIDS IN WATER AT DIFFERENT TEMPERATURES (°C)

Anion	ϕ_v^o (ion), ml mol^{-1}			
	25°	35°	45°	55°
Formate	31.95, 32.2[a]	32.20	32.42	32.50
Acetate	46.12, 46.3[a]	46.49	46.81	47.00
Propionate	60.28, 59.8[a]	60.80	61.57	61.85
n-Butyrate	76.08	76.76	77.75	78.26
n-Valerate	93 10	93.92	95.04	95.66

[a]Ref. 21.

TABLE 4—PARTIAL MOLAL EXPANSIBILITIES OF SODIUM SALTS OF FATTY ACIDS E° ($= d\phi_v^o/dT$) AND OF ACID ANIONS E_{ion}^o ($= d\phi_v^o$ ion/dT) AT DIFFERENT TEMPERATURES (°C)

Salt	E° ml mol^{-1} K^{-1}		
	30°	40°	50°
Sodium formate	0.060	0.041	0.028
Sodium acetate	0.075	0.053	0.037
Sodium n-propionate	0.092	0.101	0.046
Sodium n-butyrate	0.018	0.119	0.065
Sodium n-valerate	0.123	0.132	0.081

Anion	E_{ion}^o, ml mol^{-1} K^{-1}		
	30°	40°	50°
Formate	0.025	0.021	0.009
Acetate	0.037	0.033	0.021
n-Propionate	0.053	0.078	0.028
n-Butyrate	0.071	0.097	0.048
n-Valerate	0 081	0.114	0.064

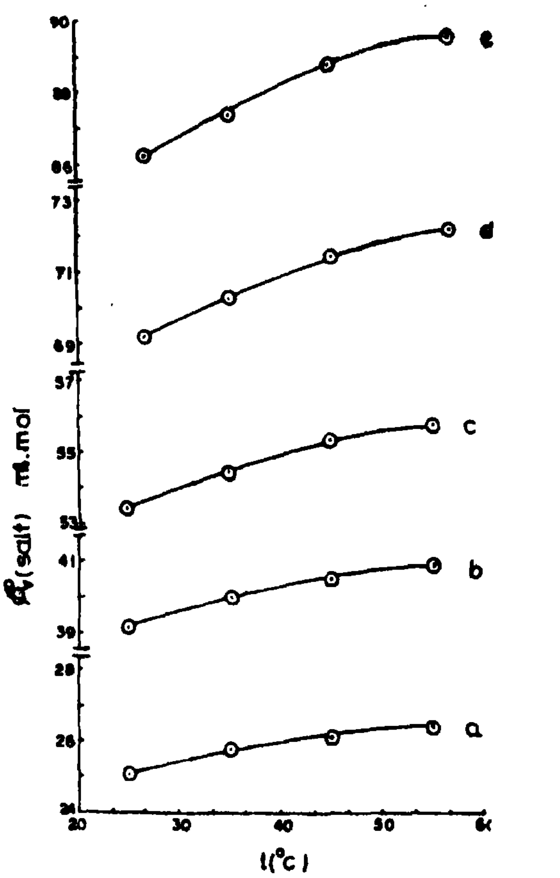


Fig. 2. Partial molal volumes of sodium salts of fatty acids in water at different temperatures: (a) sodium formate, (b) sodium acetate, (c) sodium propionate, (d) sodium n-butyrate and (e) sodium n-valerate.

TABLE 5—CONTRIBUTION OF -CH_2- GROUPS TOWARDS PARTIAL MOLAL VOLUMES AT DIFFERENT TEMPERATURES (°C)

	-CH_2- group contribution, ml mol^{-1}			
	25°	35°	45°	55°
ϕ_v^o (sodium acetate) − ϕ_v^o (sodium formate)	14.17	14.29	14.39	14.50
ϕ_v^o (sodium n-propionate) − ϕ_v^o (sodium acetate)	14.16	14.31	14.76	14.85
ϕ_v^o (sodium n-butyrate) − ϕ_v^o (sodium n-propionate)	15.80	15.96	16.18	16.41
ϕ_v^o (sodium n-valerate) − ϕ_v^o (sodium n-butyrate)	17.02	17.16	17.29	17.40

consecutive salts of the homologous series. The average value for this contribution is found to be 15.28, 15.43, 15.68 and 15.79 ml mol^{-1} at 25, 35, 45 and 55°, respectively.

Previous workers[12-14] have found out this contribution at 25° for a series of saturated homologous aliphatic alcohols, which was around 16.0 ml mol^{-1}. If we also calculate the -CH_2- group contribution to the ϕ_v^o from the work of Kaulgud *et al.*[15] on aliphatic saturated amines, it is found to be close to this value (15.95 ml mol^{-1}) at 25°.

The difference in the -CH_2- group contribution as obtained from our work and that from the work on alcohols and amines is understandable when we consider the fact that our solutes are 1 : 1 electrolytes, whereas those in the work of the others are non-electrolytes. Further, since the alcohols and amines are very similar polar molecules, the similarity in the -CH_2- group contribution in their case is expected. While comparing their results on amino acids[16] with that of uncharged organic molecules[17], Shahidi and Farrel[18] concluded that the contribution of side chains to the ϕ_v^o values is not greatly influenced by the terminal charge group. In our case, we do not find this to be true in the sense that there is a substantial difference between the -CH_2- group contribution of RCOONa salts

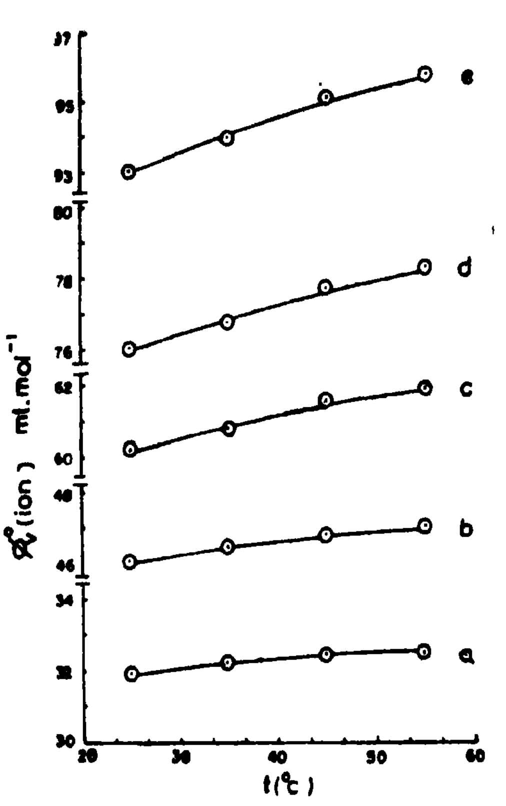


Fig. 3. Partial molal volume of acid anions of sodium salts of fatty acids in water at different temperatures: (a) sodium formate, (b) sodium acetate, (c) sodium n-propionate, (d) sodium n-butyrate and (e) sodium n-valerate.

(this work) and ROH and RNH_2 (Refs. 12-17) (although OH and NH_2 groups are not strictly charge groups, the situation is not entirely different from the sodium salts as OH and NH_2 groups are fairly polar in nature). Kaulgud *et al.*[15] while comparing the behaviour of alcohols and amines have concluded recently that the two polar head groups (*i.e.* OH and NH_2) do make a difference in the hydration behaviour of these two classes of solutes. This lends further support to our contention that the $-CH_2-$ group contribution is different for different classes of solutes. That the $-CH_2-$ group contribution also depends on the geometry of the molecules is evident from the difference of our values from that calculated from the work on various other compounds[18].

Size of the anion: It is expected that as 'n' in $CH_3-(CH_2)_n-COO^-$ increases the extent of hydrophobic hydration would go on increasing. That this is found to be so in the present study will be clear if we consider the increase of $-CH_2-$ group contribution to ϕ_v^0 as we go from formate to acetate, acetate to propionate, propionate to n-butyrate and n-butyrate to n-valerate (see also Fig. 4). The formate and acetate ions seem to affect the solvent differently than propionate, butyrate and valerate.

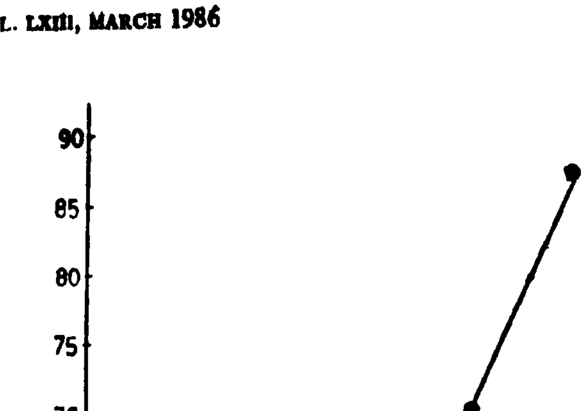


Fig. 4. Partial molal volumes of sodium salts of fatty acids in water against number of carbon atoms at 35°.

The latter ions seem to be definite structure makers. Such a conclusion was also drawn by Snell and Greyson[6] from their enthalpy and entropy of transfer work on these salts from water to D_2O.

Effect of temperature: Both the salt and ionic partial molal volumes increase with increase in temperature. This may either be due to the decrease in electrostriction with increase in temperature[19], or due to the loosening of water structure at higher temperatures. This argument is supported by the fact that the partial molal volumes of sodium formate, acetate, propionate and butyrate in 6*M* urea are much higher than the corresponding values in water at 25° (Ref. 19), assuming that increase in temperature brings about the same kind of effect as the increase in urea concentration in water, because in 6*M* urea the water structure is expected to be considerably broken down[20], and further

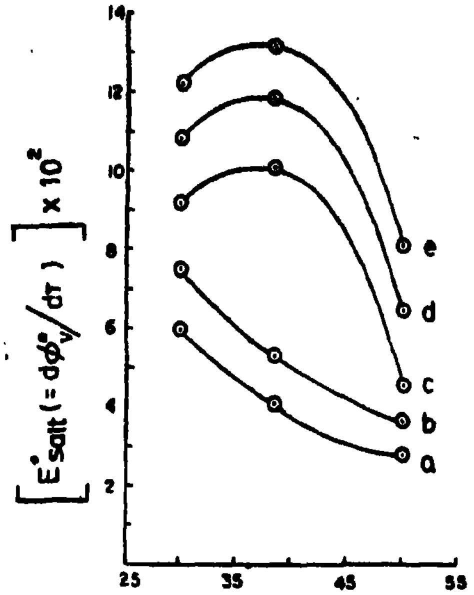


Fig. 5. Partial molal expansibilities, E° $(=d\phi^{\circ}_{v}/dT)$ of sodium salts of fatty acids in water at different temperatures: (a) sodium formate, (b) sodium acetate, (c) sodium n-propionate, (d) sodium n-butyrate and (e) sodium n-valerate.

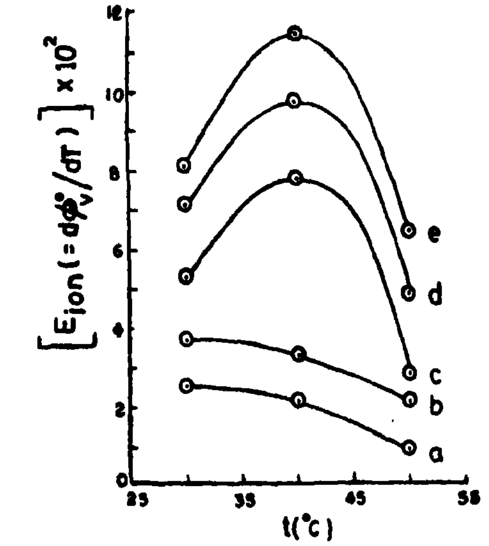


Fig. 6. Partial molal expansibilities of acid anions E°_{ion} $(=d\phi^{\circ}_{v}/dT)$ of sodium salts of fatty acids in water at different temperatures: (a) sodium formate, (b) sodium acetate, (c) sodium n-propionate, (d) sodium n-butyrate and (e) sodium n-valerate.

since electrostriction has been suggested to be less in aqueous urea than in pure water[20].

Since the ϕ°_{v} value increases with temperature in all cases (Table 1) the temperature dependence of ϕ°_{v} values does not give a clear picture about the effect of these solutes on the structure of water, particularly about the difference in behaviour of the first two homologues from the rest[9].

However, from the values of expansibilities (Table 4 and Figs. 5 and 6) this trend is clear, although qualitative. We do not of course attach much importance to the actual magnitudes of the expansibilities at different temperatures because of their doubtful accuracy. It is to be noted from Figs. 5 and 6 that beyond 40° all the salts appear to be structure breakers. This may possibly be due to the fact that at higher temperature increased thermal agitation does not allow structure formation by these salts to an extent detectable by the present technique.

Acknowledgement

Financial assistance from the U.G.C., New Delhi, and a Junior Research Fellowship to one of the authors (S.B.) are gratefully acknowledged.

References

1. F. J. Millero, *Chem. Rev.*, 1971, 71, 147.
2. F. Franks and D. J. G. Ives, *Quart. Rev.*, 1966, 20, 1.
3. L. G. Hepler, *Can. J. Chem.*, 1969, 47, 4613.
4. (a) C. Jolicoeur and P. R. Philip, *J. Solution Chem.*, 1975, 4, 3; (b) S. Cabani in "Advances in Solution Chemistry", eds. I. Bertini, L. Lunazzi and A. Dei, Plenum Press, New York, 1981, p. 13.
5. E. J. King, *J. Phys. Chem.*, 1969, 73, 1220.
6. H. Snell and J. Greyson, *J. Phys. Chem.*, 1970, 74, 2148.
7. K. J. Patil, P. V. Patil and O. B. Thakare, *Indian J. Chem., Sect. A*, 1979, 17, 177.
8. C. De Visser, G. G. Perron and J. E. Desnoyers, *Can. J. Chem.*, 1977, 55, 856.
9. D. O. Masson, *Philos. Mag.*, 1929, 8, 218.
10. F. J. Millero, *J. Phys. Chem.*, 1970, 74, 356.
11. A. J. Ellis, *J. Chem. Soc., A*, 1968, 1138.
12. D. M. Alexander, *J. Chem. Eng. Data*, 1969, 4, 252.
13. H. Høiland and E. Vikingstad, *Acta Chem. Scand., Ser. A*, 1976, 30, 182.
14. C. Jolicoeur and G. Lacroix, *Can. J. Chem.*, 1976, 54, 624.
15. M. V. Kaulgud, V. S. Vagde and A. Srivastava, *J. Chem. Soc., Faraday Trans. 1*, 1982, 313.
16. F. Shahidi and P. G. Farrell, *J. Chem. Soc., Faraday Trans. 1*, 1981, 77, 963.
17. O. Enea, P. P. Singh and L. G. Hepler, *J. Solution Chem.*, 1977, 6, 719.
18. S. Cabani, G. Conti and L. Lepori, *J. Phys. Chem.*, 1972, 76, 1338, 1343.
19. W. A. Hargraves and G. C. Kresheck, *J. Phys. Chem.*, 1969, 73, 3249.
20. S. Subramanian, T. S. Sarma, D. Balasubramanian and J. C. Ahluwalia, *J. Phys. Chem.*, 1971, 75, 815.
21. J. W. Akitt, *J. Chem. Soc., Faraday Trans. 1*, 1980, 76, 2259.
22. "Handbook of Chemistry and Physics", 59th ed., CRC Press, Cleveland, 1979.

J. Indian Chem. Soc.,
Vol. LXIII, March 1986, pp. 306-307

Thermodynamics of Non-electrolyte Solutions. II. Excess Volumes of Binary Solutions of 2,2,4-Trimethylpentane with some Aromatic Compounds at 40°

O. P. YADAV*, S. P. KHATKAR and R. C. SAINI

Department of Chemistry and Biochemistry, Haryana Agricultural University, Hissar-125 004

Manuscript received 19 June 1984, revised 9 September 1985, accepted 17 January 1986

Excess volumes of seven binary systems, *viz* 2,2,4-trimethylpentane + benzene; + toluene; + *o*-xylene; + *m*-xylene; + chlorobenzene; + benzaldehyde; and + acetophenone, have been determined at 40° over the entire range of composition by using a bicapillary pycnometer. The results have been compared with excess volumes calculated from 'graph theory'.

IN continuation of our earlier studies[1,2] on excess thermodynamic functions of binary non-electrolyte mixtures containing one of the components as an isomeric alkane, we report here the excess volumes of some binary systems of isooctane (2,2,4-trimethlypentane) with some aromatic compounds. The experimental results have been compared with the corresponding excess volumes calculated from graph theory[3,4].

Experimental

2,2,4-Trimethylpentane, benzene, toluene, *o*-xylene and *m*-xylene (each L.R. grade) were distilled over sodium metal. Chlorobenzene, benzaldehyde and acetophenone were distilled before use. The purity of these chemicals was checked by comparing their observed boiling points and densities with the corresponding literature values. The experimental details have been described elsewhere[5].

Results and Discussion

Molar excess volumes (v^E) of the studied binary systems have been calculated using the relation,

$$v^E=(M_1x_1+M_2x_2)/d-M_1x_1/d_1-M_2x_2/d_2 \quad (1)$$

where, M_i, x_i and d_i denote molecular weight, mole fraction and density, respectively of the ith component (i=1, 2) and d is density of the mixture.

Excess volumes of the studied binary systems at rounded mole fractions alongwith the error in experimental v^E have been given in Table 1. For the systems 2,2,4-trimethylpentane+benzene or + toluene, v^E values are symmetrical and positive throughout the studied composition range. The magnitude of excess volume for 2,2,4-trimethylpentane + benzene are higher than the corresponding values for n-octane + benzene system[6]. This may be explained in terms of comparatively less hindered interstitial accomodation within unlike molecules in case of the systems containing n-alkane than isomeric alkane.

The magnitude of excess volume decreases with the increase of number of substituted methyl groups on the benzene ring. This is evident from the excess volumes for the systems containing benzene, toluene, or a xylene as one of the components of the mixture (Fig. 1). For the systems containing

TABLE 1—MOLAR EXCESS VOLUME (v^E)* FOR BINARY SYSTEMS OF 2,2 4-TRIMETHYLPENTANE WITH SOME AROMATIC COMPOUNDS AT 40°

x_1	Benzene	Toluene	*o*-Xylene	*m*-Xylene	Chlorobenzene	Benzaldehyde	Acetophenone
0.1	0.18 (0.14)	0.13 (0.06)	−0.02	−0.18	−0.12 (−0.10)	−0.32 (−0.19)	−0.18 (−0.18)
0.2	0.26 (0.24)	0.19 (0.11)	−0.04	−0.21	−0.20 (−0.20)	−0.48 (−0.34)	−0.40 (−0.32)
0.3	0.34 (0.31)	0.22 (0.16)	−0.05	−0.22	−0.27 (−0.26)	−0.56 (−0.46)	−0.51 (−0.43)
0.4	0.39 (0.37)	0.23 (0.19)	−0.02	−0.19	−0.31 (−0.30)	−0.59 (−0.54)	−0.56 (−0.51)
0.5	0.41 (0.41)	0.21 (0.21)	0.00	0.00	−0.32 (−0.32)	−0.58 (−0.58)	−0.55 (−0.55)
0.6	0.37 (0.39)	0.19 (0.21)	0.01	0.16	−0.31 (−0.32)	−0.53 (−0.57)	−0.50 (−0.51)
0.7	0.30 (0.36)	0.16 (0.19)	0.02	0.19	−0.28 (−0.28)	−0.45 (−0.52)	−0.40 (−0.50)
0.8	0.22 (0.28)	0.11 (0.16)	0.01	0.15	−0.22 (−0.22)	−0.30 (−0.41)	−0.20 (−0.39)
0.9	0.13 (0.17)	0.06 (0.10)	0.01	0.09	−0.13 (−0.13)	−0.10 (−0.23)	−0.06 (−0.23)

*Error in experimental v^E = ± 0.02 ml mol^{-1}; values in parentheses calculated from 'graph theory'.

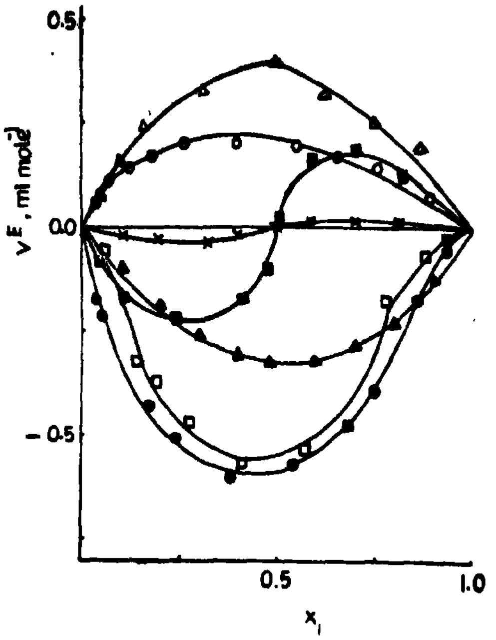


Fig. 1. Plots of v^E *vs* mole fraction of 2,2,4-trimethylpentane (x_1) for some binary systems : 2,2,4-trimethylpentane + (△) benzene, (○) toluene, (×) *o*-xylene, (■) *m*-xylene, (▲) chlorobenzene, (●) benzaldehyde, (□) acetophenone.

o- or *m*-xylene, the excess volume *versus* mole fraction plots are sigmoid with negative magnitude of v^E over the composition range rich in xylene component and positive values in the region rich in 2,2,4 trimethylpentane. In case of the binary systems containing chlorobenzene, benzaldehyde or acetophenone as a component the excess volumes are negative over the entire composition range. The negative values of excess volumes for the above systems may be due to the difference in the characteristic temperatures of the constituent components[6], which lead to a negative free volume or equation-of-state term in v^E. It is interesting to note that the presence of both electron-releasing (*i.e.* CH_3) as well as electron-withdrawing (*i.e.* Cl, CHO, $COCH_3$) groups substituted on benzene ring produce a similar effect of decrease in excess volume in comparison to when the pure benzene is one of the components. However, this effect is more pronounced in case of the electron-withdrawing substituted group.

According to graph theory [3,4] the excess volume may be calculated using the relation,

$$v^E = \alpha(1/(x_1\,{}^3\xi_1 + x_2\,{}^3\xi_2) - x_1/{}^3\xi_1 - x_2/{}^3\xi_2 \quad (2)$$

The connectivity parameters of third degree (${}^3\xi$) of component substances were calculated using the relation,

$$^3\xi = \sum_{i<j} \sum_{j<k} \sum_{k<l} (\delta_i, \delta_j, \delta_k, \delta_l)^{-\frac{1}{2}} \quad (3)$$

$\delta_i, \delta_j, \delta_k$ *etc.* denote the degrees of i, j, k *etc.* verticles of the graph of a molecule. According to the basic assumption of this theory, $1/\xi^3$ of a molecule is a measure of the probability that its surface area interacts affectively with the corresponding surface area of other molecules. The values of ${}^3\xi$ for 2,2,4-trimethylpentane, benzene and toluene were 1.021, 1.500 and 1.894, respectively. For chlorobenzene, benzaldehyde and acetophenone, the values of ${}^3\xi$ used were the same as for benzene. The parameter α in equation (2) was calculated using experimental v^E at equimolar concentration of the mixture. The excess volumes calculated from graph theory for the systems : 2,2,4-trimethylpentane + benzene ; + toluene ; + chlorobenzene ; + benzaldehyde ; + acetophenone are given in parenthesis in Table 1. The calculated values of v^E agree fairly well with the experimental values for the systems containing benzene, toluene or chlorobenzene. In case of the systems containing benzaldehyde or acetophenone there is only a qualitative agreement between the theoretical and the experimental values. For the systems containing *o*- or *m*-xylene as one of the components, no comparison could be made between the calculated and the observed excess volumes owing to the apparent weakness of this theory that it can be applied to only such systems which exhibit either positive or negative values of v^E throughout the composition range of the mixture.

Acknowledgement

The authors are grateful to C.S.I.R., New Delhi, for providing financial help.

References

1. D. V. S. Jain and O. P. Yadav, *Indian J. Chem.*, 1974, 12, 721.
2. O. P. Yadav, S. P. Khatkar and R. C. Saini, *J. Indian Chem. Soc.*, 1985, 62, 353.
3. D. H. Rouvary, *R. Inst. Chem. Rev.*, 1971, 4, 173.
4. A. T. Balaban, "Chemical Applications of Graph Theory", Academic Press, London, 1974.
5. D. V. S. Jain, B. S. Lark, S. S. Chamak and P. Chander, *Indian J. Chem.*, 1970, 8, 66.
6. P. J. Flory, *J. Am. Chem. Soc.*, 1965, 87, 1833.

J. Indian Chem. Soc.,
Vol. LXIII, March 1986, pp. 308-310

Polarographic Behaviour of some Potential Antidiabetic Compounds with Three Reduction Sites

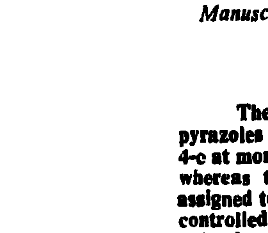
RAJEEV JAIN*

School of Studies in Chemistry, Jiwaji University, Gwalior-474 011

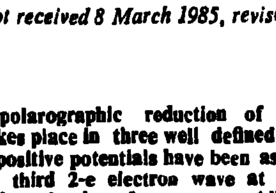
Manuscript received 8 March 1985, revised 31 October 1985, accepted 17 January 1986

The polarographic reduction of 1-(2,4-dinitrophenyl)-3,5-dimethyl-4-arylazopyrazoles takes place in three well defined reduction waves. The first two waves each 4-e at more positive potentials have been assigned to the reduction of two nitro groups, whereas the third 2-e electron wave at comparatively negative potential has been assigned to the reduction of azo group. All the three waves were found to be diffusion-controlled and irreversible. A plausible mechanism has been suggested for the reduction of azo group as evident by the number of electrons involved in the reduction and controlled potential electrolysis. The effect of substituents has been determined quantitatively by the application of Hammett equation.

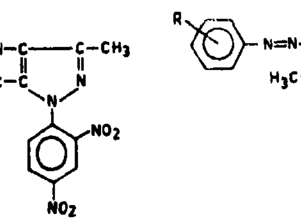
LITERATURE survey reveals that polarographic behaviour of 1-(2,4-dinitrophenyl)-3,5-dimethyl-4-arylazopyrazoles (1) has not been systematically studied inspite of their antidiabetic activity[1] and their unique structure from the electrochemical point of view. Keeping this in view these compounds have been studied polarographically in order to establish the preferential reduction of groups when they are present in a compound and to study the effect of substituents on the reduction of azo group.



(1)



(1a)



(1b)

Experimental

1 - (2,4 - Dinitrophenyl) - 3,5-dimethyl-4-arylazopyrazoles (1-14) and compounds (1a) and (1b) were synthesised by the literature method[1]. Their structures were confirmed by elemental and spectral analyses. The stock solutions ($10 \times 10^{-3} M$) of all these compounds were prepared in dimethylformamide (A.R.). Britton-Robinson buffers in the *p*H range 2.0-11.0 were prepared in distilled water using AnalaR grade chemicals. Solutions for polarographic measurements were prepared by mixing depolariser (1.0 ml), DMF (3.0 ml) (which was necessary to prevent precipitation), 1*M* KCl (1.0 ml) and appropriate buffer or NaOH solution (5.0 ml). Dissolved oxygen was removed by the passage of nitrogen gas for about 15 min.

An Elico-DC CL-25 polarograph was used and the capillary characteristics were 2.10 $mg^{2/3}s^{-1/2}$. SCE was used as the reference electrode. The number of electrons (n) involved in the reduction process was determined by the method of Devries and Kroon[2] and by controlled potential electrolysis. The temperature coefficient was calculated by Nejedly's method[3]. The uv-vis spectra of the solutions were recorded on a UV-VIS Carl Zeiss spectrophotometer.

Results and Discussion

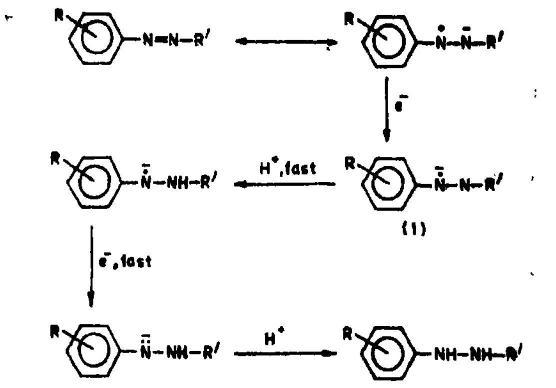
In these compounds (1-14) the possible reduction sites are the cyclic C=C and C=N groups of the pyrazole ring and excocyclic N=N and NO_2 sites. As extranuclear sites are more susceptible to reduction[4], it can be safely inferred that the reduction takes place at extranuclear N=N and NO_2 sites. This is further confirmed by the fact that simple pyrazoles are not reducible at d.m.e. under these experimental conditions whereas N=N and NO_2 groups are electroreducible.

All the compounds got precipitated in the buffered solutions of *p*H 2.0-11.0 and in acidic

medium. Therefore, studies were carried out in solutions of different strengths of NaOH. In these solutions all the compounds gave three well defined reduction waves. First, two reduction waves at more positive potential were found to be 4-e reduction waves whereas third wave was found to involve only 2-e in the electrode process. On the basis of number of electrons involved in the process as well as on the known easy reducibility of nitro group[6] in both aliphatic and aromatic compounds at the d.m.e., first two waves have been assigned to the reduction of nitro groups and the third wave to the reduction of azo group. This fact was verified by synthesising a similar compound 1-phenyl-3,5-dimethyl-4-arylazopyrazole (1a) which is not having nitro groups in the phenyl ring attached to N-atom of the pyrazole nucleus. This compound was found to give only one 2-e wave at a half-wave potential corresponding to the $E_{1/2}$ of the third wave under similar experimental conditions. This fact was further confirmed by carrying out controlled potential electrolysis on the potential corresponding to the plateau of the second wave, *i.e*, wave for the reduction of nitro group After controlled potential electrolysis for about ~12 h, the catholyte was subjected to product analysis. The catholyte was found not having any nitro group by the usual group tests and also on polarographic examination it did not give first two waves for the reduction of nitro groups but it gave only one wave corresponding to the potential of the third wave, which can be safely assigned to the reduction of azo group. These experiments are sufficient evidences to support that first two waves are for the reduction of nitro groups.

Reduction of nitro groups : Out of the two 4-e waves, first wave has been assigned to the reduction of NO_2 group present at 2-position in the phenyl ring whereas second wave to the reduction of 4-NO_2 group. For confirming the prior reduction of 2-nitro group, a compound 1-(4-nitrophenyl)-3,5-dimethyl-4-arylazopyrazole (1b) having only one nitro group at *para*-position was synthesised. On polarographic studies in similar experimental conditions it gave only two waevs, *i.e.* 4-e wave for the reduction of NO_2 group at potential corresponding to the 4-NO_2 group in case of compound 1 and second 2-e wave corresponding to wave for azo group. Both the waves for the reduction of nitro groups were diffusion-controlled and irreversible[6]. The values of i_d/C and $\alpha\, n_a$ are practically independent of concentration of depolariser. A mechanism for the reduction of nitro group, similar to that suggested by other workers[6,7-9], can be proposed for these compounds.

Reduction of azo group : All the arylazopyrazoles (Table 1) gave a single 2-e transfer, well defined cathodic waves in different strengths of NaOH solutions. The wave was found to be diffusion-controlled and irreversible by the usual polarographic experiments. Following (e, H^+, e, H^+) mechanism for the reduction of azo group based on the number of electrons involved in the reduction and independence of $E_{1/2}$ on the strength of NaOH solutions, may be proposed for these compounds.



The controlled potential electrolysis results confirm the formation of hydrazono compound. This mechanism is further supported by the work of others on azo compounds[11-14]. The maximum absorption in uv-vis spectra of 1 at 405 nm disappeared in solutions after complete electrolysis. Furthermore, the above electrolysed solution did not give any polarographic wave, thereby confirming the above reduction mechanism.

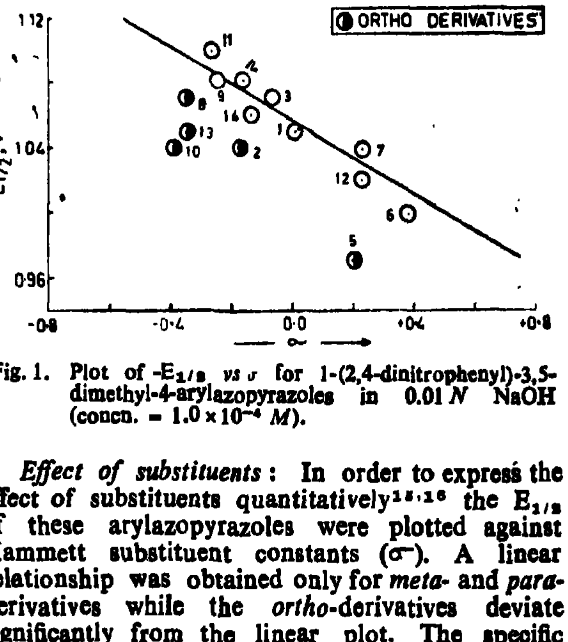


Fig. 1. Plot of $-E_{1/2}$ *vs* σ for 1-(2,4-dinitrophenyl)-3,5-dimethyl-4-arylazopyrazoles in 0.01 *N* NaOH (concn. = 1.0×10^{-4} *M*).

Effect of substituents : In order to express the effect of substituents quantitatively[15,16] the $E_{1/2}$ of these arylazopyrazoles were plotted against Hammett substituent constants (σ). A linear relationship was obtained only for *meta*- and *para*-derivatives while the *ortho*-derivatives deviate significantly from the linear plot. The specific reaction constant (ρ) was found to be 0.12 V and its positive sign indicated[17] the nucleophilic nature of the electrode process. The observed linear relationship of $E_{1/2}$ *vs* σ indicated that the substituents appreciably affected the reduction of azo group by polar and mesomeric effects through the benzene ring. For the *ortho*-derivatives, the corrected values of $E_{1/2}$ were obtained from the relationship given by Zuman[18]. The plot of corrected $E_{1/2}$ *vs* σ was linear from which the

TABLE 1—POLAROGRAPHIC CHARACTERISTICS OF SOME 1-(2,4-DINITROPHENYL)-3,5-DIMETHYL-4-ARYLAZOPYRAZOLES IN 0.01 N NaOH (CONCN. = 1.0×10^{-4} M)

Compd. no.	R	$-E_{1/2}$ V	i_d μA	α_n	I	$\Delta E_{1/2}$* V
1	H	1. 0.49	0.81	0.60	0.38	
		2. 0.67	0.85	0.67	0.40	
		3. 1.05	0.40	0.30	0.19	–
2	2-CH_3	1. 0.51	0.75	0.54	0.35	
		2. 0.72	0.70	0.54	0.33	
		3. 1.04	0.40	0.30	0.19	0.01
3	3-CH_3	1. 0.49	0.75	0.57	0.36	
		2. 0.69	0.70	0.57	0.36	
		3. 1.07	0.35	0.30	0.16	0.02
4	4-CH_3	1. 0.48	0.80	0.55	0.38	
		2. 0.69	0.75	0.57	0.36	
		3. 1.08	0.45	0.32	0.21	0.03
5	2-Cl	1. 0.55	0.75	0.55	0.36	
		2. 0.66	0.80	0.57	0.38	
		3. 0.97	0.40	0.35	0.19	0.08
6	3-Cl	1. 0.57	0.76	0.59	0.36	
		2. 0.65	0.76	0.51	0.36	
		3. 1.00	0.40	0.31	0.19	0.05
7	4-Cl	1. 0.50	0.78	0.49	0.37	
		2. 0.67	0.80	0.49	0.38	
		3. 1.04	0.45	0.27	0.21	0.01
8	2-OC_2H_5**	1. 0.48	0.60	0.41	0.28	
		2. 0.69	0.65	0.49	0.31	
		3. 1.07	0.25	0.21	0.12	0.02
9	4-OC_2H_5	1. 0.56	0.75	0.55	0.36	
		2. 0.66	0.70	0.54	0.33	
		3. 1.08	0.35	0.39	0.17	0.03
10	2-OCH_3	1. 0.50	0.70	0.60	0.33	
		2. 0.72	0.75	0.55	0.36	
		3. 1.04	0.40	0.35	0.19	0.01
11	4-OCH_3	1. 1.52	0.75	0.60	0.35	
		2. 0.71	0.82	0.67	0.67	
		3. 1.10	0.40	0.41	0.19	0.05
12	4-Br	1. 0.49	0.86	0.54	0.41	
		2. 0.66	0.80	0.54	0.38	
		3. 1.02	0.45	0.39	0.21	0.03
13	2,4-$(CH_3)_2$**	1. 0.51	0.62	0.45	0.29	
		2. 0.71	0.58	0.49	0.28	
		3. 1.05	0.20	0.28	0.09	0.00
14	3,5-$(CH_3)_2$	1. 0.48	0.68	0.50	0.32	
		2. 0.65	0.65	0.52	0.31	
		3. 1.06	0.30	0.27	0.14	0.01

*For reduction of azo group. **Slight precipitation occured.

specific reaction constant (ρ) was found to be 0.11 V, which is in good agreement with the values reported in the literature[18] for similar systems. In the case of nitro group reduction, the substituents are remote from the reduction site and hence, no systematic change in $E_{1/2}$ was observed. Polarographic *ortho*-shift (△O) was determined for methyl, methoxy, chloro and ethoxy groups and found to be positive indicating that *ortho*-derivatives are reduced at less negative potential than their *para*-analogues.

The $E_{1/2}$ values of disubstituted compounds indicated that the 2,4-disubstituted derivative does not follow the additivity principle[19], whereas the 3,5-disubstituted derivative show a reasonable additivity of 3 and 5 shifts. The smaller shift of 0.02 V in the case of *ortho*-derivatives may be attributed to the steric hindrance to coplanarity[20].

References

1. H. G. GARG and P. P. SINGH, *J. Med. Chem.*, 1968, 11, 1103.
2. T. DEVRIES and J. L. KROON, *J. Am. Chem. Soc.*, 1953, 75, 2484.
3. V. NEJEDLY, *Collect. Czech. Chem. Commun.*, 1929, 1, 319.
4. W. U. MALIK, V. K. MAHESH and R. N. GOYAL, *J. Electroanal. Chem.*, 1974, 54, 411.
5. M. FIELDS, C. VALE, JR. and M. KANE, *J. Am. Chem. Soc.*, 1949, 71, 42.
6. L. MEITES, "Polarographic Techniques", Interscience, New York, 1967.
7. M. HEYROVSKY, *J. Electroanal. Chem.*, 1972, 36, 203.
8. M. SINGH, *J. Indian Chem. Soc.*, 1983, 60, 737.
9. J. PEARSON, *Trans. Faraday Soc.*, 1948, 44, 683.
10. A. J. BARD and H. LUND, "Encyclopedia of the Electrochemistry of the Elements", Marcel Dekker, New York, 1973, Vol. XIII.
11. C. R. CASTOR and H. J. SAYLOR, *J. Am. Chem. Soc.*, 1953, 75, 1427.
12. P. J. HILSON and P. P. BIRNBAUN, *Trans. Faraday Soc.*, 1952, 48, 478.
13. B. NYGARD, *Arkiv Kemi*, 1966, 26, 167.
14. I. M. ISSA, R. M. ISSA, Y. M. TEMERK and M. R. MAKMOUD, *Electrochim. Acta*, 1973, 18, 139.
15. P. ZUMAN, "Substituent Effects in Organic Polarography", Plenum Press, New York, 1967.
16. K. ZUTSHI, G. E. RYSCHKEWITSCH and P. ZUMAN, *Inorg. Chem.*, 1983, 22, 564.
17. P. ZUMAN, *Collect. Czech. Chem. Commun.*, 1960, 25, 3225.
18. H. H. JAFFE, *Chem. Rev.*, 1953, 53, 191.
19. R. W. BROOKMAN and D. E. PEARSON, *J. Am. Chem. Soc.*, 1952, 74, 4128.
20. M. CHARTON and B. I. CHARTON, *J. Org. Chem.*, 1971, 36, 260.

J. Indian Chem. Soc.,
Vol. LXIII, March 1986, pp. 311-314

Derivatives of *cis*- and *trans*-1,3-Bis(hydroxymethyl)-2,2-dimethylcyclobutanes and the Synthesis of 6,6-Dimethyl-3-oxabicyclo[3,1,1]heptane

R. K. GAUTAM, S. KANNAN and G. S. SAHARIA*

Department of Chemistry, University of Delhi, Delhi-110 007

Manuscript received 15 December 1980, revised 8 October 1985, accepted 2 December 1985

LAH reduction of *cis*-diethyl norpinate gives *cis*-1,3-bis(hydroxymethyl)-2,2-dimethylcyclobutane, whereas Bouveault-Blanc reduction yields the *trans*-isomer. Both the isomeric diols were characterised through the formation of their bis-phenylurethanes, ditosylates, dimesylates, bis-hydrogen phthalates and bis-3,5-dinitrobenzotes. *cis*-Diol has been further used for the formation of its bis-benzoyloxy, bis-acetoxy, bis-methoxy and bis-iodo derivatives. *cis*-1,3-bis(Hydroxymethyl)-2,2-dimethylcyclobutane dimethanesulphonate has also been converted into 6,6-dimethyl-3-oxabicyclo[3, 1, 1]heptane.

THE preparation of *trans*-1,3-bis(hydroxymethyl)-2,2-dimethylcyclobutane from *cis*-diethyl norpinate by its reduction with sodium and ethanol has been reported[1] but no derivative has been mentioned. During the course of the present work, it was found that this method resulted in extremely poor yields due to the competing saponification reaction of the ester with NaOEt. By employing the following modifications the reduction of the *cis*-diethyl norpinate, however, gave the improved yield of the *trans*-diol. (i) Use of *n*-butanol in place of ethanol controls the initial vigorous reaction, ensures complete reduction but lessens the saponification effect; (ii) addition of NH_4Cl further avoids the saponification attack of the alkoxide as per the equation,

$$4NH_4Cl+4Na+RCOOR' \rightarrow 4NaCl+4NH_3+RCH_2OH+R'OH$$

and (iii) *o*-xylene used as a solvent keeps Na in a finely divided state and also provides inert medium.

Burgstahler and Sticker[2] have reported the preparation of *cis*-diol by the LAH reduction of *cis*-norpinic acid anhydride without discussing any of the derivatives except the dimesylate. During the present work, the *cis*-diol has been prepared by the LAH reduction of *cis*-diethyl norpinate and purified through column chromatography. Both the isomeric diols have been characterised through the formation of a number of their derivatives.

Dimesylate of *cis*-1,3-bis(hydroxymethyl)-2,2-dimethylcyclobutane on reaction with alkali gives 6,6-dimethyl-3-oxabicyclo[3,1,1]heptane (3a), whereas similar reaction with *trans*-isomer was not attempted due to its insufficient amount. Further support to the cyclising ability of *cis*-diol is forthcoming by the formation of isonopinone[3] and 6,6-dimethyl-3-thiabicyclo[3,1,1]heptane[3] (3b) from the dimesylate of the *cis*-diol.

The nmr spectra of the various intermediates obtained during the preparation of *trans*-norpinic acid from the ω-imide of α',α'-dicyano-β,β-dimethylglutaric acid and *cis*-norpinic acid from α-pinene have been discussed for the first time (Table 1).

Experimental

cis-*1,3-Bis(hydroxymethyl)-2,2-dimethylcyclobutane* (2a): *cis*-Diethyl norpinate (11.4 g, 0.05 mol) in dry ether (125 ml) was added dropwise to a stirred slurry of LAH (1.9 g, 0.05 mol) in anhydrous ether (200 ml). After stirring for 9 h an additional amount of LAH (1.9 g) was added and the mixture stirred for further 10 h. After cautious addition of a saturated aqueous solution of Na_2SO_4 (10 ml) and then anhydrous Na_2SO_4 (25 g), the contents were filtered and the filtrate concentrated. This was dissolved in CH_2Cl_2 and the remaining water removed by azeotropic distillation. Evaporation of the solvent followed by fractionation through column chromatography over silica gel using benzene-ethyl acetate (3 : 1) as eluent gave 2a (4.3 g, 60%) as small white plates, m.p. 61° (lit. 60°).

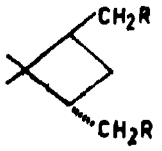
cis-*1,3-Bis(hydroxymethyl)-2,2-dimethylcyclobutane ditoluene-*p*-sulphonate* (2b) : To ice-cold solution of *cis*-diol (1.44 g, 0.01 mol) in dry pyridine (5 ml) was added with swirling at *p*-tosyl chloride (4.6 g, 0.022 mol). After chilling 0° for 10 h the mixture was allowed to stand at room temperature overnight, the contents were then poured over crushed ice and the solid obtained (m.p. 88°) on crystallisation from benzene yielded

* D/II, 42 Kidwai Nagar (East), New Delhi-110 023.

Table 1—Nmr Spectra of Compounds*

Sl. no.	Compd.	δ
1.	2, 2-Dimethylcyclobutane-1,1,3,3-tetracarboxylic acid	1.3 (6H, s, CH_3), 3.3 (2H, s, CH_2)
2.	*trans*-Norpinic acid	1.6 (3H, s, CH_3), 1.72 (3H, s, CH_3), 2.1-2.5 (4H, m, ring H)
3.	Pinic acid	1.0 (3H, s, CH_3), 1.3 (3H, s, CH_3), 1.9-2.3 (3H, m, ring CH_2 and $CHCH_2COOH$), 2.4 (2H, d, CH_2COOH), 2.8 (1H, t, $CHCOOH$), 10.4 (2H, s, COOH)
4.	Hydroxypinic acid	1.2 (3H, s, CH_3), 1.3 (3H, s, CH_3), 2-3.0 (4H, m, ring H), 4.5 (1H, d, $CHOH$)
5.	3-Carboxy-2,2-dimethylcyclobutan-aldehyde	1.1 (3H, s, CH_3), 1.4 (3H, s, CH_3), 2-3 0 (4H, m, ring H). 9.8 (1H, s, CHO), 10.6 (1H, s, COOH)
6.	*cis*-Norpinic acid	0.9 (3H, s, CH_3), 1.2 (3H, s, CH_3), 1.8-3.0 (4H, m, ring H)
7.	*cis*-Diethyl norpinate	1.1-1.4 (12H, m, CH_3), 2-3.0 (4H, m, ring H), 4.2-46 (4H, q, OCH_2),
8.	2a	1.0 (3H, s, CH_3), 1.1 (3H, s, CH_3), 2-2.6 (4H, m, ring H), 3.6 (4H, d, CH_2OH)
9.	2b	0 8 (3H, s, ring CH_3), 1.0 (3H, s, ring CH_3), 2.4 (6H, s, $ArCH_3$), 3.9 (4H, d, CH_2O), 7.2 (4H, d, ArH), 7.4 (4H, d, ArH)
10.	2c	1.1 (3H, s, ring CH_3), 1.2 (3H, s, ring CH_3), 2-2 6 (4H, m, ring H), 3.0 (6H, s, CH_3SO_2)
11.	2h	1.2 (3H, s, CH_3), 1.3 (3H, s, CH_3), 2-2.6 (4H, m, ring H) 4.4-4.5 (4H, d, CH_2O), 9.1 (6H, m, ArH)
12.	2j	1.1 (3H, s, CH_3), 1.15 (3H, s, CH_3), 4.3 (4H, d, CH_2O), 7.6-8.0 (1H, m, ArH)
13.	1a	3.5-3.8 (4H, m, CH_2OH)
14.	1e	4.3-4.6 (4H, m, CH_2O), 8-8.4 (8H, m, ArH), 11.8 (2H, s, COOH)

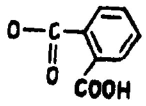
*Solvent for compounds : Pyridine (Sl. no. 1), D_2O-TFA (Sl. nos. 2,6), $CDCl_3$ (Sl. nos. 3, 5, 7, 8, 10, 11, 13, 14) and $CDCl_3$-TFA (Sl. nos. 4, 9. 12).



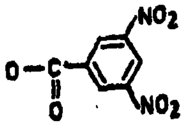
(1)

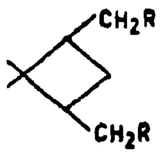
1a ; R = OH
b ; R = OTs
c ; R = OMs
d ; R = $OCONHC_6H_5$

e ; R =



f ; R =

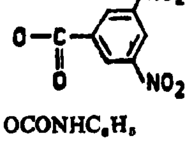




(2)

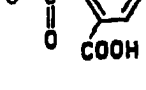
2 a ; R = OH
b ; R = OTs
c ; R = OMs
d ; R = OCH_3
e ; R = $OCOCH_3$
f ; R = $OCOC_6H_5$
g ; R = I

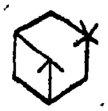
h ; R =



i ; R = $OCONHC_6H_5$

j ; R =





(3)

3 a : X = O
b ; X = S

2b (2.5 g, 60%), m.p. 92° (Found : C, 58.3 ; H, 6.3. $C_{22}H_{28}O_6S_2$ requires : C, 58.4 ; H, 6.2%).

cis-*1,3-Bis (hydroxymethyl)-2,2-dimethylcyclobutane dimethane sulphonate* (2c) : It was crystallised from ethyl acetate-petroleum ether (b.p. 60-80°) (82%) m.p. 76° (lit. 75-6°).

cis-*1,3-Bis(hydroxymethyl)-2,2-dimethylcyclobutane bis-hydrogen phthalate* (2j) : The *cis*-diol was heated at 100° with phthalic anhydride (3 g) in pyridine (5 ml) for 1 h. The contents were cooled, treated with excess of dilute sulphuric acid and the precipitated gummy mass was dissolved in chloroform and extracted with 5% aqueous sodium carbonate. The alkaline layer was acidified and extracted with chloroform. The chloroform layer was washed with water, dried (Na_2SO_4), solvent removed and the residue on crystallisation from alcohol (40%), gave 2j (45%), m.p. 162° (Found : C, 65.4 ; H, 5.5. $C_{24}H_{24}O_8$ requires: C, 65.5 ; H, 5.5%)

cis-*1,3-Bis(hydroxymethyl)-2,2-dimethylcyclobutane bis-phenylurethane* (2i) : A mixture of *cis*-diol (0.72 g) and phenyl isocyanate (1.5 g) was heated at 100° for 3 h and then stored at room temperature for 1 h. The solid so obtained on crystallisation from benzene-petroleum ether (b p. 40-60°) gave 2i (48%), m.p. 182° (Found : C, 69.0 ; H, 6.9, $C_{22}H_{26}O_4N_2$ requires : C. 69.1 ; H, 6.8%).

cis-*1,3-Bis(hydroxymethyl)-2,2-dimethylcyclobutane bis-3',5'-dinitrobenzoate* (2 h) : To an ice-cold solution of *cis*-diol (0.72 g) in dry pyridine (5 ml), 3,5-dinitrobenzoyl chloride (0.3 g) was added in small lots with shaking and the contents kept at 0° for 2 h. The solution was diluted with water, and the deposited oil was taken up in chloroform and washed with HCl (5%), water, aqueous sodium carbonate (5%) and finally with water. After drying (Na_2SO_4) and recovering chloroform, the solid on crystallisation from benzene gave 2h (45%), m.p. 172° (Found : C, 49.8 ; H, 3.7. $C_{22}H_{20}O_{12}N_4$ requires : C, 49.6 ; H, 3.8%).

cis-*1,3-Bis(methoxymethyl)-2,2-dimethylcyclobutane* (2d) : *cis*-Ditoluene *p*-sulphonate (2.26 g) was refluxed with KOH (5 g) in methanol (75 ml) for 3h ; solid potassium toluene *p*-sulphonate obtained on cooling was filtered off and methanol removed at pump. The residual product was diluted with water, extracted with ether, the ethereal solution washed with water, dried (Na_2SO_4) and solvent removed ; the residue on distillation gave 2d (38%), 90°/8 mm (Found : C, 69.7 ; H, 11.4, $C_{10}H_{20}O_2$ requires : C, 69.8 ; H, 11.6%).

6,6 - Dimethyl - 3-oxabicyclo[3.1.1]heptane (3a) : *cis*-Dimethane sulphonate (4.47 g) was refluxed with aqueous KOH (15%, 100 ml). The reaction mixture was steam distilled and the distillate extracted with ether ; the ethereal layer washed with water, dried (Na_2SO_4) and ether recovered, the residue on distillation gave 3a (75%), 60°/7 mm (Found : C. 76.1 ; H, 11.0, $C_8H_{14}O$ requires : C, 76.2 ; H, 11.1%).

cis-*1,3-Bis(acetoxymethyl)-2,2 - dimethylcyclobutane* (2e) : A mixture of *cis*-diol (0.44 g) and acetic anhydride (10 ml) was refluxed for 2 h. Then the solution was cooled, diluted with water (25 ml) and the ester extracted with chloroform. The chloroform layer was washed with aqueous sodium bicarbonate (5%), water, dried (Na_2SO_4) and solvent recovered ; the residue on distillation gave 2e (53%), 110°/1 mm (Found : C, 63.3 ; H, 8.7. $C_{12}H_{20}O_4$ requires : C, 63.2 ; H, 8.8%).

cis-*1,3-Bis(benzoyloxymethyl)-2,2 - dimethylcyclobutane* (2f) : The *cis*-diol (1.44 g) in dry pyridine (10 ml) was cooled to 0°, benzoyl chloride (3.5 g) was added in small lots with shaking and the contents kept at 0° for 2 h. The solution was diluted with water, the deposited oil taken up in chloroform and then washed with HCl (5%), water, aqueous sodium carbonate (5%) and finally with water, dried (Na_2SO_4) and solvent recovered. The oil so obtained, after fractionating through column chromatography over silica gel using benzene-petroleum ether (b.p. 60-80°) (1 : 1) as eluent and distillation gave 2f (45%), 140°/0.1 mm (Found : C, 74.8 ; H, 6.7. $C_{22}H_{24}O_4$ requires : C, 75.0 ; H, 6.8%).

cis-*1,3-Bis(iodomethyl) - 2,2 - dimethylcyclobutane* (2g) : *cis*-Ditoluene *p*-sulphonate (2.26 g) was refluxed with acetone (150 ml) containing sodium iodide (5 g) for 3 h and the sodium toluene *p*-sulphonate separated on cooling was filtered off and the filtrate diluted with water. The deposited oil was taken up in ether, the ethereal solution was washed with water, dried (Na_2SO_4) and ether recovered. The residue on distillation gave 2g (40%), 90°/1 mm (Found : C, 26.3 ; H, 4.0. $C_8H_{14}I_2$ requires : C, 26.4 ; H, 3.9%).

trans-*1,3-Bis(hydroxymethyl)-2,2 - dimethylcyclobutane* (1a) : To *cis*-diethyl norpinate (0.05 mol) and *o*-xylene (50 ml) containing ammonium chloride (0.3 mol) and n-butanol (60 ml) was added sodium (0.3 g atom) carefully. Initial vigorous reaction was controlled by external cooling and when subsided, the contents were refluxed in an oil-bath until most of sodium had reacted (6 h). The reaction mixture was cooled and methanol added slowly to destroy excess of sodium ; to hydrolyse the unreacted ester, water (90 ml) was added and refluxed for 1 h. The contents were cooled and steam-distilled to remove n-butanol and *o*-xylene ; the residue extracted with ether, dried (Na_2SO_4) and solvent removed. On distilling under reduced pressure, 1a (40%) was obtained at 120°/3 mm (lit. 125-8°/4 mm) (Found : C, 66.9 ; H, 11.2. $C_8H_{16}O_2$ requires : C, 66.7 ; H, 11.2%).

Derivatives of *trans*-diol were prepared by similar procedures as adopted for *cis*-diol.

trans-*1,3-Bis (hydroxymethyl)-2,2-dimethylcyclobutane ditoluene-p-sulphonate* (1b) : It was crystallised from benzene (50%), m.p. 83° (Found : C, 58.6 ; H, 6.1. $C_{22}H_{28}O_6S_2$ requires : C, 58.4 ; H, 6.2%).

trans-*1,3-Bis(hydroxymethyl)-2,2-dimethylcyclobutane dimethyl* p-*sulphonate* (1c): It was crystallised from ethyl acetate-petroleum ether (b.p. 60-80°) (60.0%), m. p. 69° (Found: C, 39.8; H, 6.5, $C_{10}H_{20}O_6S_2$ requires: C, 40.0: H, 6.7%).

trans-1,3-Bis(hydroxymethyl)-2,2-dimethylcyclobutane bis-phenylurethane (1d): It was crystallised from petroleum-ether (b.p. 40-60°) (50%), m.p. 176° (Found: C, 69.0; H, 6.6. $C_{22}H_{26}O_4N_2$ requires: C, 69.1; H, 6.8%).

trans-*1,3-Bis(hydroxmethyl)-2,2-dimethylcyclobutane bis-hydrogen phthalate* (1e): It was crystallised from alcohol (40%), m.p. 162° (Found: C, 65.3; H, 5.4. $C_{24}H_{24}O_8$ requires C, 65.5; H, 5.5%).

trans-*1,3-Bis(hydroxymethyl)-2,2-dimethylcyclobutane bis-3',5'-dinitrobenzoate* (1f): It was crystallised from benzene (60%), m.p. 165° (Found: C, 49.7; H, 3.6. $C_{22}H_{20}O_{12}N_4$ requires: C, 49.6; H, 3.8%).

References

1. P. C. Guha and K. Ganapathi, *Curr. Sci.*, 1936, 5, 244.
2. A. W. Burgstahler and R. E. Sticker, *Tetrahedron*, 1968, 24, 2435.
3. Carlson, G. Robert and D. Kanneth, *Tetrahedron Lett.*, 1975, 11, 947.

J. Indian Chem. Soc.,
Vol. LXIII, March 1986, pp. 315-316

New *N*-Glucosides. Syntheses of 1- and 5-Glucosyl-2,4-isodithiobiurets

S. P. DESHMUKH, B. N. BERAD and M. G. PARANJPE*

Department of Chemistry, Nagpur University, Nagpur-440 010

Manuscript received 16 December 1984, revised 6 May 1985, accepted 24 December 1985

Several 1-tetra-*O*-acetyl-β-D-glucopyranosyl-5-aryl/alkyl-2-*S*-benzyl-2,4-isodithiobiurets (4) and 1-aryl/(*H*)-5-tetra-*O*-acetyl-β-D-glucopyranosyl-2-*S*-benzyl-2,4-isodithiobiurets (7) have been prepared by the interaction of 1-tetra-*O*-acetyl-β-D-glucopyranosyl-2-*S*-benzyl isothiocarbamide with aryl/alkylisothiocyanates and 1-aryl-2-*S*-benzylisothiocarbamides with tetra-*O*-acetyl-β-D-glucopyranosyl isothiocyanate, respectively.

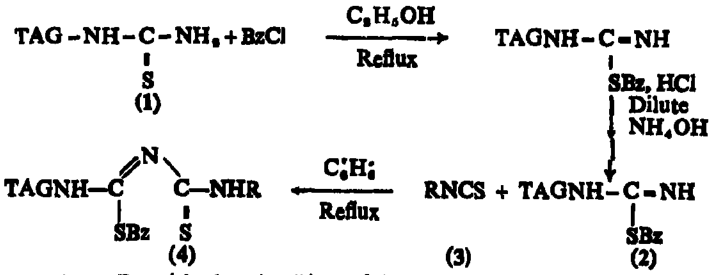
N-Glucosylated compounds are known for their physiological and pharmaceutical importance[1]. Recently, we have reported several *N*-glucosyl thiocarbamides[2] (1). Now we report the syntheses of some 1- and 5-glucosylated-2,4-isodithiobiurets.

A free base of 1-tetra-*O*-acetyl-β-D-glucopyranosyl-2-*S*-benzyl isothiocarbamide (2) (prepared by the interaction of 1 and benzyl chloride) on reaction with phenyl isothiocyanate (3a) afforded a product, m.p. 140°. It was identified as 1-tetra-*O*-acetyl-β-D-glucopyranosyl-5-phenyl-2-*S*-benzyl-2,4-isodithiobiuret (4a) on the basis of chemical characteristics and ir, nmr and mass spectral analyses as well as by polarimetry. This reaction of 2 was also extended to several other aryl/alkyl isothiocyanates (3) and corresponding products (4b-4g) were isolated.

Interaction of 1-phenyl-2-*S*-benzyl isothiocarbamide (5a) and tetra-*O*-acetyl-β-D-glucopyranosyl isothiocyanate (6) afforded a product, m.p. 121°. It was assigned the structure 1-phenyl-5-tetra-*O*-acetyl-β-D-glucopyranosyl-2-*S*-benzyl-2,4-isodithiobiuret (7a) by the usual chemical characteristics and ir, nmr and mass spectral analyses and also polarimetry. The reaction of 6 was also extended to other 1-aryl/(*H*)-2-*S*-benzyl isothiocarbamides (5) and corresponding 2,4-isodithiobiurets (7b-7e) were isolated.

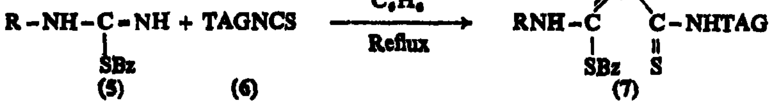
Experimental

The required aryl and alkyl isothiocyanates and 1-aryl-2-*S*-benzyl isothiocarbamides were prepared by the methods described earlier[3,4]. 1 was prepared by the interaction of ammonia and 6. The latter



where, R = (a) phenyl, (b) *o*-tolyl, (c) *m*-tolyl, (d) *p*-tolyl, (e) methyl, (f) ethyl and (g) TAG
TAG = tetra-*O*-acetyl-β-D-glucopyranosyl
Bz = benzyl

Scheme 1



where, R = (a) phenyl, (b) *o*-tolyl, (c) *p*-tolyl, (d) *p*-Cl-phenyl and (e) hydrogen

Scheme 2

was prepared by the extension of earlier known method[4] using lead thiocyanate in place of silver thiocyanate.

Preparation of **6** : A solution of tetra-*O*-acetyl-α-D-glucopyranosyl bromide (5 g) in sodium-dried xylene (30 ml) was treated with lead thiocyanate (4 g) The mixture was refluxed gently for 3 h. The solution was then allowed to cool and filtered from the lead salt and treated with petroleum ether (b.p. 60-80°) (70 ml) with stirring. Tetra-*O*-acetyl-β-D-glucopyranosyl isothiocyanate was precipitated out as a white solid (3 5 g). The crude isothiocyanate was crystallised from ethanol-water, m p. 112-114° (lit[4]. 111-113°) (Found: C, 45.87; H, 4.32; N, 3.82; S, 8.44. $C_{15}H_{19}O_9NS$ calcd. for: C, 46.28; H, 4.88; N, 3.59; S, 8.22%).

Preparation of **2**: A mixture of **1** (0.02 *M*, 8.1 g), benzyl chloride (0.02 *M*, 2.5 g) and ethanol (20 ml) were heated under gentle reflux for 90 min. The resulting acidic solution when rendered basic with dilute ammonium hydroxide yielded a granular solid **2** (8 g), crystallised from ethanol, m.p. 136° (Found: N, 5.61. $C_{32}H_{28}C_6N_2S$ calcd. fort N, 5.64%); gave a picrate, m.p. 104°.

Preparation of **4**: **3a** (0.01 *M*, 1.3 g) was added to a benzene solution of **2** (0.01 *M*, 4.9 g in 30 ml) and the mixture was refluxed over a boiling water-bath for 3 h. Then benzene was removed by distillation and the resulting syrup was triturated several times with petroleum ether followed by ethanol to afford a solid **4a** (5 g) crystallised from ethanol, m.p. 140° (Found: C, 54.82; H, 5.31; N, 6.65; S, 10.92. $C_{40}H_{33}O_9N_3S_2$ calcd. for: C, 55.15; H, 5.22; N, 6.65; S, 10.14%); tlc (silica gel, EtOH-EtOAc (1 : 1) solvent) single spot (R_f 0.75); $[\alpha]_D^{31}$ −9.10 (c 2.248 in $CHCl_3$); ν_{max} 3 340 (NH), 1 740 (C=O), 1 580 (C=N), 1 230 (S−Bz), 1 040 (C=S) and 900 cm^{-1} (β-D-glucopyranose ring[6-9]). Its nmr spectra displayed signals due to ∂ 8.4 (NH), 7.35-7.45 (ArH)[9], 2.02 (equatorial acetoxy protons[10] indicating presence of β-anomer) and 4.95-5.32 ppm (lit.[11] 4.75-5.38; β-anomer); mass spectra did not show molecular ion peak.

The other compounds prepared were, **4b**, 147°; **4c**, 143°; **4d**, 150°; **4e**, 79°d; **4f**, 62°d; **4 g**, 100°d.

Preparation of **7** : **6** (0.02 *M*, 7.7 g) was added to a benzene solution of **5a** (0 02 *M*, 4.8 g in 60 ml) and the mixture refluxed over a boiling water-bath for 6 h. The solvent was then distilled off. The resultant syrupy mass was then triturated several times with petroleum ether followed by ethanol to yield a white solid **7a** (7 g) crystallised from ethanol, m.p. 121° (Found: C, 54.79; H, 5.22; N, 6.68; S, 9.89. $C_{40}H_{33}O_9N_3S_2$ calcd. for: C, 55 15; H, 5.22; N, 6.65; S, 10.14%); tlc (EtOH-EtOAc solvent) single spot (Rf 0.72); $[\alpha]_D^{31}$ + 11.13° (c 2.3276 in $CHCl_3$); ν_{max} 3 420 (NH), 1 740 (C=O), 1 575 (C=N) and 900 cm^{-1} (β-anomer); ∂ 8.3 (NH), 7.15-7.35 (ArH), 2.12 (equatorial acetoxy protons) and 5.05-5.35 (β-anomer); mass spectrum did not show molecular ion peak.

The other compounds prepared were, **7b**, 116°; **7c**, 131°; **7d**, 123°; and **7e**, 136°.

Acknowledgement

Two of the authors (S.P.D. and B.N.B.) are grateful to U.G C. and C.S.I.R., New Delhi, respectively for the award of Junior Research Fellowship. The authors thank Prof. K. N. Munshi, for facilities.

References

1. I. Goodman, "Advances in Carbohydrate Chemistry", ed. M. L. Wolform, Academic Press, New York, 1958, Vol. 13, p. 233.
2. S. P. Deshmukh and M. G. Paranjpe, *J. Indian Chem. Soc.*, 1985, **62**, 375.
3. A. I. Vogel, "A text book of Practical Organic Chemistry", 4th ed., Longmans Green, E.L.B.S., London, 1978, p. 736.
4. E. A. Werner, *J. Chem. Soc.*, 1890, 295.
5. K. M. Harring and T. B. Johnson, *J. Am. Chem. Soc.*, 1933, **55**, 395.
6. R. M. Silverstein and G. C. Bassler, "Spectrometric Identification of Organic Compounds", John Wiley, New York, 1963.
7. N. B. Colthup, L. H. Daly and S. E. Wiberley, "Introduction to Infrared and Raman Spectroscopy", Academic Press, New York, 1963.
8. S. A. Barker, E. J. Bourne, R. Stephens and D. H. Whiffen, *J. Chem. Soc.*, 1954, 3468.
9. J. R. Dyer, "Applications of Absorption Spectroscopy of Organic Compounds", Prentice-Hall, London, 1974.
10. S. A. Barker, J. Homer, M.C. Keith and L.F. Thomas, *J. Chem. Soc.*, 1963, 1538.
11. C. A. Glass, *Can. J. Chem.*, 1965, **43**, 2652.

J. Indian Chem. Soc.,
Vol. LXIII, March 1986, pp. 317-319

Synthesis of some New Substituted Thiosemicarbazides and Triazoles as Possible Anticonvulsants

M. I. HUSAIN* and MOHD. AMIR

Chemistry Department, Lucknow University, Lucknow-226 007

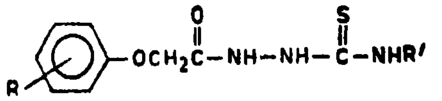
Manuscript received 20 May 1982, revised 7 July 1983, accepted 26 November 1985

Fourteen 1-*o*/*p*-anisoxyacetyl-4-arylthiosemicarbazides and their corresponding 5-(*o*/*p*-anisoxymethyl)-4-aryl-3-mercapto-1,2,4(*H*)-triazoles were synthesised. Eight of these compounds, when screened against maximal electroshock and pentylenetetrazole-induced seizures in mice at a dose of 80 mg/kg were, however, found to be inactive.

VARIOUS hydrazine derivatives[1] and semicarbazides[2] have been known to inhibit monoamine oxidase activity[3]. Monoamine oxidase inhibitors have also been reported to exhibit marked anticonvulsant activity[4]. Several mercaptotriazole[5-8] derivatives have displayed significant anticonvulsant activity. Moreover, the presence of a methoxy group in a compound imparts anticonvulsant activity. Encouraged with these observations, it is considered worthy to synthesise the title compounds.

An *o*/*p*-methoxyphenol was allowed to react with ethyl chloroacetate in presence of acetone and anhydrous K_2CO_3 to give ethyl *o*/*p*-anisoxyacetate which was condensed with hydrazine hydrate in absolute ethanol to yield *o*/*p*-anisoxyacetic acid hydrazides. The latter, on being refluxed with various aryl isothiocyanates gave thiosemicarbazides which on cyclisation under alkaline conditions afforded the desired mercaptotriazoles.

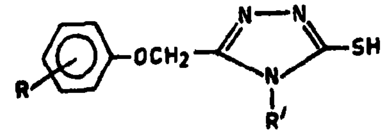
TABLE 1—1-*o*/*p*-ANISOXYACETYL-4-ARYLTHIOSEMICARBAZIDE (3)



Sl. no.	R	R′	M. p. °C	Molecular formula	N% : Found/(Calcd.)
1.*	*p*-Methoxy	Phenyl	160	$C_{16}H_{17}N_3O_3S$	12.32 (12.69)
2.	*p*-Methoxy	4-Tolyl	159	$C_{17}H_{19}N_3O_3S$	11.78 (12.17)
3.	*p*-Methoxy	4-Chlorophenyl	161	$C_{16}H_{16}N_3O_3SCl$	11.12 (11.49)
4.	*p*-Methoxy	3-Chlorophenyl	155	$C_{16}H_{16}N_3O_3SCl$	10.98 (11.49)
5.	*p*-Methoxy	4-Ethoxyphenyl	162	$C_{18}H_{21}N_3O_4S$	11.48 (11.20)
6.*	*p*-Methoxy	4-Anisyl	164	$C_{17}H_{19}N_3O_4S$	11.28 (11.63)
7.	*p*-Methoxy	α-Naphthyl	156	$C_{20}H_{19}N_3O_3S$	11.46 (11.02)
8.	*o*-Methoxy	Phenyl	150	$C_{16}H_{17}N_3O_3S$	12.23 (12.69)
9.*	*o*-Methoxy	4-Tolyl	159	$C_{17}H_{19}N_3O_3S$	12.54 (12.17)
10.	*o*-Methoxy	4-Chlorophenyl	163-65	$C_{16}H_{16}N_3O_3SCl$	11.16 (11.49)
11.	*o*-Methoxy	3-Chlorophenyl	162	$C_{16}H_{16}N_3O_3SCl$	11.82 (11.49)
12.*†	*o*-Methoxy	4-Ethoxyphenyl	163	$C_{18}H_{21}N_3O_4S$	11.62 (11.20)
13.	*o*-Methoxy	4-Anisyl	157	$C_{17}H_{19}N_3O_4S$	11.18 (11.63)
14.	*o*-Methoxy	α-Naphthyl	164	$C_{20}H_{18}N_3O_3S$	11.38 (11.02)

*ν_{max} 1 085-1 140 (C=S), 1 600 (Ar), 1 685-1 710 (C=O of sec. amide), 2 900 (CH) and 3 200-3 300 cm^{-1} (NH).
†τ($CDCl_3$) 1.3 (3H, t, CH_3 of OEt), 3.78 (3H, s, OCH_3), 3.95 (2H, q, CH_2 of OEt), 4.55 (2H, s, OCH_2CO), 6.85-7.3 (8H, m, ArH), 7.4 (1H, s, CS-*NH*Ar) and 8.7 (2H, brs, CON*H*N*H*CS).

TABLE 2—5-(o/p-ANISOXYMETHYL)-4-ARYL-3-MERCAPTO-1,2,4 (H)-TRIAZOLE (4)



Sl. no.	R	R'	M. p. °C	Molecular formula	N% : Found/(Calcd.)
1.*	*p*-Methoxy	Phenyl	168	$C_{16}H_{15}N_3O_2S$	13.13 (13.42)
2.	*p*-Methoxy	4-Tolyl	180	$C_{17}H_{17}N_3O_2S$	12.43 (12.84)
3.	*p*-Methoxy	4-Chlorophenyl	183	$C_{16}H_{14}N_3O_2SCl$	12.46 (12.08)
4.	*p*-Methoxy	3-Chlorophenyl	190	$C_{16}H_{14}N_3O_2SCl$	11.74 (12.08)
5.	*p*-Methoxy	4-Ethoxyphenyl	182	$C_{18}H_{19}N_3O_3S$	12.18 (11.76)
6.*	*p*-Methoxy	4-Anisyl	173	$C_{17}H_{17}N_3O_3S$	11.87 (12.24)
7.	*p*-Methoxy	α-Naphthyl	172	$C_{20}H_{17}N_3O_2S$	11.12 (11.57)
8.	*p*-Methoxy	Phenyl	173-175	$C_{16}H_{15}N_3O_2S$	13.15 (13.42)
9.*†	*o*-Methoxy	4-Tolyl	179	$C_{17}H_{17}N_3O_2S$	12.32 (12.84)
10.	*o*-Methoxy	4-Chlorophenyl	185	$C_{16}H_{14}N_3O_2SCl$	12.52 (12.08)
11.	*o*-Methoxy	3-Chlorophenyl	172	$C_{16}H_{14}N_3O_2SCl$	11.75 (12.08)
12.*	*o*-Methoxy	4-Ethoxyphenyl	168	$C_{18}H_{19}N_3O_3S$	12.23 (11.76)
13.	*o*-Methoxy	4-Anisyl	181	$C_{17}H_{17}N_3O_3S$	11.83 (12.24)
14.	*o*-Methoxy	α-Naphthyl	180	$C_{20}H_{17}N_3O_2S$	11.18 (11.57)

*ν_{max} 1 130 and 1 340 (C=S of amide), 1 600 (Ar), 2 900 (CH) and 3 200-3 300 cm^{-1}. †τ($CDCl_3$) 6.65 (3H, s, CH_3), 3.65 (3H, s, OCH_3), 4.75 (2H, s, $NCCH_2$), 6.7-7.25 (8H, m, ArH) and 6.33 (1H, brs, SH).

Experimental

All melting points were determined in open capillaries and are uncorrected. The purity of the compounds was checked by tlc on silica gel.

Ethyl ortho/para-*anisoxyacetates* (1) : To a solution of *o*/*p*-methoxyphenol (0.08 *M*) in anhydrous acetone (25 ml) was added ethyl chloroacetate (0.08 *M*) and anhydrous K_2CO_3 (0.08 *M*). The reaction mixture was refluxed on a steam-bath for 15 h and then cooled, filtered and the filtrate concentrated under reduced pressure. The residue thus obtained was utilised in the next step without further purification.

Ortho/para-*anisoxyacetic acid hydrazides* (2): A mixture of 1 (0.06 *M*) and hydrazine hydrate (0.09 *M*) in absolute ethanol (25 ml) was refluxed on a steam-bath for 12 h. Excess ethanol was distilled off and the solid mass thus obtained was filtered, dried and recrystallised from benzene. The hydrazides thus prepared are (i) *o*-anisoxyacetic acid hydrazide (65%), m.p. 80° (Found : N, 13.98. $C_9H_{12}N_2O_3$ calcd. for : N, 14.28%) and (ii) *p*-anisoxyacetic acid hydrazide (60%), m.p. 78° (Found : N, 13.86. $C_9H_{12}N_2O_3$ calcd. for ; N, 14.28%).

1-ortho/para-*Anisoxyacetyl-4-arylthiosemicarbazides* (3) : A mixture of 2 (0.004 *M*) and an aryl isothiocyanate (0.004 *M*) in anhydrous benzene (25 ml) was refluxed on a steam-bath for 3-5 h. Excess benzene was distilled off and the solid product thus obtained was filtered, dried and recrystallised from ethanol. The thiosemicarbazides (Table 1) so obtained were characterised by their sharp m.p.'s, elemental analysis and ir spectra.

5-(ortho/para-*Anisoxymethyl*)*-4-aryl-3-mercapto-1,2,4* (H)*-triazoles* (4) : A solution of 1-anisoxyacetyl-4-arylthiosemicarbazide (3) in 2*N* NaOH (30 ml) was refluxed for 2-3 h and then filtered and the filtrate acidified with dilute HCl. The precipitate formed was collected by filtration, washed with water and recrystallised from ethanol. The compounds thus prepared were characterised by their sharp m.p.'s, analysis and ir spectra (Table 2). The peak around 1 700 cm^{-1} (C=O of sec. amide) observed in the corresponding thiosemicarbazides was absent in hese compounds.

Acknowledgement

The authors express their sincere thanks to Prof. V. S. Misra, Head, Chemistry Department, Lucknow University, for facilities and Dr. Nityanand, Director, C.D.R.I., Lucknow and Prof. B. N. Dhawan, Division of Pharmacology, C.D.R.I., for anticonvulsant screening.

References

1. J. H. BEIL, A. HORITA and A. E. DRUKKER in "Pharmacology Agents", ed. M. GORDON, Academic Press, New York, 1964, Vol. 1, p. 359.
2. L. A. CATES, *J. Med. Chem.*, 1967, 10, 925.
3. S. P. SINGH, A. CHAUDHARI, V. I. STENBERG and S S. PARMAR, *J. Pharm. Sci.*, 1979, 65, 1978.
4. D. J. PROCKOP, P. A. SHORE and B. B. BRODIE, *Ann. N. Y. Acad. Sci.*, 1959, 80, 643.
5. A. A. B. HAZZA, N. S. HABIB, S. M. E. L. KHAWASS, Y. T. DABEES, F. M. SHARABI and G. G. TAWIL, *Sci. Pharm.*, 1978, 46, 298.
6. C. ANISWORTH, N. R. BARTON and W. R. CRIMSON, *J. Med. Chem.*, 1962, 5, 383.
7. S. S. PARMAR, M. CHAUDHRY, S. K. CHAUDHRY and S. KUMAR, *J. Pharm. Sci.*, 1977, 66, 77.
8. S. S. PARMAR, A. K. GUPTA, H. H. SINGH and T. K. GUPTA, *J. Med. Chem.*, 1972, 15, 999.

J. Indian Chem. Soc.,
Vol. LXIII, March 1986, pp. 320-322

Studies on Thiazolidinones as Potential Antitubercular Compounds

M. P. DAVE, J. M. PATEL, N. A. LANGALIA and K. A. THAKER*

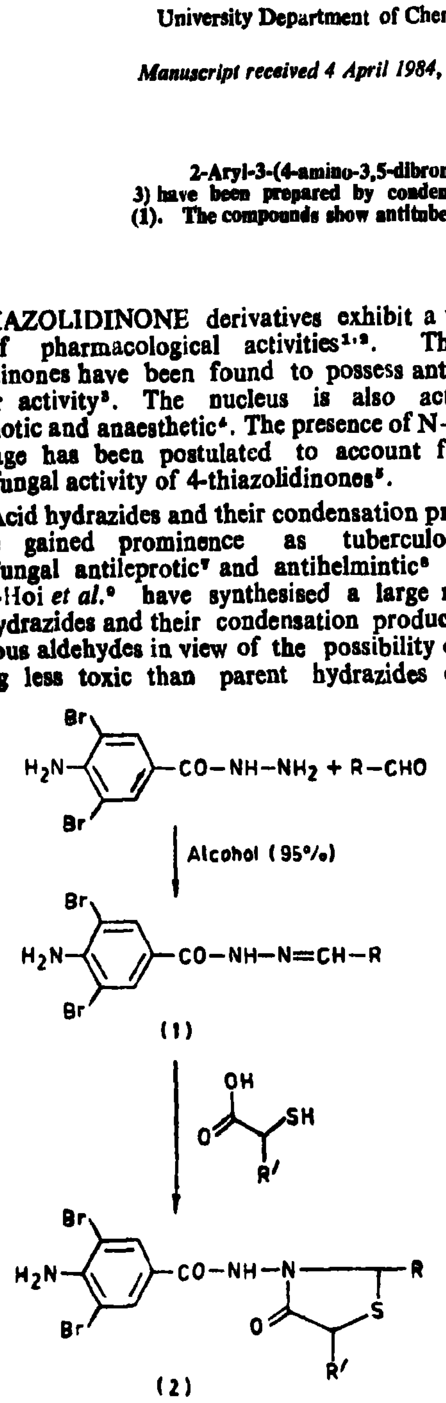
University Department of Chemistry, Bhavnagar University, Bhavnagar-364 002

Manuscript received 4 April 1984, revised 30 September 1985, accepted 2 December 1985

2-Aryl-3-(4-amino-3,5-dibromobenzamido)-5-substituted-4-thiazolidinones (2 and 3) have been prepared by condensation of mercaptoalkanoic acids with azomethines (1). The compounds show antitubercular activity, when tested against $H_{37}R_v$ strain.

THIAZOLIDINONE derivatives exhibit a variety of pharmacological activities[1,2]. Thiazolidinones have been found to possess antitubercular activity[3]. The nucleus is also active as hypnotic and anaesthetic[4]. The presence of N—C—S linkage has been postulated to account for the antifungal activity of 4-thiazolidinones[5].

Acid hydrazides and their condensation products have gained prominence as tuberculostatic[6], antifungal antileprotic[7] and antihelmintic[8] agents. Buu-Hoi *et al.*[9] have synthesised a large number of hydrazides and their condensation products with various aldehydes in view of the possibility of their being less toxic than parent hydrazides due to



where, R = different aromatic moiety and R' = CH_2COOH or H.

Scheme 1

blocking of free NH_2 group. A literature review has revealed that condensation of aromatic aldehyde with acid hydrazide of 4-amino-3,5-dibromobenzoic acid has not been studied so far.

The present communication deals with the synthesis and pharmacological studies of some 4-thiazolidinones[10] of the type 2 and 3, the Schiff[11] bases of 4-amino-3,5-dibromobenzoic acid hydrazide have been prepared with different aromatic aldehydes and condensed with thioglycolic acid and thiomallic acid. When tested, these compounds (2 and 3) show antitubercular activity against $H_{37}R_v$ strain in Lowenstein-Jensen's egg medium (4 ml). Infrared spectra of the title compounds have been taken on a Spectromom 2000 spectrophotometer. The strong bands at 1 750 and 1 760 cm^{-1} were characteristic carbonyl stretching frequency for thiazolidinone ring system. All the reaction sequences have been reported in Scheme 1

Experimental

Melting points of the compounds were determined in open capillary tubes and are uncorrected. The structure of the compounds have been established on the bases of their elemental analysis and infrared spectrum.

4-Amino-3,5-dibromo benzoic acid hydrazide : It was prepared by known method[12].

1-(4-Amino-3,5-dibromobenzoyl)-2-benzylidene hydrazine : To the solution of aldehyde (benzaldehyde) (0.01 *M*) in ethanol (50 ml ; 95%) was added 4-amino-3,5-dibromo benzoic acid hydrazide (0.01 *M*) in ethanol (50 ml ; 95%) ; the contents heated to reflux for 2 h, cooled and worked out to get the corresponding Schiff's base.

2-Phenyl-3-(4-amino-3,5-dibromo benzamido)-4-thiazolidinone : 1-(4-Amino-3,5-dibromobenzoyl)-2-benzylidene hydrazine (0.01 *M*), benzene (100 ml) and thioglycolic acid (0.012 *M*) were refluxed (25 h) using Dean and Stark separator. The solvent was

then removed, residue treated with $NaHCO_3$ solution and filtered when thiazolidinone crystallised from ethanol.

2-(2-Chloro phenyl)-3-(4-amino-3,5-dibromobenzamido)-5-carboxymethyl-4-thiazolidinone : 1-(4-Amino-3,5-dibromobenzoyl)-2-(2-chloro)benzylidene hydrazine (0.01 *M*) and thiomallic acid (0.01 *M*) were condensed in presence of anhydrous zinc chloride (0.5 g) at 160° for 2 h on oil-bath and the temperature raised to 180° for 30 min. The product so obtained was dissolved in sodium bicarbonate solution (4 *N*) and filtered ; the filtrate reprecipitated with dilute hydrochloric acid and crystallised from ethanol (95%).

TABLE 1—DATA OF COMPOUNDS 1

Sl. no.	R	M.p. °C	Yield %	N% : Found/ (Calcd.)
1.	C_6H_5	245	60	10.70 (10.58)
2.	$2\text{-}Cl\text{-}C_6H_4$	285	62	9.93 (9.73)
3.	$3\text{-}Cl\text{-}C_6H_4$	220	66	9.84 (9.73)
4.	$3\text{-}NO_2\text{-}C_6H_4$	260	58	12.79 (12.67)
5.	$4\text{-}NO_2\text{-}C_6H_4$	320	55	12.78 (12.67)
6.	$2\text{-}OCH_3\text{-}C_6H_4$	240	67	9.94 (9.81)
7.	$2\text{-}OH\text{-}C_6H_4$	280	64	10.30 (10.17)
8.	$4\text{-}OH\text{-}C_6H_4$	284	57	10.05 (10.17)
9.	$3,4\text{-}CH_2O_2\text{-}C_6H_3$	270	53	9.40 (9.52)
10.	$3\text{-}OCH_3\text{-}4\text{-}OH\text{-}C_6H_3$	244	65	9.61 (9.48)
11.	$3,4\text{-}di\text{-}OCH_3.C_6H_3$	248	59	9.31 (9.19)
12.	$3,5\text{-}di\text{-}Br\text{-}2\text{-}OH\text{-}C_6H_2$	169	67	7.48 (7.36)

The physical data of 1 and 2 are presented in Tables 1 and 2.

Biological screening : The *in vitro* antimycobacterial activity of the compounds were studied at 0, 5 and 30 $\mu g\ ml^{-1}$ (solvent : DMF) against $H_{37}R_v$ strain of *Mycobacterium tuberculosis* using Lowenstein-Jensen egg medium. The retardation of growth rate was studied upto 6 weeks at 37°. The procedure was duplicated using only solvent for control purpose.

From the experimental data it has been concluded that the thiazolidinones (2) are tuberculostatic at 30 $\mu g\ ml^{-1}$. Further, substitution in benzene ring or presence of carboxymethyl group at position-5 of the thiazolidine ring have no significant effect on tuberculostatic activity. In contrast to thiazolidinones (2), the corresponding hydrazones (1) do not inhibit the growth of *Mycobacterium tuberculosis* ($H_{37}R_v$ strain) reflecting the key role of thiazolidinone structure for tuberculostatic activity.

Results and Discussion

The *in vitro* antimycobacterial screening results show that all the compounds are inactive at 0 and 5 $\mu g\ ml^{-1}$ and active at 30 $\mu g\ ml^{-1}$. Therefore, only conclusion that can be drawn from these results is that the compounds 2 and 3 are active at higher concentration rather than at lower concentration.

TABLE 2—DATA OF COMPOUNDS 2 and 3

Sl. no.	R	R′	M.p. °C	Yield %	Analysis % : Found/(Calcd.) N	S
1.	$-C_6H_5$	H	161	71	9.04 (8.92)	6.90 (6.79)
2.	$3\text{-}NO_2\text{-}C_6H_4$	H	270	68	10.96 (10.85)	6.31 (6.20)
3.	$4\text{-}NO_2\text{-}C_6H_4$	H	203	64	10.96 (10.85)	6.35 (6.20)
4.	$2\text{-}OCH_3\text{-}C_6H_4$	H	221	75	8.47 (8.37)	6.25 (6.37)
5.	$2\text{-}OH\text{-}C_6H_4$	H	228	77	8.77 (8.62)	6.71 (6.57)
6.	$3,4\text{-}di\text{-}OCH_3\text{-}C_6H_3$	H	224	72	8.05 (7.91)	6.14 (6.03)
7.	$2\text{-}Cl\text{-}C_6H_4$	CH_2COOH	176	52	7.56 (7.45)	5.54 (5.67)
8.	$3\text{-}Cl\text{-}C_6H_4$	CH_2COOH	147	74	7.60 (7.45)	5.78 (5.67)
9.	$3,5\text{-}di\text{-}Br\text{-}2\text{-}OH\text{-}C_6H_2$	CH_2COOH	135	70	5.84 (5.97)	4.65 (4.95)
10.	$4\text{-}OH\text{-}C_6H_4$	CH_2COOH	216	69	7.85 (7.71)	6.03 (5.87)
11.	$3,4\text{-}CH_2O_2.C_6H_3$	CH_2COOH	225	65	7.62 (7.49)	5.57 (5.70)
12.	$3\text{-}OCH_3\text{-}4\text{-}OH.C_6H_3$	CH_2COOH	270	72	7.19 (7.30)	5.67 (5.56)

Acknowledgement

Authors are thankful to Bhavnagar University, for research scholarships to two of them (M.P.D. and J.M.P.). Authors are also grateful to Dr. S. B. Trivedi, Director, Tuberculosis Research Centre, Amargadh, for screening the samples.

References

1. A. R. SURREY and R. A. CULTER, *J. Am. Chem. Soc.*, 1958, 80, 578.
2. J. DORAN and H. A. SONAL, *J. Org. Chem.*, 1938, 3, 193.
3. N. M. TURKEVICH, L. Y. LADNAYA, I. V. PLESHNEV and O. L. GROM, *Khim. Issled. Farm.*, 1970, 64 (*Chem. Abstr.*, 1972, 76, 34154).
4. H. D. TROUTMANN and L. M. LONG, *J. Am. Chem. Soc.*, 1948, 70, 3436.
5. J. KINUGAWA and K. NAGASE, Jap. Pat., 8 542/1965 (*Chem. Abstr.*, 1965, 63, 5653).
6. NG. PH. BUU-HOI, NG. D. XUONG, NG. H. NAM and F. BINON, *C. R. Hebd. Seances Acad. Sci.*, 1952, 235, 329.
7. T. S. GARDNER, R. WENIS and LEC, *J. Org. Chem.*, 1961, 26, 1516.
8. Brit. Pat., 1 085 474/1947.
9. NG. PH. BUU-HOI, NG. D. XUONG, NG. H. NAM, F. BINON and R. ROYER, *J. Chem. Soc.*, 1953, 1358.
10. A. R. SURREY, *J. Am. Chem. Soc.*, 1947, 69, 2911.
11. A. A. CHILINGARYAN, *Chem. Abstr.*, 1963, 58, 6723.
12. M. CLAESEN, P. VAN DIJCK and H. VANDERHAEGHE, *J. Pharm. Pharmacol.*, 1954, 6, 127.

J. Indian Chem. Soc.,
Vol. LXIII, March 1986, pp. 323-325

Synthesis and Physiological Activity of 2*H*-[1]-Benzothiopyrano[3,4-*e*][1,3] oxazine-5-ones

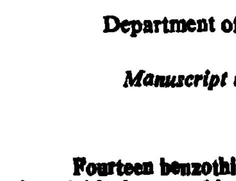
B. SUCHARITA REDDY and MALLESHWAR DARBARWAR*

Department of Chemistry, Osmania University, Hyderabad-500 007

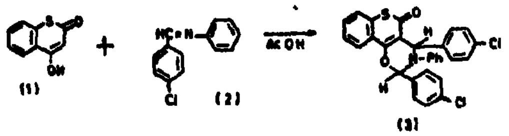
Manuscript received 5 August 1985, accepted 24 December 1985

Fourteen benzothiopyranooxazine-5-ones have been synthesised by the condensation of 4-hydroxy-1 thiocoumarin and 6-chloro-4-hydroxy-1-thiocoumarin with different Schiff bases (derived from aromatic aldehydes and aniline) in acetic acid medium. The possible reaction mechanism has been advanced. Analytical, spectral and physiological properties of the compounds have been evaluated.

1-Thiocoumarins are known to exhibit varied physiological properties, namely anticoagulant, anti-allergic, bactericidal and insecticidal activities. Oxazines are reported to act as antibiotic, amoebicidal, anaesthetic and antitubercular agents[1]. During search for compounds of better activity it was considered worthwhile to synthesise thiocoumarins with fused oxazine ring and evaluate their physiological properties. It was with this view that the following work has been undertaken. The present communication, therefore, deals with synthesis of a new heterocyclic system, *viz.* 2*H*-benzothiopyrano[3,4-*e*][1,3]oxazine-5-one.



As a representative case, 4-hydroxy-1-thiocoumarin (1)[1,2] was treated with two moles of Schiff base (2) (obtained from *p*-cholorobenzaldehyde and aniline) in acetic acid at room temperature. The contents were shaken well and a clear dark brown solution was obtained with the evolution of heat. This solution on stirring for ten minutes yielded an yellow compound 3 (m p. 256°; single spot on tlc, benzene-ethyl acetate, 1 : 1). The compound was not soluble in sodium bicarbonate solution indicating that hydroxyl group at 4-position in 1-thiocoumarin was not free and involved in the reaction. Elemental analysis indicated presence of nitrogen and sulphur (Scheme 1).

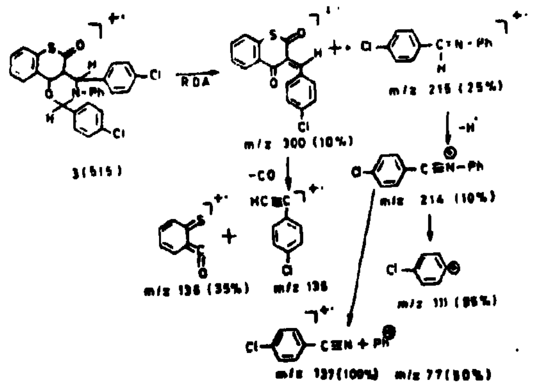


Scheme 1

Ir spectra of the compound showed absorptions at 1 640 (CO of thiocoumarin) and 1 230 cm^{-1} (C—O—C). The absorptions due to OH group of 4-hydroxy-1-thiocoumarin and that due to NH (Schiff base) were absent. In uv spectra, absorption maxima at 232 (log ϵ 4.80, Ph—S chromophore) and 316 nm (log ϵ 4.2 ; cinnamoyl chromophore) were present. Pmr spectra in TFA and $CDCl_3$ indicated signals at δ 6.2 (1H, s, NCH (Ph) O) and 8.1 (1H, s, CCH(Ph)N and a multiplet at δ 6.8-8.0 (17H, Ar). In addition, another pmr spectra of the compound (in TFA and $CDCl_3$) obtained by the reaction of 4-hydroxythiocoumarin with Schiff base (obtained from *p*-tolualdehyde and aniline) was also recorded to have an internal standard. In this spectrum, a new signal at δ 1.8 (6H, s, CH_3) was observed in addition to all signals mentioned above.

On the basis of above chemical and spectral data the structure of the compound has been assigned as 2*H*-benzothiopyrano[3,4-*e*] [1,3]oxazine-5-one (3). The compound showed characteristic fragmentation pattern in the mass spectra. The peak (M^+) was not observed in the spectrs indicating that the molecule was highly unstable under the conditions. However, the M^+ split by RDA process and as a result two fragments appeared at m/z 300 (10%) and 215 (25%). The latter ion correspond to a molecule of Schiff base. The second RDA process was followed after the ion m/z 300 lost CO to give rise to two ions at m/z 136. The ion m/z 215 lost a proton to form m/z 214 which on subsequent cleavage may give rise m/z 137 and 77 or may fragment to form m/z 111. The ion m/z 137 constituted the base peak in the mass spectrum. The possible structures of these ions and mass spectral fragmentation pattern is shown in Scheme 2.

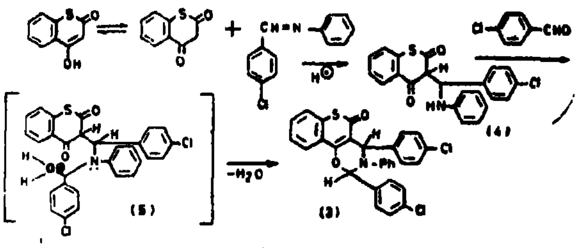
Mechanism : 4-Hydroxy-1-thiocoumarin is acidic and reacts with one molecule of protonated Schiff base to form 4. The Schiff base are known



Scheme 2

ot act as proton acceptors and also act as potential source of aldehyde in heterocyclisation reactions. Hanmanthu and Ratnam[3] reported the formation of 1,3-naphthoxazines by the reaction of Schiff bases with α-napthol and β-napthol. 4-Hydroxy-coumarin reacts similarly with Schiff bases forming coumarinooxazines[4]. The intermediate 4 further reacts with aldehyde to form 5 which cyclises by loss of a molecule of water to 3 (Scheme 3).

Adopting the above procedure thirteen benzothiopyranooxazines have been prepared by condensation of each simple and 6-chloro-4-hydroxy-1-thiocoumarins with Schiff bases obtained from aniline and different aldehydes, namely benzaldehyde, *p*-chlorobenzaldehyde, *p*-methylbenzaldehyde 2,4-dicholorobenzaldehyde, *p*-anisaldehyde, furfural and pyridine-3-aldehyde. Their m.p.'s, analytical and spectral data are presented in Table 1.



Scheme 3

Physiological activity : All the compounds have been screened for antibacterial (tube-dilution method) activity against two bacteria, namely *Bacillus subtilis* (gram+ve) and *Escherichia coli* (gram −ve) and antifungal activity (plate method) against two fungi, namely *Aspergillus niger* and *Alternaria alternata*. Among the compounds tested most active were 9-chloro-3-*N*-phenyl-2,4-di(*p*-chlorophenyl)benzothiopyranooxazine-5-one, 9-chloro- -*N*-phenyl-2,4-di-(2′,5′-dichlorophenyl) benzothiopyranooxazine-5-one, 3-*N*-phenyl-2,4-di(2′,4′ dichlorophenyl)benzothiopyranooxazine-5-one and 3-*N*-phenyl-2,4 di(*p*-chlorophenyl)benzothiopyranooxazine 5-one against both *B. subtilis* and *E. coli* at 10 ppm.

9-Chloro-2,4-di(2′,4′-dichlorophenyl)-3-*N*-phenyl benzothiopyranooxazine-5-one and 2,4-di(2′,4′-d -

TABLE 1—ANALYTICAL AND SPECTRAL DATA OF 2*H*-BENZOTHIOPYRANO[3,4-*b*] [1,3-*e*]OXAZINE-5-ONES (3)*

Sl. no.	R	Ar	M.p. °C	Yield %	Mol. formula	Analysis % : Found/(Calcd.) C	H	N	λ_{max} (log ε) nm	ν_{max} cm^{-1}
1.	–	C_6H_5	218	67	$C_{29}H_{21}O_2NS$	77.80 (77.85)	4.63 (4.7)	3.10 (3.13)	233 (4.8) 318 (4.1)	1 635 1 230
2.	–	*p*-Cl-C_6H_4	256	62	$C_{29}H_{19}O_2NSCl_2$	67.57 (67.59)	3.62 (3.69)	2.66 (2.71)	238 (4.4) 324 (3.8)	1 640 1 230
3.	–	*p*-H_3C-C_6H_4	168	68	$C_{31}H_{25}O_2NS$	78.26 (78.31)	5.20 (5.26)	2.90 (2.94)	235 (4.5) 329 (4.7)	1 640 1 232
4.	–	2,4-Cl_2-C_6H_3	165	62	$C_{29}H_{17}O_2NSCl_4$	59.62 (59.69)	2.85 (2.91)	2.36 (2 40)	237 (4.4) 321 (4.5)	1 640 1 230
5.	–	*p*-OCH_3-C_6H_4	100	67	$C_{30}H_{23}O_3NS$	73.30 (73.73)	4.88 (4.93)	2.70 (2.76)	231 (4.7) 329 (3.9)	1 635 1 232
6.	–	Furfuryl	146	66	$C_{25}H_{17}O_4NS$	70.20 (70.25)	3.92 (3.98)	3.20 (3.27)	239 (4.2) 325 (3.6)	1 640 1 230
7.	–	3-Pyridyl	175	63	$C_{27}H_{19}O_2N_3S$	72.10 (72.76)	4.18 (4.23)	9.30 (9.35)	231 (3.7) 331 (3.9)	1 635 1 232
8.	9-Chloro	C_6H_5	220	67	$C_{29}H_{20}O_2NSCl$	72.30 (72.34)	4.10 (4.15)	2.85 (2.91)	238 (4.3) 329 (3.6)	1 635 1 230
9.	9-Chloro	*p*-Cl-C_6H_4	120	67	$C_{29}H_{18}O_2NSCl_3$	63.32 (63.38)	3 25 (3.27)	2.50 (2.55)	237 (4.4) 320 (4.5)	1 640 1 230
10.	9-Chloro	*p*-H_3C-C_6H_4	178	67	$C_{31}H_{24}O_2NSCl$	73.0 (73.08)	4.36 (4.71)	2.70 (2.75)	231 (4.6) 313 (4.0)	1 650 1 235
11.	9-Chloro	2,4-Cl_2-C_6H_3	192	65	$C_{29}H_{16}O_2NSCl_5$	56.36 (56.40)	2.52 (2.59)	2.20 (2.26)	237 (4.4) 320 (4.5)	1 640 1 230
12.	9-Chloro	*p*-OCH_3-C_6H_4	236	67	$C_{30}H_{22}O_2NSCl$	68.70 (68.70)	4.37 (4.43)	2.52 (2.58)	—	1 635 1 235
13.	9-Chloro	Furfuryl	180	65	$C_{25}H_{16}O_2NSCl$	65.00 (65.07)	3.40 (3.47)	3.00 (3.03)	238 (4.2) 331 (3.9)	1 635 1 230
14.	9-Chloro	3-Pyridyl	238	62	$C_{27}H_{18}N_3SCl$	71.80 (71.84)	3.92 (3.99)	9.27 (9.31)	238 (3.9) 332 (3.9)	1 640 1 230

*Solvent of recrystallisation : acetic acid.

chlorophenyl)-3-*N*-phynylbenzothiopyranooxazine-5-one have shown an inhibition of 50% against *A. niger* and *A. alternata* at 100 ppm only.

The testing results indicate that a halogen when present in thiocoumarin ring or present in *N*-phenyl moiety enhances the activity and which is maximum when halogens are present in both the places.

Experimental

Melting points were determined in open capillaries and are uncorrected. Uv spectra were recorded in methanol on a Beckman DB spectrophotometer, ir spectra (KBr) on a Perkin-Elmer 337 spectrophotometer, pmr spectra (TFA and $CDCl_3$) on a Varian A-60 D spectrometer (TMS as internal standard) and mass spectra on a Perkin-Elmer-Hitachi-RMU-6L double focussing instrument operating at 70 eV using direct inlet system. Tlc analysis was performed on glass plates (10 × 5 cm^2) coated (250 mμ) with silica gel G (containing 13% calcium sulphate as binder).

General procedure :

2H-*Benzothiopyrano*[*3,4*-e][*1,3*]*oxazine-5-one* (3) *:* 4-Hydroxy-1-thiocoumarin (0.9 g) and Schiff base (obtained from *p*-chlorobenzaldehyde and aniline ; 2.1 g) were mixed in acetic acid and shaken well. The resulting dark brown solution was stirred at 30° for 1 h. A yellow compound that separated was filtered and recrystallised from acetic acid in the form of light yellow needles (1.8 g, 62%), m. p. 256° (Found : C, 67.57 ; H, 3.62 ; N, 2.66. $C_{23}H_{15}O_2NSCl_2$ requires : C, 67.57 ; H, 3.68 ; N, 2.71)%.

Acknowledgement

One of the authors (B.S.) expresses thanks to U. G. C., New Delhi, for the award of Teacher Fellowship (F. I. P.). Thanks are also due to Prof. C. Manoharachary for evaluating the physiological activity.

References

1. E. Ziegler and H. Junek, *Monatsh. Chem.*, 1955, **86**, 37.

2. P. S. Jamkhandi and S. Rajgopal, *Arch. Pharm.* (*Weinheim. Ger.*), 1967, **300**, 561.

3. P. Hanmanthu and C. V. Ratnam, *Indian J. Chem.*, *Sect. B*, 1977, **15**, 1019.

4. S. Y. Ditha and J. R. Merchant, *Tetrahedron Lett.*, 1978, **38**, 3607.

J. Indian Chem. Soc.,
Vol. LXIII, March 1986, pp. 326-328

Selective Extraction of Copper(II) with High Molecular Weight Carboxylic Acid and its Applications

U. S. RAY*, B. D. PRADHAN and S. B. KAR

Department of Chemistry, Visva-Bharati, Santiniketan-731 235

Manuscript received 3 April 1985, revised 6 September 1985, accepted 24 December 1985

Comparative extraction behaviour of copper(II) has been performed with high molecular weight carboxylic acids, such as versatic 9, versatic 911, versatic 10 and SRS 100 using benzene as diluent. The effect of *p*H, extractant concentration, metal ion concentration, diluent and contact time on the extraction of Cu^{II} have been studied. Copper has been quantitatively extracted at *p*H 6.0-9.0 with versatic 911 diluted with benzene. The Cu^{II}-versatic 911 ratio in the extracted species was found to be 1 : 3. Cu^{II} has been separated from Mg, Ca, Ba, Sr, Mn, Co, Ni, Zn, Cd, Hg, Pb, Al, Fe^{III}, Cr, Bi and Th. The effect of diverse anions, such as EDTA, thiocyanate, oxalate, thiosulphate, fluoride, iodide, tartrate and bifluoride has been investigated. Quantitative separations of Cu^{II} from synthetic mixtures have been reported. The proposed method has been applied to extract copper from some of the standard alloy samples.

THERE are several reports in the literature on the extraction of metal ions with carboxylic acids[1,2]. The typical high molecular weight carboxylic acids, such as versatic 9, versatic 911, versatic 10 and SRS 100 were used in this laboratory for the extraction of di-, tri-, tetra-valent metals[3-6]. The composition of the extracted species of several metals using versatic 911 as extractant were investigated by several workers[6,7]. The present study was undertaken to investigate the extraction behaviour of copper(II) with versatic 911 in benzene. The proposed method is simple, rapid, selective and can be carried out both at micro and macro levels. The method has been applied to extract copper(II) from some of the standard alloy samples. No such study has yet been reported in the literature.

Experimental

Separatory funnels (100 ml) were used for the extraction experiments. The *p*H measurements were carried out with Elico LI-10 *p*H meter.

Versatic 911, versatic 9, versatic 10 and SRS 100 (Shell Chemical, London) were used as such. Versatic 911 is a mixture of saturated tertiary monocarboxylic acids (C_9, C_{10} and C_{11}) manufactured from C_8-C_{11} olefins. The concentration and purity of versatic 911 is 5.43 *M* and 99%, respectively[7]. Versatic 911 was standardised by usual acid-alkalimetric titration. Versatic 9 is a mixture of highly branched saturated aliphatic acids (C_9) while SRS 100 consists of approximately 50% highly branched predominantly tertiary high molecular weight versatic acids (C_{18}) and approximately 50% natural oil. Versatic 10 is a mixture of isomeric tertiary monocarboxylic acids[8] (C_{10}). These cation-exchangers were suitably diluted in organic solvents and used for the extraction.

$CuSO_4$ solution (4.95 mg ml^{-1}) was prepared by dissolving $CuSO_4.5H_2O$ (AnalaR) in double-deionised water and the solution was standardised by complexometric titration with EDTA (disodium salt) using murexide (murexide-KCl 1 : 100) indicator[9]. Buffer solutions of different *p*H were prepared from sodium acetate (0.2 *M*)-acetic acid solution (*p*H range 3.5-6.75) and from ammonium chloride-ammonium hydroxide solution (*p*H range 7.0-9.5). All chemicals and solvents used were of analytical grade unless otherwise mentioned.

General procedure of extraction: The aqueous phase was made up of 9.9 mg Cu^{II} and 10 ml buffer solution. The *p*H adjustment was done by adding sodium hydroxide solution (*p*H 3.5-6.75) or ammonia solution (*p*H 7.0-9.5). The total volume of the aqueous phase was made upto 20 ml, *i.e.* leaving the ultimate concentration of Cu^{II} in the aqueous phase 7.8×10^{-3} *M*. The organic phase was prepared from 16.66% versatic 911 in benzene (9.05×10^{-1} *M*). The ratio of volumes of aqueous phase and organic phase was maintained at 2 : 1. Both the phases were taken in a separatory funnel and equilibrated. Contact time was varied from 1 to 5 min to achieve maximum extraction. The distribution ratio reached a constant value within 1 min. However, the contact time was maintained at 5 min. The two phases after equilibration were settled for 10 min. Any trace of organic phase left associated with the aqueous phase was washed

with benzene (5 ml). The resulting benzene extract was added to the separated organic phase. The amount of copper in the aqueous phase was estimated by complexometric titration. The organic phase was stripped with $2M$ HNO_3 (15 ml) for 5 min. The stripped acid extract was neutralised with ammonia and the amount of copper extracted was estimated complexometrically. Variations in procedure are indicated at appropriate places. All the experiments of extraction were carried out at $25 \pm 1°$.

Results and Discussion

Effect of variables on the extraction :

p*H* : The extraction behaviour of copper(II) at various *p*H with versatic 911 is given in Table 1. The experiments were performed at constant extractant (9.05×10^{-1} *M*) and metal ion (7.8×10^{-3} *M*) concentrations. The extraction of copper increases with increased *p*H and becomes quantitative at *p*H 6.0-9.0.

TABLE 1—EXTRACTION OF Cu^{II} AS A FUNCTION OF VERSATIC 911 AT *p*H 6.2

Versatic 911 $\times 10^{-1}$ *M*	Extraction %	Distribution ratio (D_{cu})
9.05	100	∞
4.93	100	∞
2.58	100	∞
1.75	97.80	88.9
1.32	95.6	43.45
1.06	94.3	33.08
0.89	89.2	16.52
0.67	78.1	7.13
0.53	64.4	3.62
0.27	22.1	0.57

Versatic 911 concentration : The effect of solvent concentration on extraction was studied by varying the concentration of versatic 911 from 9.05×10^{-1} to 2.7×10^{-2} *M* using benzene as diluent. The result are given in Table 1. In all the cases, metal ion concentration and *p*H were kept constant. In case of pure solvent with the increase of *p*H, the tendency of emulsion formation increases, hence to check it, different dilutions were done for different solvents. As evident from Table 1 the extraction is quantitative for a certain concentration range and then decreases with more dilution of the solvent.

Various diluents : With 9.05×10^{-1} *M* versatic solvent in various diluents, the extraction behaviour was tested keeping metal ion concentration, *p*H (6.2) and volume ratio (2 : 1) constant. Quantitative extraction was obtained with benzene diluent. Hence, the extraction of copper in benzene was preferred for different solvent systems, like versatic 911, versatic 9, versatic 10 and SRS 100.

Different carboxylic acids : The extraction of Cu^{II} at various *p*H with different carboxlic acids was tested using benzene as diluent. In each case volume ratio was kept constant. It was observed that of the various solvents (*i.e.* versatic 911, versatic 9, versatic 10 and SRS 100) used, versatic 911 gave the best result. The results are given in Table 2.

TABLE 2—EXTRACTION OF Cu^{II} WITH DIFFERENT CARBOXYLIC ACIDS AT DIFFERENT *p*H USING BENZENE DILUENT

*p*H	Versatic 911	Versatic 9	Versatic 10	SRS 100
4.0	43.4	9.0	10.6	3.2
4.5	73.5	39.5	45.9	15.1
5.0	88.6	81.3	88.2	71.4
5.5	97.8	92.7	96.4	90.3
6.0	99.65	95.2	97	93.3
6.2	99.8	97.3	97.7	95.3
6.5	99.96	99.0	99.0	97.4
7.0	100	100	100	100
7.5	100	100	100	98.7
8.0	100	100	100	93.5
8.5	100	100	100	89.9
9.0	98.1	98.0	96.16	81.3
9.5	70.9	95.6	—	—

Equilibrium time : The contact time was varied from 1 to 5 min. The quantitative extraction was obtained within 1 min and stripping was completed within 3 min. However, contact time for both extraction and stripping were kept 5 min in all the experiments.

Extracted species : The extraction experiments were carried out with constant metal ion concentration (7.8×10^{-3} *M*) at different *p*H and the corresponding distribution ratios were calculated. The stoichiometry of the extracted species was determined from the result obtained by plotting log D against log [Versatic 911] which produced a straight line of slope 1.53. Shibata and Nishimura[9] showed that versatic 911 in benzene diluent exists as dimer. Taking into account of this evidence, the extraction mechanism of Cu^{II} is proposed to be

$$Cu^{2+} + 1.5\,\overline{R_2H_2} \rightleftharpoons \overline{CuR_2.RH} + 2H^+$$

where, the barred species are in the organic phase and R_2H_2 refers to the dimeric form of versatic 911 in benzene solution. The extraction mechanism was further confirmed by plotting log D against *p*H which produced a straight line of slope 1.94. This indicates the release of two hydrogen ions during extraction which corroborates the proposed stoichiometry of the extracted species.

Extractive separation : The extraction of a definite amount of copper was carried out in presence of varying amounts of diverse ions over the *p*H range 6.2-7.05. The procedure for extraction was same as described above, except that *p*H of the solution was adjusted after the addition of diverse ions. Fe^{III}, Al, Cr, Cd, Hg and Th interfere under the recommended procedure. Fe, Al, Cr and Th were masked with ammonium bifluoride, and Cd and Hg with potassium iodide. Thus, the interference due to these ions was eliminated. Ca^{II}, Mg^{II}, Sr^{II}, Ba^{II}, Co^{II}, Ni^{II}, Mn^{II},

Zn^{II}, Pb^{II} and Bi^{III} do not interfere in the extraction of copper. Iodide, bifluoride, tartrate and thiocyanate do not interfere.

Separation of copper from synthetic mixture: The proposed method was applied for the extraction of copper(II) from some of the synthetic mixtures. Figures in the parenthesis against each ion indicate the amount of the ions present in milligram. The extraction was carried out at pH 6.2 keeping other parameters constant. In most of the cases quantitative extraction was achieved. For the interfering ions, the required amount of masking agents were added before the adjustment of pH. The results are given in Table 3.

TABLE 3—QUANTITATIVE SEPARATION OF Cu^{II}† FROM SYNTHETIC MIXTURE

pH = 6 2 ; Cu^{II} = 9.9 mg

Synthetic mixture (mg)	Cu^{II} extracted
Mg(3)+Ca(14)	99.12
Ni(10)+Zn(10)	101.26
Co(10)+Mn(10)	99.24
Ni(10)+Mn(10)	100.63
Zn(10)+Co(10)	100.25
Ni(10)+Co(10)	99 6
*Zn(6)+Cd(10)	100.25
*Al(3)+Ca(14)	98.1
*Al(3)+Bi(3)	101.26
*Zn(6)+Cd(10)+Hg (6)	99.74
Bi(3)+Mg(3)+Ni(10)	99.74
*Al(3)+Mn(6)+Bi(3)	100.75
*Al(3)+Fe(1)+Co(8)	100.25
*Mg(3)+Ca(14)+Sr(13)+Ba(13)	99.62
Mn(6)+Co(6)+Ni(6)+Zn(6)	100

†$Cu(NO_3)_2$ solution used in place of $CuSO_4$. *NH_4HF_2 used for Al, Fe, Cr, and KI for Cd and Hg as masking agents.

Extraction of copper(II) from standard alloys: In order to assess the possible analytical application of the proposed method the recommended procedure was applied for the extraction of Cu^{II} from some of the standard alloy samples The alloy samples were dissolved in acids to get the solution and then the proposed procedure was applied for the extraction. In most of the cases quantitative extractions were obtained. The results agree well with the standard data available for the alloy samples (Table 4).

TABLE 4—DETERMINATION OF Cu^{II} IN ALLOY SAMPLES

Sample	Copper extracted	Certified value	Deviation %
Brass	68.02	67.4	0.92
H. T. Brass 10 G	60.6	60.8	0.33
Aluminium bronze	85.7	85.9	0.23
Copper-nickel 180/2	67.8	68.12	0.47

Process of extraction of Cu^{II} from alloy samples:

Extraction from brass 5G (Sn+Cu+Pb+Fe+Zn): Brass sample solution was prepared according to the standard procedure. To mask iron, ammonium bifluoride was used and the extractions were carried out at pH 6.55.

Extraction from H.T. brass-10G (Cu+Fe+Sn+Pb+Zn+Al): The analytical procedure of brass was followed for the preparation of solution. A few black particles left insoluble in the solution were filtered through Whatman no. 42 filter paper and washed with hot dilute HNO_3. The volume was made upto 100 ml, and the extraction carried out at pH 6.55 using ammonium bifluoride as masking agent.

Extraction from aluminium bronze (Al+Cu+Fe): The sample (0.557 g) was treated with concentrated HNO_3 (15 ml) and water (10 ml). When vigorous reaction subsided the solution was boiled to 5 ml on a sand-bath, diluted to 50 ml and heated for 20 min to dissolve any insoluble particle left. A clear solution was obtained and the volume made upto 100 ml. Using ammonium bifluoride as masking agent at pH 7.45, quantitative extraction was achieved which agrees well with the standard value.

Extraction from copper-nickel (Cu+Ni+Mn+Fe+S): The solid (0.777 g) was treated with water (10 ml) and concentrated HNO_3 (15 ml). After vigorous reaction ceased it was heated slowly for 5 min giving a clear greenish solution. The volume was made upto 100 ml. The extraction was performed at pH 6.55 using ammonium bifluoride as masking agent.

Acknowledgement

The authors are grateful to C.S.I.R., New Delhi, for sponsoring the project and awarding a fellowship to one of them (B.D.P.). The authors thank Prof. A. K. De, Head, Department of Chemistry, Visva-Bharati, for facilities.

References

1. A. W. ASHBROOK, *Miner Sci. Eng.*, 1973, **5**, 3.
2. H. GREEN, *Talanta*, 1973, **2**, 158.
3. A. K. DE and U. S. RAY, *Sep. Sci.*, 1971, **6**, 25.
4. U. S. RAY and S. C. MODAK, *Indian J. Chem., Sect. A*, 1982, **21**, 760.
5. U. S. RAY and S. C. MODAK, *Sep. Sci.*, 1981, **16**, 67.
6. U. S. RAY and S. C. MODAK, *Indian J. Chem., Sect. A*, 1981, **20**, 933.
7. A. W. ASHBROOK, *J. Inorg. Nucl. Chem.*, 1972, **34**, 1721.
8. R. PRIBIL, 'Chelometry-Basic Determinations", Chempol, Praha, 1961.
9. J. SHIBATA and S. NISHIMURA, *J. Jpn. Inst. Met.*, 1973, **39**, 206.

J. Indian Chem. Soc.,
Vol. LXIII, March 1986, pp. 329-331

Oxidimetric Estimation of Caffeine using Aromatic Sulphonyl Haloamines

S. M. MAYANNA* and B. JAYARAM

Department of Chemistry, Central College, Bangalore-560 001

Manuscript received 5 July 1982, revised 26 August 1985, accepted 24 December 1985

The reactions between caffeine and *N*-haloamines have been found to proceed quantitatively over a wide range of experimental conditions. Simple titrimetric procedures for the a say of caffeine with *N*-haloamines have been developed. The products of oxidation are identified. The methods are also extended for the assay of caffeine in medicinal formulations, instant coffee and tea, soft drinks and alcoholic beverages.

CONSIDERABLE progress has been made in analytical chemistry with the introduction of aromatic sulphonyl haloamines as redox titrants[1,2]. *N*-Haloamines react with a surprising range of functional groups, affecting an array of molecular transformations. The well known member of the *N*-haloamines are: chloramine-T (CAT), dichloramine-T (DCT), bromamine-T (BAT), dibromamine-T (DBT), chloramine-B (CAB), dichloramine-B (DCB), bromamine-B (BAB), and dibromamine-B (DBB). The dihalogen compounds are generally employed as redox titrants in non-aqueous or partially aqueous media.

Caffeine (1, 3, 7-trimethylxanthine) is a stimulant present in pharmaceuticals, food products, plant materials and drinks. The analytical procedures reported so far, for its estimation in solution include complexometric titrations[3], chromatography[4], potentiometry[5] and spectrophotometry[6]. These methods involve sophisticated instrumentation or elaborate experimental procedures. Simple titrimetric procedures are therefore required for assaying caffeine in solution. The present communication reports the oxidimetric estimation of caffeine with DCT, BAT, DBT, CAB, BAB and DCB. A direct titration of the reductant with haloamines was not feasible, but the back titration methods developed are simple, elegant and fairly rapid.

Experimental

Caffeine (B.D.H.) was recrystallised from aqueous solution[7] before use. Caffeine solution of known concentration was prepared by dissolving the required amount of caffeine in triple-distilled water (for monohaloamines), or glacial acetic acid (for dihaloamines). CAB[8], DCB[9], DCT[10], BAB[11], BAT[12] and DBT[13] were prepared and characterised by standard procedures.

Preliminary studies :

A 10^{-3} *M* caffeine solution (5 ml) was added to a known and excess (40-60%) volume of oxidant (0.005 *N*) containing various concentrations of $HClO_4$ (0.01-0.1*M*) or NaOH (0.01-1.0*M*) or buffers[14] (*p*H 1-10) in an iodine-flask. The reaction mixture was set aside for various intervals of time with occasional shaking. 3*M* H_2SO_4 (20 ml) and 10% KI (10 ml) were then added and the liberated iodine was titrated to a starch end-point with standard $Na_2S_2O_3$ solution (0.01*M*). A blank titration was carried out with the oxidants under identical conditions.

In 30 min, the oxidation of caffeine with CAB is stoichiometric in $HClO_4$ and fairly rapid in buffer media (*p*H 1 and 2). A slight over-oxidation is noticed in buffers of *p*H 3 and 4 and slow at *p*H>4. The rate of oxidation is very slow in presence of NaOH. Oxidation of caffeine by BAT is more or less stoichiometric in $HClO_4$. In buffer media, the rate increases at *p*H > 1, reaches a maximum at *p*H 3 and then decreases. However, a reproducible stoichiometry is observed in NaOH medium (0.01-0.5*M*). Oxidation of caffeine by BAB is slow in mineral acids and in buffers (except *p*H 2, 4 and 5). However, the required stoichiometry is noticed in presence of NaOH (0.5-1.0 *M*). The oxidation of caffeine by dihaloamines in glacial acetic acid is stoichiometric and reproducible within 30 min.

The results were subjected to statistical analysis. The values of coefficient of variance (%) for different oxidants were in the limit 0.1 to 0.5. From these results it appear that the accuracy of estimation of caffeine with different oxidants is in the order, DCT > DBT > DCB > CAB > BAT = BBB.

Recommended procedure :

A known volume (25 ml) of 0.05 *N* oxidant was reacted with aliquots of caffeine in an iodine-flask, containing sufficient amount of acid or base (buffer of *p*H 2 for CAB, 0.025-0.5 *M* NaOH for BAT, 0.05-1.0 *M* NaOH for BAB and 25 ml of 50% acetic acid for dihalomines). After 30 min, 3 *M* sulphuric acid (20 ml) was added along with 10%

KI (10 ml) and the liberated iodine estimated using standard thiosulphate solution (0.01 *N*). Blank experiment was conducted at each time, and the amount of caffeine in the sample solution estimated.

Preliminary separation for assaying caffeine in different materials :

ACQ (aspirin-caffeine-quinine) tablet : Powdered tablet (0.25 g) was warmed with 0.1*N* sodium bicarbonate solution (25 ml), filtered and the residue washed. The filtrate was extracted with chloroform (3×30 ml) and the extract washed with dilute hydrochloric acid ($1\times10^{-3}N$, 3×30 ml). The residue from the chloroform extract was taken up in distilled water (100 ml) and 10 ml of the solution was used for the estimation with oxidants.

APC (aspirin, phenacetin and caffeine) tablets : Powdered tablet (0.25g) was refluxed with 2*N* H_2SO_4 (10 ml) for 1 h. The solution was then cooled, diluted with water (10 ml) and extracted with successive portions (30 ml) of chloroform until extraction is complete. The aqueous solution was preserved for the assay of phenacetin. The combined chloroform layer was extracted with 1 *N* NaOH (3 × 20 ml) and then with water (20 ml). The alkaline extract was then used for the assay of acetyl salicylic acid. The chloroform extract was evaporated and the residue was taken up in 100 ml distilled water and a 10 ml of the solution was taken for the estimation with the oxidants.

AC (aspirin-caffeine) tablet : Powdered tablet (0.25 g) was warmed with 0.1 *N* sodium bicarbonate solution (25 ml), filtered and the residue then washed. The filtrate was extracted with chloroform (3×30 ml). The solvent was evaporated and the residue dissolved in distilled water (100 ml), and a 10 ml of the solution was used for estimation with the oxidants.

Drinks (alcoholic and non-alcoholic) : The sample (10 ml) with or without added caffeine was treated with liquor ammonia (10 ml) and extracted with chloroform[16] (3 × 20 ml). Chloroform was evaporated, and the concentrate taken up in distilled water (10 ml) was estimated with the oxidants.

Instant coffee : The sample (10 g) was extracted with petroleum ether (b.p. 40-60°). The dried residue was treated with ammonium hydroxide solution (sp.gr. 0.88) and then extracted with chloroform. The extract was dried with anhydrous sodium sulphate and then filtered through a column containing aluminium oxide and magnesium oxide. The filtrate was evaporated. The solid caffeine was then dissolved in a known volume of water and used for analysis.

Instant tea : Polyphenols, pigments and other substances were removed from a known volume of an aqueous solution of the sample by precipitating with 3% lead subacetate [$2Pb(C_2H_3O_2)_2Pb(OH)_2$] solution. The filtrate and washings were collected and treated with 2 *N* H_2SO_4 to remove the excess of lead compound. It was then filtered and the acid in the solution was neutralised with dilute NaOH. A known volume of this solution was used for estimation with the oxidants.

Copper complex : An aqueous acidic solution of copper(II) chloride was added to an aqueous solution of caffeine (8 : 1 mol ratio). The mixture was stirred for several hours when dark green crystals of the complex[17] appeared. They were washed with ether and the dried sample of the complex [$CuCl_2(C_8H_{10}N_4O_2)H_2O$] was analysed for copper. A known amount of the complex (1 mg ml^{-1}) was dissolved in glacial acetic acid and used for estimation with oxidants.

Results and Discussion

In order to show the recovery capability of the present method, experiments are carried out containing known amounts (0.50-25 mg) of caffeine. Some typical results are given in Table 1. It is seen that caffeine can be estimated by the *N*-haloamine with an accuracy of about ± 1%. Table 2 indicates the determination of caffeine in various samples. The method of sample preparation described earlier is designed to remove interfering compounds. The results of spectrophotometric analysis are also included for comparison. It is seen that the values obtained by the titrimetric determination using *N*-haloamines are in agreement with those obtained by the spectrophotometric method.

TABLE 1—ESTIMATION OF CAFFEINE WITH *N*-HALOAMINES

Caffeine taken (mg)	Caffeine found (mg)					
	CAB	BAB	BAT	DCT	DBT	DCB
0.5	0.5	0.50	0.50	0 50	0.50	0.50
1.0	1.01	0.99	1.01	1.00	1.01	0.99
1.5	1.51	1.49	1.51	1.50	1.49	1.51
2.0	2.01	1.98	1.98	2.02	2.02	1.99
3.0	3.02	2.98	2.98	3.02	3.02	2.99
4 0	3.99	3.97	4.03	4.01	4.03	3.98
5.0	5.01	5.04	4.97	4.98	5.02	5.03
7.0	7.02	7.05	7.03	7.03	6.98	7.04
10.0	9.99	10.06	9.96	10.02	9.97	10.02
12 0	12.02	12.07	12 06	11.98	12.03	12.04
15.0	14.98	15.08	15.05	15.03	14.95	15.05
20.0	20.03	19.92	19.94	20.04	19.96	19.94
25.0	25.05	24.85	24.94	25.04	25.05	24.98

The stoichiometric oxidation of caffeine with the *N*-haloamines employed can be represented as

$$C_8H_{10}O_2N_4 + 2RNXNa\ (2R'NXNa \text{ or } R'NX_2) + 3\ H_2O \rightarrow$$
$$C_6H_6N_2O_4 + CH_3NHCONH_2 + 2RNH_2\ (2R'NH_2 \text{ or } R'NH_2) + 2NaX\ (\text{or } 2HX)$$

where, $R=C_6H_5SO_2$, $R'=p\text{-}CH_3C_6H_4SO_2$ and X=Cl or Br. It is observed that the monohaloamines undergo a two-electron change while dihalo compounds undergo a four-electron change in their reactions. In each case, the oxidant is reduced to the respective sulphonamide.

TABLE 2—DETERMINATION OF CAFFEINE IN SAMPLES WITH *N*-HALOAMINES

Sample	Caffeine found (mg g^{-1})						
	CAB[c]		BAB	BAT	DCT	DBT	DCT
APC tablet	62.1	(62.5)	62.0	61.98	62.90	61.99	62.0
AC tablet	39.02	(38.8)	38.4	38.4	38 6	38.50	39.01
AQC tablet	33.8	(34.0)	34.3	33.7	34.2	34.2	33.7
Cola drink[a]	100.9	(101.1)	102.0	102.0	101.5	102.0	100.7
Alcoholic beverage[a]	508.1	(510.0)	515.00	514 0	509.0	512.1	513.0
Instant coffee	37.3	(37.5)	37.2	37.8	37.3	37.2	37.8
Instant tea	26.7	(26 8)	26.6	26.99	26.9	27.0	26.6
Caffeine-copper complex[a]	1.99	(–)	2.0	1.98	2.0	1.99	1.98

[a]Concentrations are expressed as $\mu g\ ml^{-1}$. [b]Weight = 2.0 mg. [c]Caffeine by spectrophotometric method[*] given in parenthesis.

The products are dimethylalloxan and methylurea, which were detected[18] by tlc. Benzene sulphonamide formed in the reaction with CAB, BAB and DCB was detected by tlc[9]. A mixture of petroleum ether, chloroform and n-butanol (2 : 2 : 1, v/v) was the solvent, with iodine as the detecting reagent (R_f=0.88). *p*-Toluenesulphonamide, the reduced product of BAT, DCT and DBT was identified[19] by paper chromatography with benzyl alcohol saturated with water as the solvent and 0.5% vanillin in 1% HCl in ethanol as the spray reagent (R_f=0 91)

Detailed investigations showed that (i) foreign ions, such as Na, K, Zn^{II}, Ba^{II}, nitrate, phosphate, chlorate and sulphate (upto ionic strength, 0.2*M*) have no influence on the rate of oxidation, (ii) addition of chloride ion slightly accelerates the rate of oxidation and (iii) stoichiometry of oxidation is unaffected by the reversal of the addition of the reagents.

Acknowledgement

The authors are grateful to Prof. G. K .N. Reddy, Head, Department of Chemistry, Bangalore University, for his kind interest in the work.

References

1. V. J. JENNINGS, *CRC Crit. Rev. Anal. Chem.*, 1974, 407.
2. M. M. CAMPBELL and G. JOHNSON, *Chem. Rev.*, 1978, 78, 65.
3. M. GAJEWSKA, *Chem. Anal. (Warsaw)*, 1973, 18, 313.
4. G. F. PISANI, *J. Chem. Educt.*, 1976, 53, 733.
5. A. PEREIRA, JR. and M. A. PEREIRA *Estud. Agron.*, 1967, 8, 55.
6. W. M. OVERTON, L. A. LARRY and V. RAYMONDS, *J. Pharm. Sci.*, 1973, 62, 1524.
7. A. L. MOYE, *J. Chem. Educt.*, 1972, 49, 194.
8. A. CHRZASZCZEWSKA, *Chem. Abstr.*, 1955, 49, 212.
9. H. S. YATHIRAJAN, D. S. MAHADEVAPPA and RANGASWAMY, *Talanta*, 1980, 27, 52.
10. T. J. JACOB and C. G. R. NAIR, *Talanta*, 1972, 19, 347.
11. M. S. AHMED and D. S. MAHADEVAPPA, *Talanta*, 1980, 27, 669.
12. C. G. R. NAIR, R. L. KUMARI and P. I. SENAN, *Talanta*, 1978, 25, 525.
13. C. G. R. NAIR and P. INDRASENAN, *Talanta*, 1976, 23, 239.
14. A. FINDLAY, "Practical Physical Chemistry", Longmans, London, 1954, p. 268.
15. "Pharmacopia of India", Government of India, Ministry of Health, 1970, p. 21.
16. D. PEARSON, "Chemical Analysis of Food", Chemical Publishing Co., New York, 1970, p. 269.
17. G. BANDOLI, C. M. BIAGINI, D. A. CLEMENT and G. RAZZARDI, *Inorg. Chim. Acta*, 1976, 20, 71.
18. B. H. HANSEN and G. G. DRYHURST *J. Electroanal. Chem. Interfacial Electro chem.*, 1971, 30, 407.
19. D. S. MAHADEVAPPA and N. M. M. GOWDA, *Talanta*, 1975, 22, 771.

Notes

Preparation and Characterisation of Adducts of Hexamethylphosphoramide with Copper(II) Carboxylates

N. KUMAR*, B. L. KALSOTRA
and
(Miss) RENU SACHAR

Department of Chemistry, University of Jammu, Jammu-180 001

Manuscript received 17 January 1985, revised 18 October 1985, accepted 15 November 1985

HEXAMETHYLPHOSPHORAMIDE (HMPA) has four donor sites (three nitrogen atoms and one oxygen atom) but it invariably acts as a unidentate oxygen donor molecule. It forms coordination compounds with a large variety of organic compounds, Lewis acids and inorganic salts[1]. However, no work is reported on its complexes with copper(II) carboxylates except the one describing its complex with copper(II) chloroacetate[2]. This prompted us to investigate its complexes with some of the copper(II) carboxylates.

Experimental

Carboxylic acids (B.D.H.), $CuSO_4.5H_2O$ (AnalaR) and HMPA (B.D.H.) were used as such. Basic $CuCO_3.Cu(OH)_2.H_2O$ (B.D.H) was purified by washing with hot water. Solvents were purified by conventional methods. Copper(II) arylcarboxylates and chloroacetates were prepared by standard methods[3,4].

Complexes were prepared by the interaction of equimolar quantities of the requisite amounts of copper(II) carboxylates and the ligand in an appropriate organic solvent with or without refluxing. The reaction mixture on concentration deposited the desired products which were separated, washed with appropriate solvents like acetone and methanol, and dried over calcium chloride at room temperature. In some cases, the product obtained was recrystallised from a suitable organic solvent, such as methanol before drying.

Copper was estimated gravimetrically as cuprous thiocyanate. Carbon and hydrogen were determined in the Microanalytical Laboratory of this department. Molar conductance was determined on millimolar solutions in 1,4-dioxane and methanol using Elico CM 82T conductivity bridge and a conductivity cell with a cell constant of 0.50. Magnetic moments were determined by Gouy's method. Electronic spectra were scanned on a Beckman-DB spectrophotometer in chloroform. Diffuse reflectance spectra were recorded on a Carl-Zeiss DMR-21 ultraviolet, visible and near-infrared spectrophotometer. Ir spectra were recorded on a Pye Unicam SP 2000 spectrophotometer in KBr.

Results and Discussion

The complexes isolated are green crystalline compounds of 1 : 1 stoichiometry as shown by their elemental analysis (Table 1). The complexes are slightly hygroscopic and dissolve in common organic solvents giving solutions which decompose on prolonged standing. Cryoscopic molecular weight studies on these systems did not afford satisfactory results because of their insufficient solubility in benzene and nitrobenzene. The molar conductance values which lie in the range 0.025-0.624 and 18.11-85.20 $mol^{-1}\ \Omega^{-1}\ cm^2$ in 1,4-dioxane and methanol, respectively suggest that the complexes are non-ionic in nature[5,6].

The magnetic moment values of these complexes fall in the range 1.46-1.63 B.M. at room temperature (Table 1) and are similar to those of dimeric carboxylate bridged mono-adducts of copper(II) carboxylates with other oxygen donors[7]. This suggests that these complexes also have a carboxylate bridged structure similar to that of copper(II) acetate monohydrate[8]. The magnetic moment values of the present complexes are somewhat higher than those of 1.30-1.45 B.M. observed for typical dimeric adducts of copper(II) carboxylates[9]. This may be attributed to high steric requirements of the ligand which somehow cause a reduction in the magnetic exchange occurring in these systems thereby making them to acquire comparatively higher magnetic moments.

The solution and diffuse electronic spectra of the complexes show one broad band lying between 675 and 728 nm excepting copper(II) dichloroacetate adduct which shows this band at 800 nm in its diffuse reflectance spectra. This band is a characteristic of blue or green copper(II) complexes having a distorted octahedral stereochemistry and is assigned to the $d_{xz,yz} \longrightarrow d_{x^2-y^2}$ transition[10]. However, the 2nd band which appears as a shoulder around 375 nm in many dimeric complexes of copper(II) carboxylates[11] is missing in the spectra of these complexes. Since a number of non-dimeric complexes have also been found to exhibit this band[12], its presence cannot be regarded as a diagnostic feature of dimeric structure. Hence, its absence in the present complexes does not preclude the possibility that they are dimeric.

In the infrared spectra the $\nu_{P=O}$ of the complexes exhibits a negative shift of 85-138 cm^{-1} as compared to the corresponding frequency of the ligand[2] suggesting that HMPA coordinates through its oxygen atom to the metal ion in these systems[2,13]. The

TABLE 1—ANALYTICAL, MAGNETIC AND ELECTRONIC SPECTRAL DATA OF HMPA COMPLEXES OF COPPER(II) CARBOXYLATES

Sl. no.	Compd.	M. p. °C	Analysis % : Found/(Calcd.)			λ_{max} nm	μ_{eff} B.M.
			Cu	C	H		
1.	Cu(benzoate)$_2$.HMPA	238*	12.89 (13.11)	49.38 (49.53)	5.59 (5.77)	700^a	1.52
2.	Cu(*o*-methylbenzoate)$_2$.HMPA	226	12.17 (12.39)	51.26 (51.51)	6.12 (6.24)	680^b	1.59
3.	Cu(*m*-methylbenzoate)$_2$.HMPA	*	12.20 (12.39)	51.29 (51.51)	6.19 (6.24)	690^b	1.63
4.	Cu(*p*-methylbenzoate)$_2$.HMPA	247	12.27 (12.39)	51.30 (51.51)	6.09 (6.24)	682^a	1.46
5.	Cu(*o*-chlorobenzoate)$_2$.HMPA	214	11.27 (11.47)	43.17 (43.36)	4.48 (4.69)	685^a	1.60
6.	Cu(*m*-chlorobenzoate)$_2$.HMPA	249	11.39 (11.47)	43.19 (43.36)	4.50 (4.69)	680^b	1.56
7.	Cu(*p*-methoxybenzoate)$_2$.HMPA	241	11.40 (11.66)	48.27 (48.48)	5.68 (5.87)	675^a	1.50
8.	Cu(*m*-nitrobenzoate)$_2$.HMPA	248	10.92 (11.06)	41.56 (41.77)	4.41 (4.52)	685^a	1.48
9.	Cu(monochloroacetate)$_2$.HMPA	188	14.32 (14.79)	27.68 (27.93)	5.01 (5.12)	690^a 716^b	1.56
10.	Cu(dichloroacetate)$_2$.HMPA	202*	12.58 (12.74)	23.88 (24.07)	3.88 (4.01)	800^a 728^b	1.63

*Decomposes. ^{a}Diffuse reflectance spectra. ^{b}In $CHCl_3$.

frequency difference between the asymmetric and symmetric carboxylate stretches lies in the range 230-250 cm^{-1} with the exception of the complex of copper(II) dichloroacetate where this separation is 286 cm^{-1}. These values are appreciably higher than those found in the corresponding parent copper(II) carboxylates and are similar to those of binuclear complexes of copper(II) arylcarboxylates and chloroacetates with oxygen donors[14] suggesting a usual dimeric carboxylate bridged structure for these complexes.

Acknowledgement

The authors are thankful to Prof. O. P. Vig, Department of Chemistry, Panjab University, Chandigarh, for facilities, and one of them (R. S.) is grateful to U. G. C., New Delhi, for financial assistance.

References

1. H. NORMANT, *Angew. Chem.*, 1967, **6**, 1046.
2. R. C. PAUL, P. R. SHARMA and S. L. CHADHA, *Indian J. Chem., Sect. A*, 1977, **15**, 27.
3. M. KONDO and M. KUBO, *J. Phys. Chem.*, 1958, **62**, 1558.
4. J. LEWIS, Y. C. LIN, L. K. ROYSTON and R. C. THOMPSON, *J. Chem. Soc.*, 1965, 6464.
5. R. L. MARTIN and A. WHITLEY, *J. Chem. Soc.*, 1958, 1394.
6. A. B. P. LEVER, *J. Inorg. Nucl. Chem.*, 1965, **27**, 149.
7. J. CATTERICK and P. THORNTON, *Adv. Inorg. Chem. Radiochem*, 1977, **20**, 291.
8. B. N. FIGGIS and R. L. MARTIN, *J. Chem. Soc.*, 1956, 3837.
9. M. KATO, H. B. JONASSEN and J. C. FANNING, *Chem. Rev.*, 1964, **64**, 99.
10. L. DUBICKI and R. L. MARTIN, *Inorg. Chem.*, 1966, **5**, 2203.
11. A. B. P. LEVER, "Inorganic Electronic Spectroscopy", Elsevier, Amsterdam, 1968.
12. D. P. GRADDON, *J. Inorg. Nucl. Chem.*, 1960, **14**, 161.
13. A. K. MAJUMDAR, R. G. BHATTACHARYYA and D. C. BERA, *Chem. Ind. (London)*, 1971, 730.
14. K. S. BOSE and C. C. PATEL, *Indian J. Chem.*, 1970, **8**, 840.

Studies on some Mixed Ligand Complexes of Copper(II) and Nickel(II) Pyrrolidonates with some Nitrogen Donors

(Mrs.) P. R. SHUKLA* and SURESH CHANDRA

Department of Chemistry, Lucknow University, Lucknow-226 007

and

GOPAL NARAIN

Chemistry Department, Dr. Harisingh Gaur Vishwavidyalaya, Sagar-470 003

Manuscript received 3 February 1984, revised 6 November 1985, accepted 6 February 1986

A large number of transition metal complexes with various heterocyclic Schiff bases and oximes have been reported from this laboratory[1-8]. The present paper reports the studies on some mixed ligand complexes of Cu^{II} and Ni^{II} pyrrolidonates with different amines, such as aniline piperidine, α-picoline, pyridine (L), ethylenediamine, tetramethylethylenediamine (L') and diethylenetriamine or triethylenetetraamine (L").

TABLE 1—ANALYTICAL, MOLAR CONDUCTANCE AND MAGNETIC MOMENT DATA

Sl. no.	Compd.	Colour	Analysis % : Found/(Calcd.) M	C	H	N	Mol. cond. $\Omega^{-1}cm^2mol^{-1}$	μ_{eff} B.M.
1.	$[Cu(C_4H_6NO)_2(C_6H_7N)_2]$	Dark brown	15.00 (15.21)	58.13 (57.47)	6.13 (6.22)	12.89 (13.41)	2.08	2.29
2.	$[Cu(C_4H_6NO)_2(C_5H_{11}N)_2]$	Light green	16.10 (15.82)	52.95 (53.79)	10.40 (10.55)	13.48 (13.94)	1.90	1.84
3.	$[Cu(C_4H_6NO)_2(C_4H_9NO)_2]$	Brown	15.10 (15.66)	48.00 (47.34)	6.50 (6.90)	13.50 (13.80)	2.80	1.90
4.	$[Cu(C_4H_6NO)_2(C_6H_{18}N_4)]$	Dark green	18.50 (18.82)	50.10 (49.77)	8.12 (8.29)	16.23 (16.59)	Insol	2.08
5.	$Cu(C_4H_6NO)_2(C_2H_7NO)]$	Brown	20.91 (21.72)	41.76 (41.02)	6.28 (6.49)	14.16 (14.35)	Insol	1.96
6.	$[Ni(C_4N_6NO)_2(C_5H_5N)_2(H_2O)_2]$	Dark brown	13.65 (13.95)	50.93 (51.34)	6.10 (6.18)	13.12 (13.31)	5.60	3.25
7.	$[Ni(C_4H_6NO)_2(C_5H_{11}N)_2(H_2O)_2]$	Light pink	13.20 (13.56)	50.40 (49.92)	7.39 (7.85)	12.52 (12.94)	Insol	3.43
8.	$[Ni(C_4H_6NO)_2(C_6H_7N)_2(H_2O)_2]$	Yellowish green	13.41 (13.08)	52.98 (53.48)	6.59 (6.68)	12.25 (12.48)	3.50	3.41
9.	$[Ni(C_4H_6NO)_2(C_4H_9NO)_2(H_2O)_2]$	Brown	13.20 (13.43)	33.40 (32.97)	7.21 (7.32)	11.99 (12.82)	Insol	2.97
10.	$[Ni(C_4H_6NO)_2(C_2H_7NO)(H_2O)_2]$	Pink	17.85 (18.18)	38.10 (37.07)	6.91 (7.10)	11.85 (12.97)	4.35	3.23
11.	$[Ni(C_4H_6NO)_2(C_4H_{13}N_3)(H_2O)_2]$	Light pink	15 61 (15.91)	33.01 (32.54)	8.50 (8.67)	14.98 (15.18)	Insol	3.48
12.	$[Ni(C_4H_6NO)_2(C_4H_{13}N_3)(H_2O)]$	Pink	16.13 (16.87)	41.83 (41.41)	7.59 (7.76)	20.00 (20.13)	5.60	2.88
13.	$[Ni(C_4H_6NO)_2(C_6H_{18}N_4)]$	Pinkish	15.54 (15.74)	44 98 (45.07)	7.95 (8.04)	21.95 (22.53)	6.50	3.06

TABLE 2—ELECTRONIC SPECTRAL DATA AND LIGAND PARAMETER OF Ni^{II} COMPLEXES

Obs. V_3 kK	Obs. V_2 kK	Obs. V_1 kK	Obs. Dq cm^{-1}	B cm^{-1}	β	V_2/V_1	Calcd. V_2 kK	Calcd. V_3 kK
27.60	16.16 14.09	10.87 10.00	1043	944	0.875	1.47	19.57	30.00
26.30	15.15 13.50	9.61	961	895	0.828	1.57	17.30	28.50
27.01	14.70 13.50	10.20	1020	881	0.817	1.40	18.35	29.25
26.67	14.29 13.33	9.73	973	894	0.828	1.51	15.80	27.52
24.40	16.13 13.70	9.80	980	935	0.865	1.46	17.64	28.77
26.17 16.13	14.71	10.09	1009	964	0.893	1.53	17.01	28.34
25.00	17.86 13.52	10.42	1042	981	0.908	-	17.30	28.51
26.67	16.94 14.40	10.00 10.99	1049	1035	0.962	1.58	18.17	29.12

The hitherto unknown Cu^{II} and Ni^{II} pyrrolidonates have been obtained by treating sodium pyrrolidonate with an aqueous solution of corresponding metal(II) sulphate and possess the formulae $Cu(C_4H_6NO)_2.2H_2O$ and $Ni(C_4H_6NO).4H_2O$. The complexes were then prepared by suspending a known amount of these salts (1 mol) in methanol and adding to it the amine (1 mol). The solution was refluxed for 6 h and the complexes were crystallised out by repeated treatment with petroleum ether (b.p. 60-80°). The complexes are sparingly soluble in methanol, nitrobenzene and DMF, and start decomposing on heating and hence their melting points could not be determined. These have been characterised using various physiochemical methods as described. The metal was estimated using standard methods. The microanalytical estimation of C, H and N as well as the infrared spectra were recorded at C. D. R. I., Lucknow. The magnetic and electronic spectral measurements were made at Guru Nanak Dev University, Amritsar.

Results and Discussion

The elemental analysis show the complexes to possess the formula $[Cu(C_4H_6ON)_2(L')(H_2O)_2]$, $[Ni(C_4H_6ON)_2(dien)(H_2O)]$, $[Ni(C_4H_6ON)_2 trien)]$, where, C_4H_6ON = uninegative pyrrolidonate ion; L = aniline, piperidine, pyridine, α-picoline, morpholine; L' = ethanolamine, tetra-

methylethylenediamine, dien = diethylenetriamine and trien = triethylenetetraamine.

Low conductance of the complexes in nitrobenzene corresponds to their non-electrolytic nature as indicated by the formula above and suggests that the deprotonation of the NH group of free 2-pyrrolidone has occurred and it has been converted into its uninegative ion, which is capable of acting as a bidentate ligand coordinating through CO and NH groups. However, keeping in view the nature of the ligands used in the study, it is not possible for the ion to act as a bidentate ligand and hence it is suggested that it should be have only as a monodentate ligand thus conferring the usual coordination numbers of four on the Cu^{II} and six on Ni ions. The site of its coordination is the CO group, since in the ir spectra a sharp band appears at 1 690 cm^{-1} (CO) stretch, which in free ketone is seen at 1 725 cm^{-1} (Refs. 6, 7). The coordination of amines is indicated by the shifts of their relevant ir bands[8-11]. The planar and octahedral geometries of Cu^{II} and Ni^{II} complexes are confirmed by their magnetic and electronic data.

The Cu^{II} complexes are paramagentic with the magnetic moment around 1.90 B.M. The appearance of a d-d band at 16.00 kK accompanied by two shoulders at 12.00 and 10.50 kK, assignable as $^2B_{1g} \rightarrow {}^2A_{1g}$, $^2B_{1g} \rightarrow {}^2E_g$ and $^2B_{1g} \rightarrow {}^2A_{2g}$ transitions respectively, is indicative of planar steriochemistry. The values of μ_{eff} for Ni^{II} complexes lie in the range 2.97-3.20 B.M. suggesting octahedral steriochemistry. These complexes show three comparatively weak bands at 23.00, 17.50 and 9.50 kK which correspond to the three idealised (O_h symmetry) transitions such as $^3A_{2g} \rightarrow {}^3T_{1g}$ (P) (ν_3), $^3A_{2g} \rightarrow {}^3T_{1g}$ (F) (ν_2) band, $^3A_{2g} \rightarrow {}^3T_{2g}$ (ν_1), respectively. The ν_2 as well as ν_3 transitions are found to be broken down in two components which is due to the departure of the symmetry towards pseudooctahedral. The values of the ligand field parameters have been calculated using the well known equation[13], and it is found that the Dq values for complexes of ligands L are somewhat lower than those L′ or L″ which correlates well with the positions of these ligands in spectrochemical series. The β values suggest the presence of sufficient amount of covalent character on the metal-ligand band.

References

1. P. R. Shukla, V. K. Singh, A. M. Jaiswal and G. Narain, *J. Indian Chem. Soc.*, 1983, **60**, 321.
2. P. R. Shukla, J. Bhargava and G. Narain, *J. Indian Chem. Soc.*, 1983, **60**, 287.
3. P. R. Shukla, O. P. Pandey and G. Narain, *J. Indian Chem. Soc.*, 1983, **60**, 397.
4. P. R. Shukla, V. K. Singh and G. Narain, *J. Indian Chem. Soc.*, 1983, **60**, 291.
5. P. R. Shukla, J. Bhargava and G. Narain, *J. Indian Chem. Soc.*, 1983, **60**, 788.
6. W. Pelz, *Ann. Gen. Chem.*, 1960, **72**, 96.
7. F. A. Snavely, *J. Org. Chem.*, 1962, **27**, 994.
8. A. R. Kartizky, *J. Chem. Soc.*, 1959, 2049.
9. N. N. Greenwood and K. Wade, *J. Chem. Soc.*, 1960, 1130.
10. B. Chenon and C. Sandorty, *J. Chem. Soc.*, 1958, 1181.
11. N. S. Hem and A. L. G. Rees, *Nature (London)*, 1952, **169**, 110.
12. D. B. Powell and N. Sheppard, *Spectrochim. Acta*, 1961, 1768.
13. B. N. Figgis, "Introduction to Ligand Fields", Wiley Eastern, New Delhi, 1976, p. 220.

Mixed Ligand Complexes of Nickel(II), Copper(II), Palladium(II) and Platinum(II) with Pyrrole-2-carboxaldehyde and Acetylacetone

P. K. KANUNGO, N. K. SANKHLA and R. K. MEHTA*

Chemistry Department, University of Jodhpur, Jodhpur-342 001

Manuscript received 9 January 1978, revised 23 December 1985, accepted 3 March 1986

IN continuation of our earlier work[1] on mixed ligand complexes, we now report a slightly different type of mixed ligand complexes of the type described below.

Experimental

[MLL′], type of complexes (where, M = Ni^{II}, Cu^{II}, Pd^{II} or Pt^{II}; L = pyrrole-2-carboxaldehyde; and L′ = acetylacetone) were prepared by adding pyrrole-2-carboxaldehyde and acetylacetone to the metal acetate solution in 1 : 1 : 1 ratio. The coloured solid separated was filtered and recrystallised from methanol. The solid on reaction with an excess of ammonia or alkylamines gave [MLL′A] type complexes (where, A = ammonia or alkylamine molecule) which on refluxing with ethanolamine on a water-bath for 2-3 h gave [MLE.H_2O] type complexes (where, E = ethanolamine). The complexes were recrystallised from methanol.

Results and Discussion

All the complexes gave satisfactory elemental analyses. On analysis [MLE.H_2O] type complexes, in addition, indicated the presence of a water molecule per molecule of the complex. These compounds are soluble in common organic solvents. Their negligibly small molar conductance values (3.2-7.: Ω^{-1} cm^2 mol^{-1}) suggest them to be non-electrolytic in nature. The Ni^{II}, Pd^{II} and Pt^{II} complexes are found diamagnetic while Cu^{II} complexes are paramagnetic (μ_{eff} = 1.88 B.M.) at room temperature.

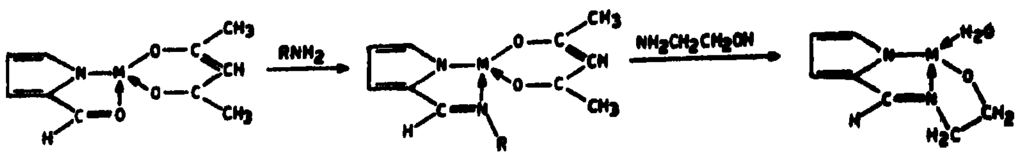


Fig. 1. Structure of mixed ligand complexes; R = H, CH_3 or C_2H_5.

The electronic absorption spectra of the mixed ligand Ni^{II} complexes in methanol gave two bands in the region 610-620 and 535-550 nm which can be assigned to the transitions $^1A_{1g} \rightarrow ^3B_{1g}$ and $^1A_{1g} \rightarrow ^3B_{2g}$, respectively. The Cu^{II} complex (solution) gave one band in the region 635-645 nm which may be assigned to the transition $^2B_{1g} \rightarrow ^2E_g$. Solution spectra of the Pd^{II} complexes exhibited three bands in the ranges 440-450, 375-380 and 315-320 nm assigned to the transitions $^1A_{1g} \rightarrow ^1B_{1g}$; $^1A_{1g} \rightarrow ^1E_{1g}$ and $^1A_{1g} \rightarrow ^1A_{2u}$, respectively. The Pt^{II} complexes also gave three bands in the region 310-320, 350-355 and 420-430 nm assignable to the transitions $^1A_1 \rightarrow ^1B_1$, $^1A_1 \rightarrow ^1A_2$ and $^1A_1 \rightarrow ^3A_2$, respectively. These data indicate a square-planar structure[3-5] for the Ni^{II}, Cu^{II}, Pd^{II} and Pt^{II} complexes.

In the ir spectra of complexes [MLL'] and [MLL'A], no bands have been observed in the region 3 300-3 100 or 3 600-3 400 cm^{-1} indicating that hydrogen of the NH group of pyrrole-2-carboxaldehyde and OH group of acetylacetone get dissociated on complexation. Spectra of the [MLL'] complexes show bands at 1 630 cm^{-1} and 1 570 cm^{-1} which can be assigned to aldehydic C=O and C=O of the acetylacetone, respectively. In the ir spectra of the [MLL'A] complexes (in which R=H), the band at 1 630 cm^{-1} disappeared and a new band around 1 600 cm^{-1} C=N of the imine linkage appeared. The band at 1 570 cm^{-1} C=O of acetylacetone remains unchanged indicating that it does not undergo condensation The appearence of the band in the region 3 300-3 100 cm^{-1} shows the presence of free N–H which was absent in the mixed ligand complexes derived from alkylamines. The ir spectra of the [MLE. H_2O] type complexes show a band around 3 400 cm^1 (OH) which confirms the presence of water molecule, and a band at 1 600 cm^{-1} (C=N). The appearence of two new bands in the region 500 480 and 570-560 cm^{-1} in the above type of complexes suggest the presence of M—O and M—N bondings[6] in them.

On the basis of the above investigations, the [MLL'], [MLL'A] and [MLE. H_2O] type complexes may be represented by the structures as shown in Fig. 1.

Acknowledgement

The authors are thankful to U.G.C., New Delhi, for the award of a fellowship to one of them (K.K.).

References

1. B. R. Singhvi, D. C. Sehgal and R. K. Mehta, *J. Indian Chem. Soc.*, in the press.
2. F. A. Cotton and G. Wilkinson, "Advanced Inorganic Chemistry", Wiley Eastern, New Delhi, 1966, p. 881.
3. L. Sacconi, *J. Inorg. Nucl. Chem.*, 1961, 19, 73.
4. S. Yamada, *Coord. Chem. Rev.*, 1966, 1, 415.
5. P. Natarajan and A. W. Adamson, *J. Indian Chem. Soc.*, 1977, 54, 25.
6. K. Nakamota, "Infrared Spectra of Inorganic and Coordinated Compounds", Wiley, New York, 1963, p. 151.

Stability Constants of Complexes of some Bivalent Metal Ions with *N*-(2-Hydroxy-3-methoxybenzylidene)-2,6-dimethylaniline and *N*-(2-Hydroxy-3-methoxybenzylidene)-2,4-dimethylaniline

P. P. SANGODKAR and M. S. MAYADEO*

Department of Chemistry, Ramnarain Ruia College, Matunga, Bombay-400 019

Manuscript received 30 July 1985, accepted 17 January 1986

FROM the literature survey on the stability constants it is seen that no work on solution stability constants of *N*-(2-hydroxy-3-methoxybenzylidene)-2,6-dimethylaniline and *N*-(2-hydroxy-3-methoxybenzylidene)-2,4-dimethylaniline has been reported so far. The present investigation is aimed at determining the stability constants of Cu^{II}, Ni^{II}, Zn^{II}, Co^{II}, Cd^{II}, and Mg^{II} with the above mentioned ligands.

Experimental

The reagents *N*-(2-hydroxy-3-methoxybenzylidene)-2,6-dimethylaniline and *N*-(2-hydroxy-3-methoxybenzylidene-2,4-dimethylaniline, were synthesised by condensing ethanolic solution of 2-hydroxy-3-methoxybenzaldehyde with 2,6-dimethylaniline and 2,4-dimethylaniline, respectively in equimolar ratios. The products were repeatedly crystallised to get analytically pure compounds. The purity of the compounds was tested by tlc and elemental analysis; m.p. 135 and 99°, respectively.

Calvin-Bjerrum[1] titration technique was used to determine the dissociation constants of the reagents and the formation constants of their metal chelates at 30±0.1° in 75 : 25 (v/v) dioxan-water medium at 0.1 *M* ionic strength.

A Elico Li-15 pH meter (division, 0.1 unit; temperature compensator range 0-100°) was employed throughout the investigation for pH determinations. The glass electrode supplied was used in combination with a dip type calomel electrode. Standardisation of the pH meter was resorted to by means of buffers 0.05 M potassium hydrogen phthalate (pH 4.019 at 30°) and 0.01 M borax (pH 9.18 at 30°). The metal ion solutions prepared from A. R. grade salts, were standardised by EDTA titrations[8]. During the titrations oxygen-free nitrogen presaturated with solvent mixture was bubbled through the solutions. The following solutions were titrated potentiometrically against standard carbonate free sodium hydroxide (1.075 M): (i) 5 ml 0.16 M $HClO_4$ + 5 ml 0.64 M $NaClO_4$ + 30 ml dioxan, (ii) 5 ml 0.16 M $HClO_4$ + 5 ml 0.64 M $NaClO_4$ + requisite amount of the reagent to give 0.004 M reagent concentration in the final solution + 30 ml of dioxan, and (iii) 5 ml 0.64 M $NaClO_4$ + 5 ml metal perchlorate (0.008 M in 0.16 M $HClO_4$) + requisite amount of the reagent to give 0.004 M reagent concentration in final solution + 30 ml of dioxan. The titrations were performed in duplicate to test for reproducibility.

Results and Discussions

Formation functions, $\bar{n}_A$, $\bar{n}$, pL were calculated using the standard expressions from the titration curves, the pK_1^H and pK_2^H values of the ligands at $\bar{n}_A$ = 0.5 and 1.5, respectively were calculated (Figs. 1a and b). The values were further corroborated from the plots of log $\bar{n}_A/(1-\bar{n}_A)$ *vs* B and log $(2-\bar{n}_A)/(\bar{n}_A-1)$ *vs* B. The formation curves of metal-ligand systems were obtained by plotting $\bar{n}$ *vs* pL (Figs. 2 and 3). From these curves the values of log K_1 and K_2 were determined. The values obtained by half-integral method were further corroborated from the plots of log $\bar{n}/(1-\bar{n})$ *vs* pL and log $(2-\bar{n})/(\bar{n}-1)$ *vs* pL. For those metal systems where difference between log K_1 and

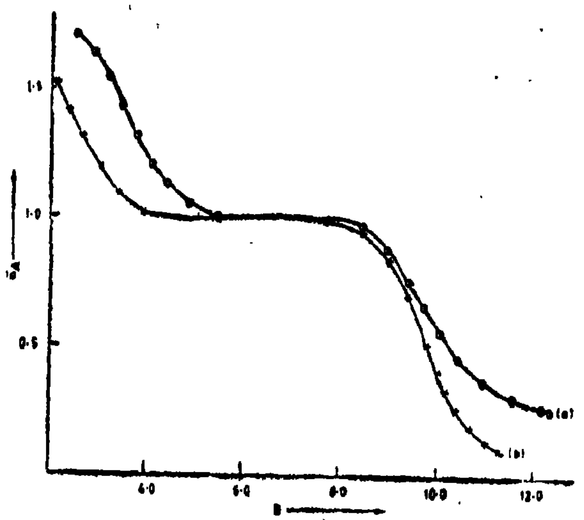


Fig. 1. Formation curves of (a) N-(2-hydroxy-3-methoxybenzylidene)-2,4-dimethylaniline and (b) N-(2-hydroxy-3-methoxybenzylidene)-2,6-dimethylaniline.

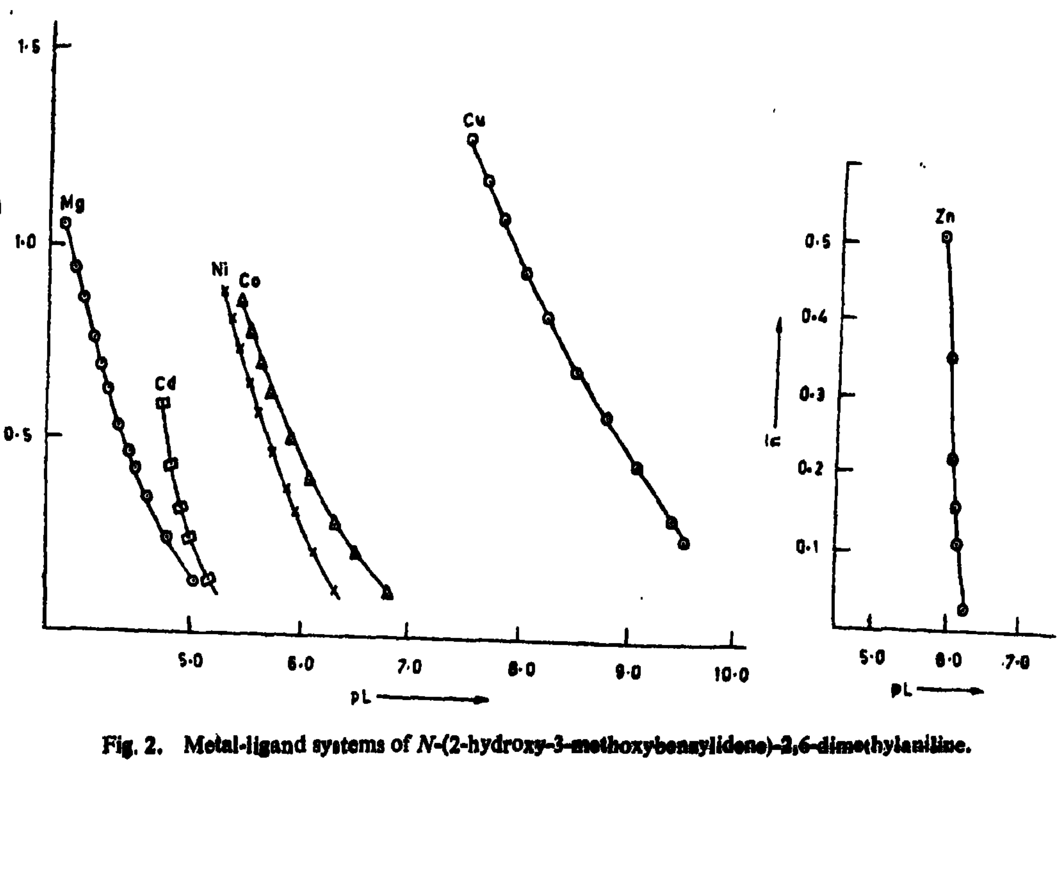


Fig. 2. Metal-ligand systems of N-(2-hydroxy-3-methoxybenzylidene)-2,6-dimethylaniline.

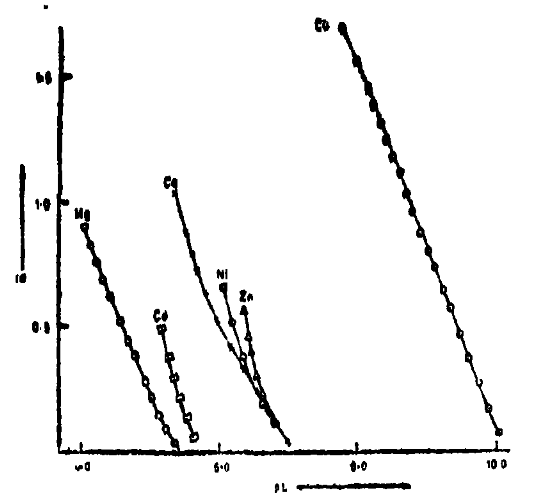


Fig. 3. Metal-ligand systems of *N*-(2-hydroxy-3-methoxybenzylidene)-2,4-dimethylaniline.

log K_2 was less than 1.78 log units, the values were better determined by least-square method.

The pK^H_{OH} values of the ligands were examined in the light of mesomeric and inductive effects of the substituents. The pK^H_{OH} value of *N*-(2-hydroxy-3-methoxybenzylidene)-2,6-dimethylaniline (b) is 9.83 and that of *N*-(2-hydroxy-3-methoxybenzylidene)-2,4-dimethylaniline (a) is 10.30. In the compound (b), the two methyl groups are flanking the azomethine nitrogen and hence bring in the steric repulsion, interfering with the coplanarity of the anilino ring with the six-membered chelate ring formed by the intra-molecular hydrogen bonding. It may thus result in the weakening of the hydrogen bond due to lesser electron donation from the methyl groups, as a result the pK^H_{OH} value of the compound (b) is less than that of compound (a), although both the compounds have two methyl groups in the anilino ring. The order of the stability constants for the ligand *N*-(2-hydroxy-3-methoxybenzylidene)-2,6-dimethylaniline is $Cu^{II} > Co^{II} > Zn^{II} > Ni^{II} > Cd^{II} > Mg^{II}$, and that for ligand *N*-(2-hydroxy-3-methoxybenzylidene)-2,4-dimethylaniline is $Cu^{II} > Zn^{II} > Co^{II} \simeq Ni^{II} > Cd^{II} > Mg^{II}$.

In the present study, graphs of stability constants of the complexes of the bivalent metal ions of the first transition series of both the ligands were plotted against atomic number of the elements (Fig. 4). It was observed that there was a monotonic rise to a maximum of Cu followed by a lower value of Zn. A similar relation was observed by Irving and Williams[8]. The plots also confirmed the observation that the stability seems to decrease with the increase in basicity of the metal, *i.e.* weakly basic metal like Cu forms stronger chelates and strongly basic metal like Mg forms weaker chelates[4]. The second ionisation potential rises along the transition series to a maximum of Cu and falls again at Zn. A correlation between second i nisation potential and complex stability was pointed out by other workers[5-7]. A similar relation was also observed in both the ligands under study (Fig. 5). Plots of log K of the same reagents

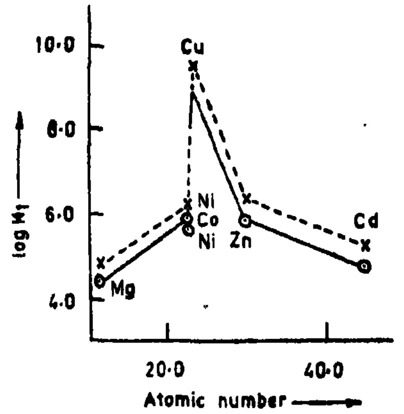


Fig. 4.
a (×)
b (◎)

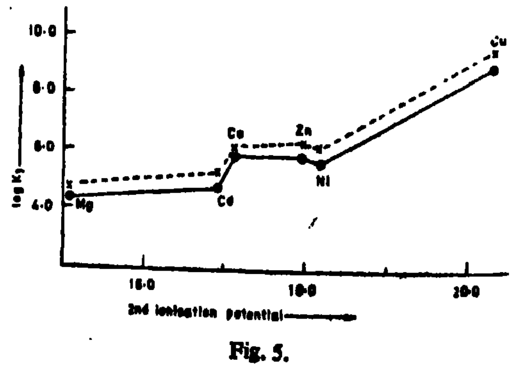


Fig. 5.
a (×)
b (◎)

TABLE 1—STEPWISE STABILITY CONSTANTS OF VARIOUS COMPLEXES

Temp. = 30 ± 0.1°, μ = 0.1 *M*

N-(2-Hydroxy-3-methoxybenzylidene)-2,6-dimethylaniline			*N*-(2-Hydroxy-3-methoxybenzylidene)-2,4-dimethylaniline		
Cation	log K_1	log K_2	Cation	log K_1	log K_2
H^+	9.83	2.10	H^+	10.30	3.325
Cu^{II}	9.00	–	Cu^{II}	9.48	8.26
Co^{II}	5.93	–	Zn^{II}	6.40	–
Zn^{II}	5.90	–	Co^{II}	6.20	–
Ni^{II}	5.73	–	Ni^{II}	6.20	–
Cd^{II}	4.77	–	Cd^{II}	5.25	–
Mg^{II}	4.37	–	Mg^{II}	4.75	–

against reciprocal of ionic radii of transition metal ions (Fig. 6) show that the ligands form weak complexes with Mg and stable complexes with Cu than with other bivalent transition metal ions.

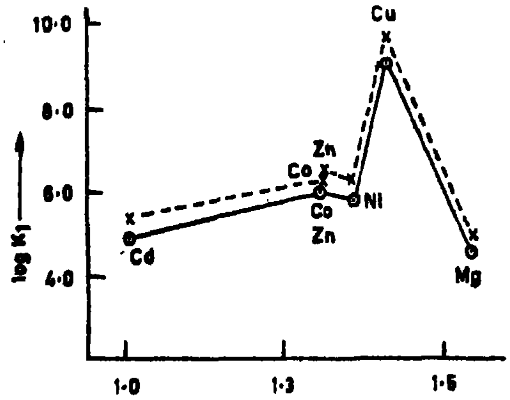


Fig. 6.
a (×)
b (⊙)

Acknowledgement

The authors wish to record their sincere thanks to Dr. D. G. Vartak, Bombay, for his valuable suggestions.

References

1. H. M. Irving and H. S. Rossotti, *J. Chem. Soc.*, 1954, 2904.
2. H. A. Flaschka, "EDTA Titrations", Pergamon, New York, p. 78.
3. H. Irving and R. J. P. Williams, *J. Chem. Soc.*, 1953, 3192.
4. A. E. Martell and M. Calvin, "Chemistry of Metal Chelates Compounds", Prentice-Hall, New York, 1956.
5. H. Irving and R. J. P. Williams, *Nature (London)*, 1948, 162, 146.
6. G. Schwarzenbach, H. Ackermann and J. Prue, *Nature (London)*, 1949, 163, 723.
7. M. Calvin and N. C. Melchoir, *J. Am. Chem. Soc.*, 1948, 70, 3270.

Studies of Formation Constants of Cinnamohydroxamic Acid Complexes with Lanthanum(III), Neodymium(III) and Samarium(III)

S. K. BRAHMA and A. K. CHAKRABURTTY*

Inorganic Chemistry Section, Jadavpur University, Calcutta-700 032

Manuscript received 26 November 1981, revised 24 December 1985, accepted 17 January 1986

THE flexibility of the coordination number of the rare earth ions[1] makes it interesting to study the nature of the rare earth-hydroxamate bond in the complexes with different types of simple and substituted hydroxamic acids[2-4]. The determination of stability constant values of some of the lanthanide-hydroxamate complexes, particularly those with NBPHA, was made previously[5]. In the present communication, the formation constant values of three lanthanide ions La^{III}, Nd^{III} and Sm^{III} with cinnamohydroxamic acid (CHA) in dioxane-water medium (3 : 1, v/v) are reported.

Experimental

The ligand cinnamohydroxamic acid (CHA) was prepared by the method described earlier[5]. The reagent was repeatedly recrystallised before use. The purity of the reagent was verified by m.p. (110-11°) determination and matching of ir spectra.

The perchlorates of the lanthanides used were prepared by digesting the corresponding oxides (Johnson Matthey, 99.9% pure) with perchloric acid and removing the excess acid by repeated evaporation. Finally, the perchlorates were dissolved in water and made up to definite volumes. Lanthanide ions were determined by oxalate precipitation and subsequent ignition to respective oxides[4]. Free perchloric acid present in the metal perchlorate solution were determined by running a known volume of the solution through a column of Amberlite IR-120 (H^+-form) and titrating the liberated acid with a standard sodium hydroxide solution[5] and subtracting the quantity of acid liberated M(III) ions.

Purified dioxane[6] and double-distilled (CO_2-free) water were used for making solutions. All other chemicals were of A R. grade.

Procedure : Experimental procedure consisted of titration of 40 ml dioxane-water (3 : 1, v/v) solutions containing 2×10^{-3} *M* metal ion, 2×10^{-3} *M* CHA and having a constant ionic strength (0.1*M*) maintained by adding requisite amounts of sodium perchlorate with a standard solution of NaOH in an inert (nitrogen) atmosphere at $30\pm0.5°$. The *p*H measurements were made with a Cambridge *p*H meter having a glass electrode (Universal type) and a calomel electrode connected to the cell by salt bridge. The acid dissociation constant of CHA was determined by a similar titration of the ligand in the absence of metal ion *p*H meter was calibrated using aqueous buffer solutions and the readings were converted to the stoichiometric hydrogen ion concentration incorporating correction for the use of mixed solvents[7] The absence of polynuclear and hydroxo-complexes in the complexation equilibrium was checked by using two different concentration of metal ions.

Results and Discussion

Successive formation constants K_1, K_2 and K_3 were evaluated by analysing the formation function,

$$\sum_{n=0}^{N} (\bar{n}-n)[L^-]^n \beta_n \quad (1)$$

by the computational method of Rossotti and Rossotti[8]. Maximum $\bar{n}$ values obtained in the present experiments was 2.5 which also supports our assumption of 1 : 3 complex formation. Mean log K values are presented in Table 1. The overall sability constants log β_3 for the rare earth-cinnamohydroxamate complexes were not comparable to

TABLE 1—FORMATION CONSTANT VALUFS OF LANTHANIDF-CINNAMOHYDROXAMATE COMPLEXES IN DIOXANE-WATER SOLVENT

Temp. = 30 ± 0.5°, μ = 0.1 *M*

pK^{H}CHA = 6.93

Metal ion	1/r(A^{o-1})	log K_1	log K_2	log K_3	log β_3
La^{III}	0.942	4.04	3.92	2.98	10.91
Nd^{III}	1.005	4.53	4.04	3.24	10.81
Sm^{III}	1.037	4.84	4.26	3.41	12.51

those of NBPHA[8] (in the same solvent mixture) or salicylhydroxamic acid[9] (in acetone-water solvent). In fact the log β_3 values of the lanthanide-NBPHA (≈22) and solicylhydroxamate complexes (≈19) were much higher than those of CHA complexes (≈11). Solid complexes of La^{III}, Nd^{III} and Sm^{III} with CHA have been prepared and analysed. The composition of these complexes were found to be Ln L_3. xH_2O (x=2 for La^{III} and 1 for Nd^{III} and Sm^{III}). The analytical data are given in Table 2.

TABLE 2—ANALYTICAL DATA OF HYDRATED LANTHANIDE-CINNAMOHYDROXAMATE COMPLEXES

Compd.	Colour	Analysis % : Found (Calcd.)		
		M	N	C
$La(C_9H_8NO_2)_3.2H_2O$	White	21.00 (21.01)	6 25 (6.35)	48.98 (49.02)
$Nd(C_9H_8NO_2).H_2O$	Pale pink	21.70 (21.85)	6 45 (6.51)	50.00 (50.25)
$Sm(C_9H_8NO_2)_3$	White	22.95 (22.98)	6 40 (6.41)	49.55 (49.50)

The ir spectra of the solid complexes showed broad bands (above 3 000 cm^{-1}), which could be ascribed to the presence of either coordinated or lattice water[10]. The $\nu_{C=O}$ of CHA (1 665 cm^{-1}) has been found to shift to 1 640 cm^{-1} in its sodium salt, whereas, for the lanthanide complexes a further shift towards lower frequencies (1 632 for La^{III}, 1 635 for Nd^{III} and 1 632 cm^{-1} for Sm^{III} complexes) were observed. The strong ν_{OH} (at 1 350 cm^{-1}) and ν_{NO} (at 976 cm^{-1}) bands of the free ligand were shifted to 1 370 and 960 cm^{-1}, respectively in the complexes. Thus, the lanthanide ions were probably attached to two coordination sites (C=O and NHO⁻) of the cinnomohydroxamate ion.

Acknowledgement

Thanks of the authors are due to Dr. M. Chaudhury of the I.A.C.S., Calcutta, for his help during this work.

References

1. S. P. SINHA, "Complexes of the Rare Earths", Pergamon Press, London, 1966.
2. S. K. BRAHMA and A. K. CHAKRABURTTY, *J. Indian Chem. Soc.*, 1980, 57, 942.
3. J. THIELE and R. H. PICKARD, *Ann. Chem.*, 1899, 194, 309.
4. S. K. BRAHMA and A. K. CHAKRABURTTY, *J. Inorg. Nucl. Chem.*, 1977, 39, 1723.
5. K. NAG and M. CHAUDHURY, *Indian J. Chem., Sect. A*, 1977, 15, 921.
6. A. I. VOGEL, "A Textbook of Practical Organic Chemistry", 3rd ed., Longmans, London, p. 177.
7. L. G. VAN UITERT and C. G. HASS, *J. Am. Chem. Soc.*, 1953, 75, 451.
8. F. J. C. ROSSOTTI and E. ROSSOTTI, "The Determination of Stability Constants", McGraw-Hill, London, 1961, p. 88.
9. N. K. DUTTA and T. SESHADRI, *Talanta*, 1970, 17, 168.
10. K. NAKAMOTO, "Infrared and Raman Spectra of Inorganic and Coordination Compounds", 3rd ed., Wiley-Interscience, New York, 1978, p. 227.

Rare Earths Complexes of some Amino Acids. A Polarographic Study

FARID KHAN*

Department of Chemistry, Doctor Harisingh Gour Vishwavidyalaya, Sagar-470 003

Manuscript received 29 November 1984, revised 30 September 1985, accepted 17 January 1986

AMINO acids have been used as complexing reagents with various metal ions[1-5]. Tewari and Shrivastava[6] reported the stability constants of La^{III}, Ce^{III}, Pr^{III}, Nd^{III} and Y^{III} complexes with L-asparagine and L-glutamine by potentiometric technique. The present paper is continuation of our previous work[7-9] and was undertaken with the view to determine the formation constants and thermodynamic parameters of Ce^{III} complexes with L-alanine, L-glutamine and L-asparagine on a dropping mercury electrode.

Experimental

All the chemicals were of A. R. grade. The solution of L-alanine (Eastman & Kodak), L-glutamine (B. D. H., England) and L-asparagine (E. Merck) were prepared in double distilled water and their purity was checked by chromatographic method[10]. The metal solution was prepared by dissolving weighted quantity of $CeCl_3.6H_2O$ (Fluka, A.G.) in distilled water and was standardised with EDTA[11]. The overall concentration of Ce^{III}, potassium chloride and gelatin in the test electrolytic solution was 1.0 m*M*, 1.0 *M* and 0.01%, respectively. The concentration of ligand was varied from 1.0 to 10.0 m*M* in each case. For the adjustment of ionic strength (μ) at 1.0 *M*, potassium chloride was used. Sodium hydroxide and hydro-

TABLE 1—STABILITY CONSTANTS AND THERMODYNAMIC PARAMETERS OF 1 : 1 COMPLEXES OF Ce^{III}

μ = 1.00 *M* KCl

Ligands	log K at temp. (°C)			ΔH k cal mol⁻¹ at temp. (difference of 10°)		ΔG k cal mol⁻¹ at temp. (°C)			ΔS cal K⁻¹ mol⁻¹ at temp. (°C)		
	25	35	45	(35-25)	(45-35)	25	35	45	25	33	45
L-Alanine	6.10	5.60	5.00	−21.14	· 40.28	−8.37	−7.94	−7.32	−42.83	−42.85	−103.65
L-Glutamine	3.72	3.15	2 65	−24.09	−37.95	−5.11	−4.47	−3.88	−63.70	−63.71	−107.14
L-Asparagine	3.52	3.60	−2.60	−21.99	−39.097	−4.83	−4.25	−3.80	−57.58	−57.60	−110.99

chloric acid were used to maintain *p*H of the test solution at 2.70 ± 0.02.

*p*H measurements were made on a Elico LI-120 digital *p*H meter. Polarograms were recorded on an automatic pen recording polarograph (C. I. C., India). The capilliary used had an 'm' value 2.18 mg s^{-1} and drop time 3.0 s at 43.0 cm effective height of mercury. Nitrogen gas was passed to remove dissolved oxygen from the solution before recording the polarograms. Measurements were made at 25, 35 and 45°.

Results and Discussion

A well defined three electron reversible reduction wave of Ce^{III} has been reported[12,13] at *p*H 2.70±0.02 in 1.0 *M* potassium chloride with 0.01% gelatin used as a maximum suppressor. The slopes of linear plots of log $i/(i_d-i)$ *vs* $E_{d.e.}$ were of the order of 21±1 mV for Ce^{III} and its complexes with all the three ligands indicating reversibility of the electrode process. The straight line plots of i_d *vs* $\sqrt{h}$ for metal ion and its complexes showed the diffusion-controlled nature of the waves. The reduction potential of Ce^{III} was −1.85 V against S.C.E. at *p*H 2.70±0.02.

The half-wave potential shifted to more negative value on increasing the concentration of ligand. The method of Lingane[14] was used to determine composition and stability constants. Thermodynamic parameters were calculated from the well known thermodynamic relations[15] and tabulated in Table 1.

The order of stability constants of Ce^{III} complexes with respect to ligands was found L-asparagine < L-glutamine < L-alanine and decrease with the increase of temperature.

Acknowledgement

The author is thankful to Head of the Department of Chemistry, for facilities.

References

1. E. M. ROGOZINA and T. M. PONIKAROVA, *Zh. Obsch. Khim.*, 1970, 40, 2357.
2. E. M. ROGOZINA and T. M. PONIKAROVA, *Zh. Obsch. Khim.*, 1968, 38, 1957.
3. S. D. MAKHIJANI and S. P. SANGAL, *J. Indian Chem. Soc.*, 1977, 54, 670.
4. B. S. SEKHON and S. L. CHOPRA, *Indian J. Chem.*, 1974, 12, 1322.
5. V. E. PLYUSHCHEV, G. V. NADEZHDINA, G. S. LOSEVA, V. V. MELLNIKOVA and T. S. PARFEROVA, *Izv. Vyssh. Uchebn. Zaved. Khim. Tekhnol.*, 1975, 18, 1029.
6. R. C. TEWARI and M. N. SHRIVASTAVA, *J. Inorg. Nucl. Chem*, 1973, 35, 3044.
7. F. KHAN and A. V. MAHAJANI, *J. Indian Chem. Soc.*, 1982, 59, 996.
8. F. KHAN and A. V. MAHAJANI, *J. Indian Chem. Soc.*, 1983, 60, 296.
9. F. KHAN, V. K. CHITALE and A. V. MAHAJANI, *J. Indian Chem. Soc.*, 1984, 61, 165.
10. A. A. KHAN and W. U. MALIK, *J. Indian Chem. Soc.*, 1963, 10, 566.
11. F. J. WELCHER, "The Analytical Uses of Ethylenediaminetetraacetic Acid", Van Nostrand, New York, 1957, pp. 174, 181.
12. L. MEITES, "Polarographic Technique", Interscience, New York, 1965, p. 628.
13. K. S. PITRE and V. K. CHITALE, "Proceedings of the Convention of Chemists : Abstract", 1980, Indian Chemical Society, Calcutta, Anal. 11.
14. J. J. LINGANE, *Chem. Rev.*, 1941, 29, 1.
15. K. B. YATSIMIRSKII and V. P. VASIL'EV, "Instability Constants of Complex Compounds", Pergamon, London, 1960, p. 60.

Physicochemical Studies of Complex Formation of Cyclopentane Tetracarboxylic Acid with Alkaline Earth Metals

A. K. MISRA*

Central Road Research Institute, New Delhi-110 020

and

K. SRINIVASULU

School of Studies in Chemistry, Vikram University, Ujjain

Manuscript received 20 May 1985, revised 16 September 1985, accepted 17 January 1986

CIS, cis, cis, cis-1,2,3,4-Cyclopentanetetracarboxylic acid (CPTA) and its different compounds were used for various purposes, such as in resins and rubber preparation[1], for plasticisers[2], and for surface treatment of metals and plasters[3]. So far, a systematic study of its complexes seems to be lacking although as a quadridentate ligand it has been of great interest in coordination chemistry. The present investigation deals with the determination of the formation constants of the all *cis*-

cyclopentanetetracarboxylic acid complexes of alkaline earth metals in aqueous medium using the Irving-Rossotti titration technique. The nature of the metal-ligand bond (in solids) of the complexes has been explained by studying their ir spectra and correlated with the formation constants of the complexes.

Experimental

A 0.05 *M* solution of the ligand, CPTA (Matheson ; m.p. 195-96°) was prepared in double distilled water. Stock solutions of metals were prepared from their metal nitrates, and standardised gravimetrically[5]. Stock solutions were diluted to 0.01*M* solutions for *p*H-metric titrations.

*p*H values were measured using a *p*H meter (*p*H 821, Electronic Corporation of India) with an expanded scale having an accuracy of ±0.02 log units and sensitivity ±0.01. The temperature was always maintained at 30±0.1°.

The following sets of solutions (total volume= 50 ml, ionic strength (μ)=0.19 *M* $HClO_4$) were titrated against carbonate-free NaOH (0.2 *M*): (i) 10 ml 0.05 *M* $HClO_4$ + 9 ml 1 *M* $NaClO_4$ + 31 ml H_2O, (ii) 10 ml 0.05 *M* $HClO_4$+10 ml 0.05 *M* ligand+9 ml 1 *M* $NaClO_4$+21 ml H_2O, and (iii) 10 ml 0.05 *M* $HClO_4$ + 10 ml 0.05 *M* ligand+ 9 ml 1 *M* $NaClO_4$+5 ml 0.01 *M* metal salt solution +16 ml H_2O. The metal to ligand ratio was kept 1 : 10 in all the titrations to satisfy the highest coordination number of the respective metal ion.

Equal volumes of equimolar solutions of the metal nitrates and ligand were mixed to isolate the complexes. The *p*H of the solutions were raised from 6.5 to 7.5 and the clear solutions were concentrated. On addition of ethanol the solid complexes were obtained which were filtered, washed several times with water-ethanol mixture and dried at 60-70°.

Results and Discussion

Proton-ligand stability constants were calculated considering four dissociable carboxylic groups in CPTA. The values of $\bar{n}H/(1-\bar{n}H)$ were plotted in the regions $0<\bar{n}H<1$, $1<\bar{n}H<2$, $2<\bar{n}H<3$, $3<\bar{n}H<4$. Such plots were linear (Fig. 1) and all the points falling on the linear curves in the above regions were considered for the calculation of log pK_1^H, log pK_2^H, log pK_3^H and log pK_4^H, the values of which come out to be 9.1709, 4.9500, 3.9313 and 2.5101, respectively. Metal-ligand stability constants of the complexes were calculated by applying least-square technique to the $\bar{n}$, *pL* data. The formation curves were drawn by plotting $\bar{n}$ *vs* *pL* values (Fig. 2) From these formation curves, the values of log K_1 and log K_2 for different metal complexes are given in Table 1.

The stability constants of alkaline earth metal complexes follow the order, $Be^{II} > Mg^{II} < Ca^{II} > Sr^{II} > Ba^{II}$ (Table 1). Be^{II} forms strongest complex in the series, while Mg^{II} has lower stability constant value than Ca^{II} as observed in case of other similar ligands[6,7].

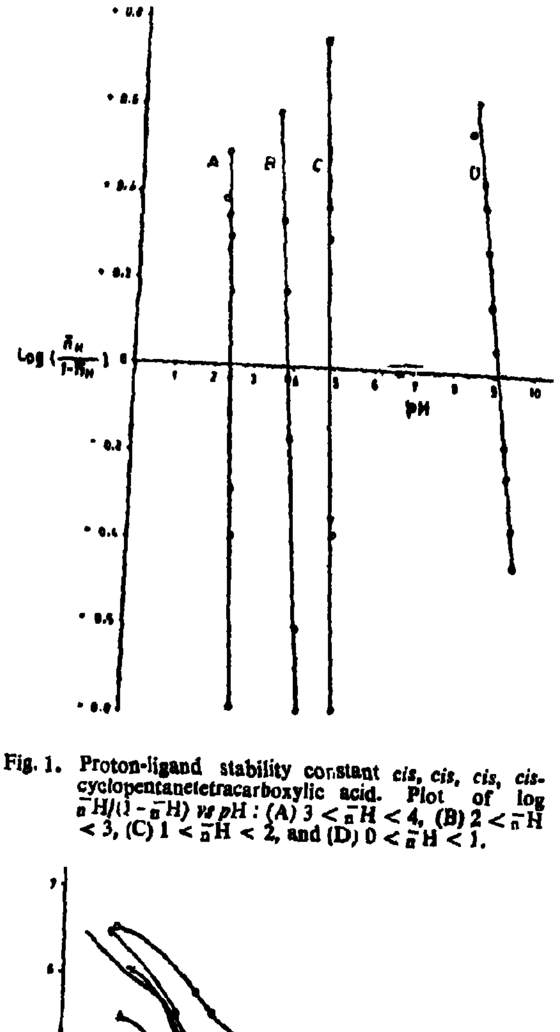


Fig. 1. Proton-ligand stability constant *cis, cis, cis, cis*-cyclopentanetetracarboxylic acid. Plot of log $\bar{n}H/(1-\bar{n}H)$ *vs* *p*H : (A) $3<\bar{n}H<4$, (B) $2<\bar{n}H<3$, (C) $1<\bar{n}H<2$, and (D) $0<\bar{n}H<1$.

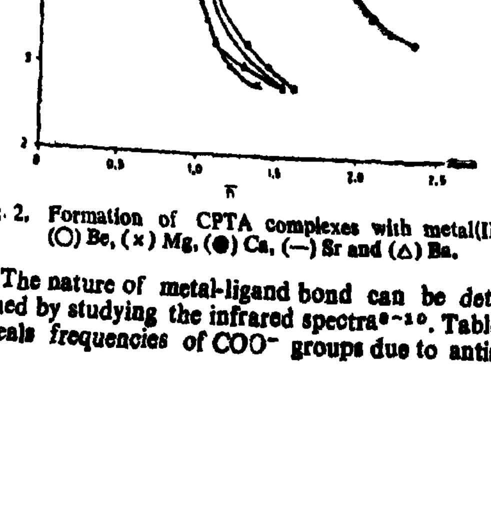


Fig. 2. Formation of CPTA complexes with metal(II): (O) Be, (×) Mg, (●) Ca, (—) Sr and (△) Ba.

The nature of metal-ligand bond can be determined by studying the infrared spectra[8-10]. Table 2 reveals frequencies of COO^- groups due to antisy-

TABLE 1—STABILITY CONSTANT OF ALKALINE EARTH METAL-CPTA COMPLEXES

μ = 0.19 *M*, temp = 30±0.1°

Metal(II)	log K_1	log K_2
Be	6.46 (±0.03)	4.90 (±0.05)
Mg	6.00 (±0.05)	–
Ca	6.15 (+0.04)	2.90 (±0.06)
Sr	5.90 (±0.05)	2.85 (±0.04)
Ba	5.38 (±0.07)	2.84 (±0.04)

TABLE 2 – INFRARED ABSORPTION PEAKS OF CARBOXYLIC GROUPS (ANTISYM. AND SYM.) AND THEIR DIFFERENCES IN ALKALINE EARTH METAL COMPLEXES

Metal(II)	ν_{COO^-} (antisym.) cm^{-1}	ν_{COO^-} (sym.) cm^{-1}	Frequency difference cm^{-1}
Be	1 600	1 379	221
Mg	1 550	1 360	190
Ca	1 540	1 388	152
Sr	1 540	1 418	122
Ba	1 526	1 408	118

mmetrical and symmetrical vibrations and their differences in CPTA-alkaline earth metal complexes. It can be seen that the differences of the frequencies in the region 1 660 to 1 525 and 1 420 to 1 360 cm^{-1} show the decrease in the order, $Be^{II} > Mg^{II} > Ca^{II} > Sr^{II} > Ba^{II}$ which is also the order of their ionic radii. This suggests that the order of decreasing stabilities of the complexes should also be same[11]. This is true for stability values except there is reversal in case of Mg^{II} and Ca^{II} complexes because Mg^{II} forms hydrate bonds in aqueous medium.

The study indicates that Be—O bond is less ionic in character than other alkaline earth metal complexes and this trend increases with the increase in their ionic radii.

References

1. R. VAN VOLKENBURGH, H. W. HYDE and C. ROYSTEN, U.S. Pat. 3 346 598/1967.
2. J.C. PETROPOULOUS and D. MEGNE, U.S. Pat. 3 211 691/1965.
3. J. W. TREBBIKCOCK, Fr. Pat. 1 335 000/1963.
4. H. M. IRVING and H. S. ROSSOTTI, *J. Chem. Soc.*, 1954, 2904.
5. A. I. VOGEL, "A Textbook of Quantitative Inorganic Analysis", Longmans, London, 1961, pp. 517-56.
6. S. CHABEREK and A. E. MARTELL, "Organic Sequestering Agents", Wiley, New York, 1959, p. 572.
7. H. KROLL and I. MATOS, *Am. Chem. Soc., Chicago*, 1958, 111.
8. D. H. BUSCH and J. C. BAILOR, JR., *J. Am. Chem. Soc.*, 1953, 75, 4574.
9. D. T. SAWYER and P. J. PAULSEN, *J. Am. Chem. Soc.*, 1958, 80, 1597.
10. D. T. SAWYER and P. J. PAULSEN, *J. Am. Chem. Soc.*, 1959, 81, 817.
11. J. C. BAILOR, JR., "The Chemistry of Coordination Compounds", Reinhold, New York, 1956, pp. 1765-77.

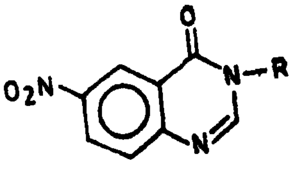
Effect of Nitro Group on the Mass Spectra of Quinazolinone Derivatives†

JALPANA ROY, BHAGAT RAM and A. P. BHADURI*

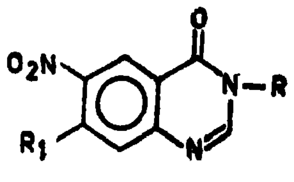
Division of Medicinal Chemistry, Central Drug Research Institute, Lucknow-226 001

Manuscript received 21 May 1979, accepted 11 September 1985

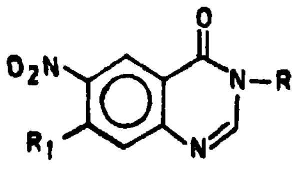
BEHAVIOUR of 4(3*H*-quinazolinone derivatives under electron impact have been studied earlier[1-3] but no attempt, however, appear to have been made to study the effect of nitro group on the phenyl part of the quinazolinone ring. In the absence of appropriate deuterated compounds, an attempt has been made to study the gross change in the breakdown pattern under electron impact ionisation conditions in the mass spectral study of this class of compounds possessing substituents on the phenyl part of the quinazolinone ring. The results obtained with the EI-MS-computor system are presented in this communication.



(1) R = CH_3



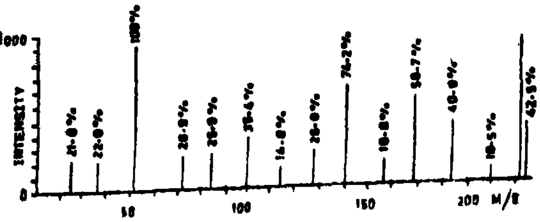
(2) R = H, R_1 = piperidyl
(3) R = H, R_1 = 2-methyl
(4) R = H, R_1 = 3-methyl
(5) R = CH_3, R_1 = piperidyl



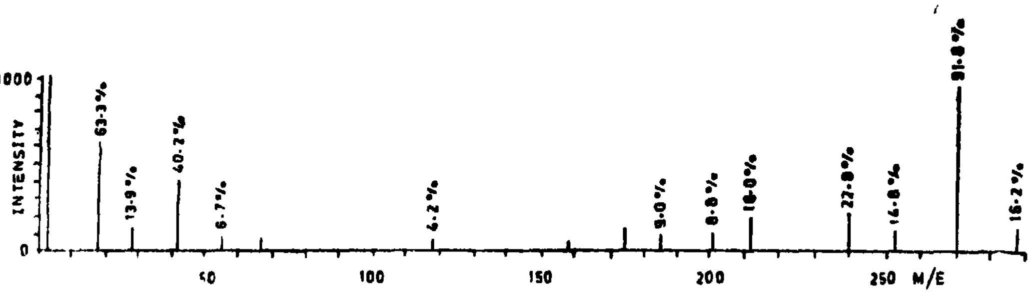
(6) R = CH_3, R_1 = morpholino

Earlier studies of various quinazolinone derivatives studied under electron impact mass spectrometry invariably led to the fragmentation of the pyrimidine part of the quinazolinone ring. Substituents such as nitro group with or without *ortho*-amino function should, in principle, exhibit their well known behaviour under electron impact[4]. Studies carried out with 1-6 revealed that the heterocyclic ring in 1 was not cleaved initially. The percentage abundance of the peaks appearing due to the loss of O, NO, NO_2 and also due to the loss of CO, CH_3CN and (CO + HCN) fragments, suggest that the predominant pathway of the breakdown appears to be mediated through the NO_2 group. In compounds 2-5, the absence of peaks

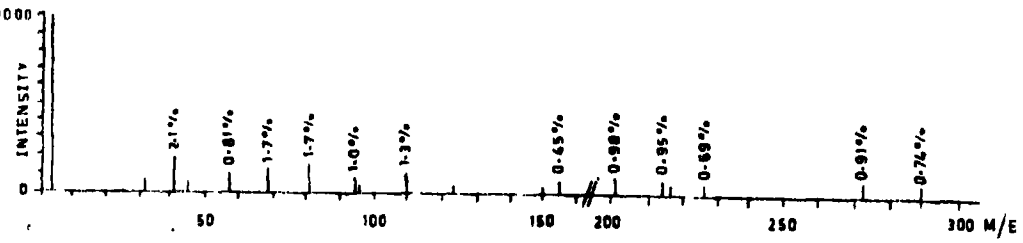
†C.D.R.I. Communication No. 2543.



(1)



(5)



(6)

for M^+-CO, M^+-CH_2CN and M^+-HCN clearly indicated that the breakdown did not initiate from the pyrimidine part of the quinazolone ring. The presence of peaks for M^+-H, M^+-CH_3, M^+-O M^+-H-O, M^+-NO, M^+-NO_2 and M^+-H-NO_2 in these compounds clearly revealed that the substituents at positions 6 and 7 participated in the breakdown of these compounds. Compound 6 disappeared immediately under the conditions used for compounds 2-5, in the mass spectrometer and so had to be recorded at lower probe temperature. The observed peaks, however, supported the aforementioned behaviour reported for 2-5. Computor print out of 1, 5 and 6 along with their percentage abundance is presented for the sake of clarity. The preparation of the compounds studied have been reported earlier[5].

References

1. T. J. Balterham, A. C. K. Triffett and J. A. Wunderlich, *J. Chem. Soc. B*, 1967, 892.
2. M. Luckner, K. Winter and L. Nover, *Tetrahedron*, 1969, 25, 2575.
3. R. R. Pradt, S. H. Bogers and A. Jordaan, *Tetrahedron*, 1967, 23, 3521.
4. R. M. Silverstein, G. C. Bassler and T. C. Morrill, "Spectrometric identification of organic compounds", New York, 1974, p. 33.
5. J. Roy, M. Seth and A. P. Bhaduri, *Indian J. Chem.*, *Sect. B*, 1978, 16, 42.

^{13}C Nmr Study of 5-Aryl-4-(3-methyl-5-styryl-4-isoxazolyl)-3-phenyl-Δ^2-1,2,4-oxadiazolines

E. RAJANARENDAR, C. JANAKIRAM RAO
and
A. KRISHNA MURTHY*

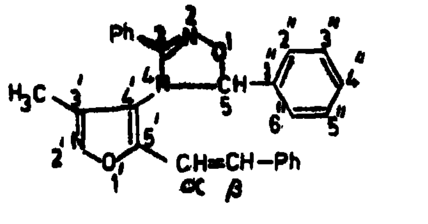
Department of Chemistry, Kakatiya University, Warangal-506 009

Manuscript received 11 April 1985, accepted 24 December 1985

THE synthesis and mass spectral behaviour[1] of 5-aryl-4-(3-methyl-5-styryl-4-isoxazolyl)-3-phenyl-Δ^2-1,2,4-oxadiazolines have been reported from these laboratories. ^{13}C nmr spectra of these compounds is discussed in this paper and this happens to be the first ever report on ^{13}C nmr data of isoxazolyloxadiazolines. ^{13}C nmr study of isoxazoloazepines has earlier been reported by us[2].

The chemical shift values of the various carbons of five isoxazolyloxadiazolines (1-5) studied, have been presented in Table 1. The assignments are based on chemical shifts, off-resonance multiplicities and internal consistency. In the spectrum of 3,5-diphenyl-4-isoxazolyloxadiazoline (1) with wide-band proton decoupling sixteen lines have been

listed in the computer printout of line frequencies. An off-resonance single frequency decoupling experiment showed that the multiplities of these lines due to proton decoupling correspond to seven singlets (quaternary carbons), eight doublets (CH carbons), and one quarter (CH_3). The fifteen aromatic CH of the three benzene rings come as five doublets.



(1)
(2) 4″-Cl
(3) 4″-OCH_3
(4) 4″-CH_3
(5) 3″-OCH_3, 4″-OH

The broadening of the methyl peak found in the range δ 9.0-10.8 ppm is most probably, due to coupling to [14]N nuclei. The signal which falls in the range 99.5-99.85 in all the compounds is assignable to the tertiary carbon atom of the oxadiazoline ring[3]. The two ethylenic carbons α and β resonate at 110 and 115, respectively. Carbon-β is more deshielded than carbon-α as it experiences the mesomeric withdrawal of electrons by the isoxazole ring C=N and hence resonates at lower field[3]. The absorption due to C′$_4$, which is part of the chromophore encompassing the isoxazole-ring double bonds and styryl moiety, is at 135.5, found in all the compounds. The peak at 158 is due to C′$_5$ which is flanked by ethylenic double bond and isoxazole ring oxygen. Assigning such a downfield absorption to this carbon is justified because it is also under the electron withdrawing influence of C=N of the isoxazole. All the five compounds show signal around 155 assignable, most probably, to C′$_3$. The most downfield signal of the spectrum at 161.30 is due to C_3 as it is an sp^2 carbon attached to two nitrogens in addition to a benzene ring.

TABLE 1—[13]C NMR CHEMICAL SHIFTS (δ) OF ISOXAZOLYLOXADIAZOLINES (1-5)[a]

Carbons	1	2	3	4	5
CH_3 (q)	9.00	10.65	9.63	9.45	9.18
3 (s)	161.20	161.25	161.00	161.29	161.50
5 (d)	99.70	98 29	99 85	99.69	98.50
α (d)	109.87	109.67	110.24	110.01	110.36
β (d)	115.20	115.73	114 32	115.60	115.62
3′ (s)	155.50	155.35	155.00	155.72	155.11
4′ (s)	135.50	136.00	135.80	135.00	135.42
5′ (s)	158.00	158.52	158.05	158 93	158.45
Miscellaneous[b]	–	–	55 29 (q.OMe)	21.01 (q.CH_3)	55.75 (q.OMe)
	–	134.20 (s, 4″)	159.40 (s, 4″)	136.50 (s, 4″)	157.05 (s, 3″)
	–	–	–	–	160.25 (s, 4″)

[a]Off-resonance muitiplicities in parenthesis. [b]Includes substituents on benzene ring in compounds 2-5.

The rest of the assignments are complicated by the presence of three aromatic rings which result in strong signals near 128 ppm which are not readily distinguished from one another.

Experimental

Instrument : Nucleus, [13]C ; frequency, 20 MHz, instrument, Varian FT-80A ; mode, FT ; lock, internal ; temperature, 30° ; solvent, (a) compounds 1-4 in $CDCl_3$ and (b) compound 5 in DMSO-d_6 ; concentration, 0.5 *M* ; tube size, 10 mm o.d. ; standard, TMS ; pulse width, 5 μs ; acquisition time, 1.0 s ; spectral width, 5 KHz ; number of transients, 80 000 and 110 000 ; number of data point, 10 000, decoupling conditions, decoupling mode (1), decoupler off set (56) ; flip angle, 45° ; repetition rate 1.0 s ; digital resolution, 1.6 points/Hz ; and resolution enhancement, sesitivity enhancement was employed, using a decreasing exponential weighting function with a time constant of 0.7 Hz, resulting in 0.45 Hz line broadening.

Acknowledgement

The authors thank Prof. E. V. Sundaram, Head, Department of Chemistry and Dean, Faculty of Science, Kakatiya University, Warangal, for facilities and Dr. J. N. Shoolery for the spectra.

References

1. B. RAJANARENDAR, C. J. RAO and A. K. MURTHY, *Indian J. Chem., Sect. B*, 1981, **20**, 839.
2. C. J. RAO, A. K. MURTHY and J. N. SHOOLERY, *Org. Magn. Reson.*, 1983, **21**, 77.
3. E. RAJANARENDAR, Ph.D. Thesis, Kakatiya University, Warangal, 1982, p. 55.

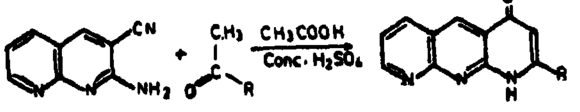
Synthesis of 2-Aryl-4(1*H*)-anthyridinones

K. MOGILAIAH, K. RAJENDAR REDDY, K VIJAYENDER REDDY and B. SREENIVASULU*

Department of Chemistry, Kakatiya University, Warangal-506 009

Manuscript received 4 July 1985, accepted 24 December 1985

SCANTY information is available in literature concerning the chemistry of anthyridines[1-4]. In the present communication, a series of hitherto unknown 2-aryl-4(1*H*)-anthyridinones are reported.



(1) (2) (3)

Scheme 1

TABLE 1—PHYSICAL DATA OF 2-ARYL-4(1*H*)-ANTHYRIDINONES (3)*

Sl. no.	R	Yield %	Molecular formula	Analysis %: Found/(Calcd.) C	H	N
1.	Phenyl	65	$C_{17}H_{11}N_3O$	74.70 (74.73)	4.05 (4.03)	15.31 (15.38)
2.	*p*-Tolyl	80	$C_{18}H_{13}N_3O$	75.20 (75.26)	4.50 (4.53)	14.56 (14.63)
3.	*p*-Methoxyphenyl	82	$C_{18}H_{13}N_3O_2$	71.20 (71.29)	4.21 (4.29)	13.85 (13.86)
4.	*o*-Hydroxyphenyl	71	$C_{17}H_{11}N_3O_2$	70.52 (70.59)	3.75 (3.81)	14.59 (14 53)
5.	*p*-Hydroxyphenyl	75	$C_{17}H_{11}N_3O_2$	70.50 (70.59)	3.79 (3.81)	14 50 (14 53)
6.	*p*-Chlorophenyl	80	$C_{17}H_{10}N_3OCl$	66.35 (66.45)	3.22 (3.26)	13.63 (13.68)
7.	*p*-Bromophenyl	78	$C_{17}H_{10}N_3OBr$	57.99 (57 95)	2.85 (2.84)	11.91 (11.93)
8.	*m*-Nitrophenyl	65	$C_{17}H_{10}N_4O_3$	64.07 (64.15)	3.11 (3.14)	17.52 (17.61)
9.	*p*-Nitrophenyl	67	$C_{17}H_{10}N_4O_3$	64.04 (64.15)	3.11 (3.14)	17.55 (17.61)
10.	2-Hydroxy-4-chlorophenyl	70	$C_{17}H_{10}N_3O_2Cl$	63 19 (63.16)	3.05 (3.10)	13.09 (13.00)
11.	2-Hydroxy-4-methylphenyl	72	$C_{18}H_{13}N_3O_2$	71.21 (71.29)	4.25 (4 29)	13 95 (13.86)
12.	α-Naphthyl	65	$C_{21}H_{13}N_3O$	77.94 (78.02)	4.00 (4.02)	13.05 (13.00)
13.	β-Naphthyl	66	$C_{21}H_{13}N_3O$	77.95 (78.02)	4.01 (4.02)	13.07 (13 00)
14.	2-Pyridyl	68	$C_{16}H_{10}N_4O$	70 00 (70.07)	3 61 (3.65)	20.57 (20.44)
15.	3-Pyridyl	70	$C_{16}H_{10}N_4O$	70.01 (70.07)	3.61 (3.65)	20 58 (20.44)
16.	4-Pyridyl	70	$C_{16}H_{10}N_4O$	7'.00 (70.07)	3.61 (3.65)	20.57 (20.44)
17.	2-Furyl	67	$C_{15}H_9N_3O_2$	68.51 (68.44)	3.38 (3.42)	15.81 (15.97)
18.	2-Thienyl	69	$C_{15}H_9N_3OS$	64 44 (6'.52)	3.21 (3.23)	15.00 (15.05)

*All compounds have high m p. 300°.

The starting compound 2-amino-3-cyano-1,8-naphthyridine (1) was obtained by the condensation of 2-aminonicotinaldehyde with malonitrile in ethanol with piperidine as catalyst[5]. Condensation of 1 with aryl methyl ketones (2) in glacial acetic acid with a trace of concentrated sulphuric acid gave 2-aryl-4(1*H*)-anthyridinones (3) in good yield (Scheme 1). All the synthesised compounds were satisfactorily characterised by elemental analyses and ir spectral data. In the ir spectra, the absence of a characteristic strong band at 2 200 cm^{-1} indicated the absence of cyano group. 3 exhibited characteristic bands at 1 680 (C=O) and 3 300 cm^{-1} (NH) and an intense band at 1 600 cm^{-1} (C=N). The spectra also exhibited bands at 1 490, 1 460, 1 400, 1 380, 1 220, 1 180, 1 100, 9:0, 870 and 730 cm^{-1}. The pertinent data of the compounds thus prepared are recorded in Table 1.

Experimental

All the melting points were taken in open capillaries and are uncorrected. Ir spectra (nujol) were recorded on a Perkin-Elmer 283 spectrophotometer. The homogeneity and purity of the compounds were tested by tlc.

2-Amino-3-cyano-1,8-naphthyridine (1): It was prepared by the condensation of 2-aminonicotinaldehyde with malonitrile by the method of Hawes and Wibberley[5] in 95% yield, m.p. 261° (lit. 260-2°); ν_{max} (nujol) 3 450, 3 250, 2 200, 1 640, 1 600, 1 5:0, 1 495, 1 440, 1 150, 1 060 and 780 cm^{-1}.

*2-Aryl-4(1*H*)-anthyridinones* (3): A mixture of 1 (0.1 mol) and appropriate aryl methyl ketone (2, 0.1 mol) was refluxed in glacial acetic acid (30 ml) in the presence of a catalytic amount of concentrated sulphuric acid for 4 h. The reaction mixture was allowed to cool and poured onto crushed ice. The separated solid was filtered and recrystallised from aqueous acetic acid to give 3.

Acknowledgement

The authors thank Prof. E. V. Sundaram, Head, Department of Chemistry and Dean, Faculty of Science, Kakatia University, Warangal, for facilites. Two of the authors (K. V. R. and B. S.) thank U. G. C., New Delhi, for financial support and the others (K. R. R. and K. M.) thank C. S. I. R., New Delhi, for the award of Junior Research Fellowship and Pool Officer, respectively.

References

1. S. CARBONI, A. DA SETTIMO, P. L. FERRACINI, I. TONETTI and D. BERTINI, *Gazz. Chim Ital.*, 1967, 97, 1274.
2. S. CARBONI, A. DA SETTIMO, D. BERTINI, P.L. FERRACINI, O. LIVI and I. TONETTI, *J. Heterocycl. Chem.*, 1972, 9, 801, and references therein.
3. S. CARBONI, A. DA SETTIMO and I. TONETTI, *J. Heterocycl. Chem.*, 1970, 7, 875.
4. P. CALUWE and T. G. MAJEWICZ, *J. Org. Chem.*, 1977, 42, 3410.
5. E. M. HAWES and D. G. WIBBERLEY, *J. Chem. Soc.* (*C*), 1967, 1564.

Syntheses and Nucleophilic Additions to Conjugated Imines of 3-(2-Methoxyphenyl)-5-(4-aminophenyl) isoxazole and 1,2-Dihydro-5-acenaphthylene-carboxaldehyde

BHARAT J. SANYAL, FREDDY H. HAVALDAR
and
PETER S. FERNANDES*

Nadkarny-Sacasa Research Laboratory, St. Xavier's College, Bombay-400 001

Manuscript received 1 April 1985, revised 9 August 1985, accepted 2 December 1985

AZOMETHINES are known to undergo addition reactions wherein a variety of reagents add on to the polarised double bond[1,2]. In continuation of our earlier work, we have carried out syntheses of some imines by reacting 3-(2-methoxyphenyl)-5-(4-aminophenyl)isoxazole with aromatic aldehydes and reacting 1,2-dihydro-5-acenaphthylenecarboxaldehyde[3] with aromatic amines. The imines **1-7** subsequently obtained gave good yields of cyano-imines (**8-14**) on treatment with potassium cyanide in the presence of traces of acetic acid. The imines (**1-7**) were also reduced to the dihydro products (**15-21**) with sodium borohydride.

Experimental

All melting points were determined in open capillary tubes and are uncorrected. The ir spectra were obtained in KBr pellets and the nmr spectrum in $CDCl_3$.

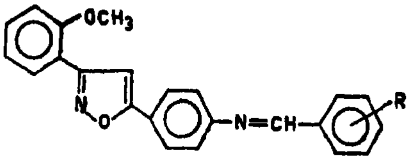
3-(2-Methoxyphenyl)-5-(4-aminophenyl) isoxazole : 4'-Nitroflavone was synthesised by the reported procedure[4]. 4'-Nitroflavone was reacted with hydroxylamine hydrochloride to yield 3-(2-hydroxyphenyl)-5-(4-nitrophenyl)isoxazole (A) (70%), m.p. 230°. Alternately, (A) was also obtained by reacting 4'-nitro-2-hydroxydibenzoylmethane with hydroxylamine hydrochloride.

Compound (A) was then methylated by using dimethyl sulphate and refluxing with fused potassium carbonate in dry acetone to yield, 3-(2-methoxyphenyl)-5-(4-nitrophenyl)isoxazole (B) (60-65%), m.p.174°.

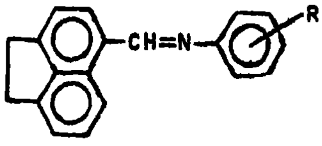
Compound (B) was then reduced by using granulated tin and conc. hydrochloric acid to yield the amine 3-(2-methoxyphenyl)-5-(4-aminophenyl) isoxazole (50%). m.p. 137° (Found : C, 72.14 ; H, 5.28 ; N, 10.47. $C_{16}H_{14}N_2O_2$ requires : C, 72.18 ; H, 5.26 ; N, 10.52%) ; ν_{max} 1 626 (C=N of isoxazole ring), 1 054 (OCH_3) and 3 500 cm^{-1} (NH of primary amine) ; δ 3.69 (2H, bs, NH_2), 3.94 (3H, s, OCH_3), 6.9 (1H, s, C=CH of isoxazole), 6.75-7.9 (8H, m, ArH).

1,2-Dihydro-5-acenaphthylenecarboxaldehyde[5] : A mixture of acenaphthene, *N*-methylformanilide, phosphorous oxychloride in *o*-dichlorobenzene was reacted to yield the desired aldehyde.

TABLE 1



1-4



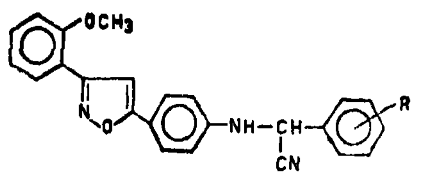
5-7

Compd. no.	R	Molecular formula	M.p. °C	Yield %	N% : Found/ (Calcd.)
1	2-Ph	$C_{23}H_{18}N_2O_3$	174	85	7.49 (7.56)
2	4-NO_2	$C_{23}H_{17}N_3O_4$	137	60.5	10.43) (10.52
3	4-OCH_3	$C_{24}H_{20}N_2O_3$	134	70	7.18) (7.29
4	H	$C_{23}H_{18}N_2O_2$	91	65	7.84) (7.90
5	4-NO_2	$C_{19}H_{14}N_2O_2$	105	80	9.13) (9.27
6	H	$C_{19}H_{15}N$	98	60	5.36 (5.45)
7	4-Cl	$C_{19}H_{14}NCl$	103	70	4.68 (4.80)

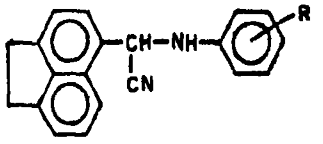
Imines **1-7** (*Table 1*) : (i) The isoxazole amine (0.01 mol) was dissolved in ethanol, acidified by adding a few drops of acetic acid, and then various aromatic aldehydes (0.01 mol) were added. The mixture was refluxed for 2 h. The product (**1-4**) separated on cooling, was filtered and crystallised from ethanol. (ii) The acenaphthylene-carboxaldehyde (0.01 mol) was dissolved in ethanol containing a few drops of acetic acid. The mixture was refluxed for 2 h. The product (**5-7**) which separated on cooling was filtered and crystallised from ethanol. The ir spectrum (KBr) showed the absorption for CH=N at 1 668 cm^{-1}.

Addition of HCN to imines **8-14** (*Table 2*) : The appropriate imine (1-7 ; 0.01 mol) was dissolved in methanol and the solution was made acidic by adding a few drops of acetic acid. Potassium cyanide (0.01 mol in 10 ml water) was added to the imine solution with continuous stirring at 0-5°. The product (8-14) obtained was filtered and recrystallised from methanol. 1-4 gave nitriles 8-11, whereas 5-7 yielded nitriles 12-14. The cyanoimines showed the absorption at 3 430 (NH) and 2 245 cm^{-1} (C≡N).

TABLE 2



8-11

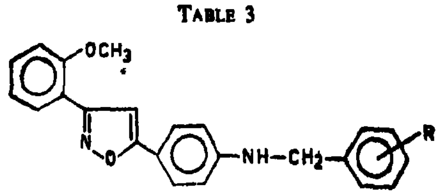


12-14

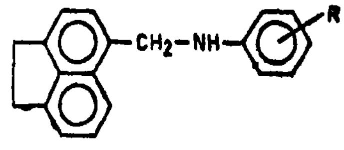
Compd. no.	R	Molecular formula	M.p. °C	Yield %	N% : ound/ (Calcd.)
8	2-OH	$C_{24}H_{19}N_3O_3$	185	80	10.50 (10.57)
9	4-NO_2	$C_{24}H_{18}N_4O_4$	197	67	13.03 (13.14)
10	4-OCH_3	$C_{25}H_{21}N_3O_3$	193	75	10.15 (10.21)
11	H	$C_{24}H_{19}N_3O_2$	158	70	10.93 (11.02)
12	4-NO_2	$C_{20}H_{15}N_3O_2$	95	70	12.85 (12.77)
13	H	$C_{20}H_{16}N_2$	135	60	9.75 (9.86)
14	4-Cl	$C_{20}H_{15}N_2Cl$	173	63	8.90 (8.79)

Reduction of imines **15-21** *with* $NaBH_4$ (*Table 3*) : Sodium borohydride (0.03 mol) was added to a methanolic solution of the imine (0.02 mol) over a period of 30 min at 5-10°. The mixture was then kept overnight at room temperature. The excess sodium borohydride was neutralised by adding water and the product extracted with ether. The ether extract was washed with water until neutral, dried over anhydrous sodium sulphate and finally evaporated. The compound (15-21) thus obtained was recrystallised from methanol. 1-4 gave the dihydro compounds (15-18), whereas 5-7 gave the dihydro compounds 19-21. The dihydro products showed the absorption at 3 300-3 250 cm^{-1} (NH).

TABLE 3



15-18



19-21

Compd. no.	R	Molecular formula	M.p. °C	Yield %	N% : Found/ (Calcd.)
15	2-OH	$C_{22}H_{20}N_2O_3$	129	55	7.44 (7.52)
16	4-NO_2	$C_{22}H_{19}N_3O_4$	209	50	10.39 (10.47)
17	4-OCH_3	$C_{24}H_{22}N_2O_3$	107	56-60	7.17 (7.25)
18	H	$C_{22}H_{20}N_2O_2$	169	45	7.79 (7.86)
19	4-NO_2	$C_{19}H_{16}N_2O_2$	84	60	9.16 (9.21)
20	H	$C_{19}H_{17}N$	115	52	5.32 (5.41)
21	4-Cl	$C_{19}H_{16}NCl$	165	56	4.82 (4.77)

The nitro substituted derivative showed the absorption at 1 520 cm^{-1} which indicates that the NO_2 group does not undergo reduction during the reaction with borohydride.

References

1. N. SINGH and P. S. SETHI, *J. Indian Chem. Soc.*, 1975, 52, 1079.
2. P. S. FERNANDES, N. N. JOSHI, A. J. MENEZES, V. D'SOUZA and V. V. NADKARNY, *J. Indian Chem. Soc.*, 1977, 54, 923.
3. L. F. FIESER and J. E. JONES, *J. Am. Chem. Soc.*, 1942, 64, 1666.
4. P.S. FERNANDES and L. COUTINHO, *J. Indian Chem. Soc.*, 1983, 60, 864.

Synthesis and Antifungal Activity of Hydroxyphenylethylidenebenzylamines

M. R. MANRAO* and SUNITA KOHLI

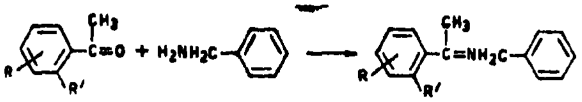
Department of Chemistry, Punjab Agricultural University, Ludhiana-141 004

Manuscript received 20 May 1985, accepted 2 December 1985

A detailed survey of the literature reveals that there are only a few instances[1,2] where imines have shown antifungal activity, and most of these imines have at least one halogen atom which

has its own effect. In order to find out whether the imines having no halogen atom are also active against fungus, some ketimines[a] were synthesised by condensing various ketones with benzylamine. But these imines were found to have little effect against fungus. It has been reported that presence of hydroxyphenyl group in some compounds increases the activity[4,5]. So it was proposed to synthesise new ketimines having hydroxyphenyl group. This paper describes the synthesis of 2-hydroxyphenylethylidenebenzylamine (1), 4-hydroxyphenylethylidenebenzylamine (2), 2,4-dihydroxyphenylethylidenebenzylamine (3), 2,5-dihydroxyphenylethylidenebenzylamine (4) and 2,6-dihydroxyphenylethylidenebenzylamine (5), their spectral studies and antifungal activity.

2-Hydroxyacetophenone, 4-hydroxyacetophenone, 2,4-dihydroxyacetophenone, 2,5-dihydroxyacetophenone and 2,6-dihydroxyacetophenone which fail to give imines with aniline and substituted anilines perhaps due to steric hinderance offered by methyl group, yielded crystalline compounds (1-5) with benzylamine in quantitative yields.



The ketimines have been identified and confirmed on the basis of elemental analysis and spectral studies. Uv spectra of these ketimines indicate three absorption bands at 212, 265 and 340 nm. The band at 265 nm is used to identify the azomethine linkage as is shown by the fact that this band completely disappears on reduction of the ketimines with sodium borohydride. Ir spectrum of 1 shows absorption band at ~ 1 620 (azomethine) and ~ 3 500 cm^{-1} (phenolic). The lowering of the absorption value in the former case is attributed to the presence of intra-molecular hydrogen bonding[6]. Nmr spectrum of 1 indicates nine aromatic protons as a multiplet between τ 2.6-3.2, three methyl protons as a singlet at τ 7.7, two methylene protons as a singlet at τ 5.2 and the phenolic proton at τ 1.8 as a singlet. In mass spectra molecular ion peaks constitute the base peaks. Another common and important peak in all the spectra is at 91 which is ascribed to $C_6H_5CH_2^+$ species. The physical data of the ketimines are recorded in Table 1.

TABLE 1

Compd. no.	R	R'	Yield %	M.p.* °C	Molecular formula**
1	H	2-OH	95	110	$C_{15}H_{15}NO$
2	4-OH	2-H	95	135	$C_{15}H_{15}NO$
3	4-OH	2-OH	95	90	$C_{15}H_{15}NO_2$
4	5-OH	2-OH	90	185	$C_{15}H_{15}NO_2$
5	6-OH	2-OH	90	115	$C_{15}H_{15}NO_2$

*Uncorrected. **All gave satisfactory elemental analyses.

Antifungal activity: The new ketimines (1-5) were tested for their antifungal activity against *Alternaria triticina*, *Alternaria tenuis*, *Puccinia striformis*, *Puccinia recondita* and *Pestalotia psidii* by employing standard method of spore germination inhibition. Four concentrations, *viz.* 1 000, 500, 250 and 100 ppm of each of the compounds have been tried against all the test fungi. All the compounds have been found to possess promising antifungal activity against the above fungi and caused 100% spore germination inhibition at 1 000 ppm. The other three concentrations were also effective (Table 2). Substitution by the second hydroxyl particularly in 6-position, increases the activity of the parent compound.

TABLE 2—ANTIFUNGAL ACTIVITY OF HYDROXYPHENYLETHYLIDENEBENZYLAMINES

Comd. no.	Conc. ppm	Activity (% spore germination inhibition) *A. triticina*	*A. tenuis*	*P. striformis*	*P. recondita*	*P. psidii*
	1 000	100.0	100.0	100.0	100.0	100.0
1	500	100.0	100.0	95.5	96.2	98.2
	250	92.2	69.2	62.1	54.4	47.3
	100	33.2	21.5	17.15	18.4	25.1
	1 000	100.0	100.0	100.0	100.0	100.0
2	500	92.7	90.1	80.5	90.0	90.2
	250	63.1	53.4	51.2	47.2	42.2
	100	29.9	20.4	20.6	15.6	32.2
	1 000	100.0	100.0	100.0	100.0	100.0
3	500	100.0	100.0	96.1	79.2	82.1
	250	74.2	70.1	69.2	65.2	64.3
	100	35.6	27.9	23.6	17.1	20.1
	1 000	100.0	100.0	100.0	100.0	100.0
4	500	100.0	100.0	92.1	100 0	83.3
	250	72.1	73.4	64.2	52.5	55.1
	100	32.3	28.1	20.3	10.3	19.2
	1 000	100.0	100.0	100.0	100 0	100.0
5	500	100.0	100.0	97.2	98.7	100.0
	250	81.2	75 9	72.0	62.2	67.3
	100	41.3	36 2	34.7	25.5	31.4

Experimental

The following general procedure was used for the synthesis of hydroxyphenylethylidenebenzylamines.

A mixture of 2-hydroxyacetophenone (0.1 mol), benzylamine (0.1 mol) and toluene (125 ml) was refluxed using a 'Dean and Stark' apparatus. Distillation of the solvent after the azotropic removal of water formed during the reaction gave the crude ketimine which was recrystallised from ethanol to yield fine yellow crystals of 2-hydroxyphenylethylidenebenzylamine (95%), m.p. 110°.

Testing of the compounds against fungus: Four concentrations (1 000, 500, 250 and 100 ppm) of 1 were taken and treated against *Puccinia striformis*. The treated spores were incubated for 18 h and per cent spore germination inhibition was calculated by

counting 200 spores of each treatment. Spores incubated in water and respective solvent in which the compound was dissolved were used as control. Percentage spore germination inhibition was calculated using the standard formula. Similarly, other ketimines (2-5) were tested for their antifungal activity against *Puccinia striformis*, *Puccinia recondita*, *Alternaria triticina*, *Alternaria tenuis* and *Pestalotia psidii*

References

1. H. PACHECO, L. CRONENBERGER, D. PILLON and J. THIOLLIERE, *Chem. Abstr.*, 1970, **72**, 111001, 111002.
2. P. PROGIL, *Chem. Abstr.*, 1969, **71**, 69660.
3. M. RAI and A. SINGH, *Indian J. Chem.*, *Sect. B*, 1976, **14**, 365.
4. J. LEE, H. ZIERING, S. D. HEINEMANN and L. BERGER, *J. Org. Chem.*, 1947, **12**, 885.
5. O. J. BRAENDEN, N. B. EDDY and B. HABACH, *Bull. World Health Org.*, 1955, **13**, 935.
6. J. FABIAN, M. LEGRAND and P. POIRIERS, *Bull. Soc. Chim. Fr.*, 1956, **287**, 1499.

Reaction of Azlactone with Veratraldehyde Schiff Bases

MANGAT RAI*, BALJIT KAUR and P. S. KALSI

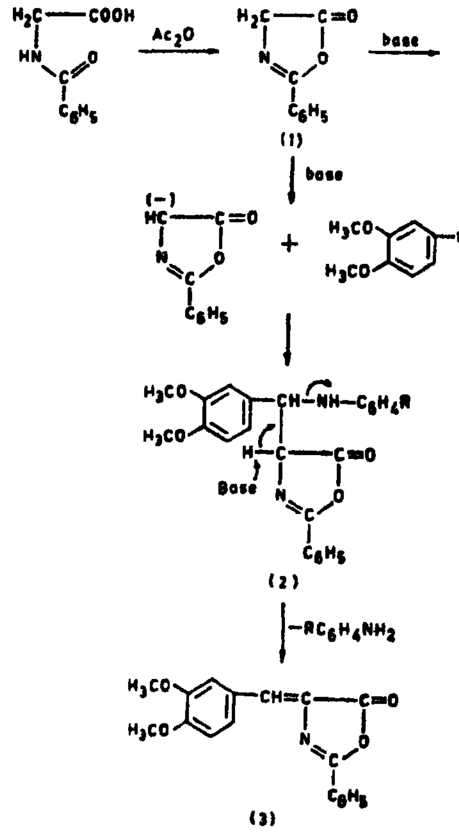
Department of Chemistry, Punjab Agricultural University, Ludhiana-141 004

Manuscript received 12 October 1984, revised 30 August 1985, accepted 24 December 1985

REACTION of azlactones, which are obtained *in situ* from α-acylamido acids, with carbonyl compounds constitutes a special case of the Perkin reaction. Cinnamalanilines and azlactone of benzoylalanine have been shown to undergo a (4+2)-cycloaddition reaction[2]. In continuation of the work on this reaction with disubstituted benzalanilines[3], this paper describes the reaction of benzoylglycine with veratraldehyde Schiff bases[4].

A crystalline product, m.p. 162°, was obtained in quantitative yield by the reaction of azlactone, prepared from hippuric acid and acetic anhydride *in situ* in presence of sodium acetate, with 3,4-dimethoxybenzalniline. On the basis of elemental analysis, ir and nmr studies, the compound has been identified as 2-phenyl-4-(3,4-dimethoxybenzal)-5-oxazolone (3). Ir spectrum of the product shows absorption bands at 1 750 and 1 670 cm^{-1} indicative of C=O and C=N linkage, respectively. Nmr spectrum ($CDCl_3$) of the product indicates 6 methoxy protons at τ 6.0 as a singlet, and a multiplet at τ 2.2-3.4 equivalent to 4 protons thereby showing that olefinic proton merges with the aromatic protons.

It seems, 3 is formed through the electrophilic addition of the enolate, produced by the abstraction of a proton by base from the active methylene part of the azlactone to the Schiff base to give an unstable adduct (2) followed by elimination of amine in the presence of base (Scheme 1).



Scheme 1

The product 3 is confirmed by m.m.p. determination (no depression) with authentic sample of 2-phenyl-4-(3,4-dimethoxybenzal)-5-oxazolone synthesised by an unambiguous route[1]. Electron-donating substituents (*p*-OEt, *p*-OMe, *p*-Me) in the *N*-phenyl nucleus facilitate the reaction as shown by higher yields of the product, whereas electron-withdrawing groups (Cl, Br) retard it. However, the same product was obtained after amine elimination in all the cases.

Experimental

Reaction of azlactone (1) *with 3,4-dimethoxybenzalaniline :* Hippuric acid (1.8 g, 0.01 mol) and 3,4-dimethoxybenzalaniline (2.41 g, 0.01 mol) were dissolved in dry benzene (50 ml) and to it acetic anhydride (A.R. ; 1.2 ml) added. The mixture was heated and allowed to stand at room temperature for 2 days. During this period most of the crude product separated out which was filtered under reduced pressure. The mother liquor on concentration yielded a further crop. The combined crude product

was recrystallised from hot benzene to give light brown crystals of 2-phenyl-4-(3,4-dimethoxybenzal)-5-oxazolone (80%), m.p. 162° (Found: C, 70.02; H, 4.82; N, 4.48. $C_{18}H_{15}NO_4$ calcd. for: C, 69.90; H, 4.85; N, 4.53%).

Reaction with 3,4-dimethoxybenzal-*p*-toluidine, 3,4-dimethoxybenzal-*p*-anisidine, 3,4-dimethoxybenzal-*p*-phenetidine, 3,4-dimethoxybenzal-*p*-chloroaniline and 3,4-dimethoxybenzal-*p*-bromoaniline was carried out by using the above procedure. The above reactions also resulted in formation of 2-phenyl-4-(3,4-dimethoxybenzal)-5-oxazolone (3) (85-70%).

References

1. A. H. Blatt, *Org. Synth.*, 1961, **2**, 55.
2. S. Mohan, B. Kumar and J. S. Sandhu, *Chem. Ind. (London)*, 1971, 671.
3. M. Rai, K. Krishan and A. Singh, *Indian J. Chem., Sect. B*, 1977, **15**, 847.
4. M. Rai, B. Kaur and B. S. Dhir, *J. Indian Chem. Soc.*, 1982, **56**, 416.

Synthesis of some New Antifungal Tetrazolyl Sulphides

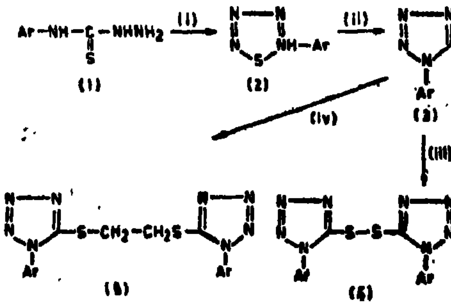
S. K. SANGAL* and ASHOK KUMAR

Department of Chemistry, Meerut College, Meerut-250 001

Manuscript received 1 April 1985, accepted 2 December 1985

A well known fact about 1,2,3,4-tetrazoles is that they have a varied spectrum of biological activities[1]. This nucleus when present in a compound imparts anticonvulsant[2], radio-protective[3] and spermatostatic[4] properties to that compound. The SH group attached to the nucleus may enhance the pharmacological activities[5]. The sulphides have been reported to possess more biological activities than the parent mercapto compounds[6]. Moreover, the heterocyclic disulphides have been known to possess significant antifungal activity[7]. Studies of pesticidal activities of bis(4-aryl-5-mercapto-1,2,4-triazol-3-yl)alkanes have indicated that activity increased[8] with the increase in the number of methylene groups. These studies in the modification of pharmacological activities of heterocyclics, prompted the authors to take up the synthesis of new tetrazolyl sulphides and to screen these compounds for their fungicidal activity. As speculated, these compounds have been found to posses significant fungicidal activity.

1-Aryl-1,2,3,4-tetrazole-5-thiols (3) have been prepared by the method of Freund and Hempel[9]. These have been converted to bis-tetrazolyl disulphides (4) and to bis-ethylene disulphides (5) according to Scheme 1.



Scheme 1

Reagents: (i) HNO_2; (ii) aqueous NaOH; (iii) Br_2; C_2H_5OH; (iv) $BrCH_2CH_2Br$; (v) anhydrous CH_3COONa.

The purity of the compounds was checked by tlc. Their characterisation has been done by ir spectra. Eighteen of the title compounds have been screened for their fungicidal activity against *A. niger* and *A. flavus*. Some of these compounds exhibited satisfactory antifungal activity.

Experimental

All the melting points are uncorrected. The ir spectra (KBr) were recorded on a Perkin-Elmer 521 spectrophotometer. 5-Aryl-amino-1,2,3,4-thiatriazoles (2) were prepared by the action of HNO_2 on 1 in cold.

Bis(1-aryl-1,2,3,4-tetrazol-5-yl)disulphides (4): The compounds were prepared by oxidation of 1-aryl-1,2,3,4-tetrazole-5-thiol (3) with bromine. To an ethanolic solution (20 ml) of 3 (0.01 *M*), a cold ethanolic solution (20 ml) of bromine (0.01 *M*) was added dropwise with stirring. The precipitate thus obtained was filtered, washed with ethanol and recrystallised (Table 1).

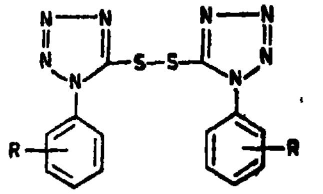
Bis(1-aryl-1,2,3,4-tetrazol-5-yl)ethylene disulphides (5): To an ethanolic solution of 3 (0.01 *M*), anhydrous sodium acetate and ethylene bromide (0.005 *M*) were added. The contents were refluxed for 4 to 5 h and then poured into cold water. The solid thus obtained was filtered, washed and recrystallised from ethanol (Table 2).

Fungicidal screening: All the nineteen compounds were evaluated for their fungitoxicity by agar plate technique[10] against *A. niger* and *A. flavus* at three different concentrations, namely 1 : 1 000 and 1 : 10 000 and 1 : 100 000. The number of replications in each was three. The percentage inhibition (after 90 h) by various compounds are recorded in Tables 1 and 2.

Results and Discussion

All the tested compounds possessed significant

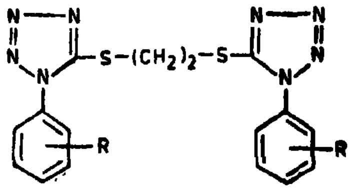
TABLE 1—BIS(1-ARYL-1,2,3,4-TETRAZOLYL) DISULPHIDES (4)



Sl. no.	R	M.p. °C	Yield %	Molecular formula	Analysis % : Found/ (Calcd.) N	S	% Inhibition (1 : 10 000) *A. flavus*	*A. niger*
1.	H	184	79.5	$C_{14}H_{10}N_8S_2$	30.9 (31.3)	18.2 (18.0)	57.2	48.5
2.	2-CH_3	224	69.2	$C_{16}H_{14}N_8S_2$	29.0 (29.3)	16.4 (16.8)	44.6	41.7
3.	4-CH_3	167	72.2	$C_{16}H_{14}N_8S_2$	–	–	38.5	36.3
4.[a]	4-Cl	195	85.3	$C_{14}H_8N_8S_2Cl_2$	26.0 (26.4)	14.8 (15.2)	50.1	45.8
5.	3-Cl	176	90.2	$C_{14}H_8N_8S_2Cl_2$	–	–	52.4	46.7
6.	2-Cl	200	76.1	$C_{14}H_8N_8S_2Cl_2$	–	–	55.6	53.8
7.	2-OCH_3	164	86.3	$C_{16}H_{14}N_8O_2S_2$	26.1 (27.0)	14.8 (15.4)	60.2	58.9
8.	3-OCH_3	238	90.0	$C_{16}H_{14}N_8O_2S_2$	–	–	57.8	51.2
9.	4-OCH_3	219	92.2	$C_{16}H_{14}N_8O_2S_2$	26.3 (27.0)	14.6 (15.4)	62.9	58.1
10.	2-CH_3,5-Cl	254	80.3	$C_{18}H_{18}N_8O_2S_2Cl_2$	22.5 (23.1)	12.9 (12.2)	58.7	56.9
11.	4-OC_6H_5	225	87.5	$C_{16}H_{18}N_8O_2S_2$	24.1 (25.0)	13.7 (14.4)	59.6	56.7
12.	4-NO_2,2-Cl	185	68.9	$C_{14}H_6N_{10}O_4S_2Cl_2$	28.3 (29.1)	13.0 (13.4)	46.7	44.5
13.	2-NO_2,4-Cl	159	66.5	$C_{14}H_6N_{10}O_4S_2Cl_2$	–	–	51.8	47.5

[a] λ_{max} 1 581 (C=N conj.), 736 (C–S–C) and 759 cm^{-1} (C–Cl).

TABLE 2—BIS(1-ARYL-1,2,3,4-TETRAZOL-5-YL)ETHYLENEDISULPHIDES (5)



Sl. no.	R	M.p. °C	Yield %	Molecular formula	Analysis % : Found/ (Calcd.) N	S	% Inhibition (1 : 100 000) *A. flavus*	*A. niger*
14.	H	95	50	$C_{16}H_{14}N_8S_2$	28.6 (29.3)	16.1 (16.7)	54.0	49.3
15.	2-OCH_3	120	61	$C_{18}H_{18}N_8O_2S_2$	24.7 (25.0)	13.6 (14.4)	59.1	50.9
16.	3-Cl	85	49	$C_{16}H_{12}N_8S_2Cl_2$	24.5 (24.8)	14.0 (14.1)	57.2	56.1
17.[a]	4-Cl	115	78	$C_{16}H_{12}N_8S_2Cl_2$	–	–	53.7	50.5
18.	4-OC_6H_5	66	86	$C_{28}H_{22}N_8O_2S_2$	22.9 (23.8)	13.1 (13.6)	62.1	55.2
19.	2-NO_2	76	79	$C_{16}H_{12}N_{10}O_4S_2$	29.0 (29.6)	12.7 (13.5)	57.5	49.8

[a] λ_{max} 1 581 (C=N conj.), 736 (C–S–C) and 759 cm^{-1} (C–Cl).

fungicidal activities at 1 : 100 000 concentration. In general, compounds having chlorine atom or methoxy group in 1-aryl nucleus exhibit higher fungitoxicity. Replacement of 4-OCH_3 group by 4-OC_2H_5 group has been found to decrease fungitoxicity. The ethylene disulphides were found to be better fungicides than the corresponding sulphides. The most active compounds of the series were 6, 7, 9 and 18 (Tables 1 and 2).

Acknowledgement

The authors are thankful to U. G. C., New Delhi, for providing financial assistance.

References

1. M. Leinzinger, B. Issekutz and E. Novak, *Arch. Exptl. Path. Pharmakol.*, 1935, 177, 397.
2. R. G. Dybenko, P. N. Kulyabko, P. V. Pel'kis, *Radiobiologiya*, 1969, 9, 633 (*Chem. Abstr.*, 1970, 542).
3. C. L. Mitchell, *Toxicol. Appl. Pharmacol.*, 1964, 6, 23.
4. M. L. Tarakhovskii, E. P. Nesynov, P. S. Pel'kis, I. E. Naigertisk, V. V. Rybakova, M. O. Lozinskii, R. G. Dubenko and A D. Grabenko, *Fiz. Aktiv. Veshchestva*, 1971, 3, 119 (*Chem. Abstr.*, 1972, 42070).
5. J. G. Horsfall and S. Rich, *Chem. Abstr.*, 1952, 46, 11543.
6. K. C. Joshi and A. B. Sen, *J. Sci. Food. Agric.*, 1952, 11, 526.
7. U. Srivastava, R. H. Khan and S. C. Bahel, *J. Antibact. Antifung. Agents Jpn.*, 1979, 7, 8.
8. S ar L. Chimetron, Fr. Pat. 1 476 5431 1967 (*Chem. Abstr.*, 1968, 69, 96725).
9. M. Freund and H. Hempel, *Chem. Ber.*, 1895, 28, 74.
10. J. G. Horsfall, *Bot. Rev.*, 1945, 11, 357.

Separation of Thorium from Trivalent Rare Earths in Monazite and its Gravimetric Determination using *o*-Carboxyphenylazo-β-naphthol

S. VATSALA and GEETHA PARAMESWARAN*

Department of Chemistry, University of Calicut, Kerala-673 635

Manuscript received 17 May 1982, revised 26 March 1984, accepted 6 February 1986

THOUGH many methods of separating thorium from the cerite earths have been developed, each method has some complexity[1-4]. Murthy and Rao[5] and Rao and Rao[6] have reported the use of *o*-chlorobenzoic acid and *o*- and *p*-aminobenzoic acid for the separation and estimation of thorium in monazite. In the present work, we report the use *o*-carboxyphenylazo-β-naphthol (CPAN) in quantitatively precipitating thorium in the presence of ten-fold excess of lanthanum in a single precipitation at *p*H 5.3. Since in Indian monazite, the ratio of ThO_2 to R_2O_3 is 1 : 8, the advantage offered by this reagent in the recovery of thorium from monazite becomes more apparent.

Experimental

Preparation of reagent: The azo dye CPAN was prepared by diazotising anthranilic acid and coupling it with β-naphthol which was purified earlier by sublimation. The dye was finally recrystallised from glacial acetic acid, m.p. 265-70°. The dye was insoluble in water and slightly soluble in most of the common organic solvents and was freely soluble in dimethyl sulphoxide (DMSO) (Found: C, 69.5; H, 4.2; N, 9.3. $C_{17}H_{12}N_2O_3$ calcd. for: C, 69.86; H, 4.11; N, 9.59%).

A solution of thorium nitrate, using $Th(NO_3)_4.4H_2O$ was prepared and standardised with 10% oxalic acid solution. Solutions of nitrates of lanthanum, uranium and zirconium oxychloride were also prepared. All the chemicals employed were of analytical grade.

Procedure: To the stock solution (20 ml) containing thorium (50 mg), acetate-acetic acid buffer was added, followed by twice the volume of DMSO. *p*H of the solution was adjusted with a *p*H meter. It was established that a minimum of 2 : 1 ratio of DMSO to water must be maintained in the reaction mixture to keep the dye in solution. The reagent (100 mg) was added to the above solution with continuous strring. The precipitate was digested over boiling water-bath for 1 h and filtered through Whatman no. 41 filter paper. The precipitate was washed several times with water, dried, ignited to ThO_2 and weighed.

Results and Discussion

Study at various p*H:* The precipitation of thorium under different conditions of *p*H was investigated. It was noticed that the precipitation was not complete when the *p*H was 5.0 or lower. The complete precipitation occurs at *p*H range 5.3-7.0.

Interference of other ions: The interference of 8-fold excess of La^{III} at various *p*H was investigated. It was noticed that the precipitation of thorium was incomplete at *p*H 5, and at *p*H 5.5 rare earths started to precipitate. The optimal *p*H for the precipitation of thorium without the interference of rare earths was found to be 5.3. The study of interfernce of Zr^{IV}, UO_2^{II}, Ce^{III} and La^{III} was carried out at *p*H 5.3. Amount of La^{III} varied from 2 to 10 times the amount of Th. It was found that none of these ions causes any interference at this particular *p*H.

Composition of thorium complex: Analysis of the metal content of the complex displayed the metal-ligand ratio to be 1 : 2. C, H, N analysis was also done (Found: Th, 28.07; C, 51.25; H, 2.94, N, 6.82. $Th[C_{17}H_{10}N_2O_3]_2$

calculated for: Th, 28.57; C, 50.24; H, 2.46; N. 6.89%). The ir spectrum of the thorium chelate indicated the absence of characteristic absorptions for OH and COOH groups. However, the strong absorption of the ligand at 1 700 cm^{-1} due to γ (C=O) is shifted to lower frequencies in the chelate and appears at 1 600 cm^{-1}. A strong band at 1 450 cm^{-1} (N=N) is shifted to 1 400 cm^{-1} in the complex. These shifts towards lower frequencies show that N=N and C=O are involved in bond formation. The TGA data also support 1 : 2 complex.

Estimation of thorium in monazite: Powdered monazite sand was converted into a mixture of thorium and rare earth sulphates by heating with concentrated H_2SO_4. Accurately weighed quantities of Travancore monazite were digested with 3-4 times its weight of concentrated H_2SO_4 for 4 h at 200-250°. The mass was extracted with ice-cold water. Thorium and rare earth metals were precipitated by oxalic acid. Reprecipitation was carried out. The precipitate was dissolved in concentrated HNO_3 and the excess acid evaporated to dryness. The residue was dissolved in water and acetate-acetic acid buffer was added to adjust the *p*H at 5.3 and Th was estimated with CPAN according to the procedure detailed above. Similar experiments was conducted using fresh samples of monazite. Th is precipitated as iodate by standard procedure[7]. Thorium iodate is converted into oxalate by using oxalic acid. Finally, thorium oxalate is ignited to ThO_2, dried and weighed.

ThO_2 contents in monazite obtained through these two methods are comparable: iodate method, 8.99%; and CPAN method, 9.00%.

References

1. A. C. NEISH, *J. Am. Chem. Soc.*, 1904, **26**, 780.
2. K. V. S. KRISHNAMURTHY and A. PURUSHOTTAM, *Rec. Trav. Chim.*, 1952, **71**, 671.
3. H. H. WILLARD, L. GORDON and C. H. VANSELOW, *Anal. Chem.*, 1949, **21**, 1323.
4. M. VENKATARAMANIAH, T. K. SATYANARAYANAMURTHY and S. V. R. BH. RAO, *J. Indian Chem. Soc.*, 1950, **27**, 81.
5. D. S. N. MURTHY and S. V. R. BH. RAO, *J. Indian Chem. Soc.*, 1950, **27**, 457.
6. B. R. L. RAO and S. V. R. BH. RAO, *J. Indian Chem. Soc.*, 1950, **27**, 459.
7. L. ERDEY, "Gravimetric Analysis", Pergamon Press, New York, 1965, Part II, p. 501.

Extractive Spectrophotometric Determination of Trace Amounts of Molybdenum with Benzyltriethylammonium Chloride

K. C. BAYAN and H. K. DAS*

Department of Chemistry, Gauhati University, Gauhati-781 014

Manuscript received 17 January 1985, accepted 2 December 1985

A number of quaternary ammonium salts have been reported to find application in the determination of a large number of metal ions in small concentration in solution. Yoshimura and Ueno[1] used benzyldimethylphenylammonium chloride in the spectrophotometric determination of cobalt(II), iron(III), copper(II) and molybdenum(V) in SCN^- solutions. The same reagent was employed for the gravimetric determination of platinum[2] and extractive spectrophotometric determination of bismuth[3] and palladium[4]. Benzyltriethylammonium chloride in SCN^- solution reacts with many metallic ions with the formation of coloured precipitate. The present work describes a highly sensitive and selective method for the extractive spectrophotometric determination of molybdenum(V) in trace concentrations using benzyltriethylammonium chloride as reagent and 1,2-dichloroethane as the extracting solvent.

Experimental

A Hilger Uvispek photoelectric spectrophotometer with matched quartz cells of 1 cm optical path was used.

The stock solution of molybdenum was prepared from molybdenum trioxide (A.R.) and was standardised by known method[5]. Test solutions of lower concentration were prepared by appropriate dilution of the stock. The reagent, benzyltriethylammonium chloride, was prepared[6] by refluxing for 1 h a mixture of ethyl acetate, dimethylformamide, triethylamine and benzylchloride. A 0.01 *M* solution of benzyltriethylammonium chloride, a 3 *M* solution of potassium thiocyanate and a saturated solution (1.8 *M*) of thiourea were prepared in distilled water. All chemicals used were of analytical grade.

Procedure: An aliquot of the solution containing 4-80 μg of molybdenum was made acidic with 18 *M* H_2SO_4 (2 ml). To this the thiourea solution (8 ml), the potassium thiocyanate solution (4 ml) and then the benzyltriethylammonium chloride solution (5 ml) were added. The total volume was made up to 25 ml with distilled water. The resulting solution after having mixed with 1,2-dichloroethane (20 ml) was shaken for 3 min, and the organic layer separated. Absorbance of the extract was measured at 465 nm against the pure solvent. Amount of molybdenum in unknown solutions was calculated from the standard calibration curve.

Results and Discussion

Benzyltriethylammonium chloride (QCl) reacts with the SCN^--complex of molybdenum(V) yielding the ion-pair $Q^+ [Mo(SCN)_6]^-$ in the form of an orange-yellow precipitate. The ion-pair is completely extractable into 1,2-dichloroethane and the extract absorbs maximum at 465 nm. Beer's law is obeyed over the concentration range 0.2-4.0 ppm of molybdenum. The reagent blank shows no absorption at this wave length. Molar absorptivity and Sandell's sensitivity are 1.79×10^4 l mol^{-1} cm^{-1} and 0.0053 μg cm^{-2}, respectively.

The complex exhibits constant and maximum absorption provided the acidity of the aqueous layer be maintained at 1-2 *M* with respect to sulphuric acid. The role of thiourea is mainly in reducing molybdenum(VI) to molybdenum(V) and in increasing the rate of formation and stability of the coloured complex[7]. A thiourea concentration below 0.13 *M* in the aqueous phase resulted in the lowering of absorbance while higher concentrations were without any significant effect. Effect of thiocyanate concentration on the absorbance was studied by using potassium thiocyanate solution of varying concentrations. It was found that concentrations below 0.18 *M* and beyond 0.88 *M* in the aqueous layer with respect to potassium thiocyanate produced low values of absorbance. As regards reagent concentration, 5 ml of a 0.01 *M* solution of benzyltriethylammonium chloride was adequate for complete extraction of the complex for the given range of molybdenum concentration. Reagent concentration below 0.003 *M* in the aqueous phase resulted in the decrease in absorbance while higher concentration could produce no change in the colour intensity.

Effect of foreign ions : A number of representative ions were examined for their interference in the determination of molybdenum by the recommended procedure. The tolerance limit (Table 1) was set at the amount required to cause less than 3 per cent error in the recovery of molybdenum by restricting the higher limit of foreign ion concentration to 1000-fold excess (w/w) to that of molybdenum.

The present method proves very rapid and simple, and provides excellent recovery of molybdenum in micro-quantities in presence of most of the common ions. Standard deviation and coefficient of variation as obtained from the absorbance of 2 ppm of molybdenum were 0.0015 and 0.416%, respectively. The method, further deserves special mention of its selectivity in the sense that interference from foreign ions is much less than that in case of other existing methods for the determination of molybdenum.

TABLE 1—EFFECT OF FOREIGN IONS ON EXTRACTION OF MOLYBDENUM

Mo taken = 40 μg

Ions added	Tolerance limit mg	Ions added	Tolerance limit mg
Cu^{II}	4	Mn^{II}	40
Ag^{I}	20	Mn^{VII}	40
Au^{III}	40	Fe^{II}	2.8
Zn^{II}	12	Fe^{III}	2
Cd^{II}	0.32	Co^{II}	40
Hg^{II}	32	Ni^{II}	40
Sn^{II}	0.20	Rh^{III}	40
Sn^{IV}	0.80	Pd^{II}	0.4
Pb^{II}	0.80	Pt^{IV}	8
As^{III}	40	Fluoride	40
As^{V}	40	Bromide	40
Sb^{III}	40	Iodide	40
Bi^{III}	40	Thiosulphate	0.4
V^{V}	4	Oxalate	40
Cr^{III}	40	Citrate	40
Cr^{VI}	32	Tartrate	40
W^{VI}	1	EDTA	40

Acknowledgement

The authors thank Prof. (Mrs.) A. Chaudhuri, Head of the Department of Chemistry, Gauhati University, for facilities, and to the U.G C., New Delhi, for awarding teacher-fellowship to one of them (K.B.).

References

1. J. YOSHIMURA and K. UENO, *Mem. Fac. Sci. Kyushu Univ., Ser. C*, 1961, 4, 63.
2. D. E. RYAN, *Can. J. Chem.*, 1956, 34, 1683.
3. K. C. BAYAN and H. K. DAS, *Curr. Sci.*, 1984, 53, 312.
4. K. C. BAYAN and H. K. DAS, *Curr. Sci.*, 1984, 53, 915.
5. A. I. VOGEL, "A Text Book of Quantitative Inorganic Analysis", 3rd. ed., E.L.B.S., London, 1964, p. 508.
6. D. A. SCOLA and N. A EDELSON, *J. Chem. Eng. Data*, 1968, 13, 453; H. MOCHIDA, K. HORII and R. KOMIYA, Jap. Pat. 21 022/1966.
7. V. KH. MASHEZOV and S. D. BESKOV, *Khim. Fiol.* 1966, 29, 363.

J. [illegible]
Vol. LXIII, March 1986, pp. 356

Book Reviews

An Introduction to Science of Corrosion and its Inhibition, S. N. Banerjee, Oxonian Press Pvt. Ltd., New Delhi, 1985, Pp. 624+xvi, Rs. 102.00.

THIS book, written for the students of the Engineering and Applied Sciences as claimed by the author, is a comprehensive text and will be useful not only to the students but also to the research students and practising corrosion technologists. The author quotes U. R. Evans, 'There are two reasons for study of metallic corrosion, intellectual and the utilitarian', and the remark by J. Ghandhy, 'The science of corrosion has made great progress in recent years. Unless the problem is fully understood and analysed by those who are confronted with it, the prevention of corrosion will remain largely a question of hit and miss, with more misses than hits'. He thus rightly justifies the coverage in the text.

The author discusses the fundamental principles of corrosion in the first four chapters. In the fifth he deals with corrosion in industries, starting with corrosion in boiler plant and going over to problems in chemical, petroleum, building and fertiliser industries. In chapters 6, 7 and 8, he elaborates various types of corrosion and deals with the factors, mechanisms and remedial measures in case of corrosion of metals under various constraints, in atmosphere, underground, immersion condition and also at high temperature. Corrosion testing and monitoring methods have been discussed in chapter 9. The last chapter contains methods of corrosion control. It covers 150 pages.

Each chapter has a set of questions. There are five useful appendices at the end of the book.

For the students a cheaper paperback will be welcome.

S. Aditya

Battery Lead Oxides and Plate Technology, Compiled by The Battery Society of India, New Delhi, 1985, Pp. 75.

THIS technical note from the Battery Society of India is a compilation of the general manufacturing processes of lead oxide and the technologies associated with the fabrication of different types of plates, used in lead-acid storage battery.

Lead oxide which is being used as active material since 1881, in the form of paste on lead-alloy grid (acting as current conductor), shows different chemical and physical modifications depending on the modes of preparation. Wide variations in their activities as well as electrochemical reversibility have been noted. Although many of the properties have been characterised there still remains a lot to be understood about their mode of functioning in a battery. Considerable research and development are being carried on not only to have a better understanding but also to improve the performance in relation to capacity and life of a lead-acid battery.

The first part of the note, namely, the battery lead oxides, has been sub-divided into four sections as historical background, developments in battery lead oxide chemistry and technology, and lastly chemical analysis of battery oxides. The different manufacturing processes have been described and compared in light of oxide characteristics. The role of additives and impurities has been discussed. Chemical methods for the analysis of oxides have been incorporated.

The second part, namely, the plate technology, has been divided into three sub-sections as flat-pasted plates, pasting process and the tubular plates. Methods of paste preparation and application, the role of composition, mixing and density as well as their chemical properties in flat plates have been discussed. The composition of the paste and the method for filling tubular plates have been described briefly.

The note contains in the Appendix various related data in tabular and graphical forms which will be of immense help to the battery technologists and shop-floor operators.

On the whole this is a useful compilation.

Ansuman Roy

J. Indian Chem. Soc.,
Vol. LXIII, April 1986, pp. 357-370

Some Coordination Polymers†

ARUN K. DEY

Department of Chemistry, University of Allahabad, Allahabad-211 002

THERE has been a phenomenal growth in technology since the World War II and rapid strides had necessarily to be made in the sciences to meet the requirements of new materials with specific properties, in order to meet the demands of growing technology. This often led to discoveries on the border lines of different disciplines, which subsequently resulted in the development of investigations of inter-disciplinary interests. During this period, inorganic chemistry underwent a renaissance and the frontiers of the subject began expanding. The chemistry of polymers which had by now already advanced sufficiently, provided an impetus for the study of a new class of compounds known as inorganic polymers.

Polymer, in general, can be defined as a substance in which many structural units are connected by valence bonds in any possible way. On the basis of this definition, inorganic polymers would include a variety of substances, like mortar, natural silicates, quartz, polyphosphates, polyphosphazenes, glasses, diamond, graphite, polymeric boron nitride, sulphur nitrides, silicones and even ionic crystal aggregates like sodium chloride. Various organometallic and metal-organic substances are often included in inorganic polymers. The oldest synthetic inorganic polymer, in fact the oldest of all synthetic polymers—was a simple alkali silicate glass used during the Badarian period in Egypt (*ca* 12 000 B.C.) used as a glaze in ornamental amulets and beads. Subsequent improvements in glass manufacture continued through centuries and reached a stage of perfection[1] during the time of Tutankhamen (1 300 B.C.). The next major discovery in the area of inorganic polymers occured about 3000 years later when Thomas Graham[2] published an account of obtaining sodium polyphosphates both in crystalline and amorphous forms.

The conventional polymers with an organic backbone are characterised by high viscosity and long range elasticity, useful for their applications in technology, but they suffer from a disadvantage that most of them break down on heating in air below 250°. On oxidation, the carbon and hydrogen oxidise to CO_2 and H_2O. Commercial products, like polyethylene, polyamide, polyester fibres, *etc.* are popular examples of organic polymers. It may be pointed out that the important Ziegler-Natta catalyst used for polymerising ethylene is the inorganic species containing Ti^{III}. The high-density polyethylene so formed, is relatively hard, stiff and consists of mainly straight chains. However, the inherent flammability of the above commercial products is a great disadvantage. The Summerland disaster in the Isle of Man on 2 August 1973 caused great concern about the desirability of such materials for household use. Inorganic polymers, on the other hand are thermally more stable and are therefore suitable for withstanding high temperatures. Moreover, they are stronger, harder, usually insoluble, but are brittle.

The term coordination polymer includes a variety of substances, and in general, can be defined as a macromolecular entity involving a metallic element which forms an integral part of the backbone. It is usual to classify the coordination polymers in this way.

The study of coordination polymers which was systematically initiated nearly four decades ago is now regarded as one of the developing frontier areas of coordination chemistry. Renewed interest has been evinced in the context of obtaining materials with high temperature resistance. The potential applications of coordination polymers are as surface coatings on metals and glasses, adhesives, high temperature lubricants, electrical insulators, semiconductors, heat shields for artificial satellite and space ships, nose cones of missiles, constructional materials in aerospace industry and space vehicle and in various other projects. Attempts are also being made to obtain polymer fibre with special properties and has been successfully tried for communication system in some countries.

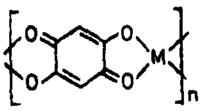
The synthesis of a coordination polymer is usually achieved by one of the following procedures : (i) a metal complex may yield a polymeric material during its formation due to the favourable donor groups present in the ligand, (ii) the ligand itself be a preformed organic polymer to which a metal ion may suitably be coordinated, and (iii) a metal ion may be coordinated with a ligand, and the monomeric metal complex reacted with another organic compound to form a polymeric complex.

In the author's laboratory, interest in the field of coordination polymers arose out of the exploration of stable polymeric materials. This led to the synthesis of several novel types of organic monomers which were used further for polymerisation with a metal ion. The ligands employed were hydroxy- and amino-anthraquinones, phthalein dyes, azo dyes with 8-quinolinol units, and Schiff bases. Some

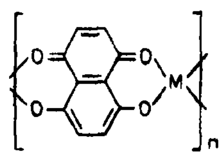
† Acharya Prafulla Chandra Ray Memorial Lecture (1980) delivered under the auspices of the Indian Chemical Society on 15th October, 1984 at Calcutta.

work on polymeric metal complexes of Mannich bases has also been done.

Frank *et al.*[3] initiated the work on metal complexes of 2,5-dihydroxy-*p*-benzoquinone. Kanda and Saito[4] prepared 1 : 1 polymeric complexes of 2,5-dihydroxy-*p*-benzoquinone with Cu^{II}, Ni^{II} and Cd^{II}. An interesting feature observed by physical measurements revealed that Cu^{II} polymers are rigid rods[5]. Jain and Singhal[6] were able to prepare a three-dimensional polymer with Zr^{IV}. Thermal studies of these polymers were carried out by Bottei and Frangman[7]. Naphthazarin and quinizarin, however, form six-membered rings. Bailes and Calvin[8] assigned polymeric octahedral structure to Co^{II} naphthazarin complex.

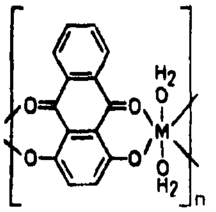


(1) 2,5-Dihydroxy-*p*-benzoquinone

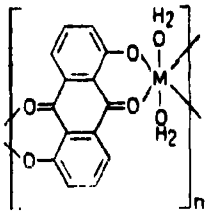


(2) 5,8-Dihydroxy-1,4-naphthaquinone (Naphthazarin)

Polymeric chelates of 1,4- and 1,5-dihydroxyanthraquinone (1,4-DHA, 1,5-DHA) were prepared by Guggiari[9] and Mangini and Stratta[10], respectively.

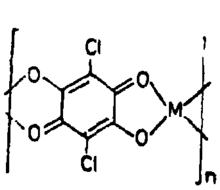


(3) 1,4-DHA

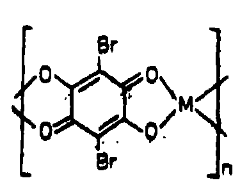


(4) 1,5-DHA

Coble and Holzclaw[11] synthesised chelate polymers of Cu^{II} with various dihydroxyquinoid ligands and compared their respective thermal stabilities on the basis of increased number of rings. Bottei and McEachen[12] compared the ir spectra and thermal stability of chloroanilic and bromoanilic acid polymers and those of 2,5-dihydroxy-*p*-benzoquinone (**1**). Copper chelates were found to be most

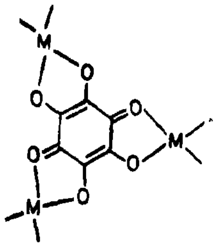


(5) Chloroanilic acid

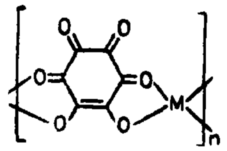


(6) Bromoanilic acid

stable and zinc chelates least thermally stable. The order of stability of polymers of ligands were chloroanilic acid > bromoanilic acid > 2,5-dihydroxy-*p*-benzoquinone. The same authors[13] also synthesised complexes of copper and cobalt with juglone, 2,5-dihydroxy-*p*-benzoquinone and naphthazarin, and attempted to establish a relationship between thermal stability and polymeric structure or ring size. Coordination polymers of tetrahydroxy-*p*-benzoquinone and rhodizonic acid were reported by Bottei and Greene[14]. Metals chosen were copper, cobalt, nickel and zinc. Except copper which forms Cu_2L, other metals yield complexes of the composition $M_2L.6H_2O$. The order of thermal stability for tetrahydroxy-*p*-benzoquinone and rhodizonic acid chelates are Co > Zn > Ni > Pb > Cu and Ni > Zn > Co > Pb > Cu, respectively. Bottei and Quane[15] investigated the thermal stability of polymers from β-hydronaphthazarin as opposed to polymers from naphthazarin and attributed the decrease in stability of the former to the decrease in electron delocalisation and aromaticity in the ring system. Similarly, Bottei and Frangman[16] attributed the lack of stability of 2,5-dihydroxy-*p*-benzoquinone chelates essentially to the same reason, as well as to the formation of a five rather than a six-membered ring. However, on these assumptions, the relative thermal stabilities of tetrahydroxy-*p*-benzoquinone and rhodizonic acid chelates could not be established. Bottei and Frangman[17] synthesised coordination polymers of 2,5-dihydroxy-*p*-benzoquinone with copper, nickel and zinc. Copper formed CuL, but other metals



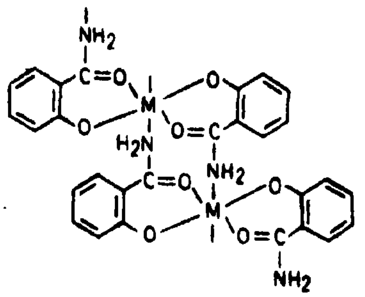
(7) Tetrahydroxy-*p*-benzoquinone



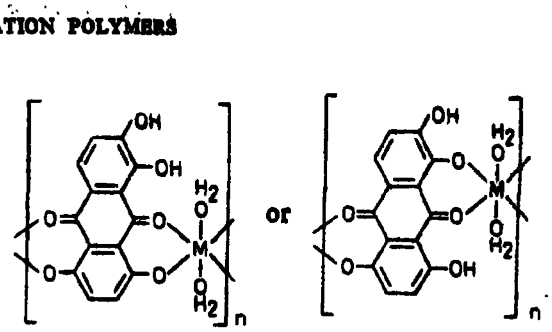
(8) Rhodizonic acid

form polymers of the general composition $ML.2H_2O$. The order of decreasing thermal stability is Zn > Co ~ Ni > Cu.

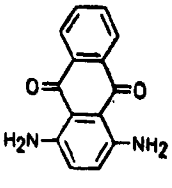
Maurya *et al.*[18] have initiated systematic study on coordination polymers from these laboratories and synthesised by refluxing ethanolic solutions of salicylamide (SAM) with Mn^{II}, ZrO^{IV}, UO_2^{VI} and Be^{II}. SAM acts as tridentate ligand although all the three donor sites are not coordinated to the same metal ion. Two SAM ions are bonded to each metal ion through the hydroxyl and carbonyl oxygens. The metal ion is linked to two such groups by the coordination through the nitrogen of of the NH_2 groups leading to a polymeric structure 9 (except Be complex).



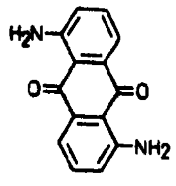
(9) Bis(salicylamido)metal complex



(10) 1,2,5,8-Tetrahydroxyanthraquinone



(11) 1,4-Diaminoanthraquinone



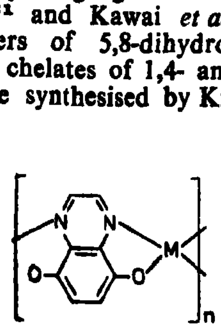
(12) 1,5-Diaminoanthraquinone

Coordination polymers of 1,4-dihydroxyanthraquinone with Hg^{II}, ZrO^{IV} and UO_2^{VI} and of 1,5-dihydroxyanthraquinone with Be^{II}, Mn^{II}, Cd^{II}, Hg^{II}, ZrO^{IV} and UO_2^{VI} ions have been investigated by the same workers. The compounds are stable, powdery in appearance, and insoluble in water, dilute mineral acids, alkalis, and in most of the common organic solvents. They are brown in colour except that uranium complexes are dark blue black. The DTA, DTG and TG thermograms indicate that the heat effect is endothermic, which reveals the sublimation of the ligands. The order of thermal stability is UO_2(390°) > ZrO(360°) > Hg(340°) *in* the case of quinizarin, and Mn(380°) > Be(370°) > UO_2(360°) > ZrO(350°) > Cd(300°) > Hg (285°) in the case of anthrarufine. The composition of the polymers is $ML.2H_2O$, however, Be^{II} polymer is ML. These have been assigned octahedral polymeric structure, on the basis of elemental analysis, ir, and reflectance spectra and thermal study.

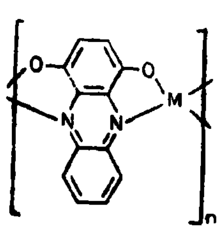
Coordination polymers of Mn^{II}, Fe^{II}, Co^{II}, Ni^{II}, Cu^{II}, Zn^{II} and Cd^{II} with 1,2,5,8-tetrahydroxyanthraquinone have been reported by Banerjie and Dey[19]. These have been prepared by homocondensation of ligand and metal acetate hydrates in DMF. Dark blue to black products obtained were amorphous solids, insoluble in practically all common organic solvents indicative of their polymeric structure. Due to their insoluble nature molecular weight determination was not possible. One-to-one metal to ligand ratio was found as expected for chain polymers. Association of $2H_2O$ per metal was established through elemental analysis, ir spectra and thermal analysis. Magnetic and spectral measurements assigned octahedral geometry around central metal.

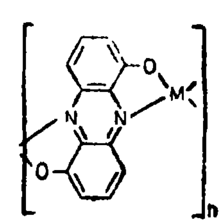
John and Dey[20] have synthesised coordination polymers of some bipositive transition metals with 1,4- and 1,5-diaminoanthraquinone. The order of thermal stability for 1,4- and 1,5-diaminoanthraquinone complexes are Co(350°) > Cu(300°) > Ni(280°) > Mn(260°) ; and Cu(360°) > Ni(320°) > Co(280°) > Mn(250°), respectively. The elucidation of their structures reveal that complexation occurs through phenolic oxygen and quinolic oxygen as indicated by ir spectra, and the polymeric chain grows.

Metal complexes of 8-quinolinol are among the most stable coordination compounds involving organic ligands. Several coordination polymers have been prepared by using ligands of bis(8-quinolinol) type. Adachi[21] and Kawai *et al.*[22] studied the metallic polymers of 5,8-dihydroxy quinoxaline. 1 : 1 Polymeric chelates of 1,4- and 1,6-dihydroxyphenazines were synthesised by Kidani[23] and Berg and Alam[24].



(13) 5,8-Dihydroxyquinoxaline

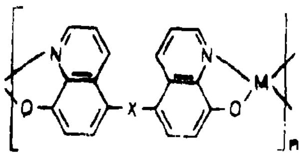




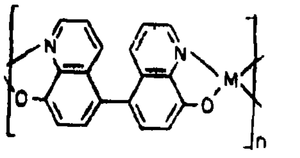
(14) 1,4-Dihydroxyphenazine (15) 1,6-Dihydroxyphenazine

Bailar *et al.*[25] synthesised a number of coordination polymers of bis(8-hydroxyquinolines). The thermal stability of the copper and zinc bis(8-quinolinol) type coordination polymers were examined by heating the sample in a stream of nitrogen and measuring the weight loss. The bis(8-hydroxy-5-quinolyl)sulphone ligand appeared to give the most stable coordinated systems with decomposition temperature of 280° and 320° for the copper and zinc polymers, respectively. Korshak *et al.*[26] followed the pattern of Bailar and reported

the synthesis of a number of coordination polymers of bis(8-hydroxy-5-quinolyl)methane as well as a number of mixed polymers. The thermal stability of a group of the first row transition metal coordination homopolymers was elucidated by noting colour changes as the sample was heated in air in a capillary tube, and also by measuring deformation of the sample with increasing temperature. Berg and Alam[27] discussed the synthesis of coordination polymers of 8,8′-dihydroxy-5,5′-biquinolinol, and the use of ligand as an analytical reagent for detecting metal ions in the microgram range. Metals like copper, zinc, cobalt, nickel, manganese and cadmium were employed. They also studied the thermal stability of these polymers by heating the samples at different temperatures in air and observing changes in colour and in infrared spectra.

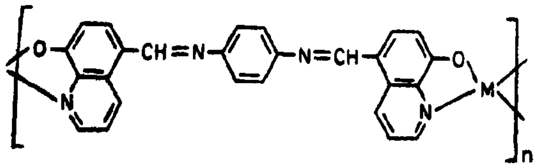


(16) Bis(8-hydroxy-5-quinolyl)methane
X = CH_2, - sulphone ; X = SO_2



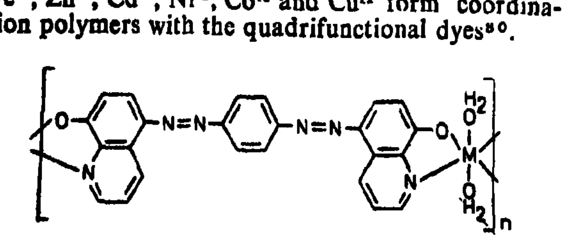
(17) 8,8′-Dihydroxy, 5,5′-biquinolinol

Poddar and Saha[28] have prepared polymeric complexes of some transition metal ions with Schiff base derived from 5-formyloxine and *p*-phenylenediamine.

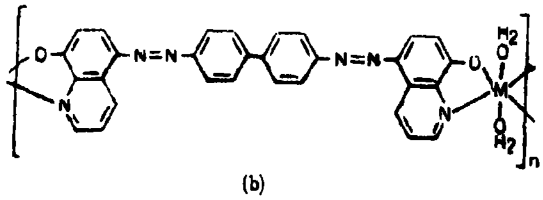


(18) 5-Formyloxine-phenylenediamine

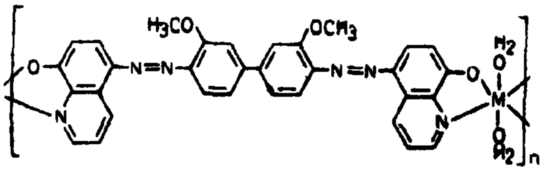
Banerjie and Dey[29] reported a new approach to link two molecules of 8-quinolinol by coupling it with tetraazonium chlorides of *p*-phenylenediamine, benzidine and *o*-dianisidine, respectively. Mn^{II}, Fe^{II}, Zn^{II}, Cd^{II}, Ni^{II}, Co^{II} and Cu^{II} form coordination polymers with the quadrifunctional dyes[30].



(a)



(b)

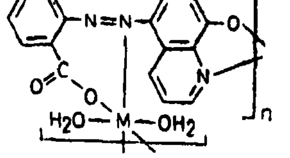


(c)

(19) Quinolinol Schiff bases

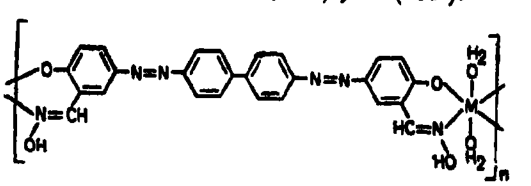
These complexes were prepared by refluxing ligand and metal acetate hydrate in dimethylsulphoxide. Dark red brown complexes are amorphous and insoluble in practically all common organic solvents. The 1 : 1 metal to ligand ratio and association of $2H_2O$ per metal ion is inferred. These are octahedral and decompose at high temperature. The order of thermal stability for the complexes of dyes from *p*-phenylenediamine, benzidine, and *o*-dianisidine is Cd(380°) > Mn(320°) > Zn(300°) ~ Fe(300°) > Co(280°) ~ Ni(280°) > Cu(260°) ; Cd(360°) ~ Zn(360°) > Mn(340°) > Co(320°) ~ Ni(320°) ~ Cu(320°) > Fe(300°) ; and Cd(400°) > Zn(380°) > Mn(360°) ~ Cu(360°) > Fe(340°) > Co(320°) > Ni(300°). The thermal stability of the complexes of dyes shows the order *p*-phenylenediamine < benzidine < *o*-dianisidine. This may be attributed to the increasing size of the amine moeity.

2-Carboxyphenyl-5-azo-8-hydroxyquinoline and 5,5′-(benzidinebisazo)salicylaldoxime have also been employed for the synthesis of coordination polymers of transition metals. Octahedral com-



(20) 2-Carboxyphenyl-5-azo-8-hydroxyquinoline

plexes show the following order of thermal stability : Co(340°) ~ Cu(340°) > Ni(320°) ; Cd(420°) > Zn(360°) ~ Mn(360°) > Co(340°) > Ni(320°) > Cu(300°).



(21) 5,5′-(Benzidinebisazo)salicylaldoxime

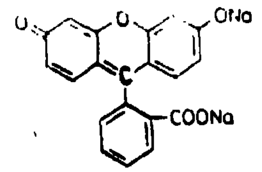
Agarwal *et al.*[81] have prepared the complexes of fluoroscein with Co^{II}, Cu^{II}, Zn^{II}, Cd^{II}, Pb^{II}, Ce^{III}, Th^{IV} and UO_2^{VI} at *p*H 3.0-4.0 and no hydroxo groups or bridges have been found to be present.

Magnetic study has been made for Co^{II} complex which is paramagnetic, whereas other complexes are largely diamagnetic. The effective magnetic moment value for Co^{II} complex has been found to be 4.77 B.M. The theoretical values for various geometries have been shown in Table 1.

TABLE 1—THEORETICAL VALUES OF MAGNETIC MOMENT FOR Co^{II} COMPLEXES

Geometry	Permissible values B.M.
Octahedral	4.7—5.2
Tetrahedral	4.4—4.8
Square planar	4.8—5.2

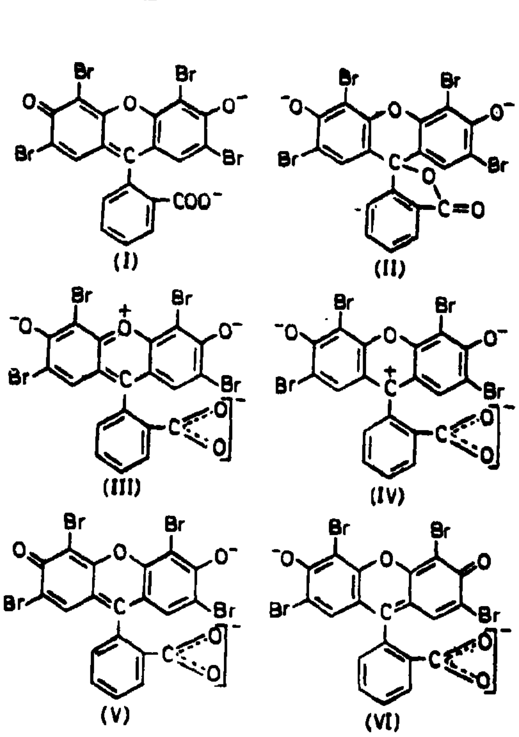
The observed magnetic moment value is at the lower limit of octahedral complexes and at the upper limit for tetrahedral complexes. However, the observed μ_{eff} value is similar to some other Co^{II} complexes having distorted square-pyramidal geometry. Structure of fluoroscein and ir study of the complexes reveal that all the three possible donor sites are involved in coordination. Evidently, since chelation is not possible for steric reasons, this type of complexation results in a three-dimensional coordinated polymeric structure. This polymerisation produces properties of insolubility in common organic solvents and high thermal stability, which is in the order Ce^{III}(460°) > Zn^{II} (360°) > UO_2^{VI}(340°) ~ Pb^{II}(340°) > Th^{IV}(320°) ~ Cd^{II}(320°) > Cu^{II}(260°) ~ Co^{II}(260°).



(22) Fluoroscein (Na-salt)

Complexes of Fe^{II}, Cu^{II}, Cd^{II}, Pb^{II}, Th^{IV} and UO_2^{VI} with disodium salt of eosin have similarly been prepared. Ir study of the ligand suggests that no single structure hitherto assigned to it, represent the true state of affairs and six resonating structures have been proposed[82].

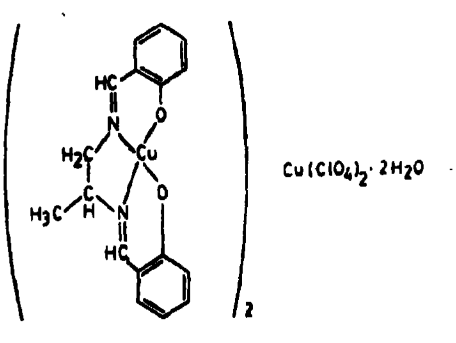
Although complexes of eosin appear to be polymeric and exhibit insolubility in common organic solvents and high thermal stability, the composition of the complexes of eosin and fluoroscein differ. Also Fe^{II} and Cu^{II} complexes probably have distorted octahedral geometry and are magnetically normal in behaviour. Order of thermal stability of the complexes is Cd(360°) > Fe(350°) > UO_2(300°) ~ Th(300°) ~ Pb(300°) > Cu(290°).



(23) Eosin and its resonating structures

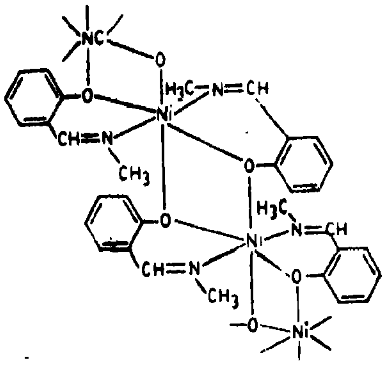
Pfeiffer and Pfitzner[83] were the first to study bis(Schiff bases) as catenating ligands. They investigated copper derivative of bis(Schiff bases) derived from diamines and salicylaldehyde which gave cryoscopic molecular weights corresponding to dimers. But later these were given a polymeric structure, since the established dimers were soluble.

Schiff base metal complexes as ligands have been described in a review by Sinn and Harris[84]. Copper(II) complex derived from *N,N'*-1,2-propylene-bis(salicylaldimine) reacts with copper perchlorate to form the trinuclear complex.

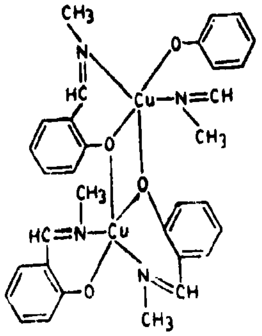


(24) *N,N'*-1,2-Propylene-bis(salicylaldimine)copper(II)

Oxygen-bridged polymeric forms of bis(*N*-methylsalicylaldimino)nickel(II) (24) have been isolated in the solid state by Harris *et al.*[85] which are paramagnetic. A corresponding copper(II) analogue is also known which exists in both monomeric and dimeric forms and the metal atoms are linked by oxygen bridges[86].

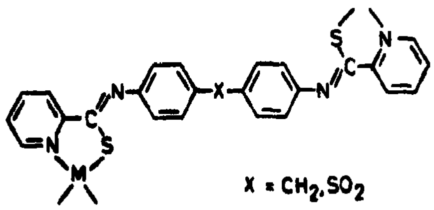


(25) Bis(*N*-methylsalicylaldimino)nickel(II)



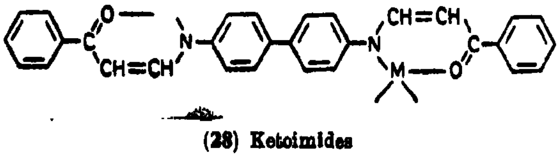
(26) Bis(*N*-methylsalicylaldimino)copper(II)

Bailar *et al.*[37] investigated thiopicolinamide, and



(27) Thiopicolinamide

ketoimides were investigated by Nesmeyanov *et al.*[38]. The analytical data for thiopicolinamide based

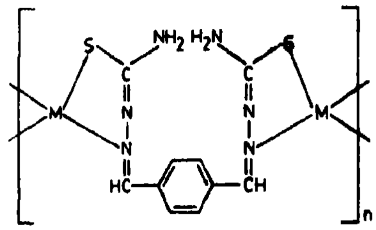


(28) Ketoimides

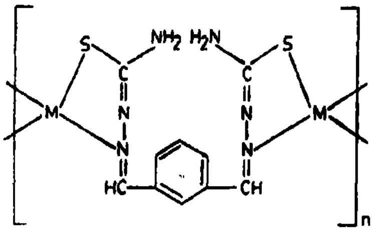
polymers with Cu, Ni or Zn metals indicate molecular weights over 5000. The powdery products are thermally stable to 250-410°. Cu^{II} polymer of ketoimide was prepared by homocondensation in DMF or by interfacial condensation technique between chlorobenzene and aqueous solution. The resultant powders were stable upto 400° for *p*-phenylenediamine and to 350° for benzidine.

Thiosemicarbazides, thiosemicarbazones and their derivatives possess various biological activities and are extensively used in the treatment of tuberculosis. Antimicrobial and antitumour activity are also shown by thiosemicarbazones. Their activity is thought to be due to their ability to form chelates with trace metals present in living systems[39,40].

Drinkard and Chakravarty[41] prepared bis-(thiosemicarbazones) of terephthalaldehyde and naphthazarin and its polymeric Zn^{II} and Ni^{II} complexes. The coordination polymers of isoterphthalaldehyde-bis(thiosemicarbazone) and terephthalaldehyde-bis(thiosemicarbazone) with Cu^{II} and Hg^{II} have been synthesised by Marcu and Dima[42], and their thermal properties and semiconducting properties were studied.

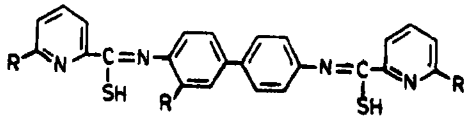


(29) Terephthalaldehyde-bis(thiosemicarbazone)



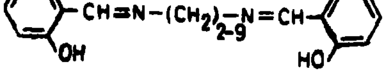
(30) Isoterphthalaldehyde-bis(thiosemicarbazone)

Thioamide[43] with variously substituted benzene rings were employed for the preparation of polymers. Zinc complexes with quadridentate Schiff bases of



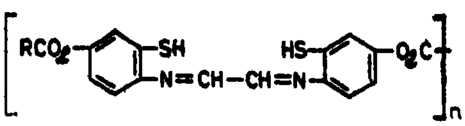
(31) Thioamide

salicylaldehyde and polymethylenediamine with 2-9 carbon atoms chain have been investigated in



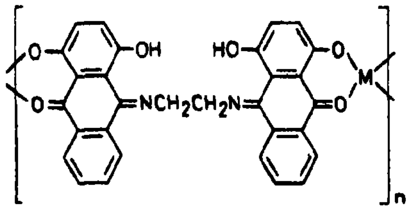
(32) Salicylaldehyde(polymethylenediamine)

detail[44]. Chelating polyesters with azomethine linkage have been synthesised[45]. Suk *et al.*[46] have



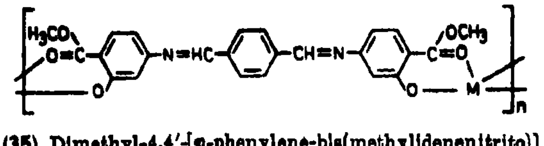
(33) Polyesters with azomethine linkage

prepared transition metal polymers such as poly [M(II)-ethylenediaminequinizarin], where M = Co, Ni and Cu. X-Ray powder method of analysis shows these to be of low molecular weight, and these were found to be insoluble in ether, benzene or acetone.



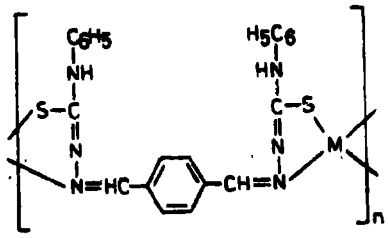
(34) Polyethylenediaminequinazarin

Marcu and Dima[47] investigated the polycoordination of dimethyl-4,4'-[p-phenylenebis(methylidenenitrito)]disalicylate with Co^{II}, Ni^{II} and Cu^{II} in DMF. The coloured polymers were found to be heat stable and semiconducting, and were amorphous, only Cu^{II} polymer having a crystallinity of 89%. The ir and esr spectra of the complexes were studied to elucidate the polymeric nature.



(35) Dimethyl-4,4'-[p-phenylene-bis(methylidenenitrito)] disalicylate

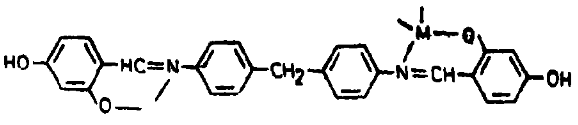
Maurya *et al.*[48] synthesised coordination chain polymers of terephthalaldehyde-bis(4-phenylthiosemicarbazone) with Be^{II}, Co^{II}, Ni^{II}, Cu^{II}, Zn^{II}, Cd^{II} and UO_2^{VI} ions by homocondensation in DMF. The variously coloured complexes Be(yellow), Co(reddish brown), Ni(reddish brown), Cu(greenish yellow), Cd(dark yellow), Zn(red) and UO_2(yellow) were powdery in appearance, and insoluble in water and in common organic solvents. Co, Ni, Cu and UO_2 complexes are octahedral while those of Be, Zn and Cd are tetrahedral. Ir spectral studies suggest coordination through thioenolic S and azomethine N. They decompose at 260-360°, the order of stability being Ni > Cd ~ Be > Co ~ Cu ~ UO_2.



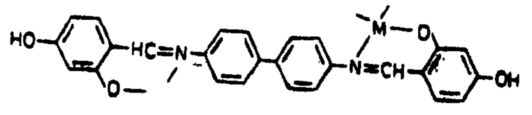
(36) Terephthalaldehyde-bis(4-phenylthiosemicarbazone)

Terephthalaldehyde-bis(4-phenylthiosemicarbazone) [TPBPTS] acts as tetradentate chelating agent coordinating through the thiolo sulphur and nitrogen of the (C=N) group of the Schiff base. Polymerisation is achieved since steric factors prevent the coordination of all the donor groups to a single metal ion, and the metal ion acts as a bridging unit between two donor groups of the ligand. Thus the polymeric chain grows through the consecutive TPBPTS-metal linkage. The polymeric chelate is neutral, since the protons from the SH groups remain ionised.

Macarovici *et al.*[49] prepared Co^{II}, Ni^{II}, Cu^{II} and Zn^{II} complexes of Schiff bases derived from resorcylaldehyde and bis(4-aminophenyl)methane or 4,4'-biaminobiphenyl.

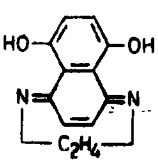


(37) Resorcylaldehyde-bis(4-aminophenyl)methane



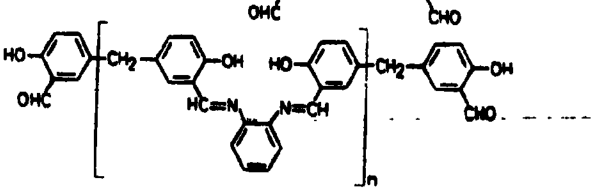
(38) Resorcylaldehyde-bis(4,4'-biaminobiphenyl)

Polyazomethine, the polymeric Schiff base ligand was synthesised by Dubský *et al.*[50] and thus established a new approach for preparing coordination polymers.

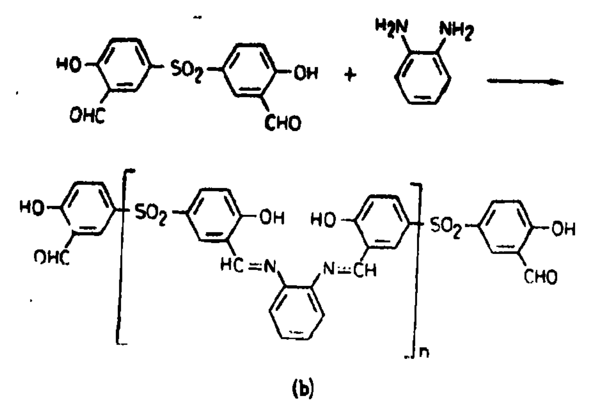


(39) Polyazomethine

Polymeric Schiff bases with long chain and high molecular weight were prepared by Aspey[51], and also by Marvel *et al.*[52]. Initial compounds had been salicylaldehyde, and o-pheylenediamine, but two different pathways had been adopted.

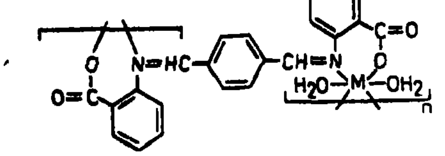


(a)



(b)

(40) Formation of salicylaldehydo(o-phenylenediamine)



(41) Long chain Schiff bases and their polymeric metal complexes

Bis(Schiff base) has been prepared from terephthalaldehyde and anthranilic acid and its complexes with bivalent metals have been synthesised by Singh *et al.*[53]. The octahedral 1 : 1 polymers are thermally stable and decompose in the order Cd(460°) > Mg(420°) ~ Zn(420°) ~ Pb(420°) > Ni(400°) ~ Co(400°) > Mn(360°) > Cu(300°).

Polymeric complexes of Schiff bases of salicylaldehyde and *p*-phenylenediamine or benzidine were investigated by Maurya *et al.*[54]. Salicylaldehydatometal complexes were condensed with the diamines in DMF, with the bipositive metal ions, like Be, Co. Ni, Cu, Zn, Cd, and UO_2. They are amorphous solids and are insoluble.

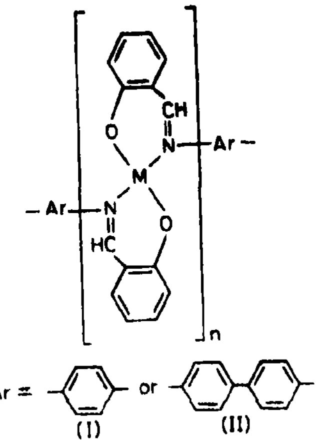
The values of the magnetic moments show that the Co^{II} and Cu^{II} complexes are paramagnetic and Ni^{II} complexes diamagnetic. The geometry of the complexes along with their thermal decomposition temperature are shown in Table 2.

TABLE 2—GEOMETRY, MAGNETIC MOMENT AND THERMAL DECOMPOSITION OF BIS(SALICYLALDEHYDATO) METAL(II)-1,4-DIAMINOBENZENE COMPLEXES

Geometry	Magnetic moment B.M.	Decomp. temp. °C
Co^{II} Tetrahedral	4.48	320
Ni^{II} Sq.-planar	Diamag.	360
Cu^{II} Sq.-planar	1.85	340
Be^{II} ...	Diamag.	400
Zn^{II} ...	Diamag.	400
Cd^{II} ...	Diamag.	340

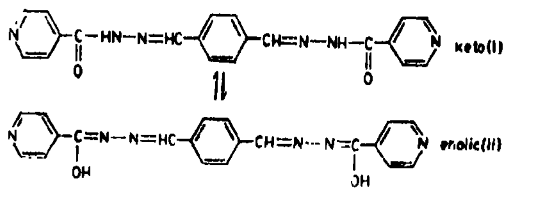
Tetrahedral geometry around the central metal is suggested except in the case of Cu and Ni, which are square-planar, while UO_2 complex is octahedral.

Order of thermal stability for *p*-phenylenediamine bases is Be(400°) ~ Zn(400°) > Co(340°) ~ Ni(340°) ~ Cd(340°) ~ UO_2(340°) > Cu(320°), and for benzidine base it is Ni(400°) > Cu(360°) ~ Cd(360°) > UO_2 (340°) > Co(320°).



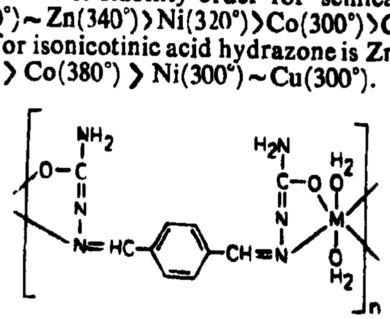
(42) Salicylaldehydodiamines

Singh *et al.*[55] have investigated in detail the syntheses of coordination polymers of terephthalaldehyde-bis(semicarbazone) and bis(isonicotinicacidhydrazone). Ethanolic NaOH solution of semicarbazide hydrochoride was added to ethanolic solution of terephthalaldehyde and refluxed to get an yellow precipitate of the Schiff base. The terephthalaldehyde bis(isonicotinicacidhydrazone) was prepared in ethanolic solution. The polymeric complexes of Co^{II}, Ni^{II}, Cu^{II}, Zn^{II} and Cd^{II} were prepared by homocondensation in DMF. The coloured amorphous solids are insoluble in water and in common organic solvents. Elemental analysis suggests 1 : 1 metal to ligand ratio and an association of $2H_2O$ per metal ion. Ir spectra suggests coordination in

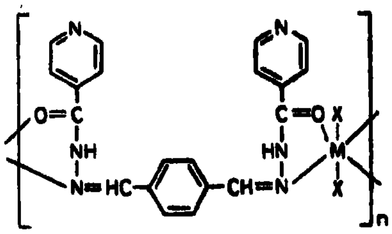


(43) Tautomeric forms of terephthalaldehyde-bis(isonicotinic acid hydrazone)

enolic form though ligand exists in keto form. Octahedral geometry around central metal has been established. The stability order for semicarbazone is Cd(340°) ~ Zn(340°) > Ni(320°) > Co(300°) > Cu(220°), and that for isonicotinic acid hydrazone is Zn(420°) > Cd(400°) > Co(380°) > Ni(300°) ~ Cu(300°).



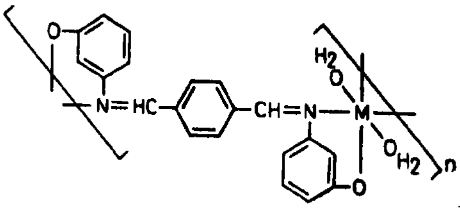
(44) Terephthalaldehyde-bis(semicarbazone)



(45) Terephthalaldehyde-(isonicotinicacidhydrazone) [X = CH_3COO^-]

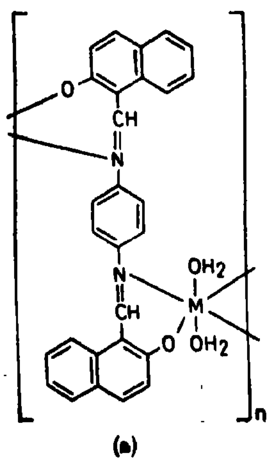
Maurya *et al.*[56] have carried out polymerisation reactions involving the formation of Schiff base metal complexes by condensation of terephthalaldehyde with benzoic or nicotinic acid hydrazides. All the complexes are paramagnetic except Zn^{II} and chelation occurs through the enolic form.

Copper and cobalt polymeric complexes of Schiff base derived from terephthalaldehyde and *m*-aminophenol have been prepared by Singh *et al.*[55].

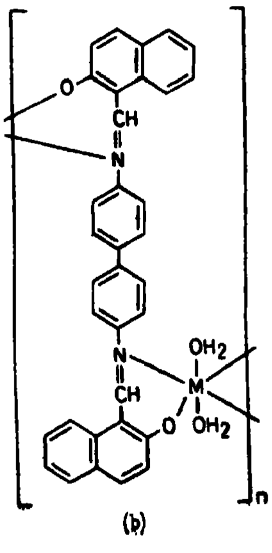


(46) Terephthalaldehyde(aminophenol)

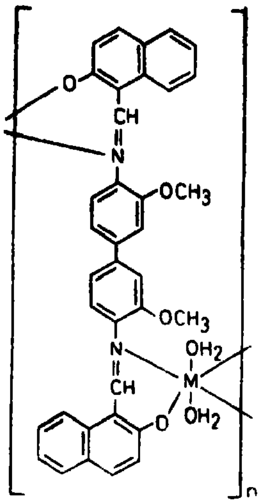
Dwivedi[57] has synthesised a number of coordination polymers by employing Schiff bases derived from aromatic diamines, like *p*-phenylenediamine, benzidine and *o*-dianisidine, and phenolic aldehyde like 2-hydroxy-1-naphthaldehyde. The polymeric complexes were synthesised by refluxing an equimolecular mixture of ligand and metal ion in DMF. The orders of thermal stability for these complexes are: bis(2-hydroxy-1-naphthalidene)-*o*-dianisidine, Zn(380°) > Mn(340°) > Co(300°)~Ni (300°)~Cu(300°) > UO_2(280°); bis(2-hydroxy-1-naphthalidene)benzidine, Mn(380°) > Ni(320°)~Co(320°) > Cu(300°); and bis(2-hydroxy-1-naphthalidene)-*p*-phenylenediamine, Mn(340°) > Ni(300°)~Cu(300°) > Co(280°).



(a)



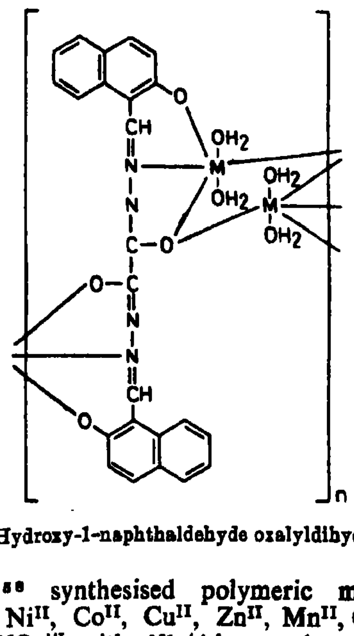
(b)



(c)

(47) Bis(2-hydroxy-1-naphthalidene)diamines

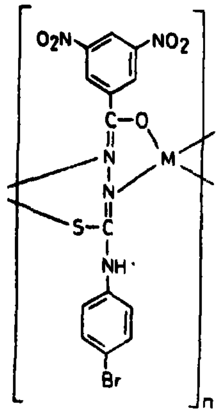
Oxalyldihydrazone of 2-hydroxy-1-naphthaldehyde was prepared by refluxing oxalyldihydrazide and the phenolic aldehyde in the ratio of 1 : 2 in ethanolic DMF (4 : 1). This yellow hydrazone is dissolved in ammoniacal DMF and the solution of metal ions added to it to obtain coloured complexes. The complexes have distorted octahedral geometry around the central metal and are thermally stable. The order of thermal stability being Zn(400°)~Ni (400°) > Co(320°)~Cu(320°).



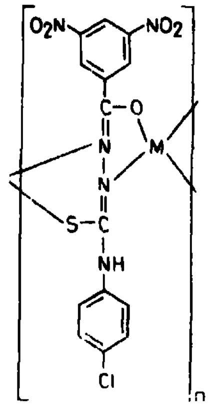
(48) 2-Hydroxy-1-naphthaldehyde oxalyldihydrazone

Pandey[58] synthesised polymeric metal complexes of Ni^{II}, Co^{II}, Cu^{II}, Zn^{II}, Mn^{II}, Cd^{II}, Pb^{II}, Fe^{II} and UO_2^{VI} with N^1-(4-bromophenyl)-N^4-(3,5-dinitrobenzoyl)thiosemicarbazide by refluxing ligand and metal (1 : 1) in DMF. Variously coloured octahedral complexes are thermally stable and decompose in the order, Zn(335°) > Mn(300°) > Cd (290°)~Cu(290°) > Fe(277°) > Co(275°) > Pb(270°)~Ni(270°) > UO_2(245°). Coordination polymers of

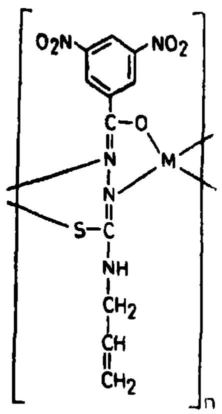
bipositive metal ions with N^1-allyl-N^4-(3,5-dinitrobenzoyl)thiosemicarbazide were prepared by the same procedure. These decompose in the order, Zn(245°) > Cd(240°) > Ni(225°)~Cu(225°) > Co(220°) > Pb(205°). Dwivedi[57] has prepared polymeric metal complexes of N^1-(4-chlorophenyl)-N^4-(3,5-dinitrobenzoyl)thiosemicarbazide. The order of thermal stability for these complexes is Cu(300°) ~Ni(300°) > Co(260°)~Zn(260°)~UO_2(260°) > Mn (240°) > Fe(200°).



(49) N^1-(4-Bromophenyl)-N^4-(3,5-dinitrobenzoyl) thiosemicarbazone

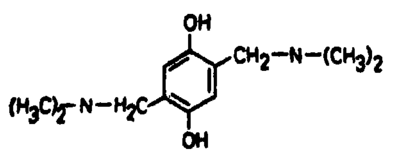


(50) N^1-(4-Chlorophenyl)-N^4-(3,5-dinitrobenzoyl) thiosemicarbazone

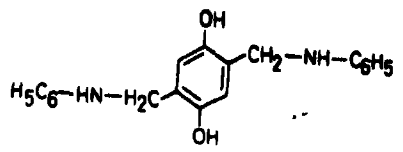


(51) N^1-Allyl-N^4-(3,5-dinitrobenzoyl)thiosemicarbazone

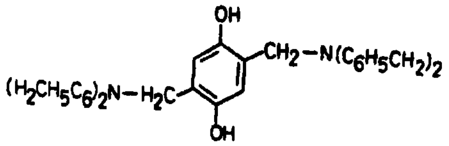
Mannich bases as ligands which have not been used so far for the synthesis of polymeric metal complexes have recently been employed for the preparation of coordination polymers of some bipositive transition metal ions in these laboratories. Gupta[59] has exploited Mannich bases derived from hydroquinone, formaldehyde, dimethylamine, benzylamine or dibenzylamine. Khanna[60] used N,N'-bis(salicylamidomethyl)piperazine for the preparation of polymeric complexes.



(a)

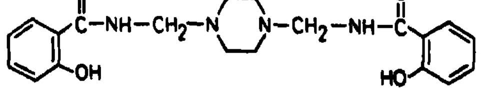


(b)



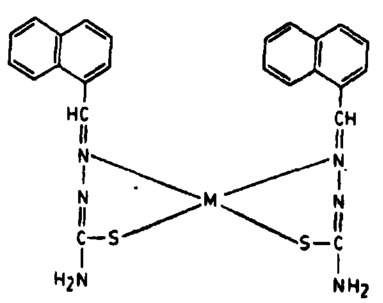
(c)

(52) Mannich bases



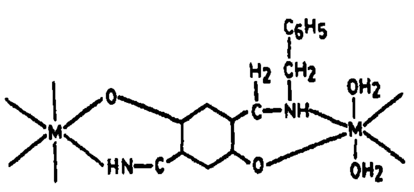
(53) Mannich bases

Gupta[59] has investigated several Schiff bases derived from naphthaldehyde, Mannich base and bipositive metal complexes of oxalic and biscyclohexylidene hydrazide. On the basis of analytical, magnetic, thermal, diffuse reflectance and infrared spectral studies, following octahedral structure has been suggested for naphthaldehyde thiosemicarbazone complexes.



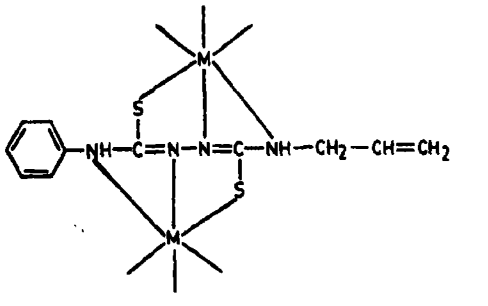
(54) Naphthaldehyde thiosemicarbazone complex

Mannich bases as potential polydentate ligands have been described by Gupta *et al.*[61]. They are synthesised by condensing hydroquinone, formaldehyde and benzylamine in dioxan medium. The polymeric metal complexes formed have the formula $[ML.2H_2O]_n$. The ir spectral data show that the ligand acts as tetradentate chelating agent, coordinating through phenolic oxygens and imino nitrogens. All the four donors do not coordinate to the same metal ion due to steric factors, thus leading to the formation of polymeric chain of ligand-metal linkages.



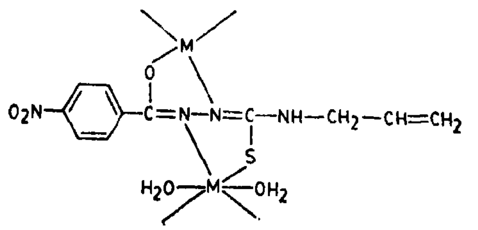
(55) 2,5-Bis(benzylaminomethyl)hydroquinone (Mannich base)

Khanna[60] and Dey *et al.*[61] synthesised several polydentate ligands for the first time involving thiosemicarbazides, hydrazones and aldimines. 1-Thioformanilido-4-allylthiosemicarbazone (TFATS) displays nine tautomeric forms. It behaves as hexadentate ligand coordinating through thioenol, sulphur and two nitrogen atoms (N_1, N_6).



(56) 1-Thioformanilido-4-allylthiosemicarbazone

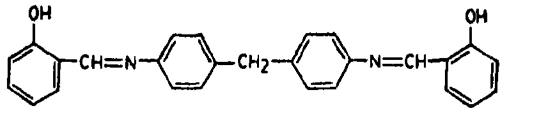
1-Isonicotinoyl- and 1-*p*-nitrobenzoyl-4-allylthiosemicarbazone (INATS, NBATS) behave as tetradentate ligands, coordinating through the thiolo sulphur and nitrogen atoms. Steric factors prevent the coordination of all the donors to a single metal ion, which therefore, acts as a bridging unit between the donor sites of the ligand and thus the polymeric chain grows through consecutive INATS or NBATS metal linkages.



(57) 1-*p*-Nitrobenzoyl-4-allylthiosemicarbazone

A prominent extra band is observed at 880 cm^{-1} due to NO_2 substituent present in benzene ring.

The aldimines are synthesised from 4,4'-methylene dianiline and salicylaldehyde.



(58) Di-salicylidene-4,4'-methylenedianiline

Schiff base is indicated by the appearance of C=N stretching band in the region 1 625-20 cm^{-1}. The coordination occurs through the azomethine nitrogen and oxygen atom of phenolic group.

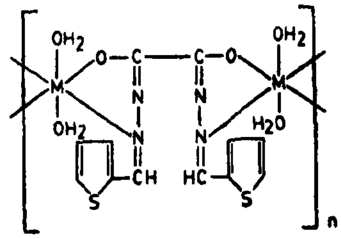
Esr spectral studies have been done for copper(II) complexes, and the esr parameters were determined. From the g values it has been inferred that $d_{x^2-y^2}$ is in the ground state, which is in conformity with band assignments in the reflectance spectra.

μ_{eff} values were also determined by substituting g, $g_\parallel$ and $g_\perp$ obtained from esr spectra for monomeric copper(II) complexes by the following equation,

$$\mu_{eff}^2 = \frac{g_\parallel^2}{4} + \frac{g_\perp^2}{2} + \frac{3KT}{\lambda_0}(g-2)$$

The values are found to be in close agreement with those obtained by magnetic susceptibility measurements.

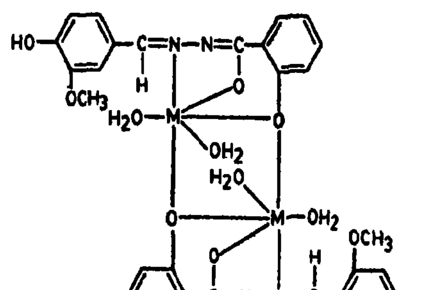
Singh and Misra[62] studied polymeric 2 : 1 metal-ligand complexes formed by thiophene-2-aldehyde-oxalyldihydrazone with bipositive cations. The analytical data indicate the composition to be $[M_2L.4H_2O]_n$. The structure has been shown as 59 and two water molecules are attached to each metal ion.



(59) Thiophene-2-aldehydeoxalyldihydrazone

The studies have also been extended employing semithio-, 4-phenylthio-semicarbazides, nicotinic or isonicotinic hydrazides with thiophene-2-aldehyde.

Singh[64] has studied systematically the metal complexes formed by 4-hydroxy-3-methoxy-benzal dehyde (vanillin) with nicotinic, benzoic or salicylic acid hydrazides. Oxobridged complexes are formed by 4-hydroxy-3-methoxybenzaldehyde salicylic acid hydrazone which are supported from ir spectral studies and lower magnetic moment values presumably due to metal-metal interaction.



(60) 4-Hydroxy-3-methoxybenzaldehydesalicylicacidhydrazone

In this brief account of some coordination polymers (summarised in the Appendix) an attempt has been made to draw the attention of workers to this interesting area of inorganic chemistry. It is hoped that further rigorous studies would provide a wealth of information on the various facets of these compounds and their industrial and biological applications.

Acknowledgement

The author expresses his appreciation for the cooperation received from the band of his dedicated collaborators, whose works have been cited in the text. He is particularly thankful to Professor B. V. Agarwala, R. D. University, Jabalpur, for his kind help in the preparation of the manuscript.

APPENDIX

SUMMARY OF STUDIES IN THE AUTHOR'S LABORATORY

Sl.	Ligand	Metal	Ref.
1.	*N'*-(4-Bromophenyl)-*N*⁴-3,5-dinitrobenzoylthiosemicarbazone	Fe^{II}, Mn^{II}, Co^{II}, Ni^{II}, Cu^{II}, Zn^{II}, Cd^{II}, Pb^{II}, UO_2^{VI}	58
2.	*N'*-Allyl-*N*⁴-(3,5-dinitrobenzoylthiosemicarbazone)	Co^{II}, Ni^{II}, Cu^{II}, Zn^{II}, Cd^{II}, UO_2^{VI}	58
2a.	Isatin thiosemicarbazone	Co^{II}, Ni^{II}, Cu^{II}	67
3.	*N'*-4-Chlorophenyl-*N*⁴-3,5-dinitrobenzoylthiosemicarbazone	Mn^{II}, Fe^{II}, Co^{II}, Ni^{II}, Cu^{II}, Zn^{II}, UO_2^{VI}	57
3a.	Vanillin thiosemicarbazone	Mn^{II}, Fe^{III}, Co^{II}, Ni^{II}, Cu^{II}	67
4.	1-Thioformanilido-4-allylthiosemicarbazone	Cu^{II}, Ni^{II}, Co^{II}, Zn^{II}, Cd^{II}	62
5.	1-Isonicotinyl-4-allylthiosemicarbazone	Co^{II}, Ni^{II}, Cu^{II}, Zn^{II}, Cd^{II}	60
6.	1-*p*-Nitrobenzoyl-4-allylthiosemicarbazone	Co^{II}, Ni^{II}, Cu^{II}, Zn^{II}, Cd^{II}	60
7.	Naphthaldehyde thiosemicarbazone	Co^{II}, Ni^{II}, Cu^{II}	59
7a.	Furfuraldehyde thiosemicarbazone	Co^{II}, Ni^{II}, Cu^{II}	67
8.	Thiophene-2-aldehyde thiosemicarbazone	Co^{II}, Ni^{II}, Cu^{II}, Zn^{II}, Cd^{II}, UO_2^{VI}	63
9.	Anisaldehyde thiosemicarbazone	Co^{II}, Ni^{II}, Cu^{II}, Cd^{II}	65
10.	Pyridine-2-carboxaldehydethiosemicarbazone	Ni^{II}, UO_2^{VI}	65
11.	2-Hydroxy-1-naphthalidene phenylthiosemicarbazone	Co^{II}, Ni^{II}, Cu^{II}	57
12.	2-Hydroxy-1-naphthalidene-4-phenylthiosemicarbazone	Co^{II}, Ni^{II} Cu^{II}	57
13.	Terephthaldehyde-bis-(4-phenylthiosemicarbazone)	Zn^{II}, Cd^{II}, Be^{II}, Co^{II}, Ni^{II}, Cu^{II}, UO_2^{VI}	48
14.	Thiophene-2-aldehyde 4-phenylthiosemicarbazone	Co^{II}, Ni^{II}, Cu^{II}, Zn^{II}, Cd^{II}, UO_2^{VI}	63
15.	Anisaldehyde-4-phenylthiosemicarbazone	Co^{II}, Ni^{II}, Cu^{II}, Zn^{II}, Cd^{I}	65
16.	Pyridine-2-carboxaldehyde-4-phenylthiosemicarbazone	Co^{II}, Ni^{II}, Cu^{II}, Zn^{II}, Cd^{II}, UO_2^{VI}	65
17.	Salicylaldehyde semicarbazone	Co^{II}, Ni^{II}, Cu^{II}, Zn^{II}, Cd^{II}, Be^{II}, UO_2^{VI}	18
17a.	Isatin semicarbazone	Cu^{II}, Ni^{II}	67
18.	Terephthaldehyde-bis-(semicarbazone)	Mn^{II}, Cu^{II}, Zn^{II}, Fe^{II}, Co^{II}, Ni^{II}, Cd^{II}, UO_2^{VI}	55
19.	Naphthaldehyde semicarbazone	Co^{II}, Ni^{II}, Cu^{II}	59
19a.	Vanillin semicarbazone	Fe^{III}, Cu^{II}	67
20.	Thiophene-2-aldehyde semicarbazone	Co^{II}, Ni^{II}, Cu^{II}	63
21.	Salicylidene-4-phenyl semicarbazone	Co^{II}, Ni^{II}, Cu^{II}, Zn^{II}	58
22.	Di-4-bromosalicylidene oxalyldihydrazone	Co^{II}, Ni^{II}, Cu^{II}, Zn^{II}	58
23.	Di-(2-hydroxy)-1-naphthalidene oxalyldihydrazone	Co^{II}, Ni^{II}, Cu^{II}, Zn^{II}	57
24.	Naphthaldehyde oxalyldihydrazone	Co^{II}, Ni^{II}, Cu^{II}	59
25.	Thiophene-2-aldehyde oxalyldihydrazone	Co^{II}, Ni^{II}, Cu^{II}, Zn^{II}, Cd^{II}, UO_2^{VI}	63
26.	Furfuraldehyde oxalyldihydrazone	Co^{II}, Ni^{II}, Cu^{II}, Zn^{II}, Cd^{II}, UO_2^{VI}	65
*26a.	Furfuraldehyde dianisidine		68
*26b.	Thiophene-2-aldehyde dianisidine		68
27.	Disalicylidene dianisidine	Mn^{II}, Co^{II}, Ni^{II}, Cu^{II}, Zn^{II}, Cd^{II}, UO_2^{VI}	58
28.	Di-4-bromosalicylidine dianisidine	Co^{II}, Ni^{II}, Cu^{II}, Zn^{II}	58
*28a.	Anisaldehyde dianisidine		68
29.	Di(2-hydroxy)1-naphthalidene dianisidine	Mn^{II}, Co^{II}, Ni^{II}, Cu^{II}, Zn^{II}, UO_2^{VI}	57
30.	Di(4-bromo)salicylidene *p*-phenylenediamine	Co^{II}, Ni^{II}, Cu^{II}	57
31.	Di(2-hydroxy-1-naphthalidene)-*p*-phenylenediamine	Mn^{II}, Co^{II}, Ni^{II}, Cu^{II}	57
*31a.	Anisaldehyde-*p*-phenylenediamine		68
32.	Salicylidene-*p*-phenylenediamine	Co^{II}, Ni^{II}, Cu^{II}	54
33.	Salicylidenediamine	Zn^{II}, Cd^{II}, Be^{II}	54
*33a.	Thiophene-2-aldehyde-*p*-phenylenediamine		68
34.	Di-5-bromosalicylidene-4,4'-methylenedianiline	Cu^{II}, Ni^{II}	60
35.	Di-salicylidene-4,4'-methylenedianiline	Cu^{II}, Ni^{II}	60
36.	Di-2-hydroxy-naphthalidene-4,4'-methylene dianiline	Co^{II}, Ni^{II}, Cu^{II}	60
*36a.	Furfuraldehyde-*p*-phenylenediamine		68
37.	(4-Bromosalicylidene)-benzidine	Co^{II}, Ni^{II}, Cu^{II}	57
*37a.	Anisaldehydebenzidine		68
b.	Thiophene-2-aldehyde-benzidine		
c.	Furfuraldehydebenzidine		
38.	Di(2-hydroxy-1-naphthalidene)benzidine	Mn^{II}, Co^{II}, Ni^{II}, Cu^{II}	57
39.	2-Hydroxy-1-naphthalidene-3,5-dinitrobenzoylhydrazone	Mn^{II}, Co^{II}, Ni^{II}, Cu^{II}, Zn^{II}, Cd^{II}, UO_2^{VI}	57
40.	Salicylidene-3,5-dinitrobenzoylhydrazone	Mn^{II}, Co^{II}, Ni^{II}, Cu^{II}, Zn^{II}, Cd^{II}, UO_2^{VI}	55

41.	Terephthaldehyde-bis-(3,5-dinitrobenzoic acid)hydrazone	Co^{II}, Ni^{II}, Cu^{II}	60
42.	Terephthaldehyde-bis-(*p*-nitrobenzoic acid)-hydrazone	Co^{II}, Ni^{II}, Cu^{II}, Zn^{II}, Cd^{II}	60
43.	*p*-Hydroxybenzaldehyde (*p*-nitrobenzoic acid)-hydrazone	Co^{II}, Ni^{II}, Cu^{II}	60
44.	*p*-Hydroxybenzaldehyde (benzoic acid)hydrazone	Co^{II}, Ni^{II}, Cu^{II}	64
45.	4-Hydroxy-3-methoxy benzaldehyde(benzoic acid)hydrazone	Co^{II}, Ni^{II}, Cu^{II}	64
46.	*p*-Hydroxybenzaldehyde (*o*-nitrobenzoic acid) hydrazone	Co^{II}, Ni^{II}, Cu^{II}	64
47.	*p*-Hydroxybenzaldehyde-(*m*-nitrobenzoic acid) hydrazone	Co^{II}, Ni^{II}, Cu^{II}	64
48.	4-Hydroxy-3-methoxy benzaldehyde (*o*-nitro benzoic acid)hydrazone	Co^{II}, Ni^{II}, Cu^{II}	64
49.	4-Hydroxy-3-methoxy-benzaldehyde (*m*-nitro-benzoic acid)hydrazone	Co^{II}, Ni^{II}, Cu^{II}	64
50.	4-Hydroxy-3-methoxy benzaldehyde (*p*-nitro-benzoic acid)hydrazone	Co^{II}, Ni^{II}, Cu^{II}	64
51.	(i) Terephthaldehyde-bis-(benzoic acid)hydrazone and (ii) terephthaldehyde-bis(nicotinic acid) hydrazone	Mn^{II}, Co^{II}, Ni^{II}, Cu^{II}, Zn^{II}	56
52.	4-Hydroxy-3-methoxy benzaldehyde(nicotinic acid)hydrazone	Co^{II}, Ni^{II}, Cu^{II}	64
53.	*p*-Hydroxy benzaldehyde (nicotinic acid)hydrazone	Co^{II}, Ni^{II}, Cu^{II}	64
54.	Thiophene-2-aldehyde (nicotinic acid)hydrazone	Co^{II}, Ni^{II}, Cu^{II}, Zn^{II}, Cd^{II}, UO_2^{VI}	63
55.	Anisaldehyde (nicotinic acid)hydrazone	Co^{II}, Ni^{II}, Cu^{II}, Zn^{II}	65
56.	*o*-Hydroxy acetophenone (isonicotinic acid)hydrazone	Fe^{II}, Co^{II}, Ni^{II}, Cu^{II}, Zn^{II}, Cd^{II}	53
57.	*m*-Hydroxybenzaldehyde (isonicotinic acid) hydrazone	Co^{II}, Ni^{II}, Cu^{II}	53
58.	Terephthaldehyde-bis-(isonicotinic acid) hydrazone	Mn^{II}, Fe^{II}, Ni^{II}, Cu^{II}, Co^{II}, Zn^{II}, Cd^{II}, UO_2^{VI}	55
59.	*p*-Hydroxybenzaldehyde (isonicotinic acid) hydrazone	Co^{II}, Ni^{II}, Cu^{II}, Zn^{II}	60
59a.	Isatin (isonicotinic acid) hydrazone	Co^{II}, Ni^{II}, Cu^{II}	67
60.	Naphthaldehyde (isonicotinic acid)hydrazone	Co^{II}, Ni^{II}, Cu^{II}	59
60a.	Vanillin (isonicotinic acid)hydrazone	Mn^{II}, Fe^{III}, Co^{II} Cu^{II}, Ni^{II}	67
61.	Thiophene-2-aldehyde (isonicotinic acid) hydrazone	Co^{II}, Ni^{II}, Cu^{II}, Zn^{II}, Cd^{II}, UO_2^{VI}	63
61a.	Furfuraldehyde(isonicotinic acid) hydrazone	Mn^{II}, Fe^{III}, Cu^{II}, Ni^{II}	67
62.	Anisaldehyde (isonicotinic acid)hydrazone	Co^{II}, Ni^{II}, Cu^{II}, Zn^{II}, Cd^{II}	65
63.	Pyridine-2-carboxaldehyde (isonicotinic acid) hydrazone	Cd^{II}, UO_2^{VI}	65
64.	*p*-Hydroxybenzaldehyde (salicylic acid)hydrazone	Co^{II}, Ni^{II}, Cu^{II}	64
65.	4-Hydroxy-3-methoxy benzaldehyde (salicylic acid)hydrazone	Co^{II}, Ni^{II}, Cu^{II}	64
66.	Oxalicacid bis(cyclohexylidene)hydrazide	Co^{II}, Ni^{II}, Cu^{II}	59
67.	2-Hydroxynaphthalidene 4-amino-2-nitrotoluol	Co^{II}, Ni^{II}, Cu^{II}, Cd^{II}	60
68.	(i) 1,4-Diaminoanthraquinone, (ii) 1,5-diaminoanthraquinone, (iii) 1-aminoanthraquinone, (iv) 1-4-*N,N'*-dimethleneaminoanthraquinone, (v) *N*-salicylideneanthranilic acid	Co^{II}, Ni^{II}, Cu^{II}	20
69.	Terephthaldehyde-bis-(anthranilic acid)	Mn^{II}, Co^{II}, Ni^{II}, Cu^{II}, Zn^{II}, Cd^{II}, Pb^{II}, Hg^{II}	58
70.	Terephthaldehyde-bis-(*o*-aminophenol)	Co^{II}, Cu^{II}	50
71.	Salicylamide	Mn^{II}, Cd^{II}, Be^{II}, ZrO^{IV}, Hg^{II}, UO_2^{VI}	18
72.	Dihydroxyanthraquinone	Mn^{II}, Cd^{II}, Be^{II}, ZrO^{IV}, Hg^{II}, UO_2^{VI}	18
73.	(i) 5,5'-(Benzidine-bis-azo)-8-hydroxyquinoline ; (ii) 5,5'-(*p* phenylenediamine bisazo)-8-hydroxyquinoline ; (iii) 5,5'-(*o*-dianisidine bisazo)-8-hydroxyquinoline	Mn^{II}, Fe^{II}, Ni^{II}, Co^{II}, Cu^{II}, Zn^{II}, Cd^{II}	30
74.	5,5'-(Benzidine-bisazo) salicylaldoxime	Mn^{II}, Co^{II}, Ni^{II}, Cu^{II}, Zn^{II}, Cd^{II}	29
75.	2-Carboxyphenyl-5-azo-8-hydroxyquinoline	Co^{II}, Ni^{II}, Cu^{II}	29
76.	1,2,5,8-Tetrahydroxy-anthraquinone	Mn^{II}, Fe^{II}, Co^{II}, Ni^{II}, Cu^{II}, Zn^{II}, Cd^{II}	19
77.	(i) *o*-Cresotic acid ; (ii) *m*-cresotic acid ; (iii) hydroxynaphthoic acid	Cu^{II}	66
78.	*Mixed ligand* 1 : 10-phenanthrolin as primary, and *o*-cresotic acid and *m*-cresotic acid as secondary ligands	Fe^{II}, Cu^{II}	66
79.	Eosin	Fe^{II}, Cu^{II}, Cd^{II}, Pb^{II}, Th^{IV}, UO_2^{VI}	32
80.	Fluorescein	Co^{II}, Cu^{II}, Zn^{II}, Cd^{II}, Pb^{II}, Ce^{III}, Th^{IV}, UO_2^{VI}	31

* Metal complexes under investigation.

References

1. N. H. RAY, "Inorganic Polymers", Academic Press, London, 1972.
2. T. GRAHAM, *Philos. Trans.*, 1833, **123**, 253.
3. R. L. FRANK, G. R. CLARK and J. N. COKER, *J. Am. Chem. Soc.*, 1950, **72**, 1827.
4. S. KANDA and Y. SAITO, *Bull. Chem. Soc. Jpn.*, 1957, **30**, 192.

5. S. KANDA, *Nippon Kagaku Zasshi*, 1960, **81**, 1847.
6. B. D. JAIN and S. P. SINGHAL, *J. Inorg. Nucl. Chem.*, 1961, **19**, 175.
7. R. S. BOTTEI and J. T. FRANGMAN, *J. Inorg. Nucl. Chem.*, 1966, **24**, 1259.
8. R. H. BAILES and M. CALVIN, *J. Am. Chem. Soc.*, 1947, **69**, 1886.
9. P. B. GUGGIARI, *Chem. Ber.*, 1912, **45**, 2442.
10. A. MANGINI and R. STRATTA, *Gazz. Chim. Ital.*, 1932, **62**, 686.
11. H. D. COBLE and H. F. HOLZCLAW, *J. Inorg. Nucl. Chem.*, 1974, **36**, 1051.
12. R. S. BOTTEI and C. P. MCEACHEN, *J. Inorg. Nucl. Chem.*, 1970, **32**, 2645.
13. R. S. BOTTEI and C. P. MCEACHEN, *J. Inorg. Nucl. Chem.*, 1970, **32**, 2653.
14. R. S. BOTTEI and D. L. GREENE, *J. Inorg. Nucl. Chem.*, 1968, **30**, 1469.
15. R. S. BOTTEI and D. QUANE, *J. Inorg. Nucl. Chem.*, 1964, **26**, 1919.
16. R. S. BOTTEI and J. T. FRANGMAN, *J. Inorg. Nucl. Chem.*, 1966, **24**, 1259.
17. R. S. BOTTEI and J. T. FRANGMAN, *J. Inorg. Nucl. Chem.*, 1966, **24**, 1259.
18. P. L. MAURYA, B. V. AGARWALA and A. K. DEY, *Inorg. Nucl. Chem. Lett.*, 1977, **13**, 145 ; *Indian J. Chem., Sect. A*, 1978, **16**, 358.
19. V. BANERJIE and A. K. DEY, *Makromol. Chem.*, 1979, **180**, 2133.
20. V. M. JOHN, Doctoral Thesis, University of Allahabad, 1982.
21. J. ADACHI, *Nippon Kagaku Zasshi*, 1955, **76**, 311.
22. S. KAWAI, H. HAMAGUCHI and M. TATSUMOTO, *Bunseki Kagaku*, 1956, **5**, 165.
23. Y. KIDANI, *Chem. Pharm. Bull. Jpn.*, 1958, **6**, 563.
24. E. W. BERG and A. ALAM, *Anal. Chim. Acta*, 1963, **28**, 126.
25. J. C. BAILAR, JR., "Inorganic Polymers", Chemical Society, London, 1961.
26. V. V. KORSHAK, S. V. VINOGRADOVA and T. M. BABCHINISTER, *Vysokomol. Soedin.*, 1960, **2**, 498.
27. E. W. BERG and A. ALAM, *Anal. Chim. Acta*, 1962, **27**, 454.
28. S. N. PODDAR and N. SAHA, *Indian J. Appl. Chem.*, 1970, **33**, 244.
29. V. BANERJIE and A. K. DEY, *Curr. Sci.*, 1977, **46**, 778.
30. V. BANERJIE and A. K. DEY, *Polymer Bull.*, 1979, **1**, 685 ; Proc. XX Int. Conf. Coord. Chem., Calcutta, 1979, I-126, p. 211 ; *Makromol. Chem., Rapid Commun.*, 1980, **1**, 41.
31. B. AGARWAL, B. V. AGARWALA and A. K. DEY, *J. Indian Chem. Soc.*, 1979, **57**, 342.
32. B. AGARWAL, B. V. AGARWALA and A. K. DEY, *Rev. Chim. Minerals*, 1979, **16**, 535.
33. P. PFEIFFER and H. PFITZNER, *J. Prakt. Chem.*, 1936, **145**, 243.
34. E. SINN and C. M. HARRIS, *Coord. Chem. Rev.*, 1969, **4**, 391.
35. C. M. HARRIS, S. L. LENZER and R. L. MARTIN, *Aust. J. Chem.*, 1958, **11**, 331.
36. D. HALL and T. N. WATERS, *J. Chem. Soc.*, 1960, 2644.
37. J. C. BAILAR, JR., K. V. MARTIN, M. L. JUDD and J. A. MCLEAN, JR., WADC Tech. Rept. No. 57/391, Pt. II, 1958.
38. A. N. NESMEYANOV, M. I. RIBINSKAYA and G. L. SLONIMSKII, *Vysokomol. Soedin.*, 1960, **2**, 526.
39. M. J. M. CAMPBELL, *Coord. Chem. Rev.*, 1979, **15**, 279 ; S. PADHYE and G. B. KAUFMAN, *Coord Chem. Rev.*, 1985, **63**, 127.
40. N. C. DESAI, H. K. SHUKLA, B. R. PAREKH and K. A. THAKER, *J. Indian Chem. Soc.*, 1984, **61**, 455.
41. W. C. DRINKARD and D. N. CHAKRAVARTY, WADC Tech. Rept. No. 59/761, p. 232, 1960.
42. M. MARCU and M. DIMA, *Rev. Roum. Chim.*, 1967, **12**, 1358 ; 1968, **13**, 359.
43. A. P. TERENTÉV, E. G. RUKHADZE, I. G. MACHOLINA and G. V. PANOVA, *Vysokomol. Soedin.*, 1964, 123.
44. G. E. BATLEY and D. P. GRADDON, *Aust. J. Chem.*, 1967, **20**, 885.
45. E. BAYER, *Chem. Abstr.*, 1968, **68**, 22400.
46. C. J. SUK and K. W. SUK, *Dochan Hwahak Hwoejee*, 1969, **13**, 29.
47. M. MARCU and M. DIMA, *Rev. Roum. Chim.*, 1970, **15**, 1365.
48. P. L. MAURYA, B. V. AGARWALA and A. K. DEY, *Polymer Bull.*, 1979, **1**, 631 ; *J. Indian Chem. Soc.*, 1980, **57**, 275.
49. G. C. MACAROVICI, A. DONITIU and M. GAL, *Ser. Chem.*, 1971, **16**, 31.
50. J. V. DUBSKÝ, A. LANGER and E. WAGNER, *Mikrochem.*, 1937, **22**, 108.
51. S. A. ASPEY, *Diss. Abstr.*, 1955, **15**, 2008.
52. C. S. MARVEL and N. TARKÖY, *J. Am. Chem. Soc.*, 1957, **79**, 6000.
53. B. SINGH, V. BANERJIE, B. V. AGARWALA and A. K. DEY, *J. Indian Chem. Soc.*, 1980, **57**, 365.
54. P. L. MAURYA, B. V. AGARWALA and A. K. DEY, *Polymer Bull*, 1980, **3**, 253 ; *Makromol. Chem.*, 1982, **183**, 511 ; Proc. XXIII Int. Conf. Coord. Chem.. Colarado, 1984, p. 354.
55. B. SINGH, P. L. MAURYA, B. V. AGARWALA and A. K. DEY, *J. Indian Chem. Soc*, 1981, **58**, 541 ; 1982, **59**, 1130 ; 1982, **59**, 29.
56. P. L. MAURYA, C. P. DUBE and B. V. AGARWALA, *J. Indian Chem. Soc.*, 1982, **59**, 1400.
57. D. K. DWIVEDI, Doctoral Thesis, University of Allahabad, 1980.
58. C. B. PANDEY, Doctoral Thesis, University of Allahabad, 1980.
59. H. K. GUPTA, Doctoral Thesis, University of Allahabad, 1983.
60. D. KHANNA, Doctoral Thesis, University of Allahabad, 1982.
61. H. K. GUPTA, P. L. MAURYA and A. K. DEY, *J. Indian Chem. Soc.*, 1982, **59**, 216.
62. D. KHANNA, B. V. AGARWALA and A. K. DEY, *Indian J. Chem., Sect. A*, 1982, **21**, 609.
63. B. SINGH, Doctoral Thesis, University of Allahabad, 1984 ; B. SINGH and H. H. MISRA, *J. Indian Chem. Soc.*, in the press.
64. H. R. SINGH, Doctoral Thesis, University of Allahabad, 1985.
65. P. S. N. REDDY, Doctoral Thesis, University of Allahabad, 1985.
66. B. AGARWAL, Doctoral Thesis, University of Allahabad, 1979.
67. P. CHATTERJEE and B. V. AGARWALA, Unpublished work.
68. H. K. DUGGAL and B. V. AGARWALA, Unpublished work.

J. Indian Chem. Soc.,
Vol. LXIII, April 1986, pp. 371-373

Studies on the Preparation and Characterisation of Bis-p-biphenyltin(IV) Carboxylates

J. C. TREHAN, R. K. SHARMA, N. KUMAR and C. P. SHARMA*

National Physical Laboratory, Hillside Road, New Delhi-110 012

Manuscript received 21 June 1985, revised 20 January 1986, accepted 6 February 1986

Bis-p-biphenyltin(IV) carboxylates of the type p-$(C_6H_5-C_6H_4)_2Sn(OCOR)_2$, where R=o-$CH_3-C_6H_4$, p-$CH_3-C_6H_4$, $CH_3-O-C_6H_4$, $CH_2-C_6H_5$ and $CH=CHC_6H_5$, have been prepared by the reaction of bis-p-biphenyltin dichloride with sodium salt of respective carboxylic acid in 1 : 2 molar ratio in methanol and acetone mixture. The complexes are characterised by elemental analysis, molecular weight determination, conductivity measurements, infrared and ^1H nmr spectroscopy. The carboxylate moiety acts as bidentate in these complexes.

ORGANOTIN carboxylates of the three known types, *viz.* $R_3SnOCOR'$, $R_2Sn(OCOR')_2$ and $RSn(OCOR')_3$ are of great commercial value owing to their utility as polyvinyl chloride stabilisers[1-5] and fungicides[6]. Their structural chemistry is also of great interest because of the varying bonding behaviour of the carboxylate moiety in different organotin carboxylates. Extensive structural investigations using ir, ^1H nmr, Mössbauer spectroscopy and *X*-ray studies made on triorganotin carboxylates, $R_3SnOCOR$, suggest that most of such compounds occur in the solid phase as coordination polymers with pentacoordinate tin[7-11]. In solution or in the liquid phase, the compounds are monomeric. Formation of the polymeric structure is also impeded by the steric hindrance presented by bulky R group or a branching R' group. Furthermore, in dialkyltin carboxylates, $R_2Sn(OCOR')_2$, the tin atom has been suggested to bear coordination number of six with the distorted *trans* arrangement of the alkyl groups and the carboxylate moiety acting as a bidentate ligand[12,13].

The present communication deals with the synthesis and structural investigation of some hitherto unknown carboxylates of bis-p-biphenyltin(IV) of the type $(p\text{-}C_6H_5-C_6H_4)_2Sn(OCOR)_2$, where R=o-$CH_3-C_6H_4$, p-$CH_3-C_6H_4$, $CH_3-O-C_6H_4$, $CH_2-C_6H_5$ and $CH=CH-C_6H_5$.

Experimental

All reagents were of AnalaR grade. Bis-p-biphenyltin(IV) dichloride was prepared by the disproportionation reaction of tetrabis-p-biphenyltin(IV) and tin tetrachloride[14].

Preparation of sodium salt of carboxylic acids : Sodium salt of carboxylic acids used in this work, were synthesised according to the preparation of sodium cinnamate. Sodium hydroxide pellets (4 g, 0.1 mol) were taken in ethanol (50 ml) and refluxed till it dissolved completely. Cinnamic acid (14.8 g, 0.1 mol) was taken in dry benzene (50 ml). Alkali solution was added slowly dropwise to the acid solution till it showed pink colour with phenolphthalein. The sodium salt of cinnamic acid was precipitated out and filtered. The precipitate was washed several times with ether and dried.

Preparation of complexes. Biscinnamatobis(p-*biphenyl*)*tin*(*IV*) *:* To a solution of sodium cinnamate (3.4 g, 0.02 mol) in methanol (50 ml) was added a solution of bis-p-biphenyltin dichloride (4.95 g, 0.01 mol) in acetone (50 ml). The mixture was refluxed for 0.5 h and filtered. Solvent was removed from the filtrate under reduced pressure to 10 ml and then petroleum ether (b.p. 60-80°) was added dropwise. A white precipitate formed was collected, dried *in vacuo* and recrystallised from a mixture of methylene chloride and petroleum ether (1 : 1) to give a white crystalline solid (80%).

Similarly other bis(p-biphenyl)tin biscarboxylates, *i.e.* o-tolyl, p-tolyl, anisyl and benzyl were prepared. Analytical data for the complexes are given in Table 1.

Infrared spectra were recorded on a Perkin-Elmer 399 grating spectrophotometer using KBr pellets in the 4 000-400 cm^{-1} region. Proton magnetic resonance spectra were recorded at ambient temperature (28°) at sweep width of 500 Hz with a Varian A-60 spectrometer. The magnetic field sweep was calibrated with a standard sample of chloroform and TMS (1%) in deuterated chloroform. Quantitative estimation of carbon and hydrogen was done by using micro-analytical apparatus. Tin was estimated as tin oxide gravimetrically.

Results and Discussion

The new bis-p-biphenyltin(IV) bis-carboxylates are obtained by the reaction of bis-p-biphenyltin dichloride with the respective sodium salt of

TABLE 1—CONDUCTIVITY AND ANALYTICAL DATA OF $(p\text{-}C_6H_5\text{-}C_6H_4)_2Sn(OCOR)_2$ COMPLEXES

Sl. no.	R	M.p. °C	Molar conductivity* Ω^{-1} cm^2 mol^{-1}	Mol. Wt. Found/ (Calcd.)	Analysis % : Found/(Calcd.) C	H	Sn
1.	$o\text{-}CH_3-C_6H_4$	48-9°	0.65	702.4 (694.7)	68.5 (69.09)	4.4 (4.60)	18.4 (17.09)
2.	$p\text{-}CH_3-C_6H_4$	83°	0.67	708.8 (694.7)	68.7 (69·09)	4.72 (4.60)	18.7 (17.09)
3.	$CH_3O-C_6H_4$	80°	0.69	720.2 (726.7)	65.92 (66.06)	4.44 (4.40)	16.7 (16.84)
4.	$CH_2-C_6H_5$	90°	0.80	700.6 (694.7)	69.23 (69.09)	4.58 (4.61)	17.62 (17.09)
5.	$CH=CH\ C_6H_5$	72°	0.83	725.6 (718.7)	89.97 (70.13)	4.40 (4.45)	15.94 (16.52)

* Concentration was 0.5 m in each case.

carboxylic acid molar ratio 1 : 2 in acetone-methanol mixture according to the following equation,

$$p\text{-}(C_6H_5-C_6H_4)_2\ SnCl_2+2NaOCOR \rightarrow$$
$$p\text{-}(C_6H_5-C_6H_4)_2\ Sn(OCOR)_2+2NaCl$$

The complexes are white crystalline solids and are fairly stable in dry and inert atmosphere. Conductance measurements and molecular weight determinations show that all the complexes are essentially non-electrolytes in nitrobenzene and are monomeric in benzene.

Infrared spectra : In the infrared spectra, the study of the region 1 700-1 300 cm^{-1} incorporating (OCO) stretching vibrations is of great diagnostic value. In this region, the difference between ν_{asym} (OCO) and ν_{sym}(OCO) may be taken as good criterion to identify the particular mode of bonding of the carboxylate ligand[15]. If this difference is of the order of ~150 cm^{-1}, the carboxylate moiety may be considered to act either as bridging or as bidentate ligand[16]. However, a difference greater than 200 cm^{-1} indicates the monodentate behaviour of the ligand[17].

The ir spectral data of all the compounds studied in the present investigation (Table 2) reveal them to be having bidentate carboxylate ligands because the difference between ν_{asym}(OCO) and ν_{sym}(OCO) is of the order ~150 cm^{-1}, thereby a coordination number of six may be assigned to tin atom.

TABLE 2—CHARACTERISTIC IR BANDS (cm^{-1})* OF $(p\text{-}C_6H_5-C_6H_4)_2$ Sn(OCOR)$_2$ COMPLEXES

Sl. no.	R	ν_{asym}(OCO)	ν_{sym}(OCO)	($\nu_{asym}-\nu_{sym}$)
1.	$o\text{-}CH_3-C_6H_4$	1 600s	1 480s	120
2.	$p\text{-}CH_3-C_6H_4$	1 610vs	1 480s	130
3.	$CH_3O-C_6H_4$	1 600vs	1 480s	120
4.	$CH_2-C_6H_5$	1 550vs	1 4.0s	130
5.	$CH=CH\ C_6H_5$	1 575s	1 430s	145

* s=strong, vs=very strong.

^{1}H nmr spectra : Proton magnetic resonance spectra of the bis-*p*-biphenyltin(IV) carboxylates show two types of signals, and correlation of the resonance signals with various groups present in the molecules has been made. The spectra exhibit the resonance signal in the form of a doublet, triplet and doublet between τ 2.0 and 3.0 due to biphenyl protons. The other proton signals characterising different carboxylate groups are a singlet due to CH_3 protons attached to benzene moiety of carboxylate τ ~7.6 and a singlet due to C_6H_5 proton τ~2.8, in *o*-tolyl complexes. In *p*-tolyl complex, there is a singlet τ~7.62 due to CH_3 protons attached to benzene nuclei of the carboxylate and a singlet which is mixed with the other benzene protons of biphenyl unit τ~2 44. In the anisyl derivative, there appears a singlet τ~6.15 due to methoxy group and a singlet τ~2 24 due to benzene nuclei characterise the phenyl acetate complex. In cinnamate complex, there are two singlet τ~3.4 and 3.6 whereas proton signals due to benzene ring of cinnamate mixed with the protons of the benzene ring of biphenyl unit.

References

1. V. YNGUE, US Pat., 2 307 092/1943 (*Chem. Abstr.*, 1943, **37**, 3532).
2. W. M. QUATTLEBAUM, JR. and C. A. NOFFSINGER, US Pat. 2 307 157/1943 (*Chem. Abstr.*, 1943, **37**, 3533).
3. G. P. MACK and E. PARKER, US Pat. 2 938 013/1960 (*Chem. Abstr.*, 1960, **54**, 20834).
4. W. A. JOHNSON, *Tin Its Uses*, 1962, **54**, 5.
5. J. G. A. LUIJTEN and S. PEZARRO, *Br. Plast.*, 1957, 183.
6. K. HARTEL, *Angew. Chem.*, 1958, **70**, 135.
7. M. W. G. DEBYE, D. E. FANTON, S. E. ULRICH and J. J. ZUCKERMAN, *J. Organomet. Chem.*, 1971, **28**, 339 and reference therein.
8. B. Y. K. HO, J. A. ZUBIETA and J. J. ZUCKERMAN, *Chem. Commun.*, 1975, 88.
9. R. H. HERBER, H. A. STOCKLER and W. T. REICHLE, *J. Chem. Phys.*, 1965, **42**, 2447.
10. D. W. ALLEN, J. S. BROOKS, R. FORMSTONE, A. J. CROWE and P. J. SMITH, *J. Organomet. Chem.*, 1978, **156**, 359.
11. C. P. SHARMA, N. KUMAR, S. CHANDRA and V. G. BHIDE, *J. Inorg. Nucl. Chem.*, 1981, **43**, 2659.

12. Y. MAEDA and R. OKAWARA, *J. Organomet. Chem.*, 1967, 10, 247.
13. A. G. MADDOCK and R. H. PLATT, *J. Chem. Soc. (A)*, 1971, 1191.
14. T. V. TALALAEVA, N. A. ZAITSEVA and K. A. KOCHESKOV, *J. Gen. Chem. USSR*, (*Engl. Transl.*), 1946, 16, 901.
15. K. ITO and H. BERNSTEIN, *Can. J. Chem.*, 1956, 34, 170.
16. N. F. CURTIS, *J. Chem. Soc. (A)*, 1968, 1579.
17. M. LINHARD and B. J. RAU, *Z. Anorg. Chem.*, 1953, 271, 121.

J. Indian Chem. Soc.,
Vol. LXIII, April 1986, pp. 374-376

Complexes of Cobalt(II), Nickel(II) and Copper(II) with 4-Substituted-1-(2-furoyl)thiosemicarbazides†

A. C. HIREMATH*, M. B. HALLI and N. V. HUGGI

Department of P. G. Studies and Research in Chemistry, Gulbarga University, Gulbarga-585 106

Manuscript received 9 January 1984, revised 30 January 1986, accepted 17 February 1986

Metal complexes of the type $MLCl_2$, where M = Co^{II}, Ni^{II} and Cu^{II} ; L = 1-(2-furoyl)-4-phenylthiosemicarbazide, 1-(2-furoyl)-4-(*p*-chlorophenyl)thiosemicarbazide or 1-(2-furoyl)-4-(*p*-bromophenyl)thiosemicarbazide, have been synthesised. Analytical data, magnetic moment, molar conductance, electronic and infrared spectral data have been explored to elucidate the structure of the complexes.

THE thiosemicarbazides and their metal complexes are of great importance due to their wide range of analytical and pharmacological applications[1-4]. As ligands, they provide three potential donor sites, *viz*. O, N and S, and form complexes with various transitional and non-transitional metal ions. The present paper deals with synthesis of Co^{II}, Ni^{II} and Cu^{II} complexes of 1-(2-furoyl)-4-phenylthiosemicarbazide (L), 1-(2-furoyl)-4-(*p*-chlorophenyl)thiosemicarbazide (L′) and 1-(2-furoyl)-4-(*p*-bromophenyl)thiosemicarbazide (L″) and their characterisation with the aid of elemental analysis, magnetic moment, molar conductance, ir and electronic spectral data.

Experimental

All the chemicals used were of AnalaR grade. The ligands L, L′ and L″ were synthesised by the literature methods[5].

Preparation of complexes : A hot ethanolic solution of the ligand (0.05 *M*) was treated with metal chloride (0.05 *M*) in the same solvent with vigorous stirring. The resulting reddish brown solution was refluxed for about 30 min, a saturated ethanolic solution of sodium acetate was then added dropwise to the reaction mixture to raise the *p*H to 5-6 (except for Cu^{II} complexes) and the reflux continued for a few minutes. The solution was concentrated and treated with an excess of distilled water to get the complexes separated as insoluble residue. These were filtered, washed with little ethanol and dried in vacuum over fused calcium chloride. The complexes are brown, reddish brown or green coloured amorphous solids stable in air, and soluble in DMF, DMSO and pyridine.

The metal, nitrogen, sulphur and chloride were estimated by standard methods. The results of analyses are shown in Table 1.

Physical measurements : The measurements of molar conductance, magnetic susceptibility, infrared spectra and electronic spectra (nujol) were made as detailed in our earlier paper[6]. The electronic spectra of the complexes in pyridine solution were recorded in the range 900-340 nm on Elico model CL-24 spectrophotometer.

Results and Discussion

All the complexes were of 1 : 1 (metal-ligand) stoichiometry (Table 1). The molar conductances in DMF ($10^{-3}M$) were in the range 6-31 Ω^{-1} cm^2 mol^{-1} suggesting non-electrolytic[7] nature of the complexes.

The μ_{eff} values (Table 1) for Co^{II} complexes are in the range 2.48-2.7 B.M. which are well within the range expected for spuare-planar Co^{II} complexes[8]. For Cu^{II} complexes, the observed values (Table 1) lie in the range 1.65-1.79 B.M. which correspond to square-planar geometry. The subnormal values may be ascribed to the spin-orbit coupling taking place by super-exchange through the bridging sulphur atoms[9] or metal-metal interaction in the dimeric or polymeric structure formed through halogen bridging[10]. Ni^{II} complexes are diamagnetic in nature suggesting their square-planar stereochemistry[11].

The solid state electronic spectra of Co^{II} complexes exhibit two prominent bands, one of medium intensity at 14 290-16 390 cm^{-1} and the second of high intensity at 18 180-19 610 cm^{-1}, attributable to $^2A_{1g} \rightarrow {}^2B_{1g}$ and $\rightarrow {}^2E_g$ transitions, respectively in square-planar geometry[12]. The relatively high intensity of the second band may be due to contributions by the charge transfer transition appearing in the region 28 570-30 000 cm^{-1}. In pyridine solution, the Co^{II} complexes exhibit only one band at 18 500-20 000 cm^{-1}, as a shoulder on a steeply raising uv

† Abstract of the paper was presented at the 20th Annual Convention of Chemists held at Cuttack, December, 1983.

TABLE 1—ELEMENTAL ANALYSIS, MOLAR CONDUCTANCE AND MAGNETIC SUSCEPTIBILITY OF THE COMPLEXES

Compd.	Colour	M.p. °C	Analysis % : Found/(Calcd.) M	N	S	Cl	Λ_M Ω^{-1} cm^{-1} mol^{-1}	μ_{eff} B.M.
$CoLCl_2$	Dark brown	255	15.60 (15.07)	10.60 (10.74)	8.72 (8.18)	18.89 (18.17)	30.5	2.48
$NiLCl_2$	Light brown	285	15.32 (15.02)	10.61 (10.75)	8.00 (8.19)	17.93 (18.71)	20.83	—
$CuLCl_2$	Brown	195	16 85 (16.05)	10.12 (10.62)	7.88 (8.09)	17.85 (17.95)	18.18	1.68
$CoL'Cl_2$	Dark green	240	13.29 (13.82)	9.20 (9.86)	7.25 (7.51)	16.84 (16.67)	28.50	2.59
$NiL'Cl_2$	Light brown	255	13.61 (13.80)	9.67 (9.88)	7.62 (7.58)	16.48 (16.70)	6.15	—
$CuL'Cl_2$	Dark brown	180	14.30 (14.75)	9.65 (9.75)	6.88 (7.43)	16.39 (16.49)	30.35	1.65
$CoL''Cl_2$	Brown	260	12.25 (12.52)	8.55 (8.94)	6.62 (6.81)	15.01 (15.11)	25.15	2.70
$NiL''Cl_2$	Reddish brown	300	12.31 (12.49)	8.77 (8.94)	6.70 (6.81)	15.41 (15.12)	12.61	—
$CuL''Cl_2$	Green	190	13.55 (13.88)	8.45 (8.85)	6.12 (6.74)	14.56 (14.96)	28.35	1.79

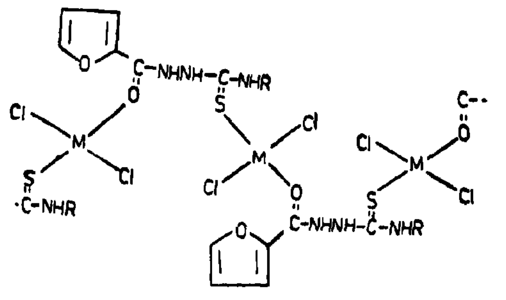
absorption tail of a charge transfer band. Hence, the change of absorption bands and absence of any band around 15 000 cm^{-1} are ascribed to the change of geometry from planar to pseudo-octahedral ones.

The diamagnetic Ni^{II} complexes exhibit a medium intensity band at 16 130-16 673 cm^{-1} and a high intensity band at 23 810-30 300 cm^{-1}, corresponding to transitions from ${}^1A_{1g} \to {}^1A_{2g}$ and $\to {}^1E_g$, respectively[13]. The high intensity of the latter band may be due to overlap of L→M charge transfer band. The Ni^{II} complexes undergo colour change from brown to yellow in pyridine thereby showing new uv absorption bands at 13 420-14 390 and 24 690-26 315 cm^{-1} which correspond to ${}^3A_{2g} \to {}^3T_{1g}$ (F)(ν_2) and $\to {}^3T_{1g}$(P)(ν_3) transition, respectively in an octahedral stereochemistry, with the disappearance of bands observed in the solid state spectra. The band due to ${}^3A_{2g} \to {}^3T_{2g}$(F)($\nu_1$) transition could not be located due to instrumental limitation. However, the values of ν_1 band have been computed (8 100-8 600 cm^{-1}). The calculated values of Racah parameter, B (981-993 cm^{-1}) and the ratio ν_2/ν_1 (1.65-1.67) for the complexes in pyridine are well within the range expected for pseudo-octahedral Ni^{II} complexes[13]. It may be concluded that the square-planar Ni^{II} complexes have undergone an axial addition of two pyridine molecules to form pseudo-octahedral structure by expanding the coordination number from four to six[14]. A single broad band (15 380-21 800 cm^{-1}) in the electronic spectra of Cu^{II} complexes (in the solid state) is well in the range for square-planar complexes. The three transitions, ${}^2B_{1g} \to {}^2A_{1g}$, $\to {}^2B_{2g}$ and $\to {}^2E_g$ are very close in energy and form a single broad band[13]. The absence of any band below 10 000 cm^{-1} rules out the posibility of tetrahedral or pseudo-tetrahedral geometry[15]. The high intense band observed at 25 000-31 000 cm^{-1} is ascribed to L→M charge transfer transition. Only one medium intensity band is observed at 12 820-16 130 cm^{-1} in the electronic spectra of Cu^{II} complexes in pyridine solution and no band is observed around 18 500 cm^{-1}. The 10Dq values calculated for the spectra in pyridine lie in the range 1 430-1 560 cm^{-1}. This implies that the square-planar configuration has changed in pyridine, thus suggesting coordination of two solvent molecules forming pseudo-octahedral structure[16].

The infrared bands for the free ligands in the region 3 230-3 125 cm^{-1} are attributed to intermolecularly hydrogen bonded NH stretch[17,18]. In the metal complexes the NH bands undergo positive shift or remain unaltered, suggesting the non-involvement of NH group in bonding with metal ion. The N–N stretching bands[19] (950-920 cm^{-1}) in the ligands show red shift in the complexes suggesting that protonation has not been possible to N–N group and no coordination has taken place through NH group[20]. In the complexes, the C=O stretching bands of the ligand (1 650-1 610 cm^{-1}) show red-shift of 10-55 cm^{-1} in the complexes suggesting the participation of C=O group in coordination[21]. The ligands exist in thione and keto form since no bands due to SH and OH stretch are observed in the region 2 600-2 400 and 3 400 cm^{-1}, respectively. The ligand bands observed at 1 295-1 255 cm^{-1} are ascribed to C–O–C (furan ring) stretching vibration[5,22]. These bands show blue-shifts in the respective complexes suggesting the non-involvement of furan ring oxygen in bonding. The ligand bands observed at 1 555-1 500, 1 390-1 350, 1 080-1 025 and 790-730 cm^{-1} are assigned to the thioamide bands I, II, III and IV, respectively[17,23]. On complexation the thioamide band I remains unaltered or show slight blue- or red-shift, since it has major contribution of NH deform and small contribution of C–N stretch. The thioamide bands II and III with some contributions of C=S stretch in the complexes have shown lower frequency shift of the order of 5-30 cm^{-1} with varying intensity. The thioamide band IV mainly due to C=S stretch has shown considerable red-shift with reduced intensity in all the complexes suggest-

ing the coordination of thioketo sulphur[24]. The 500-370 cm^{-1} bands in the far-ir region are attributed to M–O (carbonyl) stretching vibration in the complexes[25]. In all the complexes, the medium intensity bands observed at 280-220 cm^{-1} are ascribed to M–Cl stretching mode[26]. The bands observed in the region 270-225 cm^{-1} are attributed to *M–S stretching mode*[27]. *The M–S stretching* mode appears in the vicinity of M–Cl stretch where there is possibility of both vibrations to overlap. The reduced intensity of M–O and M–S stretching modes may be due to the polymeric nature of the complexes[28].

It is, therefore, evident that the ligands exhibit bidentate nature in all the complexes by bonding through the carbonyl oxygen and thioketo sulphur atoms as shown in the following structure.



where, M = Co^{II}, Ni^{II} and Cu^{II}; R = C_6H_5, $C_6H_4Cl(p)$ and $C_6H_4Br(p)$.

Acknowledgement

The authors gratefully acknowledge Prof. S. P. Hiremath, Head of the Department of Chemistry, Gulbarga University, for facilities. One of the authors (M.B.H.) is grateful to C.S.I.R., New Delhi, for a Senior Research Fellowship.

References

1. H. L. Yale, K. A. Losee, F. M. Perry and J. Bernstein, *J. Am. Chem. Soc.*, 1951, **76**, 2206.
2. B. T. Gouda and D. S. Mahadevappa, *J. Indian Chem. Soc.*, 1978, **55**, 842.
3. K. C. Agarwal, B. A. Booth and E. C. Moore, *Biochem. Pharmacol.*, 1974, **23**, 2412.
4. B. Craciuneanu and E. Florean, *Rev. Roum. Chim.*, 1968, **13**, 105, 758.
5. V. B. Jigajinni, S. C. Bennur, R. S. Bennur and V. V. Badiger, *J. Karnatak University (Sci.)*, 1975, **20**, 2.
6. A. C. Hiremath, N. V. Huggi and M. B. Halli, *Indian J. Chem., Sect. A*, 1983, **22**, 607.
7. W. J. Geary, *Coord. Chem. Rev.*, 1971, **7**, 81.
8. B. N. Figgis and J. Lewis, *Prog. Inorg. Chem.*, 1965, **6**, 192.
9. M. Patel, M. M. Patel, A. Ray and M. R. Patel, *J. Inorg. Nucl. Chem.*, 1981, **43**, 509.
10. M. M. Jostafa, A. M. Shallaby and A. A. El. Asmy, *J. Indian Chem. Soc.*, 1983, **60**, 109; C. M. Harris and R. L. Martin, *Proc. R. Soc. London*, 1958, 259.
11. M. Akabar Ali and S. G. Teoh, *J. Inorg. Nucl. Chem.*, 1978 **40**, 451, 2013.
12. C. Natarajan and M. Palaniandavar, *J. Indian Chem. Soc.*, 1983, **60**, 1.
13. A. B. P. Lever, "Inorganic Electronic Spectroscopy", Elsevier, New York, 1968; *Coord. Chem. Rev.*, 1968, **3**, 199.
14. B. B. Kaul and K. B. Pandeya, *J. Inorg. Nucl. Chem.*, 1978, **40**, 229.
15. L. W. Laue and L. T. Taylor, *J. Coord. Chem.*, 1973, **2**, 295; M. S. Patil and J. R. Shah, *J. Indian Chem. Soc.*, 1983, **60**, 79.
16. A. K. Rana and J. R. Shah, *Indian J. Chem., Sect. A*, 1982, **21**, 929.
17. C. N. R. Rao, "Chemical Applications of Infrared Spectroscopy", Academic, New York, 1963.
18. P. J. F. Griffith and G. D. Morgan, *Spectrochim. Acta, Part A*, 1972, **28**, 1899.
19. A. K. Srivastava, A. L. Varshney and P. C. Jain, *J. Inorg. Nucl. Chem.*, 1980, **42**, 47
20. J. R. Durig, S. P. Bush and H. H. Mercer, *J. Chem. Phys.*, 1966, **44**, 423.
21. R. C. Aggarwal and T. R. Rao, *J. Inorg. Nucl. Chem.*, 1978, **40**, 171.
22. R. S. Sharma and S. C. Bahel, *J. Indian Chem. Soc.*, 1982, **59**, 877.
23. K. Das, U. S. Prasad, A. K. Dubey, B. N. Keshari and L. K. Mishra, *J. Indian Chem. Soc.*, 1983, **60**, 497.
24. R. Singh, M. P. Srivastava and L. K. Mishra, *Indian J. Chem., Sect. A*, 1977, **15**, 805.
25. C. B. Mahto, *J. Indian Chem. Soc.*, 1981, **58**, 935.
26. N. Saha and K. M. Datta, *J. Indian Chem. Soc.*, 1981, **58**, 940.
27. G. Marcotrigiano, G. Peyronel and R. Battistuzzi, *J. Inorg. Nucl. Chem.*, 1975, **37**, 1975.
28. H. S. Verma, A. Pal, R. C. Saxena and J. L. Vats, *J. Indian Chem. Soc.*, 1982, **59**, 1184.

J. Indian Chem. Soc.,
Vol. LXIII, April 1986, pp. 377-379

Complexes of 2-(2′-Hydroxy-1′-naphthalidene)imino-5-*p*-anisyl-1,3,4-thiadiazole with a few Metal(II) Ions

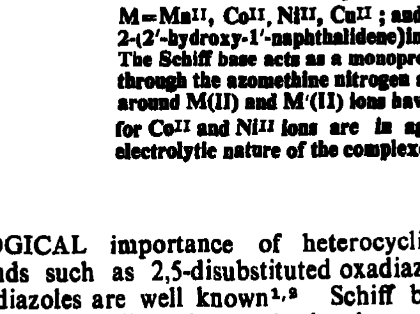
K. C. SATPATHY*, R. MISHRA and B. B. JAL

Department of Chemistry, Sambalpur University, Jyoti Vihar-768 019

Manuscript received 20 July 1984, revised 4 July 1985, accepted 15 November 1985

Two series of complexes of the type $[M(SB)_2(H_2O)_2]$ and $[M'(SB)_2]$, where $M=Mn^{II}$, Co^{II}, Ni^{II}, Cu^{II}; and $M'=Zn^{II}$, Cd^{II}, Hg^{II}, Pb^{II}; and SB=deprotonated 2-(2′-hydroxy-1′-naphthalidene)imino-5-p-anisyl-1,3,4-thiadiazole, have been prepared. The Schiff base acts as a monoprotic bidentate ligand coordinating to the metal ions through the azomethine nitrogen and the phenolic oxygen atoms. The stereochemistry around M(II) and M′(II) ions have been discussed. Crystal field parameters calculated for Co^{II} and Ni^{II} ions are in agreement with the proposed stereochemistry. Non-electrolytic nature of the complexes is evident from the molar conductance values.

BIOLOGICAL importance of heterocyclic compounds such as 2,5-disubstituted oxadiazole and thiadiazoles are well known[1,2] Schiff bases of various heterocyclic amines and related compounds are reported to be anticonvulsant, insecticidal, antibacterial and antifungal agents. It is further reported that heterocyclic organic compounds exhibit enhanced biological activity when administered in the form of metal complexes[3-5]. In view of this, in recent years, considerable attention has been paid to the metal complexes containing oxadiazole and thiadiazole moieties[6-9]. As a part of our study in search of some new Schiff base complexes with possible biological activities we further report in the present communication the preparation and characterisation of some bivalent metal complexes with 2-(2′-hydroxy-1′-naphthalidene)imino-5-*p*-anisyl-1,3,4-thiadiazole.



Experimental

The amine, 2-amino-5-(*p*-anisyl)-1,3,4-thiadiazole was prepared by literature methods[10,11]. The Schiff base 2-(2′-hydroxy-1′-naphthalidene)imino-5-*p*-anisyl-1,3,4-thiadiazole was prepared by condensation of the amine in ethanol with 2-hydroxy-1-naphthaldehyde and recrystallisation from petroleum ether-acetone, (85%), yellow, m.p. 98°, $C_{20}H_{15}O_2N_3S$; λ_{max} 245 and 310 nm; $\delta(CDCl_3)$ 3.17 (3H, s, OCH_3), 7.15 (1H, s, N=CH), 6.7 (1H, s, phenolic OH) and 7.4-7.86 (10H, m, unsym. Ar)

The complexes were prepared by refluxing the Schiff base and the hydrated metal chlorides in 2 : 1 molar ratio in ethanol. The complexes are quite stable at room temperature, and insoluble in common organic solvents. However, freshly prepared complexes are sparingly soluble in dioxane, DMF and acetone. Most of the complexes melt above 250° and a few decompose before melting. The molecular formulae of the complexes are computed basing on elemental analysis (Table 1) and physical measurements by the methods as reported earlier[12,13].

Results and Discussion

The electronic spectrum of the ligand 2-(2′-hydroxy-1′-naphthalidene)imino-5-(*p*-anisyl)-1,3,4-thiadiazole shows an intense band at ~245 nm (40 820 cm^{-1}) with a weak shoulder at 252 nm (36 680 cm^{-1}) followed by a strong intense band at ~310 nm (32 260 cm^{-1}). The former two bands may be due to n-σ^* transition in a heterocyclic thiadiazole moiety, whereas the latter band indicates a π-π^* transition in an extended conjugated system which arises due to greater delocalisation of the π-electron resulting in a bathochromic shift[14,15]. A strong and broad band appearing in the ir spectrum of the ligand at ~3 000-2 800 cm^{-1} is attributed to stretching vibration of the phenolic OH engaged in intra-molecular hydrogen bonding[16,17]. The disappearance of ν_{OH} band in the complexes indicates the coordination of the ligand through deprotonated phenolic oxygen. A strong and sharp band in the spectrum of the ligand at ~1 260 cm^{-1} is assigned to the combination mode of phenolic ν_{C-O} and δ_{O-H} vibrations. Another band at ~1 180 cm^{-1} is characteristic of phenolic ν_{C-O}[18,19]. The hypsochromic shift of both these bands on complexation suggests coordination through oxygen.

The ir spectra of the complexes $[M(SB)_2(H_2O)_2]$ display strong and broad bands at ~3 400-3 200 cm^{-1} which may be assigned to ν_{O-H} of coordinated water molecules. This is supported by

TABLE 1—ANALYTICAL DATA

Compd.	Colour	M.p. °C	Analysis % : Found/(Calcd.) C	H	N	S	M
HSB	Yellow	98	66.89 (66.48)	4.09 (4.15)	11.52 (11.63)	8.79 (8.86)	—
$[Mn(SB)_2(H_2O)_2]$	Brown	>250	59.20 (59.19)	3.89 (3.96)	10.21 (10.36)	7.99 (7.89)	6.55 (6.78)
$[Co(SB)_2(H_2O)_2]$	Greenish blue	200	58.90 (58.89)	3.89 (3.93)	10.25 (10.30)	7.78 (7.85)	7.36 (7.23)
$[Ni(SB)_2(H_2O)_2]$	Yellow	>250	58.81 (58.91)	3.83 (3.93)	10.19 (10.31)	7.89 (7.86)	7.15 (7.20)
$[Cu(SB)_2(H_2O)_2]$	Yellowish green	240d	58.44 (58.56)	3.81 (3.90)	10.31 (10.25)	7.77 (7.81)	7.68 (7.75)
$[Zn(SB)_2]$	Orange yellow	>250	60.93 (61.18)	3.66 (3.57)	10.59 (10.70)	8.01 (8.15)	8.19 (8.28)
$[Cd(SB)_2]$	Pale yellow	250	57.58 (57.60)	3.29 (3.36)	10.13 (10.09)	7.78 (7.69)	13.86 (13.52)
$[Hg(SB)_2]$	Yellowish brown	120	52.08 (52.14)	3.11 (3.04)	9.02 (9.13)	6.93 (6.89)	21.70 (21.78)
$[Pb(SB)_2]$	Yellow	175	51.93 (51.77)	3.09 (3.02)	9.11 (9.06)	6.88 (6.90)	22.28 (22.33)

SB = Deprotonated 2-(2′-hydroxy-naphthalidene)-imino-5-p-anisyl-1,3,4-thiadiazole.

appearance of bands at ~1 580 and 840 cm^{-1} characteristic of δ_{HOH} and H_2O rocking and wagging modes of vibrations, respectively[20-22]. However, in the ir spectra of the complexes of Zn^{II}, Cd^{II}, Hg^{II} and Pb^{II}, these bands were found to be absent.

Bands at ~1 650 and 1 410 cm^{-1} in the spectrum of the Schiff base may be due to $\nu_{C=N}$ mode of azomethine linkage and ν_{C-N}, respectively. The bathocromic shift of both these vibrations by 10-15 cm^{-1} in the spectra of the complexes indicates the coordination of the azomethine nitrogen to the metal ion[23,24]. The bands at ~1 620, 910 and 660 cm^{-1} appearing in the spectrum of the ligand are assigned to $\nu_{C=N-N=C}$, ν_{N-N} and ν_{C-S-C}, respectively[25-27]. These bands remain unaltered in the spectra of the complexes indicating that the hetero atoms in the thiadiazole moiety do not take part in coordination. The molar conductance values of the complexes in the range 0.5-10 Ω^{-1} cm^2 mol^{-1} in acetone (10^{-3} *M*) suggest the non-electrolytic nature of the complexes.

Thermal analysis : The general scheme of the thermal decomposition of the complexes $[M(SB)_2(H_2O)_2]$ is same. The TGA curve displays no mass loss upto 150° indicating absence of lattice water. Around 150°, a rapid loss in weight corresponding to two molecules of water is observed in the thermogram, accompanied by a sharp endothermic peak at the same temperature in the DTA curve. This suggests the presence of two molecules of water coordinated to the metal ion in the complex. The abrupt change in weight loss around 270°, with an exothermic peak at the same temperature in the DTA curve indicates the commencement of decomposition of the organic ligand. In case of the complexes of Zn^{II}, Cd^{II} and Pb^{II}, the loss in weight starts at 200-400° and the decomposition continues without any abrupt change in the weight-loss. The TGA curves of all the complexes attain stability around 600° and the weights of the residues correspond to the formation of the metal oxide. The thermal stability of the complexes is found to be in the order, Zn > Mn > Ni > Cd > Cu > Co > Pb.

Electronic spectra and magnetic properties : The Mn^{II}, Co^{II}, Ni^{II} and Cu^{II} complexes are paramagnetic with observed magnetic moments 5.9, 4.8, 3.25 and 2.03 B.M., respectively. The electronic spectrum (Fig. 1) of Mn^{II} complex displays bands at 18 180, 21 980, 25 000 and 28 570 cm^{-1} which

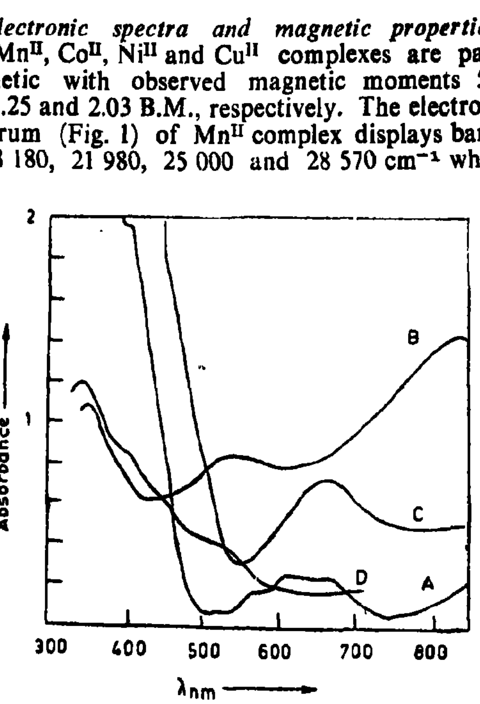


Fig. 1

may be assigned to the transitions $^6A_{1g}(S)\rightarrow{}^4T_{1g}(G)$, $\rightarrow{}^4T_{2g}(G)$, $\rightarrow{}^4A_{1g}$, $^4E_g(G)$ and $\rightarrow{}^4T_{2g}(D)$, respectively. The Co^{II} complex shows ligand field bands at ~15 040 and 17 390 cm^{-1} assignable to $^4T_{1g}\rightarrow{}^4A_{2g}(F)$ and $^4T_{1g}\rightarrow{}^4T_{1g}(P)$ transitions, respectively. A charge transfer band is also observed at ~24 390 cm^{-1}. The Ni^{II} complex yield three bands at ~11 900, 18 180 and 29 410 cm^{-1}. In an octahedral field, these bands can be assigned to

${}^6A_{1g}\rightarrow{}^4T_{2g}$, ${}^4A_{2g}\rightarrow{}^3T_{1g}(F)$ and ${}^3A_{2g}\rightarrow{}^3T_{1g}(P)$ transitions, respectively. The electronic spectrum of Cu^{II} complex shows a broad asymmetric ligand field band in the region 13 000-16 000 cm^{-1} with maxima at ~14 390 cm^{-1} corresponding to ${}^2E_g\rightarrow{}^2T_{2g}$ transition in a nearly octahedral arrangement.

Various ligand field parameters, such as ν_2/ν_1, $10D_q$, β, B, C, F_2 and F_4 have also been calculated for Co^{II} and Ni^{II} from the electronic spectral data (Table 2). The nephelauxetic ratio (β) for Co^{II} and Ni^{II} complexes were calculated to be 0.78 and 0.87, respectively which are less than unity indicating partial covalence in the metal-ligand bond. The

TABLE 2—CRYSTAL FIELD AND NEPHELAUXETIC PARAMETERS (cm^{-1}) FOR $[Co(SB)_2(H_2O)_2]$ AND $[Ni(SB)_2(H_2O)_2]$

Compd.	D_q	B	E	F_2	F_4
$[Co(SB)_2(H_2O)_2]$	831.8	756.1	3503	1256.6	100.1
$[Ni(SB)_2(H_2O)_2]$	1180	904.6	4260	1513	121.7

magnetic moment values together with the position of the ligand field absorption bands and the spectral data suggest octahedral stereochemistry for Mn^{II}, Co^{II} and Ni^{II} complexes and distorted octahedral geometry around the Cu^{II} ion[28-31].

Acknowledgement

Grateful thanks are due to the Secretary, (E & YS), Government of Orissa, for grant of study leave to one of the authors (B.B.J.).

References

1. T. YAMAZAKI, H. YOSHITAKA, T. HONDAV, F. KIMURA, Y. KAWAGUCHE, M. ICHIDA and K. NAKAGAMI, Jap. Pat. 7 709 736 (*Chem. Abstr.*, 1977, **87**, 64659).
2. L. NUESSLEIN, E. A. PIEROCH and K. ROEDER, US. Pat. 4 061 646 (*Chem. Abstr.*, 1978, **88**, 62397).
3. V. ATRE, G. V. REDDY, L. N. SHARADA and M. C. GANORKAR, *Indian J. Chem., Sect. A*, 1982, **21**, 934.
4. D. S. RAO and M. C. GANORKAR, *J. Indian Chem. Soc.*, 1981, **58**, 217.
5. V. J. TYAGARAJU, V. RANBAORE, V. ATRE and M. C. GANORKAR, *J. Indian Chem. Soc.*, 1982, **59**, 199.
6. S. S. TIWARI, A. K. SEN GUPTA and J. KUMAR, *Indian J. Pharm.*, 1970, **32**, 91.
7. B. A. RAI, U. AGRAWAL and LAXMI, *Indian J. Chem., Sect. A*, 1979, **18**, 436.
8. N. B. SINGH and J. SINGH, *Indian J. Chem., Sect. A*, 1979, **17**, 191.
9. A. K. SEN GUPTA and K. HAJELA, *J. Indian Chem. Soc.*, 1981, **58**, 690.
10. V. R. RAO and V. R. SRINIVASAN, *Indian J. Chem.*, 1970, **8**, 509.
11. M. S. GIBSON, *Tetrahedron*, 1962, **18**, 1380.
12. K. C. SATPATHY, R. MISHRA and B. B. JAL, *Indian J. Chem., Sect. A*, 1984, **23**, 697.
13. K. C. SATPATHY, B. B. JAL and R. MISHRA, *Transition Met. Chem.*, 1984, **9**, 8.
14. Y. R. SHARMA, "Elementary Organic Absorption Spectroscopy", S. Chand, New Delhi, 1980, p. 18.
15. M. R. MAHAMOUD, R. A. HAMIDE and F. A. GORD, *Indian J. Chem., Sect. A*, 1980, **19**, 144.
16. S. SATPATHY and B. SAHOO, *J. Inorg. Nucl. Chem.*, 1970, **32**, 2224.
17. B. N. KESHARI and L. K. MISHRA, *Indian J. Chem., Sect. A*, 1981, **20**, 884.
18. B. DAS and S. K. MAHAPATRA, *J. Inorg. Nucl. Chem.*, 1975, **37**, 272.
19. Y. R. SHARMA, "Elementary Organic Absorption Spectroscopy", S. Chand, New Delhi, 1980, p. 100.
20. B. SINGH, P. L. MAURYA, B. V. AGRAWALA and A. K. DEY, *J. Indian Chem. Soc.*, 1982, **59**, 30.
21. H. K. GUPTA, P. L. MAURYA and A. K. DEY, *J. Indian Chem. Soc.*, 1982, **59**, 218.
22. D. KHANNA, V. BANERJEE, B. V. AGRAWALA and A. K. DEY, *Indian J. Chem., Sect. A*, 1982, **21**, 621.
23. S. K. SAHNI, S. P. GUPTA, S. K. SANGAL and V. B. RANA, *J. Indian Chem. Soc.*, 1977, **54**, 200.
24. J. R. DYER, "Application of Absorption Spectroscopy of Organic Compounds", Prentice-Hall, New Jersey, 1965, p. 87.
25. V. B. RANA, D. P. SINGH, P. SINGH and M. P. TEOTIA, *Indian J. Chem., Sect. A*, 1982, **21A**, 528.
26. J. SINGH and N. K. SINGH, *Indian J. Chem., Sect. A*, 1982, **21**, 536.
27. L. J. BELLAMY, "The Infrared Spectra of Complex Molecules", Methuen, London, 1958, p. 354.
28. A. B. P. LEVER, "Inorganic Electronic Spectroscopy", Elsevier, Amsterdam, 1968.
29. L. SACCONI, *Transition Met. Chem.*, 1968, **4**, 199.
30. C. J. BALLHAUSEN, "Introduction to Ligand Field Theory", McGraw-Hill, New York, 1962.
31. R. S. DRAGO, "Physical Methods in Inorganic Chemistry", Reinhold, New York, 1965.

J. Indian Chem. Soc.,
Vol. LXIII, April 1986, pp. 380-383

Synthesis and Structural Studies of some Trivalent Lanthanide Metal Complexes of Salicylaldehyde (*N*-*o*-Hydroxybenzalidene)tyrosyl Hydrazone

T. R. RAO*, I. A. KHAN and R. C. AGGARWAL

Department of Chemistry, Faculty of Science, Banaras Hindu University, Varanasi-221 005

Manuscript received 7 October 1985, accepted 6 February 1986

Salicylaldehyde (*N*-*o*-hydroxybenzalidene)tyrosyl hydrazone (SalTH) has been found to form complexes of the types [M(SalTH)Cl_3(H_2O)]2H_2O and M(SalTH – 3H)-(H_2O), where M = La^{III}, Pr^{III}, Nd^{III}, Sm^{III}, Eu^{III}, Gd^{III} and Dy^{III}. The complexes have been characterised by elemental analysis, molar conductance, magnetic susceptibility, infrared, electronic and pmr spectroscopy. The nephelauxetic ratio ($\bar{\beta}$), covalency (δ) and the bonding parameter ($b^{1/2}$) have been calculated for the neodymium complexes. Infrared spectral studies show that the SalTH acts as a neutral bidentate ligand in the adduct complexes and as a tribasic pentadentate one in the neutral complexes. A coordination number six has been proposed around the metal ion in all the complexes.

RECENTLY a number of papers[1-4] have been published from our laboratories on 3d-metal complexes of isonicotinoylhydrazine, tyrosine hydrazide, *N*-benzoylglycyl hydrazide, and their Schiff bases. This work has been extended to the lanthanum(III) complexes of the above types of ligands. The synthesis and structural studies of lanthanum(III) complexes of isonicotinoyl hydrazine and *o*-hydroxyacetophenoneisonicotinoyl hydrazone have been published[5,6] since then. The present paper describes the results of our similar investigations on the complexes of salicylaldehyde (*N*-*o*-hydroxybenzalidene)tyrosyl hydrazone with La^{III}, Pr^{III}, Nd^{III}, Sm^{III}, Eu^{III}, Gd^{III} and Dy^{III}.

Experimental

Lanthanide trichlorides were obtained from Indian Rare Earths, and l-tyrosine hydrazide from Sigma. All other chemicals used were of AnalaR grade.

Preparation of ligand: Salicylaldehyde (*N*-*o*-hydroxybenzalidene)tyrosyl hydrazone was prepared by refluxing tyrosine hydrazide (25 mmol in 50 ml of methanol) and salicylaldehyde (50 mmol in 50 ml of methanol) for ~6 h. The yellow amorphous solid obtained on slow cooling of the reaction mixture to room temperature was separated by filtration, washed repeatedly with cold methanol and the crude product was recrystallised from hot methanol, m.p. 215° (Found: C, 68.48; H, 5.21; N, 10.42; N_2H_4, 7.94. $C_{23}H_{21}N_3O_4$ calcd. for: C, 68.32; H, 5.18; N, 10.33; N_2H_4, 7.88%).

Preparation of complexes: The complexes, [M(SalTH)Cl_3(H_2O)]2H_2O, were prepared by mixing ethanolic solutions of SalTH (~2.5 mmol) and the appropriate metal chloride (~2.5 mmol). Addition of a few drops of dilute HCl to the above solution resulted in the formation of a gummy solid, which, on maceration with acetonitrile yielded the microcrystalline complex. The complexes were filtered, washed successively with acetonitrile and ether and dried *in vacuo*.

The neutral complexes containing the deprotonated form of the ligand were prepared by mixing together aqueous ethanolic solutions of the ligand (1 mmol), KOH (3 mmol) and the appropriate metal chloride (1 mmol) and adjusting *p*H of the solution to 7.5 by the addition of a few drops of dilute HCl. The precipitated complexes were digested on a water-bath for ~30 min, filtered, washed successively with water and ethanol, and dried at room temperature.

Analysis: Lanthanides were gravimetrically estimated as oxides[7] as well as oxalates after decomposing the organic matter with aqua regia and subsequently with concentrated H_2SO_4. Hydrazine was estimated volumetrically after subjecting the complexes to acid hydrolysis. The C, H and N were analysed on Coleman analysers.

Physical measurements: The magnetic susceptibility measurements were carried out at room temperature on a Cahn-Faraday electrobalance and the molar conductance determined on a WTW conductivity meter. The infrared spectra were recorded on a Perkin-Elmer 621 spectrophotometer, while the electronic spectra were obtained on a Cary-14 spectrophotometer.

Results and Discussion

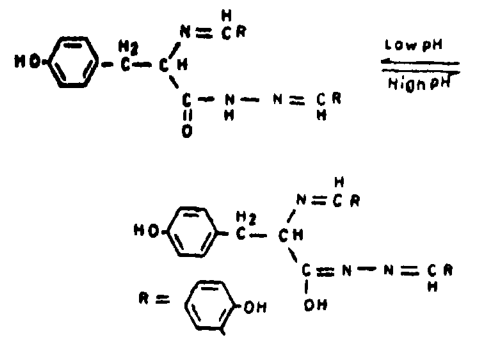
The analytical data (Table 1) show that the metal-ligand interaction gives rise to the formation

TABLE 1—ANALYTICAL AND PHYSICAL DATA OF Ln^{III} COMPLEXES OF SalTH

Compd.	Colour	M.p. °C	Analysis % : Found/(Calcd.) Metal	Cl	N	N_2H_4	Molar conductance Ω^{-1} cm^2 mol^{-1}	μ_{eff} B.M.
$[La(SalTH)Cl_3(H_2O)]2H_2O$	Light yellow	246	19.43 (19.77)	15.04 (15.14)	5.98 (5.89)	4.43 (4.55)	185.7	Diamag.
$[Pr(SalTH)Cl_3(H_2O)]2H_2O$	Yellow	228	19.12 (20.00)	14.98 (15.10)	5.96 (5.90)	4.27 (4.54)	129.8	3.30
$[Nd(SalTH)Cl_3(H_2O)]2H_2O$	Yellow	236	19.91 (20.38)	14.67 (15 03)	5.93 (5.86)	4.32 (4.59)	106.2	3.37
$[Sm(SalTH)Cl_3(H_2O)]2H_2O$	Light yellow	185d	20.91 (21.06)	14.65 (14.90)	5.88 (5.78)	4.15 (4.48)	118.0	2.04
$[Eu(SalTH)Cl_3(H_2O)]2H_2O$	Yellow	173d	20.59 (21.24)	14.26 (14.87)	5.87 (5.69)	—	129.8	3.22
$[Gd(SalTH)Cl_3(H_2O)]2H_2O$	Yellow	165d	21.40 (21.82)	14.80 (14.76)	5.82 (5.72)	4.35 (4.44)	141.6	7.38
$[Dy(SalTH)Cl_3(H_2O)]2H_2O$	Yellow	240	22.30 (22.88)	14.28 (14.65)	5.78 (5.70)	4.20 (4.40)	141.6	8.97
$La(SalTH\text{-}3H)(H_2O)$	Yellow	>300	24.81 (24.94)	—	7.54 (7.34)	5.45 (5.74)	3.0	Diamag.
$Pr(SalTH\text{-}3H)(H_2O)$	Reddish yellow	>300	24.92 (25.21)	—	7.51 (7.45)	5.62 (5.72)	2.95	3.61
$Nd(SalTH\text{-}3H)(H_2O$	Reddish yellow	>300	24.98 (25.65)	—	7.47 (7.31)	5.50 (5.69)	2.89	3.23
$Sm(SalTH\text{-}3H)(H_2O)$	Yellow	>300	26.21 (26.45)	—	7.38 (7.28)	5.34 (5.63)	9.40	2.03
$Eu(SalTH\text{-}3H)(H_2O)$	Reddish yellow	>300	26.30 (26.66)	—	7.36 (7.22)	—	10.62	3.88
$Gd(SalTH\text{-}3H)(H_2O)$	Yellow	>300	27.12 (27.33)	—	7.30 (7.21)	5.40 (5.56)	3.54	7.67
$Dy(SalTH\text{-}3H)(H_2O)$	Yellow	>300	27.35 (27.99)	—	7.24 (7.18)	5.42 (5.51)	8.88	9.22

d = Decomposes.

of two types of complexes, *viz*. the adduct complexes involving the non-deprotonated form of the ligand and the neutral complexes in which SalTH coordinates in its deprotonated form. The formation of the neutral complexes in slightly alkaline medium suggests the amide⇌imidol tautomerism of SalTH as a function of *p*H as shown below,



All the complexes are fairly stable under normal atmospheric conditions. The adduct complexes are soluble in water, methanol, DMF and DMSO but are insoluble in non-polar organic solvents like benzene and CCl_4, while the neutral complexes are soluble only in hot DMF and DMSO. The molar conductance values of the adduct complexes in 0.001 *M* DMF solution show their 1 : 2 electrolytic behaviour[8] presumably due to the solvolysis of two of the three chloride groups. The neutral complexes, however, behave as non-electrolytes in 0.001 *M* DMF solutions[8].

All the adduct complexes are found to melt/decompose at specific temperatures below 250° while the neutral complexes do not melt below 300° (Table 1). The thermolysis of the adduct complexes corresponds to the loss of two molecules of water in the temperature range 85-100° and to the loss of one more water molecule around 140°. The above observation suggests that two molecules of water are lattice-held while the third one is present within the coordination sphere resulting in its loss at a relatively high temperature.

The paramagnetic behaviour of the lanthanide(III) ions is consistent with the presence of unpaired electrons. Since these electrons are well shielded by the $5s^2p^6$ octet both in their spin and orbital motion, the magnetic moments show little deviation from the Van Vleck values[9] indicating a very little participation of the 4f-electrons in bond formation in these complexes. The Sm^{III} and Eu^{III} complexes, however, show greater values than the calculated ones presumably on account of the low J-separation[10].

Electronic spectra : The f-f transition bands show normally, unlike the d-d ones, weak perturbation due to complexation. Increase in the intensity, shift of the barycentre and splitting of certain bands due to the crystal field with respect to the aquo ions

TABLE 2—ELECTRONIC SPECTRAL DATA OF Nd^{III} COMPLEXES OF SalTH

	A		B		Assignment	Spectral parameter*
	λ_{max} cm^{-1}	ϵ	λ_{max} cm^{-1}	ϵ		
	11 455	6.5	11 428	8.0	$^4I_{9/2} \rightarrow {^4F_{3/2}}$	$^A\bar{\beta}=0.988\ 8$
	11 585	5.0	—	—	$\rightarrow {^4F_{5/2}}$	$b^{1/2}=0.076\ 8$
^{A}[Nd(SalTH)$Cl_2(H_2O)$]$2H_2O$	12 470	21.5	12 422	14.5	$\rightarrow {^2H_{9/2}}$	
	13 420	13.0	13 868	12.8	$\rightarrow {^4F_{7/2}}$	$\delta=1.698$
	18 515	13.0	18 458	13.0		
	13 605	12.0	—	—		
^{B}[Nd(SalTH-3H)(H_2O)]	14 705	3.5	14 598	3.5	$\rightarrow {^4F_{9/2}}$	$^B\bar{\beta}=0.978\ 1$
	17 095	35.0	17 005	33.5	$\rightarrow {^4G_{5/2}}, {^2G_{7/2}}$	$b^{1/2}=0.104\ 6$
	19 045	11.5	18 865	19.3	$\rightarrow {^4G_{7/2}}$	$\delta=2.239$
	19 495	8.5	19 415	17.5	$\rightarrow {^4G_{9/2}}$	

* Calculated for the hypersensitive transition $^4I_{9/2} \rightarrow {^4G_{5/2}}, {^2G_{7/2}}$

$$\bar{\beta}=\frac{1}{n}\sum_{n=1}^{n}\frac{\nu_{complex}}{\nu_{aquo}},\quad b^{1/2}=[\tfrac{1}{2}(1-\bar{\beta})]^{1/2},\quad \%\delta=\left(\frac{1-\bar{\beta}}{\bar{\beta}}\right)\times 100$$

spectral data are recorded in 0.02 *M* DMF solution.

are effects that can be observed on complex formation. The electronic spectra of the Nd^{III} complexes are recorded in 2×10^{-2} *M* DMF solutions. The spectra of the complexes show a shift of the spectral bands towards lower energy as compared to those of the aquo ions[11,12] due to the nephelauxetic effect. The band shape of the hypersensitive transition ($^4I_{9/2} \rightarrow {^4G_{5/2}}, {^2G_{7/2}}$) is almost similar in both the adduct and the neutral complex, which indicates that the complexes maintain the same coordination number. The various parameters calculated from the hypersensitive bands are given in Table 2. The nephelauxetic parameter (β) is less than unity while the bonding parameter ($b^{1/2}$) and the Sinha's parameter (δ) are positive for both the complexes indicating the presence of a moderate amount of covalency between the metal and the ligand[13,14]. Further, the relative comparison of the above parameters reveals enhanced covalency in the neutral complex compared to the adduct complex of Nd^{III}.

Infrared spectra : The coordination sites of the ligand involved in bonding with the metal ion have been determined by a careful comparison of the ir spectra of the complexes with that of the parent ligand. Since the full spectrum of the ligand is highly complex, only those bands diagnostic of coordination with the metal ion have been taken for discussion. The 3 500-3 200 cm^{-1} region of the spectra of particularly the adduct complexes, contains a broad band which may be due to the ν_{OH} and ν_{NH} bands arising from the ligand and the water molecules associated with the complexes. Hence, we have refrained from drawing any conclusion based on the bands appearing in the above region.

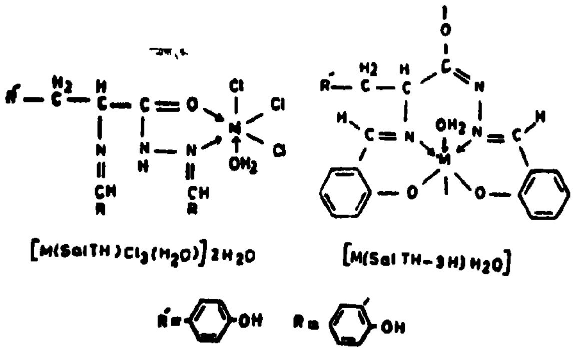
The salTH shows intense absorptions at 1 660, 1 615, 1 510 and 1 275 cm^{-1} which may be respectively assigned to the amide I, $\nu_{C=N}$, amide II and amide III bands[15]; the corresponding bands are observed in the spectra of the adducts in 1 635-1 630, 1 605-1 600, 1 500-1 495 and 1 285 cm^{-1} regions, respectively. Thus, the observed negative shifts in the C=N, amide I and amide II bands and the positive shift in the amide III band suggest coordination through the azomethine group and the carbonyl group of the ligand in all the adduct complexes. The coordination through the azomethine nitrogen atom is further substantiated by the observed positive shift of the order of 40-55 cm^{-1} in the ν_{N-N} mode of the adduct complexes compared to its position at 995 cm^{-1} in the spectrum of the parent ligand. A monodentate coordination of the N–N moiety was reported[16] to increase the ν_{N-N} mode by an order of 40-50 cm^{-1}. Further, the ν_{sym} (C–O, phenolic) band appearing at 1 235 cm^{-1} in the spectrum of the parent ligand remains almost unaltered in the spectra of all the adduct complexes suggesting the absence of phenolic OH group coordination. Thus, in all the adduct complexes, the SalTH seems to behave as a bidentate ligand coordinating through the carbonyl oxygen and the azomethine nitrogen of the hydrazide moiety.

In the spectra of the neutral complexes, all the amide bands, however, disappear while the $\nu_{C=N}$ and the ν_{N-N} bands undergo negative (10-15 cm^{-1}) and positive (40-50 cm^{-1}) shifts, respectively suggesting the coordination of the C=N and N–N moieties and the destruction of the C=O group presumably *via* the amide$\rightleftharpoons$imidol tautomerism of the ligand. The coordination of the ligand in its imidol form in all the neutral complexes has been further suggested by the appearance of new peaks characteristic of ν_{NCO}- in the 1 360 and 1 545 cm^{-1} regions of the spectra[17]. The ν_{sym} (C–O, phenolic) band appearing at 1 235 cm^{-1} in the spectrum of the parent ligand undergoes a positive shift of the order of 35-40 cm^{-1} and a new band characteristic of ν_{asym} (C–O–M) appears at 1 535-1 525 cm^{-1} region in the spectra of the neutral complexes indicating bonding through

the oxygen atoms of both the phenolic groups[18]. Thus, in all the deprotonated complexes the SalTH appears to behave as a trinegative pentadentate ligand coordinating through the imidol oxygen, the two azomethine groups and the two phenolate oxygen atoms. The non-ligand bands appearing in the 330-310 and 400-370 cm^{-1} regions in the spectra of all the complexes may tentatively be assigned to the ν_{M-N} and the ν_{M-O} modes, respectively[19,20].

Pmr spectra : In order to decide the bonding sites of the ligand involved in the complexes, the pmr spectra of a representative adduct complex, *viz.* [La(SalTH)Cl_3.H_2O]2H_2O, and a representative neutral complex, *viz.* [La(SalTH-3H)H_2O] have been recorded in DMSO-d_6 and their spectral features compared with those of the parent ligand recorded in the same solvent. The pmr spectrum of SalTH exhibits signals at δ 6.48-7.50, 8.04-8.25, 11.40 and 12.73 assignable[21] to the aromatic protons, methine protons of the azomethine moieties, imine proton of the hydrazone moiety and the phenolic hydroxyl protons, respectively. Of the two singlets observed for the methine protons, one undergoes a downfield shifting with a slight broadening while the other remains unchanged in the adduct complex. This clearly indicates the coordination of only one of the azomethine groups, *viz.* the azomethine group of the hydrazone moiety (based on the pmr and ir spectra taken together) in the adduct complexes. However, both the singlets due to the methine protons undergo a downfield shift with broadening in the neutral complex which seems to be due to the coordination of both the azomethine groups with the metal ion. The signals due to the phenolic hydroxyl protons and the imine proton of the hydrazone moiety could not, however, be located in the spectra of the complexes.

Based on the elemental analyses and the various physicochemical studies, the structures shown below have been proposed for the lanthanum(III) complexes.



Acknowledgement

The authors are thankful to the Head of the Chemistry Department, Banaras Hindu University, for providing facilities. One of the authors (I.A.K.) thanks C.S.I.R., New Delhi, for the award of Senior Research Fellowship.

References

1. R. C. AGGARWAL and T. R. RAO, *Curr. Sci.*, 1977, **46**, 625.
2. T. R. RAO, M. SAHAY and R. C. AGGARWAL, *Indian J. Chem., Sect. A*, 1984, **23A**, 214.
3. T. R. RAO, M. SAHAY and R. C. AGGARWAL, *Synth. React. Inorg. Metal-Org. Chem.*, 1985, **15**, 175.
4. T. R. RAO, M. SAHAY and R. C. AGGARWAL, *Synth. React. Inorg. Metal-Org. Chem.*, 1985, **15**, 209.
5. T. R. RAO, I. A. KHAN and R. C. AGGARWAL, *Curr. Sci.*, 1985, **54**, 218.
6. T. R. RAO, I. A. KHAN and R. C. AGGARWAL, *J. Less-Common Met.*, 1986, **115**, 325.
7. I. M. KOLTHAFF, P. J. ELVING and E. B. SANDELL, "Treatise on Analytical Chemistry", Interscience, New York, 1968, Part II, 8, pp. 29.
8. W. J. GEARY, *Coord. Chem. Rev.*, 1971, **7**, 81.
9. J. H. VAN VLECK and A. FRANK, *Phys. Rev.*, 1929, **32**, 1494.
10. S. P. SINHA, "Complexes of Rare Earths", Pergamon, New York, 1966, p. 14.
11. G. R. CHOPPIN, D. E. HENRIE and K. BUIJS, *Inorg. Chem.*, 1966, **5**, 1743.
12. S. MISUMI, S. KIDA and M. AIHARA, *Coord. Chem. Rev.*, 1968, **3**, 193.
13. S. P. SINHA, *Spectrochim. Acta*, 1966, **22**, 57.
14. D. E. HENRIE and G. R. CHOPPIN, *J. Chem. Phys.*, 1968, **49**, 477.
15. K. NAGANO, H. KINOSHITA and A. HIRAKAWA, *Chem. Pharm. Bull.*, 1964, **12**, 1198.
16. A. BRAIBANTI, F. DALLAVALLE, M. A. PELLINGHELLI and E. LEPORATI, *Inorg. Chem.*, 1968, **7**, 1430.
17. C. N. R. RAO, "Chemical Applications of Infrared Spectroscopy", Academic, New York, 1964, pp. 758-765.
18. E. SINN and C. H. HARRIS, *Coord. Chem. Rev.*, 1969, **4**, 391.
19. J. L. CHARPANTIER and T. MOELLER, *J. Inorg. Nucl. Chem.*, 1970, **32**, 3575.
20. N. NGSEE, H. W. LATZ and D. G. HENDRICKER, *J. Inorg. Nucl. Chem.*, 1977, **39**, 71.
21. R. L. DUTTA and B. R. DAS, *Indian J. Chem., Sect. A*, 1985, **24**, 498.

J. Indian Chem. Soc.,
Vol. LXIII, April 1986, pp. 384-386

Physicochemical Studies on Non-stoichiometric Oxides of Yttrium, Praseodymium and Gadolinium. Part-II

M. SAHA, RABINDRA KUMAR and S. BHAGAT*

P. G. Department of Chemistry, Bhagalpur University, Bhagalpur-812 007

Manuscript received 18 July 1985, accepted 6 February 1986

Acidity and excess oxygen of the samples obtained from solid state decomposition of nitrates of yttrium, praseodymium and gadolinium have been determined. Apparent activation energy involved in these processes have also been estimated.

It has been observed that excess oxygen varies exponentially with acidity. Apparent activation energy in case of thermal decomposition of praseodymium nitrate is significantly higher than those of nitrates of yttrium and gadolinium.

RECENTLY considerable work on physical and structural phenomena of non-stoichiometric transition metal oxides has been reported[1,2]. For the last few years we are studying the electric transport and catalytic activity of non-stoichiometric oxides of rare earth metals obtained from solid state decompositions[3,4]. Some of them are found to be semiconductor with excellent catalytic capability for chemical decompositions[5,6]. Though transition metal oxides as a reformation catalyst have been widely studied but it lacks to throw light firstly, on the mechanism of liberation of oxygen in case of rare earth oxide as reformation catalyst and secondly, the surface characterisation which must have bearing on the electronic and catalytic behaviours. Further, the thermogravimetric data besides furnishing valuable information regarding heat treatment processes of the solids, indicate unambigously about the various stages of physico-chemical changes like dehydration, decomposition *etc.* of the solid state decomposition processes.

Keeping this in view, the present investigation was undertaken to measure the physicochemical parameters, like excess oxygen and acidity of non-stoichiometric oxides of yttrium, praseodymium and gadolinium. This paper also deals with the estimation of apparent activation energies of solid state decomposition of nitrates of Y, Pr and Gd.

Experimental

Nitrates of Y, Pr and Gd of 99.99% purity (Indian Rare Earth Ltd.) were used as such.

Preparation of samples and measurements : The non-stoichiometric oxide samples of Y, Pr and Gd at 600, 700, 800 and 960° were prepared by the method as reported earlier[7]. The metal in the oxides was estimated by the usual method. Emperical formulae were derived. The results are shown in Table 1. The acidity measurements were performed by the method of Arora *et al.*[8] and the results are given in Table 1. Measurement of excess oxygen was done by the method described by Volts *et al.*[9].

TABLE 1—VALUES OF EXCESS OXYGEN, ACIDITY OF SAMPLES OBTAINED AT DIFFERENT DECOMPOSITION TEMPERATURES

Decomp. temp. °C	Emperical formula	Excess oxygen per 100 g of sample $\times 10^{-2}$	Acidity meq g^{-1}
600	$Y_2O_{3.44}$	49.4	120.45
700	$Y_2O_{3.49}$	19.0	104.37
800	$Y_2O_{3.49}$	9.5	88.83
960	$Y_2O_{3.60}$	7.6	80.80
600	$Pr_2O_{3.88}$	22.50	32.85
700	$Pr_2O_{3.99}$	15.20	36.50
800	$Pr_2O_{3.06}$	15.20	36.50
960	$Pr_2O_{3.33}$	11.4	29.20
600	$Gd_2O_{3.5}$	17.0	65.70
700	$Gd_2O_{3.70}$	9.5	58.40
800	$Gd_2O_{3.75}$	7.6	47.45
960	$Gd_2O_{3.80}$	6.65	43.8

Evaluation of activation energy of thermal decomposition : The thermogravimetric study was performed at P and D, F.C.I. Ltd., Sindri using stanton Red-Croft T.G. 750 thermobalance of sensitivity 0.1 mg per division of chart at the heating rate of 10° min^{-1}. The activation energy of solid state thermal decomposition process was evaluated, using the modified equation of Dharwadkar and Phadnis[10].

Results and Discussion

The values of excess oxygen and acidity together with the emperical compositions of the different samples are given in Table 1. Fig. 1 shows how the excess oxygen changes with the change in acidity of the different samples. Fig. 2 is a typical DTG curve of yttrium nitrate.

From Table 1 it appears that except the samples obtained from praseodymium nitrate, acidity values

decrease with rise in decomposition tempera ture. Similar is the trend of the values of excess oxy gen. This observation indicates unambigously that th e

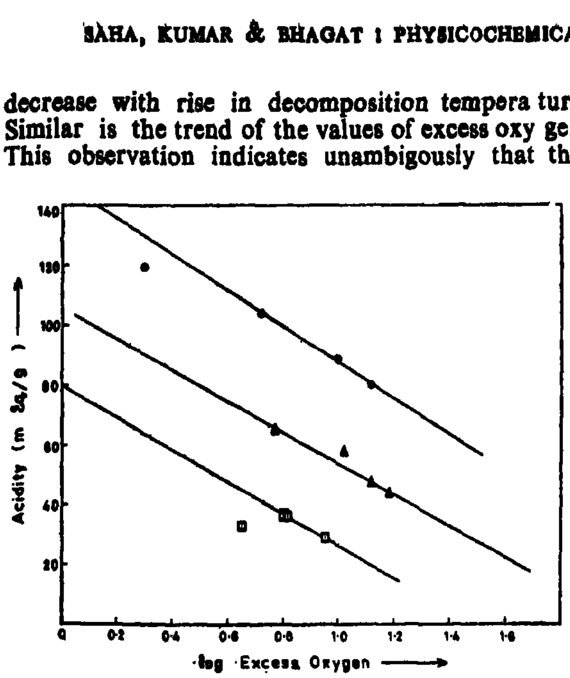


Fig. 1. Plot of acidity *vs* log (excess oxygen) : (O) yttrium oxide, (□) praseodymium oxide and (Δ) gadolinium oxide.

excess oxygen is related with the acidity of the samples somehow or other. The plot of excess oxygen *vs* acidity (Fig. 1) reveals that the acidity varies exponentially with excess oxygen.

It is also interesting to point out as is obvious from the Table 1 that though the values of acidity of the samples obtained from praseodymium nitrate seem to be more or less the same but they contain considerable amount of excess oxygen, which according to Maxim[11] signifies the chemisorbed oxygen. Thus, it is to be concluded that the samples

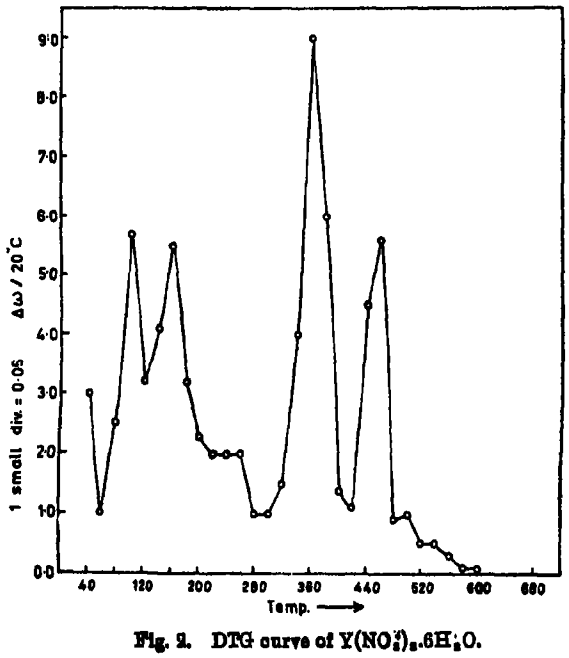


Fig. 2. DTG curve of $Y(NO_3)_3 . 6H_2O$.

obtained from praseodymium nitrate would show greater activities for the chemical changes where the excess oxygen plays the key role. The catalytic activity is to be measured to ascertain this.

From the perusal of Table 1 it is obvious that the oxygen content increases regularly with the temperature of decomposition but reverse is the trend of excess oxygen and acidity values. This shows that neither the excess oxygen nor the acidity is at all related to the oxygen content in the samples. Obviously, the catalytic activities of the samples seem to be independent of the oxygen content of the sample. This needs detailed study to corroborate the conclusion.

The study of TGA on nitrates of Y, Pr and Gd was performed. A typical DTG curve of yttrium nitrate is shown in Fig. 2. From a close look it is quite clear that decomposition takes place in four stages in case of yttrium nitrate where as the decomposition takes place in three stages in cases of praseodymium and gadolinium nitrates. Thus, it is to be concluded that the decomposition behaviour of yttrium nitrate is different from that of nitrates of praseodymium. Further, from the DTG curve itself the estimation of different temperatures leading to the formation of stable non-stoichiometric oxides has been done. It appears that the formation of stable oxides from yttrium nitrate and praseodymium nitrate occurs at the same temperature, *i.e.* 480° and that from gadolinium nitrate at 470°. It indicates that in the absence of air stable oxides are formed at the same temperature in these three cases. However, complete dehydration takes place at different temperatures which are 188, 228 and 344° for nitrates of yttrium, praseodymium and gadolinium, respectively. Probably, the half-filled f-orbital present in gadolinium causes the protonisation of water molecules developing force of attraction among the water molecules of crystallisation and nitrates molecules. Consequently, dehydration of gadolinium nitrate takes place at higher temperature as compared to nitrates of yttrium and praseodymium.

Apparent activation energies of solid state decomposition for different stages have been estimated and the results are recorded in the Table 2. The results on activation energy show that the overall value of apparent activation energy in case of decomposition of praseodymium nitrate is considerably higher than that in case of yttrium and gadolinium nitrates. However, the latter two have approximately the same values. It is worthwhile to point out that the activation energy of the reaction is a direct measure of the energy changes involved. Thus, comparatively higher thermal energy is required for the solid state decomposition of praseodymium nitrate, leading to stable oxide product as compared to the decomposition of yttrium and gadolinium nitrates with stable oxide product.

As is clear from Table 2 that the values of activation energies for solid state decomposition

TABLE 2—VALUES OF APPARENT ACTIVATION ENERGY FOR THERMAL DECOMPOSITION OF NITRATES OF YTTRIUM, PRASEODYMIUM AND GADOLINIUM

Sl. no.	Compd.	First energy of activation E_1 kcal mol^{-1}	Second energy of activation E_2 kcal mol^{-1}	Third energy of activation E_3 kcal mol^{-1}	Total energy of activation E_a kcal mol^{-1}
1.	Yttrium nitrate	21.740	4.570	13.070	39.380
2.	Praseodymium nitrate	30.077	2.816	26.154	59.047
3.	Gadolinium nitrate	12.205	4.993	19.220	36.418

corresponding to second stage are more or less same in all the three cases. It indicates that probably the second stage is the complete elemination of six molecules of water of crystallisation forming the anhydrous salt and thereafter decomposition starts. Our overall finding on acidity and excess oxygen of these samples is indicative of the exponential relationship between acidity and excess oxygen. Our observation is quite different from that of earlier worker[12]. According to him, in case of nickel oxide the acidity varies linearly with excess oxygen. How far, the acidic nature contributes towards the activity of the samples is under study. It is to be mentioned that in case of solid state decomposition of praseodymium nitrate, except the processes of dehydration and decomposition, the diffusion of oxygen predominates causing the greater changes in energy as is obvious from apparent activation energy values.

Acknowledgement

The authors are thankful to Prof. K. D. Banerji for providing the facilities. One of us (M. S.) is grateful to U. G. C., New Delhi, for granting a Teacher Fellowship.

References

1. S. METHFESSEL and D. MATHIS, "Hand Buch Der Physik", Springer-Verlag, Heidelberg, 1968, p. 389.
2. K. N. R. TAYLOR, *Contemp. Phys.*, 1970, **11**, 423 ; *Adv. Phys.*, 1971, **20**, 551.
3. S. BHAGAT and L. D. AHUJA, *Indian J. Chem.*, 1971, **9**, 358.
4. J. N. TEWARI, Ph.D. Thesis, Bhagalpur University.
5. B. YADAVA, Ph.D. Thesis, Bhagalpur University.
6. J. N. TEWARI and S. BHAGAT, *Indian J. Chem.*, in the press.
7. 'The Rare Earths", eds. H. SPEDDING and A. H. DAANE, Iowa State University, p. 578.
8. B. R. ARORA, R. K. BANERJI, N. K. MANDAL, N. C. GANGULI and S. P. SEN, *Technol.*, 1972, **9**, 8.
9. VOLTZ, *J. Phys. Chem.*, 1960, **64**, 1594.
10. S. R. DHARWADKAR and A. B. PHADNIS, *Indian J. Chem.*, 1969, **7**, 1032.
11. J. MAXIM and T. BRAUN, *J. Phys. Chem.*, 1963, **24**, 537.
12. D. N. SAHAI, D. DATTA and A. SARKAR, *Technol.*, 1978, **15**, 3, 4.

J. Indian Chem. Soc.,
Vol. LXIII, April 1986, pp. 387-389

Thermodynamics of $CoSO_4$ and $NiSO_4$ in Mixed Solvents from Conductance Method

B. K. PARIDA

Department of Chemistry, S.C.S. College, Puri-752 001

and

P. B. DAS*

State Forensic Science Laboratory, Rasulgarh, Bhubaneswar-751 010

Manuscript received 19 June 1985, revised 3 December 1985, accepted 17 February 1986

The ion-solvent interaction of $CoSO_4$ and $NiSO_4$ with organic solvent (10, 20 and 30 wt%) glycerol-, glycol- and isopropanol-water mixtures at different temperatures has been studied by conductance method. The dissociation constant has been calculated along with ΔG_t^o, ΔG_t^o (el) and ΔG^o (ch) and the ion-solvent interaction has been inferred.

THE physical properties of the mixed solvents, like glycerol-water, glycol-water and isopropanol-water, *viz.* dielectric constant, dipole moments are very much different from that of water. These organic solvents are more or less aprotic, whereas water is both an electron donor and an acceptor. These and several other properties make a study of their aqueous mixtures an interesting thing to explore, particularly of the ionic processes accompanying the solution of strong electrolytes.

In the present communication, the conductivities of $CoSO_4$ and $NiSO_4$ in glycerol-water, glycol-water and isopropanol-water mixtures at 30 to 45° have been studied at 10, 20 and 30% by weight of the organic solvent to investigate the ion-solvent interaction.

Experimental

The salts $CoSO_4$ and $NiSO_4$ used were of E. Merck (extra pure) grade. The purification of glycerol, glycol and isopropanol, preparation of the solvents, solutions and measurement of conductance had been described previously[1]. The conductance measurements were within accuracy of $\pm$ 0.002 and the concentration range was from 0.02 to 0.002 mol dm^{-3}. The temperature of the investigation was from 303 to 318 $\pm$ 0.01 K.

Results and Discussion

The Onsager equation[2] for a completely dissociated electrolytes is

$$\Lambda = \Lambda^\circ - (A + B\Lambda^\circ)\sqrt{I}$$

where, A and B are Onsager constants. It satisfactorily accounts for the change in equivalent conductivity with concentration. Correct evaluation of Λ° can be made by extrapolating to zero concentration of the plot of Λ *vs* $c^{1/2}$. However, the above method of extrapolation is unreliable in the cases of a number of electrolytes involving incomplete dissociation or ion-association. In the present case, the dielectric constant of the medium is lowered and there is a great probability of ion-association. Hence, the method of Fuoss and Krauss[3] and that of Shedlovsky[4] have been utilised to calculate the values of Λ° and the dissociation constant. The Λ° and K values calculated by both the methods are in good agreement and are given in Tables 1 and 2. The K values are found to decrease with the increase in temperature for all the solvent compositions and for both the salts. The K values also decrease with the decrease in dielectric constant caused by the increase in organic solvent. This is attributed to the incomplete dissociation or ion-association.

The standard thermodynamic parameters, ΔG_t^o have been calculated in the usual manner[5]. The plot of ΔG° *vs* solvent composition were found to be linear. The extrapolated values gave the thermodynamic parameters for aqueous solutions. The standard thermodynamic quantities (ΔG_t^o) for transfer process from water to 10, 20 and 30% of organic solvent-water could be calculated by using Feakins method[6]. The probable uncertainties in ΔG_t^o is $\pm$ 15 J mol^{-1}. The ΔG_t^o values are negative which indicates that the ion-pairs are in a lower energy-state in aquo-organic solvents than in water and hence the ion-pair formation is favoured by decreasing the dielectric constant of the medium.

Single-ion values of free energy are not available presently for the solvent mixture studied. Hence, the method adopted by Khoo and Chan[7] was followed to study ion-solvent interaction. The Born

TABLE 1—Λ° VALUE (Ω^{-1} cm^2)

Temp. °C	Glycerol-water			Glycol-water			Isopropanol-water		
	10%	20%	30%	10%	20%	30%	10%	20%	30%
				$CoSO_4$					
30	121.4	100.6	84.3	120.5	108.4	87.5	110.9	81.6	60.2
35	132.8	111.4	92.5	134.8	112.6	95.8	116.2	87.4	63.4
40	143.9	119.5	99.8	143.4	120.4	100.8	121.8	92.4	66.5
45	151.2	127.3	105.2	159.5	129.8	113.4	128.9	100.6	71.4
				$NiSO_4$					
30	130.4	102.8	83.4	126.5	100.4	86.5	114.2	80.4	62.2
35	138.5	112.4	89.9	136.4	113.5	90.4	118.5	85.2	65.8
40	144.6	114.8	100.4	139.5	119.6	95.4	124.2	89.4	70.4
45	152 6	128.4	113.2	142.6	123.4	99.8	132.2	94.5	75.4

TABLE 2—K VALUE ($\times 10^3$)

Temp. °C	Glycerol-water			Glycol-water			Isopropanol-water		
	10%	20%	30%	10%	20%	30%	10%	20%	30%
				$CoSO_4$					
30	6.3	4.2	3.7	6.9	5.1	4.0	7.5	6.2	4.6
35	6.2	4.3	3.8	6.8	5.0	4.0	7.6	6.1	4.5
40	6.1	4.3	3.6	6.8	5.0	3.9	7.4	6.0	4.4
45	6.2	4.1	3.5	6.7	4.9	3.8	7.3	6.1	4.4
				$NiSO_4$					
30	5.8	4.0	3.4	6.6	4.8	3.7	7.1	5.8	4.2
35	5.7	4.1	3.4	6.5	4.7	3.8	7.0	5.7	4.1
40	5.6	4.0	3.5	6.4	4.6	3.6	7.0	5.6	4.0
45	5.6	3.9	3.4	6.4	4.6	3.5	6.9	5.6	4.0

TABLE 3—ΔG_t° (el) VALUE (J mol^{-1})

Temp. °C	Glycerol-water			Glycol-water			Isopropanol-water		
	10%	20%	30%	10%	20%	30%	10%	20%	30%
				$CoSO_4$					
30	250	800	1288	300	520	804	740	1580	2772
35	350	890	1328	300	522	808	760	1545	2794
40	400	890	1334	405	525	810	770	1558	2844
45	450	880	1320	360	575	820	790	1588	2892
				$NiSO_4$					
30	310	700	1162	272	482	740	50	300	310
35	310	702	1181	272	490	745	100	310	320
40	315	708	1194	300	495	775	102	322	342
45	320	710	1202	310	505	795	120	334	362

TABLE 4—ΔG_t° (ch) VALUE (J mol^{-1})

Temp. °C	Glycerol-water			Glycol-water			Isopropanol-water		
	10%	20%	30%	10%	20%	30%	10%	20%	30%
				$CoSO_4$					
30	−1200	−2670	−3478	−1020	−1940	−2894	−1360	−2700	−5142
35	−1250	−2930	−3488	−1070	−2082	−2938	−1440	−2795	−4824
40	−1350	−2760	−3664	−1185	−2245	−3030	−1430	−2758	−4854
45	−1380	−2900	−3760	−1180	−2225	−3140	−1460	−2718	−4922
				$NiSO_4$					
30	−1370	−2690	−3672	−1162	−2022	−3030	−700	−1460	−2280
35	−1580	−2762	−3695	−1152	−2200	−3005	−790	−1580	−2380
40	−1595	−2858	−3694	−1280	−2285	−3205	−802	−1602	−2502
45	−1610	−2960	−3812	−1250	−2325	−3225	−860	−1624	−2542

equation was expected to fit increasingly better as the organic solvent content is increased. It was possible to split the ΔG_t° values into two parts as Roy *et al.*[8] had done, *i.e.*, 'chemical contribution' denoted in their terminology by ΔG_t° (ch) and an electrical contribution, ΔG_t° (el) could be calculated from the Born equation.

From a knowledge of ΔG_t° (el), the chemical contribution of free energy transfer ΔG_t°(ch) could be calculated by subtracting the respective electrostatic contribution values from molar quantities. ΔG_t° (el) and ΔG_t° (ch) values are given in Tables 3 and 4, respectively. ΔG_t° (ch), *i.e.* chemical contribution to the free energy of transfer is negative in all cases and hence the process is thermodynamically favourable as far as the chemical interactions are concerned. Since ΔG_t° (el) is positive (Table 3), the lower the value the greater is the ion-solvent interaction and the order for Co^{II} is glycol-water > glycerol-water > isopropanol-water, whereas for Ni^{II} it is isopropanol-water > glycol-water > glycerol-water.

Glycerol has three OH groups, glycol has two OH whereas isopropanol has only one OH group and water is both an electron donor and acceptor. So the 3-dimensional water structure is broken down in presence of Ni^{2+}, Co^{2+} and SO_4^{2-} and the order is dependent on the nature of the ion.

References

1. N. C. Das and P. B. Das, *Electrochim. Acta*, 1978, **23**, 191.
2. H. S. Harned and B. B. Owen, "Physical Chemistry of Electrolytic Solutions", Reinhold New York.
3. R. M. Fuoss and C. A. Krauss, *J. Am. Chem. Soc*, 1933, **55**, 476.
4. T. Shedlovsky, *J. Franklin Inst.*, 1938, **225**, 439.
5. N. C. Das, P. P. Misra and P. B. Das, *Acta Ciencia Indica*, 1979.
6. D. Feakins and D. J. Turners, *J. Chem. Soc.*, 1965, 4984.
7. K. H. Khoo and C. Y. Chan, *Aust. J. Chem.*, 1978, **28**, 721.
8. R. N. Roy, W. Vernon and A. L. M. Bothwell, *Electrochim. Acta*, 1977, **15**, 826.

J. Indian Chem. Soc.,
Vol. LXIII, April 1986, pp. 390-392

On Variation of the Transference Number of an Ion of a Strong Electrolyte in Solution according to Cube-root of its Concentration

B. N. GHOSH

University College of Science and Technology, Calcutta-700 009

Manuscript received 3 April 1985, accepted 17 February 1986

In previous publications it has been shown on the basis of theoretical consideration that kappa of the Debye-Hückel theory of strong electrolytes requires modification. The expression for the modified kappa, κ_m, deduced theoretically, includes within it 'the effective ionic diameter' a and varies according to cube-root of concentration of the electrolyte in solution so long as a (the effective ionic diameter) remains constant. Equations for the cationic transference numbers of the strong electrolytes deduced by using the modified κ_m have been subjected to test using the data available in the literature and have been found satisfactory.

IN papers[1-3] published previously it has been pointed out that the expression for kappa of the Debye-Hückel theory[4] of the strong electrolytes should be modified and the modified kappa, denoted by κ_m, is to be expressed as

$$\kappa_m = \left[\frac{2e^2}{DkTa}\right]^{1/3}\left[\frac{\Sigma\nu_i z_i^2}{\nu}\right]^{1/3}\left[\frac{\nu N}{1000}\right]^{1/3}(C^{1/3}-C_0^{1/3}) \quad (1)$$

$$=(B/\sqrt{\bar{a}})(C^{1/3}-C_0^{1/3}) \quad (1a)$$

In equation (1) e, D, k, T and N have their usual significance, a represents the 'effective ionic diameter', ν_i the number of ions of the species i of the electrolyte yielding ν ions per molecule, Z_i the valency of the i ions and C_0 represents that concentration of the electrolyte at which κ_m becomes zero. In equation (1a) B represents the product of the constants in equation (1).

Using this κ_m, equations have been deduced in previous publications which can account satisfactorily for the variation of the mean activity coefficient of the ions[1-3] of the strong electrolytes, their molecular conductance[2,3], their viscosity[5] and their apparent molal volume[6] with dilution.

In this paper, deduction of equations, using this modified κ_m, for the transference numbers of the ions of the strong electrolytes, composed of only two kinds of ions, has been discussed.

In previous publications[2,3] the following expression for the equivalent conductance of a strong electrolyte in solution has been deduced.

$$\lambda=\lambda_s-(A_1\lambda_0+B_2)\kappa_m \quad (1)$$

$$=\lambda_s-(A_1\lambda_0+B_2)(B/\sqrt{\bar{a}})C^{1/3} \quad (1a)$$

where, $\lambda_s=\lambda_0+(A_1\lambda_0+B_2)(B/\sqrt{\bar{a}})C_0^{1/3}$ and A_1, B_2, B are constants consisting of the universal constants and can be calculated, C_0 represents the concentration at which κ_m is zero. λ_0 has its usual significance and a the 'effective ionic diameter' expressed in Ångström unit. The aforesaid equation (1a) after substituting the values of the constants A_1, B_2 and B simplifying may be written as

$$\lambda=\lambda_s-S\left[\frac{1.22}{\sqrt{\bar{a}}}\right]C^{1/3} \quad (1b)$$

where at 25°, $S=(0.23\lambda_0+60.19)$ for a 1 : 1 electrolyte[3]. Equation (1b) may also be written as

$$(\lambda_+)+(\lambda_-)=(\lambda_{s+})+(\lambda_{s-})-S(1.22/\sqrt{\bar{a}})\,C^{1/3} \quad (1c)$$

where, λ_+ and λ_- represent the equivalent conductance of the positive and the negative ions respectively and λ_{s+} and λ_{s-} the corresponding quantities at infinite dilution. It is to be noted that

$$[(\lambda_+)+(\lambda_-)]=\lambda \text{ and } [(\lambda_{s+})+\lambda_{s-})]=\lambda_s.$$

The expressions for the equivalent conductance of the individual ions can be found from equation (1c) by splitting it up in the following way,

$$\lambda_+=\lambda_{s+}-i\,S(1.22/\sqrt{\bar{a}})C^{1/3} \quad (2)$$

$$\lambda_-=\lambda_{s-}-(1-i)\,S(1.22/\sqrt{\bar{a}})C^{1/3} \quad (2a)$$

where, i is a constant.

Equation (2) leads to the expression for the transference number of the cations as

$$T_+=\frac{\lambda_+}{(\lambda_+)+(\lambda_-)}=\frac{\lambda_+}{\lambda}=\frac{\lambda_{s+}-i\,S(1.22/\sqrt{\bar{a}})C^{1/3}}{\lambda_s-S(1.22/\sqrt{\bar{a}})C^{1/3}}$$

$$=\frac{[(\lambda_{s+})-i\,S(1.22/\sqrt{\bar{a}})C^{1/3}]}{\lambda_s}[1+(S/\lambda_s)(1.22/\sqrt{\bar{a}})C^{1/3}]$$

$$=T_+^0-(S/\lambda_s)(1.22/\sqrt{\bar{a}})[i-T_+^0]C^{1/3} \quad (2b)$$

* Present Address: 30 Regent Estate, Calcutta-700 092.

neglecting terms involving $C^{2/3}$, such as $i(S/\lambda_s)^2 (1.22/\sqrt{\bar{a}})^2 C^{2/3}$ and its higher powers.

Similarly, the expression for the transference number of the anion may be written as

$$T_- = T_-^\circ - (S/\lambda_s)(1.22/\sqrt{\bar{a}})[1 - i - T_-^\circ]C^{1/3} \quad (2c)$$

The constants $(i - T_+^\circ)$ and $\sqrt{\bar{a}}$ in equation (2b) may be put together and it may be expressed as

$$T_+ = T_+^\circ - (S/\lambda_s)(1.22)[(i - T_+^\circ)/\sqrt{\bar{a}}]C^{1/3} \quad (3)$$

$$= T_+^\circ - S_m(C)^{1/3} \quad (3a)$$

where, $S_m = (S/\lambda_s)(1.22)[(i - T_+^\circ)/\sqrt{\bar{a}}]$

A plot of T_+ against $C^{1/3}$ has been found to be linear.

From the slope and intercept of the straight line, S_m and T_+° can be found. λ_s and $\sqrt{\bar{a}}$ in equation (3) can be found from data on measurements of equivalent conductance of the electrolyte available in the literature, but i and T° are to be found from data on measurements of cationic transference number. Attention may also be drawn to the fact that $(i - T_+^\circ)/\sqrt{\bar{a}}$ is a characteristic constant of the electrolyte used and it may be related to such other fundamental property of the electrolyte as the sum of its ionic radii r_- and r_+. It has been found that for the 1 : 1 electrolytes containing a common anion, such as the Cl^- ion, the following equation holds good

$$(i - T_+^\circ)/\sqrt{\bar{a}} = -m(r_- + r_+) + m_0 \quad (4)$$

where, m and m_0 are constants.

The Debye-Hückel-Onsager equation[8] for the transference number of the cation of a strong electrolyte is expressed as

$$T = T_+^\circ + S_{(T+)}C^{\frac{1}{2}} \quad (L)$$

$$\text{where, } S_{(T+)} = \left[\frac{T_+^\circ(Z_- + Z_+) - Z_+}{(Z_- + Z_+)\lambda_s}\right]B_2^* \quad (La)$$

In equation (La), Z_- and Z_+ denote the valency of the cation and the anion respectively of the electrolyte used, and B_2 has the same significance as stated already.

The equations (3a) and (L) have been subjected to comparative test using such data as are available in the literature and are recommended for their precision.

Processing of the data and verification of the equations :

The data recorded in the Tables 1 and 2 have been collected from the literature[9]. Under the head miscellaneous of the Tables are mentioned the electrolyte, the equation used and the values of the constants in the equation. C represents molar concentration and the other terms have their usual significance. The values of T_+° and S_m in equation (3a) have been found from plots of T_+ against $C^{1/3}$ as stated already. It is to be noted that S_m is positive or negative according as T_+° is less or greater than i. In Table 3 are recorded the data used for verifying equation (4).

TABLE 1—VARIATION OF T_+ WITH CONCENTRATION FOR 1 : 1 ELECTROLYTES AT 25°

Miscellaneous	C	Values of T_+ (cationic transport number): Observed	Calcd. Eqn. (3a)	Calcd. Eqn. (L)
HCl	0.01	0.825 1	0.825 2	0.825 4
Eqn. (3a) T_+° = 0.819 9	0.02	0.826 6	0.826 6	0.827 3
S_m = −0.024 6	0.05	0.829 2	0.829 0	0.831 0
Eqn. (L) T_+° = 0.820 9	0.1	0.831 4	0.831 3	0.835 2
$S_{(T+)}$ = +0.045 07				
LiCl	0.01	0.328 9	0.329 0	0.327 9
Eqn. (3a) T_+° = 0.338 8	0.02	0.326 1	0.325 9	0.324 4
S_m = 0.047 5	0.05	0.321 1	0.321 3	0.317 5
Eqn. (L) T_+° = 0.336 4	0.1	0.316 8	0.316 8	0.310 4
$S_{(T+)}$ = −0.085 14				
NaCl	0.01	0.391 8	0.391 7	0.391 4
Eqn. (3a) T_+° = 0.397 1	0.02	0.390 2	0.390 3	0.389 4
S_m = 0.025 2	0.05	0.387 6	0.387 8	0.385 3
Eqn. (L), T_+° = 0.396 3	0.10	0.385 4	0.385 4	0.380 8
$S_{(T+)}$ = −0.049 10				
KCl	0.01	0.490 2	0.490 2	0.490 2
Eqn. (3a), T_+° = 0.490 6	0.02	0.490 1	0.490 1	0.490 1
S_m = 0.001 85	0.05	0.489 9	0.489 9	0.489 8
Eqn. (L), T_+° = 0.490 6	0.1	0.489 8	0.489 7	0.489 4
$S_{(T+)}$ = −0.003 76	0.2	0.489 4	0.489 5	0.488 9
NH_4Cl	0.01	0.490 7	0.490 7	0.490 5
Eqn. (3a), T_+° = 0.491 0	0.02	0.490 6	0.490 6	0.490 4
S_m = 0.001 35	0.05	0.490 5	0.490 5	0.490 1
Eqn. (L), T_+° = 0.490 9	0.1	0.490 7	0.490 4	0.489 8
$S_{(T+)}$ = −0.003 76				
KNO_3	0.01	0.508 4	0.508 3	0.507 2
Eqn. (3a), T_+° = 0.507 2	0.02	0.508 7	0.508 7	0.507 3
S_m = −0.006 5	0.05	0.509 3	0.509 3	0.507 6
Eqn. (L), T_+° = 0.506 9	0.1	0.510 3	0.509 9	0.507 3
$S_{(T+)}$ = +0.002 97				
$AgNO_3$	0.01	0.464 8	0.464 8	0.462 7
Eqn. (3a), T_+° = 0.462 7	0.02	0.465 2	0.465 4	0.462 0
S_m = −0.01	0.05	0.466 4	0.466 4	0.460 7
Eqn. (L), T_+° = 0.464 3	0.1	0 468 2	0.407 4	0.459 2
$S_{(T+)}$ = −0.016 04				
CH_3COONa	0.01	0.553 7	0.553 8	0.554 0
Eqn. (3a), T_+° = 0.548 9	0.02	0.555 0	0.555 0	0.555 4
S_m = −0.022 6	0.05	0.557 3	0.557 3	0.558 2
Eqn. (L), T_+° = 0.550 7	0.1	0.559 4	0.559 4	0.561 3
$S_{(T+)}$ = +0.033 36				
CH_3COOK	0.01	0.649 3	0.650 0	0.650 2
Eqn. (3a), T_+° = 0.640 5	0.02	0.652 3	0.652 4	0.653 2
S_m = −0.044	0.05	0.656 9	0.656 7	0.659 4
Eqn. (L), T_+° = 0 642 7	0.1	0.660 9	0.660 9	0.666 8
$S_{(T+)}$ = +0.074 67				

TABLE 2—VARIATION OF T_+ WITH CONCENTRATION FOR 2 : 1 AND 3 : 1 ELECTROLYTES AT 25°

Miscellaneous	C	Values of T_+ (cation transport number): Observed	Calcd. Eqn. (3a)	Calcd. Eqn. (L)
K_2SO_4	0.005	0.482 9	0.483 1	0.486 4
Eqn. (3a), T_+° = 0.478 0	0.01	0.484 8	0.484 5	0.489 4
S_m = −0.030 1				
Eqn. (L), T_+° = 0.479 0	0.025	0.487 0	0.486 8	0.493 8
$S_{(T_0)}$ = +0.104 8	0.05	0.489 0	0.489 1	0.502 4
$CaCl_2$	0.005	0.426 4	0.426 4	0.424 9
Eqn. (3a), T_+° = 0.443 8	0.01	0.422 0	0.421 8	0.419 5
S_m = 0.102	0.025	0.414 0	0.414 0	0.411 9
Eqn. (L), T_+° = 0.438 0				
$S_{(T+)}$ = −0.261 4	0.05	0.406 0	0.406 2	0.396 6

(Table 2 contd.)

$LaCl_3$		0.003 33	0.462 5	0.463 2	0.458 7
Eqn. (3a), T^o_+ =	0.485 2	0.006 67	0.457 6	0.457 3	0.451 1
S_m =	0.148				
Eqn. (L), T^o_+ =	0.477 0	0.016 7	0.448 5	0.447 4	0.435 8
$S_{(T_+)}$ =	−0.317 0	0.033 3	0.437 5	0.437 5	0.419 0

results better than equation (L). In the combined constant $(i-T^o_+)/\sqrt{\bar{a}}$, T^o_+ depends on the equivalent conductances λ_{s+} and λ_{s-} of the cations and anions respectively at infinite dilution. Since λ_{s+}, λ_{s-} and a, are all dependent on the size of the ions, so it is assumed that they may be related to the crystallographic radii r_+ and r_- of these ions of an electrolyte. An attempt was, therefore, made to correlate them and it was found that an equation of the following type holds good for the chlorides of the 1 : 1 electrolytes,

$$(i-T^o_+)/\sqrt{\bar{a}} = -m(r_-+r_+)^{1/2}+m_o \qquad (4)$$

where, $m=0.247$ and $m_o=0.437$.

TABLE 3—VARIATION OF $(i-T^o_+)/\sqrt{\bar{a}}$ WITH $(r_-+r_+)^{1/2}$ OF THE CHLORIDES OF 1 : 1 ELECTROLYTES AT 25°

Constants in eqn. (4)	Electrolyte	(r_-+r_+)	(1.22)S	λ_s	S_m	Values of $(i-T^o_+)/\sqrt{\bar{a}}$ Observed	Calcd. eqn. (4)
	LiCl	1.55	0.919	115.08	0.047 5	0.052	0.054
$m=0.247$	NaCl	1.66	0.861	126.48	0.025 2	0.029	0.027
	KCl	1.77	0.771	149.86	0.001 85	0.002 4	0.002
$m_o=0.437$	NH_4Cl	1.77	0.490	149.94	0.001 85	0.001 8	0.002
	HCl	1.98	0.453	426.17	−0.024 6	−0.054	−0.051

Discussion

Attention may be drawn to the fact that the values of λ_+ and λ_- the constituent ions of an electrolyte depend not only on interionic attraction but also on hydration which determines the size of the ions. At *infinite dilution interionic attraction* vanishes but the effect of hydration persists. The data presented in the Tables 1 and 2 involve the assumption that hydration remains constant in the concentration range 0.01 to 0.1 *N*. If, however, the hydration of the ions decreases as the concentration of the electrolyte increases to 0.1 *N* or to a still higher value, then a, in equation (3a) would decrease producing disagreement between the observed and the calculated values of T_+.

It will be noticed from the data recorded in Table 1 that for the 1 : 1 electrolytes the values of T_+ calculated by using equation (3a) agree with the observed ones better than those calculated by using the Onsager equation (L). For $AgNO_3$ the slope observed is positive while that calculated by using Onsager equation (La) is negative. For this electrolyte it may also be noted that the value of T_+ at 0.1 *N*, calculated by equation (3a) is lower than that observed. Although it is still within the limits of experimental error yet it may be taken as an indication that hydration of the Ag^+ ion is tending to decrease. The NO_3 ion which is believed to be a strong 'structure breaker' may be responsible for this effect.

The data for the unsymmetrical electrolytes, recorded in Table 2, confirm the conclusion drawn already that equation (3a) fits the experimental results better than equation (L).

It will be noticed from the data, recorded in Table 3, for the chlorides of the 1 : 1 electrolyte, that the calculated values of $(i-T^o_+)/\sqrt{\bar{a}}$ agree well with those observed. The value of (r_-+r_+) of NH_4Cl has been taken to be the same as that of KCl. It follows from equation (4) that $i=T^o_+-\sqrt{\bar{a}}\,[m(r_-+r_+)^{1/2}-m_o]$.

For 1 : 1 electrolytes having a common anion other than the chloride it is worthwhile investigating whether an equation similar to (4) holds good or not.

References

1. B. N. GHOSH, *J. Indian Chem. Soc.*, 1981, **58**, 678.
2. B. N. GHOSH, *J. Indian Chem. Soc.*, 1982, **59**, 787.
3. B. N. GHOSH, *J. Indian Chem. Soc.*, 1983, **60**, 141.
4. P. DEBYE and E. HÜCKEL, *Phys. Z.*, 1923, **24**, 183, 334.
5. B. N. GHOSH, *J. Indian Chem. Soc.*, 1983, **60**, 607.
6. B. N. GHOSH, *J. Indian Chem. Soc.*, 1984, **61**, 218.
7. H. S. HARNED and B. B. OWEN, "The Physical Chemistry of Electrolytic Solutions", 3rd ed., 1957 p. 170, Table (5-8-1).
8. Ref. 7, p. 221.
9. Ref. 7, Appendix A, p. 699, Table (6-6-1A).
10. H. S. FRANK and M. W. EVANS, *J. Chem. Phys.*, 1945, **13**, 507.
11. H. S. FRANK and W. Y. WEN, *Faraday Discuss. Chem. Soc.*, 1957-58, **24-26**, 133.

J. Indian Chem. Soc.,
Vol. LXIII, April 1986, pp. 393-396

Studies on the Suppression of Polarographic Maxima of Nitrobenzaldehydes by some Uni- and Poly-valent Cations and Anions *vis-a-vis* the Kinetics of Electrode Reaction

SARNAM SINGH SHAKYA, (Miss) INDU BALA and MUKHTAR SINGH*

Department of Chemistry, Agra College, Agra-282 002

Manuscript received 13 December 1982, revised 21 June 1984, accepted 17 February 1986

The suppression of the polarographic negative maxima of *m*- and *p*-nitrobenzaldehydes (*ortho* isomer does not yield a maximum) in borax-boric acid buffer of pH 7.1 has been attempted at 25±0.1° using some uni- and poly-valent cations and anions, *viz.* Na^+, Ca^{2+} and Al^{3+}; and CNS^-, I^-, oxalate and citrate as suppressors. The electrode reactions of the depolarisers have been found to be diffusion-controlled and irreversible in the presence of different amounts of these suppressors. The values of kinetic parameters (αn_a and $k^\circ_{f,h}$) have been calculated by Koutecky's method.

ACCORDING to Meites[1], in the presence of surfactants, the structure of the double layer at the solution-mercury (dme) interface is greatly influenced. This implies that the study of the electrode kinetics of a depolariser is greatly influenced if its reduction at the dme is studied in the presence of conventional surfactants used as maxima suppressors. It is in this background that the suppression of polarographic maxima of nitrobenzaldehydes has been contemplated by uni- and polyvalent cations and anions with a view to studying their electrode kinetics. Hence the title study has been undertaken.

Experimental

The experimental details were the same as reported earlier[2]. The number of electrons (n) involved in the reduction of *o*-, *m*- and *p*-nitrobenzaldehydes was determined by the millicoulometric method of DeVries and Kroon[3] and was found to be 8 for *ortho* and *para* isomers, and 6 for the *meta* isomer. The diffusion coefficient (D) of each depolariser was obtained from the Ilkovic equation. The kinetic parameters (αn_a and $k^\circ_{f,h}$) were calculated from the plots of log $k_{f,h}$ *vs* $E_{d.e}$. Throughout the measurements the current at the end of the drop (*i.e.* maximum current) was recorded for the reasons given by Meites[4]. The following uni- and polyvalent cations and anions were used: cations (nitrate being the anion in each case): Na^+, Ca^{2+} and Al^{3+}: anions (potassium being the cation in each case): CNS^-, I^-, oxalate and citrate. The dme had the following capillary characteristics (in 0.1*M* $NaNO_3$, in open circuit): m=3.16 mg s^{-1}, t=2.46 s, $m^{2/3} t^{1/6}$=2.5 $mg^{2/3} s^{-1/2}$, h_{corr}=36.2 cm.

Results and Discussion

In BR-buffer of *p*H 7.1, *m*- and *p*-nitrobenzaldehydes (in 4%, v/v, ethanolic solution) yield sharp and well defined maxima which lie at −0.66 and −0.56 V (*vs* sce), respectively from the potential of electrocapillary zero, which is −0.32 V (*vs* sce) under the same experimental conditions. Since $E_{1/2}$ values of *m*- and *p*-nitrobenzaldehydes at *p*H 7.1 lie on negative side of the electro-capillary zero, the maxima of these depolarizers are of negative polarity[5]. The relative heights of these maxima are in the following order: *m*-nitrobenzaldehyde>*p*-nitrobenzaldehyde.

The effect of increasing concentrations of uni- and poly-valent cations and anions on the maxima of *m*- and *p*-nitrobenzaldehydes has been studied. Typical values of E_{max} and i_{max} have been presented in Table 1 for Na^+ and I^- ions only; the results for other cations and anions mentioned are similar. A perusal of Table 1 shows that with the addition of uni- and poly-valent cations and anions, the value of i_{max} decreases and that of E_{max} gets shifted to positive potentials. Singh *et al.*[6] have put forward an explanation for this positive shift in E_{max}. After the suppression of the maxina of *m*- and *p*-nitrobenzaldehydes by the requisite amounts of uni- and poly-valent cations and anions, *o*- and *m*-nitrobenzaldehydes yield, in each case, a well defined two-step reduction wave while the *para* isomer yields a well defined three-step reduction wave at *p*H 7.1. The wave-heights of all the steps are diffusion-controlled as evidenced by the linearity of i_d *vs* $h^{1/2}_{corr}$ plots and their passing through the origin. Various criteria for ascertaining the irreversibility of the polarographic reduction of *o*-, *m*- and *p*-nitrobenzaldehydes in the presence of increasing concentrations of uni- and

TABLE 1—VALUES OF POLAROGRAPHIC CHARACTERISTICS AND KINETIC PARAMETERS (αn_a AND $k^\circ_{f,h}$) FOR IRREVERSIBLE ELECTRODE REACTIONS OF *o*-, *m*- AND *p*-NITROBENZALDEHYDES (IN 4% ETHANOLIC SOLUTIONS) IN PRESENCE OF INCREASING CONCENTRATIONS OF UNI- AND POLY-VALENT CATIONS AND ANIONS AT *p*H 7.1

[Ion] *M*	$-E_{max}$ (sce) V	$-E_{1/2}$ (sce) V	i_{max} μA	i_d μA	Slope mV	$D \times 10^6$ $cm^2 s^{-1}$	αn_a	$K^\circ_{f,h}$ $cm\ s^{-1}$
				o-Nitrobenzaldehyde				
0.0 I	—	0.375	—	20.40	62	8.91	0.82	1.52×10^{-8}
II	—	1.315	—	21.76	115		0.42	1.98×10^{-11}
Cation Na^+								
4.00 I	—	0.395	—	18.70	65	7.40	0.88	2.01×10^{-8}
II	—	1.325	—	19.72	125		0.49	2.76×10^{-11}
4.50 I	—	0.390	—	17.00	65	6.27	0.85	4.86×10^{-8}
II	—	1.305	--	18.86	128		0.44	4.02×10^{-11}
5.00 I	—	0.382	—	16.32	66	5.45	0.86	8.30×10^{-8}
II	—	1.300	—	16.66	121		0.44	4.17×10^{-11}
Anion I^-								
0.125	—	0.390	—	18.70	65	7.01	0.83	5.17×10^{-8}
0.250	—	0.386	—	19.72	63	7.80	0.85	6.26×10^{-8}
0.500	—	0.380	—	20.40	62	8.34	0.86	8.06×10^{-8}
				m-Nitrobenzaldehyde				
0.00	0.66	—	38.76	—	—	—	—	—
Cation Na^+								
0.50	0.65	—	36.04	—	—	—	—	—
1.00	0.62	—	32.64	—	—	—	—	—
2.50	0.57	—	23.12	—	—	—	—	—
4.00	0.56	—	19.86	—	—	—	—	—
4.50* I	—	0.370	—	18.70	58	8.53	0.93	6.39×10^{-7}
II	—	1.180	—	12.24	75		0.72	1.62×10^{-15}
5.00 I	—	0.365	—	18.02	57	7.98	0.94	7.92×10^{-7}
II	—	1.160	—	11.90	74		0.73	3.16×10^{-15}
5.50 I	—	0.350	—	17.68	56	7.27	0.95	8.96×10^{-7}
II	—	1.120	—	10.88	72		0.75	8.30×10^{-15}
Anion I^-								
1.00	0.62	—	32.64	—	—	—	—	—
2.00	0.60	—	28.22	—	—	—	—	—
3.50	0.58	—	24.82	—	—	—	—	—
4.20	0.58	—	21.42	—	—	—	—	—
4.25* I	—	0.440	—	21.08	57	9.10	0.94	5.17×10^{-7}
II	—	1.280	—	10.88	73		0.74	2.11×10^{-5}
4.50 I	—	0.432	—	18.02	56	6.59	0.95	6.32×10^{-7}
II	—	1.260	—	9.18	70		0.77	3.61×10^{-15}
4.75 I	—	0.415	—	17.68	56	6.11	0.96	8.71×10^{-7}
II	—	1.250	—	8.50	69		0.78	4.02×10^{-15}
				p-Nitrobenzaldehyde				
0.0	0.56	—	30.94	—	—	—	—	—
Cation Na^+								
2.0×10^{-3}	0.53	—	27.54	—	—	—	—	—
5.0×10^{-3}	0.49	—	23.80	—	—	—	—	—
2.0×10^{-2}	0.45	—	19.72	—	—	—	—	—
2.4×10^{-2}	0.44	—	18.02	—	—	—	—	—
2.8×10^{-2}* I	—	0.370	—	17.68	67	6.15	0.81	2.49×10^{-8}
II	—	1.240	—	9.52	87		0.62	4.75×10^{-14}
III	—	1.380	—	7.82	68		0.81	8.75×10^{-19}
1.00 I	—	0.335	—	17.34	66		0.88	3.41×10^{-8}
II	—	1.205	—	7.82	85	4.80	0.63	6.21×10^{-14}
III	—	1.385	—	5.78	67		0.80	9.11×10^{-19}
2.00 I	—	0.320	—	17.00	65		0.83	8.78×10^{-8}
II	—	1.195	—	7.82	88	5.49	0.65	2.82×10^{-11}

(Table 1 contd.)

Anion I^-								
4.0×10^{-4}	0.51	—	98.56	—	—	—	—	—
8.0×10^{-3}	0.50	—	22.10	—	—	—	—	—
2.50	0.48	—	20.74	—	—	—	—	—
3.00	0.48	—	19.88	—	—	—	—	—
3.10* I	—	0.382	—	19.04	67		0.81	6.02×10^{-5}
II	—	1.245	—	9.18	83	7.66	0.65	5.16×10^{-14}
III	—	1.380	—	10.88	68		0.80	4.12×10^{-19}
3.50 I	—	0.375	—	17.68	66		0.82	8.18×10^{-5}
II	—	1.280	—	8.84	82	6.51	0.66	6.29×10^{-14}
III	—	1.370	—	9.52	67		0.82	6.68×10^{-19}
3.75 I	—	0.370	—	17.00	64		0.86	9.32×10^{-5}
II	—	1.220	—	7.82	80	5.69	0.67	8.68×10^{-14}
III	—	1.360	—	8.84	65		0.83	8.96×10^{-19}

I = First wave, II = second wave and III = third wave.

* Concentration at which the maximum gets just suppressed.

poly-valent cations and anions were applied. The slope values of log plots in each case are much larger than the theoretical values expected for 8- and 6-electron reversible reduction processes. It follows from this that the polarographic reduction of *o*-, *m*- and *p*-nitrobenzaldehydes is irreversible[7]. The dependence of current on h_{corr} at different stages of the wave was also studied and the current was found to be independent of the pressure head of the mercury at the foot of the wave whereas it was proportional to $h_{corr}^{1/2}$ at the plateau of the wave, thereby supporting the irreversible nature of the polarographic reduction[8,9].

The values of αn_a and $k^o_{f,h}$ for the electrode reactions of *o*-, *m*- and *p*-nitrobenzaldehydes tend to increase with increasing concentrations of uni- and poly-valent cations and anions. This shows[10] that the reduction of *o*-, *m*- and *p*-nitrobenzaldehydes at dme is rendered less irreversible with increasing concentrations of uni- and poly-valent cations and anions.

A comparison of $k^o_{f,h}$ values at the stage where maxima of *m*- and *p*-nitrobenzaldehydes get just suppressed by uni- and poly-valent cations and anions (*ortho* isomer does not give maximum) may give a quantitative estimation of the influence of these ions on the kinetics of the electrode reactions of *m*- and *p*-nitrobenzaldehydes. From a perusal of Table 1 the following order of $k^o_{f,h}$ values in respect of various uni- and poly-valent cations and anions is obtained. Uni- and poly-valent cations : $Al^{3+} > Ca^{2+} > Na^+$. Thus, among the uni- and poly-valent cations it is Al^{3+} which suppresses the maxima of *m*- and *p*- nitrobenzaldehydes with minimum iufluence on the kinetics of the electrode reactions. Uni- and poly-valent anions : $CNS^- > I^- >$ (citrate)$^{3-}$ $>$ (oxalate)$^{2-}$. Thus, among the uni- and poly-valent anions it is CNS^- which suppresses the maxima of *m*- and *p*-nitrobenzaldehydes with minimum influence on the kinetics of the electrode reactions.

The order of $k^o_{f,h}$ values in respect of the electrode reactions of *o*-, *m*- and *p*-nitrobenzaldehydes in the presence of uni- and poly-valent cations and anions is as follows : *o*-nitrobenzaldehyde > *p*-nitrobenzaldehyde > *m*-nitrobenzaldehyde. Thus, *o*-nitrobenzaldehyde is easiest to reduce at dme.

Relative efficacies of uni- and poly-valent cations and anions in the suppression of the maxima of m- *and* p-*nitrobenzaldehydes on the basis of* αn_a *values* : At the stage where the maxima of *m*- and *p*-nitrobenzaldehydes just disappear (marked by an asterisk in Table 1), the order of αn_a values signifies[6] the extent to which the addition of uni- and poly-valent cations and anions renders the electrode reactions of *m*- and *p*-nitrobenzaldehydes more irreversible from the position in the absence of these ions. In other words, a cation or an anion for which αn_a has got a higher value at the point of just suppression of the maxima will be more effective with minimum influence on the kinetics of the electrode reactions of *m*- and *p*-nitrobenzaldehydes. On this basis, the following order of relative efficacies of various uni- and poly-valent cations and anions has been established. Uni- and poly-valent cations : $Al^{3+} > Ca^{2+} > Na^+$. Uni- and poly-valent anions : $CNS^- > I^- >$ (citrate)$^{3-}$ $>$ (oxalate)$^{2-}$.

It is interesting to note that not only uni- and poly-valent cations but also anions suppress the negative maxima of *m*-and *p*-nitrobenzaldehydes and that their (cations and anions) efficacies follow the valency rule. However, I^- and CNS^- do not follow this generalisation. This may be attributed to the fact that both I^- and CNS^- are capillary active substances[11] and as such they are more effective in suppressing the maxima. Further, the order of efficacies found on the basic of molarity is identical to that obtained on the basis of αn_a values.

References

1. L. MEITES, "Polarographic Techniques", Interscience, New York, 1965, p. 287.
2. S. S. SHAKYA, K. CHANDRA and M. SINGH, *Indian J. Chem., Sect. A*, 1982, **21**, 411.

3. T. DeVries and J. L. Kroon, *J. Am. Chem. Soc.*, 1953, **75**, 2484.
4. L. Meites, "Polarographic Techniques", Interscience, New York, 1965, p. 241.
5. J. Heyrovsky and J. Kuta, "Principles of Polarography", Academic, New York, 1966, p. 487.
6. M. Singh, G. Ram and S. K. Jha, *Indian J. Chem., Sect. A*, 1977, **15**, 406.
7. Ref. 4, p. 227.
8. P. Delahay, *J. Am. Chem. Soc.*, 1951, **53**, 4944.
9. P. Kivalo, K. B. Oldham and H. A. Laitinen, *J. Am. Chem. Soc.*, 1953, **75**, 4148.
10. Ref. 4, p. 323.
11. I. M. Kolthoff and J. J. Lingane, "Polarography", Interscience, New York, 1952, Vol. I, p. 166.

J. Indian Chem. Soc.,
Vol. LXIII, April 1986, pp. 397-399

Polarographic Examination of Active Components of *Datura stramonium*

ASHA BEGERHOTTA and N. R. BANNERJEE*

Electrochemical Laboratories, Department of Chemistry, University of Delhi, Delhi-110 007

Manuscript received 30 September 1985, accepted 6 February 1986

The polarograms, the limiting current-pH, $E_{1/2}$-pH, limiting current-concentration and slopes of log $\bar{i}$ *vs* log h plots of the principal component of *Datura stramonium* stem-, leaf- and root-extracts in cold 1% $HClO_4$ solution prove the catalytic nature of limiting currents, similar to those of atropine. From the calibration curve (limiting current-concentration) of atropine sulphate at pH 5.3 the air-dried stems, leaves and roots of the plant are found to contain respectively 1.10, 1.05 and 1.04% of atropine.

POLAROGRAPHY together with chromatography offers the most rapid and sensitive analytical technique for purposes of identification, estimation and establishment of the course of electroreduction (or -oxidation) of organic compounds present as active principles in medicinal plants[1]. Organic compounds present in these plants exhibit different behaviour at dropping mercury electrode depending upon their chemical nature.

The plant under present investigation, *Datura stramonium* (family : Solanaceae) contains an alkaloid, atropine which is well known for its wide therapeutic value[2,3]. The present work has been carried out in order to establish a routine polarographic method for the estimation of atropine in various parts of the plant.

Experimental

Polarograms were recorded (298 K) with a radiometer pen-recording polarograph, Polariter PO4. A Kalousek cell with a saturated calomel electrode (sce) was used as the reference electrode. The dropping mercury electrode (dme) made from sargent capillary was used having the following characteristics : $m = 0.952$ mg s^{-1} and $t = 4.3$ s at 60 cm height of mercury reservoir in 0.5 mol dm^{-3} KCl solution at zero applied potential (sce). The *p*H values of the solutions were measured before and after recording each polarogram on ELICO LI-10 *p*H meter with an accuracy of ± 0.1 *p*H unit.

All the reagents used were of A.R. grade. The stems, leaves and roots of the plant *Datura stramonium* were collected in July-August, separately dried in air, crushed and 40.0 g of each kept immersed in 1% perchloric acid (400 ml) for a week at room temperature and the cold extracts filtered before use. Each extract was diluted 1000 times with conductivity water after adding tetramethylammonium acetate-borate buffer (0.075 mol dm^{-3}, final strength) and tetramethylammonium bromide (0.1 mol dm^{-3}, final concentration) for obtaining the test solutions.

Results and Discussion

Polarograms of Datura stem-extract at different *p*H values exhibit single waves with their heights decreasing with increasing *p*H values (Fig. 1). The current-*p*H plot (Fig. 5) shows an exponential

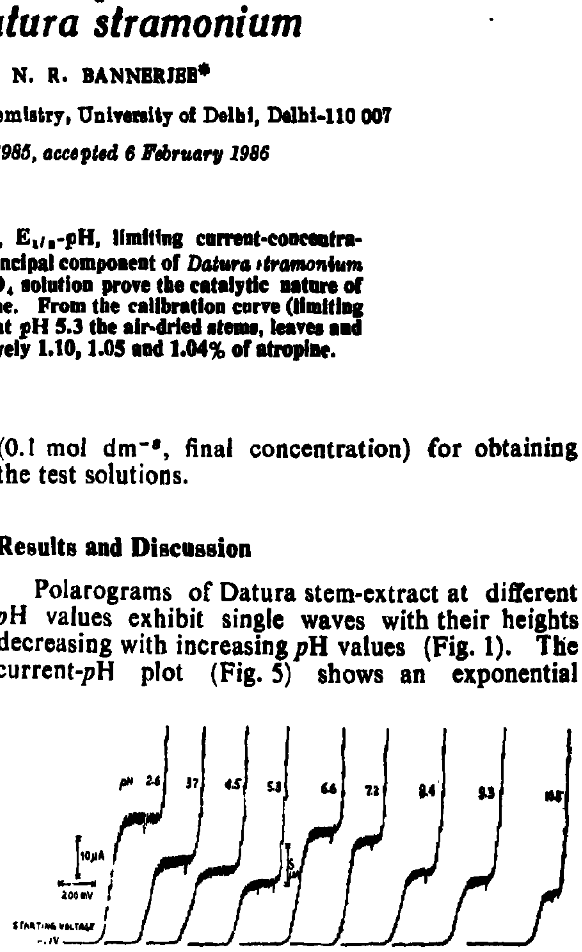


Fig. 1. *p*H-dependence of polarograms of Datura stem-extract (0.01 ml of 1% $HClO_4$ solution made up to 10 ml of test solution).

decrease of limiting current, reminiscent of an acid-base equilibrium in which the acidic component alone is electro-active. Such a behaviour is usually exhibited by catalytic hydrogen waves[4,5]. Dependence of limiting current on concentration (in terms of dilution of the extract from 1000 to 31.25) exhibits Langmuir-type behaviour, a characteristic of catalytic waves[6]. The nature of the polarographic waves has been verified by the slopes of log $\bar{i}$ *vs* log h plots over the entire wave at two *p*H's 5.3 and 8.4. The slopes range from −1.09 at 1.48V to −0.16 at 1.70V and from −0.39 at 1.52V to −0.21 at 1.82V at *p*H's 5.3 and 8.4, respectively. Polarograms of cold and diluted extracts of Datura leaves and roots at different *p*H values under the identical conditions as employed above show similar decrease in limiting currents with increasing *p*H values (Figs. 2 and 3). The current-*p*H, $E_{1/2}$-*p*H

and current-concentration plots are similar to those of the stem-extract, indicating similar nature of the active components present in the stems, leaves and roots of *Datura stramonium*. The log $\bar{i}$ *vs* log h plots for the waves of leaf-extract have similar slope values ranging from −1.09 to −0.17 at *p*H 5.3 and from −0.36 to −0.20 at *p*H 8.4. The corresponding slopes for the root-extract range from −1.09 to −0.17 and from −0.40 to −0.23 at *p*H's 5.3 and 8.4, respectively.

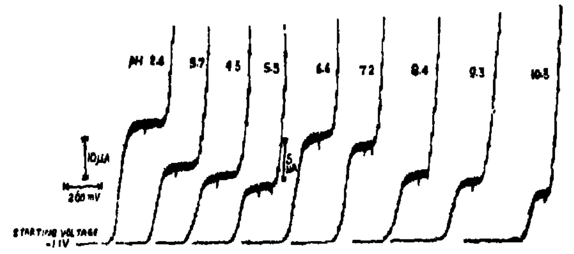


Fig. 2. *p*H-dependence of polarograms of Datura leaf-extract (0.01 ml of 1% $HClO_4$ solution made up to 10 ml of test solution).

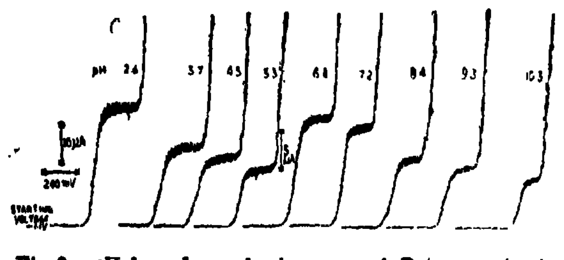


Fig. 3. *p*H-dependence of polarograms of Datura root-extract (0.01 ml of 1% $HClO_4$ solution made up to 10 ml of test solution).

The polarograms (Fig. 4) of atropine sulphate (0.1 mol m^{-3}) at different *p*H values and similar ionic strengths and buffer concentrations as employed for the extracts show striking resemblance (Figs. 1-3). The plots of current *p*H, (Fig. 5), $E_{1/2}$ -*p*H (Fig. 6), current-concentration (Fig. 7) and slope values of log $\bar{i}$ *vs* log h plots for the waves at *p*H 5.3 and 8.4 (−1.08 to −0.16 for *p*H 5.3 and from −0.40 to −0.25 for *p*H 8.4) confirm the catalytic nature of the polarographic waves and identity of the active component of the extracts of Datura stems, leaves and roots with atropine. Mixed polarogram of atropine sulphate and each extract (1 : 1) at *p*H 7.2 show single waves with enhanced current supporting the above conclusion.

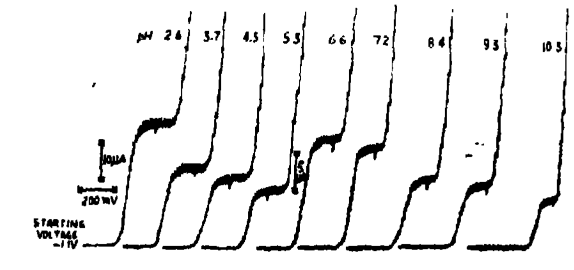


Fig. 4. *p*H-dependence of polarograms of atropine sulphate (0.1 mol m^{-3}).

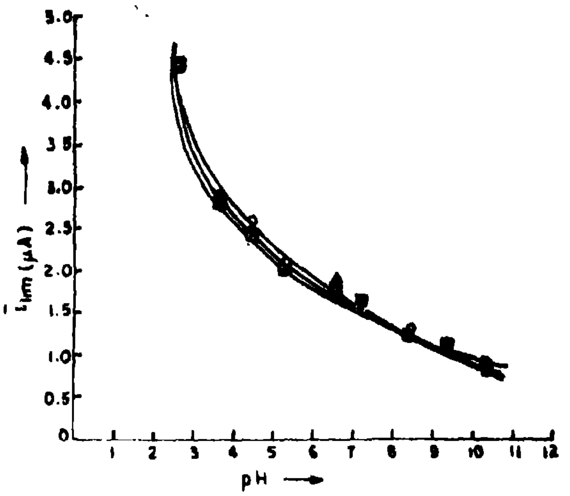


Fig. 5. Dependence of limiting current on *p*H : (○) atropine sulphate (0.1 mol m^{-3}), (●) stem-extract (0.001 ml), (△) leaf-extract (0.001 ml) and (□) root-extract (0.001 ml).

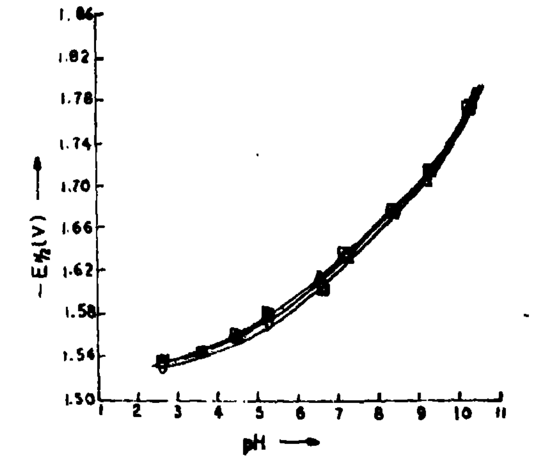


Fig. 6. Dependence of half-wave potential on *p*H : (○) atropine sulphate (0.1 mol m^{-3}), (●) stem-extract (0.001 ml), (△) leaf-extract (0.001 ml) and (□) root-extract (0.001 ml).

To determine the concentration of atropine in different parts of Datura, polarograms for different concentrations (0.1-1.7 mol m^{-3}) of atropine sulphate (*p*H 5.3) have been recorded. The calibration curve (i_{lim} *vs* concentration plot) has the slope of 3.28 μA $mmol^{-1}$. The concentration of atropine in air-dried stems, leaves and roots of *Datura stramonium* have thus, been estimated to be 1.10, 1.05 and 1.04%, respectively.

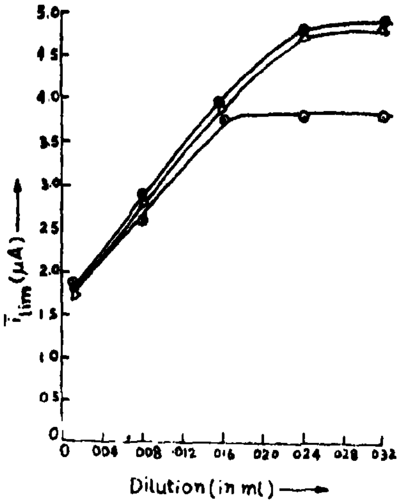


Fig. 7. Concentration (in terms of dilution) dependence of limiting currents at *p*H 5.8: (○) stem-extract, (●) leaf-extract and (Δ) root-extract.

Acknowledgement

The authors thank the Head, Department of Chemistry, University of Delhi, for his kind interest and C.A.S. for the award of Senior Research Fellowship to one of them (A.B.).

References

1. P. ZUMAN, "Organic Polarographic Analysis", Pergamon, New York, 1964, p. 230.
2. R. N. CHOPRA, "Indigenous Drugs of India", U. N. Dhur and Sons, Calcutta, 1958, p. 482.
3. A. K. NADKARNI, "Indian Materia Medica", Popular Book Depot, Bombay, 1954, p. 440.
4. S. G. MAIRANOVSKII, "Catalytic and Kinetic Waves in Polarography", Plenum, New York, 1968, p. 252.
5. Ref. 4, p. 253.
6. J. HEYROVSKÝ and J. KŮTA, "Principles of Polarography", CSAV, Prague, 1965, p. 289.

J. Indian Chem. Soc.,
Vol. LXIII, April 1986, pp. 400-403

Flow Behaviour of Bentonite Suspension. Part-I. Interaction with Electrolytes

N. K. MITRA*, A. C. DAS and A. BASUMAJUMDAR

Department of Chemical Technology, University of Calcutta, Calcutta-700 009

Manuscript received 17 August 1984, accepted 6 February 1986

Bihar bentonite, purified from non-clayey gritty matters, inorganic and organic compounds, was finally converted into mono-ionic sodium form. The purified clay was characterised by chemical analysis, CEC, DTA and X-ray for pure montmorillonitic nature. The suspension characteristics in terms of rheological behaviour were studied in presence of different electrolytes, such as LiCl, NaCl, KCl, $MgCl_2$, $CaCl_2$, $BaCl_2$, $Al(NO_3)_3$ and $ZrOCl_2$. The influence of electrolytes on the colloidal properties of the clay suspension was indicated by the determination of plastic viscosity and yield value through rotational cup and bob viscometer of McMichael type.

THE sensitivity of clay suspension towards addition of electrolytes is of paramount importance in drilling fluids, fabrication of ceramic wares by slip casting, application of unshaped refractories such as mortars, ramming masses and castables on the furnace wall before the commencement of relining. Adjustment of appropriate amount of electrolyte enables a ceramic technologist to control the suspensibility as well as the flow behaviour of clay suspension. The slip should possess low viscosity for easy flowing and high yield value (*e.g.* the minimum force required to start flow) for high green strength. Hence, the study of flow behaviour of bentonite became essential for the analysis of particle interaction.

According to Henry and Taylor[1], who studied the changes in *p*H and apparent viscosity of clay slips, the *p*H of exchange neutrality of each clay agreed closely with maximum in the *p*H-viscosity curve. Marshall[2] pointed out that the addition of increasing amounts of monovalent bases to electrodialysed montomorillonite (bentonite) increased the viscosity. The viscosity attained a maximum just before the complete neutralisation and then experienced a second rise. The first maximum was less marked with K^+ than Li^+ or Na^+. The second maximum showed a different order, *i.e.* $K^+ > Li^+ > Na^+$.

Alader[3] showed that only the external surfaces of the particles affected the stability of bentonite suspension whereas during the ion-exchange or hydration the inner portion of the particles also reacted. This observation explained the wide variation of mechanical properties of films produced from bentonite suspension. Sengupta and Indra[4] observed that the viscosity and yield value curve of bentonite suspension at various stages of neutralisation plotted against the corresponding alkali passed through a maximum and then a minimum in the same way as the buffer capacity curve.

Olphen[5] studied the effect of neutral salts, such as NaCl on the yield stress of 3% suspension of dialysed Na-Woming bentonite and concluded that the formation of structure in the pure gel can be attributed to edge-to-flat-surface association of the flat micelles caused by opposed charge of the double layer at the surfaces. Williams *et al.*[6] showed that the variations in rheological properties of natural bentonites were affected greatly by the Na/Ca ratio by the weight dilution of the colloidal fraction by minerals, and by varying amounts of soluble salts. Marshall[7] concluded that plasticity of kaolinite is a result of physical properties and that of montmorillonite a result of chemical properties. Other clay minerals are intermèdiate between kaolinite and montmorillonite depending upon the make up of the clay mineral.

The flocculation of Na-montmorillonite of five different particle sizes was studied by Kahn[8] in presence of NaCl, $CaCl_2$, $AlCl_3$ and $La(NO_3)_3$. Flocculation value (concentration of electrolyte where sharp change of viscosity occurred) of NaCl was relatively independent of particle size of Na-montmorillonite concentration whereas the flocculation value of other electrolytes was strongly affected by ion-exchange. Gabrysh *et al.*[9] studied the effects of concentration, temperature, suspension medium, hydrogen ion concentration and successive application of the shear stress on the flow behaviour of colloidal suspensions of bentonite. They concluded that at high shear rates all flow curves coincided and that temperature had no effect. Van Olphen[10] showed that the addition of NaCl to the purified 2% Na-bentonite suspensions in water initially decreases the yield stress, but beyond about 5 meq dm^{-3} increases it. The same is true for the relative viscosities and the sediment volumes of more dilute suspensions. The sequence of flocculation-deflocculation-flocculation of the clean suspensions is explained by the concept of positive edge charge of the

clay plates, allowing positive edge of negative flat-surface flocculation. The change in viscosity of Wyoming bentonite was studied by Nash[11] with variations in cation ionisation, base saturation, clay concentration, NaCl concentration and type of exchangeable cation. The viscosity changes little with decreasing cation ionisation until a certain threshold value is reached Below this value the viscosity increases rapidly, indicating that the repulsive potential barrier has been reduced to the order of the kinetic energy of the particles.

Previous workers measuring apparent viscosity, did not fully reveal the nature of suspension so far as the rheology is concerned. The properties of suspension characteristics as well as the stability of clay suspensions possess widespread practical application. Thus, the present work has been designed to study systematically the interactions of bentonite clay with different electrolytes at various concentrations.

Experimental

Bihar bentonite, greyish in colour and one of the best varieties of montmorillonite containing clays of India, was selected for the present investigation. The clay, after purifying from non-clay gritty material and associated organic and inorganic impurities, became white with slight yellowish tinge. The purified clay containing the maximum portion of 1 μ and below size fractions was always stored in a constant temperature incubator (36±1°) to avoid any extraneous moisture absorption. For the present study, bentonite was converted into Na-form and its usual characteristics are furnished in Table 1.

TABLE 1—CHEMICAL ANALYSIS AND OTHER CHARACTERISTICS OF BENTONITE IN Na-FORM

Constituents	% (w/w)	Cation exchange capacity meq/100 g	DTA peak temp.
SiO_2	51.30		156,565 (endo)
Al_2O_3	27.31		
Fe_2O_3	1.41	97.20	940 (exo)
CaO	—		
MgO	1.36		
Loss on ignition	14.89		

AnalaR and E. Merck quality salts of LiCl, NaCl, KCl, $MgCl_2$, $CaCl_2$, $BaCl_2$, $Al(NO_3)_3$ and $ZrOCl_2$ were used for the preparation of the solutions of electrolytes. In order to have the same milliequivalent of cations per ml of solution, electrolyte solutions containing mono-, di-, tri- and tetra-valent cations were prepared at 1, 0.5, 0.33 and 0.25 molar concentrations.

The suspensions were prepared at 10% concentration in a wide mouth glass stoppered reagent bottle of 250 ml capacity. A small volume of distilled water was added to make a slurry, followed by addition of required volume of the standard solution of electrolyte. Finally, the volume was made upto 100 ml with distilled water. The suspension was aged for overnight, shaken in a mechanical shaker for 3 h and then immediately used for measurement of viscosity.

The viscosity was measured in a modified McMichael viscometer utilising Reiner and Riwlin equation[12] for plastic flow in a rotational viscometer.

For yield value,

$$f = CT_0 \quad (1)$$

$$\text{Plastic viscosity } (U) = \frac{(T - T_0)S}{\Omega} \quad (2)$$

where, $S = \dfrac{\frac{1}{R_b^2} - \frac{1}{R_c^2}}{4\pi h}$ and $C = \dfrac{S}{\ln R_c/R_b}$,

R_b, R_c = Radius of the bob and cup, respectively, $U = 1/\mu$ plastic viscosity, Ω = angular viscosity, h = depth of immersion of the bob, and T = movement due to external forces (torque).

Results

From the chemical analysis, cation-exchange capacity and differential thermal analyses nature of the montmorillonite in Bihar bentonite was ascertained. The chemical analysis indicates montmorillonite is dioctahedral with Al^{3+} in the octahedral sites. Some of these sites are substituted by Fe^{3+} and Mg^{2+}. There were also substitution in the tetrahedral silica layer by Al^{3+}.

The rheological characteristics (yield value and plastic viscosity) were determined from the multipoint consistency curves, by the plot of r.p.m. *vs* torque. The nature of the flow curve did not differ to a great extent. The flow curves of 10% Na-bentonite suspension in presence of $BaCl_2$, shown in Fig. 1, is representative. The relative change of plastic

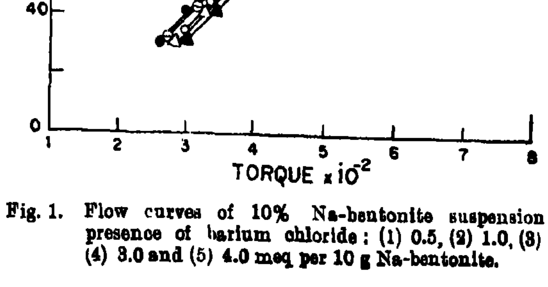


Fig. 1. Flow curves of 10% Na-bentonite suspension in presence of barium chloride: (1) 0.5, (2) 1.0, (3) 2.0, (4) 3.0 and (5) 4.0 meq per 10 g Na-bentonite.

viscosity and yield value with addition of electrolytes are shown in Figs. 2 and 3 and the results are provided in Table 2.

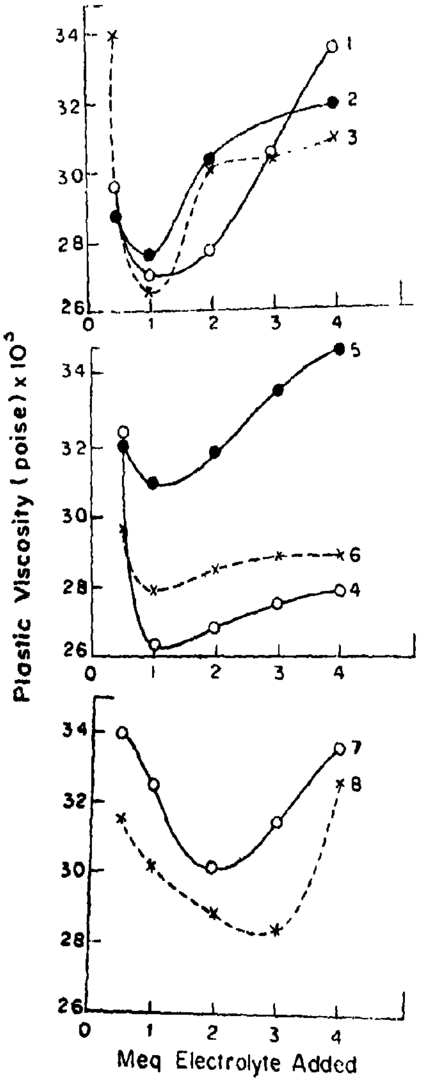


Fig. 2. Plastic viscosity relationship of 10% Na-bentonite suspension during interaction with different electrolytes: (1) LiCl, (2) NaCl, (3) KCl, (4) $MgCl_2$, (5) $CaCl_2$, (6) $BaCl_2$, (7) $Al(NO_3)_3$ and (8) $ZrOCl_2$.

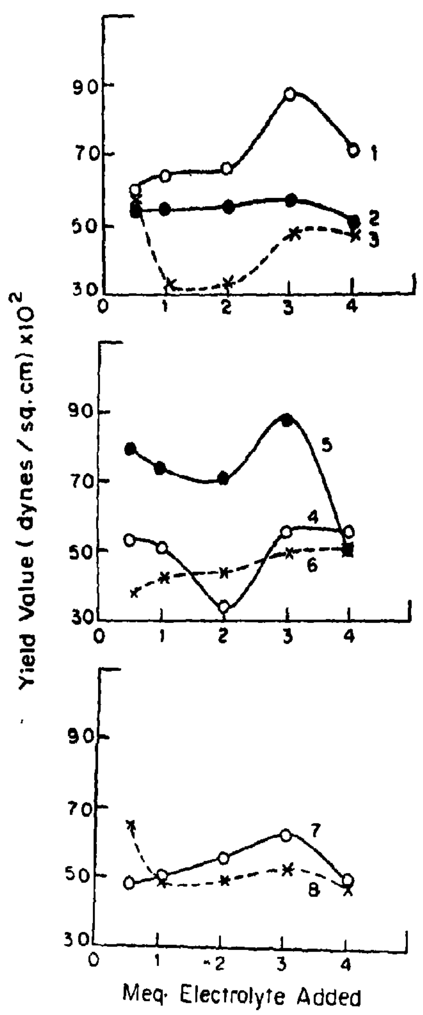


Fig. 3. Yield value relationship of 10% Na-bentonite suspension during interaction with different electrolytes; (1) LiCl, (2) NaCl, (3) KCl, (4) $MgCl_2$, (5) $CaCl_2$, (6) $BaCl_2$, (7) $Al(NO_3)_3$ and (8) $ZrOCl_2$.

Discussion

The yield value figures reveal that the nature of the flow of 10% Na-bentonite suspension changed from Newtonian to non-Newtonian during interaction with electrolytes in all cases. Higher yield value was observed with $CaCl_2$ followed by LiCl, $Al(NO_3)_3$ and $ZrOCl_2$ with specified addition of electrolytes. At the initial point of addition (0.5 meq per 10 g clay) the order of the cations with respect to plastic viscosity and yield value may be written as: $Al^{3+} > K^+ > Mg^{2+} > Ca^{2+} > Zr^{4+} > Li^+ > Ba^{2+} > Na^+$, and $Ca^{2+} > Zr^{4+} > Li^+ > K^+ > Na^+ > Mg^{2+} > Al^{3+} > Ba^{2+}$, respectively. In each case, with addition of electrolyte the plastic viscosity appreciably increased. Different cations did not produce a significant difference in plastic viscosity. This indicates the degree of interaction is approximately the same in this range. Still, Ca^{2+} and Al^{3+} showed relatively higher plastic viscosity throughout the whole range of addition. The nature of yield value curves are not identical. An upward trend followed by a decrease at the final point of addition was observed with Li^+, Na^+ and Al^{3+} whereas all other cations except Ba^{2+} showed continuous increase of yield value on gradual addition of electrolyte. The initial change of yield value was prominent with K^+, Mg^{2+} and Zr^{4+}. Thus the flow

TABLE 2—EFFECT OF GRADUAL ADDITION OF ELECTROLYTES ON FLOW BEHAVIOUR OF 10% Na-BENTONITE SUSPENSION

Electrolyte	Meq added per 10 g clay	Plastic viscosity poise $\times 10^3$	Yield value dyne cm^{-2}
	0.5	29.68	0.5971
	1	27.06	0.6848
LiCl	2	27.67	0.6552
	3	30.55	0.8600
	4	33.38	0.6961
	0.5	28.86	0.5823
	1	27.66	0.5898
NaCl	2	30.31	0.5459
	3	30.58	0.5665
	4	31.77	0.5010
	0.5	33.90	0.5869
	1	24.05	0.3276
KCl	2	30.07	0.3844
	3	30.31	0.4915
	4	30.87	0.4640
	0.5	32.29	0.5222
	1	26.25	0.4983
$MgCl_2$	2	26.86	0.3252
	3	27.52	0.5898
	4	27.86	0.5328
	0.5	32.01	0.7780
	1	31.86	0.7803
$CaCl_2$	2	30.92	0.6961
	3	33.67	0.8600
	4	34.87	0.4915
	0.5	29.58	0.3685
	1	27.92	0.4094
$BaCl_2$	2	28.56	0.4164
	3	28.86	0.4879
	4	28.87	0.4915
	0.5	33.92	0.4743
	1	32.55	0.4988
$Al(NO_3)_3$	2	30.09	0.5501
	3	31.41	0.6212
	4	33.67	0.4915
	0.5	31.54	0.6416
	1	30.20	0.4846
$ZrOCl_2$	2	28.87	0.4846
	3	28.41	0.5187
	4	32.77	0.4607

properties of the suspension may be satisfactorily controlled as per requirement by suitable addition of electrolyte and the curves will be very much helpful in predicting the rheology.

The decrease of yield value and plastic viscosity in presence of electrolytes may be explained by the fact that here both the double layers are compressed whereby effective charge is reduced. Under this condition, attraction is less than repulsion because both edge-to-face (EF) attraction and face-to-face (FF) repulsion are diminished and thus the particles are disengaged, breaking the cardhouse structure. The increase of plastic viscosity and yield value in presence of electrolytes may be explained by the fact that in presence of high concentration of low potential cations or low concentration of high potential cations both the double layers are compressed to a greater degree. Under this condition, the van der Waals attraction between edges and faces supplements the opposite charge attraction. The subtle balance between EF attraction and FF repulsion becomes favourable for the formation of cardhouse structure. Simultaneously EF association by van der Waals attraction is likely to occur, which may contribute to the resulting increase in yield value and plastic viscosity. At high salt concentration (4 meq per 10 g of clay) decrease of yield value may be due to rapid occurrence of FF association by which the number of particles in the cardhouse is reduced thereby decreasing the strength.

References

1. E. C. HENRY and N. W. TAYLOR, *J. Am. Ceram. Soc.*, 1938, **21**, 165.
2. C. E. MARSHALL, "The Colloid Chemistry of the Silicate Minerals", Academic, New York, 1949, Vol. I, p. 152.
3. A. BUZAGH, *Magy. Kem. Foly.*, 1950, **56**, 7.
4. N. C. SENGUPTA and M. K. INDRA, *J. Indian Chem. Soc., Ind. News Ed.*, 1949, **12**, 100.
5. H. V. OLPHEN, *Discuss. Faraday Soc.*, 1951, **89**.
6. F. J. WILLIAMS, M. NEZAYKO and D. J. WEINTRITT, *J. Phys. Chem.*, 1953, **57**, 6.
7. L. C. MARSHALL, *Am. Ceram. Soc. Bull.*, 1959, **34**, 54.
8. A. KAHN, *J. Colloid. Sci.*, 1958, **13** 51.
9. W. F. GABRYSH, H. EYRING, P. LINSEN and A. F. GABRYSH, *J. Am. Ceram. Soc.*, 1963, **46**, 523.
10. H. VAN OLPHEN, 'Forces Between Suspended Bentonite Particles", Natl. Acad. Sci.-Natl. Res. Council, Publ. No. 456, 1956, p. 204.
11. V. E. NASH, Clays and Clay Minerals Proceedings of the 7th National Conference on Clays and Clay Minerals, 1958, **5**, 328.
12. H. GREEN, "Industrial Rheology and Rheological Structures", Wiley, New York, 1949, p. 35.

J. Indian Chem. Soc.,
Vol. LXIII, April 1986, pp. 404-405

Debromination of Chalcone Dibromide and Stilbene Dibromide with Sodium Hydrogen Sulphide†

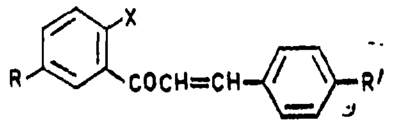
ASHOK G. DOSHI and BHANULAL J. GHIYA*

Department of Chemistry, Institute of Science, Nagpur-440 001

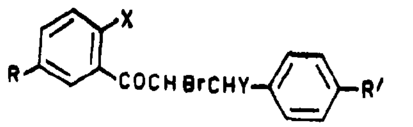
Manuscript received 22 May 1985, revised 24 December 1985, accepted 17 February 1986

Sodium hydrogen sulphide debrominated chalcone dibromide and α-bromo-β-hydroxychalcone and also stilbene dibromide in methanol to chalcone and stilbene, respectively.

DEBROMINATION of *vic*-dihaloalkanes and α,β-dibromoketones have been studied by earlier workers using the debrominating agents, like potassium iodide in acetone[1], stannous chloride in different solvents[2], sodium hydrogen selenide[3], thiourea in ethanol[4,5] and also by some recent workers using hydrated sodium sulphide under phase transfer conditions[6,7] and photochemical and chemical reduction of *vic*-dihalides *via* phase transfer of 4,4'-bipyridinium radical[8] for solar energy conversion. Use of cobalt octacarbonyl on alumina has been reported for selective dehalogenation of α-bromosulphoxides[9]. Chromium(II) acetate also brings reductive debromination in *vic*-dihaloalkanes[10] and chalcone dibromides[11].



(1)



(2)

a; R=CH$_3$, R'=OCH$_3$, X=OH, Y=Br.
b; R=X=H, R'=OCH$_3$, Y=Br.
c; R=R'=X=H, Y=Br.
d; R=CH$_3$, R'=H, X=OH, Y=Br.
e; R=CH$_3$, R'=OCH$_3$, X=OAc, Y=Br.
f; R=CH$_3$, R'=OCH$_3$, X=OAc, Y=OH.

Sodium sulphide with *vic*-dibromo derivatives of certain oximes is reported to give sulphoxide derivatives[12]. Chalcone with anhydrous sodium sulphide in dry ethanol gives thiophenes and with excess of sodium sulphide in acetyl acetone at room temperature is reported to give $PhCOCH_2CSPh$[13]. Thiourea with 2'-hydroxychalcones gives 1,3-thiamine derivatives in alkaline ethanol on refluxing for 3 h while in 10 min in DMSO[14]. Sodium polysulphide with chalcones is reported to form 2,4-dibenzoyl-3,5-diphenylthiolanes[15].

Chalcone dibromides (**2a-e**); α-bromo-β-hydroxychalcone (**2f**) or stilbene dibromide (*meso*) (0.055 mol) was treated with freshly prepared sodium hydrogen sulphide (0.01 mol) in dry methanol (30 ml). The reaction mixture was heated from 10 min to 1 h and then diluted with water. The product was crystallised from rectified spirit. **2a-d** regenerated original chalcone **1a-d**; **2e-f** gave 2-acetoxy of **1a** and stilbene dibromide gave *trans*-stilbene in 80% yield. The crude products on tlc examination gave two spots, one of chalcone and another of sulphur (stilbene and sulphur in case of stilbene dibromide).

Sodium hydrogen sulphide was prepared by saturating sodium ethoxide solution with dry H_2S and precipitating NaSH by adding dry ether. NaSH was filtered at the pump. (NaSH reacts with moisture evolving H_2S very rapidly).

The reductive debromination in the above compounds was an important observation during our study in the synthesis of thioflavonoids.

References

1. T. S. WHEELER and M. P. DODWADNATH, *Proc. Ind. Acad. Sci., India, Sect. A*, 1955, **2**, 438.
2. P. A. SONI and B. J. GHIYA, *Curr. Sci.*, 1972, **41**, 187.
3. T. K. RAJA, *Indian J. Chem., Sect. B*, 1976, **19**, 812.
4. T. C. SHARMA and M. M. BOKADIA, *Indian J. Chem., Sect. B*, 1976, **14**, 65.
5. R. S. RAGHAVAN, M. GOVINDRAJAN and K. G. SANJEEV BABU, *Current Sci.*, 1979, **48**, 1072.
6. D. LANDINI, L. MILESI, M. L. QUADRI and F. ROLLA, *J. Org. Chem.*, 1984, **49**, 152.
7. J. NAKAYAMA, H. MACHIDA and M. HOSHINO, *Tetrahedron Lett.*, 1983, **24**, 3001.
8. Z. GOREN and I. WILLNER, *J. Am. Chem. Soc.*, 1983, **165**, 7764.

† Submitted in July '83 for 71st session of Indian Science Congress, 1983, as poster paper.

9. H. ALPER and M. GOPAL, *J. Org. Chem.*, 1983, **48**, 4390.
10. K. FUKUNAGA and M. YAMAGUCHI, *Synthesis*, 1981, 879.
11. S. W. SATHE and B. J. GHIYA, Unpublished work.
12. V. P. TASHCHI, A. F. BUKASOV, T. I. ORLOVA, YU. G. PUTSYKIN and YU. A. BASKAKOV, *Khim. Geterotsikl. Soedin*, 1982, **6**, 751 (*Chem. Abstr.*, 1982, **97**, 109734).
13. R. T. LALONDE *J. Chem. Soc., Chem. Commun.*, 1982, **7**, 401.
14. V. S. JAMODE, *Indian J. Chem., Sect. B*, 1979, **17**, 629.
15. R. T. LALONDE, B. A. HORENSTEIN, K. SCHWANDLER, R. O. FRITZ and R. A. FLORENCE, *J. Org. Chem.*, 1983, **48**, 4049.

J. Indian Chem. Soc.,
Vol. LXIII, April 1986, pp. 406-407

Relative Acidity of 5-Hydroxyperinaphthindane-1,3-dione

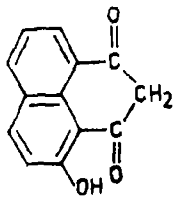
A. K. BHATTAMISHRA*, B. C. MAHANTA†, K. K. MUKHERJEE‡ and M. K. ROUT**

Physical Metallurgy Division, National Metallurgical Laboratory, Jamshedpur-831 007

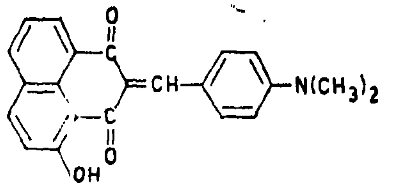
Manuscript received 19 August 1985, accepted 24 December 1985

Synthesis of p-dimethylaminobenzylidene dyes derived from 5-hydroxyperinaphthindane-1,3-dione and various acidic nuclei have been described. Utilising their absorption maxima data and that of dimethinmerocyanines and by applying Brooker's deviation theory relative acidity of 5-hydroxyperinaphthindane-1 3-dione and other acidic nuclei have been established.

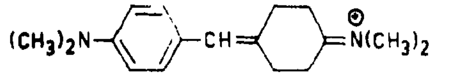
SIMILAR to merocyanines, benzylidine dyes are of great importance in dye chemistry. Just as the merocyanines are regarded as the structural hybrid of symmetrical cyanine and oxonol, the benzylidene derivatives of the cyclic keto[1] methylene compound (perinaphthindane-1,3-dione, 1, in this case) 2 may be regarded as the structural hybrid of Micher's hydrol blue (3) and the corresponding oxonol (4).



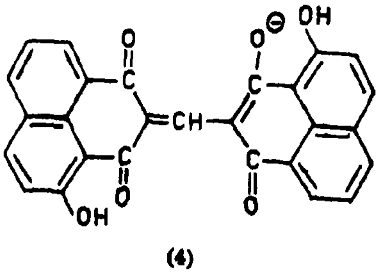
(1)



(2)



(3)



(4)

Experimental

5-Hydroxyperinaphthindane-1,3-dione (**1**) selected for this investigation was prepared according to the method of Black *et al.*[1]. Preparation of 2-(acetanilidomethylene) and 2-(3'-acetanilidoallylidene) intermediate of 5-hydroxyperinaphthindane-1,3-dione, merocyanines and oxonols have been described in our previous paper[2].

2-(p-*Dimethylaminobenzylidene*)-*5-hydroxyperinaphthindane-1,3-dione :* 5-Hydroxyperinaphthindane-1,3-dione(0.4 g) and *p*-dimethylaminobenzaldehyde (0.30 g) were refluxed in acetic anhydride for 30 min. On cooling, the product separated out and it was crystallised from ethanol, yield (70%), m.p. 220° ; λ_{max} 485 nm.

Utilising the λ_{max} data of the above dyes the deviations were calculated according to Brooker and Keyes[3].

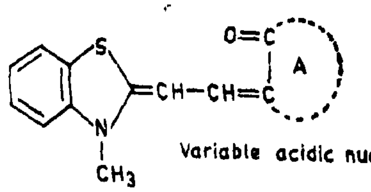
Results and Discussion

Relative acidity from the deviation of dimethin merocyanines : In order to find out the relative acidity of perinaphthindane-1,3-dione, the λ_{max} values of the dimethin merocyanines and deviations derived from a fixed basic nucleus, *i.e.* benzothiazole and variable acidic nuclei are compared. From Table 1, it is evident that the acidity of different nuclei decreases in the order : chroman-2,4-dione > thiachroman-2,4-dione > 1-phenyl-3-methylpyrazolone > indan-1,3-dione > perinaphthinadane-1,3-dione > 3-phenylrhodanine.

Relative acidity from the deviation of benzylidene dyes : The previous conclusion can also be attained by comparing the λ_{max} values of *p*-dimethylaminobenzylidene dyes derived from perinaphthindane-1,3-dione and other acidic nuclei with fixed aminobenzaldehydic nucleus (Table 2). From Table 2 it is evident that acidity decreases in the order : chroman-2,4-dione > thiachroman-2,4-dione > 1-phenyl-3-methylpyrazolone > indan-1,3-dione > perinaphthindane-1,3-dione > 3-phenylrhodanine.

† Khallikot College, Berahmpur.
‡ F. M. College, Balasore.
** Ex-Vice-Chancellor, Utkal University.

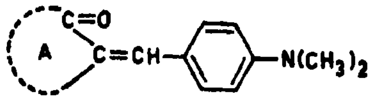
TABLE 1



Variable acidic nucleus 'A'

Nature of nucleus 'A'	λ_{max} (nm) Symmetrical trimethin cyanine of benzothiozole	Symmetrical monomethin oxonol ion of 'A'	Calculated	Observed	Deviation
Perinaphthindane-1,3-dione	565	480	522.5	500	22.5
3-Phenylrhodanine	565	520	542.5	510	32.5
Indan-1,3-dione	565	455	510	494	16.0
1-Phenyl-3-methylpyrazolone	565	443	504	490	14.0
Thiachroman-2,4-dione	565	430	497.5	485	12.5
Chroman-2,4-dione	565	430	497.5	490	7.5

TABLE 2



Variable acidic nucleus 'A'

Nature of nucleus 'A'	λ_{max} (nm) Micher's hydrol blue	Symmetrical methin oxonol ion of 'A'	Calculated	Observed	Deviation
Perinaphthindane-1,3-dione	606	480	543	485	58
3-Phenylrhodanine	606	520	563	480	83
Indan-1,3-dione	606	455	530.5	475	55.5
1-Phenyl-3-methylpyrazolone	606	443	524.5	470	54.5
Thiachromandione	606	430	518	490	28.0
Chroman-2,4-dione	606	430	518	505	13.0

Thus, from the above studies it is also confirmed that either in a series of merocyanines or benzylidene dyes, deviation is maximum for the least acidic nucleus which agrees well with the Brooker's theory of deviation.

References

1. R. BLACK, H. SHAW and T. K. WALKER, *J. Chem. Soc.*, *I*, 1931, 272.
2. A. K. BHATTAMISHRA, B. C. MAHANTA, K. K. MUKHERJEE and M. K. ROUT, *J. Indian Chem. Soc.*, 1973, **50**, 147.
3. L. G. S. BROOKER and G. H. KEYES, *J. Am. Chem. Soc.*, 1951, **73**, 5345.

J. Indian Chem. Soc.,
Vol. LXIII, April 1986, pp. 408-409

Synthesis of 3,4,5-Triphenyloxazine-2-ones

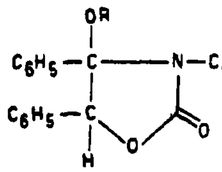
M. B. HOGALE, A. R. SHELAR, V. T. TARAPURE and M. H. JAGDALE*

Department of Chemistry, Shivaji University, Kolhapur-416 004

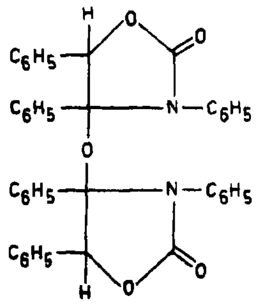
Manuscript received 6 April 1984, accepted 17 February 1986

3,4,5-Triphenyloxazine-2-ones have been prepared starting from benzoin and phenyl isocyanate in the presence of triethylamine. All the compounds were obtained in good yields.

MOST of the reactions of isocyanates involve the formation of widely differing cyclic and acyclic reaction products[1]. The reactions of isocyanates, such as formation of ureas[2], oxazines[3], imidazoles[4], carbodiimides[5] and oligodimerisation[6] are of industrial importance. A wide variety of functionally differing compounds can be synthesised by the condensation of hydroxy aldehydes or ketones and isocyanates[7,8].



(1) R=H
(2) R= -COOH$_3$
(3) R= -NHCOC$_6$H$_5$



Dimer (4)

Experimental

Physical constants yields and analytical values of compounds are reported in Table 1. Melting points were determined using a Thomas Hoover capillary melting point apparatus which was calibrated against known standards. The infrared spectra were recorded on a Baird 455 double beam spectrograph using KBr pellets. The nmr spectra were recorded on a Varian A-60 spectrometer using tetramethylsilane as an internal standard. Tlc was carried out on silica gel with isopropanol as the eluent. The chromatogram was developed by exposing tlc plates to iodine vapours.

Preparation of **1** *:* A solution of benzoin (4.25 g, 1 mol) of anhydrous benzene (10 ml) was added with constant stirring to a solution of phenyl isocyanate (2.60 ml, 1 mol) and triethylamine (0.5 ml) in benzene (10 ml) over a period of 30 min. The reaction was exothermic resulting in the formation of white crystals. After the reaction mixture was cooled to room temperature and allowed to stand overnight, the crude product was obtained which on recrystallisation with benzene gave pure product (**1**). The yield of the product was almost quantitative. Ir spectrum of **1** showed peaks at 3 400 (broad band) (OH) and 1 750 cm^{-1} (C=O). The nmr spectrum showed two singlet at δ 6.15 and 1.8 corresponding to benzylic and hydroxy protons. The presence of hydroxy group in **1** is also confirmed by preparation of its characteristic acetyl derivative (**2**).

Preparation of **3** *:* The compound of the type **3** was obtained by reacting benzoin (2.12 g, 1 mol) and phenyl isocyanate (2.60 ml, 2 mol) in the presence of triethylamine (0.5 ml) in dry benzene The white crystals obtained were recrystallised from ethanol. Ir spectrum of **3** showed peaks at 3 360-3 395 (double peak) (NH) and 1 765 cm^{-1} (C=O). A singlet was observed at δ 6.9 ppm of benzylic proton in the nmr spectrum.

TABLE 1

Compd.	M.p °C	Yield %	Molecular formula	Analysis % : Found/(Calcd.)		
				C	H	N
1	148	55.50	$C_{22}H_{17}NO_3$	76.13 (76.83)	5.15 (5.18)	4.20 (4.28)
2	158	89.50	$C_{24}H_{19}NO_4$	76.55 (76.65)	5.20 (5.27)	3.78 (3.90)
3	160	50.00	$C_{29}H_{22}N_2O_4$	74.40 (74.60)	4.56 (4.88)	6.15 (6.22)
4	180	48.75	$C_{44}H_{34}N_2O_6$	77.45 (77.58)	4.85 (4.92)	4.24 (4.26)

Preparation of **4** *:* The Dimer (**4**) was formed from benzoin (4.12 ml, 2 mol) and phenyl isocyanate (1.3 ml, 1 mol) and triethylamine (0.5 ml). The product purified from benzene showed no peak in ir spectrum corresponding to OH but a strong absorption at 1 770 cm^{-1} (C=O). Nmr spectrum showed a peak at δ 6.2 corresponding to benzylic proton.

Acknowledgement

The authors are grateful to Dr. B. B. Ghatge, National Chemical Laboratory, Pune, for useful suggestions.

References

1. S. Patai, "The Chemistry of Cyanates and other Thio Derivatives", Interscience-Wiley, New York, 1977.
2. H. D. Dakin, *J. Am. Chem. Soc.*, 1910, **44**, 48.
3. R. J. Shozda U. S. Pat., 3 514 470/1970 (*Chem. Abstr.*, 1970, **73**, 25432).
4. G. Odian and L. S. Hiraoka, *J. Polym. Sci., Part A-1*, 1970, **8**, 1309.
5. A. R. Sayigh and H. Ulrich, U. S. Pat 3 492 331/1970 (*Chem. Abstr.*, 1970, **72**, 78652).
6. C. J. Brown, *J. Chem. Soc.*, 1955, 2931.
7. R. F. Bekker, *Recl. Trav. Chim.*, 1964, **83**, 1039.
8. R. E. Strube and F. A. Mackellar, *Recl. Trav. Chim.*, 1964, **83**, 1191.

J. Indian Chem. Soc.,
Vol. LXIII, April 1986, pp. 410-411

Dipolar Cycloaddition of Chloroketene to *o*-Nitrocinnamalanilines

M. R. MANRAO*, ANIL KUMAR and P. S. KALSI

Department of Chemistry, Punjab Agricultural University, Ludhiana-141 004

Manuscript received 20 May 1985, accepted 6 February 1986

Dipolar cycloaddition of chloroketene, prepared *in situ* from monochloroacetyl chloride and triethylamine to *o*-nitrocinnamalanilines yields δ-lactams in excellent yields. The structures of these compounds are supported by elemental analyses and spectral studies. Substitution by electron-withdrawing nitro group in the C-phenyl ring seems to retard the reaction.

CHLOROKETENES[1] add to imines to give β-lactams[2-5]. When the imine function is a part of a conjugated system both 1,2- and 1,4-cycloadducts are possible. However, cinnamalanilines have been reported to undergo 1,4-cycloaddition only to give δ-lactams[4]. In continuation of our work[6-8] on the effect of nitro substituent on the reactions of conjugated Schiff bases, this paper describes the reaction of monochloroketene with *o*-nitrocinnamalanilines.

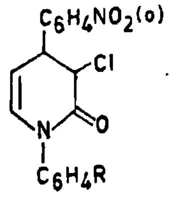
o-Nitrocinnamalanilines (3) were prepared by condensing *o*-nitrocinnamaldehyde with aniline and substituted anilines[9]. The dropwise addition of monochloroacetyl chloride (**1**) to the benzene solution of *o*-nitrocinnamalaniline and triethylamine at room temperature yielded a crystalline product. This product was identified as δ-lactam (**4**) on the basis of elemental analyses and ir studies. The band at 1 690 cm^{-1} and not at ~1 780 cm^{-1} in the infrared spectrum of the adduct was used to identify δ-lactam system. δ-Lactams synthesised from various *o*-nitrocinnamalanilines by the addition monochloroacetyl chloride in the presence of triethylamine are recorded in Table 1.

$$ClCH_2COCl \xrightarrow{(C_2H_5)_3N} ClCH=C=O$$

(1) (2)

$$(2) + o\text{-}NO_2C_6H_4CH=CH-CH=N-C_6H_4R \longrightarrow$$

(3)



(4)

The presence of electron-withdrawing nitro group in the *C*-phenyl nucleus seems to lower the reactivity of these Schiff bases (3) since out of a total nine such Schiff bases adducts were successfully obtained only in five cases, and in these cases too on the whole the yields of the adducts were comparatively lower than the corresponding adducts obtained from cinnamalanilines. On the other hand, presence of electron-withdrawing substituents in the *N*-phenyl ring of the Schiff bases seems to increase their reactivity as indicated by comparatively higher yields in case of *o*-nitrocinnamal-*p*-chloroaniline and *o*-nitrocinnamal-*p*-bromoaniline.

It was also observed that if the reaction was carried out in the absence of triethylamine 1 : 1*N*-acylated adducts were obtained in quantitative yields which changed into δ-lactam on refluxing in benzene solution. The *N*-acylated adducts also yielded δ-lactams on addition of triethylamine, but the yields were poor (20-30%) and a considerable amount of tars was obtained. Thus, it is postulated that in the presence of triethylamine the elimination process was probably favoured over the acylation of the Schiff base by acid chloride.

TABLE 1—CHARACTERISTICS OF δ-LACTAMS

Compd. no.	Substituent in *N*-phenylnucleus	M.p.* °C	Yield %	Molecular formula**
4a	H	165	60	$C_{17}H_{13}NO_3Cl$
4b	*p*-OCH$_3$	195	60	$C_{18}H_{15}NO_4Cl$
4c	*p*-OC$_2$H$_5$	145	58	$C_{19}H_{17}NO_4Cl$
4d	*p*-Cl	167	75	$C_{17}H_{12}NO_3Cl_2$
4e	*p*-Br	180	70	$C_{17}H_{12}NO_3ClBr$

* All the melting points are uncorrected.
** All the compounds gave satisfactory elemental analyses

Experimental

The following general procedure was followed for the synthesis of δ-lactams. *o*-Nitrocinnamalaniline (0.01 mol) was dissolved in benzene (25 ml) and to it added triethylamine (0.02 mol). To the

above mixture was added monochloroacetyl chloride (0.02 mol) taken in benzene (25 ml) slowly and with constant stirring at room temperature. After the addition of chloroacetyl chloride was complete, the mixture was allowed to stand at room temperature for 3-4 h. Removal of solvent under vacuum yielded a crude product which was recrystallised from ethanol to get pure crystals of δ-lactam (60%), m.p. 165°.

References

1. J. C. Sheehan and J. J. Ryan, *J. Am. Chem. Soc.*, 1951, **73**, 1204.
2. E. Ziegler, Th. Wimmer and H. Mittelbach, *Monatsh. Chem.*, 1968, **99**, 2128.
3. J. A. Deyrup and S. C. Clough, *J. Am. Chem. Soc.*, 1969, **91**, 4590.
4. F. Duran and L. Ghosez, *Tetrahedron Lett.*, 1970, 245.
5. A. K. Bose, G. Spiegelman and M. S. Manhas, *Tetrahedron Lett.*, 1971, 3167.
6. M. Rai, S. Kumar, K. Krishan and A. Singh, *Chem. Ind.* (*London*), 1979, 211.
7. K. Krishan, M. Rai, J. Singh and A. Singh, *Indian J. Chem., Sect. B*, 1977, **15**, 1041.
8. M. Rai and A. Singh, *Indian J. Chem.*, *Sect. B*, 1978, **16**, 155.
9. N. Singh and K. Krishan, *J. Indian Chem. Soc.*, 1973, **50**, 277 ; *Indian J. Chem.*, 1973, **11**, 889.

J. Indian Chem. Soc.,
Vol. LXIII, April 1986, pp. 412-413

Synthesis of Thiatriazole Derivative from 6-Methyl-1,4-benzoxazin-3(2*H*)-one

M. B. HOGALE*, N. P. DHORE and B. R. KHOT

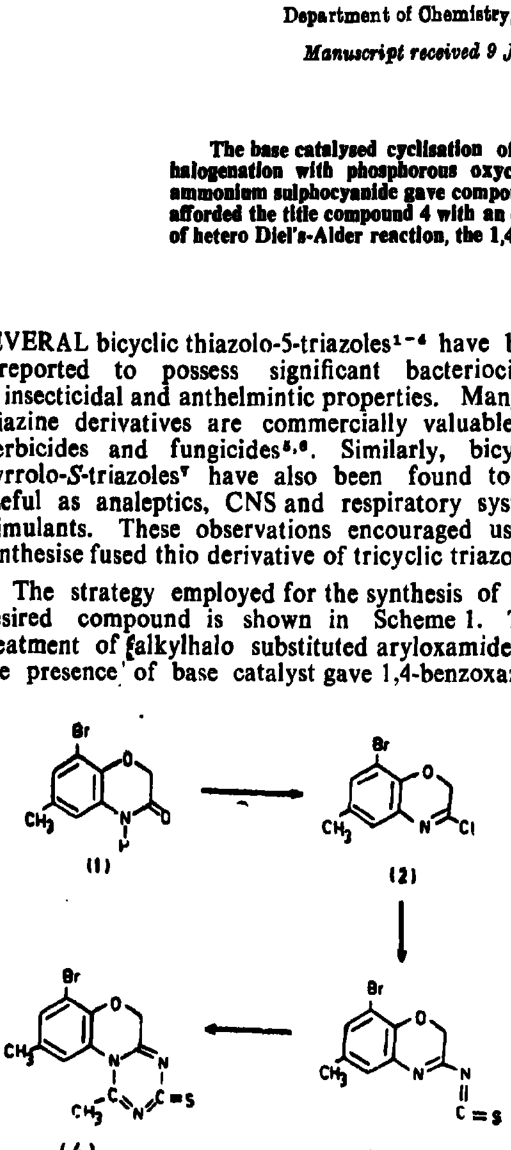
Department of Chemistry, Shivaji University, Kolhapur-416 004

Manuscript received 9 July 1985, accepted 17 February 1986

The base catalysed cyclisation of 2,6-dichloro-4-methylaryloxamide followed by halogenation with phosphorous oxychloride gave compound 2. Reaction of 2, with ammonium sulphocyanide gave compound 3, which when condensed with methyl cyanide afforded the title compound 4 with an excellent yield. This is an interesting example of hetero Diel's-Alder reaction, the 1,4-cycloaddition of isothiocyanate to acetonitrile.

SEVERAL bicyclic thiazolo-5-triazoles[1-4] have been reported to possess significant bacteriocidal, insecticidal and anthelmintic properties. Many *S*-triazine derivatives are commercially valuable as herbicides and fungicides[5,6]. Similarly, bicyclic pyrrolo-*S*-triazoles[7] have also been found to be useful as analeptics, CNS and respiratory system stimulants. These observations encouraged us to synthesise fused thio derivative of tricyclic triazole.

The strategy employed for the synthesis of the desired compound is shown in Scheme 1. The treatment of alkylhalo substituted aryloxamide in the presence of base catalyst gave 1,4-benzoxazin-


(1) (2) (4) (3)

Scheme 1

3(2*H*)-one (1) followed by halogenation with phosphorous oxychloride to give pale yellow chloro compound (2) in good yields (70%). The desired halogenation in the above compounds was evident from the absence of characteristic ir absorption bands for NH (3 200-3 300 cm^{-1}) and lactam ketone (1 695 cm^{-1}).

Compound 2, in refluxing with ammonium sulphocyanide in acetone yielded thiocyanate derivative (3), which when heated with methyl cyanide afforded 4. The uv spectrum of the triazole? (4), has the characteristic absorption band at λ_{max} 320 nm (C=S). This structure was also supported by the absence of ir band around 2 050 (N=C=S) and the presence of 1 620 (C=N) and 1 060 cm^{-1} (C=S).

Experimental

Melting points were determined in capillaries and are uncorrected. The ir spectra were recorded in nujol on a Perkin-Elmer 297 spectrophotometer and pmr on a Varian A-90 instrument using tetramethyl silane as an internal reference. All the compounds were analysed satisfactorily for C, H and N. The purity of the products, besides the elemental analysis was checked by tlc.

6-Methyl-8-bromo-1,4-benzoxazin-3(2H)-one (**1**) : 4-Methyl-2,6-dibromophenoxyacetamide (9.0 g, 0.04 mol) and triethylamine (3.0 g, 0.03 mol) in dry methanol (40 ml) was refluxed on an oil-bath for ~6 h at 110° and the solvent was then removed under reduced pressure. The residue was extracted with ether and concentrated, the solid obtained was recrystallised from ethanol to yield **2** (6.0 g, 80%), m.p. 108° (Found : C, 44.60 ; H, 3.33 ; N, 5.75. $C_9H_8NO_2Br$ requires : C, 44.63 ; H, 3.30 ; N, 5.78%) ; λ_{max} (EtOH) 256 nm ; ν_{max} (nujol) 1 695 (C=O) and 3 200 cm^{-1} (NH) ; δ (CD_3-COCD_3) 4.6 (2H, s, OCH_2), 7.25 (1H, d, *J* 3Hz, C_7-H), 7.4 (1H, d, *J* 3Hz, C_5-H) and 8.8 (1H, s, br, NH).

6-Methyl-8-bromo-1,4-benzoxazin-3-yl-chloride(**2**) : **1** (5.2 g, 0.02 mol) in phosphorous oxychloride (50 ml) and PCl_5 (1.5 g) was refluxed gently on a water-bath for ~ 3 h and $POCl_3$ was then removed under reduced pressure. The residue was triturated with ice-water (500 g). The pale

yellow solid that separated was recrystallised from ethanol (4.0 g, 80%), m.p. 130° (Found : C, 41.46 ; H, 2.68 ; N, 5.37, $C_9H_7NOClBr$ requires : C, 41.50 ; H, 2.70 ; N, 5.39%) ; ν_{max} (nujol) 1 620 (C=N), 1 600 (C=C), 780 (C–Cl) ; δ ($CDCl_3$) 2.15 (3H, s, C_6-CH_3), 4.58 (2H, s, OCH_2), 7.20 (1H, d, *J* 3Hz, C_7-H) and 7.35 (1H, d, *J* 3Hz, C_5-H).

6-Methyl-8-bromo-1,4-benzoxazin-3-yl-isothiocyanate (**3**) : A mixture of **2** (2.60 g, 0.01 mol) and NH_4SCN (0.76 g, 0.01 mol) was refluxed in acetone (30 ml) for 1 h and acetone was then removed. The residue was washed with water and recrystallised from ethanol to give **3** (2.5 g, 84%), m.p. 182° (Found: C, 59.08; H, 3.42; N, 13.70. $C_{10}H_7N_2OSBr$ requires : C, 59.10 ; H, 3.45 ; N, 13.80%) ; ν_{max} (KBr) 2 050 (N=C=S) and 1 600 cm^{-1} (CH=C) ; δ (DMSO-d_6) 2.15 (3H, s, $ArCH_3$), 4.7 (2H, s, OCH_2), 7.2 (1H, d, C_7-H) and 7.35 (1H, d, C_5-H).

*6-Methyl-8-bromo-4*H*-[1',3',5']triazolo-4'-methyl-2'-thiocarbonyl[3,4-c][1,4]benzoxazine* (**4**) : **3** (1.4 g, 0.005 mol) was added to acetonitrile (0.21 g, 0.005 mol) in absolute ethanol (50 ml) and the mixture refluxed for 5 h. The solvent was then removed and the residue washed with ice-water to precipitate the brown product which was filtered and washed with NH_4OH followed by water, and recrystallised from ethanol to furnish **4** (1.0 g, 71.5%), m.p. 220° (Found : C, 46.65 ; H, 3.22 ; N, 13.45. $C_{12}H_{10}N_3OSBr$ requires : C, 46.75 ; H, 3.24 ; N, 13.6%) ; ν_{max} (KBr) 1 620 (C=N) and 1 610 cm^{-1} (C=S) ; δ (DMSO-d_6) 1.8 (3H, s, CH_3), 2.2 (3H, s, $ArCH_3$), 4.7 (2H, s, OCH_2), 7.25 (1H, d, C_7-H) and 7.40 (1H, d, C_5-H).

References

1. S. KANO, O. NAMURA and T. TANIGUCHI, Jap. Pat. 789/1978 (*Chem. Abstr.*, 1974, **80**, 871118).
2. D. R. SHRIDHAR, M. JUGIBHUKTA, P. P. JOSHI and P. GOPAL-REDDY, *Indian J. Chem., Sect. B*, 1981, **20**, 182.
3. D. R. SHRIDHAR, *et al*, *Indian J. Chem., Sect. B*, 1981, **20**, 474.
4. H. SINGH, L. D. S. YADAV, K. S. SHARMA and D. K. SINGH, *Indian J. Chem., Sect. B*, 1983, **22**, 1177.
5. P. C. KEARNEY and D. D. KAUFMAN, "Herbicides Chemistry, Degradation and Mode of Action", Marcel Dekker, New York, 1975, Vol. 1, p. 180.
6. R. J. LUKEN, "Chemistry of Fungicidal Action", Springer-Verlag, Berlin, 1971, p. 102.
7. A. E. WICK, P. A. BARTLETT and D. DOLPHIN, *Helv. Chim. Acta*, 1971, **54**, 518.

J. Indian Chem. Soc.,
Vol. LXIII, April 1986, pp. 414-416

Studies on s-Triazines. Part-II. Preparation of 2,4-Diarylamino-6-carbethoxymethylamino and 4-(2′,4′-Diarylamino-s-triazin-6′-yl)aminoantipyrine

LINA MEHTA and HANSA PAREKH*

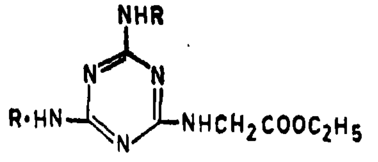
Department of Chemistry, Saurashtra University, Rajkot-360 005

Manuscript received 16 August 1985, accepted 24 December 1985

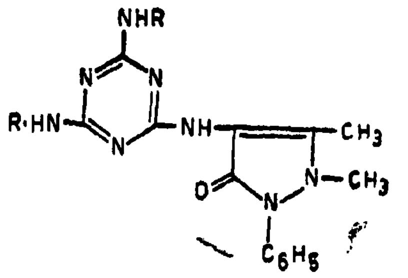
Some new 2,4,6-trisubstituted-s-triazines having carbethoxymethylamino and 4-aminoantipyrine moeity have been prepared. The constitution of the products is supported by ir and nmr spectral study.

SEVERAL workers have investigated *s*-triazine derivatives as potential therapeutic agents for diseases due to bacteria and protozoa[1], African sleeping sickness[2,3], malaria[4,5], cancer[6,7] and possess antiviral property[8]. *s*-Triazine derivatives are also used as fungicides[9,10] and weedicides[11].

In continuation of our work on *s*-triazine nucleus[12] and in order to study their therapeutic utility, we have synthesised substituted *s*-triazine derivatives of type 1 and 2 (where R=aryl) by condensing glycine ester hydrochloride and 4-aminoantipyrine with 2,4-diarylamino-6-chloro-*s*-triazine as they are having therapeutic importance.



(1)



(2)

2,4-Diarylamino-6-chloro-*s*-triazine[5,9,12,14] have been prepared by condensing cyanuric chloride (0.01 mol) with different bases (0.02 mol) in acetone at 35-40° for 1.5 h. The third chlorine of cyanuric chloride was condensed with glycine ester hydrochloride or 4-aminoantipyrine in dioxane by heating at 85-90° for 1.5 h. The structure of the compounds synthesised were supported by ir and nmr spectral study. The ir spectra were taken on a Perkin Elmer spectrophotometer using KBr pellets in the range of 4 000-600 cm^{-1}. It gave following characteristic bands: 820 (C_3N_3)[15], 1 255 (C–O–C str ester), 1 238 and 1 050 (C–O–C str Ar–O–CH_3), 3 400 and 3 260 (N–H str), 1 660 (C=O), 780 and 715 cm^{-1} (C–H bending monosubstituted benzene). The nmr spectra were taken on a EM-360 60 MHz spectrometer using $CDCl_3$ and DMSO as solvent. It gave the following T value :

2.3-3.1 (m, Ar H), 6.8 (s, N–CH_3) and 7.8 (s, C–CH_3).

Experimental

*2,4-Diphenylamino-6-carbethoxymethylamino-*s*-triazine :* 2,4-Diphenylamino-6-chloro-*s*-triazine (0.01 mol) was dissolved in dioxane (30 ml) and to it was added a solution of glycine ester hydrochloride (0.01 mol) in dioxane. The mixture was neutralised by adding sodium hydroxide solution. The product was isolated and crystallised from ethanol, (90%), m.p. 202° (Found : C, 62.57 ; H, 5.38 ; O, 8.69 ; N, 22.7. $C_{19}H_{20}O_2N_6$ calcd. for : C, 62.64 ; H, 5.49 ; O, 8.79 ; N, 23.08%).

Similarly all other 2,4-diarylamino-6-chloro-*s*-triazine were condensed. The physical constants are recorded in Table 1.

4(2′,4′-Diphenylamino-s-triazine-6′-yl)aminoantipyrine : 2,4-Diphenylamino-6-chloro-*s*-triazine (0.01 mol) was dissolved in dioxane (30 ml) and to it was added a solution of 4-aminoantipyrine (0.01 mol) in dioxane. The mixture was refluxed for 1.5 h. The acid evolved was neutralised by adding sodium hydroxide solution. The product was isolated and crystallised from ethanol, (90%), m.p. 263° (Found : C, 66.25 ; H, 5.27 ; O, 3.48 ; N, 24.57. $C_{26}H_{24}ON_8$ calcd. for : C, 66.37 ; H, 5.31 ; O, 3.53 ; N, 24.77%).

TABLE 1—PHYSICAL CONSTANTS OF 2,4-DIARYLAMINO-6-CARBETHOXYMETHYLAMINO-*s*-TRIAZINE

Sl. no.	R	Molecular formula	Yield %	M.p. °C	Nitrogen % Found/(Calcd.)
1.	Phenyl	$C_{19}H_{20}O_2N_6$	69	180	22.70 (23.08)
2.	*o*-Tolyl	$C_{21}H_{24}O_2N_6$	72	145	21.22 (21.43)
3.	*m*-Tolyl	$C_{21}H_{24}O_2N_6$	67	118	21.30 (21.43)
4.	*p*-Tolyl	$C_{21}H_{24}O_2N_6$	75	174d	21.28 (21.43)
5.	*o*-Anisyl	$C_{21}H_{24}O_4N_6$	70	150	19.78 (19.81)
6.	*p*-Anisyl	$C_{21}H_{24}O_4N_6$	66	210	19.69 (19.81)
7.	*p*-Carbethoxyphenyl	$C_{25}H_{28}O_6N_6$	60	188d	16.41 (16.53)
8.	*p*-Bromophenyl	$C_{19}H_{18}O_2N_6Br_2$	59	196d	15.95 (16.09)
9.	α-Naphthyl	$C_{27}H_{24}O_2N_6$	60	191	17.90 (18.10)
10.	*o*-Chlorophenyl	$C_{19}H_{18}O_2N_6Cl$	62	188	19.32 (19.44)
11.	*m*-Chlorophenyl	$C_{19}H_{18}O_2N_6Cl$	60	189	19.25 (19.44)
12.	*p*-Chlorophenyl	$C_{19}H_{18}O_2N_6Cl$	65	218	19.35 (19.44)
13.	*o*-Nitrophenyl	$C_{19}H_{18}O_6N_8$	72	190d	24.59 (24.67)
14.	*p*-Nitrophenyl	$C_{19}H_{18}O_6N_8$	61	>360	24.62 (24.67)
15.	*p*-Acetylphenyl	$C_{23}H_{24}O_4N_6$	60	212	18.69 (18.75)

TABLE 2—PHYSICAL CONSTANTS OF 4-(2′,4′-DIARYLAMINO-*s*-TRIAZIN-6′-YL)AMINOANTIPYRINE

Sl. no.	R	Molecular formula	Yield %	M.p. °C	Nitrogen % Found/(Calcd.)
1.	Phenyl	$C_{26}H_{24}ON_8$	90	263	24.57 (24.77)
2.	*o*-Tolyl	$C_{28}H_{28}ON_8$	87	162	22.45 (22.76)
3.	*m*-Tolyl	$C_{28}H_{28}ON_8$	80	190	22.58 (22.76)
4.	*p*-Tolyl	$C_{28}H_{28}ON_8$	91	200	22.65 (22.76)
5.	*o*-Anisyl	$C_{28}H_{28}O_3N_8$	85	138	21.15 (21.37)
6.	*m*-Anisyl	$C_{28}H_{28}O_3N_8$	89	218	21.21 (21.37)
7.	*p*-Anisyl	$C_{28}H_{28}O_3N_8$	79	198	21.25 (21.37)
8.	*p*-Carbethoxyphenyl	$C_{32}H_{32}O_5N_8$	82	242	18.35 (18.42)
9.	*p*-Bromophenyl	$C_{26}H_{22}ON_8Br_2$	71	186	17.21 (17.38)
10.	α-Naphthyl	$C_{34}H_{28}ON_8$	76	207	19.76 (19.85)
11.	*o*-Chlorophenyl	$C_{26}H_{22}ON_8Cl_2$	84	147	20.86 (21.05)
12.	*m*-Chlorophenyl	$C_{26}H_{22}ON_8Cl_2$	81	244	20.78 (21.05)
13.	*p*-Chlorophenyl	$C_{26}H_{22}ON_8Cl_2$	86	225	20.92 (21.05)
14.	*o*-Nitrophenyl	$C_{26}H_{22}O_5N_{10}$	83	>360	25.15 (25.27)
15.	*m*-Nitrophenyl	$C_{26}H_{22}O_5N_{10}$	87	231	24.91 (25.27)
16.	*p*-Nitrophenyl	$C_{26}H_{22}O_5N_{10}$	78	216d	24.95 (25.27)
17.	*p*-Acetylphenyl	$C_{30}H_{28}O_3N_8$	70	215d	20.32 (20.43)

Similarly all other 2,4-diarylamino-6-chloro-*s*-triazines were condensed. The physical constants are recorded in Table 2.

Acknowledgement

The authors are thankful to U.G.C., New Delhi, for awarding Junior Research Fellowship to one of them (L.M.) and to Saurashtra University for facilities.

References

1. H. JENSCH, U. S. Pat. 2 092 352 (*Chem. Abstr.*, 1937, 31, 8128).
2. E. A. H. FRIEDHIEM, *J. Am. Chem. Soc.*, 1944, 65, 1775.
3. C. K. BANKS, O. M. GRUHZIT, E. W. TILLILON and J. CONTROULIS, *J. Am. Chem. Soc.*, 1944, 66, 1771.
4. W. W. CUTHBERBERTSON and J. S. MOFFALT, *J. Chem. Soc.*, 1948, 561.
5. F. H. S. CURD, J. K. LANDQUIST and F. L. ROSE, *J. Chem. Soc.*, 1947, 154.
6. E. CIORANCESCH, *Rev. Chem.* (*Bucharest*), 1954, 5, 425.
7. J. H. BURCHENAL and J. F. JOHNSTON, *Proc. Soc. Exptl. Biol. Med.*, 1950, 74, 708.
8. Ciba Ltd., Brit. Pat. 754 071/1956 (*Chem. Abstr.*, 1957, 51, 8814).
9. C. N. WOLF, U. S. Pat. 2 720 480/1955 (*Chem. Abstr.*, 1956, 50, 13101).
10. C. N. WOLF, P. H. SCHULDT and M. M. BALDWIN, *Science*, 1935, 61, 121.
11. J. R. GEIGYA and H. BASEL, *Swits. Eeptl* (*Ger.*), 1956, 121, 146.
12. H. PAREKH, A. R. PARIKH and K. A. THAKER, *J. Inst. Chem., Calcutta*, 1975, 47, 63.
13. N. V. KOZLOVA, D. F. KUTEPOV, D. N. KHOKHLOV and A. I. KRYMOVA, *Zh. Obshch. Khim.*, 1968, 30, 3303.
14. M. GOI, *Yuki Gosei Kagaku Kyokai Sh*, 1960, 18, 327.
15. W. M. PADGETT II and W. F. HAMMER, *J. Am. Chem. Soc.*, 1958, 80, 803; A. R. PARIKH and K. J. MEHTA, *J. Indian Chem. Soc.*, 1979, 56, 383.

J. Indian Chem. Soc.,
Vol. LXIII, April 1986, pp. 417-419

Carbon-13 Nmr Signals of some Simple Coumarins†

AMARENDRA PATRA

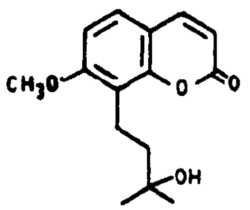
Department of Chemistry, University College of Science, University of Calcutta, Calcutta-700 009

Manuscript received 23 September 1985, accepted 17 February 1986

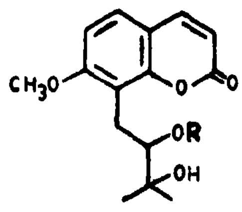
Carbon-13 nmr spectra of some simple coumarins related to osthol (1) are reported.

OSTHOL (**1**) is one of the common coumarins occasionally found from natural sources. In recent years osthol and its epoxide (**5**) have been employed for some interesting transformation studies[1-8]. This communication reports the carbon-13 nmr spectral data for osthol (**1**) and some of its derivatives (**2**-**6** and **10**) along with those of the related compounds phebalosin (**7**) and ulopterol (**8**). The spectrum of umbelliferone methyl ether[9] (**9**) (≡7-methoxycoumarin) was used as a model. Incidentally **6** as well as the *laevo* antipodes of **4** and **5** have also been reported from natural sources[10] and designated citrusal, meranzin hydrate and meranzin (≡auraptene), respectively. *Dextro* form of meranzine hydrate acetate (**10**) has also been found from plants[10].

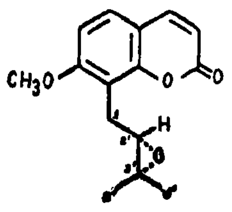
The coumarin carbons in osthol (**1**) and its derivatives **2** and **3** resonate more or less in similar positions. A comparison of these resonance positions (Table 1) with the carbon-13 resonances of umbelliferone methyl ether (**9**) indicates that the alkyl side chain at C-8 in **1**-**3** causes strong deshielding at C-8 (~16.9-18.8 ppm) along with marginal shielding of both C-7 and C-8a (~1.9-2.3 and 2.6-3.0 ppm, respectively probably by γ-effects with C-2′) as well as of C-5 (by ~2.2-2.4 ppm). The methyl of the methoxy group in **1**-**3** is pushed towards C-6 causing the shielding (γ-effect) of the latter ~5.4-5.5 ppm relative to similar carbon in **9**. Phebalosin (**7**) also exhibits coumarin carbon resonances similar to those of **4**-**6**.



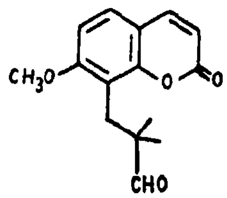
(3)



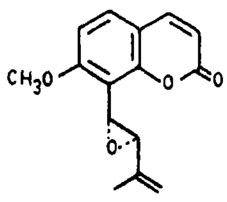
(4) R=H
(10) R=COCH$_3$



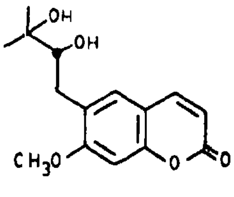
(5)



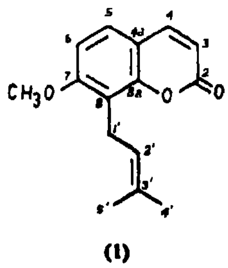
(6)



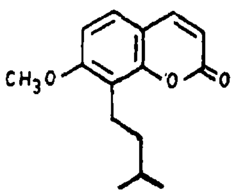
(7)



(8)



(1)



(2)

A differentiation between the resonance positions of C-4a and C-8 in **1**-**3** was made in the following way. The non-protonated sp^2 carbon signal at δ 117.4 in **1**, undergoing minor shifts in the spectra of **2** and **3**, moves upfield by about 3.5 ppm in the spectra of **4**, **5** and **10**. This is due to the shielding γ-effect of the oxygen functions at C-2′ in **4**, **5** and **10** exhibited on C-8. This study indicates that the

† Part of the final P.R.S. Report (1983) submitted to the University of Calcutta

TABLE 1—CARBON-13 NMR SIGNALS (δ) OF THE SIMPLE COUMARINS (1—10)

Carbon	1	2	3	4	5	6	7	8	9	10
C-2	160.9	161.3	161.3	160.7[a]	160.7[a]	160.7[a]	161.6	161.2	160.5	160.6[a]
C-3	112.4	112.8	112.6	112.7	112.7	112.9	113.0	112.5	112.1	112.2
C-4	143.5	143.7	143.7	143.7	143.5	143.6	143.2	143.4	142.9	143.6
C-4a	112.6	112.8	112.7	112.6	112.6	113.9	112.5	111.7	112.2	113.2
C-5	126.0	125.9	126.1	126.8	127.0	127.3	128 8	129.4	128.8	126.8
C-6	107.1	107.1	107.2	107.2	107.2	107.2	107.4	125.2	112.6	106.8
C-7	159.9	160.3	160.1	160.5[a]	160.5[a]	160.3[a]	160.0	160.6	162.2	160.2[a]
C-8	117.4	119.8	118.6	118.9	118.9	114.7	112.2	98.4	100.5	114.1
C-8a	152.4	152.8	152.7	153.1	153.1	[b]	153.6	154.4	155.4	152.8
C-1′	21.6	20.5	17.5	25.8	22.2	30.0	51.5	32.8	—	22.8
C-2′	120.9	38.	042.3	78.0	62.7	47.2	60.8	77.2	—	78.5
C-3′	132.1	28.	170.7	72.7	59.0	204.8	141.1	72.7	—	71.6
C-4′	25.4	22.4	28.8	25.3	23.8	21.3	113.1	26.0	—	25.6
C-5′	17.5	22.4	28.8	23.9	18.8	21.3	17.1	23.3	—	25.0
OCH_3	55.7	55.9	55.9	55.9	55.9	55.6	56.1	55.7	—	55.6
$OCOCH_3$	—	—	—	—	—	—	—	—	—	169.9
$OCOCH_3$	—	—	—	—	—	—	—	—	—	20.1

[a] Assignments are interchangeable. [b] C-8a resonance was ill-resolved from noise.

C-4a and C-8 resonance assignments of osthol (**1**), made earlier by Wenkert *et al.*[11], should be reversed.

The resonance assignments of the alkyl side chain carbons in **1-8** and **10** (Table 1), were made from the change in their resonance positions in the spectra of these compounds. The methylene carbon signal at δ 21.6 present in the spectrum of **1** is obviously related to C-1′. The olefinic methine carbon signal at δ 120.9 and non-protonated sp^2 carbon signal at δ 132.1 in **1** are missing in the spectrum of **2** indicating their association with C-2′ and C-3′, respectively in **1**. The methyl groups resonate at δ 17.5 and 25.4. The former signal was related to C-5′ since it suffers *cis* interaction with the methylene group and is thus expected[12] to experience some shielding effect.

The methine (C-3′) and methyl carbon (C-4′ and C-5′) signals in **2** are readily identified from the splitting pattern of the signals in the SFORD spectrum. The methylene carbons (C-1′ and C-2′) resonate at δ 20.5 and 38.0. C-2′ in **2** should resonate at lower field than C-1′ since the former experiences more deshielding α- and β-effects[12]. The assignment receives support from the following observation. The attachment of a hydroxyl function at C-3′ as in **3** causes downfield shift of the signal at δ 38.0 in **2** to δ 42.3 in **3** and upfield shift of the resonance at δ 20.5 in **2** to δ 17.5 in **3**. Since in **3**, C-1′ should experience shielding γ-effect of OH function whereas C-2′ should undergo downfield shift for the presence of OH on adjacent carbon (by β-effect) C-1′ and C-2′ in **3** are related to the signals at δ 17.5 and 42.3, respectively. Additional support to the above assignments is obtained from inspections of the spectra of **4**, **5** and **10**. The methylene signals present at δ 25.8, 22.2 and 22.8 in **4**, **5** and **10**, respectively, are undoubtedly associated with C-1′ in these compounds. The relatively low field positions of these signals compared to C-1′ resonance in **3** (at δ 17.5) are in conformity with that C-1′ in **4** as well as in **5** and **10** experience additional deshielding effect of the oxygen function at C-2′. In **5**, the methyl (C-5′) eclipsed (or so) with methylene (C-1′) should resonate at higher field. The resonances for C-1′ to C-5′ in **6** are assignable from the splitting pattern in the SFORD spectrum.

The side chain carbon resonance assignments of phebalosin (**7**) follow from comparison with similar carbon resonances in **2** and **5**. Compound **4** as well as (+)-ulopterol[13] (**8**) have the same alkyl side chain which exerts more or less similar deshielding effect (~12.6-13.4 ppm) on C-8 or C-6 as appropriate. In **8**, methyl of the methoxy group is likely to be pushed towards C-8. The magnitude of shielding (~2.1 ppm) of C-8 in **8** relative to **9** was, however, somewhat less than that observed for C-6 in **1-7**.

The hydroxyl at C-3′ in **3** causes (relative to **2**) strong deshielding of C-3′ by ~42.6 ppm, significant deshielding of C-2′ (~4.3 ppm) as well as of C-4′ and C-5′ (~6.4 ppm). It exerts ~3.0 ppm shielding effect on C-1′. The hydroxyl function at C-2′ in **4** deshields C-2′ (35.7 ppm), C-1′ (8.3 ppm) as well as C-3′ (2.0 ppm) and shields C-4′ and C-5′ by about 3.5 and 4.9 ppm, respectively, when compared with the respective carbon resonances in **3**.

Experimental

The carbon-13 nmr spectra were recorded on Varian Associates CFT-20 NMR spectrometer operating at 20 MHz in the FT mode. The compounds were submitted to proton-noise decoupling and single frequency off-resonance decoupling to establish carbon shifts and degree of protonation. The samples were run in 5 mm (o.d.) tubes using $CDCl_3$ as solvent as well as internal lock. The spectra were taken with sweep width 4000 Hz (4500 Hz for **6**), a pulse of approximately 45° flip angle and about 3 s delay between pulses All solutions were about 5-15% in concentration. The solvent signal was used as internal standard. The

chemical shifts reported are in δ (ppm) downfield from TMS ($\delta_{TMS} = \delta_{CDCl_3} + 76.9$ ppm).

Acknowledgement

The author expresses his sincere thanks to his colleague Dr. (Mrs.) J. Banerji, Chemistry Department, University College of Science, Calcutta, for providing the coumarin samples used and also to the U.G.C., New Delhi, for financial assistance.

References

1. B. R. BARIK, A. K. DEY, P. C. DAS, A. B. KUNDU and A. CHATTERJEE, *Indian J. Chem., Sect. B*, 1984, **23**, 223.
2. S. PRAKASH, M. A. KHAN, H. KHAN and A. ZAMAN, *Phytochemistry*, 1983, **22**, 1836.
3. J. BANERJI, N. BHADURI, R. N. REJ, J. N. SHOOLERY, S. MUKHERJEE and S. BHATTACHARYYA, *Indian J. Chem., Sect. B*, 1980, **19**, 841.
4. J. BANERJI, R. N. REJ, A. CHATTERJEE and A. BANERJI, *Indian J. Chem., Sect. B*, 1979, **17**, 118.
5. A. CHATTERJEE, R. N. REJ, A. BANERJI and J. BANERJI, *Chem. Ind. (London)*, 1976, 410.
6. J. BANERJI and R. N. REJ, *Chem. Ind. (London)*, 1974, 529.
7. J. BANERJI, S. C. BASA and A. CHATTERJEE, *J. Chem. Soc. (C)*, 1971, 3992.
8. S. C. BASA, J. CHATTERJEE and A. CHATTERJEE, *Tetrahedron Lett.*, 1971, 1977.
9. R. D. LAPPER, *Tetrahedron Lett.*, 1974, 4293; H. DUDDECK and M. KAISER, *Org. Magn. Reson.*, 1982, **20**, 55.
10. R. D. H. MURRAY, J. MÉNDEZ and S. A. BROWN, "The Natural Coumarins", John Wiley, New York, 1982.
11. E. WENKERT, B. L. BUCKWALTER, I. R. BURFITT, M. J. GAŠIC, H. E. GOTTLIEB, E. W. HAGAMAN, F. M. SCHELL and P. M. WOVKULICH in Topics in Carbon-13 NMR Spectroscopy, ed. G. C. LEVY, John Wiley, New York, 1976, Vol. 2, p. 81.
12. J. B. STOTHERS, "Carbon-13 NMR Spectroscopy", Academic Press, New York, 1972; G. C. LEVY and G. L. NELSON, "Carbon-13 Nuclear Magnetic Spectroscopy for Organic Chemists", Wiley-Interscience, New York, 1972.
13. B. TALAPATRA, A. BASAK and S. K. TALAPATRA, *Indian J. Chem., Sect. B.*, 1983, **22**, 465.

J. Indian Chem. Soc.,
Vol. LXIII, April 1986, pp. 420-424

Synthesis of some 2,4-Diamino-6-(substituted)-amino-5-arylazopyrimidines and their Effect on the Growth of *S. faecalis*

D. SEN*, SMRITIREKHA BHOWMIK and PURNENDU SENGUPTA†

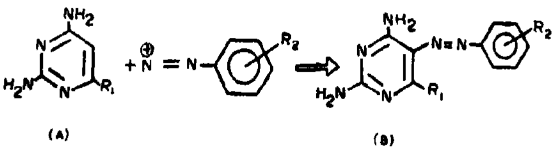
Department of Chemical Technology, University Colleges of Science and Technology, University of Calcutta Calcutta-700 009

Manuscript received 26 June 1982, revised 7 May 1985, accepted 6 February 1986

A number of 5-arylazopyrimidines have been prepared by coupling 2,4-diamino-6-(substituted)-aminopyrimidines with diazotised arylamines and their effect on the growth of *Streptococcus faecalis* has been reported. Investigations show that the above compounds inhibit the growth of *S. faecalis* and act as folic acid antagonists. The growth inhibition has also been compared with that produced by 5-unsubstituted compounds and some well known antibiotics.

IN course of our previous work, we synthesised various kinds of purine and pyrimidine derivatives[1-6] with the hope of getting compounds having antagonistic activity on nucleic acid metabolism. Many of the compounds synthesised by us were found to inhibit the growth of *S. faecalis* and other organisms[7-10].

It was observed that the presence of amino group at 2- and 4-positions of the pyrimidine ring was probably responsible for antimicrobial activity. Further, a number of 5-arylazopyrimidines have been found to possess interesting antifolic, antimicrobial, antimalarial and anticancer properties[11-17]. Pyrimidines having an amino and/or hydroxyl group at C-2 and C-4 positions and a bulky substituted amino group at C-6 position have been found to inhibit the growth of some microorganisms[18,19]. 2,4-Diamino-6-*p*-bromoanilino-5-nitropyrimidine has been found to exhibit activity against Walker 256 (WM) tumor system[20]. In view of the above observations, we became interested in studying the effect of introducing an arylazo group in 5-position and a bulky substituted amino group in 6-position of 2,4-diaminopyrimidine moiety on the biological properties of resultant compounds and our compounds (1-24 reported in the present paper) were synthesised with that view.



(A) (B)

These synthetic pyrimidines have been tested against *S. faecalis* and their growth inhibitory activity has been compared with that of 5-unsubstituted pyrimidines (Type A) and also with some well known antibiotics.

The new 5-arylazopyrimidines (1-24) were obtained by the coupling reaction of an appropriate 2,4,6-trisubstituted pyrimidine (A) with diazotised arylamine at 2-5° and *p*H 5-6 or 8-9 depending on the nature of the 5-unsubstituted compound used. Proper maintenance of *p*H was found to be essential for the reaction. The 5-arylazopyrimidines are all coloured crystalline solids and almost all the compounds are insoluble in common organic solvents at room temperature. The compounds prepared are listed in Table 1.

Experimental

Melting points were determined in capillary tubes on a copper block. M. ps. of the compounds that melted with decomposition were determined by rapidly heating the block to about 20° below the actual m.p. and then heating the block at the rate of ~ 4° min^{-1}. All the melting points reported are corrected. In crystallisation, the term alcohol always refers to 90% (w/w) ethanol. Uv spectra were recorded in absolute ethanol on a Cary 17D spectrophotometer. Before elemental analysis, the compounds were dried over P_2O_5 at 110°/1 mm for 16 h.

All the 2,4-diamino-6-(substituted-amino)pyrimidines, used as starting materials, were prepared according to the known methods[8,21] except 2,4-diamino-6-morpholino compound which was prepared as follows.

A mixture of 2,4-diamino-6-chloropyrimidine[22] (0.0069 mol) and anhydrous morpholine (0.034 mol) was slowly heated for 1 h to 130° (oil-bath temp.) and then kept at this temperature for further 2.5 h. The solid soon went into solution and a viscous substance resulted. The product was extracted with boiling toluene (2 × 20 ml). The toluene extracts were combined and slightly concentrated. On

† Present address: Department of Chemistry, Gurudas College, Calcutta-700 054.

TABLE 1—PHYSICAL CONSTANTS AND DATA ON GROWTH-INHIBITION AND ITS REVERSAL BY PGA FOR 5-ARYLAZOPYRIMIDINES (1—24 ; STRUCTURE B)

Compd. no.	R_2	Yield %	M.p. °C	Colour	Molecular formula	λ_{max} (log ε)	Inhibitor concn. ($\mu g\ ml^{-1}$) required for 50% inhibition of *S. faecalis* growth†	Percent growth* with increasing concn. of PGA** — PGA concn. $m\mu g\ ml^{-1}$: 1	20
					R_1 = *p*-Iodophenylamino				
1	*p*-Br	87.2	300 d	Yellow needles	$C_{16}H_{13}N_7BrI$	204(5.05) 256(4.78) 284(4.81) 428(4.56)	*a*	—	—
2	*o*-CH_3	85.2	250 d	Yellow powder	$C_{17}H_{16}N_7I$	202(4.76) 254(4.41) 290(4.62) 400(4.51)	*b*	—	—
3	*o*-OCH_3	72.4	246 d	Yellow powder	$C_{17}H_{16}N_7OI$	208(4.72) 292(4.49) 397(4.22)	*c*	—	—
4	*m*-OCH_3	83.7	223 d	Yellow powder	$C_{17}H_{16}N_7OI$	202(4.49) 255(4.17) 290(4.48) 400(4.37) 420(4.39)	*b*	—	—
5	*p*-SO_3H	84.6	283 d	Yellow powder	$C_{16}H_{14}N_7SO_3I$	254(4.25) 288(4.40) 426(4.28)	4.8	22	73
					R_1 = *p*-Anisidino				
6	*p*-Br	87.0	233 d	Deep yellow powder	$C_{17}H_{16}N_7OBr$	204(3.95) 232(3.67) 274(3.67) 430(3.26)	*c*	—	—
7	*o*-CH_3	88.7	214	Yellow powder	$C_{18}H_{19}N_7O$	228(3.77) 256(3.99) 280(4.14) 3.96(4.07)	*d*	—	—
8	*o*-OCH_3	81.0	119 d	Golden yellow shining crystals	$C_{18}H_{19}N_7O_2$	202(4.52) 250(4.09) 286(4.30) 442(4.28)	*e*	—	—
9	*m*-OCH_3	82.3	166 d	Yellow powder	$C_{18}H_{19}N_7O_2$	204(5.15) 276(4.85) 428(4.54)	*b*	—	—
10	*p*-SO_3H	89.1	265 d	Orange powder	$C_{17}H_{17}N_7SO_4$	202(4.76) 252(4.40) 276(4.46) 428(4.25)	0.48	11	68
					R_1 = Cyclohexylamino				
11	*p*-Br	77.5	210	Yellow shining needles	$C_{16}H_{20}N_7Br$	202(4.25) 258(4.12) 388(4.24)	0.62	17	75
12	*o*-CH_3	79.4	182	Yellow shining needles	$C_{17}H_{23}N_7$	204(4.00) 258(4.19) 392(4.29)	0.80	18	71
13	*m*-OCH_3	71.4	174	Yellow crystals	$C_{17}H_{23}N_7O$	204(4.10) 258(4.38) 388(4.42)	1.34	26	82
14	*p*-SO_3H	79.7	309 d	Yellow powder	$C_{16}H_{21}N_7SO_3$	211(4.50) 264(4.28) 394(4.39)	*f*	—	—
					R_1 = Piperidino				
15	*p*-Br	90.3	215	Orange shining plates	$C_{15}H_{18}N_7Br$	202(4.69) 213(4.63) 229(4.61) 271(4.58) 396(4.73)	*b*	—	—

(Table 1 contd.)

16	*o*-CH_3	88.1	222 d	Orange shining needles	$C_{16}H_{21}N_7$	240(4.28) 282(4.34) 395(4.36)	1.91	6	62
17	*o*-OCH_3	86.5	174	Brown shining needles	$C_{16}H_{21}N_7O$	245(3.97) 285(4.21) 325(3.74) 402(4.32)	100	15	78
18	*m*-OCH_3	84.9	164	Orange shining plates	$C_{16}H_{21}N_7O$	205(4.91) 270(4.71) 394(4.81)	58.0	28	77
19	*p*-SO_3H	84.9	247 d	Yellow powder	$C_{15}H_{19}N_7SO_3$	202(4.98) 224(4.87) 270(4.62) 394(4.58)	*g*	—	—
					R_1 = Morpholino				
20	*p*-Br	75.8	239 d	Orange shining crystals	$C_{14}H_{16}N_7BrO$	204(4.29) 234(4.15) 258(4.04) 272(4.03) 392(4.26)	40.0	12	71
21	*o*-CH_3	54.8	187	Yellow shining needles	$C_{15}H_{19}N_7O$	204(4.45) 272(3.19) 392(4.40)	72.0	19	74
22	*o*-OCH_3	47.4	201 d	Orange shining needles	$C_{15}H_{19}N_7O_2$	204(4.47) 275(4.34) 400(4.48)	14.75	22	78
23	*m*-OCH_3	94.0	171	Orange shining crystals	$C_{15}H_{19}N_7O_2$	210(4.19) 275(3.99) 394(4.05)	80.5	26	80
24	*p*-SO_3H	89.5	243 d	Yellow powder	$C_{14}H_{17}N_7SO_4$	204(5.04) 232(4.82) 255(4.64) 285(4.45) 390(4.10)	*c*	—	—
2,4-Diamino-6-*p*-iodo-anilinopyrimidine							15.9		
2,4-Diamino-6-*p*-anisidinopyrimidine							35.0		
2,4-Diamino-6-cyclo-hexylaminopyrimidine							82.0		
2,4-Diamino-6-piperidinopyrimidine							154.0		
2,4-Diamino-6-morpholinopyrimidine							865.0		
Chloramphenicol							2.15		
Tetracycline							14.25		
Streptomycin							*h*		
Neomycin							*h*		

Satisfactory analytical data for C, H and N has been obtained for all the compounds. For purification, 1-4 and 6-9 were crystallised from glacial AcHO ; 9-12, 20-22 from alcohol ; 13, 23 from absolute alcohol, 15 from pyridine-water ; 16-18 from alcohol-water ; 5, 10, 14, 19 and 24 purified by dissolving in $NaHCO_3$ solution and precipitating by acidifying with dilute HCl.

† PGA medium (PAG concn. 1.0 mμg ml^{-1} allowing half maximal growth). * Maximum growth with optimum amount of PGA (3 mμg ml^{-1}) and without inhibitor taken as 100%. ** The growth is restored gradually with increasing concentration of PGA. However, only the data with 20 mμg ml^{-1} of PGA has been incorporated in the table because maximum reversal of growth occurs at this concentration of PGA. The reversal studies were made at the inhibitor concentration indicated in column 7.

[i.e., the half-inhibitory concentration at a PGA level of 1 mμg ml^{-1}]

a-g No inhibition upto 30, 100, 200, 300, 50, 120, 80 μg ml^{-1}, respectively. Higher concentration than indicated could not be used owing to low solubility of the compounds. *h* Little or no activity.

cooling, the title compound crystallised out. It was further purified by crystallisation from toluene as white needles, (0.84 g, 62.40%), m.p. 184° (Found : C, 49.34 ; H, 6.28 ; N, 36.01. $C_8H_{13}N_5O$ requires : C, 49.22 ; H, 6.66 ; N, 35.89%).

5-Arylazopyrimidines (**1-24**) *: General method of preparation :* A solution of 2,4,6-trisubstituted-pyrimidine (0.00215 mol) was prepared by adding glacial acetic acid drop by drop with stirring to a suspension of the compound in water (100 ml) (2,4-diamino-6-cyclohexylaminopyrimidine and 2,4-diamino-6-morpholinopyrimidine dissolved in water without addition of glacial acetic acid). An ice-cold solution of an equimolar amount of the diazotised arylamine [prepared by adding a cold solution of 0.00215 mol sodium nitrite in water (5 ml) with stirring to an ice-cold solution of 0.00215 mol of the amine in 10 ml 1*N* HCl ; the diazotised solution must contain excess of HCl] was slowly added to the pyrimidine solution with stirring. The stirring was continued and after 5 min 2*N* NaOH solution was added dropwise to bring *p*H of the reaction solution to 8-9, when a heavy precipitate appeared. Stirring was further continued for 4 h. (In the case of compounds **5**, **10**, **14**, **19** and **24**, the solution became coloured at *p*H 8-9 instead of giving precipitate. In these cases after stirring for 4 h, dilute HCl was added dropwise to bring the *p*H to 5-6 when a heavy precipitate appeared). The product was filtered, washed several times with water, dried at 80° (compounds **5**, **10**, **14**, **19** and **24** were, however, dried directly after filtration without washing) and purified (*cf*. foot-note to Table 1).

Inhibition of growth of microorganism :

Assay method : All compounds were tested for antimicrobial activity against *Streptococcus faecalis* ATCC 8043. To a series of culture tubes containing different amounts of each inhibitor, basal medium[23,24] (5 ml) and folic acid were added and the volume was made upto 10 ml with water. After sterilisation, inoculation and incubation (18 h), growth was measured as turbidity with a Klett-Summerson photoelectric colorimeter. From the growth curve (Klett reading *vs* inhibitor concentration), half inhibitory concentration was determined by noting the inhibitor concentration at 50% inhibition of standard growth (Table 1). The solubilities of the compounds **1-4**, **6-9**, **14**, **15**, **19** and **24** were low and not sufficient for determination of 50% inhibition of growth.

Reversal studies : To a series of tubes containing a specific amount of the inhibitor and basal medium (5 ml), increasing amounts of PGA were added and the volume was made upto 10 ml. The amount of growth at different concentrations of PGA were noted.

Results

The results (Table 1) show that the synthesised 5-arylazo compounds inhibit the growth of *S. faecalis*. A comparison of the inhibitory activity of the compounds with the 5-unsubstituted compounds shows that a 5-arylazo group imparts additional growth inhibitory power. The antimicrobial activity depends on the nature of the substituent in the 6-position and also on the nature of the substituent on the phenyl ring in the 5-position.

The results of reversal studies in Table 1 (column 8) also show that the growth inhibitory action of the compounds can be reversed by increasing concentrations of PGA. The 5-arylazopyrimidines can, therefore, be regarded as specific antagonists of folic acid. All these compounds have a common structural feature (they all contain a 2,4-diaminopyrimidine moiety), with is very similar to the 2-amino-4-hydroxypyrimidine moiety present in PGA. It is, therefore, probable that the 2,4-diaminopyrimidine moiety present in the above types of compounds is responsible for binding of the compounds at the active site of an enzyme for which folic acid acts as a substrate.

References

1. A. Paul and D. Sen, *Indian J. Chem.*, 1963, **1**, 98.
2. A. Paul and D. Sen, *Indian J. Chem.*, 1964, **2**, 212.
3. A. Ghosh and D. Sen, *J. Indian Chem. Soc.*, 1965, **42**, 505.
4. D. Sen and S. Dutta Chowdhury, *J. Indian Chem. Soc.*, 1970, **47**, 369.
5. D. Sen and P. Sengupta, *J. Indian. Chem. Soc.*, 1973, **50**, 260.
6. D. Sen and P. Sengupta, *Indian J. Chem.*, 1975, **13**, 549.
7. P. Roy Burman and D. Sen, *Biochem. Pharmacol.*, 1964, **13**, 1487.
8. D. Sen and S. Dutta Chowdhury, *Indian J. Biochem.*, 1970, **7**, 187.
9. D. Sen and P. Sengupta, *Indian J. Biochem. Biophys.*, 1976, **13**, 365.
10. D. Sen, S. R. Bhowmik and P. Sengupta, *Indian J. Chem., Sect B*, 1983, **22**, 388.
11. G. M. Timmis, D. G. I. Felton and H. O. J. Collier, *J. Pharm. Pharmacol.*, 1957, **9**, 46.
12. E. J. Modest, H. N. Schlein and G. E. Foley, *Proc. Am. Assoc. Cancer Res.*, 1956, **2**, 134 ; *J. Pharm. Pharmacol.*, 1957, **9**, 68.
13. M. Israel, H. N. Schlein, C. L. Maddock, S. Farber and E. J. Modest, *J. Pharm. Sci.*, 1966, **55**, 568.
14. K. Tanaka, K. Kaziwara, Y. Aramaki, E. Omura, T. Arakai, M. Kawashima, J. Watanabe, T. Sugawa, Y. Sanno, Y. Sugino, Y. Ando, K. Imai, H. Yokotani and M. Ishidate, *Acta Unio Intern. Contra. Concrum*, 1959, **15**, 281 (*Chem. Abstr.*, 1959, **53**, 22498).
15. K. Tanaka, E. Omura, T. Sugawa, Y. Sanno, Y. Ando, K. Imai and M. Kawashima, *Chem. Pharm. Bull., Tokyo*, 1959, **7**, 1.
16. K. Tanaka, E. Omura, M. Kawashima, J. Watanabe, H. Yokotani, H. Ito, Y. Sugino, M. Ishidate, T. Araki, Y. Aramaki and K. Kaziwara, *Chem. Pharm. Bull., Tokyo*, 1959, **7**, 7.

17. M. Kawashima, *Chem. Pharm. Bull., Tokyo*, 1959, 7, 13, 17.
18. D. Roy, S. Ghosh and B. C. Guha, *J. Org. Chem.*, 1960, 25, 1909.
19. D. Roy, S. Ghosh and B. C. Guha, *Arch. Biochem. Biophys.*, 1961, 92, 366.
20. D. E. O'Brien and C. C. Cheng, *J. Med. Chem.*, 1966, 9, 575.
21. B. Roth, U. S. Pat. 2 577 039/1951 (*Chem. Abstr.*, 1952, 46, 5620).
22. B. Roth, J. M. Smith and M. E. Hultquist, *J. Am. Chem. Soc.*, 1950, 72, 1915.
23. A. Jones and S. Morris, *Analyst*, 1949, 74, 29.
24. "Methods of Vitamin Assay", 2nd ed., The Association of Vitamin Chemists, Interscience, New York, 1951.

J. Indian Chem. Soc.,
Vol. LXIII, April 1986, pp. 425-426

Synthesis of 3-Substituted-amino/aroyloxy-7-chloro-5-phenyl-1,3-dihydro-2*H*-1,4-benzodiazepin-2-ones as Possible Anxiolytics

Y. D. KULKARNI*, S. H. R. ABDI and V. L. SHARMA

Department of Chemistry, Lucknow University, Lucknow-226 007

and

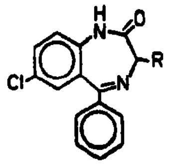
P. R. DUA and G. SHANKER

Pharmacology Division, Central Drug Research Institute, Lucknow-226 001

Manuscript received 6 June 1985, revised 11 December 1985, accepted 17 February 1986

Ten new 3-substituted-amino/aroyloxy-7-chloro-5-phenyl-1,3-dihydro-2*H*-1,4-benzodiazepin-2-ones were synthesised and tested for their acute toxicity, effect on gross behaviour and anxiolytic activity using antihypoxia and antimetrazole tests in mice. At 1/5th ALD_{50}, two compounds, one with a morpholino group and the other with a 4-methoxybenzoyloxy group at 3-position exhibited maximum antimetrazole activity similar to oxazepam and also produced significant increase of survival time in antihypoxia test which was comparable to oxazepam.

THE structure activity relationship on 1,4-benzodiazepines had been studied[1,2]. The introduction of a hydroxy, alkoxy, carboxy *etc.* groups at 3-position had yielded the compounds with significant anxiolytic activity. Esterification of 3-hydroxy group also resulted into compounds with similar activity since the hydrolysis at the ester linkage produced the parent compound as a metabolite. Moreover, several esters and amides of 3,4,5-trimethoxybenzoic acid also possessed high tranquillising activity[3,4]. These reports prompted the authors to synthesise the title compounds with an amine residue or an aroyloxy group at 3-position of 1,4-benzodiazepine moiety and to evaluate them for their anxiolytic activity.



Experimental

Melting points were determined in open capillary tubes and are uncorrected. The reactions were followed by tlc. Ir spectra were recorded on a Perkin-Elmer 157 infracord and Perkin-Elmer 177 or 137 grating instruments as KBr discs. Pmr spectra were recorded on a Varian A60D spectrometer (60 MHz) using TMS as internal standard.

5-Chloro-3-phenylanthranil[5], 2-amino-5-chlorobenzophenone[5], 2-amino-5-chlorobenzophenone oxime[6], 2-chloroacetamido-5-chlorobenzophenone oxime[6], 2-chloromethyl-4-phenyl-6-chloroquinazoline-3-oxide[6], 7-chloro-5-phenyl-1,3-dihydro-2*H*-1,4-benzodiazepin-2-one-4-oxide[7], 3-acetoxy-7-chloro-5-phenyl-1,3-dihydro-2*H*-1,4-benzodiazepin-2-one[8] and 7-chloro-3-hydroxy-5-phenyl-1,3-dihydro-2*H*-1,4-benzodiazepin-2-one[8] were prepared by the known procedures.

*3-Substituted-amino-7-chloro-5-phenyl-1,3-dihydro-2*H*-1,4-benzodiazepin-2-ones* (**1-4**) : To a solution of 7-chloro-3-hydroxy-5-phenyl-1,3-dihydro-2*H*-1,4-benzodiazepin-2-one (0.001 mol) in ethanol (20 ml) were added appropriate amine (0.0011 mol) and two drops of glacial acetic acid. The reaction mixture was heated at reflux for 18-24 h and concentrated under reduced pressure. The residue was recrystallised from aqueous ethanol in yields 50-80%. The compounds were characterised by their m.ps., elemental analyses and ir spectral data which showed the presence of bands at 3 400-3 200 (amide NH), 2 900 (CH_2), 1670 (amide C=O) and 1 640 cm^{-1} (C=N).

*3-Aroyloxy-7-chloro-5-phenyl-1,3-dihydro-2*H*-1,4-benzodiazepin-2-ones* (**7-10**) : To a suspension of an aroyl chloride (0.0015 mol) in dry benzene (25 ml) were added 7-chloro-3-hydroxy-5-phenyl-1,3-dihydro-2*H*-1,4-benzodiazepin-2-one (0.001 mol) and triethylamine (0.004 mol). The mixture was then refluxed for 8-12 h on a water-bath. Triethylamine hydrochloride was filtered off and the filtrate concentrated under reduced pressure. The residue obtained was recrystallised from aqueous methanol or benzene-petroleum ether mixture in yields 80-95%. The compounds were characterised by their m.ps., elemental analyses and ir bands at 3 150 (amide NH),

TABLE 1—3-SUBSTITUTED-AMINO/AROYLOXY-7-CHLORO-5-PHENYL-1,3-DIHYDRO-2*H*-1,4-BENZODIAZEPIN-2-ONES*

Compd. no.	R	M.p. °C	Molecular formula	ALD_{50} mg/kg i.p. (confience limit)	Anxiolytic activity[a] % increase in survival time
1	Morpholino	175-76	$C_{19}H_{18}ClN_3O_2$	681 (nil)	33.33
2	Dimethylamino	151-52	$C_{17}H_{16}ClN_3O$	825 (562-1210)	13.66
3	*N*-Phenylpiperazino	129-30	$C_{25}H_{23}ClN_4O$	825 (562-1210)	—
4	Piperidino	105-06	$C_{20}H_{20}ClN_3O$	681 (nil)	16.39
5	*N*-Methylpiperazino	111-12	$C_{20}H_{21}ClN_4O$	681 (nil)	—
6	3,4,5-Trimethoxyanilino	116-18	$C_{24}H_{22}ClN_3O_4$	681 (nil)	16.75
7[b]	Benzoyloxy	210-21	$C_{22}H_{15}ClN_2O_3$	681 (nil)	—
8	4-Methoxybenzoyloxy	178-79	$C_{23}H_{17}ClN_2O_4$	681 (nil)	35.59
9	3,4,5-Trimethoxybenzoyloxy	112-13	$C_{25}H_{21}ClN_2O_6$	>1000	—
10	4-Nitrobenzoyloxy	229-30	$C_{22}H_{14}ClN_3O_5$	825 (562-1210)	20.54
Oxazepam	—	—	—	825 (562-1210)	59.28

* All compounds analysed for C, H and N were found satisfactory.

[a] δ ($CDCl_3$) 8.50 (1H, m, NH), 7.80-7.30 (13H, m, ArH) and 4.80 (1H, s, COOHCO). [b] Mean survival time for control groups ranged from 33.4 to 37.6 min. At 1/5th ALD_{50}, no gross behavioural effect was observed in compounds while oxazepam was depressant. At 1/5th ALD_{50}, 1, 8 and oxazepam were 100% active while 9 was 60% active against metrazole induced seizures.

2 950 (CH aliphatic), 1 730 (ester C=O), 1 680 (amide C=O) and 1 625 cm^{-1} (C=N).

Pharmacological studies : Acute toxicity studies (LD_{50} determination)[9], gross behavioural effects[10] and anxiolytic activity by metrazole seizure threshold test[11] (a model[12,13] for preliminary screening of anxiolytic activity) and antihypoxia test[14] were carried out by known procedures. Oxazepan was used as standard in all these tests. The results have been summarised in Table 1.

Results and Discussion

ALD_{50} of compounds **1** and **4-8** was 681 mg/kg while for **2**, **3**, **10** and oxazepam it was 825 mg/kg. Compound **9** had an ALD_{50}>1 000 mg/kg. At 1/5th ALD_{50} none of the test compounds showed any effect on gross behaviour while oxazepam had depressant effect. The significant increase in survival time[13] and protection against metrazole seizures by **1**, **8** and oxazepam had shown that they had appreciable anxiolytic activity. Compounds **1** and **8** were, however, devoid of CNS depression. Compound **9** produced 60% protection against metrazole seizures. Among the 3-substituted-amino compounds (**1-6**) only the morpholino compound (**1**) was active and the activity might be attributed to the internal ether linkage[15] present in morpholine. Anxiolytic activity of compounds **8** and **9** confirmed the structure activity relationship studies that esterification of 3-hydroxy group retained the activity while lack of activity in **7** and **10** suggested that hydrolysis at ester linkage might not be occurring to yield oxazepam as metabolite. Complete loss of activity in **6** and less activity in **9** had indicated that introduction of a trimethoxyphenyl group was not desirable.

Thus, 7-chloro-5-phenyl-1,3-dihydro-2*H*-1,4-benzodiazepin-2-one with a 3-(4-morpholino) group (**1**) or a 3-(4-methoxybenzoyloxy) group (**8**) possess anxiolytic activity comparable to oxazepam. They are, however, devoid of CNS depression, a distinct advantage over oxazepam.

Acknowledgement

The authors express their thanks to Professor V. S. Misra, Head, Chemistry Department, Lucknow University, for facilities and Dr. Nityanand, Director and Professor B. N. Dhawan, Deputy Director, C.D.R.I., Lucknow, for pharmacological studies of the compounds.

References

1. L. H. STERNBACH, *J. Med. Chem.*, 1979, **22**, 1.
2. S. J. CHILDRESS in Burger's Medicinal Chemistry, ed. M. E. WOLFF, 4th ed., John Wiley, New York, Part III, 1981, p. 990.
3. M. MASTUI, S. OKANO and R. MITSUGAMI, Jap. Pat. 226/1962 (*Chem. Abstr.*, 1963, **58**, 482).
4. H. ROEHNERT, H. BARTH and F. CARSTENS, E. Ger. Pat. 22 180/1961 (*Chem. Abstr.*, 1963, **58**, 1410).
5. R. B. DAVIS and L. C. PIZZINI, *J. Org. Chem.*, 1960, **25**, 1884.
6. L. H. STERNBACH, S. KAISER and E. REEDER, *J. Am. Chem. Soc.*, 1960, **82**, 475.
7. S. C. BELL, T. S. SULKOWSKI, C. GOCHMAN and S. J. CHILDRESS, *J. Org. Chem.*, 1962, **27**, 562.
8. S. C. BELL and S. J. CHILDRESS, *J. Org. Chem.*, 1962, **27**, 1691.
9. H. J. HORN, *Biometrics*, 1956, **12**, 311.
10. R. A. TURNER, 'Screening Methods in Pharmacology", Academic Press, New York, 1965, p. 28.
11. E. A. SWINYARD, W. C. BROWN and L. S. GOODMAN, *J. Pharm. Exptl. Ther.*, 1952, **106**, 319.
12. H. LAL and M. W. EMMETT OGLESBY, *Neuropharmacology*, 1983, **22**, 1427.
13. M. NAKANISHI, H. YASUDA and T. TSUMAGARI, *Life Sci.*, 1973, **13**, 467.
14. C. CAILLARD, A. MENU, M. PLOTKINE and P. RASIGNOL, *Life Sci.*, 1975, **16**, 1607.
15. L. VARGHA, E. KASZTREIMER, J. BORSY, L. FARKAS, J. KUSZMAN and B. DUMBOVICH, *Biochem. Pharmacol.*, 1962, **11**, 639.

J. Indian Chem. Soc.,
Vol. LXIII, April 1986, pp. 427-429

Synthesis and Biological Activity of Heterocyclic Derivatives derived from Ethyl-2-hydroxy-quinoxaline-3-carboxylate

P. S. FERNANDES* and T. M. SONAR

Nadkarny-Sacasa Research Laboratories, St. Xavier's College, Mahapalika Marg, Bombay-400 001

Manuscript received 15 July 1985, accepted 17 February 1986

Ethyl-2-chloroquinoxaline-3-carboxylate obtained from ethyl-2-hydroxyquinoxaline-3-carboxylate upon treatment with morpholine gave ethyl-2-morpholinoquinoxaline-3-carboxylate (1). This ester upon reaction with hydrazine hydrate (99%) gave respective carboxy hydrazide (2). This hydrazide on reaction with phenyl isothiocyanates gave thiosemicarbazides (3a-c). The thiosemicarbazides on reaction with concentrated sulphuric acid or anhydrous phosphoric acid gave 2-(4-substituted)-anilino-5-((2'-morpholino)quinoxalino)-1,3,4-thiadiazoles (4a-c). The thiosemicarbazides on reaction with 4% sodium hydroxide formed 4-(*para*-substituted-phenyl)-3-mercapto-5-((2'-morpholino)quinoxalino)-1,2,4-triazoles (5a-c), and on reaction with I_2 in KI gave 2-(4-substituted)anilino-5-((2'-morpholino)quinoxalino)-1,3,4-oxadiazoles (6a-c). respectively.

SEVERAL biologically active polypeptides, such as levomycin, actinoleukin and echinomycin have been shown to possess one or more quinoxalinoyl residues[1]. Echinomycin possesses antitumour, antiviral, and antibacterial activities but its low therapeutic index has precluded any medicinal uses.

Thiosemicarbazides in general are known for their antitubercular[2], antifungal[2,3] and hypoglycemic[4] properties. In view of these, we felt, it is worth synthesising thiosemicarbazides of substituted quinoxaline series. Thiosemicarbazides are further reacted to give corresponding oxadiazoles, thiadiazoles, and triazoles. All compounds synthesised were screened for their antibacterial properties.

Ethyl-2-chloro-quinoxaline-3-carboxylate was prepared according to the reported procedures[5]. This compound upon reaction with morpholine in methanol gave ethyl-2-morpholino-quinoxaline-3-carboxylate (**1**) in good yields. Its structure was confirmed by ir, nmr and mass spectra. **1** showed a sharp peak at 1 720 cm^{-1} in its ir spectrum indicating the presence of an ester carbonyl group. Support for the structure was obtained from ^1H nmr spectra ($CDCl_3$) of **1** where CH_3 protons are found as triplet at δ 1.4, CH_2 as a quartet at 4.45, CH_2 adjacent to N (morpholino) as triplet at 3.55, CH_2 adjacent to O as a triplet at 3.8 and aromatic protons as a multiplet at 7.75.

Ethyl-2-morpholinoquinoxaline-3-carboxylate upon reaction with hydrazine hydrate (99%) gave the corresponding carboxy hydrazide (**2**) in fairly good yields. Its structure was confirmed by ir, nmr and mass spectra. **2** showed a sharp peak at 1 650 (C=O) and 3 320 cm^{-1} (NH) in its ir spectrum. The structure was confirmed from ^1H nmr spectra ($CDCl_3$) of **2** where CH_2 protons (adjacent to N of morpholino group) are found as a triplet at δ 3.5, CH_2 adjacent to O (morpholino group) are occuring as a triplet at 3.85, four aromatic protons as a multiplet at 7.7, NH_2 protons of hydrazide as a singlet at 4.05 and NH protons of hydrazide are seen as a singlet at 8.6.

Hydrazide **2** was allowed to react with substituted phenyl isothiocyanate to give corresponding thiosemicarbazides (**3a-c**). The broad peaks in the ir spectra of **3a** at 3 000-3 220 cm^{-1} may be due to NH functions and the peaks at 1 270 cm^{-1} are assigned to C=S functions.

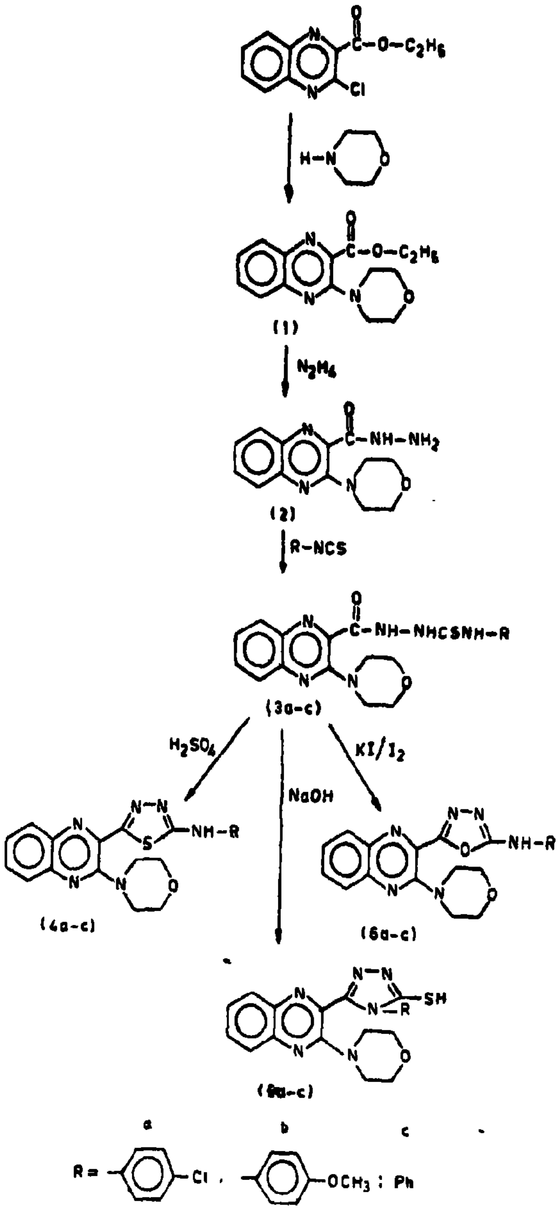
The thiosemicarbazides on reaction with concentrated H_2SO_4 or a phosphoric acid undergoes a cyclodehydration to give 2-(4-substituted)-anilino-5 ((2'-morpholino)quinoxalino) 1,3,4-thiadiazoles (**4a-c**). The ir spectrum of **4a** showed peaks at 3 200 cm^{-1} and 2 980 cm^{-1} due to two NH groups. The peaks at 1 540 and 1 580 cm^{-1} clearly indicate the conjugated C=N with the absence of C=O.

The thiosemicarbazides upon refluxing with 4% sodium hydroxide gave 4-(*para*-substituted-phenyl)-3-mercapto-5-((2'-morpholino)quinoxalino)-1,2,4-triazoles (**5a-c**). The ir spectrum of **5a** showed the absence of NH and C=O functions. Appearance of a peak due to conjugated C=N at 1 595 and 1 605 cm^{-1}, is in confirmity with the structures (**5a-c**). Thiosemicarbazide upon reaction with I_2 in KI gave 2-(4-substituted)-anilino-5-((2'-morpholino)quinoxalino)-1,3,4-oxadiazoles (**6a-c**). **6a** exhibited all the characteristic features in ir like NH at 3 200 cm^{-1}, absence of a peak due to C=O and peaks at 1 560 and 1 590 cm^{-1} due to conjugated C=N is observed. This suggests that the thiosemicarbazides have undergone oxidation to give the substituted oxadiazoles (**6a-c**).

Physical data are given in Table 1 and various reactions involved in Scheme 1.

TABLE 1—PHYSICAL DATA OF 2-MORPHOLINOQUINOXALINE-3-THIOSEMICARBAZIDE (3a-c), 2-(4-SUBSTITUTED)-ANILINO-5-((2'-MORPHOLINO)QUINOXALINO)-1,3,4-THIADIAZOLE (4a-c), 4-(*para*-SUBSTITUTED-PHENYL)-3-MERCAPTO-5-((2'-MORPHOLINO)QUINOXALINO)-1,2,4-TRIAZOLES (5a-c), AND 2-(4-SUBSTITUTED)-ANILINO-5-((2'-MORPHOLINO)QUINOXALINO)-1,3,4-OXADIAZOLES (6a-c)

Compd. no.	M.p. °C	Yield %
3a	201	58
3b	182	76
3c	162	98
4a	218	68
4b	240	77
4c	284	89
5a	235	21
5b	260	70
5c	95	85
6a	192d	72
6b	188	83
6c	156	61



Scheme 1

Experimental

All the melting points are uncorrected. Ir spectra (KBr) were taken on a Perkin-Elmer 633 spectrophotometer. For compounds **1** and **2** nmr and mass spectra were taken on Varian FT 80 and Varian 114 MAT instruments, respectively. All the compounds gave satisfactory elemental analysis.

Ethyl-2-morpholinoquinoxaline-3-carboxylate (**1**) : Diethyl malonate was oxidised with nitrous oxide to give ethyl oxomalonate[6], which upon condensation with *o*-phenylenediamine gave ethyl-2-hydroxyquinoxaline-3-carboxylate. This compound upon reaction with phosphorous oxychloride gave ethyl-2-chloroquinoxaline-3-carboxylate.

To a methanolic solution of the above crude chloro compound (0.01 mol), morpholine (0.01 mol) was added and refluxed for 2 h. Solvent was then removed under vacuum and the contents extracted with hot petroleum ether. Petroleum ether extracts were concentrated and cooled to 0° under vigourous stirring for 1 h to get the crude product, which was filtered and recrystallised from 70% methanol to get ethyl-2-morpholinoquinoxaline-3-carboxylate (34%), m.p. 66°.

2-Morpholino-quinoxaline-3-carboxy hydrazide (**2**) : The above prepared ethyl-2-morpholinoquinoxaline-3-carboxylate (0.01 mol), methanol (50 ml), and hydrazine hydrate (0.015 mol) were refluxed on a water-bath for 8 h. The reaction mixture was then concentrated under vacuum. Resultant mass was cooled to 0° for 1 h. Ice-cold water (10 ml) was then added to the solution under stirring. The solid that separated out was filtered and crystallised from ethanol (activated charcoal used) to give the corresponding hydrazide (73%), m.p. 180°.

2-Morpholinoquinoxaline-3-thiosemicarbazide (**3a-c**) : Carboxy hydrazide (**2** ; 0.001 mol) in ethanol (100 ml) was dissolved by heating. To it appropriate phenyl isothiocyanate[7] (0.001 mol) was added with stirring and then refluxed on water-bath for 3 h. Reaction mixture was concentrated to 1/3 volume and cooled. The solid separated out was collected by filtration and crystallised from ethanol to get **3a-c**.

2(4-Substituted)anilino-5((2'-morpholino)quinoxalino)-1,3,4 thiadiazole (**4a-c**) :

For compounds **4a** *and* **4c** : The appropriate thiosemicarbazide (**3a**, **3c**) (0.001 mol) was added in small portions to concentrated sulphuric acid (25 ml) at 0°. The mixture was kept stirring for

1 h. It was allowed to stand overnight at room temperature, and then poured carefully into crushed ice. To it under cooling, 10% liquor ammonia was added till *p*H was neutral. The solid separated was filtered, washed with ice-cold water and crystallised from ethanol.

For compound **4b** *:* Thiosemicarbazide (**3b** ; 0.001 mol) was added with stirring to anhydrous phosphoric acid (20 ml) during 20 min. It was heated on an oil-bath at 120° for 0.5 h, then cooled to room temperature and reaction mass poured over crushed ice. To it under stirring, 10% ammonia was added till *p*H became neutral. The solid separated was filtered, washed with water and crystallised from ethanol.

*4-(*para*-Substituted-phenyl)-3-mercapto-5-((2'-morpholino)quinoxalino)-1,2,4-triazoles* (**5a-c**) *:* The appropriate thiosemicarbazide (**3a-c** ; 0.001 mol) and 2*N* sodium hydroxide (20 ml) were refluxed for 3 h. The solution was cooled, filtered and acidified with dilute hydrochloric acid. The desired compound thus precipitated was filtered, washed with water and crystallised.

2-(4-Substituted)-anilino-5((2'-morpholino)quinoxalino)-1,3,4-oxadiazoles (**6a-c**) *:* Thiosemicarbazides (**3a-c** ; 0.001 mol) in ethanol (50 ml) were added to NaOH (5 ml, 4*N*), with cooling and shaking. A solution of iodine in KI was added dropwise with stirring and cooling till the colour of iodine persisted. The mixture was refluxed on a water-bath for 4 h and more iodine solution was added to maintain a permanent tinge of iodine. The solvent was distilled off. The reaction mixture was cooled, poured into ice-water. *p*H of the solution was made acidic by adding dilute HCl. The solid separated was filtered, washed with dilute solution of sodium thiosulphate and then with little cold water and crystallised.

Biological activity : The compounds (Table 1) were evaluated for their antibacterial activity by ditch plate technique[8], using concentration levels 2, 3 and 5 mg ml^{-1}. The test organisms employed were *Salmonella typhi*, *Staphylococcus aureus*, *Pseudomonas aeruginosa*, *Escherichia coli* and *Bacillus subtiles*. Activity levels at concentration of 2 and 3 mg ml^{-1} were negligible in most cases. Compounds **5c** and **6c** were found to inhibit all the organisms tested, though the activity against *P. aeruginosa* and *B. subtiles* were negligible. **3c** was active in all the organism at a concentration of 5 mg ml^{-1}. **5a** and **2** were totally inactive against all the organisms. **4c** though inactive against the rest showed very promising activity agaist *Salmonella* species.

References

1. K. Sato, O. Shiratori and K. Katagiri, *J. Antibiotic, Ser. A*, 1967, **20**, 270.
2. A. K. Bhat, R. P. Bhamaria, R. A. Bellave and Deliwala, *Indian J. Chem.*, 1967, **5**, 397.
3. T. Zsolnia, *Biochem. Pharmacol.*, 1962, **11**, 271.
4. E. L. Leafe, Proc. 7th Brit. Weed. Control. Conf., Glasgow, 1964 (*Chem. Abstr.*, 1966, **64**, 1279).
5. A. H. Gowenlock, G. T. Newbold and F. S. Spring, *J. Chem. Soc.*, 1945, 622.
6. H. Gilman and A. H. Blatt, *Org. Synth.*, 1941, **1**, 266.
7. H. Gilman and A. H. Blatt, *Org. Synth.*, 1941, **1**, 447.
8. C. H. Collins and P. M. Lyne, "Microbiological Methods", 3rd ed., Butterworths, London, 1970, p. 424.

J. Indian Chem. Soc.,
Vol. LXIII, April 1986, pp. 430-431

Spiro Heterocycles. Part-VII. Synthesis and Antibacterial Activity of some Fluorine containing Spiro[azetidine-2,3′-[3*H*]indole]-2′,4(1′*H*)-diones

KRISHNA C. JOSHI*, RENUKA JAIN and VANDANA SHARMA

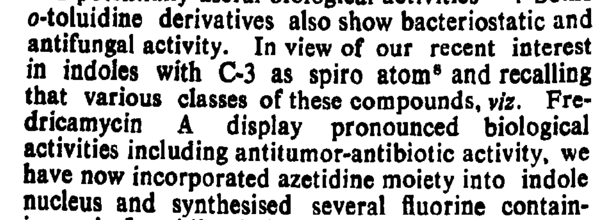
Department of Chemistry, University of Rajasthan, Jaipur-302 004

Manuscript received 2 September 1985, accepted 17 February 1986

Several new fluorine containing spiro [azetidine-2,3′-[3*H*]indole]-2′,4(1′*H*)-diones have been synthesised by the condensation of chloroacetylchloride with Schiff bases of indole-2,3-diones. The structures are supported by analysis, ir and nmr spectra, and some of the compounds have been screened for antibacterial activity.

THE β-lactam drugs are the most widely prescribed antibiotics used in medicine even after many years of their indroduction[1-3]. The naturally occurring azetidine-2-carboxylic acid has shown some unique and potentially useful biological activities[4-7]. Some *o*-toluidine derivatives also show bacteriostatic and antifungal activity. In view of our recent interest in indoles with C-3 as spiro atom[8] and recalling that various classes of these compounds, *viz.* Fredricamycin A display pronounced biological activities including antitumor-antibiotic activity, we have now incorporated azetidine moiety into indole nucleus and synthesised several fluorine containing spiro[azetidine-2.3′-[3*H*]-indole]-2′,4(1′*H*)-diones and screened them for antibacterial activity. In this, we have been further guided by the observation that incorporation of fluorine into bioactive molecules can lead to altered/enhanced biological activity.

The synthesis involved the condensation of primary amines with an appropriate indole-2,3-dione (1) resulting in the formation of the intermediate Schiff bases (2) which on cyclocondensation with chloroacetylchloride gave the spiro product (3) (Scheme 1). The formation of these compounds is evidenced by ir and nmr spectral studies. In the ir spectra, absorptions at 1 700 (C=O) and 1 650 cm^{-1} (C=N stretching) indicated the formation of 3-aryliminoindole-2-ones. Ir spectra of the final spiro compound showed disappearance of C=N absorption and appearance of absorptions at



Scheme 1

1 710 cm^{-1} (monocyclic β-lactam ring) and 745-770 cm^{-1} (C−Cl group). The indole carbonyl absorption remained as such. In the nmr spectra of the spiro compound, additional peak due to C−H proton at δ 4.2 was observed along with usual absorptions of aromatic protons in the region δ 7.3-7.9 and NH proton at δ 8.4.

Experimental

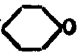
The purity of compounds was checked by tlc. Ir spectra (KBr) were recorded on a Perkin-Elmer 557 spectrophotometer. Nmr spectra were recorded on Perkin-Elmer RB-12 aud Varian A-60D instruments. TMS was taken as internal standard for pmr spectra.

3-Aryliminoindol-2-ones; *Schiff bases* (2) : These were prepared following the method of Joshi *et al.*[9] by the condensation of appropriate indole-2,3-diones with aromatic amines.

*3-Chloro-5′-fluoro-1-(4-fluorophenyl)-spiro[azetidine-2,3′-[3*H*]indole]-2′,4(1′*H*)-diones* (3) : To a well stirred solution of 5-fluoro-3-(4′-fluorophenyl)iminoindol-2-one (0.01 mol) and triethylamine (0.01 mol) in dry benzene was added chloroacetyl chloride (0.01 mol) dropwise at room temperature[10]. After addition of chloroacetyl chloride was complete, the mixture was stirred for extra 5 h and left at room temperature for 3 days. The precipitated triethylamine hydrochloride was filtered off and washed thoroughly with dry benzene. The filtrate was washed several times with dilute hydrochloric acid, then with water and then dried over anhydrous sodium sulphate. The solvent was evaporated *in vaccuo* and the residue was then recrystallised from benzene-petroleum ether (70%), m.p. 140°.

Other spiro[azetidine-2,3′-[3*H*]indole]-2′,4(1′*H*)-diones (3) were prepared in a similar manner. Their characterisation data are recorded in Table 1.

TABLE 1—PHYSICAL AND ANALYTICAL DATA OF SPIRO[AZETIDINE-2,3'-[3H]INDOLE]-2',4(1'H)-DIONES (3)

Sl. no.	X	R	R'	Mol. formula	M.p. °C	Yield %	Nitrogen % Found/(Calcd.)
1.	H	4-FC_6H_4	H	$C_{16}H_{10}ClFN_2O_2$	115	55	8.77 (8.84)
2.	5-F	C_6H_5	H	$C_{16}H_{10}ClFN_2O_2$	186	60	8.70 (8.84)
3.	5-F	4-FC_6H_4	H	$C_{16}H_9ClF_2N_2O_2$	140-142	70	8.28 (8.37)
4.	5-F	3-FC_6H_4	H	$C_{16}H_9ClF_2N_2O_2$	95	40	8.30 (8.37)
5.	5-F	4-$CF_3C_6H_4$	H	$C_{17}H_9ClF_4N_2O_2$	74	50	7.19 (7.26)
6.	5-F	4-FC_6H_4	CH_2NO	$C_{21}H_{18}ClF_2N_3O_3$	105	48	9.65 (9.68)
7.	6-F	C_6H_5	H	$C_{16}H_{10}ClFN_2O_2$	98	50	8.80 (8.84)
8.	6-F	4-FC_6H_4	H	$C_{16}H_9ClF_2N_2O_2$	103	45	8.32 (8.37)
9.	6-F	4-$CF_3C_6H_4$	H	$C_{17}H_9ClF_4N_2O_2$	78	60	7.22 (7.26)

Antibacterial activity :

The compounds (Table 1) were tested for antibacterial activity against gram-negative bacteria, *viz. E. coli, P. pyocyneus, C. frundii* and gram-positive bacteria, *viz. S. coagulase, S. viridaus* and *S. hemolyticus* by disc method[11], using ethanol as a solvent at a concentration of 10 mg ml^{-1}. The observations indicate that the compounds are not active against gram-negative bacteria except compounds of serial nos. 2, 3, 5 and 9 which show slight activity against *E. coli* (zone of inhibition between 7-10 mm in diameter). All the compounds are, however, moderately active against gram-positive bacteria (zone of inhibition between 10-17 mm), the activity against *S. hemolyticus* is maximum.

Acknowledgement

The authors are thankful to U.G.C., New Delhi, for the award of a Junior Research Fellowship to one of them (V.S.). Thanks are also due to Drs. H. N. Mangal and S. P. Garg, S. M. S. Medical College, Jaipur, for carrying out the bactericidal activity.

References

1. R. D. Hotz and D. J. Krenzer, U. S. Pat. 39 558 974.
2. T. Kemiya, *Chem. Soc. Spec. Publ.*, 1977, **28**.
3. G. Maffi, *France (Pania), Ed. Sci.*, 1959, **14**, 76.
4. L. Fowden, *J. Biochem.*, 1956, **64**, 323.
5. P. J. Peterson and L. Fowden, *Nature (London)*, 1964, **200**, 148.
6. T. Takeuchi and D. J. Propop, *Acta Biochem. Biophys.*, 1969, **175**, 142.
7. D. J. Propop, *Acta Biochem. Biophys.*, 1969, **175**, 156.
8. K. C. Joshi, R. Jain and P. Chand, *Heterocycles*, 1985, **23**, 957.
9. K. C. Joshi, V. N. Pathak and P. Chand, *J. Prakt. Chem.*, 1980, **322**, 314.
10. K. M. Hassan, A. K. El-Shafei and H. S. El-Kashef, *Z. Naturforsch, Teil B*, 1978, **33**, 1515.
11. R. Cruickshank, "Medical Microbiology", 12th. ed., 1975, Vol. II.

J. Indian Chem. Soc.,
Vol. LXIII, April 1986, pp. 432-434

Amino Acid Esters of Norethindrone as Possible Acrosin Inhibitors†

KASTURI LAL, PANNA LAL KOLEY and SUPRABHAT RAY*

Medicinal Chemistry Division, Central Drug Research Institute, Lucknow-226 001

Manuscript received 10 October 1985, accepted 17 February 1986

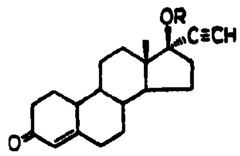
A series of amino acid esters of norethindrone (I) have been synthesised as possible acrosin inhibitors by reacting different amino acids with I in the presence of equimolar amounts of 4-*N*,*N*-dimethylaminopyridine (DMAP) and dicyclohexylcarbodiimide (DCC).

THE proteolytic enzyme 'acrosin', present on the sperm head, helps in the removal of zona pellucida, the protecting covering on the ova, during the fertilisation process[1,2]. Depletion of acrosin from the sperm surface by synthetic[3,4] and natural proteinase inhibitors[5-7] thus effectively block the penetration of the sperm at the surface of the zona. Such anti-acrosin agents, therefore, may find use in the fertility control. However, these enzyme inhibitors interfere with other biological processes as well, limiting their use.

The antiproteolytic activity of some N-protected amino acids and their esters[8,9] was utilised by Hall *et al.*[10] to produce antifertility effect. In the current study, a series of amino acid esters of norethindrone have been synthesised as pro-drugs. It has been presumed that norethindrone, a potent progestational agent, would act as a carrier of the amino acid residue to the target organs including cervix, vagina and uterine lumen, thus minimising the complications arising due to the presence of enzyme inhibitors in non-target sites. The proteolytic effect of the acrosin released from the sperm surface would hydrolyse the ester linkage and the amino acid residue thus liberated, by virtue of its anti-acrosin activity, would protect the zona pellucida and thereby block the penetration of the sperm at the zona for fertilisation. Norethindrone itself would also contribute toward antifertility activity.

Attempts to esterify norethidrone(I) with various amino acids by standard procedures[11-14] were unsuccessful. However, by using N-protected amino acids in the presence of equimolar amounts of DMAP and DCC[15] I could be esterified. Easily removable groups, such as benzyloxycarbonyl (Z) and t-butoxycarbonyl (BOC) were used to protect the amino function. Deblocking was best achieved by treating the ester with anhydrous ether saturated with dry HCl gas. Since esters with free amino groups were found unstable, they were converted to N-acetyl esters *in situ*. Norethindrone esters thus prepared are given in Table 1. These compounds have been submitted for biological screening and the result will be published separately.

TABLE 1



Compd. no.	R	M.p. °C	Yield %	Molecular formula*
1	H	—	--	—
2	Z-L-Ala	64-66	95.0	$C_{31}H_{37}NO_5$
3	BOC-L-Ala	234-35	90.0	$C_{28}H_{39}NO_5$
4	Ac-L-Ala	97-98	90.0	$C_{25}H_{33}NO_4$
5	BOC-L-Val	69-70	94.1	$C_{30}H_{43}NO_5$
6	Ac-L-Val	110-12	88.2	$C_{27}H_{37}NO_4$
7	BOC-L-Pro	97-98	94.6	$C_{30}H_{41}NO_5$
8	Ac-L-Pro	181-82	95.5	$C_{27}H_{35}NO_4$
9	BOC-L-Phe.Ala	92-94	87.5	$C_{34}H_{43}NO_5$
10	Ac-L-Phe.Ala	208-10	85.0	$C_{31}H_{37}NO_4$
11	Z-L-Leu	64-66	80.0	$C_{34}H_{43}NO_5$
12	BOC-L-Leu	84-86	85.0	$C_{31}H_{45}NO_5$
13	Ac-L-Leu	193-95	90.2	$C_{28}H_{39}NO_4$
14	BOC-L-I Leu	87-88	85.0	$C_{31}H_{45}NO_5$
15	Ac-L-I Leu	91-93	81.9	$C_{28}H_{39}NO_4$
16	BOC-L(p.Ac)Tyr	102-104	80.0	$C_{36}H_{45}NO_7$
17	Ac-L-(p.Ac).Tyr	207-208	70.0	$C_{33}H_{39}NO_6$
18	BOC-L-Try	208-210	88.0	$C_{36}H_{44}N_2O_5$
19	Ac-L-Try	148-50	78.7	$C_{33}H_{36}N_2O_4$
20	BOC-L-(ε.BOC)ORn	87-88	80.0	$C_{35}H_{52}N_2O_7$
21	Ac-L-(ε.Ac)ORn	75-77	70.0	$C_{29}H_{40}N_2O_5$
22	BOC-L-(ε.BOC)Lys	88-90	88.0	$C_{36}H_{54}N_2O_7$
23	Ac-L-(ε.Ac)Lys	74-77	90.0	$C_{30}H_{42}N_2O_5$
24	BOC-L-Met	78-80	90.0	$C_{30}H_{43}NO_5S$
25	Ac-L-Met	98-100	89.0	$C_{27}H_{37}NO_4S$
26	4-BOC.NH-$(CH_2)_3$CO	oil	90.0	$C_{29}H_{41}NO_5$
27	4-Ac.NH-$(CH_2)_3$.CO	58-60	95.9	$C_{26}H_{35}NO_4$
28	6-BOC.NH-$(CH_2)_5$.CO	oil	85.0	$C_{31}H_{45}NO_5$
29	6-Ac.NH-$(CH_2)_5$.CO	105-107	95.0	$C_{28}H_{39}NO_4$

* All the compounds gave satisfactory C, H, N analyses.

† CDRI Communication No. 3818.

Experimental

All melting points were taken in sulphuric acid bath and are uncorrected. Ir spectra (KBr) were recorded on a Perkin-Elmer 157 spectrophotometer. ^{1}H nmr spectra, in $CDCl_3$ (unless otherwise mentioned), were run on a Perkin-Elmer R-32 (90 MHz) spectrometer using TMS as internal standard (chemical shift in δ ppm). Uv spectra (methanol) were recorded on a Perkin-Elmer 202 ultraviolet-visible spectrometer. Mass spectra were obtained using a JEOL JMS-D 300 spectrometer.

N-Benzyloxy-, *N*-acetyl- and *N,N*-di-t-butoxycarbonylamino acids were prepared by the standard procedures[16-18]. *N*-t-Butoxycarbonylamino acids were obtained by the method of Schnabel[19]. Preparations of *N*-t-butoxycarbonyl-4-aminobutyric acid and *N*-t-butoxycarbonyl-6-aminocaproic acid are described.

Typical examples :

N-*t-Butoxycarbonyl-4-aminobutyric acid :* A mixture of 4-aminobutyric acid (2 g, 19.40 mmol), t-butyl azidoformate (3 ml, 21.18 mmol), 4*N* NaOH (5 ml), dioxane (10 ml) and water (10 ml) was stirred at room temperature for 4 h. The *p*H of the reaction mixture was maintained at 9-10 by occasional addition of 4*N* NaOH. The mixture was diluted with water (50 ml) and extracted with ethyl acetate (2×10 ml). The aqueous layer was cooled and acidified to *p*H 2 with citric acid. After saturating with sodium chloride the mixture was extracted with ethyl acetate (4×20 ml). The organic layer was washed with water, dried (Na_2SO_4) and the solvent distilled off under reduced pressure to give an oil which solidified upon standing (3.6 g, 91.3%), m.p. 53-4° (Found : C, 53.2 ; H, 8.3 ; N, 6.5. $C_9H_{17}NO_4$ requires : C, 53.2 ; H, 8.4 ; N, 6.9%) ; ν_{max} 3 340 (NH) and 1 700 cm^{-1} (OCONH) ; δ 1.34 (9H, s, $C(CH_3)_3$), 1.72 (2H, m, 3-CH_2), 2.27 (2H, m, 2-CH_2), 3.04 (2H, m, 4-CH_2), 5.00 (1H, br, NH) and 8.80 (1H, br, CO_2H).

N-*t-Butoxycarbonyl-6-aminocaproic acid* : It was prepared following the above procedure from 6-aminocaproic acid, (93.6%), m.p. 41-2° (Found : C, 56.8 ; H, 8.9 ; N, 6.3. $C_{11}H_{21}NO_4$ requires : C, 57.1 ; H, 9.2 ; N, 6.1%). ν_{max} (neat) 3 340 (NH) and 1700 cm^{-1} (OCONH) ; δ 1.28 (9H, s, $C(CH_3)_3$), 2.08 (2H, m, 2-CH_2), 2.90 (2H, m, 6-CH_2), 4.56 (1H, br, NH) and 8.78 (1H, br, CO_2H).

*17-(*N*-Acetylpyrrolidino-2'-carbonyl)oxy-19-norpregn-4-en-20-yn-3-one* (8) : A mixture of norethindrone (I ; 0.50 g, 1.68 mmol), *N*-acetyl-L-proline (0.40 g, 2.55 mmol), DCC (0.42 g, 2.03 mmol) and DMAP (0.225 g, 1.84 mmol) in dry CH_2Cl_2 (20 ml) was allowed to stand at room temperature for 16 h. Dicyclohexylurea was filtered off ; the filtrate extracted with 4*N* HCl (4×5 ml), 1*N* Na_2CO_3 solution (4×5 ml) and finally with brine and dried (Na_2SO_4). On removal of the solvent *in vacuo* it yielded a residue which on crystallisation from EtOAc gave 8, ν_{max} 1 745 (OCO), 1 660 (3-CO) and 1 620 cm^{-1} (C=C) ; λ_{max} 245 nm ; δ 0.89 (3H, s, 18-CH_3), 1.98 (3H, s, $COCH_3$), 2.49 (1H, s, C≡CH), 3.47 (3H, m, 5'-CH_2), 4.27 (1H, m, 2'-CH) and 5.70 (1H, s, 4-H) ; *m/z* 437 (M^+).

Norethindrone-L-2-acetamidopropanoate (4) : To a solution of norethindrone-L-2-t-butoxycarbonylaminopropanoate (0.7 g) dry CH_2Cl_2 (5 ml) was added ethereal HCl (5 ml) and the solution stirred at room temperatue for 4 h. To the residue obtained on removal of the solvents *in vacuo* pyridine (5 ml) and Ac_2O (2 ml) were added and the mixture left at room temperature for 2 h. Pyridine and Ac_2O were removed under vacuum and water added to the residue. It was extracted with EtOAc (3×20 ml) and the organic layer washed successively with 2*N* HCl (2×5 ml), aqueous $NaHCO_3$ (3×5 ml), water (4×5 ml) ; dried (Na_2SO_4) and solvent distilled off. The residue thus obtained was purified by column chromatography followed by crystallisation from ethyl acetate ; ν_{max} 3 330 (NH), 1 745 (OCO), 1 660 (3-CO) and 1 620 cm^{-1} (C=C) ; λ_{max} 243 nm ; δ 0.86 (3H, s, 18-CH_3), 1.30 (3H, d, *J* 8 Hz, $CHCH_3$), 1.91 (3H, s, $NHCOCH_3$), 2.51 (1H, s, C≡H), 4.42 (1H, m, COCH), 5.70 (1H, s, 4-H) and 6.28 (1H, d, *J* 8 Hz, NH) ; *m/z* 411 (M^+).

References

1. J. Yamane, *Cytologia*, 1935, **6**, 233.
2. L. M. Buruiana, *Naturwissenschaften*, 1956, **43**, 523.
3. L. J. D. Zeneveld, R. T. Robertson and W. L. Williams, *FEBS Lett.*, 1970, **11**, 345.
4. S. O. Newell, K. L. Polakoski and W. L. Williams, *Proc. Int. Congr. Anim. Reprod. Artif. Insemin.*, 7th., 1972.
5. L. J. D. Zeneveld, R. T. Robertson, M. Kessler and W. L. Williams, *J. Reprod. Fertil.*, 1971, **25**, 387.
6. L. J. D. Zeneveld, K. L. Polakcski, R. T. Robertson and W. L. Williams, *Proc. Int. Res. Conf. Proteinase Inhibitors*, 1st., 1970.
7. R. Stambaugh, B. G. Brackelt and L. Mastroianni, *Biol. Reprod.*, 1969, **1**, 223.
8. L. J. Loeffler, Z. Sajadi and I. H. Hall, *J. Med. Chem.*, 1977, **20**, 1578.
9. L. J. Loeffler, Z. Sajadi and I. H. Hall, *J. Med. Chem.*, 1977, **20**, 1581.
10. I. H. Hall, J. H. Drew, Z. Sajadi and L. J. Loeffler, *J. Pharm. Sci.*, 1979, **68**, 696.
11. L. F. Fieser, "Experiments in Organic Chemistry", D. C. Heath, Boston, 1977, p. 77.
12. K. Holmberg and B. Hansen, *Acta Chem. Scand.*, 1979, **33**, 410.
13. W. Szeja, *Synthesis*, 1980, 402.
14. A. A. L. Gunatilaka and S. Sotheeswaran, *J. Chem. Soc., Chem. Commun.*, 1978, 980.

15. K. LAL, P. L. KOLEY and S. RAY, *Indian J. Chem., Sect. B*, 1982, **21**, 682.

16. J. P. GREENSTEIN and M. WINITS, "Chemistry of Amino Acids", John Willey, New York, 1961, pp. 887, 2195

17. G. R PETTIT and S. K. GUPTA, *Can. J. Chem.*, 1967, **4**, 1561.

18. E. SANDRIN and R. A. BOISSONNAS, *Helv. Chim. Acta*, 1963, **46**, 1637.

19. E. SCHNABEL, *Iustus Liebigs Ann. Chem.*, 1967, **702**, 188.

NOTES

Magnetic and Spectral Behaviour of Palladium(II), Platinum(IV) and Ruthenium(III) Complexes with some Tridentate Substituted Thiosemicarbazones

R. C. SAXENA, C. L. JAIN*, R. BENJAMIN

and

S. K. SAHGAL

Department of Chemistry, M. M. H. College, Ghaziabad-201 001

Manuscript received 25 July 1984, revised 30 August 1985, accepted 17 February 1986

IN a sequence to our earlier reports[1,2] of transition metal complexes with heterocyclic thiosemicarbazones, we here report the isolation of Pd^{II}, Pt^{IV} and Ru^{III} complexes with recently synthesised tridentate ligands by following the method of Verma[3], *viz.* 1-benzaldehyde-4-thiosalicylamidothiosemicarbazone ($C_{15}H_{14}N_4OS_2$: HS-SABTZ), 1-benzaldehyde-4-(3-hydroxy-2-naphthamido)thiosemicarbazone ($C_{19}H_{16}N_4O_2S$: HO-NABTZ) and 1-benzaldehyde-4-(2-hydroxy-3-indomido)thiosemicarbazone ($C_{18}H_{15}N_4O_2S$: HO-INBTZ) and they are characterised by chemical analysis, molar conductance, magnetic and electronic and ir spectral studies in order to evaluate the stereochemistry of the ligands around the metal ions.

Experimental

[Monochloro-mono(-S-SABTZ)/(-O-NABTZ)/(-O-INBTZ) Pd^{II}] ; [bis-(-S-SABTZ)/(-O-NABTZ)/(-O-INBTZ) Pt^{IV}] dichloride ; [bis-(-S-SABTZ)/(-O-NABTZ)/(-O-INBTZ) Ru^{III}] monochloride : The acetonic solution of the ligands (2 m*M*) was mixed with ethanolic solution of $PdCl_2.2H_2O$ (0.34 g, 2 m*M*) or chloroplatinic acid (0.41 g, 1 m*M*) or ruthenium trichloride (0.207 g, 1 m*M*) and the reaction mixtures were refluxed over steam-bath for ~2 h. Subsequently on cooling, coloured products obtained were filtered, washed with several increments of ethanol and dried completely under vacuum over P_4O_{10}. The products were crystallised with acetone and were found tlc-pure and freely soluble in DMF, DMSO and nitromethane.

In all of the present complexes ionic chlorine was estimated by adding alcoholic solution of $AgNO_3$ to the isolated and weighed complex, giving a white curdy precipitate and indicating the presence of ionic chlorine outside the coordination sphere. The ionic chlorine % were found quite in good agreement. Chemicals of AnalaR grade and metal salts of John Matheun, were used. Magnetic, absorption and infrared spectral data were taken as described earlier[1,2]. The molar conductance values in 10^{-3} *M* DMF are recorded in the Table 1.

Results and Discussion

The absorption bands from Pd^{II} complexes, *viz.* 20 800, 23 800 and 28 500 (with HS-SABTZ), 19 800, 21 900 and 26 000 (with HO-NABTZ) and 21 800, 23 000 and 26 500 cm^{-1} (with HO-INBTZ) are assigned[4] to spin-allowed transitions, *viz.* ${}^1A_{1g}\rightarrow{}^1A_{2g}$, ${}^1A_{1g}\rightarrow{}^1B_{1g}$ and ${}^1A_{1g}\rightarrow{}^1E_g$, respectively. The values of μ_{eff}, Δ_1, Δ_2, Δ_3 and LFSE, *viz.* (0.42, 24 300, 5 000, 4 200 and 83.3), (0.32, 23 300, 4 100, 3 600 and 79.9) and (0.28 B.M., 25 300 cm^{-1}, 3 200 cm^{-1}, 3 000 cm^{-1} and 86.6 kcal mol^{-1}) from Pd^{II} complexes with proposed ligands HS-SABTZ, HO-NABTZ and HO-INBTZ, respectively, revealed[5] square-planer stereochemistry around Pd^{II} metal ion. The large value of Δ_1 for the complex with HO-INBTZ corresponds to a high value of LFSE, which is considered due to larger ligand field-splitting on complexation.

From absorption spectra of Pt^{IV} complexes the bands observed at 19 000, 24 500, 26 300 and 34 700 (HS-SABTZ) ; 17 500, 18 800, 25 000 and 35 200 (HO-NABTZ) and 17 200, 20 400, 24 700 and 34 800 cm^{-1} (HO-INBTZ) are tentatively assigned[6] to ${}^1A_{1g}\rightarrow{}^3T_{1g}$, $\rightarrow{}^3T_{2g}$, $\rightarrow{}^1T_{1g}$ and $\rightarrow{}^1T_{2g}$, respectively, following octahedral field with d^6 configuration. The values of μ_{eff}, 10Dq, B, β and LFSE are calculated, *viz.* (2.12, 29 950, 525, 0.59 and 30.06), (1.37, 28 750, 403, 0.56 and 32.86) and (1.37 B.M., 28 450 cm^{-1}, 387 cm^{-1}, 0.55 and 32.52 kcal mol^{-1}) for Pt^{IV} complexes with HS-SABTZ, HO-NABTZ and HO-INBTZ, respectively, revealed[6] octahedral stereochemistry. The smaller β values calculated in the range (0.55-0.59) reveal their strong covalent character which is also supported by a small value of molar conductance.

From the present Ru^{III} complexes, the absorption bands observed at 16 950, 19 600 and 23 500 (HS-SABTZ) ; 16 000, 20 400 and 22 800 (HO-NABTZ) and 17 500, 21 900 and 24 800 cm^{-1} (HO-INBTZ) are assigned to ${}^2T_{1g}\rightarrow{}^2E_g$, ${}^2T_{1g}\rightarrow{}^2A_{2g}$ and ${}^2T_{1g}\rightarrow{}^2A_{1g}$, respectively, by following $(t_{2g})^4(e_g)^1$ configuration. The separation energy between two spin-forbidden transitions assigned to ${}^2T_{1g}\rightarrow{}^2E_g$ and ${}^2T_{1g}\rightarrow{}^2A_{1g}$, corresponds[4] to 8B. The values of 10Dq have been calculated from the ratio (Dq/B) =5.1. The energy-difference (E') between the ground state and first excited state is also calculated

TABLE 1—ANALYTICAL AND INFRARED SPECTRAL DATA FOR Pd^{II}, Pt^{IV} AND Ru^{III} COMPLEXES WITH HS-SABTZ, HO-NABTZ AND HO-INBTZ

Compd.	Colour	M.p. °C	Molar conductance in 10^{-3} *M* DMF Ω^{-1} cm² mol⁻¹	Analysis % : Found/(Calcd.) C	S	Cl/N*	Metal/H*	Ir bands (cm⁻¹) and tentati[ve] assignments* $\nu_{C=N}$ of imine-N	($\nu_{C=S}$ + $\nu_{C=N}$ + γ_{CN})	$\nu_{C=}$
$C_{18}H_{14}N_4OS_2$ (HS-SABTZ)	Light yellow	137	—	54.81 (54.54)	18.54 (19.39)	17.35* (16.96)*	4.31* (4.24)*	1 650s	1 310s	750
$C_{19}H_{16}N_4O_2S$ (HO-NABTZ)	Buff yellow	127	—	62.26 (62.63)	9.18 (8.79)	15.64* (15.38)*	4.21* (4.39)*	1 685s	1 300s	760
$C_{19}H_{16}N_4O_2S$ (HO-INBTZ)	Yellowish-red	115	—	61.96 (61.53)	9.52 (9.11)	15.27* (15.95)*	4.13* (4.27)*	1 640s	1 395s	755
[Pd(-S-SABTZ)Cl]	Orange-red	202	1.43	37.74 (38.30)	14.23 (13.60)	6.32 (7.50)	23.07 (22.68)	1 650s	1 275m	730
[Pd(-O-NABTZ)Cl]	Dark red	200	5.49	45.78 (45.13)	5.86 (6.33)	6.85 (7.02)	18.90 (18.46)	1 650s	1 275ms	735
[Pd(-O-INBTZ)Cl]	Dark red	152	0.017	44.32 (43.91)	6.18 (6.50)	6.84 (7.21)	22.25 (21.63)	1 655s	1 270ms	725
[Pt(-S-SABTZ)₂]Cl₂	Orange	120	171.5	41.27 (42.11)	14.35 (14.84)	7.27 (7.56)	24.12 (23.25)	1 635s	1 270ms	740
[Pt(-O-NABTZ)₂]Cl₂	Orange	86	183.4	48.78 (49.52)	6.63 (6.95)	7.23 (7.05)	22.12 (21.16)	1 635s	1 265ms	725
[Pt(-O INBTZ)₂]Cl₂	Orange	90	175.2	48.53 (48.27)	6.95 (7.15)	7.64 (7.23)	22.16 (21.79)	1 635s	1 270s	720
[Ru(-S-SABTZ)₂]Cl	Greyish yellow	115	94.52	44.78 (45.31)	15.85 (16.11)	4.72 (4.46)	13.05 (12.72)	1 640s	1 370ms	735
[Ru(-O-NABTZ)₂]Cl	Dull grey	98	101.6	53.14 (52.86)	7.75 (7.42)	4.04 (4.11)	12.08 (11.70)	1 645s	1 360ms	730
[Ru(-O-INBTZ)₂]Cl	Dull grey	105	98.7	50.15 (49.51)	7.52 (7.33)	3.84 (4.06)	12.08 (11.77)	1 645s	1 360ms	735

* vs = very sharp, s = sharp, m = medium, ms = medium sharp.

by using the relation $E^* = (10Dq\text{-}3F_2\text{-}20F_4)$ assuming $F_2 = 10$ cm⁻¹ and $F_4 = 1\ 000$ cm⁻¹. For the Ru^{III} complexes with HS-SABTZ, HO-NABTZ and HO-INBTZ, the value of μ_{eff}, 10Dq, B and E* are calculated as (0.25, 41 769, 819 and 21 739), (0.19, 43 400, 850 and 23 370) and (0.31 B.M., 46 512 cm⁻¹, 912 cm⁻¹ and 16 482 cm⁻¹), respectively, revealing[7] inner-orbital low-spin distorted octahedral stereochemistry of the ligands around Ru^{III} metal ion.

The sharp absorption bands observed at ~1 300 and ~750 cm⁻¹ in the free ligands, assigned[8] to ($\nu_{C=S}+\nu_{C=N}+\gamma_{CN}$) and $\nu_{C=S}$, respectively, are decreased in frequency (by 20-40 cm⁻¹) as well as weakned in intensity, revealing coordination through thio-keto-sulphur atom. The absence of the band observed in free ligands at 2 320 (HS-SABTZ), 3 300 (HO-NABTZ) and 3 180 cm⁻¹ (HO-INBTZ) assigned to ν_{SH}, ν_{OH} and ν_{OH}, respectively, ascertain the participation of the sulphur atom of SH group and oxygen atom of OH group through deprotonation on complexation under study. The sharp absorption bands observed at 1 650, 1 635 and 1 640 cm⁻¹ (in the free ligands), attributed to $\nu_{C=N}$ of immine-nitrogen do not exhibit any remarkable red/blue shift in frequency as well as decrease in their intensity, indicating non-involvement of immino-nitrogen in coordination. In all of the present complexes, the medium to weak intensity bands observed in the far-ir, region, *viz.* 550-500, 450-400 and 350-250 cm⁻¹, tentatively assigned[8] to $\nu_{M\text{-amide-N}}$, $\nu_{M\text{-S}}$ and $\nu_{M\text{-Cl}}$, respectively, also confirm the square-planer and octahedral stereochemistries of ligands HS-SABTZ, HO-NABTZ and HO-INB[TZ] around Pd^{II} and Pt^{IV}, and Ru^{III} metal io[ns] respectively.

References

1. O. L. JAIN, B. L. KHANDELWAL and P. N. MUNDLEY *Inorg. Nucl. Chem.*, 1980, **42**, 1769.
2. R. C. SAXENA, C. L. JAIN and S. C. RASTOGI, *In[org.] Chim Acta*, 1975, **16**, 103.
3. R. S VERMA, *J. Indian Chem. Soc.*, 1966, **43**, 558.
4. C. K. JORGENSON, *Acta Chem. Scand*, 1957, **11**, 151.
5. V. B. RANA, *J. Inorg. Nucl. Chem.*, 1975, **37**, 248.
6. S K. SAHANI, P. C. JAIN and V. B. RANA, *India[n] Chem., Sect. A*, 1978, **16**, 699.
7. L. R. RAMIREZ, T. A. STEPHENSON and E. S. SWITK[ES] *J. Chem. Soc., A*, 1973, 1770.
8. M. J. M. CAMPBELL, *Spectrochim. Acta, Part A*, 1968, 1149.

Studies on Suppression of Polarographic Maximum of Gallium(III) by Cationic and Anionic Surfactants and by their Mixtures *vis-a-vis* the Adsorption Characteristics

(MISS) INDU BALA and MUKHTAR SINGH*

Chemistry Department, Agra College, Agra-282 002

Manuscript received 25 June 1984, revised 6 November 1985 accepted 6 February 1986

A survey of literature reveals that suppression [of] polarographic maximum of Ga^{III} by surfacta[nts] has not been attempted so far. The pres[ent] paper reports the results of our investigations

the suppression of polarographic maximum of Ga^{III} by some cationic and anionic surfactants with special reference to the additive and antagonistics effects of their mixtures. The adsorption characteristics of cationic and anionic surfactants separately as well as in their mixtures have also been studied.

Experimental

$Ga(NO_3)_3.8H_2O$ was a Fluka (A.R.) product. All other chemicals used were of analytical reagent grade and their solutions were prepared in conductivity water. The depolariser concentration was kept at 5.0×10^{-4} *M*. $NaNO_3$ (0.05 *M*) was used as the supporting electrolyte. A Toshniwal CLO2 manual polarograph in conjunction with a Toshniwal PL 50 polyflex galvanometer was used for measuring the potential and current, respectively. Hydrogen was used for deoxygenation of the solutions. All the measurements were made at $25\pm0.1^\circ$. Saturated calomel electrode (S.C.E.) was used as a reference electrode. Electrocapillary curves were obtained by the drop-time method[1]. The dme had the following capillary characteristics (in 0.05 *M* $NaNO_3$, open circuit) : $m=3.317$ mg s^{-1}, $t=3.2$ s, $m^{2/3}t^{1/6}=2.7$ $mg^{2/3}$ $s^{-1/2}$, $h_{corr}=53.2$ cm.

Results and Discussion

Representative Figs. 1a-c depict the morphology of C-V curves of Ga^{III} in the presence of increasing concentrations of cationic and anionic surfactants separately as well as in their mixtures.

Ga^{III} under the chosen experimental conditions yields sharp maximum which occurs at -1.28 V (S.C.E.) and that it lies on the negative side of the electrocapillary zero whose potential is -0.47 V (S.C.E.) under the same experimental conditions. Since the $E_{1/2}$ of Ga^{III} (≈ -1.10 V) lies on the negative side of the electrocapillary zero, the maximum of Ga^{III} is of negative polarity[2].

Effect of increasing concentrations of surfactants on the maximum : The effect of increasing concentrations of cationic and anionic surfactants, separately as well as in their mixtures, on E_{max} and i_{max} has been studied and the values are shown in Figs. 1a-c. It is seen that E_{max} gets shifted to positive potentials as the concentration of the surfactants is increased, and i_{max} decreases, from 19.10 μA (in the absence of surfactants) to different values just before the suppression of the maximum.

Relative efficacies of surfactants in suppression of the maximum : The maximum suppression point[3] (M.S.P.) is defined as the concentration of the surfactant precisely sufficient to eliminate the maximum under consideration. It is computed by plotting the value of i_{max}/i_d *vs* log of concentration of the surfactant and extrapolating to the concentration axis at which i_{max}/i_d is unity. The M.S.P. values for different surfactants separately and in their mixtures are listed in Table 1. A perusal of Table 1 reveals that M.S.P. values for cationic surfactants are much less than those for anionic ones. It follows that the amount of ionic surfactants required to suppress the maximum of similar sign is greater than that for those possessing disimilar charges[4]. Antweiler[5] has unambiguously proved that the polarographic maximum of the first kind is due to tangential streaming of the solution with respect to the drop. The success of a suppressor depends on its capability of curbing this streaming. Since the maximum in the present study lies on the negative side of the electrocapillary zero, the cationic surfactants will move right up to the mercury surface and the anionic ones are likely to move at a distance somewhere in the double layer. A cationic surfactant will prevent streaming more effectively as compared to an anionic one with identical hydrocarbon chain. This is supported

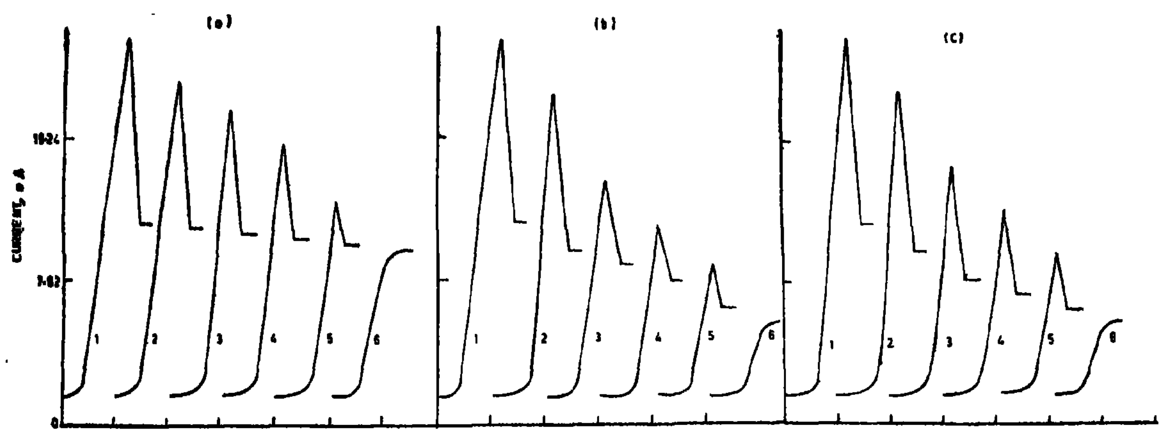


Fig. 1. C – V curves of Ga^{III} in presence of increasing concentrations of (a) LPC : (1) 0.0, (2) 1.00×10^{-6}, (3) 2.00×10^{-6}, (4) 3.00×10^{-6}, (5) 4.00×10^{-6}, (6) 4.98×10^{-6} *M* ; (b) SLS : (1) 0.0, (2) 3.00×10^{-4}, (3) 5.00×10^{-4}, (4) 1.00×10^{-3}, (5) 1.50×10^{-3}, (6) 2.00×10^{-3} *M* ; and (c) LPC+SLS : (1) 0.0, (2) $2.0\times10^{-7}+1.0\times10^{-4}$, (3) $2.5\times10^{-6}+5.0\times10^{-4}$, (4) $2.5\times10^{-6}+1.0\times10^{-3}$, (5) $2.5\times10^{-6}+1.5\times10^{-3}$, (6) $2.5\times10^{-6}+2.0\times10^{-3}$ *M*.

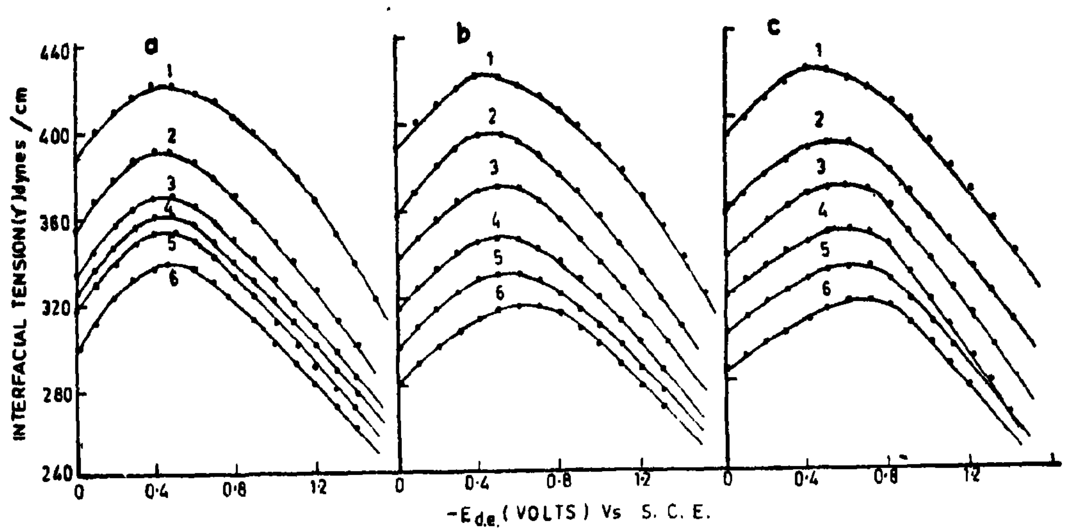


Fig. 2. Electrocapillary curves of Ga^{III} in presence of increasing concentrations of (a) LPC: (1) 0.0, (2) 1.00×10^{-6}, (3) 2.00×10^{-6}, (4) 3.00×10^{-6}, (5) 4.00×10^{-6}, (6) 4.98×10^{-6} *M*; (b) SLS: (1) 0.0, (2) 3.00×10^{-4}, (3) 5.00×10^{-4}, (4) 1.00×10^{-3}, (5) 1.50×10^{-3}, (6) 2.00×10^{-3} *M*; and (c) LPC+SLS: (1) 0.0, (2) $2.00 \times 10^{-7} + 1.0 \times 10^{-4}$, (3) $2.5 \times 10^{-6} + 5.0 \times 10^{-4}$, (4) $2.5 \times 10^{-6} + 1.0 \times 10^{-3}$, (5) $2.5 \times 10^{-6} + 1.5 \times 10^{-3}$, (6) $2.5 \times 10^{-6} + 2.0 \times 10^{-3}$ *M*.

TABLE 1—COMPARATIVE VALUES OF M.S.P. FOR THE MAXIMUM OF Ga^{III} IN RESPECT OF CATIONIC AND ANIONIC SURFACTANTS SEPARATELY AND IN THEIR MIXTURES

Surfactant	M.S.P. *M*	Cationic+Anionic surfactants	M.S.P. *M*
Cationic			
		LPC+SLS	1.97×10^{-3}
LPC	4.93×10^{-6}	LPC+Manoxol-OT	4.97×10^{-4}
CPC	8.96×10^{-6}	LPC+Tergitol-7	2.93×10^{-3}
CPB	5.93×10^{-6}	CPC+SLS	2.45×10^{-3}
CTAB	4.94×10^{-6}	CPC+Manoxol-OT	3.59×10^{-4}
CDBAC	4.96×10^{-6}	CPC+Tergitol-7	1.95×10^{-3}
Anionic			
		CPB+SLS	1.96×10^{-3}
SLS	1.95×10^{-3}	CPB+Manoxol-OT	3.57×10^{-4}
Manoxol-OT	5.12×10^{-4}	CPB+Tergitol-7	2.97×10^{-3}
Tergitol-7	1.90×10^{-3}	CTAB+SLS	2.96×10^{-3}
		CTAB+Manoxol-OT	3.56×10^{-4}
		CTAB+Tergitol-7	1.93×10^{-3}
		CDBAC+SLS	2.45×10^{-3}
		CDBAC+Manoxol-OT	2.58×10^{-4}
		CDBAC+Tergitol-7	2.95×10^{-3}

by the fact that LPC is more effective than SLS, though both the surfactants have the same carbon chain length.

On the basis of M.S.P. values, the following order for the relative efficacies of cationic and anionic surfactants in suppressing the negative maximum of Ga^{III} has been established: cationic surfactants, LPC > CTAB > CDBAC > CPB > CPC; anionic surfactants, Manoxol-OT > Tergitol-7 > SLS.

Electrocapillary curves and adsorption characteristics of surfactants : The electrocapillary curves in the presence of different concentrations of cationic and anionic surfactants separately as well as in their mixtures, have been shown in typical Figs. 2a-c. In the absence of a surfactant, the potential of the electrocapillary zero is -0.47 V (*vs* S.C.E.) under the chosen experimental conditions. In the presence of increasing concentrations of surfactants, however, a change in the shape of the electrocapillary curve occurs. The electrocapillary zero gets shifted to less negative potentials in the case of cationic surfactants and to more negative potentials in the case of anionic surfactants, but in the case of mixtures of the two, this shift occurs to more negative potentials.

The values of interfacial tension have been obtained from electrocapillary curves for the potential (-0.9 V), on the negative side of the electrocapillary zero. It is seen that interfacial tension (γ) decreases as the concentration of the surfactants increases. This implies positive adsorption as is shown by increasing positive values of ΓRT calculated by Gibb's adsorption equation[6],

$$\Gamma = -\frac{C}{RT} \cdot \frac{d\gamma}{dC}$$

The value of $d\gamma/dC$ has been obtained from γ *vs* C plots. Thus, the addition of surfactants leads to their adsorption on the electrode surface and that they are carried away by the motion of the mercury and of the electrolyte to the place of greatest surface tension They accumulate there and decrease the surface tension thereby creating a force against the streaming and ultimately bring about the suppression of the polarographic maximum.

Additive and antagonistic effects of mixtures of cationic and anionic surfactants : The additive and antagonistic effects of mixtures of cationic and anionic surfactants have been ascertained by determining their M.S.P. values separately and in their

mixtures. The M.S.P. values in respect of various surfactants, *viz.* LPC, CPC, CPB, CTAB and CDBAC (cationic) ; SLS, Manoxol-OT and Tergitol-7 (anionic) ; and the mixtures, LPC+SLS, LPC+Manoxol-OT, LPC+Tergitol-7 ; CPC+SLS, CPC+Manoxol-OT, CPC+Tergitol-7, CPB+SLS, CPB+Manoxol-OT, CPB+Tergitol-7, CTAB+SLS, CTAB+Manoxol-OT, CTAB+Tergitol-7, CDBAC+SLS, CDBAC+Manoxol-OT, and CDBAC+Tergitol-7, have been determined and listed in Table 1. A perusal of Table 1 shows that the M.S.P. values in respect of the mixtures, LPC+SLS, LPC+Manoxol-OT, LPC+Tergitol-7, CPC+SLS, CPC+Manoxol-OT, CPC+Tergitol-7, CPB+SLS, CPB+Manoxol-OT, CPB+Tergitol-7, CTAB+SLS, CTAB+Manoxol-OT, CTAB+Tergitol-7, CDBAC+SLS, CDBAC+Tergitol-7 are much larger than those for individual surfactants thereby indicating antagonistic effects of these mixtures in the suppression of the maximum of Ga^{III}. This is further supported by the fact that the values of ΓRT, in each case, at the concentration of surfactant at which the maximum gets just suppressed are lower for these mixtures than those for individual surfactants.

It is interesting to note that M.S.P. value in respect of the mixture of CDBAC and Manoxol-OT is equal to half of the individual M.S.P. value, thereby indicating that this mixture shows neither additive nor antagonistic effect in suppressing the maximum of Ga^{III}. Further, it is also interesting to note that none of the probable mixtures of the two surfactants (*i.e.* cationic and anionic) shows the additive effect in the suppression of negative polarographic maximum of Ga^{III}.

Acknowledgement

The award of a Senior Research Fellowship by C.S.I.R., New Delhi, to one of the authors (I.B.) is gratefully acknowledged.

References

1. P. Zuman and I. M. Kolthoff, "Progress in Polarography", Interscience, New York, 1962, Vol. I, p. 88.
2. J. Heyrovsky and J. Kuta, "Principles of Polarography", Academic Press, New York, 1966, p. 299.
3. E. L. Colichman, *J. Am. Chem. Soc.*, 1950, **72**, 4036.
4. W. U. Malik and R. Haque, *J. Polarogr. Soc.*, 1962, **8**, 62.
5. H. J. Antweiler, *Z. Elektrochem.*, 1937, **43**, 596 ; 1938, **44**, 719, 888.
6. J. W. Gibbs, *Trans. Connecticut Acad.*, 1876, 3 ; "Collected Works", 1928, Vol. I, p. 230 ; J. Rice, "Commentary on the Scientific Writings of Gibbs", Yale University Press, New Haven, 1937, Vol. I.

Viscosity of Electrolyte Solutions

PRIYANATH HALDAR and DILIP K. MAJUMDAR*

Department of Chemistry, Kalyani University, Kalyani-741 235

Manuscript received 5 August 1985, accepted 6 February 1986

THE search for an equation of fluidity which would account for the variation of viscosity of electrolyte solutions with concentration over a wide range dates back to the early days of solution chemistry. But till now hardly any progress has been achieved in concentrated electrolyte solutions, particularly beyond 0.1 *M*. In this respect the model proposed by Goldsack and Franchetto[1] who based their derivation of the equation of fluidity on the absolute rate theory successfully explains the viscosity results of simple electrolyte in highly concentrated solutions, extending nearly to saturation. Another approach was made by Angell[2,3] who adopted the equation of fluidity based on the free volume theory of liquids to fused salt mixtures and electrolyte solutions by proposing that the only parameter dependent on the electrolyte concentration is T_0, the glass transition temperature. Assuming a linear dependence of T_0 on the electrolyte concentrations, N in equivalent per litre, Angell[3] put forward the following equation of fluidity of electrolyte solution,

$$1/\eta = Ae^{-k'/(N_0 - N)} \quad (1)$$

where, A and k' are two parameters supposed to be independent of composition and N_0 is the hypothetical concentration at which the glass transition would occur.

Roy Choudhury and Majumdar[4] modified equation (1) by incorporating the condition that $\eta \rightarrow \eta_0$, the viscosity of the solvent as N→O, so that it becomes

$$\ln \eta_{rel} = \frac{k'N}{N_0(N_0 - N)} \quad (2)$$

Equation (2) has been shown to be valid for the concentration dependence of the viscosity of quaternary ammonium halides[4-6] in aqueous solutions for wide range of concentration for suitable values of N_0. Moreover, this equation in the dilute solution range led to Jones-Dole equation without the Falkenhagen term and one could identify the k'/N_0^2 with the B coefficient of Jones-Dole equation.

In view of these results, it would be worthwhile to test the validity of equation (2) for an electrolyte in a non-aqueous solvent and at several temperatures. We have examined equation (2) with respect to temperature dependence of the viscosity of simple electrolytes, KCl and NaCl in aqueous solutions as well as the concentration dependence of viscosity at a fixed temperature of lithium chloride in *N,N*-dimethylformamide.

Experimental

Potassium chloride (KCl) and sodium chloride (NaCl) were of AnalaR quality and the purity of the samples checked by the determination of chloride volumetrically.

N,N-Dimethylformamide (E. Merck, India) was freshly distilled under reduced pressure before use. The solvent having density 0.9350 g cm^{-3} at 35° compared favourably with the literature value. Stock solutions of the alkali halides were prepared by direct weighing and filtered to remove any suspended impurities and the concentration of the alkali halide determined by titration against standard silver nitrate solution. The solution of desired concentration was made by appropriate dilution with double-distilled water. The solution of lithium chloride in *N,N*-dimethylformamide was made by direct weighing and the desired concentration made by appropriate dilution with freshly distilled *N,N*-dimethylformamide.

All the measurements of density and time of flow were taken in a constant temperature water-bath controlled to $\pm 0.05°$. The time of flow was measured in a suspended level Ubbelohde viscometer by a stop watch reading upto 1/10th of a second. A bicapillary pycnometer was employed for the determination of density.

Results and Discussion

Viscosity of KCl and NaCl in aqueous solutions : The viscosity of KCl and NaCl in aqueous solutions were determined over a wide range of concentration extending to saturation at three different temperature, 35, 40 and 45°. It was seen that these data nicely fit equation (2). The plot of ln η_{rel} *vs* $N/(N_0 - N)$ produces straight line through the origin at the temperatures studied for suitable value of N_0 (Figs. 1 and 2). The value of N_0 was chosen

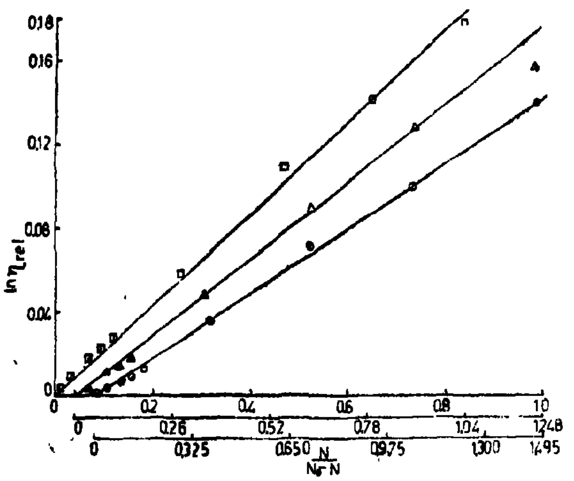


Fig. 1. Plot of ln η_{rel} *vs* $N/(N_0 - N)$ for KCl at different temperature : (⊙) 35.0, (△) 40.0 and (⊡) 45.0°.

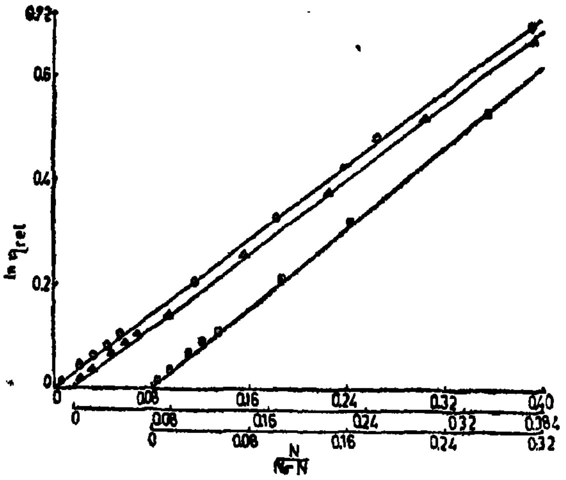


Fig. 2. Plot of ln η_{rel} *vs* $N/(N_0 - N)$ for NaCl at different temperature : (⊙) 35.0, (△) 40.0 and (⊡) 45.0°.

by trial and error method described earlier[4]. The set of N_0 and k' which produced minimum deviation between observed η_{rel} and those calculated according to equation (2) is accepted as the best choice. These values of N_0 and k' for KCl and NaCl are given in Table 1. It is seen in Table 1 that the value of N_0 increases with temperature.

TABLE 1—VALUES OF N_0 AND k' FOR ELECTROLYTES IN WATER

	Temp. °C	N_0	k'	k'/N_0^2	B*
KCl	35.0	7.2	0.6988	0.0182	0.0098
	40.0	7.8	1.0520	0.0182	(0.0242)
	45.0	9.4	2.0587	0.028	—
NaCl	35.0	19.4	34.76	0.092	0.0900
	40.0	19.9	36.50	0.090	(0.0982)
	45.0	20.2	38.71	0.096	—

* Values of B-coefficient are taken from literature (Ref. 7) and values in parentheses refer to 42.5°.

In Table 1 are given the values of k'/N_0^2 which compare favourably with the B coefficient of the Jones-Dole equation as given in the literature[7].

Viscosity of LiCl in N,N-*dimethylformamide :* The viscosity studies of LiCl in *N,N*-dimethylformamide covers a concentration range 0.3-2.5 *M* at 35°. When the relative viscosity is treated by means of Jones-Dole equation, we find steeply ascending curve as the concentration of lithium chloride increases (Fig. 3). This is not unexpected since it is already known that the Jones-Dole equation has been found to be satisfactory only upto 0.1 *M*. As the studies of the viscosity in the present investigation begins with a concentration > 0.3 *M*, it is obvious that the valid concentration range for the application of Jones-Dole equation has been far exceeded. Naturally we treat our data with Angell's equation, rearranged as equation (2). It

is seen that the plot of equation (2) produced a straight line passing through the origin for $N_0 = 27.0$ (Fig. 4). The value of N_0 has been selected

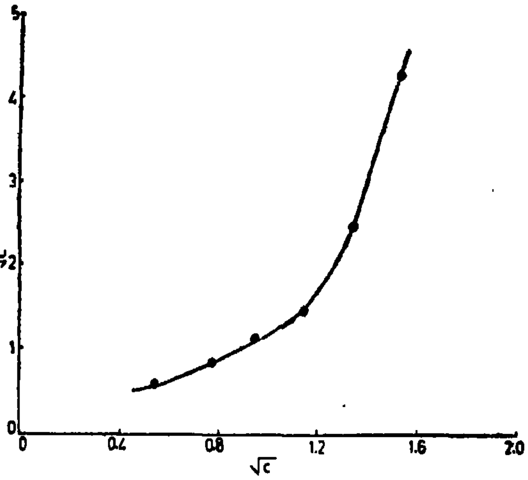


Fig. 3. Jones-Dole plot for LiCl in DMF at 35.0°.

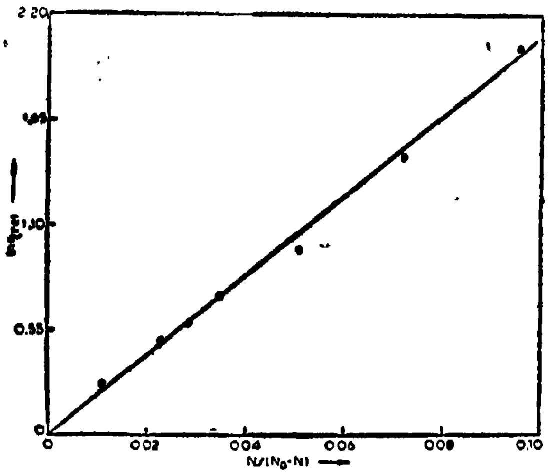


Fig. 4. Plot of $\ln \eta_{rel}$ vs $N/(N_0 - N)$ for LiCl in DMF at 35.0°.

by trial and error method, and the value of N_0 and k' are given in Table 2. Further it is seen that the

Table 2—Values of N_0 and k' for Lithium Chloride in DMF at 35.0°

	N_0	k'	k'/N_0^2
LiCl	27.0	563.92	0.77

value of k'/N_0^2 for LiCl in *N,N*-dimethylformamide is 0.7 ; this value falls in a similar range for LiCl in other amide solvent[8], *N*-methylpropionamide and *N*-methylformamide.

Acknowledgement

The authors thank U.G.C., New Delhi, for the award of a Fellowship to one of them (P.H.).

References

1. D. E. Goldsack and R. C. Franchetto, *Can. J. Chem.*, 1978, **56**, 1442.
2. C. A. Angell, *J. Phys. Chem.*, 1966, **70**, 2793.
3. C. A. Angell, *J. Chem. Phys.*, 1967, **46**, 4673.
4. K. Roy Choudhury and D. K. Majumdar, *Electrochim. Acta*, 1983, **28**, 23.
5. K. Roy Choudhury and D. K. Majumdar, *Electrochim. Acta*, 1983, **28**, 597.
6. K. Roy Choudhury and D. K. Majumdar, *Electrochim Acta*, 1984, **29**, 1371.
7. R. A. Robinson and R. H. Stokes, "Electrolyte Solutions", 2nd. ed., Butterworths, London, 1959.
8. P. P. Rastogi., *Bull. Chem. Soc. Jpn.*, 1970, **43**, 2442.

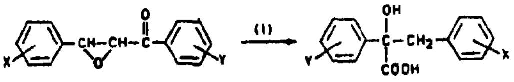
Spectral Analysis of some α-Benzylmandelic Acids

R. S. RAGHAVAN* and N. JAYACHANDRAMANI

Department of Chemistry, Pachaiyappa's College, Madras-600 030

Manuscript received 5 May 1983, revised 9 September 1985, accepted 17 February 1986

HYDROXY acids are very useful in organic synthesis, due largely to the versatility of the hydroxyl group in undergoing a variety of reactions and hence their synthesis is of considerable interest. Baker and Robinson[1] reported that chalcone epoxide on treatment with alkali yields α-benzylmandelic acid after undergoing an initial elimination reaction entailing epoxide ring opening followed by a benzil-benzilic acid type rearrangement. Bharara *et al.*[2] reported a similar observation in the case of 2-benzyloxychalcone epoxides. However, a systematic spectral analysis of α-benzylmandelic acids has not been reported in the literature. In this note, we report melting point, microanalytical, ir and nmr spectral data of seven α-benzylmandelic acids, prepared[1,2] by the action of alcoholic alkali (reflux, 4 h) on the appropriate chalcone epoxides. The latter were prepared[3,4] from the respective chalcones by treatment with alkaline hydrogen peroxide.



(1) (2)

a X=Y=H
b X=*p*-CH$_3$; Y=H
c X=*p*-Cl ; Y=H
d X=*o*-Cl ; Y=H
e X=H ; Y=*p*-Cl
f X=*m*-Cl ; Y=H
g X=*p*-CH$_3$; Y=*p*-Cl

Reagents : (i) Alcoholic NaOH reflux ; H$_2$O, H$^{\oplus}$.

Some characteristic features of the nmr spectra of the α-benzylmandelic acids are (*i*) the two methylene protons of the benzyl group are, as expected, non-equivalent and show geminal coupling (*J* 11-15 Hz), (*ii*) the protons of the chlorinated aromatic ring in **2e** and **2g** appear as AB doublets instead of the expected AA 'BB' pattern, and

(iii) except in case of **2b** and **2d**, the hydroxyl protons could not be traced.

Compound **2a** : M.p. 161-62° (ethanol) (lit[1]. 162°) (Found : C, 74.70 ; H, 5.85. $C_{15}H_{14}O_3$ requires : C, 74.38 ; H, 5.79%) ; ν_{max} 3 440 (OH) and 1 740 cm^{-1} (C=O) ; τ (80 MHz, DMSO-d_6) 2.46-2.85 (10H, m, Ar), 6.64 and 6.79 (1H, d each, J 11 Hz, benzylic).

Compound **2b** : M.p. 178-79 (ethanol) (Found : C, 74.20 ; H, 6.24. $C_{16}H_{16}O_3$ requires : C, 75.0 ; H, 6.25%) ; ν_{max} 3 419 (OH) and 1 724 cm^{-1} (C=O) ; τ (80 MHz, DMSO-d_6) 2.35-3.02 (9H, m, Ar), 5.78 (1H, s, OH), 6.70 and 6.86 (1H, d each, J 13.5 Hz, benzylic), 7.79 (3H, s, CH_3).

Compound **2c** : M.p. 203-05° (ethanol) (Found : C, 64.61 ; H, 4.62. $C_{15}H_{13}O_3Cl$ requires : C, 65.10 ; H, 4.70%) ; ν_{max} 3 424 (OH) and 1 724 cm^{-1} (C=O) ; τ (80 MHz, DMSO-d_6) 2.47-2.81 (9H, m, Ar), 6.64 and 6.77 (1H, d each, J 11 Hz, benzylic).

Compound **2d** : M.p. 136-38° (ethanol) (Found : C, 65.09 ; H, 4.71. $C_{15}H_{13}O_3Cl$ requires : C, 65.10 ; H, 4.70%) ; ν_{max} 3 450 (OH) and 1 719 cm^{-1} (C=O) ; τ (90 MHz, $CDCl_3$) 2.3-3.0 (9H, m, Ar), 4.5-5.2 (OH), 6.2 and 6.4 (1H, d each, J 15 Hz, benzylic).

Compound **2e** : M.p. 194-95° (ethanol) (Found : C, 65.24 ; H, 4.82. $C_{15}H_{13}O_3Cl$ requires : C, 65.10 ; H, 4.70%) ; ν_{max} 3 414 (OH) and 1 727 cm^{-1} (C=O) ; τ (200 MHz, DMSO-d_6) 2.38 and 2.64 (2H, d each, J 8.6 Hz, *p*-disubstd. Ar), 2.85 (5H, s, Ar), 6.59 and 6.78 (1H, d each, J 14.6 Hz, benzylic).

Compound **2f** : M.p. 129-30° (ethanol) (Found : C, 64.40 ; H, 4.62. $C_{15}H_{13}O_3Cl$ requires : C, 65.10 ; H, 4.70%) ; ν_{max} 3 424 (OH) and 1 724 cm^{-1} (C=O) ; τ (200 MHz, DMSO-d_6) 2.41-2.91 (9H, m, Ar), 6.57 and 6.82 (1H, d each, J 13.5 Hz, benzylic).

Compound **2g** : M.p. 175-76° (ethanol) (Found : C, 66.30 ; H, 5.17. $C_{16}H_{15}O_3Cl$ requires : C, 66.10 ; H, 5.16%) ; ν_{max} 3 412 (OH) and 1 723 cm^{-1} (C=O) ; τ (200 MHz, DMSO-d_6) 2.57 and 2.64 (2H, d each, J 8.5 Hz, *p*-disubstd. Ar), 2.96-3.17 (4H, m, Ar), 6.66 and 6.88 (1H, d each, J 13.2 Hz, benzylic) and 7.51 (s, OH), 7.8 (3H, s, CH_3).

All the ir spectra were measured in KBr pellets. TMS was used as internal standard in all nmr measurements.

Acknowledgement

The authors thank Dr. B. R. Pai, Consultant, Research and Development, Amrutanjan Ltd., Madras, and Dr. V. V. Krishnamurthy, Hydrocarbon Research Institute, University of Southern California, Los Angeles, U.S.A., for the spectral data. The authors are grateful to Dr. R. Balasubramanian, Lecturer in Organic Chemistry, University of Madras, for microanalytical data.

References

1. W. Baker and R. Robinson, *J. Chem. Soc.*, 1932, 1798.
2. S. C. Bharara, A. C. Jain and T. R. Seshadri, *Tetrahedron*, 1964, 20, 1141.
3. G. B. Payne and P. H. Williams, *J. Org. Chem.*, 1959, 24, 54.
4. C. A. Bunton and G. J. Minkoff, *J. Chem. Soc.*, 1949, 665 ; R. D. Temple, *J Org. Chem.*, 1970, 35, 1275.

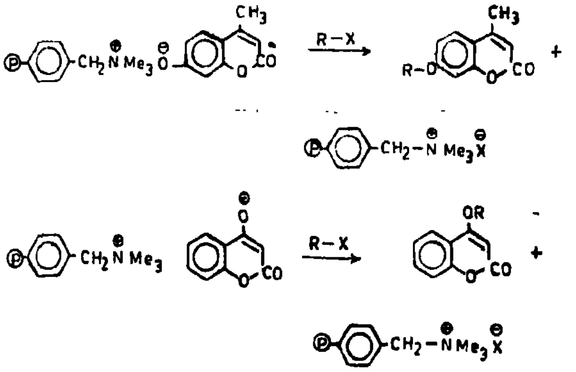
Polymer supported Hydroxycoumarin Anion. Convenient Method for *O*-Alkylation of Hydroxycoumarin

J. G. DESHMUKH, M. H. JAGDALE, R. B. MANE
and
M. M. SALUNKHE*

Department of Chemistry, Shivaji University, Kolhapur-416 004

Manuscript received 31 October 1985, accepted 17 February 1986

THE reagents supported on insoluble polymers have found wide applications during the last decade in various fields, particularly in organic synthesis[1]. In continuation of our work on polymer supported reactions[2] and in view of the importance of *O*-alkylated hydroxycoumarins as a basic compound in drug industry[3], a simple and efficient method is now reported for the *O*-alkylation of hydroxycoumarins. The use of anion-exchange resin for *O*-alkylation of hydroxycoumarins which combine the advantage of solid phase synthesis and anionic activation. Owing to the effectiveness of this system, extraordinarily mild reaction conditions can be employed.

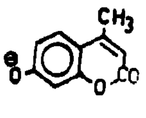
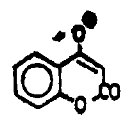


Experimental

Alkyl halide in methanol was reacted with hydroxy coumarin anion bound to the ion-exchange resin. Alkylation was complete within 6 to 10 h at room temperature giving quantitative yields of products in essentially pure form. The results are summarised in Table 1.

Amberlyst A-26 hydroxycoumarin anion : Commercial strongly basic anion-exchange resin in the

TABLE 1—*O*-ALKYLATION OF HYDROXYCOUMARINS WITH ALKYL HALIDES AT ROOM TEMPERATURE

Anion	Alkylating agent	Reaction time h	Yield %	M.p.* °C
	CH_3I	6	99	157 (159)[a]
	C_2H_5I	8	96	95
	$C_6H_5CH_2Cl$	10	99	85
	$CH_2=CHCH_2Br$	10	100	102
	$CH_3CH_2CH_2I$	10	96	82
	CH_3I	6	99	124 (124)[b]
	C_2H_5I	8	96	185 (186)[b]
	$C_6H_5CH_2Cl$	8	90	110
	$CH_2=CHCH_2Br$	6	96	100
	$CH_3CH_2CH_2CH_2I$	10	90	88
	$CH_3CH_2CH_2I$	10	95	92

*Literature value in parenthesis. [a]J. M. KAUFFMAN, *Appl. Opt.*, 1981, 19, 3431. [b]Ref. 3.

chloride form (Amberlyst A-26) packed in a column was washed with aqueous 5% sodium salt of hydroxycoumarin until complete removal of chloride ion. The resin was then successively washed with water, ethanol and benzene and finally dried *in vacuo* at 50° over phosphorus pentoxide for 12 h. The exchange capacity was determined by passing aqueous 1 *N* sodium chloride (100 ml) through the resin (0.3 g) in a column. The amount of hydroxycoumarin anion in the eluent was titrated with 0.01 *N* hydrochloric acid using methyl orange as indicator. The product I contains 1.2 mmol hydroxycoumarin per g of resin and product II 1.4 mmol hydroxy coumarin per g of resin.

Alkylation procedure : Amberlyst A-26 hydroxycoumarin anion form (containing 5 mmol hydroxycoumarin) in methanol (15 ml) was stirred with an appropriate alkyl halide (5.01 mmol) in a stoppered flask. After completion of the reaction the resin was removed by filtration and washed with methanol. The distillation of the solvent furnished corresponding alkylated product in quantitative yield in essentially pure form. The products were characterised by comparison of the melting points, ir and nmr spectra with those of authentic samples. The resin used may, in all cases, be easily regenerated by washing with hydrochloric acid.

Acknowledgement

One of the authors (J.G.D.) is grateful to U.G.C., New Delhi, and Shri Swami Vivekanand Shikshan Sanstha, Kolhapur for financial support.

References

1. A. AKELAH and D. C. SHERRINGTON, *Chem. Rev.*, 1983, **81**, 557.
2. A. R. SANDE, M. H. JAGDALE, R. B. MANE and M. M. SALUNKHE, *Tetrahedron Lett.*, 1984, **25** 3501.
3. A. K. DAS GUPTA, R. M. CHATTERJEE and K. R. DAS, *Indian J. Chem., Sect. B*, 1981, **20**, 511.

Substituted 1,8-Naphthyridines. Part-III. Synthesis and Biological Activity of some 1,8-Naphthyridine Derivatives

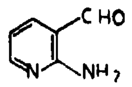
K. VIJAYENDER REDDY*, K. MOGILAIAH
and
B. SREENIVASULU

Department of Chemistry, Kakatiya University, Warangal-506 009

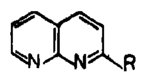
Manuscript received 16 August 1985, accepted 24 December 1985

1,8-Naphthyridine derivatives have been reported to possess antibacterial[1-6] and antimalarial[7,8] activities. Nalidixic acid (1-ethyl-3-carboxy-7-methyl-1,8-naphthyridin-4-one) has been found to be particularly effective against gram-negative bacteria[9] found in chronic urinary tract infections. Various 2,3-disubstituted-1,8-naphthyridines have been found to be associated with diuretic activity[10,11]. In view of this, it was thought worthwhile to synthesise a series of unreported 2-substituted-1,8-naphthyridines and test them for their biological activity.

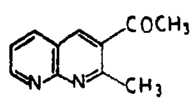
The present communication deals with a one-step synthesis of 2-aryl-1,8-naphthyridines (2), involving the Friedlander condensation of 2-aminonicotinaldehyde (1) with arylmethyl ketones in glacial acetic acid with a trace of concentrated sulphuric acid. The same reaction was also carried out in alcohol medium with a few drops of piperidine. The yields are better under acid conditions. The structures of these compounds have been established by elemental analyses and spectral data. The ir spectra of 2 showed bands at 1 600 (C=N), 1 590, 1 540, 1 420, 1 300 and 800 cm^{-1}. The mass spectra of 2 exhibited strong molecular ion peaks consistent with their elemental analyses. The mass spectra of 2-*p*-chloro-



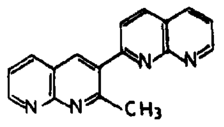
(1)



(2)



(3)



(4)

phenyl and 2-nitrophenyl 2 showed strong M^+ peaks at m/z 240 and 251, respectively. The mass spectrum of 2 ($R=p$-$Cl.C_6H_4$) showed strong M^+ peaks at m/z 240 (M^+, 84%), 239 ($M^+ - H$, 30), 205 ($M^+ - Cl$, 10), 204 $M^+ - Cl - H$, 17), 179 ($M^+ - Cl - C_2H_2$, 10), 178 ($M^+ - Cl - HCN$, 12), 177 (204 − HCN, 17), 152 (179 − HCN, 9), 151 (12), 103 (9), 102 (25), 77 (11),

* Department of Chemistry, CKM Arts & Science College, Warangal-506 006.

TABLE 1—PHYSICAL DATA OF 2-ARYL-1,8-NAPHTHYRIDINES (2)*

Sl. no.	R	M.p.** °C	Yield %	Molecular formula	N% Found/ (Calcd.)
1.	Phenyl	116	80	$C_{14}H_{10}N_2$	13.65 (13.59)
2.	4-Methylphenyl	147	80	$C_{15}H_{12}N_2$	12.81 (12.72)
3.	4-Methoxyphenyl	148	80	$C_{15}H_{12}N_2O$	11.98 (11.87)
4.	2-Hydroxyphenyl	188	78	$C_{14}H_{10}N_2O$	12.70 (12.61)
5.	4-Hydroxyphenyl	254	79	$C_{14}H_{10}N_2O$	12.76 (12.61)
6.	3-Nitrophenyl	219	90	$C_{14}H_9N_3O_2$	16.78 (16.73)
7.	4-Nitrophenyl	263	86	$C_{14}H_9N_3O_2$	16.80 (16.73)
8.	4-Bromophenyl	217	87	$C_{14}H_9N_2Br$	9.74 (9.83)
9.	2-Pyridyl	148	93	$C_{13}H_9N_3$	20.35 (20.29)
10.	3-Pyridyl	142	90	$C_{13}H_9N_3$	20.41 (20.29)
11.	4-Pyridyl	168	92	$C_{13}H_9N_3$	20.39 (20.29)
12.	2-Naphthyl	165	86	$C_{18}H_{12}N_2$	10.99 (10.94)
13.	1-Naphthyl	134	85	$C_{18}H_{12}N_2$	11.01 (10.94)
14.	4-Chlorophenyl	202	92	$C_{14}H_9N_2Cl$	11.86 (11.67)
15.	2-Hydroxy-4-chlorophenyl	161	82	$C_{14}H_9N_2OCl$	10.50 (10.30)
16.	2-Hydroxy-5-methylphenyl	190	80	$C_{15}H_{12}N_2O$	11.79 (11.86)
17.	2-Hydroxy-5-nitrophenyl	240	80	$C_{14}H_9N_3O_3$	15.70 (15.73)
18.	Biphenyl	186	83	$C_{20}H_{14}N_2$	9.91 (9.93)
19.	2-Furyl	146	90	$C_{12}H_8N_2O$	14.18 (14.29)
20.	2-Thienyl	133	92	$C_{12}H_8N_2S$	13.31 (13.20)

* All compounds gave satisfactory analyses for C and H.

** Solvents for crystallisation : Sl. no. 1,2-cyclohexane ; 5-ethylacetate ; 7,19-chloroform ; 8,12,14,18-ethanol ; 16,17-aqueous acetic acid ; and benzene for the rest.

76 (26) and 75 (27). The pmr spectrum of **2** (R = p-$Cl.C_6H_4$) in $CDCl_3$ showed two multiplets centred at δ 8.5 and 9.3 assigned to C-5 and C-7 protons, respectively. The protons at C-3, C-4 and C-6 on naphthyridine framwork appeared along with four aromatic protons as a complex multiplet at δ 7.5-8.3. Finally, the formation of **2** was confirmed by the synthesis of 2-phenyl-1,8-naphthyridine by the method of Hawes and Wibberley[12]. Physical data of these compounds are recorded in Table 1.

The condensation of acetylacetone with **1** in a 1 : 2 molar ratio in ethanol in presence of a few drops of piperidine gives 2-methyl-3-(1,8-naphthyridin-2-yl)-1,8-naphthyridine (**4**). The formation of the same compound was confirmed by adopting an alternate method involving the Friedlander condensation of 2-methyl-3-acetyl-1,8-naphthyridine (**3**) with **1** under the same conditions. The ir spectrum of **4** exhibited strong band at 1 600 cm^{-1} (C=N). The spectrum also showed bands at 1 550, 1 500, 1 370, 920 and 850 cm^{-1}. The pmr spectrum in $CDCl_3$+DMSO-d_6 resonated a three proton singlet at δ 3.1 assigned to methyl group. The C-7 protons on both the naphthyridine moieties appeared as multiplet centred at δ 9.5. The remaining seven protons appeared as a complex multiplet at δ 7.6-8.5. The mass spectrum of **4** showed strong M^+ peaks at m/z 272 (M^+, 72%), 271 (M^+ −H, 100), 245 (M^+ −H−C_2H_2, 15), 244 (M^+ −H−HCN, 12), 219 (7), 218 (11), 217 (12), 192 (8), 191 (7), 142 (4), and 129 (16).

Antibacterial activity : Twelve compounds of the series were evaluated for their bacterial activity against *Bacillus megaterium* (gram +ve) and *Proteus vulgaris* (gram −ve), using the filter paper disc method[13]. Two different concentrations of twelve compounds (360 and 600 μg/disc) were prepared and 25 Whatman filter paper (No. 1) discs (6 mm dia) were dipped and the solutions were allowed to evaporate. The paper discs with different com-

pounds were placed aseptically on petriplates containing nutrient agar seeded with different bacteria and incubated for 72 h at 37±1°. At the end of the incubation period, the zone of growth inhibition was measured an expressed in mm. At least 10 paper discs were observed and repeated twice. The results are summarised in Table 2.

Table 2—Antibacterial Activity of 2

Sl. no.*	Concn. µg/disc	Inhibition zone (mm)	
		B. megaterium	*P. vulgaris*
1.	360	1.2	3.0
	600	2.0	4.0
2.	360	1.0	3.2
	600	2.2	3.6
3.	360	–	3.0
	600	2.0	4.8
4.	360	–	1.0
	600	–	2.8
5.	360	–	–
	600	–	–
6.	360	1.4	–
	600	2.0	1.8
7.	360	–	–
	600	–	2.0
8	360	–	1.0
	600	–	2.0
9.	360	–	–
	600	1.3	1.0
10.	360	–	–
	600	1.0	1.2
11.	360	1.0	1.0
	600	1.4	1.8
12.	360	–	–
	600	1.0	1.0

(–)=No inhibition.
* Referred to as in Table 1.

Anthelmintic activity : Three selected compounds (sl. no. 9, 10 and 11) werescreened for their anthelmintic activity using the method of Seifter[14] on five Amphistone parasites, *Fischoederius cobboldii*, *Fischoederius elongatus*, *Gastrothylax crumenifer*, *Cotylophoron cotylophorum* and *Paramphistomum cervi*. All the three compounds exhibited helminthecidal property against all the organisms tested. However, the degree of toxicity varied with the compound. Compound 9 was found to be more effective in comparison with the other two, but it was less effective than the drug mebendazole. It was suggested that 80% inhibition of glucose uptake was possible as observed by the compound 9. The other two compounds (sl. no. 10 and 11) showed an inhibition of 76%. Compared to mebendazole these have very less activity. It is concluded from these results that 2-(pyridyl)-1,8-naphthyridines do have the antihelmintic property. The degree of toxicity is found to depend upon the position of the pyridyl group.

Experimental

Melting points were taken in open capillary tubes in sulphuric acid-bath and are uncorrected. The purity of all the compounds was checked by tlc. Ir spectra were run in nujol on a Perkin-Elmer 283 spectrophotometer, pmr spectra on a Varian 60 MHz spectrometer using TMS as the internal reference, and the mass spectra on a varian MAT CM-7 instrument at 70 eV.

2-Aryl-1,8-naphthyridine (**2**) *:* A mixture of 2-aminonicotinaldehyde (**1** ; 0.1 mol) and appropriate aryl methyl ketone (0.1 mol) was refluxed in glacial acetic acid (30 ml) in the presence of a catalytic amount of concentrated sulphuric acid for 3 h. The reaction mixture was allowed to cool and poured onto crushed ice. The separated solid was filtered and recrystallised from a suitable solvent to give **2** (Table 1).

2-Methyl-3-acetyl-1,8-naphthyridine (**3**) *:* To an equimolar mixture of **1** (0.1 mol) and acetylacetone (0.1 mol) was added ethanol (20 ml) and a few drops of piperidine. The mixture was refluxed for 3 h, and cooled. The separated solid was filtered and recrystallised from ethanol, (90%), m.p. 146° (lit.[15] 146-7°).

2-Methyl-3-(1,8-naphthyridin-2-yl)-1,8-naphthyridine (**4**) *: Method-A :* **1** (0.2 mol) and acetylacetone (0.1 mol) were refluxed in ethanol (20 ml) in the presence of a few drops of piperidine for 12 h. The reaction mixture was allowed to cool. The solid thus obtained was filtered and recrystallised from benzene, (65%), m.p. 184° (Found : C, 74.90 ; H, 4.38 ; N, 20.55. $C_{17}H_{12}N_4$ requires : C, 75.00 ; H, 4.41 ; N, 20.59%).

Method-B : An equimolar mixture of **1** (0.1 mol) and **3** (0.1 mol) was refluxed in ethanol (20 ml) in the presence of a catalytic amount of piperidine for 12 h. The reaction mixture was cooled, and the separated solid filtered and recrystallised from benzene.

Acknowledgement

The authors are thankful to Prof. E. V. Sundaram, Head, Department of Chemistry and Dean, Faculty of Science, for providing facilities, and to Dr. S. M. Reddy, Department of Botany, Kakatiya University, Warangal, for antibacterial activity.

References

1. A. Albert and H. Hampton, *J. Chem. Soc.*, 1968, 4937.
2. N. Suzuki and R. Dohmori, *Chem. Pharm. Bull.*, 1979, 27, 410.
3. N. Suzuki, Y. Tanaka and R. Dohmori, *Chem. Pharm. Bull*, 1980, 28, 235.
4. N. Suzuki, *Chem. Pharm. Bull.*, 1980, 28, 761.
5. H. Egawa, T. Miyamota, A. Minamida, Y. Nishimura, H. Okada, H. Uno and J. Matosumota, *J. Med. Chem*, 1984, 27, 1548.
6. J. Matsumota, Y. Nishimura and S. Nakamura, Fr. Pat. 2 531 084 (*Chem. Abstr.*, 1984, 101, 505088).
7. R. Ito, Y. Hashimoto, M. Iida and M. Namana, *Symp. Enzyme Chem. (Tokyo)*, 1950, 4, 82 (*Chem. Abstr.*, 1951, 45, 7166).
8. G. B. Balin and W. L. Tan, *Aust. J. Chem.*, 1984, 37, 1065.
9. J. Nezval and K. Halocka, *Experientia*, 1967, 23, 1048.

10. D. K. J. GORECKI and E. M. HAWES, *J. Med. Chem.*, 1977, 20, 124.
11. E. M. HAWES, D. K. J. GORECKI and D. D. JOHNSON, *J. Med. Chem.*, 1978, 16, 849.
12. E. M. HAWES and D. G. WIBBERLEY, *J. Chem. Soc. C*, 1967, 1564.
13. J. C. VINCENT and H. W. VINCENT, *Proc. Soc. Expt. Biol. Med.*, 1944, 55, 162.
14. S. SEIFTER, S. DAYTON, B. NOVIC and E. MUNTWYLER, *Arch. Biochem.*, 1950, 25, 191.
15. E. M. HAWES and D. G. WIBBERLEY, *J. Chem. Soc. C*, 1966, 315.

Chemical Examination of the Leaves of *Juniperus bermudiana* Linn. (Cupressaceae)

(MISS) F. KHATOON, IMDAD U. KHAN

and

W. H. ANSARI*

Department of Chemistry, Aligarh Muslim University, Aligarh-202 001

Manuscript received 9 July 1984, revised 20 December 1985, accepted 17 February 1986

JUNIPERUS bermudiana Linn. (Syn. *J. verginiana*) was examined only for its biflavonoid contents[1]. We have undertaken a thorough investigation of *J. bermudiana* leaves. Dried and powdered leaves (1.5 kg) procured from F. R. I., Dehradun (India), were extracted exhaustively with petroleum ether (b.p. 60-80°), benzene, ethyl acetate and acetone. Petroleum ether and benzene extracts were combined and concentrated. The residue was chromatographed over Si-gel column affording the following compounds. Identification is based on spectral studies and also comparison of m.ps. and spectral data with those reported.

n-Hexane elution : It gave a white crystalline compound (150 mg), m.p. 63°, M^+ 408, analysed for $C_{29}H_{60}$; ν_{max} (KBr) 2 880 and 1 465 cm^{-1} ; *m/e* 408 (M^+), 379, 350, 336, 322, 308, 297 and 157 ; τ (CCl_4) 8.75 (60H, s) ; confirmed its identity as nonacosane (lit.[3] m.p. 63.6-64°).

Further elution with the same solvent provided an another crystalline compound (80 mg), m.p. 84°, M^+ 429, $C_{29}H_{60}O$; ν_{max} (KBr) 3 300 (OH), 2 890, 1 460, 1 370, 1 330, 1 120, 1 080, 1 055, 850 and 710 cm^{-1} ; *m/e* 424 (M^+), 409 ($M-CH_3$), 406 ($M-H_2O$), 378 ($M-H_2O-C_2H_4$) and 297 ($M-C_9H_{19}$), and peaks of masses separated by 14 units (CH_2) with increasing intensity (characteristics of long chain alcohol) ; τ (CCl_4) 8.75 (59H, s) and 7.55 (1H, s) ; suggested it to be 1-nonacosanol (lit.[3,4] m.p. 84-5°) ; further confirmed by acetylation with Ac_2O-Py, τ (CCl_4) 8.75 (59H, s) and 8.35 (3H, s, 1-OAc).

Petrol benzene (7 : 3) elution : It afforded a LB positive white solid which on crystallisation (petrol-ether) yielded needles (70 mg), m.p. 165° (lit. m.p. 167°) ; ν_{max} (KBr) 3 350, 1 720, 1 690, 1 658, 1 640, 1 004, 914, 880, 830 cm^{-1} ; τ ($CDCl_3$) 9.01 (3H, s), 8.94 (3H, s), 8.78 (3H, s), 5.23, 5.00, 4.68 and 4.13 (m). Spectral data were found identical in all respects with those reported for sandaracopimeric acid[5,6].

Ethyl acetate extract : On further purification by solvent treatment and column chromatography followed by preparative tlc yielded three biflavonoids labelled as JBI, JBII and JBIII. Each was analysed separately by methylation and acetylation followed by pmr determination and found identical in m.p., chromatographic and spectral data with the reported biflavonoids[1].

Acetone extract : The brown residue on purification by paper chromatography (n-BuOH − AcOH − H_2O, 4 : 1 : 5) yielded a yellow compound, m.p. 181°, R_f 0.80. On hydrolysis (10% HCl), it gave an aglycone, m.p. 315°, identified as quercetin by comparing R_f, m.p. and shade in uv light of its methyl ether[7], and a sugar. The sugar was confirmed as rhamnose by pc (n-BuOH − AcOH − H_2O, 4 : 1 : 5, R_f 0.31) ; n-BuOH − ETOH − H_2O, 4 : 1 : 2, R_f 0.36 ; yellow brown colour with aniline hydrogen phthalate as spraying reagent. The glycosidic linkage was established by methylation ($Me_2SO_4-K_2CO_3$) followed by acid hydrolysis. The partial methyl ether, m.p. 195° obtained, was acetylated (Ac_2O-Py) to give an acetate, m.p. 159°. Pmr spectrum showed the oxygenation pattern of quercetin with one acetoxyl at τ 7.71 and four methoxyls at τ 6.18-6.23. Mass spectrum of the partial methyl ether provided main peaks at *m/e* 358 (M^+, 100%), 343 ($M-CH_3$), 329 ($M-HCO$), 180 and 179 (RDA fragments). The fragments *m/e* 329 and 179 confirmed OH group at C-3. Bathochromic shift[8] of 55 nm (in band I) with $AlCl_3$ further confirmed OH at C-3. The glycosidation was therefore at C-3. The structure of the compound was thus assigned as quercetin-3-*O*-rhamnoside[9]. This is the first report of the occurrence of these compounds in the family Cupressaceae.

Acknowledgement

One of the authors (I.U.K.) is thankful to U.G.C., New Delhi, for financial assistance.

References

1. S. K. ROY, M. A. QASIM, M. KAMIL, M. ILYAS and W. RAHMAN, *J. Indian Chem. Soc.*, 1984, 61, 172.
2. I. HEILBRON and H. M. BUNBURY, "Dictionary of Organic Compounds", Oxford University Press, 1953, Vol. III, p. 820.
3. C. D. HODGMAN, "A Hand Book of Chemistry and Physics", Chemical Rubber Publishing, U. S. A., 1960, p. 1128.
4. K. A. ZIRVI, K. JEWERS and M. J. NAGLER, *Planta Med.*, 1977, 32, 244.
5. L. J. GOUGH and J. S. MILLS, *Phytochemistry*, 1970, 9, 1093.
6. O. E. EDWARDS, A. NICOLSON and M. N. RODGER, *Can. J. Chem.*, 1960, 38, 663.

7. T. A. Geissman, "The Chemistry of Flavonoid Compounds", Pergamon Press, New York, 1962, p. 428.
8. Ref. 7, p. 132.
9. Ref. 7, p. 387.

Fatty Acid Composition of *Cicer soongaricum* Steph. Seed Oil

S. K. KATIYAR* and A. K. BHATIA

Regional Research Laboratory, Jammu Tawi-180 001

Manuscript received 16 April 1985, revised 6 December 1985, accepted 17 February 1986

CICER soongaricum Steph. (fam. : Leguminoseae ; local name *Sarri*) grows wild at an altitude of 3,000-5,000 m MSL in the Ladakh area of Jammu and Kashmir State. The local inhabitants in this high altitude desert consume the seeds of this plant as a dietary item. General composition of this legume has already been reported[1]. The present communication deals with the fatty acid constituents of the seeds oil.

Experimental

The seeds of *C. soongaricum* were collected during ethnobiological survey from South Pullu area (near Khardung La Pass, altitude 5 000 m MSL). The healthy and mature seeds were dried and ground upto 100-120 mesh.

The oil was solvent extracted using petroleum ether (b.p. 60-80°) and purified by the method of Folch *et al.*[2]. Methyl esters of the fatty acids were obtained by saponification of the oil, removal of

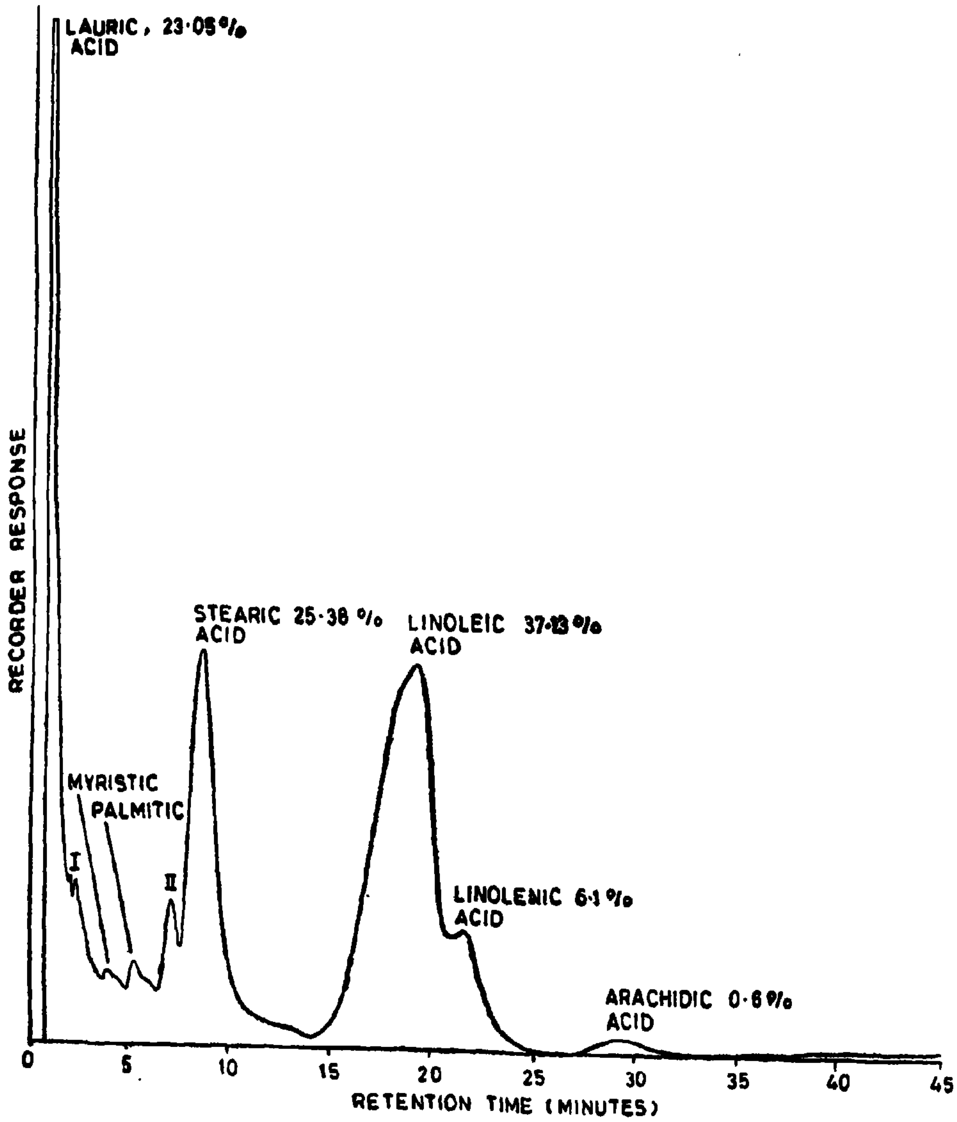


Fig. 1. Glc separation of fatty acids of *C. soongaricum* seed oil, I, II = unidentified peak.

unsaponifiable matter and esterification of the sample with 4% hydrochloric acid in methanol at 70-90° for 12-14 h[3]. Different fatty acids in the form of methyl esters were analysed through glc. The operating conditions of glc were : Pye-Unicam 204 instrument, Reoplex glass column (6 mm × 2 m), F.I.D. detector, nitrogen flow rate 35 ml min^{-1}, column temperature 180°, isothermal condition, injection port temperature 270°, detector 300°. Peak area was calculated by triangulation method. Physical characteristics of the seed oil were studied by the reported method[4].

The seeds contain 7.2% oil. Physical characteristics of the oil were : refractive index 1.472, iodine value 107, saponification value 193. The unsaponifiable matter found to be 4.5% is quite high in comparison to other reported Indian gram varieties[5].

Results and Discussion

Among the various fatty acids, linoleic acid predominated (37.13%). Stearic, lauric and linolenic acids were found to be 25.38, 23.05 and 6.10%, respectively, while myristic, palmitic and arachidic acids were in lesser concentrations. The glc graph (Fig. 1) showed two unidentified peaks, one after lauric acid (peak-I) and other after palmitic acid (peak-II) whose concentrations were 3.4 and 2.18%, respectively. It is significant to note that *C. soongaricum* seeds oil is a rich source of essential fatty acids, *viz.* linoleic and linolenic acids (43.23%). In addition of fulfilling dietary requirements, the essential fatty acids are also precursors in the biosynthesis of prostaglandins which in trace amounts are necessary for various physiological activities.

Acknowledgement

Grateful thanks are due to the Department of Environment, Government of India, New Delhi, for providing financial assistance.

References

1. S. K. KATIYAR, A. K. BHATIA, N. KUMAR and C. K. ATAL, *J. Sci. Food Agric.*, 1985, 36, 442.
2. J. FOLCH, M. LEES and G. H. SLOANE-STANLEY, *J. Biol. Chem.*, 1957, 226, 497.
3. M. KATES, *J. Lipid Res.*, 1964, 5, 132.
4. "Official Methods of Analysis", 13th. ed., Association of Official Analytical Chemists, Washington, D. C., 1980.
5. "The Wealth of India, A Dictionary of Indian Raw Materials", C. S. I. R., New Delhi, 1950, Vol. II, p. 168.

Chemical Investigation of *Holoptelea integrifolia* Planch. and *Cassia fistula* Linn.

K. M. BISWAS* and HAIMANTI MALLIK

Department of Chemistry, University of Calcutta, 92 A P.C. Road, Calcutta-700 009

Manuscript received 28 August 1985, accepted 24 December 1985

HOLOPTELEA integrifolia Planch. (Ulmaceae) is the only species of the genus *Holoptelea* occurring in India. Several triterpenoids[1-3], aliphatic alcohols[1] and acids[4] were isolated from this plant. *Cassia fistula* Linn. (Leguminosae) is one of the commonest trees of India. All its parts were previously investigated and several anthraquinones[5-10], flavonoids[6,7,9], and aliphatic alcohols[5,11], acids[11] and esters[11] were isolated. Both these plants have medicinal uses[12,13]. Reinvestigation of the stem bark of *H. integrifolia* has resulted in the isolation of 2-aminonaphthaquinone (yield, 0.0013%), friedelin (0.002%), epifriedelinol (0.0053%), β-sitosterol (0.004%) and its β-D-glucoside (0.01%), while that of the flowers of *C. fistula* yielded aurantiamide acetate (0.011%), β-sitosterol (0.006%), its β-D-glucoside (0.02%) and an uncharacterised fatty acid ester of β-sitosterol (CF-1) (0.001%). Although 2-aminonaphthaquinone is synthetically known[14], to our knowledge, there is no previous report of its natural occurrence.

Holoptelea integrifolia *Planch.* :

Air dried and powdered stem bark of *H. integrifolia* (1.5 kg), collected from Midnapore district in West Bengal during October was extracted in a Soxhlet apparatus for 40 h each first with petroleum ether and then with chloroform. The petroleum ether extract on concentration and cooling deposited a yellowish white solid which was collected by filtration. Chromatography of the solid on a silica gel column gave friedelin (eluate : petroleum ether-benzene, 1 : 1) and epifriedelinol (benzene), and that of the concentrate of the filtrate furnished the same two compounds and β-sitosterol (benzene-chloroform, 1 : 1). The concentrate of the chloroform extract on similar chromatography afforded 2-aminonaphthaquinone (chloroform-methanol, 49 : 1) and β-sitosterol-β-D-glucoside (chloroform-methanol, 9 : 1).

2-Aminonaphthaquinone crystallised in orange-red needles, m.p. 205° (lit.[14] 205°) from chloroform-petroleum ether ; λ_{max} (EtOH) (log ε) 233 (3.98), 266 (4.19), 333 (3.20) and 445 nm (3.44) ; ν_{max} (KBr) 3 370-3 180 (NH), 1 685 (C=O), 1 625, 1 570, 1 420, 1 365, 1 270, 1 220, 1 125, 980, 825 and 720 cm^{-1} ; δ ($CDCl_3$) 5.16 (2H, br s, exchangeable with D_2O, 2-NH_2), 5.97 (1H, s, H-3), 7.55-7.78 (2H, m, H-6 and H-7) and 7.97-8.11 (2H, m, H-5 and H-8) ; *m/e* (rel. int.) 173 (100, M^+), 146 (93, M − HCN), 145 (49, M − CO), 118 (43, M − HCN − CO), 117 (93, M − 2CO), 105 (96, M − HCN − CHCO), 104 (91, M − HCN − CH_2CO), 77 (88) and 76 (79). On treatment with ethanolic 0.5 *N* HCl, 2-aminonaphthaquinone furnished 2-hydroxynaphthaquinone, crystallising from chloroform-petroleum ether as yellow needles, m.p. 190° d (lit.[15] 192° d). The formation of 2-hydroxynapthaquinone by acid hydrolysis of 2-aminonaphthaquinone indicates that the latter behaves as a vinylogous amide, not as an amine. The insolubility of 2-aminonaphthaquinone in dilute acids and its resistance to acetylation at room temperature with acetic anhydride and pyridine also support this view.

The other isolates were identified by direct comparison with their authentic samples as well as their spectral data (ir, uv, nmr, *etc.*).

Cassia fistula Linn. :

Air dried and powdered flowers of *C. fistula* (1 kg), collected from Midnapore district of West Bengal in May were extracted in a Soxhlet apparatus for 40 h each with petroleum ether and chloroform successively. The petroleum ether extract on concentration and cooling deposited a solid which was separated by filtration. Chromatography of the solid over a silica gel column gave aurantiamide acetate (eluate : chloroform-methanol, 49 : 1) and that of the concentrate of the filtrate gave CF-1, an uncharacterised fatty acid ester of β-sitosterol (petroleum ether-benzene, 1 : 1), and β-sitosterol (benzene). The concentrate of the chloroform extract on column chromatography over silica gel afforded a further amount of aurantiamide acetate along with β-sitosterol-β-D-glucoside (chloroform-methanol, 9 : 1).

Aurantiamide acetate, a modified phenylalanine dipeptide, crystallising from chloroform-petroleum ether as clusters of hairy needles, m.p. 185° (lit[16]. 185°), $[\alpha]_D$-44° (*c* 0.12 in $CHCl_3$), was identified from its spectral properties and finally by direct comparison with an authentic sample[16]. The ir spectrum of CF-1 indicated the presence of an ester C=O (1 735 cm^{-1}) and its ^1H nmr spectrum exhibited signals at δ 1.22 (~24H, s), 2.23 (2H, t, *J* 6 Hz) and 4.3-4.7 (1H, m). Its hydrolysis with ethanolic 1*N* HCl afforded β-sitosterol. Thus, CF-1 appeared to be an ester of β-sitosterol and a fatty acid. It could not be characterised owing to paucity of material.

Acknowledgement

The authors thank Professor S. K. Talapatra of this Department, for providing an authentic sample of aurantiamide acetate, and are grateful to the U.G.C., New Delhi, for the award of a Junior Research Fellowship to one of them (H.M.).

References

1. G. Misra, S. C. Bhatnagar and S. K. Nigam, *Planta Med.*, 1974, **26**, 394.
2. G. Misra, S. C. Bhatnagar and S. K. Nigam, *Planta Med.*, 1975, **27**, 290.
3. G. Misra, *Planta Med.*, 1977, **31**, 232.
4. G. S. Grover and J. T. Rao, *J. Inst. Chem., Calcutta*, 1983, **55**, 2.
5. A. Kumar, C. S. Pande and R. K. Kaul, *Indian J. Chem.*, 1966, **4**, 460.
6. A. D. Patil, *Indian J. Chem., Sect., B*, 1982, **21**, 626.
7. V. Narayanan and T. R. Seshadri, *Indian J. Chem.*, 1972, **10**, 379.
8. G. D. Agarwal, S. A. I. Rizvi, P. C. Gupta and J. D. Tiwari, *Planta Med.*, 1972, **21**, 150.
9. T. V. Pamanabha Rao and V. Venkateswarlu, *Bull. Natl. Inst. Sci. (India)*, 1965, 28.
10. Y. Selvaraj and M. S. Chander, *J. Indian Inst. Sci.*, 1978, **60**, 179.
11. G. D. Agarwal, S. A. I. Rizvi, P. C. Gupta and R. D. Tiwari, *Proc. Nat. Acad. Sci. (India), Sect. A*, 1970, **40**, 388.
12. K. R. Kirtikar and B. D. Basu, "Indian Medicinal Plants", Lalit Mohan Basu and Co., Allahabad, 1935, Vol. II, p. 857.
13. K. R. Kirtikar and B. D. Basu, "Indian Medicinal Plants", Lalit Mohan Basu and Co., Allahabad, 1935, Vol. III, p. 109.
14. L. F. Fieser and J. L. Hartwell, *J. Am. Chem. Soc.*, 1935, **57**, 1483.
15. R. H. Thomson, "Naturally Occurring Quinones", Academic Press, London, 1971, p. 202.
16. S. K. Talapatra, A. K. Mallik and B. Talapatra, *Phytochemistry*, 1980, **19**, 1199.

Chemical Investigation of *Alstonia congensis* Engl.—Isolation of Rhazine

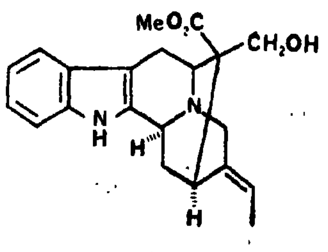
Avijit Banerji* and Sukla Jana

Pure Chemistry Department, University College of Science, University of Calcutta, Calcutta-700 009

Manuscript received 23 September 1985, accepted 17 February 1986

THE major source of indole alkaloids in nature are plants belonging to different genera of the family Apocynaceae. Several species of the genus *Alstonia* (family : Apocynaceae) occur widely in tropical countries of Asia and Africa. The extract of different species of this genus are reputed as antimalarials and in many cases as a tonic for general debility. In the present communication we report the systematic investigation of the stem-bark of *Alstonia congensis* and the characterisation of one of the constituent alkaloids as rhazine[1] (**1**).

Sun-dried stem-bark of *Alstonia congensis* (collected from Africa) was powdered, defatted with petrol and then extracted with methanol at room temperature for 20 days. The concentrated methanolic extract was churned with aqueous 5% citric acid solution and the mixture filtered. The aqueous extract was basified with NH_3 solution at 0° to *p*H 9 and extracted with chloroform. The concentrated chloroform extract was chromatographed over alumina. An alkaloid, $C_{21}H_{24}N_2O_3$ (M^+ 352), m.p. 235-36° d, was obtained from the benzene-chloroform (1 : 1) eluates. Its mass spectrum showed prominent peaks at *m/z* 352 (M^+), 351($M-1$), 337($M-CH_3$), 321($M-OCH_3/CH_2OH$), 170, 169, 168 and 154, respectively. The latter fragments are characteristic of the tetrahydro-β-carboline moiety. Its uv spectrum further corroborated this view, showing λ_{max} at 291, 280-283 and 227 nm (log ε 3.78, 3.87 and 4.52) which suffered a hypsochromic shift to 290, 273-274 and 222 nm (log ε 3.81, 3.93 and 4.56) in presence of a trace of acid. It showed ir bands at 3 150-3 400 (br, OH), 1 705 and 1 215 (ester C=O), 1 445, 840 and 730 cm^{-1}, respectively. The spectroscopical data (uv, ir, ms, ^1H nmr) indicated that the alkaloid was probably identical with rhazine[1].



(1)

Finally its identity was established as rhazine by direct comparison (m.m.p., co-tlc and superimposable ir) with an authentic sample. The complete ^{1}H nmr assignment of rhazine, which to our knowledge has not been reported so far is given here. 200 MHz ^{1}H nmr (recorded in $CDCl_3$ on a Bruker WP-200) δ 1.66 (3H, dd, *J* 6.7 and 1.9 Hz, C(18)H) ; 1.70-2.05 (3H, br m, C(14)H_2 and OH) ; 2.70 (1H, ddd, *J* 13, 4.3 and 1.9 Hz, C(15)H) ; 2.95 (3H, s, CO_2CH_3), 3.31 (1H, dd, *J* 15.5 and 1.6 Hz, C(6)H) ; 3.00-3.12 (2H, m, C(5)H and C(6)H) ; 3.60-3.62 (2H, br, CH_2OH) ; 3.69 and 3.84 (AB-system each of 1H, d, *J* 10.5 Hz, N – C(21)H_2) ; 4.31 (1H, dd, *J* 10.4 and 0.8 Hz, C(3)H) ; 5.41 (1H, br q, *J* 6.7 Hz, C(19)H) ; 7.06 (1H, dt, J_o 7.0, J_m 1.5 Hz, C(10)H) ; 7.13 (1H, dt, J_o 7.0, J_m 1.5 Hz, C(11)*H*) ; 7.30 (1H, br dd, J_m 1.5 Hz, partially obscured by $CHCl_3$ signal, C(12)H) ; 7.44 (1H, br dd, J_o 8.6, J_m 1.5 Hz, C(9)H) and 7.98 (1H, br s, NH).

The concentrate of the benzene eluate afforded a non-alkaloidal compound, m.p. 184-85°, as white granules. It showed characteristic bands at 3 300-3 500 (br) for hydroxyl group in the ir spectrum. The spectroscopical data (uv, ir, ms) indicated that the compound was an aliphatic diol, $C_{28}H_{58}O_2$ (M^+ 426). A number of other alkaloidal components have been isolated. These are being characterised.

Acknowledgement

The authors thanks C.S.I.R., New Delhi, for the award of a Junior Research Fellowship to one of them (S. J.).

Reference

1. A. CHATTERJEE, J. BANERJI and A. BANERJI, *Indian J. Pharm. Educt.*, 1977, 80, and references cited therein.

A New Flavonol Glycoside from the Mature Tubers of *Cyperus rotundus* L.

N. B. SINGH and P. N. SINGH*

Botany Department, University of Allahabad, Allahabad-211 002

Manuscript received 22 November 1985, accepted 17 February 1986

WE have previously reported[1] a new saponin from mature tubers of *Cyperus rotundus* L. We now report the isolation of a flavonol glycoside (1) $C_{28}H_{32}O_{15}$, m.p. 196° d from the same source. This glycoside has not been isolated earlier from any plant source.

1 on acid hydrolysis gave an aglycone and rhamnose. The aglycone $C_{16}H_{12}O_7$, m.p. 284° gave all characteristic colour reactions of a flavonol[2] and was identified as rhamnetin on the basis of uv, ir, nmr and mass fragmentation pattern and con-chromatography with an authentic sample.

Methylation of 1 followed by acid hydrolysis gave 5,7,3',4'-tetramethoxyquercetin confirming the attachment of sugar at 3-position. The glycoside was fully methylated, hydrolysed and the resulting partially methylated sugars were identified as 2,3-di-*O*-methylrhamnose and 2,3,4-tri-*O*-methylrhamnose[3,4]. This established the glycoside as a (1→4) trioside of rhamnose linked at 3-position of the aglycone. On this basis, 1 was identified as rhamnetin 3-*O*-rhamnosyl (1→4) rhamnopyranoside.

Experimental

The tubers of *Cyperus rotundus* L. were extracted with ethanol, concentrated and extracted with ether and ethyl acetate, respectively. Extraction with ethyl acetate and chromatography over silica gel with C_6H_6 – EtOAc (1 : 1) gave 1, m.p. 196°d (EtOH) ; λ_{max} (EtOH) 255 and 355 ; ($AlCl_3$) 260 and 400 ; ($AlCl_3$ – HCl) 270 and 400 ; (NaOAc) 255 ; (NaOAc/H_3BO_3) 260 and 390 nm.

On hydrolysis, 1 gave rhamnetin and rhamnose (pc in EtOAc-pyridine-H_2O, 12 : 5 : 4 and EtOAc – PrOH – H_2O, 3 : 1 : 1). Methylation and acid hydrolysis gave 5,7,3',4'-tetramethoxyquercetin, identified by m.m.p. and co-chromatography with an authentic sample. 1 was methylated with Me_2SO_4 in aqueous NaOH and the methylated glycoside hydrolysed with 4*N* H_2SO_4. The partially methylated sugars were identified by pc (BuOH – EtOH – H_2O, 5 : 1 : 4).

References

1. P. N. SINGH and S. B. SINGH, *Phytochemistry*, 1980, 19, 2056.
2. L. HORHAMMER and R. HANSEL, *Arch. Pharm.*, 1955, 288, 315.
3. E. L. HIRST and J. K. N. JONES, *Faraday Discuss. Chem. Soc.*, 1949, 7, 268.
4. J. K. N. JONES, *J. Chem. Soc.*, 1946, 788.

J. Indian Chem. Soc.,
Vol. LXIII, May 1986, pp. 451-459

Synthesis of some Novel Boron-Schiff Base and Allied Derivatives†

J. P. TANDON

Department of Chemistry, University of Rajasthan, Jaipur-302 004

Synthesis of some novel boron Schiff base and allied derivatives is described. These have been prepared by the different molar reactions of trialkoxy or phenoxy-boranes, oxybis(diacetoxy borane), 2-isopropoxybenzo-1,3-dioxa-2-borole, 2-isopropoxy-1,3-dithia-2-borole, 2-isopropoxy-1,3-thiaza-2-borole, phenylboronic acid, boron trifluoride diacetic acid and boron trifluoride etherate with ligands of stereochemical as well as biological significance, *viz.* Schiff bases; azines, semi- and thio-semicarbazones and *S*-methyl or benzyldithiocarbazates. The mode of bonding in the resulting complexes has been deduced on the basis of uv, ir, mass and multinuclear resonance (^{1}H, ^{13}C, ^{11}B, ^{19}F) studies and some of these have been examined for their biocidal activity.

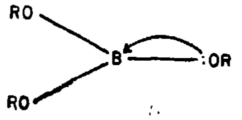
THE boron-nitrogen chemistry has been the focal point of attraction for the chemists during the last two decades and a large number of complexes having B-N bonds have been synthesised on account of their applications in diverse fields such as industry[1,2], agriculture[3,4] and medicine[5,6]. Probably due to the isoelectronic and isosteric nature of B-N and C-C bonds, the B-N chemistry is very extensive and diverse.

The chemistry of Schiff base complexes has attracted a great deal of attention ever since Pfeiffer carried out his pioneering research in 1930's. Schiff base complexes have subsequently been found to play an essential role in many biological processes, *viz.* transamination, decarboxylation, condensation, β-elimination and racemisation which are known to involve Schiff base intermediates. These find applications as algaecides and plant growth regulators[7] and their pharmacological applications as anticancer, antituberculostatic and antiinflammation agents as well as their uses as antiviral, antibiotic[8] and anaesthetic agents[9] have been described.

A variety of boron-Schiff base and allied derivatives can be synthesised by using trialkoxy- or phenoxy-boranes, oxybis(diaxetoxyboranes), 2-isopropoxybenzo-1,3-dioxa-2-borole, 2-isopropoxy-1,3-dithia-2-borole, 2-isopropoxy-1,3-thiaza-2-borole, phenyl boronic acid, boron trifluoride diacetic acid and boron trifluoride etherate as the starting materials.

Synthesis of boron derivatives involving alkoxy boranes :

In trialkoxyboranes, the electrophilic character of boron atom is reduced due to the back coordination from oxygen to boron (+M effect) and accordingly these behave as weak Lewis acids.



However, the aryloxyboranes behave as good Lewis acids due to − M effect and these form only the addition compounds.

The reactions of triisopropoxyborane with the Schiff bases derived by the condensation of β-diketones with alkyl or arylamines and hydroxyalkyl or arylamines are quite slow, whereas similar reactions with triethoxyborane are fast enough as well as straightforward. This is due to the fact that the covalent character increases with the greater +I effect of the alkyl group.

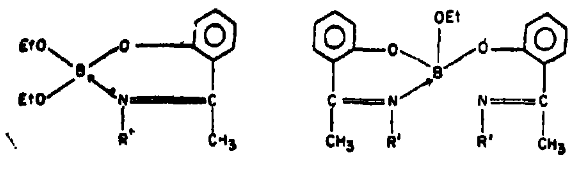
The reactions of triethoxyborane with *o*-hydroxy acetophenonealkyl or arylimines ($HOC_6H_4CCH_3 : NR'$) in 1 : 1, 1 : 2 and 1 : 3 molar ratios[10] can be represented by the following general equation,

$$B(OEt)_3 + nHOC_6H_4CCH_3 : NR' \xrightarrow[4,\ 6\ \text{or}\ 10\ h]{\text{Benzene}} B(OEt)_{3-n}(OC_6H_4CCH_3 : NR')_n + nEtOH$$

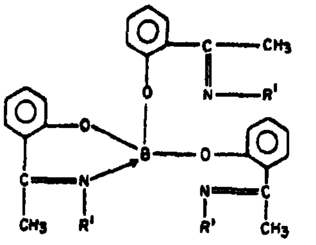
where, n=1, 2 or 3 ; R'=CH_3, C_2H_5, n-C_3H_7, n-C_4H_9, C_6H_5, *o*-$CH_3C_6H_4$, *m*-$CH_3C_6H_4$, *p*-$CH_3C_6H_4$, ClC_6H_4.

†Acharya J. C. Ghosh Memorial Lecture (1982) delivered under the auspices of the Indian Chemical Society on November 5, 1985 at Raipur.

The resulting derivatives can be structurally represented as



(1:1 derivative) (1:2 derivative)



(1:3 derivative)

The diethoxymono-Schiff base and monoethoxyboron-bis-Schiff base derivatives undergo alcohol interchange reactions in presence of excess of tertiary butanol and these show the labile nature of ethoxy groups present in these derivatives.

$$B(OEt)_{3-n}(OC_6H_4CCH_3 : NR')_n + Bu^tOH \xrightarrow[\text{(excess)}]{30\text{ h}} B(OBu^t)_{3-n}(OC_6H_4CCH_3 : NR')_n + nEtOH$$

where, $n = 1$ and 2.

However, reactions of triethoxyborane with bifunctional tridentate Schiff bases[11], such as 4-(hydroxy alkyl or aryl)amino-3-pentene-2-one, 3-(hydroxy alkyl or aryl)amino-1-phenyl-2-butene-1-one and *o*-hydroxyacetophenone hydroxyalkylimines take place in 1 : 1 and 1 : 2 molar ratios only.

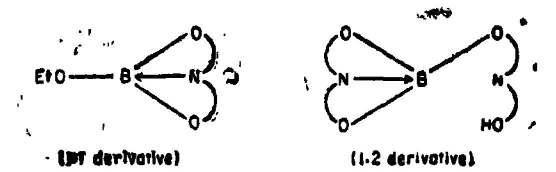
$$B(OEt)_3 + RCOCHCCH_3NHX'OH \longrightarrow B(OEt)(RCOCHCCH_3NX'O) + 2EtOH$$

$$B(OEt)_3 + 2RCOCHCCH_3NHX'O \longrightarrow B(RCOCHCCH_3NHX'O)(RCOCHCCH_3NHX'O) + 3EtOH$$

where, $R = CH_3$ and C_6H_5 ; $X' = CH_2CH_2$, $CH(CH_3)CH_2$, $CH_2CH_2CH_2$, $CH(CH_2CH_3)CH_2$ and C_6H_4.

The reactions of Schiff bases derived from 2,4-pentanedione are quite slow, whereas similar reactions with the Schiff bases of 1-phenyl-1,3-butanedione are comparatively faster due to the $-I$ effect of the phenyl ring.

The 2 : 3 molar reactions of these Schiff bases with triethoxyborane simply result in the formation of a mixture of 1 : 1 and 1 : 2 derivatives. The former can be separated from the resulting mixture by crystallising out from benzene-n-hexane (5 : 3) mixture. The non-formation of 2 : 3 derivatives can possibly be attributed to the steric factors as the two boron atoms cannot accommodate the third ligand moiety in between.



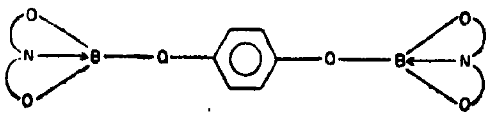
(1:1 derivative) (1:2 derivative)

where, HONOH = donor set of the bifunctional tridentate Schiff base.

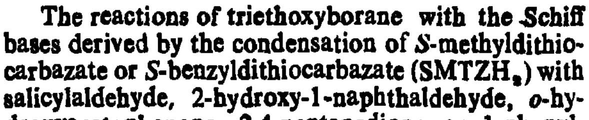
However, the reaction of ethoxy boron mono Schiff base derivative with 1,4-dihydroxybenzene in 2 : 1 molar ratio proceeds as follows,

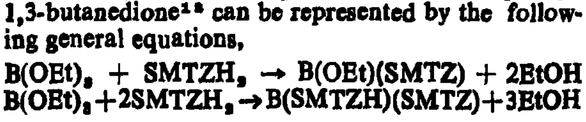
$$2B(OEt)(C_6H_5COCHCCH_3NX'O) + HOC_6H_4OH \rightarrow (C_6H_5COCHCCH_3NX'O)B\text{-}O\text{-}C_6H_4\text{-}O\text{-}B(C_6H_5COCHCCH_3NX'O) + 2EtOH$$

The formation of such a derivative can be explained on the basis of the smaller size of 1,4-dihydroxybenzene as compared to the Schiff base molecule.



Similar reactions of triethoxyborane with ligands having ONO and ONS donor systems, *i.e.* semicarbazones and thiosemicarbazones[12] take place in 1 : 1 and 1 : 2 molar ratios.



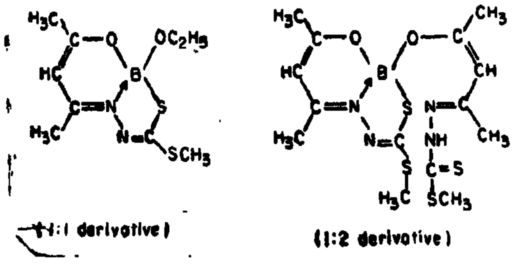


where X = O or S ; $Y = NH_2$.

The reactions of triethoxyborane with the Schiff bases derived by the condensation of *S*-methyldithiocarbazate or *S*-benzyldithiocarbazate ($SMTZH_2$) with salicylaldehyde, 2-hydroxy-1-naphthaldehyde, *o*-hydroxyacetophenone, 2,4-pentanedione or 1-phenyl-1,3-butanedione[13] can be represented by the following general equations,

$$B(OEt)_3 + SMTZH_2 \rightarrow B(OEt)(SMTZ) + 2EtOH$$

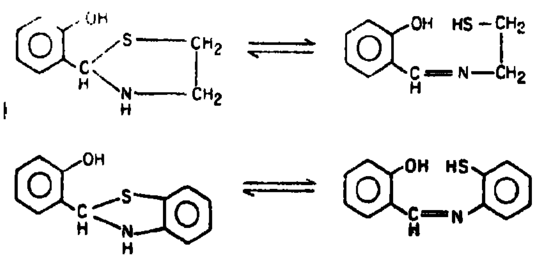
$$B(OEt)_3 + 2SMTZH_2 \rightarrow B(SMTZH)(SMTZ) + 3EtOH$$



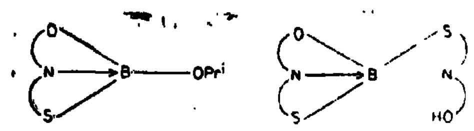
(1:1 derivative) (1:2 derivative)

In the ^{1}H nmr spectrum of 1:1 boron derivative, the disappearance of NH (δ 10.75) and SH (4.45) proton signals shows chelation of boron through oxygen and sulphur atoms, whereas in 1 : 2 derivative, these proton signals appear at δ 10.52 and 4.26 due to the existence of the resonating NH or SH proton of one of the ligand moiety. Further, two sets of proton signals are observed for every proton in 1 : 2 derivative with one set remaining at almost the same position as in the ligand itself. This clearly shows that one of the ligand moieties acts as a tridentate and another one as unidentate species.

The condensation of aromatic aldehydes or β-diketones with 2-aminoethanethiol, 2-aminopropanethiol or *o*-aminobenzenethiol results in the formation of cyclic products containing a thiazoline ring[14,15]. However, in presence of metallic or non-metallic ions, isomerisation of these ligands to their tautomeric Schiff base form takes place[16,17].



The triisopropoxyborane undergoes facile reactions with benzothiazolines[18] in 1: 1 and 1: 2 molar ratios and the resulting products can be structurally represented as



(1:1 derivative) (1:2 derivative)

where, HO-N-SH = donor set of the ligand molecule.

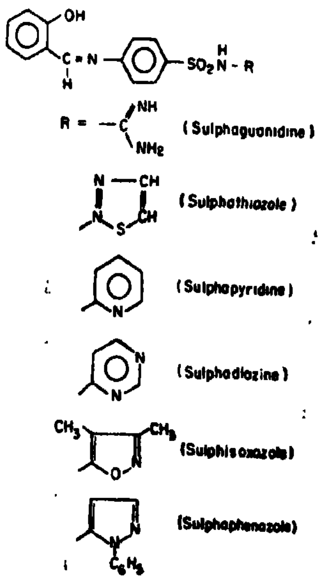
In the ligands, the absence of γ_{SH} in the region 2 660-2 550 cm^{-1} and the appearance of a strong and sharp γ_{NH} band in the region 3 350-3 250 cm^{-1} are indicative of their benzothiazoline form in the solid state. However, the disappearance of γ_{NH} band as well as the absence of γ_{SH} band in the ir spectra of 1 : 1 boron complexes show the chelation of sulphur as well as nitrogen of the ligand moieties to the central boron atom. Further, in the case of boron complexes, a strong band around 1 610 cm^{-1} is observed and this is due to the coordinated azomethine group.

The ligands derived by the condensation of *o*-mercaptoaniline with 2,4-pentanedione ($C_{11}H_{13}ONS$), salicylaldehyde ($C_{13}H_{11}ONS$) and β-hydroxynaphthaldehyde ($C_{17}H_{13}ONS$) show the NH proton signals at δ 5.80, 5.65 and 5.40, respectively and these disappear completely in the corresponding boron complexes.

In the ligands $C_{13}H_{11}ONS$ and $C_{17}H_{13}ONS$, the phenolic OH proton resonance signal appears as broad signals at δ 9.25 and 9.9, respectively and which disappear in the 1: 1 boron complexes. Thus, its deprotonation supports the coordination of phenolic oxygen to boron. However, in 1 : 2 complexes, these peaks are observed in the form of hydrogen bonded OH protons indicating the non-involvement of phenolic proton in the complex formation. A downfield shift in the resonance signal of alkyl and aryl protons is also observed and this is due to the deshielding of protons on account of the coordination of azomethine nitrogen to the boron atom.

The ^{11}B nmr chemical shift (δ 8.80) of the 1 : 2 derivatives shows the tetracoordinated state of boron.

The sulphonamides have long been known to possess significant biocidal activity and the Schiff bases derived from them are also expected to inherit these characteristics. These can be structurally represented as follows,



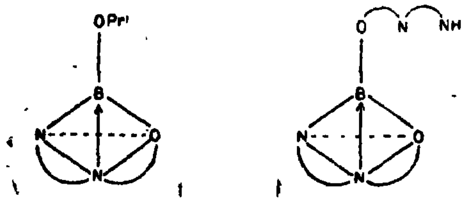
These Schiff bases react with boron isopropoxide in 1 : 1 and 1 : 2 molar ratios as indicated below[19],

$$B(OPr^i)_3 + H\widehat{ON}\widehat{NH} \rightarrow B(ONN)(OPr^i) + 2Pr^iOH$$

$$B(OPr^i)_3 + 2H\widehat{ON}\widehat{NH} \rightarrow B(\widehat{ON}\widehat{N})(H\widehat{ON}\widehat{N}) + 3Pr^iOH$$

where, $H\widehat{O\text{-}N}\text{-}\widehat{NH}$ = donor system of the sulphonamide Schiff base.

The resulting boron Schiff base derivatives can be structurally represented as

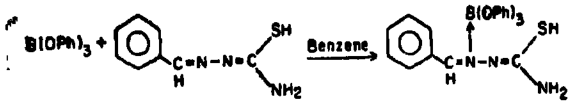


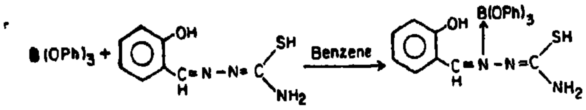
(1:1 derivative) (1:2 derivative)

The [11]B nmr signals appear at δ 2.83 and 2.06 corresponding to the tetracoordinated state of boron in these derivatives.

Synthesis of boron derivatives involving aryloxyboranes :

Aryloxyboranes differ markedly from their alkoxy counterparts due to the greater $-M$ effect of the phenyl ring and thereby behave as stronger Lewis acids. As a consequence of this, a number of adducts with nitrogen donor ligands are formed[20,21]. Thus, with the Schiff bases, the triphenoxyborane forms 1 : 1 adducts only.

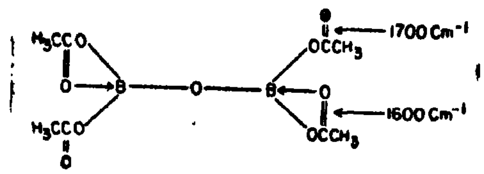




Synthesis of boron derivatives involving B-O-B bonding :

A new series of boron complexes having B-O-B linkage can be obtained by the reactions of oxybis(diacetoxyborane) with a variety of Schiff bases. The reaction product of boric oxide with acetic anhydride was identified as triacetoxyborane by Pictet and Geleznoff[22]. Dimroth[23] repeated its preparation and found the ratio of acetic acid to boric acid as 2 : 1. He, therefore, concluded that the product was oxybis(diacetoxyborane) and not the triacetoxyborane. The oxybis(diacetoxyborane) structure was subsequently established by Hayter[24] on the basis of molecular weight and *X*-ray diffraction measurements.

The structure of oxybis(diacetoxyborane) has now been very well supported by [11]B nmr and ir spectral studies[25,26]. Taking into account the inductive effect, [11]B resonance signal should appear at a slightly lower field in the spectrum of oxybis(diacetoxyborane) than the boron signal in the spectra of alkoxy and aryloxyboranes (δ -14 to -19). It is not, however, so and the chemical shift for the boron signal in this compound is observed at δ 1.1 $\pm$ 1.0. This is rather due to the shielding of the boron atom through chelation by one of the acetoxy carbonyls.



The oxybis(diacetoxyborane) undergoes facile reactions with different types of Schiff bases to produce a variety of simple or mixed type of derivatives[27-31].

$$H_3BO_3 + 5Ac_2O \longrightarrow (AcO)_2B\text{-}O\text{-}B(OAc)_2 + 6AcOH$$

$$(AcO)_2B\text{-}O\text{-}B(OAc)_2 + H\widehat{ONX}H \xrightarrow[15\text{-}16\ h]{Toluene} (\widehat{ONX})B\text{-}O\text{-}B(OAc)_2 + 2AcOH$$

$$(AcO)_2B\text{-}O\text{-}B(OAc)_2 + 2H\widehat{ONX}H \xrightarrow[17\text{-}19\ h]{Toluene} (\widehat{ONX})B\text{-}O\text{-}B(\widehat{ONX}) + 4AcOH$$

Mixed derivatives :

$$(\widehat{ONX})B\text{-}O\text{-}B(OAc)_2 + C_6H_4(OH)_2 \xrightarrow[10\text{-}12\ h]{Benzene} (\widehat{ONX})B\text{-}O\text{-}B(O_2C_6H_4) + 2AcOH$$

[11]B nmr spectra of 1 : 1 benzothiazoline derivatives show two sharp peaks at δ 18.4 and 2.8 confirming the existence of boron atoms in tri- and tetracoordinated states, respectively, whereas 2 : 1 products give only one signal at δ 2.06 suggesting the tetracoordinated state of both the boron atoms.

Synthesis of boron derivatives of unsymmetrical boranes :

A variety of Schiff base and allied derivatives of unsymmetrical boranes can be prepared by the reactions of 2-isopropoxybenzo-1,3-dioxa-2-borole with azomethines as well as Schiff base derived from azines, semi- and thiosemi-carbazones and *S*-methyl and *S*-benzyldithiocarbazates[32]. These reactions are quite facile in the medium of dry benzene as shown below,

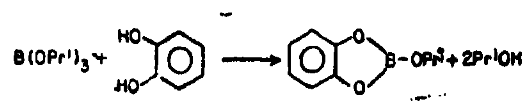
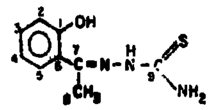
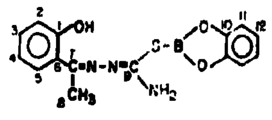


TABLE 1—^{13}C NMR DATA OF LIGAND AND ITS BORON COMPLEX

Structure	Chemical shift in δ (ppm)											
	1	2	3	4	5	6	7	8	9	10	11	12
	150.92	115.30	128.91	119.03	126.58	116.94	115.67	12.61	178.91			
 (In CDCl$_3$)	150.8	115.6	130.5	118.7	128.2	117.2	115.71	14.5	180.2	150.8	107.5	119.1

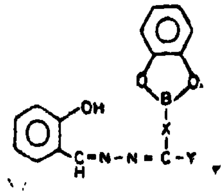
$$\overline{OC_6H_4OB}\text{-}OPr^i + \widehat{NX}H \longrightarrow \overline{OC_6H_4OB}(\widehat{NX}) + Pr^iOH$$

$$\overline{OC_6H_4OB}\text{-}OPr^i + H\widehat{ON}\widehat{X}H \longrightarrow \overline{OC_6H_4OB}\ (H\widehat{ON}\widehat{X}) + Pr^iOH$$

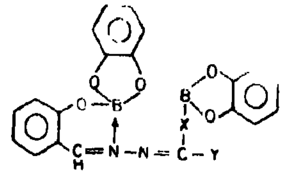
$$2\,\overline{OC_6H_4OB}\text{-}OPr^i + H\widehat{ON}\widehat{XH} \longrightarrow [\overline{OC_6H_4OB}]_2\,(\widehat{ON}\widehat{X}) + 2Pr^iOH$$

where, $\widehat{NX}H$ and $H\widehat{ON}\widehat{X}H$ = donor systems of Schiff bases ; X = O or S.

The resulting complexes are coloured solids with sharp melting points and are monomeric in nature. ^{11}B nmr spectral studies indicate the presence of tricoordinated boron in the 1 : 1 derivatives and tri- as well as tetracoordinated states in the 2 : 1 derivatives[23].



(1:1 derivative)

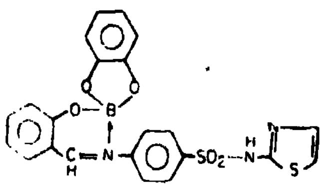


(2:1 derivative)

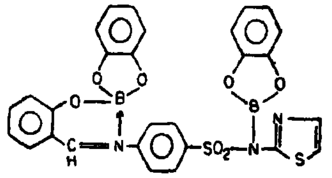
where, X=O or S ; Y=NH_2, SCH_3 or $SCH_2C_6H_5$.

The negligible shifting of azomethine carbon signal (marked by 7) in ^{13}C nmr spectra (Table 1) of the complex [$\overline{OC_6H_4OB}$)(HO.$C_6H_4C(CH_3)$: NNC : SNH_2] as compared to the ligand clearly substantiates the fact that azomethine moiety is not involved in coordination. However, a shift in the carbon signal (marked by 9) attached with sulphur indicates the involvement of sulphur atom in complexation with boron atom.

Similar reactions of 2-isopropoxybenzo-1,3-dioxa-2-borole with salicylaldehyde sulphathiazoles[24] result in the isolation of the following derivatives,



(1:1 derivative)



(2:1 derivative)

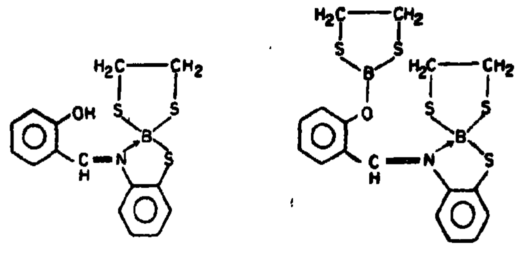
Further, to confirm the molecular association of these derivatives, the mass spectrum (Chart 1) of one representative compound, *viz.* *o*-hydroxyacetophenone azinatoboron complex was recorded. The molecular ion peak is observed at *m/e* 386, which corresponds to their monomeric nature.

Organoboranes containing sulphur play an important role in the synthetic organic chemistry. These find uses as synthetic intermediates due to their ready availability and ease of reactivity and are thus unique among organometallic reagents. The unsymmetrical borane derivatives containing sulphur can be prepared by the reactions of 2-isopropoxy-1,3-dithia-2-borole with monofunctional bidentate Schiff bases in 1 : 1 and bifunctional tridentate Schiff bases[25] in 1 : 1 and 2 : 1 molar ratios as

$$\overline{SCH_2CH_2SB}\text{-}OPr^i + HSN \rightarrow \overline{SCH_2CH_2SB}(SN) + Pr^iOH$$

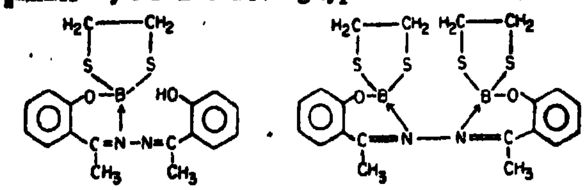
$$\overline{SCH_2CH_2SB}\text{-}OPr^i + HSNOH \rightarrow \overline{SCH_2CH_2SB}\,(HONS) + Pr^iOH$$

$$2\overline{SCH_2CH_2SB}\text{-}OPr^i + HSNOH \rightarrow [\overline{SCH_2CH_2SB}]_2\,(ONS) + 2Pr^iOH$$



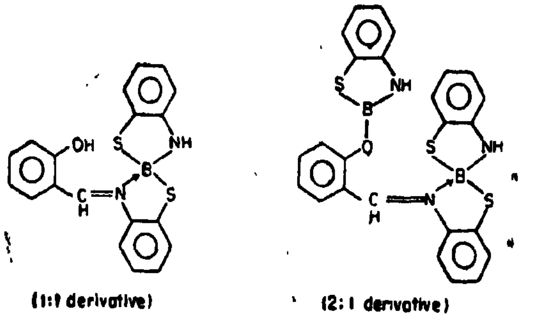
(1:1 derivative) (2:1 derivative)

Similar reactions with the Schiff bases derived from azines[86] yield the following type of derivatives,



(1:1 derivative) (2:1 derivative)

2-Isopropoxybenzo-1,3-thiaza-2-borole also undergoes facile reactions with bifunctional tridentate benzothiazolines in 1 : 1 and 2 : 1 molar ratios and the structures of the resulting products can be indicated as



(1:1 derivative) (2:1 derivative)

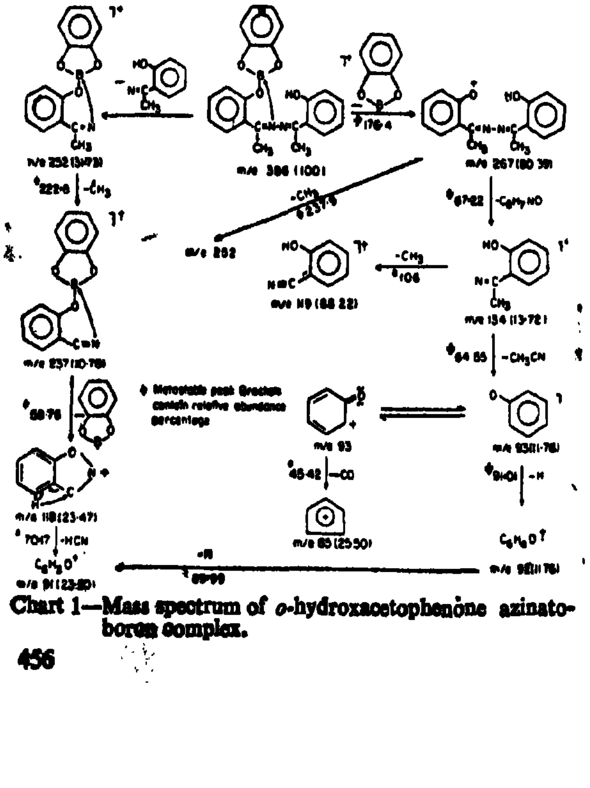


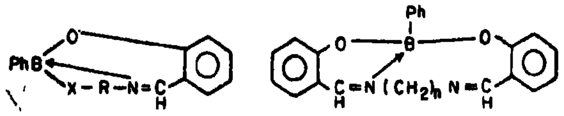
Chart 1—Mass spectrum of *o*-hydroxacetophenone azinatoboron complex.

Synthesis of boron derivatives of phenyl(dihydroxy)borane :

Another series of organoboron derivatives of Schiff bases can be obtained by the reactions of phenyl(dihydroxy)borane with different types of azomethines[87]. These reactions are carried out in presence of benzene over a Stark's assembly and the water liberated is collected azeotropically with benzene.

$$PhB(OH)_2 + HONXH \rightarrow PhB(ONX) + 2H_2O$$

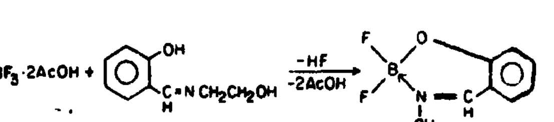
$$PhB(OH)_2 + HONNOH \rightarrow PhB(ONNO) + 2H_2O$$



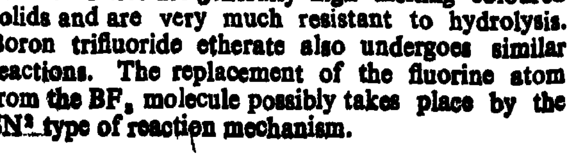
where, X = O or S ; R = CH_2CH_2, C_6H_4, N = C.NH_2, N = $\overset{|}{C}SCH_3$ and N = $\overset{|}{C}SCH_2C_6H_5$; n = 1, 2 or 3.

Synthesis of boron derivatives involving B-F bonding :

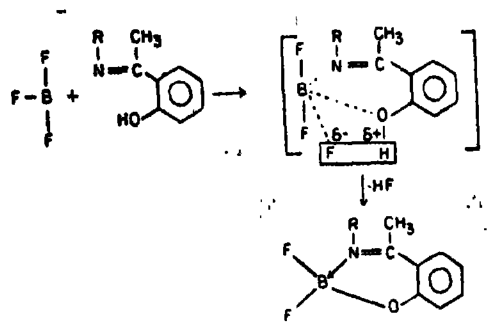
Boron trifluoride diacetic acid ($BF_3.2AcOH$) or boron trifluoride etherate (BF_3Et_2O) also undergoes reactions with different types of Schiff bases[88,89]. However, replacement of fluorine is not so facile. The boron trifluoride diacetic acid reacts with *N*-alkyl or aryl salicylaldimines as follows,



Schiff bases having the phenolic group are capable of replacing the fluorine, whereas those having an alcoholic group, such as *N*-(2-hydroxypropyl) benzaldimine, do not undergo such a replacement reaction.

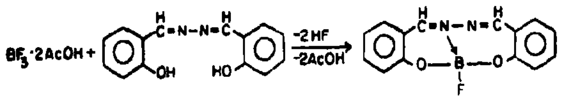


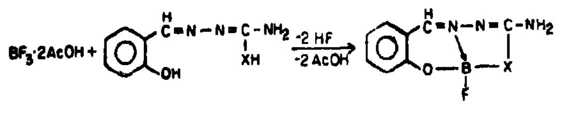
In the resulting derivatives, further replacement of fluorine is not possible even under drastic conditions due to the stable tetracoordinated state of boron. These are generally high melting coloured solids and are very much resistant to hydrolysis. Boron trifluoride etherate also undergoes similar reactions. The replacement of the fluorine atom from the BF_3 molecule possibly takes place by the S_N2 type of reaction mechanism.



where, R = alkyl or aryl group.

The reactions of BF_3.2AcOH with Schiff bases derived from azines and semi- or thiosemi-carbazones can be depicted by the following equations,





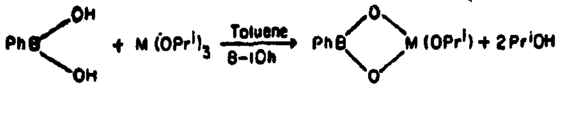
where, X = O, S.

In ^{19}F nmr spectra, only a singlet is observed at δ 28 in the case of semicarbazone and δ 23 in the case of thiosemicarbazone derivatives, and this shows the presence of only a single fluorine atom in the resulting complexes.

Synthesis of boron derivatives involving M-O-M' type of bonding :

A number of papers and patents[40,41] appear in the literature on the use of metalloboraxones, stannoboranes as well as compounds having Sn-O-M type of linkage as plastic stabilisers, bactericides, fungicides, lubricants and water repellents. The possibility of synthesising inorganic polymers with heterometalloxane backbone structure has further stimulated interest in the synthesis of such binuclear derivatives.

The equimolar reactions of phenylboronic acid with boron or aluminium isopropoxide yield the following type of derivatives,



where, M = B or Al.

The resulting monoisopropoxy derivatives further react with ligands having a phenolic group, such as Schiff bases, azines, semi- or thiosemicarbazones or *S*-benzyldithiocarbazates so as to produce the desired products.

$$PhBO_2Al(OPr^i)+HONXH \xrightarrow[8\text{-}10\,h]{Toluene} PhBO_2Al(ONXH)+Pr^iOH$$

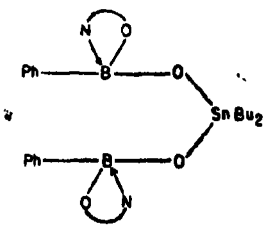
These complexes are coloured solids with high m.ps. and in the ^{11}B nmr spectrum, a sharp peak at δ 23.20 suggests the tricoordinated state for the boron atom.

For the synthesis of derivatives having B-O-Sn type of bonding, phenylboronic acid is first of all allowed to react with monofunctional bidentate Schiff base in equimolar ratio.

$$PhB(OH)_2+HON \xrightarrow[9\text{-}10\,h]{Benzene} [PhB\,(NO)\,OH]+H_2O.$$

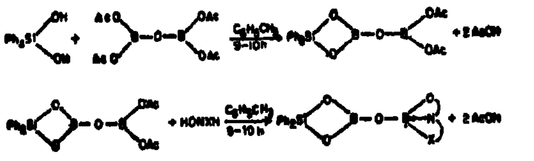
The resulting derivative then undergoes reaction with dibutyltin oxide in 2 : 1 molar ratio to yield B-O-Sn type of derivatives.

$$2PhB\,(NO)\,OH+OSnBu_2 \xrightarrow[9\text{-}10\,h]{Benzene} [PhB(\,ON\,)O]_2SnBu_2 + H_2O.$$



The ^{11}B nmr signal appears at δ 2.2 suggesting the tetracoordinated state for both the boron atoms.

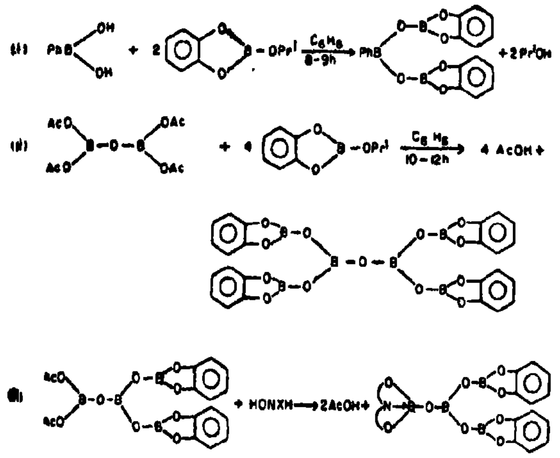
Equimolar reactions of diphenylsilanediol with oxybis(diacetoxyborane) and bifunctional tridentate Schiff base result in the synthesis of the following type of derivatives,



where, HONXH=bifunctional tridentate Schiff base molecule.

The ^{11}B nmr spectra give two peaks at δ 20.5 and 1.4 suggesting the tri- and tetra-coordinated states for the boron atoms in the resulting complexes.

Similarly, the reaction of 2-isopropoxybenzo-1,3-dioxa-2-borole with phenylboronic acid or oxybis-diacetoxy borane yields B-O-B type of binuclear derivatives.



Biological studies :

The application of boron compounds in the cancer therapy[42] has revoked considerable interest due to the unique nuclear property of non-radio-active isotope to absorb thermal neutrons ^{10}B which has an exceptionally large cross section capture area. Alkylboronic acids have been shown to act as reversible enzyme inhibitors and the extent of inhibition depends on the alkyl chain length[43]. The uses of organoboranes as insecticides, fungicides, plant growth agents[44], soil conditioners, herbicides and weed killers have also been described.

A few representative boron Schiff base complexes have been screneed for their activity on pathogenic gram-negative and gram-positive bacteria[45]. The results show that the organoboron complexes of Schiff bases derived from *S*-benzyl dithiocarbazates, sulpha drugs and semicarbazones and thiosemicarbazones inhibit the growth of gram-positive as well as gram-negative bacteria even at very low concentrations. It has also been shown that the complexation increases the activity as the boron complexes are much more active than the ligands themselves. In general, the complexes derived from thio-Schiff bases or those containing sulphur show greater activity than those, which do not have it. The fungicidal activity of boron thiosemicarbazone complexes is appreciably higher than the two well known fungicides, Bevistin and PCNB, which have been reported to be quite active against phytopathogens.

Acknowledgement

The author sincerely thanks his present as well as earlier coworkers, Drs. R. V. Singh, H. B. Singh, S. R. M. Tripathi, P. K. Singh, (Miss) L. Bahl and K. K. Chaturvedi for carrying out the experimental work. Financial support from C.S.I.R. and U.G.C., New Delhi, is also gratefully acknowledged.

References

1. M. Minami and A. Kitamure, *Chem. Abstr.*, 1974, **80**, 133012.
2. P. H. R. B. Lemon, *Br. Plastics*, 1963, **36**, 336 (*Chem. Abstr.*, 1965, **63**, 11786).
3. H. Nakamura, Y. Iitaka, T. Kitachara, T. Okazaki and Y. Okami, *J. Antibiot.*, 1977, **30**, 714.
4. M. Grassberger, *Chem. Abstr.*, 1979, **91**, 39316.
5. Y. Oka and I. Yanagisawa, *Nucl. Technol.*, 1981, **55**, 642.
6. A. H. Soloway, R. L. Wright and J. R. Messer, *J. Pharmacol. Exp. Ther.*, 1961, **134**, 177 (*Chem. Abstr.*, 1962, **56**, 872).
7. H. A. Cyba, U. S. Pat, 3 398 170/1968 (*Chem. Abstr.*, 1968, **69**, 6363).
8. T. Snami and S. Umezava, *Bull. Chem. Soc. Jpn.*, 1956, **29**, 975.
9. H. Theiss, H. Schoemberger and K. Borah, *Arch. Pharm.*, 1966, **299**, 1031.
10. J. P. Tandon and H. B. Singh, *Indian J. Chem., Sect. A*, 1979, **17**, 620 ; 1979, **18**, 529.
11. J. P. Tandon and H. B. Singh, *Synth. React. Inorg. Metal-Org. Chem.*, 1977, **7**, 547 ; 1978, **8**, 265 ; *Acta Chim. (Budapest)*, 1978, **98**, 81.
12. J. P. Tandon and P. K. Singh, *J. Inorg. Nucl. Chem.*, 1981, **43**, 1755.
13. J. P. Tandon and P. K. Singh, *Proc. Indian Acad. Sci.*, 1984, **93**, 53.
14. H. Jadamus, Q. Fernando and H. Freiser, *J. Am. Chem. Soc.*, 1964, **86**, 3056.
15. R. G. Charles and H. Freiser, *J. Org. Chem.*, 1953, **18**, 422.
16. L. F. Lindoy and S. E. Livingstone, *Inorg. Chim. Acta*, 1967, **1**, 365.
17. C. C. Lee, A. Shama and L. J. Theriot, *Inorg. Chem.*, 1971, **10**, 1669.
18. J. P. Tandon, K. K. Chaturvedi and R. V. Singh, *Synth. React. Inorg. Metal-Org. Chem.*, 1984, **14**, 1085 ; *J. Prakt. Chem.*, 1984, **326**, 817.
19. J. P. Tandon, K. K. Chaturvedi and R. V. Singh, *J. Prakt. Chem.*, 1985, **325**, 144.
20. T. Colelough, W. Gerrard and M. F. Lappert, *J. Chem. Soc.*, 1956, 3006.
21. H. Beyer and H. Noth, *Chem. Ber.*, 1960, **93**, 1078.
22. A. Pictet and A. Glezeneff, *Chem. Ber.*, 1903, **36**, 2269.
23. O. Dimroth, R. Ruchti, R. Sagstetter, J. Hetzer, H. Bernzott, C. Bamberger, O. Rehmann and R. Schweizer, *Justus Liebigs Ann. Chem.*, 1925, **446**, 97 (*Chem. Abstr.*, 1926, **20**, 1052).
24. R. G. Hater, A. W. Laibengayer and P. G. Thompson, *J. Am. Chem. Soc.*, 1957, **79**, 4243.
25. J. P. Onak, H. Landesman, R. E. Williams and I. Shapiaro, *J. Phys. Chem.*, 1959, **63**, 1533.
26. L. A. Duncenson, W. Gerrard, M. F. Lappert, H. Pyazora and H. Shafferмann, *J. Chem. Soc.*, 1958, 3652.
27. J. P. Tandon, S. M. Tripathi and R. V. Singh, *J. Chin. Chem. Soc.*, 1980, **27**, 51.
28. J. P. Tandon, K. K. Chaturvedi and R. V. Singh, *Synth. React. Inorg. Metal-Org. Chem.*, 1983, **12**, 155.

29. J. P. TANDON and H. B. SINGH, *Synth. React. Inorg. Metal-Org. Chem.*, 1985, **15**, 391.
30. J. P. TANDON and H. B. SINGH, *J. Inorg. Nucl. Chem.*, 1980, **42**, 793.
31. J. P. TANDON, P. K. SINGH and H. B. SINGH, *Indian J. Chem., Sect. A*, 1981, **20**, 202.
32. J. P. TANDON, R. V. SINGH and L. BAHL, *Acta Chim. Hung.*, 1984, **115**, 251 ; *Indian J. Chem., Sect. A*, 1983, **22**, 951.
33. J. P. TANDON and L. BAHL, *Indian J. Chem., Sect. A*, 1986, **25**, 54.
34. J. P. TANDON, L. BAHL and R. V. SINGH, *Synth. React. Inorg. Metal-Org. Chem.*, 1984, **14**, 1135.
35. J. P. TANDON, R. V. SINGH and L. BAHL, *Synth. React. Inorg. Metal-Org. Chem.*, 1983, **13**, 613.
36. J. P. TANDON, R. V. SINGH and L. BAHL, *J. Prakt. Chem.*, 1985, in the press.
37. J. P. TANDON and S. R. M. TRIPATHI, *Indian J. Chem., Sect. A*, 1979, **17**, 618.
38. J. P. TANDON and P. K. SINGH, *Indian J. Chem., Sect. A*, 1982, **21**, 833.
39. J. P. TANDON and S. R. M. TRIPATHI, *Inorg. Nucl. Chem. Lett.*, 1978, **4**, 917.
40. G. WEISSENBERGER, *Chem. Abstr.*, 1967, **67**, 1068.
41. J. ELLERMANN, *Z. Anorg. Allg. Chem.*, 1979, **34**, 975.
42. G. I. LOCHES, *Am. J. Roentgenol*, 1936, **36**, 1.
43. V. K. ANTONOV, T. V. IVANINA, I. V. BEREZIN and K. MARTINEK, *Dokl. Akad. Nauk SSSR*, 1968, **183**, 1435.
44. R. A. WILDES and T. F. NEALES, *J. Exp. Bot.*, 1969, **20**, 591.
45. J. P. TANDON, L. BAHL and S. K. SINHA, *Curr. Sci.*, 1984, **53**, 566.

J. Indian Chem. Soc.,
Vol. LXIII, May 1986, pp. 460-462

Alkaline Earth Metal Complexes. Reactions of Calcium Ions with Common Plant Acids

A. K. BANERJEE*, T. V. R. K. RAO and S. K. ROY

Chemistry Department, Patna University, Patna-800 005

Manuscript received 2 May 1981, revised 30 January 1986, accepted 3 March 1986

Calcium complexes of citric, malic and tartaric acids and their mixed ternary ones, have been investigated by conductometric titration and elemental analysis of the isolated solid compounds. Conductometric titration data indicated the formation of binary 1 : 1 and 1 : 2 calcium-citrate, and 1 : 2 calcium-malate and -tartarate complexes. The 1 : 1 : 1 stoichiometry of the ternary calcium malatocitrate, calcium malatosuccinate, calcium tartaratocitrate, calcium tartaratomalate and calcium tartaratosuccinate, and 1 : 1 : 2 calcium malatosuccinate complexes have been indicated by such study. The 1 : 1 calcium citrate, 1 : 2 calcium-malate and -tartarate complexes have been isolated in solid state.

CALCIUM occurs in plants and animals and its reactions with naturally occurring compounds would be helpful in understanding the mechanism of absorption, transport and storage of calcium in bio-systems. In the present paper, the binary and ternary complexes of calcium with plant acids, *viz.* citric, malic, succinic and tartaric acids are being reported on the basis of conductometric evidences.

The specificity of tartaric acid for calcium is well known[1]. Interaction of calcium with citric acid has been intensively studied in literature[2-4]. The complex formations of alkaline earth cations with malic, citric and tartaric acids have been reported in literature[5-7]. We have isolated 1 : 1 calcium-citrate, 1 : 2 calcium-malate and -tartarate complexes. A 1 : 2 calcium-citrate complex has also been studied by conductometric titrations.

Experimental

All the neutral calcium salts were prepared by the usual methods and were tested for purity by elemental analysis. The standard acid solutions were prepared in conductivity water. The suspensions of known weights of the neutral calcium salts of citric, malic and tartaric acids in conductivity water (100 ml), were titrated conductometrically, against standard solutions of the plant acid component with the help of Systronics 303, a direct reading conductivity meter using a conductivity cell of black platinised platinum electrodes. The instrument was calibrated with standard KCl solution. After each addition of the titrant, a time period of 3 min for stirring followed by one 1 min for settling down, was allowed before taking the reading.

The solid complexes were isolated by the general method of interaction of water suspension of neutral calcium salts of the acids with an excess of the corresponding acid solutions, till a clear solution was obtained. In case of malic acid complex, owing to the higher solubility of calcium malate, an excess of acid solution was added even beyond the visible dissolution point. The clear solutions, thus obtained, were filtered, concentrated on water-bath and crystallised. The crystals were filtered, washed with cold distilled water to remove any adhered free acid and dried in an air-oven at 100° temperature.

Results

The neutral calcium citrate, malate and tartarate salts prepared have been found to be of molecular formula $Ca_3C_{12}O_{14}H_{10}.4H_2O$, $CaC_4O_5H_4.H_2O$ and $CaC_4O_6H_4.4H_2O$ respectively, by elemental analysis. The results are as follows : 1 : 1 calcium citrate complex (Found : Ca, 15.23 ; C, 30.26 ; H, 3.94. $Ca(C_6O_7H_6).2H_2O$ requires : Ca, 15.04 ; C, 27.07 ; H, 3.76%) ; 1 : 2 calcium malate complex (Found : Ca, 13.23 ; C, 27.97 ; H, 4.78. $Ca(C_4O_5H_5)_2.2H_2O$ requires Ca, 11.69 ; C, 28.07 ; H, 4.09%) ; 1 : 2 calcium tartarate complex (Found : Ca, 9.53 ; C, 27.12 ; H, 4.00. $Ca(C_4O_6H_5)_2.2H_2O$ requires : Ca, 10.69 ; C, 25.67 ; H, 3.74%).

Colour, m.p./decomp. temp. of the complexes are given in Table 1. Conductometric titration data are presented in Table 2.

Discussion

The curve of calcium citrate ($Ca_3(cit)_2.4H_2O$)-citric acid titration showed two breaks at 1 : 1 and 1 : 4 mole ratios between calcium citrate and citric acid. These correspond to a 1 : 1 and 1 : 2 mole ratios between Ca^{2+} and cit^{3-} ions. The curves for calcium malate *vs* malic acid titration and calcium tartarato-tartaric acid titration showed only

TABLE 1—PHYSICAL PROPERTIES OF COMPLEXES

Compd.	Colour	Decomp. temp. °C	Colour change during decomp.	M.p. of the corresponding acid from which complexes prepared °C
Calcium citrate complex (1 : 1)	Shining white	230	Grey	
Calcium citrate complex (1 : 2)	White	155	Pale yellow	
Calcium malate complex (1 : 2)	Shining white	138-39[a]	Pale yellow	
Calcium tartarate complex (1 : 2)	Shining white	139[a]	Pale yellow	
Calcium malatocitrate (1 : 1 : 1)	White	235	Yellow	153 (citric)
Calcium malatosuccinate (1 : 1 : 1)	White	255	Grey	185 (succinic)
Calcium malatotdisuccinate (1 : 1 : 2)	White	260	Grey	185 (succinic)
Calcium tartaratocitrate (1 : 1 : 1)	White	260	Yellow	153 (citric)
Calcium tartaraomalate (1 : 1 1)	White	240	Pale yellow	100 (malic)
Calcium tartaratosuccinate (1 : 1 : 1)	White	195	Yellow	185 (succinic)

[a]Melted.

TABLE 2—CONDUCTOMETRIC TITRATION OF Ca-CITRATE, Ca-MALATE AND Ca-TARTARATE

Initial volume = 100 ml

Complex g	Titrant	Inflection point (ml) : Found/(Calcd.) 1 : 1	1 : 2
Ca-citrate			
0.114	0.4 *M* Citric acid	0.6 (0.5)	2.2 (2.0)
Ca-malate			
0.344	0.5 *M* Malic acid[b]	3.2 (3.6)	–
0.268	0.4 *M* Citric acid[b]	3.8 (3.5)	–
0.2746	0.5 *M* Succinic acid[b]	2.6 (2.9)	5.8 (5.8)
Ca-tartarate			
0.188	0.5 *M* Tartaric acid[a]	1.75 (1.45)	–
0.188	0.5 *M* Malic acid[a]	1.7 (1.45)	–
0.188	0.4 *M* Citric acid[a]	1.6 (1.8)	–
0.188	0.5 *M* Succinic acid[a]	1.48 (1.45)	–

At [a]32°, [b]30°.

one break in the vicinity of 1 : 1 mole ratio between the reactants indicating the formation of 1 : 2 calcium malate and 1 : 2 calcium tartarate complexes. In case of calcium citrate-citric acid titration, the visible dissolution of the original suspension took place between the Ist and 2nd breaks. In case of calcium malate-malic acid titration, the visible dissolution took place before the lone break point. In calcium tartarate-tartaric acid titration, the visible dissolution took place beyond the break point. Thus, conductometric titrations provided evidence of various complexes, *viz.* 1 : 1 calcium citrate, 1 : 2 calcium citrate, 1 : 2 calcium malate and 1 : 2 calcium tartarate.

In all of the above titrations, the specific conductivity continued to increase with the addition of the titrant; at the break points, however, the rate of increase of specific conductivities decreased. The volume of titrant in all the cases were so adjusted that there could not possibly be any dilution effect.

The elemental analysis of the solid compounds isolated were found to be in closer agreement to the values required for 1 : 1 calcium citrate, 1 : 2 calcium malate and 1 : 2 calcium tartarate complexes together with two molecules of water in each case. The water molecules seem to be strongly associated to the metal ions, for they could be released at temperatures much higher than 100°. The m.p./decomp. temp. of the complexes (Table 1) as compared to those of the starting ingredients, suggest them to be genuine compounds and not the stoichiometric mixtures of the starting ingredients. Our attempts to isolate the 1 : 2 calcium citrate complex, as shown by conductometry, have met with failure. However, the m.p. (155°) of a dry residue, obtained by evaporating a solution containing calcium citrate and citric acid in 1 : 4 molar ratio to dryness was 2° higher than the m.p. of citric acid (153°), indicating, thus, the dry residue to be a genuine compound and not the mixture of calcium citrate and citric acid. The dry residue on treatment with absolute ethanol yielded the 1 : 1 calcium citrate complex. Thus, our observations suggest the formation of 1 : 1 calcium citrate, 1 : 2 calcium malate and 1 : 2 calcium tartarate complexes in aqueous solution and their isolability in the solid state ; and a 1 : 2 calcium citrate complex, existing perhaps, only in aqueous solution.

In the titrations carried out for mixed ligand ternary complexes, the initially taken suspension ultimately went into solutions indicating non-replacement chemical interactions between the reactants. A replacement reaction under the experimental conditions would have resulted in the precipitation of the calcium salt of the titrant acid. For comparative purpose a titration in which there would be a replacement, was also carried out, *e.g.* calcium malate was titrated against tartaric acid. The suspension of calcium malate initially went into solution but was immediately followed by the precipitation of calcium tartarate (replacement). The plots for the titrations, calcium malate *vs* citric

acid, calcium tartarate *vs* citric, malic and succinic acids showed only one break in the vicinity of 1 : 1 mole ratio between the neutral calcium salt and the titrant free acid, suggesting a 1 : 1 complexation between the reactants. The plot for calcium malate against succinic acid titration showed two breaks at 1 : 1 and 1 : 2 mole ratio between the reactants suggesting a 1 : 1 and 1 : 2 complexation between calcium malate and succinic acid. Since the neutral calcium malate and tartarate have a 1 : 1 stoichiometry between the metal ion and the carboxylate anion in them, the complexes corresponding to the 1 : 1 break, seem to have a 1 : 1 : 1 stoichiometry among the calcium ions and the two different acid anions. The 1 : 2 break in calcium malate *vs* succinic acid titration suggests a complex of 1 : 1 : 2 stoichiometry among the calcium ions, malic acid and succinic acid, respectively. In the titrations with calcium malate, the visible dissolution of the original suspension took place before the break points, whereas in titrations with calcium tartarate, the visible dissolution took place beyond the break points. Complexation as the primary factor for 1 : 1 break in case of titrations of calcium tartarate with different acids has been mentioned earlier. In the case of replacement titration (calcium malate *vs* tartaric acid), the specific conductivity initially increased with the addition of the titrant, followed by visible dissolution. But around the 1 : 1 mole ratio between the reactants, the precipitation of calcium tartarate started with the decreased in specific conductivity till the replacement was complete. Beyond this, calcium tartarate formed, started to dissolve slowly with further addition of the titrant (tartaric acid) with a gradual increase in specific conductivity, resulting roughly in a V-shaped curve. Thus various complexes indicated are (i) calcium malatocitrate (1 : 1 : 1), (ii) calcium malatosuccinate (1 : 1 : 1), (iii) calcium malatodisuccinate (1 : 1 : 2), (iv) calcium tartaratocitrate (1 : 1 : 1), (v) calcium tartaratomalate (1 : 1 : 1) and (vi) calcium tartaratosuccinate (1 : 1 : 1).

The mixed ligand ternary complexes could not be isolated in the solid state, suggesting thus, their probable existence only in aqueous solution. However, the neutral calcium salts and the free acid solutions were mixed in exact mole ratios corresponding to the conductometric breaks. The clear solutions thus obtained were evaporated to dryness on water-bath. The melting/decomposition temperatures of these dry residues (Table 1) have generally been found to be higher than the m.p./decom. temp. of the free acids from which they were prepared, supporting conclusions drawn from conductometric titrations.

Acknowledgement

Authors express their gratefulness to U.G.C., New Delhi, for sponsoring the scheme.

References

1. R. J. P. Williams, *J. Chem. Soc.*, 1952, 3770.
2. Euler and Bolin, *Z. Phys. Chem.*, 1909, 61, 1.
3. E. Shorr, T. P. Alamy, M. H. Sloan, H. Taussky and V. Toscani, *Science*, 1942, 96, 587.
4. J. Muss and H. Lebel, *Medd*, 1936, 13, 17.
5. R. K. Cannas and A. Kibrick, *J. Am. Chem. Soc.*, 1938, 60, 2314.
6. N. Joseph, *J. Biol. Chem.*, 1946, 164, 529.
7. M. Bobtelsky and J. Jordan *J. Am. Chem. Soc.*, 1945, 67, 1824.
8. F. Defrancesco and C. Defrancesco, *Rev. Soc. Ital. Sci. Aliment*, 1978, 7, 381.

J. Indian Chem. Soc.,
Vol. LXIII, May 1986, pp. 463-465

Study of the Complexes obtained from Interaction between Copper(II) Chelates of 2-Hydroxyaromatic Ketones and Aralkyl Monoamines

RABINDER NATH

Defence Research and Development Establishment, Gwalior-474 002

and

R. P. BHATNAGAR*

School of Studies in Chemistry, Jiwaji University, Gwalior-474 011

Manuscript received 10 October 1984, revised 14 April 1986, accepted 23 April 1986

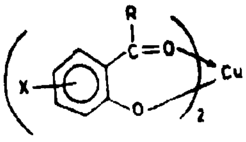
The title interaction has been studied in ethanol medium under reflux conditions and also in restricted amount of the solvent at room temperature. Square-planar Schiff base complexes result under the first set of conditions. But at room temperature diamine adducts seem to be formed. A mechanism envisaging an initial rapid coordination of the primary amine to the central metal ion has been proposed for the Schiff base complex formation reaction.

A primary amine is expected to interact with transition metal chelate in at least two distinct ways. Either it may coordinate with the central metal ion to form a new compound with expanded coordination number or it may react with the coordinated ligand first, with subsequent possibilities of the formation of Schiff base complexes. Though convincing evidence for the former type of interaction is lacking, Nunez and Eichhorn[1] postulated the formation of adducts as intermediates in such reactions. However, the latter course of reaction has been suggested by some workers[2-5] for metal chelates with hydroxy-aromatic carbonyl compounds.

Adduct formation should be possible in cases where stereochemical and energetic factors favour a slow condensation reaction. Using copper(II) chelates 2-hydroxyaromatic ketones, interaction with alkyl monoamines has been investigated in order to confirm or discard the possibilities of adduct formation as postulated by Nunez[1] and Janecke[6].

Experimental

All chemicals were of reagent gradequality. The 2-hydroxyaromatic ketones were prepared by Frus



1 ; X = H, R = CH_3
2 ; X = 5-CH_3, R = CH_3
3 ; X = 5-Cl, R = CH_3
4 ; X = 5-Cl, R = C_6H_5

reaction from appropriate phenolic esters. Copper(II) chelates (1-4) were prepared by the reported methods[7,8].

The Schiff base complexes were first obtained in ethanolic medium by condensing each of the above copper(II) chelates separately with benzyl and β-phenylethyl amines as detailed below :

Interaction of chelates with the primary amines under reflux conditions : Copper(II) chelates of the carbonyl compound (0.01 mol) was suspended in ethanol (~ 50 ml) and the amine (0.02 mol) incorporated into the mixture. The mixture was refluxed for 15 min and cooled. Reddish-brown complexes separated were purified by recrystallisation from benzene-ethanol (1 : 1) mixture. Compounds so prepared (Cu-1 to Cu-8) have been listed in Table 1 along with their analytical and magnetic data. Identical compounds could also be obtained by reacting copper(II) acetate with requisite quantity of the Schiff base in presence of an external base.

Interaction of Cu^{II} chelates at 20° with primary amines in presence of excess ethanol : Freshly prepared and dried Cu^{II} chelates (0.01 mol) was taken with about four times the volume of ethanol. The mixture was thoroughly ground in a mortar for 5 min. Appropriate amine (0.02 mol) was then allowed to drop into the mixture in a mortar with constant trituration and the contents were quickly transferred to a sintered glass crucible and filtered under efficient suction. The solid in the crucible was again moistured with methanol/ethanol (2 ml) and stirred thoroughly. The solvent

TABLE 1—ANALYTICAL AND MAGNETIC DATA OF COPPER(II) COMPLEXES

Compd. no.	Reactants		Molecular formula	Analysis % : Found/(Calcd.)		μ_{eff}[a] B.M.
	Chelate	Amine		N	Cu	
Cu-1	1	Benzyl	$C_{30}H_{28}N_2O_2Cu$	5.20 (5.47)	12.08 (12.41)	1.60
Cu-2	1	β-Phenylethyl	$C_{32}H_{32}N_2O_2Cu$	5.26 (5.19)	11.42 (11.47)	1.59
Cu-3	2	Benzyl	$C_{32}H_{32}H_2O_2Cu$	5.50 (5.19)	11.36 (11.37)	1.59
Cu-4	2	β-Phenylethyl	$C_{34}H_{36}N_2O_2Cu$	5.21 (4.93)	10.75 (11.19)	1.59
Cu-5	3	Benzyl	$C_{30}H_{26}N_2O_2Co_2Cu$	5.04 (4.82)	10·80 (10.94)	1.59
Cu-6	3	β-Phenylethyl	$C_{32}H_{30}N_2O_2Cl_2Cu$	5.00 (4.60)	10.18 (10.43)	1.64
Cu-7	4	Benzyl	$C_{40}H_{30}N_2O_2Cl_2Cu$	3.39 (3.97)	9.25 (9.01)	1.54
Cu-8	4	β-Phenylethyl	$C_{42}H_{34}N_2O_2Cl_2Cu$	4.14 (3.82)	8.80 (8.67)	1.58

[a]At 239 k.

was then removed by suction. It was repeated 2-3 times. Products were dried finally in a vacuum desiccator.

Characterisation of the complexes prepared by the above methods was done by micro-analysis of the elements and estimation of copper as cupric oxide after igniting the complex to a constant weight.

Infrared spectra were taken with a Perkin-Elmer 577 spectrophotometer using KBr pallets. A Beckman 25 uv-vis spectrometer was used for electronic spectra measurements. Electrolytic conductance was measured in chloroform as solvent at room temperature. Magnetic susceptibility was measured by Gouy's method.

Results and Discussion

The compounds were found to be non-electrolytes.

Infrared frequencies characteristic of these complexes are listed in Table 2. The broad band envelope in 2 800-200 cm^{-1} region, present in cases of free Schiff bases due to intra-molecular H-bonded phenolic group[9], was absent in the prepared compounds. Deprotonation and simultaneous formation of Cu—O bond can thus be inferred. The $\nu_{C=N}$ mode absorbed at marginally lower frequencies[10] (1 610-1 590 cm^{-1}) as compared to those of the free Schiff bases (1 620-1 600 cm^{-1}). This indicates involvement of azomethine nitrogen in bonding[11].

TABLE 2—PRINCIPAL IR BANDS (cm^{-1}) OF COPPER(II) COMPLEXES

Compd. no.	$\nu_{C=N}$	$\nu_{C=C}$	δ_{CH_2}	δ_{CH_2}	ν_{C-O}	ν_{Cu-N}	ν_{Cu-O}
Cu-1	1 590	1 570, 1 525	1 435	1 360	1 320	415	312
Cu-3	1 610	1 580, 1 530	1 447	1 345	1 325	370	340
Cu-4	1 610	1 590, 1 530	1 460	1 340	1 315	360	337
Cu-5	1 597	1 585, 1 520	1 450	1 345	1 318	360	335
Cu-6	1 592	1 555, 1 515	1 445	1 363	1 315	365	340
Cu-7	1 590	1 555, 1 505	1 440	–	1 317	360	327
Cu-8	1 595	1 575, 1 520	1 450	–	1 325	355	335

New bonds in the 415-355 and 390-315 cm^{-1} regions were assigned respectively to Cu ← N and Cu—O stretching modes[12]. Presence of several bands in 520-450 cm^{-1} region and slight increase in intensity and frequency shift were observed. These are probably due to the out-of-plane ring deformations. Metal ligand stretching mode due to vibrational coupling also is likely to give some of these absorptions.

Uv-vis absorption spectra (Table 3) was strikingly similar for all the eight compounds showing bands in 630-615, 380-360 and 308-304 nm regions. The lowest energy band in the visible region was due to the merger of the

$$^2B_{1g} \rightarrow {}^2A_{1g},\ {}^2B_{1g} \rightarrow {}^2B_{2g} \text{ and } {}^2B_{1g} \rightarrow {}^2E_g$$

transitions in a D_{4h} symmetry[14,15]. The strong absorption at 350-360 nm is expected to be due to ligand-copper(II) charge transfer[17]. The highest

TABLE 3—UV-VISIBLE SPECTRAL DATA OF COMPLEXES

Compd. no.	λ_{max}[a] (nm)		
	1	2	3
Cu-1	615 (215)	360 (9 210)	308 (11 760)
Cu-2	620 (204)	360 (8 600)	308 (12 950)
Cu-3	620 (216)	370 (10 790)	305 (12 950)
Cu-4	625 (216)	370 (11 350)	305 (14 750)
Cu-5	630 (209)	370 (12 770)	350 (14 165)
Cu-6	625 (310)	370 (14 190)	303 (14 460)
Cu-7	625 (225)	380 (12 120)	305 (12 260)
Cu-8	625 (175)	380 (11 425)	303 (12 600)

[a]Figures in parentheses represent molar extinction coefficients.

The band in the visible region appeared as a broad shoulder preceding the intense band around 370 nm.

energy band appearing at almost a constant wave length (~ 305 nm) is caused by π-π^* transitions of the amine aromatic rings[18,19].

The μ_{eff} values (Table 1) of 1.54-1.64 B.M. for these compounds were appreciably lower than the spin-only value of 1.73 for a d^9 system. This may be due to the quenching of the unpaired spin in the metal ion as unpaired spins on the adjacent Cu^{II} ions coupled by super exchange type of interaction involving a π-electronic pathway across the bridging oxygen atoms[22] arising from partial dimerisation of the Cu^{II} complexes in solid state.

Reaction carried out at room temperature gave solids of colours varying from bright green to olive green. However, the correct stoichiometry could be determined only for compounds obtained by the intraction of benzylamine and chelates 1, 2 and 3 (Cu-9 : $C_{30}H_{32}N_2O_4Cu$, Cu-10 : $C_{32}H_{36}N_2O_4Cu$, and Cu-11 : $C_{30}H_{30}N_2O_4Cl_2Cu$). Their characterisation by infrared spectral data suggest them to be adducts of amines with the metal-ketone complexes. Their complexes gave a doublet of medium intensity having a maxima in 3 310 to 3 250 cm^{-1} region (which is ~ 50 cm^{-1} lower than those for pure amines[23,24]). Additional new bands at 1 590-1 560 and 1 212-1 190 cm^{-1} regions were also obtained due to δ_{NH} and ν_{CN} vibration modes[25,26]. The broad intense band at 1 625 ± 5 cm^{-1} was due to ν_{CO} mode[27]. The magnetic moment values of these compounds are found to be in the range 1.84-1.90 B.M.

These adducts are relatively unstable and decompose even during preparation, as observed in adducts of β-phenylethyl amine with metal-ketone complexes. However, the adducts changed into tetracoordinated Schiff base complexes on refluxing in ethanolic solutions. The reaction can thus be envisaged as the initial bonding of amine to the metal in the chelate to give adduct as intermediate which facilitates the nucleophilic attack on the carbonyl group resulting in the removal of a molecule of water.

References

1. L. J. Nunez and G. L. Eichhorn, *J. Am. Chem. Soc.*, 1962, **84**, 901.
2. R. H. Holm, G. W. Everett, Jr. and A. Chakravarty, *Prog. Inorg. Chem.*, 1966, **7**, 83.
3. E. J. Olszewski and B. F. Martin, *J. Inorg. Nucl. Chem.*, 1965, **27**, 1043.
4. M. M. Patel and R. P. Patel, *Indian J. Chem.*, *Sect. A*, 1976, **14**, 909.
5. S. Ekk, *Inorg. Chem.*, 1976, **15**, 358.
6. W. P. Jencks, *Prog. Phys. Org. Chem.*, 1964, **2**, 63.
7. D. P. Gradon and G. M. Mockler, *Aust. J. Chem.*, 1968, **21**, 617.
8. E. Uhlig and U. Dinjus, *Z. Anorg. Allg. Chem.*, 1973, **397**, 297.
9. H. H. Freedman, *J. Am. Chem. Soc.*, 1961, **83**, 2900.
10. K. Dey and K. C. Ray, *J. Indian Chem. Soc.*, 1973, **50**, 631.
11. J. E. Kovacic, *Spectrochim. Acta*, *Part A*, 1967, **23**, 183.
12. A. B. P. Lever and E. Mantovani, *Can. J. Chem.*, 1973, **51**, 1967.
13. K. Nakamoto, C. Udovich and J. Tukemoto, *J. Am. Chem. Soc.*, 1970, **92**, 3973.
14. J. P. Fackler, F. A. Cotton and D. W. Barnum, *Inorg. Chem.*, 1963, **2**, 97.
15. L. Sacconi and M. Ciampolini, *J. Chem. Soc.*, 1964, 276.
16. T. P. Cheeseman, D. Hall and T. N. Waters, *J. Chem. Soc.*, A, 1966, 694.
17. C. A. Agambar and K. G. Orrel, *J. Chem. Soc.*, 1969, 897.
18. K. K. Chatterjee and B. E. Douglas, *Spectrochim. Acta*, 1965, **21**, 1625.
19. M. El-Bayoumi, J. El-Asser and F. Abdel-Halim, *J. Am. Chem. Soc.*, 1971, **93**, 586.
20. B. N. Figgis, *Nature* (*London*), 1958, **182**, 1568.
21. D. Hall and T. N. Waters, *J. Chem. Soc.*, 1964, 2644.
22. J. Kato, H. B. Jonasson and J. C. Fanning, *Chem. Rev.*, 1964, **64**, 99.
23. A. P. Gray and R. C. Lord, *J. Chem. Phys.*, 1957, **26**, 690.
24. C. T. Spencer and L. T. Taylor, *Inorg. Chem.*, 1973, **12**, 644.
25. J. C. Evans, *Spectrochim. Acta*, 1960, **16**, 428.
26. N. B. Kolthup, *J. Opt. Soc. Am.*, 1950, **40**, 397.
27. A. K. Sengupta and S. K. Nath, *Indian J. Chem.*, *Sect. A*, 1960, **19**, 166.
28. D. Hopgood and D. L. Leussing, *J. Am. Chem. Soc.*, 1949, **91**, 3740.
29. A. M. Shallaby, M. M. Mostafa and M. M. Bekheit, *Indian J. Chem.*, *Sect. A*, 1979, **17**, 516.
30. P. Bamfield, *J. Chem. Soc.*, *A*, 1969, 2021.

J. Indian Chem. Soc.,
Vol. LXIII, May 1986, pp. 466-468

Synthesis and Structural Studies of Salicylaldazine Complexes of Oxovanadium(IV), Manganese(II), Iron(II), Cobalt(II), Nickel(II), Copper(II) and Zinc(II)

R. C. AGGARWAL*, N. K. SINGH and R. P. SINGH**

Department of Chemistry, Banaras Hindu University, Varanasi-221 005

Manuscript received 25 November 1985, revised 10 April 1986, accepted 23 April 1986

Neutral complexes of the type M(SA).nH$_2$O, where M = VO^{II}, Mn^{II}, Fe^{II}, Co^{II}, Ni^{II}, Cu^{II} or Zn^{II}; SA = dianion of salicylaldazine; n = 1 for VO^{II} and Zn^{II}, and 2 for other metal ions, have been prepared. The complexes are non-electrolytes as is evident from low values of their molar conductance (10-15 Ω^{-1} cm^{2}mol^{-1}) in DMF solutions. The magnetic moment values and electronic spectral data suggest that the Mn^{II}, Fe^{II}, Co^{II} and Ni^{II} complexes are outer-orbital octahedral while Cu^{II} complex is distorted octahedral. Infrared spectral studies indicate that SA^{2-} behaves as a tetradentate ligand bonding through the two azomethine nitrogens and both the phenolic oxygens. TGA and ir studies show that the water molecule(s) are coordinated in all the complexes except the Zn^{II} complex where it is present in the lattice. *X*-ray powder diffraction studies of Cu(SA).2H$_2$O and Zn(SA).H$_2$O suggest that they are not isomorphous and belong to hexagonal and orthorhombic crystal systems, respectively.

THE 3d metal(II) complexes of salicylaldazine *o*-HO-C$_6$H$_4$CH=N-N=CHC$_6$H$_4$OH-*o*(H$_2$SA)[1-3] have been prepared but no definite conclusions have been drawn about the mode of bonding of the ligand and the stereochemistry of the complexes. In view of the inadequacy of the previous work and our continuing interest in transition metal complexes of salicylaldimines[4,5], the research work on the title complexes was undertaken and the results of these investigations are reported in the present paper.

Experimental

All chemicals used were of AnalaR quality. Salicylaldazine (H$_2$SA) was prepared by the literature procedure[6]. Purity of the ligand was checked from its m.p. 213° (lit[6]. 213-14°) (Found: N$_2$H$_4$, 13.50. Calcd. for C$_{14}$H$_{12}$O$_2$N$_2$: N$_2$H$_4$, 13.33%).

Preparation and analysis of complexes: VO(SA).H$_2$O was prepared by adding hydrazine hydrate to a methanolic solution of bis(salicylaldehydato)-aquooxovanadium(IV)[7] in 1 : 1 mo ar ratio and warming the reaction mixture for ~ 15 min. The complex thus precipitated was filtered, washed with methanol and finally with CHCl$_3$, and dried at room temperature. The other M(SA).nH$_2$O complexes, where M=Mn^{II}, Co^{II}, Ni^{II}, Cu^{II} and Zn^{II}, were prepared by reacting aqueous solutions of the respective metal chloride with H$_2$SA dissolved in minimum quantity of aqueous NaOH in 1 : 1 molar ratio. Fe(SA).2H$_2$O was prepared similarly employing methanolic solutions and carrying out the reaction under hydrogen atmosphere. The complexes precipitated immediately and were filtered, washed with very dilute acetic acid and finally with chloroform, and dried *in vacuo*.

The complexes were analysed for metal, nitrogen, hydrazine and water content. Experimental details pertaining to the analyses, molar conductance, magnetic susceptibility, electronic and ir spectral measurements were the same as described in our earlier paper[4]. The results are given in Tables 1 and 2. The *X*-ray powder photograph for Cu(SA).2H$_2$O and Zn(SA).H$_2$O were obtained on a Philips *X*-ray generator using nickel filtered CuK$_\alpha$ radiation and a Debye-Scherrercamera.

Results and Discussion

The analytical data (Table 1) show that H$_2$SA yields neutral complexes of the general formula M (SA).nH$_2$O, where n = 1 for Zn^{II} and VO^{II}, and 2 for other metal ions. The complexes do not melt but decompose in the temperature range 200-300°. The complete loss of water molecule(s) at ~110° in the case of Zn^{II} complex and at relatively higher temperatures (160-170°) in the case of other complexes showed that the water molecule(s) are lattice-held in the former and coordinated in the latter complexes[8]. These findings about the nature of water molecules in the hydrated complexes is supported by the presence of a band in 755-800 cm^{-1} region, characteristic of coordinated water in complexes of all metal ions except that of Zn^{II}

**Present address: Chemistry Department, U.P. (P.G.) College, Varanasi.

TABLE 1—ANALYTICAL, MAGNETIC MOMENT AND MOLAR CONDUCTANCE DATA OF COMPLEXES

Compd.	Colour	Analysis % : Found/Calcd.)			Weight loss %[a] Found/ (Calcd.)	μ_{eff}[b] B.M.	Molar conductance in DMF Ω^{-1} cm^2 mol^{-1}
		Metal	N	N_2H_4			
$VO(SA).H_2O$	Brown	15.10 (15.77)	8.71 (8.67)	–	5.40 (5.57)	1.70	11.5
$Mn(SA).2H_2O$	Orange yellow	16.95 (16.70)	8.41 (8.51)	9.60 (9.73)	10.71 (10.94)	6.04	10.0
$Fe(SA).2H_2O$	Dark brown	17.02 (16.93)	8.64 (8.49)	9.75 (9.70)	10.54 (10.91)	5.00	11.5
$Co(SA).2H_2O$	Dark pink	17.53 (17.70)	8.51 (8.41)	10.10 (9.61)	10.53 (10.81)	4.97	14.0
Co(SA)	Brownish red	20.10 (19.84)	9.46 (9.43)	–	–	4.83	–
$Ni(SA).2H_2O$	Yellow	17.10 (17.64)	8.70 (8.42)	9.34 (9.62)	10.56 (10.82)	3.24	13.6
Ni(SA)	Yellowish green	19.40 (19.78)	9.02 (9.44)	–	–	2.95	–
$Cu(SA).2H_2O$	Light brown	19.46 (18.82)	8.24 (8.30)	–	10.89 (10.67)	1.87	15.0
Cu(SA)	Brown	21.21 (21.08)	9.58 (9.29)	–	–	1.86	–
$Zn(SA).H_2O$	Yellow	20.80 (20.34)	8.60 (8.71)	9.93 (9.96)	5.40 (5.60)	Diamag.	12.8

[a]Temp. 110° for Zn^{II} complex and 160–170° for other complexes. [b]At 298 k.

TABLE 2—ELECTRONIC SPECTRAL DATA AND LIGAND FIELD PARAMETERS OF COMPLEXES

Compd.	λ_{max} cm^{-1}	Assignments	10 Dq cm^{-1}	B' cm^{-1}	β	$\beta°$	LFSE $kJmol^{-1}$
$VO(SA).H_2O$	12 900, 15 380	$d_{xy} \rightarrow d_{yz}, d_{xz}$; $d_{x^2-y^2}$	15 380	–	–	–	73.4
$Fe(SA).2H_2O$	16 600	$^5T_{2g} \rightarrow {^5E_g}$ (D)	16 600	–	–	–	79.2
$Co(SA).2H_2O$	10 800	$^4T_{1g}$ (F) $\rightarrow$ $^4T_{2g}$ (F)	–	–	–	–	–
Co(SA)	9 525, 21 050	$^4T_{1g}$ (F) $\rightarrow$ $^4T_{2g}$ (F), $^4T_{1g}$ (P)	10 810	854	0.878	12.20	103.1
$Ni(SA).2H_2O$	10 530, 17 600	$^3A_{2g}$ (F) $\rightarrow$ $^3T_{2g}$ (F), $^3T_{1g}$ (F)	10 530	896	0.850	15.10	150.7
Ni SA)	10 700	$^3A_{2g}$ (F) $\rightarrow$ $^3T_{2g}$ (F)	10 700	–	–	–	153.0
$Cu(SA).2H_2O$	14 300	$^2E_g \rightarrow T_{2g}$	14 300	–	–	–	102.3
Cu(SA)	15 400	$^2E_g \rightarrow {^2T_{2g}}$	15 400	–	–	–	110.2

(Ref. 9). The complexes are insoluble in water and in organic solvents, such as ethanol, methanol, THF and acetone, and slightly soluble in DMF and DMSO. The molar conductance values (10-15 Ω^{-1} cm^2 mol^{-1}) of the complexes in DMF show their non-ionic nature[10].

Magnetic moment: The μ_{eff} values (Table 1) indicate that the hydrated as well as anhydrous complexes of Fe^{II}, Co^{II} and Ni^{II} are spin-free and have octahedral geometry[11]. The magnetic moment of Mn^{II} complex corresponds to five unpaired electrons while μ_{eff} values of Cu^{II} and VO^{II} complexes correspond to one unpaired electron indicating spin-free nature of the former complex but giving no specific information about the stereochemistry of the latter.

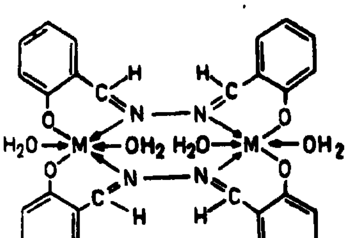
Electronic spectra: The uv spectra of H_2SA in nujol show three bands at 27 400, 34 500 and 45 450 cm^{-1} while the spectra of the complexes in the 20 000-50 000 cm^{-1} region also show three bands at 23 250-23 800, 33 000 and 40 000-44 400 cm^{-1}. The 27 400 cm^{-1} band of the ligand corresponding to the 30 300 cm^{-1} band of free salicylaldehyde[12] is considerably red-shifted (23 250-23 800 cm^{-1}) in the complexes due to the formation of salicylaldazinato ion and its subsequent participation in chelate ring formation around the metal ion[13] (1). The number and position of the d-d transition bands and assignments thereof (Table 2) suggest the octahedral geometry for the hydrated as well as anhydrous complexes of VO^{II}, Fe^{II}, Co^{II}, Ni^{II} and Cu^{II} (Refs. 14-18). The broadness of the d-d transition band and $\nu_{o\mu}$ ν_{xt} ratio of 1.36-1.44 (Ref. 19) in Cu^{II} complexes indicate that they are tetragonally distorted. The visible spectrum of Mn^{II} complex yields no d-d transition bands because these bands appear to have submerged into the strong intra-molecular transitions of the salicylaldazinato ion.

The D_q values of the complexes suggest that SA lies between water and ammonia in the spectrochemical series while $\beta°$ values indicate 12.2-15.1% covalency in the metal-ligand bond.

Infrared spectra: The infrared spectra of the ligand in nujol show a broad band at 3 450 cm^{-1} assigned to ν_{OH} which is shifted to 3 700 cm^{-1} in the chloroform solution, indicating the presence of hydrogen bonding in the ligand in the solid state.

The spectra of the hydrated complexes show a broad band in 3 400-3 470 cm^{-1} region which may be attributed to ν_{OH} of the water molecules present in these complexes. A single $\nu_{C=N}$ band observed at 1 625 cm^{-1} in the spectra of the ligand suffered a negative shift of 10-25 cm^{-1} in the spectra of the complexes, indicating coordination through both the symmetrical azomethine nitrogen atoms. Satapathy and Sahoo[8] reported two $\nu_{C=N}$ bands at 1 613 and 1 595 cm^{-1} in the case of Fe^{II} complex but we observed only one band at 1 600 cm^{-1} in the spectrum of Fe(SA).$2H_2O$, which suggests that both the C=N groups of the ligand are involved in coordination in the above complex just as in other complexes. The coordination through both the azomethine nitrogens is further supported by a positive shift of 55-100 cm^{-1} in N—N stretching frequency in the spectra of the complexes[20]. A positive shift of 13-50 cm^{-1} in ν_{C-O} band in the complexes as compared to the ligand (1 272 cm^{-1}) and appearance of a new band due to ν_{asym} (C—O) in the region 1 530-1 545 cm^{-1} in the spectra of the hydrated complexes and around 1 550 cm^{-1} in the anhydrous complexes indicate the presence of C—O—M moiety in these complexes and also the unidentate nature of the C—O group in former complexes and its bridging bidentate nature in the latter[21,22]. The 960 cm^{-1} band appearing in the oxovanadium(IV) complex is assigned to $\nu_{V=O}$[23] while the non-ligand bands appearing in this and other complexes in the regions 250-465 and 325-390 cm^{-1} are tentatively assigned to ν_{M-O}[24,25] and $\nu_{M\leftarrow N}$[26,27] modes, respectively.

X-Ray powder diffraction: The indexing of the X-ray diffraction lines were done by Hess-Lipson's method[28] and it was found that most of the prominent diffraction lines could be satisfactorily indexed for hexagonal and orthorhombic symmetries for Cu(SA).$2H_2O$ and Zn(SA).H_2O, respectively. The lattice parameters calculated for the above symmetries are: a=10.267Å, C=16.05Å, V= 732Å^3 for Cu(SA).$2H_2O$ and a = 7.492Å, b= 12.58Å, c=16.08 and V=1515Å^3 for Zn(SA).$2H_2O$. The powder X-ray diffraction photograph of these complexes show that they are not isomorphous.



M(SA).$2H_2O$
M = Fe, Co, Ni, Cu

1

Based on the composition and physicochemical studies, the following structure (1) could be proposed for the M(SA).nH_2O complexes.

Acknowledgement

The authors thank the Head of the Department of Chemistry, Banaras Hindu University, for providing facilities. One of the authors (R.P.S.) is also thankful to U.G.C., New Delhi, for the award of a Teacher Research Fellowship.

References

1. L. HUNTER and J. A. MARRIOT, *J. Chem. Soc.*, 1937, 2000.
2. C. S. MARVEL and P. V. BONSIGNORA, *J. Am. Chem. Soc.*, 1959, 81, 2668.
3. S. SATAPATHY and B. SAHOO, *J. Inorg. Nucl. Chem.*, 1970, 32, 2223.
4. R. C. AGGARWAL, N. K. SINGH and R. P. SINGH, *Inorg. Chem. Acta Lett.*, 1979, 32, L87.
5. R. C. AGGARWAL, N. K. SINGH and R. P. SINGH, *Inorg. Chem.*, 1981, 20, 2794.
6. H. CAJAR, *Chem. Ber.*, 1898, 31, 2807.
7. J. J. R. F. DA SILVA, R. WOOTTON, *J. Chem. Soc., A*, 1970, 3369.
8. A. C. FABRETTI, G. C. FRANCHINI, C. P. PRETI and G. TOSI, *Can. J. Chem.*, 1977, 55, 344.
9. I. NAKAGAWA and T. SHIMANOUCHI, *Spectrochim. Acta*, 1964, 20, 429.
10. W. J. GEARY, *Coord. Chem. Rev.*, 1971, 7, 81.
11. B. N. FIGGIS and J. LEWIS in "Modern Coordination Chemistry", eds. J. LEWIS and R. G. WILKINS, Interscience, New York, 1960, p. 403.
12. K. K. ROHTAGI and S. K. SENGUPTA, *J. Inorg. Nucl. Chem.*, 1972, 34, 3061.
13. L. SACCONI, P. PACLETTI and F. MAGGIO, *J. Am. Chem. Soc.*, 1957, 79, 4067.
14. A. SYAMAL, *Coord. Chem. Rev.*, 1975, 16, 309.
15. T. M. DUNN in "Modern Coordination Chemistry", eds. J. LEWIS and R. G. WILKINS, Interscience, New York, 1964, p. 290.
16. A. D. LIEHR, *J. Phys. Chem.*, 1963, 67, 1314; R. W. MATHEWS and R. A. WALTON, *Inorg. Chem.*, 1971, 10, 1433.
17. L. SACCONI, *Transition Met. Chem.*, 1968, 4, 199.
18. L. SACCONI and M. CIAMPOLINI, *J. Chem. Soc.*, 1964, 276.
19. C. K. JORGENSEN, *Acta Chem. Scand.*, 1955, 9, 1362.
20. A. BRAIBANTI, F. DALLAVALLE, M. A. PELLINGHELLI and E. LEOPORATI, *Inorg. Chem.*, 1968, 7, 1430.
21. H. YAMADA, *Bull. Chem. Soc. Jpn.*, 1959, 32, 1051.
22. E. SINN and C. M. HARRIS, *Coord. Chem. Rev.*, 1969, 4, 391.
23. J. SELBIN, L. H. HOLMES, JR. and S. P. MCGLYNN, *J. Inorg. Nucl. Chem.*, 1963, 25, 1359.
24. D. N. SATHYANARAYANA and C. C. PATEL, *Indian J. Chem.*, 1968, 6, 523.
25. N. OHKAKU and K. NAKAMOTO, *Inorg. Chem.*, 1971, 10, 798.
26. B. BEEROFF, M. J. M. CAMPBELL and R. GRZESKOWIAK, *J. Inorg. Nucl. Chem.*, 1974, 36, 55.
27. A. B. P. LEVER and E. MANTOVANI, *Inorg. Chem.*, 1971, 10, 817.
28. B. D. CULLITY, "Elements of X-ray Diffraction", Addison-Wesly, Massachusetts, 1959, 301.

J. Indian Chem. Soc.,
Vol. LXIII, May 1986, pp. 469-471

Potentiometric and Structural Studies on Chromium(II), Manganese(II), Iron(II), Cobalt(II), Nickel(II), Copper(II), Zinc(II) and Cadmium(II) Complexes with Butan-3-semicarbazone-1-carboxylic Acid

J. K. VERMA*

Government College, Daman-396 210

and

G. S. P. VERMA

Ranchi University, Ranchi-834 008

Manuscript received 28 August 1984, revised 24 February 1986, accepted 31 March 1986

The potentiometric studies on Cr^{II}, Mn^{II}, Fe^{II}, Co^{II}, Ni^{II}, Cu^{II}, Zn^{II} and Cd^{II} chelates with butan-3-semicarbazone-1-carboxylic acid were carried out according to Calvin-Bjerrum technique in 75% (v/v) dioxane-water medium at 25, 35 and 45° (μ = 0.1*M* $NaClO_4$). The stability constant suggests that high temperature favours the formation of the chelates and follows the order $Cu^{II} > Zn^{II} > Ni^{II} > Co^{II} > Fe^{II} > Mn^{II} > Cr^{II} > Cd^{II}$. The negative ΔG values suggest spontaniety of the reaction. The positive ΔS values indicate that the entropy term is favourable for the chelate ring formation. The solid chelates have been characterised on the basis of analytical, conductance, magnetic and electronic and infrared spectral data. The analytical data suggest 1 : 2 metal-ligand composition. The chelates are non-electrolytes and monomers. The infrared data reveal that the ligand behaves as a monobasic tridentate ligand which deprotonates during complexation and coordinates through azomethine nitrogen and carbonyl oxygen. The magnetic and electronic spectral data suggest a spin-free octahedral geometry around metal(II) ions.

A perusal of literature[1] reveals that no work has been done on Cr^{II}, Mn^{II}, Fe^{II}, Co^{II}, Ni^{II}, Cu^{II}, Zn^{II} and Cd^{II} chelates with butan-3-semicarbazone-1-carboxylic acid (HBSC). The potentiometric studies has been carried out according to Calvin-Bjerrum titration technique[2] in 75% (v/v) dioxane-water medium at 25, 35 and 45° (μ=0.1 *M* $NaClO_4$). The solid chelates have been characterised on the basis of analytical, conductance, magnetic and electronic and infrared spectral data.

Experimental

A Systronic digital *p*H meter (accuracy 0.01 *p*H unit) was used for the *p*H measurements which was calibrated as reported earlier[3]. Following titrations were carried out in 75% (v/v) dioxane-water medium at 25, 35 and 45° (μ=0.1 *M* $NaClO_4$) with 0.052 *M* carbonate-free sodium hydroxide: (i) 0.02 *M* $HClO_4$ + 0.08 *M* $NaClO_4$, (ii) 0.02 *M* $HClO_4$ + 0.08 *M* $NaClO_4$ + 0.004 *M* HBSC and (iii) 0.02 *M* $HClO_4$ + 0.08 *M* $NaClO_4$ + 0.004 *M* HBSC + 0.001 *M* metal(II) ion. The *p*H meter reading (B) was corrected from the relationship $pH^{corr} = B + \log U_H$, where $\log U_H$ is the correction factor and is given by the equation, $\log U_H = (0.007406)\, t + 0.828$.

The ligand HBSC was prepared by the standard method[5]. Its purity was ascertained from the measurement of its m.p. (173.8°). Metal chlorides were used for preparing metal(II) chelates except of Fe^{II} for which ferrous ammonium sulphate was used. The ethanolic solution of the ligand in appropriate ratio was added to an ethanolic solution of the metal(II) ion with constant stirring. The reaction mixture in each case was digested on a water-bath for 45-60 min. The crystals of metal(II) chelates which separated on cooling the reaction mixtures were filtered, washed with ethanol and dried in vacuum desiccator. Hydrogen gas was bubbled through the reaction mixture to prevent any possible oxidation of Fe^{II}, Mn^{II}, Cr^{II} and Co^{II}.

Carbon, nitrogen and hydrogen were estimated by the micro-analytical method. Metal(II) ions were estimated by the standard method[6]. The physical measurements were carried out as reported earlier[7].

*D-1, Motidaman Fort, Daman-396 220.

Results and Discussion

The average number of proton associated with the ligand ($\bar{n}_A$) was determined by employing the method of Irving and Rossotti[8]. The value of $\bar{n}_A$ was found to be less than 2 suggesting that the ligand dissociates in two steps. This could be due to basic property of the tertiary nitrogen (CH=N) which accepts a proton in the perchloric medium at low pH and the protonated species dissociates in two steps[8]. The values of the metal-ligand stability constants were computed as usual[8]. In all the cases studied, the values of $\bar{n}$ were always less than 2 showing the formation of only 1 : 1 and 1 : 2 complexes. The stability constant (Table 1) increases with temperature in each case indicating that high temperature favours complexation. The values follow the order $Cu^{II} > Zn^{II} > Ni^{II} > Co^{II} > Fe^{II} > Mn^{II} > Cr^{II} > Cd^{II}$ which is in agreement with Irving-William order[10]. The thermodynamical parameters were evaluated as described earlier[8]. The negative ΔG values suggest spontaniety of the reactions and the positive ΔS values indicate that the entropy term is favourable for the chelate ring formation.

TABLE 1—PROTON-LIGAND, STABILITY CONSTANT AND THERMODYNAMIC DATA

Compd.	Temp °C	log K_1	log K_2	$-\Delta G$ kcal mol^{-1}	ΔH kcal mol^{-1}	ΔS cal K^{-1} mol^{-1}
$Cr(BSC)_2$	25	6.83	3.07	13.47		
	35	6.98	3.13	14.29	11.06	82.31
	45	7.15	3.32	15.12		
$Mn(BSC)_2$	25	6.89	3.33	13.94		
	35	7.07	3.42	14.78	11.27	84.59
	45	7.22	3.52	15.63		
$Co(BSC)_2$	25	7.14	3.78	14.89		
	35	7.31	3.92	15.83	13.01	93.92
	45	7.49	4.03	16.76		
$Fe(BSC)_2$	25	6.96	3.63	14.48		
	35	7.15	3.76	15.37	12.30	89.89
	45	7.30	3.88	16.27		
$Ni(BSC)_2$	25	7.23	3.97	15.30		
	35	7.41	4.14	16.28	13.88	97.92
	45	7.57	4.29	17.23		
$Cu(BSC)_2$	25	7.41	4.24	15.89		
	35	7.58	4.42	16 91	14.74	102.76
	45	7.73	4.60	17.94		
$Zn(BSC)_2$	25	7.32	4.16	15.65		
	35	7.50	4.32	16.66	14.31	100.53
	45	7.68	4.46	17.67		
$Cd(BSC)_2$	25	6.74	2.91	13.16		
	35	6.86	3.04	13.95	10.60	79.72
	45	6.99	3.15	14.76		
HBSC	25	9.08	3.28	16.85		
	35	8.98	2.99	16.87	−16.25	2.01
	45	8.86	2.75	16.89		

The analytical data (Table 2) indicate 1 : 2 metal-ligand stoichiometry. The low molar conductance values are ascribed to the non-electrolytic nature of the chelates. The observed molecular weight values suggest a monomeric character. The magnetic data (Table 2) of Fe^{II}, Co^{II}, Ni^{II} and Cr^{II} chelates suggest the formation of six-coordinated complexes with spin-free octahedral geometry around the metal(II) ions[11]. The μ_{eff} value of Mn^{II} chelate corresponds to five unpaired electron and indicates spin-free tetrahedral or octahedral geometry around Mn^{II} ion. The magnetic moment of Cu^{II} complex indicates the presence of one unpaired electron. However, the excess over spin-only value is attributed to spin-orbit coupling. Zn^{II} and Cd^{II} complexes are diamagnetic.

The electronic spectrum of ligand exhibits bands at 27 780 and 26 540 cm^{-1} assignable to $\pi \rightarrow \pi^*$ and $n \rightarrow \pi^*$ transitions, respectively[12]. These bands are also present in the spectra of the metal(II) chelates with slight change in position and intensity. The

TABLE 2—ANALYTICAL, CONDUCTANCE, MAGNETIC AND ELECTRONIC SPECTRAL DATA

Compd.	Mol. wt. Found/ (Calcd.)	Analysis % : Found/(Calcd.) Metal	N	C	H	Λ_M Ω^{-1} cm^2 mol^{-1}	μ_{eff} B.M.	λ_{max} cm^{-1}	d-d Transition (Assignment)
$Cr(C_6H_{10}N_3O_3)_2$	445 (396)	13.19 (13.13)	21.15 (21.21)	36.42 (36.36)	5.13 (5.05)	6.80	4.84	14 290	$^5E_g \rightarrow ^5T_{2g}$
$Mn(C_6H_{10}N_3O_3)_2$	340 (390)	13.83 (13.77)	21.02 (21.06)	36.16 (36.09)	4.96 (5.01)	5.30	5.93	17 860 20 410	$^6A_{1g} \rightarrow ^4T_{1g}$ (G) $^6A_{1g} \rightarrow ^4T_{2g}$ (G)
$Fe(C_6H_{10}N_3O_3)_2$	345 (399)	13.88 (13.97)	19.94 (21.01)	35.96 (36.01)	4.92 (5.00)	4.80	5.63	11 900	$^5T_{2g} \rightarrow ^5E_g$
$Co(C_6H_{10}N_3O_3)_2$	460 (402)	14.56 (14.63)	20.93 (20.85)	35.68 (35.74)	4.88 (4.96)	9.10	4.96	12 350 21 280	$^4T_{1g}$ (F) $\rightarrow ^4A_{2g}$ (F) $^4T_{1g}$ (F) $\rightarrow ^4T_{1g}$ (P)
$Ni(C_6H_{10}N_3O_3)_2$	455 (402)	14.66 (14.58)	20.80 (20.86)	35.69 (35.76)	5.02 (4.97)	4.6	2.86	11 760 15 630 20 830	$^3A_{2g} \rightarrow ^3T_{2g}$ $^3A_{2g} \rightarrow ^3T_{1g}$ (F) $^3A_{2g} \rightarrow ^3T_{1g}$ (P)
$Cu(C_6H_{10}N_3O_3)_2$	355 (407)	15.65 (15.59)	20.55 (20.65)	35.41 (35.33)	4.85 (4.91)	8.3	1.92	15 630	$^2E_g \rightarrow ^2T_{2g}$
$Zn(C_6H_{10}N_3O_3)_2$	427 (409)	15.89 (15.97)	20.60 (20.52)	35.26 (35.18)	4.94 (4.89)	4.6	Dia		
$Cd(C_6H_{10}N_3O_3)_2$	506 (456)	24.66 (24.62)	18.48 (18.40)	31.62 (31.55)	4.44 (4.38)	5.3	Dia		

electronic spectral data (Table 2) suggest nearly an octahedral structure for these metal(II) chelates. The assignment of d-d transition bands were made as per the literature[13]. The broadening of d-d band in Cu^{II} chelate could be due to Jahn-Teller effect[14]. The fourth band in Co^{II} chelate could not be recorded due to the limited spectral range of the instrument. The transitions ${}^6A_{1g} \rightarrow {}^4T_{2g}$ (D) and ${}^6A_{1g} \rightarrow {}^4T_{1g}$ (P) in the spectrum of Mn^{II} chelate are eclipsed by the intraligand bands.

The weak band at 2 730 cm^{-1} in the infrared spectrum of the ligand due to H-bonded νOH stretching mode of the carboxylic group[15] disappears in the metal(II) chelates indicating the deprotonation of carboxylic OH during the formation of the complexes. In the ligand the asymmetric and symmetric stretching vibration of the carboxylate group, ν_{as}(COO) and ν_s(COO) appear at 1 750 and 1 480 cm^{-1}. In the chelates these bands occur at 1 640-1 620 and 1 470-1 460 cm^{-1}, with difference $\triangle\nu$(COO) of 160-170 cm^{-1} and indicate the presence of monodentate carboxylate group[16]. The band at 1 580 cm^{-1} in the ligand, assignable to $\nu_{C=N}$ stretching mode[17], shifts by 10-25 cm^{-1} towards lower frequency region in the chelates indicating the coordination through azomethine nitrogen. The bands at 1 710, 1 530 and 1 2 0 cm^{-1} in the ligand are assigned to amide-I (mainly due to $\nu_{C=O}$), amide-II (due to $\nu_{C-N} + \delta_{NH}$) and amide-III (due to $\nu_{C-N} + \delta_{NH_2}$) modes, respectively[18]. In the complexes, the amide-I band is lowerd by 10-20 cm^{-1} and amide-II and amide-III bands shift by 10-30 cm^{-1} towards higher frequency region. These change in the amide group frequencies indicate that the carbonyl group is bonded to metal ion through oxygen[19]. The low intensity bands appearing at 480-460 cm^{-1} and 360-350 cm^{-1} in the complexes are attributedt to ν_{M-O} and ν_{M-N} stretching modes, respectively[16].

References

1. R. H. Holm, G. W. Everett, Jr. and A. Chakravarty, *Prog. Inorg. Chem.*, 1966, 83 ; B. O. West, "New Pathways in Inorganic Chemistry", Cambridge University Press, London, 1968, p. 303.
2. H. Irving and H. S. Rossotti, *J. Chem. Soc.*, 1954, 2906.
3. J. K. Verma and R. B. Patel, *J. Indian Chem. Soc.*, 1982, 59, 43.
4. U. B. Rao and H. B. Mathur, *J. Inorg. Nucl. Chem.*, 1971, 33, 2919 ; *Indian J. Chem.*, 1969, 7, 1234.
5. A. I. Vogel, "A Text Book of Practical Organic Chemistry", Longmans Green, London, 1966, p. 344.
6. A. I. Vogel, "A Text Book of Quantitative Inorganic Analysis", Longmans Green, London, 1968.
7. J. K. Verma and G. S. P. Verma, *Indian J. Chem., Sect. A*, 1982, 21, 825.
8. H. Irving and H. S. Rossotti, *J. Chem. Soc.*, 1953, 3397.
9. J. K. Verma, R. B. Patel and Keemtilal, *J. Inst. Chemi., Calcutta*, 1982, 54, 175.
10. H. Irving and R. J. P. William, *Nature (London)*, 1948, 162, 746.
11. F. A. Cotton and G. Wilkinsons, "Advanced Inorganic Chemistry", Wiley Eastern, New Delhi, 1970.
12. L. D. Dave, C. Mathew and V. Oommen, *Indian J. Chem., Sect. A*, 1982, 21, 645.
13. A. B. P. Lever, "Inorganic Electronic Spectroscopy", Elsevier, London, 1968 ; B. N. Figgis, "Introduction to Ligand Fields", Wiley Eastern, New Delhi, 1976 ; C. J. Ballhausen, "Introduction to Ligand Field Theory", McGraw-Hill, New York, 1962.
14. I. M. Procter, B. J. Hathway and P. Nichols, *J. Chem. Soc., A*, 1968, 1678.
15. L. Pauling, "The Nature of Chemical Bond", Oxford University Press, London, 1959, pp. 12, 478 ; R. M. Silverstein, C. G. Bassler and T. C. Morrill, "Spectrometric Indentification of Organic Compounds", Wiley, New York, 1974, pp. 3, 100.
16. K. Nakamoto, "Infrared Spectra of Inorganic and Coordination Compounds", Wiley, New York, 1970, p. 222 ; K. Dey and K. C. Ray, *J. Indian Chem. Soc.*, 1973, 50, 66 ; N. F. Curtic, *J. Chem. Soc. A*, 1968, 1579.
17. L. J. Bellamy, "The Infrared Spectra of Complex Molecules", Chapman Hall, Londou, 1957, p. 227.
18. R. D. B. Fraser and W. C. Price, *Proc. R. Soc.*, 1976, 66, 1410 ; S. C. Jain, M. S. Gill and M. S. Rao, *J. Indian Chem. Soc.*, 1976, 53, 537.
19. B. Beecroft, M. J. Campbell and R. C. Kabiak, *J. Inorg. Nucl. Chem.*, 1974, 36, 55 ; G. D. Prasad, D. N. Sathyanarayan and C. C. Patel, *Spectrochim. Acta, Part A*, 1972, 38, 2311; M. Nonoyama, S. Tomito and K. Yamaski, *Inorg. Chim. Acta*, 1975, 12, 33.

J. Indian Chem. Soc.,
Vol. LXIII, May 1986, pp. 472-474

Fluoro Complexes of Hexavalent Uranium. Part-XI. Complexes of Dioxouranium(VI) containing Fluoride and Malonate

M. C. CHAKRAVORTI* and (Miss) MANJU CHOWDHURY

Department of Chemistry, Indian Institute of Technology, Kharagpur-721 302

Manuscript received 3 February 1986, revised 17 March 1986, accepted 2 April 1986

The salts of the new types $M_2[UO_2F_2(C_3H_2O_4)]$, $M_4[UO_2F_2(C_3H_2O_4)_2]$ and $M_2[(UO_2)_2F_4(C_3H_2O_4)]$, where M = K and NH_4, have been prepared by crystallising solutions containing UO_2F_2 and the alkali malonates in different mole ratios. The thermogravimetric analysis of the ammonium salts have been carried out. Molecular conductances of the salt solutions indicate that the complex ions are decomposed in dilute solution to a great extent. The mode of bonding of malonate group in the complexes has been examined by ir spectra.

MALONATO complexes of uranyl ion have received only scanty attention. The trihydrate, $UO_2(C_3H_2O_4).3H_2O$ has been prepared[1] by heating $UO_3.nH_2O$ with excess of malonic acid solution. Its thermal decomposition has been studied[1]. Complexes of the type $[UO_2(C_3H_2O_4)_2]^{2-}$ have been reported[2,3] with alkali and alkaline earth metals. The structures of $(NH_4)_2[UO_2(C_3H_2O_4)_2].H_2O$ and $Ba[UO_2(C_3H_2O_4)_2].3H_2O$ have been studied[4,5] by *X*-ray. An adduct of uranyl malonate with urea has been prepared[6]. A number of peroxomalonato complexes have been reported[7]. In continuation to our studies on the mixed complexes of UO_2^{2+} containing fluoride and carboxylate ions[8-10], we report in this communication the isolation and characterisation of fluoromalonato complexes of UO_2^{2+} of the new ions $[UO_2F_2(C_3H_2O_4)]^{-2}$, $[UO_2F_2(C_3H_2O_4)_2]^{4-}$ and $[(UO_2)_2F_4(C_3H_2O_4)]^{2-}$.

Experimental

Uranyl nitrate, hydrogen peroxide, hydrofluoric acid (40%) and malonic acid used were of AnalaR or G.R. (E. Merck) quality. Preparation of the acid $H[UO_2F_3].H_2O$, starting from $UO_2(NO_3)_2.6H_2O$, has been described in our earlier publications[8,11]. Uranyl fluoride was prepared by heating $H[UO_2F_3].H_2O$ in a platinum crucible at 150° to a constant weight. Potassium malonate was prepared by neutralising malonic acid with potassium hydroxide followed by complete evaporation and drying in a desiccator over caustic soda. A solution of ammonium malonate was prepared by neutralising molanic acid with ammonium hydroxide and reducing the volume on a water-bath avoiding complete evaporation.

***Analysis*:** Methods of analysis of uranium potassium and fluorine are described in our previous papers[8,12]. Uranium content of the ammonium salts was also determined by igniting the compounds and weighing as U_3O_8. Nitrogen was analysed by Dumas' method. Total fluoride and malonate content was determined by passing the salt solution through a column of cation-exchange resin (Dowex 50-X8, A. R. grade, J. T. Baker Chemical Co., Phillipsberg) in hydrogen form and titrating the effluent with standard alkali solution using phenolphthalein as indicator. Uranyl ion remained fixed on the resin.

Physical measurements: Thermogravimetric analysis was done using a manual thermobalance. The sample (~100 mg) was heated at a rate of 2° per min. The conductivity measurements were made with a Systronics 303 direct reading conductivity meter using a polythene body conductivity cell. Ir spectra were recorded in KBr pellets using a Perkin-Elmer 598 spectrophotometer in the range of 4 000-400 cm^{-1}.

Preparation of complexes: $(NH_4)_2[(UO_2)_2F_4(C_3H_2O_4)]$, $(NH_4)_2[UO_2F_2(C_3H_2O_4)]$ and $(NH_4)_4[UO_2F_2(C_3H_2O_4)_2]$. A concentrated solution of UO_2F_2 (1.0 g) was mixed with concentrated solutions of ammonium malonate in the mole ratio 1 : 1, 1 : 3 and 1 : 10, respectively, and kept in the desiccator over sulphuric acid. The yellow crystals separated after 1 day were filtered. The yields were 0.6, 0.6 and 0.8 g, respectively.

The potassium salts were prepared by following the same methods as those used for the corresponding ammonium salts replacing ammonium malonate by appropriate amounts of potassium malonate. The yields were 0.5, 0.6 and 0.8 g, respectively.

All the compounds were dried by pressing between folds of filter paper and then keeping in a

TABLE 1—ANALYTICAL DATA OF COMPLEXES

Compd.	Analysis % : Found/(Calcd.) U	F	Alkali metal or N	Equivalent of total anion[a] per U atom Found/(Calcd.)	Molecular conductance[b] Ω^{-1} mol^{-1} cm^{2}
$K_2[(UO_2)_2F_4(C_3H_2O_4)]$	59.7 (59.8)	9.7 (9.5)	10.0 (9.8)	3.00 (3.0)	460
$K_3[UO_2F_3(C_3H_2O_4)]$	48.6 (48.8)	7.9 (7.8)	16.2 (16.0)	3.98 (4.0)	450
$K_4[UO_2F_2(C_3H_2O_4)_2]$	35.5 (35.6)	5.8 (5.7)	23.6 (23.4)	5.95 (6.0)	600
$(NH_4)_2[(UO_2)_2F_4(C_3H_2O_4)]$	63.2 (63.1)	10.1 (10.0)	3.8 (3.7)	2.95 (3.0)	420
$(NH_4)_3[UO_2F_3(C_3H_2O_4)]$	53.5 (53.4)	8.6 (8.5)	6.3 (6.2)	3.99 (4.0)	450
$(NH_4)_4[UO_2F_2(C_3H_2O_4)_2]$	40.8 (40.7)	6.6 (6.5)	10.3 (10.2)	6.00 (6.0)	590

[a]Total fluoride and malonate. [b]In 1×10^{-3} M aqueous solution at 25°.

desiccator over concentrated sulphuric acid. The analytical data of the complexes are given in Table 1.

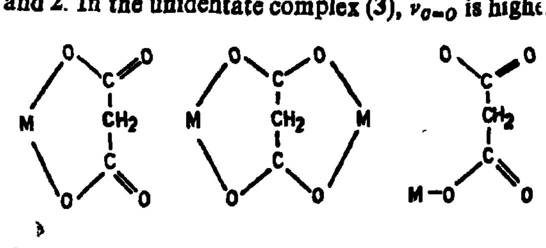
Results and Discussion

The compounds are yellow crystalline substances, stable in air and soluble in water, but insoluble in common organic solvents. The salts $M_2[(UO_2)_2F_4(C_3H_2O_4)]$ and $M_3[UO_2F_3(C_3H_2O_4)]$(where M=K and NH_4) can be recrystallised unchanged from water. However, recrystallisation of $M_4[UO_2F_2(C_3H_2O_4)_2]$ (where M=K and NH_4) from water gave yellow products, the analyses of which did not correspond to any simple stoichiometry. The molecular conductances of the salts (Table 1) indicate that the complex ions are highly dissociated in dilute solutions.

On passing dilute solutions of the salts through a column of cation-exchange resin in hydrogen form the complex ions are completely broken up. Elution with water brought out all fluoride and malonate in the effluent. Uranyl ion was adsorbed on the bed which could be finally eluted out with dilute hydrochloric acid.

The thermograms of the three ammonium salts were recorded up to 600°. The compounds $(NH_4)_4[UO_2F_2(C_3H_2O_4)_2]$ and $(NH_4)_3[UO_2F_3(C_3H_2O_4)]$ begin to decompose at about 130°. The TGA curves of both the compounds gave horizontals stretching approximately between 340 and 460° corresponding to the formation of UO_2F_2 with the losses of 47.7 and 31.2% which correspond to the losses of two molecules and one molecule of ammonium malonate, respectively (calculated losses 47.3 and 30.9%, respectively). The compound $(NH_4)_2[(UO_2)_2F_4(C_3H_2O_4)]$ begins to decompose at about 180°. The TGA curve of this compound gave a horizontal stretching between 360 and 450° corresponding to the formation of UO_2F_2 with a loss of 18.6% which corresponds to the loss of one molecule of ammonium malonate (calculated loss 18.3%). U_3O_8 was finally obtained by heating all the complexes upto about 520°.

The X-ray structure analysis of a very few complexes containing coordinated malonate has been made[4]. From the available data it appears that the carboxylate ion is mainly coordinated as shown in 1 and 2. In the unidentate complex (3), $\nu_{C=O}$ is higher



Bidentate (1) Bridged tetradentate (2) Unidentate (3)

than ν_{as} (CO_2^-) and ν_{C-O} is lower than ν_s (CO_2^-). As a result, the separation between the two ν_{COO} is much larger in unidentate complexes than in the free ion[18]. The ir spectral band positions of the complexes are recorded in Table 2. If the 1 655 and 1 580 cm^{-1} bands in potassium malonate are taken as ν_{as} (COO) and the 1 440 and 1 410 cm^{-1} bands as ν_s (COO), the separation of the two ν_{COO} bands in the two complexes $K_3[UO_2F_3(C_3H_2O_4)]$ and $K_4[UO_2F_2(C_3H_2O_4)_2]$ is smaller than the free ion value. It may be suggested that the two complexes contain bidentate malonate rather than unidentate. The ratio of UO_2^{2+} : malonate in the complex $K_2[(UO_2)_2F_4(C_3H_2O_4)]$ is 2 : 1, which suggests that it is a di - or poly-nuclear complex containing presumably bridging malonate. The antisymmetric and the symmetric COO bands in this complex appear closer to the free ion value. The exact way in which malonate is coordinated in this complex is difficult to conclude from the ir spectra. The fact that the spectra of these three complexes show the presence of traces of water (probably coming from KBr) which is evident from the appearance of weak bands near 3 400 cm^{-1}, would

TABLE 2—IR SPECTRAL BANDS OF COMPLEXES (cm^{-1})

Compd.	$\nu(UO_2)^a$	$\nu_{as}(COO)^b$	$\nu_s(COO)$
$K_2[(UO_2)_2F_4(C_3H_2O_4)]$	940 vs, 910 vs	1 640 vs	1 450 vs
$K_2[UO_2F_2(C_3H_2O_4)]$	925 vs, 890 vs	1 580 vs	1 410 vs
$K_4[UO_2F_2(C_3H_2O_4)_2]$	890 vs	1 590 vs	1 420 vs
$(NH_4)_2[(UO_2)_2F_4(C_3H_2O_4)]$	900 vs	1 640 vs	1 460 vs[c]
$(NH_4)_2[UO_2F_2(C_3H_2O_4)]$	890 vs	1 590 vs	1 400 vs[c]
$(NH_4)_4[UO_2F_2(C_3H_2O_4)_2]$	890 vs	1 590 vs	1 400 vs[c]
$K_2C_3H_2O_4$[d]		1 655 vs, 1 580 vs	1 440 vs, 1 410 vs, 1 365 vs

Overlapped with ν_{C-C}, ν_{CO} and ν_{O-C-O} bands. [b]Overlapped with δ_{H_2O}. [c]Overlapped with NH_4^+ bands. [d]Included for comparison.

suggest that any attempt to decide the mode of coordination of malonate from the position of the ν_{as} (COO) band would only be a guess. The analysis of the ir spectra of the three ammonium compounds would also be difficult since the symmetrical COO band would be overlapped with the ν_4 mode of NH_4^+ which appears at about 1 400 cm^{-1}. However, it may be suggested that the malonate ion in $(NH_4)_2[(UO_2)_2F_4(C_3H_2O_4)]$, $(NH_4)_2[UO_2F_2(C_3H_2O_4)]$ and $(NH_4)_4[UO_2F_2(C_3H_2O_4)_2]$ is coordinated in the same manner as in the corresponding potassium compounds.

The assignment of the UO_2^{2+} bands in the complexes is also difficult since malonate gives absorption bands in the expected region. No attempt for the assignment of the U-F bands was made since malonate gives a number of bands below 650 cm^{-1}. It is, however, possible that some or all the complexes contain bridging fluoride.

References

1. L. V. VOLODKINA, A. V. DUBROVIN, K. M. DUNAEVA and V. I. SPYTSYN, *Zh. Neorg. Khim.*, 1982, 27, 2612.
2. J. A. HERRERO, J. BERMUDEZ and E. GUTIERREZ RIOS, *An. Quim.*, 1977, 73, 1271.
3. J. A. HERRERO, J. BERMUDEZ and E. GUTIERREZ RIOS, *Quim. Ind.*, 1972, 18, 15.
4. G. BOMBIERI, F. SENETOLLO, E. FOZSELLINI and A. DELPRA, *J. Inorg. Nucl. Chem.*, 1980, 42, 1423.
5. R. M. ROJAS, A. DELPRA, G. BOMBIERI and F. BENETOLLO, *J. Inorg. Nucl. Chem.*, 1979, 41, 541.
6. V. E. KARASEV, I. M. ORLOVA, G. M. PODNEBESNOVA and R. N. SHCHELOKOV, *Koord. Khim.*, 1979, 5, 541.
7. A. M. CURVICH, L. P. POLOZHENSKAYA, L. F. SOLNTSEVA and N. P. OSICHEVA, *Radiokhimiya*, 1971, 13, 588.
8. M. C. CHAKRAVORTI, P. K. BHARADWAJ, S. C. PANDIT and B. K. MATHUR, *J. Inorg. Nucl. Chem.*, 1978, 40, 1365.
9. M. C. CHAKRAVORTI, M. CHOWDHURY and P. K. BHARADWAJ, *Inorg. Chim. Acta*, 1980, 42, 247.
10. M. C. CHAKRAVORTI and M. CHOWDHURY, *J. Indian Chem. Soc.*, 1985, 62, 399.
11. M. C. CHAKRAVORTI and N. BANDYOPADHYAY, *J. Inorg. Nucl. Chem.*, 1972, 34, 2867.
12. M. C. CHAKRAVORTI and P. K. BHARADWAJ, *J. Inorg. Nucl. Chem.*, 1978, 40, 1643.
13. K NAKAMOTO, "Infrared and Raman Spectra of Inorganic and Coordination Compounds", Wiley, New York, 1978, p. 232.

J. Indian Chem. Soc.,
Vol. LXIII, May 1986, pp. 475-478

Studies on Dioxouranium(VI) Complexes with some Schiff Bases

P. S. PRABHU and S. S. DODWAD*

Physical Chemistry Laboratory, Institute of Science, Madame Cama Road, Bombay-400 032

Manuscript received 16 July 1984, revised 30 May 1985, accepted 3 March 1986

Uranyl complexes of some Schiff bases obtained by condensing salicylaldehyde with 2-aminopyridine, aniline and nitroanilines and 5-methylsalicylaldehyde with 2-aminopyridine are synthesised and characterised by elemental analysis, spectral and conductance data and magnetic susceptibility study. All the complexes are orange-red in colour, microcrystalline in nature and form compounds of the type $[UO_2(LH)_2](NO_3)_2$ and $[UO_2(L)_2]$, where LH and L are Schiff base molecules, L representing the ligand containing pyridyl nitrogen in the structure. The bonding with the metal in the complexes takes place from oxygen and hydroxyl oxygen in the two types of ligands and the imine nitrogen of the ligands. Pyridyl nitrogen does not take part in coordination. The studies show that the complexes formed are 1 : 2 adducts and that the complexes have coordination number eight and six, respectively.

METAL complexes with Schiff base ligands obtained from salicylaldehyde or substituted salicylaldehyde with various aromatic amines have been extensively studied[1-5]. Solution study of a number of Schiff base complexes with various divalent metal ions have been studied by Dodwad *et al.*[6,7] in this laboratory. The authors have reported uranyl complexes of some Schiff bases elsewhere[8]. In the present investigation, the authors wish to report some more uranyl complexes with different series of Schiff bases.

Experimental

Uranyl nitrate hexahydrate used for preparing the complexes was of AnalaR grade. Salicylaldehyde, 2-aminopyridine, aniline and nitroanilines of L. R. grade were purified by conventional methods. 5-Methylsalicylaldehyde was prepared by the method suggested by Duff[9].

Preparation of Schiff bases: These were prepared by mixing calculated quantities of the corresponding aldehyde and the amine in ethanolic medium and the resulting solution was refluxed for 0.5-1 h. On cooling, solidification occurred rapidly. The solids were separated and recrystallised from methylated spirit. The Schiff bases were crystallised as light yellow to orange coloured crystals.

Preparation of complexes: The complexes were prepared by refluxing one part of uranyl nitrate and two parts of Schiff base in ethanolic medium for 1-2 h. On cooling, the orange-red to red coloured complexes were separated, filtered, washed with ethanol and dried (fused $CaCl_2$) in vacuum.

Analysis: Uranium in the complexes was estimated gravimetrically as U_3O_8. Nitrogen was estimated by microanalytical method. The results of elemental analysis are given in Table 1.

Physical measurements: The conductance measurements of all the complexes in DMF were made on a Philips PR 9500 conductivity bridge having a cell constant 0.6831 cm^{-1}. Molar conductance of the complexes were calculated (Table 1). The ir spectra (nujol) of the ligands and their

TABLE 1—ANALYSIS AND CONDUCTANCE DATA OF URANYL COMPLEXES OF SCHIFF BASES

Ligand	Complex	Colour of complex	Analysis % : Found (Calcd.) U	N	Conductivity Ω^{-1} cm^2 mol^{-1}
Salicylidene-2-iminopyridine (1)	$[UO_2(C_{12}H_9ON_2)_2]$ (6)	Red	35.32 (35.84)	8.63 (8.43)	*
5-Methyl salicylidene-2-iminopyridine (2)	$[UO_2(C_{13}H_{11}ON_2)_2]$ (7)	Red	33.92 (34.39)	8.51 (8.09)	*
Salicylanil (3)	$[UO_2(C_{13}H_{11}ON)_2(NO_3)_2]$ (8)	Orange	30.00 (30.20)	7.72 (7.12)	121.031
4'-Nitrosalicyanil (4)	$[UO_2(C_{13}H_{10}O_3N_2)_2(NO_3)_2]$ (9)	Orange red	26.72 (27.10)	10.00 (9.56)	129.631
3'-Nitrosalicyanil (5)	$[UO_2(C_{13}H_{10}O_3N_2)_2(NO_3)_2]$ (10)	Orange	26.64 (27.10)	9.82 (9.56)	127.031

* Insoluble in DMF : Non-electrolytes.

TABLE 2—SELECTED IR FREQUENCY (cm^{-1}) OF SCHIFF'S BASES AND THEIR URANYL COMPLEXES

Compd. no.*	Aromatic C–H stretch	C=N stretch	Aromatic C=C stretch	C–O stretch	OH bending	O=U=O ν_3	O–NO_2
1	3 070 w	1 615 sh	1 590 s	1 380 m			
			1 560 m	1 190 s	1 280 sh	—	—
			1 500 m				
2	3 070 w	1 610 sh	1 580 s	1 380 m			
			1 555 s	1 210 s	1 280 s	—	—
			1 490 m				
3	3 080 w	1 620 s	1 600 sh	1 380 sh			
			1 580 sh	1 190 s	1 280 s	—	—
			1 485 sh				
4	—	1 605 sh	1 590 sh	1 380 s			
			1 570 sh	1 180 s	1 280 s	—	—
			1 510 sh				
5	3 130 w	1 635 sh	1 615 sh	1 385 sh			
			1 585 sh	1 200 sh	1 285 sh	—	—
			1 530 sh				
6	3 100 w	1 625 s	1 600 sh	1 390 sh			
			1 575 sh	1 190 sh	—	920 s	—
			1 525 s				
7	3 100 w	1 625 sh	1 595 m	1 380 s			
			1 575 m	1 210 m	—	905 sh	—
			1 545 m				
8	3 100 w	1 640 s	1 620 m	1 390 sh			
			1 600 m	1 190 m	1 280 s	920 s	1 245 sh
			1 490 sh				
9	3 100 w	1 640 s	1 600 s	1 380 sh			
			1 520 s,b	1 180 m	1 280 s	930 s	1 240 sh
			1 480 sh			(ν_1 = 860 sh)	
10	3 130 w	1 660 s	1 630 sh	1 390 m			
			1 550 s	1 200 m	1 290 s	940 s	1 250 sh
			1 500 m				

* As in Table 1.
b = broad, m = medium, sh = sharp, s = strong, w = weak.

complexes were recorded on a Perkin-Elmer 700 spectrophotometer in the region 4000-650 cm^{-1} and their tentative assignments are presented in Table 2. From the frequencies of UO_2, the force constant and the bond length values were calculated and reported in Table 3.

TABLE 3—ABSORPTION FREQUENCY, FORCE CONSTANT AND BONDLENGTH VALUES OF URANYL COMPLEXES OF SCHIFF'S BASES

Compd. no.*	ν_3, OUO cm^{-1}	f_{UO} m dyne/Å	R_{UO} Å
6	920	7.03	1.73
7	905	6.80	1.74
8	920	7.03	1.73
9	930	7.18	1.73
10	940	7.33	1.72

* As in Table 1.

Results and Discussion

The complexes obtained are orange-red to red in colour, microcrystalline and are insoluble in common organic solvents. This insolubility hampered the molecular weight determination. However, they are soluble in DMF. The results of elemental analysis (Table 1) suggest that these complexes have 1 : 2 stoichiometry.

Conductance : It is found that the complexes of type-1 are insoluble in DMF and did not permit the conductance measurements and hence can be regarded as non-electrolytes. It is observed that the molar conductance of the remaining complexes in DMF at the concentration of $10^{-3}M$ fall in the range of 120-130 Ω^{-1} cm^2 mol^{-1} indicating that they behave as 1 : 2 electrolytes. Such results were also observed by Jain *et al.*[10]. The DMF solvent molecules displace the weakly coordinated nitrate groups from the coordination sphere[11].

Magnetic measurements : Magnetic susceptibilities of the uranyl complexes were measured by a modified form of Gouy's balance, described by Prasad[12]. It was observed that all the complexes are diamagnetic in nature. This indicates that all of them are spin-paired complexes of hexavalent uranium.

Infrared spectra : The spectra of Schiff bases and their complexes exhibit a weak band characteristic of aromatic C—H stretching vibration in the region 3 130-3 070 cm^{-1}. In the ligands as well as their complexes, a strong, sharp or medium band is observed in the region 1 630-1 480 cm^{-1} (C=C stretching). The spectra of the complexes and the ligands show a strong, sharp or medium band in the region 1 390-80 and 1 210-1 180 cm^{-1} (C—O stretching). Two characteristic frequencies, *viz.* 940-905 and 860 cm^{-1}, in the complexes, can be predicted[13,14] for UO_2^{2+} ion. A strong or sharp band is observed for all the reagents in the region 1 285-80 cm^{-1} (OH bending)[15]. This band is also observed in the complexes of type-2.

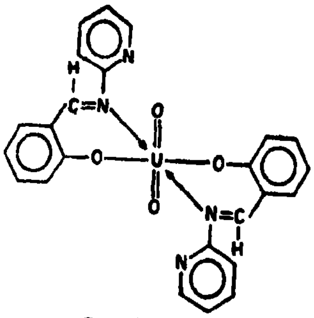
Absence of measurable absorption in the infrared region characteristic of OH absorption (3 650-3 590 cm^{-1}) has been attributed to the existence of intra-molecular hydrogen bonding[16].

Some of the Schiff bases studied in the present investigation exhibit the property of thermochromism and photochromism[17,18]. This property has also been attributed to the existence of intramolecular hydrogen bonding[19,20] between the phenolic proton and the imine nitrogen.

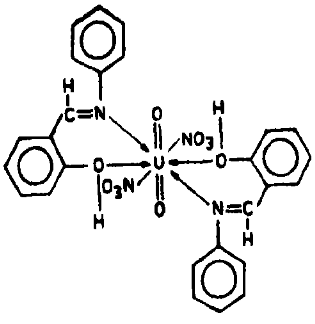
The formation of a bond between the oxygen of the OH group and the metal, in all the complexes, increases the electron density on the latter. Consequently, the ν_{C-N} will shift towards higher wave number side to increase in C–N bond order[21,22]. A strong and sharp band observed in the region 1 635-05 cm^{-1} (C=N stretch)[23] in the Schiff bases is observed in the region 1 660-25 cm^{-1} of the complexes. The observable shift obtained in the C=N stretch after complexing confirms the formation of coordinate bond from oxygen of the OH group and imine nitrogen to the metal ion in the complexes of type-2 and formation of a covalent bond in the complexes of type-1. A sharp band for the complexes of type-2 appearing in the region 1 250-40 cm^{-1} (NO_3 group) is absent in ligands. This band is not observed in the complexes of type-1.

Reagents of type-1 are basic in nature due to the presence of pyridyl nitrogen in their structure. Hence, deprotonation of phenolic hydrogen takes place readily during complexation. A band around 1 280 cm^{-1} characteristic of OH bending vibration and absorption characteristic of NO_3 group are absent in the complexes formed from reagents of type-1. These complexes are found to be non-electrolytes as seen from the conductance data. Pyridine nitrogen does not involve[6] in coordination. All these facts lead to the conclusion that in the complexes derived from reagents of type-1, oxygen of phenol and imine nitrogen are involved in bond formation and also that NO_3 ions are absent. In view of these observations, these complexes can be regarded as having coordination number six. The complexes exhibit a strong band in the region 940-905 cm^{-1} characteristic of ν_{as} (O=U=O). From these, the force constant (f) value of ν_{as} (O=U=O) and the U–O bond length (R_{u-o}) for all the complexes have been calculated[24]. The R_{u-o} values fall in the range 1.73-1.74 Å which are comparable to those (1.60-1.92 A) observed for other dioxouranium(VI) complexes[25].

With the help of analytical, conductance and infrared spectral data it may be suggested that the Schiff base complexes derived from reagents of type-1 and type-2 have coordination number six and eight, respectively, and their structures are represented as



Complex type-1



Complex type-2

References

1. M. A. Pujar and T. D. Bharamagoudar, *J. Indian Chem. Soc.*, 1980, 57, 462.
2. M. D. Hobday and T. D. Smith, *Coord. Chem. Rev.*, 1973, 9, 311.
3. O. A. Osipev, V. I. Minkin, D. Sh. Verkhovodova and M. I. Knyazhanskii, *Chem. Abstr.*, 1968, 68, 87107.
4. N. S. Biradar and V. H. Kulkarni, *J. Less-Common Met.*, 1972, 26, 355.
5. K. Dey and K. C. Ray, *Inorg. Chim. Acta*, 1974, 10, 139.
6. S. S. Dodwad, I. R. Patil and M. G. Datar, *Indian J. Chem., Sect. A*, 1983, 22, 83.
7. S. S. Dodwad, I. R. Patil and M. G. Datar, *J. Indian Chem. Soc.*, 1984, 61, 595.
8. P. S. Prabhu and S. S. Dodwad, *J. Indian Chem. Soc.*, 1983, 60, 546.
9. J. C. Duff, *J. Chem. Soc.*, 1941, 547.
10. S. C. Jain, M. S. Gill and G. S. Rao, *J. Indian Chem. Soc.*, 1981, 58, 210.
11. J. V. Quagliano, J. Fujita, G. Franz, D. J. Phillips, J. A. Walamslay and S. Y. Tyree, *J. Am. Chem. Soc.*, 1961, 83, 3370.
12. Prasad, *Proc. Indian Acad. Sci., Sect. A*, 1944, 20, 224.
13. J. Selbin, *Angew Chem.*, 1966, 5, 712.
14. B. M. Gatehouse and A. E. Comyns, *J. Chem. Soc.*, 1958, 3965.
15. A. M. Shallaby and M. M. Mostafa, *Indian J. Chem., Sect. A*, 1979, 17, 516.
16. S. P. Hendricks, D. R. Wulf, G. E. Hilbert and U. Liddel, *J. Am. Chem. Soc.*, 1936, 58, 1991.

17. M. D. COHEN and G. M. J. SCHMIDT, *J. Phys. Chem.*, 1962, **66**, 2442.
18. M. D. COHEN, G. M. J. SCHMIDT and S. FLAVIAN, *J. Chem. Soc.*, 1964, 2041.
19. G. M. J. SCHMIDT, *Acta Crystallogr.*, 1957, **10**, 793.
20. M. D. COHEN, Y. HIRSHBERG and G. M. J. SCHMIDT in "Hydrogen Bonding", ed. D. HADZI, Pergamon Press, London, 1959, p. 293.
21. C. B. SINGH and B. SAHOO, *J. Inorg. Nucl. Chem.*, 1974, **36**, 1259.
22. N. S. BIRADAR and V. H. KULKARNI, *Rev. Roum. Chim.*, 1970, **15**, 1993.
23. D. H. BUSCH and J. C. BAILAR, JR., *J. Am. Chem. Soc.*, 1956, **78**, 1137.
24. S. P. McGLYNN, J. K. SMITH and W. C. NEELY, *J. Chem. Phys.*, 1961, **35**, 105.
25. W. H. ZACHARIASEN, *Acta Crystallogr.*, 1954, **8**, 847.

J. Indian Chem. Soc.,
Vol. LXIII, May 1986, pp. 479-480

Stabilities and Thermodynamics of Beryllium(II), Oxovanadium(II) and Zirconium(IV) Complexes of (L)-2-Aminobutanedioic acid-4-amide

(Mrs.) SUSHMA SHARMA, K. K. SAXENA and R. S. SAXENA*

Department of Chemistry, Malaviya Regional Engineering College, Jaipur-302 017

Manuscript received 22 September 1984, revised 20 August 1985, accepted 3 March 1986

The stability constants of Be^{II}, VO^{II} and Zr^{IV} complexes of (L)-2-aminobutanedioic acid-4-amide have been determined in aqueous medium at different temperatures, *viz.* 25, 35 and 45° and varying ionic strengths $\mu = 0.1$, 0.2, 0.5 and 1.0 *M* KNO_3 employing Calvin Melchior's extension of Bjerrum's method and refined by least-square treatment. The thermodynamic functions $\Delta G°$, $\Delta H°$ and $\Delta S°$ accompanying complex formation have also been evaluated at 35°.

IN continuation of the earlier work by Sexena and coworkers[1-5] on the electrochemical behaviour of amino acids and their metal complexes, this communication reports the formation, composition and stability constants of Be^{II}, VO^{II} and Zr^{IV} complexes with (L)-2-aminobutanedioic acid-4-amide at different temperatures, *viz.* 25, 35 and 45° and ionic strengths $\mu = 0.1$, 0.2, 0.5 and 1.0 *M* KNO_3 by *p*H-metric titration technique.

Experimental

(L)-2-Aminobutanedioic acid-4-amide (H_2A) (B.D.H., England) and $BeSO_4.4H_2O$, $VOSO_4.H_2O$, $ZrSO_4.H_2O$ and NaOH were of AnalaR grade. Their solutions were prepared in double-distilled water whose strengths were checked by standard methods[6].

Procedure: *p*H measurements were made on EC digital *p*H meter (accuracy ± 0.01) with combined glass-calomel electrode. The temperature of the cell was maintained by a thermostat. Requisite amounts of KNO_3 were added to the solution mixture for maintaining ionic strengths. The initial *p*H of the solutions of Be^{II}, VO^{II}, Zr^{IV} salts and the ligand were measured and found to be in the vicinity of 3.80, 3.19, 2.50 and 5.96, respectively. At these acidic *p*H values, the metal salt solution did not indicate any hydrolysis. The experimental procedure as described earlier[1] involves a series of *p*H titrations of the ligand with standard NaOH solution in the absence and presence of metal ions at different metal-ligand ratios.

For qualitative detection of complex formation, stoichiometric *p*H titrations were performed for the following solutions containing the metal and ligand in different molar ratios of 1 : 1, 1 : 2 and 1 : 4 against 0.1 *M* NaOH (total vol. 25 ml): (i) $4 \times 10^{-3} M$ H_2A, (ii) $4 \times 10^{-3} M$ H_2A + $4 \times 10^{-3} M$ M^{n+}, (iii) $4 \times 10^{-3} M$ H_2A + $2 \times 10^{-3} M$ M^{n+} and (iv) $4 \times 10^{-3} M$ H_2A + $1 \times 10^{-3} M$ M^{n+}

After each addition of the titrant NaOH, *p*H meter readings were noted. Curves were plotted between *p*H and moles of alkali required per mole of ligand 'm', and from the inflections in the curves, metal-ligand combining ratio was obtained. The stability constants of metal-ligand complexes were evaluated by employing Calvin and Melchior's extension[7] of Bjerrum's[8] *p*H titration technique keeping the ratio of metal to ligand constant at 1 : 5, using $4 \times 10^{-3} M$ $HClO_4$ for initial lowering of the buffer region and preventing hydrolysis.

Formation function $\bar{n}$ and free ligand concentration [A] were calculated by using the standard expression from the titration curves drawn. The pK_1 and pK_2 values of the dissociation of the ligand at different temperatures and ionic strengths have already been reported by the authors[9] and used in the calculations.

Results and Discussion

The formation curves were obtained by plotting $\bar{n}$ *vs* −log A. The stability constants are determined by noting −log A values at $\bar{n}$ = 0.5 and 1.5, which indicated the formation of 1 : 1 and 1 : 2 metal-ligand complexes. It was observed that Be^{II}, VO^{II} and Zr^{IV} complexes with the ligand were formed in the *p*H ranges 3.8-7.2, 3.3-6.5 and 2.2 to 4.0, respec-

TABLE 1—STABILITY CONSTANTS AND THERMODYNAMIC FUNCTIONS OF Be^{II}, VO^{II} AND Zr^{IV} COMPLEXES WITH (L)-2-AMINOBUTANEDIOIC ACID-4-AMIDE

Metal		Temp. 25°	35°					45°
		μ 0.1	0.0	0.1	0.2	0.5	1.0	0.1
	log K_1	6.25	6.55	6.60	6.65	6.85	7.10	6.85
	log K_2	4.95	5.25	5.30	5.35	5.55	5.80	5.65
Be^{II}	log β	11.20	11.80	11.90	12.00	12.40	12.90	12.50
	log $β^a$	11.28	11.80	11.88	12.04	12.35	12 79	12.55
	log K_1	7.05	7.25	7.30	7.35	7.45	7.70	7.50
	log K_2	6.45	6.55	6.60	6.85	7.00	7.20	6.80
VO^{II}	log β	13.50	13.80	13.90	14.20	14.45	14.90	14.30
	log $β^a$	13.54	13.70	13.79	14.05	14.25	14.99	14.10
	log K_1	8.50	8.70	8.75	8.80	8.90	9.00	9.00
	log K_2	7.55	7.65	7.70	7.75	7.90	8.05	7.90
Zr^{IV}	log β	16.05	16.35	16.45	16.55	16.80	17.05	16.90
	log β	16.09	16.36	16.48	16.36	16.84	16.96	17.00

^{a} Represents stability constant obtained by least-square treatment. Uncertainty limit upto ± 0.02 - 0.04.

tively, beyond which slight precipitation occurred. The log K_1 and log K_2 values of metal-ligand complexes were determined at temperatures 25, 35 and 45° and ionic strengths 0.1, 0.2, 0.5 and 1.0 *M* and further refined by least-square treatment (the difference between log K_1 and log K_2 being less than 1.78) (Table 1) which shows the following order of stabilities : $Be^{II} < VO^{II} < Zr^{IV}$.

Stability constants gradually increase with rise in temperature showing thereby that higher temperature favours the formation of complexes and their stability. Further, log K values are found to increase with the increase in ionic strengths (Table 1). Thermodynamic stabilities were obtained by the extrapolation of measured formation constants to zero ionic strength.

TABLE 2—THERMODYNAMIC FUNCTION OF METAL-LIGAND COMPLEXES AT 35° AND ZERO IONIC STRENGTH

Metal complex	$-\Delta G^0$ kcal mol^{-1}	ΔH^0 kcal mol^{-1}	ΔS^0 cal K^{-1} mol^{-1}
Be^{II}	16.6 (±0.6)	27.7 (±0.8)	144.0 (±4.5)
VO^{II}	19.5 (±0.8)	18.0 (±0.6)	121.6 (±4.4)
Zr^{IV}	23.0 (±0.7)	18.7 (±0.4)	135.6 (±3.8)

Thermodynamic parameters, such as free energy (ΔG^0), enthalpy (ΔH^0) and entropy (ΔS^0) accompanying complexation are determined at 35° with the help of standard equations[10] and are summarised in Table 2. The negative values of ΔG^0 show that the reaction tends to proceed spontaneously. The positive values of enthalpy indicate the endothermic nature of the reaction suggesting that higher temperature favours chelation process, in fair agreement with increasing stability with temperature. The positive values of entropy also favour the chelation process.

References

1. R. S. SAXENA and S. K. DHAWAN, *Revista Chim.*, 1982, 33, 780.
2. R. S. SAXENA and R. D. PARIKH, *Monatsh. Chem.*, 1984, 115, 141.
3. R. S. SAXENA and S. K. DHAWAN, *J. Indian Chem. Soc.*, 1983, 60, 733.
4. R. S. SAXENA, A. GUPTA, K. C. GUPTA and T. KAUR, *Acta Chim. Acad. Sci. Hung.*, 1983, 113, 139.
5. R. S. SAXENA and G. L. KHANDELWAL, *Indian J. Chem., Sect. A*, 1977, 15, 757.
6. A. I. VOGEL, "A Textbook of Quantitative Inorganic Analysis", Pergamon Press, London, 1964, pp. 518, 546.
7. M. CALVIN and N. C. MELCHIOR, *J. Am. Chem. Soc.*, 1948, 70, 3270.
8. J. BJERRUM, "Metal Ammine Formation in Aqueous Solutions", P. Hasse, Copenhagen, 1941.
9. K. K. SAXENA, S. SHARMA and R. S. SAXENA, *Afinidad*, 1985, 62, 91.
10. K. B. YATSIMIRSKII and V. P. VASIL'EV, "Instability Constants of Complex Compounds", Pergamon, Oxford, 1960.

J. Indian Chem. Soc.,
Vol. LXIII, May 1986, pp. 481-484

Kinetics of Oxidation of Benzene azodimethylaniline and Methyl Orange by Chromic Acid in Presence of 1,10-Phenanthroline and 2,2'-Bipyridyl

P. V. SUBBA RAO*, K. SRINIVAS and K. SRIRAMA MURTY

School of Chemistry, Andhra University, Waltair-530 003

Manuscript received 12 October 1984, revised 6 May 1985, accepted 2 April 1986

The title reaction studied spectrophotometrically was found to be first order with respect to both the reactants. The reaction is catalysed by H^+ ion and the order with respect to H^+ ion was found to be unity in both the cases. 1,10-Phenanthroline was found to have greater catalytic effect than 2,2'-bipyridyl and a plot of $1/k_1$ *vs* 1/[phen] was a straight line with a positive slope and intercept on $1/k_1$-axis, whereas a plot of $1/k_1$ *vs* 1/[bipy] was also a straight line but passing through the origin. A decrease in the activation energies was observed when compared to that of uncatalysed reaction and the decrease was more in the case of 1,10-phenanthroline-catalysed reaction than that of 2,2'-bipyridyl-catalysed one. Plausible mechanism has been proposed to explain the catalytic behaviour of these ligands.

THE accelerating effects of 1,10-phenanthroline and 2,2'-bipyridyl on chromium(VI) oxidations were known for a long time[1]. The accelerating effects of these ligands on chromium(VI) oxidations were explained by postulating that these ligands stabilise the transition state and also the intermediate oxidation states of chromium. However, no systematic kinetic investigation of this accelerating effect on chromic acid oxidations has been, so far, reported. With a view to having a clear insight into the mechanism of catalysis of chromic acid oxidations by these ligands, the present authors have taken up a detailed kinetic study of oxidation of benzene azodimethylaniline (BADMA) and methyl orange (p-SO_3H BADMA) by chromic acid in the presence of 1,10-phenanthroline and 2,2'-bipyridyl. Michaelis type of kinetics was observed with 1,10-phenanthroline as catalyst but not in the case of 2,2'-bipyridyl used as catalyst. Interestingly, Michaelis type of kinetics is very rarely observed in chromic acid oxidations.

Experimental

Double-distilled water was used for the preparation of all solutions. E. Merck 'pro analysi' chromium trioxide was used for the preparation of chromium(VI) solution and it was standardised by the improved iodometric method[2]. BADMA was prepared by the reported method[3] and its solution in 5% acetic acid was standardised with standard titanous chloride solution[4]. Perchloric acid and 1,10-phenanthroline (both E. Merck, pro analysi) and 2,2'-bipyridyl (AnalaR) were used. Sodium perchlorate solution was prepared by neutralising requisite quantity of standard perchloric acid solution with standard sodium hydroxide solution.

The experiments were carried out under pseudo-first order conditions by isolating the aromatic azo compound and the course of reaction was followed by measuring the optical density of the unreacted azo compound at 510 nm. Temperature of the reaction mixture was maintained constant to ± 0.1°. The rate constants were reproducible within ± 3%.

Stoichiometry and product analysis: The stoichiometry of the reaction in the presence and absence of 1,10-phenanthroline and 2,2'-bipyridyl was found to be 4 moles of chromium(VI) to 3 moles of azo compound. In agreement with the stoichiometric results, the oxidation product was found to be the corresponding nitroso compound as evidenced by the spot test[5]. Under the experimental conditions employed by the present authors, the extent of the uncatalysed reaction was negligible. Hence, no correction due to uncatalysed reaction was made in calculating the rate constants for the catalysed reaction.

Results and Discussion

The order with respect to each of the azo compounds is unity as revealed by the straight line graphs obtained at different initial concentrations of each of the azo compounds for log (O.D) *vs* time plots, and they were found to be parallel to each other (Table 1). The order with respect to chromium(VI) is unity as revealed by the straight lines obtained passing through origin when k_1 was

plotted against [Cr^{VI}] (Table 2). Plots of k_1 *vs* concentration of hydrogen ion was straight line passing through the origin in each showing that the reaction is of first order with respect to hydrogen ion. These results are presented in Table 3.

TABLE 1—DEPENDENCE OF RATE ON CONCENTRATION OF SUBSTRATE

[Phen] = $8.0\times10^{-4}M$, [Bipy] = $2.0\times10^{-3}M$, [$HClO_4$] = $0.1M$, μ = 0.5, Acetic acid = 3% (v/v), Temp. = 25±0.1°, [Cr^{VI}] = $1.0\times10^{-4}M$ when Phen used and is $2.0\times10^{-4}M$ when Bipy used as ligand.

[Substrate] $\times10^4M$	k_1 $\times10^2$ min^{-1}	k'_1 $\times10^2$ min^{-1}
0.51[a]	3.68	3.74
0.56[b]	3.35	3.52
0.64[a]	3.74	3.72
0.74[b]	3.41	3.51
0.99[a]	3.70	3.74
1.11[b]	3.38	3.52
1.65[a]	3.72	3.76
1.85[b]	3.35	3.54

*Bipy used as ligand.
BADMA as substrate.
[b]Methyl orange as substrate.

TABLE 2—DEPENDENCE OF RATE ON CONCENTRATION OF CHROMIUM(VI)

[Methyl orange] = $0.99\times10^{-4}M$, [BADMA] = $1.11\times10^{-4}M$, [$HClO_4$] = $0.1M$, [Phen] = $8.0\times10^{-4}M$, μ = 0.5, Acetic acid = 3% (v/v), Temp. = 25±0.1°, [Bipy] = $2.0\times10^{-3}M$.

Cr^{VI} $\times10^4M$	k_1 $\times10^2$ min^{-1}	k'_1 $\times10^2$ min^{-1}	k_2 $\times10^2$ min^{-1}	k'_2 $\times10^2$ min^{-1}
1.0	3.70	3.38	2.12	1.55
1.5	5.02	4.55	–	–
2.0	7.05	6.41	3.74	3.52
2.5	8.91	7.98	–	–
3.0	10.42	9.45	5.92	5.21
3.5	12.10	11.34	–	–
4.0	14.24	12.96	7.30	7.12
5.0	–	–	9.42	8.44
6.0	–	–	11.23	10.57

k_1 and k'_1 = Pseudo-first order rate constants when Phen used as ligand.
k_2 and k'_2 = Pseudo-first order rate constants when Bipy used as ligand.
k_1 and k_2 = Pseudo-first order rate constants when methyl orange used as substrate.
k'_1 and k'_2 = Pseudo-first order rate constants when BADMA used as substrate.

TABLE 3—DEPENDENCE OF RATE ON HYDROGEN ION CONCENTRATION

[Methyl orange] = $0.99\times10^{-4}M$, [BADMA] = $1.11\times10^{-4}M$, [Phen] = $8.0\times10^{-4}M$, μ = 0.5, Acetic acid = 3% (v/v), Temp. = 25±0.1°, [Bipy] = $2.0\times10^{-3}M$, [Cr^{VI}] = $1.0\times10^{-4}M$ when Phen used as ligand and is $2.0\times10^{-4}M$ when Bipy used as ligand.

[$HClO_4$] M	k_1 $\times10^2$ min^{-1}	k'_1 $\times10^2$ min^{-1}	k_2 $\times10^2$ min^{-1}	k'_2 $\times10^2$ min^{-1}
0.1	3.70	3.38	3.74	3.52
0.2	6.63	6.34	7.52	6.68
0.3	10.86	9.71	11.48	8.95
0.4	14.07	12.52	14.81	14.10
0.5	17.36	15.96	18.72	17.50

k_1, k'_1, k_2, k'_2 defined as in Table 2.

Effect of varying ligand: The pseudo-first order rate constant (k_1) was determined at different initial concentrations of 1,10-phenanthroline or 2,2′-bipyridyl, keeping the concentrations of all other reactants constant. While the plot of k_1 *vs* [2,2′-bipyridyl] is a straight line passing through origin at all concentrations employed (Table 4), the plot of k_1 *vs* [phen] is linear only at lower

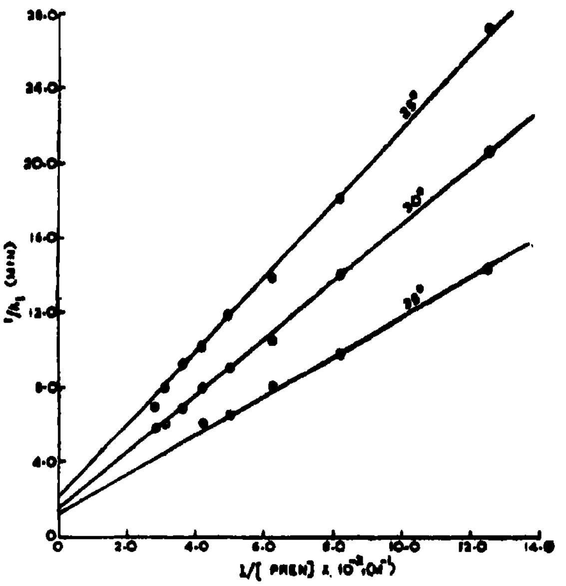


Fig. 1. Plots of $1/k_1$ *vs* $1/$[Phen]; [Cr^{VI}] = $1.0\times10^{-4}M$, [Methyl orange] = $0.99\times10^{-4}M$, [$HClO_4$] = $0.1M$, μ = 0.5.

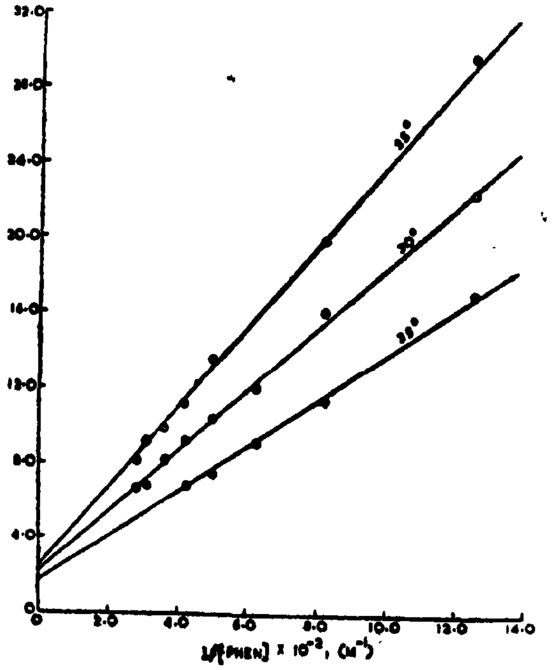


Fig. 2. Plots of $1/k_1$ *vs* $1/$[Phen]; [Cr^{VI}] = $1.0\times10^{-4}M$, [BADMA] = $1.11\times10^{-4}M$, [$HClO_4$] = $0.1M$, μ = 0.5.

TABLE 4—EFFECT OF VARYING THE CONCENTRATION OF BIPYRIDYL ON RATE

$[Cr^{VI}] = 2.0 \times 10^{-4} M$, [Methyl orange] $= 0.99 \times 10^{-4} M$, [BADMA] $= 1.11 \times 10^{-4} M$, $[HClO_4] = 0.1 M$, $\mu = 0.5$, Acetic acid = 3% (v/v), Temp. = $25 \pm 0.1°$.

[Bipy] $\times 10^3 M$	k_1* $\times 10^3$ min^{-1}	k'_1** $\times 10^3$ min^{-1}
2.0	3.74	3.52
3.0	5.97	5.05
4.0	7.05	6.98
5.0	8.83	9.10
6.0	10.50	10.31
7.0	12.48	12.42

*Methyl orange used as substrate.
**BADMA used as substrate.

1,10-phenanthroline concentrations. At higher concentrations of the ligand, curvature was observed showing a definite trend towards the attainment of limiting rate at still higher concentrations of 1,10-phenanthroline. Further, a plot of $1/k_1$ *vs* 1/[Phen] is a straight line with a definite positive intercept on $1/k_1$-axis (Figs. 1 and 2). Ionic strength was found to have negligible effect on the rate of the reaction.

The dependence of rate on the concentrations of Cr^{VI}, the substrate and 1,10-phenanthroline or 2,2'-bipyridyl suggests their participation in the transition state. The authors believe that Cr^{VI} forms, in a preequilibrium, a 1 : 1 complex with 2,2'-bipyridyl or 1,10-phenanthroline which acts as a more powerful oxidising species than the uncomplexed Cr^{VI}. Such complexes were reported earlier with pyridine and 1,10-phenanthroline by Sisler *et al.*[6,7]. The complex in the subsequent rate-determining step oxidises the aromatic azo compounds forming $Cr^{IV}L$. $Cr^{IV}L$ is reduced to $Cr^{III}L$ in fast steps. The detailed schematic mechanism is given in Sheme 1.

$$HCrO_4^- + L \overset{K_1}{\rightleftharpoons} Cr^{VI}L$$

$$Cr^{VI}L + H^+ + Ar{-}N{=}N{-}Ar' \xrightarrow[k]{r.d} Ar{-}N{=}\overset{+}{N}(O^-){-}Ar' + Cr^{IV}L$$

$$2(Cr^{IV}L + ArN{=}N{-}Ar' \longrightarrow \underset{L}{Cr^{III}}L + (Ar{-}N{-}N{-}Ar')^{+\cdot})$$

$$2(Cr^{VI} + (Ar{-}N{-}N{-}Ar')^{+\cdot} \longrightarrow Cr^{V}L + Ar{-}N{=}\overset{+}{N}(O^-){-}Ar')$$

$$2(2Cr^{V}L \longrightarrow Cr^{IV}L + \underset{L}{Cr^{VI}}L)$$

$$Cr^{VI} + Ar{-}N{=}\overset{+}{N}(O^-){-}Ar' \longrightarrow Cr^{IV}L + Ar{-}NO + Ar'{-}NO$$

$$2(Cr^{IV}L + Ar{-}N{=}\overset{+}{N}(O^-){-}Ar' \longrightarrow Cr^{III}L + Ar{-}\overset{+\cdot}{N} + Ar'{-}NO)$$

$$2(Cr^{VI} + Ar{-}\overset{+\cdot}{N} \xrightarrow{L} Cr^{V}L + Ar\ \ NO)$$

$$4Cr^{III}L + 8L \longrightarrow 4Cr^{III}L_3 \text{ (in several fast steps)}$$

$$4Cr^{VI} + 3Ar{-}N{=}N{-}Ar' + 8L \xrightarrow{4L} 4Cr^{III}L_3 + 3Ar{-}NO + 3Ar'{-}NO$$

Scheme 1

The rate law from Scheme 1 is represented as

$$-d[Ar{-}N{=}N{-}Ar']/dt = \frac{k\,K_1[HCrO_4^-]\,[L]\,[H^+]\,[ArN{=}N{-}Ar']}{1+K_1\,[L]} \quad (1)$$

$$k_1 = \frac{k\,K_1\,[HCrO_4^-]\,[L]\,[H^+]}{1+K_1\,[L]}, \text{ when } [HCrO_4^-] >> [ArN{=}NAr'] \quad (2)$$

$$1/k_1 = \frac{1}{kK_1\,[Cr^{VI}]\,[L]\,[H^+]} + \frac{1}{k\,[Cr^{VI}]\,[H^+]} \quad (3)$$

From the equation (2) plots of $1/k_1$ *vs* 1/[L] must be straight lines with positive intercepts on $1/k_1$-axes. The authors believe that an obtainment of intercept in the case of 1,10-phenanthroline and its absence in the case of 2,2'-bipyridyl-catalysed reaction can be explained by assuming that the stability constant in the former case has appreciable magnitude and the equation (2) is obeyed. But in the case of bipyridyl-catalysed reaction, the stability constant may be small in magnitude and the product K_1 [L] may be negligible in comparison with one in the denominator of the right-hand side of equation (1). Consequently, the plot of $1/k_1$ *vs* 1/[L] will be a straight line passing through origin in the case of bipyridyl-catalysed reaction. It is interesting to note that 1,10-phenanthroline, in general, forms stronger complexes with metal ions than bipyridyl[8].

The authors consider that the higher rates observed in the presence of 1,10-phenanthroline may be due to the greater stabilisation of transition state involving Cr^{VI}, ligand and substrate. 1,10-Phenanthroline which forms stronger complex is likely to stabilise the transition state more, leading to greater acceleration. This may be due to the presence of a better π-electron system in 1,10-phenanthroline than in 2,2'-bipyridyl. The rate acceleration may also be due to the stabilisation of Cr^{IV} by these ligands.

Activation parameters : The data of the activation energy calculated for the reaction are presented in Tables 5 and 6. The data of the uncatalysed reaction are presented in Table 7. The data clearly show that the catalysed reaction has lower activation energy than the uncatalysed reaction and the decrease in the activation energy is greater in the case of 1,10-phenanthroline-catalysed reaction

TABLE 5—ACTIVATION PARAMETERS WITH LIGAND AS 1,10-PHENANTHROLINE

$\mu = 0.5$

Temp. (± 0.1)°C	k* $\times 10^{-4}$ l^2 mol^{-2} min^{-1}	E_a(± 0.3) kcal mol^{-1}	k'** $\times 10^{-4}$ l^2 mol^{-2} min^{-1}	E'_a(± 0.3) kcal mol^{-1}
25	5.00		4.40	
30	5.32	2.20	4.75	2.80
35	5.64		5.13	

* Methyl orange used as substrate.
** BADMA used as substrate.

TABLE 6—ACTIVATION PARAMETERS WITH LIGAND AS 2,2'-BIPYRIDYL

$\mu = 0.5$

Temp. (±0.1)°C	k* ×10⁻² l^2 mol^{-1} min^{-1}	E_a(±0.5) kcal mol^{-1}	k'** ×10⁻² l^2 mol^{-1} min^{-1}	E_a(±0.5) kcal mol^{-1}
25	1.87		1.76	
30	2.09	4.0	1.98	4.2
35	2.59		2.48	

* and ** As in Table 5.

TABLE 7—ACTIVATION PARAMETERS FOR UNCATALYSED REACTION

$[Cr^{VI}] = 6.82 \times 10^{-4} M$, $[HClO_4] = 2.0 M$, $\mu = 2.0$, Acetic acid = 40% (v/v), Substrate = BADMA

Temp. (±0.1)°C	k_1 ×10³ min^{-1}	E_a (±1.0) kcal mol^{-1}
30.5	30.23	
35.0	38.86	10.0
40.0	46.06	

TABLE 8—VALUE OF STABILITY CONSTANT AND ITS ENTHALPY FOR CHROMIUM(VI)-1,10-PHENANTHROLINE COMPLEX

Temp. °C	k_1 ×10⁻² mol^{-1}	ΔH (±0.5) kcal mol^{-1}
25	10.45	
30	9.13	−4.80
35	8.01	

showing that the ligand stabilises the transition state more than the bipyridyl ligand. From the slopes and intercepts of the plots of $1/k_1$ *vs* 1/[Phen] the authors calculated the values of the stability constants for chromium(VI)-1,10-phenanthroline complex at three temperatures. Using these data, the enthalpy of formation ΔH of $Cr^{VI}L$ was calculated from the integrated expression of Van't Hoff (Table 8).

References

1. S. V. ANANTHA KRISHNAN and H. JAYARAMAN, *Indian J. Chem.*, 1964, 2, 146; S. V. ANANTHA KRISHNAN and R. V. VARADARAJAN, *Indian J. Chem.*, 1970, 8, 423; V. M. SADAGOPARAMANUJAM, S. SUNDARAM and N. VENKATASUBRAMANIAM, *Indian J. Chem.*, 1973, 11, 889.
2. G. GOPALA RAO and C. R. VISWANATHAM, *Curr. Sci.*, 1942, 11, 102.
3. A. I. VOGEL, "Elementary Practical Organic Chemistry", Quantitative Organic Analysis, Longmans Green, London, 1971, Part III, p. 754.
4. A. I. VOGEL, "Practical Organic Chemistry", ELBS, London, 1968, p. 265.
5. F. FEIGL, "Spot tests in Organic Analysis", Elsevier, New York, 1966, p. 290.
6. H. H. SISLER, J. D. BUSH and O. E. ACCOUNTIUS, *J. Am. Chem. Soc.*, 1948, 70, 3827; H. H. SISLER, W. C. L. MING, E. METTER and F. R. HURLEY, *J. Am. Chem. Soc*, 1953, 75, 446; O. E. ACCOUNTIUS, J. D. BUSH and H. H. SISLER, *Inorg. Synth.*, 1953, 4, 94.
7. H. H. SISLER, N. EL-JADIR and D. H. BUSCH, *J. Inorg. Nucl. Chem.*, 1961, 16, 257.
8. H. IRWING and D. H. MELLOR, *J. Chem. Soc.*, 1962, 5222.

J. Indian Chem. Soc.,
Vol. LXIII, May 1986, pp. 485-489

Kinetics of Hydrolysis of *N*,*N*′-Di-*p*-methoxyphenylphosphorodiamidic Chloride

V. SAHNI and S. PRABHA*

School of Studies in Chemistry, Jiwaji University, Gwalior-474 011

Manuscript received 12 December 1984, accepted 31 March 1986

Hydrolysis of *N*-(*p*-methoxyphenyl)phosphorodiamidic chloride has been studied in the acid region, 0.01 to 8.0 *M* HCl at 40° (acetic acid-water 20%, v/v). Ionic strength effect differentiates two contributory forms, the neutral as well as the conjugate acid form, the former being reactive as the zwitterionic form. Rates are reduced on adding DMF and DMSO. The frequency factor ($10^{1?}$) being on the borderline of uni- and bimolecular mechanisms also favours the zwitterionic form, so that the transition state may be possible with dispersal of +ve charge. The value of E (15.05 kcal mol^{-1}), however, requires a bimolecular hydrolysis, although involving a short-lived transition state. Effect of metal ions is used to strengthen specific acid catalysis suggested by neutral electrolyte effect studies. A maximum at 4.0 *M* acid and other parameters used in comparative kinetic data favour P—N bond cleavage for this diester. Coplanarity of *p*-CH_3O substituent with the rest of the matrix is highlighted by the highest magnitude of rates due to acid catalysis in the series of diesters examined.

THE hydrolysis of a diester with C—N—P linkage has been pursued to account for the most suitable pathway(s) depending upon the presence of the neutral (modified) and the conjugate acid species. The polar neutral form has been suggested in the case of aminophosphates (monoesters mainly) by Chanley and Feageson[1]. So the objective was to find out their presence and contribution in the diesters. It may be worthwhile to mention that a detailed kinetic study led us to postulate the zwitterion for *N*-(*p*-methoxyphenyl)phosphorodiamidic chloride.

Experimental

N-(*p*-Methoxyphenyl)phosphorodiamidic chloride was prepared by stirring *p*-anisidine and PCl_5 (1 : 1) in benzene, for about 7 h. It was recovered by repeated precipitation with ammonia and HCl, m.p. 146° (Found : C, 53.8 ; H, 6.80 ; N, 7.95 ; P, 9.49. $C_{14}H_{16}N_2PO_3Cl$ calcd. for : C, 51.45 ; H, 4.90 ; N, 8.57 ; P, 9.49%).

All chemicals used were either of AnalaR or G. R. (S. M.) quality. Deuterium oxide was procured from Bhabha Atomic Research Centre, Trombay and its isotopic purity as reported was >99.4%.

Kinetics of hydrolysis of *N*,*N*′-di-*p*-methoxyphenylphosphorodiamidic chloride has been investigated in the acid range 0.01-8.0 *M* HCl in 20% (v/v) acetic acid at 40°. The progress of the reaction was followed by estimating the rate of appearance of inorganic phosphate[2]. The concentration of the diester was maintained at 5×10^{-4} mol dm^{-3} throughout the study, except when its concentration effect was determined.

Results and Discussion

The first order rate constants for the hydrolysis of *N*-(*p*-methoxyphenyl)phosphorodiamidic chloride increases with the increase in acid molarity upto 4.0 *M*, at which a maximum appears. After this, the rates decrease gradually. This decrease in rates, after the maximum, is attributed either to negative electrolyte effect or decrease in water activity, or both.

In order to determine and distinguish between the operative reactive forms, ionic strength studies[3] have been carried out using appropriate proportions of sodium chloride and HCl. The first order rate coefficients have been summarised in Table 1. The diamidic-chloride does behave like other diesters and gives three linear curves (Fig. 1), which on extrapolation, give intercepts of different magnitudes. It is noticed that, these values when further modified, correspond to a linear curve, indicating constant contribution of the neutral form (Fig. 2). Thus, the rates *via* the neutral form for this diester are expected to be rather constant, but the overall

TABLE 1—OBSERVED AND CALCULATED RATES FOR HYDROLYSIS OF *N*-(*p*-METHOXYPHENYL)-PHOSPHORODIAMIDIC CHLORIDE AT 40°

Sl. no.	Acid M	10^3 k_{N^+} min^{-1}	10^3 $k_{H^+}C_{H^+}$ min^{-1}	ke Found/ (Calcd) $\times 10^3$ min^{-1}
1.	0.01	3 98	-	3.84 (3.98)
2.	0.10	3.98	0.35	4.42 (4.33)
3.	0.50	3.98	1.62	5.83 (5.60)
4.	1.00	3.98	2.89	6.21 (6.87)
5.	2.00	3.98	4.62	4.67 (8.60)
6.	3.00	3.98	5.53	5.63 (9.51)
7.	4.00	3.98	5.89	9.76 (9.87)
8.	5.00	-	5 87	4.88 (4.11)[a]
9.	6.00	-	5.63	3.72 (3.46)[a]
10.	7.00	-	5.24	2.67 (2.76)[a]
11.	8.00	-	4.77	1.85 (2.09)[a]

[a] n is 1 in equation (5).

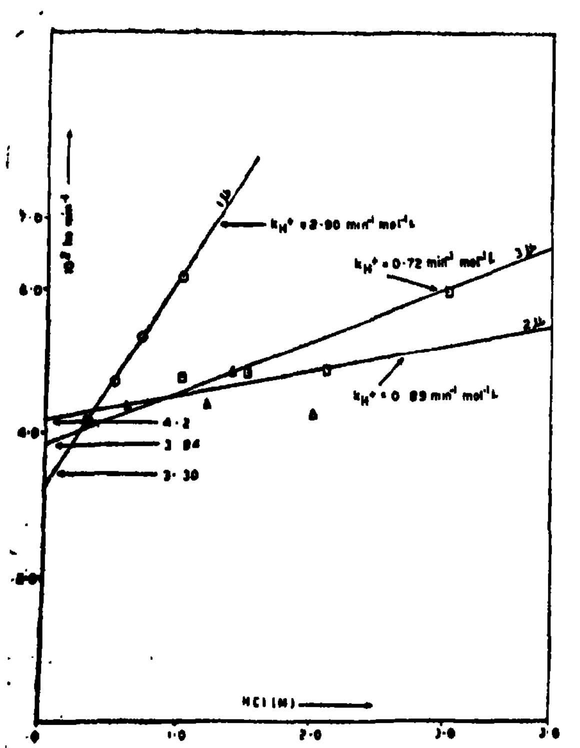


Fig. 1. Hydrolysis of di-*p*-anisidine phosphate at constant ionic strength at 40° : (O) 1, (△) 2 and (□) 3 μ.

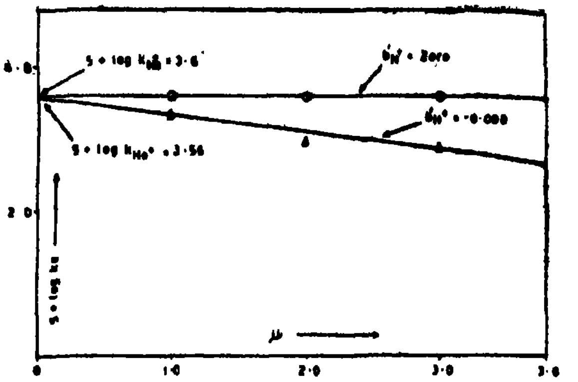


Fig. 2. Hydrolysis of di-*p*-anisidine phosphate *via* conjugate acid and neutral species : (O) $5+\log k_{N^+}$ and (△) $5+\log k_{H^+}$.

magnitude of these is quite high and significant. Here the 2nd empirical term of Debye-Hückel equation[4] for the calculation of rates *via* the neutral form is reduced to

$$5+\log k_N = 5+\log k_{N0} \quad (1)$$

Further, this neutral form has been considered to participate better as a modified zwitterionic form so that equation (1) may be further modified as

$$5+\log k_{N^+} = 5+\log k_{N0^+} \quad (2)$$

However, the neutral form is accompanied by the conjugate acid form. For the latter, the rates rise with the increase in acid molarity. However, slopes of these linear curves, *i.e* acid-catalysed rates decrease with the decrease in μ, indicating $-$ve ionic strength effect on the acid-catalysed species. This form is, however, reactive in the entire acid range, although the rates decrease after 4.0 M. These specific acid-catalysed rates are, therefore, based on the equation,

$$5+\log k_{H^+} = 5+\log k_{H^+0} - b'_{H^+}.\mu \quad (3)$$

The latter parameter is a negative quantity because the slope of the linear curve in modified plot (Fig. 2) is also $-$ve. These bimolecular rates have been modified into unimolecular rates by multiplying them with the concentration of acid so that

$$\log k_{H^+}C_{H^+} = \log k_{H^+0} + \log C_{H^+} - b'_{H^+}.\mu \quad (4)$$

On the basis of equations (2) and (4), rates have been specifically calculated and are found to agree closely with the observed rates (Table 1) especially in the low acid region. Thus, both modified neutral and conjugate acid forms of this diester are present and are contributory.

The lowering in rates after the maximum, *i.e.* 4.0 M, is attributed to both, negative ionic strength effect and decrease in water activity. The number

of water molecules involved is only one at each acid molarity, and this has been determined by applying the modified form of Brönsted-Bjerrum equation,

$$ke_{calcd.} = k_{H^+O} \cdot C_{H^+} \exp. b_{H^+} \mu (aH_2O)_n \quad (5)$$

where, n is the number of water molecules involved. Concepts of Hammett[6] and Zücker-Hammett[7] leading to slopes, zero and 1.19, are favourable for the participation of water in the rate-determining step. Parameters of Bunnett[8] ($w=11.09$ and $w^*=3.31$) emphasise that water acts as a nucleophile too, in addition to the above behaviour. Value of Φ(1.65) based on the plot of Bunnett and Olsen[9], postulates further that water acts as a proton-transfer agent, when the proton attaches to N of the C—N—P linkage.

Arrhenius parameters[10] (Table 2) being nearly the same, before and after the maximum, account for the absence of maximum protonation. Both E (energy of activation) and E-based $\Delta S^{\neq}$ (entropy of activation) favour the presence and participation of water molecule in the formation of a transition state. The frequency factor is just near the border line of uni- and bi-molecular reactions. However, all the other Arrhenius parameters postulate a bimolecular mechanism.

TABLE 2—ARRHENIUS PARAMETERS FOR HYDROLYSIS OF N-(p-METHOXYPHENYL)PHOSPHORODIAMIDIC CHLORIDE IN AQUEOUS HYDROCHLORIC ACID

HCl M	E kcal mol^{-1} (kJ mol^{-1})	A s^{-1}	$\Delta S^{\neq}$ e.u. (JK mol^{-1})	$\Delta G^{\neq}$ kcal mol^{-1} (kJ mol^{-1})
3.0	15.05 (62.96)	7.11×10^{11}	−26.99 (126.8)	23.28 (23.28)
5.0	13.22 (55.31)	1.91×10^{11}	−32.53 (102.0)	23.40 (23.38)

The hydrolysis *via* the neutral form by both uni- and bi-molecular modes will result in creation of charges, so that the rates are enhanced by a changeover from less to more polar solvent. However, in the present study, the results are just the opposite. Thus, it is possible that both the reactive forms exist as charged structures initially and this then is dispersed during a bimolecular attack. According to qualitative theory of Hughes and Ingold[11] this dispersal may be decided by solvent effect studies and it results in the decrease in rates to some extent by an increase in the polarity of the solvent.

In order to confirm the above, solvent effect study has been made using solvents of different polarities. At low acid molarity (0.1M), increase in the percentage of a protic solvent, like acetic acid, brings about a lowering in rates. This lowering suggests the formation of a transition state, in which there is either a reduction or dispersal of charge. Use of dipolar aprotic solvents[12], like DMF and DMSO, also brings about a lowering in the magnitude of rates. Such an effect is possibly due to its strong interaction with the hydrogen ions of the acid present (HCl) as well as its association with water molecules. In the former, there is depletion of H_3O^+ ions due to the formation of $DMFH^+$ like species, so that the net effect is a decrease in velocity of hydrolysis in this phase.

All the above results and reasonings either suggest an altogether different pathway or require the existence of the neutral form as its cationic state, *i.e.* zwitterion in the acid range, hydrolysing by a bimolecular pathway. Such a structure will bring about a dispersal of the +ve charge, so that when solvents are varied as above, the rates may be lowered to some extent. Solvent-isotope[13] effect studies made in D_2O lead to lowering in rates, suggesting a specific acid-catalysed reaction.

The rate of hydrolysis is lowered[14] when different electrolytes are used in the low as well as high acid region. In the acid range, the reaction requires the presence of electrophilic species, like H^+. The following order of decreasing strengths in water has been observed for a series of electrolytes: $H^+ > Na^+, K^+$. The decrease in rates due

TABLE 3—COMPARATIVE KINETIC DATA FOR HYDROLYSIS OF SOME DIAMIDATES *via* THEIR CONJUGATE ACID SPECIES

Sl. no.	Diesters (C—N—P)	Temp. °C	ke $\times10^3$ min^{-1}	Maxima M	E kcal mol^{-1}	$-\Delta S^{\neq}$ e.u.	Molarity	Fission	Ref.
1.	o-CH_3-aniline	50	*d*	1.0	11.40^a	38.66	2	P−N	15
2.	p-CH_3-aniline	50	8.42	5.0	9.15^c	37.29	2	P−N	16
3.	p-Br-aniline	90	27.50	4.0	9.15^b	55.98	2	P−N	17
4.	p-Cl-aniline	90	19.40	4.0	9.15^b	56.78	2	P−N	17
5.	m-NO_2-aniline	98	2.58	3.5	16.61^b	31.90	2	P−N	18
6.	p-NO_2-aniline	98	0.06	2.0	14.64^a	44.91	2	P−N	19
7.	p-CH_3O-aniline	40	9.76	4.0	15.05^b	26.29	2	P−N	This work
8.	p-OC_2H_5-aniline	98	18.57	4.0	5.72^b	70.55	2	P−N	20

a,b,c = At 1.0, 3.0 and 5.0 M, respectively. d = Data not available.

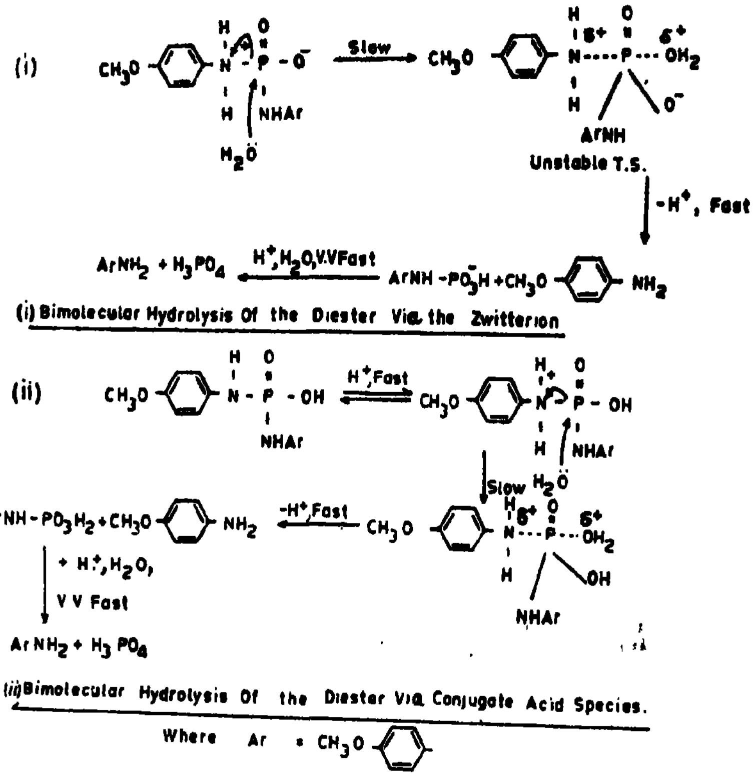


Chart 1.

to different electrolytes, like LiCl, NaCl, is in accordance with the reasoning that they act as soft electrophilic centres as compared to the aquated ion. This nature makes the hydrolysis difficult, because the leaving group ($H_3CO-Ph-N^+H_3$) is comparatively of the harder type.

The concentration effect study was also carried out at low as well as at high acid molarities. Rates are found to be insensitive to concentration changes. Thus the reaction is proved to be of the first order type. The second reaction partner, water, in this bimolecular reaction is always present in excess, so that it is better to refer the rates as pseudo-first order rates.

Existence of an isokinetic relationship[14] (β= 187.5°) and comparative kinetic data (Table 3) showing similarity in behaviour suggest P—N bond cleavage for this diester. P—N bond rupture is also justified by the formation of a suitable *p*-anisidine molecule during hydrolysis. The maximum reactivity of the present diester requires participation of the *p*-MeO group in one way or the other. Since the ester has been shown to involve the modified neutral form, *i.e.* the zwitterion in the acid region upto 4.0 *M*, the acid catalysis leading to highest rates allows the stabilisation of the +ve charge by the *p*-MeO group (+M). It also requires the coplanarity of the *p*-MeO substituent with the site of protonation (NH) *via* the aryl matrix. The order of acid catalysis as seen from Table 3 can be shown as: *p*-CH_3O > *p*-CH_3 > *p*-Br > *p*-Cl > *p*-OC_2H_5 > *m*-NO_2 > *p*-NO_2.

On the basis of the above discussion, it may be possible to postulate the following plausible routes of hydrolysis in the acid range *via* the two reactive forms (Chart 1).

Acknowledgement

One of the authors (V.S.) is thankful to U.G.C., New Delhi, for granting a Junior Research Fellowship.

References

1. J. D. CHANLEY and E. FEAGESON, *J. Am. Chem. Soc.*, 1958, 80, 2686.
2. R. J. L. ALLEN, *Biochem. J.*, 1940, 34, 858.
3. K. J. LAIDLER, "Reaction Kinetics", Pergamon, London, 1963, Vol. II, pp. 63, 225.
4. F. A. LONG and W. F. MCDEVIT, *Chem. Rev.*, 1952, 51, 119.
5. P. W. C. BARNARD, C. A. BUNTON, D. KELLERMAN, M. M. MHALA, B. SILVER, C. A. VERNON and V. A. WELCH, *J. Chem. Soc., B*, 1966, pp. 227, 229.
6. L. P. HAMMETT, "Physical Organic Chemistry", McGraw-Hill, New York, 1940.
7. L. ZÜCKER and L. P. HAMMETT, *J. Am. Chem. Soc.*, 1939, 61, 2791.
8. J. F. BUNNETT, *J. Am. Chem. Soc.*, 1961, 83, 4956.
9. J. F. BUNNETT and OLSEN, *Can. J. Chem.*, 1966, 44, 1899, 1917.
. S. ARRHENIUS, *Z. Phys. Chem.*, 1889, 4, 226.
. E. D. HUGHES and C. K. INGOLD, *J. Chem. Soc.*, 1935, 244.

12. E. M. KOSOWER, "An Introduction to Physical Organic Chemistry", Wiley, New York, 1968, pp. 51, 69, 334.

13. R. D. GILLIOM, "Introduction to Physical Organic Chemistry", Addison Wesley, 1970, p. 200.

14. N. B. CHAPMAN and J. SHORTER, "Advances in Linear Free Energy Relationship", Plenum Press, London, 1972, pp. 204, 309.

15. A. N. SAGNE, Ph.D. Thesis, Jiwaji University, 1972.

16. A. K. BHOITE, Ph.D. Thesis, Jiwaji University, 1977.

17. N. AGARWAL, Ph.D. Thesis, Jiwaji University, 1983.

18. K. KULSHRESTHA, Ph.D. Thesis, Jiwaji University, 1982.

19. P. JAIN, Ph.D. Thesis, Jiwaji University, 1982.

20. A. K. BHADORIA, Ph.D. Thesis, Jiwaji University, 1982.

J. Indian Chem. Soc.,
Vol. LXIII, May 1986, pp. 490-494

Infrared Investigations of β-Picoline-halogen Charge-transfer Complexes

S. K. BAROOAH and I. HAQUE*

Department of Chemistry, Dibrugarh University, Dibrugarh-786 004

Manuscript received 6 February 1978, revised 3 February 1986, accepted 2 April 1986

The infrared spectra (4 000 – 400 cm^{-1}) of β-pic-I_2, β-pic-ICl, β-pic-IBr, β-pic-Br_2 and β-pic-BrCl charge-transfer complexes have been studied in a range of solvents. The solid β-pic-I_2 complex has been found to undergo solid state transformation 2β-pic-I_2 → (β-pic_2-I)$^+I_3^-$. In polar solvents all the complexes ionise.

$$2\beta\text{-pic-IX} \rightleftharpoons (\beta\text{-pic}_2\text{-I})^+ + IX_2^-$$

$$2\beta\text{-pic-BrX} \rightleftharpoons (\beta\text{-pic}_2\text{-Br})^+ + BrX_2^-$$

But no evidence for ionisation have been found in non-polar solvents. Assuming a C_s symmetry point group for these complexes all the observed bands have been assigned. The vibrations at 1 044 and 620 cm^{-1} of β-picoline have been found to be quite sensitive to complex formations. The effect of solvent and acceptor on these two vibrations have been discussed.

THE effect on vibrational spectra of halogens due to the formation of charge-transfer complexes with various donors have been the subject of many investigations[1,2]. Contrary to this, very little work has been done on the vibrational spectra of the donors. The most intensely studied donor molecules are benzene[3], trimethylamine[4], pyridine[5], dioxane[6], and a few others. The vibrational frequencies of the benzene and dioxane molecules donot shift on complex formation except some change in intensities. But infrared spectra of trimethylamine and pyridine have been found to change remarkably. The β-picoline-halogen complexes have not been extensively studied. The infrared spectra of equimolar β-picoline-iodine solutions have been examined over a small frequency range around 1 000 cm^{-1} by Glusker and Thomson[7] and they observed changes in the frequencies of a number of β-picoline bands providing evidence of complex formation. The far-infrared spectra of β-picoline-ICl have also been examined[8]. In this paper, the infrared spectra of β-picoline-halogens in the frequency range 4 000-400 cm^{-1} are presented in solutions of various solvents and also in mulls. The nature of the species present is discussed, the frequencies are assigned and the solvent and acceptor effects on the ring vibrations are also discussed.

Experimental

β-Picoline was dried over KOH and BaO for several days and distilled under reduced pressure. Iodine (AnalaR) was resublimed and dried over P_2O_5. Iodine bromide and bromine chloride were prepared as described in literature[9]. Chloroform, carbon tetrachloride, methylene chloride acetonitrile (all A.R. grade) were dried over $CaCl_2$ and distilled from fresh P_2O_5. Spectroscopic grade benzene, and carbon disulphide were used without further purifications.

Preparation : β-Picoline-iodine was prepared as described[10] previously (Found ; I_2, 72.0. β-pic-I_2 calcd. for : I_2, 73.16%). β-Picoline-ICl and -IBr complexes were prepared by mixing equimolar quantities of β-picoline and ICl or IBr in carbon tetrachloride or methanol solutions at 0°, and then recrystallised from methanol and dried over P_2O_5 in vacuum : β-pic-ICl, m.p. 56.5° (Found : N, 5.42 ; C, 27.99 ; H, 2.78 ; total halogen, 62.3. Calcd. for : N, 5.47 ; C, 28.1, H, 2.73 ; total halogen, 63%). β-pic-IBr, m.p. 62.5° (Found : N, 4.52 ; C, 23.84 ; H, 2.32 ; total halogen, 68.8. Calcd. for : N, 4.66 ; C, 24.00 ; H, 2.33 ; total halogen, 69%). As the bromine and bromine chloride complexes of β-picoline were found to be very much unstable in the solid state no attempt was made to take the spectra of solid compounds.

Infrared spectra were recorded on a Specord 75 IR grating spectrophotometer using KBr window cells. For solutions, path length of the cells varied

from 0.02 to 0.04 mm. All the measurements were made on freshly prepared solutions. The accuracy in the wave numbers was within ± 2 cm^{-1}. The spectral resolution in the solution spectra was better than 2 cm^{-1} at 3 200 cm^{-1} and better than 1 cm^{-1} at 2 500-400 cm^{-1}.

Table 1, reporting only those bands which can be clearly distinguished from the solvent background.

The vibrational spectra of solid β-picoline-iodine in mulls are found to be quite different from that of the equimolar solutions of β-picoline and iodine in non-polar solvents, such as carbon tetrachloride

TABLE 1—IR SPECTRA (cm^{-1})* OF β-PICOLINE-IODINE IN VARIOUS MEDIA

1 : 1 β-pic−I_2 in CCl_4	1 : 1 β-pic−I_2 in CS_2	1:1 β-pic−I_2 in CH_2Cl_2	1 : 1 β-pic−I_2 in C_6H_6	1 : 1 β-pic−I_2 in $CHCl_3$	In β-pic	Solid in mull	β-pic−I_2 in dioxane	Interpretation**
3 084 w	3 087 vw							A′ ν (CH)
3 064 m	3 064 m							A′ ν (CH)
	3 050 w							A′ ν (CH)
3 020 w								A′ ν (CH)
2 960 w	2 960 vw							A′ Me
2 924 w								A′ Me
	2 860 m							A″ sym CH stretch in Me GP
2 743 w								1 250+1 450
2 610 vw								1 380+1 250
	2 500 w							1 260+1 240
1 916 m	1 916 m			1 916vw				1 230+700
1 900 w	1 910 m							988+915
	1 886 w							1 100+785
				1 730 w				1 100+640
1 716 w	1 716 w							1 031+700
		1 600 m	1 600 w			1 600 m	1 600 w	A′ ν (CC)
		1 587 s	1 584 m	1 584 w		1 584 m		988+629
		1 580 w	1 580 w			1 580 w	1 580 m	A′ ν (CC)
1 480 s	1 480 sh	1 480 s					1 480 w	A′ ν (CC, CN)
1 450 w								A″ asym CH bending in Me GP
			1 430 w			1 423 w		452+915
1 416 m								A′ ν (CC, CN)
1 384 w	1 384 w	1 386 w						A″ sym CH bending in Me GP
1 250 m	1 260 w							A′ α (CC)
	1 240 w							A′ α (CC)
1 223 w								A′ β (CH)
1 194 s	1 193 s	1 193 s	1 192 s	1 192 m		1 186 s	1 193 s	A′ β (CH)
	1 164 w							700+452
1 127 s	1 127 s	1 128 s	1 126 s	1 127 s		1 122 s	1 126 w	A′ β (CH)
1 102 s	1 100 m	1 099 s	1 100 s	1 100 m		1 092 m		A′ ϕ (CC)
		1 058 s			1 059 m	1 058 s	1 059 vw	(β-pic_2-I^+)
1 052 s	1 053 s	1 055 s	1 050 s	1 053 s	1 053 s			A′ Ring
1 031 w	1 031 w	1 031 w				1 028 s		A′ β (CH)
	988 w							A′ γ (CH)
	915 w							535+452
			850 s					A″ γ (CH)
		823 sh				824 m	817 vw	(β-pic_2I^+)
	814 m	815 sh	814 m	813 w	813 w	810 m	805 w	A″ γ (CH)
	785 s	791 s	789 s			791 s	792 s	A′ Ring
711 s	711 vw						710 s	A″ γ (CH)
720 s	700 s			695 m	700 sh	686 s	696 s	A″ γ (CH)
		652 m			651 sh	650 s	653 vw	(β-pic_2I^+)
641 s	641 s	645 s	643 w	642 m	643 s	645 s	645 s	A′ X-sensitive
533 w	533 m	533 w	535 w				535 vw	A″ component of e_{2u} of 404
	460 m	456 m			463 m			A″ X-sensitive

* s = strong, w = weak, m = medium, vw = very weak, sh = shoulder,
** β-pic = β-picoline, sym = symmetrical, asym = asymmetrical, GP = group, Me = methyl.

Results and Discussion

The spectral data over the frequency range 400-4 000 cm^{-1} in a range of solvents and in mulls of β-picoline-iodine complex are presented in and benzene. Solid β-picoline iodine in mulls shows a strong band at 1 058 cm^{-1} and another at 650 cm^{-1} and no band is observed at 530 cm^{-1} (Fig. 1). But equimolar solutions of I_2 and

β-picoline in CCl_4 and in CS_2 show bands at ~1 053, 640 and 534 cm^{-1}. Although the shifting of the first two bands may be attributed to the solvent effect but the absence of the band at 530 cm^{-1}, which is usually quite strong, cannot be explained. In polar solvents, such as excess of β-picoline, acetonitrile and also in methylene chloride solutions a pair of bands is observed near 1 050 cm^{-1}, *i.e.* at ~ 1 050 and 1 063 cm^{-1} and also a pair of bands is observed in the vicinity of 640 cm^{-1}. Besides, a band at 530 cm^{-1} is also observed in all the three solvents. The bands at 1 058 and 650 cm^{-1} observed in polar solvents and also in mulls correspond to $(\beta\text{-pic}_2\text{-I})^+$ frequencies[11]. It may be assumed that the complex is ionised[8,12] in excess of β-picoline and also in other polar solvents and the additional bands are due to the presence of $(\beta\text{-pic}_2\text{-I})^+$ ion. In non-polar solvents all the observed bands may be accounted for β-pic-I_2. In the case of solid β-pic-I_2, possibly it undergoes solid state transformations to $(\beta\text{-pic}_2\text{-I})^+ I_3^-$, like hexamethylenetetramine-iodine complex[13]. This is also observed visually as the colour of the solid changes from orange to dark brown. Moreover, the spectra of the solid compound in mulls are identical to that of the $(\beta\text{-pic}_2\text{-I})^+$ in $(\beta\text{-pic}_2\text{-I})\ BF_4$ (Ref. 11). Further evidence for the formation of I_3^- ion in the solid state is obtained by taking the uv spectra of solid β-picoline-iodine complex showing an intense band at ~ 363 nm[14,15]. This band is identified as $\pi_g - \delta_u$ transition for the I_3^--ion. In methylene chloride solution, it gives two bands at ~ 363 and 504 nm. The latter being the blue-shifted iodine band.

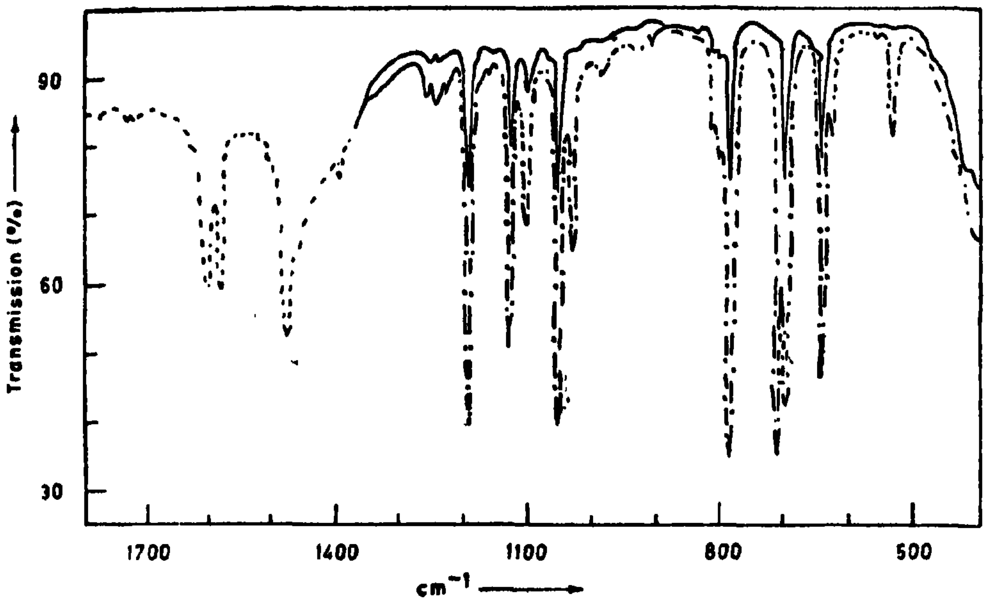


Fig. 1. Composite ir spectra: (–) solid β-pic-I_2 in nujol mull (–) and (—.—) equimolar solution of I_2 and β-picoline in CS_2.

The spectra of β-pic-IBr and β-pic-ICl are identical both in mulls and in non-polar solvents. In polar solvents, in both the cases, additional bands at ~ 1 060 and 551 cm^{-1} are observed but they are generally weak. Assuming the complex is unionised in non-polar media and in mulls and ionised in polar media, all the bands are accounted for. Similar observations are also made for β-pic-Br_2 and β-pic-BrCl complexes. In all the cases the spectra of freshly prepared solutions may be entirely accounted for by the equilibria,

$$2\text{-}\beta\text{-pic-IX} \rightleftharpoons (\beta\text{-pic}_2\ \text{I})^+ + IX_2^-, \text{ and}$$

$$2\text{-}\beta\text{-pic-BrX} \rightleftharpoons (\beta\text{-pic}_2\text{Br})^+ + BrX_2^-.$$

Assignments: The bands found in the unionised compounds may be readily assigned by comparing with the spectra of β-picoline[15-17]. The symmetry point group of β-picoline is C_s if the methyl group is regarded as point mass. By comparing with the compounds of pyridine and γ-picoline this C_s point group may be assumed to retain by the β-picoline-halogen complexes also. The infra-red data support the C_s symmetry.

For C_s symmetry, the vibration fall into two groups A′ and A″ and the 42 fundamental vibrations fall into the classes 29A′ + 13A″; of these vibrations, 4A′ + 2A″ comprises of five intermolecular modes and the halogen-halogen stretching vibrations and they are expected to fall in the far-infrared region. Table 2 which shows the assignments for the observed bands of the complexes, also includes those for the β-picoline. The β-picoline bands at ~ 1 044 and 785 cm^{-1} which we have assigned as ring modes donot agree with the assignments made

TABLE 2 — ASSIGNMENT OF FUNDAMENTAL VIBRATIONAL FREQUENCIES (cm^{-1}) OF β-PICOLINE COMPLEXES AND COMPARISON WITH β-PICOLINE

Designation	β-pic	β-pic-I_2	β-pic-IBr	β-pic-ICl	β-pic-Br_2	β-pic-BrCl
A′						
ν (CH)	3 087	3 087	3 087	3 097	3 093	
ν (CH)	3 050	3 060	3 067	3 066	3 067	3 073
ν (CH)	3 030		3 017	3 030	3 035	3 020
ν (CH)	2 995	3 010	2 997	3 000	2 985	
Me	2 950	2 960	2 950	2 950	2 950	
Me	1 927	1 916	1 923	1 932	1 950	1 916
ν (CC)	1 595	1 600	1 601	1 603	1 600	1 604
ν (CC)	1 577	1 587	1 580	1 580	1 580	1 586
ν (CC, CN)	1 480	1 480	1 480	1 480	1 480	1 483
ν (CC, CN)	1 413	1 416	1 423	1 440	1 410	1 416
β (CH)	1 341		1 345	1 347	1 337	
β (CH)	1 332		1 336	1 336	1 332	1 330
β (CH)	1 226	1 233	1 234	1 24[illegible]	1 223	1 236
β (CH)	1 194	1 189	1 195	1 197	1 190	1 192
β (CH)	1 126	1 122	1 126	1 130	1 128	1 129
ϕ (CC)	1 108	1 095	1 100	1 100	1 106	1 102
Ring	1 044	1 050	1 057	1 060	1 065	1 063
β (CH)	1 031	1 032	1 031	1 031	1 031	1 033
γ (CH)	985	988	990	990	985	990
Ring	785	788	785	785	785	793
X-sen	629	645	648	649	649	649
A″						
Asym CH stretch in Me GP	2 980	2 960	2 923	2 922	2 923	
Sym CH stretch in Me GP	2 868	2 860	2 851	2 850	2 873	
Asym CH bending in Me GP	1 455	1 430			1 460	1 460
Sym CH bending in Me GP	1 383	1 387	1 387	1 387	1 383	1 380
γ (CH)	924	915	924	930	924	
γ (CH)	857	855	857	857		
γ (CH)	711	697	697	710	712	720
Component of e_{2u} of 404	535	535	535	533	533	535
X-sen	452	467	467	468	460	454

by others[15-17]. By comparision with the vibrations of pyridine, these two vibrations have been found to be quite similar to the vibrations 992 and 605 cm^{-1} of pyridine which shifts to higher frequencies on complex formation with halogens.

Effect of environment : As the polarity of the environment increases the transfer of charge from the donor to the acceptor should also increase[1]. As a result, the shifts of the vibration frequencies of the β-picoline should increase. This is actually observed in all the complexes for the $\sim$ 1 044 and 629 cm^{-1} bands. It is obvious from Table 2 that the frequency shifts of the 1 044 and 629 cm^{-1} bands are dependent on a common factor, and should be directly related to each other. Fig. 2 shows the plots of 1 044 cm^{-1} against 629 cm^{-1} bands for the complexes β-pic-ICl and β-pic-IBr in a variety of environments. This is also observed for the different complexes Fig. 2.

Frequency shift : With the change of acceptor, the 1 044 and 629 cm^{-1} bands of β-picoline shift to different positions. There seems to be no corelation between the extent of the adjacent coordination atom. The explanation may be given in terms of charge-transfer from the ring to the acceptor.

The charge-transfer takes place from the nitrogen $2sp^2$ lone-pair orbital to the vacant np_z antibonding orbital of halogen, thereby modifying the π-bonding of the ring. This transfer of charge should increase with the increase in acid strength of halogen[1]. The acid strength in order of increasing strength are $Cl_2 < Br_2 < I_2 < IBr < BrCl < ICl$. This has been observed in the case of dioxane-halogen complexes[6]. But in our case a slight drift is observed. It is observed that the change in frequency is greater for ICl complex than for IBr, which is even greater for I_2 complexes. It is also found to be greater for the BrCl than for the Br_2 complexes. Since I_2 has a greater acid-strength than Br_2, it is expected that the shift of 1 044 or 629 cm^{-1} band will be larger for I_2 than for Br_2 complex. But in practice, exactly the opposite effect is observed. A possible explanation for this anamoly may be given in terms of a back-transfer of charge from the π_g-antibonding orbital of

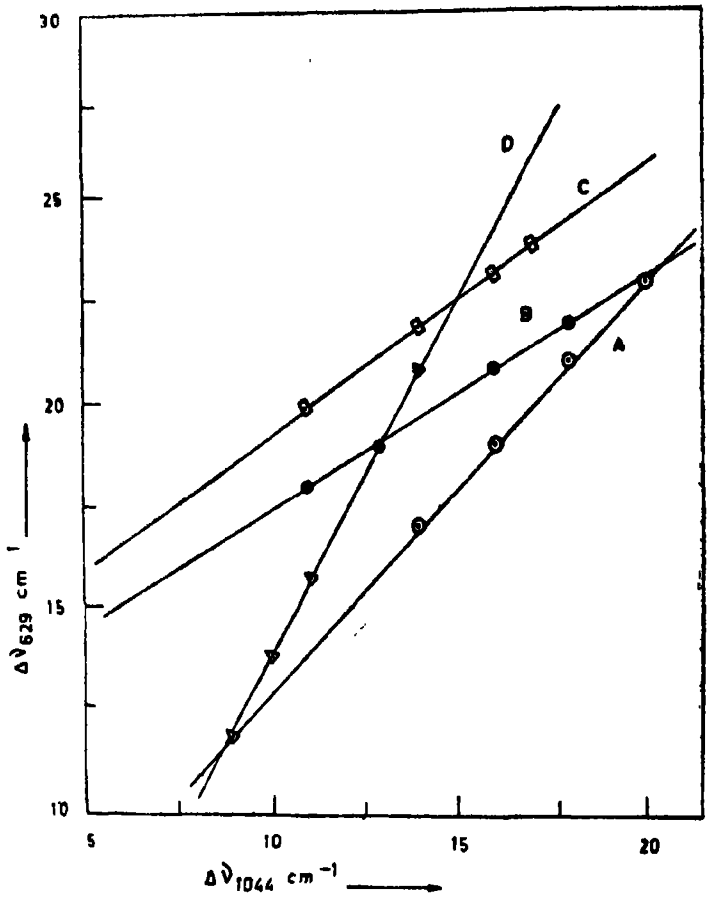


Fig. 2. Plot of $\Delta\nu_{1044}$ against $\Delta\nu_{629}$ in a variety of solvents: A(O) β-pic-ICl, B(●) β-pic-IBr, C(□) β-pic-Br_2 and D(△) β-pic-I_2.

bromine to the lowest unoccupied π-orbital of β-picoline.

Acknowledgement

The authors wish to acknowledge the Dibrugarh University for a financial grant to one of them (S. B.), and the C.S I.R.O., Australia and C.D R.I., Lucknow, for elemental analysis.

References

1. R. S. MULLIKAN and W. B. PERSON, "Molecular Complexes. A Lecture and Reprint Volume", Wiley-Interscience, New York, 1969.
2. R. FOSTER, "Organic Charge-Transfer Complexes", Academic Press, London 1969.
3. W. B. PERSON, C. F. COOK and H. B. FRIEDRICH, *J. Cnem. Phys.*, 1967, 46, 2521.
4. H. YADA, J. TANAKA and S. NAGAKURA, *J. Mol. Spectrosc.*, 1962, 9, 461.
5. I. HAQUE and J. L. WOOD, *Spectrochim. Acta. Part A*, 1967, 23, 959.
6. J. W. ANTHONSEN, *Spectrochim. Actā, Part A*, 1976, 32, 963.
7. D. L. GLUSKER and H. W. THOMSON, *J. Chem. Soc.*, 1955, 471.
8. R. F. LAKE and H. W. THOMSON, *Proc. R. Soc., London, Ser. A*, 1967, 297, 440; J. YARWOOD and W. B. PERSON, *J. Am. Chem. Soc.*, 1968, 3930.
9. J. CORNOG and R. A. KARGES, *Inorg. Synth.*, 1939, 1, 165.
10. J. P. SAXENA and M. R. GELARA, *Indian. J. Chem.*, 1968, 6, 562.
11. S. K. BAROOAH, Ph. D. Thesis, Dibrugarh University, 1981.
12. I. HAQUE and J. L. WOOD, *Spectrochim. Acta, Part A*, 1967, 23, 2523.
13. G. A. BOWMAKER and F. S. HANNA, *Aust. J. Chem.*, 1971, 24, 2239.
14. S. CORTER, N. A. B. GRAY and J. L. WOOD, *J. Mol. Struct.*, 1971, 7, 481.
15. B. R. PANDEY and R. S. TRIPATHI, *Indian J. Pure. Appl. Phys.*, 1971, 9, 346.
16. E. SPINNER, *J. Chem. Soc.*, 1963, 3860.
17. D. GANDOLFO and J. ZAREMBOWITCH, *Spectrochim. Acta, Part. A*, 1977, 33, 615.
18. W. GABES and D. J. STUFFENS, *Spectrochim. Acta, Part A*, 1974, 30, 1835.

J. Indian Chem. Soc.,
Vol. LXIII, May 1986, pp. 495-498

Polarographic Study of Cinchomeronic Acid in various Aquo-organic Mixtures

P. YADAGIRI SWAMY, G. VEERABHADRAM and K. S. SASTRY*

Department of Chemistry, University College of Science, Osmania University, Hyderabad-500 007

Manuscript received 30 April 1985, revised 4 March 1986, accepted 2 April 1986

The polarographic reduction of cinchomeronic acid has been studied in 1 : 1 aquo-organic mixtures of various organic solvents of methanol, ethanol, n-propanol, dioxane, dimethyl formamide, dimethyl sulphoxide and ethylene glycol in buffered and unbuffered solutions. The limiting current is found to decrease, while the half-wave potential is found to shift to more negative values in the presence of organic solvent. Similar behaviour is also observed with the increase in the percentage of ethanol. The limiting current is diffusion-controlled and the reduction process is found to be irreversible. The kinetic parameters have been deduced using Meites-Israel method.

THE electrochemical reduction of pyridine carboxylic acids[1-4] was a subject of many investigations. The polarographic reduction of pyridine dicarboxylic acids was attempted by Tissier and Agoutin[5]. They studied the variations of diffusion current and half-wave potential with *p*H, and deduced the values for the three equilibrium constants of cinchomeronic acid. Campanella and Chiacchierini[6] made polarographic studies of dipicolinic acid, and interpreted the data on the basis of equilibria among the six species in which the acid could exist in aqueous solution. Brown *et al.*[7] investigated the electrochemical reduction of picolinic and dipicolinic acids and their aldehydes at a mercury pool cathode to hydroxymethylpyridines.

In the present work, the polarographic study of cinchomeronic acid has been conducted in various aquo-organic mixtures to understand the effect of medium on the diffusion current, half-wave potential and kinetics. Aquo-organic mixtures of (1 : 1) methanol, ethanol, n-propanol, dioxane, dimethyl formamide, dimethyl sulphoxide and ethylene glycol and various percentages of ethanol with water in buffered and unbuffered solutions were used for this purpose.

Experimental

Cinchomeronic acid was obtained from SIGMA (U.S.A.). All the chemicals used were of A.R. grade. The organic solvents were used after necessary purifications as given in literature[8-10]. The concentration of cinchomeronic acid was 1m*M*. The buffer solution of *p*H 1.34 was obtained by mixing hydrochloric acid and sodium acetate. The buffer solution of *p*H 3.01 was obtained for Britton-Robinson[11] modified universal buffer solutions. Potassium chloride was used as a supporting electrolyte. The *p*H values of the solutions were checked with a Elico LI-120 digital *p*H meter. Triton-x-100 (5×10^{-4}%) was used as a maximum suppressor. The polarograph was a CLO ?A manual polarograph with Toshniwal a PL50 polyflex galvanometer. The viscocity of the solution was measured with an Ostwald's viscometer, and the values obtained are comparable with the reported values.

Purified nitrogen gas was passed through the solution to flush out O_2 before each polarogram was taken. The capillary delivered 2.835 mg of mercury per sec at a corrected mercury column height of 17.08 cm. The drop time was 3.8 sec (in distilled water, open circuit). The potentials were measured against a saturated calomel electrode (SCE). The measurements were made at a constant temperature of 30±0.1° maintained with a thermostat.

Results and Discussion

The polarographic behaviour of 1m*M* of cinchomeronic acid in the presence of 1 : 1 aquo-organic mixtures of various organic solvents, *viz.* methanol, ethanol, n-propanol, dioxane, dimethyl formamide, dimethyl sulphoxide and ethylene glycol has been studied both in buffered and unbuffered solutions (at *p*H 1.34 and 3.01). In all these cases a single well defined cathodic wave is obtained. The limiting current is found to decrease with the increase in

*p*H of buffer solution, while the half-wave potential shifted to more negative values. This indicates that the electrode reaction is governed by the rate of proton transfer[13], which becomes slower at higher *p*H values. A shift of the half-wave potential towards more negative value indicates that the electrodic reaction is increasingly difficult at higher *p*H values. The polarograms of cinchomeronic acid in the presence of various organic solvents at *p*H 1.34 are shown in Fig. 1.

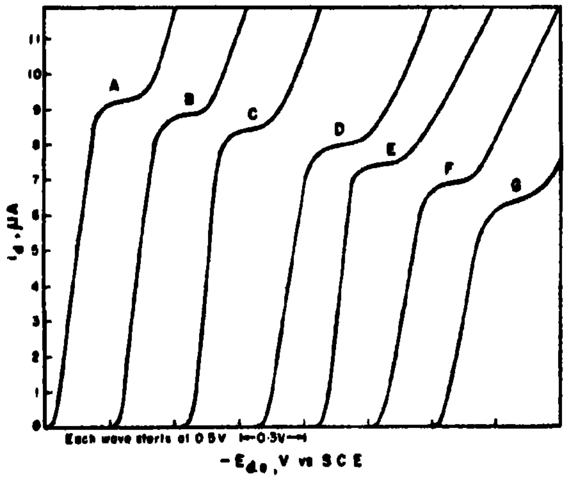


Fig. 1. Polarograms of cinchomeronic acid at a *p*H of 1.34 in aquoorganic mixtures of various organic solvents: (A) methanol; (B) dioxane; (C) ethanol; (D) dimethyl formamide; (E) n-propanol; (F) dimethyl sulphoxide; (G) ethylene glycol.

There is a marked decrease in the value of diffusion current with the addition of the organic solvent, and the extent of decrease depends on the nature of the organic solvent. This decrease in the diffusion current may be attributed to the increase in the viscosity of the solution. The $i_d\ \eta^{1/2}$ values are given in Table 1. The half-wave potential is shifted to more negative value in the presence of organic solvents (Table 1). The diffusion-controlled nature of the polarographic wave is evident from the linearity of i_d *vs* $h^{1/2}$ plots. The conventional log plots, *i.e.* $-E_{d.e}$ *vs* log $i/(i_d-i)$ are straight lines but their slopes are more than the theoretically expected values for a reversible wave. This indicates the irreversible nature of the electrodic reaction.

The $k^{\circ}_{f,h}$ (formal heterogeneous rate constant) values are calculated using the method of Meites and Israel[18] and are shown in Table 1. The diffusion coefficient value necessary for the calculation of $k^{\circ}_{f,h}$ is deduced by the procedure given in the literature[15]. The values of $k^{\circ}_{f,h}$ are found to decrease in the presence of organic solvents and with the increase in the chain length of the alcohol. The deduced αn_a (α—transfer coefficient, n_a = number of electrons involved in the rate determining step) values are shown in Table 1, which are comparable to the values deduced in the absence of organic solvents. This shows that the mechanism of electrochemical reaction is similar even in the presence of organic solvents, although a marked shift in diffusion current and $E_{1/2}$ is observed.

TABLE 1—EFFECT OF VARIOUS AQUOORGANIC MIXTURES (1 : 1) ON THE POLAROGRAPHIC WAVE OF 1 m*M* OF CINCHOMERONIC ACID

Solvent	i_d μA	$-E_{1/2}$ V	$i_d\ \eta^{1/2}$	r A	αn	$k^{\circ}_{f,h}$ cm s^{-1}
			*p*H = 1.34			
Water	11.98	0.647	10.66	10.92	1.161	1.56×10^{-11}
Methanol	9.24	0.643	10.70	10.91	1.096	3.83×10^{-11}
Ethanol	8.43	0.646	11.71	9.12	1.093	2.91×10^{-11}
n-Propanol	7.49	0.657	10.94	10.40	1.078	2.16×10^{-11}
Dioxane	8.80	0.635	11.50	9.45	1.154	1.94×10^{-11}
Dimethyl formamide	7.99	0.728	11.35	9.69	1.162	0.26×10^{-11}
Dimethyl sulphoxide	6.99	0.651	11.25	9.84	1.085	2.30×10^{-11}
Ethylene glycol	6.50	0.640	10.79	10.73	1.072	4.32×10^{-11}
			*p*H = 3.01			
Water	10.64	0.812	9.52	13.82	1.020	9.98×10^{-14}
Methanol	8.24	0.842	9.56	13.72	0.993	9.73×10^{-14}
Ethanol	7.49	0.850	10.41	11.68	0.977	8.71×10^{-14}
n-Propanol	6.61	0.863	9.65	13.45	0.956	8.22×10^{-14}
Dioxane	7.86	0.840	10.30	11.86	1.001	7.95×10^{-14}
Dimethyl formamide	7.05	0.908	10.01	12.52	0.962	1.39×10^{-14}
Dimethyl sulphoxide	6.18	0.882	9.95	12.65	0.935	6.21×10^{-14}
Ethylene glycol	5.75	0.844	9.43	13.76	0.940	7.84×10^{-14}
			Unbuffered media			
Water	8.34	0.836	7.68	24.08	1.121	1.92×10^{-14}
Methanol	6.37	0.830	7.39	23.08	1.098	1.66×10^{-14}
Ethanol	5.49	0.835	7.63	21.56	1.078	1.52×10^{-14}
n-Propanol	4.74	0.843	6.87	26.01	1.062	1.47×10^{-14}
Dioxane	5.92	0.818	7.76	20.98	1.113	1.46×10^{-14}
Dimethyl formamide	5.12	0.871	7.27	23.62	1.057	0.56×10^{-14}
Dimethyl sulphoxide	4.24	0.827	6.83	26.72	1.046	3.72×10^{-14}
Ethylene glycol	3.74	0.829	6.21	32.51	1.035	4.23×10^{-14}

The effect of change of concentration of ethanol on the polarographic reduction of cinchomeronic acid has been studied at *p*H 3.01. Various percentages of ethanol with water have been used for this purpose. The limiting current is found to decrease with increase in the alcohol content of the medium as shown in Fig. 2 without the actual process being altered essentially. This decrease

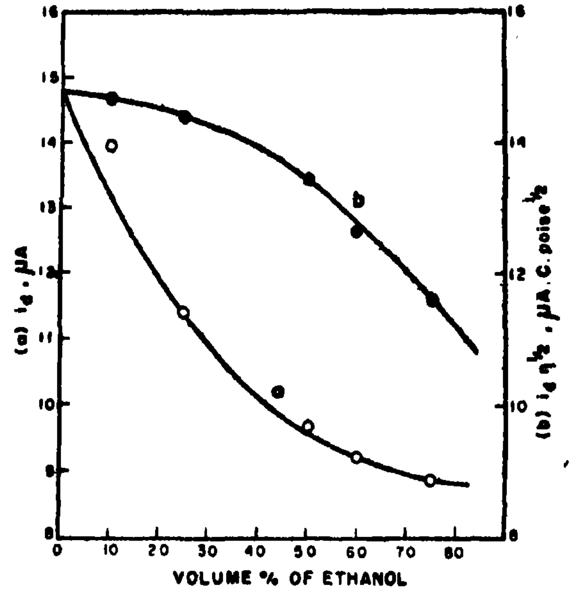


Fig. 2. Plots of (a) i_d and (b) $i_d\,\eta^{\frac{1}{2}}$ volume percentage of ethanol for the polarographic reduction of cinchomeronic acid at *p*H 3.01.

may be attributed to the decrease in the effective diffusion coefficient which may result either from an increase in the viscosity of the solution or a change in the size of the solvated species[14]. Since in different cases these two effects may tend either to reinforce or compensate each other, a quantitative estimation of the individual influences may be difficult.

The plots of $i_d\eta^{1/2}$ ethanol concentration are shown in Fig. 2. The increase in the volume of the reducible species is most probably due to a higher tendency of these species to be solvated by the ethanol molecules than water[15]. The change in current should accordingly be the resultant effect of the increase in viscosity and the molecular volume which in turn lowers the diffusion coefficient. The equations of Ilkovic[16] and Stokes–Einstein[17] can be used to order to get the following form[15].

$$i_d = 708\,n\,cm^{2/3}t^{1/6}\left(\frac{3.38 \times 10^{-8}}{(4/3\,\pi r^3 N)}\,1/3\,\eta\right)^{1/2} \quad (1)$$

where, i_d = diffusion current (μA), n = number of electrons involved in the reduction process, c = concentration of the depolariser (m*M*), r = radius of the diffusing particle (cm), m = flow rate (mg s^{-1}), N = Avagadro number. Equation (1) can be simplified as

$$r = k^3 / i_d^2\eta, \quad (2)$$

where, $k = (3.53\,n\,cm^{2/3}\,t^{1/6})\,10^{-4}$. The data of Table 2 show that the radius of the reduced species increases with increase in the ethanol content of the medium.

TABLE 2—EFFECT OF ETHANOL CONCENTRATION ON THE POLAROGRAPHIC WAVE OF 1 m*M* OF CINCHOMERONIC ACID

Ethanol %	i_d μA	$-E_{1/2}$ V	$i_d\,\eta^{1/2}$	r A	αn_a	$k^\circ_{f,h}$ cm s^{-1}
10	13.98	0.841	14.68	5.82	0.988	12.42
25	11.42	0.846	14.39	5.98	0.985	10.74
50	9.68	0.859	13.46	6.92	0.972	8.85
60	9.24	0.867	12.66	7.77	0.966	7.92
75	8 91	0.880	11.58	9.33	0.954	5.92

The half-wave potential is found to shift to more negative values with increase in the precentage of ethanol as shown in Table 2 and Fig. 3. This can be attributed to several factors, namely, dielectric

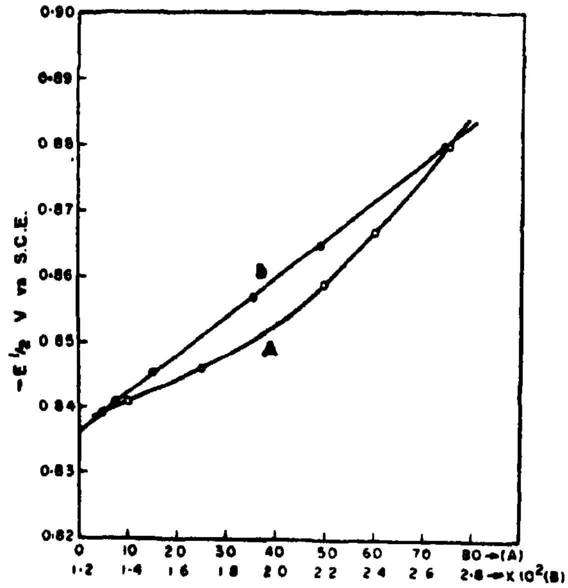


Fig. 3. Plots of $E_{\frac{1}{2}}$ *vs* (A) volume percentage of ethanol, and (B) reciprocal dielectric constant, for the polarographic reduction of cinchomeronic acid at *p*H 3.01.

constant (ϵ), solvation of ions, and absorption of organic solvent at the electrode surface. The variation of $E_{1/2}$ with ϵ is given by the Takahashi relation[18],

$$E_{1/2(S)} = E_{1/2(W)} - K\left(\frac{1}{\epsilon_{(W)}} + \frac{1}{\epsilon_{(S)}}\right) \quad (3)$$

where, $E_{1/2(W)}$ and $E_{1/2(S)}$ are the half-wave potentials in aqueous and aquoorganic mixtures, respec-

tively, and K is a constant. If the dielectric constant were the dominant factor, the shift in $E_{1/2(s)}$ would be a linear function $1/\epsilon_{(s)}$. The plots of $E_{1/2(s)}$ vs $1/\epsilon_{(s)}$ are linear (Fig. 3) which shows that the dielectric constant is indeed the dominant factor fo the changes observed in the present study.

The addition of ethanol to water causes a destruction of the normal structure of water[18] which influences the hydration layer surrounding the ions, leading to a shift of $E_{1/2}$ to less negative values. However, the shift of $E_{1/2}$ to more negative values observed in the present work may also be due to the absorption of the organic solvent molecules to some extent at the electrode surface. The accumulation of solvent molecules near the electrode surface retards the adsorption of the reducible species and also blocks the reactive centres on the electrode surface. Thus, the reduction process requires higher energy and hence the $E_{1/2}$ shifts to more negative potentials.

The kinetic parameters $k^0_{f,h}$ and the n_a values are given in Table 2. $k^0_{f,h}$ values are found to decrease with increase in the concentration of ethanol, which shows the increase in irreversibility. This is further supported by the decrease in n_a values with increase in the percentage of ethanol.

Acknowledgement

The authors wish to thank Prof. T. Navaneeth Rao, In-charge, Physical Chemistry Section and Prof. M. L. N. Reddy, Head, Department of Chemistry for their keen interest. One of the authors (P. Y. S.) wishes to express his gratitude to U. G. C., New Delhi, for the award of a research fellowship.

References

1. P. C. Tompkins and C. L. A. Schmidt, *Univ. California, Pub. Physiol.*, 1944, 8, 229.
2. H. H. G. Jellinek and J. R. Urwin, *J. Phys. Chem.*, 1954, 58, 168.
3. J. Volke and V. Volkova, *Collect. Czech. Chem. Commun.*, 1955, 20, 1332.
4. H. Lund, *Acta Chem. Scand.*, 1963, 17, 972.
5. C. Tissier and Agoutin, *J. Electroanal. Chem. Interfacial Electrochem.*, 1973, 47, 499.
6. L. Campanella, E. Chiacchierini and M. Palchetti, *Rev. Roum. Chim.*, 1972, 17, 647.
7. O. R. Brown, J. A. Harrison and K. S. Sastry, *J. Electroanal. Chem.*, 1975, 58, 387.
8. A. J. Vogel, "A Text Book of Practical Organic Chemistry". 3rd. ed., Longmans, London, 1971, pp. 166, 169, 170.
9. J. E. Lind and R. M. Fuoss, *J. Phys. Chem.*, 1961, 65, 999.
10. K. Zutshi and B. Maheshwari, *J. Indian Chem. Soc.*, 1979, 56, 813.
11. H. T. S. Britton, "Hydrogen Ions", 4th. ed., Chapman & Hall, London. 1955, pp. 353, 365.
12. M. M. Ghoneim, Y. M. Temerk and K. A. Idriss, *Indian J. Chem.*, 1978, 16, 300.
13. L. Meites and Y. Israel, *J. Am. Chem. Soc.*, 1961, 83, 4903; L. Meites, "Polarographic Techniques", 2nd. ed., Interscience, New York, 1967, p. 145.
14. H. Sadek, R. M. Issa and B. H. Abdet, *Electrochim. Acta*, 1971, 16, 401.
15. M. M. Ghoneium, R. M. Issa, I. M. Issa and M. Khattab, *Indian J. Chem.*, *Sect. A*. 1977, 15, 19.
16. D. Ilkovic and J. Heyrovsky, *Collect. Czech. Chem. Commun.*, 1955. 20, 782.
17. A. Einstein, *Ann. Phys.*, 1905, 15, 549; 1906, 19, 371; *Electrochem.*, 1908, 14, 235.
18. R. Takahashi, *Talanta*, 1925, 12, 122.

J. Indian Chem. Soc.,
Vol. LXIII, May 1986, pp. 499-502

Batch Dilatometer for Measurement of Excess Volumes of Ternary Mixtures and Ternary Volume Effects in Benzene—Carbon tetrachloride—Cyclohexane Mixtures at 298.15 K

BHAJAN S. LARK*, SURJIT SINGH and SATINDER KAUR

Department of Chemistry, Guru Nanak Dev University, Amritsar-143 005

Manuscript received 13 December 1982, accepted 3 March 1986

A new batch dilatometer for measurement of excess volumes of ternary mixtures is described and used for the measurement of this property for 35 mixtures of benzene-carbon tetrachloride-cyclohexane at 298.15 K. Two summing methods for the binary contributions have been analysed and ternary volume effects have been calculated for these mixtures which show that mutual adjustments of the molecules become poorer.

A batch dilatometer for the direct determination of excess volume of ternary mixtures (V_t^E) has been designed and described. The apparatus is an extension of the batch dilatometer for binary mixtures introduced by Lark and Palta[1]. The advantage of this dilatometer is simplicity in its operation and absence of greased stoppers. The dilatometer was tested by measuring excess volumes of a number of binary mixtures consisting of benzene-cyclohexane, which agreed very well with the results already reported from these laboratories[2]. Presently the dilatometer has been used to determine V_t^E of 35 mixtures of benzene (1)-carbon tetrachloride (2)-cyclohexane (3) at 298.15 K. The results have been used to determine the ternary volume effects which may be defined as the excess volume in excess of the contributions of the compository binary mixtures. The magnitudes of ternary effects present a case study of the dilution effects caused by the addition of a component to the binary mixtures of other two components. In the system under investigation, benzene and carbon tetrachloride have specific interactions and make charge-transfer complex. The addition of cyclohexane having no specific interaction with either benzene or carbon tetrachloride is expected to cause dilution of the specific interactions. The ternary effect for a given mixture

$$\Delta V^E = V_t^E - V_{123}^E \qquad (1)$$

if any may be evaluated from equation (1), where V_t^E is the experimental value of the excess volume of a ternary mixture and V_{123}^E is the corresponding value obtained by the summation of the three compository binary contributions. Two such summing up procedures have been reported in literature.

First method is due to Nissema[3] in which the sum of the binary contributions V_{123}^E is given by

$$V_{123}^E\ (a) = \sum_{i=1}^{3} x_i V_i^E \qquad (2)$$

where, V_i^E is the partial molar excess volume of the i-th. component in the ternary mixture which is obtained from the partial molar excess volumes of component i in the (i, j) and (i, k) binary mixtures; j and k are components next and previous to i, in the cyclic order of 1, 2, 3 (*i.e.* j, k = 1, 2, 3 but $k \neq j \neq i$) and are obtained from equation (3),

$$V_i^E = \frac{x_j}{x_j + x_k} (V_i^E)_{ij} + \frac{x_k}{x_k + x_j} (V_i^E)_{ik} \qquad (3)$$

where, $(V_i^E)_{ij}$ is the partial molar excess volume of i-th. component in (i, j) binary mixture at mole fraction $x_i/(x_i+x_j)$ of the i-th. component. The contribution V_i^E is obtained by differentiating equation (4) representing the binary data,

$$V_{ij}^E = x_i x_j [A_{ij} + B_{ij}(x_i - x_j) + C_{ij}(x_i - x_j)^2] \qquad (4)$$

where, A, B and C are constants determined by least-square fitting of the experimentally determined binary V^E data.

The second method has been reported by Rastogi[4] which evaluates the binary contributions

by the expression,

$$V^E_{123}(b)=\tfrac{1}{2}[(x_1+x_2)V^E_{12}+(x_2+x_3)V^E_{23}+(x_3+x_1)V^E_{31}] \quad (5)$$

where, V^E_{ij} is the excess volume of the compository binary mixture (i, j) at the mole fraction $x_i/(x_i+x_j)$ of the i-th. component in the binary mixture.

The results of the two procedures may be compared by assuming the three compository binary mixtures (1, 2) (2, 3) and (3, 1) obeying the following equations,

$$V^E_{12}=x_1x_2[A_{12}+B_{12}(x_1-x_2)+\dots] \quad (6)$$

$$V^E_{23}=x_2x_3[A_{23}+B_{23}(x_2-x_3)+\dots] \quad (7)$$

$$V^E_{31}=x_3x_1[A_{31}+B_{31}(x_3-x_1)+\dots] \quad (8)$$

One mole of an equimolar (1, 2, 3) ternary mixture statistically contains 1/3 mole of each of compository (1, 2), (2, 3) and (3, 1) equimolar binary mixtures, and the excess volume per mole of an equimolar binary mixture (i, j) is given by

$$V^E_{ij}=\tfrac{1}{4}A_{ij} \quad (9)$$

consequently V^E_{123}, in terms of the binary contributions should be given as

$$V^E_{123}=\tfrac{1}{3}(\tfrac{1}{4}A_{12})+\tfrac{1}{3}(\tfrac{1}{4}A_{23})+\tfrac{1}{3}(\tfrac{1}{4}A_{31})=\tfrac{1}{12}(A_{12}+A_{23}+A_{31}) \quad (10)$$

For an equimolar ternary mixture, both equations (2) and (5) predict the expected sum, but when any of the components is absent, equation (2) predicts correct excess volume of the then left over binary mixture, but equation (5) predicts half the required value, *viz.* putting $x_3=0$ and $x_1=x_2=0.5$, equation (5) gives,

$$V^E_{12}(b)=\tfrac{1}{2}(0.5+0.5)V^E_{12} \quad (11)$$

Consequently the ternary effect, as defined by equation (12),

$$V^E(a \text{ or } b)=V^E_t-V^i_{123}(a \text{ or } b) \quad (12)$$

will be different except for equimolar ternary mixture, when equation (5) is used for summing up the binary contributions. The differences will be the largest at extremal conditions. This is shown to be true for the data discussed later in the paper.

Experimental

The three solvents used were of A R. grade and were further purified by the methods described elsewhere[7]. The purity of the compounds was checked by determining their refractive indices and densities, which agreed well with the literature values. The solvents were thoroughly degassed before use. The newly designed dilatometer is illustrated in Fig. 1. Two limbs A and B (capacity 3-4 ml) hold two liquids, and are connected to each other through a tube T, containing mercury (M) which keeps the components apart and unmixed. These limbs have ground glass discs D and D′ with pin holes in their centre. After filling, these can be sealed with teflon caps E and E_1 and metal discs F and F_1, and clamped. The third component is filled in the bulb C, which is fused in the middle of

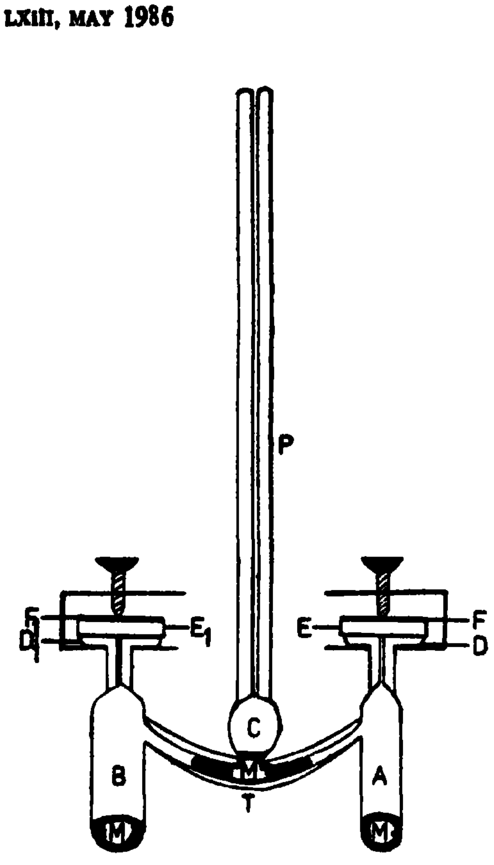


Fig. 1. The dilatometer.

the connecting tube T and carries a capillary P of uniform bore (vol/cm = 0.00578 cm^3). The filling of the dilatometer and other details are the same as described for the earlier reported dilatometer for binary mixtures. The measurements were carried out at 298.15 ± 0.01 K, in a 150 lit water thermostat.

Estimation of uncertainties: The experimentally determined excess volume of a ternary mixture V^E_t has been evaluated from the various measurable quantities appearing in the equation (13),

$$V^E_t=\frac{\Delta h(w/\rho l)}{\frac{w_1}{M_1}+\frac{w_2}{M_2}+\frac{w_3}{M_3}} \quad (13)$$

where, Δh is the difference in the levels of the liquid in the capillary (Fig. 1) before and after mixing, w is the weight of the mercury thread of length l filled in the capillary during calibration, ρ its density at the temperature of calibration; w_1, w_2 and w_3 are the weights of the three components filled in the dilatometer, and M_1, M_2 and M_3 are the corresponding molecular weights. The equation derived for the uncertainty in V^E, caused by the uncertainty in weights of the three components (± 0.00014 g), weight of mercury (±0.00014 g) and the length of the mercury thread (± 0.0014 cm)

is as follows,

$$dV^E = \left[\left(\frac{d\Delta hw/\rho l}{A}\right)^2+\left(\frac{\Delta h/\rho l dw}{A}\right)^2 + \left(\frac{\Delta h(w/\rho l^2)dl}{A}\right)^2 \sum_{i=1}^{3}\left(\frac{B}{A^2}\ \frac{dwi}{M_1}\right)^2+C^2\right]^{\frac{1}{2}}$$

where,
$$A = \sum_{i=1}^{3} \frac{w_i}{M_i}$$
$$B = \Delta hw/\rho l$$

where, C is the uncertainty caused due to temperature variation of ±0.01 K, determined by finding the shift of the level in the capillary for 0.1° rise of temperature at a mean value of 298.15 K. The overall uncertainty for representative mixtures comes out to be ±0.003 $cm^3\ mol^{-1}$.

Results and Discussion

The experimental excess volumes of ternary mixtures at 298.15 K, as a function of x_1 and x_2 are summarised in Table 1. The V^E data for the compository binary mixtures as represented by equations (15-17) were taken from literature[1,6,8].

TABLE 1—TERNARY EXCESS VOLUME (V^E) AND TERNARY EFFECTS (V^E) FOR BENZENE (1) – CARBONTE TRACHLORIDE (2) – CYCLOHEXANE (3) MIXTURES AT 298.15 K

x_1	x_2	V^E_t	$\Delta V^E(a)$	$\Delta V^E(b)$	ΔV^E (Eqn. 18)	$\delta V^E \times 10^3$
		cm³ mol⁻¹				
0.0551	0.6641	0.164	0.014	0.036	0.013	1
0.0564	0.5958	0.186	0.013	0.047	0.015	−2
0.0584	0.6495	0.165	0.010	0.032	0.014	−4
0.0660	0.2674	0.232	0.013	0.086	0.017	−4
0.0718	0.1982	0.236	0.015	0.095	0.015	0
0.0757	0.5407	0.213	0.023	0.053	0.021	2
0.0812	0.1207	0.235	0.011	0.100	0.012	−1
0.0828	0.5959	0.195	0.024	0.037	0.021	3
0.0943	0.5294	0.219	0.026	0.044	0.026	0
0.1982	0.0585	0.415	0.016	0.188	0.015	1
0.2069	0.0595	0.427	0.018	0.193	0.016	2
0.2078	0.0660	0.422	0.015	0.186	0.017	−2
0.2120	0.0688	0.432	0.021	0.193	0.018	3
0.2146	0.7108	0.082	0.016	−0.014	0.017	−1
0.2380	0.7131	0.067	0.016	−0.003	0.013	3
0.2396	0.7173	0.055	0.009	−0.008	0.011	−2
0.2402	0.6915	0.086	0.021	−0.005	0.017	4
0.4023	0.5279	0.115	0.031	0.017	0.017	4
0.4192	0.0722	0.569	0.031	0.248	0.031	0
0.4266	0.4944	0.125	0.029	0.016	0.031	−2
0.4491	0.4614	0.144	0.035	0.023	0.036	−1
0.5630	0.3081	0.223	0.048	0.059	0.047	0
0.6331	0.0750	0.484	0.033	0.209	0.032	1
0.6705	0.1982	0.245	0.035	0.080	0.041	−6
0.6874	0.2753	0.082	0.013	0.026	0.017	−4
0.6880	0.2516	0.133	0.027	0.046	0.025	2
0.6995	0.2793	0.051	0.009	0.017	0.010	−1
0.7044	0.2596	0.080	0.012	0.025	0.016	−4
0.7403	0.2144	0.100	0.014	0 033	0.018	−4
0.7521	0.0989	0.299	0.030	0.122	0.028	2
0.7694	0.0476	0.368	0.023	0.169	0.017	6
0.7823	0.0454	0.352	0.021	0.162	0.016	5
0.7861	0.0519	0.333	0.022	0.151	0.017	5
0.7933	0.1618	0.101	0.011	0.035	0.015	−4
0.8111	0.0644	0.263	0.018	0.113	0.017	1

$$V^E_{12}=x_1x_2[0.021468-0.024701(x_1-x_2)+0.02637(x_1-x_2)^2] \quad (15)$$

$$V^E_{23}=x_2x_3[0.65809-0.00659(x_2-x_3)+0.0279(x_2-x_3)^2] \quad (16)$$

$$V^E_{31}=x_3x_1[2.5887-0.1195(x_3-x_1)+0.0044(x_3-x_1)^2] \quad (17)$$

The ternary effects $\Delta V^E(a)$ and $\Delta V^E(b)$ as defined by equation (12) were calculated, and have been included in Table 1 (columns 4 and 5). $\Delta V^E(a)$ values which represent the real ternary effects have been fitted by the method of least-squares to the equation,

$$\Delta V^E(a)=x_1x_2x_3[1.800+1.102(x_1-x_2)+0.358(x_2-x_3)] \quad (18)$$

The deviations of the $\Delta V^E(a)$'s from the recalculated values have been included in Table 1 (column 7). These deviations have standard mean value of ±0.003 $cm^3\ mol^{-1}$ which is of the order of estimated uncertainties in ternary volumes. The ternary effects are much larger than the individual deviations from the recalculated values and are thus much significant.

From the comparison of data in columns 4 and 5 (Table 1) it is found that ΔV^E values as predicted by equation (2) are all positive, whereas equation (5) predicts some negative values too. This may be ascribed to the failure of equation (5) to yield correct summation of binary contributions which is expected to give large deviations near extremal concentrations (small concentration of one of the components). Also, the positive $\Delta V^E(b)$ values are sometimes 10 times as large as $\Delta V^E(a)$ values. The real ternary effects $\Delta V^E(a)$ vary from 5 to 25% of the corresponding V^E_t values. As all the ΔV^E values are positive, the mutual interactions of any compository binary mixture are weakened by the presence of the third component. To understand the mutual dilution effects in different mixtures

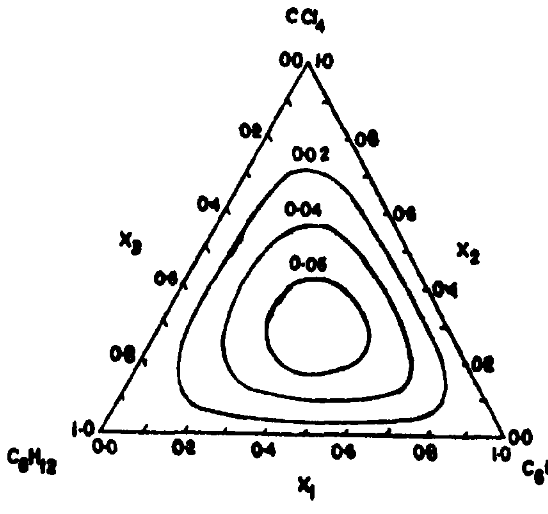


Fig. 2. Ternary effect $\Delta V^E(a)$ ($cm^3\ mol^{-1}$) as a function of composition; $\Delta V^E(a)$ values shown on the contours.

equivolume contours have been drawn on an equilateral triangle (Fig. 2). The three sides of the triangle represent three mole fractions. Such contours for selected values of $\Delta V^E(a)$ and x_1 were obtained through solution of equation (18) using numerical methods. It is apparent from Fig. 2 that $\Delta V^E(a)$ is maximum for mole fractions 0.40, 0.29 and 0.31 of the respective 1, 2, 3 components. When to such a mixture any one of the three components is added, the ternary effect is reduced.

The positive ternary effect, no doubt, is indicative of the reduced mutual interactions of the ternary mixtures, but this does not indicate the approach to ideal behaviour, as the condition of zero excess volume is disobeyed more and more. It may be said that in the present system studied, the mutual geometrical adjustments between the three kinds of molecules become poorer. V_t^E for eight such mixtures at 303.15 K have also been reported earlier[6]. These values when compared with the corresponding V_t^E values at 298.15 K from the present data are found to be consistently slightly higher, the $\Delta V_t^E(a)$ values calculated for these eight mixtures showed that these vary from about 15 to 30% of the corresponding V_t^E values.

References

1. R. C. Palta and B. S. Lark, *J. Indian Chem. Soc.*, 1979, 56, 322.
2. M. Karvo and A. Nissem, *Finn. Chem. Lett.*, 1979, 132; A. Nissema, *Ann. Acad. Sci. Fenn., Ser. A2*, 1970, 153.
3. R. P. Rastogi, *J. Sci. Ind. Res.*, 1980 39, 480.
4. O. Kiyohara and G. C. Benson, *J. Chem. Thermodyn.*, 1977, 9, 807.
5. G. A. Bottomley and R. L. Scott, *J. Chem. Thermodyn*, 1974, 6, 973.
6. R. P. Rastogi, J. Nath and M. L. Yadava, *J. Chem. Thermodyn.*, 1974, 6, 1197.
7. J. A. Riddick and E. E. Toops, Jr., "Organic Solvents: Physical Properties and Methods of Purification", Wiley-Interscience, New York, 1967, Vol. VIII.

J. Indian Chem. Soc.,
Vol. LXIII, May 1986, pp. 503-506

Theoretical Study of Azaheterocyclic Systems : Azafluoranthenes

SUKANTA KUMAR PAL and N. K. DAS GUPTA*

Chemistry Department, Visva-Bharati, Santiniketan-731 235

Manuscript received 27 June 1985, accepted 2 April 1986

The molecules azafluoranthenes have been studied using SCFMO method of Pariser and Parr and Pople modified by Dewar and Harget. The ground state and other properties have been predicted and compared with experimental results where available. The $\pi^* \leftarrow \pi$ spectra for 1-aza- and 3-aza-fluoranthene predicted by the CI method are in good agreement with experimental results and better than those of Michl.

IN the study of nonbenzenoid hydrocarbons, fluoranthene molecule plays an important role and it has been studied theoretically by many authors[1,2]. In this paper, we report the results of our calculation on azafluoranthenes (Fig. 1) using P-P-P method, predicting the ground state and other properties and correlate them with experimental results where available. The aim of this paper is also to see how far the properties of azafluoranthenes have been changed from fluoranthene due to substitution of =CH– group in fluoranthene molecule by =N– .

Method and parameter :

The method is well known and has been described elsewhere[3]. The procedure is the self-consistent field approach due to Pariser and Parr[4] and Pople[5] modified by Dewar and Harget[6,7] within the zero-differential overlap approximation and using semi-empirical evaluation of integrals.

The resonance integrals (β_{ij}), the bond length (r_{ij}) and the two-centre two-electron repulsion integrals (γ_{ij}), for bonded atoms were adjusted at each interaction according to the relation,

$$r_{ij}\ (\text{Å}) = a - bp_{ij} \qquad (1)$$

$$\text{and } \beta_{ij} = -K_{ij} S_{ij}^{AB} \qquad (2)$$

where, p_{ij} is the π-bond order, S_{ij} overlap integral between 2 p_π Slater type orbitals at centres i and j for nuclei type A and B. The values of parameters a, b and K are given in Table 1. For non-bonded atoms, β_{ij} is set equal to zero.

TABLE 1—VALUES OF PARAMETERS

Bond	K	a/A	b/A	Atoms	I_i eV	γ_{ii} eV
C–C	6.927	1.512	0.174	C	11.16	11.134
C–N	6.9612	1.448	0.178	N	14.12	12.341

The two-centre two-electron repulsion integrals (γ_{ij}) were evaluated from Ohno's formula[8]. One centre-two electron repulsion integrals γ_{ii} were calculated using the relation of Pariser[9],

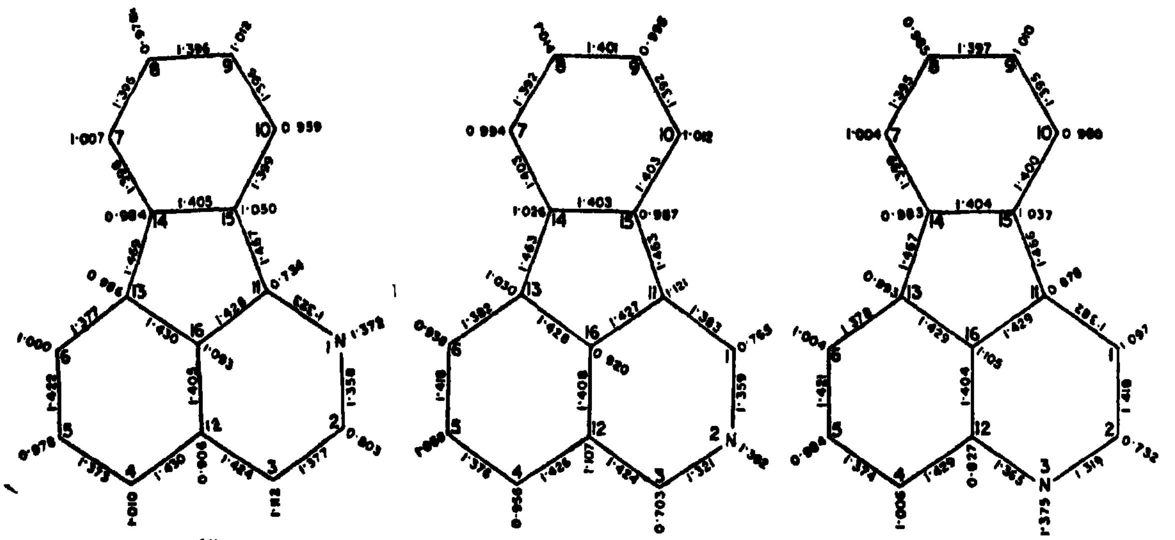
$$\gamma_{ii} = I_i - A_i \qquad (3)$$

where, I and A represent the valence state inonisation potential and electron affinity of atoms concerned, respectively. The values of I and A are taken from the work of Hinze Jaffe[10]. Table 1 also contains the values of I_i and A_i.

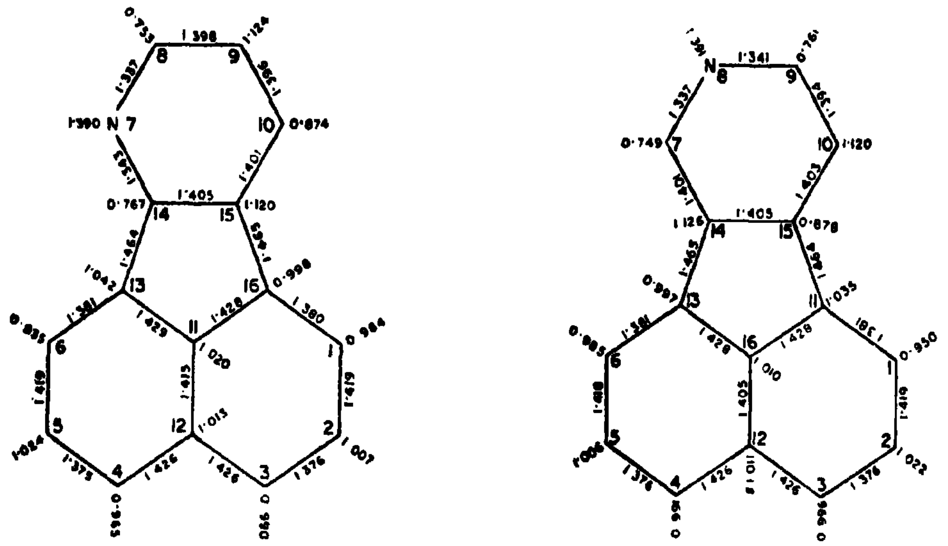
γ_{ij} for non-bonded centre were kept at the values calculated from the initial and ideal geometry of the molecules assumed to be planar with bond lengths equal to 1.40 Å.

Results and Discussion

$\pi^* \leftarrow \pi$ Spectra, ionisation potential, electron affinity and π-dipole moment : $\pi^* \leftarrow \pi$ Spectra have been studied for these molecules using both SCF and configuration interaction, CI, methods. In the CI method, instead of using Ohno's formula for evaluation of two-centre two-electron repulsion integrals the formula of Mataga and Nishimoto[11] was used. Because in the context of configuration interaction, the use of the formula of Mataga and Nishimoto for γ_{ij} is more effective in predicting the



(1) (2) (3)



(4) (5)

Fig. 1. Azafluoranthene : (1) 1-aza and (2) 2-aza, (3) 3-aza, (4) 7-aza and (5) 8-aza.

$\pi^* \leftarrow \pi$ spectra for a large number of compounds[9,18]. The values of K for β_{C-C} used in the CI procedure was changed from 6.927 to 9.1846 eV (Ref. 12), and for β_{C-N} it is 6.9612 eV, same as used in the SCF procedure. With this modification we utilised the SCF procedure to generate the initial vectors, β-integrals and γ-integrals to be used in the CI procedure where all the configurations arising from one-electron excitations involving orbitals obtained in a prior self-consistent field calculation. The calculated $\pi^* \leftarrow \pi$ spectral transitions for these molecules have been presented in Table 2 along with the oscillator strength (f), which was obtained from the relation[18],

$$f = 1.085 \times 10^{-5} \bar{\nu} \mu^2 \quad (4)$$

where, $\bar{\nu}$ is the transition energy in cm^{-1} and μ is the dipole length for the corresponding transition in Å. The experimental values are presently available only for 1-aza- and 3-aza-fluoranthenes and they have been included in Table 2. On comparison, it is clear that the present work is in good agreement with the experimental ones, specially the results obtained by CI method which is better than the work of Michl[14] who also used limited configuration interaction.

According to Koopmans' theorem[15], the ionisation potential (IP) can be approximated by the highest occupied orbital energy (e_i). But the predicted value of IP is 1 or 2 eV higher than the experimental value. In case of electron affinity (EA), it can also be approximated by the lowest unoccupied orbital energy (e_j). Here too the predicted value of EA differs from the experimental value of EA by 1 or 2 eV. Hence, a correction

TABLE 2 – $\pi^* \leftarrow \pi$ SPECTRAL TRANSITIONS, ΔE (eV) AND OSCILLATOR STRENGTH (f^a) OF AZAFLUORANTHENES (AzaF)

Molecule	Experimental transitions[c]		Present work: CI method		Present work: SCF method		Other work[b]	
	ΔE	log ε	ΔE	f	ΔE	f	ΔE	f
1-AzaF			3.15	0.01			3.17	0.0093
	3.39	3.80	3.40	0.48	3.45	0.09	3.44	0.56
	4 03	3.05	3.92	0.04	3.68	0.70	4.16	0.013
	4.42	4.05	4.33	0.15	4.51	0.62	4.41	0.15
	4.88	3.95	4.98	0.06	4.80	0.25	5.16	0.096
			5.18	0.65	5.12	0.38	5.32	0.37
	5.32	4.40	5.39	1.17	5.28	0.30	5.48	1.3
			(0.084)		(0.169)		(0.157)	
2-AzaF			3.39	0.04			3.38	0.44
			3.48	0.45	3.83	0.65	3.50	0.51
			3.86	0.03	3.86	0.28	4.06	0.024
			4.46	0.26	4.64	0.61	4.57	0.29
			4.88	0.26	4.88	0.57	5.08	0.06
			5.08	0.24	4.96	0.27	5.13	0.13
			5.18	0.30	5.05	0.08	5.26	0.54
			5.39	0.91	5.46	0.29	5.45	0.86
3-AzaF[b]	3.08	2.22	3.11	0.05			3.15	0.057
	3.53	3.74	3.53	0.35	3.45	0.08	3.60	0.40
	3.86	3.01	3.79	0.18	3.70	0.60	3.91	0.23
	4.40	4.38	4.42	0.20	4.12	0.82	4.51	0.25
	4.84	4.30	5.01	0.30	4.99	0.02	5.13	0.44
	5.02	4 24	5.13	0.15	5.10	0.29	5.23	0.33
	5.41	4.44	5.41	0 89	5.36	0.33	5.38	0.23
	6.04	4.56	5.89	0.77	6.03	0.42	5.68	0.78
			(0.098)		(0.142)		(0.188)	
7-AzaF			3.31	0.01			3.30	0.023
			3.63	0.39	3.82	0.43	3.73	0 45
			3.84	0.08	3.98	0.48	3.94	0.099
			4.34	0.48	4.11	0.37	4.56	0 50
			4.86	0.07	4.80	0.39	5.06	0.0013
			5.00	0.02	5.10	0.43	5.07	0.072
			5.28	0.62	5.19	0.29		
			5.41	1.23	5 61	0.02	5.48	1.3
			5.86	0.45	5.71	0.24	5.57	0.67
8-AzaF			3.31	0.10			3.34	0.17
			3.52	0.40	3.70	0.68	3.59	0.42
			3.83	0.08	3.91	0.25	3.94	0.096
			4.46	0.14	4.06	0.55	4.63	0.079
			4.96	0.13	4.81	0.53	5.10	0.20
			5.05	0.002	4.96	0 15	5 15	0 067
			5.23	0.56	5.24	0.22	5.36	0.73
			5.37	1.01	5.40	0.32	5.46	0.92
			5.78	0.62	5.84	0.24		

[a]Ref. 13. [b]Ref. 14. [c]For 1-AzaF, Ref. 17 ; and for 3-AzaF, ref. 14 and J. MICHL, *Thor. Chim Acta*, 1969, 20, 66.
Figures in Parenthesis indicate standard deviation.

term is to be added in both the cases of IP and EA in order to obtain their correct values. The following relation between ionisation potential and highest occupied orbital energy and electron affinity and lowest unoccupied orbital energy are in common use in the literature.

$$IP = -(e_i + C) \quad (5)$$

$$\text{and} \quad EA = -(e_j + D) \quad (6)$$

where, C and D are correction terms. Birss and Dasgupta[16] used a value of C to be 1.88 eV and they predicted the ionisation potential of a large number of aromatic hydrocarbons and heterocyclic systems. The value of D is 1.38 being the difference between the lowest unoccupied orbital energy and the electron affinity of chrysene. The predicted values of IP and EA are presented in Table 3 which also contains the calculated value of $E_{\frac{1}{2}}$, the half-wave reduction potential from the relation proposed by Birss and Dasgupta[16],

$$E_{\frac{1}{2}} = -0.833\, e_j - 3.46 \quad (7)$$

The theoretical π-dipolemoment calculated by us is also included in Table 3. (Experimental values are not presently available).

Heat of atomisation, bond energy and stability : 'Dewar' resonance energy (RE) has been calculated from the relation,

$$RE = \Delta H_a - \Delta H'_a \quad (8)$$

TABLE 3—HEAT OF ATOMISATION (ΔH_a), π-BOND ENERGY ($E_{\pi b}$), RESONANCE ENERGY (RE), IONISATION POTENTIAL (IP), ELECTRON AFFINITY (EA), HALF-WAVE REDUCTION POTENTIAL ($E_{1/2}$) AND π-DIPOLEMOMENT (μ)

Molecule*	ΔH_a eV	$E_{\pi b}$ eV	RE eV	RE/bond	IP eV	EA eV	$E_{1/2}$ V	μ D
1-AzaF	133.368	23.785	2.326	0.1224	7.85	0.99	1.57	1.51
2-AzaF	133.455	23.833	2.413	0.1270	7.79	0.80	1.73	1.35
3-AzaF	133.385	23.800	2.342	0.1233	8.01	1.05	1.52	1.30
7-AzaF	133.419	23.818	2.376	0.1251	7.95	0.76	1.76	1.02
8-AzaF	133.430	23.825	2.387	0.1256	7.81	0.92	1.63	1.62

*AzaF = Azafluoranthene.

where, ΔH_a is the heat of atomisation of the molecule and $\Delta H'_a$ is the heat of atomisation of the molecule when π-electrons are localised. In the absence of experimental value of ΔH_a, it can be estimated from the relation,

$$\Delta H_a = E_{\pi b} + E_{\sigma b} + n_{C-H} E_{C-H} \quad (9)$$

where, $E_{\pi b}$, $E_{\sigma b}$ and E_{C-H} are the π-bond energy, σ-bond energy and C—H bond energy, respectively, and n_{C-H} is the number of C—H bond. The value of $\Delta H'_a$ has been evaluated from the relation,

$$\Delta H_a = n'E_{C-C} + n''E_{C=C} + n_{C-H} E_{C-H} \quad (10)$$

where, n', n'', E_{C-C} and $E_{C=C}$ represent the number of C—C bonds, number of C=C bonds, C—C bond energy and C=C bond energy, respectively. The values of n_{C-H} and E_{C-H} are the same as in equation (9). The values of E_{C-H}, E_{C-C} and $E_{C=C}$ are taken from Dewar and Harget[6,7]. The values of ΔH_a and $E_{\pi b}$, resonance energy and resonance energy per bond (RE/bond) have been included in Table 3. From Table 3 it is clear that the resonance energy of azafluoranthenes are comparable to that of fluoranthene (2.353 eV) and it is expected that they are stable aromatic molecule which they are.

Charge density and bond length : Calculated charge density and bond length have been shown in Fig. 1. For 1-aza-, 2-aza- and 3-aza-fluoranthene, the distribution of charge density on nitrogen and *ortho*, *para* and *meta* carbon atoms resemble that of quinoline and isoquinoline[19]. For the other two molecules, the similar situation is also observed.

In case of azaheterocyclic system, the charge density on carbon atoms *meta* to nitrogen atom is higher than that on other carbon atoms. In 1-aza- and 3-aza-fluoranthene, the charge density on centres C_3 and C_1, respectively, is highest. Hence, electrophilic attack is most probable on these centres. But experimental results[17,18] show that centres C_2 is the most suitable place for electrophilic attack in both the cases and the charge density on this centre is the second highest.

Acknowledgement

The authors express their sincerest thanks to U.G.C., New Delhi, for financial support in the form of a Junior Research Fellowship to one of them (S. K. P.). Thanks are also due to Mr. Sunirmal Ghosh for some preliminary work.

References

1. A. DAS GUPTA and N. K. DAS GUPTA, *Can. J. Chem.*, 1976, **54**, 3227.
2. N. K. DAS GUPTA and F. W. BIRSS, *Bull. Chem. Soc Jpn.*, 1978, **51**, 1211, and references therein.
3. R. G. PARR, "Quantum Theory of Molecular Electronic Structure", Benjamin, New York, 1965.
4. R. PARISER and R. G. PARR, *J. Chem. Phys.*, 1953, **21**, 466, 767.
5. J. A. POPLE, *Trans. Faraday Soc.*, 1953, **49**, 1375.
6. M. J. S. DEWAR and A. J. HARGET, *Proc. Roy. Soc. London, Ser. A*, 1970, **315**, 443, 457.
7. M. J. S. DEWAR and N. TRINAJSTIC, *Theor. Chim. Acta*, 1970, **17**, 235.
8. K. OHNO, *Theor. Chim. Acta*, 1964, **2**, 219.
9. R. PARISER, *J. Chem. Phys.*, 1953, **21**, 368.
10. J. HINZE and H. H. JAFFE, *J. Am. Chem. Soc.*, 1962, **84**, 540.
11. N. MATAGA and K. NISHIMOTO, *Z. Phys. Chem.*, 1957, **13**, 140.
12. N. K. DAS GUPTA, A. DAS GUPTA and F. W. BIRSS, *Indian J. Chem., Sect. B*, 1982, **21**, 334.
13. L. SALEM, "Molecular Orbital Theory of Conjugated System", Benjamin, New York, 1966, p. 358.
14. J. MICHL, *Theor. Chim. Acta*, 1969, **15**, 315.
15. T. KOOPMANS, *Physica*, 1934, **1**, 104.
16. F. W. BIRSS and N. K. DAS GUPTA, *Indian J. Chem., Sect. B*, 1979, **17**, 610.
17. N. CAMPBELL and K. F. REID, *J. Chem. Soc. London*, 1958, 4743.
18. C. F. KOELSCH and A. P. STEINHAUER, *J. Org. Chem.*, 1953, **18**, 1516.
19. J. MICHL, *Theor. Chim. Acta*, 1969, **20**, 66.

J. Indian Chem. Soc.,
Vol. LXIII, May 1986, pp. 507-509

Synthesis of *p*-Camphorene

O. P. VIG and G. L. KAD*

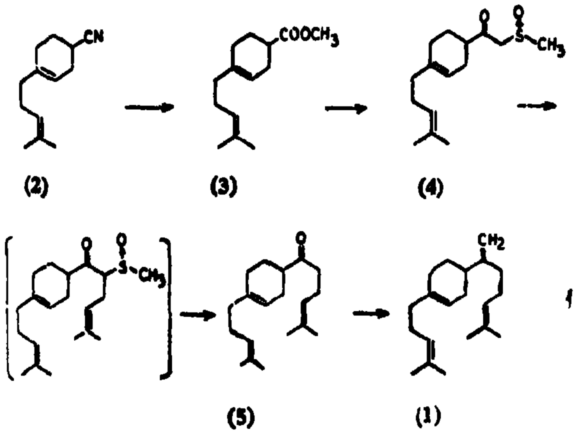
Department of Chemistry, Panjab University, Chandigarh-160 014

Manuscript received 27 April 1984, accepted 2 April 1986

p-Camphorene is synthesised by the application of Wittig reaction with methylenetriphenylphosphorane on 1(4-methyl-3-pentenyl)-4-(5-methyl-4-hexe-1-one)cyclohex-1-ene (5), the cardinal intermediate, which was procured by the formation of β-ketosulphoxide and then its subsequent alkylation with 1-bromo-3-methyl-2-butene of the compound 1 (4-mehyl-3-pentenyl)-4-carbmethoxycyclohex-1-ene (3). The alkylated material was submitted to reductive cleavage with aluminium amalgam in aqueous THF at 65° to furnish 5.

p-Camphorene, a monocyclic diterpene hydrocarbon, was first found in the higher boiling fraction of camphor oil[1]. Since then it has been isolated from a number of oils, such as volatile oil of *Dacrydium biforme*[2], Japanese tall oil[3] and oil of hops[4]. Semmler and Jonas[5] showed it to be identical with dimyrecene[6]. The characteristic structural features of this diterpene possessing structure (1) is the presence of a methylene and two isopropylidene groupings alongwith a unsubstituted double bond in the specific positions within the cyclohexane ring. Literature does not record any direct and clean synthesis of this hydrocarbon.

Here, we report a facile and unambiguous synthesis of *p*-camphorene, making use of β-ketosulphoxide as the cardinal intermediate. The sequence of reactions employed in accomplishing the synthesis is depicted in Scheme 1.



Scheme 1

The starting material, 1(4-methyl-3-pentenyl)-4-cyano-cyclohex-1-ene (2), was procured according to the procedure laid down in the literature[8]. The compound 2 on alcoholysis[9] provided 1(4-methyl-3-pentenyl)-4-carbmethoxy-cyclohex-1-ene (3) in 80% yield. The resulting ester was converted into1-(4-methyl-3-pentenyl)-4-(1-oxo-2-methylsulphinyl-ethyl)cyclohex-1-ene (4) by making use of methylsulphinylcarbanion (obtained from equimolar quantities of sodium hydride and dimethyl sulphoxide)[10].

Alkylation of the β-keto sulphoxide (4) with 1-bromo-3-methyl-2-butene in dry dimethylformamide employing sodium hydride as a base[11] resulted in the corresponding alkylation product which was not isolated. This, upon reductive cleavage with aluminium amalgam[10] in aqueous THF afforded the ketone, 1(4-methyl-3-pentenyl)-4-(5-methylhex-4-en-1-oxyl)cyclohex-1-ene (5) in 57% yield after chromatographic purification. This ketone was submitted to Wittig reaction with methylenetriphenylphosphorane according to the procedure of Corey *et al.*[12]. The resulting product was chromatographed over neutral alumina and subsequently distilled under vacuum to afford 1 in 74% yield, identified by comparison of its ir spectral data with those reported for the natural compound in the literature[4].

Experimental

Boiling points are uncorrected. Ir spectra of the films were recorded on a Perkin-Elmer infrared spectrophotometer having sodium chloride optics.

1(4-Methyl-3-pentenyl)-4-carbmethoxy-cyclohex-1-ene (3) *:* A slow stream of hydrogen chloride gas was bubbled into a mixture of the solution of 2 (10 g) in methanol (26.3 ml) and water (2 ml).

The resulting heat of solution caused the solvent to reflux. After the temperature had subsided (15 min), the reaction mixture was treated with water (4.7 ml), warmed on a steam-bath for 20 min and poured into an excess of cold water. The solution was extracted with solvent ether. The ethereal layer was washed successively with water, sodium bicarbonate solution, saturated brine solution and dried (Na_2SO_4). The solvent was expelled and the residue was distilled under vacuum to afford 1(4-methyl-3-pentenyl)-4-carbmethoxy-cyclohex-1-ene (3; 9.4 g, 80%), b.p. 130-32° / 4 mm (Found: C, 75 23; H, 9.72. $C_{14}H_{22}O_2$ requires: C. 75.67; H, 9.91%); η_D^{28} 1.4740; ν_{max} 1 745 (ester), 835 and 810 cm^{-1} (triply substituted double bond).

1(4-Methyl-3-pentenyl)-4-(1-oxo-2-metholsulphinyl-ethyl)cyclohex-1-one (4): In a three-necked flask, equipped with rubber stopper, a magnetic stirrer and a three-way stop cock, sodium hydride (3.9 g, 50%) was washed with n-hexane to remove the mineral oil. After replacing the air in the apparatus by nitrogen, DMSO (40 ml) was added *via* syringe. The reaction mixture was heated at 75-80° until the evolution of hydrogen ceased (30 min). To methylsulphinyl carbanion thus formed, was added an equal volume of dry THF (40 ml) and the contents were cooled in ice-bath, followed by dropwise addition with strring of the ester (3; 9.0 g) over a period of several minutes. After stirring for 1 h more at room temperature, the reaction mixture was poured into cold water (200 ml), acidified at lower temperature with calculated quantity of hydrochloric acid (10.5 ml) and thoroughly extracted with chloroform. The organic extract was washed with water and dried (anhydrous $CaCl_2$). Solvent evaporation, followed by vacuum distillation afforded semi-solid β-ketosulphoxide (4; 6.0 g, 65%), b.p. 180-90°/4 mm. However, all attempts to crystallise it proved unsuccessful (Found: C, 67.32; H, 8.78; S. 11.80. $C_{15}H_{24}O_2S$ requires: C, 67.15; H, 8.95; S, 11.94%); ν_{max} 1 695 (carbonyl), 1 010-40 (sulphinyl), 825 and 780 cm^{-1} (triply substituted double bond).

1(4-Methyl-3-pentenyl)-4(5-methyl-4-hexe-1-one)-cyclohex-1-ene (5): Dry dimethylformamide (40 ml) was added to sodium hydride (0.36 g, 50%) under an atmosphere of nitrogen. The resulting slurry was cooled, stirred and the solution of 4 (4.0 g) in dry dimethylformamide (20 ml) was added to it slowly so as to keep the ensuing reaction under control. Stirring was continued at room temperature till the conversion of 4 into the anion was complete (ceasation of hydrogen evolution). At this stage, the reaction mixture was again cooled and 1-bromo-3-methyl-2-butene (2.75 g) (prepared by the addition of hydrobromic acid to isoprene) added to it dropwise. After continuing the stirring for another 30 min at room temperature, the contents were put into cold water (100 ml) and extracted with chloroform. The organic layer was washed with saturated brine solution and dried (anhydrous $CaCl_2$). The residue, left after the removal of the solvent from the dried organic phase, was placed under vacuum for 1 h to yield the alkylated β-ketosulphoxide (which was not isolated).

The above alkylated β-ketosulphoxide (4.0 g) was dissolved in aqueous tetrahydrofuran (240 ml, 10%). The solution was taken in a three-necked flask provided with a reflux condenser and a mechanical stirrer. Freshly prepared aluminium amalgam (obtained by immersing 3.3 g aluminium in 2% mercuric chloride for 15 s) was added to this well stirred solution in the form of small pieces. The contents were then refluxed at 65° for 90 min. Thereafter, the reaction mixture was filtered and the residual solid washed well with tetrahydrofuran. The combined filterate was concentrated under reduced pressure and extracted with ether. The ethereal extract was washed with water, dried and the solvent expelled. The residual oil was chromatographed over alumina (50 g) with benzene-petroleum ether (1:4) as eluent and carefully fractionated under vacuum to obtain the desired ketone (5, 57% with respect to 4), b.p.140-142°/4 mm (Found: C, 82.76; H, 10.42, $C_{18}H_{30}O$ requires: C, 8.321; H, 10.95%); η_D^{28} 1.4355; tlc showed a single spot (solvent system: benzene: n-hexane; 1:1); ν_{max} 1 710 (carbonyl), 835, 815 and 795 cm^{-1} (triply substitued double bond).

p-*Camphorene* (1): Sodium hydride (0.48 g, 50%) was washed with n-hexane to remove the mineral oil and freshly distilled dimethyl sulphoxide (6 ml) was added to it under nitrogen atmosphere. The contents were heated with stirring (75-80°) until hydrogen gas ceased to evolve (nearly 45 min). The resulting solution was cooled in an ice-water-bath and methyltriphenylphosphonium iodide (4.05 g) dissolved in dimethyl sulphoxide (12 ml) was introduced to it to furnish a dark red solution of the desired phosphorane. After stirring the above mixture at room temperature for 10 min, the ketone (5; 2.74 g) in dry tetrahydrofuran (5 ml) was added and the stirring was continued for 2 h. The reaction mixture was left overnight at room temperature and heated at 50° for 1 h with stirring. The contents were poured into cold water and extracted with petroleum ether (4×25 ml). The combined extract was washed with water and dried. The solvent having been evaporated, the residue was purified by chromatography over neutral alumina (20 g) using petroleum ether (b.p. 40-60°, 80 ml) as eluent. It was followed by distillation under reduced pressure to obtain 1 (2.0 g, 74%), b.p. 172-74°/ 5 mm (Found: C, 87.93; H, 12.07. $C_{20}H_{32}$ requires: C, 88.23; H, 11.77%); η_D^{28} 1.4894; ν_{max} 3 070, 1 650, 892 (methylene), 835, 815 (trisustituted double bond), 2 900, 1 450, 1 380, 1 120, 925 and 750 cm^{-1}.

References

1. F. W. SEMMLER and I. ROSENBURG, *Chem. Ber.*, 193, 46, 768.
2. R. E. CORBETT and L. C. K. WONG, *Chem. Abstr.*, 1956, 50, 5854.
3. S. ITO, *Chem. Abstr.*, 1959, 53, 1183.
4. H. LAMMENS and M. VERZELE, *Chem. Abstr.*, 1969, 70, 78185.
5. F. W. SEMMLER and K. G. JONAS, *Chem. Ber.*, 1913, 46, 1566.
6. C. HARRIES, *Chem. Ber.*, 1902, 35, 3264.
7. J. L. SIMONSEN, L. N. OWEN and D. H. R. BARTON, "The Terpenes", Cambridge, 1950, Vol. III, p. 334.
8. T. SASAKI, S. EGUCHI and T. ISHII, *J. Org. Chem.*, 1969, 34, 3749.
9. J. O. RODIN, M. A. LEAFER and R. M. SILVERSTEIN, *J. Org. Chem.*, 1970, 35, 3152.
10. E. J. COREY and M. CHAYKOVSKY, *J. Am. Chem. Soc.*, 1964, 86, 1639; 1965, 87, 1345.
11. P. G. GASMAN and G. D. RICHMOND, *J. Org. Chem.*, 1966, 31, 2355.
12. E. J. COREY, R. GREENWALD and M. CHAYKOVSKY, *J. Org. Chem.*, 1963, 28, 1128.

J. Indian Chem. Soc.,
Vol. LXIII, May 1986, pp. 510-511

Azatriterpenes. VI. Synthesis of 2-Eno[2,3-*g*]pyrazolo-[1,5-*a*]pyrimidines of Pentacyclic Triterpenes

K. LAXMAN RAO, T. V. P. R. SUBBA RAO and T. SUNDARA RAMAIAH*

Department of Chemistry, Nizam College, Hyderabad-500 001

and

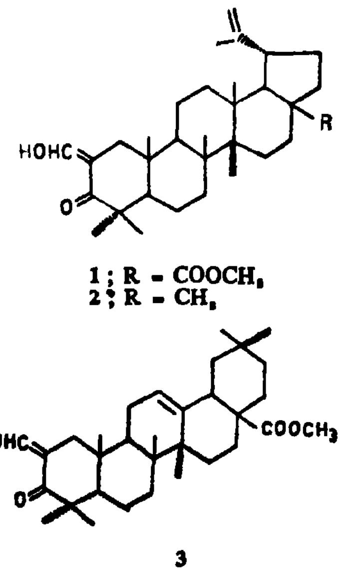
S. K. RAMRAJ

Department of Chemistry, V. V. College, Hyderabad-500 001

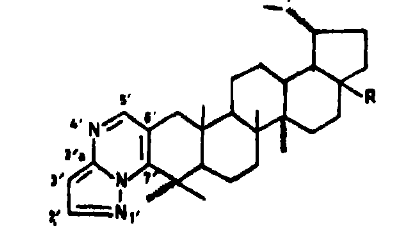
Manuscript received 15 March 1985, revised 13 November 1985, accepted 23 April 1986

Condensation of 3-aminopyrazole with 2-hydroxymethylene derivatives of methyl betulonate (1), lupenone (2) and methyl oleanonate (3) in absolute ethanol furnished their respective 2-eno[2,3-*g*]pyrazolo[1,5-*a*]pyrimidines (4, 5 and 6). They were characterised by elemental and spectral data.

RING-A fused heterocycles of triterpenoids were synthesised earlier in our laboratory[1-3] with a view to induce biological activity to biologically inert triterpenoids, as fusion of heterocyclic ring or incorporation of hetero atom into steroidal nucleus had modified their physiological activity[4-7]. Sykes and Bajwa synthesised a number of new steroidal heterocycles by the condensation of 2-amino-1,3,4-thiadiazole[8], 4-amino-1,2,4-triazole[9], 3-aminopyrazole[10], 3-amino-1,2,4-triazole[11] *etc.* with various steroidal β-ketoaldehydes.

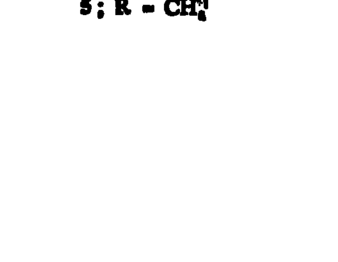


1 ; R = $COOCH_3$
2 ; R = CH_3



3

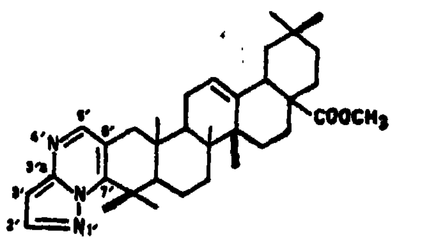
In the present investigation, 2-hydroxymethylene derivatives of methyl betulonate[3] (1), lupenone (2) and methyl oleanonate[3] (3) were condensed with 3-aminopyrazole in absolute ethanol. Sykes and Bajwa observed the formation of angularly and linearly fused pyrazolopyrimidines (7, 8) in the condensation of 3-aminopyrazole with 2-hydroxymethylene derivatives of 3-oxo steroids[10]. The 5′-proton showed signal at δ 8.15 in the angularly fused product (7) whereas the 7′-proton showed a signal at δ 8.37 in the linearly fused product (8). In the present case, the nmr spectra of all the three 2-eno[2,3-*g*]pyrazolo[1,5-*a*]pyrimidines (4, 5 and 6) showed signal at δ 8.15 characteristic of 5′-H. This confirms the angularly fused nature of the products.



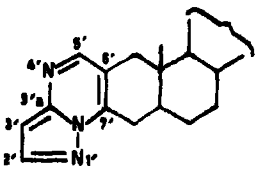
4 ; R = $COOCH_3$
5 ; R = CH_3

Experimental

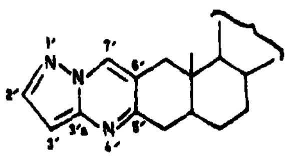
The melting points were recorded using Bio-Chem melting point apparatus and are uncorrected. Nmr spectra were recorded in $CDCl_3$ on a EM-360 60 MHz spectrometer with TMS as the internal standard. Ir spectra were recorded on a Perkin-



6



7



8

Elmer Infra Cord 237 spectrophotometer and uv spectra on a Perkin-Elmer 137 spectrophotometer.

2-Hydroxymethylene-lup-20(29)-en-3-one (2) : To lupenone (2 g) in dry benzene (25 ml) freshly distilled dimethyl formamide (5 ml), freshly distilled ethyl formate (5 ml) and sodium methoxide solution (25 ml) prepared from sodium (5 g) were added and refluxed for 8 h. The reaction mixture was cooled, acidified and extracted with ether. The ether extract furnished the 2-formyl derivative as colourless solid (1.5 g) crystallising from methanol as colourless needles (2), m.p. 180-82° (Found : C, 82.55 ; H, 10.60. $C_{31}H_{48}O_2$ requires : C, 82.30 ; H, 10.62%) ; δ 8.6 (1H, s, CHO) ; ν_{max} 3 150 cm^{-1} (chelated OH) and 1 680 cm^{-1} (CHO) ; λ_{max} (EtOH) 284 nm, underwent a bathochromic shift of 20 nm in base (EtOH-0.1 *N* NaOH).

A Typical experiment for the condensation of 3-aminopyrazole with β-keto aldehyde of pentacyclic triterpenes (1-3). *Isolation of 2-eno[2,3-g]pyrazolo-[1,5-a]pyrimidines* (4-6) : A solution of the triterpene β-keto aldehyde (800 mg) and 3-aminopyrazole (200 mg) in absolute ethanol (30 ml) was refluxed for 12 h. The mixture was evaporated to dryness *in vacuo*. The residue was adsorbed over neutral alumina (Acme) and eluted with petroleum ether (500 ml) and benzene (1.5 1). Petroleum ether eluate did not yield any residue. Benzene eluate yielded 2-eno[2,3-*g*]pyrazolo[1,5-*a*]pyrimidines (500 mg) which were finally purified by crystallisation from $CHCl_3$-MeOH as colourless needles. Methyl 2-eno[2, 3-*g*]pyrazolo[1, 5-*a*]pyrimidine-lup-20(29)-en-28-oate (4), m.p. 140-45° (Found : C, 77.02 ; H, 9.42 ; N, 7.98. $C_{35}H_{49}O_2N_3$ requires : C, 77.34 ; H, 9.02 and N, 7.73%) ; δ 6.60 (1H, d, *J* 2 Hz, 3'-H), 8.0 (1H, d, *J* 2 Hz, 2'-H), 8.15 (1H, s, 5'-H), 4.7 (2H, d, *J* 6.5 Hz, C=CH_2), 3.65 (3H, s, COOMe) and 0.9-2.5 (18H, 6 × Me). 2-Eno-[2,3-*g*]pyrazolo[1,5-*a*]pyrimidine-lup-20(29)-ene (5) : m.p. 225-30° (Found : C, 81.36 ; H, 10.02 ; N, 8.01. $C_{34}H_{49}N_3$ requires : C, 81.77 ; H, 9.82 and N, 8.41%) ; δ 6.60 (1H, d, *J* 2 Hz, 3'-H), 8.0 (1H, d, *J* 2 Hz, 2'-H), 8.15 (1H, s, 5'-H), 4.7 (2H, d, *J* 6.5 Hz, C=CH_2) and 0.9-2.5 (21H, 7×Me). Methyl 2-eno-[2,3-*g*]pyrazolo[1,5-*a*]pyrimidine olean-12-en-28-oate (6) : m.p. 260-65° (Found : C, 77.62 ; H, 9.12 ; N, 7.88. $C_{35}H_{49}O_2N_3$ requires : C, 77.34 ; H, 9.02 and N, 7.73%) ; δ 6.60 (1H, d, *J* 2 Hz, 3'-H), 8.0 (1H, d, *J* 2 Hz, 2'-H), 8.15 (1H, s, 5'-H), 5.3 (1H, t, 12-H), 3.65 (3H, s, COOMe) and 0.9-2.5 (21H, 7×Me).

Acknowledgement

The authors are grateful to Prof. M. C. Ganorkar, Head, Department of Chemistry, Nizam College, Hyderabad, for facilities. One of the authors (S.K.R.) thanks V. V. Education Society, Hyderabad, for encouragement and Director, R.S.I.C., Lucknow, for nmr spectra, and the other (T.V.P.R.) thanks U.G.C., New Delhi, for financial assistance.

References

1. K. L. RAO, S. K. R. RAJ and T. S. RAMAIAH, *J. Indian Chem. Soc.*, 1978, 55, 102.
2. CH. GOVARDHAN, R. P. REDDY, T. S. RAMAIAH and T. V. R. RAO, *J. Indian Chem. Soc.*, 1983, 60, 858.
3. K. L. RAO, T. S. RAMAIAH, K. S. REDDY, S. K. RAMRAJ and T. V. P. R. SUBBA RAO, *J. Indian Chem. Soc.*, 1985, 62, 137.
4. R. O. CLINTON, A. J. MANSON, F. W. STONES, H. C. NEUMANN, R. G. CHRISTIAN, R. L. CLARKE, J. H. ACKERMAN, D. F. PAGE, J. W. DEAN, W. B. DICKINSON and C. CARABATEAS, *J. Am. Chem. Soc.*, 1961, 83, 1478.
5. E. CASPI and D. M. PIATAK, *Can. J. Chem.*, 1963, 41, 2294.
6. R. HIRSCHMANN, N. G. SLEINBERG, E. F. SHOENWALDT, W. J. PALEVEDA and M. TISCHLER, *J. Med. Chem.*, 1964, 7, 352.
7. H. SINGH and V. V. PARASHAR, *Tetrahedron Lett.*, 1966, 983.
8. J. S. BAJWA and P. J. SYKES, *J. Chem. Soc., Perkin Trans. 1*, 1978, 1618.
9. J. S. BAJWA and P. J. SYKES., *J. Chem. Soc., Perkin Trans. 1*, 1979, 1816.
10. J. S. BAJWA and P. J. SYKES, *J. Chem. Soc., Perkin Trans. 1*, 1980, 481.
11. J. S. BAJWA and P. J. SYKES, *J. Chem. Soc., Perkin Trans. 1*, 1979, 3085.

J. Indian Chem. Soc.,
Vol. LXIII, May 1986, pp. 512-514

Gravimetric Determination of Palladium(II), Copper(II) and Nickel(II), and Palladium(II), Copper(II) and Manganese(II) from Ternary Mixtures, using 2-Hydroxy-1-acetonaphthoneoxime and 1-Hydroxy-2-acetonaphthoneoxime†

V. V. BALAKRISHNA*

Department of Chemistry, Sri Venkateswara University Post-Graduate Centre, Kurnool-518 001

and

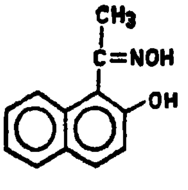
N. APPALA RAJU

Department of Chemistry, Sri Venkateswara University, Tirupati-517 502

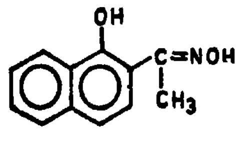
Manuscript received 30 July 1985, revised 24 February 1986, accepted 23 April 1986

2-Hydroxy-1-acetonaphthoneoxime and its isomer 1-hydroxy-2-acetonaphthoneoxime have been used as reagents for the gravimetric determination of palladium(II), copper(II) and nickel(II) as well as palladium(II), copper(II) and manganese(II) from ternary mixtures. The results obtained are fairly accurate.

2-Hydroxy-1-acetonaphthoneoxime (2-HANO), and its isomer, 1-hydroxy-2-acetonaphthoneoxime (1-HANO) have been extensively studied in these laboratories[1-7]. 2-HANO gives a yellow precipitate with Pd^{II} (*p*H 1.5-2.5), a buff coloured precipitate with Cu^{II} (*p*H 3.5-6.0), a greenish yellow precipitate with Ni^{II} (*p*H 8.0-10.0) and a dark green precipitate with Mn^{II} (*p*H 8.0-10.0). Similarly, 1-HANO gives a deep yellow precipitate with Pd^{II}, grey precipitate with Cu^{II}, greenish yellow precipitate with Ni^{II} and dark green precipitate with Mn^{II} under similar experimental conditions. Accordingly, procedures were developed for the gravimetric determination of these metals when present either singly or in binary mixtures[1,3,4]. The present paper deals with their determination in ternary mixtures.



2-HANO



1-HANO

Experimental

The reagents were prepared by the procedures reported earlier[1,6]. A 1% (w/v) solution of 1-HANO in rectified spirit was used, while in case of 2-HANO a 1% (w/v) solution was prepared in 1 : 1 aqueous ethanol. Stock solutions of copper sulphate, nickel sulphate and manganese chloride were prepared using AnalaR samples and were standardised[8]. In the case of palladium chloride, a solution was prepared by dissolving palladium chloride (Reachim, USSR) (1 g) in concentrated HCl (10 ml) and making up in a one litre standard flask, and the palladium content was determined using dimethylglyoxime[8]. Solutions for the study of interference by diverse ions were prepared such that each ml contained about 10 mg of the metal ions. In case of Au^{III} and Pt^{IV} the solutions were prepared such that each ml contained about 1 mg of the metal ions. A *p*H of 1.5 was maintained with 2 *M* HCl in case of Pd^{II}. Similarly, sodium acetate-acetic acid buffer and ammonium chloride-ammonium hydroxide buffer were used to maintain the *p*H at 4.5 and 8.5, respectively in the cases of Cu^{II}, Ni^{II} and Mn^{II}. The determinations gave very good results under those *p*H conditions.

Determination of Pd^{II}, Cu^{II} and Ni^{II} from ternary mixtures: Aliquots of the standard solutions of palladium chloride, copper sulphate and nickel sulphate were pipetted out into a clean 250 ml beaker and diluted to about 150 ml with distilled water. The *p*H was adjusted to 1.5 with 2 *M* HCl and the reagent (1-HANO or 2-HANO) was added dropwise with

† Presented at the 69th Session of Indian Science Congress held at Mysore in January, 1982.

constant stirring (1 ml per mg of the metal). The precipitate was digested on a hot-water-bath for 15 min, filtered on a sintered crucible (IG-4), washed with aqueous ethanol (4 : 1), dried at 110-20° and weighed as $Pd(C_{12}H_{10}O_2N)_2$ in case of 1-HANO and as $Pd(C_{12}H_{10}O_2N)_2.H_2O$ in case of 2-HANO. The filtrate was concentrated to about 150 ml, a few ml of 1 *N* NaOH was added to neutralise the solution and copper was precipitated at *p*H 4.5 and weighed as $Cu(C_{12}H_{10}O_2N)_2$ after digestion, washing and drying. The filtrate was concentrated again to 150 ml and nickel was precipitated at *p*H 8.5 and weighed as $Ni(C_{12}H_{10}O_2N)_2$ after digestion, washing and drying. The gravimetric factors for Pd^{II}, Cu^{II} and Ni^{II} are 0.2099, 0.1370 and 0.1278, respectively. In case of palladium complex with 2-HANO, the gravimetric factor is 0.2028 corresponding to the formula $Pd(C_{12}H_{10}O_2N)_2.H_2O$. Results are shown in Table 1.

Study of interference by diverse ions: Cu^{II}, Ni^{II}, Mn^{II} and Pt^{IV} did not interfere in case of Pd^{II}, but Au^{III} interfered. Similarly, Cd^{II}, Ni^{II}, Zn^{II}, Cr^{III} and Mn^{II} did not interfere in case of Cu^{II}. Mn^{II} interfered in case of Ni^{II} and Ni^{II} interfered in case of Mn^{II} as both are precipitated under similar conditions. Even masking with cyanide was of no use. The interference due to Co^{II} in case of both Ni^{II} and Mn^{II} was overcome by the use of a solution of 1 *M* ammonium thiocyanate. Six determinations each of 10.57 mg of Pd^{II}, 10.02 mg of Cu^{II}, 11.30 mg of Ni^{II} and 11.77 mg of Mn^{II} with 1-HANO gave standard deviations of 0.05_2, 0.02_6, 0.02_8 and 0.05_9 mg, respectively; the relative mean errors being ±0.19, ±0.10, ±0.09 and ±0.25%, respectively. Similarly, six determinations each of 11.09 mg of Pd^{II}, 10.02 mg of Cu^{II}, 15.54 mg of Ni^{II} and 11.77 mg of Mn^{II} with 2-HANO gave standard deviations of 0.03_2, 0.04_5, 0.03_7 and 0.06_2 mg, respectively; the relative mean errors being ±0.36, ±0.54, ±0.19 and ±0.08%, respectively.

TABLE 1—DETERMINATION OF Pd^{II}, Cu^{II} AND Ni^{II} IN TERNARY MIXTURES

Metal	Computed value (mg) 2-HANO	Computed value (mg) 1-HANO	Experimental value (mg) 2-HANO	Experimental value (mg) 1-HANO	Error, % 2-HANO	Error, % 1-HANO
Pd	(DMG method)					
	5.55	5.29	5.56	5.31	−0.18	+0.38
	11.09	10.57	11.10	10.54	+0.09	−0.28
	16.64	21.14	16.68	21.18	+0.24	+0.18
Cu	(Iodometric method)					
	10.02	10.02	10.00	10.04	−0.20	+0.20
	18.04	20.04	18.08	20.08	+0.22	+0.20
	24.05	30.06	24.02	30.11	−0.12	+0.16
Ni	(DMG method)					
	15.54	11.30	15.52	11.25	−0.13	−0.34
	26.64	22.60	26.72	22.50	+0.30	−0.44
	37.74	33.90	37.62	33.82	−0.32	−0.24

Determination of Pd^{II}, Cu^{II} and Mn^{II} in ternary mixtures: The procedure followed was similar as described above except that a standard solution of manganese sulphate was used in place of a standard solution of nickel sulphate in the ternary mixture. The gravimetric factor for Mn^{II} is 0.1207. Results are shown in Table 2.

Results and Discussion

From the Tables 1 and 2 it is evident that 5.0-25.0 mg of the metal ions can be determined

TABLE 2—DETERMINATION OF Pd^{II}, Cu^{II} AND Mn^{II} IN TERNARY MIXTURE

Metal	Computed value (mg) 2-HANO	Computed value (mg) 1-HANO	Experimental value (mg) 2-HANO	Experimental value (mg) 1-HANO	Error, % 2-HANO	Error, % 1-HANO
Pd	(DMG method)					
	5.55	5.29	5.58	5.33	+0.76	+0.57
	11.09	10.57	11.12	10.63	+0.54	+0.57
	16.64	21.14	16.66	21.02	+0.12	+0.54
Cu	(Iodometric method)					
	10.02	10.02	9.98	9.99	−0.40	−0.30
	18.04	20.04	18.02	20.00	−0.22	−0.20
	24.05	30.06	24.00	30.01	+0.12	−0.16
Mn	(DMG method)					
	9.31	9.31	9.29	9.28	−0.21	−0.32
	11.77	11.77	11.71	11.82	−0.34	+0.42
	23.53	23.53	23.44	23.45	−0.38	−0.30

(with fair accuracy) with the reagents studied. The results presented are comparable to those obtained with 2-hydroxy-4-methoxy-5-methyl-chalconeoxime[9] in case of determination of Pd^{II}, Cu^{II} and Ni^{II} in ternary mixtures. No results are available for comparison with ternary mixtures containing Pd^{II}, Cu^{II} and Mn^{II} as only these two reagents happen to be used for the purpose. The present study indicates that both the reagents studied are suitable for the determination of Pd^{II}, Cu^{II} and Ni^{II} or Pd^{II}, Cu^{II} and Mn^{II} in ternary mixtures. Though 2-HANO happens to be as good as 1-HANO in its potentiality as a gravimetric reagent, 1-HANO scores over 2-HANO in view of ease in its preparation and greater stability of its alcoholic solution.

References

1. R. C. Hussain and N. Appala Raju, *Proc. Indian Acad. Sci., Sect. A*, 1976, 84, 144.
2. R. C. Hussain, Ph.D. Thesis, S. V. University, 1977.
3. V. V. Balakrishna, R. C. Hussain and N. Appala Raju, *Proc. Indian Acad. Sci., Sect. A*, 1978, 87, 291.
4. V. V. Balakrishna and N. Appala Raju, *Curr. Sci.*, 1979, 48, 724.
5. V. V. Balakrishna and N. Appala Raju, *Curr. Sci.*, 1980, 49, 227.
6. N. V. K. N. Prasada Rao, V. V. Balakrishna and N. Appala Raju, *Indian J. Chem., Sect. A*, 1980, 19, 607.
7. V. V. Balakrishna, Ph.D. Thesis, S. V. University, 1980.
8. A. I. Vogel, "A Text Book of Quantitative Inorganic Analysis", Longmans, London, 1975, pp. 358, 481, 512, 434.
9. B. K. Deshmukh, C. N. Vyas and R. B. Kharat, *J. Indian Chem. Soc.*, 1975, 52, 385.

Notes

Polynuclear Alkali Metal Complexes with Nickel(II)- and Cobalt(II)-salicylaldehyde

A. K. BANERJEE*, SHEO SATYA PRAKASH

and

S. K. ROY

Chemistry Department, Patna University, Patna-800 005

Manuscript received 22 September 1984, revised 2 January 1986, accepted 3 March 1986

USING $Ni(SalH)_2$ and $Co(SalH)_2$ as 'metal complex ligands'[1-3], in this paper, we describe a few oxygen bridged polynuclear[4] complexes of alkali metal salts of 1-nitroso-2-naphthol and 8-hydroxyquinoline.

Experimental

The complexes were prepared by refluxing a mixture of $Ni(SalH)_2$ or $Co(SalH)_2$ and alkali metal salts in the ratio of 1 : 2 in absolute ethanol for 2-3 h. The whole thing went into solution and the adducts precipitated from hot solutions.

Results and Discussion

Analytical data suggest the general formula $[M_a(SalH)_2(M_bL)_2]$, where M_a = Ni or Co, and M_bL = Li, Na or K salts of deprotonated 8-hydroxyquinoline or 1-nitroso-2-naphthol. The colour of the adducts are different from those of the metal complex ligands. The higher decomposition temperatures of these adducts, compared to that of the metal complex ligands, indicated strong bonding between oxygen atom of metal complex ligands and the alkali metal ions. The adducts were stable under dry condition. The colour, decomposition temperatures and other properties of the adducts are given in Table 1.

The magnetic moment of octahedral trimer $[Ni(SalH)_2]_3$ is 3.35 B.M., whereas the adducts have moments 3.5-3.8 B.M. These higher magnetic moments may be due to the change in geometry. $Co(SalH)_2$ is also an octahedral tetramer with magnetic moment 5.0 B.M. For the corresponding trinuclear alkali metal adducts, the magnetic moments have been observed in the range 4.5-4.75 B M. The lower magnetic moment values suggest a change in geometry from octahedral to tetrahedral.

Infrared spectral measurements were made in nujol for the ligands and complexes between 4 000 and 600 cm^{-1}. Selected absorption bands are given in Table 1. In salicylaldehyde molecule, due to intra-hydrogen bonding, the C=O (aldehydic carbonyl) frequency show up at 1 665 cm^{-1}. The C—O (phenolic) stretch is observed in the free ligand at 1 282 cm^{-1}; on complexation with transition metals, this band shifts to higher energy by about 40-50 cm^{-1}, indicating phenolic oxygen coordination

TABLE 1

Compd.	Colour	Decomp. temp. °C	Analysis % : Found/(Calcd.) N	Ni/Co	Na/K	Magnetic moment at 29°	Selected ir bands (cm^{-1}) C=O	C–O
$Ni(SalH)_2$≡L	Green	270				3.35		
$(LiIN2N)_2$.L	Brown	280	3.85 (4.20)	8.4 (8.8)		3.50	1 640	1 345
$(NaIN2N)_2$.L	Brown	285	4.2 (4.0)	7.95 (8.40)	6.4 (6.6)	3.55	1 640	1 340
$(KIN2N)_2$.L	Dark brown	290	3.9 (3.8)	8.3 (8.0)	10.4 (10.8)	3.65	1 630	1 340
$(Li8HQ)_2$.L	Green	278	2.2 (2.3)	9.3 (9.6)		3 60	1 630	1 330
$(Na8HQ)_2$.L	Green	282-83	2.05 (2.20)	8.8 (9.1)	3.2 (3.6)	3.65	1 630	1 330
$(K8HQ)_2$.L	Dark green	285	1.89 (2.01)	8.4 (8.7)	5.4 (5.8)	3.80	1 635	1 330
$Co(SalH)_2$≡L'	Yellow	275				5.00		
$(LiIN2N)_2$.L'	Red	300	4.0 (4.2)	8.45 (8.90)		4.50	1 645	1 340
$(NaIN2N)_2$.L'	Red	285	3.8 (4.0)	8.0 (8.4)	6.2 (6.6)	4.65	1 640	1 335
$(K1N2N)_2$.L'	Red	290	3.84 (3.80)	7.6 (8.0)	9.8 (10.8)	4.75	1 640	1 335
$(Li8HQ)_2$.L'	Dark brown	285	2.1 (2.8)	9.4 (9.7)		4.55		
$(Na8HQ)_2$.L'	Brown	280	2.35 (2.20)	9.4 (9.2)	3.2 (3.6)	4.70		1 330
$(K8HQ)_2$.L'	Dark brown	285	2.0 (2.1)	8.5 (8.8)	5.4 (5.8)	4.70	1 640	1 335

of the salicylaldehyde. This upward shift is due to the maintenance of a ring current arising out of electron delocalisation in the chelate ring.

In case of $Ni(SalH)_3$, which is a trimer, the aldehydic C=O and the phenolic C—O, both split into two ; the aldehydic C=O show up at 1 655 and 1 636 cm^{-1}, whereas phenolic C—O can be spotted out at 1 355 and 1 322 cm^{-1}. Looking into the crystal structure of $[Ni(SalH)_2]_3$, it is found that half the oxygen atoms of aldehydic and phenolic ones, are bridged oxygens, *i.e.* one oxygen attached to two Ni^{II} ions. The other half (6 oxygen atoms, comparising of 3 aldehydic and 3 phenolic oxygen atoms) oxygen atoms are terminal ones, *i.e.* they are attached to only one Ni^{II} ion. The Co^{II}-salicylaldehyde is also polynuclear, where two aldehydic C=O at 1 655 and 1 627 cm^{-1} and two phenolic C—O at 1 354 and 1 321 cm^{-1} have been reported. It can be generalised that in metal salicylaldehydes, when they are monomers, the aldehydic $\nu_{C=O}$ and phenolic ν_{C-O} show only one normal peak at 1 650 cm^{-1} and 1 320 cm^{-1}, respectively ; whereas when it is a polymer with oxygen bridges, both the aldehydic and phenolic frequencies split into two, one at the normal region and the other at a slightly higher frequency. In these polynuclear alkali metal transition metal-salicylaldehydes, the aldehydic $\nu_{C=O}$ and phenolic ν_{C-O} have been observed not to be in their normal range (Table 1), but invariably higher. This is very suggestive that all these oxygens are bridged ones, bridging the transition metal and, most probably, the alkali metal.

The visible absorption spectrum of $[Ni(SalH_2]_3$ shows typical octahedral absorption bands at 450, 600, and 900 nm. The electronic spectra of alkali metal adducts is different in nature and show one strong band at ~600 nm with a shoulder at 550 nm ; but the two other peaks of $[Ni(SalH)_2]_3$ are missing. This suggests that the octahedral structure $[Ni(SalH)_2]_3$ has been converted to tetrahedral structure in its alkali metal adducts. The visible absorption spectrum of $[Co(SalH)_2]_4$ shows only one band at 550 nm, which is typical of an octahedral cobalt (II) complex. In its alkali metal adducts, this 550 nm band of $Co(SalH)_2$ shift to ~ 650 nm. It is very likely that octahedral $[Co(SalH)_2]_4$ break up into tetrahedral structure in its alkali metal adducts.

The magnetic properties and electronic spectral studies of alkali metal adducts reveal a break in polymerised system of $[Ni(SalH)_2]_3$ and $[Co(SalH)_2]_4$. Accordingly, the octahedral structure of polymeric nickel-salicylaldehyde and cobalt-salicylaldehyde are converted into a tetrahedral structure of $Ni(SalH)_2$ and $Co(SalH)_2$ in their alkali metal adducts. The bonding between salicylaldehyde $M(SalH)_2$ and alkali metal salts, is most likely through the oxygen atoms of aldehydic and phenolic groups, tetrahedrally situated in these cases.

References

1. S. J. GRUBER, C. M. HARRIS and E. SINN, *Inorg. Nucl. Chem. Lett.*, 1967, 3, 465.
2. S. J. GRUBER, C. M. HARRIS and E. SINN, *Inorg. Chem.*, 1968, 7, 268.
3. S. J. GRUBER, C. M. HARRIS and E. SINN, *Inorg. Nucl. Chem. Lett.*, 1968, 4, 107.
4. A. K. BANERJEE, D. PRASAD and S. K. ROY, *J. Indian Chem. Soc.*, 1982, 5'', 1303.

Highly unsaturated 'N_2O_2' Ligand System and its Transition Metal Complexes

S. BALASUBRAMANIAN and C. N. KRISHNAN*

Department of Inorganic Chemistry, A. C. College Campus, University of Madras, Madras-600 025

Manuscript received 7 February 1985, revised 3 February 1986, accepted 3 March 1986

THE synthesis of some of the 'N_2O_2' type ligands involve the condensation of β-diketones like acetylacetone, substituted acetylacetone, benzoylacetone, dibenzoylmethane, dipivaloylmethane, 3,5-heptanedione *etc.*[1-4], with aliphatic diamines. However, there are not many reports on the synthesis of the Schiff base ligands with γ-diketones. The conjugated azomethines are considered to be significant because of their relevance to biologically important processes. Rhodopsin, a compoun[d] containing conjugated azomethine, is an importan[t] intermediate involved in the chemistry of vision[5]. There has been considerable interest in the synthesi[s] and study of quadridentate Schiff base complexe[s] with 'N_2O_2' donors[6,7]. The stereochemistry of the metal complexes of these ligands is found to vary with the length of the methylene chain[8]. The present investigation aims at the synthesis and characterisation of a highly unsaturated ligan[d] derived from benzilmonohydrazone and a γ-diketone, *viz.* acetonylacetone and its nickel(II), copper(II) and cobalt(II) complexes.

Experimental

5,8-Dimethyl-1,2,11,12-tetraphenyl-3,4,9,10-tetrazadodeca-2,4,8,10-tetraen-1,12-dione (DTTHD): Benzilmonohydrazone (BMH) (15 g) was dissolved i[n] dry benzene (100 ml) and acetonylacetone (8 ml) was added to it and heated under reflux on a water-bath for 12 h. The dark red solution was cooled t[o] 0°. The solid separated was filtered, washed severa[l] times with ether, recrystallised from benzene-petro[l] mixture and finally dried *in vacuo*, m.p. 120° (Found : C, 77.87 ; H, 6.00 ; N, 10.24. $C_{34}H_{30}N_4O_2$ calcd. for : C, 77.56 ; H, 5.70 ; N, 10.64%).

General method of preparation of the complexes To a solution of the ligand DTTHD (0.002 mol) in ethanol (50 ml) metal(II) perchlorate (0.002 mol) was added and the solution was refluxed for 5 h cooled and filtered. The resulting microcrystallin[e] solid was filtered, washed with water and ethe[r]

and finally dried *in vacuo* at 100°. The analytical data of the complexes (Table 1) confirm the 1 : 1 stoichiometry for metal-ligand.

TABLE 1—ANALYTICAL DATA OF COMPLEXES

Complex	Analysis % : Found/(Calcd.)	
	Metal	N
$[Ni(DTTHD)](ClO_4)_2$	7.30 (7.49)	7.00 (7.15)
$[Cu(DTTHD)](ClO_4)_2$	7.62 (7.51)	6.97 (7.14)
$[Co(DTTHD)](ClO_4)_2$	7.94 (8.05)	7.04 (7.10)

Results and Discussion

The electronic spectrum of the ligand recorded in benzene solvent, indicated two peaks at 27 100 and 38 910 cm^{-1}, and the molar extinction coefficient was found to be 3 651 cm^{-1} mol^{-1}. These bands are assigned to the transitions $n \rightarrow \pi^*$ and $\pi \rightarrow \pi^*$, respectively. The ir spectra of the ligand showed very strong absorptions at 1 670 (C=O) and at 1 630 cm^{-1} (C=N). The weak band due to C—H stretch is observed at 3 040 cm^{-1}. The medium absorptions appearing in the region 1 580-1 600 cm^{-1} are attributed to the combination of C=C and C=N frequencies The disappearance of the free NH_2 absorption of the starting material coupled with the analytical data has confirmed that the 2 : 1 condensation of the hydrazone with the acetonylacetone has indeed taken place.

The nmr spectrum of the ligand recorded in $CDCl_3$/TMS showed aromatic multiplets in the region δ 7.2-8.0 and methyl and methylene signals at δ 1.66 and 2.06, respectively. This is in accordance with the values expected from the ligands of similar type[9]. The mass spectrum exhibited the molecular ion peak (M^+) at m/z 526, thus supporting the proposed molecular formula for the ligand.

The metal chelate obtained from this ligand are expected to be quite stable as in the case of Schiff base complexes derived from acetylacetone due to the polarisation of ligand electrons and the formation of M-L π-bond.

The conductance values (125-150 Ω^{-1} cm^2 mol^{-1}) of all the complexes in DMF show their 2 : 1 electrolyte nature[10]. The magnetic moments obtained by Gouy method give a clue to the nature of the stereochemistry around the metal ions. The nickel(II) complex was found to be paramagnetic with a magnetic moment of 3.2 B.M., while copper(II) complex showed a value of 1.8 B.M. The esr spectra recorded for the microcrystalline copper(II) and cobalt(II) complexes at room temperature show $g_{||}$=2.218, $g_{\perp}$=2.048. $A_{||}$= 170×10^{-4} cm^{-1} and g_1=2.348 ; and g_0=2.075, respectively.

The electronic spectra of the complexes were recorded in DMF solution. A broad band at 20 833 cm^{-1} characteristic for the square-planar nickel(II) complexes has been observed in the case of $[Ni(DTTHD)](ClO_4)_2$, while $[Cu(DTTHD)](ClO_4)_2$ and $[Co(DTTHD)](ClO_4)_2$ showed broad bands at 16 500 and 15 750 cm^{-1}, respectively. A distorted planar geometry can be envisaged for these complexes.

The ir spectra of the complexes indicate a positive shift of 10-15 cm^{-1} in the case of both C=O and C=N frequencies, thus confirming the N_2O_2 coordination in these complexes. The perchlorate absorption in the 1 100 cm^{-1} region is also observed.

Acknowledgement

The financial assistance from U.G.C., New Delhi, is gratefully acknowledged.

References

1. P. J. McCarthy, R. H. Hovey, K. Ueno and A. E. Martell, *J. Am. Chem. Soc.*, 1955, 77, 5820.
2. J. P. Fackler, Jr., *Prog. Inorg. Chem.*, 1966, 7, 361.
3. J. J. Fortman and R. E. Sievers, *Coord. Chem. Rev.*, 1971, 6, 331.
4. K. C. Joshi and V. N. Pathak, *Coord. Chem. Rev.*, 1977, 22, 37.
5. G. Wald, *Science*, 1968, 162, 230.
6. R. H. Holm, G. W. Everett, Jr. and A. Chakravarty, *Prog. Inorg. Chem.*, 1966, 7, 83.
7. M. D. Hobday and T. D. Smith, *Prog. Inorg. Chem.*, 1972, 7, 385.
8. M. Hariharan and F. L. Urbach, *Inorg. Chem.*, 1979, 8, 556.
9. S. Balasubramanian, Ph.D. Thesis, University of Madras, 1984.
10. W. J. Geary, *Coord. Chem. Rev.*, 1971, 7, 81.

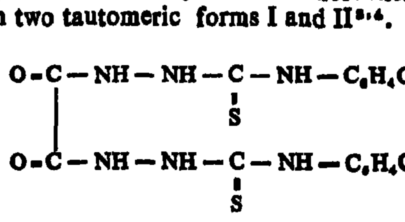
Complexes of *p*-Chlorophenyloxalylthiosemicarbazide with Manganese(II), Iron(II), Cobalt(II), Nickel(II), Copper(II), Cadmium(II) and Mercury(II)

(Miss) AMNA, RAM ADHAR RAI and (Mrs.) LAKSHMI*

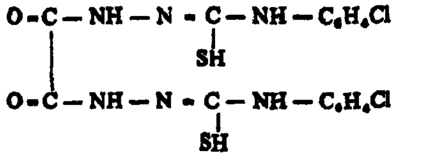
Department of Chemistry, Gorakhpur University, Gorakhpur-273 009

Manuscript received 18 November 1982, revised 24 February 1986, accepted 31 March 1986

THE ligands having —N—C=S group with nitrogen and sulphur as donor sites have been the subject of two reviews[1,2]. Thiosemicarbazide exists in two tautomeric forms I and II[3,4]. As the



(I)



(II)

chelating behaviour of *p*-chlorophenyloxalythiosemicarbazide has not been reported so far, its extensive studies are needed. The present paper reports the preparation of some new complexes of bivalent Mn, Fe, Co, Ni, Cu, Cd and Hg. The complexes have been characterised with the help of ir, uv-visible, magnetic susceptibility and analytical data.

Experimental

All the chemicals used were of AnalaR grade. The ligand was prepared by the reported method[5].

Preparation of complexes $(C_{16}H_{14}Cl_2N_6O_2S_2)M(II).xH_2O$: An aqueous solution of $MCl_2.xH_2O$ (1 mmol) was mixed with a solution of ligand (1 mmol) in DMF with continuous stirring and digested on steam-bath for 1 h. The solid product precipitated was washed with water and dried in vaccum.

The complexes are insoluble in most organic solvents. However, Ni^{II}, Co^{II} and Cu^{II} complexes are soluble in DMF. All the complexes decompose above 280°.

Elemental analysis data are given in Table 1. Infrared spectra (KBr) of the ligand and the complexes in the range 4 000-200 cm^{-1}, were recorded with a Perkin-Elmer 521 spectrophotometer, and electronic spectra (nujol of the complexes were obtained in the range 200-900 nm with a Carry 14 spectrophotometer from I.I.T., Kanpur. Magnetic susceptibilities were determined with the help of Faraday balance at room temperature using ferrous ammonium sulphate as the standard.

Results and Discussion

The stoichiometry ML has been established for all the complexes from the results of elemental analysis. Upon coordination through N–H group, the band at 3 320 and 3 100 cm^{-1} either disappeared or became broad in all the complexes, showing coordination of metal ion through NH group. A strong band at 1 670 cm^{-1} becomes broad and weak, which further suggest contribution of δ_{NH} in coordination. Band at 1 580 or 1 540 cm^{-1} either disappear or becomes broad and weak in all the complexes, showing the chelation through –N–C=S moiety (thioamide band I)[6,7]. The assignment of the vibrational modes at 1 360, 1 250, 1 150 and 750 cm^{-1} is summarised in Table 2. A band at 830 cm^{-1} disappears in all the complexes showing the contribution of δ(–N–N–C(=S)–). Bands at 540 and 450 cm^{-1} disappear in all the complexes, showing the contribution of τ(N–N). Two new bands at 500 and 370 cm^{-1} appear in all the complexes showing the presence of ν(M–N) and ν(M–S), respectively.

Effective magnetic moment of the Cu^{II} complex was found in the normal range 1.88 B M. The uv-visible spectrum shows three bands at 34 482, 35 211 and 25 000 cm^{-1}. The former two bands are charge transfer band o high energy, and the band at 25 000 cm^{-1} may be assigned as d-d transition, $^2B_{1g} \rightarrow {}^2A_{1g}$ for square-planar Cu^{II} complex.

In the case of Fe^{II} complex observed value of magnetic moment is found to be 5.27 B.M. In uv-visible spectra, the bands at 34 482 and 21 551 cm^{-1} correspond to charge-transfer band and d-d transition, respectively. The band at 21 551 cm^{-1} can be assigned as $^5A_{1g} \rightarrow {}^5B_{1g}$ in the square-planar complex of Fe^{II}.

The observed value of magnetic moment in Mn complex is found to be 4.90 B.M. indicating the

TABLE 1—ANALYTICAL AND MAGNETIC MOMENT DATA FOR *p*-CHLOROPHENYLOXALYLTHIOSEMICARBAZIDE-METAL COMPLEXES

Compd.	Colour	Analysis % : Found/(Calcd.)					Decomp. temp. °C	Magnetic moment B.M.
		C	H	N	S	M		
L	White	43.23 (42.01)	3.80 (3.06)	19.33 (18.38)	19.22 (19.01)	–	200[a]	–
[MnL].2H$_2$O	White	35.82 (35.04)	2.83 (2.55)	16.12 (15.33)	12.18 (11.68)	10.32 (10.02)	283	4.90
[FeL].4H$_2$O	Dark bluish green	33.01 (32.82)	2.85 (2.39)	14.60 (14.36)	11.21 (10.94)	10.72 (9.55)	282	5.27
[CoL.2H$_2$O].H$_2$O	Dark green	34.41 (32.73)	3.44 (2.63)	14.94 (14.73)	12.40 (11.23)	10.80 (10.34)	284	4.80
[NiL.2H$_2$O]	Yellowish green	35.02 (34.80)	3.11 (2.53)	14.11 (15.22)	12.29 (11.60)	11.37 (10.64)	290	2.84
[CuL].4H$_2$O	Reddish brown	33.10 (32.40)	2.85 (2.36)	14.37 (14.18)	11.50 (10.82)	12.02 (10.72)	285	1.88
[CdL].3H$_2$O	White	31.60 (30.79)	2.85 (2.25)	14.71 (13.522)	11.74 (10.26)	19.90 (18.03)	284	–
[HgL].2H$_2$O	Yellow	28.40 (27.68)	2.02 (2.01)	11.19 (12.11)	10.98 (9.22)	29 80 (28.90)	287	–

[a]M.p.

TABLE 2—ASSIGNMENTS AND SHIFTS OF IR BANDS (cm^{-1}) OF THE LIGAND AND COMPLEXES

Ligand	Complex	Assignments	Shifts in the frequency and change in intensity
3 320m	–	In ligand due to ν(N–H) asym and ν(N–H) sym	Disappears or broadening
3 100m	–		Disappears or broadening
1 670s I	1670±10	Contribution of δ(NH)	Broadening of δ(N–H) band
1 580m I	–	Chelation through N=C=S moiety thioamide band I	Disappears or becomes broad
1 540m I	–		
1 360m II	1360±10	Coordination through N=C=S and contribution of thioamide band II	Shifting by 10 cm^{-1}
1 250m	1250–20	Showing the election drift from N–N(azide) band	Shifts to lower wave number
1 150m III	1150±10	Coordination through NCS group, band III	
830w	–	Contribution of δ(N–N–C–)	Disappears
750w IV	–	Coordination through (C=S) group, band IV	Disappears
540m	–	Contribution of τ(N–N)	Disappears
450m	–	Contribution of τ(N–N)	Disappears
	500	ν(M–N)	
	340+30	ν(M–S)	

possibility of spin-free configuration (b_{2g}^1 e_g^2 a_{1g}^1 b_{1g}^1). Orbital configuration to the magnetic moment in square-planar complexes, is expected to be small as orbital angular momentum among the d-orbital is largely quenched by low symmetry D_{4h}. Thus the absence of transition band and the value of magnetic moment (4.90 B.M.) suggest square-planar arrangement of the ligand around Mn^{II} ion.

The observed value of magnetic moment 2.84 B.M., suggests the presence of two unpaired electron in Ni^{II} complex. There are bands at 31 250, 37 593, 20 576 and 19 230 cm^{-1} in the electronic spectrum of Ni^{II} complex. Bands at 31 250 and 37 593 cm^{-1} may be due to charge-transfer band. The band at (486 nm) 20 576 cm^{-1} suggest the existence of ground state $^3A_{2g}$ for octahedral Ni^{II} complex[10]. Because the ratio of the frequencies 20 576 to 19 230 cm^{-1} is found to be more sensitive to give the free ion value of B' 616 cm^{-1} compared to the reported value of B 1 080 cm^{-1} for Ni^{II} complex[9]. The band at 20 576 (ν_2) and 19 230 cm^{-1} (ν_1) can be assigned due to $^3A_{2g} \rightarrow {}^3T_{1g}(P)$ and $^3A_{2g}(F) \rightarrow {}^3T_{1g}(F)$ transitions for Ni^{II} octahedral complex. The value of 10 Dq is found to be 20 328 cm^{-1} which is extremely high compared to the reported value 12 000 cm^{-1} for enthylenediamine for octahedral Ni^{II} complex[9].

The value of magnetic moment observed in the Co^{II} complex 4.80 B.M., suggest the octahedral geometry of the complex[9]. There are two bands in the electronic transition at 20 408 and 18 867 cm^{-1}. The bands at 20 408 and 18 867 cm^{-1} may be assigned to $^4T_{1g}(F) \rightarrow {}^4T_{1g}(P)$ and $^4T_{1g}(F) \rightarrow {}^4T_{2g}$ transitions. The ratio of frequencies 20 408 to 18 867 cm^{-1} is found to be more sensitive to give the free ion value of B' 739 cm^{-1}, compared to the reported value of B 1 120 cm^{-1} for Co^{II} complex.

Acknowledgement

The authors thank Prof. R. P. Rastogi, Head of the Chemistry Department, University of Gorakhpur, for providing facilities and valuable suggestions. The instrumentation facilities from I.I.T., Kanpur and R.R.L., Jammu, are also gratefully acknowledged.

References

1. M. A. ALI and S. E. LIVINGSTONE, *Coord. Chem. Rev.*, 1974, 13, 101.
2. M. J. M. CAMPBELL, *Coord. Chem. Rev.*, 1975, 15, 279.
3. S. K. SAHNI, P. C. JAIN and V. B. RANA, *Indian J. Chem.*, 1978, 699.
4. S. E. LIVINGSTONE and J. E. OLUKA, *Transition Met. Chem.*, 1977, 2, 163.
5. S. S. SINGH and S. S. TIWARI, *Indian J. Appl. Chem.*, 1970, 33, 273.
6. I. SUZUKI, *Bull. Chem. Soc. Jpn.*, 1962, 95, 1499.
7. C. N. R. RAO, "Chemical Application of Infrared Spectroscopy", Academic, New York, 1963, p. 300.
8. F. A. COTTON and G. WILKINSON, "Advanced Inorganic Chemistry", Willey, New York, 1966, pp. 841-843.
9. B. N. FIGGIS, "Introduction to Ligand Fields", Wiley, New York, 1966, pp. 220, 226, 223, 316, 52, and Table 3.3.
10. C. J. BALLHAUSEN, "Introduction to Ligand Field Theory", Interscience, New York, 1966.

Thermodynamic Stability of some Rare Earths Complexes with Tyrosine. A Polarographic Study

FARID KHAN

Department of Chemistry, Doctor Harisingh Gour Vishwavidyalaya, Sagar-470 003

Manuscript received 17 December 1983, revised 20 August 1985, accepted 3 March 1986

VARIOUS complexing reagents have been employed in the polarographic determination of rare earths[1-6]. In continuation, the author now reports the thermodynamic stability of Ce^{III},

Pr^{III} and Nd^{III} complexes with tyrosine on a dropping mercury electrode.

Experimental

All chemicals used were AnalaR grade. The ligand solution was prepared in double-distilled water. The metals solutions were prepared by dissolving their oxides in minimum amount of hydrochloric acid and were standardised with EDTA[7]. The overall concentrations of potassium chloride, gelatin and rare earth metal ion in the test electrolytic solution were kept constant at 1.0*M*, 0.01% and 2.0 m*M*, respectively. The concentration of ligand was varied from 1.0 to 10.0 m*M* in each case. Ionic strength (μ) was fixed at 1.0, adjusted with potassium chloride. Hydrochloric acid and sodium hydroxide were used to adjust *p*H of the test solution at 2.70 ± 0.02.

Polarograms were recorded on an automatic pen recording polargraph (C.I.C., India), the capillary used had a'm' value of 2.15 mg s^{-1} and drop time of 3.10 s at 44.0 cm effective height of the mercury ($m^{2/3} t^{1/6} = 2.15 mg^{2/3} s^{-1/2}$). Pure nitrogen gas was passed through the solution for removing the dissolved oxygen. A Elico LI-120 digital *p*H meter was used to measure *p*H of the solution. All the measurements were made at 25 and 35°, thermostatically controlled.

Results and Discussion

Ce^{III}[8], Pr^{III} and Nd^{III}[9-10] give a well defined three-electron reversible reduction waves at *p*H 2.70 ± 0.02 in 1.0 *M* potassium chloride with 0.01% gelatin being used as a maximum suppressor. The difference of $E_{3/4} - E_{1/4}$ was 20 ± 1 mV for Ce^{III}, Pr^{III}, Nd^{III} and their complexes indicating the reversibility[11] of the electrode process. The nature of the waves for metal ions and their complexes was found to be diffusion-controlled as revealed from the straight line plots of i_d *vs* $\sqrt{h}$.

The half-wave potential shifted to more negative value on increasing the concentration of ligand. The method of Lingane[12] was used to determine the formation of 1 : 1 complexes of Ce^{III}, Pr^{III} and Nd^{III} with tyrosine. Thermodynamic parameter (ΔG) was calculated from the thermodynamic relations[13] and given in Table 1.

TABLE 1—STABILITY CONSTANTS (LOG K) AND FREE ENERGY CHANGE (ΔG) OF Ce^{III}, Pr^{III} AND Nd^{III} COMPLEXES WITH TYROSINE

μ = 1.0 KCl	log K		ΔG kcal $mole^{-1}$	
	25°	35°	25°	35°
Ce^{III}	3.52	3.00	−4.83	−4.25
Pr^{III}	4.35	4.12	−5.96	−5.84
Nd^{III}	4.60	4.35	−6.30	−6.16

The order of stability of complexes was found to be $Ce^{III} < Pr^{III} < Nd^{III}$, which is due to lanthanide contraction[6].

The gain in the free energies suggest that the complexes are not facilitated at higher temperature[6].

Acknowledgement

The author thanks to the Head of the Department of Chemistry for facilities.

References

1. F. KHAN and A. V. MAHAJANI, *J. Indian Chem. Soc.*, 1982, 59, 996.
2. F. KHAN and A. V. MAHAJANI, *J. Indian Chem. Soc.*, 1983, 60, 295.
3. F. KHAN, V. K. CHITALE and A. V. MAHAJANI, *J. Indian Chem. Soc.*, 1983, 60, 296.
4. F. KHAN and A. V. MAHAJANI, *J. Indian Chem. Soc.*, 1983, 60, 297.
5. F. KHAN and A. V. MAHAJANI, *J. Indian Chem. Soc.*, 1983, communicated.
6. F. KHAN and A. V. MAHAJANI, *J. Inst. of Chem. Calcutta*, 1982, 54, 209.
7. F. J. WELCHER, "The Analytical Uses of Ethylene Diamine Tetraacetic Acid", Van Nostrand, New York, 1957, pp. 174, 181.
8. K. S. PITRE and V. K. CHITALE, "Abstract : Convention of Chemists, 1980", Indian Chemical Society, Calcutta, Anal. 11.
9. C. R. ESTEE and G. GLOCKER, *J. Am. Chem. Soc.*, 1948, 70, 1344.
10. K. S. PITRE and V. K. CHITALE, "Abstract : Convention of Chemists, 1979", Indian Chemical Society, Calcutta, Anal. 5.
11. L. MEITES, "Polarographic Technique", 2nd ed., Interscience, New York, 1965, pp. 224-228.
12. J. J. LINGANE, *Chem. Rev.*, 1941, 29, 1.
13. K. B. YATSIMIRSKII and V. P. VASILEV, "Instability Constants of Complex Compounds", Pergamon Press, New York, 1960, p. 60.

Thermal Decomposition of $CeCl_3.7H_2O$

INDU B. SHARMA*, S. BATRA, SAROJ BALLA and R. K. GUPTA

Department of Chemistry, University of Jammu, Jammu-180 001

Manuscript received 19 April 1984, revised 19 September 1985, accepted 31 March 1986

A number of hydrates of cerium chloride including the heptahydrate cerium chloride ($CeCl_3.7H_2O$) are known to exist[1]. On heating, cerium chloride is reported to lose water followed by HCl. The present investigation deals with the study of the thermal decomposition of $CeCl_3.7H_2O$, both isothermal and non-isothermal to understand the nature of coordination of water molecules and the identity of the ultimate decomposition product. The final decomposition product has been analysed by *X*-ray diffractometry.

Experimental

$CeCl_3.7H_2O$ (G.R., E. Merck, 98.5%) was used without further purification. For the isothermal study, a known amount of the compound (500 mg)

was heated at constant temperatures, 393, 413 and 433 K with ±0.2 K variation in a manually operated thermo-balance and loss in weight was observed. Simultaneous thermal analysis (DTA, TG and DTG) was carried out with a Paulik-Paulik-Erdey MOM derivatograph. The curves were recorded at a heating rate of 10 K/min, while the weight of the sample taken was 100 mg. The identity of the final product was established by *X*-ray diffraction study.

Results and Discussion

Thermoanalytical studies: The simultaneous DTA-TG-DTG curves of $CeCl_3.7H_2O$ at the heating rate of 10 K/min in the static air atmosphere are given in Fig. 1. The thermal changes can be

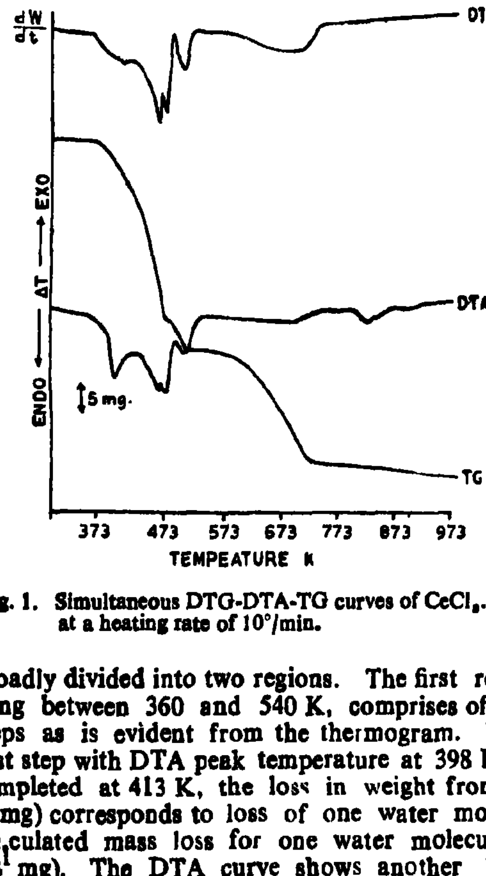


Fig. 1. Simultaneous DTG-DTA-TG curves of $CeCl_3.7H_2O$ at a heating rate of 10°/min.

broadly divided into two regions. The first region, lying between 360 and 540 K, comprises of four steps as is evident from the thermogram. In the first step with DTA peak temperature at 398 K and completed at 413 K, the loss in weight from TG (5 mg) corresponds to loss of one water molecule (calculated mass loss for one water molecule is 4.8 mg). The DTA curve shows another broad endothermic peak in the region lying between 443 and 488 K. This broad peak is resolved into two endotherms, which suggests two seperate transitions occuring in the region, with peak temperatures at 463 and 473 K. The total weight loss as calculated from the TG curve, corresponding to these temperatures, is 20.5 and 5 mg, showing the loss of four and one water molecules at these steps, respectively. The TG curve emphasises that the first two changes corresponding to the 398 and 463 K peak temperatures do not lead to any stable product formation as the products continue losing weight with change in temperature while the third step (with peak temperature at 473 K) leads to a stable product over a small region of temperature. The fourth step in this region with the DTA peak temperature at 513 K is associated with 5 mg weight loss corresponding to the loss of another water molecule resulting in the complete dehydration.

In the second DTA region with broad endothermic zone lying between 545 and 730 K, the weight loss as calculated from the TGA is 0 mg which corresponds to the decomposition of the sample to CeO_2. The d values and their relative intensities as calculated from the room temperature *X*-ray diffraction studies of the sample drawn at 730 K are given in Table 1. These values when compared with the known values for CeO_2 show that the product formed is CeO_2 (Ref. 2). The DTA curve of the product exhibits a phase transformation at 825 K without any loss of weight as is evident from the TG and DTG curves. The room temperature *X*-ray diffraction study of the product of the phase transformation shows that it is again CeO_2, showing that the process of transformation is reversible.

TABLE 1—*X*-RAY DIFFRACTION DATA OF THE PRODUCT OF THERMAL DECOMPOSITION OF $CeCl_3.7H_2O$ AT 730 K AND THE REPORTED DATA FOR CeO_2

Decomposition product		Reported data for CeO_2	
d, Å	Intensity	d, Å	Intensity
3.119	100	3.124	100
2.699	40	2.706	29
1.912	58	1.913	51
1.631	44	1.632	44
1.563	9	1.562	5
1.353	7	1.353	5
1.241	14	1.241	15
1.210	9	1.210	6
		1.104	12
		1.041	9
		0.957	5
		0.915	13
		0.902	7
		0.856	7
		0.825	6
		0.816	5

Isothermal studies: The DTA shows that the first endothermic change is completed at 433 K. To study the mechanism of the process, loss in weight of $CeCl_3.7H_2O$ at 393, 413 and 433 K at different intervals of time was measured and the results are plotted in Fig. 2. The samples attained constant weight after 60, 45, and 30 min at 393, 413 and 433 K, respectively. The kinetic data obey the Avrami-Erofeev equation[3,4] in the form, $-\log(1-\alpha) = (kt)^{1/n}$, where α is the fraction of the reaction completed at any time t. Applicability of the equation is shown in Fig. 3, where

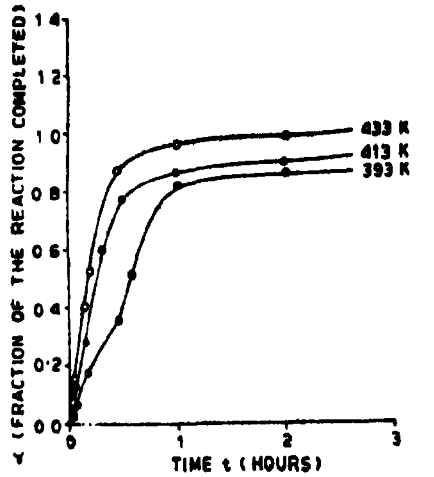


Fig. 2. Plots of α (fraction of the reaction completed) *vs* time t at various temperatures for the isothermal decomposition of $CeCl_3.7H_2O$.

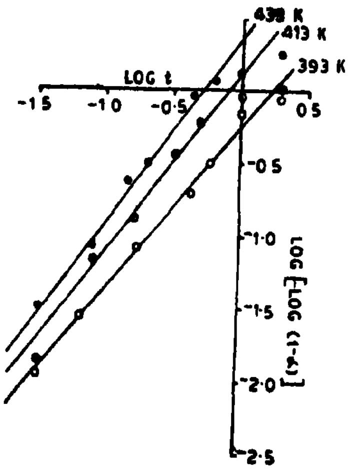


Fig. 3. Plots of log-log (1–α) *vs* time t for the isothermal decomposition of $CeCl_3.7H_2O$.

log-log (1 – α) is plotted *vs* log t. The energy of activation, as calculated from the Arrhenius plots, comes out to be 14 kcal mol^{-1}. The applicability of the Avrami-Erofeev equation suggests that in these dehydration steps complete random nucleation of the product occurs first, followed by the growth of the nuclei in three dimensions.

Mechanism of dehydration : The specific reaction rate constant values at different temperatures for the various changes in DTA were calculated from the Borchordt and Daniels first order equation[6],

$$k = \frac{\Delta T}{A - a}$$

where, ΔT is the difference in temperatures between the sample and the reference materials (peak height). A is the total area of the curve and a is the area of the curve at any temperature T. The energies of activation as calculated from the plots of log k *vs* 1/T are 36, 59, 55, 55, and 18 kcal mol^{-1} for the changes corresponding to the peak temperatures of 398, 463, 473, 513 and 683 K, respectively. The energy of activation for the phase transformation process in CeO_2 is 17 kcal mol^{-1}.

The order of the reaction (n) was calculated from the thermogravimetric results by applying the Horowitz-Metzger equation[6],

$$C_s = (n)^{\frac{1}{1-n}} = \frac{W_s - W_f}{W_0 - W_f}$$

where, W_s is the weight of the substance at the peak temperature, W_0 is the initial weight and W_f is the final weight of the sample. The values of the order of the reaction for the various changes corresponding to the DTG peak temperature 403, 463, 473, 513 and 683 K are 0.7, 0.5, 0.7, 0.5 and 0.6, respectively. The Coats Redfern equation[7,8],

$$\log \frac{C^{-1}}{T^2} = \log \frac{2R}{\phi E}\left(1 - \frac{2RT}{E}\right) - \frac{E}{2.303RT}$$

was applied to determine the energy of activation from TGA,

where, $C^{-1} = \log\left(\frac{W_{oc} - W}{W_{oo}}\right)^{-1}$, and W_{oo} = total mass loss for the particular stage, W = mass loss at temperature T, Z = pre-exponential factor, R = gas constant and ϕ = heating rate in Ks^{-1}. The energies of activation, calculated by plotting log C^{-1}/T^2 *vs* 1/T, corresponding to the DTG peak temperatures given above were found to be 30, 38, 90, 61 and 16 kcal mol^{-1}, respectively. The values of the energy of activation as calculated from the TG data when compared with the corresponding values from DTA show fair agreement except for the second and third steps of dehydration. The discrepancy is due to the fact that the two steps lack sharp transition. These transitions are almost continuous, which is substantiated by the TGA, where mass losses for the steps are continuous, and the DTA, where these are part of a broad endothermic region.

The loss of water molecules in different stages suggests that the nature of their bonding is different. The first two stages in which five water molecules are lost exhibit comparatively lower energy of activation. The energies of the activation for the loss of the sixth and seventh molecules are comparatively higher and this suggests that these water molecules are structurally bound. However, the decomposition process, where $CeCl_3$ decomposes to CeO_2, exhibits low energy of activation both in the DTA and TGA.

References

1. J. W. MELLOR, "A Comprehensive Treatise on Inorganic and Theoretical Chemistry", Longmans Green, London, 1952, Vol. V, p. 639.

2. "X-ray Diffraction Data Card no. 4-0591, Powder Diffraction File, International Centre for Diffraction Data, Pennsylavania, 1979.
3. A. AVRAMI, *J. Chem Phys.*, 1941, 9, 177.
4. B. V. BROFSEV, *Compt. Rend. Acad. Sci. URSS*, 1946, 52, 511.
5. H. J. BORCHARDT and F. DANIELS, *J. Am. Chem. Soc.*, 1957, 79, 41.
6. H. H. HOROWITZ and G METZGER, *Anal. Chem.*, 1963, 35, 1964.
7. A. W. COATS and J. P. REDFERN, *Nature (London)*, 1964. 201, 68.
8. W. W. WENDLANDT, "Thermal Methods of Analysis", John Wiley, New York, 1974, p. 48.

Conductivity of Electrolytes in Dioxane-Water Mixtures at different Temperatures

P. P. MISRA, N. C. DAS and P. B. DAS*

Department of Chemistry, Ravenshaw College, Cuttack-753 003

Manuscript received 7 November 1979, revised 7 March 1986, accepted 2 April 1986

A substantial body of data on the conductances of ions in many aquoorganic solvents, like propylene carbonate, trifluoroethanol, sulpholane, DMSO, DMF and acetone *etc.*[1] have recently been reported. But no study on the conductance of electrolytes in dioxane-water mixtures is reported as yet, although dioxane is a good solvent having a dielectric constant 2.5 at 25°. In the present communication, the conductivity of KCl, KBr, KNO_3, $KBrO_3$, KIO_3, K_2SO_4, NaCl, NaBr, $NaNO_3$, $NaBrO_3$, $NaIO_3$ and Na_2SO_4 at 10, 20 and 30 wt % of dioxane and at 30, 35, 40 and 45° ±0 1°, have been studied. The study gives information regarding the ion-solvent interactions from the mobilities and Walden product of the ions in the solvent. Assumption of Stoke[2] relating Walden product $\Lambda^\circ\eta_0$ with the radii of the anions has been employed to estimate the single ion mobilities and ionic Walden product.

Experimental

The salts and dioxane used were of E. Merck (extra pure) quality. Preparation of the solvents, solutions and conductance measurements were the same as described earlier[3]. The conductance measured was accurate up to ±2 in 1000. The concentration range for uniunivalent salts from 0.01 to 0 001 and for unibivalent salts from 0.02 to 0 002 mol dm^{-3}.

Results and Discussion

The Debye-Hückel-Onsager conductance equation is found to be valid as the plot of Λ *vs* $C^{1/2}$ is linear and the theoretical slope, $(A+B\ \Lambda^\circ)$ differs from that of the observed one by only 2%. The Λ° values has been obtained from the extra-polated

TABLE 1—IONIC WALDEN PRODUCT $(\lambda^\circ_i\ \eta_0)/\Omega^{-1}\ cm^2\ P$

Temp. °C	Wt % dioxane anion when paired with K^+	10	20	30	Anion when paired with Na^+	10	20	30
30	Cl^-	0.65	0.63	0.63	Cl^-	0.63	0.63	0.63
35		0.63	0.65	0.62		0.61	0.63	0.63
40		0.66	0.65	0.64		0.63	0.63	0.63
45		0.66	0.64	0.65		0.61	0.63	0.63
30	Br^-	0.60	0.58	0.59	Br^-	0.57	0.57	0.58
35		0.58	0.59	0.58		0.56	0.56	0.58
40		0.62	0.61	0.59		0.56	0.58	0.58
45		0.59	0.59	0.60		0.56	0.55	0.57
30	NO_3^-	0.56	0.53	0.54	NO_3^-	0.53	0.53	0.53
35		0.53	0.56	0.53		0.50	0.53	0.54
40		0.56	0.56	0.54		0.52	0.51	0.53
45		0.55	0.54	0.55		0.52	0.50	0.52
30	BrO_3^-	0.47	0.44	0.45	BrO_3^-	0.42	0.43	0.44
35		0.45	0.46	0.40		0.43	0.42	0.44
40		0.49	0.49	0.44		0.42	0.44	0.43
45		0.46	0.44	0.45		0.43	0.41	0.42
30	IO_3^-	0.57	0.54	0.55	IO_3^-	0.53	0.53	0.54
35		0.55	0.55	0.53		0.52	0.53	0.54
40		0.55	0.59	0.55		0.52	0.54	0.54
45		0.56	0.54	0.55		0.53	0.52	0.53
30	SO_4^{2-}	0.84	0.80	0.67	SO_4^{2-}	0.81	0.79	0.66
35		0.81	0.82	0.78		0.80	0.78	0.66
40		0.83	0.81	0.79		0.79	0.77	0.78
45		0.83	0.80	0.80		0.80	0.77	0.78
30	K^+	0.70	0.71	0.70	Na^+	0.62	0.61	0.60
35		0.71	0.69	0.70		0.63	0.62	0.60
40		0.69	0.69	0.70		0.62	0.61	0.60
45		0.70	0.71	0.69		0.62	0.61	0.61

*Present address : Director, State Forensic Science Laboratory, Rasulgarh, Bhubaneswar-751 010.

values at zero concentration. Λ° has also been obtained by Fuoss and Kraus's and Shedlovsky's methods[4]. But the Λ° values are almost the same. The Walden product is almost constant at all temperatures and at all solvent compositions. This constancy is presumably due to the contribution of the positive temperature coefficient of the conductivity with the negative temperature coefficient of the viscosity of the solvent. Hence, it is very difficult to predict about the structure breaking or promoting nature in the solvent, with in the temperature range studied.

The Walden product[5] may be given by the equation,

$$\Lambda^\circ\eta_0 = (\lambda^\circ_+ + \lambda^\circ_-)\eta_0 = \frac{eF}{6\pi}\left(\frac{1}{r_+}+\frac{1}{r_-}\right)$$

where, e is the electronic charge of the ion, F the force acting on the particle, and r_+ and r_- are the radii of the cation and anion, respectively. Ionic Walden products, $\lambda^\circ_+\eta_0$ and $\lambda^\circ_-\eta_0$ for the individual ions and hence the single ion mobilities were, therefore, estimated by plotting $\Lambda^\circ\eta_0$ *vs* the inverse of the radii of the anions[6]. Linear relations were found to exist at all solvent compositions and at all temperatures. By extrapolating the straight line to $1/r_- = 0$, $\lambda^\circ_+\eta_0$ for K^+ and Na^+ were estimated. Then on subtracting these values from $\Lambda^\circ\eta_0$, the values of $\lambda^\circ_-\eta_0$ for Cl^-, Br^-, NO_3^-, BrO_3^-, IO_3^-, SO_4^{2-} were evaluated (Table 1). It is evident that the values of $\lambda^\circ_-\eta_0$ of the same anions are different when paired with K^+ and Na^+. This indicates that the spheres of solvation of Na^+ and K^+ are not equally affected.

TABLE 2—IONIC MOBILITIES λ_i-Ω^{-1} cm^2 (AT 35° ONLY)

(K⁺)				(Na⁺)			
Cl^-	73.11	61.65	53.57	Cl^-	68.78	60.65	52.57
Br^-	67.31	57.73	49.32	Br^-	64.40	54.80	48.34
NO_3^-	61.51	54.80	45.07	NO_3^-	57.53	51.84	44.92
BrO_3^-	50.74	54.10	34.02	BrO_3^-	48.33	41.09	33.42
IO_3^-	62.01	53.82	45.07	IO_3^-	59.84	51.86	44.92
SO_4^{2-}	93.21	80.24	66.33	SO_4^{2-}	92.06	76.32	56.13
K_s^+	80.05	67.52	60.38	Na^+	72 50	60.67	51.02

K^+ = 74.93 and Na^+ = 51.52 at 25° (Ref. 7).

Then, on dividing the respective ionic Walden products by the viscosity of the solvent, mobility of each ion was estimated. Only the data at 35° are given for illustration. Table 2 shows that the limiting equivalent conductances of all the anions have greater magnitude when paired with K^+ and less in case of Na^+. The lesser mobilities may be interpreted as a measure of ion-solvent interaction. Table 2, therefore, suggests that following order of ion-solvent interaction exists in dioxane-water mixtures: $BrO_3^- > NO_3^- > IO_3^- > Br^- > Cl^- > SO_4^{2-}$ and $Na^+ > K^+$.

References

1. R. L. BLOKHRA and Y. P. SUHGEL, *J. Indian Chem. Soc.*, 1978, 55, 497.
2. D. A. MCINNES, "The Principle of Electrochemistry", Dover, New York, 1961.
3. N. C. DAS and P. B. DAS, *Electrochim. Acta*, 1978, 23, 191.
4. N. C. DAS P. P. MISRA and P. B. DAS, *Acta Ciencia Indica*, 1979, 95, 136.
5. P. WALDEN, *Z. Phys. Chem.*, 1906, 55, 206.
6. P. P. MISRA and P. B. DAS, *Experientia*, 1979, 35, 457.
7. H. S. HAMED and B. B. OWEN, "Physical Chemistry of Electrolytic Solution", Reinhold, New York, 1953.

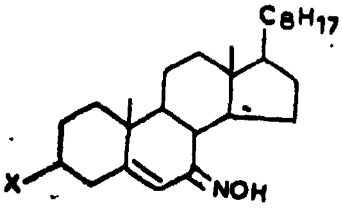
BF_3-catalysed Beckmann Rearrangement of Steroidal unsaturated Ketoximes

SHAFIULLAH and JAVED A. ANSARI*

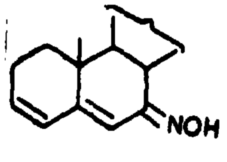
Steroid Research Laboratory, Department of Chemistry, Aligarh Muslim University, Aligarh-202 001

Manuscript received 2 April 1985, revised 31 October 1985, accepted 23 April 1986

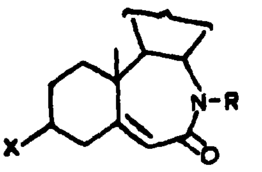
BF_3-catalysed Beckmann rearrangement of α,β-unsaturated steroidal ketoxime is reported to afford an unusual product in addition to usual amide[1]. This together with our earlier studies[2,3] promted us to undertake the Beckmann rearrangement of 3β-chlorocholest-5-en-7-one oxime (1), its 3β-acetoxy analogue (2) and cholesta-3,5-dien-7-one oxime (3). Contrary to our expectation, the reaction followed the usual course and afforded lactams and in some cases their N-acyl derivatives.



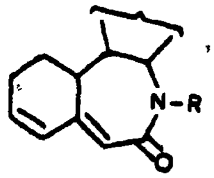
1; X = Cl
2; X = OAc



3



4; X = Cl, R = H
6; X = OAc, R = Ac
7; X = OAc, R = H



5; R = H
8; R = H

The oxime (1) on treatment with BF_3-etherate in acetic anhydride afforded 3β-chloro-7a-aza-B-homocholest-5-en-7-one (4) and 7a-aza B-homocholesta-3,5-dien-7-one (5). On similar treatment, the oximes 2 and 3 gave the corresponding lactams (7 and 5) and the N-acyl derivatives (6 and 8), respectively. The structures of these compounds were established on

the basis of microanalysis, spectral data (uv, ir, pmr) and comparison with authentic samples in known cases.

Experimental

All melting points were observed on a Koflar apparatus and are uncorrected. Ir spectra were obtained in KBr with a Pye-Unicam SP3-100 spectrophotometer. Uv spectra were recorded on a Pye-Unicam PU-8800 spectrophotometer. Pmr spectra were run in CCl_4 on a Varian A60 instrument with Me_4Si as the internal standard.

Beckmann rearrangement of the oxime 1 ; A suspension of the oxime 1 (2.0 g) in acetic anhydride (15 ml) was treated with BF_3-etherate (5 ml) during a period of 15 min with mechanical stirring. The dark solution thus obtained was kept for 1 h at 10-15° and then at room temperature overnight. The mixture was poured into 50 ml of chilled water. The resulting oily material was extracted with ether and washed with water, sodium bicarbonate solution (5%) and again with water. The organic layer was dried over sodium sulphate (anhydrous) and evaporated to dryness. The oily residue was chromatographed over silica gel (40 g). Elution with petroleum ether-ethyl acetate (7 : 1) afforded 4 which was recrystallised from methanol (0.9 g, 45%), m.p. 171° (lit.[5] 171°) (Found : C, 74.70 ; H, 10.11 ; N, 3.20. $C_{27}H_{44}$NOCl calcd. for : C, 74.74 ; H, 10.15 ; N, 3.23%).

Further elution with petroleum ether-ethyl acetate (3 : 1) gave 5, which was recrystallised from methanol (0.75 g, 37.5%), m.p. 170° (lit.[5] 170-71°) (Found : C, 81.61 ; H, 10.79 ; N, 3.50. $C_{27}H_{45}NO$ calcd. for : C, 81.61 ; H, 10.83 ; N, 3.52%).

Beckmann rearrangement of the oxime 2 : The oxime 2 (2.0 g) on treatment with BF_3-etherate (5 ml) in acetic anhydride (15 ml) afforded two products on tlc. After usual work up of the reaction mixture, the oily residue was chromatographed over silica gel (40 g). Elution with petroleum ether-ethyl acetate (10 : 1) provided 6 which was recrystallised from methanol (0.65 g, 32.5%), m.p. 103° (Found : C, 74.51 ; H, 9.80 ; N, 2.80. $C_{31}H_{49}NO_4$ calcd. for : C, 74.55 ; H, 9.82 ; N, 2.80%) ; λ_{max} (CH_3OH) 223 nm ; ν_{max} (KBr) 1 740 (CH_3COO), 1 690 (CO—N), 1 670, 1 620 (C=C—CO—N), 1 240 and 1 040 cm^{-1} (C—O) ; δ (CCl_4) 6.0 (1H, s, C_6-H), 4.55 (1H, mc, C_3-αH), 3.25 (1H, m, C_8-H), 1.98 (3H, s, CH_3COO), 1.85 (3H, s, CH_3CO), 1.12 (3H, s, C_{10}-CH_3), 0.80 (3H, s, C_{13}-CH_3), 0.98 and 0.96 (remaining methyl protons).

Continued elution with petroleum ether-ethyl acetate (4 : 1) furnished 7 which was recrystallised from petroleum ether (0.9 g, 45%), m.p. 196° (lit.[6] 197-98°) (Found : C, 75.97 ; H, 10.26 ; N, 3.05. $C_{29}H_{47}NO_3$ calcd. for : C, 76.15 ; H, 10.28, N, 3.06%).

Beckmann rearrangement of the oxime 3 : The reaction of the oxime 3 (2.0 g) with BF_3-etherate (5 ml) in acetic anhydride (15 ml) was carried out as described above. The residue was chromatographed over silica gel (40 g). Elution with petroleum ether-ethyl acetate (8:1) afforded 8 which was recrystallised from methanol (0.8 g, 40.0%), m.p. 123° (Found : C, 79.26 ; H, 10.24 ; N, 3.18. $C_{29}H_{45}NO_2$ calcd. for : C, 79.27 ; H, 10.25 ; N, 3.19%) ; λ_{max} (CH_3-OH) 272 nm ; ν_{max} (KBr) 1 695 (CO—N), 1 670 and 1 610 cm^{-1} (C=C—CO—N) ; δ (CCl_4) 6.0 (2H, br s, C_3-H and C_4-H), 5.58 (1H, s, C_6-H), 3.3 (1H, m, C_8-H), 2.07 (3H, s, CH_3CO), 1.12 (3H, s, C_{10}-CH_3), 0.74 (3H, s, C_{13}-CH_3), 0.83, and 0.91 (other methyl protons).

Continued elution with petroleum ether-ethyl acetate (3 : 1) gave the product 5 which was recrystallised from methanol (0.7 g, 35.0%), m.p. 170° (lit[5]. 170-71°).

Acknowledgement

The authors thank Prof. M. S. Ahmad, Chairman, Department of Chemistry, for facilities. One of the authors (J.A.A.) is thankful to U.G.C., New Delhi, for financial assistance.

References

1. J. ROMO and A. ROMO-DE-VIVAR, *J. Am. Chem. Soc.*, 1959, 81, 3446.
2. M. S. AHMAD, SHAFIULLAH and ISLAMUDDIN, *Indian J. Chem.*, 1974, 12, 1323.
3. SHAFIULLAH and ISLAMUDDIN, *Acta Chim. Acad. Sci. Hung.*, 1979, 10, 319.
4. C. W. SHOPPEE, G. KRUGER and R. N. MARRINGTON, *J. Chem. Soc.*, 1962, 1050.
5. M. S. AHMAD and A. H. SIDDIQUI, *Aust. J. Chem.*, 1968, 21, 1371.
6. M. S. AHMAD and A. H. SIDDIQUI, *Indian J. Chem.*, 1968, 6, 403.

Synthesis of some Di-, Tri- and Tetra-peptides containing Methionine, Valine and Glycine

A. M. EL-NAGGAR*, M. R. ZAHER and F. A. KORA

Chemistry Department, Faculty of Science, Al-Azhar University, Nasr-City, Cairo, Egypt

Manuscript received 18 November 1983, accepted 23 April 1986

METHIONINE is frequently present in biologically active polypeptides, *e.g.* ACTH, MSH, bradykinin and eledoisin[1,2]. Recently, we have reported the synthesis of *N*-tosylamino acids and dipeptide derivatives and some compounds were found to display antimicrobial activities[3-5]. In view of the above observations and in continuation of our studies in the same field[3-5], we synthesised a new series of *N*-tosyl-di-, -tri- and -tetra-peptides (3-33) containing methionine, valine, and glycine

with different sequences. The synthetic peptides (3-33) are necessary intermediate compounds for subsequent synthesis of higher peptides analogous to some antibiotics and other pharmacologically active compounds. The biological activity of the synthesised peptides (3-33) and their copper(II) complexes has been studied.

L-Methionine methyl ester hydrochloride (1) was prepared using the thionyl chloride method and obtained in higher yield (90%) than that reported earlier[6,7]. The synthesis of methionyl- and methionine-peptides was achieved by the application of HCl, L-Met-OMe (1) and Tos-L-Met (2) *via* the DCC method and no side reaction was observed. *N*-Tosyldipeptide methyl esters (3-9) were prepared in good yields (55-73%) using DCC. Treatment of these dipeptide methyl esters with methanol saturated with ammonia afforded the desired *N*-tosyldipeptide amides (10-13). However, it was observed that during the synthesis of Tos-L-Met-L-Met-NH_2 (10) a byproduct was isolated, which was recrystallised from methanol, (15%), m p. 221-23° (Found : N, 14.39. $C_{11}H_{21}N_3O_2S_2$ requires : N, 14.40%) ; R_f 0.31, $[\alpha]_D^{25}$ + 10.2 (C, 0.1 LMF) ; gave positive ninhydrin reaction and was identified as L-Met-L-Met-NH_2. The remaining *N*-tosyldipeptide amides (11-13) were chromatographically homogeneous and did not respond to ninhydrin reaction.

Hydrazinolysis of the methyl esters (3-9) in methanol or ethanol gave the corresponding *N*-tosyldipeptide hydrazides (14-20).

The reaction of Tos-Gly-Gly (22) with L-Met-OMe.HCl (1) and Tos-L-Met (2) with HCl. Gly-Gly-OMe (21) in the presence of DCC gave the corresponding tripeptides (23 and 24). Synthesis of *N*-tosyltripeptide methyl esters (25-29) was achieved starting from the hydrazides (14-20), which were converted into the corresponding dipeptide azides. The azides on coupling with amino acid methyl esters gave the tripeptide derivatives (25-29), which were easily isolated and purified. The protected tetrapeptides (32, 33) were prepared in 70-72% yield by the treatment of Tos-Gly-Gly-Gly (31) with HCl. L-Met-OMe (1), and Tos-L-Met (2) with HCl. Gly-Gly-Gly-OMe (1), and Tos-L-Met (2) with HCl. Gly-Gly-Gly-OMe (30) using DCC.

The dipeptide methyl esters (3-9) containing L-methionine as the N- or C-terminal amino acid in the dipeptide gave deep blue coloured 1 : 1 complexes with Cu^{II} (λ_{max} 620-640 nm). The dipeptide amides (10-13) gave deep violet coloured 1 : 1 complexes with Cu^{II} (λ_{max} 560-575 nm). Similarly, the dipeptide hydrazides (14-20) gave violet coloured 1 : 1 complexes with Cu^{II} (λ_{max} 560-575 nm). A comparison of the blue copper complexes of *N*-tosyldipeptide methyl esters with violet copper complexes of their corresponding dipeptide amides and dipeptide hydrazides strongly supports the view that the amide and hydrazide groups participate in the complex formation of dipeptide amides and dipeptide hydrazides of methionine. Similar observations have been reported by us[8-11] in the case of copper(II) complexes of di- and tri-peptide amides and hydrazides of serine, glycine, lysine and ornithine. The tripeptide methyl esters (23-29) gave pale violet or deep violet coloured 1 : 1 complexes with Cu^{II} (λ_{max} 560-570 nm). The tetrapeptide methyl esters (32, 33) gave red or reddish violet coloured 1 : 1 complexes with Cu^{II} (λ_{max} 540-550 nm).

From the above results, it is evident that the di-, tri-, and tetra-peptide methyl esters containing methionine form normal complexes with Cu^{II} as has been observed for di-, tri- and tetra-peptides of glycine and alanine[12]. However, in the case of dipeptide amides and dipeptide hydrazides, the amide and hydrazide groups participate in the complex formation.

The structures of 3 - 33 were assigned on the basis of elemental analyses, chromatographic studies, spot tests, ir and nmr spectra. The ir spectra of all the peptides displayed characteristic bands at 3 360, 3 280, 3 080 (NH, CONH, SO_2NH) ; 2 950, 2 860 (SCH_3) ; 1 650, 1560 (amide I, II and III) ; 1 760, 1 720 (C=O) ; 1 720, 1 440, 1 270 and 1 090 cm^{-1} (SO_2NH) in support of their structures. The nmr spectra of all *N*-tosyl-di-, -tri- and -tetrapeptides exhibit four aromatic protons in the range δ 7.6-8.41, three methyl (SCH_3) protons at 3.49 ; the NH amide proton at δ 5.64 and other protons assignable to aromatic and amino acid and peptide residues.

The peptides 3-20, 23-29, 32 and 33 have been prepared for the first time. Methods used for studying copper(II) complexes were the same as described earlier[8-11,13,14].

Biological screening: The antimicrobial activity of the peptides (3-33) was determined using the hole plate and filter paper disc methods[15-17]. Tos-L-Val-L-Met-OMe (7), Tos-L-Met-L-Met-N_2H_3 (20) and Tos-L-Met-Gly-Gly-OMe (24) were found to possess high antimicrobial activities against *Bacillus subtilis* (ICC-strain), *B. cereus* (NRRL-B-569) and *B. mycoids* (USSR) at minimal inhibitory concentration values ranging from 25 to 50 μg ml^{-1}, and inactive against *Escherichia coli* (NRRL-B-210), *Salmonella typhosa* (NRRL-B-573) and *Penicillium chrysogenum* (MIC 250-500 μg ml^{-1}). However, the remaining peptides were inactive at test concentrations (250-500 μg ml^{-1}). Other pharmacological studies are in progress.

Experimental

Samples for analyses were dried at 70°/10 mm over anhydrous P_2O_5 for 36 h. Melting points were determined on an electrothermal melting point apparatus and are uncorrected. All thin layer chromatograms (R_f value) were made on silica gel-G (B.D.H.) using n-butanol-pyridine-acetic acid-water (15 : 10 : 3 : 12) as solvent system and iodine-potassium iodide (20%) as detection reagent. Benzi-

TABLE 1—PHYSICAL DATA OF N-TOSYL-DI-, -TRI- AND -TETRA-PEPTIDES CONTAINING METHIONINE (3-33)†

Compd. no.	Peptide*	Yield** %	M.p. °C	R_f	Mol. formula	Elemental Analysis N %: Found	(Calcd.)	$[\alpha]_D^{25}$***
3	Tos-L-Met-Gly-OMe	60[a]	117–119	0.79	$C_{15}H_{22}N_2O_5S_2$	7.48	7.59	+35 (c, 0.1 A
4	Tos-L-Met-L-Val-OMe	73[a]	130–132	0.54	$C_{18}H_{28}N_2O_5S_2$	6.74	6.90	+40.5 (c, 0.3 A)
5	Tos-L-Met-L-Leu-OMe	67[b]	106–108	0.68	$C_{19}H_{30}N_2O_5S_2$	6.51	6.60	+22.7 (c, 0.1 A)
6	Tos-Gly-L-Met-OMe	59[c]	146–148	0.76	$C_{15}H_{22}N_2O_5S_2$	7.48	7.50	+47.5 (c, 0.1 A)
7	Tos-L-Val-L-Met-OMe	69[c]	119–121	0.75	$C_{18}H_{28}N_2O_5S_2$	6.74	6.82	+30.6 (c, 0.2 A)
8	Tos-L-Leu-L-Met-OMe	55[c]	83–85	0.72	$C_{19}H_{30}N_2O_5S_2$	6.51	6.55	+17.5 (c, 0.8 A)
9	Tos-L-Met-L-Met-OMe	58[c]	128–130	0.73	$C_{18}H_{28}N_2O_5S_3$	6.25	6.30	+80.5 (c, 0.2 B)
10	Tos-L-Met-L-Met-NH$_2$	48[a]	137–139	0.59	$C_{17}H_{27}N_3O_4S_3$	9.69	9.79	+ 7.3 (c, 0.2 B)
11	Tos-Gly-L-Met NH$_2$	70[a]	209–211	0.68	$C_{14}H_{21}N_3O_4S_2$	11.69	11.78	+ 9.8 (c, 0.2 B)
12	Tos-L-Val-L-Met-NH$_2$	67[d]	186–188	0.60	$C_{17}H_{27}N_3O_4S_2$	10.47	10.50	+19.3 (c, 0.3 A)
13	Tos-L-Leu-L-Met-NH$_2$	65[a]	219–221	0.64	$C_{18}H_{29}N_3O_4S_2$	10.12	10.23	+ 9.5 (c, 0.5 B)
14	Tos-L-Met-Gly-N$_2$H$_3$	75[d]	144–146	0.53	$C_{14}H_{22}N_4O_4S_2$	14.97	15.04	+22.6 (c, 0.4 C)
15	Tos-L-Met-L-Val-N$_2$H$_3$	79[d]	163–165	0.62	$C_{17}H_{28}N_4O_4S_2$	13.46	13.50	+28 (c, 0.6 C)
16	Tos-L-Met-L-Leu-N$_2$H$_3$	84[a]	193–195	0.54	$C_{18}H_{30}N_4O_4S_2$	13.02	13.12	+25.5 (c, 0.3 C)
17	Tos-Gly-L-Met-N$_2$H$_3$	69[d]	170–172	0.59	$C_{14}H_{22}N_4O_4S_2$	14.97	15.10	+18 (c, 0.7 A)
18	Tos-L-Val-L-Met-N$_2$H$_3$	81[d]	174–176	0.62	$C_{17}H_{28}N_4O_4S_2$	13.46	13.47	+41.5 (c, 0.9 C)
19	Tos-L-Leu-L-Met-N$_2$H$_3$	79[d]	149–151	0.56	$C_{18}H_{30}N_4O_4S_2$	13.02	13.08	+15 (c, 0.5 C)
20	Tos-L-Met-L-Met-N$_2$H$_3$	79[a]	202–204	0.49	$C_{17}H_{28}N_4O_4S_3$	12.50	12.58	+ 6.5 (c, 0.2 A)
23	Tos-Gly-Gly-L-Met-OMe	63[a]	200–202	0.93	$C_{17}H_{25}N_3O_6S_2$	9.74	9.89	+ 8.6 (c, 0.3 A)
24	Tos-L-Met-Gly-Gly-OMe	67[a]	222–224	0.89	$C_{17}H_{25}N_3O_6S_2$	9.74	9.76	+10.5 (c, 0.3 A)
25	Tos-Gly-L-Met-Gly-OMe	75[a]	129–131	0.90	$C_{17}H_{25}N_3O_6S_2$	9.74	9.85	+ 4.7 (c, 0.5 A)
26	Tos-L-Met-Gly-L-Met-OMe	74[a]	182–184	0.85	$C_{20}H_{31}N_3O_6S_3$	8.31	8.35	+20.5 (c, 0.6 B)
27	Tos-L-Met-L-Met-Gly-OMe	63[a]	123–125	0.86	$C_{20}H_{31}N_3O_6S_3$	8.31	8.39	+24.5 (c, 0.6 B)
28	Tos-Gly-L-Met-L-Met-OMe	68[a]	167–169	0.88	$C_{20}H_{31}N_3O_6S_3$	8.31	8.42	+30.8 (c, 0.3 B)
29	Tos-L-Met-L-Met-L-Met-OMe	63[a]	134–135	0.83	$C_{22}H_{35}N_3O_6S_4$	7.52	7.30	+52.5 (c, 0.2 B)
32	Tos-Gly-Gly-Gly-L-Met-OMe	72[a]	191–193	0.87	$C_{19}H_{28}N_4O_7S_2$	11.47	11.58	+23.6 (c, 0.6 B)
33	Tos-L-Met-Gly-Gly-Gly-OMe	70[a]	118–120	0.86	$C_{19}H_{28}N_4O_7S_2$	11.47	11.60	+72 (c, 0.2 A)

*Abbreviations are those proposed by IUPAC-IUB Commission on Biochemical Nomenclature, *J. Biol. Chem.*, 1970, **242**, 6489; 1975, **250**, 3215.

**Crystallisation solvent: [a]ethanol-water, [b]benzene-petroleum ether, [c]methanol-water, [d]absolute ethanol.

***Measured in the solvent: (A) = acetone, (B) = ethanol, (C) = DMF.

†Gave satisfactory C and H analyses.

dine, ninhydrin, silver nitrate and hydroxamate reactions were used for detection of amino acid and peptide derivatives on Whatman No. 1 paper chromatograms (spot reactions)[17]. Optical rotations were measured in acetone (A), ethanol (B) and DMF (C), on a Bellingham Stanley polarimeter using 1 dm tube at 25° The ir spectra (KBr) were recorded on a Unicam SP 1200 spectrophotometer, and the nmr spectra on a Varian T-60 A spectrophotometer and shifts reported (δ p.p.m.) relative to internal TMS.

HCl.L-Met-OMe (1) *and Tos L-Met* (2): The compounds were prepared by the procedures described earlier[6,18].

N-*Tosyldipeptide methyl esters* (3-9): *General procedure*: To a cold solution (0°) of HCl.L-Met-OMe (1) or any other amino acid methyl ester hydrochloride (0.013 mol) in THF (250 ml) was added Et$_3$N (1.5 ml) and the solution stirred for 30 min at 0°. The reaction mixture was cooled to −5° and Tos-L-Met (2) or any other tosylamino acid (0.011 mol) and DCC (2.06 g) were added to it successively and the mixture stirred for 3 h at 0°, left for 24 h in a refrigerator at 5°, and then for 24 h at room temperature. The precipitated dicyclohexylurea was filtered off and the filtrate treated with glacial acetic acid (0.5 ml) and set aside for 30 min at 20° to precipitate the dissolved dicyclohexylurea. It was filtered, the solvent removed *in vacuo* from the filtrate and the residue recrystallised from ethanol, methanol or their mixtures with water. The dipeptides (3-9) were soluble in DMF, dioxan, THF and alcohols, and insoluble in water and ether. All the dipeptide methyl ester (3-9) were homogeneous on tlc, responded positively to benzidine, and hydroxamate reactions and gave negative ninhydrin test.

N-*Tosyldipeptide amides* (10-13): *General procedure*: *N*-Tosyldipeptide methyl ester (6-9; 0.001 mol) was dissolved in methanol (150 ml) and the solution saturated with ammonia (0°). The saturated ammonia mixture was placed in a pressure-bottle and kept at room temperature for 48 h. The solvent was removed to dryness under reduced pressure and the residue recrystallised from ethanol, methanol or their mixtures with water. The resultant *N*-tosyl dipeptide amides (10-13) were soluble in DMF, nitromethane, THF and alcohols, and were chromatographically homogeneous (detection with iodine solution and benzidine).

N-*Tosyldipeptide hydrazides* (14-20): *General procedure*: *N*-Tosyldipeptide methyl ester (3-9; 0.013 mol) was dissolved in ethanol (200 ml) and hydrazine hydrate (85%, 0.035 mol) added to it. The reaction was left for 24 h at room temperature and for 12 h at 5°. The

precipitated hydrazide was filtered and washed several times with cold methanol and finally recrystallised from ethanol-water (1 : 1) mixture. The dipeptide hydrazides (14-20) were chromatographically homogeneous (detection with benzidine, iodine solution and silver nitrate) and gave negative hydroxamate reactions.

HCl.Gly-Gly-OMe (21) *and Tos-Gly-Gly* (22): The compounds were prepared by the procedures described earlier[19,20].

*Tos-Gly-Gly-*L*-Met-OMe* (23): It was prepared from Tos-Gly-Gly (22; 0.01 mol), HCl.L-Met-OMe (1, 0.011 mol) and DCC (0.01 mol) using the method described for the preparation of 3-9. The product was purified by repeated recrystallisation from ethanol-water to give chromatographically homogeneous 32 (detection with benzidine and hydroxamate reaction).

*Tos-*L*-Met-Gly-Gly-OMe* (24): Tos-L-Met (2; 0.01 mol) and HCl.Gly-Gly-OMe (30; 0.011 mol) were dissolved in THF (150 ml) containing Et_3N (3 ml). The mixture was cooled to −5°, DCC (3.5 g) added to it and the reaction mixture worked up as described for 32. The tripeptide 24 was chromatographically homogeneous (detection with benzidine and iodine solution).

N-*Tosyltripeptide methyl esters* (25-29): *General procedure*: *N*-Tosyldipeptide hydrazide (14-20; 0.006 mol) was dissolved in a mixture of acetic acid (8 ml), 5 *N* HCl (4 ml) and water (45 ml) and cooled to −5°. Sodium nitrite (0.53 g) in water (5 ml) was added to it and the mixture stirred for 5 min at −5°. The dipeptide azide was extracted with ethyl acetate (75 ml) and the extract washed successively with H_2O, 5% $NaHCO_3$ and water, and dried (Na_2SO_4). Compounds 25-29 were prepared by the addition of ethyl acetate solution of the azide to a cooled (−3°) solution of the free amino acid methyl ester (prepared from 0.01 mol of the amino acid methyl ester hydrochloride and 0.9 ml Et_3N as described earlier[11]) in ethyl acetate (25 ml), and keeping the reaction mixture for 24 h at 0° and for another 24 h at room temperature. It was washed successively with 0.5 *N* HCl, water, 5% $NaHCO_3$, water, and dried (Na_2SO_4). The solvent was removed and the residue recrystallised from ethanol, methanol or their mixtures with water. All tripeptide methyl esters (25-29) were found to be chromatographically homogeneous (detection with benzidine, iodine solution and hydroxamate reaction) and gave negative ninhydrin reaction.

HCl.Gly-Gly-Gly-OMe (30) *and Tos-Gly-Gly-Gly* (31): The compounds were prepared by the procedures described earlier[20,21].

*Tos-Gly-Gly-Gly-*L*-Met-OMe* (32): Tos-Gly-Gly-Gly (31; 0.005 mol) and HCl.L-Met-OMe (1; 0.0055 mol) were dissolved in THF (100 ml) containing Et_3N (1.5 ml). The reaction mixture was cooled to 0°, DCC (1.3 g, 0.005 mol) added to it and the mixture worked up as described for 23. The tetrapeptide (32) was purified by repeated recrystallisation from ethanol-water to give tlc-pure product. The tetrapeptide (32) was hydrolysed (6 *N* HCl, 100°, 24 h) followed by subsequent chromatography and the hydrolysate yielded two positive spots with ninhydrin corresponding to glycine and methionine.

*Tos-*L*-Met-Gly-Gly-Gly-OMe* (33): It was prepared from Tos-L-Met (2; 0.01 mol) and HCl.Gly-Gly-Gly-OMe (30; 0.011 mol) in THF (50 ml)-dioxan (30 ml) mixture using the method described for the prepartion of 24. The product was purified by recrystallisation several times from methanol and finally from ethanol-water. The tetrapeptide was chromatographically homogeneous (detection with benzidine, iodine solution and hydroxamate reactions). Complete acid hydrolysis of 33 gave similar results as reported for 32.

References

1. S. GUTTMANN and R. A. BOISSONNAS, *Helv. Chim. Acta*, 1959, 42, 1257.
2. E. SCHRODER and K. LUBKE, "The Peptides", Academic, New York, 1965, Vol. 1, p. 241.
3. A. M. EL-NAGGAR, A. F. EL-HADDAD, A. M. GOMMAA, M. F. BADIE and M. S. LATIF, *Acta Pharm. Jugosl.*, 1982, 32, 247.
4. A. M. EL-NAGGAR, A. F. EL-HADDAD, M. F. BADIE, M. S. LATIF and A. M. GOMMAA, *Afinidad*, 1983, 40, 379.
5. A. M. EL-NAGGAR, M. R. ZAHER and F. A. KORA, *Egypt. J. Chem.*, 1981, 24, 145
6. M. BRENNER and R. W. PFISTER, *Helv. Chim. Acta*, 1951, 34, 2085.
7. G. KUPRYSZEWSKI and T. SOKOLOWSKI *Acta Biochim. Pol.*, 1957, 4, 85.
8. A. M. EL-NAGGAR, *Egypt. J. Chem.*, 1973, 16, 229, 313.
9. A. A. EL-NAGGAR, Y. A. SHEHATA and M. R. ZAHER, *Roczniki Chemii*, 1977, 51, 233.
10. A. M. EL-NAGGAR, M. R. ZAHER, and F. A. KORA, *Egypt. J. Chem.*, 1980, 23, 994.
11. A. M. EL-NAGGAR, M. R. ZAHER and S. A. EL-GHAFFAR, *Indian J. Chem., Sect. B*, 1983, 22, 392.
12. M. I. PLEKHAN, *Zh. Obshch. Khim.*, 1951, 21, 313.
13. E. M. SALEM, A. M EL-NAGGAR and M. A. ZEWAIL, *J. Appl. Chem. Biotechnol.*, 1974, 24, 745.
14. A. M. EL-NAGGAR, M. R. ZAHER and A. M. ABDEL-SALAM, *J. Appl. Chem. Biotechnol.*, 1976, 26, 305.
15. H. J. CARLSON, *J. Bacteriol.*, 1948, 55, 607.
16. J. G. VINCENT and H. W. VINCENT, *Proc. Exptl. Biol.*, 1944, 55, 162.
17. A. M. EL-NAGGAR, F. S. M. AHMED and M. F. BADIE, *J. Heterocycl. Chem*, 1981, 18, 91.
18. B. G. BARRAS and D. T. ELMORE, *J. Chem. Soc.*, 1957, 3134.
19. H. N. RYDON and P. W. SMITH, *J. Chem. Soc.*, 1955, 2542.
20. A. M. EL-NAGGAR, M. R. ZAHER and S. A. EL-GHAFFAR, *Bull. Soc. Chim. (Beograd)*, 1982, 47, 253.
21. F. A. KORA, Ph.D. Thesis, Al-Azhar University, 1982.

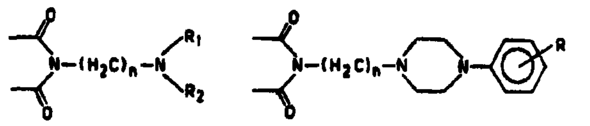
Synthesis and Pharmacology of some 2-[3-(4-Aryl-1-piperazinyl)propyl]-1*H*-benz[*de*]isoquinolin-1,3(2*H*)-diones/2,5-pyrrolidinediones

B. M. KHADILKAR and S. D. SAMANT*

Organic Chemistry Laboratory, University Department of Chemical Technology, Matunga, Bombay-400 019

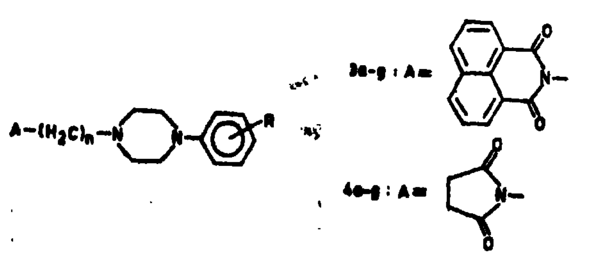
Manuscript received 5 July 1985, accepted 23 April 1986

OUR continued interest in ω-aminoalkylimides (1) led to the preparation of a number of *N*-[ω-(4-aryl-1-piperazinyl)alkyl]imides (2) and their pharmacological evaluation[1-3]. These compounds show varying degree of CNS depressant activity.



(1) (2)

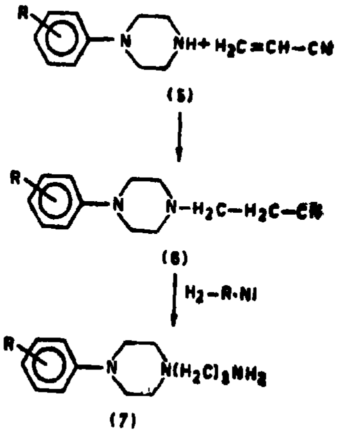
During these studies it was noted that the pharmacological activity was governed by the nature of the three moities present in the basic pharmacophore (1), namely, the imide part, the alkylene bridge and the terminal amine residue. It was found that the chain length of the alkylene bridge and the nature of the imide part were crucial for the activity. Propylene chain was ideal for the CNS depressant activity. Moreover, it is a known fact that lipophilicity—lipophobicity balance is one of the important parameters for the desired activity. Increase in the lipophilicity of a drug may increase the activity due to better crossing of the blood-brain barrier. With these things in mind, 2-[3-(4-aryl-1-piperazinyl) propyl]-1*H*-benz[*de*]isoquinolin-1,3-(2*H*)diones (3) which contained a bulky lipophilic naphthalimide as the imide part were prepared. Some similar naphthalimides have been recently reported to have antidepressant[4], antiinflammatory[4], local anaesthetic[5], cytostatic[6] and rhodenticidal[7] activities. Succinimide, being the simplest imide, a parallel series of 1-3-(4-aryl-1-piperazinyl)propyl-2, 5-pyrrolidine diones (4) was also prepared.

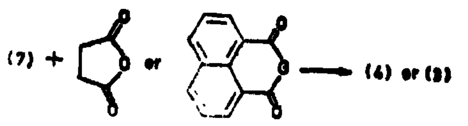


1-Substitutedphenylpiperazines (5) were heated with acrylonitrile to obtain 4-aryl-1-(2-cyanoethyl)-piperazines (6) which were reduced catalytically to the corresponding 4-aryl-1-(3-aminopropyl)piperazines[8] (7). 7 were subsequently condensed with the appropriate anhydrides to obtain the title compounds (3 and 4).

Pharmacology :

All the compounds showed mild sedative action in mice. However, it did not warrant further screening. These compounds, however, showed promising hypotensive activity. Cats of either sex, weighing between 2.5-4 kg were anaesthetised by i.p. injection of urethane (400 mg/kg) and chloralose (50 mg/kg). The trachea was exposed and cannulated. The cannula was connected to Mary's Tambur for recording respiration. Left common carotid artery was cannulated and the cannula was connected to a mercury manometer for recording B.P. The test compounds were injected in the form of their aqueous solutions of their hydrochloride salts, i.v., at the dose of 0.5-1.0 mg/kg. All the compounds showed good hypotensive activity in normotensive cats and the onset of action was quick. 4 showed fall in B.P. of about 80-100 mm of Hg with duration of action about 30 min. 3 were found to lower the B P. by about 60-80 mm of Hg ; however, the duration of action was only about 5-10 min. Within each series variations in the activity with respect to the substitutents were marginal.





Experimental

All melting points reported are uncorrected. Ir spectra were recorded on a Beckmann Acculab-10 spectrophotometer. Pmr spectra were recorded on a Varian-60 spectrometer using TMS as the internal standard. 1-Arylpiperazines (5) were prepared by the Pollard method[8]. Reaction of 5 with acrylonitrile and subsequent reduction of the cyanocompounds (6) to the corresponding amine derivatives (7) is known[8].

1-[3-(4-(4-Methylphenyl)-1-piperazinyl)propyl]-2,5-pyrrolidinedione.HCl (4d) : 7d (2.32 g, 0.01 mol) and succinic anhydride (1.0 g, 0.01 mol) were refluxed in dry pyridine (30 ml) for 10 h. Acetic anhydride(5 ml) was added and the mixture was further refluxed for 5 h. The solution was concentrated *in vacuo* and the residue was taken in ethanol (50 ml). The solution was filtered and dry HCl gas was passed through the solution when the hydrochloride of the product separated out. The solution was cooled and filtered. The product was crystallised from ethanol (2.3 g, 60%), m.p. 221-22 ; ν_{max} (KBr) 1 690 and 1 760 cm^{-1} (CONCO) ; δ (D_2O) 2.0 (2H, m, $NCH_2CH_2CH_2N$), 2.22 (3H, s, $PhCH_3$), 2.64 (4H, s, $COCH_2CH_2CO$), 3.2-3.66 (12H, m, $N(CH_2CH_2)_2N$, $NCH_2CH_2CH_2N$) and 6.82-7.3 (4H, dd, *J* 9Hz, Ar*H*).

Compounds 4a-g were prepared similarly by condensing succinic anhydride with appropriate 7 (Table 1).

TABLE 1—1-[3-(4-SUBSTITUTED-PHENYL-1-PIPERAZINYL)-PROPYL]-2,5-PYRROLIDINEDIONES.HCl (4)*

Compd. no.	R	Yield %	M.p. °C
4a	H	65	237-38
4b	2-CH_3	58	217-18
4c	3-CH_3	58	245-46
4d	4-CH_3	60	221-22
4e	2-Cl	55	198-99
4f	3-Cl	55	213-14
4g	4-Cl	59	238-39

* Showed satisfactory elemental analyses.

2-[3-(4-(4-Methylphenyl)-1-piperazinyl)propyl]-1H-benz[de]isoquinolin-1,3(2H)dione(3d) : 7d (2.32 g, 0.01 mol) and naphthalic anhydride (1.98 g, 0.01 mol) were heated in an oil-bath at 160-70° for 1 h. The mixture was cooled and the oily residue boiled in ethanol when a yellow solid separated. The solution was cooled and filtered. The residue was crystallised from CH_2Cl_2-petroleum ether (b.p 60-80°) (70 : 30, v/v), (2.7 g, 70%), m.p. 140-41° ; ν_{max} (KBr) 1 655 and 1 695 (CONCO) ; δ ($CDCl_3$) 1.9 (2H, m, $NCH_2CH_2CH_2N$), 2.25 (3H, s, $PhCH_3$), 2.56 (6H, m, $CH_2N(CH_2)_2$), 2.9 (4H, t, $ArN(CH_2)_2$), 4.22 (2H, t, $CH_2N(CO)_2$), 6.7 and 7.0 (4H, dd, *J* 8Hz, p-$CH_3C_6H_4$) and 7.5-8.6 (6H, m, naphth-*H*).

TABLE 2—2-[3-(4-SUBSTITUTED-PHENYL-1-PIPERAZINYL)-PROPYL]-1H-BENZ[de]ISOQUINOLIN-1,3-(2H)-DIONES (3)*

Compd. no.	R	Yield %	M.p. °C
3a	H	75	142-43
3b	2-CH_3	70	145-46
3c	3-CH_3	60	115-16
3d	4-CH_3	70	140-41
3e	2-Cl	65	150-51
3f	3-Cl	65	98-99
3g	4-Cl	69	143-44

* Showed satisfactory elemental analyses.

Compounds 3a-g were prepared similarly by condensing naphthalic anhydride with appropriate 7 (Table 2).

Acknowledgement

The financial support of U.G.C., New Delhi, under FAT to one of the authors (S.D.S.) is gratefully acknowledged. The authors are indebted to Dr. A. Y. Nimkar, Bombay College of Pharmacy, Bombay, for pharmacological help.

References

1. S. D. SAMANT and R. A. KULKARNI, *J. Indian Chem. Soc.*, 1981, 58, 692.
2. S. D. SAMANT and R. A. KULKARNI, *J. Indian Chem., Soc.*, 1979, 56, 1002.
3. S. D. SAMANT and R. A. KULKARNI, *J. Indian Chem., Soc.*, 1978, 55, 819.
4. W. PETER and V. BERTHOLD, US Pat. 3 940 397/1976.
5. A. DA SETTIMO, G. PRIMOFIORE, O LIVI, I. TONETTI, N. TELLINI and P. BIANCHINI, *Farmaco Ed. Sic.*, 1982, 37, 105 (*Chem. Abstr.*, 1982, 96, 142671).
6. M. F. BRANA, A. M. SANZ, J. M. CASTELLANO, C. M. ROLDAN, and C. ROLDAN, *Eur. J. Med. Chem. Chim. Ther.*, 1981, 16, 207.
7. C. M. ROLDAN, B. M. FERNANDEZ and C. J. M. BERLANGA, Can. Pat. 1 030 147/1978.
8. C. B. POLLARD and L. G. MCDOWELL, *J Am. Chem. Soc.*, 1934, 56, 2199.
9. S. HAYAO and R. N. SHUT, *J. Org. Chem.*, 1961, 26, 3415.

Chemical Examination of *Nymphaea stellata* Willd.

K. S. MUKHERJEE*, P. BHATTACHARYA, R. K. MUKHERJEE
and
P. K. GHOSH**

Department of Chemistry, Visva-Bharati, Santiniketan-731 235

Manuscript received 18 October 1985, accepted 25 April 1986

NYMPHAEA stellata Willd. (Nymphaeaceae)[1-3], popularly known as *Chit-shaluk* or *Sapla*, grows abundantly in the hotter parts of India. The plant is medicinally very important and its flower has an acrid, cooling, bitter-sweetish taste and is used in removing impurities from the blood. A decoction of flowers is prescribed in the palpitation of heart. The powdered root-stock is used as body strengthening medicine, hair-tonic and in the treatment of dyspepsia, diarrhoea and piles. Survey of literature reveals that no phytochemical work seems to have been done on this plant. Accordingly, a chemical investigation of the aerial parts (leaves and stems) of this plant has been undertaken.

**Present address : Govt. Quinine Factory, Mungpoo, Darjeeling, West Bengal.

The air dried powdered aerial parts (leaves and stems) of *N. Stellata* Willd. was extracted successively with light petrol (b.p. 60-80°) and ethanol. The concentrated petroleum ether (b.p. 60-80°) extract was chromatographed over silica gel. Elution of the column with benzene afforded a solid, crystallised from methanol, m.p. 135-36°. It gave positive Leibermann-Burchardt test for sterol and was identified as β-sitosterol by comparative studies (m.m p. co-ir and co-tlc) with an authentic sample and through the preparation of acetate, m.p. 127-28°.

The concentrated ethanolic extract on chromatography over silica gel and on elution with ethyl acetate furnished a solid crystallised from methanol in fine plates, $C_{17}H_{19}O_3N$ (M^+285), m.p. 220-22°; ν_{max} (KBr) 3 250 (phenolic OH) and 3 400 cm^{-1} (NH); λ_{max} (EtOH) 281 (log ε 3.80) and 254 nm (log ε 2.68) similar to benzylisoquinoline alkaloids[3]; mass spectrum is typical of benzylisoquinoline type of alkaloids[4], significant peaks *m/e* 285 (M^+), 178 and 163. From the study of these data as well as from the formation of dimethyl ether derivative, m.p. 200°, on treatment with diazomethane, it was identified as coclaurine[5].

Acknowledgement

The authors are thankful to R.S.I.C., Bose Institute, Calcutta, for mass spectral analysis. Financial assistance from U.G.C., New Delhi, is also gratefully acknowledged.

References

1. R. N. Chopra, S. L. Nayar and I. C. Chopra, "Glossary of Indian Medicinal Plants", C. S. I. R., New Delhi, 1956, p 177.
2. K. R. Kirtikar and B. D. Basu, "Indian Medicinal Plants", 1933, Vol. 1, p. 113.
3. M. Sharma, "The Isoquinoline Alkaloids", Academic, New York, 1972. p. 83.
4. H. Budzikiewicz, C. Djerassi and D. H. Williams, "Structure Elucidation of Natural Products by Mass Spectrometry", 1964, Vol. 1, p. 173.
5. I. Heilbourn, A. H. Cook, H. M. Bunbury and D. H. Hey, 'Dictionary of Organic Compounds", Eyre and Spotiswoode, London, 1965, Vol. 2, p. 722.

Chemical Investigation of *Alysicarpus bupleurifolius* DC

RAKA JAIN* and R. K. GUPTA

Indian Grassland and Fodder Research Institute, Jhansi-284 001

Manuscript received 31 October 1985, accepted 23 April 1986

ALYSICARPUS bupleurifolius DC (Leguminosae) is an annual herb[1]. In India it occurs widely in the Himalayas ascending North West upto 1200 m in Kumaon. The plant has not been chemically examined so far. In view of its wide availability in Bundelkhand area and also an important forage legume[2], its phytochemical investigation was undertaken. Isolation and identification of a mixiture of hydrocarbons (C_{27}-C_{34}), aliphatic alcohols (C_{28}-C_{34}), β-sitosterol-D-glucoside, D (+)-pinitol and *meso*-inositol are reported here. The identity of the compounds was established on the basis of m.m.p. co-tlc, ir and mass spectra and comparison with authentic samples.

Experimental

The plant, collected from the Institute campus during August-September, was found to contain, crude protein 11.1%, calcium 1.36% and phosphorus 0.09%. Air dried, powdered aerial part of the plant was exhaustively extracted with ethanol (95%) and the combined extracts were concentrated *in vacuo* and fractionated with hexane-benzene, ethyl acetate and acetone.

Hexane fraction: It was chromatographed over a column of silica gel. Elution with different solvents and their mixtures yielded the following substances.

Hydrocarbons (C_{27-34}): Elution with hexane afforded a colourless waxy product, m.p. 65-67°. Ir spectrum indicated the presence of long chain n-alkanes[3]. It was analysed by glc us ng OV-1 column and temperature programming from 120 to 300° at 2°/min, injection temperature 250°, detector temperature 350°. A tentative carbon number was assigned to each peak on the basis of the retention time of standard alkane (C_{27}-C_{33}) and the use of parafilm[4]. It was also confirmed by field ionisation mass spectrum (fims)[5].

Alcohols (C_{28}-C_{34}): Futher elution with hexane-benzene (4 : 1) afforded a colourless waxy solid, m.p. 83-84°; ν_{max} (KBr) 3 400, 2 920, 2 850, 1 450, 1 375, 1 040, 740 and 720 cm^{-1}. Glc analysis showed it to be a mixture of mainly seven components. The eims showed a series of peaks at odd mass corresponding to $C_nH^+_{2n+1}$, $C_nH^+_{2n-1}$ and $C_nH_{2n+1}O^+$ ions and prominent event mass ion peaks at *m/z* 392, 406, 420, 434, 448, 462 and 478. These peaks corresponded to the molecular ions of the olefins produced by dehydration of the corresponding alcohols. Hence, the solid was shown to be a mixture of straight chain aliphatic alcohols. The field desorption mass spectrum (fdms)[6] of the solid confirmed the molecular weights as 410, 424, 438, 452, 466, 480 and 494. It formed an acetate ν_{max} (KBr) 2 900, 2 850, 1 730 ($OCOCH_3$), 1 460, 1 360, 1 240, 740 and 720 cm^{-1}. The fdms of the acetate mixture showed peaks at *m/z* 452, 466, 480, 494, 508, 522 and 536 which represented the molecular ions of the acetates of the respective alcohols. Thus from the above data, the waxy solid was found to be a mixture of straight chain aliphatic alcohols (C_{28}-C_{34}).

Benzene fraction :

β-Setosterol-D-glucoside, m.p. 300° (MeOH), $[\alpha]_D^{30°}$-43° ; tetraacetate (Ac_2O/Py), m.p. 166-67° ; acid hydrolysis furnished β-sitosterol (m.m.p. and co-tlc) and D-glucose (co-pc). The compound was shown to be identical with β-sitosterol-D-glucoside.

Acetone fraction :

It was chromatographed on silica gel column. Elution with different solvents and their mixture yielded two compounds : D(+)-Pinitol, m.p. 186°, identical (ms and ir) with an authentic specimen, pentacetate, m.p. 98° ; and meso-inositol, m.p. 218-219°, identical (ms and ir) with an authentic sample, hexaacetate, m.p. 215°.

Acknowledgement

The authors are thankful to Dr. K. P. Madhusudanan, C.D.R.I. for mass spectral analysis and helpfull discussions. Encouragement given by Dr. B. D. Patil is also gratefully acknowledged.

References

1. J. D. Hooker, "Flora of British India", L. Reeve and Co., London, 1879, Vol. II, p. 158.
2. *Biol Abstr*. 1949, 23, 29938.
3. J. R. Dyer, "Application of Absorption Spectroscopy to Organic Compounds", Prentice-Hall of India, New Delhi, 1978, p. 38.
4. P. Gaskin, J. MacMillen, R. D. Firn, R. J. Pryce, *Phytochemistry*, 1971, 10, 1155.
5. G. W. Wood, *Tetrahedron*, 1982, 38, 1125.

3-(*p*-Acetophenyl)-1-phenyltriazene-*N*-oxide. A New Reagent for Gravimetric Determination of Nickel(II) and Palladium(II) and their Separation from Binary Mixture

K. B. SARAN, B. C. ROY and S. LAHIRI*

Department of Chemistry, Jadavpur University, Calcutta-700 032

Manuscript received 11 May 1982, revised 25 February 1986, accepted 31 March 1986

THE so-called hydroxytriazene has been recently shown from ir spectra to exist predominently in the tautomeric *N*-oxide form[1]. Such ligands have been used both as analytical reagents and as complex former[2-7]. We recommend in this communication a new triazene derivative, 3-(*p*-acetophenyl)-1-phenyltriazene-*N*-oxide for the gravimetric determination of Ni^{II} and Pd^{II}. The reagent reacts with Ni^{II} and Pd^{II} quantitatively in the *p*H ranges, 6-10 and 1.5-10, forming deep yellow, $Ni(C_{14}H_{12}O_2N_3)_2$ and buff coloured, $Pd(C_{14}H_{12}O_2N_3)_2$ complexes, respectively. The determinations of both the metal ions in the presence of large number of foreign ions and from their binary mixture have been described.

Experimental

3-(p-Acetophenyl)-1-phenyltriazene-N-oxide : T reagent was prepared by coupling phenylhydrox amine suspended in cooled acidified water w diazo salt of *p*-aminoacetophenone at 0°. The of the reaction mixture containing yellow pasty m was raised around 5 by saturated sodium acet solution and kept for 1 h. The light yell compound was recrystallised from hot ethan m.p. 158° (Found : N, 16.32 ; C, 65.60 ; H, 5.2 $C_{14}H_{13}O_2N_3$ requires : N, 16.47 ; C, 65.88 ; 5.10%).

Ni^{II} and Pd^{II} solutions : MCl_2 (E. Merck, M Ni or Pd) was dissolved in hydrochloric acid a the metal content was determined gravimetrica with dimethylglyoxime[8].

A Cambridge bench model *p*H meter was us to record the acidity of the solutions. Infrar spectra (nujol) were recorded in a Perkin-Elmer 1 spectrophotometer.

Procedure : Ni^{II} and Pd^{II} (3.0-40 mg) w precipitated from hot solutions (200 ml) using least 1.5 times the theoretical amounts of reagent warm ethanol (15 ml) at the *p*H range 6-10 a 1.5-10 respectively, adjusted by dilute sodiu hydroxide solution. The deep yellow Ni^{II}-compl and buff coloured Pd^{II}-complex were digested boiling water-bath for 30 min and filtered through weighed Gooch crucibles no. 4 and respectively, washed with hot water, dried 110-20° and weighed as $M(C_{14}H_{12}O_2N_3)_2$. T gravimetric factors for nickel and palladium 0.1036 and 0.1732, respectively.

The standard deviations for several determin tions of Ni^{II} and Pd^{II} (9.0 mg each) were fou to be ± 0.28 and ± 0.33%, respectively.

Separation and determination of Ni^{II} and Pd present in a binary mixture : Pd^{II} was first dete mined from the binary mixture (150-200 ml) at *p* 2.0 using reagent 3-4 times of the total metal io in the usual way. The volume of the filtrate a the washing was then reduced to 200 ml and N was determined following the procedure described.

Procedure in presence of diverse ions : Ni^{II} a Pd^{II}(9.0mg each) could be determined at *p*H 7.0 a 3.0, respectively in the presence of the followi foreign ions using tartrate (1.0-1.5 g) as maski agent : Al^{III}, Bi^{III}, As^{III} Ag^{I}, Pb^{II} and Sn^{I} 30 mg each ; Be^{II}, Zn^{II}, Mg^{II}, MoO_4^{2-}, WO_4^{2} VO_3^-, ZrO^{II}, HfO^{II}, Nb^{V}, Ta^{V}, Rh^{III}, Pt^{IV}, Cs and TiO^{II}, 50 mg each. However Fe^{III} (30 m Hg^{II} and Cd^{II} (50 mg each) and UO_2^{II} (50 m needed ascorbic acid plus phosphoric acid, pot assium iodide and ammonium acetate as the maski agents, respectively. Cr^{II}, Mn^{II}, Cu^{II} and Co donot interfere with the determination of Pd but with Ni estimation. Anions, such as F^- (500 m SCN^- (100 mg), AsO_4^{3-} (100 mg), BO_3^{3-} (100 m oxalate and citrate (100 mg each) and PO (200 mg) are tolerable in both the cases. Disodiu

EDTA and CN^- interfere. Even trace amount of Au^{II} interferes with Pd^{II} estimation.

Results and Discussion

The precipitations of Ni^{II} and Pd^{II} complexes commence at pH 5.0 and 1.0 and are quantitative within the pH ranges 6-10 and 1.5-10, respectively. At least 1.5 times the theoretical amounts of the reagent are needed for complete precipitation of metal ions. Ethanolic solution of the reagent was found stable for several weeks. The complexes are insoluble in water but soluble in organic solvents. Nickel and palladium complexes melt with decomposition at 253 and 285°, respectively. Analytical results indicate molecular formula, $M(C_{14}H_{12}O_3N_2)_2$.

Infrared spectral bands of the reagent at 1 670, 3 205 and 1 290 cm^{-1} are due to C=O, N–H and N–O stretching vibrations, respectively. In the spectrum of Ni^{II} or Pd^{II} complexes, the position of C=O band remains unchanged while N–H band disappears and a lowering in frequency of N–O band is observed, suggesting the bonding through N of N–H group after displacement of proton and through O of N–O group.

References

1. T. Mitsuhashi, Y. Osamura and C. Simamura, *Tetrahedron Lett.*, 1965, 30, 2593.
2. D. N. Purohit, *Talanta*, 1967, 14, 353.
3. N. R. Biswas, B. C. Roy and S. Lahiri, *J. Indian Chem. Soc.*, 1979, 56, 473.
4. K. B. Saran, B. C. Roy and S. Lahiri, *Indian J. Chem., Sect. A*, 1985, 24, 541.
5. N. M. Banerjee, B. C. Roy and S. Lahiri, *J. Indian Chem. Soc.*, 1984, 61, 617.
6. R. L. Dutta and R. Sharma, *J. Indian Chem. Soc.*, 1983, 60, 325.
7. S. Lahiri, N. R. Biswas and B. C. Roy, *J. Indian Chem. Soc.*, 1981, 58, 1138.
8. A. I. Vogel, "A Text book of Quantitative Inorganic Analysis", 3rd Ed., Longmans, London, 1961, pp. 511, 526.

Use of some Visual Indicators for Direct Titrations with Dibromamine-T

G. SOBHANA DEVI and P. INDRASENAN*

Department of Chemistry, University of Kerala, Trivandrum-695 034

Manuscript received 3 June 1985, revised 3 February 1986, accepted 3 March 1986

REDOX titrations in nonaqueous or partially aqueous media are, as a rule, followed potentiometrically. A search through the literature has revealed that the use of visual indicators for titrations in such media is very limited[1-7]. As part of our investigations on novel redox titrants, we explore the possibility of using some visual indicators for direct titrations with dibromamine-T, a typical oxidimetric titrant in aqueous acetic acid medium[8-11].

Experimental

Dibromamine-T (DBT) was prepared[8] by bromination of chloramine-T (B.D.H.). A decinormal solution (~0.025 *M*) of DBT was prepared by dissolving the dry sample (8.2 g) in anhydrous acetic acid (1 dm^3) and was standardised by the usual iodometric method and stored in an amber-coloured bottle. The six indicator solutions used for the titrations, *viz.*, amaranth, indigo carmine, methyl orange, methyl red, *p*-ethoxychrysoidine and quinoline yellow were prepared by dissolving the dye stuffs in appropriate solvents by standard methods[12]. Standard solutions (~0.1 *N*, 500 ml) of potassium antimony tartarate (8.1 g), sodium sulphite (8.2 g), ascorbic acid (4.4 g), hydrazine sulphate (1.6 g), benzhydrazide (2.7 g), isoniazid (1.7 g), phenylhydrazinehydrochloride (1.8 g), semicarbazidehydrochloride (1.4 g), aniline (0.78 g), phenol (0.78 g) and anthranilic acid (1.1 g) were prepared by dissolving the specified amount of these substances in water. As^{III} solution was prepared by dissolving As_2O_3 (2.5 g) in 1 *N* sodium hydroxide, neutralising it with 1 *N* sulphuric acid and making upto 500 ml with water. Standard solution (500 ml) of Fe^{II} was prepared by dissolving 19.6 g of ferrous ammonium sulphate (19.6 g) in 2 *N* sulpuric acid and standard solution (500 ml) of 8-hydroxyquinoline (1.8 g) prepared in aqueous acetic acid (50%, v/v). The strengths of these reductant solutions were checked by standard methods[13,14].

The metal oxinates of Al^{III}, Cd^{II}, Co^{II}, Mg^{II}, Mn^{II}, Ni^{II} and Zn^{II} were prepared by standard methods[13,15]. To the solutions of the metal salts (2 *M*), an ethanolic solution of 8-hydroxyquinoline (6 *M* for Al^{III} and 4 *M* for others) was added in small portions with stirring. The precipitated oxinates were filtered, washed with water and dried over P_4O_{10}. Metal anthranilates of Mn^{II}, Co^{II}, Ni^{II}, Zn^{II} and Cd^{II} were prepared by mixing a solution of sodium anthranilate (4 *M*) and the respective metal salts (2 *M*) in neutral or weakly acid medium. The metal anthranilates were filtered, washed with 0.2% solution of sodium anthranilate and finally with ethanol and dried over P_4O_{10}. Standard solutions of the metal oxinates and anthranilates were prepared by dissolving the required amounts in 500 ml of 2 *N* hydrochloric acid to give approximately 0.1 *N* solutions. The strengths of these solutions were checked by the bromate-bromide method[13,14].

The titrations were carried out at room temperature by the following method. To measured aliquots (10-20 ml) of the reductant solution taken in a flask, 2 *N* hydrochloric acid (5 ml) and other reagents such as potassium bromide (0.5 g), sodium acetate (0.5 g), *etc.*, if required, were added. After

diluting the reaction mixture with water to give an overall volume of 100 ml, 2 drops of suitable indicator was added. It was then titrated with standard solution of dibromamine-T to a sharp permanent colour change. A blank titration was done concurrently in each case and no indicator correction was found necessary.

Results and Discussion

The results of the titrations are presented in Table 1. During the redox reaction, DBT is reduced to *p*-toluenesulphonamide as per the half cell reaction,

TABLE 1—DIRECT VISUAL TITRATIONS USING DIBROMAMINE-T (TEN REPLICATES)

Reductant*	Range of concentration studied mmol	Relative mean deviation %	Standard derivation µmol	Average error %
Arsenic(III)	0.51 – 0.99	0.23	2.63	0.21
Antimony(III)	0.49 – 0.99	0.23	2.39	0.22
Iron(II)	0.90 – 1.90	0.14	1.62	0.14
Sulphite	0.41 – 0.84	0.14	1.59	0.14
Ascorbic acid	0.48 – 0.98	0.14	1.75	0.14
Hydrazine	0.31 – 0.58	0.15	1.77	0.15
Benzhydrazide	0.27 – 0.54	0.07	0.90	0.07
Isoniazid	0.25 – 0.52	0.15	1.93	0.15
Phenylhydrazine	0.23 – 0.46	0.14	1.57	0.14
Semicarbazide	0.24 – 0.50	0.22	2.21	0.16
Aniline	0.17 – 0.35	0.12	1.29	0.12
Phenol	0.23 – 0.43	0.09	1.14	0.09
Oxine	0.22 – 0.46	0.14	1.19	0.14
Anthranilic acid	0.15 – 0.31	0.10	1.10	0.10
$Al(C_9H_6ON)_3$	0.08 – 0.16	0.29	1.82	0.15
$Mg(C_9H_6ON)_2.2H_2O$	0.12 – 0.26	0.18	1.85	0.18
$Mn(C_9H_6ON)_2.2H_2O$	0.12 – 0.26	0.09	1.08	0.09
$Co(C_9H_6ON)_2.2H_2O$	0.12 – 0.25	0.15	1.63	0.15
$Ni(C_9H_6ON)_2.2H_2O$	0.13 – 0.25	0.14	1.55	0.14
$Zn(C_9H_6ON)_2.2H_2O$	0.13 – 0.25	0.14	1.65	0.14
$Cd(C_9H_6ON)_2.2H_2O$	0.11 – 0.24	0.27	2.35	0.19
$Mn(C_7H_6O_2N)_2$	0.08 – 0.17	0.13	1.26	0.11
$Co(C_7H_6O_2N)_2$	0.08 – 0.17	0.14	1.37	0.14
$Ni(C_7H_6O_2N)_2$	0.08 – 0.16	0.14	1.34	0.14
$Zn(C_7H_6O_2N)_2$	0.07 – 0.16	0.14	1.25	0.13
$Cd(C_7H_6O_2N)_2$	0.08 – 0.17	0.13	1.38	0.13

*Quinoline yellow indicator used for all reductants except the metal oxinates, for which methyl red used.

$$RNBr_2 + 2H^+ + 4e^- \rightleftharpoons RNH_2 + 2Br^-$$

where, $R=CH_3C_6H_4SO_2$. The formal potential of the redox couple involved in the oxidant system in glacial acetic acid medium has been reported to be + 1.3 V at 25°, which indicates that DBT is a moderately strong oxidant[9]. From the data presented in Table 1, it is evident that all the 26 reductants can be determined very accurately and precisely by the present direct visual titration method using dibromamine-T as the titrant. Although all the 6 visual indicators are suitable in almost all the systems studied, quinoline yellow is found to be the best for all but the metal oxinates. In the case of metal oxinates, quinoline yellow does not give sharp end-point due to the colour of the complex in solution. The solutions of all the oxinates in 2 *N* hydrochloric acid have yellowish green colour, which will mask the colour change from yellow to colourless during the titration using quinoline yellow indicator. Therefore, in this case, methyl red is found to be the most suitable indicator.

Except the systems in which bromination is the actual reaction, all the other systems do not require any addition of bromide. Thus, bromide is to be added for aniline, phenol, oxine, anthranilic acid, and metal oxinates and anthranilates. For all other reductants, there is no need to add bromide, which is a clear advantage of dibromamine-T over other reagents developed earlier. In the case of Fe^{II}, addition of phosphoric acid (5 ml) is essential to remove Fe^{III} formed *via* complexation and hence, a sharp colour change of the quinoline yellow indicator is possible at the end-point. Moreover, presence of acetate is needed for anthranilic acid and metal anthranilates. In these cases, acetate acts as a catalyst.

All the reductants undergo the usual reactions reported elsewhere. In conformity with the reported reactions, one equivalent of DBT is consumed per mole of Fe^{II} ; 2 equiv. for As^{III}, Sb^{III}, sulphite and ascorbic acid ; 4 equiv. for hydrazine, benzhydrazide, isoniazid, phenylhydrazine, semicarbazide and oxine ; 6 equiv. for aniline, phenol and anthranilic acid ; 8 equiv. for metal oxinates of Mg^{II}, Mn^{II}, Co^{II}, Ni^{II}, Zn^{II} and Cd^{II} ; and 12 equiv. for metal oxinate of Al^{III} and metal anthranilates of Mn^{II}, Co^{II}, Ni^{II}, Zn^{III} and Cd^{II}.

Acknowledgement

One of the authors (G.S D.) is thankful to the authorities of the University of Kerala, for awarding a fellowship.

References

1. L. ERDY, T. MEISEL and G. RADY, *Acta Chim. Acad. Sci. Hung.*, 1961, **26**, 71.
2. G. P. RAO and A. R. V. MURTHY, *Z. Anal. Chem.*, 1961, **180**, 169.
3. N. V. RAO, K. M. M. K. PRASAD and P. V. RAMANA, *Chem. Anal.*, 1976, **21**, 291.
4. N. V. RAO, A. B. AVADHANULU, C. B. R. SARMA and K. S. KRISHNA, *J. Indian Chem. Soc.*, 1975, **52**, 1048.
5. K. K. VERMA, J. AHMED, M. P. SAHASRABUDHEY and S. BOSE, *J. Indian, Chem. Soc.*, 1977, **54**, 699.
6. B. C. VERMA and S. KUMAR, *J. Indian Chem. Soc*, 1979, **56**, 1032.
7. B. C. VERMA, S. KUMAR and B. S. ATWAL, *Zh. Anal. Khim.*, 1980, **35**, 386.
8. C. G. R. NAIR and P. INDRASENAN, *Talanta*, 1976, **23**, 239.
9. B. T. GOWDA and D. S. MAHADEVAPPA, *J. Indian Chem. Soc.*, 1978, **55**, 342.
10. B. T. GOWDA, and D. S. MAHADEVAPPA, *Indian J. Chem.*, *Sect. A*, 1978, **16**, 635.

11. D. S. MAHADEVAPPA, K. S. RANGAPPA, B. T. GOWDA and N. M. M. GOWDA *Microchem. J.*, 1980, **26**, 132.
12. A. I. VOGEL "A Text Book of Quantitative Inorganic Analysis", Longmans, London, 1964.
13. C. L. RULFS, E. P. PRZYBYLOWICZ and C. E. SKINNER, *Anal. Chem.*, 1954, **26**, 408.
14. I. M. KOLTHOFF and R. BELCHER, "Volumetric Analysis", Interscience, New York, Vol. III, 1957.

Effects of Aquatic Toxic Trace Elements on the Quality of Foodfish

ANDREW K. KOLI*, RONALD WHITMORE and WILLIAM CONYERS

Department of Natural Sciences, South Carolina State College, Orangeburg, South Carolina 29117, U.S.A.

Manuscript received 16 October 1981, revised 20 January 1986, accepted 3 March 1986

THE recent discovery of relatively high levels of mercury in fish in North America has focused intense concern on numerous of other potentially toxic elements, such as mercury, copper, zinc, iron, manganese, magnesium, chromium, nickel, calcium, sodium, potassium and others which may be ubiquitous in ecosystems. Trace elements from anthropogenic activities and natural processes enter the marine environment. Such discharges are known to contain organic and inorganic micropollutants including toxic trace elements[1]. The fish which live in polluted water may accumulate trace elements, some of which are toxic, from the water *via* their food chains. The fish feeding on small marine organisms, on algae, and on bottom sediments, readily accumulate trace elements, thus endangering human health[2].

Samples of saltwater fish from the Atlantic Coast of South Carolina were collected. The species composition of the collections generally reflects the fish populations of the water sampled. Since nutritionally and recreationally fish constitute most important segment of the aquatic ecosystem, toxic elements in fish are obviously of great concern[3].

Experimental

Source of materials: Samples of fish from the Atlantic Coast of South Carolina were collected during the summer 1978. The species composition of the collections generally reflects the fish populations of the water sampled. The fish collected were sheepshead (*Diplodus holbrooki*), sea bass (*Monrone saxatilis*), whiting (*Uopycis regius*), grouper (*Garrupa nigrital*), toad fish (*Opsanus tau*), dolphin (*Coryhaena hippurus*), cod (*Gadus morphua*), mullet (*Mugil cephalus*), Red snapper (*Lutianus aya*), silver snapper (*Lutianus grisens*), speckled trout (*Salvenlinus fontinalis*), and flounder (*Lophopsetta maculata*). The whole fresh fish were placed on ice in an ice-chest and given an identification number, the date of collection and the place of collection, and were then transported to the laboratory for weighing and storage. The whole fish were weighed and placed in plastic bags and stored in a freezer.

Wet digestion; Frozen fish samples were thawed and dissected. The pieces of edible muscle tissue, about (~10 g), were weighed accurately and placed in clean dry Erlenmeyer flasks which were closed with polyethlene stoppers. Sample flasks were digested in a constant temperature shaking water-bath at 58° until clear solution in nitric acid (reagent grade) was obtained (50-60 min). Sample flasks were removed from the bath and allowed to cool. The digests were diluted to 100 ml total volume with deionised water[4].

Trace elements determination: The trace element contents of the digest were determined by flame atomic absorption spectrophotometer using a Perkin-Elmer 5000 and Perkin-Elmer 306 spectrophotometers[2]. Determination of trace elements were measured as parts per million. Standard solution of each element was used in determination.

TABLE 1—TRACE ELEMENT LEVELS (ppm) IN SALTWATER FISH FROM THE ATLANTIC COAST OF SOUTH CAROLINA

Species	Whole body wt. g	Fe	Zn	Cu	Ni	Cr	Hg	Mn	Mg	Ca	Na	K
Sea bass	215.7	0.36	0.18	0.09	0.33	0.25	0.50	0.03	12.21	14.93	72.0	550
Sea bass	209.5	0.34	0.16	0.08	0.30	0.15	0.40	0.02	10.21	9.86	68.0	500
Whiting	167.2	0.34	0.32	0.08	0.10	0.15	0.50	0.03	11.99	23.90	79.5	500
Sheepshead	1 560.8	0.49	0.26	0.09	0.10	0.38	0.12	0.02	14.31	15.48	48.5	650
Mullet	446.3	0.72	0.16	0.05	0.20	0.40	0.15	0.12	14.42	30.10	75.5	600
Grouper	1 564.1	0.78	0.55	0.09	0.22	0.30	0.52	0.07	14.43	22.31	102.0	600
Grouper	744.5	0.63	0.25	0.04	0.20	0.10	0.12	0.04	10.18	12.68	59.5	500
Flounder	287.0	0.42	0.13	0.08	0.20	0.20	0.17	0.02	14.37	9.49	47.0	700
Dolphin fillet	363.6	0.74	0.24	0.13	0.15	0.20	0.20	0.11	9.48	10.82	30.0	200
Toad fish	611.2	0.57	0.19	0.10	0.25	0.15	0.21	0.05	10.40	6 99	24.5	700
Cod fillet	620.4	0.33	0.45	0.11	0.25	0.20	0.22	0.06	10.33	6.90	47.0	300
Red snapper	1 344.7	0.45	0.16	0.08	0.18	0.22	0.23	0.07	13.72	13.87	45.0	750
Red snapper	696.7	0.39	0.08	0.05	0.15	0.20	0.14	0.02	13.71	5.61	39.0	300
Silver snapper	230.0	0.48	0.19	0.10	0.15	0.45	0.32	0.02	15.03	8.90	57.0	700
Speckled trout	325.3	0.31	0.20	0.07	0.15	0.10	0.12	0.03	13.27	8.96	53.0	600

The trace elements determined were Fe, Cu, Zn, Mn, Mg, Ca, Hg, Cr, Ni, Na and K (Table 1). Mercury was determined by flameless atomic absorption spectrophotometry procedures outlined by Hatch and Ott[5], and Uthe *et al.*[6] as modified for use with a Perkin-Elmer Coleman MAS —50 mercury analyser.

Results and Discussion

The purpose of this study was to determine whether the fish from the Atlantic Coast of South Carolina have elevated concentrations of toxic trace elements and can become dangerous for human consumption. The fish species were analysed. Trace elements Fe, Cu, Zn, Mn, Mg, Ca, Hg, Cr, Ni, Na and K were determined. Those species for which fish of widely differing weights were analysed, larger fish had higher concentrations of trace elements than smaller fish. It seems that salt-water rather than fresh-water fish have more trace element contents. Variations in trace element levels found in this study probably reflect differences between species and differences in size, life histories, dietary habits and the concentration in the marine environment.

Acknowledgement

Supported by a research grant SEA/CR Grant No. SC-X-120-06-82, U. S. Department of Agriculture, in cooperation with Cooperative State Research Service, USDA. Authors thank Dr. R. L. Hurst, Vice-President for 1890 Research and Extension and Dr. J. H. Walker, Jr., Associate Research Director.

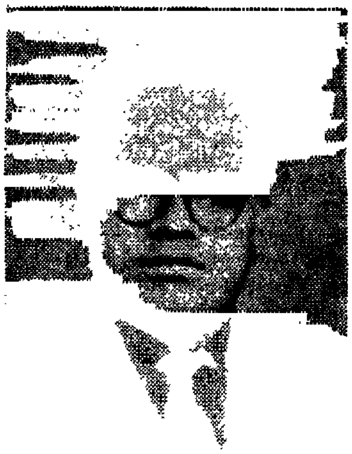
References

1. A. P. GRIMANIS, D. AZFIROPOULOS and M. V. GRIMANIS, *Environ. Sci. Technol.*, 1978, **12**, 723.
2. A. K. KOLI, S. S. SANDHU, W. T. CANTY, K. L. FELIX, R. J. REED and R. WHITMORE, *Bull Environ. Contam. Tox.*, 1978, **20**, 328.
3. D. J. LISK, *Advances in Agronomy*, 1972, **24**, 267.
4. A. BOHN and R. O. MCELROY, *J. Fish. Res. Bd., Canada*, 1976, **33**, 2836.
5. W. R. HATCH and W. L. OTT, *Anal. Chem.*, 1968, **40**, 2085.
6. J. F. UTHE, F. A. ARMSTRONG and M. P. STAINTON, *J. Fish. Res. Bd., Canada*, 1970, **27**, 805.

OBITUARY

J. Indian Chem. Soc.,
Vol. LXIII, May 1986, pp. 537-539

Anant Jagannath Mukhedkar



PROF. Anant Jagannath Mukhedkar was born on January 6, 1932. After a brilliant school and college record, he joined for Ph.D. under Prof. S. K. K. Jatkar. He obtained the Ph.D. degree in 1958 and worked on optical rotation of amino acids and amino acid complexes of copper and nickel.

Prof. Mukhedkar joined the staff of the Chemistry Department, University of Poona, as a Lecturer in 1959. He became a Reader in 1961 and a Professor in 1977. Prof. Mukhedkar was the first Nehru Memorial Research Fellow (1967) when he worked at the Bristol University (U.K.) in the group of Prof. F. G. A. Stone, on problems in organometallic chemistry.

Prof. Mukhedkar was one of the eminent inorganic chemists of India. He had varied research interests which included topics such as molecular structure, organometallic chemistry, reactions of coordinated ligands and homogeneous catalysis, magnetic materials and heterogeneous catalysis. He had to his credit 55 research papers in national and international journals. He was the author of ten books on inorganic, analytical and industrial chemistry for graduate and post-graduate courses. Twentyfive students obtained their Ph.D. under his guidance. Prof. Mukhedkar was largely responsible for the establishment of good teaching and research in Inorganic Chemistry at the University of Poona.

Prof. Mukhedkar lectured extensively in many Indian universities. He chaired many National and International Conferences and Symposia on inorganic chemistry. He was member of learned bodies, such as Indian Chemical Society and Royal Society of Chemists, and Fellow of the Maharashtra Academy of Sciences.

Prof. Mukhedkar died on October 10, 1985.

N. S. Narasimhan

Sisir Kumar Guha



SISIR Kumar Guha, D.Sc., C. Chem., F.R.S.C., formerly a Senior Professor of Chemistry, Patna Government Science College, passed away in his Patna residence on December 4, 1985. By his death, a silent and devoted teacher and research chemist was lost in this country.

Sisir Kumar was born on May 20, 1898 in a highly respectable and distinguished Guha family of Bajrajogini, Vikrampur, District Dacca (now Bangladesh). He received his early education in Dacca Collegiate School, later on in Dacca College and finally in the Dacca University from where he obtained his M.Sc. degree in 1923. He gathered much inspiration in his B.Sc. degree class while reading in Dacca College from his Professor Dr. E. R. Watson, I.E.S., and at the M.Sc. stage in

Dacca University, he constantly received encouragement at the hands of Professor (Sir) Jnan Chandra Ghosh and his another generous teacher Professor Anukul Chandra Sircar, M.A.. P R.S., Ph.D., from whom he listened to fruitful ideas for investigations to mould his future career. His neat and methodical work in the laboratory besides his great interest in extracurricular activities, both in his school and college days, gave ample indication of his making a headway in later life.

He joined Patna College in Bihar and Orissa Educational Service in 1923, as a Lecturer in Chemistry. Here, inspite of very meagre facilities for lack of space and proper equipments, he devoted himself heart and soul to create a field for research for which he received prompt support from Dr. K. S. Caldwell, I.E.S., Professor and Head of the Chemistry Department, Patna College.

In 1927, Sisir Kumar was transferred to the newly established Government Science College where he was one of the founder members of the Chemistry Department. There, in addition to heavy teaching and administrative work, he continued his research work with a strong determination. He became Assistant Professor of Chemistry in 1932. He was awarded the D.Sc. degree in 1947 by the Dacca University for his thesis, "Studies on thioindigoid, azine and azonium dyes—A correlation of colour with constitution". In 1947, Sisir Kumar became a Professor in the Chemistry Department, a post which he held until his retirement from Bihar Educational Service in 1954. But his service was retained in his own capacity for 5 years more by the Patna University and he retired in 1959. Thereafter, he acted as a research guide during 1959-79. He also worked as a Retired Scientist of C.S.I.R., New Delhi, during 1965-67 from which he detached himself due to various difficulties.

Dr. Guha made substantial and valuable contribution to the chemistry of thioindigoid, azine and azonium dyes during the last five decades. He pioneered in working out a complete relationship between colour and chemical constitution of asymmetrical and symmetrical thioindigoid dyes in several important series as far as different types of substituents are concerned. The results are embodied in some 53 papers, almost all appearing the *J. Indian Chem. Soc.* and a few in *J. Chem.* Soc. and *Chem. Ber.* between 1924 and 1980. Besides being reviewed for a decade in the Annual Reports on the Progress of Applied Chemistry, London, his findings were also incorporated in a good number of standard books of reference, including Colour Index, 3rd. ed., 1970-71, a monumental work in the dyestuff field. Some of his observations have also been translated into practice in U.S.S.R. and U.S.A. factories.

He enjoyed the Fellowship of the Royal Institute of Chemistry, London, from October 1952 to 1972, after which he was made a Life Member. From 1976, Sisir Kumar was authorised to use the style and title of 'Chartered Chemist'. On account of financial stringency in the beginning of his service life, Sisir Kumar could not securely retain his fellowship of the Indian Chemical Society before 1946, although he was elected a Fellow once in 1929 and again in 1937 and most reluctantly discontinued, which he heartily felt very much.

He worked as the Superintendent, 'Newton House' (Science College Hostel), Patna from 1928 to 1938. Those students who enjoyed the privilege of staying under his supervision there, and those who read under him during 1923-1959 in Patna College and Science College will never forget his paternal care, endearing behaviour, encouragement and proper guidance. He was not only a good teacher but an ardent research worker throughout his life. He was associated with the Universities of Calcutta, Vanaras and Bihar for nearly a decade and everywhere he proved himself as a hard working and honest teacher.

Dr. Guha sometimes felt in solitary mood that he could have worked out more on the ideas of his on line of study, had he been attached to a research institute. Dr. U. P. Basu, D.Sc., F.N.A., Director, Bengal Immunity Research Institute, Calcutta, wrote to him (letter dated November 29, 1956) : "Recently, I had been in U.S.S.R. and went round various factories also. It was a pleasure to note that some of your observations as published in 1938 and 1939 are being translated into practice. I am feeling proud that the work of an Indian Chemist is finding recognition in far away countries'.

In 1935, Dr. K. S. Caldwell, I.E.S., the Principal, Science College, Patna, gave Sisir Kumar his personal set of *J. Chem.* Soc. (1909-1934) because he admired the way in which Guha found time to continue to work and also for his devotion to teaching and research. Subsequently, this invaluable set was presented by Guha to one of his most deserving and brilliant pupil and capable colleague, Prof. J. N. Chatterjea, D.Sc., F.N.A., for making best use of them. Dr. Guha also gave his personal valuable set of *J. Indian Chem. Soc.* for 23 years (1961-1984) to the Chemistry Department, College of Commerce, Patna (Magadh University) for the facility of studies and development of research ideas where most of his old students are on the staff of the Chemistry Department.

Sisir Kumar led a quiet life at Patna devoting his time and energy to his first love, pursuit of research in his own line of study. In his last days, he felt very happy due to the success of many of his beloved pupils who made their mark as successful professors, research chemists and administrators in different parts of India and abroad.

His congenial temperament, tolerant habit, social nature, systematic work and above all his sincere desire to help the students held him in high esteem and he was an example to the younger generation of students. Being a man of clean heart and deep religious temperament. Sisir Kumar often responded to the needy with his humble mite and made silent handsome donations for pious acts.

Dr. Guha shared 64 years (1921-85) of his life in the company of Mrs. Biva Guha who not only boldly faced with strong determination the weal and woe of conjugal life but also helped her husband as a successful assistant to develop uniform dyed shades on wool and on cotton in connection with research publications.

His recreation was music and gardening. He is survived by his wife and three well established sons.

B. R. Guha

K. S. Nargund



IN the death of Dr. K. S. Nargund on December 5, 1985, Bombay chemistry circle indeed the chemists all over the world lost an eminent Chemist, a devoted teacher and an affectionate gentleman. To his innumerable students that are scattered all over the country, he was a venerable father figure.

Born on March 5, 1898, Dr. Nargund had his early education in Fergusson College, Poona, and the Indian Institute of Science, Bangalore. He began his teaching career in Gujarat College, Ahmedabad in 1927 and then went to England in 1928 to work under the guidance of Dr. Thorpe for his Ph.D. on "Three carbon tautomerism". He came back to Gujarat College and finally retired from Karnataka University, Dharwar, where he was the head of the Chemistry Department. His research work in Chemistry did not end with his retirement. He came to be associated with Parle College, Bombay, where he conducted successfully Ph.D. programmes for as many as 50 students. The number of his research papers published in various chemistry journals was above 150 and his Ph.D. students above 75. He continued to preside over the Department of Chemistry till he was over eighty. No wonder that many institutions honoured and felicitated him during his long career. Sardar Patel University, Anand, honoured him by a D.Sc. degree and Karnataka University, Dharwar, presented him a scroll of honour in its Jubilee year (1976), Parle Tilak Vidyalaya honoured him on its Diamond Jubilee (1981) at the Hands of Dr. Raja Ramanna in 1983. The Bombay Municipal Corporation felicitated him in 1983 as a senior citizen. Bombay University and College Teachers Union also felicitated him in 1981.

The finest tribute is being paid to him by his students, who have been keeping up the academic values cherished by him throughout his long life-steady devotion to duty, affection for students, selfless service to the community and an extraordinarily moral and upright conduct.

L. P. Ghalsasi

J. Indian Chem. Soc.
Vol. LXIII, May 1986.

ANNOUNCEMENT

The Indian National Science Academy invites applications from scientists for partial financial assistance to participate in some important International Conferences abroad during the year 1987-88. Scientists interested to avail of financial support from the Academy for participation in International Conferences to be held during the year 1987-88 are requested to apply in the prescribed proforma. The proforma is available from the Office of *The Executive Secretary, Indian National Science Academy, Bahadur Shah Zafar Marg, New Delhi-110 002.*

The grant scheme is operated under three different categories, *viz.*: (1) for International Conferences sponsored by the International Council of Scientific Unions (ICSU) and its affiliated bodies, (ICSU Conferences); (2) for International Conferences sponsored by other agencies, hence categorised as Non-ICSU Conferences; (3) for applicants who are interested for partial travel assistance only, for participation in any International Conference abroad. The applicants must be below 35 years of age. This is categorised as INSA-COSTED Travel Grant.

Category-1: Scientist who has been invited to deliver a plenary lecture/preside over a session of a scientific conference or whose paper has been accepted for presentation, and who will also be provided maintenance allowance during his/her stay abroad and partial travel expenses by some agency, will be given preference over others. INSA's financial support, in case of selection is limited to a maximum of half the international travel, 50% of the maintenance allowance for the duration of the conference and registration fee, wherever necessary. The prescribed application form duly completed should be despatched latest by 31st January each year for consideration by a committee of the Academy during the year.

Category-2: Scientist who has been invited to deliver a plenary lecture/preside over a session or whose paper has been accepted for presentation and who will also be provided maintenance allowance during his/her stay abroad and partial travel expenses by some agency, will be given preference over others. INSA's financial support in case of selection is limited to a maximum of Rs 5,000/-only. Applications for Category 2 should be received in the Academy for consideration three months prior to the date of commencement of the Conference.

Category-3: Under this category the scientist who is interested to avail partial travel assistance only for participation in any International Conference and is also below 35 years of age may send his/her formal request on a prescribed application form at least three months prior to the date of commencement of the conference. The applicant should fulfil the following eligibility criteria before sending his/her application, (i) his/her age should be below 35 years on the date of commencement of the conference and he/she should hold Doctorate Degree, (ii) his/her paper should have been accepted for presentation, (iii) his/her local hospitality and partial travel expenses has to be borne by the organisers or some other agency.

Candidates selected will be supported partially for their travel cost, jointly by INSA and COSTED (Committee on Science & Technology in Developing Countries). The applications will be screened once a quarter during the year.

J. Indian Chem. Soc.,
Vol. LXIII, June 1986, pp. 541-546

Dye-Surfactant Interactions. A Spectral Study†

R. C. KAPOOR

Chemical Laboratories, University of Jodhpur, Jodhpur-342 001

LUMINESCENCE, which includes fluorescence, phosphorescence and chemiluminiscence, is a very fertile field of research and provides some of the most sensitive methods of analysis. Fluorescence results from a rapid emission of light energy from a molecule which has become excited by the absorption of light. This process tends to be favoured if the compound satisfies the following conditions: (i) the longest wavelength of absorption in uv or visible region corresponds to a $\pi-\pi^*$ transition, (ii) it possesses an excited singlet state which has a half-life of nearly 10^{-8} s, and (iii) it has excited singlet state S, and triplet state T which are well separated.

The structural requirements for fluorescence of an organic compound are based on three main factors, *viz.* the nature of carbon skeleton, the geometrical arrangement of the molecule, and the type and position of substituents. In addition to the structural factors, environmental factors also affect the fluorescence spectrum of a compound[1]; these are *p*H, temperature, solvent molecule, presence of other molecules, and instrumental factors. Generally it is observed that fluorescing molecules have rigid, non-crowded, planar structure. It can also be expected that if a fluorescing molecule is bounded to a polymer, this would retard intra-molecular twisting, resulting in enhanced fluorescence.

Strongly fluorescent dyes belong to a few classes, of which those derived from the xanthene, acridine, phenazine, diphenylmethane and triphenylmethane groups are the most important[2]. These also display a tendency to aggregate into dimers or oligomers, due to high electric polarisation which becomes prominent at concentrations greater than 10^{-4} *M* (Ref. 3). The absorption spectra of the majority of organic dyestuffs in aqueous solutions do not obey Beer's law, while it is generally obeyed in alcoholic solution[4]. The deviation from Beer's law has been explained by the hypothesis of reversible dimerisation or polymerisation. The bonding energy in the dissolved state will be the difference between the affinities of the dye molecule for another of its own species and for the solvent. Since the energy of such bond is of the order of thermal energy at room temperature, the influence of concentration on the deviation from Beer's law depends strongly and reversibly on temperature.

The aggregation of dye molecules affect the efficiency of their fluorescence[5]. They also exhibit metachromic effect during this process, wherein their colour also undergoes change. The metachromic colour appears to return to the original colour at a higher temperature in a reversible manner suggesting a reversible dissociation of the dye aggregate[6].

Surfactants can be defined as a class of substances which have a tendency to aggregate in solution. Two regions characterise the chemical structure of a surfactant. One is the hydrocarbon chain, while the other is the water-soluble group. The peculiar structure causes the surfactant molecules to aggregate in a unique pattern, when present at above a certain concentration, in water. During the process of aggregation, the hydrophobic part of the molecules remain inside the cluster, avoiding contact with water, while the hydrophilic groups remain outside in contact with the solvent. The clusters thus assume colloidal dimensions which are better known as micelle. Micelle gets easily adsorbed at interfaces and, therefore, such a solution penetrates porous materials, disperses solid particles, emulsifies oil, and produces foam when stirred. The process of micelle formation is assumed to start when the surfactant reaches a certain concentration level in water (better known as critical micelle concentration, cmc). It is also believed that micelles exist in equilibrium with the monomer molecules or ions[7]. Many dyes, polynuclear hydrocarbons, proteins and lipophilic substances are stabilised in presence of micelles, while displaying marked spectral and colour changes[8,9].

Observing changes in the fluorescence can be a sensitive way to monitor the interaction between dyes and surfactants. With this end in view, the following groups of dyes were selected to study their interaction with certain surfactants: (i) *xanthine:* ethyl eosin, phloxine B, rose Bengal, erythrosine, 2', 7'-dichlorofluorescein, rhodamine B, pyronine B; (ii) *acridine:* acridine orange, acridine yellow, acriflavin; (iii) *diphenylmethane:* auramine O; (iv) *azine:* safranine O; (v) *triphenylmethane:* brilliant blue G, brilliant blue R, fuchsin acid.

The following surfactants were employed for these studies: (i) *non-ionic:* Triton X-100 (polyoxyethylene tert-octylphenol) (Eq-10), Brij-35 (polyoxyethylene (23) lauryl ether), Tween-40 (polyoxyethylene sorbitain monopalmitate), Tween-60 (polyoxyethylene sorbitain monostearate), Tween-80 (polyoxyethylene sorbitain monooleate); (ii)

† Acharya P. C. Ray Memorial Lecture (1983) delivered under the auspices of the Indian Chemical Society on November 5, 1985 at Raipur.

anionic : DBSS (dodecylbenzene sodium sulphonate), DSSS (dioctyl sodium sulphosuccinate), SLS (sodium lauryl sulphate), Aerosol-OT, Monoxol-OT ; (iii) *cationic :* CTAB (cetyltrimethylammonium bromide), CDBAC (cetyldimethylbenzylammonium chloride), CPB (cetylpyridinium bromide), CPC (cetylpyridinium chloride).

Anionic dyes' interactions :

Ethyl eosin[10] *:* Fluorescence studies indicate that initially, both the cationic and non-ionic surfactants bring about a decrease in the fluorescence intensity of ethyl eosin, which is accompanied by a shift in the λ_{max} towards longer wave length. Further addition of surfactant produces enhancement in the fluorescence intensity upto a limiting value. Fig. 1 shows the influence of CPB on the fluorescence spectrum of ethyl eosin. Addition of

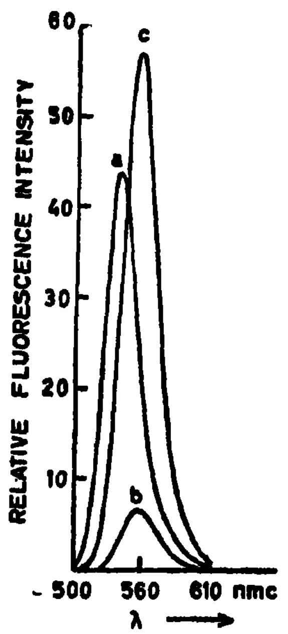


Fig. 1. Influence of CPB on fluorescence spectrum of ethyl eosin : (a) 0.00, (b) 0.014 and (c) 0.090% CPB.

anionic surfactants do not produce any change in the fluorescent behaviour of the dye solution. On the other hand, the fluorescence intensity of the dye solution increases on the addition of ethanol alone. The intensity reaches an optimum value when the solution medium contains 50% ethanol.

The absorption spectrum of the dye solution also undergoes similar changes. However, the quantum of changes are smaller. The influence of CPB on aborption spectrum of ethyl eosin is shown in Fig. 2.

Phloxine B[11] *:* Initially, the addition of non-ionic surfactants result in an increase in the fluorescence intensity of the dye solution. Subsequent additions of the surfactant cause a decline in intensity which is accompanied by a shift in the λ_{max} towards longer wave length. Brij-35 influences the behaviour in a different manner ; a continuous decrease, in fluorescence intensity of the dye, takes place on its addition.

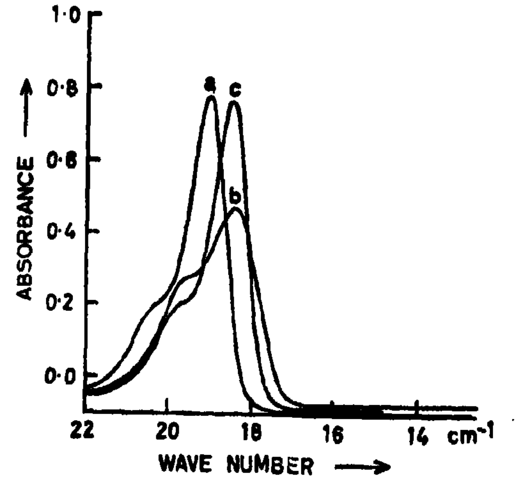


Fig. 2. Influence of CPB on absorption spectrum of ethyl eosin : (a) 0.00, (b) 0.004 and (c) 0.050% CPB.

Cationic surfactants, initially, cause a decrease in the fluorescence intensity of the dye solution, followed by a shift in the λ_{max} towards longer wave length. Subsequent addition of the surfactant results in enhancement of the fluorescence intensity. Addition of anionic surfactant has negligible influence on the fluorescence behaviour of the dye solution.

Rose Bengal[12] *:* Initially, the fluorescence intensity of the dye solution declines on the addition of non-ionic or cationic surfactant. Further addition of the surfactant results in an increase in intensity of the fluorescence. A shift in the λ_{max} is observed in between the two transitions. The influence of Tween-40 on the fluorescence spectrum of Rose Bengal solution is displayed in Fig. 3.

Addition of anionic surfactants has negligible influence on the fluorescence behaviour of the dye solution.

Erythrosine[13] *:* The fluorescence intensity appears to increase markedly on the addition of non-ionic surfactants. A shift in the λ_{max} towards longer wave length is also observed. The influence of the addition of Tween-20 on the fluorescence spectrum of erythrosine is shown in Fig. 4. In contrast, the addition of cationic surfactants produces an initial decrease in its fluorescence intensity which can even fall to zero value. Further addition of surfactant results in a rise in fluorescence intensity reaching to a limiting value. The anionic surfactants do not influence the fluorescent behaviour of the dye.

The absorption behaviour of the dye is also influenced similarly. Fig. 5 displays the changes in the absorption spectrum of erythrosine that occur on the addition of Brij-35.

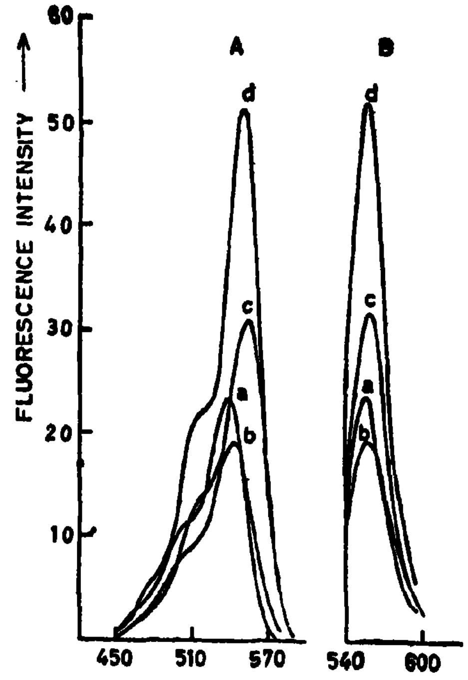


Fig. 3. Influence of Tween-40 on fluorescence spectrum of Rose Bengal solution (10^{-5} M): (a) 0.00, (b) 0.01, (c) 0.03 and (d) 0.3% Tween-40; (A) excitation and (B) emission spectra.

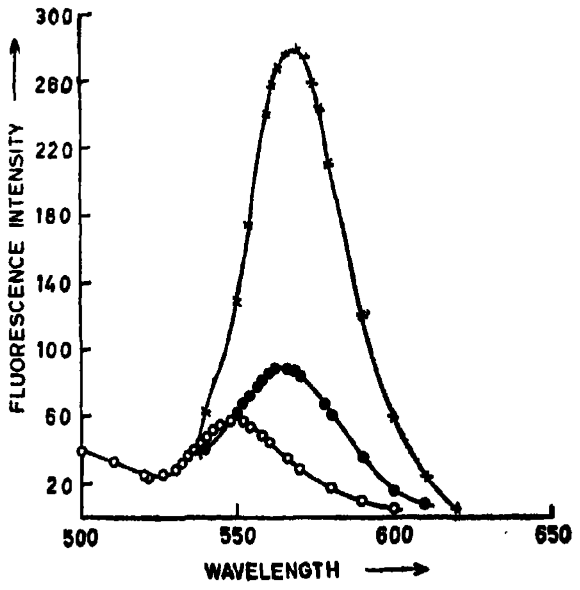


Fig. 4. Changes occuring in fluorescence spectrum of erythrosine (10^{-5} M) on the addition of Tween-20: (O) 0.00, (●) 0.005 and (×) 0.800% Tween-20.

2',7'-Dichlorofluorescein[11] : The behaviour of 2',7'-dichlorofluorescein appears at variance with other anionic dyes. Successive addition of any non-ionic surfactant produces a continuous decrease in the fluorescence intensity of the dye which finally reaches zero value. During initial addition,

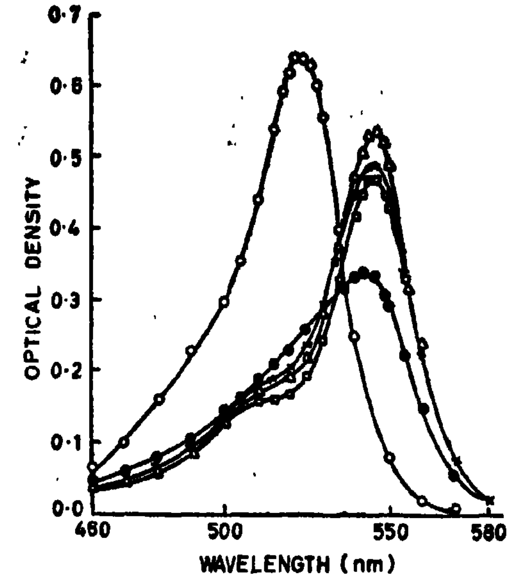


Fig. 5. Influence of addition of Brij-35 on absorption spectrum of erythrosin : (●) 0.00, (□) 0.01, (×) 0.02, (▲) 0.05 and (O) 0.2% Brij-35.

the cationic surfactants also bring about a decrease in fluorescence intensity but the same rises during subsequent additions. A shift in the λ_{max} towards longer wave length is also observed. The anionic surfactants do not exert any influence on the spectrum of the dye, except Monoxol-OT which causes a decrease in the fluorescence intensity.

Cationic dyes' interactions :

Pyronin-B[11] : Both the non-ionic and anionic surfactants, when added to the dye solution, cause an increase in its fluorescence intensity. The addition of cationic surfactants brings about a small increase, followed by a decrease in fluorescence on further addition of the surfactant.

Rhodamine-B[14] : The non-ionic surfactants, if added continuously, bring about a proportional increase in the fluorescence intensity of the dye solution. On the other hand, small amounts of anionic surfactants diminish the fluorescence intensity, which again increases on further addition of the surfactant. The behaviour is apparent from Fig. 6.

The fluorescence intensity of rhodamine-B increases slightly on the addition of cationic surfactant but no significant change in the fluorescence behaviour is noticeable.

Acridine orange[11] : The addition of non-ionic surfactant brings about a large increase in the fluorescence intensity of acridine orange solution. Initially, addition of small amounts of anionic surfactants result in decreased intensity of fluorescence. Further addition of surfactant results in an increase in intensity. The cationic surfactants also cause increase in fluorescence intensity which is

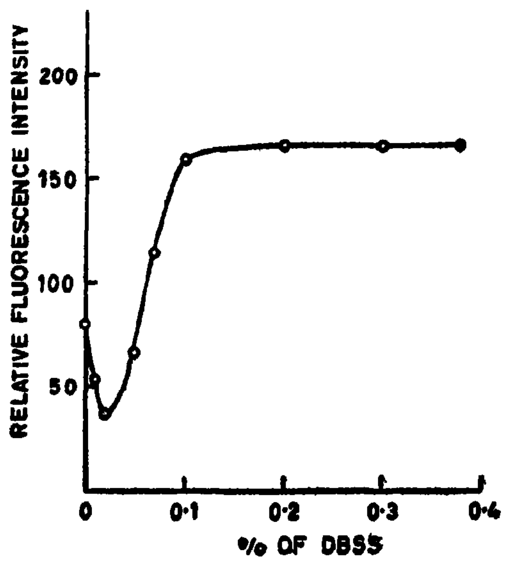


Fig. 6. Variation in fluorescence intensity of rhodamine B on varying the concentration of DBSS.

associated with a small shift in the λ_{max} towards longer wave length.

Acriflavin[11] : The fluorescence intensity of acriflavin is enhanced on the addition of non-ionic surfactants. The cationic surfactants also exert a similar influence. The addition of anionic surfactants results in an initial decrease in fluorescence intensity which is accompanied by a red-shift of 10 nm in the λ_{max}. Subsequent addition of surfactant results in a large increase in the fluorescence intensity.

Acridine yellow[15] : The addition of non-ionic surfactants causes an initial increase followed by a decrease in the λ_{max} of the dye. A red-shift in the λ_{max} is also observed. The anionic surfactants cause a large increase in the absorbance of the dye which is associated with a red-shift in the λ_{max}. The absorbance reach a maximum, and then fall slightly, on further addition of the surfactant.

The cationic surfactants have a marginal influence on the absorbance of acridine yellow. A slight increase or decrease in the maximum absorbance region is observed.

Auramine-O[16] : Initially, on adding small amounts of non-ionic surfactant, there occurs a slight increase in the flourescence intensity of auramine-O solution which is accompanied by a small red-shift in the λ_{max}. A large increase in fluorescence intensity follows on further addition of the surfactant. Similar influence is observed on the addition of ethanol to the dye solution.

Anionic surfactants also produce similar effect on the fluorescence spectrum of auramine-O. Here the magnitude of shift in the λ_{max} is larger. The cationic surfactants exert only marginal influence on the fluorescence intensity of the dye. However, some surfactants cause slight increase in fluorescence intensity while others diminish the intensity to a small extent.

Safranine-O[17] : The non-ionic surfactants display an extraordinary influence on the fluorescence intensity of safranine-O. Initially, in presence of small amount of surfactant .a slight increase in the fluorescence intensity is observed, which is accompanied by a decrease in the wave length of the λ_{max}. Further addition of the surfactant is accompanied by a large enhancement in fluoresecnce intensity. Similar phenomenon is observed on increasing the concentration of ethanol in a solution of safranine-O. The influence of the addition of Tween-80 (non-ionic) on the fluorescence emission spectrum of safranine-O is shown in Fig. 7.

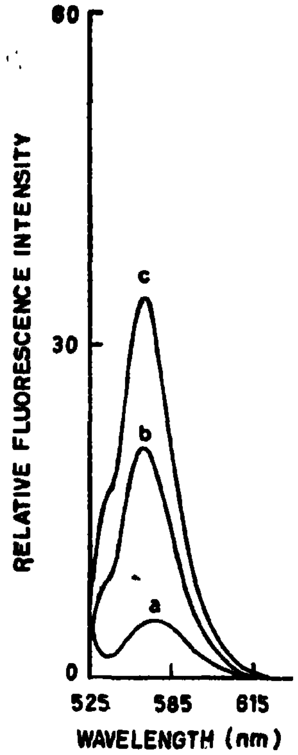


Fig. 7. Influence of addition of Tween-80 on fluorescence emission spectrum of safranine-O (2×10^{-6} *M*) : (a) 0.00, (b) 0.08 and (c) 0.27% Tween-80.

During the initial addition of anionic surfactant, a decrease in the fluorescence intensity of the dye is observed which is accompanied by a blue-shift in the λ_{max}. A large increase in the fluorescence intensity occurs on further addition of the surfactant. The cationic surfactants exert negligible influence on the fluorescence behaviour of safranine-O.

Ampholytic dyes' interaction :

Brilliant blue-G[11] : All the non-ionic surfactants, on being added to the solution of brilliant blue-G,

increase its fluorescence intensity. The process is accompanied by a blue-shift in the λ_{max}. The anionic surfactants behave similarly. However, the cationic surfactants do not display any uniform pattern.

Brilliant blue-R[11] : A large increase in fluorescence intensity is observed on the addition of either non-ionic or anionic surfactant. A concurrent blue-shift in the λ_{max} is also observed. The cationic surfactants, however, do not show a uniform pattern. CPB and CPC decrease while the addition of CTAB or CDBAC results in an increase in the fluorescence intensity of brilliant blue-R.

Fuchsin acid[18] : Cationic and anionic surfactants exert considerable influence on the fluorescence and absorption spectra of the dye solution. Addition of anionic surfactants results in an increase in the fluorescence intensity of fuchsin acid. Amongst the cationic surfactants, CPB and CPC lessen the fluorescence while CTAB and CDBAC enhance it. A blue-shift of 5 nm in the λ_{max} is concurrently observed. The non-ionic surfactants also enhance the fluorescence intensity of the dye accompanied by a blue-shift in the λ_{max}.

The absorption spectrum of fuchsin acid solution is markedly altered due to addition of surfactants. Initially, all the surfactants decrease the absorbance of the dye. The effect is least marked on the addition of non-ionic surfactants and maximum with cationic surfactants. The absorbance increases on further addition of the surfactant. Maximum enhancement is caused by TX-100.

Discussion

In the experiments made, it is observed that the non-ionic surfactants exert considerable influence on the fluorescence, and absorption characteristics of the dyes. Generally, these surfactants enhance both the fluorescence intensity and the absorbance of the dye molecules. However, the surfactant appears to exert maximum influence on the spectral characteristics of the dye when the surfactants and the dye possess opposite charges. This is due to initial charge-neutralisation and subsequent breaking up of the multimeric form of the dye to its monomeric form. When both the dye and the surfactant have similar charge, the effect is minimum. Even in this, the order of influence is : cationic dye-cationic surfactant $>$ anionic dye-anionic surfactant. When the dye possesses both cationic and anionic nature, it behaves more like cationic or anionic. For example, fuchsin acid possesses both anionic and cationic charges on the ion, yet it behaves predominently as an anionic dye.

A preferential interaction of the anionic dye, such as ethyl eosin or erythrocine with cationic surfactants, would normally be expected due to the presence of attractive forces. In such cases, the fluorescence intensity decreases and drops almost to zero level at a particular concentration of the surfactant. It appears that, initially, the interaction between the dye multimer and the surfactant causes a change in the molecular geometry of the dye, resulting in inactivation of the fluorescing sites. The dye multimer, in its changed conformation, appears susceptible to disaggregation on further addition of the surfactant. This explains the enhancement in fluorescence intensity of the dye solution on further addition of the surfactant. Similar explanation would apply for the preferential interaction between cationic dyes, like acridine orange or safranine-O, and anionic surfactants.

Enhancement in the fluorescence intensity of the dye during the addition of non-ionic surfactant appears to be due to disaggregation of the multimeric form of the dye to its monomeric form. In the multimeric form, the possibility of inter-system crossing reduces the fluorescence intensity. The hydrophilic part of the surfactant would interact preferentially with the multimeric form of the dye. At low concentration of the surfactant, the dye monomeric-multimeric equilibrium can establish inside the surfactant micelle. However, at higher concentration, complete disaggregation of the dye molecules would occur. This explains, the often encountered, initial decrease and subsequent increase in the fluorescence intensity of the dye solution on increasing the concentration of non-ionic surfactant.

The shifts occuring in the absorption and emission peaks of the dye spectra towards longer, or sometimes shorter wave length, are due to dye-surfactant interaction in the vicinity of the critical micelle concentration (cmc) of the surfactant. A red-shift indicates the presence of attractive forces while a blue-shift in the λ_{max} is indicative of repulsive forces. Both types of forces are present in the solution environment and the observed shift in spectrum is due to their resultant.

Some surfactants show anomalous behaviour. For example, Brij-35 and TX-100 often behave differently from other non-ionic surfactants due to the presence of ether linkage. Similarly, DBSS and DSSS may behave differently from other anionic surfactants due to their bulkier bidentate character. Presence of nucleophilic pyridine nucleus in CPB and CPC causes them to behave differently from other cationic surfactants.

The results described here indicate a pattern of action of surfactants during their interaction with dyes. More work is needed to refine the picture.

Acknowledgement

The results described here have been obtained from the painstaking work of the following students : V. N. Mishra, M. K. Jain, Seema Vyas, Ramesh Bharadwrj, M. C. Goud, Vikram Narula. Thanks are due to U. G. C., New Delhi, for providing funds.

References

1. J. W. BIDGES in "Fluorescence of Organic Compounds", ed. E. J. BOWEN, Van Nostrand, London, 1968.
2. G. G. GUILBAULT, "Practical Fluorescence, Theory, Methods and Technique", Marcel Dekker, New York, 1973, p. 291.
3. M. KASHA, *Radiation Res. Suppl.*, 1954, **50**, 97.
4. E. RABINOWITCH and L. F. EPSTEIN, *J. Am. Chem. Soc.*, 1948, **70**, 3683.
5. L. MICHAELIS, *J. Phys. Coll. Chem.*, 1950, **54**, 1.
6. L. MICHAELIS and S. GRANICK, *J. Am. Chem. Soc.*, 1945, **67**, 1212.
7. P. H. ELWORTHY and K. V. MYSELS, *J. Colloid Interface Sci.*, 1966, **21**, 331.
8. R. L. REEVES, *J. Am. Chem. Soc.*, 1975, **97**, 6019, 6025.
9. H. CHOUCHUNG and A. LUKTON, *J. Phys. Chem.*, 1975, **79**, 1985.
10. S. VYAS and R. C. KAPOOR, *Tenside Detergent*, 1984, **21**, 8.
11. M. K. JAIN, Ph.D. Thesis, University of Jodhpur, 1980.
12. R. C. KAPOOR, M. K. JAIN and V. N. MISHRA, *J. Lumin.*, 1981, **22**, 429.
13. R. C. KAPOOR and V. N. MISHRA, *J. Lumin.*, 1978, **17**, 175.
14. R. C. KAPOOR and V. N. MISHRA, *J. Indian Chem. Soc.*, 1976, **53**, 965.
15. M. C. GOUD, Ph. D. Thesis, submitted to University of Jodhpur, 1984.
16. S. VYAS and R. C. KAPOOR, *Polym. Photochem.*, 1984, **4**, 473.
17. S. VYAS, Ph. D. Thesis, submitted to University of Jodhpur, 1984.
18. S. VYAS and R. C. KAPOOR, communicated.

J. Indian Chem. Soc.,
Vol. LXIII, June 1986, pp. 547-564

Prediction of Thermodynamic Behaviours of Aqueous Electrolytes at all Temperatures†

UTPAL SEN

Central Electrochemical Research Institute, Karaikudi-623 006

Based upon structurally modified continuum theory, two simple approaches have been described for theoretical prediction of the free energy, entropy and heat capacity of hydration of ions and electrolytes at all temperatures. The treatments are consistent with the assumptions that the effective size of an ion in water does not change with temperature and that the Born relationship and its various derivations accurately describe the electrical part of the hydration thermodynamic functions.

In the first approach, the ionic radii of an electrolyte are fixed by the experimental hydration energies at 25°. Consequently we are able to calculate the entropy of hydration over a wide interval of temperature with only one arbitrary structural entropy parameter. This structural parameter can then be used with the continuum relationships to predict the change of the free energy of hydration with temperature to a high degree of accuracy. Even the prediction of the heat capacity of hydration, which is given directly from the second derivative of the Born equation, is accurate for electrolytes at higher temperatures.

In the second approach, even the single arbitrary parameter used in the first approach has been done away with. Here one sees the solution process of a gaseous solute ion as the combination of the two steps: (i) the formation of a cavity of a suitable size in the solvent to accommodate the solute ion and (ii) the introduction into the cavity of the solute ion which interacts with the solvent. In this approach, the thermodynamic functions associated with the cavity formation have been calculated using the scaled particle theory and it has been assumed that the specific interaction free energy occurring in the near vicinity of the ion in solution, which the traditional Born equation can not recognise, is sufficiently strong and relatively temperature insensitive. As in the earlier approach, the thermodynamic prediction through this simple approach is highly accurate for free energy, entropy as well as heat capacity at a wide range of temperature.

ACCURATE prediction of some fundamental thermodynamic properties of electrolytes in solution from purely theoretical consideration has been for long one of the most important objectives of the various theories of electrolytes. In the past, many have tried to reach this goal through various means. It has now become gradually understandable that the thermodynamic and other behaviours of electrolytes in solution can best be visualised perhaps with the help of various models based on which different properties can be theoretically calculated and compared with the corresponding experimental values. Consequently, different kinds of electrolyte solution models have been proposed from time to time. A number of excellent reviews[1-5] did discuss about these models quite extensively and the same need not be repeated here. Since in the present work some unified theory consistent with many of these classical concepts would be proposed, it seems worthwhile to recall the essence of some of these traditional models as well as the present state of the problem.

Classical approaches :

Born continuum model : When the solvent medium is considered as a structureless continuous dielectric, the free energy of solvation may be regarded as equivalent to the difference in the electrostatic energy of a gaseous ion and that of an ion in the medium of dielectric constant D. In order to evaluate this quantity, one may use the Born model[6] where the ions are represented as charged incompressible hard spheres and the solvent as a fluid with dielectric constant D which is uniform even in presence of ionic fields. The free energy increase accompanying the charging of a single gaseous ion, *i.e.* in a medium of dielectric constant unity is $(Ze)^2/2r$ where Ze is the charge earned by the ion and r is its effective radius. If the same ion is charged in a medium of dielectric constant D, the free energy change is $(Ze)^2/2Dr$, and so the increase of free energy accompanying the transfer of the gaseous ion to the particular medium which may be equated to the free energy of solvation is given by the Born equation,

$$\Delta G^{0}_{S} = W_{M+} = [(Ze)^2/2r][\frac{1}{D} - 1] \quad (1)$$

Modifications of the Born model : Although one can agree with the conclusion of Wu and Friedman[7] that a change in the size of the ion on solvation does not invalidate the Born equation, the

† Rev. Fr. L. M. Yeddanapalli Memorial Lecture (1983) delivered under the auspices of the Indian Chemical Society on November 5, 1985 at Raipur.

problem of choosing the correct solution radius of the solute ion remains to be solved. One conclusion is, however, quite certain that equation (1) gives too high negative value for the free energy of hydration (ΔG_s°) when applied to salts (*i.e.* the neutral ensemble of the cations and the anions) and when r is taken as the crystallographic radius of the ion. Attempts have, therefore, been made to use a larger value of r for the ion in solution in the Born equation to bring down the calculated value of ΔG_s° to the experimental value.

Another weak point of the original Born equation is the assumption that the dielectric constant of the solvent to be constant in the neighbourhood of the ion. The treatment has been modified by Webb[8] who allowed the variation of the dielectric constant and also for the work required to compress the solvent in the vicinity of the ion; further, by expressing the effective ionic radius as a function of the partial molal volume of the ion, it was possible to derive values of free energy of hydration without making any other assumptions concerning the effective ionic radius.

Debye and Pauling[9] modified the Born equation and suggested

$$\Delta G_s^\circ = 1/2\,(Ze)^2\left[\frac{1}{D}\left\{1/(r+\delta)\right\} + \frac{1}{D'}\left\{\frac{1}{r} - \frac{1}{(r+\delta)}\right\} - \frac{1}{r}\right] \quad (2)$$

where, the first term in brackets comes from the field free energy in solution outside of the $(r+\delta)$ sphere, δ being the increment of the radius, the second term $(1/D')$ comes from the field free energy in solution in the annual space between r and $(r+\delta)$, and the last form comes from the field free energy about the ion in vacuum. If D' is taken as 1, equation (2) reduces to the Born equation with r replaced by $(r+\delta)$,

$$\Delta G_s^\circ = [(Ze)^2/2(r+\delta)]\left[\frac{1}{D}-1\right] \quad (3)$$

The use of radius $(r+\delta)$ in the Born equation, however, corresponds to a physical model in which the charged sphere representing the ion has a different size in the vacuum and in solution.

Refinement of the Born model: The Born original model is so simple and the results obtained with it so promising that there have been a great many efforts to refine it. It has often been suggested that either the Born model or the Debye-Pauling model can at best form a basis for calculating the 'electrostatic' part of the ionic solvation energy and that this must be added to another contribution such as one would have for the discharged ion (*i.e.* a neutral species of same size)[10-13]. That is, the ionic solvation free energy is given by an equation,

$$\Delta G_s^\circ = \Delta G_{el}^\circ + \Delta G_{non\ el}^\circ \quad (4)$$

where, the first term of the right is the electrostatic contribution and the second is the non-electrostatic contribution, which may be estimated, for example, on the basis of the solvation energy of an uncharged species that is isoelectronic with the ion (and isostructural as well if ion is polyatomic).

Many other attempts of the refinement of the above models have been reviewed elsewhere[8] and it been considered that it is hard to improve on the Born model for estimating the part of solvation energetics that is particular to ionic solute. It has also been concluded that the most that one can probably learn from a theory of ion solvation based on electrostatic models in which the molecular properties of the solvent do not appear is that the thermodynamic coefficients of ion solvation can be related to those of the corresponding uncharged species.

Structural model of Frank and Wen: On the basis of wide variety of evidences, Frank and Wen[14] have proposed that surrounding a solute molecule there are three regions that can be fairly well distinguished from each other. Close to the solute molecule there is an increase in solvent structure. The nature of the structure enhancement seems to be different for polar and non-polar solutes. For highly polar solutes, such as ions, it seems probable that ice-like structure is formed, lying outside this is a region where the solvent suffers disordering as a result of the opposing effects of the ion and of the surrounding water molecules. The third region comprises the essentially unperturbed water molecules. Although these concepts provide great insight into the nature of solvation and allow important qualitative predictions to be made, it is difficult to use them as a basis for quantative calculations. These have usually been carried out on the basis of a simpler model in which only two zones are considered. The inner one generally consists of a single of water molecules, and calculations are made of the interactions between the ion and these molecules. The outer zone consists of the remaining water molecules; the interactions here are much smaller and are usually treated on the basis of a continuous model.

Molecular models: It has often been thought that a more promising approach to the theories of solvation is from a molecular model point of view. Since the pioneering work of Bernal and Fowler[15] many such theories have been proposed mainly in relation to the prediction of heat of hydration of ions. Several contributions have been suggested[1]: (i) formation of a cavity in the solvent, (ii) strong interaction between the ion and the solvent molecules of the first (and sometimes second) coordination shell, (iii) interactions between the solvent molecules in the coordination shell, (iv) weaker interactions between the hydration complex and the rest of the solvent molecules, and (v) further changes in the structure of water. Of course, none of these interactions is simple to calculate, especially in view of the uncertainty in the true ionic raddi, in the coordination number of the ions and in the orientation of the water molecules in the coordination shell. Because of

the continuous exchange with the rest of the solvent, the water molecules in the coordination shell do not form a stable cavity with the ion; and it is only on a time average that a structure may be attributed to the hydration complex.

Most of the molecular theories consider the solvent water molecule as a sphere containing a certain number of point charges or as suggested by Buckingham[16] characterised by its radius, dielectric constant, polarisability, and dipole and quadrupole moments. Apparently, to avoid the ambiguity of the Born model regarding the discrete structure of the solvent and to account for the variations in the interactions of dissolved ions and the solvent using the point charge, dipole model was suggested.

Hamiltonian models : Many of the solvation models considered above comprised one particle, representing the ion, immersed in a medium representing the solvent. In a more detailed model one may represent the medium itself by an assembly of a large number of identical particles representing the solvent molecules. As soon as this is done the methods of classical electrostatics employed in earlier models become inadequate for calculating the properties of the model system, and one must use the method of statistical mechanics.

To proceed, one needs to know, for a classical system, the Hamiltonian function for the assembly of one ion with N solvent particles,

$$H_{N+1}(P_1......P_{N+1}, r_1......r_{N+1}) = \sum_{i=1}^{N+1} (P_i^2/m_i) + U_{N+1}(r_1 ...\ r_{N+1}) \quad ... \quad (5)$$

for each set of moments, P_1, P_2... .. and locations r_1, r_2 of the (N+1) particle system. In equation (5), U_{N+1} is the potential of the interaction of the (N+1) particles in the specific configuration. If the particles representing the ion or the solvent molecules are not spherical, then each r_i must specify the orientation as well as the location of the particle. If angular moments are important, then each P_i must specify the angular momentum as well as the transitional momentum, and the kinetic energy term in equation (5) must be written to include the contributions from angular moments. Finally, if quantum mechanical effects are to be accounted for, one employs the standard transcription to convert the Hamiltonian function H_{N+1} to the appropriate Hamiltonian operator[17,18].

A basic theorem in statistical mechanics is that the Helmholtz free energy A (N+1, V, T) of the system of (N+1) particles in volume V at temperature T is given by

$$\exp[-\beta A(N+1, V, T)] = \int dp_1 \int dp_2 ...... \int dr_1 ... \int dr_{N+1} \times \exp[-\beta H_{N+1}(p_1, ..., r_{N+1})] \quad (6)$$

where, $\beta = 1/kT$ and, of course, ΔA for a solvation process may be obtained by forming the ratio of equation (6) applied to the initial and final states of the process. Again, there is a well known transcription of equation (6) for use in cases in which quantum mechanical effects are included[19].

In such a model, it is easy enough to use the mass m_i (and when appropriate, the moment of intertia I_i) corresponding exactly to that of the real ion or solvent molecule, but the potential energy function U_{N+1} is generally not well known, and in order to use equation (6), one needs to make some assumption about its form. This way of proceeding, in which one assumes a definite functional form for the Hamiltonian and then proceeds to a more or less exact evaluation of the integral in equation (6), may be called the study of Hamiltonian models.

Enormous progress has been made in recent years in the development of approximate but accurate methods of evaluating the integral in equation (6), whether directly through the use of the other exact relations. However, these methods are applicable only to models in which the potential function is pair-wise additive,

$$U_{N+1} = \frac{1}{2} \sum_{i=1}^{N+1} \sum_{j=1}^{N+1} u_{ij}(r_i, r_j) \quad (7)$$

and are practical especially in the case that the pair potential u_{ij} depends only on the distance between the particles i and j. Of course, a model subject to both of these conditions cannot represent a hydration system very realistically. In the real system, there are not only orientation dependent forces involving charge-dipole, dipole-dipole, and higher order multipole interactions, but the molecular polarisability make U_{N+1} not pairwise additive. Of course, for a still more detailed model in which the particles are the ion nucleous, the nuclei of the N-solvent molecules, and all of the electrons, the Hamiltonian will indeed have a potential function that is pairwrise additive, but the possibility of accurate evaluation of the thermodynamic properties of such a model is remote.

Recent trends :

Hybrid models : Prompted by the failures of many of the above models to represent the various aspects of the ion-solvent phenomenon on one account or other, proposals have also been put forward which combine more than one of the above concepts for solving some particular parts of the problem by one model and some other by a different model. In some of such hybrid models, the interaction of an ion and its first nearest neighbour solvent molecules (primary solvation sheath) is calculated in terms of inter-molecular forces, just as for a Hamiltonian model, while the interaction of this complex with the remaining solvent is calculated as in the theory of the Born model, perhaps the allowance for this non-electrostatic part of the solvation of the complex. There have been many studies of models of this sort[8] which illustrate what effects they may include. There are, however,

important problems with calculations of this type which need to be overcome before they can provide a reliable interpretation of hydration phenomenon more detailed than that from Debye-Pauling model.

In one of these above approaches, Muirhead-Could and Laidler[20] represented the solvent water molecule by a particle having charges at the locations of the atoms in an actual water molecule and chosen so that the model particle will have the same dipole movement as an isolated real water molecule. They assume that the complex formed by the solute ion and the solvent molecules is symmetrically constructed, with the distance from the centre of the ion to the centre of each oxygen atom of the coordinated water molecules given by the sum of the crystal radius of the ion and that of the water molecule.

The two layer hydration model of Bockris and Saluja[21] which may be considered as a statistical thermodynamic model with a difference of degree, stresses the need for the distinction between the coordination number (*i.e.* time average number of water molecules in the first hydration shell) and the solvation number (*i.e.* the solvent molecules which move with the ion during its migration jump in the solution) for an individual ion in solution. They attempted to obtain these numbers from experimental data involving spectroscopy, compressibility and ionic vibration potential[22]. Bockris and Saluja[8] also proposed that there would be two types of coordination water molecules, solvational and non-solvational, in the first layer would be consisting of partially liberated (from the characteristic hydrogen bonded structure) water molecules. There had been however some reservations[23] about the significant of the hydration numbers evaluated from ionic vibration potential together with the compressibility data.

In the hydration model syggested by Goldman and Bates[24] for theoretical calculation of the standard state thermodynamic functions associated with the transfer of ions from gas to water also, two different regions around the dissolved ion are treated differently in calculating their respective contributions to the solvation energy of the ion. In the first hydration region in the near vicinity of the ion where the water molecules are assumed to be discrete, an off-centred dipole is used to allow the possibility that the positive and negative ions of the same size and valency be unequally hydrated. A Born continuum treatment is subsequently used to calculate the secondary hydration effects. In this approach the values of the model parameters are obtained by fitting the model to experimental gas phase single ion hydration data[25,26].

Some other examples of hybrid model did consider a limited number of solvent molecules in the theoretical calculations. In these cases, the system of the solute and a small number of solvent molecules are treated as a 'supermolecule'. Such approaches have been used extensively by Pullman and Pullman and their coworkers[27]. Recently, related studies have been reported by Jorgensen[28]. Combinations of supermolecule and continuum approaches have been reported by Newton[29], Kollman and Kuntz[30] and also by Schnuelle and Beveridge[31,32]. Their statistical thermodynamic supermolecule continuum model for theoretical treatment of solvation energy and solvation effects on molecular structure and properties involve the calculation of partition function for a dissolved molecule and its first solvation shell[33]. The thermodynamic properties of the system follow from the partition function in the usual manner[33]. The general expression for the partition function (*Zi*), respresentative of the systems, involves E_1^{eff} the energy of supermolecular assembly of solvent (particle 1) and vicinal solvent molecules (particles 2-M) imbedded in polarisable dielectric in the integral. Maintaining a statistical thermodynamic super-molecule continuum calculation within computationally tractable limits requires special considerations of the evaluation of the configurational energy, E_1^{eff}, and the evaluation of the integrals over configurational coordinates of solvent molecules (configurational averaging). The most accurate but lengthy computational method of quantum mechanics can be avoided by several approximations, *viz.* shell method, cell method and site method. In the shell method, the range of configurational integration is restricted to the first solvation shell. The cell method involves restricting the configurational freedom of solvent molecules to mutually exclusive region of the configurational space of the first solvation shell. The site method involves assuming particular sites in the first solvation shell for solvent molecules, disposing the solvent molecules with their centre of gravity coincident with these sites, and carrying out a configurational averaging over orientational conditions.

A convenient approach to accurate energy evaluation is available from the large basis set *ab initio* molecular orbital study of ion-water and water-water interactions by Popkie *et al.*[34,35]. The results for ion hydration obtained by Sehnuelle and Beveridge[31,32] suggests a relatively small contribution from configurational averaging. This may indicate that the configurational averaging of water in the vicinity of highly ionic sites on a dissolved molecule will in absence of other intra-molecular perturbation, such as steric effects, also contribute little to free energy of the system. At attempt to simplify the super-molecule approach by treating the solvent molecules as fixed point charges on atomic centres was reported by Noell and Morokuma[36]. However, this point charges model at the present stage is not useful for practical calculations since it keeps the solvent molecules in arbitrarily fixed positions.

Among other recent approaches to study ion-solvent interactions Claverie *et al.*[37] considered these different models: (i) a discrete model, according to which a finite number of solvent molecules are placed around the solute molecule and the total interactions energy is calculated by simplified formulas, (ii) a continuum model, according to which the solvent surrounding the solute

is simulated by a continuum medium (the method of calculation takes into account the actual shape and charge distribution of the solute molecule), and (iii) a discrete-continuum combined model, according to which a small number of solvent molecules (corresponding to so called solvation sites) interacting strongly with the solute are treated as discrete, while the remaining solvent is simulated by a continuous medium. Apparently, the discrete model gives a representation of the 'structure' of the solvent molecules around the solute and provides satisfactorily the primary solvation sites. The continuum model gives the solvation energy with good accuracy, and the combination of discrete and continuum model should be especially appropriate for studying ionic molecules.

Chan *et al.*[38] considered a model electrolyte solution comprised of a mixture of ions of equal size, modeled as hard spheres plus embedded point charges, in a dipolar solvent, modeled as hard sphere (of different size to these of the ions) plus embedded points dipoles. The statistical mechanics of this model was treated in the mean spherical approximation (MSA) which is natural extension of the Debye-Hückel theory of electrolytes to include discrete charges and dipoles of finite size. The authors have been able to recover a familiar empirical correction to the Born energy, indicate the pitfalls in assuming empirical functional forms to describe dielectric saturation and to demonstrate derivations from the continuum discription of ion-ion interaction at close separations where because of the discrete nature of the solvent, the solvent molecules can no longer screen Coulomb potential property. However, due to this inherent inability to handle the non-linearities, the fluctuation potential and image effects the MSA cannot be relied upon to give accurate quantitative description of ion dipole systems.

Warshell[39] recently presented a new model referred to as the 'surface constrained soft sphere dipoles' (SCSSD) model in order to overcome some of the problems in the theoretical treatment of solvent effect. On one hand, it avoids the problems of dielectric continuum approaches by explicitly including solvent molecules. On the other hand, it overcomes the extreme inefficiency of the super-molecule approaches by drastically simplifying the solvent molecules while retaining their main physical features. This is done by representing the solvent molecules as soft sphere point dipoles and minimising the solute-solvent energy with respect to the orientations and positions of these dipoles while constraining the surface dipoles to have positions of the bulk molecules. This model, however, like any other dipole model cannot reproduce the hydrogen bond network of aqueous solutions, though by adjusting the density and dipole length it is possible to constrain the dipole model to reproduce the solvation energies observed in aqueous solutions.

Recently, some forceful attempts have been made to obtain a structural view of liquid water and aqueous solutions by the application of various simulation technqiues and consequently to evaluate ion-hydration phenomenon[40]. Either for Monte Carlo or molecular dynamics simulations which belongs to the above process a representation of water-solute interaction potential is required, and if the solute molecules are to be allowed to move in the molecular dynamics calculation the solute-solute potential is also needed. The thermodynamic production through above process no doubt needs lengthy computer calculations[40].

In spite of all those efforts it is apparent that the important goal of the theory of electrolytes to predict some fundamental thermodynamic property of ions in solution from first principles is still far enough. The two stumbling blocks to use continuum model, *viz.* (i) obtaining or even difining the ionic radius to the required degree of accuracy, and (ii) lack of detailed knowledge of the dielectric constant in the vicinity of an ion are yet to be removed. The molecular approaches as well as the hybrid models are also most of the time complicated and success is very limited in certain specific cases with adjustable parameters. A number of features of the electrolyte behaviour have, however, been qualitatively correlated with a more structurally based model, such as Frank-Wen proposal[14], but the attractive features of the approaches have not yet been translated into a quantative theory. The quantum mechanical approach considering the proper Hamiltonian and also various simulation methods are quite complicated and need elaborate computations.

We have however found that the continuum theory is capable of an accurate description of the thermodynamic properties of electrolytes when allowance is made for proper standard states and structural properties of ion-solvent interactions. The present paper describes two different approaches based upon structurally modified continuum theory which can be used to calculate the thermodynamic behaviour of electrolytes. In the first approach, we shall consider a structural entropy parameter along with the Born entropy term to represent the entropy of hydration. In the second approach, even this single arbitrary parameter will be eliminated. A temperature insensitive specific ion-solvent interaction free energy term will be introduced in addition to the Born free energy to represent the total free energy of interactions. Comparisons between the theoretically predicted thermodynamic quantities with those obtained directly from experiments will be provided in both the cases.

Definitions :

Dissolution of gaseous ions (electrolytes) into some solvent is commonly known as solvation process. Thermodynamic functions, such as the free energy, entropy *etc.*, associated with such transfer process are called solvation functions. In the case of aqueous solutions the process is called

as hydration. Thus,

$$M^+(g, 1\text{ atm.}, T)+X^-(g, 1\text{ atm.}, T)+Aq = M^+(aq, 1\text{ m}, T)+X^-(aq, 1\text{ m}, T) \quad (8)$$

The thermodynamic quantities associated with the transfer of one mole of M^+X^- (gas) at 1 atm. pressure to the hypothetical unimolal solution are known as the standard state thermodynamic quantities for hydration process.

The basic necessity for understanding the thermodynamics of the solvation process is to know about the standard state free energy of solvation (ΔG°_S) for solute ions (or electrolytes) at different temperatures. The various temperature derivatives of ΔG°_S at constant pressure could subsequently generate the standard entropy (ΔS°_S), enthalpy (ΔH°_S) and heat capacity ($\Delta C^\circ_{p(S)}$) of solvation. Thus,

$$\Delta S^\circ_S = -[\delta(\Delta G^\circ_S)/\delta T]_p \quad (9)$$

$$\Delta H^\circ_S = [\delta(\Delta G^\circ_S/T)/\delta(1/T)]_P = \Delta G^\circ_S - T[\delta(\Delta G^\circ_S)/\delta T]_P \quad (10)$$

$$\Delta C^\circ_{p(S)} = T[\delta(\Delta S^\circ_S)/\delta T]_P = [\delta(\Delta H^\circ_S)/\delta T]_P \quad (11)$$

The electrical work involved in the transfer of a spherically symmetrical charge from a vacuum to another medium having a dielectric constant, D, is given by the Born charging equation[8]. It will be assumed that such electrical work can be equated to free energy[41]. For an electrolyte consisting of the cations and anions, having ionic solution radii equal to r_c and r_a, respectively, equation (1) becomes

$$\Delta G^B_T = \frac{-Ne^2}{2}\left[1-\frac{1}{D}\right]\left[\frac{n_c Z_c^2}{r_c}+\frac{n_a Z_a^2}{r_a}\right] \quad (12)$$

In general, to avoid the presently arbitrary and non-thermodynamic division of thermodynamic functions into cationic and anionic contributions, the electrolyte form of the equation will be used when possible. The entropy and heat capacity of hydration relationships based on equation (2) become

$$\Delta S^B_T = \frac{Ne^2}{2}\,\frac{1}{D^2}\left(\frac{\delta D}{\delta T}\right)_P\left[\frac{n_c Z_c^2}{r_c}+\frac{n_a Z_a^2}{r_a}\right] \quad (13)$$

$$\Delta C^B_{p_T} = \frac{Ne^2}{2}\,\frac{1}{DT}\left[\frac{T^2}{D}\,\frac{\delta^2 D}{\delta T_2}-\frac{2T^2}{D^2}\left(\frac{\delta D}{\delta T}\right)^2\right]_P \left[\frac{n_c Z_c^2}{r_c}+\frac{n_a Z_a^2}{r_a}\right] \quad (14)$$

where $Ne^2/2$ has the value 166 027 Å cal mol^{-1} and Z is the number of unit charge.

The first approach (Theory no. 1) :

The greatest disagreement among various authors on use of the Born free energy equation is on the subject of the effective dielectric constant near an ion. The numerous attempts to modify the Born relationship in this respect will not be repeated here. Instead, the position will be taken that the Born equation is regorously correct, when modified by the proper considerations of the hydration process. In our first approach, the first[42] step will be the transfer of an ion gas into some void in the solvent without any distrubance of the solvent. The second step would be to introduce ion-solvent interactions. It is customary to envision some kind of electrostatically induced collapse of the solvent taking place due to the presence of the incorporated solute ion. Our present-day knowledge of electrolytes in water also suggests that such process eventually form a more or less rigid so called primary hydration sheath of water molecules around the ionic species in solution and that the primary hydration sheath of water molecules is perhaps followed by a so called secondary region of water differing from the bulk solvent. For the present, we shall describe such structural hydration effects in terms of an entropy parameter C_S, which represents the entropy loss of water rearranged from the bulk of the solvent into close association with the ions. This entropy term C_S which is designed to as well include statistical entropy terms related to the change of standard state when a gaseous solute ion comes into the solution state. It could also be assumed that C_S is independent of temperature and dependent only upon the electrolyte.

The resulting equations for the thermodynamic properties of hydration of a neutral ensemble of ions become

$$\Delta G^\circ_T = \Delta G^B_T + C_S T \quad (15)$$

$$\Delta S^\circ_T = \Delta S^B_T - C_S \quad (16)$$

$$\Delta C^\circ_{p_T} = \Delta C^B_{p_T} \quad (17)$$

or in more details,

$$\Delta G^\circ_T = -(Ne^2/2R_Z)\left(1-\frac{1}{D}\right)+C_S T \quad (18)$$

$$\Delta H^\circ_T = -(Ne^2/2R_Z)\left[1-\frac{1}{D}-\frac{T}{D^2}\left(\frac{\delta D}{\delta T}\right)_P\right] \quad (19)$$

$$\Delta S^\circ_T = (Ne^2/2R_Z)(1/D^2)(\delta D/\delta T)_P - C_S \quad (20)$$

$$\Delta C^\circ_{p_T} = (Ne^2/2R_Z)\left[(T/D^2)(\delta D^2/\delta T^2)_P - (2T/D^3)\left(\frac{\delta D}{\delta T}\right)^2\right] \quad (21)$$

where,

$$(Ne^2/2R_Z) = (Ne^2/2)(n_c Z_c^2/r_c + n_a Z_a^2/r_a) \quad (22)$$

Method of calculation : The constant C_S, can be evaluated from the entropy data at one temperature and the data at other temperatures used to check the validity of the treatment. Calculation of Born hydration functions requires knowledge of the radius parameter ($Ne^2/2R_Z$). The parameter could also be evaluated by fitting equations (13) and (16) to the entropy data alone. However, it is useful and will be revealing to define the radius parameter for the electrolyte in terms of a free energy of hydration[43]. From equation (15), we

may have

$$(Ne^2/2)/R_Z = -(\Delta G_f^\dagger - C_S T)/\left(1-\frac{1}{D}\right) \qquad (23)$$

The term $(\Delta G_f^\dagger - C_S T)$ can be approximated by initially neglecting $-C_S T$, which only amounts to ~5% of the observed free energy of hydration $\Delta G_f^\dagger$. Using ΔG^o_{298}, the calculated entropy of hydration $\Delta S_f^\dagger$ can be compared with the experimental value, ΔS_f^o, at all temperatures for which data are available and a preliminary value of C_S obtained. This value of $-C_S$ is then used to derive a value of $(\Delta G_f^\dagger - C_S T)$ and the whole process repeated until $-C_S$ does not change. In fact, the equation converges rapidly and only one or two trials are required. The standard experimental free energies, ΔG^o, at any other temperature can be used as well, but 25° is the most convenient. When the values of C_S and the radius parameter of any electrolytic water systems have been known the corresponding various thermodynamic functions can be calculated from equations (18) to (21).

Results and discussion : Since the free energy of hydration changes only 5-10% for most electrolytes over the temperature range under discussion (0-300°), a more sensitive test of present theory can be obtained by examination of the differences in hydration energy between two temperatures,

$$M^+(g, 1\ atm., T_2) + X^-(g, 1\ atm., T_2) + MX(aq, 1\ m, T_1) = M^+(g, 1\ atm., T_1) + X^-(g, 1\ atm., T_1) + MX(aq, 1\ m, T_2) \qquad (24)$$

Experimentally, this difference in the free energy of hydration can be obtained from the free energy functions,

$$(\Delta G_{f,2} - \Delta G_{f,1}) = \left(\frac{G_{f,2} - H^o_{298}}{T_2}\right)_{aq} T_2 + \sum_{gases}\left(\frac{G_{f,1} - H^o_{298}}{T_1}\right) T_1 - \left(\frac{G_{f,1} - H^o_{298}}{T_1}\right)_{aq} T_1 - \sum_{gases}\left(\frac{G_{f,2} - H^o_{298}}{T_2}\right) T_2 \qquad (25)$$

From equations (12), (15) and (18)), it follows that

$$\Delta G_{f,2} - \Delta G_{f,1} = (\Delta G^B_{T_2} - G^B_{T_1}) + C_S(T_2 - T_1) \qquad (26)$$

where,

$$(\Delta G^B_{T_2} - \Delta G^B_{T_1}) = -\left(\frac{1}{D_2} - \frac{1}{D_1}\right)\left[\frac{(\Delta G^\dagger - C_S T)}{(1 - 1/D)}\right] \qquad (27)$$

Figs. 1 and 2 illustrate such a test of the basic free energy relationship. T_1 is set at 25°. These relationships predict that the difference between the observed free energy differences and the Born energy differences (equation 26) should be a linear function of T, with a slope of C_S. The agreement between theory and experiment illustrated in Figs. 1 and 2 is essentially perfect to within the average

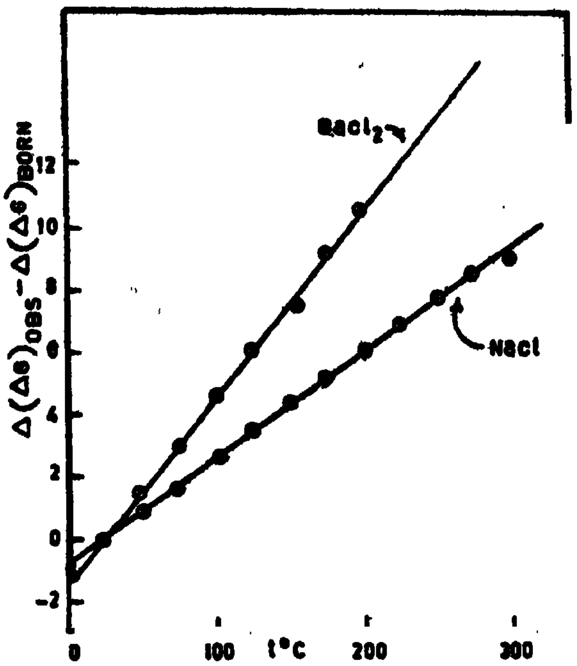


Fig. 1. Free energy diagram showing the differences between observed and Born energies of hydration at 25° and t°C (kcal mol⁻¹); straight lines predicated from Theory no. 1 and points calculated from experimental data.

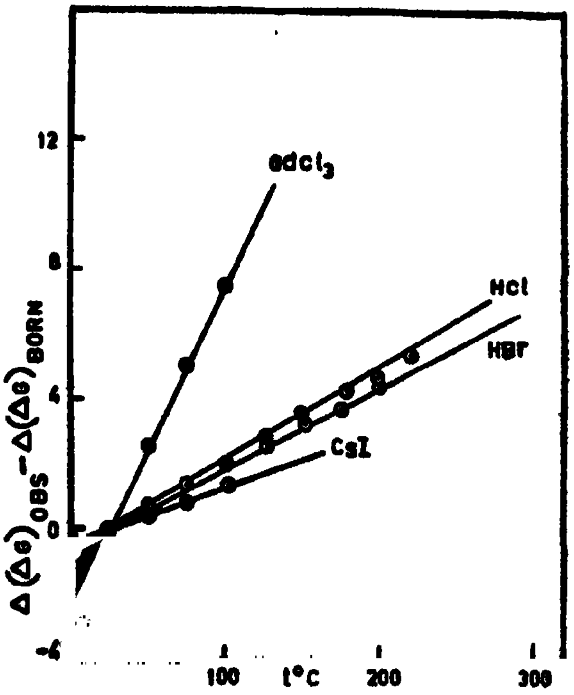


Fig. 2. Free energy diagram showing the differences between observed and Born energies of hydration at 25° and t°C (kcal mol⁻¹); straight lines predicated from Theory no. 1 and points calculated from the experimental data.

experimental error of a few tens of calories. In this test, the values of C_S were the same as those evaluated from the entropy data.

One of the basic assumptions in the present treatment is that the radius parameter $(Ne^2/2)/R_Z$ in equation (22) is temperature independent. In Table 1 the values of $1/R_Z$ has been calculated for some electrolytes, both to test this assumption and to note the size of the ions involved. Although we have deliberately refrained from considering individual ions in the basic derivations fixing up of the radius of any particular ion will enable one to compare the ionic radii of many cations and anions in solution. The known experimental values of ΔG^o at 25°, was obtained by the relationship,

TABLE 1—TEMPERATURE TEST OF THE RADIUS FUNCTION ($1/R_z$), Å^{-1}

Temp. °C	NaCl	BaCl$_2$	HCl	HBr	GdCl$_3$	CsI
0	1.111 7	2.811 5	2.092 8	—	6.638 9	0.820 6
25	1.112 0	2.818 7	2.092 7	2.026 6	6.638 95	0.821 2
50	1.112 1	2.814 0	2.092 6	2.026 5	6.639 6	0.821 8
75	1.112 1	2.818 9	2.092 5	2.025 2	6.689 8	0.821 2
100	1.112 1	2.818 5	2.092 5	2.025 2	6.689 9	0.821 0
150	1.111 9	2.818 9	2.092 6	2.025 7		
200	1.111 6	2.818 5	2.098 5	2.026 7		
250	1.112 0					
300	1.114 4					

$$\Delta G_f^o = \left[\frac{\overline{G^o} - \overline{H^o_{298}}}{T}\right]_{aq} T - \sum \left[\frac{G^o - H^o_{298}}{T}\right] T + \Delta H^o_{298} \quad (28)$$

where, ΔH^o_{298} is the hydration enthalpy. Table 1 obviously demonstrates that the radius parameter is temperature independent.

In Figs. 3 and 4, the calculated values of the entropy of hydration (ΔS^o_h) of a number of electrolytes have been plotted with the corresponding known experimental values at different temperatures. The ability of the model to quantitatively predict the entropy and its temperature variation over so large a range of temperature with only one arbitrary constant leads strong support to the validity of this use of the Born equation.

Differentiating equation (15) one would obtain,

$$[\partial(\Delta S)/\partial T]_P = [\partial(\Delta S^B)/\partial T]_P \quad (29)$$

Since, $[\partial(\Delta S/\partial T]_P = \Delta C_p/T$, it follows that

$$\Delta C_p = \Delta C_p^B \quad (30)$$

that is, the entropy constant, C_S, cancels out in consideration of the heat capacities, except for a small effect in determination of the radius parameter. However, the errors in the various derivatives of the dielectric constant data, as well as in the experimental heat capacities themselves, make it unnecessary to be so precise in our evaluation of

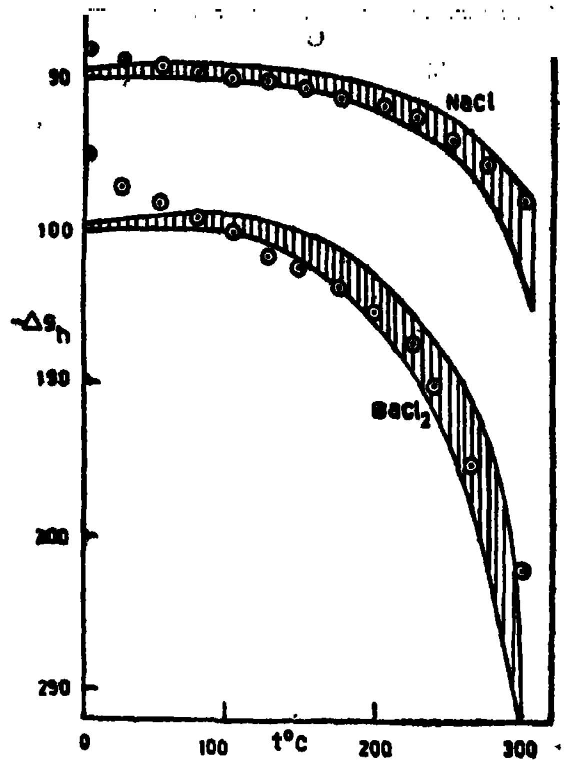


Fig. 3. Comparison of observed (symbols) and predicated (shaded band) entropy of hydration (ΔS^o_h, cal mol^{-1} K^{-1}) (Theory no. 1); width of the band was fixed from the uncertainties in dielectric constant data.

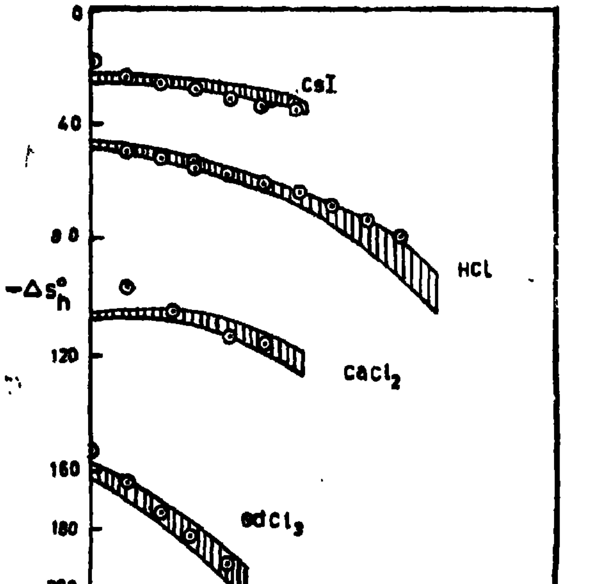


Fig. 4. Comparison of observed (symbols) and predicated (shaded band) entropy of hydration (ΔS^o_h, cal mol^{-1} K^{-1}) (Theory no. 1). The width of the band was fixed from the uncertainties in dielectric constant data.

$(Ne^2/2)R_Z$. Consequently, to a very good approximation,

$$\Delta C_p^s = \frac{1}{DT}\left[\frac{T^2}{D}\left(\frac{\delta^2 D}{\delta T^2}\right)_P - \frac{2T^2}{D^2}\left(\frac{\delta D}{\delta T}\right)^2\right]\left[\frac{\Delta G^\circ_{298}}{1-1/D}\right] \quad (31)$$

is obtained from equations (14) and (22) and involves no arbitrary constants. In Figs. 5 and 6

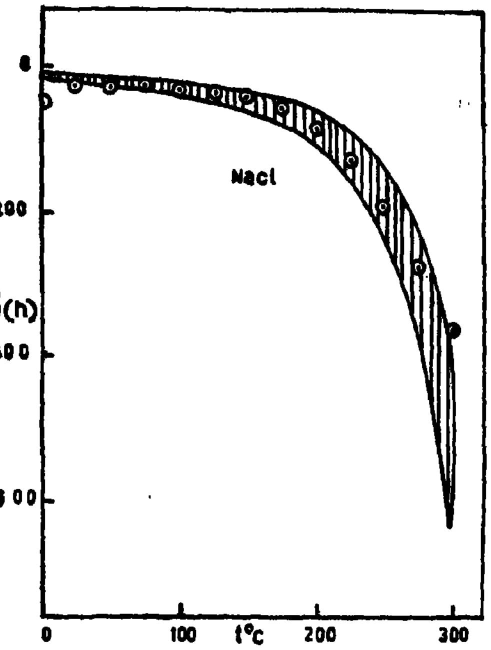


Fig. 5. Predicated (band) and observed (symbols) heat capacities of hydration ($\Delta C^\circ_{p(h)}$, cal mol^{-1} K^{-1}) (Theory no. 1).

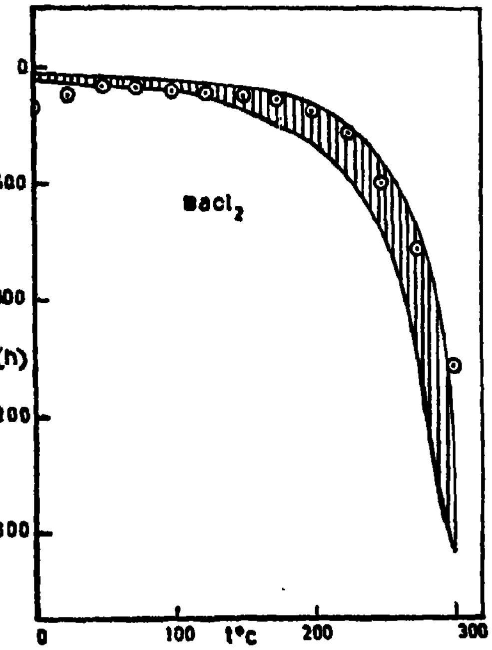


Fig. 6. Predicated (band) and observed (symbols) heat capacities of hydration ($\Delta C^\circ_{p(h)}$, cal mol^{-1} K^{-1}) (Theory no. 1).

the experimental heat capacities of hydration and a band of values predicated from equation (31) have been plotted for NaCl(aq) and $BaCl_2$(aq). The agreement is good above 75° or so.

Since one of the advantages of the proposed treatment lies in the accuracy of the predicted thermodynamic functions, it is necessary to define clearly the adopted values of D which are being used. Table 2 lists the values of D and its first and second temperature derivatives at different temperatures used in the calculations. In Table 3, the values of $1/R_Z$ and C_S for different electrolytes which may be used in the various thermodynamic predictions for aqueous electrolytes at different temperatures have been listed.

TABLE 2—SMOOTHED DIELECTRIC CONSTANT DATA FOR WATER[a]

Temp. °C	D	$-(dD/dT)^c$	$(d^2D/dT^2)^d$
0	87.74[a]	0.400 1	0.001 88
25	78.304[a]	0.356 0	0.001 64
50	69.91[a]	0.318 5	0.001 45
75	62.43[a]	0.285 5	0.001 28
100	55.72[a]	0.254 6	0.001 13
125	49.85[b]	0.214 5	0.000 98
150	43.89[b]	0.205 5	0.000 84
175	39.03[b]	0.186 6	0.000 70
200	34.59[b]	0.169 2	0.000 57
225	30.58[b]	0.156 9	0.000 43
250	26.75[b]	0.147 1	0.000 29
275	23.15[b]	0.141 0	0.000 15
300	19.66[b]	0.139 0	0.000 02
325	16.21[b]	0.140 5	−0.000 11
350	12.60[b]	0.143 7	−0.000 21
370	9.74[b]	0.149 0	−0.000 23

[a]Ref. 44. The values : [a] ±0.05, [b] ±0.01, [c] ±0.0120, [d] ±0.00020.

TABLE 3—RADIUS FUNCTION ($1/R_Z$) AND ENTROPY PARAMETERS (C_S) FOR DIFFERENT ELECTROLYTES

Electrolytes	$1/R_Z$ Å^{-1}	C_S cal mol^{-1}
HCl	2.029 3	28.4
LiCl	1.296 5	44.3
NaCl	1.112 1	34.2
KCl	0.992 7	26.6
RbCl	0.954 3	24.3
CsCl	0.909 2	24.6
AgCl	0.174 5	33.3
TlCl	1.001 2	26.5
InCl	1.017 3	27.3
CuCl	1.615 4	32.9
$BeCl_2$	4.669 9	90.1
$MgCl_2$	3.800 5	68.0
$CaCl_2$	3.322 1	65.4
$BaCl_2$	2.813 7	61.3
$TiCl_2$	3.709 0	72.7
VCl_2	3.805 9	74.3
$CrCl_2$	3.790 2	72.7
$MnCl_2$	3.708 9	68.6
$FeCl_2$	3.851 3	82.3
$CoCl_2$	3.935 6	76.5
$CuCl_2$	4.062 3	69.3
$ZnCl_2$	3.930 6	66.2
$HgCl_2$	3.681 6	60.3

(Table 3 contd.)

$CdCl_2$	8.651 8	67.9
$SnCl_2$	8.292 8	62.4
$PbCl_2$	8.198 4	57.8
$RuCl_2$	4.008 6	67.8
$PdCl_2$	8.985 1	77.7
$AlCl_3$	8.260 5	90.5
YCl_3	6.784 6	108.0
$LaCl_3$	6.887 8	99.6
$TiCl_3$	7.598 8	105.8
VCl_3	7.844 8	106.9
$CrCl_3$	8.151 0	96.5
$MnCl_3$	8.119 0	100.0
$FeCl_3$	7.918 1	99.9
$CoCl_3$	8.247 1	100.0
$NiCl_3$		
$BiCl_3$	6.748 8	86.0
$GaCl_3$	6.071 8	152.9
$InCl_3$	7.474 7	68.8
$TlCl_3$	7.797 2	78.4
$GdCl_3$	6.689 5	101.8
$MoCl_3$	7.694 8	102.6
$RuCl_3$	7.865 1	101.0
$SnCl_4$	18.029 0	112.6

The second approach (Theory no. 2) :

In an recent work, it has been found that the overall interaction phenomenon in electrolyte-solvent system can be conveniently split into two additive parts, (i) the interaction due to the presence of an ionic species of finite size into a uniform dielectric solvent system, and (ii) the so called specific interactions occuring at various distances apart from the incorporated ion which may result in the formation of the so called multi-layer solvation zones around the solute ion[46]. The free energy involved in the first part of the interaction process as mentioned above may be conveniently estimated with the help of Born charging equation[8]. A prior fixation of the value of the interaction free energy for the second part (denoted as ΔG^*), on the other hand, seems to be difficult and may require various kinds of speculation. It has been, however, realised that ΔG^* which apparently has its major contribution in the strong interactions in the vicinity of a dissolved ion would be relatively insensitive to temperature variations[47]. Consequently, some interesting possibilities arise for accurate theoretical predictions of the related thermodynamic properties of the system at different temperatures[48-50].

According to the above theory[50] proposed on the basis of the scaled particle approach[51] which has been extremely successful in thermodynamic predictions for solvation processes with neutral gases as solutes, the solvation process of electrolytes (or ions) can be seen as the simple combination of two steps, (i) the formation of a cavity of appropriate size in the solvent system for the accommodation of the solute species, and (ii) the introduction of the solute ion into the cavity which interacts with the surrounding solvent. Consequently, when this interaction process is again subdivided as stated above into the (i) Born-type electrostatic interaction and (ii) the sum of the other various kind of specific interactions occurring in the various regions around the incorporated solute ions, which the Born continuum model cannot recognise, the standard free energy of solvation, ΔG^o_S, for electrolytes can be represented as,

$$\Delta G^o_S = \Delta G^C + \Delta G^i + \Delta G_X \quad (32)$$

$$\Delta G^o_S = \Delta G^C + (\Delta G^B + \Delta G^*) + \Delta G_X \quad (33)$$

where, ΔG^C, ΔG^i, ΔG^B, ΔG^* and ΔG_X are the Gibbs free energy of cavity formation, of all interactions, of Born type electrostatic interactions, of specific interactions which the Born equation cannot recognise, and the free energy change due to the standard state conversion, respectively. The various temperature derivatives of equation (33) eleminates the unknown term ΔG^* which is assumed to be temperature independent (*i.e.* $[\partial(\Delta G^*)/\partial T]_P = 0$, and gives equations for entropy, enthalpy and heat capacity of hydration. Thus,

$$\Delta S^o_S = \Delta S^C + \Delta S^B + \Delta S_X \quad (34)$$

$$\Delta C^o_{p_S} = \Delta C^C_p + \Delta C^B_p + \Delta C_{p_X} \quad (35)$$

It can be easily seen that every term in the right sides of the above two equations are defined and can be calculated without difficulty, as described below.

Method of calculations : In order to use equations (32) to (35) for thermodynamic prediction, one must know how to calculate the thermodynamic functions for cavity formation. A number of ways including the one which involves the scaled particle theory (SPT) may be available for the estimation of the work associated with cavity formation and its temperature derivatives. The use of SPT is generally believed to lead to the most accurate values[50]. Moreover, the method can be easily simplified by assuming both the solute species and the solvent molecules to be incompressible hard spheres[51]. This simplification, however, hardly affects the accuracy in the results, particularly in the case of ion species as the solute as in the present case where the interaction energy in the transfer process predominates. Followings are the expressions for various thermodynamic functions for cavity formation[51],

$$\Delta G^C = K_0 + K_1 d_{12} + K_2 d_{12}^2 + K_3 d_{12}^3 \quad (36)$$

$$\Delta H^C = B_0 + B_1 d_2 + B_2 d_2^2 + B_3 d_2^3 \quad (37)$$

$$\Delta S^C = (\Delta H^C - \Delta G^C)/T \quad (38)$$

$$\Delta C^C_p = C_H \Delta H^C - (C_0 + C_1 d_2 + C_2 d_2^2 + C_3 d^3) \quad (39)$$

The values of K, B and C coefficients can be obtained using standard equations[51]. The values of these coefficients for various solvents at different temperatures and the corresponding solvent diameter (d_1) have been calculated and listed elsewhere[48-49,52]. Twice Pauling's crystal radius values[53] have been used for d_2 and $d_{12} = (d_1 + d_2)/2$

i.e. the sum of the radii of both the solute species and the solvent molecule.

After having calculated the various cavity functions one has to calculate the thermodynamics of interaction as depicted in equations (33) to (35). For the calculation of the Born interaction function in this approach, one need not modify the Born equation by fixing the radius parameter but can use the original equation with crystal radius of the ionic solute and the bulk dielectric constant. The thermodynamic functions for the change of standard state from one atmosphere gas to hypothetical unimolal solution can be calculated by the following equations,

$$\Delta G_x = RT\ln(RTM_1/1000\ V_1) \qquad (40)$$

$$\Delta S_x = \alpha_p RT - R - R\ln(RTM_1/1000V_1) \qquad (41)$$

$$\Delta C_{p(X)} = 2\alpha_p RT - R + RT^2(\delta\alpha_p/\delta T)_P \qquad (42)$$

where, M_1, V_1 and α_p are the molecular weight, molal volume and coefficient of cubical thermal expansion of the solvent, respectively.

In equation (33), all terms except the specific interaction free energy ΔG^* can be calculated and with the help of the corresponding known experimental free energy of hydration the values ΔG^* at different temperature can be easily generated.

It may be noted that like the earlier approach the ionic solute radius has been assumed to be temperature-independent. The crystal radius value was used both for the SPT equations for cavity and the Born equation for electrostatic interaction thermodynamic functions.

Results and discussion : The values of ΔG^* for some typical 1 : 1, 2 : 1, 3 : 1 electrolytes obtained from equation (33) at different temperatures have been listed in Table 4. It may be evident from Table 4 that the value of ΔG^* is fairly constant upto around 100° or so. Above that temperature, there may be a slight tendency that the value would increase with temperature. Considering the much greater uncertainties in the available experimental values of free energy of hydration at higher temperatures, this small magnitude of the apparent increment in the values of ΔG^* at high temperatures would for the time being be ignored.

TABLE 4—TEMPERATURE TEST FOR THE SPECIFIC INTERACTION FREE ENERGY TERM, ΔG^* (kcal mol^{-1})

Temp. °C	NaCl	$BaCl_2$	$GdCl_3$	CsI
0	81.2	206.9	687.4	30.4
25	80.8	206.0	686.6	29.2
50	80.8	205.9	686.4	28.6
75	81.0	206.2	686.7	28.4
100	81.2	206.8	687.1	28.3
125	81.5	207.2		
150	82.2	208.3		
175	82.7	209.3		
200	83.4	210.4		
225	84.2			
250	85.0			
275	85.9			
300	86.6			

In Figs. 7, 8 and 11, the calculated values of ΔG^C, ΔS^C and ΔC_p^C have been plotted against temperature. Figs. 9 and 10 show the comparision between the calculated and the experimental values of ΔS_h^o for different electrolytes at different temperatures. It is evident that as in the case of prediction by Theory no. 1 (Figs. 3 and 4), the agreement is good throughout the temperature range. The comparison of the predicted values of $\Delta C_{p(h)}^{o\prime}$ for hydration with those of the experimental values[48] can be seen in Figs. 12 and 13. A comparision between predicted and observed entropy of hydration of a number of other salts may be seen elsewhere.

Comparative assessment of the two theories :

One of the main objectives of the present work is to construct a theory of electrolyte solution which will be able to predict with sufficient accuracy the thermodynamic behaviours of electrolytes and ions in solution at all temperatures. Presently, though useful thermodynamic data for various electrolytes at room temperature may be available, the corresponding data at elevated temperatures are not easily available. The necessary compilation obviously has not been done. Considering the fact that so much time has been spent to obtain thermodynamic data of various electrolytes in solution at room temperature alone one could easily see the enormous volume of experimental work necessary for collecting such thermodynamic data at various

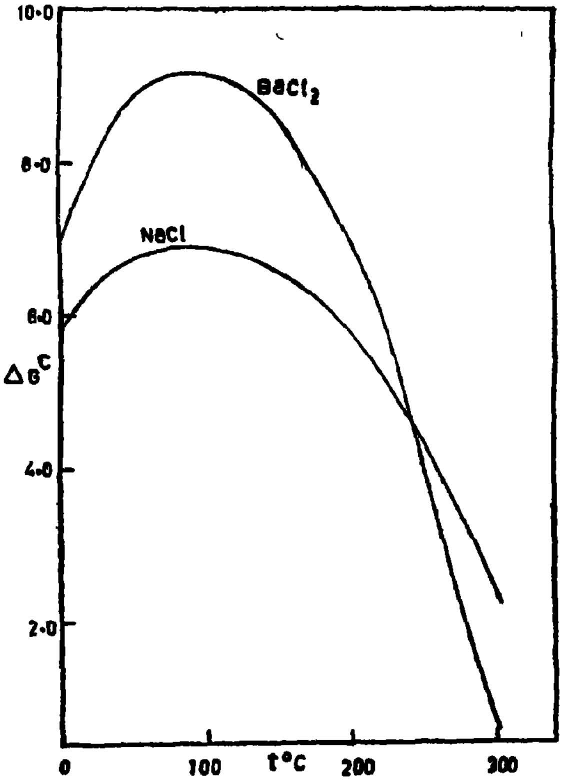


Fig. 7. Variation of ΔG^C, (kcal mol^{-1}) with temperature.

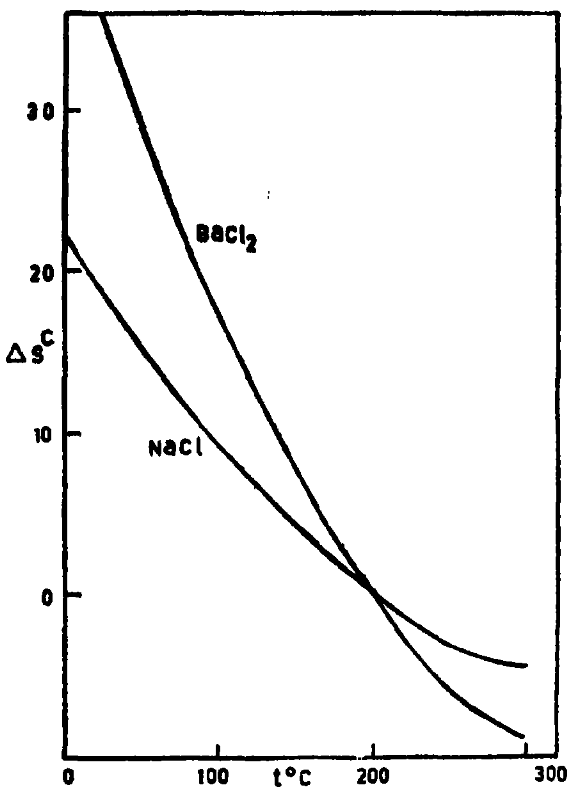


Fig. 8. Variation of $\Delta S°$ (cal mol^{-1} K^{-1}) with temperature.

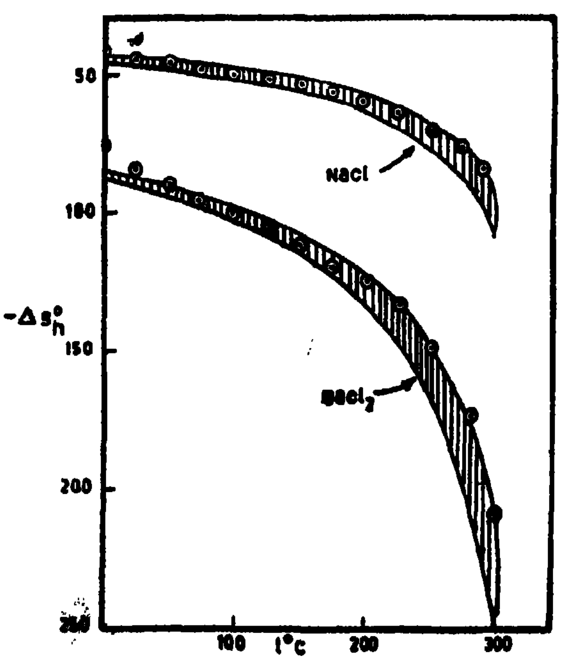


Fig. 9. Predicted (band) and observed (symbols) entropies of hydration $\Delta S^°_h$, cal mol^{-1} K^{-1} (Theory no. 2).

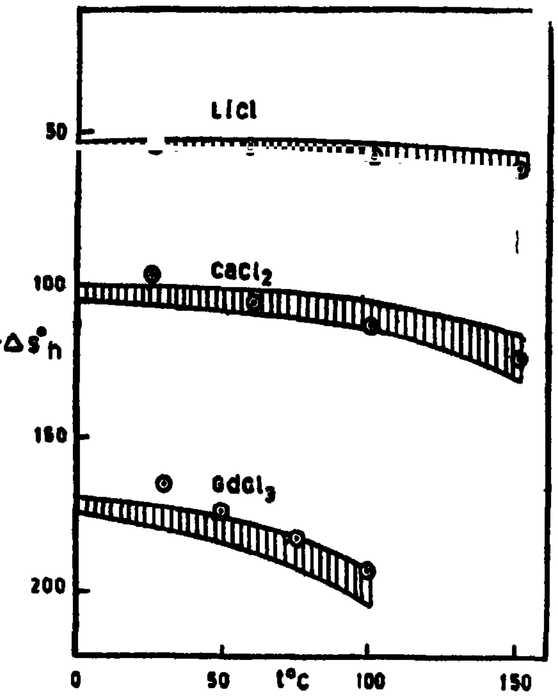


Fig. 10. Predicted (band) and observed (symbols) entropies of hydration $\Delta S^°_h$, cal mol^{-1} K^{-1} (Theory no. 2).

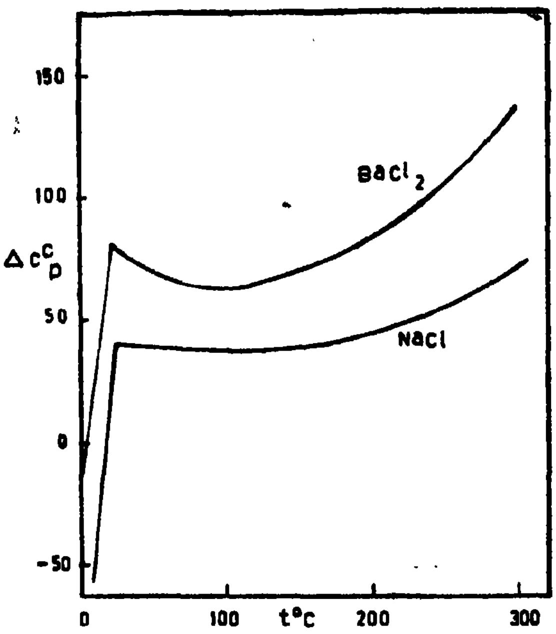


Fig. 11. Variation of $\Delta C^°_p$ (cal mol^{-1} K^{-1}) with temperature.

elevated temperatures. Perhaps only an appropriate theory can provide some relief in lessening the burden of immediate experimental works one would need in this regard.

The success of the above two theories in predicting the entropy, heat capacity and also the free

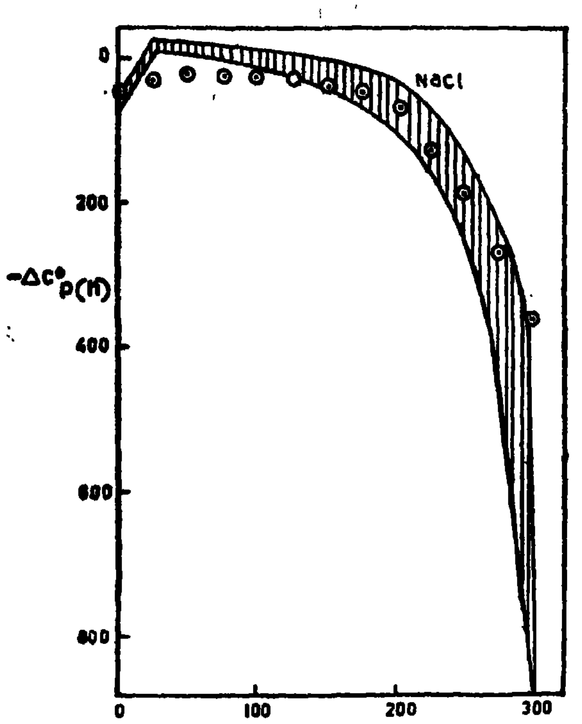


Fig. 12. Predicted (band) and observed (symbols) heat capacities of hydration, $\Delta C^{\circ}_{p(h)}$, cal mol^{-1} K^{-1} (Theory no. 2).

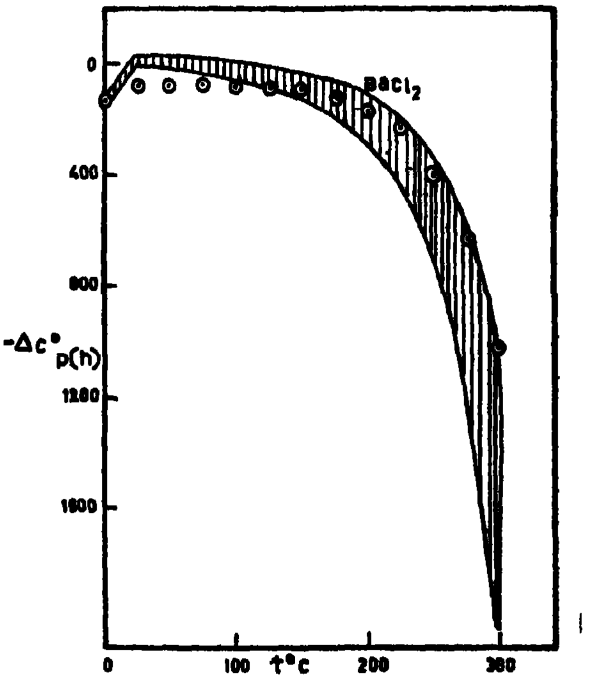


Fig. 13. Predicted (band) and observed (symbols) heat capacities of hydration, $\Delta C^{\circ}_{p(h)}$, cal mol^{-1} K^{-1} (Theory no. 2).

energy of transfer from one temperature to another could provide the answer to this long felt prime need of a short cut procedure to obtain thermodynamic data for electrolytes in solution at elevated temperatures without going through the lengthy and different experiments.

In Theory no. 1, we have to know the experimental free energy of hydration at least at one temperature for fixing the effective temperature independent solution radii of ions and subsequently to determine the entropy parameter C_S which is again insensitive to temperature change. These terms will be needed for the theoretical predictions of thermodynamic data for electrolytes. The value of C_S will be different for different electrolyte though it is not adjustable as such. Because of this dependence on the experimental hydration energy, the theory itself cannot provide any thermodynamic means for splitting the cationic and the anionic contributions from the thermodynamic data of the neutral electrolyte. On the otherhand, Theory no. 2 is capable of accurately predicting hydration entropy and heat capacity of electrolytes in solution at different temperatures without using any arbitrary parameters of taking help of any experimental thermodynamic data. It also gives accurate predictions for temperature effect on the free energy of hydration. The absolute value of the free energy of hydration of electrolyte at different temperatures, however, can be predicted only with the help of experimental free energy of hydration at one temperature[46]. Because of this unique feature of complete independence from experimental thermodynamic data as well as arbitrary parameters, Theory no. 2 provides us with the unique opportunity to have the theoretical means to identify the ionic hydration data at various temperatures without taking recourse to any non-thermodynamic assumptions[48].

The only method available until recently for fixing the ionic scale of the entropy of hydration at different temperatures is due to Criss and Cobble[64]. The method of the choice has been purely arbitrary and the authors themselves recognised their arbitrary assignments are not necessarily unique and there is a probability the entropies of ions will have absolute values different from those assigned by them at elevated temperatures[65]. The agreement in the values of the ionic entropies assigned by the arbitrary method of Criss and Cobble[64] and the predicted values by our approach (Theory no. 2) around 25° is, however, good. But as we go to higher temperatures around 100° or more the disagreement is almost total (Fig. 14). We, however, recommend our predicted values for ionic hydration entropies at higher temperatures from various considerations[48]. It may be noted that the experimental values of hydration entropies of the neutral ensemble of the cations and anions agree very well with the corresponding predicted values. Therefore, the problem may be with the arbitrary method of dividing the electrolyte thermodynamic

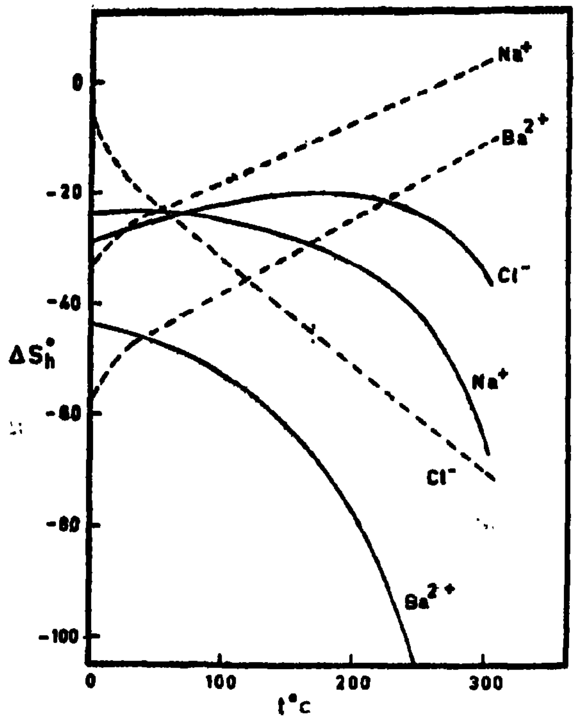


Fig. 14. Temperature behaviours of the entropy of hydration (ΔS°_{h}, cal mol^{-1} K^{-1}) of a few typical ions. Continuous lines represent this work and broken line represent Ref. 54.

values to the corresponding cationic and anionic contributions. Table 5 contains the predicted hydration entropy values for various ions at different temperatures. The effect of surfaces dipole potential[56] in the process of ionic transfer from vacuum to the solvent is negligible particularly at higher temperatures and hence has not been considered[48].

Prediction of the ionic hydration entropy involves the ionic crystal radius. In the data presented in Table 5, Pauling's crystal radius values[33] have been used. It may be noted here that sometimes the experimental crystal radius values of Gourary and Adrian[57] gives better results in some of the predictions. However, experimental radius values are available only for limited number of ions and hence the Pauling's radius values have been used for our calculations. The values of the radius for the multi-atom ions were in many cases taken from the compilation by Millero[58].

TABLE 5—PREDICTED VALUES OF STANDARD ENTROPY OF HYDRATION OF IONS (ΔS°_{h}) AT DIFFERENT TEMPERATURE (°C)

Ions	r_c	ΔS°_{h}, cal mol^{-1} K^{-1}				
		0°	25°	50°	75°	100°
H^+	—	3.8	4.5	5.1	5.8	7.3
Li^+	0.60	26.1	27.2	28.8	30.5	32.6
Na^+	0.95	23 4	23.5	23.9	24.4	25.2
K^+	1.33	24.5	23.6	23.1	22.7	22.6
Rb^+	1.48	25.5	24.3	23.4	22.6	22.2
Cs^+	1.69	27.5	25.7	24.2	23.0	22.0
Cu^+	0.96	23.8	23.4	23.7	24.2	25.0
Ag^+	1.26	24.1	23.4	23.0	22.7	22.7
Au^+	1.37	24.7	23.8	23.1	22.6	22.4
Ga^+	1.13	23.5	23.2	23.1	23.1	23.5
In^+	1.32	24.4	23.6	23.0	22.6	22.5
Tl^+	1.40	24.9	23.9	23.2	22.6	22.3
F^-	1.36	24.7	23.7	23.1	22.7	22.5
Cl^-	1.81	28.8	26.6	24.9	23.3	22.1
Br^-	1.95	30.8	27.9	25.8	23.9	22.3
I^-	2.16	33.3	30.2	27.4	25.0	22.9
OH^-	1.38	24.8	22.8	23.1	22.6	22.3
CN^-	1.92	30.1	27.6	25.6	23.7	27.2
NO_3^-	2.03	31.5	28.7	26.4	24.2	22.5
SCN^-	2.27	35.0	29.2	28.4	25.6	23.2
ClO_4^-	2.29	35.5	29.4	28.6	25.7	23.3
BPh_4^-	4.69	91.0	76.6	63.6	51.8	41.2
NH_4^+	1.48	25.5	24.3	23.4	22.6	22.2
HMo_4^+	3.47	58.8	50.5	43.1	36.8	30.3
NEt_4^+	4.00	72.6	61.6	51.9	42.9	34.9
NPr_4^+	4.52	87.9	74.0	61.6	51.1	40.1
NBu_4^+	4.94	101.6	85.1	70.4	56.9	44.8
$NPen_4^+$	5 80	114.3	95.4	78.5	63.0	49.2
$NHeX_4^+$	5.65	127.4	106.0	86.9	69.4	53.8
$NHep_4^+$	5.92	138.1	114.7	93.8	74.6	57.5
$AsPh_4^+$	4.70	93.6	78.7	65.8	53.0	42.1
Be^{2+}	0.31	121.4	134.1	48.5	164.9	184.7
Mg^{2+}	0.65	65.0	70.7	77.2	84.6	93.6
Ca^{2+}	0.99	49.4	52.5	56.2	60.5	65.9
Sr^{2+}	1.13	46.4	48.8	51.7	55.1	59.6
Ba^{2+}	1.35	43.7	45.1	47.0	49.4	52.7
Cd^{2+}	0.97	49.9	53.2	56.9	61.4	67.0
Mn^{2+}	0.80	56.1	60.5	65.5	71.2	78.4
Pb^{2+}	1.20	45.3	47.3	49.9	53.0	57.1
Hg^{2+}	1.10	44.3	49.4	52.5	56.2	60.8
Cu^{2+}	0.74	59.2	64.0	59.5	75.9	83.7
Fe^{2+}	0.76	58.1	62.8	68.1	74.3	81.8
Zn^{2+}	0.74	59.2	64.0	69.5	75.9	83.7
Co^{2+}	0.74	59.2	64.0	69.5	75.9	83.7
Ni^{2+}	0.72	60.3	65.3	71.0	77.6	85.7
Sn^{2+}	1.12	46.6	49.0	51.9	55.5	60.0
Cr^{2+}	0.84	54.4	58.4	63.1	68.5	75.3
Pd^{2+}	0.86	53.6	57.5	62.0	67.3	73.8
Ra^{2+}	1.40	43.3	44.5	46.2	48.4	51.4
Ge^{2+}	0.93	51.1	54.6	58.6	63.4	69.3
Ti^{2+}	0.90	52.1	55.8	60.0	65.0	71.1
S^{2-}	1.84	43.1	42.6	42.6	43.0	44.3
Al^{3+}	0.50	166 8	184.0	204.0	226.9	254.4
Fe^{3+}	0.64	132.9	146.8	162.4	180.2	201.7
Cr^{3+}	0.69	124.7	137.3	151.5	167.8	187.1
Mn^{3+}	0.66	129.6	142.8	157.7	174.8	195.5
Co^{3+}	0.63	135.0	148.9	164.5	182.5	204.2
Ni^{3+}	0.62	137.0	151.1	167.0	185.3	207.3
Co^{3+}	1.11	85.6	92.6	100.7	108.5	121.7
Ga^{3+}	0.62	137.0	151.1	167.0	185.3	207.3
In^{3+}	0.81	108.9	119.4	131.3	144.9	161.5
Tl^{3+}	0.95	95.9	104.5	114.4	125.8	139.7
Sc^{3+}	0.81	108.9	119.4	131.3	144.9	161.5
Y^{3+}	0.93	97.5	106.4	116.5	128.2	142.4
Gd^{3+}	1.02	90.9	98.8	107.8	118.3	131.1
La^{3+}	1.15	83.5	90.2	97.9	107.8	118.0
Th^{3+}	1.14	84.0	90.8	98.6	107.7	118.9
U^{3+}	1.11	85.6	92.6	100.7	108.5	121.7
Np^{3+}	1.09	86.7	93.9	102.2	111.8	123.7
Cr^{4+}	0.56	257.8	286.1	317.9	355.0	398.4
Mn^{4+}	0.54	266.8	296.2	329.2	367.1	412.7
Ti^{4+}	0.68	215.1	238.2	264.2	294.1	330.1
Ge^{4+}	0.53	271.6	301.6	335.2	373.8	420.3
Zr^{4+}	0 80	185.5	204.9	226.8	252.0	282.4
Sn^{4+}	0.71	206.7	228.8	253.7	282.2	316.7
Ce^{4+}	1.01	151.4	166.3	183.3	202.8	226.6
Pb^{4+}	0.84	177.6	196.0	216.8	240.7	269.6
U^{4+}	0.97	156.7	172.3	190.1	210.5	235.3
Np^{4+}	0.95	159.5	175.5	193.7	214.6	240.0
V^{5+}	0.59	377.1	419.2	466.6	520.9	586.2
As^{5+}	0.47	469.7	522.8	582.5	650.9	733.1

(Table 5 contd.)

Sb^{5+}	0.62	359.6	399.6	444.6	496.3	558.4
Bi^{5+}	0.74	304.0	337.3	374.8	417.9	469.8
Nb^{5+}	0.70	320.4	355.7	395.4	441.0	495.9
Cr^{6+}	0.52	608.3	677.5	755.2	844.3	951.4
Mo^{6+}	0.62	512.6	570.5	635.5	710.1	799.8
Mn^{7+}	0.46	929.7	1 036.4	1 156.2	1 293.6	1 458.6

		125°	150°	175°	200°	225°
H^{+}	—	9.8	13.3	15.9	18.2	20.6
Li^{+}	0.60	35.2	38.4	42.3	47.0	53.9
Na^{+}	0.95	26.4	27.9	30.0	32.6	36.5
K^{+}	1.33	22.8	23.2	24.1	25.4	27.8
Rb^{+}	1.48	22.1	22.1	22.7	23.6	25.5
Cs^{+}	1.69	21.5	21.0	21.1	21.6	22.9
Cu^{+}	0.96	26.3	27.8	29.8	32.3	36.2
Ag^{+}	1.26	23.2	23.8	24.9	26.4	29.0
Au^{+}	1.37	22.6	22.9	23.7	24.9	27.0
Ga^{+}	1.13	24.3	25.2	26.7	28 6	31.7
In^{+}	1.32	22.8	23.3	24.2	25.6	28.0
Tl^{+}	1.40	22.4	22.7	23.4	24.5	26.7
F^{-}	1.36	22.6	23.0	23.8	25.0	27.3
Cl^{-}	1.81	21.3	20.6	20.4	20.5	21.7
Br^{-}	1.95	21.2	20.1	19.7	19.6	20.4
I^{-}	2.16	21.3	19.7	18.8	18.3	18.6
OH^{-}	1.38	22.5	22.8	23.6	24.8	27.0
CN^{-}	1.92	21.2	20.2	19.8	19.7	20.6
NO_3^{-}	2.03	21.2	20.0	19.3	19.1	19.7
SCN^{-}	2.27	21.4	19.6	18.4	17.7	17.8
ClO_4^{-}	2.29	21.4	19.6	18.4	17.6	17.7
BPh_4^{-}	4.62	32.3	23.2	16.0	10.0	5.4
NH_4^{+}	1.48	22.1	22.1	22.7	23.6	25.5
NMe_4^{+}	3.47	25.3	20.2	16.3	13.2	11.0
NEt_4^{+}	4.00	28.2	21.4	16.0	11.7	8.4
NPr_4^{+}	4.52	31.6	22.8	16.0	10.3	5.9
NBu_4^{+}	4.94	34.5	24.2	16.0	9.2	3.9
$NPen_4^{+}$	5.30	37.5	25.6	16.2	8.8	1.8
$NHex_4^{+}$	5.65	40.5	27.0	16.3	7.4	0.8
$NHep_4^{+}$	5.92	43.0	28.2	16.5	6.7	−1.1
$AsPh_4^{+}$	4.70	32.8	23.4	16.0	9.8	5.1
Be^{2+}	0.31	208.5	237.1	270.7	310.8	363.0
Mg^{2+}	0.65	104.7	117.9	133.6	152.4	179.3
Ca^{2+}	0.99	72.7	80.9	90.0	102.7	120.0
Sr^{2+}	1.13	65.3	72.3	80 7	90.9	105.9
Ba^{2+}	1.35	57.0	62.4	69.1	77.3	89.6
Cd^{2+}	0.97	74.0	82.4	91.7	104.7	122.3
Mn^{2+}	0.80	87.1	97.7	110.2	125.3	146.9
Pb^{2+}	1.20	62.8	68.7	76.5	86.1	100.1
Hg^{2+}	1.10	67.2	73.9	81.8	134.8	158.6
Cu^{2+}	0.74	93.3	104.8	118.4	134.8	158.3
Fe^{2+}	0.76	91.1	102.3	115 5	131.4	154.3
Zn^{2+}	0.74	93.3	104.3	118.4	134.8	158.3
Co^{2+}	0.74	93.3	104.3	118.4	134.8	158.3
Ni^{2+}	0.72	95.6	107.4	121.4	138.3	162.5
Sn^{2+}	1.12	65.8	72.8	81.4	91.7	106.8
Cr^{2+}	0.84	83.5	93.5	105.4	119.7	140.3
Pd^{2+}	0.86	81.9	91.6	102.5	117.5	137.2
Ra^{2+}	1.40	55.6	60.6	67.0	74.9	86.6
Ge^{2+}	0.93	76.6	85.5	95.3	108.8	127.3
Ti^{2+}	0.90	78.8	86.7	96.3	112.2	131.4
S^{2-}	1.84	46.5	49.3	53.4	58.7	66.9
Al^{3+}	0.50	287.7	327.6	374.4	430.5	510.3
Fe^{3+}	0.64	227.0	258.0	294.4	338.0	400.3
Cr^{3+}	0.69	211.3	240.0	273.7	314.1	371.8
Mn^{3+}	0.66	220.5	250.4	285.8	328.0	388.3
Co^{3+}	0.63	230.4	261.9	299.0	343.3	406.5
Ni^{3+}	0.62	234.04	266.0	303.6	348.7	412.9
Ce^{3+}	1.11	136.0	153.1	173.6	198.2	233.6
Ga^{3+}	0.62	234.0	266.0	303.6	348.7	412.9
In^{3+}	0.81	181.7	205.9	234.5	268.6	318.1
Tl^{3+}	0.95	156.7	177.1	201.3	230.3	269.9
Sc^{3+}	0.81	181.7	205.9	234.5	268.6	318.1
Y^{3+}	0.93	159.3	180.7	205.4	235.1	277.6
Gd^{3+}	1.02	146.8	165.7	188.1	215.0	230.7
La^{3+}	1.15	131.7	148.2	167.9	191.6	225.7
Th^{3+}	1.14	132.7	149.4	169.3	193.2	227.6
U^{3+}	1.11	136.0	153.1	173.6	198.2	233.6
Np^{3+}	1.09	138.2	155.7	176.6	201.7	237.7
Cr^{4+}	0.56	451.3	514.9	589.5	678.6	805.7
Mn^{4+}	0.54	467.6	533.6	611.0	703.5	835.3
Ti^{4+}	0.68	378.5	425.7	487.0	560.3	664.8
Ge^{4+}	0.53	476.3	543.5	622.3	716.2	824.0
Zr^{4+}	0.80	319.2	363.3	415.3	477.0	566.1
Sn^{4+}	0.71	358.2	408.1	466.8	536.5	637.0
Ce^{4+}	1.01	255.3	290.0	330.8	379.6	449.7
Pb^{4+}	0.84	304.5	346.5	395.9	455.0	539.4
U^{4+}	0.97	265.4	301.5	344.1	395.1	468.0
Np^{4+}	0.95	270.7	307.0	351.1	403.3	477.7
V^{5+}	0.59	664.9	759.3	870.2	1 002.6	1 191.3
As^{5+}	0.47	832.0	950.3	1 090.1	1 256.6	1 493.7
Sb^{5+}	0.62	638.2	728.1	828.5	954.5	1 134.0
Bi^{5+}	0.74	532.2	607.4	695.6	80.10	951.3
Nb^{5+}	0.70	562.1	641.5	734.8	846.3	1 005.2
Cr^{6+}	0.52	1 080.3	1 233.0	1 416.4	1 633.2	1 941.3
Mo^{6+}	0.62	907.7	1 037.3	1 189.3	1 370.8	1 629.6
Mn^{7+}	0.46	1 657.1	1 895.4	2 174.8	2 508.6	2 983.9

		250°	275°	300°	325°	350°	370°
Li^{+}	0.60	68.5	78.5	104.1	150.8	247.0	418.1
Na^{+}	0.95	42.1	51.1	66.8	96.3	154.8	254.1
K^{+}	1.33	31.3	37.2	48.1	69.6	109.6	176.2
Rb^{+}	1.48	28.4	33.6	43.2	62.8	98.1	156.4
Cs^{+}	1.69	25.1	29.4	37.6	55.3	85.5	134.7
Cu^{+}	0.96	41.7	50.6	66.2	95.3	158.1	251.2
Ag^{+}	1.26	32.8	29.2	50.8	73.3	115.3	187.0
Au^{+}	1.37	30.5	36.2	46.7	67.6	106.3	170.5
Ga^{+}	1.13	36.2	43.5	56.5	81.4	129.6	210.6
In^{+}	1.32	32.5	37.5	48.5	70.1	110.4	177.7
Tl^{+}	1.40	29.9	35.4	45.7	66.2	103.9	166.4
F^{-}	1.36	35.4	36.5	47.0	68.1	107.1	171.9
Cl^{-}	1.81	23.5	27.3	34.9	51.9	79.6	124.5
Br^{-}	1.95	21.8	25.1	43.3	73.6	114.3	114.3
I^{-}	2.16	19.6	22.3	28.4	43.9	66.1	101.3
OH^{-}	1.38	30.3	35.9	46.3	67.1	105.5	169.1
CN^{-}	1.92	22.2	25.6	32.7	49.1	74.3	116.3
NO_3^{-}	2.03	20.9	24.0	30.6	46.6	70.6	109.0
SCN^{-}	2.27	18.5	20.9	26.7	41.9	62.3	95.5
ClO_4^{-}	2.29	18.3	20.7	26.4	41.6	62.2	94.5
BPh_4^{-}	4.62	1.0	−1.0	0.7	22.0	29.1	37.5
NH_4^{+}	1.48	28.4	33.6	43.2	62.8	98.1	156.4
NMe_4^{+}	3.47	9.1	9.0	12.1	28.4	39.9	56.1
NEt_4^{+}	4.00	5.4	4.4	6.8	25.0	34.1	46.2
NPr_4^{+}	4.52	1.7	−0.1	1.6	22.5	29.8	38.7
NBu_4^{+}	4.94	−1.3	−3.9	−2.5	20.8	27.0	33.9
$NPen_4^{+}$	5.30	−4.0	−7.2	−6.1	19.6	24.9	30.3
$NHex_4^{+}$	5.65	−6.6	−10.5	−9.7	18.5	23.2	27.8
$NHep_4^{+}$	5.92	−8.8	−13.1	−12.5	17.8	22.0	25.2
$AsPh_4^{+}$	4.70	0.4	−1.7	−21.7	28.5	28.5	36.5
Be^{2+}	0.31	447.3	569.6	775.2	1 148.3	1 985.6	3 528.4
Mg^{2+}	0.65	216.6	274.4	371.9	549.1	921.3	1 575.3
Ca^{2+}	0.99	144.1	181.6	245.2	361.5	603.7	1 027.9
Sr^{2+}	1.13	126.6	159.5	215.0	317.1	528.5	898.8
Ba^{2+}	1.35	106.7	133.3	180.1	265.9	441.8	748.9
Cd^{2+}	0.97	146.9	185.3	250.2	368.9	616.2	1 049.5
Mn^{2+}	0.80	177.1	223.8	302.8	446.7	747.9	1 276.5
Pb^{2+}	1.20	119.6	150.3	202.5	298.7	497.5	844.8
Hg^{2+}	1.10	130.1	163.7	220 8	325.6	543.0	923.3
Cu^{2+}	0.74	191.0	241.6	327.1	482.7	808.8	1 381.5
Fe^{2+}	0.76	186.1	235.4	316.6	470.1	787.5	1 344.6
Zn^{2+}	0.74	191.0	241.6	327.1	462.7	808.8	1 381.5
Co^{2+}	0.74	191.0	241.6	327.1	482.7	808.8	1 381.5
Ni^{2+}	0.72	196.1	248.2	336.1	496.0	831.4	1 420.3
Sn^{2+}	1.12	127.9	160.9	216.9	319.9	533.3	906.4
Cr^{2+}	0.84	168.9	213.3	288.5	425.6	712.1	1 214.3

(Table 5 contd.)

Pd^{2+}	0.86	165.1	208.5	281.9	415.7	695.5	1 186.1
Ba^{2+}	1.40	103.0	129.1	178.6	256.5	425.9	721.4
Ge^{2+}	0.93	153.0	193.1	260.8	384.6	642.9	1 095.4
Ti^{2+}	0.90	158.0	199.4	269.4	397.4	664.4	1 132.6
S^{2-}	1.84	78.0	98.0	131.6	195.8	328.2	544.5
Al^{3+}	0.50	621.1	792.1	1 079.8	1 600.8	2 701.4	4 648.5
Fe^{3+}	0.64	486.6	619.9	844.1	1 251.2	2 109.8	3 628.7
Cr^{3+}	0.69	451.7	575.8	788.2	1 160.8	1 956.6	3 359.7
Mn^{3+}	0.66	472.0	601.3	818.6	1 213.4	2 045.7	3 518.3
Co^{3+}	0.63	494.2	629.7	857.4	1 271.0	2 143.3	3 681.5
Ni^{3+}	0.62	502.1	638.5	862.5	1 291.5	2 177.9	3 741.1
Ce^{3+}	1.11	282.8	359.0	487.8	722.6	1 215.0	2 081.5
Ga^{3+}	0.62	502.1	638.5	862.5	1 291.5	2 177.9	3 741.1
In^{3+}	0.81	385.7	490.7	667.6	989.2	1 666.2	2 859.2
Tl^{3+}	0.95	329.6	419.8	569.6	843.8	1 420.2	2 435.1
Sc^{3+}	0.81	385.7	490.7	667.6	989.2	1 666.2	2 859.2
Y^{3+}	0.93	336.6	427.9	581.8	861.9	1 450 8	2 487.9
Gd^{3+}	1.02	307.3	390.5	530.7	785.8	1 322.5	2 266.8
La^{3+}	1.15	273.1	346.6	470.9	697.6	1 172.6	2 008.4
Th^{3+}	1.14	275.4	349.7	475.0	703.7	1 182.9	2 026.2
U^{3+}	1.11	282.8	359.0	487.8	722.6	1 215.0	2 081.5
Np^{3+}	1.09	287.9	365.6	496.7	735.8	1 237.3	2 120.0
Cr^{4+}	0.56	981.9	1 258.8	1 710.4	2 539.2	4 290.0	7 381.5
Mn^{4+}	0.54	1 018.1	1 300.0	1 773.6	2 633.2	4 449.0	7 655.6
Ti^{4+}	0.68	809.7	1 033.4	1 409.2	2 091.6	3 532.4	6 075.6
Ge^{4+}	0.53	1 037.2	1 324.5	1 807.0	2 682.8	4 533.1	7 800.4
Zr^{4+}	0.80	689.1	879.0	1 196.00	1 778.3	3 002.0	5 161.5
Sn^{4+}	0.71	775.7	898.9	1 349.8	2 003.4	3 383.0	5 818.1
Ce^{4+}	1.01	546.9	697.0	949.7	1 409.2	2 377.1	4 084.4
Pb^{4+}	0.84	656.5	837.4	1 141.4	1 693.8	2 858.8	4 914.8
U^{4+}	0.97	569.2	725.6	990.0	1 467.1	2 475.3	4 253.6
Np^{4+}	0.95	581.1	740.9	1 009.5	1 498.0	2 527.5	4 343.6
V^{5+}	0.59	1 458.0	1 856.6	2 534.4	3 764.5	6 364.0	10 956.1
As^{5+}	0.47	1 822.4	2 329.3	3 180.4	4 724.9	7 989.7	13 758.1
Sb^{5+}	0.62	1 388.0	1 767.0	2 411.9	3 582.4	6 055.9	10 425.1
Bi^{5+}	0.74	1 159.7	1 481.2	2 021.4	3 002.0	5 073.3	8 731.5
Nb^{5+}	0.70	1 225.6	1 565.6	2 136.7	3 173.3	5 363.4	9 231.5
Cr^{6+}	0.52	2 369.9	3 029.9	4 138.0	6 148.8	10 399.9	17 912.4
Mo^{6+}	0.62	1 988.6	2 542.0	3 471.2	5 157.5	8 722.0	15 020.8
Mn^{7+}	0.46	3 642.8	4 658.9	6 364.3	9 459.2	16 003.7	27 570.8

Criss and Cobble[54] observed that ionic entropies at higher temperatures are linearly related to ionic entropies at other temperatures and proposed their correspondence relationship,

$$S_{t_2} = a + b\, S_{t_1} \qquad \ldots (43)$$

where, S_{t_2} and S_{t_1} are the entropies at temperatures t_2 and t_1, respectively, and a and b are the coefficients of the linear equation and are constant for a particular pair of temperatures. They however obtained the ionic entropies from the experimental partial molal entropy data of the corresponding salt consisting of the particular cations and anions. Some arbitrary means were used for the division into the ionic parts and it was assumed that the cations and anions will follow a separate linear relationship to produce different correspondence curves for cations and anions[54,55]. We have shown that if one could fix the ionic scale of entropy properly the cations and anions will have the same correspondence curves[48]. It is also possible to plot the entropy of hydration of ions to a linear correspondence curve. Fig. 15 shows a few typical correspondence plots with entropy of hydration. The entropy of hydration values at 100° were taken

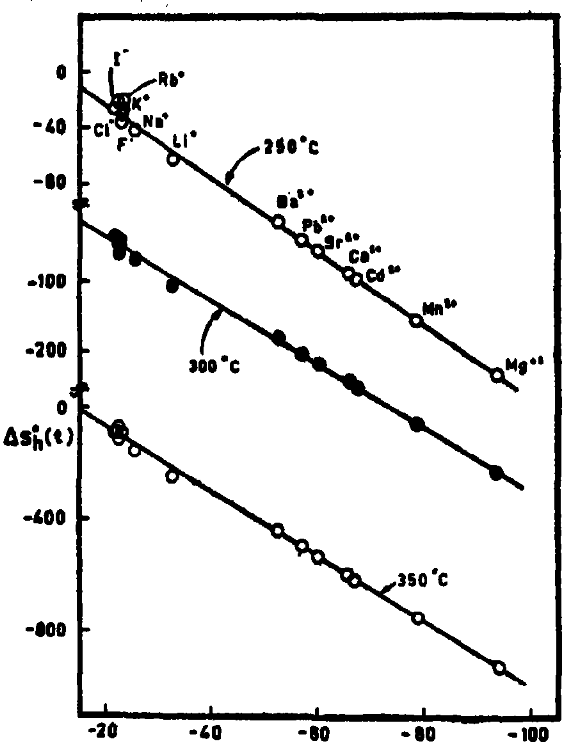


Fig. 15. Correspondence diagram illustrating the linear relationship between the predicted entropies of hydration of ions (ΔS_h°, cal mol^{-1} K^{-1}) at 100° and at other temperatures.

as reference temperature values. The values of the coefficients a (intercept) and b (slope) for each temperature plots with 100° as the reference temperature have been listed in Table 6.

TABLE 6—CORRESPONDENCE CONSTANTS a (in cal mol^{-1} K^{-1}) AND b FOR THE CALCULATED ENTROPY OF HYDRATION (ΔS°_h) OF IONS AT DIFFERENT TEMPERATURE

Temp. C°	a	b
0	−14.76	0.529
25	−10.92	0.599
50	−7.37	0.741
75	−3.75	0.861
100*	0.00	1.000
125	3.88	1.161
150	8.27	1.351
175	12.58	1.563
200	17.62	1.822
225	23.84	2.178
250	32.01	2.666
275	43.71	3.410
300	62.23	4.655
325	92.37	6.867
350	164.87	11.640
370	296.17	20.056

* Reference tem. (see equation 43).

The theory should also provide proper guidance for fixing the ionic scale for heat capacity of hydration at different temperatures. But the large limits of uncertainties of the second temperature derivatives of the solvent dielectric constant particularly at higher temperatures have been proved to be a serious handle to the accurate heat capacity predictions (Figs. 5, 6 and 12, 13). Detail discussion about heat capacity predictions by different theories will appear elsewhere[52].

Conclusion :

From the two simple but highly successful approaches described in the present communication, it may be concluded that in spite of the various criticisms put forward from time to time[2,59] against its use for thermodynamic predictions, the Born equation[6] even in its original primitive form can provide us the basis of a theory of electrolytic solution which can accurately predict the various thermodynamic behaviours of ions and electrolytes in solution at all temperatures. Moreover, the use of the primitive Born model makes the mathematical calculations for prediction strikingly simple. This remarkable success of the Born equation perhaps indicates that particularly at some higher temperature and thereafter the thermodynamic behaviours of ions in solution is directed mainly by the electrostatic field effect and the so called structural effect is only significant at some lower temperatures where the solvent hydrogen bonding is sufficiently strong. The same observation has been varified recently, by experiments with high temperature aqueous electrolyte solutions[45]. Yet another advantage of the present approaches is that they can be universally applied to non-aqueous and mixed-solvent systems[47].

Further works in this line which may reveal the possible constituents of temperature insensitive quantities C_s and ΔG^* or their slight variations at extreme temperatures and also their relationship with the so called solvation numbers would be no doubt interesting.

References

1. J. E. Desnoyers and C. Jolicoeur, "Modern Aspects of Electrochemistry", eds. J. O'M Bockris and B. E. Conway, Plenum, New York, 1969, Vol. 5.
2. C. V. Krishnan and H. L. Friedman in "Water, a Comprehensive Treatise," ed. F. Franks, 1973, Vol. 3, Ch. 1.
3. P. P. S. Saluja in "International Rev. Sci.", ed. J. O'M Bockris, Butterworths, 1976, Series 2, Vol. 6, Ch. 1.
4. W. G. Brchards in Ref. 2, 1979, Vol 6, Ch. 3.
5. U. Sen, D.Sc. Thesis, Calcutta University, 1980.
6. M. Born, *Z. Physik*, 1920, **1**, 45.
7. Y. C. Wu and H. L. Friedman, *J. Phys. Chem.*, 1966, **70**, 501.
8. T. J. Webb, *J. Am. Chem. Soc.*, 1976, **48**, 2589.
9. P. Debye and L. Pauling, *J. Am. Chem. Soc.*, 1925, **47**, 2129.
10. C. L. DeLigny and M. Alfenaar, *Recl. Trav. Chim.*, 1965, **84**, 81 ; 1967, **86**, 929.
11. H. L. Friedman and G. R. Haugen, *J. Am. Chem. Soc.*, 1954, **76**, 2060.
12. G. R. Haugen and H. L. Friedman, *J. Phys. Chem.*, 1968, **72**, 4549.
13. R. M Noyes, *J. Am. Chem. Soc.*, 1962, **84**, 513.
14. H. S. Frank and W. Y. Wen, *Faraday Discuss. Chem. Soc.*, 1957, **24**, 133.
15. J. D. Bernal and R. H. Fowler, *J. Chem. Phys.*, 1933, **1**, 575.
16. A. D. Buckingham, *Faraday Discuss. Chem. Soc.*, 1957, **24**, 157.
17. J. O. Hirschfelder, C. F. Curtiss and R. B. Bird, "Molecular Theory of Gas and Liquids", Wiley, New York, 1954, Ch. 4.
18. L. D. Landen and E. M. Lifschitz, "Quantum Mechanics", Pergamon, London, 1958.
19. L. D. Landen and E. M. Lifschitz, "Statistical Physics", Addison-Wisley, Reading, 1958.
20. J. S. Muirhead-Gould and K. J. Laidler, *Trans. Faraday Soc.*, 1967, **63**, 944.
21. J. O'M Bockris and P. P. S. Saluja, *J. Phys. Chem.*, 1972, **76**, 2298.
22. R. Zana and E. Yeager, *J. Phys. Chem.*, 1967, **71**, 521.
23. E. Yeager and R. Zana, *J. Phys. Chem.*. 1975, **79**, 1926.
24. S. Goldman and R. G. Bates, *J. Am. Chem. Soc.*, 1972, **94**, 1476.
25. I. Dzidic and P. Kebarle, *J. Phys. Chem.*, 1970, **74**, 1466.
26. M. Arshadi, R. Yamdagni and P. Kebarle, *J. Phys. Chem.*, 1970, **74**, 1475.
27. A. Pullman and B. Pullman, *Quar. Rev. Biophys.*, 1975, **7**, 506.
28. W. L. Jorgensen, *J. Am. Chem. Soc.*, 1978, **100**, 1057.
29. M. D. Newton, *J. Chem. Phys.*, 1973, **58**, 5833 ; *J. Phys. Chem.*, 1975, **79**, 2795.
30. P. Kollman and I. D. Kuntz, *J. Am. Chem. Soc.*, 1976, **98**, 6820.
31. G. W. Schnuelle and D. L. Beveridge, *J. Phys. Chem.*, 1975, **79**, 2566.
32. D. L. Beveridge and G. W. Schnuelle, *J. Phys. Chem.*, 1974, **78**, 2064 ; 1975, **79**, 2562.
33. E. A. Moelwyn-Hughes, "Physical Chemistry", 2nd ed., Pergamon, London, 1961, Ch. 8.
34. H. Popkie, H. Kistenmacher and E. Clementi, *J. Chem. Phys.*, 1973, **59**, 1325.
35. H. Kistenmacher, H. Popkie and E. Clementi, *J. Chem. Phys.*, 1973, **59**, 5842; 1975, **61**, 799.
36. J. O. Noell and K. Morokuma, *Chem. Phys. Lett.*, 1975, **36**, 465.
37. P. Claverie, J. P. Daudey, J. Langert, B. Pullman, D. Piazzola and M. J. Huron, *J. Phys. Chem.*, 1978, **82**, 405.
38. D. Y. C. Chan, D. J. Mitchel and B. N. Ninham, *J. Chem. Phys.*, 1979, **70**, 2946.
39. A. Warshell, *J. Phys. Chem.*, 1979, **83**, 1640.
40. D. W. Wood in Ref. 2, Vol. 6, Ch. 6.
41. G. N. Lewis and M. Randall, "Thermodynamics", 2nd ed., revised by K. Pitzer and L. Brewer, McGraw-Hill, New York, 1961, p. 502.
42. U. Sen and J. W. Cobble, in the press ; J. W. Cobble and R. C. Murray, *Faraday Discuss. Chem. Soc.*, 1978, **64**, 144.
43. W. M. Latimer, *J. Chem. Phys.*, 1955, **23**, 90.
44. U. Sen and J. W. Cobble, unpublished results.
45. J. W. Cobble, R. C. Murray and U. Sen, *Nature (London)*, 1981, **291**, 566.
46. U. Sen, *J. Am. Chem. Soc.*, 1979, **101**, 2531.
47. U. Sen, *J. Am. Chem. Soc.*, 1980, **107**, 2181.
48. U. Sen, *J. Chem. Soc., Faraday Trans. 1*, 1981, **77**, 2863.
49. U. Sen, *Can. J. Chem.*, 1984, **62**, 2721.
50. U. Sen, "Proceedings Sir J. C. Ghosh Memorial Conference on Strong Electrolytes", Calcutta, 1982.
51. R. A. Pierotti, *Chem. Rev.*, 1976, **76**, 717.
52. U. Sen, in the press.
53. L. Pauling, "The Nature of the Chemical Bonds", 3rd. ed., Cornell Univ. Press, Ithaca, 1960, p. 574.
54. C. M. Criss and J. W. Cobble, *J. Am. Chem. Soc.*, 1964, **86**, 5385.
55. C. M. Criss and J. W. Cobble, *J. Am. Chem. Soc.*, 1964, **86**, 5390.

56. J. E. B. RANDLES, *Faraday Discuss. Chem. Soc.*, 1956, **52**, 1578.

57. B. S. GOURARY and F. J. ADRIAN, *Solid State Phys.*, 1960, 10, 127.

58. F. J. MILLERO in "Water and Aqueous Solutions", ed. R. A. HORNE, Wiley-Interscience, New York, 1972, Ch. 18.

59. B. E. CONWAY, *Annu. Rev. Phys. Chem.*, 1966, 17, 481.

J. Indian Chem. Soc.,
Vol. LXIII, June 1986, pp. 565-567

Infrared and Thermal Studies of Dibenzyl Sulphoxide Complexes of Dioxouranium(II)

R. K. AGARWAL* and PRAVESH KUMAR

Department of Chemistry, Lajpat Rai Post-Graduate College, Sahibabad-201 005

Manuscript received 9 September 1985, revised 10 April 1986, accepted 6 May 1986

Coordination compounds of dibenzyl sulphoxide (DBzSO) with UO_2X_2 (X=Cl, Br, I, NO_3, NCS or CH_3COO) have been prepared and characterised by elemental analysis, molecular weight, conductance, infrared and TG data. Such study indicate the monomeric nature of the adducts $UO_2X_2.2DBzSO$, where the UO_2^{II} is bonded to the oxygen atom of DBzSO ligand. Force constant and U–O bond distance have also been calculated.

SULPHOXIDE, with the general formula R_2SO (R=alkyl or aryl) have large dipole moment (~4.0D). They are excellent nucleophiles capable of coordinating to the metal ions, through either sulphur or oxygen[1]. In recent years, a number of sulphoxide complexes of transition and non-transition metal ions are reported[1,2]. Comparatively less is known about the compounds of dioxouranium(II) with sulphoxides[3-12]. In all these complexes, sulphoxides coordinate UO_2^{II} through their oxygen atoms. In this paper, some details of ir and thermal studies of dibenzyl sulphoxide (DBzSO) complexes of dioxouranium(II) are given. There seems to be no prior reports on these complexes in the literature.

Experimental

All chemicals used were of analytical grade. Uranyl nitrate, uranyl chloride and uranyl acetate were available commercially, while uranyl bromide was prepared from uranyl acetate by treating it with hydrobromic acid[13]. Uranyl iodide was obtained by treating uranyl nitrate with barium iodide in dry ether[14]. Uranyl thiocyanate was prepared by mixing an ethanolic solution of uranyl nitrate and potassium thiocyanate, when potassium nitrate was precipitated[10]. The ligand DBzSO (Merck) was used as such.

Preparation of complexes : All the complexes were obtained by the following general method. The uranyl salt (1 mmol) dissolved in acetone (25 ml) was mixed with ligand (2 mmol) in acetone (20 ml). After concentrating the solution by evaporation in dry air, the complexes separated out as crystals. The crystal were filtered off, washed with acetone and finally with ether and dried in vacuum.

The elemental analyses of complexes and other experimental methods used were same as in the earlier paper[15]. Results are reported in Tables 1-3.

Results and Discussion

The analytical data (Table 1) correspond to the general formula, $UO_2X_2.2DBzSO$ (X=Cl, Br, I, NO_3, NCS or CH_3COO) for the complexes. All the complexes were coloured, non-hygroscopic crystalline solids soluble in polar solvents and with the exception of $UO_2I_2.2DBzSO$, they were stable in air. The latter complex decomposed slowly giving out iodine vapour. The electrical conductivity values 3.2-5.9 Ω^{-1} cm^2 mol^{-1} in nitrobenzene indicate the complexes as non-electrolytes. Molecular weights of the complexes determined cryoscopically in freezing nitrobenzene further confirm the monomeric nature of the complexes (Table 1).

In general, the ir spectra of the halo-complexes closely resemble each other, while those of the nitrate, thiocyanate and acetate complexes show extra bands due to the corresponding anionic species (Table 2). The strong S=O stretching band in free non-coordinated DBzSO at 1 032 cm^{-1} (Refs. 16, 17) were not observed in the ir spectra of the complexes $UO_2X_2.2DBzSO$ wherein a new band in the region 960-970 cm^{-1} was observed. The C–S stretching band of DBzSO at 682 cm^{-1} is shifted to a slightly higher wave number in the complexes. Such shift of the S=O and of the C–S bands are indicative of the decrease in the double bond character of the S=O bond and on electron shift from the aryl group to the sulphur atom of the ligand. The ir data thus suggest coordination from the oxygen atom of the DBzSO[16,17]. A very strong absorption attributed to phenyl-S stretch by previous workers[18] has been identified at 1 079 cm^{-1} in free DBzSO which does not suffer any significant change on complexation. It indicates the absence of coordination from the sulphur atom of the ligand. In the far-ir region, the ν_{U-O} bands are identified at 410-400 cm^{-1} region[19,20]. In addition to these ligand vibration modes, ν_1 and ν_3 vibrations of the uranyl ion[21] in

TABLE 1—ANALYTICAL AND PHYSICAL DATA OF UO_2X_2.2DBzSO COMPLEXES IN NITROBENZENE

Compd.	Analysis % : Found/(Calcd.)			Λm	Average mol. wt.
	U	S	Anion	Ω^{-1} cm^2 mol^{-1}	Found/(Calcd.)
UO_2Cl_2.2DBzSO	29.86 (29.71)	7.82 (7.99)	8.89 (8.86)	3.2	801 (786)
UO_2Br_2.2DBzSO	26.58 (26.74)	6.91 (7.19)	17.16 (17.97)	3.9	890 (859)
UO_2I_2.2DBzSO	23.87 (24.18)	6.84 (6.50)	24.91 (25.81)	5.9	984 (963)
$UO_2(NO_3)_2$.2DBzSO	27.54 (27.36)	7.81 (7.49)	—	3.6	854 (839)
$UO_2(NCS)_2$.2DBzSO	27.80 (28.13)	14.98 (15.13)	13.17 (13.71)	4.2	846 (829)
$UO_2(CH_3COO)_2$.2DBzSO	27.76 (28.06)	7.84 (7.54)	—	4.7	848 (832)

TABLE 2—PERTINENT IR DATA (cm^{-1}), FORCE CONSTANTS, U–O BOND DISTANCE OF DBzSO COMPLEXES OF UO_2X_2

Compd.	ν(Phen–S)	ν(S=O)	ν(U–O)	ν_1(U=O)	ν_3(U=O)	U–O force constant m dyne/A	Force constant due to interaction between bonds m dyne/A	U–O (calcd.) distance A
DBzSO	1 079s	1 032vs	—	—	—	—	—	—
UO_2Cl_2.2DBzSO	1 076m	960s	410m	830	920	6.763 2	−0.269 5	1.741 1
UO_2Br_2.2DBzSO	1 080m	965s	405m	835	930	6.879 3	−0.307 1	1.737 3
UO_2I_2.2DBzSO	1 075s, b	970s	400m	830	925	6.801 6	−0.307 8	1.740 5
$UO_2(NO_3)_2$.2DBzSO	1 072s	955s	407m	837	928	6.879 6	−0.275 9	1.737 3
$UO_2(NCS)_2$.2DBzSO	1 080m	960s	405m	832	925	6.817 2	−0.292 1	1.739 9
$UO_2(CH_3COO)_2$.2DBzSO	1 075m	970s	410m	825	920	6.724 2	−0.308 5	1.742 3

s=strong, m=medium, w=weak, b=broad, sh=shoulder, v=very.

TABLE 3—THERMOANALYTICAL RESULTS OF UO_2X_2.2DBzSO

X	Sample weight mg	Residual mass mg	Ligand's mass loss (%) 170-230°		Ligand's mass loss (%) 260-330°		Residual (%) 610°	
			Theor.[a]	Exp.	Theor.[b]	Exp.	Theor.[c]	Exp.
Cl	29.64	11.11	43.07	44.61	57.42	59.12	85.08	87.48
Br	28.82	9.18	38.76	40.16	51.68	53.06	81.58	82.41
NO_3	25.42	8.62	40.89	41.93	53.86	54.98	82.86	83.91
NCS	27.16	9.23	40.78	42.16	54.37	55.96	83.17	83.98
CH_3COO	26.91	9.02	40.68	41.98	54.24	55.83	83.09	83.51

[a] Calculated for loss of 1.5 mol of ligand. [b] Calculated for total loss of ligand. [c] Calculated as U_3O_8.

their UO_2X_2.2DBzSO complexes are observed at 837-825 and 930-920 cm^{-1}, respectively.

In the $UO_2(NCS)_2$.2DBzSO complex, the C–N and C–S stretching band appear at 2 050 and 800 cm^{-1}, respectively. On the basis of the high relative intensity of the C–N band, it may be concluded that the thiocyanate group is N-bonded[22,23] to the UO_2^{II} ion. The two ir bands at ~1 550 and 1 475 cm^{-1} in the spectra of the complex $UO_2(CH_3COO)_2$.2DBzSO is attributed to the anti-symmetric and the symmetric stretching vibration of COO^- group.

Examination of the ir spectra of $UO_2(NO_3)_2$.2DBzSO reveals the absence of ionic nitrate group[24]. This is evident from the splitting of the ν_3 band at ~1 360 cm^{-1} of the ionic nitrates into ν_1 (~1 280 cm^{-1}) and ν_4 (~1 520 cm^{-1}) in the complex. The nitrate group in this complex appears to be bidentate since the ir bands due to this group occur almost in the same region as in case of $UO_2(NO_3)_2.2H_2O$, $K[UO_2(NO_3)_3]$ and other uranyl nitrate complexes containing bidentate nitrate group[15,25]. Bands at ~1 030, and ~810 and ~730 cm^{-1} in this complex are assigned to ν_2, ν_6 and ν_3, ν_5 modes, respectively of the coordinated nitrate groups[26]. Thus uranium appear 8-coordinated in this complex. Uranium was also found 8-coordinated in the complexes[25,28], $Rb[UO_2(NO_3)_3]$, $UO_2(NO_3)_2.(Ph_3PO)_2$ and $UO_2(NO_3)_2.2H_2O$. In all other uranium(VI) complexes of DBzSO, the coordination number of uranium was 6.

In the present studies, it has been observed that the ν_1 mode of the uranyl ion appears as of weak intensity and ν_3 mode strong intensity in the ir

spectra (Table 3). A group theoretical consideration[27] shows that a linear and symmetrical triatomic UO_2^{II} ion possessing $D_{\infty h}$ symmetry gives rise to three fundamental modes of vibrations. Wilson's G – F matrix method[28] has been used to determine the stretching and interaction force constants. The results are in turn used to calculate the U – O bond distance following Badger's formula[29]. The force constants, bond distances and spectral data used herein are summarised in Table 2. It is apparent from the calculated data that the U – O bond length decreases with the increase in the value of symmetric stretching frequency (ν_1)[30]. A plot of $(\nu_1+\nu_3)$ *vs* force constants gave a straight line with the increase in the symmetric stretching vibrations on complexation ; the U – O force constant and the force constant due to the interaction between the bonds were also found to increase. Further, the U – O bonds distances in uranyl salts generally range from 1.60 to 1.92 Å depending on the nature of the equatorial ligands[31]. The calculated values of the U – O bond distances in the present complexes are close to 1.73±0.01 Å.

The thermograms of the complexes indicate virtually no change in weight upto 170°. At 173-230°, a loss of 39-43% is observed which corresponds to 1.5 mole of the ligand DBzSO, followed by a further loss of 53-59% at 260-360° showing the complete loss of DBzSO molecules leaving a residue of UO_3. The oxide U_3O_8 was finally formed at ~610°. Above this temperature there is no observable change in weight.

Acknowledgement

The authors are grateful to C.S.I.R., New Delhi, for financial assistance, and thankful to Dr. G. D. Sharma, Principal, L. R. (Post-Graduate) College, Sahibabad, for taking interest in the work.

References

1. J. Gopalakrishnan and C. C. Patel, *J. Sci. Ind. Res.*, 1968, **27**, 475.
2. J. A. Davies, *Adv. Inorg. Chem. Radiochem.*, 1981, **24**, 115.
3. F. A. Cotton and R. Francis, *J. Am. Chem. Soc.*, 1960, **82**, 2986.
4. J. O. Edward and J. A. Streitar, *Science*, 1968, **142**, 1651.
5. V. Krishnan and C. C. Patel, *Indian J. Chem.*, 1964, **2**, 416.
6. V. Krishnan and C. C. Patel, *J. Inorg. Nucl. Chem.*, 1965, **27**, 244.
7. S. M. Sinitsyna and N. M. Sinitsyn, *Dokl. Chem.*, 1966, **166**, 467.
8. G. Kaufmann and M. J. F. Leroy, *Bull. Soc. Chim. Fr.*, 1966, 3770.
9. V. V. Savant and C. C. Patel, *J. Inorg. Nucl. Chem.*, 1969, **31**, 2819.
10. V. V. Savant and C. C. Patel, *J. Inorg. Nucl. Chem.*, 1972, **34**, 1462.
11. P. A. Vigato, U. Casellato and M. Vidali, *Gazz. Chim. Ital.*, 1977, **107**, 61.
12. B. B. Mishra, S. R. Mohanty, N. V. V. S. Murti and S. Raychaudhri, *Inorg. Chim. Acta*, 1978, **28**, 275.
13. S. S. Sandhu and S. S. Sandhu, Jr., *Indian J. Chem.*, 1973, **11**, 369.
14. N. V. Sidwick, "The Chemical Elements and their Compounds", Oxford, London, 1950.
15. A. K. Srivastava, S. Sharma and R. K. Agarwal, *Inorg. Chim. Acta*, 1982, **61**, 235.
16. T. N. Srivastava, N. Bhakru and R. K. Agarwal, *J. Inorg. Nucl. Chem.*, 1981, **43**, 402.
17. R. K. Agarwal, P. Kumar and H. K. Rawat, *Thermochim. Acta*, 1985, **88**, 397.
18. R. M. Silverstein and G. C. Bassler, "Spectrometric Identification of Organic Compounds", 2nd. ed., Wiley, New York, 1967.
19. J. P. Day and L. M. Venanzi, *J. Chem. Soc. A*, 1960, 1363.
20. J. R. Ferraro and A. Walker, *J. Chem. Phys.*, 1966, **45**, 550.
21. L. Cattalini, U. Croatto, S. Degetto and E. Tondello, *Inorg. Chim. Acta Rev.*, 1971, **5**, 19.
22. Z. M. S. Al-Kazaz, K. W. Bagnall and D. Brown, *J. Inorg. Nucl. Chem.*, 1973, **35**, 1501.
23. J. L. Burmeister, *Coord. Chem. Rev.*, 1966, **1**, 205 ; 1968, **3**, 225.
24. B. M. Gatehouse, S. E. Livingstone and R. S. Nyholm, *J. Chem. Soc.*, 1957, 4222.
25. G. Topping, *Spectrochim. Acta*, 1965, **21**, 1743.
26. R. K. Agarwal, J. R. Chopra and S. C. Rastogi, *J. Indian Chem. Soc.*, 1985, **62**, 154.
27. V. K. Rastogi, A. N. Pandey, S. L. Gupta and R. C. Saxena, *Indian J. Pure Appl. Phys*, 1980, **18**, 379.
28. L. B. Wilson, *J. Chem. Phys.*, 1939, **7**, 1047 ; 1941, **9**, 76.
29. R. M. Badger, *J. Chem. Phys.*, 1934, **2**, 128 ; 1935, **3**, 710.
30. C. L. Garga, S. D. Gupta and K. V. Narasinhan, *Indian J. Pure Appl. Phys.*, 1970, **8**, 108.
31. W. H. Zachariasen, *Acta Crystallogr.*, 1954, **7**, 783.
32. J. I. Bullock, *J. Inorg. Nucl. Chem.*, 1967, **29**, 2257.

J. Indian Chem. Soc.,
Vol. LXIII, June 1986, pp. 568-572

Chromium(VI) Dioxydichloride Complexes with Sulphur Ligands found in Coal

MADANMOHAN SINGH GILL and RAJENDAR D. VERMA*

Department of Chemistry, Panjab University, Chandigarh-160 014

Manuscript received 6 November 1985, revised 14 March 1986, accepted 8 May 1986

CrO_2Cl_2 forms complexes with sulphur ligands having composition $CrO_2Cl_2.2L$ where, $L=(C_2H_5)_2S$, $(n\text{-}C_3H_7)_2S$, $(n\text{-}C_4H_9)_2S$, $(n\text{-}C_5H_{11})_2S$, $(n\text{-}C_6H_{13})_2S$, C_4H_4S and $C_6H_4SCH : CH$. The complexes are non-electrolytes and monomeric in dilute solutions. The ^1H nmr and the ir data of the complexes are discussed.

A number of complexes of CrO_2Cl_2 with phosphorus halides[1], amides[2], titanium tetrachloride[3] and nitrogen bases[4,5] have been reported. Complexes of CrO_2Cl_2 with sulphur ligands have not been prepared. As a part of our study on hydrodeheterogenation of model compounds found in coal utilising metal complexes of the heteroatom species, we have prepared and characterised complexes of sulphur ligands found in coal, with CrO_2Cl_2. The ligands used are R_2S ($R=C_2H_5$, $n\text{-}C_3H_7$, $n\text{-}C_4H_9$, $n\text{-}C_5H_{11}$, $n\text{-}C_6H_{13}$), thiophene and benzo[b]thiophene. These are found in coal tar which is recovered from coal on gasification[6,7].

Experimental

Dialkyl sulphides (R_2S; $R=C_2H_5$, $n\text{-}C_3H_7$, $n\text{-}C_4H_9$, $n\text{-}C_5H_{11}$ and $n\text{-}C_6H_{13}$) were prepared by literature methods[8]. Purity of the ligands was checked by recording their ^1H nmr in CCl_4 (Ref. 9). Thiophene and benzo[b]thiophene (E. Merck) were used as such. Chromium(VI) dioxydichloride was prepared by the reported method[10], and repeatedly distilled; fraction distilling at 117°/740 mm was collected for use. Carbon tetrachloride, dimethyl sulphoxide, nitromethane, nitrobenzene and diethyl ether were purified and dried before use.

Preparation of complexes : In a typical preparation, to an ice-cold solution of a known weight (25-30 mmol) of the base in dry CCl_4 (~50 ml) was added dropwise a stoichiometric amount of an ice-cold solution of CrO_2Cl_2 in CCl_4. The contents were magnetically stirred for ~2 h; the reaction was exothermic. In case of thiophene and bezo[b]thiophene, fine powdered solids were formed, but in case of dialkyl sulphides, solid sticky mass was obtained, which on trituration with dry ether gave fine powder. The isolated complexes were filtered under dry N_2, washed repeatedly with dry diethyl ether and finally dried under vacuum.

Analytical methods : Chromium in the complexes was estimated by heating them to 900-1 000° and weighing the residue as Cr_2O_3. Chlorine was estimated by Volhard's method. Sulphur was estimated as $BaSO_4$ after fusing the known weight of the complex with fusion mixture (Na_2O_2 and Na_2CO_3 in 1 : 2 ratio). Analytical data and colour of the complexes are given in Table 1.

TABLE 1—PHYSICAL PROPERTIES AND ANALYTICAL DATA OF COMPLEXES OF CHROMIUM(VI) DIOXYDICHLORIDE

Compd.*	Colour	M.p. °C	Molecular weight: Concn. × 10³ M	Molecular weight: Found/(Calcd.)	Analysis % : Found/(Calcd.): Cr	Cl	S
$A.2(C_2H_5)_2S$	Blackish brown	80	4.182 0	317.15 (335.4)	15.01 (15.50)	21.02 (21.17)	19.00 (19.08)
$A.2(n\text{-}C_3H_7)_2S$	Dark brown	85	2.295 2	389.05 (391.48)	12.82 (13.28)	18.04 (18.13)	16.28 (16.34)
$A.2(n\text{-}C_4H_9)_2S$	Dark brown	92	7.344 5	443.99 (447.60)	10.85 (11.61)	15.66 (15.86)	13.91 (14.29)
$A.2(n\text{-}C_5H_{11})_2S$	Dark brown	107	6.961 6	492.129 (503.70)	9.62 (10.32)	13.62 (14.09)	12.31 (12.70)
$A.2(n\text{-}C_6H_{13})_2S$	Dark violet	119	2.580 0	558.40 (559.82)	9.07 (9.28)	12.81 (12.68)	11.28 (11.43)
$A.2C_4H_4S$	Black	>300	2.714 7	39.64 (323.28)	15.72 (16.08)	20.92 (21.96)	19.57 (19.79)
$A.2C_6H_4SCH : CH$	Deep grey	>300	0.135 0	15.83 (423.40)	11.98 (12.28)	15.92 (16.76)	14.89 (15.11)

* $A=CrO_2Cl_2$.

Physical measurements : The ir spectra of the complexes were recorded in nujol and hexachlorobutadiene between KBr plates using a Perkin-Elmer 621 spectrophotometer in the range 4 000-400 cm^{-1}. The ^1H nmr spectra of the ligands and their complexes were recorded on a Varian EM 390 (90 MHz) spectrometer using TMS as external reference. Molecular weight of the complexes was determined in dimethyl sulphoxide solution cryoscopically. The molar conductance of millimolar solutions in dimethyl sulphoxide and nitromethane was determined at 25° using Toshniwal CLOI/02A conductivity bridge and dip type conductance cell with a cell constant of 0.521 cm^{-1}. Thermal analysis was carried out in an atmosphere of air by means of MOM Budapest Derivatograph (Type : Paulik, Paulik and Erdey) containing Pt-Rh thermocouples.

Results and Discussion

All the complexes are moisture-sensitive solids except $CrO_2Cl_2.2C_4H_4S$ and $CrO_2Cl_2.2C_6H_4$-SCH : CH. The complexes are insoluble in common non-polar organic solvents but dissolve in dimethyl sulphoxide, nitrobenzene, nitromethane, chloroform and dichloromethane except $CrO_2Cl_2.2C_6H_4SCH$: CH which is soluble only in dimethyl sulphoxide and dimethyl formamide.

The analytical results (Table 1) show that the complexes of CrO_2Cl_2 with sulphur ligands have 1 : 2 stoichiometry. The molecular weights of the complexes (Table 1) in dimethyl sulphoxide correspond very nearly to the monomeric formula weight in very dilute solutions but a considerable decrease in molecular weights of the complexes at higher concentration can be attributed to their association. Molecular weights of $CrO_2Cl_2.2C_4H_4S$ and CrO_2-$Cl_2.2C_6H_4SCH$: CH found very low even at very low concentration, indicate their associative nature in dimethyl sulphoxide. The molar conductance values of the millimolar solutions of these complexes in various solvents (DMSO, 8-18 ; $MeNO_2$ 2-7 Ω^{-1} cm^2 mol^{-1}) reveal their non-electrolytic nature.

Infrared study : The ir spectra of the complexes along with tentative assignment are presented in Table 2. ν_{C-H} and ν_{C-S} have been assigned as discussed by earlier workers[11-13]. However, their interpretation in $CrO_2Cl_2.2R_2S$ (R = ethyl, n-propyl, n-butyl, n-pentyl and n-hexyl) is not straight forward, owing to the occurrence of different rotational isomers of the ligands. In these complexes, the bands at 1 240 and 785-790 cm^{-1} are attributed to CH_2 wagging and rocking modes, respectively for *gauche* conformation, other vibrations attributed to CH_2 *trans* form. This may indicate that complexes consist of mixtures of *trans* and *gauche* isomers,

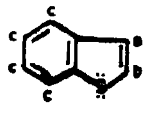
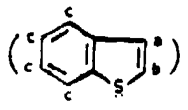
Table 2—IR Spectral Data* of Complexes of Chromium(VI) Dioxydichloride** with Tentative Assignments

$A.2L_1$	$A.2L_2$	$A.2L_3$	$A.2L_4$	$A.2L_5$	$A.2C_4H_4S$	$A.2C_6H_4SCH:CH$	Assignment
2 940sb	2 960sb	2 975sb	2 960sb	2 940sb	2 960sb	2 980sb	ν_{asym} (C–H)
2 880m	2 890m	2 890w	2 880m	2 880m	2 880w	2 880w	ν_{sym} (C–H)
					1 600s	1 625s	$\nu_{C=C}$
1 460s	1 460vs	1 470s	1 470s	1 465s	1 460vs	1 465vs	δ_{asym} (C–H)
1 870s	1 880s	1 890s	1 885m	1 885m	1 880s	1 880vs	δ_{sym} (C–H)
1 240 w	1 240m	1 240w	1 240w	1 240w			ρ_w (CH_2 *gauche*)
					1 240w	1 260w	$\nu_{C=S}+\nu_{C=C}$
					1 225w	1 210w	ρ_w (CH)
					1 170w	1 170w	
1 155wb	1 160m	1 165w	1 165wb	1 165wb			ρ_w (CH_2 *trans*)
1 070m	1 065wb	1 080w	1 090w	1 090w			ρ_t (CH_2 *trans*)
930sb	930sb	940sb	935sb	930sb			$\nu_{Cr=O}+\rho_r$ (CH_2)
					935vs	985vs	$\nu_{Cr=O}$
785w	785s	790w	785w	790w			ρ_r (CH_2 *gauche*)
					780m	785s	ρ_r (CH)
720s	720m	720s	725s	725s			$\nu_{C-S}+\rho_r$ (CH_2 *gauche*)
					720w	725w	$\nu_{C-S}+\rho_r$ (CH)
500sb	500sb	520sb	525sb	525sb	585s	585s	ν_{Cr-S}
440w	440w	450w	450w	430w	440w	435w	ν_{Cr-Cl}

* s = strong, b = broad, w = weak, m = medium, v = very.

** $A = CrO_2Cl_2$: $L_1 = (C_2H_5)_2S$, $L_2 = (n\text{-}C_3H_7)_2S$, $L_3 = (n\text{-}C_4H_9)_2S$, $L_4 = (n\text{-}C_5H_{11})_2S$ and $L_5 = (n\text{-}C_6H_{13})_2S$.

TABLE 3—^{1}H NMR SPECTRA OF LIGANDS AND COMPLEXES

Ligand	Chemical shift (δppm) H_a	H_b	H_c	Complex*	Chemical shift (δppm) H_a	H_b	H_c
$(\overset{a}{C}H_3\overset{b}{C}H_2)_2S$	1.36	2.69	—	$A.2(\overset{a}{C}H_3\overset{b}{C}H_2)_2S$	1.40	3.00	—
$(\overset{a}{C}H_3\overset{c}{C}H_2\overset{b}{C}H_2)_2S$	1.06	2.56	1.66	$A.2(\overset{a}{C}H_3\overset{c}{C}H_2\overset{b}{C}H_2)_2S$	1.09	2.86	1.69
$(\overset{a}{C}H_3(\overset{c}{C}H_2)_2\overset{b}{C}H_2)_2S$	0.96	2.56	1.56	$A.2(\overset{a}{C}H_3(\overset{c}{C}H_2)_2\overset{b}{C}H_2)_2S$	0.99	2.86	1.59
$(\overset{a}{C}H_3(\overset{c}{C}H_2)_3\overset{b}{C}H_2)_2S$	0.96	2.56	1.46	$A.2(\overset{a}{C}H_3(\overset{c}{C}H_2)_3\overset{b}{C}H_2)_2S$	0.96	2.84	1.49
$(\overset{a}{C}H_3(\overset{c}{C}H_2)_4\overset{b}{C}H_2)_2S$	0.90	2.46	1.38	$A.2(\overset{a}{C}H_3(\overset{c}{C}H_2)_4\overset{b}{C}H_2)_2S$	0.90	2.74	1.36
	7.29	7.59	—	A·2 	7.38	7.81	—
	8.00	8.23	7.78	A·2 	8.08	8.41	7.76

* $A = CrO_2Cl_2$.

differing only in configuration of the ligand. Bands at 1 240 cm^{-1} in $CrO_2Cl_2.2C_4H_4S$ and 1 260 cm^{-1} in $CrO_2Cl_2.2C_6H_4SCH:CH$ have been assigned to $\nu_{C=S}+\nu_{C=C}$ which appears in the range 1 270-1 200 cm^{-1} (Ref. 13). In pure chromium(VI) dioxydichloride $\nu_{Cr=O}$ and ν_{Cr-Cl} appear at 984 and 465 cm^{-1}, respectively[14,15]. The most predominant feature in the ir spectra of all the complexes is a very sharp and broad band in the region 930-940 cm^{-1} and a weak band in the region 430-450 cm^{-1} assigned to $\nu_{Cr=O}$ and ν_{Cr-Cl}, respectively. Broadening of $\nu_{Cr=O}$ band is due to appearance of CH_2 rocking vibration in the same region. Another important feature of the spectra of the complexes is the presence of ν_{C-S} which appears in the complexes in the region 720-725 cm^{-1}. This is slightly lower in position relative to the ν_{C-S} in free ligands (735 cm^{-1}) (Ref. 12). These shifts to lower region indicate the formation of Cr–S bond in the complexes, appearing in the region 500-535 cm^{-1}.

^{1}H nmr study : ^{1}H nmr spectra of dialkyl sulphides and their complexes were recorded in $CDCl_3$ solution, while those of thiophene, benzo[b]-thiophene and their complexes in DMSO solution. Proton chemical shifts of the ligands and their complexes are shown in Table 3. H_b protons in the complexes appear at δ 0.20-0.31 down-field as compared to H_b protons in pure ligands. Coordination by the ligands reduce the electron density around C_b, resulting in its deshielding relative to the uncomplexed ligands, causing H_b protons to undergo resonance at a lower applied magnetic field. Other signals of the protons do not differ much from those of the corresponding ligands.

Thermal study : Thermal decomposition of the complexes has been studied upto 900°. Detachment of the ligands from the complexes should be an endothermic process, however, TG and DTG curves show that decomposition takes place exothermally in three steps. This may be due to the fact that the thermal decomposition being studied in an atmosphere of air and the ligand that is removed from the complex gets decomposed by air exothermally, and this exothermal step overpower the endothermic step which is recorded by the derivatograph. DTG minima (Fig. 1) have been projected on TG curves to get inflection points (marked by small arrows on TG curves). Complexes start decomposing around 90°. In the range 440-515°, Cr_2O_3 residue is formed which has been analysed. Experimental and theoretical losses in each step agree well. The intermediates were not characterised. General mode of decomposition may be represented as

$$2CrO_2Cl_2.2L \xrightarrow[-2L]{90-240^\circ} 2CrO_2Cl_2.L$$

$$2CrO_2Cl_2.L \xrightarrow[-2L]{240-260^\circ} 2CrO_2Cl_2$$

$$2CrO_2Cl_2 \xrightarrow[-2Cl_2,\ -\frac{1}{2}O_2]{260-515^\circ} Cr_2O_3$$

where, L = ligand molecule.

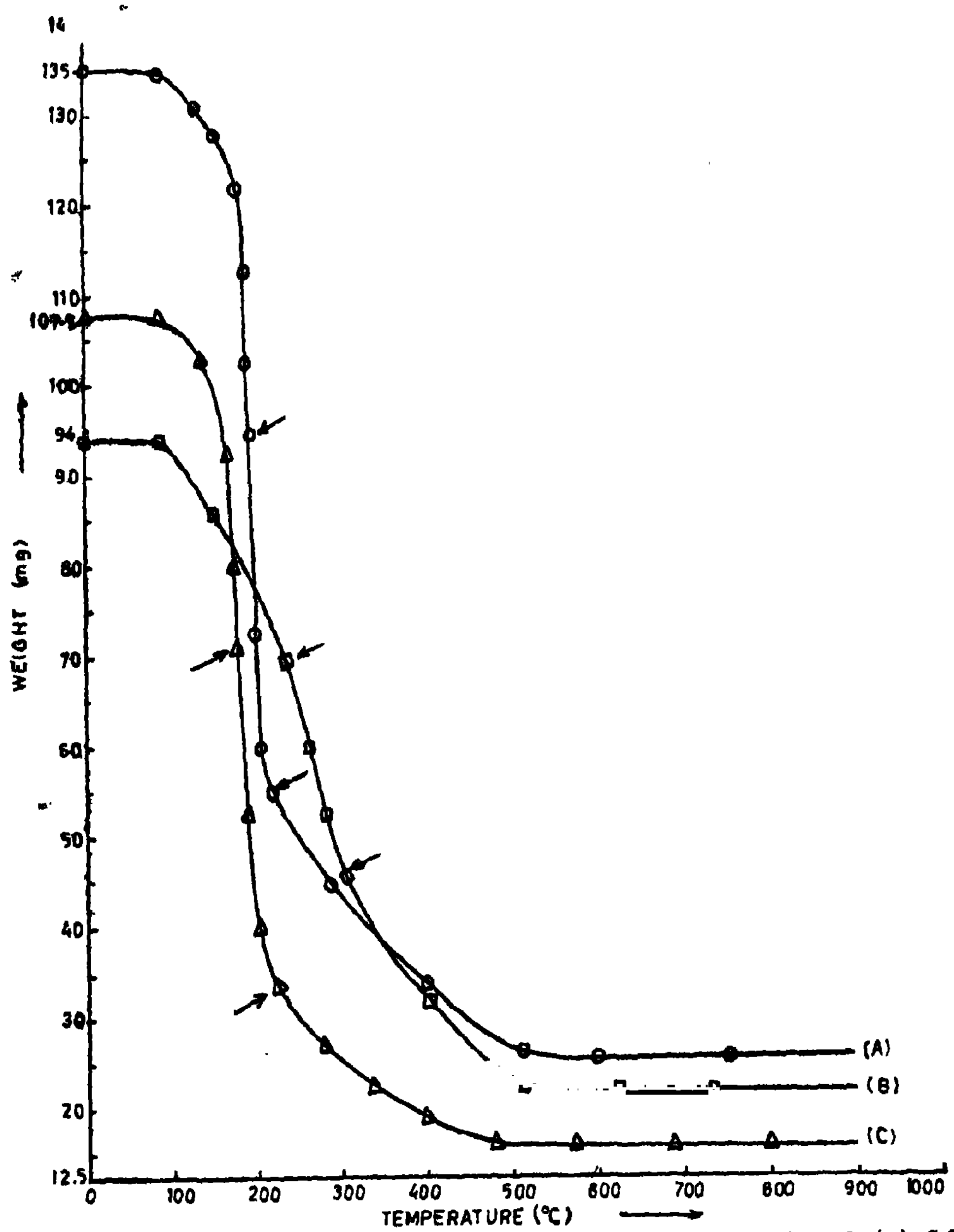


Fig. 1. TG curves of complexes : (○) $CrO_2Cl_2.2(n\text{-}C_3H_7)_2S$ (A), (□) $CrO_2Cl_2.2(n\text{-}C_5H_{11})_2S$ (B), and (▵) $CrO_2Cl_2.2(C_4H_4)S$ (C).

Acknowledgement

One of the authors (M.S.G.) expresses his sincere thanks to C.S.I.R., New Delhi, for the award of Senior Research Fellowship.

References

1. H. S. Fry and J. L. Donnelly, *J. Am. Chem. Soc.*, 1918, 40, 578.
2. R. C. Paul, O. Khosla and R. Dev, *Indian J. Chem.*, 1969, 7, 1254.
3. E. P. J. Elenius, A. Merretoja and P. Kosonen *Chem. Abstr.*, 1965, 63, 10989.
4. J. Bernard, M. Camelet and C. R. Hebd, *Sinc. Acad Sci., Paris*, 1964, 258, 5881.
5. J. S. Banait, G. Singh and S. S. Pahil, *J. Indian Chem Soc.*, 1978, 55, 516.
6. "Encylopedia of Chemical Technology", eds. R. E. Kirk and E. Othmer, Interscience, New York, 1954, Vol. 13 p. 295.
7. Ref. 6, p. 493.
8. L. Brandsma and H. E. Wijers, *Recuils*, 1963, 82, 68.
9. "The Sadtler Handbook of Proton NMR Spectra", ed. W. W Simon, Sadtler Research Laboratories, Pennsylvania, 1978.

10. H. H. Sisler and E. Marchi, *Inorg. Synth.*, 1964, **2**, 205.
11. D. Welti and D. Whittaker, *J. Chem. Soc.*, 1962, 4372.
12. R. J. H. Clark and W. Errington, *Inorg. Chem.*, 1966, **5**, 650.
13. S. H. H. Chaston and S. E. Livingston, *Aust. J. Chem.*, 1967, **20**, 1065.
14. H. Stammreich, K. Kawai and Y. Tavers, *Spectrochim. Acta*, 1959, **15**, 438.
15. F. A. Millar, G. L. Carlson and W. B. White, *Spectrochim. Acta*, 1959, **15**, 709.

J. Indian Chem. Soc.,
Vol. LXIII, June 1986, pp. 573-574

Optical Absorption and Electron Spin Resonance Spectral Studies of Copper(II) Chalcone Complexes in different Solvents

CH. RAMAKRISHNAIAH, R. SESHADRI NAIDU and R. RAGHAVA NAIDU*

Department of Chemistry, School of Mathematical and Physical Sciences, Sri Venkateswara University, Tirupati-517 502

Manuscript received 28 January 1985, revised 24 April 1986, accepted 8 May 1986

Optical absorption and electron spin resonance spectral studies on copper(II) complexes of 2'-hydroxy-, 2',2-dihydroxy-, 2'-hydroxy-4-methoxy- and 2'-hydroxy-4-chlorochalcones in chloroform, dioxan, dimethyl formamide and pyridine indicate axial interaction of all these solvents with copper(II), and such interaction is greatest with pyridine. Monomeric nature of all the complexes in these solvents is indicated from magnetic moment data.

CHALCONES have been found to possess various germicidal[1,2], bactericidal[3], fungicidal[4] and carcinogenic[5] activities. Methoxy- and hydroxy-chalcones can arrest the destruction of adrenaline[6]. Furthermore, naphthyl- and phenanthryl-chalcones possess potential bactericidal and carcinogenic activity[7]. The *ortho*-hydroxychalcones have good chelating properties, and were exploited as analytical reagents for the separation and determination of metal ions[8-12]. The present paper describes the electronic and esr spectral studies of Cu^{II} complexes of *ortho*-hydroxychalcones, *viz*. 2'-hydroxychalcone, 2',2-dihydroxychalcone, 2'-hydroxy-4-methoxychalcone and 2'-hydroxy-4-chlorochalcone in different solvents, *viz*. chloroform, dioxan, dimethyl formamide and pyridine.

Experimental

The copper(II) complexes of 2'-hydroxy-, 2',2-dihydroxy-, 2'-hydroxy-4-methoxy- and 2'-hydroxy-4-chlorochalcones were prepared according to the procedure described in the literature[13]. Spectroscopic grade chloroform, dioxan, dimethyl formamide and pyridine were used as solvents. A Shimadzu-UV-180 spectrophotometer was used to record the electronic spectra. Esr spectra were recorded at room temperature (300 K) with a Varian E-4 X-band spectrometer employing 4 to 8 gauss modulation and operating at a frequency of 9.5 GHz. DPPH has been used as the g-marker.

Results and Discussion

Cu^{II} complexes of 2'-hydroxychalcone, 2',2-dihydroxychalcone, 2'-hydroxy-4-methoxychalcone and 2'-hydroxy-4-chlorochalcone were insoluble in water and soluble in chloroform, dioxan, dimethyl formamide and pyridine. The results of elemental analysis gave 1 : 2 Cu – ligand stoichiometry.

The optical absorption spectra of all the complexes in chloroform, dioxan, dimethyl formamide and pyridine consist of intense charge transfer absorption bands in the 300-450 nm region. The electronic spectra (nujol) of the complexes gave absorption maxima in the region 19 225-24 265 cm^{-1} and these bands were assigned to $^2B_{1g} \rightarrow {}^2E_g$ ($d_{x^2-y^2} \rightarrow d_{xz}, d_{yz}$) transition[18]. In our present investigation, the band pertaining to the above transition is lowered and appeared in the region 14 493-15 152 cm^{-1} (Table 1). Shifting of λ_{max} to longer wavelength could be attributed to the axial interaction of the solvent molecules with copper(II), the extent of which fall in the order, chloroform $<$ dioxan $<$ dimethyl formamide $<$ pyridine. This observation is in agreement with the observations made by earlier investigators[14,15].

The room temperature esr spectra of the Cu^{II} chalcone complexes in chloroform, dioxan, dimethyl formamide and pyridine consist of four absorption lines. These four lines in the multiplet correspond to the (2I+1=4) spin orientations of the copper

TABLE 1—OPTICAL ABSORPTION DATA OF COPPER-CHALCONE COMPLEXES

Compd. no.	Compd.	λ_{max} (cm^{-1}) Chloroform	Dioxan	DMF	Pyridine	Nujol
1	$Cu(C_{15}H_{11}O_2)_2$	15 088	14 925	14 870	14 706	22 215
2	$Cu(C_{15}H_{11}O_3)_2.H_2O$	14 981	14 815	—	14 493	19 225
3	$Cu(C_{16}H_{13}O_3)_2$	14 970	14 910	14 881	14 600	24 265
4	$Cu(C_{15}H_{10}O_2Cl)_2$	15 152	14 870	14 815	14 706	22 215

nuclei with I=3/2. The esr spectra of the most copper(II) complexes in solution at room temperature normally exhibit four hyperfine lines with spin-dependent line widths due to the tumbling motion of the microcrystalline units. This tumbling motion in solution will average the anisotropic g and A values observed in solids. The values of ⟨ g ⟩ for Cu^{II} chalcone complexes increase in the order, chloroform ⟨ dioxan ⟨ dimethyl formamide ⟨ pyridine (Table 2), correspond to increased axial interactions with these solvents. The ⟨ A ⟩ values of copper(II) chalcone complexes (Table 2) fall in the order, chloroform ⟩ dioxan ⟩ dimethyl formamide ⟩ pyridine, indicating that the stronger the solvated complex, the smaller is the value of unpaired electron's wave function at the nucleus. Apparently, the bonding solvent pulls the electron away from the copper.

TABLE 2—ESR, BONDING AND MAGNETIC PARAMETERS OF COPPER-CHALCONE COMPLEXES* IN DIFFERENT SOLVENTS**

Parameter	1	2	3	4
$\langle g \rangle$	2.088 4[a]	—	2.087 6	2.086 8
	2.104 2[b]	—	2.102 2	2.103 3
	2.118 8[c]	2.108 5	2.105 7	2.109 9
	2.116 4[d]	2.119 3	2.118 1	2.115 5
$\langle A \rangle \times 10^4$ (cm^{-1})	50.51[a]	—	49.51	49.01
	45.19[b]	—	44.66	44.78
	41.94[c]	41.86	44.04	42.85
	41.50[d]	40.82	43.12	41.09
α^2	0.526 5[a]	—	0.518 1	0.518 0
	0.528 8[b]	—	0.520 7	0.524 2
	0.530 2[c]	0.520 0	0.524 9	0.526 7
	0.535 5[d]	0.535 8	0.547 9	0.528 6
K	0.226 4[a]	—	0.222 8	0.220 6
	0.227 4[b]	—	0.223 9	0.225 4
	0.228 0[c]	0.223 5	0.225 7	0.226 6
	0.229 4[d]	0.230 4	0.235 6	0.227 3
$\chi_M \times 10^6$ CGS	1 364[a]	—	1 363	1 362
	1 385[b]	—	1 382	1 384
	1 397[c]	1 392	1 387	1 392
	1 401[d]	1 405	1 403	1 400
μ_{eff} (B.M.)	1.808[a]	—	1.808	1.807
	1.822[b]	—	1.821	1.822
	1.831[c]	1.827	1.824	1.827
	1.838[d]	1.845	1.834	1.832

* Compd. no. as in Table 1. **Solvents: [a]chloroform, [b]dioxan, [c]DMF [d]ypridine.

Bond nature and magnetic parameters: In a spectrum taken in solution the isotropic nuclear hyperfine splitting ⟨ A ⟩ is related to the covalency of the unpaired electron by the equation,

$$\langle A \rangle = P(-\alpha^2 K_o + \langle g \rangle - 2.002\,3)$$

where, α^2 is the fraction of time the unpaired electron is on the copper atom, P is 0.036 cm^{-1} and K_o is about 0.43. The α^2 values (Table 2) for the present copper complexes indicate covalent nature of the copper(II) ligand bonds. The α^2 values suggest the fall of the covalent character slightly in the order, chloroform ⟩ dioxan ⟩ dimethyl formamide ⟩ pyridine. The greater interaction of pyridine with copper causes a back donation on the in-plane ligands which results in an increase in α^2 values in this solvent, compared to the other three solvents.

The values for paramagnetic susceptibility (χ_M), magnetic moment (μ_{eff}) and the Fermi contact term (K) were calculated using the expressions,

$$\chi_M = N\beta^2 \langle g^2 \rangle S(S+1)/3KT$$

$$\mu_{eff} = \langle g \rangle \sqrt{S(S+1)}$$

$$K = \frac{\langle A \rangle}{P} + \langle g \rangle - 2.002\,3$$

The magnetic moment values of the copper(II) chalcone complexes clearly indicate the absence of any antiferromagnetic coupling. The values further indicate that the complexes are mononuclear[16] in these solvents.

References

1. S. S. MISHRA and R. S. TEWARI, *Indian J. Appl. Chem.*, 1972, 35, 95.
2. S. S. MISHRA, *J. Indian Chem. Soc.*, 1973, 50, 68.
3. P. F. DEVITT, A. TIMONEY and M. A. VICKARS, *J. Org. Chem.*, 1961, 26, 4941.
4. N. P. BUU-HOI and N. D. XUONG, *J. Org. Chem.*, 1958, 23, 39.
5. S. C. KUSHAWAHA, DINAKAR and J. B. LAL, *Indian J. Chem.*, 1967, 5, 82.
6. C. W. WILSON and D. E. FLOYD, *J. Pharmacol. Exp. Ther.*, 1949, 95, 399.
7. M. KAMODA, *J. Agric. Chem. Soc. Jpn.*, 1954, 28, 791.
8. K. SYAMASUNDAR, *Proc. Indian Acad. Sci.*, 1964, 60, 259.
9. K. SYAMASUNDAR, *Proc. Indian Acad. Sci.*, 1968, 67, 90.
10. R. R. NAIDU, *Curr. Sci.*, 1968, 37, 342.
11. R. R. NAIDU, *Talanta*, 1975, 22, 615.
12. R. S. NAIDU and R. R. NAIDU, *Proc. Indian Acad. Sci., Sect. A*, 1975, 82, 142.
13. R. S. NAIDU and R. R. NAIDU, *J. Inorg. Nucl. Chem.*, 1979, 41, 1625.
14. R. L. BELFORD, M. CALVIN and G. BELFORD, *J. Chem. Phys.*, 1957 26, 1165.
15. C. KESAVULU, R. S. NAIDU and R. R. NAIDU, *Polyhedron*, 1985, 4, 761.
16. M. KATO, H. B. JONASSEN and J. C. FANNING, *Chem. Rev.*, 1964, 99.

J Indian Chem. Soc.,
Vol. LXIII, June 1986, pp. 575-577

A Study on the Effect of Phosphate, Molybdate and Humic acid Application on the Availability of Iron Manganese and Molybdenum in Laterite Soil

DIPTENDRA NARAYAN THAKUR and BISWANATH DAS*

Department of Agricultural Chemistry & Soil Science, Bidhan Chandra Krishi Viswavidyalaya, Kalyani-741 235

Manuscript received 17 January 1982, revised 10 February 1986, accepted 8 May 1986

A typical laterite soil of West Bengal was treated with phosphate, molybdate and humic acid singly as well as in combination and incubated at moisture saturation. Both phosphate and humic acid application showed considerable increase in Mo availability. Mo application decreased the DTPA-extractable Fe but increased the available Mn content of the soil. Phosphate application decreased both available Fe and Mn. Humic acid did not change the available Fe content but available Mn content was increased. Combined application of HA – Mo, P – Mo and HA – P as well as P – HA – Mo enhanced availability of Mo and Mn in the soil but available Fe content was found to be depressed. With the increase in incubation period, amount of available Mo and Fe gradually increased but Mn content showed a decreasing trend after initial increase.

MICRONUTRIENTS play a vital role in crop and animal production. With the present day trend of intensive cultivation using high yielding varieties of crops and with application of heavy doses of high analysis fertilisers, micronutrients are becoming limiting factor in crop production.

Availability of molybdenum in soil is very small but its role in plant nutrition is immense. Laterite soils in India are particularly low in total as well as available molybdenum content[1]. These soils are also known[2] to fix molybdate ions and phosphates due to their great affinity for ferric oxide and amorphous material which are abundant in them. High amount of phosphate fertilisation also creates problems in such soils through interactions of micronutrient elements with various components in soil as well as within the plant. Organic matter[3] also greatly influences the availability of micronutrients in soil and their uptake by plants.

In the present investigation, the effect of P, Mo and humic acid application on the changes in acid-NH_4 oxalate extractable Mo and DTPA extractable Fe, Mn in laterite soil on incubation for varying periods of time under moisture saturation have been studied.

Experimental

The soil used in the present investigation was collected from a land (Viswa Bharati Agricultural Farm, Birbhum) which has been brought into cultivation for two years using only moderate dose of N-fertilisers. The heavy, medium-textured and lateritic type soil was air-dried, ground and sieved (0.2 mm). Some physicochemical properties of the soil necessary for an understanding of the results of the present experiment are moisture saturation, 48% ; *p*H 5.8 (1 : 2.5, soil : water) ; available P, 1.05 ppm ; available Mo, trace ; DTPA-extractable Fe and Mn, 317 and 55 ppm, respectively ; free oxide, 2.6% ; organic carbon, 0.7% ; CEC 7.56 me/100 g.

The soil was treated with two levels of Mo (0, 5 ppm) as $Na_2MoO_4.2H_2O$, three levels of P (0, 40, 80 ppm) as KH_2PO_4, and two levels of humic acid (0, 600 ppm) singly as well as in different combinations. The samples were kept at room temperature and under saturated moisture condition by adding adequate amount of glass-distilled water. The three sets of sample were kept for 7, 21 and 42 day for analysis of extractable Mo, Fe and Mn.

Extraction : The soil (10 g) was shaken with acid ammonium oxalate solution (100 ml) for 8-10 h or overnight and then filtered and analysed for Mo. The extractant was produced according to the procedure developed by Grigg[4]. An aliquot of the filtrate (40-60 ml) was taken in a porcelain evaporating dish and the solution was evaporated to dryness on a steam-bath. The residue was ignited for 3-4 h at 450° to destroy the oxalate and then cooled. It was subsequently dissolved in 6.5 *M* HCl (10 ml).

For extraction of Fe and Mn, soil sample (10 g) was shaken with the DTPA-extractant solution[5] (20 ml) for 2 h and filtered. The filtrate was digested with concentrated HNO_3 (3 ml) and concentrated H_2SO_4 (5 ml). The resulting material was taken in redistilled water and analysed for Fe and Mn.

Estimation of Mo, Fe and Mn : Molybdenum was estimated colorimetrically by thiocyanate

TABLE 1—EFFECT OF P, Mo AND HUMIC ACID APPLICATION ON DTPA-EXTRACTABLE Fe, Mn AND AVAILABLE Mo CONTENT (ppm) IN SOIL

Treatments	Period of incubation (day)								
	7			21			42		
	Mo	Fe	Mn	Mo	Fe	Mn	Mo	Fe	Mn
$P_0HA_0Mo_0$	Trace	344	52.60	0.040	352	32.66	0.080	400	22.66
$P_0HA_0Mo_1$	0.240	288	68.00	0.290	344	36.00	0.330	360	32.66
$P_0HA_1Mo_0$	0.040	280	77.33	0.080	340	50.00	0.110	360	22.66
$P_0HA_1Mo_1$	0.245	328	73.33	0.300	348	61.33	0.355	364	25.03
$P_1HA_0Mo_0$	0.065	324	43.33	0.080	336	35.66	0.100	352	19.33
$P_1HA_0Mo_1$	0.285	288	62.00	0.315	352	43.33	0.330	364	28.66
$P_1HA_1Mo_0$	0.040	316	64.66	0.110	364	40.68	0.155	368	18.33
$P_1HA_1Mo_1$	0.275	304	86.60	0.315	376	45.75	0.375	380	20.00
$P_2HA_0Mo_0$	0.080	292	40.66	0.110	316	41.00	0.120	348	31.66
$P_2HA_0Mo_1$	0.275	264	50.00	0.355	312	43.33	0.400	352	33.00
$P_2HA_1Mo_0$	0.100	275	63.33	0.110	316	53.33	0.165	328	28.66
$P_2HA_1Mo_1$	0.285	280	63.33	0.330	304	50.00	0.420	348	30.00

TABLE 2—MEAN EFFECTS OF P, Mo AND HUMIC ACID APPLICATION ON THE AVAILABLE Mo, Fe AND Mn CONTENT IN SOIL

Level of application ppm	Mo (ppm) Incubation period (day)				Fe (ppm) Incubation period (day)				Mn (ppm) Incubation period (day)			
	7	21	42	Mean	7	21	42	Mean	7	21	42	Mean
P_0 (0)	0.181	0.178	0.219	0.176	310.0	346.0	371.0	342.3	67.81	44.99	25.75	46.18
P_1 (40)	0.166	0.205	0.204	0.207	308.0	357.0	366.0	343.7	64.15	41.34	20.34	41.94
P_2 (80)	0.185	0.226	0.276	0.229	277.8	312.0	344.0	311.3	54.33	46.91	30.83	44.02
HA_0 (0)	0.158	0.198	0.227	0.194	300.0	335.4	362.7	332.7	52.76	38.66	27.99	39.80
HA_1 (600)	0.164	0.208	0.263	0.215	297.2	341.3	358.0	332.2	71.43	47.80	23.28	47.51
Mo_0 (0)	0.054	0.088	0.122	0.088	305.2	337.3	359.3	333.9	56.98	42.21	23.05	40.74
Mo_0 (5)	0.265	0.318	0.365	0.316	292.0	339.3	361.3	330.9	67.21	46.62	28.22	47.85
Mean	0.160	0.183	0.267		298.6	338.3	360.3		62.09	44.08	25.63	

coloured compounds through reduction with chlorostanous acid[6]. Iron was determined by reduction of ferric-iron to the ferrous state with hydroxylamine hydrochloride and subsequent formation of an intense red ferrous chelate with *o*-phenanthroline as described by Jackson[7]. Mn was estimated colorimetrically by the periodate method[7].

A Spectronic-20 spectrophotometer was used for all absorbance measurements. All reagents and chemicals used were of A.R. quality.

Results and Discussion

The analytical data for DTPA extractable Fe, Mn and acid ammonium oxalate extractable Mo are given in Table 1. Table 2 contains the mean effect of the treatments on nutrient availability.

Available Mo : Application of Mo increased the extractable Mo content in soil, the magnitude of increase being 258.6% over the corresponding value in the control. About 4% of added Mo appeared to remain in the available pool. The results show that the application of P resulted in increase of extractable Mo, both in Mo treated and untreated soil. At higher level of P, the availability is also higher. Humic acid application has a definite effect on molybdenum availability as observed in the present investigation and the magnitude of increase being 10.8% over the control. It has been reported by Szilagyii[8] that humic acid can render molybdenum unavailable to plants. He also reported that humic acid also reduces Fe^{III} to Fe^{II} form. Present investigation, however, indicates that there is an increase in Mo availability. As the soil contains more iron in Fe^{III} form, the beneficial effect of humic acid seems to lie on the partial reduction of Fe^{III} to Fe^{II} and consequent release of some adsorbed or chemically fixed molybdate on the free oxides of iron in soil.

It is a general observation that in all cases there is an increase of Mo availability with the increase of incubation period. As the soil was kept in saturated moisture condition, an anaerobic environment was set up, causing partial reduction of ferric iron, which is largely responsible for adsorbtion of molybdenum.

The combined application of HA – Mo – P, P – Mo, and HA – P on the content of available Mo content in the soil has been found to be beneficial. The interaction effect of P – HA – Mo on the available Mo content in soil show a positive effect.

DTPA-extractable Fe : The results show that application of P, result in decrease in the extractable Fe content. Higher dose of P resulted in greater decrease. The magnitude of decrease is found to be 9.8% over the control. Humic acid application decreased extractable Fe content in the initial period of incubation but there was almost no

change in the mean effect by humic acid application. The application of Mo decreased the extractable Fe content slightly.

It is a general observation in all the cases that there is a gradual increase in extractable Fe content with the increase in the period of incubation.

There is an increase of extractable Fe content due to combined effect of Mo – P and Mo – HA, but the interactions of P – HA – Mo and HA – P have a depressive effect on extractable Fe content in soil. Presence of phosphate appears to keep iron fixed with the humic colloids making it unavailable, especially during short period of incubation of the soils.

DTPA-extractable Mn : The DTPA-extractable Mn content was found to decrease due to application of phosphorus, and the magnitude of decrease being 9.8 and 4.7% for P_1 and P_2 level, respectively. Humic acid application shows a beneficial effect on the extractable Mn content in soil, the magnitude of increase being 16.2% over the control. Mo application has a beneficial effect on the extractable Mn content in the soil, which continued more or less uniformly throughout the period of incubation, the magnitude of increase being 13.7% over the control.

Unlike extractable Fe content in all the cases, there was a gradual decrease in Mn content with the increase in the incubation period.

The combined effect of P – Mo application caused a depressive effect over that of control in the initial period of incubation, but beneficial effect was found in the later stages. The depressive effect of P – HA application on the extractable Mn content was found only in latter stages of incubation. The interaction of P – HA – Mo has been found to be beneficial in all the stages of incubation.

Acknowledgement

The authors are thankful to C.S.I.R., New Delhi, for providing financial help, in the form of a Research Fellowship to one of them (D.N.T).

References

1. R. K. Chatterjee and C. Dakshinamurti, *J. Sci. Ind. Res.*, 1962, **21**, 597.
2. H. M. Breisenauer, A. A. Tabikh and P. R. Stout, *Soil Sci. Soc. Am. Proc.*, 1963, **27**, 553.
3. A. N. Pathak, H. Shanker and R. B. Misra, *J. Indian Soc. Soil Sci.*, 1968, **16**, 399.
4. J. L. Grigg, *Analyst*, 1953, **78**, 470.
5. W. L. Lindsay and W. B. Norvell, *Soil Sci. Am. J.*, 1978, **42**, 421.
6. G. Fujimato and G. D. Sherman, *Agron. J.*, 1951, **43**, 425.
7. M. L. Jackson, "Soil Chemical Analysis", Prentice-Hall, London, 1967.
8. M. Szilagyii, *Geochem. Int.*, 1967, 1165.

J. Indian Chem. Soc.,
Vol. LXIII, June 1986, pp. 578-580

Complexes of Manganese(II), Cobalt(II), Nickel(II) and Copper(II) with Schiff Base derived from 2-Acetylfuranglyoxal and o-Phenylenediamine

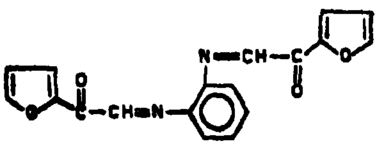
V. S. SHRIVASTAVA* and G. C. SAXENA

Chemical Research Laboratories, R. B. S. College, Agra-282 002

Manuscript received 12 December 1984, revised 28 August 1985, accepted 8 May 1986

The complexes having general formulae M(PFGA)Cl_n, where M = Mn^{II}, Co^{II}, Ni^{II} and Cu^{II}; PFGA = *N,N-o*-phenylenebis(2-furylglyoxalimine); and n = 2, have been prepared and characterised by elemental analysis, molar conductance, megnetic moment data, electronic and infrared spectral studies.

A number of papers dealing with the studies of metal complexes of the Schiff bases derived from heterocyclic glyoxalic aldehyde with various aromatic amines[1-3] appeared in the literature. But the chemistry of *N,N-o*-phenylenebis(2-furylglyoxalimine) seems to be comparatively of recent orgin. The present paper reports the synthesis and characterisation of Mn^{II}, Co^{II}, Ni^{II} and Cu^{II} metal complexes of the Schiff base,



Experimental

The Schiff base ligand was prepared by the condensation of *o*-phenylenediamine and 2-acetylfuranglyoxal in 1 : 2 molar ratio in ethanolic medium on a water-bath. The Schiff base *N,N-o*-phenylenebis(2-furylglyoxalimine) (PFGA) separated on keeping the solution overnight. It was then filtered and crystallised from ether, m.p. 75°.

Preparation of complexes : The similar procedure was adopted for the preparation of all the complexes, reported herein for the sake of brevity only one reaction in detail.

*Bis[*N, N-*o-phenylenebis (2-furylglyoxalimine)-manganese(II) chloride] :* To an ethanolic solution of $MnCl_2.4H_2O$ (0.38 g, 1.9 mmol) was added an ethanolic solution of Schiff base (0.64 g, 2.0 mmol). The reaction mixture (~50 ml) was refluxed for ~4 h and the light green compound separated upon keeping the solution overnight.

Physical measurements : The molar conductance of the complexes was recorded using a conductivity bridge and a dip type cell having cell constant 0.5 cm^{-1}. The solution was prepared in acetone and DMF. The magnetic susceptibility measurement was made on a Gouy balance at room temperature. The ir spectra (KBr) were recorded on a Perkin-Elmer 577 grating spectrophotometer in the range 200-4 000 cm^{-1}.

Results and Discussion

The reaction of metal chlorides and ligand (PFGA, $C_{18}H_{12}O_4N_2$) may be depicted as

$$C_{18}H_{12}O_4N_2 + MCl_2 \rightarrow [M(C_{18}H_{12}O_4N_2)Cl_2]$$

where, M = Mn^{II}, Co^{II}, Ni^{II} and Cu^{II}.

All the complexes are light green solids and their molar conductance measurements (Table 1) show them to be non-electrolyte[4-6].

The magnetic moments (μ_{eff}) values (Table 1) for the complexes are slightly higher than the spin-only value of the respective metal ion complex indicating the spin-free octahedral geometry around the metal ions[7-10], which are close to spin-only magnetic moment, indicating the paramagnetic nature of the chelates.

Electronic spectra : A general feature of the electronic spectra of these complexes is a shift of absorption bands towards the lower energy side due to nephelauxetic effect. The value of nephelauxetic parameter (β) has been calculated by the method of Jorgenson[11] using the relation, $\beta = \nu_{complex}/\nu_{aquo}$. Another parameter, the percentage covalency (δ)[12] has also been calculated for these complexes with the help of the expression,

$$\delta = \frac{(1-\beta)}{\beta} \times 100.$$

The results are presented in Table 2.

* Present address : Department of Chemistry, University of Rajasthan, Jaipur-302 004.

TABLE 1—ANALYTICAL AND PHYSICAL DATA OF Mn^{II}, Co^{II}, Ni^{II} AND Cu^{II} SCHIFF BASE COMPLEXES

Sl. no.	Compd.	Colour	M.p. °C	Analysis% : Found/(Calcd.) Metal	Cl	C	H	N	Conductivity $m\Omega^{-1}$ cm^2 mol^{-1}	μ_{eff} B.M.
1.	$[Mn(C_{18}H_{12}O_4N_2)Cl_2]$	Light green	208	12.86 (12.88)	15.98 (15.92)	48.41 (48.43)	2.75 (2.69)	6.85 (6.28)	0.092 4	5.92
2.	$[Co(C_{18}H_{12}O_4N_2)Cl_2]$	Green	150	13.61 (13.40)	16.45 (16.13)	50.0 (49.09)	2.92 (2.72)	6.75 (6.36)	0.068 0	4.08
3.	$[Ni(C_{18}H_{12}O_4N_2)Cl_2]$	Dark green	232	12.09 (12.92)	15.86 (15.81)	48.08 (48.11)	3.06 (2.67)	6.22 (6.24)	0.062 8	2.86
4.	$[Cu(C_{18}H_{12}O_4N_2)Cl_2]$	Light green	229	13.98 (13.88)	14.66 (15.64)	48.06 (47.58)	2.81 (2.64)	6.22 (6.17)	0.072 6	1.86
5.	Ligand (PFGA) $C_{18}H_{12}O_4N_2$	Black	75	—	—	62.79 (67.50)	4.04 (3.75)	8.67 (8.75)	—	—

TABLE 2—VALUE OF AVERAGE NEPHELAUXETIC RATIO (β) AND AVERAGE COVALENCY PARAMETER (δ) OF PFGA SCHIFF BASE COMPLEXES

Compd. no.*	β	δ %
1	0.86	16.279 0
2	0.84	19.047 0
3	0.70	42.555 0

* As in Table 1.

remains unaltered even on complexation. Three new bands appear in the spectra of the complexes at 560, 420 and 270 cm^{-1} due to M–N, M–O and M–Cl stretching modes, respectively[17-19].

On the basis of analytical, conductance, magnetic, electronic and infrared spectral data, a structure in which metal ions have six coordination number may be proposed.

TABLE 3—SOME CHARACTERISTIC IR BANDS (cm^{-1}) OF PFGA SCHIFF BASE COMPLEXES

Sl. no.	Compd.	$\nu_{C=O}$	$\nu_{C=N}$	ν_{C-O-C}	ν_{M-N}	ν_{M-O}	ν_{M-Cl}
1.	$[Mn(C_{18}H_{12}O_4N_2)Cl_2]$	1 620s	1 590w	1 015m	580m	420w	290w
2.	$[Co(C_{18}H_{12}O_4N_2)Cl_2]$	1 610s	1 580m	1 020w	580s	420s	260w
3.	$[Ni(C_{18}H_{12}O_4N_2)Cl_2]$	1 610s	1 590m	1 020w	560w	430m	270m
4.	$[Cu(C_{18}H_{12}O_4N_2)Cl_2]$	1 620m	1 590m	1 010m	580s	430m	290m
5.	$C_{18}H_{12}O_4N_2$ (Ligand)	1 660m	1 610m	1 010s	—	—	—

m = medium, s = strong, w = weak.

The usefulness of the electronic spectra in ascertaining the nature and bonding involved in these complexes are limited. Taking the free-ion as the standard, the ligand causes a slight red-shift (nephelauxetic effect) of the absorption spectral bands[13]. The magnitude of this shift is dependent upon the change in the inter-electronic repulsion parameters[14]. The value of β which is less than one, points towards the very slight incidence of covalency in the metal-ligand bond.

Infrared studies : The ir spectra of the ligand (Table 3) exhibit two strong bands at 1 610 and 1 660 cm^{-1} due to $\nu_{C=N}$ and $\nu_{C=O}$[15-16]. These bands show the negative shift in the spectra of the corresponding metal complexes indicating the involvement of C=N and C=O groups in complexation, whereas the ν_{C-O-C} at 1 010 cm^{-1}

Acknowledgement

The authors wish to thank Dr. A. K. Rai, Department of Chemistry, University of Rajasthan, Jaipur, for facility, and also thank Prof. K. N. Mehrotra, Agra University, Agra, for helpful discussions.

References

1. P. B. SHUKLA and R. TAKRU, *J. Indian Chem. Soc.*, 1980, **57**, 252.
2. M. K. HUSSAN, M. I. ISMAIL and Z. H. KHALIL, *Curr. Sci.*, 1980, **49**, 935.
3. M. K. HASSAN, M. I. ISMAIL and Z. H. KHALIL, *Ann. Chim.*, 1981, **71**, 387.
4. R. S. NYHOLM, R. G. CUNNINGHAME and M. L. TOBE, *J. Chem. Soc., Dalton Trans.*, 1972, 229.
5. A. P. AMES and P. G. SEARS, *J. Phys. Chem.*, 1955, **59**, 16.
6. W. J. GEARY, *Coord. Chem. Rev.*, 1971, **7**, 81.

7. B. N. Figgis and J. Lewis, *Prog. Inorg. Chem.*, 1964, **6**, 197.
8. N. S. Gill and R. S. Nyholm, *J. Chem. Soc.*, 1959, **39**, 97.
9. B. N. Figgis and J. Lewis, *Prog. Inorg. Chem.*, 1964, **6**, 102.
10. O. Siiman and H. B. Gray, *Inorg. Chem.*, 1974, **13**, 1158.
11. C. K. Jorgensen and B. R. Judd, *J. Mol. Phys.*, 1964, **81**, 281.
12. S. P. Sinha, *Spectrochim. Acta*, 1966, **22**, 57.
13. S. P. Sinha and H. H. Smidtke, *J. Mol. Phys.*, 1965, **10**, 7.
14. D. E. Henrie and G. R. Choppin, *J. Chem. Phys.*, 1968, **49**, 477.
15. J. E. Kovacic, *Spectrochim. Acta, Part A*, 1967, **23**, 183.
16. G. C. Percy and D. A. Thorunton, *J. Inorg. Nucl. Chem.*, 1972, **34**, 3357.
17. P. Singh, V. Singh, G. P. Pokhariyal, R. Pal and R. P. Mahesh, *J. Indian Chem. Soc.*, 1980, **57**, 259.
18. G. Devoto, M. Massacesi, G. Ponticelli and R. Ruggerj, *J. Inorg. Nucl. Chem.*, 1977, **39**, 855.
19. G. Panticelli, *J. Inorg. Nucl. Chem.*, 1977, **39**, 45.

J. Indian Chem. Soc.,
Vol. LXIII, June 1986, pp. 581-585

Oxidation of Methionine by Sodium *N*-Bromobenzenesulphonamide in Aqueous Solution. A Kinetic and Mechanistic Study

S. ANANDA, K. S. RANGAPPA and D. S. MAHADEVAPPA*

Department of Chemistry, University of Mysore, Manasagangotri, Mysore-570 006

Manuscript received 1 July 1985, revised 17 February 1986, accepted 8 April 1986

Kinetics of oxidation of DL-methionine (Mt) in the presence of HCl, $HClO_4$, H_2SO_4 and NaOH by sodium *N*-bromobenzenesulphonamide (BAB) have been investigated at 40° (and 30° in alkaline medium). The rate law is identical in the three acids,

$$-\frac{d[BAB]}{dt} = k[BAB][H^+]^2$$

In alkaline medium, the rate law shows a first order dependence each on [BAB] and $[OH^-]$. Effect of halide (Cl^- or Br^-) ion was studied. Addition of the reaction product, benzenesulphonamide retards the rate. Variation of ionic strength has no effect on the rate. The solvent isotope effect was studied using D_2O. Activation parameters have also been determined. Methioninesulphone is identified as the reaction product. Mechanisms proposed and the derived rate laws are in agreement with the observed kinetics.

RECENTLY, bromamine-B (sodium *N*-bromobenzenesulphonamide, $C_6H_5SO_2NBrNa.1.5H_2O$, hereinafter abbreviated as BAB) has been introduced[1] as an oxidimetric reagent in aqueous medium. A review of literature shows that although the reactions of aromatic sulphonyl chloramines have been extensively investigated, there is meagre information on the reaction of corresponding bromamines. Oxidation of α-amino acids[2] and dimethyl sulphoxide[3] by BAB has been kinetically studied. As a part of our board programme on the mechanistic aspects of oxidation of substrates by aromatic bromamines, we report the kinetics of oxidation of methionine by the title reagent in acid and alkaline media.

The oxidation of amino acids is of utmost importance, both from chemical point of view and from its bearing on the mechanism of amino acid metabolism. There are very few reports on the kinetics of oxidation of amino acids by halogen compounds. Kumar *et al.*[4] have studied the mechanism of oxidation of some amino acids by alkaline CAT. Wright[5] reported oxidation of amino acids by OCl^- ion and showed that chlorination occurred in acid medium while alkalinity increased the tendency towards oxidation of the compounds.

Methionine (Mt) is an optically active essential sulphur-containing amino acid, important in biological transmethylation processes. It is used in pharmaceuticals, cosmetics, nutrition and biochemical studies and as a food and feed supplement. Methionine has been oxidised to the sulphoxide by iodine[6], bromine[7], $KBrO_3$[8] and ICl[6], while $NaClO_2$[9], H_2O_2[10] and bromate mixture[7] convert it into the sulphone. Analytical methods have been devised for the estimation of this amino acid using aromatic *N*-haloamines[11]. However, except for the work of Gensch and Higuchi[6] and Young and Hsieh[12], no kinetic data are available for the oxidation of Mt with any of the reagents. A nearer example is the study of Mann-Pope reaction, *i.e.* conversion of sulphides with *N*-haloamines in buffered water-ethanol mixtures, by Ruff and Kucsman[13]. The present studies report for the first time the mechanism of oxidation of a sulphur-containing amino acid with bromamine-B.

Experimental

Bromamine-B was prepared by the reported procedure[1]. The purity of BAB was checked iodometrically through an assay of its active bromine content and was further characterised by its ^{13}C FT-nmr spectrum obtained on a Bruker WH 270 MHz spectrometer with D_2O as solvent, TMS as the external standard, (ppm relative to TMS) at 143.38 (C-1, carbon attached to S atom): 134.30 (C-4, *para* to the hetero atom) 131.26 (C-2,6) and 129.31 (C-3,5).

An aqueous solution of BAB was standardised iodometrically and preserved in brown bottles to prevent its photochemical deterioration. Chromatographically pure DL-methionine (Merck) was further assayed by the perchloric acid method[14] and its aqueous solution was prepared. All other reagents were of AnalaR grade. The ionic strength of the

system was kept at a high value by using a concentrated solution of sodium perchlorate. Heavy-water (D_2O, 99.2%) employed for solvent isotope studies was supplied by the Bhabha Atomic Research Center (Trombay).

Stoichiometry : Varying ratios of BAB to amino acid in the presence of $HClO_4$, HCl, H_2SO_4 and NaOH were equilibrated at 40° for acids (and at 30° in alkali) for 24 h. The unreacted BAB in the reaction mixtures was determined by iodometric titration. The analysis showed that one mole of methionine reacted with two moles of BAB. The observed reaction stoichiometry is represented as

$$CH_3SCH_2CH_2CH(NH_2)COOH + 2\,ArSO_2NBrNa + 2\,H_2O \longrightarrow$$

$$CH_3-\underset{\underset{O}{\|}}{\overset{\overset{O}{\|}}{S}}-CH_2CH_2CH(NH_2)COOH + 2\,ArSO_2NH_2 + 2\,NaBr \qquad (1)$$

where, Ar is C_6H_5.

Product analysis: Benzenesulphonamide ($ArSO_2NH_2$) was detected by paper chromatography. Benzyl alcohol saturated with water was used as the solvent with 0.5% vanillin in 1% HCl solution in ethanol as spray reagent (R_f=0.905). The identification of methioninesulphone was also made through paper chromatography by employing n-butanol-glacial acetic acid-water (4 : 1 : 5, v/v) as solvent and 0.2% solution of ninhydrin in butanol-water-acetic acid (95 : 4 : 0.5, v/v) as spray reagent (R_F=0.17). Kinetic procedure followed was as reported in the earlier communications[2,3].

Results

The kinetics of oxidation of methionine by BAB were investigated at several initial concentrations of the reactants, in acid and alkaline media.

Acid medium :

At constant $[H^+]$, with the substrate in stoichiometric excess, plots of log [BAB] *vs* time were linear ($r > 0.998\,0$), indicating a first order dependence of rate on [oxidant] (Table 1). Values of the pseudo-first order rate constants, k', are given in Table 1.

TABLE 1—EFFECT OF CONCENTRATION ON RATE OF OXIDATION OF METHIONINE BY BAB IN ACID MEDIA AT 40°

$[HClO_4]=[HCl]=0.07$ *M*, [Mt]=0.01 *M*, $\mu=0.5$ *M*, $[H_2SO_4]=0.035$ *M*

$[BAB]_0 \times 10^3$ *M*	$k', \times 10^4\ s^{-1}$		
	$HClO_4$	HCl	H_2SO_4
3.0	3.76	13.92	2.06
4.0	3.80	14.08	2.12
5.0	3.93	14.18	2.19
6.0	3.96	14.21	2.24
7.0	4.08	14.34	2.31
8.0	4.11	14.41	2.39
Average	3.94±0.14	14.17±0.18	2.21±0.12

The values of k' were unaffected with increase in $[Mt]_0$, indicating that the rate was independent of [amino acid] (Table 2).

TABLE 2—EFFECT OF VARYING [Mt] ON RATE OF REACTION AT 40°

$[HClO_4]=[HCl]=0.07$ *M*, [BAB]=0.005 *M*, $\mu=0.5$ *M*, $[H_2SO_4]=0.035$ *M*

$[Mt]_0 \times 10^2$ *M*	$k', \times 10^4\ s^{-1}$		
	$HClO_4$	HCl	H_2SO_4
1.0	3.96	14.18	2.19
1.5	3.74	14.08	2.16
2.0	3.67	13.91	2.23
2.5	3.18	13.86	2.18
3.0	2.87	13.74	2.20
Average	3.47±0.45	13.94±0.16	2.19±0.02

The rate increased with increase in $[H^+]$ (Table 3). Plots of log k' *vs* log $[H^+]$ were linear in all the three acid media with a slope of two ($r > 0.999\,0$). This is also confirmed by plotting k' *vs* $[H^+]^2$ when the straight line obtained passes through the origin.

TABLE 3—EFFECT OF $[H^+]$ ON RATE OF REACTION AT 40°

$[BAB]_0=0.005$ *M*, $[Mt]_0=0.01$ *M*, $\mu=0.5$ *M*

$[H^+] \times 10^2$ *M*	$k', \times 10^4\ s^{-1}$		
	$HClO_4$	HCl	H_2SO_4
4.0	—	5.57	0.71
5.0	2.20	8.89	—
6.0	3.02	12.9	—
7.0	4.19	17.5	2.19
8.0	5.42	22.2	—
9.0	7.32	28.0	—
10.0	8.93	—	4.27
14.0	—	—	8.42
16.0	—	—	10.99

The rate increased with addition of $[Cl^-]$ or $(Br^-]$ (Table 4). Plots of log k' *vs* log [halide] are straight lines with slopes less than unity ($r > 0.988$) in all three acid media, indicating a fractional order dependence on $[Cl^-]$ (order =0.5 – 0.6) and $[Br^-]$ (order=0.3 – 0.4).

TABLE 4—EFFECT OF HALIDE ION ON RATE OF REACTION AT 40°

$[BAB]_0=0.005$ *M*, $[Mt]_0=0.01$ *M*, $\mu=0.5$ *M*, $[HClO_4]=[HCl]=0.07$ *M*, $[H_2SO_4]=0.035$ *M*

$[Cl^-]$ *M* $[Br^-] \times 10^3$ *M*	$k', \times 10^4\ s^{-1}$		
	$HClO_4$	HCl	H_2SO_4
0.00 (0.0)	3.79 (3.79)	— (13.90)	2.19 (2.19)
0.02 (2.0)	4.38 (5.34)	— (18.20)	2.90 (2.81)
0.04 (5.0)	5.97 (6.86)	— (20.16)	4.06 (3.76)
0.06 (10.0)	7.68 (9.95)	— (26.14)	5.02 (5.36)
0.07	—	13.90	—
0.08	10.00	16.05	5.81
0.09	—	17.50	—
0.12	—	19.20	—

Values in parenthesis refer to Br^-.

Presence of ClO_4^- and SO_4^{2-} ions had no effect on the rate. This was confirmed by further addition of $NaClO_4$ and Na_2SO_4 to the reaction mixture.

Variation of ionic strength of the medium (0.08 – 0.65 *M*) or addition of the reaction product, benzenesulphonamide (upto 0.008 *M*) had no significant effect on the rate.

The reaction was also studied in aqueous methanol of varying composition. An increase in methanol content (0.30%) increases the rate of reaction. A plot of log k' *vs* 1/D, where D is the dielectric constant of the medium, gave a straight line with a positive slope (r > 0.987 2).

Kinetic studies were carried out in D_2O containing $HClO_4$ and k'_{D_2O} was found to be 8.06×10^{-4} s^{-1} while the corresponding k'_{H_2O} was 3.96×10^{-4} s^{-1} leading to the normal solvent isotope effect, $k'_{H_2O}/k'_{D_2O} = 0.49$.

The reaction was studied at different temperatures (30-45°). From the straight line plot of log k' *vs* 1/T (r = 0.996 6) for $HClO_4$, r = 0.999 9 for HCl and r = 0.994 5 for H_2SO_4, activation parameters were computed (Table 5).

Table 5—Kinetic and Thermodynamic Parameters for Oxidation of Methionine by BAB in Acidic and Alkaline Media

	$HClO_4$	HCl	H_2SO_4	NaOH
log A	10.1	12.7	10.0	9.0
$\Delta H^{\neq}$ kJ mol^{-1}	64.8	73.0	65.4	58.7
$\Delta S^{\neq}$ JK mol^{-1}	– 94.9	– 65.7	– 106.0	– 121.9
$\Delta G^{\neq}$ kJ mol^{-1}	94.2	93.4	98.8	90.9

Addition of reaction mixture to aqueous acrylamide solution did not initiate polymerisation, showing the absence of free radical species.

Alkaline medium :

At constant NaOH and substrate concentrations, the reaction showed a first order dependence on $[BAB]_0$ (r > 0.997 0 ; Table 6). The values of k' were unaffected with increase in [Mt], indicating that the rate was independent of [amino acid]. Values of k' increased with increase in [NaOH] and a plot of log k' *vs* log [NaOH] was linear with a slope of unity (r = 0.997 6), indicating a first order dependence of rate on hydroxide ion concentration (Table 7). Here the reactive $(OH^-)_R$ was determined by the relation, $[OH^-]_R = [OH^-]_T - [OH^-]_{Mt}$, where $[OH^-]_T$ is the total concentration and $[OH^-]_{Mt}$ the hydroxyl ion concentration neutralised by the amino acid.

Addition of the reaction product, benzenesulphonamide ($ArSO_2NH_2$) retards the reaction rate, indicating that it is involved in an equilibrium (Table 7). A plot of log k' *vs* log $[ArSO_2NH_2]$ gave a straight line (r = 0.988 6) with a slope of – 0.56.

Addition of chloride to the reaction mixture and variation of ionic strength had no effect on the rate.

Table 6—Effect of Varying Concentrations of $[BAB]_0$, $[Mt]_0$, on Rate of Reaction at 30°

$[NaOH]_R = 0.01$ *M*, $\mu = 0.50$ *M*

$[BAB]_0$ $\times 10^3$ *M*	$[Mt]_0$ $\times 10^3$ *M*	k' $\times 10^4$ s^{-1}
3.00	10.00	20.70
4.00	10.00	20.30
5.00	10.00	19.70
6.00	10.00	19.50
7.00	10.00	19.12
8.00	10.00	18.96
5.00	3.00	19.46
5.00	6.00	19.78
5.00	10.00	19.92
5.00	15.00	19.96
5.00	20.00	20.04
5.00	30.00	20.15

Table 7—Effect of Varying $[OH^-]_R$ and $[ArSO_2NH_2]$ on Rate of Reaction at 30°

$[BAB]_0 = 0.005$ *M*, $[Mt]_0 = 0.01$ *M* $\mu = 0.5$ *M*

$[OH^-]_R$ $\times 10^3$ *M*	k' $\times 10^4$ s^{-1}	$[ArSO_2NH_2] \times 10^3$ at $[NaOH]_R = 0.01$ *M*	k' $\times 10^4$ s^{-1}
2.50	4.18	1.0	15.10
5.00	8.10	2.0	11.52
6.25	10.40	3.0	9.07
7.50	13.43	4.0	7.45
10.00	19.70	5.0	6.14
12.50	23.10	6.0	5.54
15.00	30.00	—	—

An increase in methanol content (0 – 30%) increases the rate of reaction. A plot of log k' *vs* 1/D gave a straight line (r = 0.997 0) with a positive slope.

Solvent isotope studies were made in D_2O medium. It was found that $k'_{D_2O} = 1.93 \times 10^{-3}$ s^{-1}, while $k'_{H_2O} = 1.97 \times 10^{-3}$ s^{-1} and the solvent isotope effect $k'_{H_2O}/k'_{D_2O} = 1.02$.

Discussion

It is interesting to note that, oxidation of methionine by BAB in acid and alkaline media obeys zero order kinetics in $[Mt]_0$, indicating that the substrate is oxidised in a fast step. The results in acid media are similar to those obtained for the oxidation of dimethyl sulphoxide[8] by this bromamine, but the mechanism is different in alkaline medium for these substrates.

Acid medium :

Bromamine-B ($ArSO_2NBrNa$) is analogous to CAT[15] and behaves like a strong electrolyte in aqueous solutions. It may be assumed that similar equilibria exist in acid solutions,

$$ArSO_2NBrNa \rightleftharpoons ArSO_2NBr^- + Na^+ \quad (2)$$

$$ArSO_2NBr^- + H^+ \overset{K_a}{\rightleftharpoons} ArSO_2NHBr \quad (3)$$

$$K_a = 1.5 \times 10^{-5} \text{ l mol}^{-1} \text{ at } 25°.$$

$$2ArSO_2NHBr \overset{K_d}{\rightleftharpoons} ArSO_2NH_2 + ArSO_2NBr_2 \quad (4)$$

$$K_d = 5.8 \times 10^{-2} \text{ at } 25°.$$

Dibromamine-B ($ArSO_2NBr_2$) and the free acid hydrolyse to give hypobromous acid (HOBr),

$$ArSO_2NBr_2 + H_2O \rightleftharpoons ArSO_2NHBr + HOBr \quad (5)$$

$$ArSO_2NHBr + H_2O \overset{K_h'}{\rightleftharpoons} ArSO_2NH_2 + HOBr \quad (6)$$

$$K_h' = 4.21 \times 10^{-9}\ mol\ l^{-1}.$$

$$HOBr \overset{K_a}{\rightleftharpoons} H^+ + OBr^- \quad (7)$$

$$K_a = 2.0 \times 10^{-9}\ l\ mol^{-1}\ at\ 25^\circ.$$

The possible oxidising species in acidified BAB solutions are therefore $ArSO_2NHBr$, $ArSO_2NBr_2$ HOBr and Br_2. The probability of the dibromo compound as the reactive species can be ruled out, as the rate follows a strict first order dependence on [BAB]. Since the added benzenesulphonamide did not retard the reaction, it may be assumed that HOBr is not primarily involved in the rate determining step. Detailed calculations of Hardy and Johnston[16] have shown that the free acid is present in higher concentrations in acid media and it is the most likely oxidising species to be involved in the reaction sequence.

Formation of species of the type $ArSO_2\overset{+}{N}H_2Cl$ has been reported[17] with CAT and the protonation constant for the reaction,

$$ArSO_2NClH + H^+ \rightleftharpoons ArSO_2\overset{+}{N}ClH_2 \quad (8)$$

is found to be 1.02×10^2 at 25°.

The rate dependence on $[H^+]^2$ and [BAB] indicates a protonation step involving the oxidant, since the rate is independent of $[Mt]_0$. Scheme 1 accounts for the observed kinetics.

$$ArSO_2NBr^- + 2H^+ \overset{K_1}{\rightleftharpoons} ArSO_2\overset{+}{N}H_2Br \quad (i)$$

(fast ; $K_1 = k_1/k_{-1}$)

$$ArSO_2\overset{+}{N}H_2Br + H_2O \overset{k_2}{\rightleftharpoons} ArSO_2NH_2 + H_2OBr^+ \quad (ii)$$

(forward reaction is rate limiting)

$$Mt + H_2OBr^+ \underset{(fast)}{\overset{k_3}{\rightleftharpoons}} Products \quad (iii)$$

Scheme 1

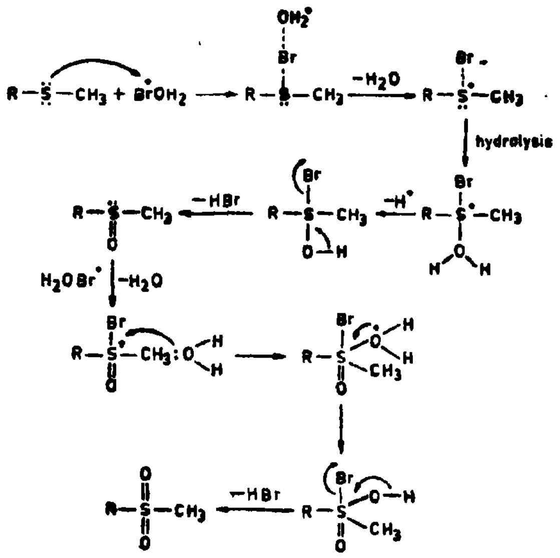
Assuming steady state for $ArSO_2\overset{+}{N}H_2Br$, Scheme 1 leads to the rate law (9), in the form,

$$-\frac{d\,[BAB]}{dt} = k[BAB][H^+]^2 \quad (9)$$

$$where,\quad k = \frac{k_1k_2[H_2O]}{k_{-1} + k_2[H_2O]}$$

An explanation of the observed solvent isotope effect can be given from Scheme 1. It may be noted that the protonation step (i) is followed by the rate limiting hydrolysis step (ii), where the normal kinetic isotopic effect $k_H'/k_D' > 1$, while the solvent isotopic effect k_{H_2O}'/k_{D_2O}' is predicted to be<1 for pre-equilibrium proton transfer followed by the slow step. Thus, the observed isotope effect is composite of solvent isotope effect and the primary isotope effect of step (ii).

Thus assuming H_2OBr^+ as the reactive species, reaction Scheme 2 can be proposed in which the substrate is attacked at the nucleophilic sulphur site by the oxidant to form a sulphurane intermediate. The latter is attacked by the dipolar solvent. Elimination of H^+ and HBr results in the formation of methionine sulphoxide, which is oxidised by the second molecule of the oxidant. The four-electron stoichiometry shown for the reaction clearly rules out the formation of a sulphimide as a minor product which was noticed by Ruff and Kucsman[18] during the oxidation of sulphides by CAB.



where, $R = CH_2CH_2CHNH_2COOH$

Scheme 2

Scheme 3 explains the results obtained in the presence of halide (X^-) ion. The tight ion-pair formed in step (i) produces the inter-halogen compound ClBr or Br_2 which would oxidise the substrate in a fast step.

$$ArSO_2NBr^- + 2H^+ + X^- \overset{K_4}{\rightleftharpoons} ArSO_2\overset{+}{N}H_2Br \cdots X^- \quad (i)$$

$$ArSO_2\overset{+}{N}H_2Br \ldots X^- \underset{slow}{\overset{k_5}{\longrightarrow}} ArSO_2\overset{+}{N}H_2 + BrX \quad (ii)$$

$$BrX + CH_3S(CH_2)_2CH(NH_2)COOH + 2H_2O \underset{fast}{\overset{k_6}{\longrightarrow}}$$

$$CH_3SO_2(CH_2)_2CHNH_2COOH + 2H^+ + Br^+ + X^- \quad (iii)$$

where, X^- is Cl^- or Br^-.

Scheme 3

Scheme 3 leads to rate law (10) in the form,

$$Rate = \frac{k_5K_4[BAB][H^+]^2[X^-]}{1 + K_4[H^+]^2[X^-]} \quad (10)$$

which at constant [H^+] reduces to

$$\text{Rate} = \frac{k_3 K_4 [BAB][X^-]}{1+K_4[X^-]} \qquad (11)$$

Equation (10) is transformed into equation (12) for a double reciprocal plot of k' *vs* [Cl^-] in the form at constant [H^+],

$$\frac{1}{k'} = \frac{1}{k_3 K_4 [H^+]^2 [Cl^-]} + \frac{1}{k_3} \qquad (12)$$

From the straight line obtained ($r=0.994\,0$), k_3 and K_4 are 42.8×10^{-4} s^{-1} and 1 460 l^2 mol^{-2} in presence of HCl, at [H^+]= 0.07 *M*. These values are comparable with those obtained during the oxidation of dimethylsulphoxide[2,3] with BAB ($k_3 = 41.27\times10^{-4}$ s^{-1} and $K_4 = 1\,100$ l^2 mol^{-2}), thus establishing the values of the formation constant and decomposition constant of the species, $ArSO_2\overset{+}{N}H_2Br...Cl^-$.

Mechanism in alkaline medium : Oxidation of Mt by BAB in alkaline medium shows a first order dependence on the [oxidant] and a fractional order retardation with respect to the product of oxidation, benzenesulphonamide ($ArSO_2NH_2$). Further, the rate is independent of substrate concentration. Scheme 4 is able to explain the observed results.

$$ArSO_2NBrNa + OH^- \underset{k_{-1}}{\overset{k_1}{\rightleftharpoons}} ArSO_2NH^- + NaOBr \qquad \text{(i)}$$
(fast)

$$NaOBr + H_2O \underset{k_{-2}}{\overset{k_2}{\rightleftharpoons}} NaOH + HOBr \qquad \text{(ii)}$$
(slow ; forward reaction is rate limiting)

$$HOBr + Mt \xrightarrow{k_3} Y \qquad \text{(iii)}$$
(fast)

$$Y + HOBr \xrightarrow{k_4} \text{Products} \qquad \text{(iv)}$$
(fast)

Scheme 4

There is ample evidence[16] to indicate the participation of hypobromous acid in reactions involving alkaline BAB solutions. From Scheme 4, assuming steady state conditions for [NaOBr] and with the approximation [RNH^-]≈[RNH_2], rate law (13) can be derived in agreement with experimental results.

$$-\frac{d[BAB]}{dt} = \frac{k_1 k_2 [BAB][OH^-]}{k_{-1}[RNH_2]+k_2} \qquad (13)$$

It is interesting to note that contrary to expectations, the rate of reaction has not increased in D_2O medium though OD^- is a stronger base than OH^- ion. The near equivalence of rates in the two media indicates that any increase in reaction rate is offset by the rate limiting hydrolysis, for which $k'_H/k'_D > 1$ is expected. Mechanism of oxidation of Mt by BAB in alkaline medium is similar to that of Scheme 2, except that the active species involved is HOBr.

References

1. M. S. Ahmed and D. S. Mahadevappa, *Talanta*, 1980, **27**, 669.
2. D. S. Mahadevappa, S. Ananda, A. S. A. Murthy and K. S. Rangappa, *Indian J. Chem.*, *Sect. A*, 1984, **23**, 17.
3. D. S. Mahadevappa, S. Ananda, A. S. A. Murthy and K. S. Rangappa, *Tetrahedron*, 1984, **40**, 1673.
4. A. Kumar, A. K. Bose and S. P. Mushran, *Monatsh. Chem.*, 1926, **20**, 524 ; 1936, **30**, 1661.
5. N. C. Wright, *Biochem. J.*, 1926, **20**, 524 ; 1936, **30**, 1661.
6. K. H. Gensch and T. Higuchi, *J. Pharm. Sci.*, 1967, **56**, 177.
7. A. P. Deliyannis, *Chem. Abstr.*, 1962, **56**, 13188.
8. F. Jancik, F. Buben and J. Korbl, *Chem. Abstr.*, 1957, **51**, 8369.
9. P. Spacu and H. Dumitrescu, *Chem. Abstr.*, 1973, **79**, 62459.
10. C. F. Dent, *Biochem. J.*, 1947, **41**, 240.
11. D. S. Mahadevappa and N. M. M. Gowda, *Talanta*, 1977, **24**, 270 ; *Microchem. J.*, 1983, **28**, 235.
12. P. R. Young and H. Hsieh, *J. Am. Chem. Soc.*, 1978, **100**, 7121.
13. F. Ruff and A. Kucsman, *J. Chem. Soc.*, *Perkin Trans. 2*, 1982, 1075.
14. A. I. Vogel, "Quantitative Organic Analysis", Longmans & Green, London, 1958, p. 508.
15. E. Bishop and V. J. Jennings, *Talanta*, 1958, **1**, 197.
16. F. F. Hardy and J. P. Johnston, *J. Chem. Soc.*, *Perkin Trans. 2*, 1973, 742.
17. S. S. Narayanan and V. R. S. Rao, *Radiochem. Radioanal. Lett.*, 1981, **49**, 193.

J. Indian Chem. Soc.,
Vol. LXIII, June 1986, pp. 586-588

Kinetics of Oxidative Decarboxylation of Benzilic acid by *N*-Bromosaccharin

U. MISHRA, (MS) K. SHARMA and V. K. SHARMA*

Department of Chemistry, Govt. Science College, Rewa-486 001

Manuscript received 28 September 1984, revised 12 March 1986, accepted 8 May 1986

Kinetics of oxidative decarboxylation of benzilic acid by *N*-bromosaccharin in binary solvent mixture of acetic acid-water in the presence of mercuric acetate has been investigated. The reaction is first order in oxidant and fractional order in substrate. Increase in [H^+] increases the rate. Addition of sodium perchlorate, sodium sulphate and sodium acetate accelerates the rate whereas saccharin shows retarding effect. Activation parameters are evaluated and probable mechanism involving 1 : 1 complex formation is suggested.

OXIDATIVE decarboxylation of hydroxy acids by various *N*-haloimides have been studied[1-6]. *N*-Bromosaccharin (NBSA), a new haloimide, has been employed in the oxidation[7-9] and bromination[10] of organic compounds. The present investigation deals with the oxidation of benzilic acid (BA) in acetic acid-water mixture in the presence of mercuric acetate by NBSA kinetically and a suitable mechanism is proposed.

Experimental

NBSA was prepared by brominating the alkaline solution of saccharin[11]. Its solution was prepared in glacial acetic acid (G.R.) and was standardised iodometrically[12]. The solution of benzilic acid (E. Merck) was prepared in glacial acetic acid. Other chemicals used were of standard grade.

The calculated volumes of reactants were mixed after attaining the desired temperature. The rate of reaction was followed from the aliquot portions of the reaction mixture taken at different intervals iodometrically.

Stoichiometry and product analysis: The stoichiometry of the reaction shows that one mole of benzilic acid is equivalent to one mole of NBSA. Under the experimental condition, the final products of oxidation were identified as benzophenone and saccharin.

Results and Discussion

Kinetic studies were arranged under the conditions [BA] and [$Hg(OAc)_2$] $\gg$ [NBSA]. All the investigations were made in the presence of mercuric acetate in order to avoid any possible bromine oxidation. Mercuric acetate acts as a scavenger for Br^- formed in the reaction and exists as $HgBr_4^{2-}$ and unionised $HgBr_2^{13}$ and thus ensuring only NBSA oxidation. Preliminary experiments were performed in the range $4.0\text{-}20.0 \times 10^{-3} M$ of [$Hg(OAc)_2$]. The plot of k_1 *vs* [$Hg(OAc)_2$] shows that initially the reaction is first order dependence in mercuric acetate and then tends to limiting rate, *i.e.* zero order dependence at [$Hg(OAc)_2$]$=10.0 \times 10^{-3} M$. Hence, all the studies were made at $10.0 \times 10^{-3} M$ mercuric acetate concentration.

The characteristic features of the oxidation can be summarised as follows. (i) Polymerisation test with acrylonitrile is negative ruling out the formation of free radical. (ii) On the five-fold variation of the concentration of NBSA, the first order rate constants for different initial concentration of NBSA at constant [BA], [$Hg(OAc)_2$] and [HOAc] are obtained almost constant (Table 1) suggesting first order dependence in oxidant which is further evidenced from linear plots of log (a-x) *vs* time.

TABLE 1—DEPENDENCE OF RATE ON NBSA AT 30°

[BA]$=2.50 \times 10^{-2} M$, [$Hg(OAc)_2$]$=1.00 \times 10^{-2} M$, [HOAc]$=$ 70% (v/v)

[NBSA] $10^3 M$	1.00	1.25	2.50	3.33	5.00
$10^3 k_1$ min^{-1}	4.37	4.34	4.40	4.44	4.36

The fractional order in benzilic acid was found from the slope (=0.80) of the plot of log k_1 *vs* log [BA] which may be due to the complex formation between BA and oxidant species as evidenced by a linear plot of k_1^{-1} *vs* $[BA]^{-1}$ with a positive intercept on y-axis (Fig. 1). (iii) The rate studies were made at different [H^+] by taking H_2SO_4 and $HClO_4$ (Table 2). With increase in concentration of acid,

* 20/5 Kothi Road, Rewa-486 001.

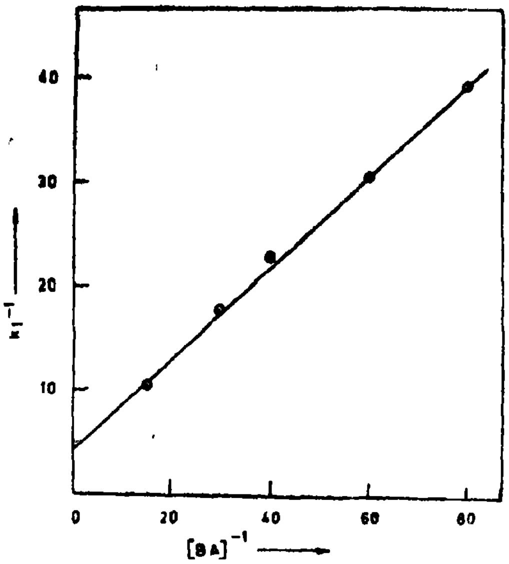


Fig. 1. Plot of k_1^{-1} *vs* $[BA]^{-1}$; $[NBSA]=2.50\times10^{-3}$ *M*, $[Hg(OAc)_2]=1.00\times10^{-3}$ *M*, HOAc-H_2O=70% (v/v), temp.=30°.

TABLE 2—DEPENDENCE OF RATE ON $[H^+]$ AT 30°

$[NBSA]=2.50\times10^{-3}$, *M*, $[BA]=2.50\times10^{-3}$ *M*, $[Hg(OAc)_2]=1.00\times10^{-3}$ *M*, [HOAc]=70% (v/v)

[Acid] 10³ *M*	0.00	1.0	5.0	15.0	20.0	25.0	50.0
A-10³ k_1 min⁻¹	4.40	6.36	8.06	12.44	—	16.29	26.39
B-10³ k_1 min⁻¹	4.40	6.23	10.37	23.92	31.06	45.15	—

A=H_2SO_4, B=$HClO_4$.

the rate of reaction increases indicating a participation of H^+ ion in the mechanism. (iv) The effect of varying composition of binary solvent mixture of acetic acid-water on the rate of oxidation has been studied. It is noted that with increase in acetic acid reaction rate decreases. (v) Addition of saccharin retards the rate of oxidation (Table 3).

TABLE 3—DEPENDENCE OF RATE ON [SACCHARIN] AT 30°

$[NBSA]=2.50\times10^{-3}$ *M*, $[Hg(OAc)_2]=10.0\times10^{-3}$ *M*, $[BA]=2.50\times10^{-3}$ *M*, [HOAc]=70% (v/v)

[Saccharin] 10³ *M*	0.0	1.66	2.00	2.50	3.33	4.00
10³ k_1 min⁻¹	44.17	21.82	17.75	14.72	11.22	9.67

The plot between k_1^{-1} and [Saccharin] is obtained linear with positive intercept suggesting inverse dependence of rate on [Saccharin]. (vi) The effect of neutral salts like sodium sulphate, sodium acetate and sodium perchlorate enhance the rate of oxidation. (vii) The title oxidation was carried out at four different temperatures (30-45°) and activation parameters are obtained from the Arrhenius plot. The value of different parameters, *viz.* E, A and $\Delta S^{\neq}$ are 17.98±0.78 kcal mol⁻¹, $11.87\pm0.99\times10^{9}$ s⁻¹ and −14.16±4.92 e.u., respectively. The value of energy of activation is more or less close to those obtained for other hydroxy acids[14,15] and hence, it is supposed that above oxidation might follow a mechanism in which formation of reversible complex between the reactants is followed by the rate determining step involving C−C fission.

Mechanism : The reactive oxidant species of *N*-bromosaccharin in aqueous acetic acid are likely to be unprotonated NBSA, protonated NBSA, H_2O^+Br, CH_3COO^+HBr and molecular bromine, hence the oxidation may be a reaction between benzilic acid and any one of the above species.

$$NBSA+H_3O^+ \overset{K_1}{\rightleftharpoons} NBSAH^+ + H_2O \qquad (1)$$

The protonated species because of weaking of N−Br bond might solvolyse further to give H_2O^+Br or its analogous acetyl derivtaive CH_3COO^+HBr

$$NBSAH^+ + H_2O \rightleftharpoons H_2O^+Br + \text{Saccharin} \qquad (2)$$

$$NBSAH^+ + CH_3COOH \rightleftharpoons CH_3COO^+HBr + \text{Saccharin} \qquad (3)$$

The present investigation was carried out at 70% [HOAc] and with the decrease in [HOAc], enhancement of rate was observed which excludes the possibility of CH_3COO^+HBr as oxidising species. Molecular bromine is also not likely to be reactive species as clean first order dependence on NBSA at all concentration was observed.

With increase in the concentration of H^+ rate enhancement was observed both in H_2SO_4 and $HClO_4$. This favours the protonated NBSA as the reactive species in the present oxidation study. These observations lead to the mechanism,

$$BA + NBSAH^+ \overset{K_2}{\rightleftharpoons} \text{Complex} + \text{Saccharin} \qquad (4)$$

$$\text{Complex} \xrightarrow{k} C_6H_5COC_6H_5 + CO_2 + HBr \qquad (5)$$

The mechanism, thus involves one or more pre-equilibria for the formation of the oxidant species followed by a slow rate determining dissociation of complex formed between benzilic acid and Br^+ to give the products. Applying equilibrium conditions for the formation of oxidant species k_{obs} is given as as

$$k_{obs} = \frac{k\,K_1K_2\,[BA]\,[H_3O^+]}{[\text{Saccharin}]\{1+K_1[H_3O^+]\}+K_1K_2[BA][H_3O^+]} \qquad (6)$$

$$\frac{1}{k_{obs}} = \frac{[\text{Saccharin}]\,\{1+k_1[H_3O^+]\}}{k\,K_1K_2[BA][H_3O^+]} + \frac{1}{k} \qquad (7)$$

The plots of $1/k_{obs}$ *vs* 1/[BA] or [Saccharin] are obtained linear with positive intercept on y-axis establishing the validity of step (6) and also it explains all the experimental results.

References

1. P. Kuselan and N. Venkatasubramanian, *Indian J. Chem., Sect. A*, 1983, **22**, 292.
2. J. Jha, P. D. Sharma and Y. K. Gupta, *Inorg. Chem.*, 1983, **22**, 1393.
3. A. L. Jain and K. K. Banerji, *J. Indian Chem. Soc.*, 1982, **59**, 654.
4. A. K. Mathur and K. K. Banerji, *Indian J. Chem., Sect. A*, 1981, **20**, 529.
5. K. K. Banerji, *Indian J. Chem., Sect. A*, 1977, **15**, 615.
6. R. Natarajan and N. Venkatasubramanian, *Indian J. Chem.*, 1975, **13**, 261.
7. P. Manikyamba and E. V. Sundaram, *Indian J. Chem., Sect. A*, 1980, **19**, 1122.
8. K. Vijaymohan, P. Raghunath Rao and E. V. Sundaram, *J. Indian Chem. Soc.*, 1984, **61**, 225.
9. U. Mishra and K. Sharma, "Abstract : Convention of Chemists 1984", Indian Chemical Society, Calcutta, Phy(P) 88.
10. S. P. Srinivasan and N. S. Gnanapragasam, *J. Indian Chem. Soc.*, 1983, **60**, 1106.
11. J. M. Bachhawat and N. K. Mathur, *Indian J. Chem.*, 1971, **9**, 1335.
12. M. Z. Barkat and M. F. Abdelwahab, *Anal. Chem.*, 1954, **26**, 1973.
13. J. C. Bailar, "The Chemistry of Coordination Compounds", Reinhold, New York, 1956, p. 6.
14. R. Dayal, K. K. Banerji and G. V. Bakore, *Indian J. Chem.*, 1971, **9**, 1017.
15. G. V. Bakore and B. P. Rishi, *Indian J. Chem.*, 1966, **4**, 4.

J. Indian Chem. Soc.,
Vol. LXIII, June 1986, pp. 589-591

Dielectric Study of Solvent Effect in Carboxylic Acids

V. SHANMUGASUNDARAM* and P. THIYAGARAJAN

Department of Physics, Annamalai University, Annamalainagar-608 101

Manuscript received 27 November 1978, accepted 8 May 1986

The dielectric constant variation method has been used to evaluate the dipole moment (μ), the Kirkwood correlation factor (g) and the association constant (K) of carboxylic acids in various solvents. From that, the effect of solvents on solute molecules are discussed.

IN order to study the interaction of the neighbouring dipole, Kirkwood in colloboration with Frohlich[1] introduced a rigorous statistical mechanical model which gives the relation for the dielectric constant of a polar liquid as

$$g\mu^2 = \frac{9\,KT}{4\,\pi N}\;\frac{(\epsilon-\epsilon_\alpha)(2\epsilon+\epsilon_\alpha)}{(\epsilon_\alpha+2)^2}$$

where, ϵ is the dielectric constant of the solute, ϵ_α the dielectric constant of the induced polarisation, T the absolute temperature, K the Blotzmann's constant, N the Avogadro's number, μ the dipole moment of the solute and g the Kirkwood correlation factor. The physical meaning of g is the measure of the local ordering, that is the measure of the short-range inter-molecular forces, which leads to dipole-dipole interaction. If there is no specific interactions one has g=1, and the above equation reduces to the Onsager equation[2] of dielectrics. For associating compounds where the occurrence of hydrogen bonding makes the relevant assumption that only certain specific angle between the dipole of the neighbouring molecule are possible, the inter-molecular interaction may be represented by means of a simplified models. For polymers, the same model can be used if each segment is used as a separate entity of which the orientation of the dipole moment is correlated with the dipole moment of the other segments. In many cases, these models contain undetermined parameters so that the value of g is often calculated as an empirical quantity by the above equation and the dipole moment μ by the method Few and Symth[3]. The unknown parameters can be found from the experimental values of g. However, an experimental determination of g with concentration will give the quantitative information regarding the undetermined parameters and hence, the nature of the inter-molecular interaction in polar liquids.

Malecki[4] studied the correlation factor g and the non-linear correlation factor due to the saturation effects in liquid complexes and from that he was able to decide whether the complex is of charge-transfer type or proton-transfer type *etc.* The static dielectric constant behaviour of mono-alcohols and their solutions in non-polar solvent[5-8] was studied with special reference to the variation of g with concentration. And the variation of g of the acetic acid was discussed in the higher concentration by Sabesan and Varadarajan[9].

Experimental

A WTW 01 dipolmeter at a frequency of 2 MHz was used to measure the dielectric constants keeping the cell temperature at 30°. The refractive indices were determined at 30° by Abbe's refractometer. Pure grade (E. Merck) solvents and solutes were purified by standard methods.

The evaluation of molar polarisation includes the measurement of dielectric constant (ϵ), refractive index (n) and density (d) of the mixtures at the different concentrations in the solvents.

Method of calculation : Considering each kind of polymer as a separate compound neglecting any specific correlation between the total dipole moment of the polymer, the dielectric equation can be written as

$$\frac{(\epsilon-1)(2\epsilon+1)}{12\pi\epsilon} = \frac{N\alpha_o}{1-f_o\alpha_o} + \sum_{n=1}^{\alpha} \frac{N_n}{1-f_n\alpha_n} \left(\alpha_n + \frac{\overline{\mu_n^2}}{3\,KT}\;\frac{1}{1-f_n\alpha_n}\right) \quad (2)$$

where, the suffix zero refers to the non-polar solvents and n refers to the polymer containing n-polar units. The average value of $\overline{\mu_n^2}$ is taken over all configurations of the multimeter. By substituting the appropriate values of α_o, α, $\frac{1}{1-f_o\alpha_o}$ and $\frac{1}{1-f_n\alpha_n}$ in equation (2),

$$\frac{\epsilon-1}{12\pi\epsilon} = \frac{N_o(\epsilon_o-1)\,M_o}{4\pi\,(2\epsilon+\epsilon_o)d_oN_A} + \frac{(\epsilon\alpha-1)\,M_1}{4\pi(2\epsilon+\epsilon_\alpha)d_1N_A}\sum_{n=1}^{n} n\,N_n + \frac{(2\epsilon+1)(\epsilon_\alpha+2)^2}{27\,KT\,(2\epsilon+\epsilon_\alpha)^2}\sum_{n=1}^{\alpha} Nn\,\overline{\mu_n^2} \quad (3)$$

Since there is no correlation between the different chain, g_n represents the total correlation between permanent moment of the segment in the n-mer and its surroundings.

The Kirkwood correlation factor, g, can be written as

$$g=\frac{\sum_{n=1}^{\infty} n\,N_n g_n}{\sum_{n=1}^{\infty} n\,N_n}=\frac{\sum_{n=1}^{\infty} N n\,\overline{\mu_n^2}}{\mu^2 \sum_{n=1}^{n} n\,N_n} \quad (4)$$

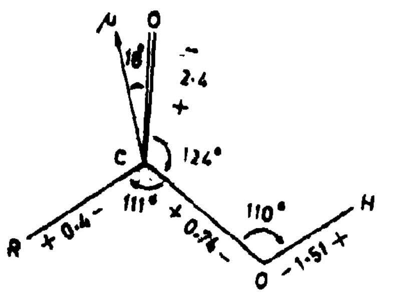
By using the mole fraction of the solvent X_1 and that of the solute X_2, the equation for the Kirkwood correlation factor, g, is given by

$$g=\left[\frac{9\,KT}{4\pi N}\,\frac{(2\epsilon+\epsilon_\infty)^2}{2X_2(\epsilon_\infty+2)^2(2\epsilon+1)}\right]\left[\phi\frac{\epsilon-1}{\epsilon}-\frac{3X_1\phi_1(\epsilon_1-1)}{2\epsilon+\epsilon_1}-\frac{3X_2\phi_2(\epsilon_\infty-1)}{(2\epsilon+\epsilon_\infty)}\right] \quad (5)$$

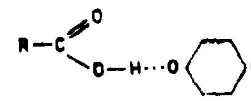
where, ϵ_1 and ϕ_1, and ϵ and ϕ are the dielectric constant and molar volume of the solvent and the solution, respectively.

Results and Discussion

The calculated values of dipole moment μ, Kirkwood correlation factor g and the association constant K, for the carboxylic acids in various solvents are given in the Table 1. From the literature, it has been found that there is no general agreement regarding the dipole moment of the carboxylic acids. By using the molecular parameters[18], bond angles and bond moment, the theoretical value of μ for a monomer acid is found to be 1.712 D.



It has been generally assumed by earlier workers[10,11] that the acetic acid in the pure liquid state exists in a cyclic hydrogen bonded dimer. However, the existance of non-zero dipolemoment value indicates that a portion of the dimeric units should be non-cyclic. And the experimental value of μ for carboxylic acid molecule found to be very much less than the theoretical value, shows the simultaneous existance of both ring dimers and open polymers[12]. Many physicochemical studies[13-14,17] reveal that the association is a mixture of non-polar dimer association and polar chain association. When the acids are diluted with the non-interacting solvents, such as CCl_4 and C_6H_6, there is no possibility for the formation of hydrogen bonding between the solute and solvent molecules but the polymer may break and form open dimer. The non-zero dipolemoment definitely indicates that even at infinite dilution the molecules are not cyclic dimer. The higher value of μ in C_6H_6 may be due to the π-electron interaction with the solute. The dioxane has a powerful anionoid centre capable of breaking down the molecular aggregates of the solute molecules and hence there is a predominance of monomer species. And these are bonded with the sp^3 bond of the dioxane leading to a higher value of μ than the theoretically calculated value.



From the above, it has been observed that the experimental value of μ follows the order, $\mu_{CCl_4} < \mu_{C_6H_6} < \mu_{dioxane}$.

The Kirkwood correlation factor g which is a measure of local ordering have both values, greater than unity and less than unity in the case of carboxylic acids (Fig. 1), and shows the parallel and antiparallel alignment with the neighbouring dipole. From the predominant configuration of an open dimer structure*, the calculated value of g is found to be 0.05 which is far below the experimental values. The higher values of g shows the presence of more number of monomers in addition to closed dimer, open dimer, trimer *etc.* In all cases, the value of g less than unity in CCl_4 and C_6H_6 shows that the dipole-dipole interaction of the aggregates of the solute makes the dipole almost anti-parallel with the field. But in dioxane, g is

TABLE 1—DIPOLE MOMENT, KIRKWOOD CORRELATION FACTOR AND DIMERISATION CONSTANT OF CARBOXYLIC ACIDS IN VARIOUS SOLVENTS

Substance	CCl_4			C_6H_6			Dioxane		
	μ Debye	g	K $dm^3\ mol^{-1}$	μ Debye	g	K $dm^3\ mol^{-1}$	μ Debye	g	K $dm^3\ mol^{-1}$
Formic	0.84	0.96	2.87	1.69	1.01	9.58	2.10	1.09	4.87
Acetic	0.85	0.82	1.97	1.12	0.78	8.78	1.78	1.12	1.46
Benzoic	0.89	0.52	0.68	1.02	0.46	2.76	1.92	1.15	11.89

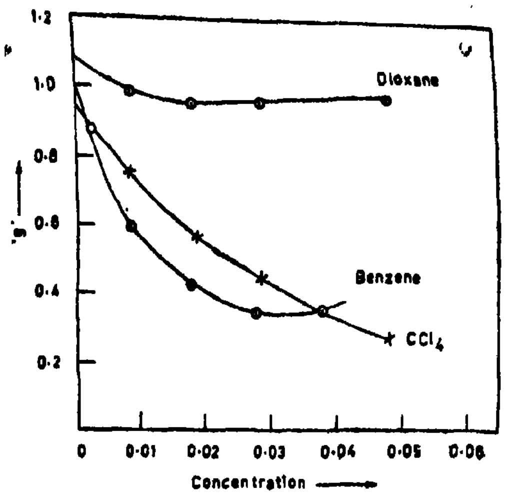


Fig. 1. Variation of g with concentration of formic acid in various solvents.

found to be greater than one in all cases, which indicates the predominance of monomer species which are H-bonded with the solvent, and tends to keep the dipoles parallel to the field. Therefore, it is observed that the interaction between the dipoles are greater in dioxane than the non-interacting solvents CCl_4 and C_6H_6. The association constants K for all cases are also given in Table 1.

From the above, it is inferred that CCl_4 can be considered as the best solvent for studying the inter-molecular interactions. Though benzene and dioxane have zero dipolemoment, they cannot be used as a solvent.

Acknowledgement

One of the authors (P.T.) is thankful to U.G.C., New Delhi, for the award of Junior Research Fellowship.

References

1. H. Frohlich, "Theory of Dielectrics", Oxford University Press, London, 1958.
2. L. J. Onsagar, *J. Am. Chem. Soc.*, 1936, 58, 1486.
3. A. V. Few and J. W. Smith, *J. Chem. Soc.*, 1949, 2781.
4. J. Malecki, *J. Chem. Soc., Faraday Trans. 2*, 1976, 104.
5. P. Bordewijk, Ph.D. Thesis, University of Leiden, 1968.
6. W. Dannhauser, *J. Chem. Phys.*, 1968, 48, 1911.
7. P. Bordewijk, F. Gransch and C. Bottcher, *Trans. Faraday Soc.*, 1970, 66, 293.
8. W. Dannhauser, R. Guerring and A. F. Fluckinger, *J. Chem. Phys.*, 1970, 52, 6447.
9. R. Sabesan and R. Varadarajan, *Indian J. Pure and Appl. Phys.*, 1977, 15, 588.
10. K. Venkateswarlu and S. Sriraman, *Trans. Faraday Soc.*, 1957, 53, 433.
11. G. V. L. Murthi and T. R. Seshadri, *Proc. Indian Acad. Sci., Sect. A*, 1942, 16, 51.
12. H. A. Phol, M. E. Hobbs and P. M. Cross, *J. Chem. Phys.*, 1941, 9, 408.
13. M. I. Batuev, *Dokl. Akad. Nauk. SSSR*, 1948, 59, 1170.
14. M. Blinc and R. Blinc, *J. Polym. Sci.*, 1958, 32, 506.
15. L. W. Reeves, *Trans. Faraday Soc.*, 1959, 55, 1684.
16. C. P. Smyth and H. E. Rogers, *J. Am. Chem. Soc.*, 1930, 52, 1824.
17. L. W. Reeves and W. G. Schneider, *Trans. Faraday Soc.*, 1958, 54, 314.
18. C. P. Smyth, "Dielectric Behaviour and Molecular Structure", McGraw-Hill, New York, 1955.

J. Indian Chem. Soc.,
Vol. LXIII, June 1986, pp. 592-593

Deuterium Labelling Studies with Unsaturated Acids and Nitriles†

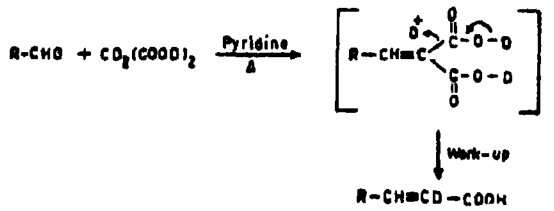
UDAY V. DESAI and RAMCHANDRA B. MANE*

Department of Chemistry, Shivaji University, Kolhapur-416 004

Manuscript received 25 June 1985, revised 20 January 1986, accepted 8 May 1986

α-Deuteriated α,β-unsaturated acids have been prepared by Knoevenagel condensation of aldehydes with deuteriated malonic acid. The decarboxylation of α,β-unsaturated cyano acid with pyridine/D_2O yields α- and γ-labelled nitriles. The deuterium incorporation is studied by pmr spectroscopy.

DEUTERIATED compounds are useful for chemical as well as for biological work. α-Deuteriated enoic acids have been prepared earlier by deuterium exchange reaction under basic condition but the incorporation is poor[1]. Manitto *et al.*[2] have reported the preparation of α-deuteriated cinnamic acids by Hofmann elimination of the quaternary ammonium salts in presence of deuterium oxide. In continuation with our work[3] on the deuterium labelled acids, we report here a simple and efficient method for the preparation of α-deuteriated unsaturated acids by Knoevengel condensation[4] of suitable aldehydes with deuteriated malonic acid (prepared by exchange with D_2O). During this reaction in pyridine, decarboxylation of the substituted malonic acid occurs and the α-position is protonated. Since only deuterons are present in the reaction medium the resulting acid is α-deuteriated (Chart 1). The



R		%D
(1)	o-ClC_6H_4	68
(2)	o-$NO_2C_6H_4$	70
(3)	p-$OMeC_6H_4$	66
(4)	p-MeC_6H_4	65
(5)	p-OH, m-$OMeC_6H_3$	60*

* Keeping with piperidine and pyridine.

Chart 1

deuterium incorporation is determined by comparing the relative intensities of carefully determined integrals of the various signals. If 100% pure deuteriated malonic acid is used one should be able to get 100% α-deuteriated enoic acid by this method.

The decarboxylation of α,β-unsaturated malonic and cyano acids has been the subject of many investigations. Corey [5,6] and others[7] have suggested isomerisation of the double bond to β,γ-position of the acid which then undergoes decarboxylation to yield β,γ- and α,β-unsaturated acids. We planned to use this for the multiple labelling of unsaturated nitriles. During the equilibriation of the α,β- and β,γ-isomers of the cyano acid (6), the γ-position (methyl group) and the α-position can get labelled (Chart 2).

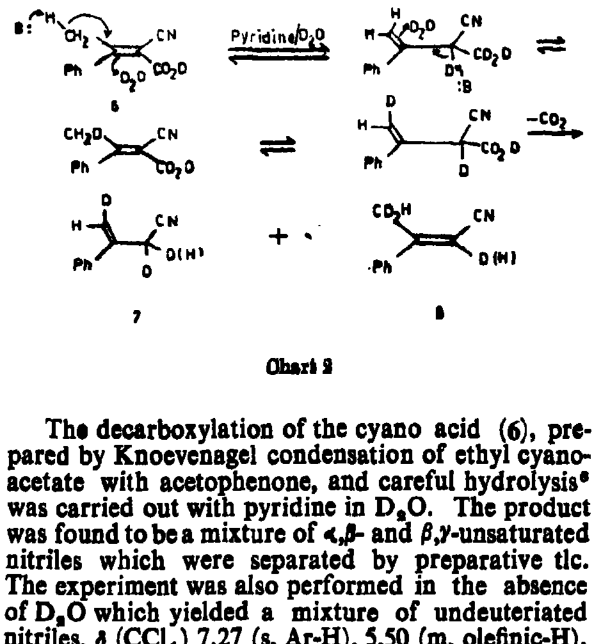


Chart 2

The decarboxylation of the cyano acid (6), prepared by Knoevenagel condensation of ethyl cyanoacetate with acetophenone, and careful hydrolysis[8] was carried out with pyridine in D_2O. The product was found to be a mixture of α,β- and β,γ-unsaturated nitriles which were separated by preparative tlc. The experiment was also performed in the absence of D_2O which yielded a mixture of undeuteriated nitriles, δ (CCl_4) 7.27 (s, Ar-H), 5.50 (m, olefinic-H), 3.43 (t, *J* 1.5 Hz, methylene-H), 2.43 (d, *J* 1.5 Hz, CH_3). Comparison of the methyl and methylene proton intensities gives the % of β,γ- and α,β-unsaturated nitriles as 83 and 17, respectively. The pmr of the deuteriated nitriles showed extensive labelling of α- as well as the γ-positions. Pmr of β,γ-unsaturated nitrile (7) δ (CCl_4, 60 MHz) 7.25(100 mm, s, Ar-H), 5.47 (15 mm, d, *J* 5 Hz, partially

† Presented at the Annual Convention of Chemists, Madras, 1981.

labelled olefinic-H), 3.4 (6 mm, broad triplet, partially labelled methylene-H), clearly indicates that the γ-position is labelled to the extent of 62.5% and the α-position 85%. Pmr of α,β-unsaturated nitrile (8) δ ($CDCl_3$, 100 MHz) 7.46 (193 mm, s, Ar-H), 5.64 (5 mm, bs, labelled olefinic-H), 2.46 (37 mm, broad multiplet indicative of coupling to D, labelled-CH_3). The integrated intensities indicate that the α-position is 87% labelled and the γ-position 68%. Since it is possible to convert β,γ-unsaturated nitrile into α,β-unsaturated nitrile, this represents an efficient method for α- and γ-labelling of α,β-unsaturated nitriles. The extensive labelling is explained in Chart 2.

Experimental

Typical procedure : Deuteriated malonic acid (0.5 g), anisaldehyde (0.5 g) and dry pyridine (4 drops) were heated on a water-bath for 4 h. The reaction mixture was cooled, diluted with water and acidified with dilute hydrochloric acid. The precipitated acid was filtered, dried and recrystallised from aqueous ethanol to yield pure α-deuteriated *p*-methoxycinnamic acid (0.570 g). The nmr integration of the signal at δ 6.35 (α-H) was compared with that at δ 7.62 (β-H and Ar-H) which indicated 66% deuterium at the α-position. The incorporation is not 100% since the deuteriated malonic acid used was only 69-70% deuteriated.

α,γ-Deuteriated-β-methylcinnamonitrile (8) *:* 2-Cyno-3-phenyl-2-butenoic acid[8] (6 ; 1.1 g), D_2O (1 ml) and pyridine (10 ml) were refluxed for 3 h. The reaction mixture was cooled and acidified with dilute hydrochloric acid and extracted with ether. The ether layer was washed with water and dried over anhydrous sodium sulphate. The ether was distilled off to give a mixture of α,β- and β,γ-unsaturated nitriles (8 and 7, 0.79 g), which were separated by preparative tlc on silica gel. The compounds were characterised by comparison of spectral data with the known undeuteriated nitriles.

Acknowledgement

The authors thank Department of Atomic Energy, Government of India, for the fellowship to one of them (U.V.D.), and R.S.I.C., I.I.T., Bombay and N.C.L., Pune, for pmr spectra.

References

1. J. G. Atkinson, J. J. Csakuary, G. T. Herbert and R. S. Stuart, *J. Am. Chem. Soc.*, 1968, 90, 498.
2. P. Manitto, D. Monti and P. Gramatica, *Chem. Commun.*, 1978, 668.
3. J. A. Elvidge, J. R. Jones, R. B. Mane and M. Saljoughian, *J. Chem. Soc., Perkin Trans. 1*, 1978, 1191.
4. H. O. House, "Modern Synthetic Reactions", 2nd. ed., W. A. Benjamin, p. 646.
5. E. J. Corey, *J. Am. Chem. Soc.*, 1952, 74, 5897.
6. E. J. Corey and G. Fraenkel, *J. Am. Chem. Soc.*, 1953, 75, 1168.
7. J. Klein and A. Y. Meyer, *J. Org. Chem.*, 1964, 29, 1038.
8. G. S. K. Rao and J. Alexander, *Indian J. Chem.*, 1972, 10, 789.

J. Indian Chem. Soc.,
Vol. LXIII, June 1986, pp. 594-596

Studies on 4-Thiazolidinones. Part-I. Preparation of 2-Aryl-3-[2′-isopropyl-5′-methylphenoxyacetylamino]-5H/methyl-4-thiazolidinones

K. P. RODA, R. N. VANSDADIA and HANSA PAREKH*

Department of Chemistry, Saurashtra University, Rajkot-360 005

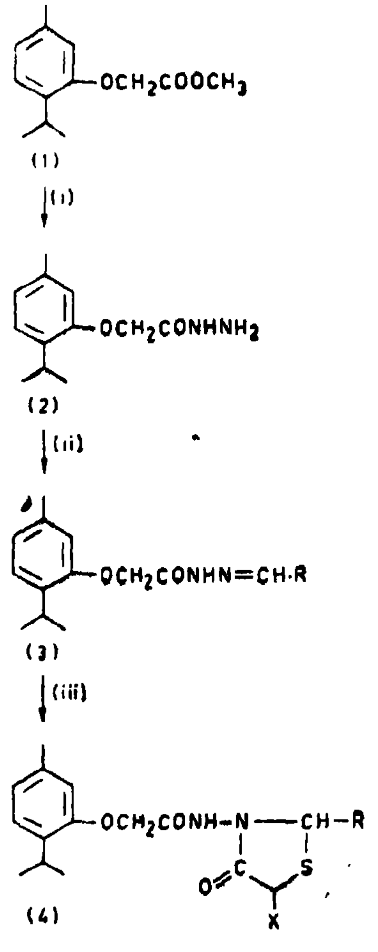
Manuscript received 16 August 1985, revised 8 January 1986, accepted 8 May 1986

Some new 4-thiazolidinones have been prepared having 2-isopropyl-5-methylphenoxyacetylamino moiety. The Schiff base from 2-isopropyl-5-methylphenoxyacetylhydrazide were condensed with thioglycolic and thiolactic acid. The constitution was supported by ir spectra.

4-THIAZOLIDINONE derivatives have been found to have many physiological activities, *viz.* anticonvulsant[1], antithyroid[2], local anaesthetic[3], analgesic[4], sedative[5] and antiviral activity[6]. Thymol derivatives also possess antituberculostatic[7], anthelmintic[8] and antiseptic[7] activities. With a view to achieve better therapeutic activity, we have synthesised 4-thiazolidinone derivatives of type **4**.

Thymol was condensed with chloroacetic acid and esterified (**1**), which was treated with hydrazine hydrate to get 2-isopropyl-5-methylphenoxyacetylhydrazide (**2**). The hydrazide was then condensed with different aromatic aldehyde to get the Schiff-bases (**3**). This on treatment with thioglycolic and thiolactic acid gave substituted 4-thiazolidinones (**4**). The constitution of the product was supported by ir spectra.

The schematic presentation of the reaction sequences is given below.



R = Aryl X = H/CH_3

Reagents : (i) $NH_2NH_2.H_2O$, (ii) RCHO, (iii) HS.CHX.COOH.

Ir spectra : The ir spectra were taken on KBr pellet in the range 600-4 000 cm^{-1}. The Schiff base gave characteristic bands at 1 680 (C=O str), 1 600 cm^{-1} (C=N str), and thiazolidinone gave same bands at 1 650 cm^{-1} (C=O str of thiazolidinone ring) and 1 590 cm^{-1} (C–N str).

Experimental

2-Isopropyl-5-methylphenoxyacylhydrazide : A mixture of 2-isopropyl-5-methylphenoxyacetate (0.01 mol) in methanol (10 ml) and hydrazine hydrate (0.01 mol) was refluxed on water-bath for 3 h. The product was isolated and crystallised from hot water, (76%), m.p. 78° (Found : C, 64.4 ; H, 8.0 ; N, 12.58. $C_{12}H_{18}O_2N_2$ calcd. for : C, 64.80 ; H, 8.11 ; N, 12.61%).

*2-Isopropyl-5-methylphenoxy-*N*-benzalamino acetamide :* Benzaldehyde (0.01 mol) was condensed with the above hydrazide (0.01 mol) in methanol (20 ml), then acetic acid (2-3 drops) was added to it and refluxed for 5 h at 70-80°. The product was isolated and crystallised from 95% ethanol, (67%),

TABLE 1

Sl. no.	R	Schiff base of type 3			Thiazolidinones of type 4					
					X=H			X=CH₃		
		Yield %	M.p. °C	N% Found	Yield %	M.p. °C	N% Found	Yield %	M.p. °C	N% Found
1.	Phenyl	67	156	8.95	56	149	7.20	52	139	6.95
2.	4-Hydroxyphenyl	68	124	8.48	54	98	6.50	59	104	6.68
3.	2-Hydroxyphenyl	62	144	8.50	52	133	6.82	54	133	6.70
4.	4-Methoxyphenyl	62	152	8.14	49	121	6.60	48	149	6.49
5.	3,4-Dimethoxyphenyl	54	176	7.49	52	168	6.10	58	163	6.00
6.	Cinnamyl	58	170	8.24	59	130	6.62	55	122	6.52
7.	2-Chlorophenyl	62	134	8.02	48	170	6.57	59	179	6.42
8.	4-Chlorophenyl	60	177	8.04	50	172	6.62	55	144	6.38
9.	2,4-Dichlorophenyl	68	218	7.30	51	209	6.10	58	208	5.85
10.	3,5-Dichloro-2-hydroxyphenyl	63	192	6.92	52	182	5.88	56	176	5.69
11.	4-Aminophenyl	60	220	12.10	58	110	10.48	48	98	10.10
12.	2-Nitrophenyl	53	177	11.70	53	169	9.72	52	165	9.40
13.	4-Nitrophenyl	66	185	11.78	51	121	9.70	56	130	9.42
14.	3-Methoxy-4-hydroxyphenyl	56	140	7.78	53	107	6.40	52	131	6.19
15.	3-Methoxy-2-hydroxyphenyl	52	145	7.76	50	138	6.41	49	117	6.17
16.	4-Methoxy-3-hydroxyphenyl	57	152	7.78	58	118	6.45	52	110	6.21
17.	3,4,5-Trimethoxyphenyl	62	124	6.91	48	192	5.80	56	184	6.69
18.	4-Dimethylaminophenyl	58	207	11.75	56	152	9.78	59	149	9.42
19.	2-Hydroxy-1-naphthyl	51	175	7.36	48	146	6.08	52	155	5.92

m.p. 156° (Found : C, 73.49 ; H, 6.91 ; N, 8.95. $C_{19}H_{22}O_2N_2$ calcd. for : C, 73.54 ; H, 7.09 ; N, 9.03%).

Similarly, other substituted Schiff bases were prepared (Table 1).

2-Phenyl-3-(2'-isopropyl-5'-methylphenoxyacetylamino)-4-thiazolidinone : Thioglycolic acid (0.1 mol) was added to 2-isopropyl-5-methylphenoxy-*N*-benzalaminoacetamide (0.05 mol) in dry benzene (25 ml) and refluxed for 6 h. The contents were poured in water, and the upper organic layer washed with sodium bicarbonate solution and water, dried with anhydrous sodium sulphate and benzene was distilled off. The product was isolated and crystallised from 95% ethanol, (56%), m.p. 149° (Found : C, 65.56 ; H, 5.90 ; N, 7.20 ; S, 8.23. $C_{21}H_{24}O_3N_2S$ calcd. for : C, 65.62 ; H, 6.25 ; N, 7.29 ; S, 8.33%).

Similarly, other substituted 4-thiazolidinones were prepared. Physical constants are recorded (Table 1).

2-Phenyl-3-(2'-isopropyl-5'-methylphenoxyacetylamino)-5-methyl-4-thiazolidinone : Thiolactic acid (0.1 mol) was added to 2-isopropyl-5-methylphenoxy-*N*-benzalaminoacetamide (0.05 mol) in dry benzene (25 ml) and refluxed for 6 h. The product was isolated as mentioned above and crystallised from 95% ethanol, (52%), m.p. 139° (Found : C, 66.30 ; H, 6.50 ; N, 6.95 ; S, 7.9. $C_{22}H_{26}O_3N_2S$ calcd. for : C, 66.33 ; H, 6.53 ; N, 7.03 ; S, 8.04%).

Similarly, other substituted 4-thiazolidinones were prepared (Table 1).

Acknowledgement

The authors are thankful to U.G.C., New Delhi, for awarding Junior Research Fellowship to one of them (K.P.R.) and to the Gujarat State Government for awarding research scholarship to the other (R.N.V.), and to Saurashtra University for facilities.

References

1. H. D. TROUTMAN and L. M. LONG, *Zh. Obshch. Khim.*, 1948, **70**, 3436.
2. S. N. GOLUBOVA, *Ukr Biokhim. Zh.*, 1953, **25**, 325.
3. F. P. LUDENA and J. O. HOPPE, *J. Am. Pharm. Assoc.*, 1951, **40**, 132.
4. G. SATZINGER, U. S. Pat. 3 072 670/1963 (*Chem. Abstr.*, 1963, **58**, 12569).
5. K. ENRICO, *Gazz. Chem. Ital.*, 1949, **79**, 621.
6. A. K. SHEINKMAN, *Microbiol. Zh.*, 1971, **33**, 88.
7. K. J. MEHTA, Ph. D. Thesis, Saurashtra University, 1979, p. 60.
8. Y. INZAWA, *Supporo. Med. J.*, 1952, 3, 48.

J. Indian Chem. Soc.,
Vol. LXIII, June 1986, pp. 596-599

Synthesis of Polynitroaryl Derivatives of 3-Aryl-1*H*,4*H*-dihydro-4,6,6-trimethyl-pyrimidine-2-thiols as Possible Fungicides

S. K. SANGAL*, ASHOK KUMAR, PAWAN RASTOGI and OM PRAKASH

School of Chemistry, Meerut College, Meerut-250 001

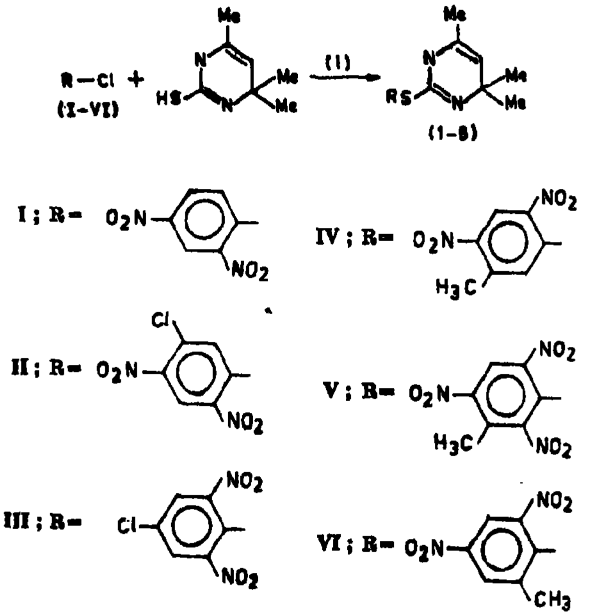
Manuscript received 20 July 1983, revised 6 March 1986, accepted 7 June 1986

Fortyeight new 3-aryl-1,4-dihydro-2-polynitroarylmercapto-4,6,6-trimethylpyrimidines (1-6) have been prepared in good yields by the condensation of appropriate active chlorobenzene and pyrimidine-2-thiol (A) in the presence of anhydrous sodium acetate in absolute ethanol. Mass spectra of three compounds (1b, 1e and 1g) have revealed that in addition to NO_2 and Me radical's loss from the molecular ion, the predominant fragment ions appear at respective *m/z* values which correspond to the molecular ions of pyrimidine thiols Ab, Ae and Ag, respectively. The further fragmentation pattern has been studied and it has been observed that loss of Me gives base peak in each case.

PYRIMIDINE nucleus has been employed as a basis for the synthesis of chemotherapeutic agents and a large number of its derivatives have been reported to possess various biological properties, such as antitumor[1], antimalarial[2], diuretic[3], anti-inflammatory[4], antithyroid[5] and antifungal[6].

The thiol group attached to a heterocyclic nucleus may enhance fungitoxicity[7]. The sulphides have been reported to be more biologically active than the parent mercapto[8] compounds. These observations coupled with the fact that polynitroaryl sulphides possess strong fungicidal activity, prompted us to undertake the synthesis of polynitroaryl derivatives of 3-aryl-1,4-dihydro-4,6,6-trimethyl-pyrimidine-2-thiols. Thus, we report in the present paper, the synthesis of fortyeight title compounds (1-6) which were obtained in good yields by the condensation of appropriate active chlorobenzenes (polynitrochlorobenzenes) and pyrimidine thiols (A) in the presence of excess of anhydrous sodium acetate and absolute alcohol.

Structures of the final compounds were confirmed by their melting points, elemental analysis, ir spectral data and mass spectral fragmentation of a few compounds. In the ir spectra of **1**, absorption band due to SH ($\sim$2 600 cm^{-1}) disappeared and in addition these compounds showed sharp and strong absorption peaks due to NO_2 groups appearing at 1 570-80 and 1 350-60 cm^{-1}. Mass spectra of three compounds **1b**, **1e** and **1g** were also recorded in order to give further support to the structures and to study their fragmentation pattern. The molecular ions do not appear as base peak in all the three cases. Base peaks are observed at respective *m/z* values obtained by the loss of Me



1a-6a, Ar=C_6H_5; 1b-6b, Ar=$C_6H_5-CH_2$; 1c-6c, Ar=*o*-$CH_3-C_6H_4$; 1d-6d, Ar=*m*-$CH_3-C_6H_4$; 1e-6e, Ar=*p*-$CH_3-C_6H_4$; 1f-6f, Ar=*m*-Cl-C_6H_4; 1g-6g, Ar=*p*-Cl-C_6H_4; 1h-6h, Ar=2,3-dichlorophenyl.

Reagents : (i) Anhydrous CH_3COONa, absolute ethanol.

Scheme 1

radical from the molecular ions of the corresponding pyrimidine thiols (Ae) which are the predominant peaks and undergo a variety of fragmentations. The other important losses from molecular ion were due to Me and NO_2 radicals.

* 184 Abu Lane, Meerut-250 001.

All these processes have been shown in Chart 1 by taking the example of 1e.

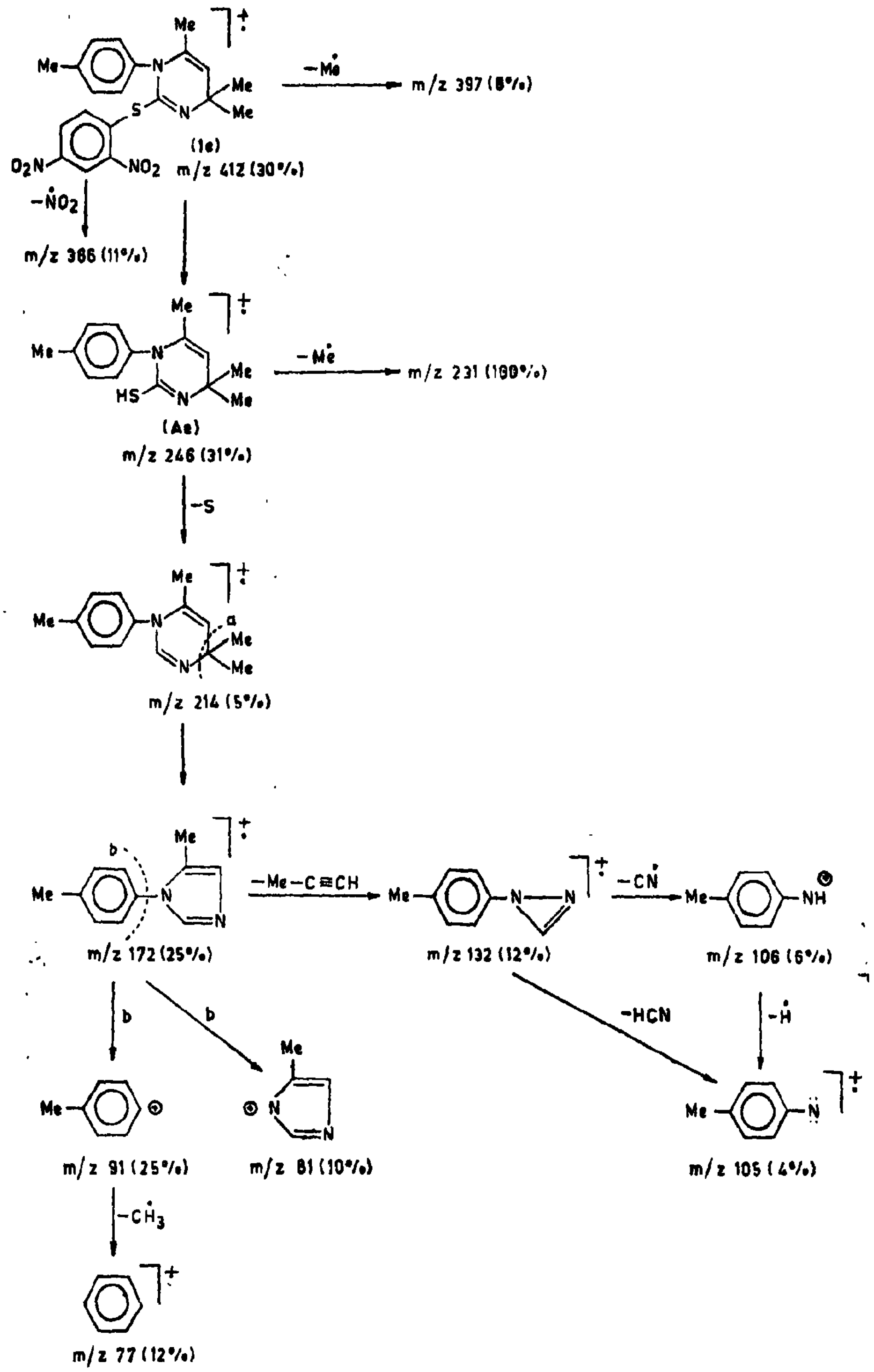


Chart 1

It is noteworthy here that the predominant peak appears at *m/z* 246 due to the molecular ion of 3-*p*-tolyl-1,4-dihydro-4,6,6-trimethylpyrimidine-2-thiol (Ae) and then this ion suffers a loss of Me radical to give the base peak at *m/z* 231. This ion also undergoes a loss of S to give an ion of poor

intensity (5%) at m/z 214. The ion at m/z 214 reveals a loss of C_2H_2 to yield an intense ion at m/z 172 which can be explained due to the formation of 2-methyl-1-*p*-tolylimidazole, a stable compound. The ion due to imidazole derivative can undergo variety of fragmentation as shown in Chart 1. As after getting molecular ion due to thiol (**Ae**, m/z 246) all the further fragments are explained from this molecule. Mass spectrum of **Ae** was separately recorded and all peaks were found to be identical with those observed in the mass spectrum of **1e**.

The mass spectral data of three compounds (**1b**, **1e**, **1g**) have been listed in Table 1.

It is interesting to mention here that peaks appearing at m/z 91 in **1b** and **1e**, the two isomeric compounds, differ in their relative abundance. **1b** and **1e** show relative intensity as 100 and 25%, respectively, thereby *indicating that the former* corresponds to tropylium cation (which is obtained from benzyl cation and is more stable) and the latter to *p*-tolyl cation (lesser stable). Thus, the two isomeric compounds may be distinguished by this study.

TABLE 1—MASS SPECTRAL DATA OF **1b**, **1e** AND **1g** (ARRANGED TO DISPLAY THE COINCIDENCE OF FRAGMENT IONS IN COMPOUNDS)

m/z (% intensity)

1b	1e	1g
412(84)	412(80)	432/434(42)*
397(8)	397(8)	417/419(10)
366(10)	366(11)	386/388(13)
246(95)	246(31)	266/268(45)
231(100)	231(100)	251/253(100)
214(4)	214(5)	—
172(26)	172(25)	192/194(22)
132(15)	132(12)	152/154(15)
106(5)	106(6)	126/128(4)
105(8)	105(5)	125/127(4)
91(100)	91(25)	111/113(20)
81(6)	81(10)	101/103(5)

* Typical chlorine isotopic profile loss of chlorine radical from *m/z* 192/194.

TABLE 2

Compd. no.	M.p.* °C	Yield %	Formula**
1a	159-61	80	$C_{19}H_{18}N_4O_4S$
1b	163	85	$C_{20}H_{20}N_4O_4S$
1c	167	90	$C_{20}H_{20}N_4O_4S$
1d	157	82	$C_{20}H_{20}N_4O_4S$
1e	169-71	70	$C_{20}H_{20}N_4O_4S$
1f	155	74	$C_{19}H_{17}N_4O_4ClS$
1g	170	84	$C_{19}H_{17}N_4O_4ClS$
1h	205	69	$C_{19}H_{16}N_4O_4Cl_2S$
2a	107	75	$C_{19}H_{17}N_4O_4ClS$
2b	115	80	$C_{20}H_{19}N_4O_4ClS$
2c	126	86	$C_{20}H_{19}N_4O_4ClS$
2d	101	78	$C_{20}H_{19}N_4O_4ClS$
2e	110	66	$C_{20}H_{19}N_4O_4ClS$
2f	98	65	$C_{19}H_{16}N_4O_4Cl_2S$
2g	119	82	$C_{19}H_{16}N_4O_4Cl_2S$
2h	147	60	$C_{19}H_{16}N_4O_4Cl_2S$
3a	104	85	$C_{19}H_{17}N_4O_4ClS$
3b	112	88	$C_{20}H_{19}N_4O_4ClS$
3c	118	90	$C_{20}H_{19}N_4O_4ClS$
3d	104-5	92	$C_{20}H_{19}N_4O_4ClS$
3e	114-5	80	$C_{20}H_{19}N_4O_4ClS$
3f	95	75	$C_{19}H_{16}N_4O_4Cl_2S$
3g	120	78	$C_{19}H_{16}N_4O_4Cl_2S$
3h	161	68	$C_{19}H_{16}N_4O_4Cl_2S$
4a	181	88	$C_{20}H_{20}N_4O_4S$
4b	174	75	$C_{21}H_{22}N_4O_4S$
4c	135	82	$C_{21}H_{22}N_4O_4S$
4d	127	80	$C_{21}H_{22}N_4O_4S$
4e	156	78	$C_{21}H_{22}N_4O_4S$
4f	196	81	$C_{21}H_{21}N_4O_4ClS$
4g	202	80	$C_{21}H_{21}N_4O_4ClS$
4h	235	60	$C_{21}H_{20}N_4O_4Cl_2S$
5a	209	90	$C_{20}H_{19}N_5O_6S$
5b	215	80	$C_{21}H_{21}N_5O_6S$
5c	185	85	$C_{21}H_{21}N_5O_6S$
5d	198	88	$C_{21}H_{21}N_5O_6S$
5e	226	82	$C_{21}H_{21}N_5O_6S$
5f	231	75	$C_{21}H_{20}N_5O_6ClS$
5g	217	79	$C_{21}H_{20}N_5O_6ClS$
5h	269	69	$C_{21}H_{19}N_5O_6Cl_2S$
6a	149	79	$C_{20}H_{20}N_4O_4S$
6b	155	68	$C_{21}H_{22}N_4O_4S$
6c	162	85	$C_{21}H_{22}N_4O_4S$
6d	160	81	$C_{21}H_{22}N_4O_4S$
6e	157	60	$C_{21}H_{22}N_4O_4S$
6f	149	70	$C_{21}H_{21}N_4O_4ClS$
6g	165	78	$C_{21}H_{21}N_4O_4ClS$
6h	187	74	$C_{21}H_{20}N_4O_4Cl_2S$

* Solvents used for crystallisation; aqueous EtOH for **1b**, **2b**, **2c**; C_6H_6 for **2d**, **2h**, **3a**, **3b**, **5b**, **5h**; EtOH for the rest of the compounds. ** Satisfactory N and S analysis obtained for all the compounds.

Experimental

Melting points were taken in open capillaries in H_2SO_4 bath and are uncorrected. Ir (KBr) spectra were recorded on a Beckmann IR-20 spectrophotometer. Mass spectra were scanned on Hitachi RUM-60, MS-12 and Varian MAT-731 spectrometers.

Polynitrohalogenobenzenes: The following reactive halogeno compounds were used for condensation with pyrimidine-2-thiols: 1-chloro-2,4-dinitrobenzene, 1,3-dichloro-4,6-dinitrobenzene, 1,4-dichloro-2,6-dinitrobenzene, 1-chloro-5-methyl-2,4-dinitrobenzene, 1-chloro-5-methyl-2,4,6-trinitrobenzene, and 1-chloro-2-methyl-4,6-dinitrobenzene. All of the compounds were prepared by methods reported earlier[9-13].

Substituted-pyrimidine-2-thiols: 3-Aryl-4,6,6-trimethyl-1,4-dihydro-pyrimidine-2-thiols (A) were prepared according to the reported method[14]. A brief procedure for the synthesis of **Ae** is described. A mixture of mesityl oxide (49 g, 0.5 *M*), ammonium thiocyanate, (38 g, 0.5 *M*), *p*-toluidine (53.5 g, 0.5 *M*) and water (100 ml) was agitated in a reaction flask. HCl (55 g) was added in 10 min at 20°. The buff coloured crystalline product precipitated when heated to reflux. The precipitate was washed with water and crystallised twice from ethanol (104.6 g), m.p. 191° (lit. 191°); M^+, m/z 246 (calculated mol. wt. 246), major peaks m/z 246 (30%), 231 (100%), 215 (5%); 214 (5%), 172 (26%), 132(12%), 106 (6%), 105 (5%), 91 (27%), 81 (9%) and 77 (12%). The

mass spectral fragementation of Ae confirms its structure.

3-Aryl-1, 4-dihydro-2-(polynitroaryl)mercapto-4,6,6-trimethylpyrimidines (**1-6**) *: General procedure :* Pyrimidine-2-thiol (A ; 0.005 *M*) was dissolved in minimum volume of boiling absolute ethanol. Anhydrous sodium acetate was added in excess and boiling was continued for about 30 min. To the boiling mixture, an ethanolic solution (0.005 *M*) of polynitrochlorobenzene (**I-VI**) was added in portions. The contents were refluxed for 5-6 h (refluxing time for the completion of the reaction was monitored by tlc). The contents of the reaction flask were then poured into cold water and kept overnight. The grey to brown coloured solid material so obtained was filtered, dried and recrystallised. All the characterisation data of the compou nds are given in Table 2.

Acknowledgement

Financial assistance to one of the authors (A.K.) is gratefully acknowledged under the F.A.T. programme from U.G.C., New Delhi.

References

1. C. Heidelberger, N. C. Chaudhuri, P. Danneberg, D. Mooren, L. Griesbach, R. Duchinsky, R. J. Schnitzer, E. Pleven and J. Scheiner, *Nature (London)*, 1957, 179, 663.
2. N. Tokutake, Brit. Pat. 1 468 868/1977 (*Chem. Abstr.*, 1977, 87, 102870).
3. V. Papesh and E. F. Schroeder, U. S. Pat. 2 729 669/1956 (*Chem. Abstr.*, 1956, 50, 11870).
4. W. Hepworth and T. W. Thompson, *Chem. Abstr.*, 1968, 69, 7724.
5. D. S. Matteson, M. S. Bleenbaum, R. A. Bechtold, J. D. Campbell and R. J. Willsek, *J. Org. Chem.*, 1978, 43, 950.
6. G. W. Anderson, I. F. Halverstadt, W. H. Miller and R. O. Roblin, *J. Am. Chem. Soc.*, 1945, 67, 2197.
7. J. G. Horsfall and S. Rich, *Contributions Boyce Thomson Inst.*, 1951, 16, 313 (*Chem. Abstr.*, 1952, 46, 11543).
8. K. C. Joshi and A. B. Sen, *J. Sci. Food Agric.*, 1952, 11, 526.
9. E. Jungfleisch, *J. Chem. Soc.*, 1868, 21, 345.
10. S. M. Sane and S. S. Joshi, *J. Chem. Soc.*, 1924, 2493.
11. G. S. Hammond and F. Modic, *J. Am. Chem. Soc.*, 1953, 75, 1385.
12. F. Reverdin and P. Crepieux, *Chem. Ber.*, 1906, 39, 2505.
13. O. Dressel and L. Delerta, *Chem. Ber.*, 1904, 37, 2094.
14. R. A. Mathes, F. D. Stewart, Jr. and F. Swedish, *J. Am. Chem. Soc.*, 1953, 75, 1747.

J. Indian Chem. Soc.,
Vol. LXIII, June 1986, pp. 600-602

Synthesis of 2-Carbomethoxy- and 2-(2-Benzimidazolyl)chromones

K. R. S. REDDY, G. SRIMANNARAYANA* and N. V. SUBBA RAO

Department of Chemistry, University College of Science, Osmania University, Hyderabad-500 007

Manuscript received 26 December 1984, revised 30 June 1985, accepted 8 May 1986

ortho-Hydroxyacetophenones on refluxing with diethyl oxalate in methanol containing sodium methoxide gives methylchromone-2-carboxylate (2). 2 admixed with _o_-phenylenediamine on heating in polyphosphoric acid gives 2-(2-benzimidazolyl)-chromone (4) _via_ the anilide (3). Compounds (2-4) inhibited the growth of _A. niger_ by 70-80% at 100 ppm.

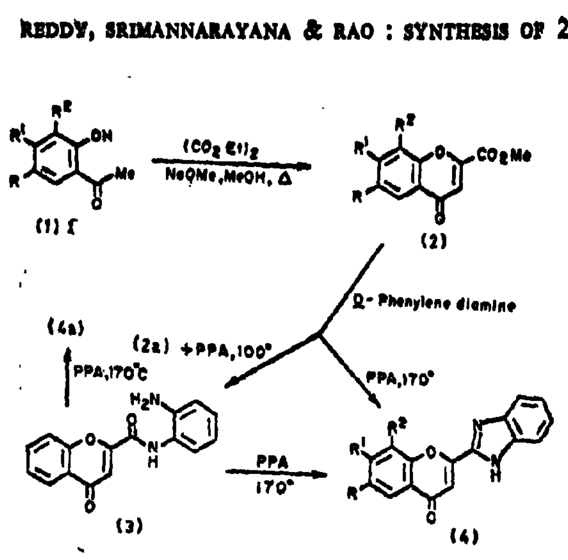
SEVERAL derivatives of chromone-2-carboxylic acid and 2-(2-benzimidazolyl)chromones have been reported to possess interesting physiological properties. A typical chromone-2-carboxylic acid, disodium chromoglycate was reported to be an effective drug in the treatment of allergic bronchial asthma[1]. Another chromone-2-carboxylic acid derivative, *N*-(p-sulphamidophenyl)chromone-2-carboxamide was found to be an excellent analgesic, more active than acetylsalicylic acid[2]. Further, heterocyclic benzimidazoles, such as thiazolylbenzimidazole, were reported to exhibit very high antifungal activity against a wide range of foliage diseases[3]. These considerations prompted us to synthesise methylchromone-2-carboxylate and 2-benzimidazolylchromones and to assess their physiological activity.

The condensation of *ortho*-hydroxyacetophenones and diethyl oxalate was widely used by earlier workers[4,5] in the synthesis of ethylchromone-2-carboxylates. Making use of this method, sodium methoxide has been employed instead of the sodium ethoxide in the condensation of *o*-hydroxyacetophenones (1) and diethyl oxalate ; the products were methyl-chromone-2-carboxylates (2) and not the ethylchromone-2-carboxylates. No attempt was made to isolate the intermediate diketone. The transesterification is complete and evidently the ester-exchange takes place with the substrate diethyl oxalate, and no ethylchromone-2-carboxylate could be found in tlc from the filtrate after recrystallisation of 2. This phenomenon was already noticed by Ellis[6] and also in our laboratories[7]. As methylchromone-2-carboxylates are not sufficiently soluble in $CDCl_3$, the spectra have been recorded in trifluoroacetic acid solutions. The low-field shift of H-3 of the methylchromone-2-carboxylates around δ 7.2 is in agreement with the reported value[8] for ethylchromone-2-carboxylate in which H-3 resonates at δ 7.13. The ir and uv data are given in Table 1. The ester carbonyl and chromone carbonyl appear around ν_{max} (nujol) 1 770 and 1 660 cm^{-1}, respectively. The uv absorption spectra reveal an intense band around λ_{max} (EtOH) 240 nm and less intense band around λ_{max} (EtOH) 310 nm. The data is in agreement with the earlier reported[9] data for ethylchromone-2-carboxylate. Thus, the condensation of *o*-hydroxyacetophenones and diethyl oxalate *in the presence of sodium methoxide as a basic catalyst* is a facile method for the synthesis of methylchromone-2-carboxylate.

By modifying the patented procedure[10], the methylchromone-2-carboxylate (2) was condensed with orthophylenediamine in polyphosphoric acid (PPA) medium at 170° for 1 h resulted in the corresponding 2-(2-benzimidazolyl)chromones (4). The condensation of methylchromone-2-carbo xylate (2a) with *o*-phenylenediamine using polyphosphoric acid at 100° instead of 170° for 4 h, resulted in the isolation of the anilide, 2-[*N*-(*o*-aminophenyl)carba-

TABLE 1—METHYLCHROMONE-2-CARBOXYLATES (2)

Compd. no.	M.p. °C	Yield %	λ_{max} (log ϵ) (EtOH)	ν_{max} cm^{-1}	δ(CF_3 COOH) ppm			CH_3 in R, R[1], R[2] (s)
					CO_2CH_3 (s)	H-3 (s)	Ar-H (m)	
2a	190	80	250(3.91), 315(3.52)	1 764, 1 666	3.60	7.00	7.10-8.10	—
2b	148	70	241(4 26), 320(3.79)	1 775, 1 650	3.90	7.33	7.37-8.00	2.30
2c	172	65	235(4.18), 309(3.87)	1 778, 1 664	3.67	7.03	7.15-8.20	2.50
2d	206	80	236(4 24), 307(3.99)	1 770, 1 647	4.16	7.38	7.40-8.20	4.30
2e	234	65	254(4.39), 313(4.13)	1 767, 1 667 1 695	3.75	7.10	7.20-8.00	2.00



(1-4) a; R=R¹=R²=H
b; R¹=R²=H, R=CH₃
c; R=R¹=H, R²=CH₃
d; R=R²=H, R¹=OCH₃
e; R=R²=H, R¹=NHCOCH₃

Scheme 1

moyl]chromone (3). The anilide (3) was not formed in the absence of PPA.

The methylchromone-2-carboxylates and 2-(2-benzimidazolyl)chromones synthesised above have been tested for their antibacterial activity against *Staphylococcus aureus*, *Bacillus coli* and *Bacillus subtilis* using tube dilution method and fungistatic activity against *Aspergillus niger* using plate method. 6-Methyl-, 8-methyl-, 7-methoxy-, and 7-amino-2-(2-benzimidazolyl)chromones are active against all the three bacteria at 100 ppm dilution. In general, methylchromone-2-carboxylates seem to be active against *Bacillus coli* only at 100 ppm. It is interesting to note that while 2-(2-benzimidazolyl)chromones have remarkable activity, of the order of 60-80% inhibition at 100 ppm, even methylchromone-2-carboxylates also exhibits considerable activity of the same order. Even at 20 ppm dilution, methylchromone-2-carboxylates and 2-(2-benzimidazolyl)-chromones inhibited the growth of fungus to the extent of 50%.

Experimental

The m.p.s. are uncorrected. The uv spectra (EtOH) of the compounds were recorded on a Beckman-DB spectrophotometer. The ir spectra were recorded on a Perkin-Elmer Infracord-132, equipped with sodium chloride cells. The pmr spectra were recorded on a Varian-60 MHz in trifluoroacetic acid using TMS as internal standard. All the compounds gave satisfactory elemental analysis.

Methylchromone-2-carboxylates (2) : Sodium (2.0 g) was dissolved in dry methanol (25 ml) with stirring. After cooling, a solution of *o*-hydroxyacetophenone (1) (0.01 mol) in diethy oxalate (6 ml), methanol (25 ml) and benzene (25 ml) was added to it and the mixture was refluxed for 8 h. After cooling, ether (100 ml) was added. The sodium salt was filtered, washed with anhydrous ether, dissolved in water and the solution acidified. The resultant precipitate was filtered, dried and recrystallised from methanol to yield (2) (Table 1) as colourless needles.

2-(2-Benzimidazolyl)chromones (4) : Intimately mixed powder of methylchromone-2-carboxylate (2) (0.005 mol) and *o*-phenylene diamine (0.005 mol) was heated with polyphosphoric acid (10 g) at 170° for 1 h. After keeping it overnight, it was treated with crushed ice and neutralised with ammonia. The resulting yellow solid, was taken into ethyl acetate and repeatedly extracted with hydrochloric acid (3%). The acid solution was neutralised with ammonia and extracted with ethyl acetate. The ethyl acetate solution was washed with water and dried over anhydrous sodium sulphate. On removing the solvent, the yellow substance obtained on recrystallisation from ethyl acetate-benzene (1 : 1) gave 4 as yellow needles. The physical, uv and ir data are presented in Table 2. In the mass spectrum of 4b, $M^{+\cdot}$ 276(10) and the base peak at m/z 160 arise due to fission at 2-position, with proton transfer, of chromone and benzimidazole junction. The $M^{+\cdot}$ 276 suffers retro-Diels-Alder fragmentation giving m/z 134.

2-N-(*o-Aminophenyl)carbamoylchromone* (3) : 2a (2.0 g) and *o*-phenylenediamine (1.0 g) were powdered, intimately mixed and heated with polyphosphoric acid (10 g) at 100° for 4 h. After leaving overnight, it was treated with crushed ice and neutralised with ammonia. The deep orang-yellow solid was filtered, washed with water and recrystallised from ethyl acetate to yield 3 as orange-yellow needles. The physical, uv and ir data are presented in Table 2. In the mass spectrum, M^+ appeared at 280, which itself is base-peak. The

TABLE 2—2-(2-BENZIMIDAZOLYL)CHROMONES (4) AND ITS PRECURSOR (3)

Compd. no.	M.p. °C	Yield %	λ_{max} (log ε) (EtOH)	ν_{max} cm⁻¹
4a	224	40	230(4.36), 284(3.95), 333(3.92)	1 684, 1 629
4b	234	30	231(4.34), 280(3.92), 337(3.95)	1 675, 1 623
4c	195	30	230(4.40), 284(3.94), 338(4.22)	1 681, 1 637
4d	222	35	229(4.48), 257(4.22), 279(4.05), 336(4.07)	1 661, 1 613
4e	244	25	230(4.46), 279(3.72), 342(4.32)	1 650, 1 630
3a	292	70	231(4.34), 276(3.96), 436(4.54)	1 692, 1 618

other fragments *m/z* 121(83) and 160(80) arise due to RDA breakdown with proton transfer.

Conversion of **3a** *to* **4a** *:* **3a** (1.0 g) was powdered and heated with polyphosphoric acid (5.0 g) at 170° for 1 h. After leaving it overnight, the reaction mixture was worked up. The yellow substance obtained was recrystallised with ethyl acetate-benzene (1 : 1) to yield yellow needles of **4a**.

References

1. H. Cairus, C. Fitzmaurice, D. Hunter, P. B. Johnson, J. King, T. B. Lee, G. H. Lord, R. Minshull and J. S. G. Cox, *J. Med. Chem.*, 1972, **15**, 583.
2. T. Pierre, S. Afri. Pat. 6 801 155/1968 (*Chem. Abstr.*, 1969, **70**, 96826).
3. P. Bessot and J. Picot, *Chem. Abstr.*, 1964, **60**, 8881.
4. B. Puetzer, C. H. Nield and R. H. Barry, *J. Am. Chem. Soc.*, 1945, **67**, 832.
5. V. A. Zagorvskii, D. A. Zykov and E. K. Corlova, *Zh. Obshch. Khim.*, 1961, **31**, 568 (*Chem. Abstr.*, 1961, **55**, 25937).
6. G. P. Ellis in "Chromenes, Chromanones and Chromones", ed. G. P. Ellis, Interscience, New York, 1977, p. 581.
7. K. A. Kumar and G. Srimannarayana, *Indian J. Chem., Sect. B*, 1984, **23**, 969.
8. G. Barker and G. P. Ellis, *J. Chem. Soc. C*, 1970, 2609.
9. C. Zarowski and G. B. Hess, *J. Am. Chem. Soc.*, 1949, **71**, 1711.
10. J. Olande, Fr. Pat. 1 488 228/1967 (*Chem. Abstr.*, 1968, **69**, 36130).

J. Indian Chem. Soc.,
Vol. LXIII, June 1986, pp. 603-604

Polyacetylenes and Terpenoids from *Erigeron karwinskyanus*

D. K. MATHELA and C. S. MATHELA*

Department of Chemistry, Kumaun University, Nainital-263 002

and

JYRKI TASKINEN

Orion Pharmaceutical Co., Research Laboratories, P O Box 8, Espoo 10, Finland

Manuscript received 26 March 1985, revised 27 January 1986, accepted 8 May 1986

Four mono- and fourteen sesqui-terpene hydrocarbons and all isomers of two acetylenic esters have been identified in the steam volatile oil of *Erigeron karwinskyanus* DC.

THE problem of insectiside resistance has necessitated research on new approaches. One of the promising methods is the use of naturally occurring antifeedants *i.e.* secondary plant metabolites which would be preferable because of their least harmful effect on the environment[1]. The screening for the antimicrobial activity of various plant extracts has shown that the steam volatile oil of the plant *Erigeron karwinskyanus* possesses high activity against certain plant pathogens, *viz. Aspergillus, Penicillium* and *Fusarium* species[2]. This prompted us to take up the chemical examination of the steam volatile extract of this plant. It was observed that the significant antimicrobial activity of the steam volatile oil of *E. karwinskyanus* is accredited to the naturally occurring acetylenic compounds in the oil. Cosmene, matricaria ester and a lactone have been identified in the oil of *E. karwinskyanus*[3]. In a previous paper[4], we reported a new pyrone glucoside in the ethanolic extract of this species. However, no detailed study on the essential oil was reported. Present communication deals with polyacetylenic and terpenoid composition of the steam-volatile oil from the aerial part of *E. karwinskyanus* and variation of the yield and composition of oil from the different plant parts during different months.

Experimental

Plant material: The plants were collected locally and identified[5].

Extraction of oil: The plants were collected at different stages of growth and divided into three parts, *viz.* leaves, stalks and flowers. After steam-distillation of each part separately, the essential oils were obtained by the extraction of the distillate with petrol (b.p. 40-60°). The ether extract was dried over anhydrous Na_2SO_4 and the solvent was removed to get essential oil. The oil from the complete aerial part was also extracted for the gc-ms analysis.

Analysis of oil: Si-gel was used for the column chromatography. Ir spectra were recorded in a Perkin-Elmer 298 spectrophotometer. The oil was analysed by gc-ms using a Carlo Erba 2300 gas chromatograph (25 m×0.3 mm capillary column, FFAP phase) connected to a JEOL JN S-D 300 mass spectrometer with a data system JMA 2000. Mass spectra were recorded at 70 eV. The column temperature was 60° upto first 6 min, raised to 100° and programmed at 4°/min upto 200°. The injection, interface and ion source temperature were 250, 220 and 230°, respectively. The high resolution ms were measured at resolution 5000 and the methane was used as reagent gas in the CIMS study. For comparison of the change in composition at different stages of growth of the plant and in its different parts, the gc study of the oils under identical conditions was also carried out.

Results and Discussion

The maximum percentage oil yield in different plant parts is as follows: flowers (0.16, November), leaves (0.09, July), stalks (0.05, July) and complete aerial part (0.1, November).

The gc-ms study of the oil from the aerial part of the plant was carried out. The constituents were identified by comparing their ms with the published spectra[6]. Four monoterpene and fourteen sesquiterpene hydrocarbons, *viz.* β-pinene, myrcene, *trans*-ocimene, cosmene, α-copaene, γ-cadinene, β-cubebene, caryophyllene, β-elemene, humulene, γ-muurolene, *trans*-β-farnesene, α-cadinene, guaiene, δ-cadinene, bergamotene, *ar*-curcumene and *allo*-aromadendrene were identified (Table 1). Besides the terpenoids, the acetylenic esters were also

TABLE 1—Gc-Ms DATA ON MONO- AND SESQUI-TERPENE HYDROCARBONS

Gc retention time min	Parent ion m/e	Important ions m/e	Compd.
1.8	186	98, 69, 121, 79	α-Pinene
1.4	136	41, 93, 69, 121	Myrcene
2.4	186	93, 121, 105, 80	*trans*-Ocimene
2.5	134	119, 91, 77, 105	Cosmene
6.8	204	105, 119, 161, 189	α-Copaene
7.9	204	161, 105, 91, 119	γ-Cadinene
8.9	204	161, 105, 91, 120	β-Cubelene
9.1	204	41, 93, 69, 133	Caryophyllene
9.2	204	81, 68, 93, 121	β-Elemene
11.0	204	93, 121, 147, 81	Humulene
11.3	204	161, 105, 91, 119	γ-Muurolene
11.8	204	69, 93, 81, 133	*trans*-β-Farnesene
12.0	204	161, 105, 119, 133	α-Cadinene
12.4	204	161, 105, 204, 189	Guaiene
13.0	204	161, 134, 204, 105	δ-Cadinene
13.2	204	93, 119, 69, 135	Bergamotene
13.8	202	119, 132, 202, 145	*ar*-Curcumene
19.4	204	51, 91, 161, 105	*allo*-Aromadendene

TABLE 2—Gc-Ms DATA ON ACETYLENIC ESTERS

gc retention time min	Parent ion m/e	Other fragment m/e	Compd.
3.1	176	147, 91, 161, 91	*cis*-Lachnophyllum ester
3.9	174	103, 159, 143, 77	*cis*-2-*cis*-8-Matricaria ester
4.8	176	147, 91, 119, 105	*trans*-Lachnophyllum ester
5.1	174	103, 159, 143, 63	*cis*-2-*trans*-8-Matricaria ester
6.1	174	159, 143, 103, 77	*trans*-2-*cis*-8-Matricaria ester
8.1	174	103, 159, 77, 143	*trans*-2-*trans*-8-Matricaria ester

identified. The fractionation of the oil by column chromatography over Si-gel gave a major fraction which showed *ir* bands at 2 235, 2 200, 1 735 and 1 175 cm^{-1} indicating it to contain polyacetylenic esters. On gc-ms of this fraction, the electron-impact and chemical-ionisation mass spectra and high resolution mass spectra showed the presence of four acetylenic esters of molecular formula $C_{11}H_{10}O_2$ and two of $C_{11}H_{12}O_2$, indicating the presence of four geometrical isomers of 2,8-decadiene-4,6-diynoic acid methyl ester (matricaria esters) and two geometrical isomers of 2-decene-4,6-diynoic acid methyl ester (lachnophyllum esters), respectively (Table 2). The results show that the oil mainly consists of acetylenic esters, matricaria ester being the chief constituent, followed by lachnophyllum ester and sesquiterpene hydrocarbons. The monoterpenes constitute only a low percentage of the oil.

The gc analysis of the oils from flowers, leaves and stalks under identical conditions also indicate that the polyacetylenic esters are the major constituents of all the oils and are maximum in the flowers (in November) followed by the oil from the leaves and stalks.

Acknowledgement

The authors are grateful to Dr. P. S. Green, The Royal Botanic Gardens, Kew, for the verification of the plant material.

References

1. A. F. ROSE, B. A. BUTT and T. GERMY, *Phytochemistry*, 1980, **19**, 563.
2. C. S. MATHELA, unpublished results.
3. F. BOHLMANN, T. BURKHARDT and C. ZDERO, "Naturally Occurring Acetylenes", London, 1973, p. 347.
4. D. K. MATHELA, A. K. PANT and C. S. MATHELA, *Phytochemistry*, 1984, **23**, 2090.
5. The plant was confirmed by DR. P. S. GREEN, The Royal Botanic Gardens, Kew (voucher no. H 257/79 deposited at the herbarium of R. B. G.).
6. K. YAMAGUCHI, "Spectral Data of Natural Products", Elsevier, New York, 1970, Vol. I; E. STENHAGEN, S. ABRAHAMSSON and F. W. MCLAFFERTY, "Registry of Mass Spectral Data", Willey, New York, 1974.

J. Indian Chem. Soc.,
Vol. LXIII, June 1986, pp. 605-606

Hot Amperometric Titration for Estimation of Trace Amounts of Lanthanum and Cerium

S. C. LAVALE

Post Graduate Chemistry Department, Government College, Betul-460 001

Manuscript received 30 September 1985, revised 3 June 1986, accepted 18 June 1986

Trace amounts of La^{III} and Ce^{III} have been estimated quantitatively with xylenol orange (XO) using hot amperometric titration technique. In hot condition, the increase in reversibility and ease of reduction facilitate the metal-ligand complexation. The titrations have been performed at pH 5.5, $\mu=0.2$ and temp. = 70°. The stiochiometric ratio of metal-XO complex is found to be 1 : 1. Many ions donot interfere the titration procedure.

IN continuation to our work[1-3] on the estimation of trace quantity of rare earths by electrometric technique, the present paper reports the use of xylenol orange (XO) as amperometric reagent for the estimation of La^{III} and Ce^{III}. Xylenol orange has been extensively used as complexometric and spectrophotometric reagent[4-8]. The titrations have been performed in hot experimental set-up, as the results were not reproducible at room temperature.

Experimental

The chemicals used were of AnalaR quality. La^{III} and Ce^{III} solutions were prepared and standardised[8]. A fresh solution of XO was prepared whenever used. Britton-Robinson buffer was prepared by the known method[9]. Amperometric titrations were done on a mannually operated polarograph. Titrations were performed in a thermostatic bath at 70±0.5°.

Polarography of XO : XO gave two-stage reduction in the pH range 4.6-11.0. Polarograms of different concentrations of XO in Britton-Robinson buffer at pH 5.5, temp. = 70±0.5° and $\mu=0.2$ were taken. The diffusion current was found to be proportional to the concentration of XO. A slight positive shift in half-wave potential was observed, which might be due to easier reduction and increased degree of reversibility of the electrode process.

Procedure of amperometric titration : Sets of solutions containing known amounts of La^{III} and Ce^{III} at $\mu=0.2$ in appropriate quantity of Britton-Robinson buffer of pH 5.5 were prepared. The plateau potential on the wave of XO, *i.e.* − 1.25 V *vs* S.C.E. was applied at which La^{III} and Ce^{III} were not electroactive. For titration, titre was taken in a thermostatic bath at 70±0.5° and titrant (XO) was added dropwise and current was noted.

Current-volume plots were reversed L shaped (Fig. 1). The end-point indicated metal-XO complexation ratio of 1 : 1.

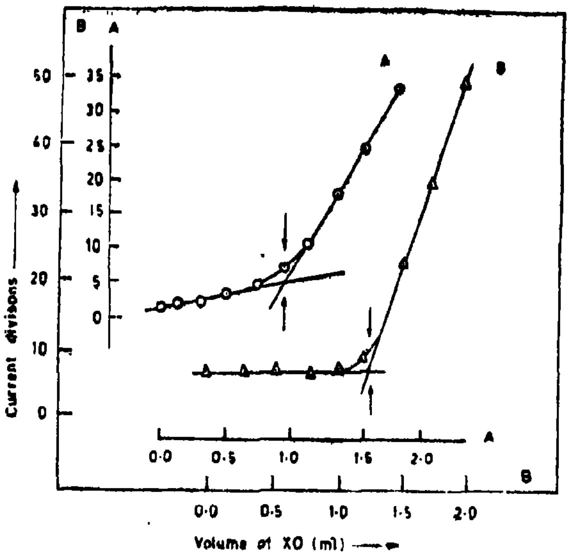


Fig. 1. Amperometric titration curves of La^{III} and Ce^{III} with xylenol orange : (A) 0.005 mM La^{III} *vs* 0.005 M XO, and (B) 0.012 5 mM Ce^{III} *vs* 0.01 M XO.

Results and Discussion

The results of the estimation of La^{III} and Ce^{III} are tabulated (Table 1). Ce^{III} and La^{III} were determined in the concentration range 0.5-7.0 μM with an error less than ±0.80%. The statistical data support the precision, confidence and ultility of the procedure.

Effect of diverse ions : For interference studies, known amount of foreign ion was added to the definite amount of metal ion solution and the solutions were amperometrically titrated following the procedure as described above. Titrations of 1-2 mg of La^{III} and Ce^{III} were not in any way hampered by the presence of large excess (mg) of the ions, *viz.* K (146), Na (115), Ca^{II} (75), Mg^{II} (73), Ba^{II} (46), Pb^{II} (39), Tl^{I} (20) and Ag^{I} (11). However, it is

TABLE 1—AMPEROMETRIC ESTIMATION OF La^{III} AND Ce^{III} WITH XO AT −1.25 V vs S.C.E.

pH = 5.5, μ = 0·2 (KCl), temp. = 70 ± 5°

Concn. of La^{III} or Ce^{III} μM	% Error	
	La^{III}	Ce^{III}
0.5	−0.40	−0.85
1.0	−0.63	+0.87
1.5	+0.53	+0 24
2.0	−0.46	−0.20
2.5	+0.63	+0 47
3.0	+0.75	−0.52
4.0	−0.77	+0.44
5.0	+0.41	−0.85
6 0	−0.80	+0.28
7.0	+0.26	−0.30

Standard deviation for La^{III} = ±0.18, and Ce^{III} = ±0.10.

observed that Ti^{IV}, Co^{II}, Ni^{II}, Cu^{II}, Zn^{II}, Cd^{II} and Fe^{II} ions interfered seriously.

Conclusion : Amperometric method described above can be considered as a good analytical tool for the estimation of trace amount La^{III} and Ce^{III} using XO as titrant. The conditions under which the estimations made are of practical significance.

Acknowledgement

Author mention his special thanks to Dr. K. S. Pitre, Reader, Dr. H. S. Gour Vishwavidhayalay, Sagar, for his kind guidance and helpful discussions. Assistance received from U. G. C., New Delhi, is gratefully acknowledged.

References

1. S. C. LAVALE and K. S. PITRE, *Bull. Chem. Soc. Jpn.*, 1982, 55, 2282.
2. S. C. LAVALE and K. S. PITRE, *J. Indian Chem. Soc.*, 1982, 59, 965.
3. S. C. LAVALE, *J. Electrochem. Soc. India*, 1984, 33-4, 374.
4. S. C. HONG and H. S. CHANG, *Hua Hsuch Tung Pao*, 1964, 52, 469.
5. K. N. MUNSHI and A. K. DEY, *Microchim. Acta*, 1968, 5, 1059.
6. R. NAYAN and A. K. DEY, *J. Inorg Nucl. Chem.*, 1974, 36, 2545.
7. P. M. TULYPA and L. G. KARYAKA, *Zh. Neorg. Khim.*, 1978, 23, 1243.
8. R. NAYAN, *Indian J. Chem., Sect. A*, 1981, 20, 382.
9. P. ZUMAN, "Polarography in Medicine Biochemistry and Pharmacy", Interscience, New York, 1958, p. 731.

NOTES

Oxomolybdenum(V) Complexes with 2-(2'-Pyridyl)benzimidazole

S. P. GHOSH, A. K. SINHA, C. P. SINGH
and
L. K. MISHRA*

Department of Chemistry, Patna University, Patna-800 005

Manuscript received 16 December 1985, revised 14 March 1986, accepted 9 April 1986

COMPLEXES of various metal ions with 2-(2'-pyridyl)-benzimidazole (PBzH) are known[1-6]. In present paper, we report the preparation and characterisation of complexes of oxomolybdenum(V) with 2-(2'-pyridyl)benzimidazole.

Experimental

The ligand was prepared as reported in previous paper[1]. The starting complexes $(NH_4)_2[MoOCl_5]$ and $(NH_4)_2[MoOBr_5]$ were prepared as reported in literature[7].

(PBzH)H₂[MoOX₅], (X=Cl or Br) : $(NH_4)_2[MoOX_5]$ (~10 g) was dissolved in concentrated HCl (48% HBr) (40-50 ml) and treated with 1 : 1 molar ratio of PBzH dissolved in hot concentrated HCl/HBr. From the resulting solutions, crystalline salts of pentahalooxomolybdenum(V) separated gradually. The products were filtered through sintered glass crucible, washed with concentrated cold acid and dried in a desiccator over KOH.

[MoO(PBzH)X₃], (X=Cl or Br) : $(PBzH)H_2[MoOX_5]$ (~5.0 g) was refluxed in dry methanol or propanol (40-50 ml) for ~1 h. The compound slowly went into solution from which brick-red compound separated out gradually. It was filtered, washed with dry methanol and dried as above.

[Mo₂O₃(PBzH)₂X₄], (X=Cl or Br) : $(NH_4)_2[MoOX_5]$ (~3-4 g) was dissolved in 95% ethanol (30-40 ml) and refluxed with 1 : 1 molar ratio of ligand on a steam-bath for 1 h. The resulting solution on concentration and cooling gave brick-red or brown precipitate. It was filtered, washed with ethanol and dried as above.

The results of elemental analyses and magnetic moment values at room temperature (303-5K) are given in Table 1.

Reflectance spectra of the solid complexes were determined on a Hilger and Watts UV Spek H700 spectrophotometer using $MgCO_3$ as standard. Ir spectra (KBr) were recorded on Perkin-Elmer 237 and 577 spectrophotometers and magnetic susceptibility by Gouy method as reported earlier[8].

Results and Discussion

The pentahalo salts (PBzH)H₂[MoOX₅] (X=Cl or Br) at reflux temperature, in dry methanol, ethanol *etc.* undergo dehydrohalogenation reaction forming trihalo complexes, [MoO(PBzH)X₃] (X=Cl or Br). However, in hydrated ethanol, oxobridged dinuclear complexes $[Mo_2O_3(PBzH)_2X_4]$ (X=Cl or Br) are formed. These oxobridged complexes can be reconverted into original mononuclear complexes, [MoO(PBzH)X₃] (X=Cl or Br) on refluxing them with concentrated HCl/HBr. The complex salts (PBzH)H₂[MoOX₅] (X=Cl or Br) and trihalo complexes [MoO(PBzH)X₃] are paramagnetic while oxobridged complexes $[Mo_2O_3(PBzH)_2X_4]$ are either diamagnetic or feebly paramagnetic. The magnetic moment values of [MoO(PBzH)X₃] (X=Cl or Br) are found in the range 1.65-1.69 B.M. which fall in the range of values shown by mononuclear oxomolybdenum(V) complexes[7-10]. The diamagnetism of oxomolybdenum(V) complexes possessing

TABLE 1

Compd.	Colour	μ_{eff}^{*} B.M.	Analysis % : Found/(Calcd.) Mo	N	Halogen	Spectral band positions (cm⁻¹) $^2B_2\rightarrow{}^2E(I)$	$^2B_2\rightarrow{}^2B_1$	$^2B_2\rightarrow E(II)+L-M$
$(PBzH)H_2[MoOCl_5]$	Yellowish green	1.65	19.81 (19.72)	8.52 (8.64)	36.72 (36.44)	13 700mb	19 610m	22 780m
$(PBzH)H_2[MoOBr_5]$	Brown	1.63	13.43 (13.54)	6.10 (5.93)	56.61 (56.38)	14 080wb	20 830s	—
$[MoO(PBzH)Cl_3]$	Brick red	1.69	23.31 (23.20)	9.98 (10.16)	25.61 (25.72)	13 830mb	19 610m	24 390sh
$[MoO(PBzH)Br_3]$	Brick red	1.65	17.48 (17.54)	7.78 (7.68)	44.12 (43.84)	14 290sb	19 610m	24 890sh
$[Mo_2O_3(PBzH)_2Cl_4]$	Reddish brown	Dia.	24.80 (24.85)	10.72 (10.88)	18.46 (18.37)	13 890wb	19 610m	22 780m
$[Mo_2O_3(PBzH)_2Br_4]$	Reddish brown	0.84	19.52 (20.21)	8.61 (8.84)	33.51 (33.65)	—	—	—

* Temp.=303-5 K.
s=strong ; w=weak ; m=medium ; sh=shoulder ; b=broad.

$Mo_2O_3^{4+}$ species is quite common as explained by Cotton and Curtis[11]. The feeble paramagnetism of complex $[Mo_2O_3(PBzH)_2Br_4]$ can be attributed to bulky volume of the bonded ligand molecule. In this case, the angle of twist of Mo–O–Mo bond may be greater than $\pi/4$ due to bulky volume of the bromine which causes incomplete pairing of spins of $Mo_2O_3^{4+}$ species[11].

Both mono- and di-nuclear complexes display electronic reflectance bands at 13 330-14 300, 19 610-20 800 and 22 390-24 400 cm^{-1} attributable to $^2B_2 \rightarrow ^2E(I)$, $^2B_2 \rightarrow ^2B_1$ and $^2B_2 \rightarrow ^2E(II)+C-T$ transitions, respectively, similar to ligand field bands of octahedral molybdenum(V) complexes[12-14].

Ir spectra : From the studies of ir spectra of PBzH and its complexes with metal ions, the coordination of the ligand has been suggested from tertiary pyridine nitrogen of benzimidazole part[15,16]. The N–H stretching mode of PBzH (3 249 cm^{-1}) is shifted to lower frequency only by 5-30 cm^{-1} in complexes but raised to higher frequency in complex salt $(PBzH)H_2[MoOCl_5]$ by 30 cm^{-1} suggesting that NH nitrogen is not involved in coordination. The $\nu_{C=N}$ of PBzH (1 638 cm^{-1}) is shifted to lower frequency in complexes suggesting the coordination of ligand through tertiary pyridine nitrogen of benzimidazole part[16]. The pyridine ring breathing mode of vibration of ligand (996 cm^{-1}) is raised to higher frequency (5-25 cm^{-1}) which has been taken to be diagonostic of the coordinated pyridine nitrogen[15,16].

The complexes $(PBzH)H_2[MoOX_5]$ and $[MoO(PBzH)X_3]$ (X=Cl or Br) display strong and sharp $\nu_{Mo=O}$ stretch at 990-975 cm^{-1} while the dinuclear complexes $[Mo_2O_3(PBzH)_2X_4]$ (X=Cl or Br) exhibit $\nu_{Mo=O}$ as strong and broad band at ~965 cm^{-1}. The observed order of wave number and nature of $\nu_{Mo=O}$ vibration are in good agreement with $\nu_{Mo=O}$ occurring in oxomolybdenum(V) complexes containing MoO^{3+} and $Mo_2O_3^{4+}$ species[17,18]. Due to a number of ligand vibrations between 850 and 650 cm^{-1} the Mo–O–Mo vibration could not be located definitely (the region 800-650 cm^{-1} is the range of vibration[17,18]). In far-infrared region, the ligand and its complexes display a number of bands between 600 and 400 cm^{-1}. The new ir bands located at 370-300 cm^{-1} have been tentatively assigned to ν_{Mo-N} and ν_{Mo-X} in these complexes[19].

References

1. S. P. GHOSH and L. K. MISHRA, *Inorg. Chim. Acta*, 1973, 7, 547.
2. S. P. GHOSH, P. BHATTACHARJEE and L. K. MISHRA, *J. Indian Chem. Soc.*, 1974, 51, 47.
3. S. P. GHOSH, P. BHATTACHARJEE, L. DUBEY and L. K. MISHRA, *J. Indian Chem. Soc.*, 1977, 54, 230.
4. S. P. GHOSH and K. M. PRASAD, *J. Indian Chem. Soc.*, 1979, 56, 660.
5. S. P. GHOSH and A. MISHRA, *J. Indian Chem. Soc.*, 1975, 52, 791.
6. R. L. DUTTA and T. RAY, *J. Indian Chem. Soc.*, 1981, 58, 709 and references therein.
7. T. A. GEORG and C. D. SEIBOLD, *J. Am. Chem. Soc.*, 1972, 94, 6859.
8. P. C. H. MITCHELL, *Quart. Rev.*, 1966, 20, 103.
9. H. K. SAHA and M. C. HALDAR, *J. Inorg. Nucl. Chem.*, 1971, 33, 3719 ; 1972, 34, 3097.
10. A. KAY and P. C. H. MITCHELL, *J. Chem. Soc., Dalton Trans.*, 1978, 1888 ; 1970, 2421.
11. F. A. COTTON and N. F. CURTIS, *Inorg. Chem.*, 1965, 4, 241.
12. A. SABATINI and J. BERTINI, *Inorg. Chem.*, 1966, 5, 204.
13. R. N. JOWITT and P. C. H. MITCHELL, *J. Chem. Soc.*, 1970, 1702.
14. C. R. HARE and H. B. GRAY, *Inorg. Chem.*, 1962, 1, 363.
15. T. J. LANE, I. NAKAGAWA, J. L. WALTER and A. J. KANDATHIL, *Inorg. Chem.*, 1962, 1, 267.
16. B. CHISWELL, F. LIONS and B. S. MORRIS, *Inorg. Chem.*, 1964, 3, 110.
17. R. M. WING and K. P. CALLAHAN, *Inorg. Chem.*, 1969, 8, 871.
18. C. M. FRENCH and J. H. GARSIDE, *J. Chem. Soc.*, 1962, 2006.
19. K. NAKAMOTO, "The Infrared Spectra of Inorganic and Coordination Compounds", Wiley Eastern, New Delhi, 1967.

Studies on Quaternary Complexes of some Rare Earth Metals

A. S. GAHLAUT, BEENA CHATURVEDI

and

R. C. SHARMA*

Department of Chemistry, Agra University, Agra-282 004

Manuscript received 23 September 1985, revised 25 March 1986, accepted 23 April 1986

OUR recent studies[1-3] on quaternary complex formation of lanthanide ions indicated that inspite of being high electropositive in nature, the lanthanides are capable of extending their coordination sphere to acquire an unusual coordination number, greater than six. The present paper includes our extended studies on 1 : 1 : 1 : 1 Ln^{III}-NTA/EDTA/CDTA-SUA-PDA quaternary systems which have not yet been studied potentiometrically.

Experimental

Solutions of all the chemicals (A. R., B. D. H./E. Merck) were prepared in double-distilled water. Standard solutions of lanthanide nitrates were prepared and standardised[4,5]. Solutions of di- and tri- potassium salts of NTA and EDTA/CDTA, respectively, were prepared by dissolving their calculated amounts in the required volume of potassium hydroxide. The concentrations of these solutions were further checked potentiometrically against 0.1 *M* KOH solution. All other solutions were prepared by direct-weighing method.

A Toshniwal CL46 digital *p*H meter with electrodes assembly was used and standardised

against (0.05 *M*) potassium hydrogen phthalate solution at 15±1°. The ionic strength (μ 0.1 *M* KNO_3) of the solution was maintained constant. The *p*H values were plotted against m (mole of base added per mole of metal ion or ligand) Fig. 1.

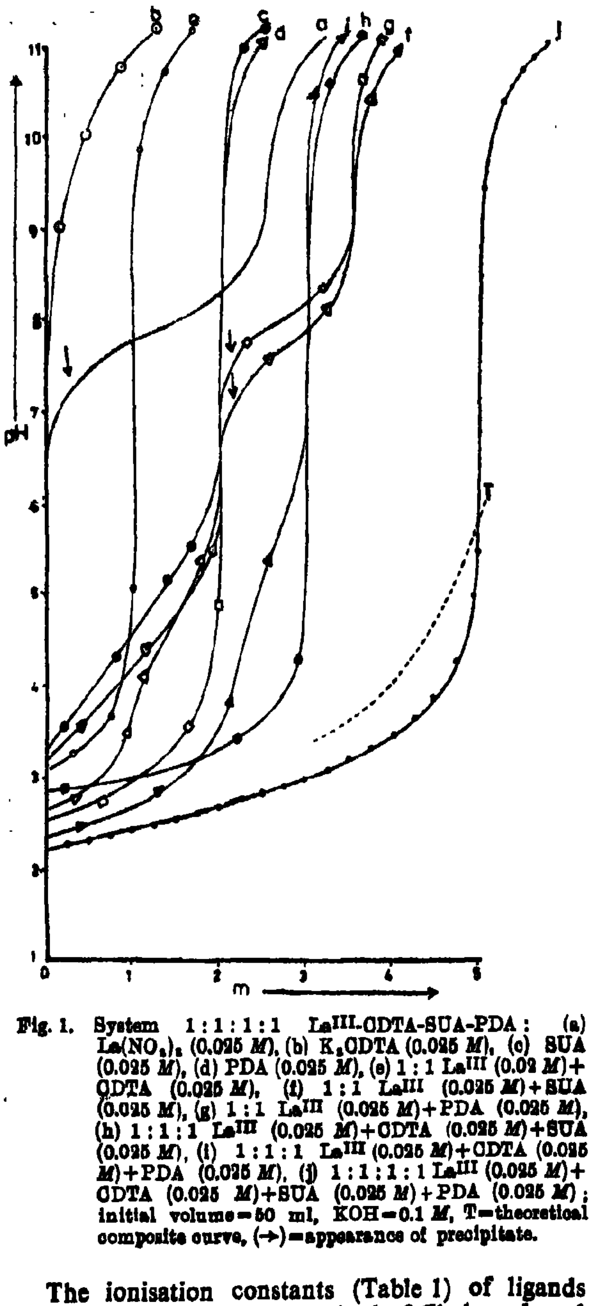


Fig. 1. System 1 : 1 : 1 : 1 La^{III}-CDTA-SUA-PDA : (a) $La(NO_3)_3$ (0.025 *M*), (b) K_2CDTA (0.025 *M*), (c) SUA (0.025 *M*), (d) PDA (0.025 *M*), (e) 1 : 1 La^{III} (0.02 *M*)+CDTA (0.025 *M*), (f) 1 : 1 La^{III} (0.025 *M*)+SUA (0.025 *M*), (g) 1 : 1 La^{III} (0.025 *M*)+PDA (0.025 *M*), (h) 1 : 1 : 1 La^{III} (0.025 *M*)+CDTA (0.025 *M*)+SUA (0.025 *M*), (i) 1 : 1 : 1 La^{III} (0.025 *M*)+CDTA (0.025 *M*)+PDA (0.025 *M*), (j) 1 : 1 : 1 : 1 La^{III} (0.025 *M*)+CDTA (0.025 *M*)+SUA (0.025 *M*)+PDA (0.025 *M*); initial volume = 50 ml, KOH = 0.1 *M*, T = theoretical composite curve, (→) = appearance of precipitate.

The ionisation constants (Table 1) of ligands were calculated by the method of Chabereck and Martell[6] and the formation constants (Table 1) of the resulting quaternary species by the method of Ramamoorthy and Santappa[7].

Results and Discussion

A representative *p*H-titration curves for the 1 : 1, 1 : 1 : 1 and 1 : 1 : 1 : 1 mixtures of Ln^{III}, (NTA/EDTA/CDTA), SUA, PDA is shown in Fig. 1. An initial lowering in the buffer region right from beginning as compared to that exhibited by the curves representing binary and ternary systems followed by an inflection at m = 5, may be correlated to the simultaneous attachment of all the three ligands to the metal ion, contributing one proton from K_2NTA/K_2EDTA/K_2CDTA and two each from SUA and PDA forming 1 : 1 : 1 : 1, Ln^{III}-(NTA/EDTA/CDTA)-SUA-PDA quaternary species in solution.

TABLE 1—PROTON-LIGAND CONSTANTS AND FORMATION CONSTANTS OF M^{III}-NTA/EDTA/CDTA-SUA-PDA QUARTERNARY COMPLEXES (M = La, Pr, Nd)

Constant	SUA	PUA	K_2NTA	K_2EDTA	K_2CDTA
pK_1^H	8.96	2.40	9.86	9.81	10.18
pK_2^H	5.44	4.80	—	—	—

	La^{III}	Pr^{III}	Nd^{III}
$\log K^M_{M\text{-NTA-SUA-PDA}}$	15.62	15.72	15.84
$\log K^M_{M\text{-EDTA-SUA-PDA}}$	15.95	16.02	16.09
$\log K^M_{M\text{-CTDA-SUA-PDA}}$	16.18	16.34	16.50

The orders of the formation constant (log $K_{MLL'L''}$) have been found to be $La^{III} < Pr^{III} < Nd^{III}$ for the lanthanide ions, and NTA < EDTA < CDTA for the aminopolycarboxylic acids, arising out of decreasing size and increasing ionic potential (charge/radius ratio) of the lanthanide ions with the increase of atomic number. The increased stability of CDTA in comparison to EDTA complexes (as both the ligands being hexadentate), is probably due to the extra-stabilisation caused by the presence of an aryl ring in CDTA.

Acknowledgement

The authors feel grateful to Prof. K. N. Mehrotra, Agra University, and Prof. J. P. Tandon, Rajasthan University, Jaipur, for facilities and interest.

References

1. P. C. DWIVEDI, S. P. TRIPATHI and R. C. SHARMA, *J. Indian Chem. Soc.*, 1984, 61, 23.
2. P. C. DWIVEDI, S. P. TRIPATHI and R. C. SHARMA, *Ann. Soc. Sci. Bruxelles*, 1983, 97, 11.
3. R. KUMAR, R. C. SHARMA and G. K. CHATURVEDI, *J. Inorg. Nucl. Chem.*, 1981, 43, 2503.
4. S. P. TRIPATHI, G. K. CHATURVEDI and R. C. SHARMA, *Zh. Chem.*, 1978, 109, 288.
5. M. A. TISHCHENKO, I. I. ZHELTVAI and N. S. POLUEKTOV, *Zh. Neorg. Khim.*, 1974, 19, 1798.
6. S. CHABERCK and A. E. MARTELL, *J. Am. Chem. Soc.*, 1952, 74, 5052.
7. S. RAMAMOORTHY and M. SANTAPPA, *Indian J. Chem.*, 1971, 9, 381.

J. INDIAN CHEM. SOC., VOL. LXIII, JUNE 1986

Magnetic Study of Uranyl Complexes of some Schiff Bases

P. S. PRABHU and S. S. DODWAD*

Department of Chemistry, Institute of Science, M. Cama Road, Bombay-400 032

Manuscript received 24 July 1984, revised 16 April 1986, accepted 8 April 1986

URANYL complexes of Schiff bases obtained by condensing salicylaldehyde and substituted salicylaldehyde with aromatic amines, like 2-aminopyridine, aniline and nitroanilines, have been isolated and characterised. The complexes have the formula ML_2 and $M(LH)_2(NO_3)_2$ where $M = UO_2$ and L and LH = Schiff base. The magnetic susceptibility values of all the ligands and their complexes have been compared with the computed ones, obtained by adding the experimental molar susceptibilities of the components, assuming strict additivity. The percentage deviations between the observed and the computed values clearly show that they are outside the experimental error, and therefore are significant. These deviations have been discussed in the light of Van Vleck's equation for the molar susceptibility of polyatomic molecule.

Experimental

Magnetic susceptibilities of the uranyl complexes were measured by a modified form of Gouy's balance, described by Prasad *et al.*[1]. The values of specific susceptibility (χ) and molar susceptibility (χ_m) of uranyl complexes were determined. The molar magnetic susceptibilities were then computed using Pascal's additivity law. The computed values were found to be higher than the experimental values. This deviation from Pascal's law is regarded as a measure of ligand field strength in terms of χ_p values. The calculated percentage-deviation values are reported in Table 1.

Discussion

It is evident from the results that all the complexes are diamagnetic. This indicates that all of them are spin-paired complexes of hexavalent uranium. Assuming the Pascal's additivity law, molar magnetic susceptibilities of all these complexes were computed. The computed values are found to be higher than the experimental values (Table 1). These deviations are beyond the experimental error and therefore are significant.

According to Van Vleck[2], the susceptibility of a polyatomic molecule without a resultant spin is given by the equation,

$$\chi_m = \chi_d + \chi_p$$

where, χ_d represents the diamagnetic term and is a function of $\sum_n \bar{r}^2$ (the radius of all electronic orbits in the molecule), and χ_p represents the second order paramagnetism, independent of temperature, arising on account of the mixing of the ground and excited states of electrons in the molecule. If the metal-nitrogen-bond in the complex is sufficiently strong, the associating units will come very close to the metal atom, thus decreasing the value of $\sum_n \bar{r}^2$ and hence that of the diamagnetic susceptibility of the molecule.

Freed and Kasper[3] and Lawrence[4] have observed that χ_p term is definitely present in uranyl complexes. Van Vleck[2] attributed this paramagnetism to the matrix elements of the magnetic moment operator $\beta(L+2S)$ between the ground state and higher states. The contribution from the spin magnetic moment is zero since all spins are paired off in the ground state. As the largest orbital contribution comes from the two $5f\sigma$ bonding electrons, Eisenstein and Pryce[5] have assumed that f-electrons are responsible for the magnetism of the uranyl ion. Belford and Belford[6,7] have shown, from the orbital overlap integral calculations, that the $5f\sigma$ uranium orbitals do not overlap much with the oxygen orbitals as the 6d orbitals do, and that considerable π bonding also might be involved.

Since the nature of various ligands complexing with the uranyl ion, are similar in structure, it is concluded that comparison of χ_p values will be possible. Examination of results show that the χ_p

TABLE 1—MAGNETIC SUSCEPTIBILITY DATA OF URANYL COMPLEXES OF SOME SCHIFF BASES

Compd.	Mol. weight	χ	χ_m (observed)	χ'_m (computed)	$\Delta\chi_m = (\chi_m - \chi'_m) = (\chi_p)$	$\%\Delta\chi_m$
$[UO_2(C_{13}H_{11}ON)_2](NO_3)_2$ (Salicylanil)	788	0.217 8	171.62	210.18	−38.56	−22.46
$[UO_2(C_{14}H_{13}ON)_2](NO_3)_2$ (*p*-Methylsalicylanil)	816	0.229 5	187.27	233.66	−46.39	−24.77
$[UO_2(C_{13}H_{10}O_3N_2)_2](NO_3)_2$ (*m*'-Nitrosalicylanil)	878	0.198 3	174.10	216.88	−42.78	−24.57
$[UO_2(C_{13}H_{10}O_3N_2)_2](NO_3)_2$ (*p*'-Nitrosalicylanil)	878	0.197 4	173.31	216.70	−43.39	−25.08
$[UO_2(C_{12}H_9ON_2)_2]$ (Salicylidene-2-iminopyridine)	664	0.158 3	105.11	156.60	−51.49	−48.98
$[UO_2(C_{13}H_{11}ON_2)_2]$ (*p*-Methylsalicylidene-2-iminopyridine)	692	0.176 4	122.06	180.16	−58.10	−47.59

value varies with the nature of the ligand. Considering the temperature independent paramagnetism χ_p term as a measure of ligand field strength, the following order of ligand field strength has been established : salicylanil > *m'*-nitrosalicylanil > *p*-methylsalicylanil > *p'*-nitrosalicylanil > *p*-methylsalicylidene-2-iminopyridine > salicylidene-2-iminopyridine.

An attempt has been made to examine the magnetic susceptibility values of isomeric substituted complexes. The values of χ_m suggest that introduction of substitutent in salicylanil (in the salicylaldehyde ring as well as in the amine ring) in various positions causes an increase in the diamagnetic susceptibility value. Langevin's theory postulates that a decrease in the effective positive charge will result in an increase in the diamagnetic susceptibility. An order of increase in the susceptibility values as a result of substitution of different groups at isomeric positions is represented as follows : salicylanil < *p*-methylsalicylanil ; salicylanil < *p'*-nitrosalicylanil < *m'*-nitrosalicylanil ; salicylidene-2-iminopyridine < *p*-methylsalicylidene-2-iminopyridine.

According to French[8], if the substituent is *ortho-para* directing, the *ortho* compound should have higher susceptibility than either *meta* or *para* compound, while when the substituent is *meta* directing, the compound has the highest susceptibility values than the other substituents. This difference is attributed to the presence of higher electron density at *ortho* position in compounds containing two-electron repelling groups *ortho* to each other, and in *meta* compound to a higher electron density at *meta* position when the two groups are *meta* to each other. The order indicates that the authors findings are in partial agreement with the above findings.

Percentage deviation and symmetry of the molecule : In the Schiff base complexes studied, coordination occurs through nitrogen[9-12] and that the bonds involved are of coordinate convalent type. These bonds are likely to cause contraction of the electronic orbits whereby value of $\sum_n \bar{r}^2$ of the molecule is decreased. Since diamagnetic susceptibility is a radical function, the decrease in the value of $\sum_n \bar{r}^2$ would lower the diamagnetic susceptibility of complex molecule. This view is supported by the negative deviations observed by the authors.

It is thus clear that the observed deviations from additivity may be due to the changes in the χ_d term of Van Vleck equation. Further, since the bond between component molecule is strong, it is likely to bring about a change in symmetry of the component molecule. χ_p term, which is also dependent on the symmetry of the molecule, is likely to be affected due to this type of bonding. Thus the observed deviation from additivity may be on account of the changes in terms χ_d and χ_p both. The deviation is therefore the net result of the two opposing effects χ_d and χ_p having opposite signs. Since, the symmetry of complex formed may be entirely different from that of the constituent molecule, the change in the χ_p term would obviously be more significant.

It appears that the χ_p term is more significant in bringing about a change in the molar susceptibility of the complex. This term is dependent on the symmetry of the molecule ; and hence, greater the symmetry of the molecule, the smaller will be its contribution to χ_m in the Van Vleck's equation. It is therefore expected that greater the symmetry of the molecule, smaller will be the deviation[13] from additivity and vice-versa. Hence, all the complexes reported in this investigation appeared to be distorted.

References

1. M. Prasad, S. S. Dharmatti and S. V. Gokhale, *Proc. Indian Acad. Sci., Sect. A*, 1944, **20**, 224.
2. J. H. Van Vleck, "The Theory of Electric and Magnetic Susceptibilities", Oxford University Press, Oxford, 1932.
3. S. Freed and C. Kasper, *J. Am. Chem. Soc.*, 1930, **52**, 4671.
4. R. W. Lawrence, *J. Am. Chem. Soc.*, 1934, **56**, 776.
5. J. C. Eisenstein and M. H. L. Pryce, *Proc. R. Soc., Ser. A*, 1955, **229**, 20.
6. R. L. Belford, *J. Chem. Phys.*, 1961, **34**, 318.
7. R. L. Belford and G. Belford, *J. Chem. Phys.*, 1961, **34**, 1330.
8. C. M. French, *Trans. Faraday Soc.*, 1945, **41**, 676.
9. N. S. Biradar and V. H. Kulkarni, *J. Less-Common Met.*, 1972, **26**, 355.
10. N. S. Biradar, V. H. Kulkarni and N. N. Sirmokadam, *Karnatak Univ. J. Sci.*, 1972, **17**, 14.
11. M. A. Pujar and T. D. Bharamagoudar, *J. Indian Chem. Soc.*, 1980, **57**, 462.
12. N. S. Biradar and A. L. Locker, *Indian J. Chem.*, 1973, **11**, 833.
13. J. V. Navangule and M. G. Datar, *J. Univ. Bombay*, 1970.

Thioarsenites of Less-common Metals. Electrometric Investigations on the Composition of Uranyl Thioarsenites as a Function of *p*H

SHIVA PRASAD

Department of Chemical Engineering, Centre of Science and Technology, Federal University of Paraíba, Campina Grande, Paraíba, Brazil

Manuscript received 30 December 1985, revised 8 April 1986, accepted 8 May 1986

THE composition of heavy metal arsenites precipitated by the addition of sodium arsenite solutions to heavy metal salts is governed mainly by *p*H. The investigation of these compounds is difficult because of the adsorption of arsenic oxide by metallic hydroxides ; the conversion of orthoarsenite to pyro- and meta-arsenite takes place with great ease, and these dissolve in excess of alkali and acid[1]. Consequently, analytical methods have failed to give a correct view of their composition.

Literature on thioarsenites is meagre. Some of the thioarsenites are probably best described as double sulphides, whereas others, *e.g.* Ag_3AsS_3 and $TlAsS_2$, form anions[2]. In view of insufficient and conflicting reports on the composition of thioarsenites and in absence of any reference on the formation of uranyl thioarsenites, it was considered worthwhile to carry out a systematic study on the formation and composition of uranyl thioarsenites. These studies carried out by electrometric techniques, have yielded more conclusive evidences on the composition of such compounds[3-5].

Experimental

Uranyl acetate, arsenous oxide, sodium sulphide, ammonium sulphide and hydrochloric acid of extra-pure grade were used, and their solutions prepared in carbonate-free conductivity water. The standard solution of Na_3AsS_3 was prepared by digesting analysed sample of As_2S_3 in Na_2S solution of required strength[6]. Calculated amounts of HCl were then added to Na_3AsS_3 solutions in definite molecular proportions in order to vary the *p*H.

*p*H measurements were carried out using a Metrohm Herisau (Switzerland) *p*H meter and Schott Gerate glass combination electrode. The conductance of solutions was measured by employing a Metrohm conductometer. The solution (25 ml) was taken in the cell thermostated at $25 \pm 0.1°$. Using different concentrations of reactants, a series of *p*H and conductometric titrations were performed both by direct and reverse methods in aqueous and aqueous alcoholic media.

Results and Discussion

The solution of Na_3AsS_3 was prepared by digesting As_2S_3 in Na_2S solution in the molar ratio 1 : 3. The *p*H of the Na_3AsS_3 solution was found to be 12.6. HCl was mixed with Na_3AsS_3 in the molar ratio 1 : 1, whereupon $Na_4As_2S_5$ was formed and *p*H of the solution found to be 10.5.

$$2Na_3AsS_3 + 2HCl = Na_4As_2S_5 + 2NaCl + H_2S$$

Sodium orthothioarsenite titrations : A series of *p*H titrations were carried out using different concentrations of uranyl acetate (*p*H 4.1) and Na_3AsS_3 (*p*H 12.6). In direct titrations (Fig. 1, curve 1), when Na_3AsS_3 solution was used as titrant, a gradual decrease in *p*H value was observed till at the stoichiometric end-point (in case of a simple double decomposition reaction). A sharp downward jump in *p*H was observed at 3 : 2 molar ratio of UO_2^{2+} : AsS_3^{3-}, corresponding to the formation of the yellow precipitate of uranyl orthothioarsenite, $3UO_2S.As_2S_3$ around *p*H 7.0. In case of reverse titrations (Fig. 1, curve 2), at first the *p*H gradually increased till in the vicinity of the end-point, when the last traces of uranyl got removed through precipitation ; further addition of alkali thioarsenite

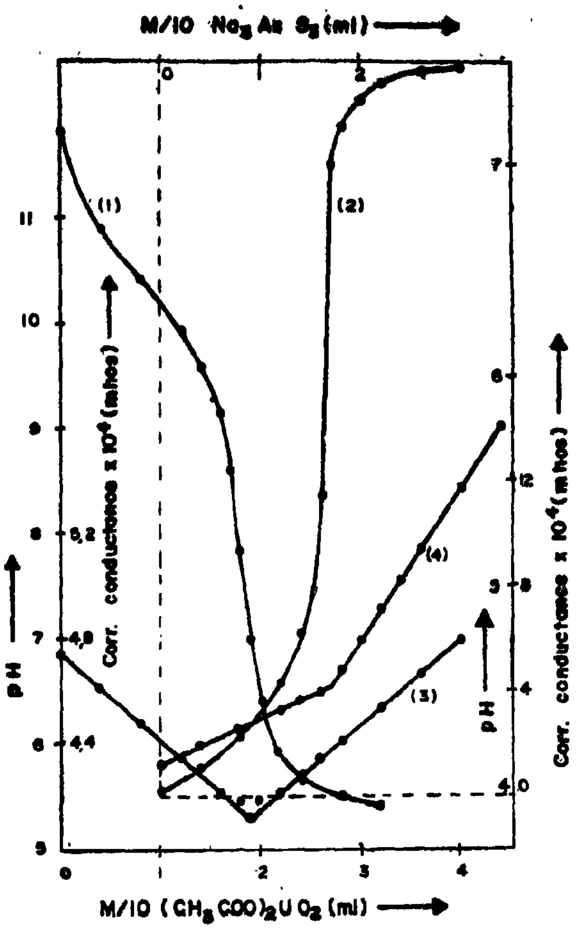


Fig. 1. Orthothioarsenite titrations : (1) and (3) 0.1 *M* $(CH_3COO)_2UO_2$ added to 25 ml of 0.005 *M* Na_3AsS_3, (2) and (4) 0.1 *M* Na_3AsS_3 added to 25 ml of 0.01 *M* $(CH_3COO)_2UO_2$.

caused a marked jump in *p*H and resulting in precipitation of $3UO_2S.As_2S_3$ according to the reaction,

$$2Na_3AsS_3 + 3(CH_3COO)_2UO_2 = (3UO_2S.As_2S_3) + 6CH_3COONa$$

Employing similar concentrations of the reactants, direct and reverse conductometric titrations (Fig. 1, curves 3 and 4) were carried out. Well defined breaks are obtained at the stoichiometric end-points, suggesting the formation of the same compound $3UO_2S.As_2S_3$.

Sodium pyrothioarsenite titrations : In the direct *p*H-metric titrations of sodium pyrothioarsenite (*p*H 10.5) and uranyl acetate (*p*H 4.1) solutions (Fig. 2, curve 1), well defined breaks at the point corresponding to the formation of uranyl pyrothioarsenite were obtained around *p*H 5.5. The reverse titration curves (Fig 2, curve 2) also supported the formation of uranyl pyrothioarsenite according to the reaction,

$$Na_4As_2S_5 + 2(CH_3COO)_2UO_2 = (2UO_2S.As_2S_3) + 4CH_3COONa$$

Both direct and inverse conductometric titrations (Fig. 2, curves 3,4) showed the formation of the compound $2UO_2S.As_2S_3$.

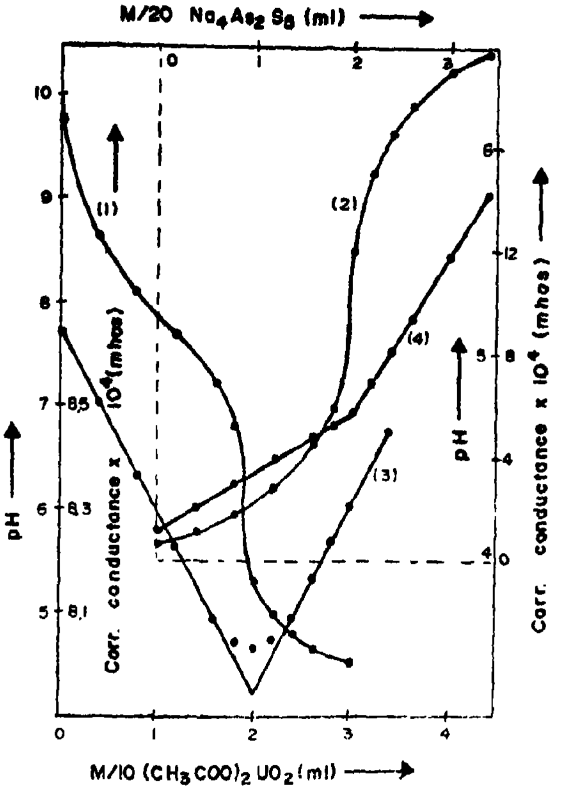


Fig. 2. Pyrothioarsenite titrations: (1) and (3) 0.1 M $(CH_3COO)_2UO_2$ added to 25 ml of 0.004 M $Na_4As_2S_5$, (2) and (4) 0.2 M $Na_4As_2S_5$ added to 25 ml of 0.008 M $(CH_3COO)_2UO_2$.

Investigations on the formation of metal-thioarsenite were not successful because the compound formed was not stable and decomposed to a yellow precipitate of As_2S_3.

Analytical study : The different uranyl arsenites were prepared by mixing stoichiometric amounts of uranyl acetate and the respective sodium thioarsenites. The precipitates obtained were washed several times with aqueous 10% (v/v) ethanolic solution and dried in a vacuum desiccator for 40 h. A known amount (2 g) of each of the above was digested with concentrated HNO_3 (15 ml) to dryness on a steam-bath. The treatment was repeated several times. The residue was dissolved in minimum quantity of HCl and then analysed[7] for U and As. Sulphur in the uranyl thioarsenites was determined gravimetrically[7]. The compositions of the compounds established through the above analysis were found to be the same as that obtained by the electrometric methods.

The present electrometric and analytical investigations confirm the formation and precipitation of $3UO_2S.As_2S_3$ and $2UO_2S.As_2S_3$ around pH 7.0 and 5.5, respectively.

Acknowledgement

The author expresses his sincere thanks to the CNPq, Brasília, for the financial aid.

References

1. F. Ephraim, "Textbook of Inorganic Chemistry", Gurney and Jackson, London, 1949, p. 745.
2. J. C. Bailar, "Comprehensive Inorganic Chemistry", Pergman Press, Oxford, 1973, Vol 11, p. 619.
3. S. Prasad, *Anal. Asoc. Quím. Argentina*, in the press.
4. S. Prasad, *Can. J. Chem.*, 1981, 59, 563.
5. S. Prasad, *An. Acad. Bras. Ciênc.*, 1982, 54, 339.
6. S. Prasad, *Rev. Latinoamer. Quím.*, 1984, 15, 50.
7. A. I. Vogel, "A Textbook of Quantitative Inorganic Analysis", Longmans Green, London, 1968, pp. 540, 367, 466.

Kinetics of Oxidation of Aliphatic Secondary Alcohols by *N*-Bromosaccharin

V. MANOHARAN* and N. VENKATASUBRAMANIAN

Department of Chemistry, Vivekananda College, Madras-600 004

Manuscript received 2 September 1982, revised 8 August 1983, accepted 6 May 1986

N-BROMOSACCHARIN (NBSA) has been used sporadically as an oxidising agent in organic chemistry[1]. While the mechanism of oxidation of organic compounds by *N*-bromosaccinimide (NBS) has been fairly well established[2-4], the reactions of NBSA have not been elucidated from the mechanistic point of view. We have therefore attempted to study the reactions of a variety of organic substrates with NBSA with a view to arrive at the mechanisms of the reactions and also to compare the reactivities of the two reagents NBS and NBSA. We report in this note the results on the kinetics of the oxidation of aliphatic secondary alcohols by NBSA.

Experimental

N-Bromosaccharin was prepared by the addition of bromine to the sodium salt of saccharin at 0°. All other reactants were commercial samples, purified by either distillation or crystallisation. Acetic acid (A.R.) was further purified[5]. The kinetics were followed under pseudo-unimolecular conditions (alcohol$\gg$NBSA) by estimating the unreacted NBSA at various intervals of time by an iodometric procedure. The rate constants reported are the average of at least three kinetic runs and are reproducible within ±5%.

Results and Discussion

The kinetics of oxidation of propan-2-ol, taken as a typical substrate, follows the rate law

* Present address: Department of Chemistry, Government Arts College, Nandanam, Madras-600 035.

$-d[NBSA]/dt = k_2[NBSA][Propan\text{-}2\text{-}ol]$ in binary solvent mixtures of acetic acid and water in presence of 0.02 *M* mercury(II) acetate, added to prevent the interaction of the product Br^- ions with the oxidant[8]. The ionic strength was maintained constant at 0.25 *M* with $HClO_4$. The data in Table 1 reveal the individual rate dependence on the reactants. Although being acid-catalysed, no specific dependence on $[H^+]$ could be seen for the reaction. (10^4k_1 in presence of 0.05 *M* and 0.2 *M* $HClO_4$ are 3.24 and 3.46 s^{-1}, respectively, in 50% aqueous acetic acid in presence of 0.02 *M* mercury(II) acetate at 30°). Hg^{II} is also involved only as a complexing agent for the Br^- and does not oxidise the alcohol under the experimental conditions. The reaction rate also does not vary significantly with the increasing ionic strength of the medium. The reaction is indeed susceptible to variations in the polarity of the medium obtained by varying the acetic acid concentration in the solvent mixture. (10^4k values in 30 and 70% acetic acid are 1.69 and 3.70 s^{-1}, respectively. The concentrations of alcohol, NBSA, $Hg(OAc)_2$ are 0.02, 0.002 and 0.02 *M*, respectively, the ionic strength being 0.25). The rate of oxidation increases with decreasing dielectric constant of the medium. Added saccharin decreases the rate of oxidation perceptibly (Table 2) indicating a prior equilibrium step involving the oxidant.

TABLE 1—ORDER DEPENDANCE FOR OXIDATION OF PROPAN-2-OL BY *N*-BROMOSACCHARIN AT 30°

Solvent: 50% HOAc – 50% H_2O, $[Hg(OAc)_2] = 0.02$ *M*, $\mu = 0.25$

[NBSA] *M*	[Propan-2-ol] *M*	10^4 k_1 s^{-1}	10^3 k_2 dm^3 mol^{-1} s^{-1}
0.001	0.020	2.62	1.31
0.002	0.020	2.63	1.31
0.003	0.020	2.63	1.31
0.004	0.020	2.62	1.31
0.002	0.040	5.02	1.26
0.002	0.050	6.15	1.23
0.002	0.100	12.9	1.29

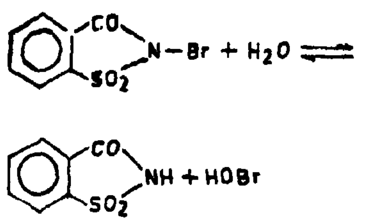
TABLE 2—EFFECT OF ADDED SACCHARIN ON THE RATE OF OXIDATION OF PROPAN-2-OL BY NBSA IN 50% HOAc – 50% H_2O AT 30°

$[Propan\text{-}2\text{-}ol] = 0.02$ *M*, $[Hg(OAc)_2] = 0.02$ *M*, $[NBSA] = 0.002$ *M*, $\mu = 0.25$

[Saccharin] *M*	10^4 k_1 s^{-1}
—	2.71
0.002	2.10
0.008	0.98
0.050	0.25

The effect of structural variations in the alcohol $R-CH_2CHOH-CH_3$ on the rate of oxidation, has been studied with a number of alcohols where R is an electron-withdrawing or an electron-releasing substituent. As in other oxidations with N-halogen compounds, these reaction rates are also considerably affected by the nature of the substituent introduced (Table 3). A linear free energy correlation of the reaction rate with σ^* (Taft substituent constant) yields a reaction constant ρ^* equal to -2.3, a value similar to other alcohol oxidations by Br_2 or NBS[6,7]. The thermodynamic parameters for the reaction are also included in the Table 3.

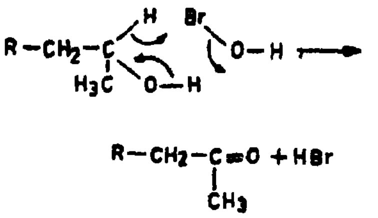
On the basis of the rate law and other observations mentioned above, the following mechanism is proposed for the oxidation.



(1)

$$R-CH_2-CHOH-CH_3 + HOBr \xrightarrow{slow} R-CH_2-CO-CH_3 + H_2O + HBr \quad (2)$$

The finer details of the slow step are more likely to be



(3)

rather than the one involving the formation of $R-CH_2-CHOBr-CH_3$ as an intermediate[8]; as in the latter case, one would expect a positive ρ^*

TABLE 3—SUBSTITUENT EFFECTS AND ACTIVATION PARAMETERS FOR THE OXIDATION OF ALCOHOLS BY NBSA

$(R\text{-}CHOH-CH_3)$ R	10^3 k_2[*] dm^3 mol^{-1} s^{-1}	E_a kcal mol^{-1}	$\Delta H^{\ne}$ kcal mol^{-1}	$\Delta S^{\ne}$ cal K^{-1} mol^{-1}
CH_3	1.32	14.8	14.2	20
CH_2-CH_3	8.4	12.1	11.6	27
$n\text{-}C_3H_7$	3.8	10.7	10.1	32
$n\text{-}C_5H_{11}$	2.8	13.8	13.2	22
C_6H_5O	0.211	—	—	—
CH_2Cl[a]	0.187	—	—	—

* At 30°. [a] For $ClCH_2-CHOH-CH_2Cl$.

(consistent with an E_2 type of elimination reaction) and base catalysis would also have been observed.

Further, a good linear correlation of the rates of oxidation of the aliphatic alcohols by NBSA with the rate constants for the oxidation of similar systems by NBS[8] underscores a formal similarity of the two transition states.

References

1. N. K. Mathur and C. K. Narang, "Determination of Organic Compounds with N-Bromosuccinimide and Allied Reagents", Academic Press, London, 1975.
2. N. Venkatasubramanian and V. Thiagarajan, *Tetrahedron Lett.*, 1967, 35, 3349.
3. N. Venkatasubramanian and V. Thiagarajan, *Can. J. Chem.*, 1969, 47, 694.
4. N. Venkatasubramanian and V. Thiagarajan, *Indian J. Chem.*, 1970, 8, 809.
5. K. J. P. Orton and A. E. Bradfield, *J. Chem. Soc.*, 1928, 960; 1927, 983.
6. N. S. Srinivasan and N. Venkatasubramanian, *Indian J. Chem.*, 1972, 10, 1014.
7. I. R. L. Barker and P. Auckett, *Chem. Ind.* (*London*), 1967, 198.
8. N. C. Deno and N. H. Potter, *J. Am. Chem. Soc.*, 1967 89, 3550.

Equilibrium Studies of Interaction of Oxovanadium(II), Manganese(II), Cobalt(II), Nickel(II) and Copper(II) with *o*-Hydroxyacetophenone, 4-Methyl-5-hydroxy-6-acetylcoumarin and 1-(2′-Furyl)-3-(4′-methyl-5′-hydroxycoumarin-6′-yl)propane-1,3-dione

K. T. KENDRE, N. R. MANJRAMKAR

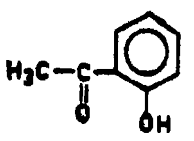
and

Y. H. DESHPANDE*

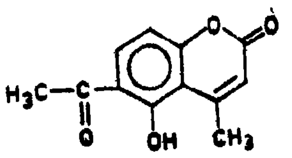
Department of Chemistry, Marathwada University, Aurangabad-431 004

Manuscript received 20 December 1980, revised 14 April 1986, accepted 23 April 1986

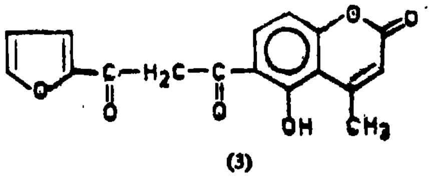
UNSATURATED lactones are well known for their selective inhibition of growth of plant and animal tissues, for toxicity in fish, antibacterial and haemorrhagic activity and for their effect on central nervous system. Coumarins belong to this class of compounds[1]. It was, therefore, decided to investigate the interactions of coumarins with metal ions commonly present in the living systems and to study the effect of substitution of various ring systems on coumarin moiety. The following ligands were selected for the present study.



(1)



(2)



(3)

Experimental

The ligands **1**, **2** and **3** were prepared by following the procedures reported earlier[2-4]. The metal ions were used in the form of their perchlorates, except for vanadium, where vanadyl sulphate was used. The concentrations of the metal ions were determined complexometrically[5] by EDTA titrations. Dioxane was purified[6]. All other reagents were of AnalaR grade. The titrations were carried out in nitrogen atmosphere. The experimental procedure involved potentiometric titration of the solution of known amount of the ligands (**1**, 1.023×10^{-3}; **2**, 1.005×10^{-3}; **3**, 1.006×10^{-3} *M*), known amounts of free $HClO_4$ (5.234×10^{-3} *M*), in the absence and presence of known amounts of the metal ions (VO^{II}, 1.187×10^{-3}; Mn^{II}, 1.327×10^{-3}; Co^{II}, 1.167×10^{-3}; Ni^{II}, 1.062×10^{-3}; Cu^{II}, 9.704×10^{-3} *M*) with sodium hydroxide solution (2.469×10^{-1} *M*) at 0.1 *M* ($NaClO_4$) ionic strength.

Results and Discussion

The $\bar{n}_A$, $\bar{n}$ and pL values were calculated by the method of Irving and Rossotti[7]. The results are stated in Table 1. The pK value of phenol in 50 : 50 (v/v) water-dioxane system was 12.0. In *o*-hydroxyacetophenone in spite of the electron withdrawing CH_3CO group, the value was found to be 12.06, probably due to the intra-molecular hydrogen bonding. The acidities of the coumarin and the diketone derivatives were comparatively higher than that of *o*-hydroxyacetophenone because of the electron withdrawing oxygen atoms attached to adjacent rings. Weak hydrogen bonding in the diketone derivative lowers its acidity to some extent.

With the exception of the VO^{II} complexes of acetophenone and diketone derivatives, the difference ($\log K_1 - \log K_2$) was less than 1.78, suggesting the formation of 1 : 1 and 1 : 2 complexes by simultaneous equilibria[8]. In the VO^{II} complexes of the acetophenone and diketone derivatives, the 1 : 1 and 1 : 2 complexes were formed in stepwise manner. VO^{II} and Cu^{II} were found to form more stable complexes with all the three ligands (Table 1). Higher stability of these complexes could be attributed to the Jahn-Teller distortion[9]. The $\log K_2$ value of Cu^{II} complex of the

TABLE 1—PROTON-LIGAND AND METAL-LIGAND STABILITY CONSTANTS*

Cations	Ligands 1		Ligands 2		Ligands 3	
	log K_1	log K_2	log K_1	log K_2	log K_1	log K
H^+	12.06	—	9.85	—	10.25	—
VO^{2+}	11.34	8.59	9.77	9.24	9.88	7.76
Mn^{2+}	6.22	5.88	4.68	4.12	5.00	4.24
Co^{2+}	6.86	6.43	5.25	4.57	5.15	5.07
Ni^{2+}	6.65	5.71	5.95	4.91	5.18	4.74
Cu^{2+}	8.64	7.92	7.75	—	6.90	6.48

* For proton association (H^+), K_1 corresponds to the species LH, while for metal ions K_1 and K_2 correspond to the species ML_1 and ML_2, respectively.

coumarin derivative could not be evaluated due to the commencement of precipitation at pH ≃4.7. With the exception of Mn^{II} complexes, the log K_1 values of the diketone complexes were slightly less than those of the acetophenone and coumarin derivatives. This was probably due to the bigger size of the diketone molecule which caused steric hindrance in the complex formation process.

Acknowledgements

The authors are thankful to Dr. K. A. Thakar, Professor and Head, Chemistry Department, Marathwada University, Aurangabad, for constant encouragement and Dr. D. V. Jahagirdar for valuable discussions. One of the authors (K.T.K.) is thankful to U. G. C., New Delhi, for the award of a Teacher Fellowship, and the authorities of the J. E. S. College, Jalna, for granting study leave.

References

1. G. RODIGHIERO and C. ANTONELLO, *Bool. Chim. Farm*, 1958, **97**, 592.
2. D. B. INGLE, Ph.D. Thesis, Marathwada University, 1969.
3. S. M. SETHNA, N. M. SHAH and R. C. SHAH, *J. Chem. Soc.*, 1938, 228.
4. N. R. MANJRAMKAR, Ph.D. Thesis, Marathwada University, 1970.
5. H. A. FLASCHKA, "EDTA Titrations", Pergamon, New York, 1978.
6. A. I. VOGEL, "A Text Book of Practical Organic Chemistry", 3rd. ed., Longmans, London, p. 177.
7. H. IRVING and H. ROSSOTTI, *J. Chem. Soc.*, 1953, 3397; 1954, 2904.
8. J. B. SCARBOUGH, "Numerical Mathematical Analysis", Oxford University Press, 1930, p. 364.
9. F. A. COTTON and G. WILKINSON, "Advanced Inorganic Chemistry", 2nd. ed., Interscience, New York, p. 688.

Potentiometric and Biocidal Studies of Ternary Complexes of some Transition Metals with *N*-Pyridylanthranilic Acid (NPA) and some Bidentate Ligands

MADHU OBEROI, SARITA CHATURVEDI, RAVI CHATURVEDI and G. K. CHATURVEDI*

Chemical Laboratories, Agra College, Agra-282 002

Manuscript received 11 April 1984, revised 4 March 1986, accepted 9 April 1986

A survey of the literature reveals the description of chelates of a number of bivalent metals/lanthanide[1,2] ions with anthranilic acid. The synthesis and chelating behaviour of *N*-phenylanthranilic acid have been investigated by Harris and Sweet[3].

In this communication, the synthesis of a new ligand, *N*-pyridylanthranilic acid (NPA) from 2-aminopyridine and *o*-chlorobenzoic acid has been described and its proton dissociation constant (NPA, $pK_1=3.46\pm0.04$; IMDA, $pK_1=3.11\pm0.09$, $pK_2=9.45\pm0.11$) were determined by the method of Chaberck and Martell[4]. The binary and ternary complex formation of some bivalent metals with the synthesised ligand and a number of bidentate ligands have been studied potentiometrically, and the values of formation constants of the resulting complexes, evaluated by the respective methods of Thompson and Loraas[5] and Ramamoorthy and Santappa[6], are recorded.

The insoluble ternary complex, 1 : 1 : 1 Cu^{II}-NPA-HQ has also been isolated and characterised by elemental analysis and ir spectra. The biocidal activity of metal ions, the ligands, and the Cu^{II} complex towards some selected fungi and bacteria are evaluated (Table 3).

Experimental

All the chemicals used were either of BDH or E. Merck grade unless stated otherwise. The metal

* Department of Chemistry, College of Basic Sciences and Humanities, G. B. Pant University of Agriculture and Technology, Pantnagar-263 145.

nitrate solutions were prepared and standardised[7]. For the potentiometric studies, the solution of IMDA was prepared by direct-weighing and HQ was used as monohydrochloride obtained by adding calculated amount of standard HCl solution in the calculated weighed amount of HQ.

Synthesis of NPA : The light yellow crystalline needle shaped NPA was synthesised[8] by condensing potassium salt of *o*-chlorobenzoic acid and 2-aminopyridine, m.p. 140° (Found : C, 67.20 ; H, 4.66 ; N, 12.99. $C_{12}H_{10}N_2O$ calcd. for : C, 67.28 ; H, 4.67 ; N, 13.08%). The 1 : 1 : 1 Cu^{II}-NPA-HQ was also analysed (Found : C, 57.40, H, 3.80 ; N, 9.55 ; Cu, 14.31. $CuC_{21}H_{15}N_3O_3.H_2O$ calcd. for : C, 57.46 ; H, 3.87 ; N, 9.57 ; Cu, 14.48%).

Potentiometric studies : The potentiometric titrations of metal ions, ligands, binary and ternary systems were carried out employing the technique reported earlier[8].

Results and Discussion

System 1 : 1 : 1 M^{II}-NPA-IMDA/HQH^+ : Curves for the system Cu^{II}-NPA-IMDA/HQH^+ have been discussed as representative (Figs. 1 and 2) ; curves for other systems involving Ni^{II}/Zn^{II}/Cd^{II} being similar have been avoided.

An inflection at m = 1 in the curve (a) (NPA) and (b) (IMDA) in Fig. 1 and curve (b) (HQH^+) in Fig. 2, can be attributed to the titration of carboxy-proton forming the potassium salt of the respective acids in case of NPA and IMDA, and hydrochloride-proton in case of HQH^+. Two inflections at m = 1 and 3 (curve (c)) in case of 1 : 1 M^{II}-NPA system may be ascribed to the formation of a soluble 1 : 1 M^{II}-NPA complex in the lower *p*H range, undergoing decomposition on further alkalisation giving metal hydroxide and free ions of the acid in solution.

TABLE 1

System	log K_{ML}	G° kcal mol⁻¹ K⁻¹	log $K_{MLL'}$	G° kcal mol⁻¹ K⁻¹
1 : 1 Cu^{II}-NPA/1 : 1 : 1 Cu^{II}-NPA-IMDA	2.32±0.06	−3.16	13.24±0.14	−18.04
1 : 1 Ni^{II}-NPA/1 : 1 : 1 Ni^{II}-NPA-IMDA	2.20±0.16	−2.99	12.54±0.20	−17.09
1 : 1 Zn^{II}-NPA/1 : 1 : 1 Zn^{II}-NPA-IMDA	1.96±0.08	−2.67	12.50±0.18	−17.03
1 : 1 Cd^{II}-NPA/1 : 1 : 1 Cd^{II}-NPA-IMDA	1.37±0.16	−1.86	12.37±0.20	−16.86

M = Cu^{II}, Ni^{II}, Zn^{II} and Cd^{II}. L = NPA. L′ = IMDA.

TABLE 2

NPA		HQ		Cu^{II}-NPA-HQ	
ν_{max}	Assignments	ν_{max}	Assignments	ν_{max}	Assignments
2 760w	NH stretch	3 100s	OH	3 300b	Splitting of NH
2 550w	CH stretch of COOH	3 270s	OH stretch	1 580s	OH stretch in H−OH
1 650b	C=O stretch	1 685s	Aromatic	1 510s	C=C, C−H
1 550s	NH stretch	1 510s	—	1 390s	M−OH
1 400m	—	1 660s	C=C	1 300m	—
1 330s	C−H stretch	1 610s	C=N	1 185s	M−OH
1 000s	C−N stretch			775s	C=O
915s	C−C stretch			580w	M−N
770s	NH rock				
750s	C−H bend				
640m	Pyridyl N			525m	M−O
				475m	

TABLE 3—MINIMUM INHIBITORY CONCENTRATION (MIC in $\mu g\ ml^{-1}$) OBSERVED AGAINST INDICATED FUNGI AND BACTERIA

Compd.	Fungi			Bacteria		
	D. tetramera	*A. nigricans*	*C. albicans*	*B. subtillis*	*S. aureus*	*E. coli*
$Cu(NO_3)_2$	50	50	—	50	50	50
NPA	12.5	—	—	6.25	6.25	25
HQ	12.5	25	25	12.5	25	—
1 : 1 Cu^{II}-HQ	12.5	50	25	12.5	25	50
1 : 1 : 1 Cu^{II}-NPA-HQ	12.5	12.5	12.5	6.25	6.25	—

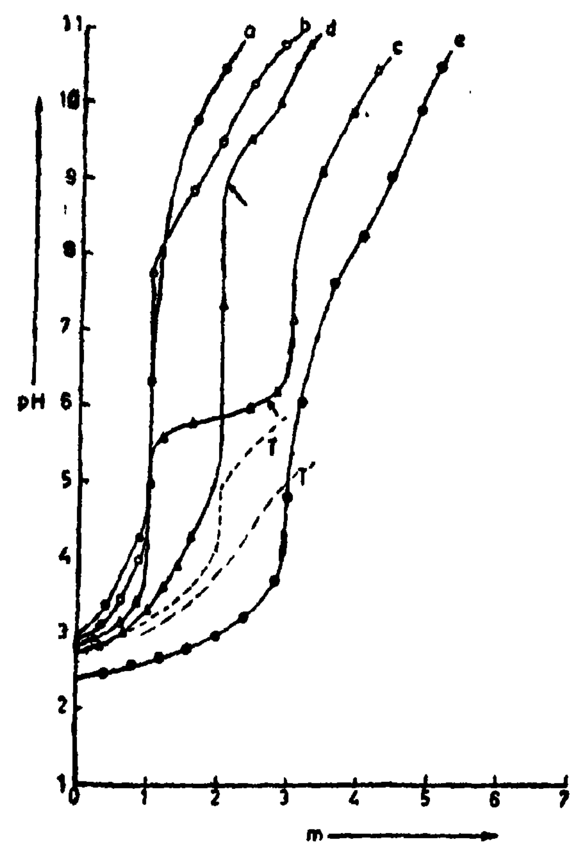


Fig. 1. System 1 : 1 : 1 Cu^{II}-NPA-IMDA : (a) NPA, (b) IMDA, (c) 1 : 1 Cu^{II}-NPA, (d) 1 : 1 Cu^{II}-IMDA and (e) 1 : 1 : 1 Cu^{II}-NPA-IMDA ; T, T' = theoretical composite curve, (→) appearance of precipitate.

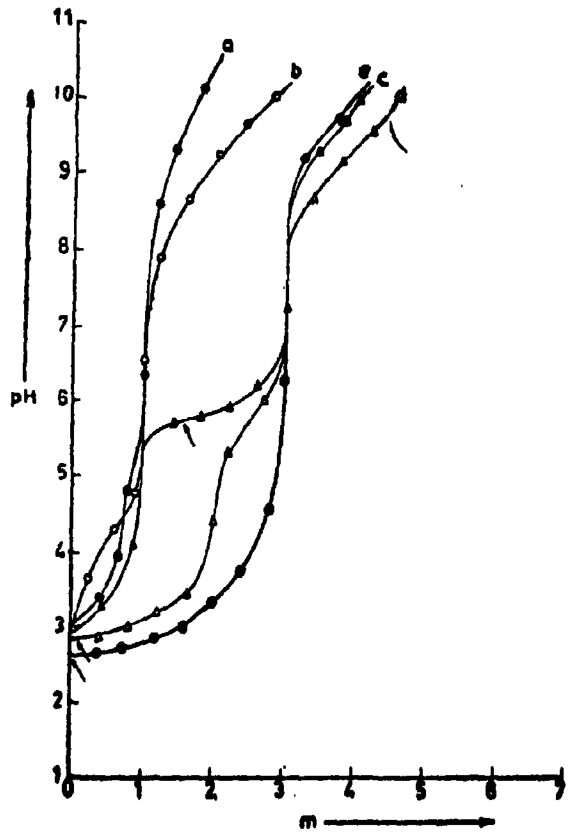


Fig. 2. System 1 : 1 : 1 Cu^{II}-NPA-HQ : (a) NPA, (b) HQ, (c) 1 : 1 Cu^{II}-NPA, (d) 1 : 1 Cu^{II}-HQ and (e) 1 : 1 : 1 Cu^{II}-NPA-HQ ; (→) Appearance of precipitate.

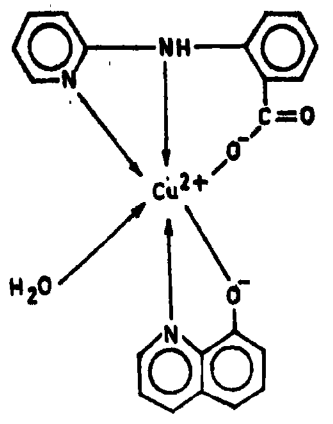
Curve (d) representing the titration of 1 : 1 M^{II}-IMDA system in Fig. 1 and 1 : 1 M^{II}-HQH^{+} in Fig. 2, give a well defined inflection at m = 2 accompanied by the formation of a precipitate in Cu^{II}-HQH^{+} system, which may be attributed to the formation of a soluble 1 : 1 M^{II}-IMDA and 1 : 1 M^{II}-HQH^{+} complex species in the respective systems.

An inflection at m = 3 exhibited by the curve (e) (Figs. 1 and 2) can be ascribed to the formation of 1 : 1 : 1 M^{II}-NPA-IMDA/HQH^{+} complex. The formation of a soluble complex 1 : 1 : 1 M^{II}-NPA-IMDA is further evidenced by non-superimposable nature of the composite curve T and T'[8], non-formation of a heterogeneous phase throughout the titration and the development of a characteristic orange-yellow colour of the solution near the inflection. Its formation is further corroborated by the constancy observed in the values of formation constant (Table 1).

In the system 1 : 1 : 1 Cu^{II}-NPA-HQH^{+} (Fig. 2), a sharp inflection at m = 3 accompanied by the formation of precipitate, support the formation of a ternary species during which carboxy protons of NPA, phenolic and hydrochloride protons of HQH^{+} are made labile. The composition of the proposed 1 : 1 : 1 Cu^{II}-NPA-HQH^{+} complex has been substantiated by the analytical data.

IR spectra : Ir spectral studies of NPA, HQ, and Cu^{II}-NPA-HQ ternary complex were made (Table 2). The OH stretching frequency at 3 270 cm^{-1} observed in free HQ and the OH (COOH) frequency at 2 500 cm^{-1} and the frequency at 640 cm^{-1} for pyridyl nitrogen in free NPA, are absent in the spectra of the complex, indicating the involvment of phenolic group of HQH^{+}, COOH and pyridyl nitrogen of NPA in the complex formation. In place of characteristic frequencies at 2 760, 1 550 and 770 cm^{-1} assigned to the NH in NPA, a new absorption band appears at 3 300 cm^{-1} in the spectra of complex, indicating the participation of NH group in the complex formation. The absorption frequencies at 580, and 525 and 475 cm^{-1} are attributed to M – N and M – O bonds in the complex, respectively. The presence of coordinated water molecule in the complex is revealed by a band occurring at 1 580 cm^{-1}.

On the basis of analytical and ir data the following structure may by proposed for the ternary complex.



Acknowledgement

The authors express their gratitude to Prof. J. P. Tandon, Rajasthan University, Jaipur, and to Dr. S. M. L. Gupta, Agra College, Agra, for their valuable suggestions. The authors also thank the C. S. I. R., New Delhi, for financial help.

References

1. A. YOUNG and T. R. SWEET, *J. Am. Chem. Soc.*, 1958, **80**, 800.
2. M. CEFOLA, A. S. THOMPA, A. V. CELLIANO and P. S. GENTILE, *Inorg. Chem.*, 1962, **1**, 290.
3. W. HARRIS and T. R. SWEET, *J. Phys. Chem.*, 1956, **60**, 509.
4. S. CHABERCK and A. E. MARTELL, *J. Am. Chem. Soc.*, 1952, **74**, 5052.
5. L. C. THOMPSON and J. A. LORAAS, *Inorg. Chem.*, 1963, **2**, 89.
6. S. RAMAMOORTHY and M. SANTAPPA, *Indian J. Chem.*, 1971, **9**, 381.
7. A. I. VOGEL, "A Text Book of Quantitative Inorganic Analysis", Longmans, London, 1962, pp. 431, 418, 468, 430.
8. S. KHANNA, B. KUMAR and G. K. CHATURVEDI, *Indian J. Chem., Sect. A*, 1980, **19**, 766.
9. A. E. MARTELL, S. CHABERCK, JR., S. C. COURTNEY, S. WESTERBACK and H. HYTIAMEN, *J. Am. Chem. Soc.*, 1967, **79**, 3036.

Phytochemical Investigation of *Cassia mimosoides* Linn

K. S. MUKHERJEE*, P. BHATTACHARYA, R. K. MUKHERJEE and P. K. GHOSH**

Department of Chemistry, Visva-Bharati University, Santiniketan-731 235

Manuscript received 30 April 1985, revised 6 September 1985, accepted 8 May 1986

CASSIA mimosoides Linn.[1] (leguminosae) is a small tree occurring throughout India and its roots are extensively used as an indigenous drug in the treatment of spasm of stomach. Literature survey revealed that the roots and seeds of this plant was investigated earlier[2]. A chemical investigation of the aerial parts (leaves and stems) of this plant was, therefore, undertaken.

** Present address: Govt. Quinine Factory, Mungpoo, Darjeeling, West Bengal.

The air-dried powdered aerial parts (leaves and stems) of *C. mimosoides* were successively extracted with petroleum ether (b.p. 60-80°) and chloroform. The concentrated petroleum ether extract was chromatographed over silica gel. Elution of the column with petroleum ether (b.p. 60-80°)-benzene (1 : 1) mixture afforded a white crystalline solid, m. p. 88°; ν_{max} (KBr) 3 300 cm^{-1}; *m/z* 452 (M^+), 434, and 421. It was identified as n-hentriacontanol by the usual comparison (m.m.p., co-tlc and co-ir) with an authentic sample.

The concentrated chloroform extract of the defatted aerial parts was subjected to chromatographic separation over silica gel with solvents of increasing polarity. The benzene-chloroform (1 : 1) eluate furnished a yellow solid, m.p. 195°, $C_{15}H_{10}O_4$ (M^+ 254); ν_{max} (KBr) 1 660 (non-chelated C=O) and 1 625 cm^{-1} (chelated C=O). It responded to methanolic magnesium acetate test[3] for anthraquinones and was characterised as chrysophanol[4] by direct comparison (m.m.p., co-tlc and co-ir) with an authentic sample. Continued elution of the column with the same solvent mixture yielded a very small amount of a solid which crystallised from glacial acetic acid as yellow leaflets, m.p. 160-2°, $C_{16}H_{12}O_5$ (M^+ 284); λ_{max} (EtOH) 257, 267, 275 sh, 288, 390, 415 and 435 nm; ν_{max} (KBr) 1 670, 1 638 and 1 675 cm^{-1}. It responded to the test[3] for anthraquinone. Further characterisation of this solid was not possible due to paucity of the material.

Acknowledgement

Sincere thanks are due to R.S.I.C., Bose Institute, Calcutta, for mass spectral analysis. Financial assistance from U.G.C., New Delhi, is gratefully acknowledged.

References

1. R. N. CHOPRA, S. L. NAYAR and I. C. CHOPRA, "Glossary of Indian Medicinal Plants", C. S. I. R., New Delhi, 1956, p. 54.
2. S. S. SUBRAMANIAN and S. NAGARJAN, *Indian J. Pharm.*, 1970, **32**, 70.
3. L. NIHOUL, *J. Pharm. Belg.*, 1960, **15**, 49.
4. H. HEILBRON and H. N. BUNBURY, "Dictionary of Organic Compounds", Eyre and Spottiswoode, London, 1965, Vol. 2, p. 707.

Chemical Examination of *Ammannia baccifera* Linn. (Lythraceae)

S. M. THAKKAR, V. K. DESHMUKH*, A. N. SAOJI and N. J. DURAGKAR

Department of Pharmaceutical Sciences, Nagpur University, Nagpur-440 010

Manuscript received 2 July 1985, revised 7 October 1985, accepted 17 February 1986

AMMANNIA baccifera Linn., (family : Lythraceae) is an important medicinal plant. Survey of literature reveals that no work has been reported so

far, and therefore a systematic chemical examination of its fruits, leaves and roots of this plant was undertaken.

Fruits :

Air-dried powder (1.5 kg) of the fruit was extracted successively with petroleum ether (b.p. 60-80°), chloroform and methanol. The petroleum ether extract (36 g) was a semi-solid, a part (17 g) of which was chromatographed over silica gel (500 g). Elution with petroleum ether gave a hydrocarbon (200 mg), m.p. 64-7° ; ν_{max} (KBr) 2 960-2 840 (C–H stretch of alkanes) and 1 450 cm^{-1} (C–H bend of alkanes) ; *m/e* 436 (M^+) 421 (M^+-CH_3), 407, 393, 379 and 365. It was identified as hentriacontane[7].

Further elution with petroleum ether-benzene (7 : 3) gave a white solid (360 mg), m.p. 84-8° ; ν_{max} (KBr) 3 400 (OH), 2 930, 2 860 and 1 465 cm^{-1} ; *m/e* 448 (M^+-H_2O), 433 ($M^+-H_2O+CH_3$), 419, 405 and 391. It was characterised as dotriacontanol[7]. The petroleum ether-benzene (1 : 1) eluate yielded a solid (30 mg), m.p. 112-6° ; ν_{max} (KBr) 3 400, 2 930, 2 860 and 1 475 cm^{-1} ; *m/e* 436 (M^+-H_2O), 418 (M^+-2H_2O)[1,2], 404, 390, 376, 362 and 348-52. It indicated to be a C_{30}-straight-chain diol, and formed a diacetate, $C_{34}H_{66}O_4$, ν_{max} 1 735 cm^{-1}. It appears to be 1,30-triacontanediol[8].

The chloroform extract on similar chromatographic analysis yielded dotriacontanol in petroleum ether (b.p. 60-80°)-benzene (4 : 1) eluate, while ethyl acetate eluate furnished a solid, m.p. 278-80° which responded to positive L.B. test for sterol. It was identified as β-sitosterol-β-D-glucoside from m.m.p., co-tlc and co-ir studies with authentic sample.

Leaves :

Air-dried powder (1.0 kg) of the leaves was extracted successively with petroleum ether, chloroform, acetone and methanol in a Soxhlet apparatus. Concentrated petroleum ether extract on usual chromatographic resolution over silica gel afforded hentriacontane, dotriacontanol and β-sitosterol while no compound could be isolated from the chloroform extract.

Acetone extract on concentration deposited a solid which was crystallised as needless (2 g) from pyridine. The compound did not melt up to 350° and was insoluble in common organic solvents ; λ_{max} (MeOH) 255 and 362, (MeOH+NaOAc) 278 and 355, (MeOH+$AlCl_3$) 272 and 380 nm ; ν_{max} (KBr) 3 480, 1 720, 1 620, 1 580, 1 500 cm^{-1} ; δ(DMSO-d_6) 7.5 (s) and 3.5 (br, s, D_2O exchangeable, OH). The compound was identified as ellagic acid by comparison with the reported spectral data[3]. The mother-liquor (25 g) remaining after the separation of ellagic acid was chromatographed over silica gel (500 g), and the ethyl acetate-acetone (19 : 1) eluate afforded a yellow solid (60 mg), m.p. 306-11°, which gave positive ferric chloride test for phenolic compound. It was found to be identical with the authentic sample of quercetin in tlc, m.p., m.m.p. and ir spectrum.

Roots :

Powdered roots (550 g) were extracted with petroleum ether (b.p. 60-80°). On concentration, the extract gave a solid which was crystallised repeatedly from ethyl acetate-benzene to yield white plates (0.9 g), m.p. 306-11° ; ν_{max}(KBr) 3 400-3 100 (OH), 1 690 (C=O), 1 640 and 882 cm^{-1} (isopropyline group)[4]. It responded to L.B. test for triterpene and was identified as betulinic acid by comparison of its mass[5] and pmr[6] spectra with those reported in literature. The mother-liquor (6.0 g) remaining after the separation of solid on chromatographic analysis over silica gel (200 g) gave a white solid (40 mg), m.p. 204-9°. It was found to be identical in all respects (co-tlc, m.m.p., ir spectra) with the reference sample of lupeol.

References

1. E. Ryhage and E. J. J. Stenhagen, *Lipid Res.*, 1960, **1**, 361.
2. A. Kinmann and C. Wakselman, *Bull. Soc., Chim. Fr.*, 1967, **3**, 937.
3. B. O. Sowemino, F. H. Segelman, M. Tinwa, H. Wagner, G. J. Persinous and N. R. Fransworth, *J. Pharm. Sci.*, 1973, **62**, 1358.
4. L. J. Bellamy, "Infrared Spectra of Complex Molecules", Methuen, London, 1964.
5. H. Budzikiewicz, J. M. Wilson and C. Djerassi, *J. Am. Chem. Soc.*, 1963, **85**, 3698.
6. M. Shamma, R. E Glick and R. J. Mamma, *Org. Chem.*, 1962, **27**, 4512.
7. W. Karrer, "Konstitution and Vorkommen der organischen Pflanzenstoffe, Band 12", Birkhauser Verlag, Basel, 1958.
8. H. A. Szymanski, "Interpreted IR Spectra", Plenum Press, Data Division, New York, 1966, Vol. II.

Extraction Studies of Ruthenium(III) and Platinum(IV) with *S*-Benzyldithiocarbazate

N. S. BHAVE*, K. P. KARIYA

and

(Miss) N. AMBADKAR

Department of Chemistry, Nagpur University, Nagpur-440 010

Manuscript received 16 April 1985, revised 14 April 1986, accepted 23 April 1986

A number of spectrophotometric reagents are known for the determination of ruthenium and platinum. Many sulphur containing reagents are found to be good extractants for these two metals[1-3]. But no attempt has yet been made to study the colour reaction of ruthenium or platinum with *S*-benzyldithiocarbazate (BDTC). The present investigation describes BDTC as new sensitive spectrophotometric reagent for micro determination of Ru^{III} at *p*H 2 and Pt^{IV} at *p*H 0.3. The Ru^{III} and Pt^{IV} complexes gave λ_{max} at 425 and 352 nm, respectively. The composition and stability constants of the extractable species were determined.

Experimental

Standard solutions of Ru and Pt were prepared by dissolving the corresponding chlorides (A.R.) in HCl and standardised by the usual method[9,10]. BDTC was synthesised[11] and purified by crystallisation from benzene. Spectrophotometric measurements were made with a Beckman DU2 spectrophotometer with optically matched quartz cells (1 cm). A Elico LI-10 *p*H meter was used for *p*H measurements.

Procedure : To a sample solution containing 50 μg of Ru^{III} or 97.55 μg of Pt^{IV} was added of 1.0×10^{-2} *M* BDTC solution (4 ml) in acetone. For Ru, the *p*H of the solution was adjusted to 2.0. For Pt^{IV}, 0.1 *M* stannous chloride solution (2 ml) was added and *p*H adjusted to 0.3. The solution was heated to 100° for 1 h on a water-bath and then allowed to cool and equilibrated by shaking for 15 min with chloroform (10 ml). The absorbance of the dry extracts were measured at 425 nm for Ru^{III} and 352 nm for Pt^{IV} using the reagent blank.

Results and Discussion

It was found that 80-fold and 30-fold molar excess of BDTC were necessary for complete extraction of Ru^{III} and Pt^{IV}, respectively. Same concentration of the reagent was maintained in the subsequent studies. The Ru^{III} and the Pt^{IV} complexes with BDTC gave same λ_{max} in solvent, like benzene, toluene, *p*-xylene, cyclohexane, chloroform, carbon tetrachloride and carbon disulphide, but the absorbance values were different. Chloroform was found to be the best solvent as the complexes showed highest distribution ratio in it.

A minimum of 70 min heating time was required to develop the maximum colour intensity and the extracts were stable for at least 5 h at 27±2°. The period of equilibration was varied from 0.5 to 20 min and the extraction was found to be quantitative after 10 min. The complexes obey Beer's law upto 8.4 and 11.1 ppm of Ru^{III} and Pt^{IV}, respectively. The molar absorptivities of the Ru^{III} and Pt^{IV} complexes were found to be 4.2×10^{3} and 9.3×10^{3} dm^{3} mol^{-1} cm^{-1}, respectively. Sensitivities in term of Sandell's defination[12], were 0.023 8 μg cm^{-2} Ru^{III} and 0.020 96 μg cm^{-2} Pt^{IV}. Relative errors were ±2.1% for Ru^{III} and ±1.1% for Pt^{IV}.

Effect of foreign ions : Among the cations (added as chloride, nitrate or sulphate), 100-fold of Be^{II}, Mg^{II}, Ca^{II}, Sr^{II}, Be^{II}, Cu^{II}, Rh^{III}, U^{VI}, Th^{IV} and alkali metal ions do not interfere. Ni^{II}, Zn^{II} and Pd^{II} interfere seriously in Ru^{III}; and Pd^{II}, Cd^{II}, Fe^{III} and Hg^{II} interfere seriously in Pt^{IV}. Among anions, 300-fold excess of acetate, tartarate, borate, molybdate, bromide, iodide, triocyanate (added as alkali metal salts) donot interfere. Tolerance limit of nitrite and fluoride ions are quite low in case of Pt^{IV}.

Stoichiometry and stability of complexes : The molar composition of Ru^{III} and Pt^{IV} chelates of BDTC was determined by mole ratio method[12,13] and Job's method[14] of continuous variation. The two method indicated the formation of 1 : 1 complex in either of the case. The log K values (K = stability constant) for Ru^{III} and Pt^{IV} complexes were found to be 4.8±0.05 and 5.5±0.05, respectively.

Acknowledgement

Authors are thankful to the Head of the Department of Chemistry, Nagpur University, for facilities.

References

1. H. Garniak, *Z. Anal. Chem.*, 1975, 275, 205.
2. H. S. Gowda and P. G. Ramappa, *Curr. Sci.*, 1976, 45, 218.
3. W. Geilmann and R. Neeb, *Z. Anal. Chem.*, 1956, 152, 96.
4. J. Das and K. Datta, *Indian J. Chem.*, 1976, 14, 917.
5. J. T. Pyle and S. K. Majumdar, *Anal. Chem.*, 1964, 39, 1796.
6. A. I. Busev and A. N. Shishkov, *Natural.*, 1970, 3, 71.
7. S. Gangopadahyay, P. K. Gangopadhaya and S. C. Shoma, *Z. Anal. Chem.*, 1976, 281, 148.
8. S. B. Gawali and V. M. Shinde, *Z. Anal. Chem.*, 1976, 280, 29.
9. A. I. Vogel, "A Text Book of Quantitative Inorganic Analysis", Longmans, London, 1961.
10. J. Brandstater and J. Vrestal, *Coll. Czech. Chem. Commun.*, 1961, 26, 392 ; 1962, 27, 1798.
11. M. Akbar Ali and M. T. H. Tarafdar, *J. Inorg. Nucl. Chem.*, 1977, 39, 1785.
12. E. B. Sandell, "Colorometric Determination of Traces of Metals", Intersciences, New York, 1959, p. 83.
13. J. H. Yoe and A. L. Jones, *Ind. Eng. Chem. Anal. Ed.*, 1944, 16, 111.
14. P. Job, *Ann. Chim.*, 1928, 9, 113.

Cation Exchange Chromatographic Separation of Nickel in Mixed Solvents

A. G. GAIKWAD and S. M. KHOPKAR*

Department of Chemistry, Indian Institute of Technology, Bombay-400 076

Manuscript received 20 September 1985, revised 8 April 1986, accepted 28 April 1986

THE cation exchange chromatographic studies of nickel were attempted in mixed solvents[1-3] with hydrochloric acid. Nitric acid[4] and hydrobromic acid[5] were also used with methanol and acetone. Such methods were not selective as ions forming anionic complexes showed strong interferences. Thus work on the separation of less common elements from nickel was lacking. Such studies are reported in this paper.

TABLE 1—CATION-EXCHANGE STUDIES OF NICKEL IN MIXED SOLVENTS

Organic solvent with 2 *M* HCl	%	Peak elution volume V_{max} ml	Total elution volume V_t ml	Ni recovery %	Elution constant (E)	Volume distribution coefficient D_v	Weight distribution coefficient D_w
HCl 2 *M*		75	250	98.9	0.58	1.74	1.21
Methanol	20	75	250	100.3	0.58	1.74	1.21
	40	75	250	99.9	0.58	1.74	1.21
	60	100	250	87.7	0.39	2.55	1.77
	80	100	250	81.6	0.39	2.55	1.77
Ethanol	20	75	250	100.0	0.58	1.74	1.21
	40	100	250	84.5	0.39	2.55	1.77
	60	125	250	54.3	0.30	3.86	2.88
	80	150	250	27.4	—	—	—
2-Propanol	20	75	250	100.1	0.58	1.74	1.21
	40	75	250	99.9	0.58	1.74	1.21
	60	150	250	72.3	0.24	4.17	2.90
Acetone	20	75	250	97.6	0.58	1.74	1.21
	40	100	250	95.5	0.39	2.55	1.77
	60	125	250	84.0	0.30	3.86	2.88
	80	100	250	66.8	0.39	2.55	1.77

TABLE 2—SEPARATION OF NICKEL FROM MULTICOMPONENT MIXTURES IN MIXED SOLVENT SYSTEMS

Sl. no.	Element	Amount added mg	Amount found mg	Recovery %	Eluant
1.	Zn	10.0	10.0	100.0	0.1 *M* HCl in 80% THF
	Pb	9.40	9.40	100.0	0.25 *M* HCl in 80% acetone
	Cu	8.80	8.70	98.8	1 *M* HCl in 80% ethanol
	Ni	10.0	9.90	99.0	2 *M* HCl
2.	Fe	9.20	9.20	100.0	0.25 *M* HCl in 80% acetone
	Cu	8.80	8.70	98.8	0.5 *M* HCl in 80% THF
	Mn	10.20	10.10	99.0	0.75 *M* HCl in 90% acetone
	Ni	10.0	10.0	100.0	2 *M* HCl
3.	Bi	10.0	10.0	100.0	0.25 *M* HCl in 20% THF
	Ca	7.50	7.45	99.3	0.5 *M* HCl in 40% 2-propanol
	U	10.0	9.98	99.8	1 *M* HCl in 80% acetone
	Ni	10.0	9.85	98.5	2 *M* HCl in 80% THF
	Th	12.50	12.50	100.0	1 *M* H_2SO_4

Experimental

The apparatus, reagents and column used were similar to one described earlier[9]. A stock solution of nickel was prepared by dissolving nickel sulphate (AnalaR) (5.65 g) in distilled water (250 ml) containing 1% sulphuric acid, and was standardised as usual. It contained 5.1 mg ml^{-1} of nickel.

General procedure : An aliquot containing 10 mg of nickel was passed through the column. After washing the column, nickel was eluted with mineral acids, salts and the mixtures of 2 *M* HCl with methanol, ethanol, 2-propanol, acetone, 1,4-dioxane or tetrahydrofuran (Table 1). The effluent lot was collected in twelve fractions (25 ml), and nickel fron each fraction was determined complexometrically.

Results and Discussion

The selectivity scale for eluant was HCl > H_2SO_4 > HNO_3 > $HClO_4$, while in the presence of 2 *M* HCl the selectivity scale for mixed solvents was methanol > THF > acetone > dioxane > propanol > ethanol. Hydrochloric acid was used with advantage with methanol, ethanol, 2-propanol and 1,4-dioxane (20-40%). However, acetone and tetrahydrofuran were poor eluants in high concentrations (Table 1).

Separatian of Ni from binary mixtures : It was noted that 2 *M* HCl in 80% methanol was efficient eluant for Ni, but not for Sc, Y, Th, La and Ce. Similarly, 2 *M* HCl and 80% acetone was best eluant for Ni but not for Mg, Ca, Sr, Ba and Al. Hence, in such mixtures, Ni was first eluted by these eluants and other ions were eluted in binary mixtures with 4-8 *M* HCl. Further more it was observed that 1 *M* HCl in 90% THF was efficient eluant for Fe^{III}, Mn, Co, Cu^{II}, U^{VI} and Ga^{III} but not for Ni^{II}, so also 0.25 *M* HCl in 80% 1,4-dioxane was efficient eluant for In^{III}, Bi^{III}, Pb^{II}, Cd^{II}, Zn^{II} and Hg^{II} but not for Ni^{II}, hence these ions were eluted first with these eluants followed by the elution of Ni with 2 *M* HCl.

Separation of Ni from multicomponent mixtures : Ni was separated from multicomponent mixtures by exploiting the difference in elution with HCl in the presence of different concentration of different kinds of non-aqueous solvents. It was possible to separate Ni from complex mixtures containing Zn, Pb, Cu, Fe, Mn, Bi, Cd, U and Th. The details of such separation are shown in Table 2.

The separation of Ni from Cu, Fe, Mn, Cd and Al is important as they are generally associated with one another in alloys. The isolation of Ni from Zr, Th, Ce, U and Ba has practical application. The overall operation for the separation and determination does not exceed 3 h. The results are reproducible.

References

1. F. W. E. Strelow and C. H. S. W. Weinert, *Anal. Chim. Acta*, 1976, **83**, 179.
2. M. Simek and J. Hanak, *Scripta Chem.*, 1971, **1**, 119.
3. F. W. E. Strelow, *Anal. Chim. Acta*, 1980, **113**, 323.
4. F. W. E. Strelow, A. H. Victor, J. Steyn and H. H. Lachmann, *Talanta*, 1976, **23**, 178.
5. F. W. E. Strelow, C. H. S. W. Weinert and T. N. N. Walt, *Talanta*, 1974, **21**, 1183.
6. A. G. Gaikwad and S. M. Khopkar, *Indian J. Chem., Sect. A*, 1983, **22**, 905.

Aas Determination of Tin in various Samples after Extraction with Liquid Anion-exchanger

SUPRA BANDYOPADHYAY and ARABINDA K. DAS*

Department of Chemistry, Burdwan University, Burdwan-713 104

Manuscript received 15 July 1985, revised 3 June 1986, accepted 18 June 1986

VARIOUS carboxylates of tin(II) compounds have been reported[1]. The present communication reports the extraction behaviour of tin as $Sn(Ox)_2^{2-}$ with liquid anion-exchanger, Aliquat 336, in benzene. The determination of tin have been carried out by atomic absorption spectrophotometry (aas).

Experimental

Aliquat 336 (Fluka, A.G.) liquid anion-exchanger was used without further purification. A stock solution of $SnCl_2.2H_2O$ (AnalaR) was prepared and the solution was standardised[2] before use. All other chemicals used were of analytical grade. A Shimadzu 646 atomic absorption spectrophotometer with a tin hollow cathode lamp was used, and the conditions were optimised according to its manual. The *p*H values were measured with a Systronics 331 expanded *p*H meter.

The general procedure was based upon solvent extraction technique. The aqueous phase was made up from a 5.0 ml of the solution containing 237.38 μg of tin ; 0.05 *M* oxalic acid solution (2.0 ml) was added, *p*H of the resulting solution adjusted to 2.3 and finally phthalate-buffer (1.5 ml) added. Then the aqueous phase was made up to 10 ml and was equilibrated in a separatory funnel with 5% (v/v) Aliquat 336 in benzene (10 ml) for 5 min. The two layers were allowed to settle for 10 min. The organic phase was then separated carefully to another separatory funnel. In order to remove the organic solvent entrained in the separated aqueous phase, the latter was washed with benzene (5 ml). The resulting extract was mixed with the earlier separated organic phase. Then 2 *M* HNO_3 (10 ml) was added to the organic phase and the mixture was shaken for 5 min. The two phases were allowed to settle. The aqueous phase was carefully separated and again washed with benzene (5 ml) to remove any entrained solvent present in the separated aqueous phase. The amount of tin extracted was estimated by aas in presence of 1000-fold excess $NaNO_3$ which enhanced the tin absorption by about 20%[3].

Results and Discussion

Extraction of tin complex became quantitative in the *p*H range 2.0-2.6. Quantitative extraction of tin occurs with benzene (97.3%), and extractions with other solvents show 94.6% in carbon disulphide, 91.9% in toluene, 83.8% in nitrobenzene, 75.7% in 1,2-dichloroethane, 70.3% in isobutyl methyl ketone, 59.5% in amyl alcohol and 35.1% in chloroform. It was found that the extraction increased with increasing extractant concentration and was complete at 5% Aliquat 336. The extraction time was quantitative within 2 min and stripping complete within 3 min, and it was maintained 5 min in both the cases. For the determination of tin, tolerance limits (within an error of ±2%) for various ions are as follows : Al^{III}, Cr^{III}, Cu^{II}, Mn^{II}, Pb^{II} (all 40-fold) ; Zn^{II}, Cd^{II}, Hg^{II}, sulphate (all 80-fold) ; Fe^{III}, phosphate (all 12-fold).

The extraction of $Sn(Ox)_2^{2-}$ is quantitative provided the Aliquat 336 – tin mole ratio is ≥ 2. Plot of log D against log [Aliquat 336] provides a straight line with slope around 2. Thus the simple extraction mechanism of Sn^{II} may be represented as

$$2[R_4N^+]_o + [Sn(Ox)_2^{2-}]_a \rightleftharpoons [(R_4N)_2Sn(Ox)_2]_o$$

where, *o* = organic phase and *a* = aqueous phase.

Analyses of tin in different samples : Several samples were analysed for tin contents after decomposition by the standard methods (Table 1). Solder, a certified sample (59.9% Sn), was decomposed[4] and

Table 1—Determination of Tin in various Samples

Sample	Amount taken g	Sn found* mg g^{-1}	Standard deviation
Solder	0.101 00	594.658	±0.048
Toothpaste	8.344 08	0.161	±0.011
Vegetable oil	9.558 20	0.016	±0.002

* Average of 4 determinations

analysed to check the present method. In toothpastes, fluoride is usually added as its tin salt (SnF_2). With this end in view a fluoride-toothpaste (Hindustan Ciba-Geigy) was decomposed[5] and analysed by the proposed method. Vanaspati (hydrogenated fat) is commonly available in a tinned can. In an ordinary groceteria, it is stored in the old tinned can for long time and may be contaminated with metallic tin. Such Vanaspati (Hindusthan Lever) sample was decomposed[6] and analysed by the present method.

References

1. J. D. DONALDSON and A. JELEN, *J. Chem. Soc., A*, 1968, 1448, 2244.
2. J. BASSETT, R. C. DENNEY, G. H. JEFFERY and J. MENDHAM, "Vogel's Textbook of Quantitative Inorganic Chemistry including Elementary Instrumental Analysis", 4th. ed., ELBS, London, 1978, p. 889.
3. E. J. AGAZZI, *Anal. Chem.*, 1965, 37, 364.
4. F. D. SNELL, C. T. SNELL and C. A. SNELL, "Colorimetric Methods of Analysis including Photometric Methods", Van Nostrand, Princeton, 1959, Volume IIA, p. 180.
5. "Standard Methods of Chemical Analysis", ed. N. H. FURMAN, 6th. ed., Van Nostrand, Princeton, 1962, Vol. I, p. 1087.
6. "Standard Methods of Chemical Analysis", ed. F. J. WELCHER, 6th. ed., Van Nostrand, Princeton, 1963, Vol. II, Part B, p. 1422.

Accession Number.
85921
Date 23.11.87

J. Indian Chem. Soc.,
Vol. LXIII, June 1986, pp. 625-626

Book Review

Chemistry in Engineering and Technology, J. C. Kuriacose and J. Rajaram, Tata McGraw-Hill Publishing Co. Ltd., New Delhi, 1984, Vol. 1, Pp. 672+xx, Rs. 30.00

THIS is the volume 1 of *Chemistry in Engineering and Technology* in two volumes written by two experienced teachers of an Institute of Technology, covering the chemistry curriculum for the students who have chosen to become engineers/technologists.

The volume 1 contains nine chapters covering the topics atomic structure, nuclear structure and radioactivity, nature of the chemical bond, states of matter, thermodynamics, phase equilibria, electrochemistry, chemical kinetics and catalysis, and photochemistry. In each of the chapters, the authors have dealt with fundamentals to provide good foundation needed for understanding the principles of chemistry, and all the time stressed the application-aspect. There are in each chapter a number of well-chosen worked-out problems and exercises for practice by the students at the end of each. The students will find the answers to the problems at the end of the book.

The book will be very useful not only to the students of Engineering and Technology but to students of Chemistry in general.

S. Aditya

Chemistry in Engineering and Technology, J. C. Kuriacose and J. Rajaram, Tata McGraw-Hill Publishing Co. Ltd., New Delhi, 1984, Vol. 2, Pp. 696+xxiii, Rs. 30.00

CHEMISTRY in Engineering and Technology volume 2, is a commendable effort by Kuriacose and Rajaram. The book is not voluminous and the discussion on organic and inorganic chemistry, and chemistry of materials has been confined within little less than 700 pages. The job is not an enviable one. However, the authors have done quite well in putting forward the fundamentals of organic and inorganic chemistry in a brief but lucid manner. Students of engineering and technology who specialise in other disciplines generally find chemistry either too difficult or uninteresting due to lack of proper text or reference books designed for them. This book certainly will help to alleviate the situation. Authors have been throughtful to include the chapter on water and its treatment, corrosion and the like which are of great importance in today's life.

Formulas are well written and mistakes are few except some printing mistakes. The heading of chapter 16 in the contents portion reads Population of the Environment and its control while it should be Pollution *etc.*

In the chapter of Chemistry of Metals and Non-metals, a number of subjects has been discussed. The chapter on protective coatings deals extensively with oil-based paints, but lacks discussion on water-based coatings. This omission is rather serious as this branch of coating industry is expanding at a rapid rate at the expense of old oil-based coatings which require solvents for their application and cause pollution. The chapter on High Polymers is also far from satisfactory. It includes a separate discussion on silicones, but ignores polyethylene, polyvinylchloride and polystyrene, the three most used plastics which an engineer or a technologist would come across in everyday life.

The price of the book is unbelievably low. Unfortunately this may not prove to be an advantage. The binding is very poor ; it will be of not much benefit to the user and will certainly afford lesser satisfaction to the authors, if the book had to remain on the shelf and can not be read more than a few times without being afraid of losing pages that become loose on little handling.

T. K. Raha

Atomic Absorption Spectrometry, B. Welz, (English translation by C. Skegg), VCH Verlagsgesellechaft, Weinheim, 1985, pp. XIII+506, DM 160, ISBN 3 527 261931

THE book under review is the second English edition of the third revised German edition published under the title *Atomabsorptionsspektrometric* by Verlag Chemie in 1983. Although this book is primarily aimed to help the analytical chemists and spectroscopists in their day to day work, it will be of great help to the teachers and students of all discipline who are interested in the work of atomic absorption spectrometry (AAS).

The book has been divided into eleven chapters besides bibliography on the subject. The first two chapters deal with the theoretical aspects of AAS. Chapter Three describes the techniques of AAS, such as flame, graphite furnace, hydride, cold vapour and miscellaneous atomisation technique. Chapter Four deals with the optics of the instruments, and chapter Five deals with the measurement and read-out system. Chapter Six describes some of the important terms associated with AAS measurement followed by several methods of calibration and standardisation, and preconcentr-

methods applicable for trace metals analysis. Chapter Seven deals with the various types of interferences, both physical and chemical, which include spectral overlapping, molecular band overlapping, radiation scattering on particules and non-specific interferences likely to be associated during the elemental analysis. Chapter Eight deals with the applications of various techniques, *e.g.* flame, graphite furnace, hydride and cold vapour techniques. Chapter Nine is a very important chapter in which the related techniques involving atomic spectra in the analytical chemistry has been discussed. The comparative as well as merits and demerits of AAS, AES, AFS, graphite-AAS and AES, and ICPS has been focused in brief and lucid manner. Chapter Ten deals with the conditions and instrumental parameters for 59 individual elements which can be carried out by AAS. Lastly, chapter Eleven presents the application of AAS in the analysis of elements present in various types of materials, *e.g.* body fluids and tissues, food stuffs and drugs, soils, fertilisers and plants, water, enviornmental samples, rocks, minerals and ores, metals and platings, coal, oil and petrochemicals, glass, ceramic and cement, plastics, textile-paper, radioactive materials, phermaceuticals, and other industrial products.

There is a good collection of references on the work on AAS in the bibliography section. The authors have tried to incorporate the up-to-date references but a number of important references relating to AAS and its applications published earlier in reputed journals are left out.

I feel that the book will be of great help to the students, teachers and chemists of all discipline dealing with AAS instruments for research work and routine analysis.

N. R. Sen Gupta